



IMPERIAL INSTITUTE
OF
AGRICULTURAL RESEARCH, PUSA.

PROCEEDINGS
OF THE
ROYAL SOCIETY OF LONDON

SERIES A

CONTAINING PAPERS OF A MATHEMATICAL AND
PHYSICAL CHARACTER.

VOL. CXXIV.

LONDON:

PRINTED FOR THE ROYAL SOCIETY AND SOLD BY
HARRISON AND SONS, LTD., ST. MARTIN'S LANE,
PRINTERS IN ORDINARY TO HIS MAJESTY.

JULY, 1929.

LONDON :
HARRISON AND SONS, LTD., PRINTERS IN ORDINARY TO HIS MAJESTY,
ST. MARTIN'S LANE.

CONTENTS.

SERIES A. VOL. CXXIV.

Minutes of Meetings, May 2, 9, 30; June 6, 13, 20, 27, 1929.

No. 793.—May 2, 1929.

	PAGE
Magnetostriction and the Phenomena of the Curie Point. By R. H. Fowler, F.R.S., and P. Kapitza	1
The Theory of Cracking Petroleum. By H. A. Wilson, F.R.S.	16
The Dispersion of Double Refraction in Quartz. By T. H. Havelock, F.R.S.	46
The Spectrum of H_2 : The Bands Analogous to the Parhelium Line Spectrum.— Part III. By O. W. Richardson, F.R.S., and P. M. Davidson	50
The Spectrum of H_2 : The Bands Analogous to the Parhelium Line Spectrum.— Part IV. By O. W. Richardson, F.R.S., and P. M. Davidson	69
Stress Systems in an Infinite Strip. By R. C. J. Howland. Communicated by L. N. G. Filon, F.R.S.	89
On the Intensity of Total Scattering of X-Rays. By I. Waller and D. R. Hartree. Communicated by R. H. Fowler, F.R.S.	119
The First and Second Order Equations of the Quantum Theory. By H. T. Flint. Communicated by O. W. Richardson, F.R.S.	143
Internal Friction in Certain Tidal Currents. By S. F. Grace. Communicated by J. Proudman, F.R.S.	150
The Relativistic Theory of an Atom with Many Electrons. By J. A. Gaunt. Com- municated by R. H. Fowler, F.R.S.	163
Perturbation Theory in Quantum Mechanics.—II. By A. H. Wilson. Com- municated by R. H. Fowler, F.R.S.	176
The Emission of Soft X-Rays by Different Elements at Higher Voltages. By O. W. Richardson, F.R.S., and F. S. Robertson	188
The Suspension of Sand in Water. By H. E. Hurst. Communicated by G. C. Simpson, F.R.S.	196
The Transfer of Heat by Radiation and Turbulence in the Lower Atmosphere. By D. Brunt. Communicated by G. C. Simpson, F.R.S.	201
The Influence of Nitrogen Peroxide on the Combination of Hydrogen and Oxygen. By H. W. Thompson and C. N. Hinshelwood. Communicated by Sir Harold Hartley, F.R.S.	219
The Action of Metastable Atoms of Helium on a Metal Surface. By M. L. E. Olliphant. (Plate 1) Communicated by Sir Ernest Rutherford, P.R.S.	228

No. 794.—June 4, 1929.

	PAGE
The Criterion for Turbulence in Curved Pipes. By G. I. Taylor, F.R.S.	243
Analysis by X-Ray Spectroscopy. By C. E. Eddy, T. H. Laby, and A. H. Turner. (Plate 2.) Communicated by Sir Ernest Rutherford, P.R.S.	249
The Soft X-Ray Emission from Various Elements after Oxidation. By L. P. Davies. Communicated by O. W. Richardson, F.R.S.	268
The Third Positive Carbon and Associated Bands. By R. K. Asundi. (Plate 3.) Communicated by O. W. Richardson, F.R.S.	277
Hydrodynamic Forces acting on a Cylinder in Motion, and the Idea of a "Hydro- dynamic Centre." By W. G. Bickley. Communicated by G. I. Taylor, F.R.S.	296
Gaseous Combustion in Electric Discharges. Part III.—The Cathodic Combustion of Dry Carbonic Oxide Detonating Gas. By G. I. Finch and D. L. Hodge. Communicated by Prof. W. A. Bone, F.R.S.	303
The Connection between the Zig-Zag Structure of the Hydrocarbon Chain and the Alternations in the Properties of Odd and Even Numbered Chain Compounds. By A. Müller. Communicated by Sir William Bragg, F.R.S.	317
On the Stability of Unimolecular Films. Part I.—The Conditions of Equilibrium. By C. G. Lyons and E. K. Rideal. Communicated by Sir William Hardy, F.R.S.	322
On the Stability of Unimolecular Films. Part II.—The Mechanism of Film Ex- pansion. By C. G. Lyons and E. K. Rideal. Communicated by Sir William Hardy, F.R.S.	333
On the Stability of Unimolecular Films. Part III.—Dissolution in Alkaline Solu- tions. By C. G. Lyons and E. K. Rideal. Communicated by Sir William Hardy, F.R.S.	344
The Electrical Condition of Hot Surfaces during the Adsorption of Gases. Part III. —A Platinum Surface at Temperatures up to 850° C. By G. I. Finch and J. C. Stimson. Communicated by Prof. W. A. Bone, F.R.S.	356
On Einstein's Unified Field Theory. By G. C. McVittie. Communicated by A. S. Eddington, F.R.S.	366
A Collision Problem in the Wave Mechanics. By C. G. Darwin, F.R.S.	375
A Photoelectric Method of Measuring the Light of the Night Sky with Studies of the Course of Variation through the Night. By Lord Rayleigh, F.R.S.	395
The Quantum Theory of Dispersion in Metallic Conductors. By R. de L. Kronig. Communicated by R. H. Fowler, F.R.S.	400
On the Interpretation of the Relativity Wave Equation for two Electrons. By N. F. Mott. Communicated by R. H. Fowler, F.R.S.	422
The Scattering of Fast Electrons by Atomic Nuclei. By N. F. Mott. Communicated by N. Bohr, For. Mem. R.S.	425
Infra-Red Investigations of Molecular Structure. Part I.—Apparatus and Technique. By C. P. Snow and A. M. Taylor. Communicated by T. M. Lowry, F.R.S.	442

	PAGE
Infra-Red Investigations of Molecular Structure. Part II.—The Molecule of Nitric Oxide. By C. P. Snow, F. I. G. Rawlins and E. K. Rideal. Communicated by T. M. Lowry, F.R.S.	453
The Arc Spectrum of Germanium. By K. R. Rao. Communicated by A. Fowler, F.R.S.	465

No. 795.—July 1, 1929.

A Study of the Catalysis by Silver of the Union of Hydrogen and Oxygen. By D. L. Chapman, F.R.S., and W. K. Hall	478
A Detailed Study of the "Radioactive Decay" of, and the Penetration of α -Particles into, a Simplified One-Dimensional Nucleus. By R. H. Fowler, F.R.S., and A. H. Wilson	493
The Process of Coagulation in Smokes. By H. S. Patterson, R. Whytlaw-Gray, F.R.S., and W. Cawood	502
The Structure and Electrification of Smoke Particles. By H. S. Patterson, R. Whytlaw-Gray, F.R.S., and W. Cawood	523
Ionisation by Collision in Monatomic Gases. By J. S. Townsend, F.R.S., and S. P. MacCallum	533
The Magnetic Anisotropy of Naphthalene Crystals. By S. Bhagavantam. Communicated by Sir C. V. Raman, F.R.S.	545
The Influence of Hydrogen Ion Concentration on the Adsorption of Weak Electrolytes by Pure Charcoals. By H. J. Phelps and R. A. Peters. Communicated by Sir Harold Hartley, F.R.S.	554
The Effect of a Nuclear Spin on the Optical Spectra. By J. Hargreaves. Communicated by R. H. Fowler, F.R.S.	568
A Comparison between the Behaviour at the Ac_3 Point of Single Crystal Iron and Polycrystal Iron, both in the Strained and Unstrained State. By H. Quinney. Communicated by G. I. Taylor, F.R.S.	591
The Absorption Spectra of Halogens and Inter-halogen Compounds in Solution in Carbon Tetrachloride. By A. E. Gillam and R. A. Morton. Communicated by E. C. C. Baly, F.R.S.	604
On the Emission of Soft X-Rays by Different Elements, with Reference to the Effect of Adsorbed Gas. By U. Nakaya. Communicated by O. W. Richardson, F.R.S.	616
On the Criteria for the Stability of Small Motions. By R. A. Frazer and W. J. Duncan. Communicated by H. Lamb, F.R.S.	642
Further Investigations of the Spectrum of Ionised Nitrogen (N II). By L. J. Freeman. Communicated by A. Fowler, F.R.S.	654
The Structure of the High Pressure Carbon Bands and the Swan System. By R. C. Johnson and R. K. Asundi. Communicated by T. R. Merton, F.R.S.	668
On the Direct Determination of the Electrostatic Moments of Molecules. By R. J. Clark. Communicated by Sir Ernest Rutherford, P.R.S.	689

	PAGE
Further Studies in the Emission of Electrons from Cold Metals. By T. E. Stern, B. S. Gossling, and R. H. Fowler, F.R.S.....	609

OBITUARY NOTICE.

Micaiah John Muller Hill (with portrait)	i
Index	vii

PROCEEDINGS OF THE ROYAL SOCIETY.

SECTION A.—MATHEMATICAL AND PHYSICAL SCIENCES.

Magnetostriction and the Phenomena of the Curie Point.

By R. H. FOWLER, F.R.S., and P. KAPITZA.

(Received March 8, 1929.)

Section 1. Introduction.—Heisenberg's† theory of ferro-magnetism claims no more than to show us the nature of the origin of this phenomenon—that is to say, where it will be found in the quantum-mechanical theory of a solid when the necessary complicated calculations can be made. He shows that it arises from the exchange degeneracy of the electrons in the different electronic systems of the lattice, and the modest claims he makes for his theory will be acknowledged by everyone.

In spite of the crude stage of present development, which we are not in a position to improve, we may perhaps be allowed to embroider a little round Heisenberg's theme. In reflecting on his theory we have tried to see whether it can also provide a natural home for the associated phenomena of the Curie point and for magnetostriction. The thermal phenomenon of recalescence has already been incorporated by Weiss‡ in his theory. Since Heisenberg's contribution is merely to explain the origin of Weiss's molecular field, his theory will naturally be expected to account for the large change of specific heat on passing through the Curie point, which is the essence of the phenomenon of recalescence. We shall, therefore, merely call attention at a later stage to the origin of this extra specific heat and note how satisfactorily it fits into Heisenberg's theory. On the other hand, there has hitherto been no theory of the relatively large change of volume on passing through the Curie point or of the phenomena of magnetostriction, nor has any theoretical relation been traced between them. Both these effects, notably the former, are far too large to be explained by magnetic forces, just as the normal magnetic forces between

† Heisenberg, 'Z. Physik,' vol. 49, p. 619 (1928).

‡ Weiss, *loc. cit.*, below.

the systems of the metallic lattice can only provide fields which are insignificant compared with Weiss's molecular field. It is almost obvious that the exchange effects of Heisenberg's theory of ferromagnetism must also explain these changes of volume. There is no reasonable alternative.

In his paper on ferromagnetism Heisenberg does not mention the phenomena of the Curie point or magnetostriction, which after all are secondary effects even if surprisingly large ones. For our purpose therefore we have worked through again Heisenberg's calculation of the partition function for a magnetised crystal, retaining terms which are irrelevant in his primary investigation because they do not depend on the applied magnetic field. We can then examine theoretically in the usual way the size of the crystal as a function of the magnetisation. As a result we think we may claim that the change of size at the Curie point and magnetostriction will both fit satisfactorily into Heisenberg's theory. We cannot, of course, go beyond a very rough quantitative comparison.

It is proper, especially as our theory is only qualitative, that we should be able to describe in general terms, but precisely, the origin of these changes of size. This we think can be done as follows: Consider the interaction of two atoms, for example two normal hydrogen atoms, as developed by Heitler and London.[†] At a given distance apart the system has two different possible energies, one corresponding to an attraction (at distances not too small) and the other to a repulsion. The difference of energy is large compared with the magnetic energy due to the spins. In this particular example the greater energy (the repulsion) corresponds to a wave function antisymmetrical in the electrons (ignoring their spins) and the other energy to a symmetrical wave-function. The complete wave-functions must, of course, be antisymmetrical in the electrons, and therefore the greater energy corresponds to a solution symmetrical in the spins of the electrons and the lesser to an antisymmetrical one. Now consider a number of such pairs set parallel to each other in a magnetic field. The magnetic field will alter the distribution of the axes of the electron-magnets, and therefore the relative numbers of pairs which are symmetrical or antisymmetrical in the spins. It will therefore alter the average repulsion or attraction of the pairs, and that too by an amount out of all proportion to the direct effect of the magnetic forces corresponding to the magnetisation produced. We cannot describe the details of the process in such a simple way when we have groups of more than two atoms in close interaction, but the effects differ only in complication and remain the same in kind. The

[†] Heitler and London, 'Z. Physik,' vol. 44, p. 455 (1927).

magnetisation compels a new selection from the various possible energies of interaction, and this results in comparatively large changes in the forces of attraction and repulsion at given distances, and so in changes of size in the magnetised crystal.

We proceed in Section 2 to a description of the results of Heisenberg's theory carried through rather more completely in the way we require here. There is nothing substantially new in this section and any reader familiar with Heisenberg's paper may omit it, though we find it makes his theory easier to ourselves to present one important step somewhat differently.

Section 2. A Summary of Heisenberg's Theory revised for the Calculation of Magnetostriction, etc.—The essential feature of Heisenberg's calculations is the construction of a partition function for a lattice of $2n$ similar interacting systems, each containing one electron free to orientate itself, taking explicit account of the magnetisation exhibited by the various possible states. This partition function, if it could be calculated exactly, would, of course, contain within itself all the equilibrium properties of the metal. To see how the size of the metal depends on the magnetisation one should strictly be able to calculate this partition function with some accuracy. We shall find that we cannot yet attain any such accuracy even when there is no magnetisation, but that, if we carry through the computation of the partition function as completely as possible with Heisenberg's approximations, we can get far enough to elucidate the nature of the effects in question and to see that they fit satisfactorily into Heisenberg's theory.

We group together all states which correspond to a given total electronic spin momentum of $sh/2\pi$ ($n \leq s \leq 0$). All these states are associated with a particular partition of $2n$, namely, $2 + 2 + \dots$ ($n - s$ times) $\dots + 2 + 1 + 1 + \dots$ ($2s$ times) $\dots + 1$. All quantities associated with this partition are characterised by a suffix σ . There are (allowing for Pauli's principle) f_σ possible states with various energy values where

$$f_\sigma = \frac{2n!}{(n+s)! (n-s)!} - \frac{2n!}{(n+s+1)! (n-s-1)!}. \quad (1)$$

We now neglect interactions except between the closest pairs, and assume that each atom in the lattice has z closest neighbours. Then the f_σ energy values of the states of the system of $2n$ atoms which correspond to a total spin of s units have a mean value E_σ given by

$$E_\sigma = -z \frac{s^2 + n^2}{2n} J_0 + J_E + E_M. \quad (2)$$

J_0 and J_E are the typical interaction integrals of the perturbation theory:—

$$J_0 = \frac{1}{2} \iint \psi_k^\kappa \psi_k^\lambda \psi_l^\kappa \psi_l^\lambda \left\{ \frac{2\varepsilon^2}{r_{kl}} + \frac{2\varepsilon^2}{r_{\kappa\lambda}} - \frac{\varepsilon^2}{r_{\kappa k}} - \frac{\varepsilon^2}{r_{\kappa l}} - \frac{\varepsilon^2}{r_{\lambda k}} - \frac{\varepsilon^2}{r_{\lambda l}} \right\} d\tau_k d\tau_l,$$

where k, l refer to the two electrons and κ, λ to the two (neighbouring) nuclei, ψ is the unperturbed wave-function for the specified electron near the specified nucleus and $d\tau$ is an element of the configuration space of the specified electron. J_E is the straightforward statical energy of interaction of the $2n$ systems which need not be more closely specified—it is necessarily positive. The last term E_M is the energy contribution of the magnetic forces themselves. It is neglected here, but it must play a part in a complete theory and give the phenomena of large scale magnetisation.†

To construct a partition function we require to know not merely E_σ but (strictly) the whole set of f_σ energies belonging to σ . In the absence of precise knowledge of this distribution Heisenberg assumes that they form an approximately Gaussian distribution about E_σ with a mean square deviation Δ_σ^2 (which can be calculated)

$$\Delta_\sigma^2 = zJ_0^2 \frac{(n^2 - s^2)(3n^2 - s^2)}{4n^3}. \quad (4)$$

Thus the number of states belonging to σ with energy between $E_\sigma + x$, and $E_\sigma + x + dx$ is assumed to be

$$\frac{f_\sigma}{\sqrt{(2\pi)} \Delta_\sigma} e^{-\frac{1}{2}x^2/\Delta_\sigma^2} dx. \quad (5)$$

Any one of these states is capable of $2s + 1$ orientations in an external magnetic field H , with the corresponding magnetic energy

$$E' = \frac{-e}{m^*c} \frac{h}{2\pi} Hm \quad (-s \leq m \leq s). \quad (6)$$

We can now write down the complete partition function

$$K = \sum_{s=0}^n \sum_{m=-s}^s \frac{f_\sigma}{\sqrt{(2\pi)} \Delta_\sigma} \int_{-\infty}^{+\infty} \exp \left[-\frac{E_\sigma + x + E'}{kT} - \frac{1}{2} \frac{x^2}{\Delta_\sigma^2} \right] dx. \quad (7)$$

On using the abbreviations

$$\alpha = \frac{e}{m^*c} \frac{h}{2\pi} \frac{H}{kT}, \quad \beta = \frac{zJ_0}{kT}, \quad (8)$$

† A step in the direction of such a theory (not in connection with Heisenberg's theory) has already been made by Mahajani, 'Phil. Trans.,' A, vol. 228, p. 63 (1929). He discusses with success the phenomena observed on the magnetisation of a single crystal of iron.

and evaluating the integral we find

$$K = \sum_{s=0}^n \sum_{m=-s}^{m=s} f_s \exp \left[\alpha m + \beta \frac{s^2 + n^2}{2n} - \frac{J_E}{kT} + \frac{1}{2} \frac{\Delta \sigma^2}{k^2 T^3} \right], \quad (9)$$

$$= \sum_{s=0}^n \sum_{m=-s}^{m=s} f_s \exp \left[\alpha m + \frac{\beta s^2}{2n} - \frac{\beta^2}{8zn^3} s^2 (4n^2 - s^2) \right] \\ \times \exp \left[\frac{1}{2} n \beta + \frac{3n\beta^2}{8z} - \frac{J_E}{kT} \right]. \quad (10)$$

By certain transformations this is reduced to

$$K = O(1) \left[\sum_{m=-n}^m \sum_{m=-s}^{m=s} \frac{2n!}{(n+m)!(n-m)!} \exp \left\{ \alpha m + \frac{\beta m^2}{2n} - \beta^2 \frac{m^2 (4n^2 - m^2)}{8zn^3} \right\} \right] \\ \times \exp \left\{ \frac{1}{2} n \beta + \frac{3n\beta^2}{8z} - \frac{J_E}{kT} \right\}, \quad (11)$$

where $O(1)$ denotes a factor not seriously different from unity, which makes a negligible contribution to $\log K$ when n is large.

Before following Heisenberg in his next step it is wise to pause and examine the nature of the partition function K which he has constructed. By (11) it is seen to be, for given n , a function only of α , β , J_E and T , that is of H , V , T and these variables alone. We know that $\log K$ is equivalent to a thermodynamic function which in this instance is such that

$$p = kT \frac{\partial}{\partial V} \log K, \quad I = kT \frac{\partial}{\partial H} \log K, \quad (12)$$

I being the total magnetisation.† These values are completely unambiguous. We could now safely follow Heisenberg in his next step, retaining, however, factors in which he was not interested. The step is to evaluate K on the assumption that there is a sharp maximum in the terms of the series (11) near some value $m = m_0$, using an elegant approximation and verifying subsequently that the maximum is sufficiently sharp. It is, however, almost as simple mathematically and more direct physically to evaluate (11) by direct attack, assuming that for values that matter m is sufficiently different from n to justify the use of Stirling's theorem. This can be justified *a posteriori*.

† See for example Fowler, 'Statistical Mechanics' (1929), §§ 2.74, 12.3. The account of I there given is based on Debye, 'Phys. Z.', vol. 27, p. 67 (1926), and is given explicitly for dielectric polarisation for which precisely the same theory is required. The corresponding magnetic theory is given by Weiss or Langevin.

We start therefore by writing the summand of (11) in the form $\exp[f(m)]$ or in full

$$\exp \left[\alpha m + \beta \frac{m^2}{2n} - \beta^2 \frac{m^2(4n^2 - m^2)}{8zn^3} + 2n \log 2 - (n+m) \log \left(1 + \frac{m}{n} \right) - (n-m) \log \left(1 - \frac{m}{n} \right) \right],$$

and finding its maximum value. Stationary values are given by the roots in m of the equation $f'(m) = 0$, or

$$\alpha + \beta \left(1 - \frac{\beta}{z} \right) \frac{m}{n} + \frac{\beta^2}{2z} \frac{m^3}{n^3} = \log \frac{1 + m/n}{1 - m/n}, \quad (13)$$

which is precisely Heisenberg's equation

$$\frac{m}{n} = \tanh \frac{1}{2} \left\{ \alpha + \beta \left(1 - \frac{\beta}{z} \right) \frac{m}{n} + \frac{\beta^2}{2z} \frac{m^3}{n^3} \right\}, \quad (14)$$

of which the roots are $m = m_0$, say. There now follows the usual proof (which we leave to the reader) that there may be (a) one or (b) three real roots of (14) which correspond mathematically to (a) the maximum of the summand, or (b) the maximum, a minimum and a subordinate maximum of the summand. In the latter case they correspond, of course, physically to the stable, an unstable and a metastable state, the maximum (stable state) corresponding to the greatest value of m_0 of the same sign as α . We are only interested here in this dominant root. The series is easily summed to the approximation required by replacing it in the usual way by

$$\exp f(m_0) \int_{-\infty}^{+\infty} \exp \left[\frac{1}{2} (m - m_0)^2 f''(m_0) \right] dm,$$

which is sufficiently nearly, written in full,

$$\exp \left[\alpha m_0 + \frac{1}{2} \beta \left(1 - \frac{\beta}{z} \right) \frac{m_0^2}{n} + \frac{\beta^2 m_0^4}{8zn^3} + 2n \log 2 - n \log \left(1 - \frac{m_0^2}{n^2} \right) - m_0 \log \frac{1 + m_0/n}{1 - m_0/n} \right].$$

Therefore from (11)

$$\log K = 2n \left[\frac{1}{2} \alpha \frac{m_0}{n} + \frac{1}{4} \beta \left(1 - \frac{\beta}{z} \right) \frac{m_0^2}{n^2} + \frac{1}{16} \frac{\beta^2}{z} \frac{m_0^4}{n^4} + \log 2 - \frac{1}{2} \log \left(1 - \frac{m_0^2}{n^2} \right) - \frac{1}{2} \frac{m_0}{n} \log \frac{1 + m_0/n}{1 - m_0/n} + \frac{1}{4} \beta + \frac{3\beta^2}{16z} - \frac{J_E}{2nkT} \right]. \quad (15)$$

Equation (15) looks far removed from Heisenberg's formula, but on using (13) and (14) in the terms involving logarithms, it reduces at once to

$$\log K = 2n \left[\log 2 + \log \cosh \frac{1}{2} \left\{ \alpha + \beta \left(1 - \frac{\beta}{z} \right) \frac{m_0}{n} + \frac{\beta^2 m_0^3}{2zn^3} \right\} \right. \\ \left. - \frac{1}{2} \beta \left(1 - \frac{\beta}{z} \right) \frac{m_0^2}{n^2} - \frac{3\beta^2 m_0^4}{16zn^4} + \frac{1}{2} \beta + \frac{3\beta^2}{16z} - \frac{J_E}{2nkT} \right], \quad (16)$$

which is what Heisenberg would have obtained by his method of approximation if he had kept all the terms in m_0/n . It must be remembered that so far in all these formulæ m_0 is merely a parameter introduced for mathematical convenience and must be regarded as a function of T , V and H . It must strictly, therefore, be varied in any differentiation with respect to any of these variables, but from the method of construction of (15) or (16) based on (13), namely, $f'(m_0) = 0$, it follows that

$$\frac{\partial \log K}{\partial (m_0/n)} = 0. \quad (17)$$

Such variations can therefore always be omitted, but this is hardly obvious unless the complete form of $\log K$ is used. Equation (17) is not true for example of Heisenberg's abbreviation, which makes this abbreviation somewhat obscure.

From the thermodynamic relation (12) and equation (15) for $\log K$ we derive at once

$$1 = kTm_0 \frac{\partial \alpha}{\partial H} = m_0 \cdot \frac{\epsilon h}{2\pi m^* c}, \quad (18)$$

which is, of course, Heisenberg's result, that the magnetisation is m_0 double-magnetons, where m_0 is the proper root of (14). To fit the fact of the existence and position of the Curie point for iron it is necessary, as Heisenberg has shown, that β should be positive and of order unity when the temperature is of the order 1000°K .

Now that we know the meaning of m_0 —that it represents in suitable units the natural saturation value of the magnetisation—we see that m_0/n is the same as Weiss' σ/σ_0 and is itself an important physical quantity, the ratio of the natural magnetisation to the limiting magnetisation of which the specimen is capable (at low temperatures or in very strong fields). It is probably wise to give this ratio a symbol of its own and we write

$$m_0/n = \zeta.$$

Section 3. The Nature of the Curie Point and the Change in Specific Heat there.—The nature of the Curie point of a ferromagnetic substance is well

known. All the phenomena agree in indicating that at temperatures below the temperature of the Curie point the normal stable state of the material is the magnetised state, the magnetisation being given by the non-zero root of equation (14) of the Weiss-Heisenberg theory. Ordinary material which is apparently unmagnetised can only be unmagnetised in bulk. It must consist of a collection of micro-crystals each fully magnetised but orientated at random, so that the large scale magnetisation is zero. The actual state of the material probably corresponds closely to the theoretical magnetisation for the temperature in question in zero external field. At temperatures above the Curie point the normal stable state is unmagnetised on both the small and large scales and the material is merely strongly paramagnetic. Below the Curie point the state of zero magnetisation which exists is unstable and no doubt is not found in the microcrystals. What we call magnetisation in bulk at such temperatures does not therefore involve any fundamental change of state from zero to finite magnetisation among the microcrystals but merely a change of orientation in their magnetisation. This is accompanied by the steady growth of the effective external field applied to each of them, from zero for the apparently unmagnetised material to $\frac{1}{2}\pi I/V + H$ ($= H_c$, say) for the material magnetised to the extent I/V per unit volume. The so-called natural saturation value of I is, of course, not the greatest magnetisation of which the substance is capable, but the fraction ζ of this quantity—that is the stable magnetisation given by equation (14) for the temperature in question and the value of α corresponding to H_c .

We are now in a position to study the energy content of the material for given α , so far at least as it depends on the terms involving the magnetisation. Note that it is the energy for given α (usually $\alpha = 0$) with which we are concerned in the phenomena of the Curie point. We apply the general formula :

$$E = kT^2 \frac{\partial}{\partial T} \log K \quad (19)$$

to equation (15) or (16), and retain only the terms in ζ . We need only, in virtue of (17), vary T where it occurs explicitly and in α and β . The contribution in which we are interested might be called E_I . Since

$$\frac{\partial \alpha}{\partial T} = -\frac{\alpha}{T}, \quad \frac{\partial \beta}{\partial T} = -\frac{\beta}{T},$$

we find

$$E_I = -2nkT \left[\frac{1}{2}\alpha \zeta + \frac{1}{4}\beta \left(1 - \frac{2\beta}{z}\right) \zeta^2 + \frac{1}{8} \frac{\beta^2}{z} \zeta^4 \right]. \quad (20)$$

In the use of this equation ζ must be determined from (14). If we consider one gram-molecule of the substance, $2nk = R$.

We follow Heisenberg's wise example and attempt only to account for the broad outline of the phenomenon of the variation of specific heat near the Curie point. For this purpose it will be sufficient to establish the value of the discontinuity in C_v . When $T > T_c$ and $\alpha = 0$, $\zeta = 0$, $E_I = 0$ and therefore $(C_v)_I = 0$. When $T < T_c$, $\xi > 0$ and $E_I < 0$, but as $T \rightarrow T_c$, E_I rapidly approaches zero. Therefore $(C_v)_I > 0$. At much lower temperatures the main term in E_I , namely, $\beta T \zeta^2$ becomes constant and $(C_v)_I$ should fall to small values, but the theory cannot yet extend so far. As $T \rightarrow T_c$

$$(C_v)_I \sim -RT_c \left[\frac{1}{4}\beta (1 - 2\beta/z) \right]_c [d\zeta^2/dT]_c.$$

Since as $T \rightarrow T_c$,

$$\beta (1 - \beta/z) \rightarrow 2,$$

the first factor after T_c is approximately $\frac{1}{2}$. From (14) we find for the remaining factor

$$\left[\frac{d\zeta^2}{dT} \right]_c \rightarrow -\frac{3}{T_c}$$

with the same sort of accuracy. Thus

$$(C_v)_I \rightarrow \frac{3}{2}R$$

to a rough approximation. We might expect it to be rather less. We may say that the theory requires a step down in C_v somewhat less than 3 calories per degree per gram-molecule as the temperature rises through the Curie point from below. The latest observations are†

Substance.	ΔC_v calories per degree per gram.	ΔC_v calories per degree per gram- atom of metal.
Nickel (Ni)	0.0285	1.7
Magnetite (Fe_3O_4)	0.079	6.1
Iron (Fe)	0.122	6.8

Even these experimental values are perhaps open to some doubt ; but they are certainly sufficiently reliable to show that while the data for nickel can fit into a theory containing one magnetisable electron per atom the data for iron do not. This, however, is what we should expect for the values of the completely saturated magnetisation in nickel and in iron are given by Weiss as

† Weiss, Piccard and Carrard, 'Arch. Sci. Phys., Geneva,' vol. 42, p. 378 ; vol. 43, pp. 22, 113, 199 (1917).

equivalent to 3 and 10 of his magnetons respectively ; that is to $\frac{2}{3}$ and 2 Bohr magnetons. Heisenberg's one-electron theory is adequate for nickel and the value of ΔC_0 fits into the theory. For iron and magnetite a two- or perhaps a three-electron theory is required. This has not yet been constructed. But it seems clear that such a theory will only differ from the present in complication of detail and will give a value of ΔC_0 per gram-atom metal twice (or three times) as great as the one-electron theory, in agreement with the observed values.

The thermo-magnetic effects observed by Weiss† on magnetisation at any temperatures are, of course, mainly residual effects arising from the changes in E_I consequent on changes in H_0 , and so, *via* (14), in ζ . These changes in H_0 may be due to changes in H or in the large scale magnetisation or in both. They have been fully discussed by Weiss and are mentioned here only for completeness.

Section 4. The Change of Size at the Curie Point.—According to the theory of Heitler and London β and J_E should give to a first approximation the *whole* of the interaction of neighbouring atoms so far as it can be regarded as arising from the one electron per atom which we have allowed to be present. Since there are many more electrons per atom to interact many of which would not have magnetic properties we need not be surprised if the main interaction comes from terms other than β which the theory has so far of necessity overlooked.

It is possible to make rough estimates ; on account of the Curie point β must be about 2 at 1000°K in iron, which means that J_0 must be about $1/50$ volt or $2J_0$ about $1/5$ volt. If the whole of the attractive forces were derived from β the energy of binding of the atoms in the lattice would also be of the order of $1/5$ volt. There appears to be no data‡ at all for vapour pressure or heat of evaporation of iron, or of metals of the iron group. Zinc has a latent heat of about 1.45 volts. Copper has a boiling point temperature more than twice that of zinc, so that its latent heat will be of the order of double that of zinc, say 3 volts. Experiments by Langmuir indicate 6 volts for the heat of evaporation of platinum and as much as 9 volts for that of tungsten. These values are no doubt higher than the value for iron. The boiling point of iron is close to that of copper, so that it appears to be safe to estimate the heat of evaporation of an iron atom at 3 volts. This is some 15 times the value which might be derived from our β .

† Weiss, 'J. Phys. Rad.', vol. 1, p. 161 (1921); Weiss and Forrer, 'Ann. Phys.' vol. 5, p. 153 (1926). [*Le phénomène magnéto-calorique.*]

‡ The data used below will all be found in 'Landolt-Börnstein,' ed. 5, p. 1332 ff.

It appears therefore that we have omitted from $\log K$ important attractive forces which are not concerned with the magnetic effects. Remembering the way in which the theory was initially simplified there is nothing surprising or contradictory in this. The extra terms should, perhaps, be regarded as arising from the interactions of other groups of electrons incapable of change of orientation. There is nothing in the size of the factor 15 which makes this impossible. Or perhaps the metal crystal should rather be regarded as a construct out of metal ions (with magnetic properties) and free electrons. These points future calculations must examine. In the meantime we shall not go far wrong in estimating from (15) changes of size in the crystal, if we retain the terms depending on α and ζ and replace the others by empirical terms, representing reasonably closely the true main structural forces.

We shall take the corrected $\log K$ to be of the form

$$\log K' = 2n \left[\log 2 + \log \cosh \frac{1}{2} \left\{ \alpha + \beta \left(1 - \frac{\beta}{z} \right) \zeta + \frac{\beta^2}{2z} \zeta^3 \right\} - \frac{1}{4} \beta \left(1 - \frac{\beta}{z} \right) \zeta^2 - \frac{3\beta^2}{16z} \zeta^4 + \frac{A}{V^p} - \frac{B}{V^q} \right]. \quad (22)$$

The terms in A and B are those typical of the ionic lattice theory, but they will sufficiently represent the facts here. We may suppose to a sufficient approximation that TA and TB are independent of the temperature— that is, we are neglecting the heat motion of the lattice elements. The equation determining the size is

$$p = kT \frac{\partial}{\partial V} \log K' (H, V, T) = 0. \quad (23)$$

Above the Curie point in zero field we may take this equation to be equivalent to

$$\frac{Ap}{V^p} - \frac{Bq}{V^q} = 0. \quad (24)$$

Some way below the Curie point where ζ is already fairly large it is equivalent to

$$\frac{Ap}{V^p} - \frac{Bq}{V^q} - V \frac{\partial \beta}{\partial V} \left[\frac{1}{4} \left(1 - \frac{2\beta}{z} \right) \zeta^2 + \frac{1}{4} \frac{\beta}{z} \zeta^4 \right] = 0, \quad (25)$$

the ratio of $A : B : \beta$ being unaltered to our approximation by the change of temperature. If A and B are taken positive, the term A/V^p represents the negative potential energy of the attractive forces and is of the order of the whole negative energy per atom, or some 15 times β . Also $q > p$. If δV is

the increase in volume in the magnetised state, we find from (24) and (25) after reduction that

$$\frac{\delta V}{V} = \frac{1}{q-p} \left(\frac{V \partial \beta / \partial V}{-V \partial (AV^{-p}) / \partial V} \right) \left[\frac{1}{2} \left(1 - \frac{2\beta}{z} \right) \zeta^2 + \frac{1}{8} \frac{\beta}{z} \zeta^4 \right]. \quad (26)$$

The orders of these factors are fairly easily estimated, though, of course, not very closely. The first, $(q-p)$, might be as large as 3, a fair mean value being 2. The second being the ratio of the V rates of variation of energy terms of similar origin is probably nearly in the ratio of the energies themselves, i.e., about $\frac{1}{18}$. The complete change of volume due to magnetisation on going through the Curie point should therefore be of the order $\frac{1}{18}$. The observed change of length in a wire appears to be $\frac{1}{360} - \frac{1}{810}$, and therefore the change of volume $\frac{1}{180} - \frac{1}{270}$. It is important, however, to notice that the observed change is a *contraction* as the temperature rises through the Curie point, that is, as the wire is demagnetised. It is therefore necessary that $\partial \beta / \partial V > 0$. This is somewhat surprising, though by no means impossible, for a range of values of V , that is, for a range of distance apart of the interacting atoms. But it is not possible to say more until more detailed calculations can be made.

This sign of $\partial \beta / \partial V$ makes β contribute to the *repulsive* forces between the atoms at metallic distances. It was, therefore, with the less regret that we concluded above that major sources of attractive forces had been omitted from the theory. It is impossible for β to do both jobs! In this intriguing situation it is satisfactory that it is possible to check the sign of $\partial \beta / \partial V$ directly which can be done by observing the change of position of the Curie point under pressure or tension (that is, with change of volume), but no such experiment appears to have been reported.

We have mentioned above that the observed change of length of iron at the Curie point is between $\frac{1}{360} - \frac{1}{810}$. We have little doubt that this is the correct order of magnitude, but accurate data do not seem to exist. The phenomenon was recorded long ago by Barrett† and it seems to be agreed on his evidence that there is a large change of length at the Curie point, but the only exact measurements we have been able to find are those of Charpy and Grenet.‡

The curves they have obtained for the change of length could easily be interpreted as supporting strongly the estimate given above, but such an interpretation would not be fair. Their curves show also a large effect of

† Barrett, 'Phil. Mag.,' vol. 46, p. 472 (1873).

‡ Charpy and Grenet, 'Bull. Soc. Encouragement Industrie Nat.,' p. 464 (1903). We are much indebted to Mr. C. E. Guillaume for information about the literature.

impurities both on the temperature and on the magnitude of the main change of length, and the change usually occurs in such a way that the effect of the Curie point cannot be disentangled with certainty from that of the $\beta \rightarrow \gamma$ transition point at a temperature some 100° C. higher. It is only possible to test the theory if the extensometer readings are accompanied by magnetic observations so as to correlate the change of length exactly with the changes of magnetic state. Charpy and Grenet do give one such set of double observations which would provide an excellent confirmation of the theory, but they refer to a nickel-iron alloy which might have more complicated properties. We must be content to point out the need for new measurements and the interest which would attach to them.

Section 5. Magnetostriction.—It appears never yet to have been pointed out that magnetostriction—the change of length observed on actually magnetising iron in bulk—must be related to the change of length at the Curie point in exactly the same way as Weiss's thermo-magnetic effects are related to the change of specific heat at the Curie point. Both the Curie point phenomena are primary effects resulting from the change over from the unmagnetised to the magnetised state on the microscale. Both the other phenomena are residual or secondary effects due to the changes of magnetisation arising from changes in the external fields which act on the microcrystals. In discussing magnetostriction it is obvious that at this stage it is only the order of the effect which we can hope to account for, and then only for saturated magnetisation. The growth of the effect, as shown by the curve of change of length against magnetization, must be a complicated phenomenon depending on the gradual switch over in the directions of magnetisation of the microcrystals. The effect itself was shown by Webster† to depend in magnitude and sign on the orientation of the magnetisation with respect to the crystallographic axes of the specimen. This also we cannot yet attempt to investigate.

Using now the value given above for the primary change of length near the Curie point, we may take (26) in the rough form

$$\frac{\delta l}{l} = \frac{1}{240} \zeta^2,$$

for the value of ζ corresponding to ordinary temperatures is about 0.9. Corresponding to a small increase in ζ such as is due to H_1 on magnetisation in bulk, we have then

$$\frac{\delta l}{l} = 7.5 \times 10^{-3} \delta \zeta.$$

† Webster, 'Roy. Soc. Proc.,' A, vol. 109, p. 570 (1925).

The value of $\delta\zeta$ is to be calculated from (14) as the result of a change $\delta\alpha$ in α . We find

$$\delta\zeta \left[\frac{1}{1-\zeta^2} - \frac{1}{2}\beta \left(1 - \frac{\beta}{z} \right) - \frac{3\beta^2}{2z} \zeta^2 \right] = \frac{1}{2}\delta\alpha = \frac{e\hbar}{4\pi mc} \frac{H_1}{kT}.$$

At ordinary temperatures, $T = 300^\circ \text{ K}$, we may assign the rough values $\frac{1}{2}, \frac{1}{3}, 1$ to the terms in []. We then find

$$\delta\zeta = 4.7 \times 10^{-3},$$

$$\frac{\delta l}{l} = 3.5 \times 10^{-5},$$

an increase of length on magnetisation, in excellent agreement with the greatest value $+ 2.0 \times 10^{-5}$ found by Webster.

The theory is not yet fit for any closer application.

Section 6. Remarks on the Interaction of Atoms of Closed Groups of Electrons.

—It may perhaps be not without interest to conclude with some remarks about the structure of metals which arise from the requirements of Heisenberg's theory. In the theory of the interaction of atomic systems the interaction integral J_0 , with which we have been so much concerned here, plays a great part. For hydrogen and helium it is necessarily true that $J_0 < 0$, as was pointed out by Heitler and London (*loc. cit.*). It is the sign of J_0 which determines the sign of the energy difference of the symmetrical and antisymmetrical† wave-functions. It is the negative sign of J_0 (coupled with a normal variation with distance) which compels two helium atoms to repel each other and makes helium an inert gas; for in normal helium the closed configurations of the electrons allow only of a wave-function antisymmetrical in certain pairs of electrons from different atoms, a solution of the wave equation which belongs to a positive interaction energy for negative J_0 . The same considerations no doubt hold for other inert gases, which consist entirely of closed configurations of electrons. We may certainly presume that they do so. But there is not the same necessity as for helium, in which the wave-functions of the normal state have no nodes. It is essential, however, that $J_0 > 0$ for a ferromagnetic substance, and Heisenberg has shown that this can occur if the principal quantum number n of the most lightly bound electrons is sufficiently large, probably if $n \geq 3$. It appears to us that additional evidence for positive J_0

† Throughout this section symmetrical or antisymmetrical are used to mean "symmetrical or antisymmetrical in the space co-ordinates of the electrons." When the spins are included the complete wave-functions are, of course, all antisymmetrical.

can often be drawn from simple considerations as to whether or not the element in question exists at ordinary temperatures as a nearly perfect monatomic gas. The arguments of course only apply to atoms with closed configurations of electrons, but there are many of these besides the inert gases. The normal free atoms Be, Mg, Ca, Sr, Ba, Zn, Cd, Hg, Pd, Pt, are all known to have this property. We believe that we may conclude that J_0 is positive for the interaction of a pair of normal atoms of any one of these elements, for otherwise the element would be able to exist (at least as an alternative) as a monatomic gas at ordinary temperatures. Mercury is the most doubtful. Its properties suggest that J_0 is positive but exceptionally small. It is not suggested that this evidence is conclusive, for the fact that Be, . . . , Hg are not observed freely as monatomic gases might be due not so much to the sign of J_0 , *i.e.*, to the effect of interactions in gas collisions as to the catalysing effect of the walls of any container. It is well recognised too that the molecular state of least energy may arise from the combination of excited states of the atoms.†

The most interesting examples of the group are palladium and platinum, for these normal atoms consist of closed configurations in exactly the same sense as the normal atoms of an inert gas, yet they are metals instead. For example, xenon has the grouping 2, 8, 18, 18, 8; and palladium 2, 8, 18, 18. There is the important difference that the normal state of an inert gas is removed from the nearest excited state by a much larger energy step than in palladium, but it is difficult to resist the speculation that two normal palladium atoms, unlike two normal atoms of an inert gas, can form a molecule because J_0 is positive, and that for the same reason the molecule can proceed, by addition of further atoms, to construct the crystalline metal.

† Heitler and Herzberg, 'Z. Physik,' vol. 53, p. 52 (1929).

The Theory of Cracking Petroleum.

By H. A. WILSON, F.R.S., Rice Institute, Houston, Texas.

(Received February 2, 1929.)

In cracking petroleum the oil is kept at nearly constant temperature and pressure for a certain time and is then separated by fractional distillation into gas, gasoline and heavier fractions.

Usually the oil is passed, through a long pipe heated in a furnace, into a reaction chamber from which the cracked oil is withdrawn continuously. The fraction of the oil converted into gasoline depends mainly on the pressure and the temperature in the reaction chamber, the time taken to pass through the chamber and on the nature of the oil.

The oils used consist almost entirely of mixtures of various types of hydrocarbons, including paraffins, naphthenes, olefines, diolefines and aromatic bodies.

In this paper the theory of the cracking of hypothetical oils consisting only of paraffins and unsaturated hydrocarbons is considered.

It is assumed that the oil remains in the reaction chamber long enough for chemical equilibrium to be established between the hydrocarbons supposed to be present and the fractions of the oil coming out of the reaction chamber as liquid, vapour, gas, gasoline and unsaturated hydrocarbons are calculated.

The theory of chemical equilibrium in mixtures of paraffins and unsaturated hydrocarbons worked out in two previous papers* is made use of in these calculations. These papers will be denoted by E I and E II.

The theoretical results for these hypothetical oils are compared with the results obtained in the cracking of real petroleums, and it is found that there is a good general agreement between the theoretical and practical results. It is therefore concluded that the hypothetical oils resemble actual oils sufficiently closely for the theory of the cracking of the hypothetical oils to represent the main features of actual cracking.

Assuming that the theory of the cracking of the hypothetical oils can be applied to real cracking operations conclusions can be drawn as to the results which should be possible in practical cracking.

* "Chemical Equilibrium in a Mixture of Paraffins," 'Roy. Soc. Proc.,' A, vol. 116, p. 501 (1927); "Chemical Equilibrium in a Mixture of Paraffins and Unsaturated Hydrocarbons," 'Roy. Soc. Proc.,' A, vol. 120, p. 247 (1928).

The composition of a hypothetical oil may be represented by the formula CH_x so that x denotes the number of hydrogen atoms per carbon atom in the oil. If the oil entering the reaction chamber is CH_{x_1} and if $\text{CH}_{x'}$ and CH_{x_2} are the compositions of the liquid and vapour coming out of the reaction chamber then if q denotes the fraction by weight of the oil coming out in the liquid state we have

$$12/(12 + x_1) = 12q/(12 + x') + (1 - q) 12/(12 + x_2)$$

for $12/(12 + x)$ is the fraction the weight of the carbon in the oil is of the weight of the oil, and, of course, the carbon entering the chamber must be equal to that leaving it. We assume here that no coke is deposited in the reaction chamber. When appreciable amounts of coke are deposited the effect of such deposits can be easily allowed for, as will be seen later. The above equation gives $q = (x - x_1)(12 + x')/(x - x')(12 + x_1)$. Thus the fraction of the oil coming out in the liquid state can be calculated when x_1 , x and x' are known.

In the two previous papers, E I and E II, it was shown that in the vapour of a mixture of paraffins and unsaturated hydrocarbons, in a state of chemical equilibrium, the molar amounts of the members of each homologous series present form a geometrical progression with the ratio f between successive terms. Thus if p_n denotes the partial pressure of the vapour of the paraffin $\text{C}_n\text{H}_{2n+2}$ then $p_n = p_1 f^{n-1}$. Also if p'_n denotes the partial pressure of the olefine C_nH_{2n} then $p'_n = p'_1 f^{n-2}$, and in the same way for $\text{C}_n\text{H}_{2n-2}$, $p''_n = p''_1 f^{n-3}$ and so on for the other series.

Also it was shown that if p, p', p'', \dots , denote the sums of the partial pressures for each series so that $p = p_1/(1 - f)$, $p' = p'_1/(1 - f)$, $p'' = p''_1/(1 - f)$, etc., then $p' = yp$, $p'' = y^2p$, $p''' = y^3p$, and so on. Here y is the molar fraction of the vapour consisting of the unsaturated bodies. Thus the total pressure P is given by $P = p + p' + p'' + \dots$, so that $P = p + yp + y^2p + \dots = p/(1 - y)$ and so $P = p_1/(1 - f)(1 - y)$.

The fraction y is given by the equation

$$y = \frac{1}{2} - \sqrt{\frac{1}{4} - Kf^2/P(1 - f)},$$

K is an equilibrium constant given by $\log K = -7400/T + \log T + C$ where T denotes the absolute temperature and C is a constant. I have assumed that y for the liquid is equal to y for the vapour. This must be very nearly true because the molar amounts of the different types of hydrocarbons all form geometrical progressions having the same ratio and the corresponding terms in each series have nearly equal physical properties. It follows also from this that the molar fraction y must be roughly equal to the fraction by weight of

the unsaturated bodies in the oil. With the values of f and y which occur in the cases considered in this paper the unsaturated weight fraction is between $0.95y$ and $1.30y$. The value of y is therefore calculated using the value of f for the vapour, and the value so obtained is used to calculate x' for the liquid in equilibrium with the vapour.

The value of the fraction f at any temperature and pressure may be obtained by means of the charts given in E I which give the values of $x = 4 - 2f$ for the vapour and for the liquid when in equilibrium with each other. In E II the constant C was put equal to 4 but it is found that the calculated results agree better with the facts with $C = 3$ so this new value will be used in the present paper.

Knowing f the value of y can be calculated by means of the equation given above using the value of K given by $\log K = -7400/T + \log T + 3$.

The value of x in the composition CH_x of the vapour can be calculated from y and f . If the vapour contains M mols of CH_4 then it contains $Mf^{m-n-2}y^{m+1}$ mols of $\text{C}_n\text{H}_{2(n-m)}$. Here $m = -1$ for the paraffins $\text{C}_n\text{H}_{2n+2}$, $m = 0$ for the olefines C_nH_{2n} , $m = +1$ for the diolefines $\text{C}_n\text{H}_{2n-2}$, and so on for the other series.

The number of mols of hydrogen in the vapour is therefore equal to

$$M(4 + 6f + 8f^2 + \dots)(1 + y + y^2 + \dots),$$

which is equal to

$$\frac{2M}{1-y} \left\{ \frac{1}{1-f} + \frac{1}{(1-f)^2} \right\}.$$

The number of mols of carbon in the vapour is equal to

$$\begin{aligned} & M(1 + 2f + 3f^2 + \dots) \\ & + yM(2 + 3f + 4f^2 + \dots) \\ & + y^2M(3 + 4f + 5f^2 + \dots) \\ & + \dots, \end{aligned}$$

which is equal to

$$\frac{M}{(1-f)^2(1-y)} + \frac{yM}{(1-f)(1-y)^2}.$$

Hence x the mols of hydrogen per mol of carbon is given by

$$x = \frac{2}{1-y} \left\{ \frac{1}{1-f} + \frac{1}{(1-f)^2} \right\} \bigg/ \left\{ \frac{1}{(1-f)^2(1-y)} + \frac{y}{(1-f)(1-y)^2} \right\}.$$

or

$$x = 2(2-f)(1-y)/(1-yf).$$

The charts in E I give x for a mixture of paraffins only for which $y = 0$

when there is equilibrium between the liquid and vapour. From the values of x given by the charts we get f since $f = 2 - x/2$. It should be noted that the charts give x for the mixture of paraffins only, but the x given by the above equation is that for the mixture of paraffins and unsaturated bodies. The maximum possible value of y is $\frac{1}{2}$ and when $y = \frac{1}{2}$ then $x = 2(2-f)/(1 - \frac{1}{2}f) = 2$. Thus when $y = \frac{1}{2}$ we have $x = 2$ whatever the value of f .

In the case of vapour not in contact with liquid the value of f will be determined by the composition of the vapour. Thus if all the oil evaporates in the reaction chamber and no coke is deposited so that only vapour comes out then we must have $x = x_1$ where CH_{x_1} is the composition of the oil used. We have then $y = \frac{1}{2} - \sqrt{\frac{1}{4} - Kf^2/P(1-f)}$ and $x = 2(2-f)(1-y)/(1-yf)$. These two equations enable f to be calculated but it is more convenient to use them to calculate K for assumed values of f and then find the temperature corresponding to the values of K calculated. Eliminating y we get

$$K = \frac{P(1-f)}{f^2} \left\{ \frac{1}{4} - \left(\frac{1}{2} - \frac{2(2-f) - x_1}{2(2-f) - fx_1} \right)^2 \right\}.$$

By means of this equation the value of K corresponding to any value of f can be calculated and then the temperature is given by $\log K = -7400/T + \log T + 3$. In this way the variation of the fraction f with the temperature can be found.

In order to calculate the gas and gasoline fractions for the liquid and vapour it is necessary to know how these fractions depend on the composition. The plan adopted is to first calculate these fractions for the mixture of paraffins only, and then to correct the values obtained for the effect of the presence of the unsaturated bodies. It is necessary first to consider the theory of chemical equilibrium in the liquid phase.

When different liquid hydrocarbons are mixed there is very little change of total volume or evolution of heat. The change of total volume is very small compared with the total volume, so that to obtain an approximate theory of such mixtures we may assume that the volume of the mixture is equal to the sum of the volumes of the bodies in it, and that the internal energy of the mixture is equal to the sum of the internal energies.*

Let m_1, m_2, m_3, \dots denote the numbers of gram molecules or mols of the hydrocarbons in such a mixture, and let v_1, v_2, v_3, \dots denote the volumes of one

* These assumptions are equivalent to the assumption that the liquid is a "perfect solution."

mol of the hydrocarbons in the pure state, so that the volume of the mixture is given by

$$V = m_1 v_1 + m_2 v_2 + m_3 v_3 + \dots = \Sigma m v.$$

Also let u_1, u_2, u_3, \dots denote the internal energies per mol in the pure state so that the internal energy U of the mixture is given by

$$U = m_1 u_1 + m_2 u_2 + m_3 u_3 + \dots = \Sigma m u.$$

In Planck's thermodynamical theory of dilute solutions he obtains similar expressions for V and U for a dilute solution but the v 's and u 's are not equal to the molar volumes and energies in the pure state. But the values of the v 's and u 's in Planck's theory of dilute solutions depend only on the temperature and pressure which is also true of the v 's and u 's defined above. It follows that the theory of the mixture of liquids may be worked out in exactly the same way as the theory of dilute solutions so that it will be sufficient to merely state the results which follow from the theory.

Let $c_n = m_n/\Sigma m$ denote the concentration of the n th constituent of the mixture, ϕ_n its entropy per mol, and let $\psi_n = \phi_n - (u_n + p v_n)/T$ where p and T denote the pressure and absolute temperature. Also let Φ denote the entropy of the mixture and $\Psi = \Phi - (U + pV)/T$ then we have $\Psi = \Sigma m_n (\psi_n - R \log c_n)$ as in the theory of dilute solutions.

If more than one phase is present then we may denote the m 's in the different phases by m, m', m'', \dots , and the other quantities for the different phases may be distinguished in the same way so that Ψ for all the phases is given by

$$\Psi = \Sigma m (\psi - R \log c) + \Sigma m' (\psi' - R \log c') + \dots$$

or

$$\Psi = \Sigma \Sigma m (\psi - R \log c).$$

The condition of equilibrium at constant temperature and pressure is $\delta\Psi = 0$ which gives $\Sigma \Sigma (\psi - R \log c) \delta m = 0$. The δm 's are proportional to the numbers of molecules involved in the small virtual change indicated by δ , and so, in ordinary cases, are proportional to integers ν , so that

$$\Sigma \Sigma (\psi - R \log c) \nu = 0.$$

The equilibrium constant K is defined by $\log K = \Sigma \Sigma \nu \log c$ so that the condition of equilibrium may be written $\log K = \Sigma \Sigma \nu \psi / R$.

The condition of equilibrium among the members of any homologous series in a liquid mixture may now be obtained in just the same way as for the vapour. Let A_n denote a molecule of the member of the series containing n carbon atoms and consider the reaction $A_{n-1} + A_{n+1} = 2A_n$. The condition of equilibrium is $\log K = \log c_n^2 / c_{n-1} c_{n+1} = (2\psi_n - \psi_{n-1} - \psi_{n+1}) / R$. Provided

ψ_n is equal to the mean of ψ_{n-1} and ψ_{n+1} this gives $c_n^2 = c_{n-1} c_{n+1}$, so that the c 's form a geometrical progression and $c_n = c_{n_1} f^{n-n_1}$ where f is a fraction less than unity and nearly independent of n , and n_1 is the smallest value of n for the homologous series in question.

In the case of a liquid mixture consisting entirely of the paraffins $C_n H_{2n+2}$ we have $c_n = c_1 f^{n-1}$. If the mixture contains x hydrogen atoms to one atom of carbon then

$$x = (4c_1 + 6c_2 + 8c_3 + \dots)/(c_1 + 2c_2 + 3c_3 + \dots) = 4 - 2f$$

exactly as in the case of the vapour of a mixture of paraffins discussed in E I.

In the paper just mentioned the percentages by weight of the different paraffins in the vapour corresponding to different values of x from 2.2 to 2.8 were given on page 503. We see now that these percentages will also hold good for the liquid phase. x for the liquid is usually between 2.0 and 2.20 so the percentages corresponding to 2.05, 2.10 and 2.15 have been calculated and are given in the following table.

Table I.

$x =$	2.05.	2.10.	2.15.
n			
1	0.063	0.284	0.636
2	0.130	0.506	1.10
3	0.186	0.705	1.50
4	0.239	0.882	1.83
5	0.289	1.04	2.09
6	0.337	1.18	2.32
7	0.382	1.31	2.49
8	0.425	1.41	2.62
9	0.465	1.51	2.73
10	0.503	1.59	2.80
11	0.538	1.66	2.85
12	0.572	1.72	2.86
13	0.605	1.77	2.87
14	0.635	1.80	2.86
15	0.660	1.84	2.83

The percentage of "gasoline" in the mixture was taken to be the sum of the percentages for the values of n from 5 to 12 together with enough of the percentages of the propane C_3H_8 and butane C_4H_{10} to make the vapour pressure of the gasoline equal to one atmosphere at 104° F. The vapour pressure was calculated in the usual way by assuming the partial pressure of each hydrocarbon in the vapour equal to its vapour pressure multiplied by its molar fraction in the liquid.

The fractions of the propane and butane required were found to be as follows:—

Table II.

$x =$	2.05	2.10	2.15	2.20	2.30	2.40	2.50	2.60	2.70	2.80
C_2H_6	1.00	1.00	1.00	1.00	1.00	0.80	0.50	0.40	0.30	0.20
C_3H_8	0.19	0.10	0.07	0.05	0.02	0	0	0	0	0

The percentage of "gas" in the mixture was taken to be the sum of the fractions of the percentages of CH_4 , C_2H_6 , C_3H_8 and C_4H_{10} not included in the gasoline.

The "gasoline" defined as above is a mixture of $C_{12}H_{26}$, $C_{11}H_{24}$, ..., C_5H_{12} , C_4H_{10} with a trace of C_3H_8 when x is less than 2.30. It would begin to boil at $104^\circ F.$ and its "end point" would be equal to the boiling point of $C_{18}H_{38}$ which is $421^\circ F.$

The following are the percentages of gas and gasoline got in this way:—

Table III.

$x =$	2.05	2.10	2.15	2.20	2.30	2.40	2.50	2.60	2.70	2.80
Gas	0.36	1.40	3.10	5.40	11.5	21.0	32.6	43.2	54.4	64.7
Gasoline	3.8	12.4	22.7	33.0	49.0	56.5	55.0	50.5	42.7	34.2

In fig. 1 the relations between x and the gas and the gasoline percentages are shown graphically.

When oil is kept at a constant temperature in a closed vessel the gas gradually increases with the time, but the gasoline rises to a maximum value and then diminishes. Fig. 2 shows the variation of the gas and gasoline with the time

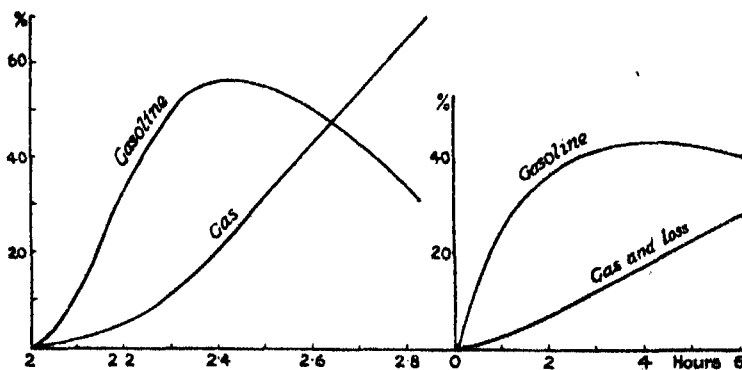


FIG. 1.

FIG. 2.

for a residual base petroleum at 800° F. The oil used filled one-half of the closed vessel. These results are taken from Cross' "Handbook of Petroleum," p. 288.

We should expect coke and highly unsaturated bodies to be slowly produced from the oil so that the percentage of hydrogen in the oil vapour should gradually increase with the time. The variation of the gas and gasoline with the time should therefore be similar to the variation of the gas and gasoline in the vapour as x in CH_x increases. We should therefore expect the curves in fig. 2 to be similar to those in fig. 1 which show the variation of the gas and gasoline in oil vapour with x . Part of the oil in the closed vessel is liquid or coke so that the percentages in fig. 2 should be less than in fig. 1. It will be seen that the curves in fig. 1 are very similar to those in fig. 2 in agreement with the theory. For example the ratio of gasoline to gas, when the gasoline has its maximum value is 2.44 in fig. 2 and 2.46 in fig. 1. Also when the gasoline has one-half its maximum value the ratio of gasoline to gas is 8.8 in fig. 2 and 7.0 in fig. 1.

The charts in E I give the values of x for the liquid and vapour phases when both are present and in equilibrium at any temperature and pressure. By means of the charts and fig. 1 above we can therefore get the percentages of gas and gasoline in the liquid and vapour phases at any temperature and pressure. The following tables give values got in this way for several temperatures and pressures. The numbers are the percentages by weight for a mixture of paraffins only.

Table IV.—Gasoline percentage.

Temperature.	7.5 atmospheres.		15 atmospheres.		30 atmospheres.		60 atmospheres.	
	Vapour.	Liquid.	Vapour.	Liquid.	Vapour.	Liquid.	Vapour.	Liquid.
° F.								
750	54	3.8	56	6.0	56.5	9.0	55.5	13.3
800	51	3.3	55	5.3	56.5	8.0	56.5	11.3
850	—	—	52	4.5	55	7.0	56.5	10.5
900	—	—	—	—	54	6.0	56	9.2
950	—	—	—	—	52	5.3	55	8.3
1000	—	—	—	—	50	4.8	54	7.2
1050	—	—	—	—	—	—	52	6.3

Table V.—Gas percentage.

Temperature.	7.5 atmospheres.		15 atmospheres.		30 atmospheres.		60 atmospheres.	
	Vapour.	Liquid.	Vapour.	Liquid.	Vapour.	Liquid.	Vapour.	Liquid.
° F.								
750	15.7	0.37	20.0	0.65	24.3	0.97	31.0	1.52
800	13.3	0.35	16.8	0.55	21.0	0.93	27.1	1.30
850	—	—	14.3	0.45	18.1	0.75	23.9	1.17
900	—	—	—	—	16.2	0.63	20.8	1.00
950	—	—	—	—	14.3	0.56	18.2	0.90
1000	—	—	—	—	12.4	0.50	16.2	0.80
1050	—	—	—	—	—	—	14.3	0.65

These tables give the percentages by weight of gasoline and gas for the mixtures of paraffins when there is equilibrium between the liquid and vapour. In the case of a mixture of paraffins and unsaturated hydrocarbons the values of the fraction f must be very nearly the same as for the mixtures of paraffins only. This is so because the physical properties of the corresponding hydrocarbons in the different homologous series are nearly equal, as was explained in E I.

Although the fraction f must be nearly the same for the mixture of paraffins and unsaturated bodies as for the mixture of paraffins only it does not follow that the percentages of gas and gasoline are also the same.

If we take the gas to include all of the CH_4 , C_2H_6 , C_3H_8 , C_2H_4 , C_3H_6 and C_3H_4 in the oil, then the weight of the gas containing one mol of CH_4 is

$$16 + 30f + 44f^2 + 28y + 42yf + 40y^2.$$

The total weight of the vapour containing one mol of CH_4 is equal to

$$\begin{aligned} & 16 + 30f + 44f^2 + \dots \\ & + 28y + 42yf + 56yf^2 + \dots \\ & + 40y^2 + 54y^2f + 68y^2f^2 + \dots \\ & + 52y^3 + 66y^3f + 80y^3y^2 + \dots \\ & + \dots \\ & = (16 - 4y - 2f - 10yf)/(1 - f)^2(1 - y)^2. \end{aligned}$$

The gas fraction F' of the weight is therefore given by

$$F' = (1 - f)^2(1 - y)^2 \frac{8 + 14y + 20y^2 + 15f + 21yf + 22f^2}{8 - 2y - f - 5yf},$$

For the mixture of paraffins only $y = 0$ and the gas fraction F is

$$F = (1 - f)^2 (8 + 15f + 22f^2) / (8 - f).$$

Hence

$$\frac{F}{F'} = \frac{(8 + 15f + 22f^2)(8 - 2y - f - 5yf)}{(1 - y)^2(8 - f)(8 + 14y + 20y^2 + 15f + 21yf + 22f^2)}.$$

By means of this expression the following values of F/F' have been calculated.

Table VI.

y .	$f = 1$.	0.9.	0.8.	0.7.	0.6.
0.5	1.33	1.40	1.46	1.51	1.53
0.4	1.21	1.22	1.26	1.29	1.30
0.25	1.09	1.10	1.12	1.12	1.12
0.1	1.026	1.028	1.030	1.030	1.031

By means of these ratios the gas fraction can be obtained from the gas fraction for the mixture of paraffins only, in the cases where the gas consists of all the compounds present for which $n = 1, 2$ or 3 . In some cases the gas contains a fraction of the bodies for which $n = 4$, but this fraction is small unless x is greater than 2.4 and it is not enough to make an appreciable difference.

When f is between 0.75 and 0.6 the vapour consists almost entirely of gas and gasoline, so that the gasoline fraction for the mixture of paraffins and unsaturated bodies can be obtained by adding to the gasoline fraction for paraffins the difference between the two gas fractions. For the larger values of f this difference is quite small so that the correction of the gasoline fraction may still be made in the same way. This correction, so made, probably slightly overestimates the gasoline in a few cases, but the error is less than 1 per cent. of gasoline and makes no appreciable difference. Since the correcting factor is nearly independent of the fraction f its value can usually be got with sufficient accuracy from that of y or the unsaturated fraction alone.

By means of the methods described above the gas, gasoline, liquid and unsaturated fractions in the oil coming out of a reaction chamber may be calculated.

The following table gives the values of these fractions for four hypothetical oils having assumed compositions $\text{CH}_{2.1}$, $\text{CH}_{2.15}$, $\text{CH}_{2.2}$ and $\text{CH}_{2.25}$. These hypothetical oils contain higher percentages of hydrogen than real petroleum. This is because real oils contain naphthenes C_nH_{2n} and possibly aromatic hydrocarbons such as benzene C_6H_6 . If, for example, an oil contained only

naphthenes and unsaturated hydrocarbons it would contain less than 2 atoms of hydrogen to 1 of carbon.

The values of the fraction f for the vapour and for the liquid at the given temperature and pressure are first got from the charts in E I. The value of y for both phases is then calculated by means of $y = \frac{1}{2} - \sqrt{\frac{1}{4} - Kf^2/(1-f)P}$ where f is the value for the vapour and K is given by $\log K = -7400/T + \log T + 3$. x for the vapour and x' for the liquid are next obtained by means of the equation

$$x = 2(2-f)(1-y)/(1-yf).$$

The liquid fraction is then given by

$$q = (x - x_1)(12 + x')/(x - x')(12 + x_1).$$

The percentages of gasoline and gas are then got from the tables of percentages in the liquid and vapour. The gas percentages are corrected by dividing them by the value of the factor F/F' (Table VI) as explained above and the gasoline percentages are also corrected.

When x_1 is greater than x no liquid remains and then the temperatures corresponding to assumed values of f are found by means of

$$K = \frac{P(1-f)}{f^2} \left\{ \frac{1}{4} - \left(\frac{1}{2} - \frac{2(2-f) - x_1}{2(2-f) - fx_1} \right)^2 \right\},$$

together with $\log K = -7400/T + \log T + 3$. The percentages of gas and gasoline corresponding to the values of f are got from Table II and corrected by means of the factor F/F' .

The table gives the percentages by weight in the oil coming out of the reaction chamber except that the percentage of unsaturated bodies is the molar percentage which is roughly equal to the percentage by weight. The percentage of unsaturated bodies will be nearly the same in the gas and in the gasoline as in the total oil.

The oil is assumed to have been in the reaction chamber long enough for equilibrium to have been established between all the bodies present, and it is also assumed that no coke is deposited in the reaction chamber. The lowest temperature given at which the liquid is zero is that at which the liquid just disappears.

Table VII.

Pressures 7.5 atmospheres. $x = 2.25$.

Temperature.	Liquid.	Gasoline.	Gas.	Unsaturated.
° F.	per cent.	per cent.	per cent.	per cent.
750	12.4	48.4	12.6	14.2
766	0	53.8	14.2	17.0
800	0	57.5	16	22.5
900	0	60	34	33.2
1000	0	47	52	37.9

Pressure 7.5 atmospheres. $x = 2.20$.

Temperature.	Liquid.	Gasoline.	Gas.	Unsaturated.
° F.	per cent.	per cent.	per cent.	per cent.
750	33.1	37.9	9.6	14.2
790	0	54.2	12.3	24.0
800	0	57	13	26.5
900	0	61	31	36.9
1000	0	50	48	40
1050	0	42	58	40.6

Pressure 7.5 atmospheres. $x = 2.15$.

Temperature.	Liquid.	Gasoline.	Gas.	Unsaturated.
° F.	per cent.	per cent.	per cent.	per cent.
750	54.0	27.1	6.8	14.2
800	13.9	46.7	9.7	30.0
804	0	54.2	10.8	33
850	0	60	19	37.8
900	0	61	29	40.4
1000	0	51	47	42.6
1050	0	44	55	43.2

Pressure 7.5 atmospheres. $x = 2.10$.

Temperature.	Liquid.	Gasoline.	Gas.	Unsaturated.
° F.	per cent.	per cent.	per cent.	per cent.
750	75	16.5	3.9	14.2
800	48.7	29.2	5.9	30
809	0	53.8	10.2	39
850	0	61	17	41.6
900	0	63	28	44
1000	0	53	46	45.3
1050	0	46	54	45.9

Table VII—(continued).

Pressure 15 atmospheres. $x = 2.25$.

Temperature.	Liquid.	Gasoline.	Gas.	Unsaturated.
° F.	per cent.	per cent.	per cent.	per cent.
750	36.3	37.9	12.8	5.6
800	23.1	43.7	12.7	9.8
843	0	52.9	13.1	18
900	0	58	19	25
1000	0	58	41	33.7
1100	0	48	51	37.6

Pressure 15 atmospheres. $x = 2.20$.

Temperature.	Liquid.	Gasoline.	Gas.	Unsaturated.
° F.	per cent.	per cent.	per cent.	per cent.
750	52.9	29.3	9.6	5.6
800	42.4	34.0	9.6	9.8
850	19.9	43.2	10.5	19.4
868	0	52.5	11.5	27
900	0	58	16	30.3
1000	0	59	33	37.2
1100	0	50	50	40

Pressure 15 atmospheres. $x = 2.15$.

Temperature.	Liquid.	Gasoline.	Gas.	Unsaturated.
° F.	per cent.	per cent.	per cent.	per cent.
750	69.7	20.8	6.4	5.6
800	61.8	24.2	6.5	9.8
850	44.8	31.2	7.3	19.4
875	19.8	43	9.2	28.6
882	0	53.1	10.9	32
1000	0	61	30	40.6
1100	0	52	47	42.6

Pressure 15 atmospheres. $x = 2.10$.

Temperature.	Liquid.	Gasoline.	Gas.	Unsaturated.
° F.	per cent.	per cent.	per cent.	per cent.
750	86.7	12.2	3.2	5.6
800	81.5	14.2	2.7	9.8
850	70.0	19.8	4.2	19.4
875	53.1	26.8	5.5	28.6
888	0	52.6	9.4	39.0
1000	0	62	28	44
1100	0	53	46	45.3

Table VII--(continued).

Pressure 30 atmospheres. $x = 2.25$.

Temperature.	Liquid.	Gasoline.	Gas.	Unsaturated.
° F.	per cent.	per cent.	per cent.	per cent.
750	49.2	33.2	12.9	2.2
800	41.5	36.6	12.6	4.0
850	32.2	38.6	12.4	7.1
900	16.8	46.3	13.2	12.4
952	0	53.8	13.7	19
1000	0	59	19	25.5
1100	0	60	33	32.5
1200	0	60	48	37

Pressure 30 atmospheres. $x = 2.20$.

Temperature.	Liquid.	Gasoline.	Gas.	Unsaturated.
° F.	per cent.	per cent.	per cent.	per cent.
750	63.9	26.3	9.5	2.2
800	57.7	28.6	9.5	4.0
850	50.2	30.9	9.4	7.1
900	38.0	35.8	9.9	12.4
950	11.1	47.3	12.3	23.4
960	0	53.5	12.3	26.5
1000	0	58	15	30
1100	0	62	31	36
1200	0	53	46	40

Pressure 30 atmospheres. $x = 2.15$.

Temperature.	Liquid.	Gasoline.	Gas.	Unsaturated.
° F.	per cent.	per cent.	per cent.	per cent.
750	78.8	19.1	6.2	2.2
800	74.0	20.7	6.2	4.0
850	68.5	21.9	6.3	7.1
900	59.2	25.1	6.9	12.4
950	39.1	34.4	8.2	23.4
975	0	53.7	10.8	33.5
1000	0	58	13	35.2
1100	0	62	29	40
1200	0	54	44	42.2

Table VII—(continued).

Pressure 30 atmospheres. $x = 2.10$.

Temperature.	Liquid.	Gasoline.	Gas.	Unsaturated.
° F.	per cent.	per cent.	per cent.	per cent.
750	93.7	12.0	2.8	2.2
800	90.3	12.7	3.0	4.0
850	86.7	13.1	3.2	7.1
900	80.5	14.7	3.7	12.4
950	67.3	20.8	4.8	23.4
980	28.5	39.6	7.8	37
983	0	53.9	10.1	40
1000	0	58	11	41
1100	0	63	27	44
1200	0	56	41	45

Pressure 60 atmospheres. $x = 2.25$.

Temperature.	Liquid.	Gasoline.	Gas.	Unsaturated.
° F.	per cent.	per cent.	per cent.	per cent.
750	60.9	29.5	13.3	0.89
800	55.1	32.0	13.0	1.6
850	49.0	33.8	12.7	2.8
900	41.1	36.8	12.6	5.2
950	30.5	41.0	12.3	8.3
1000	17.2	46.5	12.1	13.5
1040	0	53.0	13	21
1100	0	58	19	25
1200	0	58	38	32
1300	0	53	44	36
1400	0	44	55	44

Pressure 60 atmospheres. $x = 2.20$.

Temperature.	Liquid.	Gasoline.	Gas.	Unsaturated.
° F.	per cent.	per cent.	per cent.	per cent.
750	74.0	24.0	9.5	0.9
800	69.3	25.7	9.4	1.6
850	64.5	26.6	9.2	2.8
900	58.2	28.8	9.2	5.2
950	49.7	31.9	9.2	8.3
1000	38.7	36.3	9.3	13.5
1050	20.5	43.7	10.3	22.8
1063	0	53.4	11.9	27.0
1100	0	57	15	30
1200	0	60	28	36
1300	0	56	41	39
1400	0	46	53	41

Table VII—(continued).

Pressure 60 atmospheres. $x = 2.15$.

Temperature.	Liquid.	Gasoline.	Gas.	Unsat.
° F.	per cent.	per cent.	per cent.	per cent.
750	87.3	18.4	5.6	0.9
800	83.7	19.2	5.7	1.6
850	79.8	19.5	5.8	2.8
900	75.4	20.7	6.0	5.2
950	69.0	22.7	6.0	8.3
1000	60.5	25.8	6.0	13.5
1060	35.0	36.1	7.5	26.0
1072	0	54	11.5	31
1100	0	56	13	34
1200	0	61	27	39
1300	0	56	39	42
1400	0	47	52	43

Pressure 60 atmospheres. $x = 2.10$.

Temperature.	Liquid.	Gasoline.	Gas.	Unsat.
° F.	per cent.	per cent.	per cent.	per cent.
750	100	13.0	2.0	0.9
800	98	12.9	2.0	1.6
850	95.4	12.2	2.3	2.8
900	92.6	12.5	2.4	5.2
950	88.8	13.3	2.8	8.3
1000	82.4	15.3	3.3	13.5
1075	26.2	41.2	8.2	33
1078	0	53	10.7	35
1100	0	55	12	38
1200	0	61	24	43
1300	0	58	37	45
1400	0	48	51	46

The variation of the liquid, gasoline, gas and unsaturated fractions with the temperature for the oil $\text{CH}_{2.15}$ at 60 atmospheres is shown in fig. 3.

Commercial cracking processes are usually classified as liquid and vapour phase. In liquid phase processes the pressure is high enough to keep the greater part of the oil in the liquid state. The results in the above table for which the liquid fraction is greater than 50 per cent. may be said to be results for liquid phase cracking. In liquid phase cracking the temperatures used are between 750° F. and 900° F. Below 750° F. the cracking proceeds too slowly, and above 900° F. the pressure required to keep the oil liquid is usually too great and the formation of volatile products may proceed too rapidly for safety.

The calculated gasoline fractions for which the liquid fraction is greater than about 60 per cent. are, roughly speaking, nearly independent of the

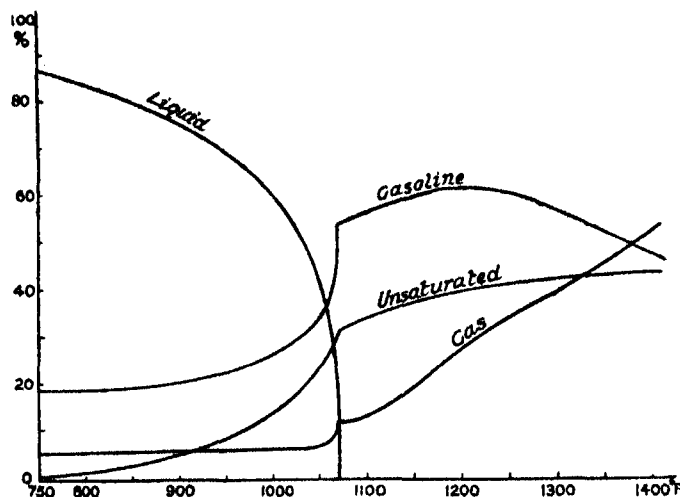


FIG. 3.

pressure and temperature but depend greatly on the composition of the oil. The gasoline fractions for the oils $\text{CH}_{2.1}$, $\text{CH}_{2.15}$, $\text{CH}_{2.2}$ and $\text{CH}_{2.25}$, are about 12 per cent., 20 per cent., 28 per cent. and 35 per cent. These hypothetical oils may therefore be said to correspond to oils of densities 1.000, 0.92, 0.87 and 0.82 respectively, which give about the same gasoline fractions (by weight) in liquid phase cracking. The corresponding percentages by volume are about 17, 25, 32 and 38. The four oils correspond roughly to heavy crude or fuel oil, crude oil, gas oil and kerosene.

It is found in practice in liquid phase cracking that the gasoline fraction increases slightly with the temperature, is nearly independent of the pressure and increases with the volatility of the oil. We see that these results are in good agreement with those deduced from the theory.

It is found in practice that a pressure of 50 or 60 atmospheres is required for the liquid phase cracking of kerosene at about 850° F. while 25 or 30 atmospheres may be used with "gas oil." It will be seen in the above table that the oil $\text{CH}_{2.2}$ is 50 per cent. liquid at 850° F. and 30 atmospheres, while the oil $\text{CH}_{2.25}$ is 49 per cent. liquid at 850° F. and 60 atmospheres according to the theory. In this respect also therefore the oil $\text{CH}_{2.25}$ corresponds to kerosene and the oil $\text{CH}_{2.2}$ to gas oil.

The more volatile oils give a larger gasoline fraction in liquid phase cracking

because they give a larger vapour fraction. The equilibrium percentage of gasoline in the vapour is about 50 per cent. whereas in the liquid it is only about 10 per cent.

The calculated gas fractions in liquid phase cracking vary with the temperature, pressure and quality of the oil in very much the same way as the gasoline fraction. The ratio of gasoline to gas is usually between 7 and 3. It increases with the pressure as we should expect. Thus at 60 atmospheres and 800° F. with the oil $\text{CH}_{2.1}$ it is 6.5, whereas at 15 atmospheres and 800° F. it is 5.3. The gas fractions calculated are usually somewhat larger than those reported in practice in liquid phase cracking. For example in Cross' "Handbook of Petroleum (1928)," p. 327, typical results obtained at 50 atmospheres and about 850° F. with six different oils are given. The average "loss" got by subtracting the total weight of the liquid products obtained from the weight of the oil used in these six cases is 7 per cent. This loss may be supposed to be mainly gas. The gasoline fractions for these six oils were about 30 per cent. by volume or, say, 26 per cent. by weight. The oil $\text{CH}_{2.2}$ at 60 atmospheres and 850° F. gives 9.2 per cent. of gas by weight which is greater than 7 per cent. The gas calculated includes C_3H_8 , C_3H_6 , and C_3H_4 , and it is probable that these bodies partly remain dissolved in the gasoline and only escape slowly from it. This may be the reason that the gas fractions calculated are often a little greater than those reported. The gas is frequently very roughly estimated in commercial work.

The unsaturated fraction in liquid phase cracking is determined by the temperature and pressure according to the theory. The following are the values of the unsaturated fraction at 750° F., 800° F., and 850° F. as given in the above table.

Table VIII.

Temperature.	7.5 atmospheres.	15 atmospheres.	30 atmospheres.	60 atmospheres.
° F.				
750	14.2	5.6	2.2	0.9
800	30.0	9.8	4.0	1.6
850	—	19.4	7.1	2.8

The calculated value of this fraction increases rapidly with the temperature and falls as the pressure increases.

In vapour phase cracking the theoretical unsaturated fraction when the oil is just completely vapourised is about 17. per cent. with the oil $\text{CH}_{2.26}$, 26

per cent. with $\text{CH}_{2.2}$, 32 per cent. with $\text{CH}_{2.15}$, and 39 per cent. with $\text{CH}_{2.1}$, and is nearly independent of the pressure.

At higher temperatures it increases and approaches limiting values of about 39 per cent., 41 per cent., 43 per cent., and 46 per cent. with the oils $\text{CH}_{2.25}$, $\text{CH}_{2.2}$, $\text{CH}_{2.15}$ and $\text{CH}_{2.1}$.

These theoretical results on the unsaturated fraction are in general agreement with the facts reported. The unsaturated fraction is said to approach 50 per cent. in the products of low pressure, high temperature vapour phase processes. In gasoline made at about 7.5 atmospheres and 750° F. it is said to be about 20 per cent., and in gasoline made in liquid phase processes at 50 atmospheres to be only about 5 per cent. Such estimates are very rough. It is generally believed that the unsaturated fraction increases rapidly with the temperature and falls with increasing pressure in agreement with the present theory.

In vapour phase cracking the temperature is raised so that the oil is entirely converted into vapour. In the above table we see that the lowest temperature at which this happens varies from 1075° F. for the oil $\text{CH}_{2.1}$ at 60 atmospheres to 766° F. for the oil $\text{CH}_{2.25}$ at 7.5 atmospheres. At any given pressure this temperature is nearly the same for any oil. Thus at 15 atmospheres it is 843° F., 868° F., 882° F. and 888° F. for the four hypothetical oils $\text{CH}_{2.25}$, $\text{CH}_{2.2}$, $\text{CH}_{2.15}$ and $\text{CH}_{2.1}$. At this temperature at which the oil is just converted into vapour the gasoline fraction is nearly 53 per cent. for any oil at any pressure according to the theory. The gas fraction is nearly independent of the pressure but varies from 10 per cent. for the oil $\text{CH}_{2.10}$ to 13.5 per cent. for the oil $\text{CH}_{2.25}$.

These theoretical results may be compared with those reported for the Dubb's cracking process in Cross' "Handbook of Petroleum (1928)," pp. 331-4. In this process the oil is heated by passing it through a coil of pipe in a furnace and it then enters a large reaction chamber. The temperature used is between 850° F. and 900° F. and the pressure is about 15 atmospheres. It is stated that either nothing but coke and vapour can be produced, or coke, vapour and fuel oil. To change from coke, fuel oil and vapour to coke and vapour it is only necessary to slightly raise the temperature. This shows that the oil just evaporates completely between 850° F. and 900° F. at 15 atmospheres. The vapour obtained contains about 50 per cent. of gasoline whatever oil is used. These results agree very well with those calculated. The calculated temperatures at which the four hypothetical oils just evaporate are between 850° F. and 900° F. and the calculated gasoline fraction is 53 per cent.

In the Dubb's process an appreciable amount of coke is usually obtained. If, for example, 10 per cent. of coke were deposited in the reaction chamber we should expect to get $0.53 \times 90 = 47.7$ per cent. of gasoline when operating so as to produce only coke and vapour. The effect of coke formation is merely to increase the hydrogen content of the oil, for example, if 1.98 per cent. of carbon were deposited from the oil $\text{CH}_{2.1}$ it would be converted into $\text{CH}_{2.16}$, and if 5.83 per cent. of carbon were deposited it would be converted into $\text{CH}_{2.25}$. But since the gasoline fraction is the same for $\text{CH}_{2.1}$ as for $\text{CH}_{2.25}$ the formation of coke should make no difference to the gasoline fraction for the vapour formed.

When the temperature is raised above that at which the oil just evaporates the calculated gasoline fraction increases to a maximum of about 60 per cent. and then falls at still higher temperatures. The maximum value occurs at 900° F. at 7.5 atmospheres and at 1200° F. at 60 atmospheres. The gas fraction increases rapidly with the temperature.

It is found in practice in low pressure vapour phase cracking that the gas fraction increases rapidly as the temperature is raised. At sufficiently high temperatures any oil gives practically nothing but coke and gas. The formation of coke increases the hydrogen content so that at high temperatures the unsaturated fraction may become small when much coke is deposited.

It is important to note that the calculated results in the above table are based on the assumption that no coke is formed. Coke formation increases x in CH_x so that for any oil x may become greater than 2.25 when much coke is formed. There is no difficulty in calculating the results to be expected from any hypothetical oil of composition CH_x when any given percentage of coke is formed at any temperature and pressure, but it does not seem to be worth while at present to carry the calculations beyond the point at which x becomes equal to 2.25.

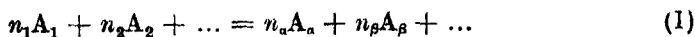
Since there appears to be a good general agreement between the calculated results for the hypothetical oils and the results obtained with actual oils we may conclude that the theory of the cracking of the hypothetical oils represents the main features of actual cracking. It follows from this that in actual cracking operations approximate equilibrium must be actually attained.

That approximate chemical equilibrium is attained when hydrocarbons are kept at sufficiently high temperatures was first suggested by Berthelot* in 1866. His views, however, have not met with general acceptance. Many facts supporting the theory of an approach to a state of equilibrium are described in Cross' "Handbook of Petroleum (1928)," pp. 281-288.

* 'Ann. Chim. Physique,' vol. 9, p. 445 (1866).

The view which seems to the writer to be most probably correct is that, when the rate of coke formation is small, approximate equilibrium is established among the liquid and gaseous hydrocarbons. The deposition of coke continually increases the hydrogen content of the oil and so disturbs the equilibrium, but this effect is small when the rate of coke formation is small.

Any chemical reaction in a mixture of gases may be represented by the equation



where A_1, A_2, \dots , represent molecules and n_1, n_2, \dots , are integers. In the thermodynamical theory of chemical equilibrium it is shown that the condition of equilibrium is $\log K = \Sigma n\psi/R$ where K is the equilibrium constant given by $\log K = \Sigma n \log c$. c_1, c_2, \dots , are the concentrations of A_1, A_2, \dots , and ψ_1, ψ_2, \dots , are the thermodynamic potentials and R is the gas constant.

If the equilibrium constant is very large the reaction should go on until practically only the bodies on the right-hand side of (1) remain whereas if K is very small it should go in the reverse direction until only the bodies on the left of (1) remain. In such cases, where K is very large or very small it is sometimes supposed that the theory is inapplicable and the reaction is said to be irreversible. This supposition is erroneous because what happens is exactly what the theory predicts, viz., that the reaction should go practically completely one way or the other. The theory applies equally to all reactions and it is impossible for a reaction to proceed beyond the equilibrium point indicated by the theory because this would involve a decrease of the entropy.

When the equilibrium constant K is not either very small or very large then the reaction must stop while appreciable amounts of all the bodies on both sides of equation (1) remain. It follows that, when K can be shown to be neither very small nor very large, then when the conditions are such that the bodies present react appreciably chemical equilibrium must be approached. Such states of chemical equilibrium, of course, are not states of static equilibrium but states of dynamical equilibrium in which the reactions proceed both ways at equal rates.

In the case of a mixture of paraffins and unsaturated hydrocarbons it can be shown that K is neither very large nor very small, and it therefore follows that chemical equilibrium must be approached at temperatures at which the reactions proceed appreciably.

A question of practical importance in liquid phase cracking is the amount of a given oil which can be cracked in unit time at any temperature and pressure with a reaction chamber of given volume. In considering this problem it will

be sufficiently exact to regard the oil as consisting of a mixture of paraffins only because in liquid phase cracking the unsaturated fraction is small.

The number of barrels of an oil which can be treated in a given time depends on the volume of the reaction chamber, the volume per barrel of the oil when in the reaction chamber and on the time which it is necessary to keep the oil in the chamber. It is found that the rate of reaction in oil is about doubled for a rise of 25° F. It follows that the time required is about halved by a rise of 25° F.

The volume of the equilibrium products formed from one barrel of oil in the reaction chamber can be calculated by assuming that the vapour can be regarded as a perfect gas and by allowing for the expansion of the liquid.

If p_n denotes the partial pressure of C_nH_{2n+2} in the vapour we have $p_n = p_1 f^{n-1}$ where f is a fraction. If m_n denotes the mols of C_nH_{2n+2} present in a volume V then $p_n V = m_n RT$ where R is the gas constant for one mol and T is the absolute temperature. Hence $m_n = V p_1 f^{n-1} / RT$. The molecular weight of C_nH_{2n+2} is equal to $14n + 2$ so that the average molecular weight of the paraffins present in the vapour is equal to $\Sigma m_n (14n + 2) / \Sigma m_n$ or to $\Sigma (14n + 2) f^{n-1} / \Sigma f^{n-1}$ which is equal to $2 + 14/(1 - f)$ or in terms of x in CH_x to $2 + 28/(x - 2)$. Knowing the average molecular weight of the vapour its density at any pressure P in atmospheres and temperature $T^\circ K$ may be easily calculated. The density in pounds per cubic foot is equal to $MP/1.314T$ where M is the average molecular weight. The volumes of the liquid and vapour formed from one barrel of oil in the reaction chamber and the total volume are given in the following table. The oil of composition $CH_{2.1}$ was taken to be of density unity so that the weight of one barrel or 5.615 cubic feet was taken to be 350 pounds. The weights of one barrel of the oils having $x = 2.15, 2.20$ and 2.25 , were taken to be 322, 305 and 287 pounds respectively. The liquid in the reaction chamber was assumed to have density one at the ordinary temperature and densities 0.72, 0.70 and 0.68 at 800° F., 850° F. and 900° F. The fractions (q) of the oil in the liquid state are given in Table VII so that knowing the densities of the vapour and of the liquid it is easy to calculate the volumes.*

As the oil passes through the reaction chamber its volume increases due to the formation of vapour of the volatile hydrocarbons which are produced in it. The volumes given above are the equilibrium final volumes calculated on

* The values of the liquid and gasoline fractions used in calculating the numbers given in Tables IX and XI were those computed for a mixture of paraffins only. They only differed slightly from the corresponding values in Table VII.

Table IX.

	Temperature.	Pressure.	Volume of liquid.	Volume of vapour.	Total volume.
	° F.	atmospheres.	cu. ft./barrel.		
$x = 2.10$	800	15	6.6	41.0	47.6
	800	30	7.0	14.6	21.6
	850	30	7.0	18.0	25.0
	800	60	7.5	2.98	10.5
	850	60	7.6	4.94	12.5
	900	60	7.6	6.04	13.6
$x = 2.15$	800	15	5.1	81.2	86.3
	800	30	5.6	35.6	41.2
	850	30	5.5	39.6	45.1
	800	60	6.2	13.9	20.1
	850	60	6.1	16.0	22.1
	900	60	6.1	17.7	23.8
$x = 2.20$	800	15	3.7	116.0	119.7
	800	30	4.2	53.6	57.8
	850	30	4.0	58.2	62.2
	800	60	4.9	23.4	28.2
	850	60	4.8	25.5	30.3
	900	60	4.6	27.8	32.4
$x = 2.25$	800	15	2.4	148.0	150.4
	800	30	3.0	70.0	73.0
	850	30	2.7	75.2	77.9
	800	60	3.7	31.9	35.6
	850	60	3.5	34.7	38.2
	900	60	3.3	36.9	40.2

the assumption that no appreciable amount of coke is deposited. In reality coke is slowly deposited so that exact equilibrium is not attained and the percentage of hydrogen in the liquid and vapour continues to gradually increase.

The part of the oil which is converted into vapour will pass through the reaction chamber in a shorter time than that which remains liquid. If the reaction chamber is a vertical cylinder and the oil is pumped in at the lower end and allowed to escape at the top then the bubbles of vapour formed will rise through the liquid with increasing velocity as they grow larger. When the volume of vapour formed is large the liquid and vapour in the upper part of the chamber may form a foam in which the liquid and vapour move up with nearly the same velocity. If the reaction chamber is a horizontal cylinder and the oil is let in at one end and out at the other the liquid level will be that of the outlet. The bubbles of vapour formed will rise through the liquid and escape into the space above the liquid level. In this way the vapour is separated from the liquid to a considerable extent.

It is clear that no accurate estimate of the time taken to pass through the reaction chamber can be made. We may, however, suppose that the volume of the chamber divided by the equilibrium volume of the oil pumped in per unit time is a relative measure of the time taken to pass through. This time may be called the apparent time. For example, at 60 atmospheres and 850° F. the equilibrium volume per barrel of the oil for which $x = 2.20$ is 30.3 cubic feet so that with a reaction chamber of volume 1000 cubic feet, when pumping two barrels of oil per minute the apparent time is $1000/(2 \times 30.3) = 16.5$ minutes. For the oil for which $x = 2.10$ the corresponding time is $1000/(2 \times 12.5) = 40$ minutes.

In practice the time of passing through the reaction chamber is usually considerably longer than necessary. As the chamber gradually fills up with coke the time is diminished but the gasoline does not diminish appreciably until the chamber is nearly full of coke. The rate at which the oil is pumped in is frequently limited by the heating capacity of the furnace rather than by the cracking capacity of the reaction chamber. If the oil is pumped in so rapidly that the time in the reaction chamber is less than that required for approximate equilibrium to be reached the production of gasoline per unit time is not reduced but is increased, but the fraction of the oil converted into gasoline is reduced.

If the fraction of gasoline in the oil is denoted by g then the rate of formation of gasoline will be nearly proportional to $\bar{g} - g$ where \bar{g} is the equilibrium value of g . Thus we have $dg/dt = a(\bar{g} - g)$, where a is a constant depending mainly on the temperature. This gives $g = \bar{g}(1 - e^{-at})$ where t is the time of passing through the chamber.

The production of gasoline per unit time is equal to g times the amount of oil P pumped through in unit time, and $t = V/Pv$ where V is the volume of the reaction chamber and v that of unit quantity of oil in the chamber. Thus the gasoline production G is given by

$$G = Pg = P\bar{g}(1 - e^{-aV/Pv}).$$

This shows that G increases with P until when P is very large it becomes equal to $\bar{g}aV/v$ and so is then independent of the amount of oil pumped through. The production of gasoline can always be increased by increasing the amount of oil pumped through provided the temperature is not allowed to fall. But increasing the amount will diminish the fraction of the oil converted into gasoline unless the time in the reaction chamber is greater than that required for approximate equilibrium to be reached.

As an example suppose $\bar{g} = 40$ per cent., $V = 1000$ cubic feet, $v = 20$ cubic feet per barrel of oil, and $a = 0.1$ with t in minutes. The following table gives the calculated values of G , t and g in this case.

Table X.

P.	G.	t.	g.
Barrels per minute.		Minutes.	Per cent.
1	0.398	50	39.8
2.5	0.87	20	34.6
5	1.3	10	25.2
10	1.6	5	15.7
20	1.8	2.5	8.85
40	1.9	1.25	4.70
80	1.94	0.63	2.43
1000	2.00	0.05	0.20

We see that the production of gasoline increases with the amount of oil pumped through at first rapidly and then more and more slowly. When the amount pumped through is small the gasoline is nearly proportional to it. In practice when P is kept constant and t diminishes, due to deposition of coke, G remains nearly constant showing that P is less than about 2.0 in the above case. It follows that if the amount of oil pumped through could be increased the production of gasoline would also be increased.

There is, of course, no definite time during which the oil must be kept in the reaction chamber. For purposes of comparison we shall take the apparent time to be 64 minutes at 800°F. , 16 minutes at 850°F. , and 4 minutes at 900°F. With these times the equilibrium composition should be very nearly reached.

Table XI gives the amounts of the four hypothetical oils which could be cracked *with these apparent times* and the gasoline production in each case for a reaction chamber of 100 cubic feet capacity. The volume of the reaction chamber required to crack 1000 barrels of oil per day is also given in cubic feet.

It appears that the gasoline production is nearly proportional to the pressure and is increased nearly four times by a rise of 50°F. It is nearly independent of the composition of the oil used. A less volatile oil gives a smaller percentage of gasoline but a larger amount of it can be pumped through. It is important to remember that the numbers in the above table depend on the assumed apparent times. The amount of gasoline can always be increased by pumping more oil through, but this reduces the percentage of the oil converted into gasoline. For example, if it was decided to work with times only half as

Table XI.

No.	Temperature.	Pressure.	Barrels per day.	Gasoline, barrels per day.	Volume of chamber for 1000 barrels per day.
	° F.	atmospheres.			cu. ft.
2-10	800	15	47	5.9	2130
2-10	800	30	104	13.2	960
2-10	850	30	360	46	278
2-10	800	60	214	29	467
2-10	850	60	720	93	139
2-10	900	60	2650	337	38
2-15	800	15	26	5.4	3850
2-15	800	30	55	11.2	1820
2-15	850	30	200	41	500
2-15	800	60	112	23	893
2-15	850	60	407	81	246
2-15	900	60	1514	306	66
2-20	800	15	19	5.5	5260
2-20	800	30	39	11	2570
2-20	850	30	145	42	690
2-20	800	60	80	21	1250
2-20	850	60	297	80	339
2-20	900	60	1110	309	90
2-25	800	15	15	5.6	6670
2-25	800	30	31	11	3230
2-25	850	30	116	42	863
2-25	800	60	63	20	1590
2-25	850	60	236	80	467
2-25	900	60	895	317	112

long the amount of oil which could be cracked would be doubled and the amount of gasoline produced would be nearly but not quite doubled.

The practical rule which follows from these theoretical results is that the amount of oil which should be pumped into the reaction chamber per day is inversely proportional to the gasoline fraction. For example, if in cracking a gas oil 2000 barrels per day of the oil is pumped through the reaction chamber and 600 barrels of gasoline is obtained, then when cracking a heavy oil which gives only 250 barrels of gasoline per day, when 2000 barrels per day is pumped through, the amount of the heavy oil pumped through should be increased to $2000 \times 600/250$ or 4800 barrels per day. It is assumed here, of course, that the temperature and pressure are the same in each case. At a given temperature and pressure the gasoline production for a given reaction chamber should be about the same for any kind of oil provided the gasoline fraction is not less than about 10 per cent.

When an appreciable amount of coke is deposited in the reaction chamber in liquid phase cracking the hydrogen content of the oil is increased and so the gasoline fraction is also increased. But it does not follow that coke production increases the amount of gasoline which can be produced per day in a given reaction chamber. For example, with a reaction chamber of 100 cubic feet capacity at 850° F. and 60 atmospheres and with the apparent time of 16 minutes the oil $\text{CH}_{2.1}$ gives 93 barrels of gasoline per day, when no coke is formed. If 1.98 per cent. of coke were deposited in the chamber the oil would be changed to $\text{CH}_{2.15}$ and so only 81 barrels of gasoline could be produced per day. With 5.83 per cent. of coke the oil would become $\text{CH}_{2.25}$ and 80 barrels per day could be produced. Thus coke formation may actually diminish the production of gasoline according to the theory, because it increases the volume per barrel in the reaction chamber so that the amount of oil pumped through per day may have to be reduced, and the effect of this may more than compensate for the increased percentage of gasoline obtained.

A serious further reduction of the production of gasoline due to coke is due to the time wasted in cleaning out the reaction chamber.

If a small quantity of a mixture of hydrocarbons containing a high percentage of hydrogen is added to the oil then the theory indicates a considerable increase in the percentage yield of gasoline. For example, if 6.3 per cent. of gas of composition CH_3 were added to the oil $\text{CH}_{2.1}$ its composition would be changed to $\text{CH}_{2.15}$, so that it would give $1.063 \times 20.4 = 21.7$ per cent. of gasoline and $1.063 \times 5.4 = 5.7$ per cent. of gas instead of 12.9 per cent. of gasoline and 2.7 per cent. of gas. But the production of gasoline per day in a reaction chamber of given volume would be slightly diminished since that for the oil $\text{CH}_{2.15}$ is slightly less than that for the oil $\text{CH}_{2.1}$, as shown above. In the same way if 13.3 per cent. of gas CH_3 were added to the oil $\text{CH}_{2.1}$ it would be changed to $\text{CH}_{2.20}$ and so would give 1.133×27.8 per cent. = 31.5 per cent. of gasoline and $1.133 \times 8.1 = 9.2$ per cent. of gas. Thus it appears that if about 5 per cent. of gas CH_3 were added to the oil $\text{CH}_{2.1}$ then 5 per cent. of gas would be produced so that the gas produced could be used to mix with the oil and the percentage of gasoline obtained would be about 20. But the daily production would not be increased because, owing to the increased volume per barrel of oil in the reaction chamber the amount of oil pumped through would have to be reduced to prevent the apparent time becoming too short.

No experimental results are available for comparison with these theoretical calculations on the effect of adding gas to the oil.

In order to get the gas to combine with the oil it would probably be necessary to devise a special apparatus in which the gas and oil would be intimately mixed together. Merely pumping the gas through the reaction chamber might not be sufficient, because, as explained above, the vapour tends to pass through rapidly and to separate from the liquid.

In any cracking process the theoretically possible maximum yield of gasoline would be obtained if the oil were converted into nothing but gasoline and carbon. If the composition of the oil is CH_{x_1} and that of the gasoline CH_{x_2} , then we have $x_1/(12 + x_1) = x_2F/(12 + x_2)$, where F is the fraction of the oil converted into gasoline. This gives $F = x_1(12 + x_2)/x_2(12 + x_1)$. For example if $x_2 \approx 2.25$ and $x_1 = 2.15$, we get $F = 96$ per cent. by weight or about 110 per cent. by volume.

It ought to be possible to obtain nearly the theoretically possible yield by returning to the reaction chamber or "recycling" all the products formed except the gasoline. In this way only gasoline and the coke formed in the reaction chamber would be produced from the oil. The principal reasons why the theoretically possible yield is not obtained in practice, at present, are because the gas is allowed to escape and fuel oil containing a good deal of hydrogen is made instead of coke. But when the gas is allowed to escape it is not necessarily advantageous to make coke instead of fuel oil because the gas fraction is greater when coke is made.

A cracking process which gives a high gasoline fraction is not necessarily better than another process giving a lower fraction. The products obtained are gas, gasoline, oil less volatile than gasoline and coke. The oil less volatile than gasoline can be returned to the reaction chamber and cracked again. Thus the fraction of the oil which is used up is the sum of the gas, gasoline and coke fractions. A measure of the efficiency of a cracking process is therefore the fraction which the gasoline fraction is of the sum of the gas, gasoline and coke fractions. For example, in liquid phase cracking at 60 atmospheres and 850°F . the oil $\text{CH}_{2.1}$ gives 2.2 per cent. of gas and 12.3 per cent. of gasoline according to the theory. The coke formed under these conditions in practice is negligible. The fraction of the oil used up, converted into gasoline is therefore $12.3/(12.3 + 2.2) = 85$ per cent. by weight.

With the same oil at 15 atmospheres and 868°F ., if no coke is deposited, the theory gives 52.5 per cent. of gasoline and 11.5 per cent. of gas. The fraction of the oil used up converted into gasoline would therefore be $52.5/(52.5 + 11.5) = 82$ per cent. But under these conditions probably some coke would be formed which would change the composition of the vapour. If we suppose

5.83 per cent. of coke formed the vapour would be changed to $\text{CH}_{2.25}$ and we should get $52.9 \times 0.9417 = 49.8$ per cent. of gasoline and $13.1 \times 0.9417 = 12.3$ per cent. of gas. The fraction of the oil used up converted into gasoline would therefore be $49.8 / (49.8 + 12.3 + 5.83) = 73.4$ per cent. Thus in this case according to the theory the high pressure liquid phase process giving a gasoline fraction of only 12.3 per cent. is more efficient than the vapour phase process giving a gasoline fraction of 49.8 per cent. In these calculations of the efficiency we have supposed that the gas is not returned to the reaction chamber.

The quality of the gasoline produced is important and it may be worth while in practice to use a less efficient process which gives gasoline of better quality.

The quality of the gasoline depends partly on the nature of the hydrocarbons present in it so that the present theory, depending as it does on the theoretical properties of hypothetical oils containing only paraffins and unsaturated hydrocarbons cannot give complete information as regards quality.

The quality is affected by the presence of unsaturated bodies which it is usually considered advisable to remove more or less completely from the gasoline. The indications of the theory as to the unsaturated fraction have already been sufficiently discussed.

The quality also depends to some extent on the relative amounts of the fractions boiling between different limits present in the gasoline. The theory gives definite information on this question.

As an example the theoretical compositions of the gasoline obtained from the oil $\text{CH}_{2.15}$ at 850° F. and 60 atmospheres, at 882° F. and 15 atmospheres and at 7.5 atmospheres and 1025° F. will be considered.

At 850° F. and 60 atmospheres x for the liquid is 2.089 and for the vapour 2.425 according to the charts in E I. The liquid fraction is 80 per cent. The liquid contains 10.5 per cent. of gasoline and the vapour 56.5 per cent. Taking 20 per cent. of the percentages of each paraffin in the vapour from the table in E I and adding them to 80 per cent. of the percentages in the liquid we find the composition of the gasoline. Since the other types of hydrocarbons have nearly the same boiling points as the corresponding paraffins they need not be considered. At 882° F. and 15 atmospheres the oil is all vapour for which $x = 2.30$ so that the percentages of the different paraffins may be got immediately from the table of percentages in E I. At 7.5 atmospheres and 1025° F. the oil is all vapour for which $x = 2.80$. In this case only 0.2 of the butane is included in the gasoline. The following are the percentages got in this way.

Table XII.

	60 atmospheres and 850° F.	15 atmospheres and 882° F.	7.5 atmospheres and 1025° F.
C_4H_{10}	11.8	11.4	7.9
C_5H_{12}	12.1	12.0	29.6
C_6H_{14}	12.0	12.2	21.3
C_7H_{16}	11.8	12.1	14.7
C_8H_{18}	11.4	11.7	10.2
C_9H_{20}	11.0	11.2	6.9
$C_{10}H_{22}$	10.4	10.6	4.5
$C_{11}H_{24}$	10.0	9.9	3.0
$C_{12}H_{26}$	9.7	9.1	2.0

It appears that the first two gasolines are practically identical in composition but the third one is considerably different according to the theory. The numbers in the above table may be taken to mean the percentages of paraffins together with other hydrocarbons of equal volatility.

The above theory is not a complete theory of cracking because it does not take into account naphthenes and aromatic hydrocarbons. These bodies have an important effect on the quality of the gasoline and the writer hopes to develop the theory so as to include them in it.

The Dispersion of Double Refraction in Quartz.

By T. H. HAVELOCK, F.R.S.

(Received February 4, 1929.)

1. Recent experimental determinations of double refraction in quartz and new dispersion formulæ for the ordinary index have suggested re-calculation of a certain relation between the ordinary and extraordinary indices which I gave some years ago.* The main object of this note is to show that it is possible to calculate the double refraction of quartz over a considerable range of wave-length with an accuracy which seems well within the range of experimental error.

The relation to which I refer is a simple expression for double refraction due to crystalline structure, obtained by specifying the effective force at a point in the medium as the force within a cavity of suitable shape; but that need not be considered further here. For a uniaxial crystal the relation is

$$\frac{1}{n_1^2 - 1} - \frac{1}{n_2^2 - 1} = C, \quad (1)$$

where n_1 is the ordinary and n_2 the extraordinary index, and C is a constant independent of wave-length. It may be remarked that in the more detailed analysis, made later by Ewald, of the electromagnetic theory of a crystalline lattice, the same relation (1) was obtained again as a first approximation for double refraction due to structure. It is not my intention to discuss this relation in the light of present knowledge of crystalline structure, but simply to show how it may be used in the particular case under consideration.

2. In the paper quoted, I showed that (1) is in fact satisfied very well for quartz over a large range of wave-length. The data used were measurements of n_1 and n_2 by Martens and by Carvallo, and the mean value of C over the range 3580 to 10970 A.U. was found to be 0.01441, with a maximum variation of two units in the fifth decimal place. Recent writers, both on the double refraction and on dispersion formulæ, have used Gifford's measurements for quartz.† I have therefore recalculated C from Gifford's results from 1852 to 7950, and Carvallo's from 8320 to 21719; the calculations have not been made for every available wave-length, but for a selection sufficient to give a

* 'Roy. Soc. Proc.,' A, vol. 80, p. 28 (1907).

† 'Roy. Soc. Proc.,' A, vol. 70, p. 329 (1902); also vol. 84, p. 193 (1910).

fair idea of the relation (1). The results are shown in the following table, giving the wave-length, the double refraction, and the quantity C calculated from the experimental values of the two indices.

λ .	$n_2 - n_1$.	C .
1852	0.014173	0.014210
2144	0.012238	0.014221
2312	0.011813	0.014268
2748	0.010603	0.014297
3034	0.010239	0.014341
3302	0.009987	0.014385
3610	0.009770	0.014385
3961	0.009600	0.014412
4046	0.009560	0.014411
4341	0.009430	0.014387
4800	0.009317	0.014422
4861	0.009288	0.014402
5270	0.009211	0.014421
5461	0.009171	0.014413
5893	0.009110	0.014424
6563	0.009017	0.014405
6708	0.009013	0.014424
7066	0.008986	0.014435
7682	0.008937	0.014435
7950	0.008908	0.014421
8320	0.008888	0.014419
9050	0.008883	0.014407
10420	0.00875	0.014393
11590	0.00869	0.014378
12290	0.00865	0.014367
13960	0.00855	0.014325
16150	0.00845	0.014325
18490	0.00828	0.014232
21719	0.00810	0.014226

It should be stated that Gifford claims accuracy for the fifth decimal place in his values of n_1 and n_2 ; presumably Carvalho's values in the infra-red are less accurate. The table covers a very wide range and is a severe test for simple relation like (1). There seems to be a definite falling off in the value of C at both ends of the scale, which may prove of interest from a theoretical point of view. However if we limit ourselves to the range 3961 to 8320, the values are remarkably constant. The mean value of C in this range is 0.014416, practically the same as obtained previously from other data. The chief divergences in this range are irregular and may fairly be taken to cast doubt upon the experimental values of n_1 and n_2 . For instance, the value at 4341 is too low and that at 7066 too high, and we shall see later that this remark is confirmed by recent experimental determinations in the neighbourhood of these two wave-lengths.

3. In using (1) to calculate the double refraction we must, of course, know

either n_1 or n_2 . But this need not be an experimental determination, for there are dispersion formulæ for the ordinary refractive index of quartz of sufficient accuracy within the range with which we are concerned. It should be noted that in calculating the difference $n_2 - n_1$ by means of (1) we do not need to know n_1 to a specially high degree of accuracy; for an error in n_1 means a corresponding error in n_2 and only a relatively small error in the difference. For instance in quartz, it is easily seen that an error of one unit in the fifth decimal place for n_1 would give an error of about four units in the seventh decimal place for the double refraction, which is certainly well within the range of experimental error.

The dispersion formula for the ordinary index which we shall use is a recent one given by Coode-Adams,* namely

$$n_1^2 = 3.53445 + \frac{0.008067}{\lambda^2 - 0.0127493} + \frac{0.002682}{\lambda^2 - 0.000974} + \frac{127.2}{\lambda^2 - 108}. \quad (2)$$

This formula was devised in connection with a certain dispersion formula for the natural rotation of quartz; that particular theory need not be discussed here, except that reference may be made to an alternative view given in a later paper by Livens and Bradshaw.† We use (2) solely as a formula which gives Gifford's values of n_1 with great accuracy in the range concerned, the average error in the value of n_1 being one unit in the fifth decimal place. We proceed now to use (2), together with

$$\frac{1}{n_1^2 - 1} - \frac{1}{n_2^2 - 1} = 0.014416, \quad (3)$$

to calculate $n_2 - n_1$ for any required wave-length.

4. In a recent paper Harris‡ has given experimental values of the double refraction for many wave-lengths, and compared his values with those of Gifford in the same range; it should be said that Harris' method gives the double refraction directly without making separate determinations of n_1 and n_2 . In the calculations made from (2) and (3) a selection has been made from the wave-lengths used by Harris, together with some of Gifford's values. In the following table the first column gives the wave-length. The second gives the experimental value of the double refraction, those marked with G being from Gifford and the remainder from Harris. The third column gives

* 'Roy. Soc. Proc.,' A, vol. 117, p. 209 (1927).

† 'Roy. Soc. Proc.,' A, vol. 122, p. 245 (1928).

‡ 'Phil. Mag.,' vol. 7, p. 80 (1929).

the double refraction calculated from (2) and (3), except that for Gifford's wave-lengths his value of n_1 was used directly in (3).

λ .	$(n_2 - n_1)$ exp.	$(n_2 - n_1)$ calc.
G. 3961	0.009600	0.009603
3992.265	0.009571	0.009588
G. 4046	0.009560	0.009564
4174.244	0.009498	0.009511
G. 4341	0.009430	0.009449
4341.844	0.009438	0.009449
4413.691	0.009415	0.009425
G. 4861	0.009288	0.009298
4866.063	0.009293	0.009296
5009.171	0.009261	0.009264
5383.916	0.009188	0.009188
5628.602	0.009148	0.009145
G. 5893	0.009110	0.009105
6047.303	0.009091	0.009086
G. 6438	0.009044	0.009038
G. 6563	0.009017	0.009025
G. 6708	0.009013	0.009008
7011.389	0.008974	0.008980
G. 7066	0.008987	0.008974
7166.052	0.008963	0.008970
G. 7950	0.008909	0.008906

A study of this table will show that there is agreement as far as the fifth decimal place in a majority of the cases. In the remainder the difference is not more than one unit in the fifth place except in one or two cases, and then the experimental values are not consistent among themselves; for instance the values at 4341 and 7066 are clearly out of place on the experimental side. There is also some indication that Harris' values for the short wave-lengths, for example, 3992, may be too low.

5. It has been shown that it is possible to calculate the double refraction of quartz for wave-lengths between 4000 and 8000 with great accuracy, probably within possible experimental error, by means of a relation between the two indices, namely, $(n_1^2 - 1)^{-1} - (n_2^2 - 1)^{-1} = \text{constant}$, together with a dispersion formula for the ordinary index.

The Spectrum of H₂: The Bands Analogous to the Parhelium Line Spectrum.—Part III.

By O. W. RICHARDSON, F.R.S., Yarrow Research Professor of the Royal Society, and P. M. DAVIDSON, B.A., King's College, London.

(Received March 13, 1929.)

Synopsis.

§ 10. The system ${}^1K \rightarrow 2{}^1S$. A strong system, $\nu_e = 21427$. In the description of this system is included a rather full account of the manner in which the data for the rotational energy interval tables are obtained and set out. This is generally applicable to similar tables in Parts II-IV. § 11. The system ${}^1L \rightarrow 2{}^1S$. This is a very similar system to the preceding but weaker, $\nu_e = 23057$. § 12. The system ${}^1M \rightarrow 2{}^1S$. Strength intermediate between the two preceding systems. Similar in many ways but differentiated by a change of structure of rotational terms with vibrational energy of initial state, $\nu_e = 23191$. § 13. The system ${}^1N \rightarrow 2{}^1S$. A strong system but has only two progressions, $n' = 0$ and 1. General type similar to preceding three $\nu_e = 24896$.

§ 10. *The System ${}^1K \rightarrow 2{}^1S$.*

This is the first of several band systems having P and R branches in which there is not so much disparity between the strength of the two sets of branches as in the $3{}^1A \rightarrow 2{}^1S$ and $3{}^1C \rightarrow 2{}^1S$ systems and in fact in most of the systems so far described. The consideration of these systems has been postponed up to the present as the progressions are very much interwoven and they are not so easy to classify as the systems already dealt with. The present one is a very strong system and contains some of the strongest lines in the spectrum, and we do not think there is any doubt that the three progressions of which it is constituted belong to the same system. Gale, Monk and Lee's wave numbers of the lines are given in Table XVII. The number which precedes the wave number is the intensity as measured by Kapuscinski and Eymers,* and that which follows it, in brackets, is the eye estimate of Gale, Monk and Lee.† In some cases where the line is not resolved by Kapuscinski and Eymers, rough estimates of the constituents are given based on their data and on Gale, Monk

* 'Roy. Soc. Proc.,' A, vol. 122, p. 58 (1929).

† 'Astrophysical Journal,' vol. 57, p. 89 (1928).

Table XVII.

ν' \downarrow	m \downarrow	$\nu'' \rightarrow$	0.	1.	2.	3.	4.	5.	6.	7.
0	1	R	126 21446.79 (8)	20126.45 (1)	20.1 18646.99 (5)	17600.32 (1)		15207.32 (0)		
		P								
	2	R	57 21461.43 (5)	8.9 20135.02 (2)	9.0 18655.19 (2)			15154.46 (1)		
		P	35.1 21396.56 (4)	4.7 20070.07 (0)	7.8 18790.26 (2)	17645.14 (1)				
	3	R	138 21440.31 (9)	35.0 20127.64 (6)	18651.17 (4)	17603.81 (00)	Interference	15223.35 (1)		
		P	83.0 21330.49 (9)	7.7 20018.09 (2)	21.1 18741.52 (6)	17499.09 (2)		15113.77 (1a)		
	4	R								
		P	17.7 21259.07 (5)		5.1 18690.35 (2)			15064.45 (0)		
	5	R								
		P	19.8 21173.61 (3)	Interference	8.8 18606.34 (3)	17375.75 (1)		15007.75 (0)		
1	1	R	79.0 23675.90 (5)	12.6 22357.53 (2)	44.0 21076.13 (5)	36.0 19829.35 (6)		17436.24 (1a)	16298.82 (0)	
		P								
	2	R	83.0 23677.92 (5)	3.7 22361.53 (1)	13.8 21081.77 (3)	52.0 19836.46 (9)				
		P	10.9 23619.12 (3)	3.1 22302.72 (00)	5.5 21022.84 (2)	19777.54 (2a)		17387.14 (1)		
	3	R	56.4 23667.96 (5)	12.6 22365.91 (3)	59.6 21078.81 (6)	52.0 19836.46 (9)			16307.00 (00a)	15195.00 (00)
		P	23.7 23559.80 (2)	36.5 22247.21 (5)	13.3 20970.62 (2)	26.0 19728.21 (5)		17342.83 (1)		
	4	R								
		P	3.0 23455.67 (1)		20006.89 (0)	12.6 19668.86 (1)	18463.55 (0a)			
	5	R								
		P				12.0 19603.36 (2)	2.9 18403.25 (1)		16099.13 (0)	

F 2

Table XVII—(continued).

$\pi' \downarrow$	$\pi'' \rightarrow$	0.	1.	2.	3.	4.	5.	6.	7.
1	B	35-7 25900-26 (3)	318 — 24581-06 (0)	3-6 25300-41 (0)	about 15 22053-06 (4)	about 22 20840-59 (4)	40 19660-83 (9)	8-9 18513-13 (0)	17397-61 (1)
	P								
2	B	17-3 25906-07 (1)	47 24589-58 (3)	8-3 25309-75 (0a)	6-6 22064-55 (1)	12-4 20852-77 (1)	14-2 19674-02 (2)	18527-75 (0)	17413-42 (0)
	P								
3	B	63-2 25894-65 (4)	318 — 24581-06 (0)	12-5 25305-44 (3)	21-3 22063-07 (3)	49-5 20853-98 (5)	44-5 19677-06 (7)	3-2 18533-76 (0)	12-0 17421-59 (2)
	P	7-1 25784-04 (1)	47-5 24471-46 (3)			20743-43 (1a)		10-0 18423-08 (2a)	
4	B	15-5 25870-80 (1)	52 24563-84 (2)	4-5 25291-88 (1)	about 17 22053-06 (4)	11-4 20848-57 (1)	16-6 19675-87 (1)		
	P		19-5 24406-78 (1)		21-1 21897-08 (3)			5-8 18378-30 (1a)	
5	B	26-7 25833-14 (2)	63-8 24538-39 (4)	8-3 23273-91 (1a)	11-4 22040-15 (2a)	45 20840-10 (4)	29-5 19672-11 (2)		
	P		20-2 24328-23 (3)		21829-97 (1a)	20629-00 (1)		11-5 18325-66 (4)	
6	B	25900-10 (0)	24509-16 (1a)	23251-16 (0)		3-1 20831-24 (0)	12-0 19668-85 (1)		
	P		24241-04 (0)					2-8 18270-32 (0a)	
7	B	25775-02 (1)	7-5 24494-08 (2)	23244-75 (0)			4-6 19664-29 (0a)		
	P							2-8 18215-57 (1)	

and Lee's eye estimates. Data for a blend of which the line forms part have a bar over them.

A very remarkable feature of this band system is the distribution of intensity of the lines. Keeping to any single branch there is the alternation in intensity corresponding to a 3 to 1 weight ratio which we have found to characterise all the bands of this spectrum hitherto examined. But in addition to this there are other curious alternations. The intensity diagram does not take the simple form of a parabolic maximum with an axial minimum observed in the previous systems, but there are maxima along two branches with two intervening minima as shown in fig. 7. In this figure the numbers in each rectangle

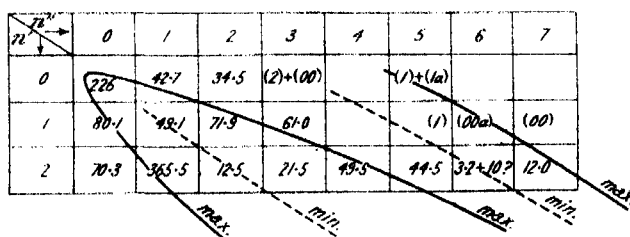


FIG. 7.

are the sums of Kapuscinski and Eymers' measures of the intensities of the strong R (3) and P (3) lines except those in brackets which are the intensity estimates of Gale, Monk and Lee, no measurements being available for these lines. There is another curious feature of this alternation in that the bands which have R (m) strong tend to have P (m) weak and vice versa. This is well shown by the R (3) and P (3) lines of the 1' progression where for $n'' = 0$ R (3) = 56.4, P (3) = 23.7, for $n'' = 1$, R (3) = 12.6, P (3) = 36.5, for $n'' = 2$, R (3) = 58.6, P (3) = 13.3 and for $n'' = 3$, R (3) = about 35, P (3) = 26.0. These peculiarities cannot be due to the progressions having been wrongly combined together into a band system as they are well marked features of the single progressions.

The properties of the system are set out in Table XVIII.

It is perhaps desirable to say a few words about the meaning of the rotational energy intervals given in this and similar tables and the manner in which they are obtained. We know from the progression vibration intervals that the lines numbered (m) end on the final level for which the number is (m) and $j = m - \frac{1}{2}$. Thus any P (m) line has a wave number given by $P(m) = \nu_0 + F'(\mu) - F''(m)$, where we suppose for the moment that the number μ and the corresponding j value of the initial state are unknown. The next line will

Table XVIII.

Initial vibration state.	0'.	1'.	2'.	Initial f values.
F (9) — F (8) for P lines		$j \downarrow$	$a \overline{\quad}$	$7\frac{1}{2}$
F (8) — F (7)			$s \overline{\quad}$	$6\frac{1}{2}$
F (7) — F (6)	$j \downarrow$		$a \overline{\quad}$	$5\frac{1}{2}$
F (6) — F (5)		$s \ 4\frac{1}{2}$	$s \overline{\quad}$	$4\frac{1}{2}$
F (5) — F (4)	$a \ 3\frac{1}{2}$	$a \ 3\frac{1}{2}$	$a \overline{\quad}$	$3\frac{1}{2}$
F (4) — F (3)	$s \ 2\frac{1}{2}$	$s \ 2\frac{1}{2}$	$s \overline{\quad}$	$2\frac{1}{2}$
F (3) — F (2)	$a \ 1\frac{1}{2}$	$a \ 1\frac{1}{2}$	$a \overline{\quad}$	$1\frac{1}{2}$
2B' for m small	$s \ \frac{1}{2}$	$s \ \frac{1}{2}$	$a \overline{\quad}$	$\frac{1}{2}$
I for m small $\times 10^{40}$				
ν_0				
$\Delta\nu_0$				
Next $\Delta = 2x\omega_0$				
ϵ about				
σ				

Note.—The top level of 1' is queried because there are not enough lines to base anything very definite on.

have the wave-number $P(m+1) = \nu_0 + F'(\mu+1) - F''(m+1)$. Thus $P(m+1) - P(m) = F'(\mu+1) - F'(\mu) - \{F''(m+1) - F''(m)\}$. Very accurate values of the final intervals $F''(m+1) - F''(m)$ have been tabulated in Part I. From them and the differences of the vibration numbers of successive lines the values of the successive energy intervals can be obtained. If we use the double intervals such as are given by $P(m+2) - P(m) = F'(\mu+2) - F'(\mu) - \{F''(m+2) - F''(m)\}$ no theoretical assumptions as to the level structure are involved. All that is assumed is that the lines are successive lines of a band and that there are no missing levels as in the He_2 spectrum. The alternating intensity of these bands shows, however, that all levels are represented. The single level differences such as $F'(\mu+1) - F'(\mu)$ do involve the assumption as to the structure of the very small lowest final level $F''(1)$ which was made in Part I. This assumption is, of course, amply verified. This does not determine μ . The data in the tables are given in a form which

does not involve assigning a value to μ . Thus $F(5) - F(4)$ means that level interval got from the two successive lines numbered P (5) and P (4) in the table, i.e., those two P lines which end on the $m = 5$ and $m = 4$ final levels. The same data can be got from pairs of R lines if both branches are really coming from the same levels. The data in the table are, in general, the mean of a number got in various ways. Where both P and R lines are present those have to satisfy the combination rule $R(m) - P(m+2) = F''(m+2) - F''(m)$ and we can at once write down the j values from our knowledge of the j values for the final states, since for R lines $j \rightarrow j-1$ and for P lines $j \rightarrow j+1$.

The rotational energy level intervals are remarkably close together compared with those of the bands hitherto described. P (2) occurs, at any rate in the $0'$ and $1'$ progressions, so that for them $\sigma = 0$ and the $j = \frac{1}{2}$ level is present. The differences of the intervals are not constant but increase with m . However, for the intervals which have been found in the $0'$ progression this change is not very great so that for the three lowest levels $F(m) = B(j - \epsilon)^2$ will be a good approximation. If we apply this we have $2B = 21.96$, $2B(1 - \epsilon) = 21.45$, giving $\epsilon = +0.0232$. To the accuracy of the data and interpretation this is the same as $\epsilon = 0$. We shall adopt this for all the progressions as the terms are of the same type. The values of the constant $2B$ for the upper state when the rotational energy is small are much smaller than any hitherto encountered and the moments of inertia are correspondingly high. They appear, in fact, to be nearly six times as large as the value 0.480 for unexcited H_2 . From the values of the ν_0 's for the three progressions we find for the upper level $\omega_0' = 2239.17$, say, about 2239 , and $x\omega_0 = 6.38$, say about 6 . That the weight ratio of the alternate rotational states is practically 3 to 1 is shown by Table XIX in which the measured intensities of R (1) + R (3) are compared with six times the intensities of R (2) for the strong $2'$ progression.

Table XIX.

ν''	0.	1.	2.	3.	4.	5.	6.	7.
R (1) + R (3)....	96.9	318	16.1	about 36	about 71	84.5	7.1	(1) + (3)
6R (2)	103.8	282	19.3	39.6	74.4	85.2	$6 \times (0)$	$6 \times (0)$

Any apparent exceptions to this rule are believed to be due to coincidences of which there are a fair number in the system. The numbers in brackets in

Table XX.

n' \downarrow	m \downarrow	$m'' \rightarrow$	0.	1.	2.	3.	4.	5.	6.	7.	8.
0	1	E	19-6 28074-26 (3)	7-6 21755-92 (1)	7-0 20474-44 (1)	19227-90 (1A)	4-5 18014-73 (2)				
		P									
	2	E	19-6 28074-26 (3)	4-0 21757-96 (0A)	20478-13 (0)		17982-83 (0)				
		P	2-6 28015-03 (1)	6-9 21699-61 (1)	20419-64 (0)		3-7 18018-24 (1)				
	3	E	15-9 28068-82 (3)	22 21746-27 (4)	9-0 20469-77 (1a)		6-3 17917-50 (3A)				
		P	10-3 28068-10 (3)	15-2 21645-54 (2)	11-2 20368-97 (3)						
	4	E					Interference				
		P	2-0 28882-19 (00a)	21575-04 (0)							
	5	E									
		P	4-6 22792-13 (1)	5-0 21492-42 (1)		18908-10 (1)					
2	1	E	26720-47 (0)	25410-13 (00)	4-6 24126-94 (0)	2-0 22832-19 (00a)	21668-82 (0)		19341-96 (1)		
		P									
	2	E									
		P	26678-14 (00) F	25356-78 (0a)	1-6 24077-06 (00a)		7-6 21619-80 (1)		19294-76 (0)		
	3	E							19335-79 (0a)		
		P	26612-35 (1)	10 25299-81 (1)	3-5 24107-55 (0a)	22864-95 (00) F			7-5 19251-81 (1)		17058-20 (0)
	4	E									
		P	26530-80 (00)	25222-96 (0)	6-2 24023-10 (1)		21507-70 (0a)	1-8 20334-94 (0)	2-8 19194-23 (0)		
	5	E									
		P	26420-92 (0)	18-1 25180-26 (1)	23564-63 (00)		5-3 21431-93 (1)				

Table XIX are the eye estimates of Gale, Monk and Lee on the conventional scale, actually intensity measures being lacking.

§ 11. *The System $^1L \rightarrow 2^1S$.*

This is a weaker system but otherwise is very similar to $^1K \rightarrow 2^1S$. So far we have only found two progressions and it seems probable that these are the $0'$ and $2'$ progressions, the missing one being the intervening $1'$ progression. This is not so surprising as in the $^1L \rightarrow 2^1S$ system there are no lines in the $1'$ progression which are as strong as the strongest lines in the $0'$ and $2'$ progressions. When in addition one considers the comparative weakness of the two $^1L \rightarrow 2^1S$ progressions which have been found and the alternating intensity

Table XXI.

Initial vibration state.	$0'$.	$1'$.	$2'$.	Initial j values.
$F(5) - F(4)$ for P lines	$a \downarrow 3\frac{1}{2}$ 61.87		$a \downarrow 3\frac{1}{2}$ 51.78	$3\frac{1}{2}$
$F(4) - F(3)$	$s \downarrow 2\frac{1}{2}$ 38.85	23.02	$s \downarrow 2\frac{1}{2}$ 32.54	$2\frac{1}{2}$
$F(3) - F(2)$	$a \downarrow 1\frac{1}{2}$ 19.47		$a \downarrow 1\frac{1}{2}$ 16.51	$1\frac{1}{2}$
$2B'$ for m small	$s \downarrow \frac{1}{2}$ 19.4		$s \downarrow \frac{1}{2}$ 16.3	$\frac{1}{2}$
I for m small $\times 10^{40}$	2.86		3.40	
ν_0	23057.22	(24890)	26714.81	
$\Delta\nu_0$ probably about	(1835)		(1825)	
ϵ about	0		0	
σ	0		0	

Table XXII.

$n' \downarrow \quad n'' \rightarrow$		0.	1.	2.	3.	4.	5.	6.	7.	8.
0	1K	39	$11\frac{1}{2}$	19	$1\frac{1}{2}$					
	1L	$11\frac{1}{2}$	$8\frac{1}{2}$	6	2					
2	1K	4	13	$9\frac{1}{2}$	4	5		4		
	1L	$1\frac{1}{2}$	$2\frac{1}{2}$	1	$\frac{1}{2}$	$1\frac{1}{2}$		3		

among the *bands* of a progression which characterises these two systems it is evident that the intervening progression may be a very rudimentary affair consisting of a few weak lines and very difficult to locate. The lines and their intensities are set out in the usual way in Table XX.

The properties of the system are set out in Table XXI. The rotational energy levels are even closer than in ${}^1\text{L} \rightarrow 2{}^1\text{S}$. The terms are of the same type as in ${}^1\text{L} \rightarrow 2{}^1\text{S}$. P (2) occurs so that $\sigma = 0$ and the $j = \frac{1}{2}$ level is present. The differences of the energy intervals are increasing with m but not very fast, so that $F(m) = B(j - \epsilon)^2$ will be a satisfactory approximation for the two lowest intervals. This gives $2B_0 = 19.38$ and $\epsilon = -0.00464$. These are the same, respectively, as 19.4 and 0 to the accuracy of the data. The higher vibrational level by the same method gives $2B_2 = 16.03$ and $\epsilon = -0.03$. Probably $2B_2 = 16.3$ and $\epsilon = 0$ are better values than these. The moments of inertia, for zero rotation, are the highest which have appeared so far. On the assumption that there is a $1' \rightarrow n''$ progression not yet found, the value of the double interval between the two ν_0 's is 3657.59, so that the vibrational intervals are in the neighbourhood of 1835 and 1825 unless $x\omega_0$ has a very exceptional value.

The distribution of intensity among the *bands* is similar to that in ${}^1\text{K} \rightarrow 2{}^1\text{S}$. This can be seen from fig. 8 in which the upper figure in each rectangle gives

$n' \downarrow \quad n'' \rightarrow$		0.	1.	2.	3.	4.	5.	6.	7.	8.
0	${}^1\text{K}$	39	$11\frac{1}{2}$	24	$5\frac{1}{2}$		$4\frac{1}{2}$			
	${}^1\text{L}$	$11\frac{1}{2}$	10	6	2	$6\frac{1}{2}$				
1	${}^1\text{K}$	20	$11\frac{1}{2}$	$18\frac{1}{2}$	27	$1\frac{1}{2}$	3	$1\frac{1}{2}$	$\frac{1}{2}$	
2	${}^1\text{K}$	$13\frac{1}{2}$	$27\frac{1}{2}$	7	18	$17\frac{1}{2}$	$22\frac{1}{2}$	$9\frac{1}{2}$	$3\frac{1}{2}$	
	${}^1\text{L}$	$2\frac{1}{2}$	$3\frac{1}{2}$	$2\frac{1}{2}$	$\frac{1}{2}$	3	$\frac{1}{2}$	$3\frac{1}{2}$		$\frac{1}{2}$

FIG. 8.

the sum of Gale, Monk and Lee's intensity estimates for all the lines of the corresponding band of ${}^1\text{K} \rightarrow 2{}^1\text{S}$ and the lower the similar value for ${}^1\text{L} \rightarrow 2{}^1\text{S}$. In doing this, lines classed as (0) are given the value $\frac{1}{2}$ and those classed as (00) the value $\frac{1}{4}$. It will be seen that in each case the strongest band is the $0' \rightarrow 0''$, and in the $2'$ progression the maximum strength is at $2' \rightarrow 1''$. It

would appear from fig. 8 that in the $2'$ progression the band intensities have more alternations in $^1L \rightarrow 2^1S$ than in $^1K \rightarrow 2^1S$. This seems to be due to the fragmentary nature of the bands compared with the more robust $^1K \rightarrow 2^1S$ system. We have seen that in that system there is a definite alternation with final vibrational number in one set of branches such as P which tends to be compensated by an opposite alternation in the other set such as R'. Thus if only one set of branches is strongly developed there will be an increase in alternation from this cause. To test this we can make a comparison by including in the sums the intensity estimates for those corresponding lines only which are common to the two bands. This is done in Table XXII. It will now be seen that in the $2'$ progression the figures are quite parallel for both systems which suggests that the greater degree of alternation apparent in the $2'$ progression in 1L as compared with 1K is due to the weak development of the R branches in $2' \rightarrow n''$ of 1L . On the other hand both methods indicate that in the $0'$ progressions 1K has one more alternation than 1L .

The alternation in intensity in the lines in the ratio 3 to 1 which is present in every band of the H_2 spectrum hitherto described is present also in this system. Thus in $0' \rightarrow 1''$ of $^1L \rightarrow 2^1S$ we have the intensities of $R(1) + R(3) = 22 + 7.6 = 6 \times 4.9$, whereas $R(2) = 4.0$. This agreement is not as good as it should be and it seems likely that $R(3)$ is too strong. If this line were a blend it might help to remove the difference as regards vibrational alternation in intensity between the $0'$ progressions of 1K and 1L just referred to. There are not enough sequences of lines in this faint system whose intensities have been measured and which are free from blends to test this relation accurately; but in $0' \rightarrow 0''$ we have $P(3) + P(5) \div 6 = 2.5$, whereas $P(4) = 2.0$, in $2' \rightarrow 2''$ we have $R(1) + P(3) \div 6 = 1.8$, whereas $P(2) = 1.6$, and in $0' \rightarrow 1' R(1) + P(3) \div 6 = 3.8$ and $P(2) + R(2) \div 2 = 5.4$ and generally it can be seen that the intensity estimates are about what would be required by a 3 to 1 weight ratio.

§ 12. The System $^1M \rightarrow 2^1S$.

This system is closely allied to the two preceding systems $^1K \rightarrow 2^1S$ and $^1L \rightarrow 2^1S$ but it has some individual features of its own particularly in the upper initial vibrational levels. It is stronger than $^1L \rightarrow 2^1S$ and weaker than $^1K \rightarrow 2^1S$. The R branches are stronger than the P branches throughout the system. The lines and intensities are set out in the usual way in Table XXIII. It will be seen that the alternation in intensity in the bands of a progression is again present. Thus in the $0'$ progression the $0''$ band is strong.

Table XXIII.

$\begin{smallmatrix} n' \\ \downarrow \\ n'' \end{smallmatrix} \rightarrow$	0.	1.	2.	3.	4.	5.	6.	7.
1 E	36.4 23216.41 (3)	21.1 21697.03 (3)	Interference	19368.83 (04)	18.4 18165.85 (4)	17.5 16976.03 (5)		
2 E	30.4 23328.36 (3)	8.3 21911.91 (1)	10.0 20431.97 (2)		10.0 18175.18 (1)	11.0 16996.32 (1a)		
3 E	8.9 23151.20 (2)	6.2 21834.84 (1)	20554.99 (1)		7.9 18097.93 (1)			
4 E	64.2 23230.80 (4)	20.9 21918.18 (1)	35.8 20641.59 (2)	19399.10 (004)	24.9 18190.12 (3)			
5 E	23.2 23099.23 (5)	30.7 21786.06 (3)	29.5 20510.10 (4)		26.2 18058.64 (5)			
6 E	23227.87 (1)	4.1 21920.84 (0)	5.0 20443.91 (0)		3.2 18205.74 (1)			
7 E	23086.00 (1)	7.3 21723.01 (1)	7.6 20457.15 (0)		8.2 18013.87 (2)			
8 E	5.8 23964.05 (1)	17.4 21664.36 (3)	13.2 20398.73 (2)		17.3 17968.06 (4)			
9 E		6.6 21568.27 (1)	3.7 20340.22 (0)		6.0 17920.33 (3)			
10 E	25374.22 (0)	10.6 24055.96 (2)		5.3 21527.84 (1)		2.7 17937.29 (1)		
11 E		6.5 24048.05 (1)		21522.96 (0a)		17936.10 (0)		
12 E	8.1 23334.27 (0a)	17.4 24021.79 (1)		6.7 21502.76 (0)	7.1 20233.60 (1a)	6.8 17973.40 (1)		
13 E		23945.61 (0)		7.3 21426.71 (00)	14.7 20217.55 (2)	2.6 17987.15 (1)		
14 E								
15 E				21269.71 (0)		19041.13 (0)		
16 E						19001.60 (1a)		

1	R	(27511.01)	9.7 26192.64 (1)	13.7 24911.08 (1)		Interference	5.7 21271.42 (1)	6.5 20123.80 (0)	Interference
	P								
2	R		26174.30 (1a)	7.6 24894.43 (1)				6.6 20112.25 (0)	18998.00 (0)
	P	27472.50 (0) F	* 26155.14 (0) F	24876.06 (0) F	23430.36 (00) F		21240.20 (0) F		
3	R		26186.62 (2)	21.8 24860.33 (2)	7.6 23617.88 (1)		10 21232.31 (2)	16.4 20098.33 (3)	8.9 18978.42 (1)
	P					22354.06 (0)		17.0 20033.91 (4)	
4	R								
	P				22431.59 (00) F	86.2 22276.33 (4)	21108.79 (00) F		
5	R								
	P			24617.47 (00) F		22194.97 (0) F	21016.43 (3) F*		

* Broad.

the 1'' band weaker, the 2'' band stronger, and 3'' band very weak, the 4'' band strong and the 5'' band not so strong. There is again the same tendency for the P (*m*) lines to be stronger in the bands for which the R (*m*) lines are weaker and vice versa. Thus in $0' \rightarrow 0''$ $R(3) = 56.2$ $P(3) = 28.2$ in $0' \rightarrow 1''$ $R(3) = 20.9$ $P(3) = 30.7$ and in $0' \rightarrow 2''$ $R(3) = 35.8$ $P(3) = 29.5$, and in fact in $0' \rightarrow 1''$ the P branch is stronger than the R branch, whereas it is weaker in $0' \rightarrow 0''$ and in $0' \rightarrow 2''$. The $0'$ progression is the strongest and the $1'$ progression the weakest, as in the ${}^1K \rightarrow 2{}^1S$ and the ${}^1L \rightarrow 2{}^1S$ systems.

The properties of the system are set out in Table XXIV. The rotational energy levels are of the same type as those of ${}^1K 2 \rightarrow {}^1S$ and ${}^1L \rightarrow 2{}^1S$, the

Table XXIV.

Initial vibration state \rightarrow	0	1	2
$F(6) - F(5)$ for P lines	$j \downarrow$ $s \ 4\frac{1}{2}$ $\overline{112.15}$	$j \downarrow$	$j \downarrow$
$F(5) - F(4)$	$a \ 3\frac{1}{2}$ $\overline{79.72}$ $\left. \begin{array}{l} 112.15 \\ 79.72 \end{array} \right\} 32.43$	$a \ 3\frac{1}{2}$ $\overline{47.04}$	$a \ 3\frac{1}{2}$ $\overline{36.03}$
$F(4) - F(3)$	$s \ 2\frac{1}{2}$ $\overline{51.80}$ $\left. \begin{array}{l} 79.72 \\ 51.80 \end{array} \right\} 27.92$	$s \ 2\frac{1}{2}$ $\overline{29.08}$ $\left. \begin{array}{l} 47.04 \\ 29.08 \end{array} \right\} 17.96$	$s \ 2\frac{1}{2}$ $\overline{18.53}$ $\left. \begin{array}{l} 36.03 \\ 18.53 \end{array} \right\} 17.50$
$F(3) - F(2)$	$a \ 1\frac{1}{2}$ $\overline{25.38}$ $\left. \begin{array}{l} 51.80 \\ 25.38 \end{array} \right\} 26.42$	$a \ 1\frac{1}{2}$ $\overline{\text{not known}}$	$a \ 1\frac{1}{2}$ $\overline{-0.27}$ $\left. \begin{array}{l} 18.53 \\ -0.27 \end{array} \right\} 18.80$
	$s \ \frac{1}{2}$ $\overline{\quad}$	$s \ \frac{1}{2}$ $\overline{\quad}$	$s \ \frac{1}{2}$ $\overline{\quad}$
$2B'$ for <i>m</i> small	26	18 to 20	18 to 19
I for <i>m</i> small $\times 10^{40}$	2.1_s	3.1 to 2.8	3.1 to 2.9
ν_0	23191.66	25367.7 or 25370.08	27513.84
$\Delta\nu_0$	2176.0 or 2178.42		2146.1 or 2143.76
Next $\Delta = 2\pi\omega_0$	29.9 or 34.66		
ϵ	$+0.04 = 0$	$+0.38 = +\frac{1}{2}?$	$+0.94 = +1$
σ	0	?	?

differences of the intervals increasing slowly at first and then more rapidly as *m* increases. P (2) occurs in the strong $0'$ vibrational level so that for this level at least $\sigma = 0$ and the $j = \frac{1}{2}$ rotational level is present. For the $1'$ and $2'$ vibrational levels the P (2) lines have not been found with certainty, but we assume that they are capable of existing and that $\sigma = 0$ for these levels also. If this assumption, which leads to a very simple description of this band system, should turn out to be incorrect the values of ϵ which we find for these higher vibrational

levels would be changed. Subject to this reservation, we assume that for the two lowest rotational intervals $F(m) = B(j - \epsilon)^2$ will be a satisfactory approximation. In this way we find for the $0'$ vibrational level that $2B_0 = 26.42$, which is the same as 26, and $\epsilon = +0.04$ which is the same as $\epsilon = 0$ to the accuracy of the data. From the P (2) line these data give $\nu_0 = 23191.66$ which should be correct to about 0.1 wave number. For the $1'$ vibrational level the same method of treatment gives $2B = 17.96$ which is equivalent to $2B = 18$ and $\epsilon = +0.38$. This is probably the same as $\epsilon = +\frac{1}{2}$ to the accuracy of the data, owing to the uncertainty as to the exact manner in which B_1 is varying with m or j : If we adopt $2B = 18$ and $\epsilon = +\frac{1}{2}$ we find from the R (1) line that $\nu_0 = 25370.08$ and if we adopt $2B = 18$ and $\epsilon = +0.374$ we find $\nu_0 = 25367.7$. $2B_1$ might be as high as 20 so that two alternative values are given in Table XXIV. There is thus an uncertainty of several units in this ν_0 . With the $2'$ level data we find as a first approximation in a similar way $2B_2 = 17.5$ and $\epsilon = +0.94$. This is the same as $\epsilon = +1$ to the accuracy of the data. If $\epsilon = +1$ exactly then $F'(2) = B_2(1\frac{1}{2} - 1)^2 = B_2(\frac{1}{2} - 1)^2 = F'(1)$ and $R(1) - P(2) = F'(2) - F'(1) + F''(2) - F''(1) = F''(2) - F''(1)$. This would enable the P (2) lines to be calculated from the R (1) lines and the known intervals in the final 2^1S level. Finkelburg* has some weak lines close to the calculated positions. These have been inserted in Table XXIII. Except for the one which is queried the lines agree amongst themselves, but if they are really the P (2) lines the $j = \frac{1}{2}$ and $j = 1\frac{1}{2}$ levels do not exactly coincide but the $j = \frac{1}{2}$ level is 0.27 wave number above the $1\frac{1}{2}$ level. If this is the position of the $j = \frac{1}{2}$ level it gives $\epsilon = +1.014 = +1$ and $2B_2 = 19.0 \pm 0.1$ instead of the preliminary value 17.5. Finkelburg has such a large number of these weak lines that it is difficult to be certain of their reality as a progression so that the value of $2B_2$ is given in the table as 18 to 19. With $2B_2 = 19$ and $\epsilon = +1$ we have for the $2'$ level $\nu_0 = 27513.84$. This should be reliable to within 0.4 wave-number whether the P (2) lines are real or not. The apparent values of the moments of inertia are again very high and as in the preceding system they increase with increasing vibration and diminish with increasing rotation. One third of $2x\omega_0$ for this system = 10 or 11.6 is nearly equal to $2x\omega_0$ for $^1K \rightarrow 2^1S$ (12.75) which recalls a similar relation in the $^1A \rightarrow 2^1S$, $^1B \rightarrow 2^1S$ and $^1C \rightarrow 2^1S$ systems. The value of ω_0 the vibration frequency at zero amplitude for the 1M state is 2195.75 or 2190.95 according to whether we assume $\epsilon = +\frac{1}{2}$ or $\epsilon = +0.374$ for the $1'$ vibration level.

* 'Z. Physik,' vol. 52, p. 27 (1929).

The change in ϵ from 0 to $+\frac{1}{2}$ and then to $+1$ as the vibration number changes from 0 to 1 and then to 2 is a curious and interesting feature of this band system.

An intensity diagram for this system is shown in fig. 9 where the numbers

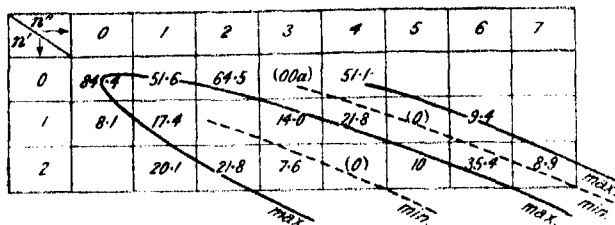


FIG. 9.

are the sums of Kapuscinski and Eymers intensity measures for the R (3) and P (3) lines of each band, except those in brackets which are Gale, Monk and Lee's eye estimates of weak lines which have not been measured by Kapuscinski and Eymers. By comparison with fig. 7 it will be seen that the intensity distribution is of the same type as in $^1K \rightarrow 2^1S$ and possesses two lines of maxima and minima respectively. The tendency to opposite alternation in intensity with final vibration number in the P and R branches respectively has been described already.

The bands of this system possess the alternation in intensity in the lines of each band corresponding to a weight ratio of 3 to 1 in the rotational terms which is such a marked feature of the whole H_2 spectrum. This is shown for example by the intensity data in Table XXV where the sums of the intensity measures of Kapuscinski and Eymers for the R (1) + R (3) lines or P (3) + P (5) lines divided by 6 are set against those of the intervening R (2) lines or P (4) lines, and $1\frac{1}{2}$ times the sums of the intensities of P (2) + P (4) lines are set against the intervening P (3) lines, where such data are available.

Table XXV.

$n' \rightarrow$	0	0	0	1	2	2		0	0
$n'' \rightarrow$	0	1	4	1	2	6		1	4
$\frac{1}{6}\{R(1) + R(3)\}$	15.3	7.0	7.2	4.7	5.9	4.2	$\frac{1}{6}\{P(2) + P(4)\}$	20.3	24.2
R (2)	30.4	8.3	10	6.5	7.6	6.6	P(3)	30.7	26.2
$\frac{1}{6}\{P(3) + P(5)\}$	7.1*	8.0	7.2						
P (4)	7.6*	7.3	8.2						

* Data for $0' \rightarrow 2''$ band and not for $0' \rightarrow 0''$ as tabulated.

On account of the temperature effect the number opposite R (2) or P (3) should be somewhat greater than the number above it, the R (3) line being considerably stronger than the R (1) line owing to the magnitude of I in the initial states of these bands. It is very satisfactory that the $0' \rightarrow 0''$ R (2) line is nearly twice as strong as it ought to be as this line is also required as R (1) of $1' \rightarrow 2''$ of the ${}^1C \rightarrow 2{}^1S$ system where it is a little more than twice as strong as it should be.

§ 13. The System ${}^1N \rightarrow 2{}^1S$.

This has a good deal of resemblance to the three preceding systems 1K , 1L and ${}^1M \rightarrow 2{}^1S$. It is a powerful system extending right across the visible spectrum and containing many strong lines but it consists of only two progressions. The lower, which is believed to be a $0'$ progression, starts at $\lambda = 3715.990$ and the upper which is believed to be a $1'$ progression, starts at $\lambda = 4009.561$. The reason for assigning these initial vibrational numbers is that if they were incorrect there should be a strong progression with similar properties starting near $\lambda = 4360$ A.U. but no such progression exists. The next upper initial vibrational level may have too much energy to be capable of existence. The wave-numbers of the lines preceded by Kapuscinski and Eymers' intensity measures and followed by Gale, Monk and Lee's eye estimates are given in Table XXVI.

The properties of the system are set out in Table XXVII. It will be seen that the energy intervals are of the same character as those for the three preceding systems, 1K , 1L and ${}^1M \rightarrow 2{}^1S$, their differences increasing slowly at first and then more rapidly as j increases. The values of B' are larger and the values of I smaller, for m small, than for those systems. In this respect 1N is intermediate between 1K , 1L , 1M and 1A , 1B , 1C , but, as in other respects, closer to the former group. For m small the terms are very close to the form Bj^2 with the values of j in Table XXVII. These have been determined by the transitions to the final $2{}^1S$ level. These are governed by the rules, so far found universal, that $\Delta j = 0$ or ± 1 and $s \rightarrow a$ and $a \rightarrow s$ transitions are not allowed. The values of ν_0 are got from the P (2) lines, using $P(2) = \nu_0 + F'(\frac{1}{2}) - F''(\frac{1}{2})$ and taking $F'(\frac{1}{2})$ to be $\frac{1}{4}B'$. The ν_0 for the $0'$ progression may thus be in error by about $\frac{1}{4}$ wave-number but for the $1'$ progression it should not exceed the errors of measurement. Since the rotational terms are close to the form Bj^2 , $\varepsilon = 0$ or thereabouts and since the P (2) line, which comes from the initial $j = \frac{1}{2}$ level is present, $\sigma = 0$.

Table XXVI.

$\pi^+ \pi^- \rightarrow$	0.	1.	2.	3.	4.	5.	6.	7.
1 R	12.7 24088-37 (2)	20.0 23615-01 (4)	6.7 22333-43 (1)	37.1 21036-78 (5)	41.5 19873-74 (9)			
2 P						Interference		
3 R	24965-00 (1a)	16.8 23646-69 (2)	22368-91 (00)	13.4 21123-59 (2)	20.3 19911-82 (4)		5.7 17586-73 (1)	
4 P	14.5 24857-55 (2)	6.6 23541-14 (2)	22261-26 (1a)	14.1 21016-02 (5)	16.2 19804-30 (5)		17479-18 (2)	
5 R								
6 P	82.5 24817-19 (3)	83.0 23677-92 (5)	22401-28 (0)	27.6 21158-92 (4)	52.0 19949-79 (8)		9.5 17629-46 (1a)	
7 R								
8 P								
9 R								
10 P								
11 R								
12 P								
13 R								
14 P								
15 R								
16 P								
17 R								
18 P								
19 R								
20 P								
21 R								
22 P								
23 R								
24 P								
25 R								
26 P								
27 R								
28 P								
29 R								
30 P								
31 R								
32 P								
33 R								
34 P								
35 R								
36 P								
37 R								
38 P								
39 R								
40 P								
41 R								
42 P								
43 R								
44 P								
45 R								
46 P								
47 R								
48 P								
49 R								
50 P								
51 R								
52 P								
53 R								
54 P								
55 R								
56 P								
57 R								
58 P								
59 R								
60 P								
61 R								
62 P								
63 R								
64 P								
65 R								
66 P								
67 R								
68 P								
69 R								
70 P								
71 R								
72 P								
73 R								
74 P								
75 R								
76 P								
77 R								
78 P								
79 R								
80 P								
81 R								
82 P								
83 R								
84 P								
85 R								
86 P								
87 R								
88 P								
89 R								
90 P								
91 R								
92 P								
93 R								
94 P								
95 R								
96 P								
97 R								
98 P								
99 R								
100 P								

Table XXVII.

Initial vibration state \rightarrow	0. j \downarrow	1. j \downarrow
F (7) — F (6) for P lines	$a \ 5\frac{1}{2}$ <u>195.88</u> $s \ 4\frac{1}{2}$ 55.56 $a \ 3\frac{1}{2}$ <u>140.32</u> } 37.02 $s \ 2\frac{1}{2}$ 32.13 $a \ 1\frac{1}{2}$ <u>102.70</u> } 33.64 $s \ \frac{1}{2}$ 36.93	$a \ 5\frac{1}{2}$ <u>180.37</u> $s \ 4\frac{1}{2}$ 72.21 ? $a \ 3\frac{1}{2}$ <u>108.16</u> } 32.37 $s \ 2\frac{1}{2}$ 25.94 $a \ 1\frac{1}{2}$ <u>75.79</u> } 24.78 $s \ \frac{1}{2}$ 49.85 $s \ \frac{1}{2}$ 25.07
2B' for m small	35 ± 2	24.9 ± 0.1
I for m small $\times 10^{40}$	1.6 ± 0.1	2.22 ± 0.01
ν_0	24896.51	26879.78
$\Delta \nu_0 = \omega_0 - x\omega_0$	1983.27	
ϵ about	0	0
σ	0	0

The intensity distribution has the same features as that presented by the 1K , 1L , $^1M \rightarrow 2^1S$ systems. In Table XXVIII we have set out the sums of Kapuscinski and Eymers' measures of the strong R (3) and P (3) lines of the system by the usual double entry method. It will be seen that in the 0' progression there are three maxima separated by intervening minima and only two maxima and one minimum in the 1' progression.

Table XXVIII.

$n' \downarrow \quad n'' \rightarrow$	0.	1.	2.	3.	4.	5.	6.	7.
0	82.5	102.7	33.0	104.4	119.0		21.9	9.7
1	29.1	47.5	49.6	2.8	28.6	31.2	32.5	5.6

It is clear from an examination of the intensity data in Table XXVI that the strength in the P branches in a progression varies with the final vibration number of the band in a different way from that in the R branches. The behaviour is, however, very complicated. It seems, in fact, as if the systems

were trying to accomplish the impossible task of making P weak where R is strong and vice versa as in $^1K \rightarrow 2^1S$, and at the same time making P and R strong and weak together as in 1A and $^1C \rightarrow 2^1S$. As we have seen this is not the only way in which this system seems to be intermediate between these two groups.

There is plenty of evidence that the weight ratio has the usual value 3 to 1 for the alternate rotational states of this system. In Table XXIX we have set out the values of $\frac{1}{2}$ the sum of Kapuscinski and Eymers' intensity measures of R (1) + R (3), P (3) + P (5) and P (5) + P (7) compared with the intervening R (2), P (4) and P (6) respectively as well as $1\frac{1}{2}$ times the sum of P (2) + P (4) compared with the intervening P (3). The only case in which there is a disparity which is very seriously beyond what might be due to temperature effects is in the line P (6) of $1' \rightarrow 3''$ which is about four times as strong as it should be. It is satisfactory that this line is also claimed as P (5) $0' \rightarrow 0''$ of $^1L \rightarrow 2^1S$ where it is about twice as strong as it should be. There are four other cases with considerable discrepancies but these might arise from a variety of causes.

Table XXIX.

$n' \rightarrow$	0					0	0	0	0	0	1	1	1	1	1	
$n'' \rightarrow$	1					0	1	2	3	4	0	1	2	4	6	
$\frac{1}{2}\{R(1) + R(3)\}$	18.8					$\frac{1}{2}\{P(3) + P(5)\}$	23.9	3.9	10.8	20	19.2	9.1	15.3	6.6	6.8	8.8
$R(2)$	16.8					$P(4)$	22.6	3.6	13.7	18.9	27	10	15	7.6	6.9	10.7

$n' \rightarrow$	0	0	0	0	1	1					0	0	1	1	1
$n'' \rightarrow$	0	2	3	4	1	3					0	1	1	2	6
$\frac{1}{2}\{P(5) + P(7)\}$	13.6	7.0	8.5	9.5	9.3	1.1				$1\frac{1}{2}\{P(2) + P(4)\}$	55.7	15.3	35.3	24.2	28.4
$P(6)$	14.4	6.7	5.5	10.3	10.6	4.6				$P(3)$	82.5	19.7	47.5	27.1	32.5

The remaining band systems will be described in Part IV of this paper and will include, among others, a strong band system in the infra-red region.

The Spectrum of H₂: The Bands Analogous to the Parhelium Line Spectrum.—Part IV.

By O. W. RICHARDSON, F.R.S., Yarrow Research Professor of the Royal Society, and P. M. DAVIDSON, B.A., King's College, London.

(Received March 13, 1929.)

Synopsis.

§ 14. The system ${}^1\text{O} \rightarrow 2\,{}^1\text{S}$. Similar to ${}^1\text{A} \rightarrow 2\,{}^1\text{S}$ but weaker and with $\epsilon = 0$. Lowest level $j = \frac{1}{2}$. Branches P and R. $\nu_e = 22814$. § 15. The progression ${}^1\text{Q} \rightarrow 2\,{}^1\text{S}$. Of the same type as ${}^1\text{O} \rightarrow 2\,{}^1\text{S}$ but with a much larger value of B. Lowest level $j = 1\frac{1}{2}$. Branches P and R. $\nu_e = 21843$. § 16. The progression $\lambda 4142\cdot801$. Single branches. If Q lowest $j = 3\frac{1}{2}$, $\nu_0 = 24367$. § 17. The progression $\lambda 4097\cdot433$. Single branches. If Q lowest $j = 2\frac{1}{2}$, $\nu_0 = 24447$. § 18. The infra-red system. These bands are close to where the bands whose initial states are the initial states of Werner's ultra-violet bands should lie. P and R but no Q branches.

§ 14. *The System ${}^1\text{O} \rightarrow 2\,{}^1\text{S}$.*

Gale, Monk and Lee's* wave-numbers of the lines of this system preceded by Kapuscinski and Eymers'† intensities and followed by Gale, Monk and Lee's (in brackets) are set out in Table XXX. It is not a very strong system and consists of three progressions. It is intermediate in character between the groups of systems ${}^1\text{A}$, ${}^1\text{B}$ and ${}^1\text{C} \rightarrow 2\,{}^1\text{S}$ and ${}^1\text{K}$, ${}^1\text{L}$ and ${}^1\text{M} \rightarrow 2\,{}^1\text{S}$, but nearer to ${}^1\text{A}$, ${}^1\text{B}$ and ${}^1\text{C}$ than to ${}^1\text{K}$, ${}^1\text{L}$ and ${}^1\text{M}$. There is no great disparity between the strength of the P and R branches in this system. There is a disagreement in the intensity data for the line $2' \rightarrow 1''$ P (5). Gale, Monk and Lee's estimate is (1) and Kapuscinski and Eymers' measure is 112.

The properties of the system are set out in Table XXXI.‡ The transitions to the final states are governed by the rules $\Delta j = 0$ or ± 1 and s to a and a to s not allowed with the j , s and a allocations to the levels shown in the table. In each initial vibrational level the strong lines start from $j = 1\frac{1}{2}$ or $3\frac{1}{2}$ and the weak lines from $j = \frac{1}{2}$ or $2\frac{1}{2}$. In the $n' = 0$ initial vibrational level P (2) is

* 'Astrophysical Journal,' vol. 67, p. 89 (1928).

† 'Roy. Soc. Proc.,' A, vol. 122, p. 58 (1929).

‡ The precise meaning of these energy intervals and the methods of obtaining them is explained fully in Part III.

Table XXX.

$\begin{smallmatrix} n \\ m \end{smallmatrix}$ $\begin{smallmatrix} \rightarrow \\ \downarrow \end{smallmatrix}$	$\begin{smallmatrix} n \\ m \end{smallmatrix}$ $\begin{smallmatrix} \rightarrow \\ \downarrow \end{smallmatrix}$	0.	1.	2.	3.	4.	5.	6.	7.	8.
0	R	5-2 22813-30 (1)	11-6 21494-98 (0)	4-0 20213-54 (0)						
	P		21575-44 (0)	2-7 20295-69 (0)						
	R	22715-27 (0)	21398-87 (0)							
	P		24 21671-27 (4)	12-0 20394-70 (2)	19152-26 (0)	3-6 17943-20 (2)				
	R	19-8 22697-15 (2)	29-7 21384-60 (3)	8-0 20107-99 (1)						
1	R	6-7 22699-45 (1)	11-4 21392-50 (1)	4-1 20120-69 (0)						
	P		39-3 21417-44 (4)	15-0 20151-83 (2)						
	R	18-7 22717-07 (4)	23775-18 (1)		8-2 21246-88 (3)	2-3 17719-08 (1)				
	P	36-2 25093-50 (1)				17-0 20033-91 (4)		17708-41 (2)		
	R	16-0 25151-59 (3)				20098-31 (0a)		17773-21 (0a)		
2	R	36-0 25825-38 (4)	6-4 23912-77 (1)	7-1 22636-12 (1)			7-5 19008-37 (1)			
	P	48-4 24977-88 (4)	28-2 23964-78 (5)		6-0 21145-86 (1)	26-0 19936-73 (4)		17864-39 (0)	18504-37 (0)	
	R	24959-26 (1)	5-1 23632-27 (0)	22380-49 (0)	3-4 21142-48 (1)					
	P	65 24958-70 (5)	2-0 23638-94 (0)	22392-40 (1)						
	R	[27135-18]	118 25816-82 (4)	4-8 24535-26 (00)	5-4 23288-85 (1)			18632-08 (0a)		
3	R	48-9 27270-83 (3)	38-4 25959-15 (3)		5-2 23439-19 (1a)					
	P	19-9 27019-01 (1)	* 23706-36 (3)	2-2 24429-82 (0)					5-3 18545-94 (1)	17464-67 (1)
	R									
	P									
	R	42-5 27098-97 (3)	112-0 25704-31 (1)	3-2 24438-76 (0)	23206-20 (0)	4-6 22005-96 (1)			2-1 18597-38 (0a)	

* Together with H₅ = 170-0.

be wrong by 5 units either way. The absence of the P (2) lines and the uncertainty in B_1 makes a corresponding uncertainty in the ν_0 for this vibrational level. Using $R(1) = 25093.50 = \nu_0 + F'(1\frac{1}{2}) - F''(\frac{1}{2})$ and putting $F'(1\frac{1}{2}) = 9/8 \times 2B_1 = 56.25$ and $F''(\frac{1}{2}) = 4.86$ gives $\nu_0 = 25042$ which might be wrong by about 5 units either way. The $n' = 2$ progression is the least satisfactory in the system, in fact it is probably the least satisfactory progression of any described in this series of papers. In the $2' \rightarrow 0''$ and $2' \rightarrow 1''$ bands the P (3) and P (5) lines are so strong that the intervening P (4) lines should occur on account of the 3 to 1 weight ratio which is universal in this spectrum and in the $2' \rightarrow 1''$ bands the same applies to R (1), R (3) and R (2), but we have not been able to find them. There are two possible reasons for this difficulty. One is that this progression is interwoven with the various $0' \rightarrow n''$ progressions which come from the $4'$ electronic level which have been described in Part II and it may be that the missing R (2) and P (4) lines have been given by mistake to one of them. The other reason is that the progression itself has a definite abnormality. The R (1) line of $2' \rightarrow 0''$ is entirely absent although R (3), P (3) and P (5) of the same band are strong and R (1) of $2' \rightarrow 1''$ seems abnormally strong. The absence of R (1) from $2' \rightarrow 0''$ is the more remarkable as it springs from the same level as P (3). Thus both its initial and final levels are known to occur. The absence of the R (2) and P (4) lines is not more remarkable than the absence of this line and may be another feature of the same or a related abnormality. On account of the absence of these lines we only have the rotational energy interval between $j = 3\frac{1}{2}$ and $j = 1\frac{1}{2}$ for this vibrational level. It is 251.59 and is very close to the corresponding quantity for the $n' = 1$ vibrational level. This strongly suggests that all three vibrational levels have the same rotational term structure. As the P (2) lines are unknown, if they exist, this would make σ doubtful but we should have $\epsilon = 0$ and $2B_2$ about 50 with an uncertainty of about ± 5 as in the $n' = 1$ level. From the wave-number of the $2' \rightarrow 0''$ R (1) line, calculated by the combinations from P (3) or from the R (1) of $2' \rightarrow 1''$, and $R(1) = \nu_0 + F'(1\frac{1}{2}) - F''(\frac{1}{2})$ using $F'(1\frac{1}{2}) = 9/8 \times 2B_2 = 56.25$ and $F''(\frac{1}{2}) = 4.86$ we find $\nu_0 = 27084$ for this vibrational level. This may be wrong by several units as in the ν_0 of the $1'$ vibrational level.

These values of ν_0 give $\omega_0 x = 124$ and $\omega_0 - \omega_0 x = 2290$ so that the vibrational frequency for zero amplitude is $\omega_0 = 2414$. As there is an uncertainty, owing to lack of sufficient data and ignorance of the precise interpretation which should be put on such data as are available, of several units in the ν_0 's of the $n' = 1$ and 2 levels we have thought it well to check

these results by using instead of the ν_0 's the wave-numbers of the R (1) lines of the 0'' band of each progression. These are set out in Table XXXI and lead to $\omega_0 - \omega_0 x = 2280$, $\omega_0 x = 119$ and $\omega_0 = 2399$. These, of course, are only rough but they confirm the values given already. The large value of $x\omega_0 = 124$ is very nearly the same as that for ${}^1C \rightarrow 2{}^1S$.

The values of $2B$ and l for the initial levels of this system are very similar to those for the 1A , 1B and 1C levels and also they are probably not vastly different for j small and j large.

The intensity diagram for this system, shown in fig. 10, gives the sums of Kapuscinski and Eymers' measures for the strong R (3) and P (3) lines of all

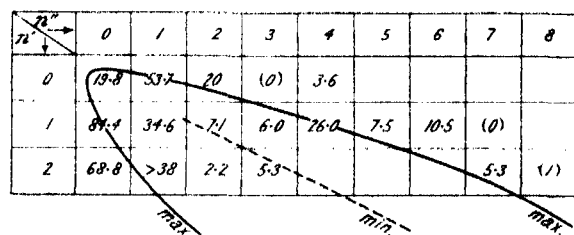


FIG. 10.

the bands by the usual double entry method. It is quite similar to the diagrams for the 1A , 1B and ${}^1C \rightarrow 2{}^1S$ systems except that the minimum in the $2'$ level instead of being confined to 1 or 2 bands has developed into a considerable area. In this system as in 1A , 1B and ${}^1C \rightarrow 2{}^1S$ the general tendency is for P and R branches of the various bands to be strong or weak together.

Except in the $2'$ progression, there is good evidence that the weight ratio of alternate rotational states is 3 to 1. This is shown in Table XXXII where $\frac{1}{2}$ the sum of Kapuscinski and Eymers' intensities of various R (1) and R (3) or P (3) and P (5) lines are compared with the intensities of the intervening R (2) or P (4) lines respectively.

Table XXXII.

$n' \rightarrow$	1.		0.	0.	0.	1.
$n'' \rightarrow$	0.		0.	1.	2.	1.
$\frac{1}{2} \{R(1) + R(3)\} \rightarrow$	12.0	$\frac{1}{2} \{P(3) + P(5)\}$	6.4	11.5	3.8	5.0
$\quad \quad R(2) \rightarrow$	16		6.7	11.4	4.1	5.1

§ 15. *The Progression $1Q \rightarrow 2^1S$.*

There is not very much of this, as we have only been able to find one progression so far, but it has some interesting characteristics. The wave-numbers of the lines preceded by Kapuscinski and Eymers' intensity measures and followed by Gale, Monk and Lee's eye estimates are given in Table XXXIII.

Table XXXIII.

m ↓	$n'' \rightarrow$	0.	1.	2.	3.
1	R	13.1 21922.71 (2)		9.0 19322.85 (1)	18076.20 (0)
	P				
2	R				
	P				
3	R	22198.54 (00)			18400.57 (00)
	P	54.3 21806.54 (5)	14.4 20493.95 (3)		11.8 17975.00 (3)
4	R				
	P	7.4 21844.49 (1)	20537.44 (1a)		18027.62 (00)
5	R				
	P	25.4 21931.77 (4)	10.0 20631.95 (2)		18134.00 (1)

The properties are set out in Table XXXIV. No P (2) lines have been found so that σ is uncertain and the lowest known initial rotational level has $j = 1\frac{1}{2}$. The energy level intervals are approximately in the ratio 2 : 3 and suggest $\epsilon = 0$ or thereabouts with the j values given. These and the s and a assignments satisfy the usual rules $\Delta j = 0$ or ± 1 and $s \rightarrow a$ and $a \rightarrow s$ barred for the transitions to the final 2^1S states. Since the rotational term values are given approximately by $F(j) = B(j^2 - \sigma^2)$ whatever value σ may have it is evident that $2B$ has a value in the neighbourhood of 75. This might be in error by about ± 5 units. In any event this value of $2B$ for j small is distinctly greater, and the value of I correspondingly less, than for any of the systems which come from an initial 3 electron state, although some of the systems described in Part II which come from 4 electron states probably have values of $2B_0$ which are not very different from this.

If we adopt $\epsilon = 0$, $\sigma = 0$ and $2B = 75$ as approximately correct, we get

Table XXXIV.

Initial vibration state.	Probably 0'.
F (5) — F (4) for P lines	$\begin{array}{c} j \\ \downarrow \\ \alpha \quad 3\frac{1}{2} \end{array}$
F (4) — F (3)	$\begin{array}{c} 238.95 \\ \alpha \quad 2\frac{1}{2} \end{array}$
	$\begin{array}{c} 153.01 \\ \alpha \quad 1\frac{1}{2} \end{array}$
2B for j small	About 75.
I for j small	About 7.4×10^{-41}
ν_0	About 21843.
ϵ	()
σ	?

from $R(1) = 21922.71 = \nu_0 + F'(1\frac{1}{2}) - F''(\frac{1}{2})$, $\nu_0 = 21843$, using $F''(\frac{1}{2}) = 4.86$ and $F'(1\frac{1}{2}) = 84.38$. Even if these assumptions are correct this value might be wrong by ± 5 units. It is a curious fact that this ν_0 is the same as the ν_0 for $3^1B \rightarrow 2^1S$ which, adopting assumptions similar in principle to these, was determined in Part I, p. 62, as 21839, and Part II, p. 473, as 21849, and the mean of these is 21844. This suggests that this progression may be the P' and R' branches corresponding to the Q branches which constitute $1^1B \rightarrow 2^1S$. However, this seems very doubtful. In the first place there is the great disparity between the values of 2B, for j small, for the two systems. In the second place the ν_0 's have been evaluated on the assumptions that σ was in the neighbourhood of 0 for both systems. But if they are to be combined into a P'QR' system it would be natural to assume that σ was at least equal to something comparable with 1. In any event some such value of σ seems to be required for $3^1B \rightarrow 2^1S$ from which the $j = \frac{1}{2}$ level is definitely missing in the initial state. If we assume $\sigma = 1$ and apply the formula $F(j) = B(\sqrt{j^2 - \sigma^2} - \epsilon)^2$ to the rotational level data of this progression, we find $2B = 84.56$, $\epsilon = +0.164$ and $\nu_0 = 21889(0.12)$. Applying the same method to the corresponding levels of the 0' progression of $1^1B \rightarrow 2^1S$, assuming that the branches are Q, we find $2B_0$ for j small = 47.96, $\epsilon = +0.378$ and $\nu_0 = 21861(18)$. The agreement of the ν_0 's has now disappeared.

The intensity distribution among the 14 lines which constitute this progression is very peculiar. In the 0'' band either the P(3) line is much too strong or P(4) is much too weak to agree with the 3 to 1 weight ratio. Of

course P (3) might be a blend but we have no grounds for suspecting it. In fact the evidence is rather to the contrary as there is only one unclassified line within 100 wave-numbers of it with strength greater than (1) on the scale of Gale, Monk and Lee. The intensity of this line 4605·364 (2) is given by Kapuscinski and Eymers as 4·5 and is much less than 1/3 of the surplus strength in P (3). Moreover in the 1'' band the R (1) line is missing although the strength of P (3) requires that it should be present. On the other hand the R (1) line appears in the 2'' band, in which every other line fails, and in about the strength which it was expected to have in the 1'' band where it is absent. This is something like the behaviour of the 2' progression of $^{10}\text{O} \rightarrow 2\ ^{18}\text{S}$ where the R (1) line of the 0'' progression was missing, the R (1) line of the 1'' progression abnormally strong and the R (2) and P (4) lines all absent. Here the R (1) line of the 1'' band is absent, the R (1) line of the 2'' band is too strong, the P (4) lines are too weak and the R (2) lines are missing.

§ 16. *The Progression starting from $\lambda = 4142\cdot801$.*

The lines of this progression preceded by Kapuscinski and Eymers' intensity measures and followed by Gale, Monk and Lee's eye estimates are set out in Table XXXV. This is a well-defined, although not very strong, progression and is remarkable for the fact that it has no lines which end on values of $m'' < 4$ (or $j'' < 3\frac{1}{2}$). It seems likely that the bands consist only of Q branches since we can find no evidence of the corresponding R branches if they are P, or P branches if they are R and it is unlikely that such a well-defined progression would consist only of unaccompanied P or R branches. However, this likelihood is diminished owing to the existence of a progression having a good deal of similarity to this which is described in § 17.

The properties on the assumption that the branches are Q are set out in Table XXXVI. If the branches were P the j values would all have to be reduced by 1, if they were R the j values would all have to be increased by 1. The energy level intervals are very nearly in the proportion 1 : 2 : 3 which is what would be given by $B(j - \epsilon)^2$ with $\epsilon = 3$ with the j values necessary for the interpretation of the lines as Q branches. This, however, could only be correct if σ were in the neighbourhood of zero and the 3 missing levels of this initial state suggest $\sigma = 3$. Accordingly two alternative interpretations are given in the table. Assuming $\sigma = 3$ and using $F(j) = B(\sqrt{j^2 - \sigma^2} - \epsilon)^2$ we obtain $2B$ for j small = about 52, the corresponding $I = 1\cdot06 \times 10^{-40}$, $\epsilon = 1\cdot69$ or say $1\frac{1}{2}$ and $\nu_0 = 24367$. If on the other hand we take $\sigma = 0$ we find $2B$ for j small = about 75, the corresponding $I = 7\cdot4 \times 10^{-41}$, $\epsilon = 3$ or

Table XXXVI.

Initial vibration state.	Probably 0' or 1'.
	j if Q lines ↓
F (7) — F (6)	a $6\frac{1}{2}$ 219·53
F (6) — F (5)	s $5\frac{1}{2}$ 149·21
F (5) — F (4)	a $4\frac{1}{2}$ 70·07
	s $3\frac{1}{2}$ 70·32
2B for j small	About 52 or about 75.
1 for j small	About $10\cdot6 \times 10^{-41}$ or about $7\cdot4 \times 10^{-41}$.
ϵ if Q lines	About $1\frac{1}{2}$ or about 3.
σ	About 3 or about 0.
ν_0 if Q lines	24367 or 24358.

thereabouts and $\nu_0 = 24358$. Each of these alternatives would, of course, require a corresponding modification if the branches should prove to be P or R instead of Q.

There is good evidence that the weight ratio 3 to 1 for a to s states holds for these bands. In the upper part of Table XXXVII are set out $1\frac{1}{2}$ times the sum of Kapuscinski and Eymers' intensities of P, R or Q (4) and (6) lines against the intervening P, R or Q (5) and $1/6$ the sum of similar data for P, R or Q (5) and (7) against the intervening Q (6). The disparity between the pairs of numbers compared is about what is to be expected if the maximum intensity, if there were no alternation (*i.e.*, if the weight ratio were 1:1), occurred at $m = 6$, which is a reasonable position for it; except that in $n'' = 3$ Q (4) + Q (6) are too high compared with Q (5). This is due to Q (4) being too high which is satisfactory because this line 20314·59 (2) also has to do duty as ${}_3\alpha_2$ P (2) in the orthohelium like bands.*

This progression possesses the property of alternation of intensity of the bands as a whole with final vibration number which is a feature of ${}^1K \rightarrow {}^2S$ and most of the systems which have followed it in this account. This is shown by the figures in the bottom row of Table XXXVII which give the sums of Gale, Monk and Lee's eye estimates for all the lines in the band having the final vibration number lying immediately above it. In this

* Richardson and Das, 'Roy. Soc. Proc.,' A, vol. 122, p. 694 (1929).

Table XXXVII.

$n'' \rightarrow$	0.	2.	3.		0.	1.	2.	3.
$1\frac{1}{2} \Sigma \begin{matrix} P \\ \text{or } R \end{matrix} \begin{matrix} Q(4) \\ \text{or } R \end{matrix} + \begin{matrix} P \\ \text{or } R \end{matrix} \begin{matrix} Q(6) \\ \text{or } R \end{matrix}$	34.7	25.4	21.0	$\frac{1}{2} \Sigma \begin{matrix} P \\ \text{or } R \end{matrix} \begin{matrix} Q(5) \\ \text{or } R \end{matrix} + \begin{matrix} P \\ \text{or } R \end{matrix} \begin{matrix} Q(7) \\ \text{or } R \end{matrix}$	11.1	1.7	6.6	3.6
P, Q or R (5)	31.1	19.4	11.2	P, Q or R (6)	17.2	2.2	10.5	6.4

$n'' \rightarrow$	0	1	2	3	4	5	6
Σ^2	$9\frac{1}{2}$	$2\frac{1}{2}$	8	$4\frac{1}{2}$	$1\frac{1}{2}$	$7\frac{1}{2}$	1

summation (0) is given the value $\frac{1}{2}$ and (00) the value ($\frac{1}{4}$). Evidently there are maxima of intensity at $n'' = 0, 2 +$, and 5 and minima at $n'' = 1$ and 4. The fact that the strongest band of all is the one with $n'' = 0$ makes it pretty certain that its initial vibration state is either $n' = 0$ or $n' = 1$. It is just possible that it might be the $n' = 1$ progression of $^1Q \rightarrow 2^1S$, but the fact that, on any hypothesis, the lowest rotational state has $j > 1\frac{1}{2}$ is difficult to reconcile with this view. On the whole it seems most likely that it is a $0'$ progression of an entirely new system.

§ 17. The Progression starting from 4097.433 (3).

Superficially this is very like the one just described and they lie close together in the spectrum. They also appear to consist of single branches. On the assumption that they are R we have looked for the corresponding P lines and on the assumption that they are P for the corresponding R lines, but without finding anything definite enough to support either assumption. Accordingly we shall describe them provisionally as Q branches. This involves making them belong to a different system from the progression just described which starts from $\lambda = 4142.801$, if that is also made to consist of Q branches. We are not really satisfied with this arrangement. These two progressions have so much in common that we think it is not unlikely that they are really different branches of the same bands. The lowest final rotational level in the present progression is $m'' = 3$ or $j'' = 2\frac{1}{2}$ as against $m'' = 4$ or $j'' = 3\frac{1}{2}$ in the one starting from 4142.801. This suggests that the two may be related as P and Q or Q and R. If the present is Q, then 4142.801 would be P, if on the other hand it is R, then 4142.801 would be Q. The wave-numbers of the lines,

preceded by Kapuscinski and Eymers' intensities and followed by Gale, Monk and Lee's, are set out in Table XXXVIII.

Table XXXVIII.

$m \quad n'' \rightarrow$ \downarrow	0.	1.	2.	3.	4.
1					
2					
3	32.7 24398.66 (3)	5.9 23086.09 (1)	9.3 21809.48 (2)	20566.99 (0)	19357.95 (0a)
4	10.0 24479.87 (1)	23172.98 (0a)	21901.17 (1)		
5	33.7 24580.27 (1)	3.3 23280.55 (1)	9.0 22014.85 (2)	20782.31 (0a)	
6	8 24696.90 (1)	23406.11 (0a)	9.3 22147.95 (3)	20922.09 (0)F	19728.21 (5)

The properties of the initial level are collected in Table XXXIX. The j values are assigned on the assumption that the branches are Q and all the values of B, I, ϵ , σ and ν_0 are also based on this assumption. If the branches

Table XXXIX.

Initial vibration state.	Probably 0 or 1.
	j if Q lines \downarrow
F (7) -- F (6)	$a \quad 6\frac{1}{2}$ 354.04
F (6) -- F (5)	$s \quad 5\frac{1}{2}$ 303.50
F (5) -- F (4)	$a \quad 4\frac{1}{2}$ 252.08
F (4) -- F (3)	$s \quad 3\frac{1}{2}$ 196.27
	$a \quad 2\frac{1}{2}$
3B for j small	58
2B for j large	50
I for j small	$9.5_s \times 10^{-41}$
I for j large	1.11×10^{-40}
ϵ	-0.24
σ	2
ν_0	24430

are R the j values will all be raised 1, and if they are P they will be lowered 1, and corresponding alterations will be required in the values of B , I , ϵ , σ and ν_0 . The values in the table have been obtained as follows. The value $\sigma = 2$ is assumed in order to account for the absence of the levels $j = \frac{1}{2}$ and $j = 1\frac{1}{2}$. We then apply the formula $F(j) = B\{\sqrt{j^2 - \sigma^2} - \epsilon\}^2$ with $\sigma = 2$ to the three lowest levels, the j values, of course, being determined by the assumption that the branches are Q and the known j values of the final levels. The two lowest energy intervals give $2B = 58.9$ or say 58 and $\epsilon = -0.24$. These data enable $F'(2\frac{1}{2})$ to be calculated; its value is 89 and if $Q(3) = 24398.66 = \nu_0 + F'(2\frac{1}{2}) - F(2\frac{1}{2})$ we find $\nu_0 = 24430$ since $F''(2\frac{1}{2}) = 121.01$.

We regard the theoretical treatment both of this and the preceding progression as very provisional and hope to return to the matter in a subsequent communication.

There is good evidence that the weight ratio 3 to 1 for the alternate rotational levels holds in these bands. Thus in the strongest band which ends on the $0''$ vibrational level we have, using Kapuscinski and Eymers' intensity measures

$$\frac{1}{8} \left\{ \begin{array}{c} \text{P} \\ \text{Q}(3) + \text{or} \\ \text{R} \end{array} \begin{array}{c} \text{P} \\ \text{Q}(5) \\ \text{R} \end{array} \right\} = 11.1 \text{ whereas the intervening } m'' = 4 \text{ line has}$$

$$\text{intensity } 10.9 \text{ and } 1\frac{1}{2} \text{ times } \left\{ \begin{array}{c} \text{P} \\ \text{Q}(4) + \text{or} \\ \text{R} \end{array} \begin{array}{c} \text{P} \\ \text{Q}(6) \\ \text{R} \end{array} \right\} = 28.4 \text{ whereas the intervening } m = 5 \text{ line has intensity } 33.7.$$

The intensity distribution is similar to that of the progression which starts at $\lambda = 4142.801$. The maximum strength is in the $0''$ band, there is then a minimum at $1''$ followed by a second smaller maximum at about $2''$. The main difference is that the $5''$ band completely fails in this progression whereas it is a well defined band which gives rise to a third maximum in 4142.801 . The fact that the maximum intensity in this progression is in the band which ends in $0''$ makes it fairly certain that the vibration number of the initial state is either 0 or 1. Most of the strength of the $n'' = 4$, $m'' = 6$ line $19728.21(5)$ belongs to another system.

§ 18. The Infra-red System.

It is probable that there is a great deal more of this system beyond the present limit of the infra-red measurements. It is obviously a very important system as the fragment which we have contains all the very strong lines that have been measured in the infra-red and it maintains its strength in almost

every direction right up to the limit of the infra-red measurements. The very strong lines lie in three bands of two progressions whose $n'' = 0$ R (1) lines are at $\nu = 13402.1$ and 15211.77 respectively. There is a weaker progression whose $n'' = 0$ R (1) line would be at $\nu = 17246.14$ if it existed and the last line but six and the last line but one of Gale, Monk and Lee's tables are in about the right position and have the correct separation for the R (1) and P (3) lines of the $n'' = 0$ band of a lower progression which should thus start with its $n'' = 0$ R (1) line at $\nu = 11350.5$. The frequencies of the lines of the bands followed by Gale, Monk and Lee's eye estimates and preceded by Kapuscinski and Eymers' measurements of the intensities, when such exist, are set out in Table XL.

The four progressions have been assigned, for reasons which will appear later, the initial vibration number 1 ?, 2 ?, 3 ? and 4 ?. Whether the first number should be 1 is very problematical, but 2 and 3 are obviously two pro-

Table XL.

n' ↓	m ↓	$n'' \rightarrow$	0.	1.	2.	3.	4.
1?	1	R	11350.5 (1a)				
	3	P	11234.3 (0c)				
2?	1	{ R P	13402.1 (4)	12083.8 (8)			
	2	{ R P	13447.8 (2a) 13317.3 (3)	12131.5 (3) 12000.9 (7)			
	3	{ R P	13470.4 (1) 13286.0 (9)	12157.8 (2) 11973.5 (10)			
	4	{ R P	 13255.5 (2a)	12189.5 (0) 11948.6 (3)			
	5	{ R P	 13203.6 (1a)	 11904.0 (3)			
	6	{ R P	 13157.7 (1)	 11866.8 (00)			
	7	{ R P	 13115.2 (1)	 11834.3 (000)			

Table XL—(continued).

n' ↓	m ↓	$n'' \rightarrow$	0.	1.	2.	3.	4.
3?	1	$\begin{cases} R \\ P \end{cases}$	15211.77 (3a)	13893.4 (9)	12612.1 (00)		
	2	$\begin{cases} R \\ P \end{cases}$	[H α] 15142.64 (2)	13915.3 (2) 13826.2 (4)			
	3	$\begin{cases} R \\ P \end{cases}$	15237.22 (2) 15095.67 (4)	13924.7 (3a) 13783.1 (10)	12506.6 (0b)		
	4	$\begin{cases} R \\ P \end{cases}$	15039.34 (2)	13732.4 (2a)	12460.6 (00b)		
	5	$\begin{cases} R \\ P \end{cases}$	14970.53 (2)	13670.9 (2)			
	6	$\begin{cases} R \\ P \end{cases}$	14885.15 (1a)	13594.3 (1)			
	1	$\begin{cases} R \\ P \end{cases}$	[17246.14]	15927.80 (1)	14646.38 (2)		
	2	$\begin{cases} R \\ P \end{cases}$					
	3	$\begin{cases} R \\ P \end{cases}$	[17245.71] 45.2 17129.89 (8) ?	15933.16 (0a) 13.9 15817.47 (3)	14656.57 (0) 14540.88 (3a)	[13298.44]	12089.5 (00)
	4	$\begin{cases} R \\ P \end{cases}$	15.0 17047.15 (4) ?	15740.49 (1)	14468.48 (1a)		
4?	5	$\begin{cases} R \\ P \end{cases}$	28.0 16978.52*(10) ?	9.5 15679.29 (1)	14413.75 (1)		

gressions with consecutive initial vibration numbers and if 1 and 4 are real and belong to the same system they must have initial vibration numbers less and greater by 1 than 2 and 3 respectively. Thus if n' is the initial vibration number assigned to the progression starting with $n'' = 0$ $R(1) = 13402.1$ the others must be $n' - 1$, $n' + 1$ and $n' + 2$ respectively. In spite of the strength of the P (m) lines we do not feel very convinced of the reality of the $4' \rightarrow 0''$ band. The entire failure of the R (m) lines is suspicious. 17129.89

has a defect of 0.13 wave-number and 16978.52 has the quite inadmissible defect of 0.45. This is especially strange as this line was measured by Gale, Monk and Lee on the interferometer. The intensities are about in the right proportion for P (3), P (4) and P (5) lines of a band, which does not favour the idea of a perturbation. 16978.52 shows the Zeeman effect and probably 17129.89 also does. This is uncertain, as this line is not resolved from 17130.78 by Merton and Barratt and probably would also not be resolved by Croze. On the whole we are inclined to attribute these three P (m) lines of $4' \rightarrow 0''$ to some other system. The line 15740.49, P (4) of $4' \rightarrow 1''$ has a defect of 0.28, but this is not unreasonable as it is also claimed by ${}_3\alpha_3$ Q (4) of the orthohelium like bands. The value is about right for ${}_3\alpha_3$ Q (4) to which therefore 15740.49 should be given; it may, however, be concealing the line of the present bands.

The properties, etc., of the system are set out in Table XLI. The bands have P and R but no Q branches. In the strong $2' \rightarrow n''$ and $3' \rightarrow n''$ progressions P (2) is present, so that the lowest possible j value, viz. $j = \frac{1}{2}$, occurs in the initial state. As the P (m) and R (m) lines are definitely identifiable by their final rotational term differences, this determines the initial j values. These satisfy $\Delta j = 0$ or ± 1 . There are no Q branches, so that $\Delta j = 0$ is excluded. This is because transitions between s and a rotational levels are not allowed. Since there are no other branches such as P', Q' or R' the initial levels must be single. The energy level intervals have a very unusual detailed structure but they are evidently modifications of the type with the intervals approximately in the ratio 1 : 2 : 3, etc. This is most evident at the 3' vibrational level. At the 4' level the type has changed to — 1 : 1 : 3 : 5, etc. It is, of course, possible that this rather weak $4' \rightarrow n''$ progression does not belong to this system but we have no other use for it. Similar changes of type of rotational structure, with increasing vibration number, have been found in some of the systems already described, for example in $3^1\text{C} \rightarrow 2^1\text{S}$. Since the $j = \frac{1}{2}$ initial level is present $\sigma = 0$ and the rotational term structure requires ϵ in the neighbourhood of zero, the terms for j small being approximately of the form Fj^2 , with j semi-integral. From $\text{P}(2) = \nu_0 + F'(\frac{1}{2}) - F''(\frac{1}{2})$ where P (2) occurs and from $\text{R}(1) = \nu_0 + F'(1\frac{1}{2}) - F''(1\frac{1}{2})$ in the other two cases the values of ν_0 can be found since the values of $F'(\frac{1}{2})$ and $F''(1\frac{1}{2})$ are known with precision (see Part I). The resulting accuracy depends on the accuracy with which $F'(\frac{1}{2})$ and $F'(1\frac{1}{2})$ may be estimated. Since $F''(\frac{1}{2}) = 2B \div 8$, even a rough value of B will not introduce much error so that the ν_0 's for the $n' = 2$ and $n' = 3$ progressions should be reliable to one wave-number or

possibly better. In the other two cases only rough values are given owing to the uncertain elements present in the rotational term structure in both cases.

The values of ν_0 thus found are very curious. Their first differences furnish the sequence of numbers 2046, 1826.6 and 2034, and these have the second differences $+219$ and -207 . These numbers for the second difference are large but no larger than some we have met with already, for example in $^1\text{A} \rightarrow 2^1\text{S}$ and in $^1\text{C} \rightarrow 2^1\text{S}$. What is really remarkable about them is the change of sign, as these second differences are usually supposed to be essentially positive, the first differences steadily diminishing as the vibration numbers increase. This result is not due to errors introduced by the uncertain elements which enter into the determination of the ν_0 's. If the ν 's for the R (1) lines, which keep roughly the same distance from the ν_0 's, are taken and treated in the same way an exactly parallel set of figures is obtained. These are shown at the bottom of Table XLI. If we take $2x\omega_0$ to be $+219$ we have ω_0 the frequency at zero amplitude of the initial state of this system $= 2376$ or thereabouts.

We have not drawn an intensity diagram for this system because we think that so much of it lies in the unknown part of the infra-red that it might be misleading. We can, however, say something about the general intensity distribution. In both the $n' = 2$ and $n' = 3$ progressions the $n'' = 1$ band is stronger than the $n'' = 0$ band. These are not features which characterise $n' = 0$ progressions or $n' = 1$ progressions, but they do characterise $n' = 2$ or 3 progressions in these parhelium-like systems (see, for example, the intensity diagrams of ^1A , ^1B and $^1\text{C} \rightarrow 2^1\text{S}$ in Parts I and II). They are therefore in favour of the assigned initial vibrational numbering. This is further confirmed by the fact that in the $n' = 2$ progression the $n'' = 1$ band is only slightly stronger than the $n'' = 0$ band, whereas it is much stronger in the $n' = 3$ progression and in the $n' = 4$ progression the maximum of intensity appears to have moved still further to the right in Table XL (if we disregard the strong P lines in the $0''$ band of this progression, the inclusion of which is almost certainly wrong).

There is evidence that the 3 to 1 weight ratio of successive rotational states holds in this system, but it is not so precise as in the other systems as most of the system is beyond the long wave limit of Kapuscinski and Eymers' measurements. For example, in the $n' = 3$ progression we find in the $n'' = 0$ band R (1) has intensity (3) R (2) is absent, whilst R (3) has intensity (2) and in the $n'' = 1$ band R (1) = (9), R (2) = (2) and R (3) = (3) according to Gale, Monk and Lee's eye estimates. The strong lines are those which end on the

levels with m odd, *i.e.*, those which come from $j = 1\frac{1}{2}, 3\frac{1}{2}$, throughout the system.

There is one further peculiar fact about this system. It lies almost exactly where we should expect to find the bands which arise from the transitions from the C to the B states of Dicke and Hopfield. The position of these can be found as follows :—

From the data given by Hori* we can find the wave numbers of the lines which would correspond in the $C \rightarrow B$ system to any set of lines such as the R (1) lines in our infra-red system. In the Lyman bands the line Hori calls Q (1) which is really a P (1) line goes from the rotational level denoted by a and $j = \frac{1}{2}$ of the B electronic levels to that denoted by a and $j = 1\frac{1}{2}$ of A (see fig. 11). In the Werner bands the line Hori calls Q (1) goes from the level denoted by a and $j = 1\frac{1}{2}$ of C to that denoted by a and $j = 1\frac{1}{2}$ of A. The difference of these transitions should go from the level a and $j = 1\frac{1}{2}$ of C to the level a and $j = \frac{1}{2}$ of B. This would correspond to the line we call R (1) in our infra-red system. In Hori's tabulation of the Werner bands there are no bands which end on the vibrationless state ($n'' = 0$) of A. Accordingly we start with the Q (1), really P (1), line of the Lyman band which goes from $n' = 3$ of B to $n'' = 1$ of A. The wave-number of this is $\nu = 89764$. This line starts from the $j = \frac{1}{2}$ level of our final levels. The first three of our final vibrational differences (Part I, Table IV) for this level are 1318.34_5 , 1281.47_5 and 1246.71_5 and their sum is 3846.53_5 . If we subtract this from 89764 we get 85917 which is therefore the wave-number of the P (1) line of the $0' \rightarrow 1''$ band of the $B \rightarrow A$ system. Now the Q (1) line of the $0' \rightarrow 1''$ band of the $C \rightarrow A$ system has $\nu = 94860$. These two lines have the same final state, namely, a and $j = 1\frac{1}{2}$, $n'' = 1$ of A. Subtracting them we get 8943 as the frequency of the line which starts on the level a and $j = 1\frac{1}{2}$ and ends on a and $j = \frac{1}{2}$ in the $0' \rightarrow 0''$ band of the $C \rightarrow B$ system. This is the (R 1) line of that system. These R (1) lines have the same initial states as Hori's Q (1) lines of the $A \rightarrow C$ system. We have determined the average values of the vibrational intervals for Hori's Q (1) lines for the C levels as follows, using Hori's tabulated wave-numbers :— $C_1 - C_0 = 2308$, $C_2 - C_1 = 2167$, $C_3 - C_2 = 2045$ and $C_4 - C_3 = 1907$. The R (1) lines of the $C \rightarrow B$ system will have the same intervals as these and accordingly starting from 8943 we get the wave-numbers of the various R (1) lines of $C \rightarrow B$ shown in Table XL where they are set over the corresponding lines of this infra-red system.

The most serious misfit is at the $3' \rightarrow 0''$ transition where the present data

* 'Z. Physik,' vol. 44, p. 846 (1927).

Table XLII.

$\pi \rightarrow$	0.	1.	2.	3.	4.
$\pi \rightarrow 0'' R(1)$ lines of $C \rightarrow B$	8943	11251	13418	15463	17370
$\pi \rightarrow 0'' R'_2(1)$ lines of infra-red system		11350.5	13402.1	15211.77	[17246.14]

are most certain. The present initial level has, however, quite different properties from those which Hori finds for Dieke and Hopfield's C level. The $j = \frac{1}{2}$ rotational level is present and all the levels are single, whereas Hori has $j = \frac{1}{2}$ absent and all the levels are double. The present rotational structure is what would occur if only transitions from the levels from which Hori's Q lines come were allowed, but there is no known exclusion principle which would stop transitions from the other levels; we should in fact get Q' branches in

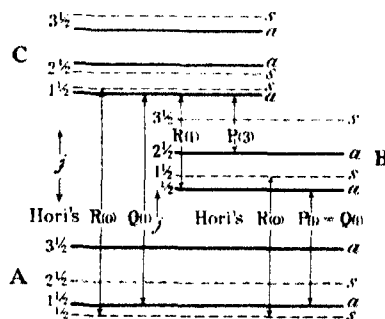


FIG. 11.

the present system. These have been looked for without success. Also his values of B (or B') are larger than ours and have a beautiful regularity which we do not find. It is a most remarkable fact that two such levels, one alone present in the ultra-violet, the other alone present in the infra-red spectrum, both presumably electronic 2 levels, should lie so close together. It is quite impossible to reconcile Hori's analysis with the properties we find. If the states are not different, then Hori's analysis is quite wrong, and this we are loath to believe.

Stress Systems in an Infinite Strip.

By R. C. J. HOWLAND, M.A., M.Sc., University College, London.

(Communicated by L. N. G. Filon, F.R.S.—Received November 28, 1928.)

The problem of determining the stresses and displacements in a rectangular strip of elastic material whose long edges are acted upon by any system of tractions was attacked by Filon,* who gave a solution which is almost complete if the breadth of the strip is small compared with its length. The problem was treated as one of "generalised plane stress,"† i.e., the stresses and displacements considered were means taken with respect to the thickness. It was found possible to express these mean stresses and displacements by series so that the boundary conditions over the long edges were completely satisfied while the *total* forces and couples over the short edges could be adjusted. In the limiting case of an infinitely long strip the series were replaced by integrals which proved in many cases more convenient for calculation.

The cognate problem of finding the stresses and displacement produced by forces acting within the strip instead of on its edges appears to have received but little attention. An attempt to find the solution for an isolated force acting at a central point and in the direction of the length of the strip was recently made by E. Melan,‡ but he was unable to satisfy the boundary conditions without introducing shears on the edges.

In the present paper a satisfactory solution is given for the much more general problem of a force, either longitudinal or transverse, acting at any point of the strip. The stresses due to any distribution of force over the strip may be deduced by integration.

The method used is essentially that of Prof. Filon, whose results are first expressed in a compact and convenient form which he has himself suggested. The solutions are obtained by the use of the stress function while the strip is, from the start, regarded as of infinite length so that Fourier integrals are used instead of Fourier series. The stress function corresponding to an isolated force is then written down as if the elastic plate were unbounded in all directions and the resulting stresses along the edges of the strip are annulled by Filon's method.

* 'Phil. Trans.,' A, vol. 201, pp. 63–155 (1903).

† The term is due to Love, 'Theory of Elasticity,' 4th ed. (Cambridge, 1927), p. 138.

‡ 'Z. angew. Math.,' vol. 5, pp. 314–318 (1925).

Fundamental Formulæ.

We consider an infinite plane strip of elastic material, isotropic and uniform and of constant thickness. We take axes of x and y in a plane parallel to the faces of the strip and placed so that the boundaries of the strip are represented by the lines $y = \pm b$. We suppose a system of generalised plane stress produced by forces acting upon the edges of the strip. Then the mean stresses are given by

$$\left. \begin{aligned} \bar{x}\bar{x} &= \frac{\partial^2 \chi}{\partial y^2}, & \bar{y}\bar{y} &= \frac{\partial^2 \chi}{\partial x^2} \\ \bar{x}\bar{y} &= -\frac{\partial^2 \chi}{\partial x \partial y} \end{aligned} \right\}, \quad (1)$$

where χ is a stress function satisfying the equation

$$\nabla^4 \chi = 0, \quad (2)$$

and the boundary conditions.

The mean displacements \bar{u} and \bar{v} are to be found from

$$\left. \begin{aligned} 2\mu\bar{u} &= -\frac{\partial \chi}{\partial x} + (1-\sigma)\frac{\partial \psi}{\partial y} \\ 2\mu\bar{v} &= -\frac{\partial \chi}{\partial y} + (1-\sigma)\frac{\partial \psi}{\partial x} \end{aligned} \right\}, \quad (3)$$

where μ is the Modulus of Rigidity, σ is the modified form of Poisson's Ratio which appears in the theory of Generalised Plane Stress, while ψ is to be found from the equation

$$\frac{\partial^2 \psi}{\partial x \partial y} = \nabla^2 \chi, \quad (4)$$

with the additional restriction that

$$\nabla^2 \psi = 0. \quad (5)$$

We proceed to construct eight special forms of stress function from which can be built up a solution satisfying arbitrary boundary conditions of normal stress and shear.

Consider first the function

$$\chi_1 = (Ay \sinh my + B \cosh my) \cos mx,$$

which is even in both x and y and is a solution of (2). It will satisfy the conditions for zero shear on the edges $y = \pm b$ if

$$A (\sinh mb + mb \cosh mb) + Bm \sinh mb = 0.$$

Hence, C being any constant, we may write

$$\chi_1 = C[(\sinh mb + mb \cosh mb) \cosh my - my \sinh mb \sinh my] \cos mx.$$

This holds for all values of m so that, provided that the integral converges, a more general solution is

$$\chi_1 = \int_0^\infty [(\sinh mb + mb \cosh mb) \cosh my - my \sinh mb \sinh my] \cos mx f(m) dm. \quad (6)$$

To obtain a given distribution of normal force over the boundaries $y = \pm b$, we have to make

$$\frac{\partial^2 \chi_1}{\partial x^2} = \phi_1(x), \quad y = \pm b.$$

$\phi_1(x)$ being a specified function. This requires that

$$\phi_1(x) = -\frac{1}{2} \int_0^\infty m^2 (\sinh 2mb + 2mb) f(m) \cos mx dm, \quad (7)$$

which is an integral equation to determine $f(m)$.

Now, for even functions, we have the reciprocal integral equations

$$\left. \begin{aligned} \phi_1(x) &= \sqrt{\frac{2}{\pi}} \int_0^\infty F(m) \cos mx dm \\ F(m) &= \sqrt{\frac{2}{\pi}} \int_0^\infty \phi_1(x) \cos mx dx \end{aligned} \right\}. \quad (8)$$

If in these we put

$$F(m) = -\frac{1}{2} \sqrt{\frac{\pi}{2}} m^2 (\sinh 2mb + 2mb) f(m), \quad (9)$$

the value of $f(m)$ is given as

$$f(m) = -\frac{4}{\pi m^2 \sinh 2mb + 2mb} \int_0^\infty \phi_1(x) \cos mx dx. \quad (10)$$

Substitution in (6) gives the required value of χ_1 . In writing down this and subsequent formulæ it will be convenient to use the following abridged notation

$$\left. \begin{aligned} s &= \sinh mb, & c &= \cosh mb \\ S &= \sinh my, & C &= \cosh my \\ \Sigma &= \sinh 2mb + 2mb \\ \Sigma' &= \sinh 2mb - 2mb \end{aligned} \right\}. \quad (11)$$

The solution may now be written

$$\chi_1 = \frac{4}{\pi} \int_0^\infty \frac{mysS - (s + mbc)C}{m^2 \Sigma} \cos mx dm \int_0^\infty \phi_1(u) \cos mu du. \quad (12)$$

Leaving aside, for the moment, all questions of convergence, we proceed to find formulæ for the displacements. Provided that we may differentiate under the integral sign, we have

$$\nabla^2 \chi_1 = \frac{8}{\pi} \int_0^\infty \frac{sC}{\Sigma} \cos mx \, dm \int_0^\infty \phi_1(u) \cos mu \, du.$$

and a solution of (4) is

$$\psi = \frac{8}{\pi} \int_0^\infty \frac{sS}{m^2 \Sigma} \sin mx \, dm \int_0^\infty \phi_1(u) \cos mu \, du.$$

As this is a harmonic function, it is the value of ψ required. We then find from (3)

$$\left. \begin{aligned} 2\mu \bar{u}_1 &= \frac{4}{\pi} \int_0^\infty \frac{mysS + \{(1-2\sigma)s - mbc\}C}{m\Sigma} \sin mx \, dm \int_0^\infty \phi_1(u) \cos mu \, du \\ 2\mu \bar{v}_1 &= \frac{4}{\pi} \int_0^\infty \frac{\{2(1-\sigma)s + mbc\}S - mysC}{m\Sigma} \cos mx \, dm \int_0^\infty \phi_1(u) \cos mu \, du \end{aligned} \right\} \quad (13)$$

Proceeding in this way, we find the following eight solutions, of which the first is the one already obtained and is repeated to make the list complete:—

I.— χ is even in x and even in y .

$$(a) \quad \widehat{xy} = 0, \quad \widehat{yy} = \phi_1(x) \quad \text{when } y = \pm b.$$

$$\left. \begin{aligned} \chi_1 &= \frac{4}{\pi} \int_0^\infty \frac{mysS - (s + mbc)C}{m^2 \Sigma} \cos mx \, dm \int_0^\infty \phi_1(u) \cos mu \, du \\ 2\mu \bar{u}_1 &= \frac{4}{\pi} \int_0^\infty \frac{mysS + \{(1-2\sigma)s - mbc\}C}{m\Sigma} \sin mx \, dm \int_0^\infty \phi_1(u) \cos mu \, du \\ 2\mu \bar{v}_1 &= \frac{4}{\pi} \int_0^\infty \frac{\{2(1-\sigma)s + mbc\}S - mysC}{m\Sigma} \cos mx \, dm \int_0^\infty \phi_1(u) \cos mu \, du \end{aligned} \right\} \quad (14)$$

$$(b) \quad \begin{aligned} \widehat{yy} &= 0, & \widehat{xy} &= \psi_2(x) \quad \text{when } y = b; \\ \widehat{yy} &= 0, & \widehat{xy} &= -\psi_2(x) \quad \text{when } y = -b. \end{aligned}$$

$$\left. \begin{aligned} \chi_2 &= \frac{4}{\pi} \int_0^\infty \frac{ycS - bsC}{m\Sigma} \cos mx \, dm \int_0^\infty \psi_2(u) \sin mu \, du \\ 2\mu \bar{u}_2 &= \frac{4}{\pi} \int_0^\infty \frac{\{2(1-\sigma)c + mbs\}C + mycS}{m\Sigma} \sin mx \, dm \int_0^\infty \psi_2(u) \sin mu \, du \\ 2\mu \bar{v}_2 &= \frac{4}{\pi} \int_0^\infty \frac{\{(1-2\sigma)c + mbs\}S - mycC}{m\Sigma} \cos mx \, dm \int_0^\infty \psi_2(u) \sin mu \, du \end{aligned} \right\} \quad (15)$$

II.— χ is even in x but odd in y .

$$(a) \quad \begin{aligned} \widehat{xy} &= 0, \quad \widehat{yy} = \phi_3(x), \quad \text{when } y = b; \\ \widehat{xy} &= 0, \quad \widehat{yy} = -\phi_3(x), \quad \text{when } y = -b. \end{aligned}$$

$$\left. \begin{aligned} \chi_3 &= \frac{4}{\pi} \int_0^\infty \frac{mycC - (c + mbs)S}{m^2\Sigma'} \cos mx \cdot dm \int_0^\infty \phi_3(u) \cos mu \cdot du \\ 2\mu\bar{u}_3 &= \frac{4}{\pi} \int_0^\infty \frac{\{(1-2\sigma)c - mbs\}S + mycC}{m\Sigma'} \sin mx \cdot dm \int_0^\infty \phi_3(u) \cos mu \cdot du \\ 2\mu\bar{v}_3 &= \frac{4}{\pi} \int_0^\infty \frac{\{2(1-\sigma)c + mbs\}C - mycS}{m\Sigma'} \cos mx \cdot dm \int_0^\infty \phi_3(u) \cos mu \cdot du \end{aligned} \right\} (16)$$

$$(b) \quad \widehat{xy} = \psi_4(x), \quad \widehat{yy} = 0, \quad \text{when } y = \pm b.$$

$$\left. \begin{aligned} \chi_4 &= \frac{4}{\pi} \int_0^\infty \frac{ysC - bcS}{m\Sigma'} \cos mx \cdot dm \int_0^\infty \psi_4(u) \sin mu \cdot du \\ 2\mu\bar{u}_4 &= \frac{4}{\pi} \int_0^\infty \frac{\{2(1-\sigma)s - mbc\}S + mysC}{m\Sigma'} \sin mx \cdot dm \int_0^\infty \psi_4(u) \sin mu \cdot du \\ 2\mu\bar{v}_4 &= \frac{4}{\pi} \int_0^\infty \frac{\{(1-2\sigma)s + mbc\}C - mysS}{m\Sigma'} \cos mx \cdot dm \int_0^\infty \psi_4(u) \sin mu \cdot du \end{aligned} \right\} (17)$$

III.— χ is odd in x but even in y .

$$(a) \quad \widehat{xy} = 0, \quad \widehat{yy} = \phi_5(x), \quad \text{when } y = \pm b.$$

$$\left. \begin{aligned} \chi_5 &= \frac{4}{\pi} \int_0^\infty \frac{mysS - (s + mbc)C}{m^2\Sigma} \sin mx \cdot dm \int_0^\infty \phi_5(u) \sin mu \cdot du \\ 2\mu\bar{u}_5 &= \frac{4}{\pi} \int_0^\infty \frac{\{mbc - (1-2\sigma)s\}C - mysS}{m\Sigma} \cos mx \cdot dm \int_0^\infty \phi_5(u) \sin mu \cdot du \\ 2\mu\bar{v}_5 &= \frac{4}{\pi} \int_0^\infty \frac{\{2(1-\sigma)s + mbc\}S - mysC}{m\Sigma} \sin mx \cdot dm \int_0^\infty \phi_5(u) \sin mu \cdot du \end{aligned} \right\} (18)$$

$$(b) \quad \begin{aligned} \widehat{xy} &= \psi_6(x), \quad \widehat{yy} = 0, \quad \text{when } y = b; \\ \widehat{xy} &= -\psi_6(x), \quad \widehat{yy} = 0, \quad \text{when } y = -b. \end{aligned}$$

$$\left. \begin{aligned} \chi_6 &= \frac{4}{\pi} \int_0^\infty \frac{bsC - ycS}{m\Sigma} \sin mx \cdot dm \int_0^\infty \psi_6(u) \cos mu \cdot du \\ 2\mu\bar{u}_6 &= \frac{4}{\pi} \int_0^\infty \frac{\{2(1-\sigma)c - mbs\}C + mycS}{m\Sigma} \cos mx \cdot dm \int_0^\infty \psi_6(u) \cos mu \cdot du \\ 2\mu\bar{v}_6 &= \frac{4}{\pi} \int_0^\infty \frac{mycC - \{(1-2\sigma)c + mbs\}S}{m\Sigma} \sin mx \cdot dm \int_0^\infty \psi_6(u) \cos mu \cdot du \end{aligned} \right\} (19)$$

IV.— χ is odd in both x and y .

$$(a) \quad \begin{aligned} \widehat{xy} &= 0, \quad \widehat{yy} = \phi_7(x), & \text{when } y = b; \\ \widehat{xy} &= 0, \quad \widehat{yy} = -\phi_7(x), & \text{when } y = -b. \end{aligned}$$

$$\left. \begin{aligned} \chi_7 &= \frac{4}{\pi} \int_0^\infty \frac{mycC - (c + mbs)S}{m^2\Sigma'} \sin mx \cdot dm \int_0^\infty \phi_7(u) \sin mu \cdot du \\ 2\mu\bar{u}_7 &= \frac{4}{\pi} \int_0^\infty \frac{\{mbs - (1-2\sigma)c\}S + mycC}{m\Sigma'} \cos mx \cdot dm \int_0^\infty \phi_7(u) \sin mu \cdot du \\ 2\mu\bar{v}_7 &= \frac{4}{\pi} \int_0^\infty \frac{\{2(1-\sigma)c + mbs\}C - mycS}{m\Sigma'} \sin mx \cdot dm \int_0^\infty \phi_7(u) \sin mu \cdot du \end{aligned} \right\} \quad (20)$$

$$(b) \quad \widehat{xy} = \psi_8(x), \quad \widehat{yy} = 0, \quad \text{when } y = \pm b.$$

$$\left. \begin{aligned} \chi_8 &= \frac{4}{\pi} \int_0^\infty \frac{bcS - ysC}{m\Sigma'} \sin mx \cdot dm \int_0^\infty \psi_8(u) \cos mu \cdot du \\ 2\mu\bar{u}_8 &= \frac{4}{\pi} \int_0^\infty \frac{\{2(1-\sigma)s - mbc\}S - mysC}{m\Sigma'} \cos mx \cdot dm \int_0^\infty \psi_8(u) \cos mu \cdot du \\ 2\mu\bar{v}_8 &= \frac{4}{\pi} \int_0^\infty \frac{mysS - \{(1-2\sigma)s + mbc\}C}{m\Sigma'} \sin mx \cdot dm \int_0^\infty \psi_8(u) \cos mu \cdot du \end{aligned} \right\} \quad (21)$$

Suppose now that the upper and lower edges of the strip are acted upon by any arbitrary distributions of normal force and shear, expressed by the equations

$$\left. \begin{aligned} \widehat{yy} &= \alpha(x), & \widehat{xy} &= \beta(x), & y &= b; \\ \widehat{yy} &= \gamma(x), & \widehat{xy} &= \delta(x), & y &= -b \end{aligned} \right\} \quad (22)$$

Then the stress function is given by

$$\chi = \sum_{r=1}^8 \chi_r \quad (23)$$

when the χ_r are given by equations (14) to (21) and

$$\left. \begin{aligned} \phi_1(x) &= \frac{1}{4} \{ \alpha(x) + \alpha(-x) + \gamma(x) + \gamma(-x) \} \\ \phi_2(x) &= \frac{1}{4} \{ \beta(x) - \beta(-x) - \delta(x) + \delta(-x) \} \\ \phi_3(x) &= \frac{1}{4} \{ \alpha(x) + \alpha(-x) - \gamma(x) - \gamma(-x) \} \\ \phi_4(x) &= \frac{1}{4} \{ \beta(x) - \beta(-x) + \delta(x) - \delta(-x) \} \\ \phi_5(x) &= \frac{1}{4} \{ \alpha(x) - \alpha(-x) + \gamma(x) - \gamma(-x) \} \\ \phi_6(x) &= \frac{1}{4} \{ \beta(x) + \beta(-x) - \delta(x) - \delta(-x) \} \\ \phi_7(x) &= \frac{1}{4} \{ \alpha(x) - \alpha(-x) - \gamma(x) + \gamma(-x) \} \\ \phi_8(x) &= \frac{1}{4} \{ \beta(x) + \beta(-x) + \delta(x) + \delta(-x) \} \end{aligned} \right\} \quad (24)$$

The solution is therefore complete provided that all the necessary conditions of convergence are satisfied. These conditions will now be investigated.

The Convergence Problem.

Consider first the integral for χ_1 , equation (14), and suppose that $\phi_1(u)$ is finite and integrable. Then, since $|\cos mu| \leq 1$, $\int_0^\infty \phi_1(u) \cos mu \, du$ will be less in absolute value than $\int_0^\infty |\phi_1(u)| \, du$ for all values of m . If this last integral converges, then when $m \rightarrow \infty$ we have

$$\left| \int_0^\infty \phi_1(u) \cos mu \, du \right| < C, \quad (25)$$

where C is a positive constant. The inequality (25) may be satisfied when $\phi_1(u)$ conforms to less stringent conditions than those stated.

Again, when m is large, we have

$$2s \sim e^{mb}, \quad 2c \sim e^{mb}, \quad 2S \sim e^{mv}, \quad 2C \sim e^{mv}, \quad 2\Sigma \sim e^{2mb}.$$

Hence, apart from a constant factor, the principal part of the integral in χ_1 is less than

$$\left| \frac{e^{m(y-b)}(y-b)}{m} \cos mx \right|,$$

which is less than $\frac{b}{m} e^{m(b'-b)}$ if $y < b'$. The last expression is independent of both x and y and tends exponentially to 0 as $m \rightarrow \infty$. Hence the integral converges at the upper limit, and this convergence is uniform with respect to both x and y .

Passing to the lower limit, we have for the integrand when m is small

$$\frac{1}{\pi} y^2 \int_0^\infty \phi_1(u) \, du + O(m^2)^*$$

which remains finite when $m \rightarrow 0$.

Differentiation under the integral sign with respect to x or y introduces additional powers of m which do not affect the convergence at either limit. It follows that such differentiations are valid and that χ_1 satisfies both the differential equation (2) and the boundary conditions. The validity of the formulæ for \bar{u}_1 and \bar{v}_1 may be established in the same way.

* The notation is that of the Tract, "Orders of Infinity," by G. H. Hardy, 'Cambridge Mathematical Tracts,' No. 12.

In the integrals for the other stress functions the conditions at the upper limits are the same as in χ_1 . Those at the lower limits are sometimes less simple. For the purpose of the present problem, a complete investigation is not necessary, but some general remarks will be of assistance in dealing with the special cases.

Consider, for example, χ_2 . When m is small, this may be written

$$\chi_2 = \frac{4}{\pi} \int_0^\infty \left\{ \frac{y^2 - b^2}{4mb} + 0(m) \right\} dm \int_0^\infty \psi_2(u) \sin mu \cdot du,$$

and there is not convergence unless the second integral is $0(m)$. This will, however, clearly be so if $\psi_2(u)$ is zero for sufficiently large values of u , or if it tends to zero sufficiently fast when $u \rightarrow \infty$. χ_2 will then be convergent, and it is easy to verify that the corresponding integrals for the stresses and displacements will also converge.

Similarly in χ_3 we have, when m is small

$$\chi_3 = \frac{4}{\pi} \int_0^\infty \left\{ \frac{3}{4m^2b^3} y \left(\frac{1}{2}y^2 - b^2 \right) + 0(1) \right\} dm \int_0^\infty \phi_3(u) \cos mu \cdot du,$$

and there will be convergence only if

$$\int_0^\infty \phi_3(u) du = 0,$$

i.e., if the forces applied to the boundaries are self-equilibrating. It is easy to see the meaning of this condition, for the stress function

$$\frac{3}{4b^3} y \left(\frac{1}{2}y^2 - b^2 \right)$$

corresponds to a unit bending moment across every section of the beam, so that the lack of convergence is an expression of the fact that unbalanced transverse forces would lead to transverse reactions at infinity and thus to an infinite bending moment. The convergence will be restored if the strip is supported at a finite distance.

It should, however, be observed that the terms producing the divergence may be removed from the integrand, provided that this removal does not produce divergence at the upper limit. For they are themselves solutions of (2) and correspond to stress-systems which do not violate the boundary conditions.

The other five stress functions do not show any essentially new features. χ_4 and χ_7 converge under the same conditions as χ_2 ; χ_6 and χ_5 converge

conditionally ; while the non-convergent part of χ_6 is trivial, as it disappears in the formulæ for the stresses.

Further discussion of the convergence and of its relation to the stresses at infinity will be reserved for the special problems that follow.

Solution for an Isolated Longitudinal Force.

Suppose now that a force P acts at the point $(0, \eta)$ in a direction parallel to the positive direction of the x -axis. If the plate extended to infinity in all directions, the solution would be*

$$\left. \begin{aligned} \chi_0 &= \frac{P}{4\pi} \left[\frac{1-2\sigma}{1-\sigma} x \log r - 2(y-\eta) \theta \right] \\ r &= \sqrt{x^2 + (y-\eta)^2}, \quad \tan \theta = \frac{y-\eta}{x} \end{aligned} \right\} \quad (25)$$

where

The corresponding stresses are

$$\left. \begin{aligned} \widehat{xx} &= \frac{P}{4\pi} \frac{x}{r^2} \left[\frac{2}{1-\sigma} \cdot \frac{(y-\eta)^2}{r^2} - \frac{3-2\sigma}{1-\sigma} \right] \\ \widehat{yy} &= \frac{P}{4\pi} \frac{x}{r^2} \left[\frac{1-2\sigma}{1-\sigma} - \frac{2}{1-\sigma} \cdot \frac{(y-\eta)^2}{r^2} \right] \\ \widehat{xy} &= -\frac{P}{4\pi} \frac{y-\eta}{r^2} \left[\frac{1-2\sigma}{1-\sigma} + \frac{2}{1-\sigma} \frac{x^2}{r^2} \right] \end{aligned} \right\} \quad (26)$$

To annul the stresses \widehat{yy} , \widehat{xy} along the lines $y = \pm b$, and so obtain the solution for the strip, we now write

$$\chi = \chi_0 + \chi_5 + \chi_6 + \chi_7 + \chi_8 \quad (27)$$

where χ_5 to χ_8 are given by equations (18) to (21) with the following values for the functions :

$$\phi_5(x) = \frac{P}{4\pi} \cdot \frac{x}{1-\sigma} \left[\frac{b_1^2}{(x^2 + b_1^2)^2} + \frac{b_2^2}{(x^2 + b_2^2)^2} - \frac{1-2\sigma}{2} \left\{ \frac{1}{x^2 + b_1^2} + \frac{1}{x^2 + b_2^2} \right\} \right], \quad (28)$$

$$\phi_7(x) = \frac{P}{4\pi} \cdot \frac{x}{1-\sigma} \left[\frac{b_1^2}{(x^2 + b_1^2)^2} - \frac{b_2^2}{(x^2 + b_2^2)^2} - \frac{1-2\sigma}{2} \left\{ \frac{1}{x^2 + b_1^2} - \frac{1}{x^2 + b_2^2} \right\} \right], \quad (29)$$

* Love, 'Theory of Elasticity,' 4th ed., p. 209. The notation has been changed to correspond with that used in the previous sections of this paper.

$$\psi_6(x) = \frac{P}{4\pi(1-\sigma)} \left[\frac{b_1 x^2}{(x^2 + b_1^2)^2} + \frac{b_2 x^2}{(x^2 + b_2^2)^2} + \frac{1-2\sigma}{2} \left\{ \frac{b_1}{x^2 + b_1^2} + \frac{b_2}{x^2 + b_2^2} \right\} \right], \quad (30)$$

$$\psi_8(x) = \frac{P}{4\pi(1-\sigma)} \left[\frac{b_1 x^2}{(x^2 + b_1^2)^2} - \frac{b_2 x^2}{(x^2 + b_2^2)^2} + \frac{1-2\sigma}{2} \left\{ \frac{b_1}{x^2 + b_1^2} - \frac{b_2}{x^2 + b_2^2} \right\} \right], \quad (31)$$

where

$$b_1 = b - \eta, \quad b_2 = b + \eta. \quad (32)$$

We have now to evaluate $\int_0^\infty \phi_5(u) \sin mu \cdot du$ and three similar integrals.

These depend on integrals of the types

$$\int_0^\infty \frac{u \sin mu}{(u^2 + b_1^2)^2} du, \quad \int_0^\infty \frac{u \sin mu}{u^2 + b_1^2} du.$$

To evaluate the first of these, consider the complex integral

$$\int \frac{u}{(b_1^2 + u^2)^2} e^{imu} du,$$

taken round a contour enclosed by the real axis in the u -plane and a large semicircle above this axis. The part of the integral due to the semicircle clearly tends to 0 as the radius tends to infinity and we are left with

$$\int_{-\infty}^\infty \frac{u}{(b_1^2 + u^2)^2} e^{imu} du = 2\pi i \times \text{residue at } u = ib_1.$$

The residue is easily found to be $\frac{me^{-mb_1}}{4b_1}$. Hence, since the integrand is an even function of u , we have

$$\int_0^\infty \frac{u}{(b_1^2 + u^2)^2} \sin mu \cdot du = \frac{\pi m e^{-mb_1}}{4b_1}. \quad (33)$$

Now take the integral $\int \frac{u}{b_1^2 + u^2} e^{imu} \cdot du$ round the same contour. The part due to the semicircle tends to 0, by Jordan's lemma, and we obtain

$$\int_{-\infty}^\infty \frac{u}{b_1^2 + u^2} e^{imu} \cdot du = 2\pi i \frac{e^{-mb_1}}{2},$$

whence

$$\int_0^\infty \frac{u}{b_1^2 + u^2} \sin mu \cdot du = \frac{1}{2} \pi e^{-mb_1}. \quad (34)$$

The other integrals required may be evaluated in the same way, the results being

$$\int_0^\infty \frac{u^2}{(b_1^2 + u^2)^2} \cos mu \cdot du = \frac{\pi e^{-mb_1}}{4b_1} (1 - mb_1), \quad (35)$$

$$\int_0^\infty \frac{1}{b_1^2 + u^2} \cos mu \cdot du = \frac{\pi e^{-mb_1}}{2b_1}. \quad (36)$$

Using these results, and those obtained by changing b_1 to b_2 , we may now write

$$\left. \begin{aligned} \int_0^\infty \phi_5(u) \sin mu \cdot du &= \frac{P}{16(1-\sigma)} (B_1 + B_2) \\ \int_0^\infty \phi_7(u) \sin mu \cdot du &= \frac{P}{16(1-\sigma)} (B_1 - B_2) \\ \int_0^\infty \phi_6(u) \cos mu \cdot du &= \frac{P}{16(1-\sigma)} (B_1' + B_2') \\ \int_0^\infty \phi_8(u) \cos mu \cdot du &= \frac{P}{16(1-\sigma)} (B_1' - B_2') \end{aligned} \right\}. \quad (37)$$

where

$$\left. \begin{aligned} B_1 &= \{mb_1 - (1 - 2\sigma)\} e^{-mb_1} \\ B_2 &= \{mb_2 - (1 - 2\sigma)\} e^{-mb_2} \\ B_1' &= \{2(1 - \sigma) - mb_1\} e^{-mb_1} \\ B_2' &= \{2(1 - \sigma) - mb_2\} e^{-mb_2} \end{aligned} \right\}. \quad (38)$$

Substituting in the formulæ for χ_5 to χ_8 we have finally

$$\left. \begin{aligned} \chi_5 &= \frac{P}{4\pi(1-\sigma)} \int_0^\infty \frac{mysS - (s + mbc)C}{m^2 \Sigma} (B_1 + B_2) \sin mx \cdot dm \\ \chi_6 &= \frac{P}{4\pi(1-\sigma)} \int_0^\infty \frac{bsC - ycS}{m \Sigma} (B_1' + B_2') \sin mx \cdot dm \\ \chi_7 &= \frac{P}{4\pi(1-\sigma)} \int_0^\infty \frac{mycC - (c + mbs)S}{m^2 \Sigma'} (B_1 - B_2) \sin mx \cdot dm \\ \chi_8 &= \frac{P}{4\pi(1-\sigma)} \int_0^\infty \frac{bcS - ysC}{m \Sigma'} (B_1' - B_2') \sin mx \cdot dm \end{aligned} \right\}, \quad (39)$$

and the complete solution is given by these, together with (25) and (27). There is no divergence at the lower limits since in χ_7 , the only critical integral, we have

$$(B_1 - B_2) = 0(m),$$

and this is sufficient for convergence. It should also be noticed that the

additional exponential factors in B_1 , B_2 , B_1' , B_2' will greatly increase the convergence at the upper limit.

Stresses at Infinity.

In order to find the limiting values of the stresses when $x \rightarrow \infty$ we have to find the values of limits of the type

$$\lim_{x \rightarrow \infty} \int_0^{\infty} F(m) \sin mx \cdot dm, \quad (A)$$

$$\lim_{x \rightarrow \infty} \int_0^{\infty} F(m) \cos mx \cdot dm. \quad (B)$$

Provided that $F(m)$ tends to 0 when $m \rightarrow \infty$, the limit of (A) is well known to be*

$$\frac{\pi}{2} \lim_{m \rightarrow 0} mF(m).$$

To evaluate (B), we integrate by parts and write

$$\int_0^{\infty} F(m) \cos mx \, dm = \frac{1}{x} \left[F(m) \sin mx \right]_0^{\infty} - \frac{1}{x} \int_0^{\infty} F'(m) \sin mx \, dm.$$

In all the integrals occurring here, both $F(m)$ and $F'(m)$ tend exponentially to 0 as $m \rightarrow \infty$. Thus it is clear that the limit (B) is 0.

From this last result, it easily follows that \widehat{xy} tends to 0 when $x \rightarrow \infty$. It is also obvious that \widehat{yy} tends to 0, since two differentiations with respect to x in any one of the stress functions will give an integral of type (A) in which $F(m) = 0(m)$. Passing to \widehat{xx} , we find that χ_5 makes no contribution. But

$$\frac{\partial^2 \chi}{\partial y^2} = \frac{P}{4\pi(1-\sigma)} \int_0^{\infty} \frac{m(bsC - ycS) - 2cC}{\Sigma} (B_1' + B_2') \sin mx \cdot dm.$$

and the limit of this when x tends to ∞ is

$$\frac{\pi}{2} \lim_{m \rightarrow 0} \left\{ -\frac{Pm}{4\pi(1-\sigma)} \cdot \frac{2cC}{\Sigma} (B_1' + B_2') \right\} = -\frac{P}{4b}.$$

In the same way, we obtain from χ_7 a contribution to \widehat{xx} of amount

$$\frac{3P(b_1 - b_2)}{8b^3} \cdot y,$$

while χ_8 makes no contribution.

* Carslaw, 'Fourier Series and Integrals,' London, 1921, p. 200.

There is thus at $+\infty$ a total thrust $\frac{1}{2}P$; as this comes from χ_6 , which is odd in x , there will be a total tension $\frac{1}{2}P$ at $-\infty$, and the applied force is automatically balanced. The term arising from χ_7 corresponds to a bending moment $\frac{1}{2}P(b_1 - b_2) = -\frac{1}{2}P\eta$, produced by the unsymmetrical position of the force.

If we require the applied force to be balanced by stresses at infinity in one direction only, we have only to add terms corresponding to tensions and moments transmitted from infinity. Thus, the stress-function

$$\bar{\chi} = \frac{P}{8b^3} y^2 (b^2 + \eta y)$$

gives the stresses

$$\widehat{xx} = \frac{P}{4b} + \frac{3P\eta}{4b^3} y, \quad \widehat{xy} = \widehat{yx} = 0,$$

so that there is across any transverse section of the beam a uniform tension of total amount $\frac{1}{2}P$ and a bending moment equal to

$$\frac{3P\eta}{4b^3} \int_{-b}^b y^2 dy = \frac{1}{2}P\eta.$$

If $\bar{\chi}$ is added to χ , the stresses at $x = +\infty$ are removed and the applied force is balanced by stresses at $x = -\infty$ alone. This corresponds more closely to conditions occurring in practice.

Distributions of Longitudinal Force.

If x is changed to $x - \xi$ is (39) and (25) the new value of χ will correspond to the stresses produced by a force P applied at the point (ξ, η) and acting parallel to the axis of x . If we then multiply χ by a function $f(\xi, \eta)$ and then integrate with respect to ξ and η over a region entirely within the strip the result will be the stress function corresponding to the application of longitudinal forces of intensity $f(\xi, \eta)$ over the part of the strip covered by the integration. It is clear that this process can be justified if $f(\xi, \eta)$ is bounded and the region of integration finite. If these conditions were not satisfied the validity of the processes might need to be specially investigated.

Transverse Force.

A force P , acting at $(\eta, 0)$ in the direction of the y -axis, will produce in an infinite plate a stress-system given by the function

$$\chi_0' = \frac{P}{4\pi} \left[2x\theta + \frac{1-2\sigma}{1-\sigma} (y-\eta) \log r \right], \quad (40)$$

where r and θ are defined as in (25). This gives for the stresses

$$\left. \begin{aligned} \widehat{xx} &= \frac{P}{4\pi} \frac{y-\eta}{r^2} \left[\frac{1-2\sigma}{1-\sigma} - \frac{2}{1-\sigma} \frac{x^2}{r^2} \right] \\ \widehat{yy} &= \frac{P}{4\pi} \frac{y-\eta}{r^2} \left[\frac{2}{1-\sigma} \cdot \frac{x^2}{r^2} - \frac{3-2\sigma}{1-\sigma} \right] \\ \widehat{xy} &= -\frac{P}{4\pi} \frac{x}{r^2} \left[\frac{1-2\sigma}{1-\sigma} + \frac{2}{1-\sigma} \cdot \frac{(y-\eta)^2}{r^2} \right] \end{aligned} \right\} \quad (41)$$

To obtain the solution for the strip, we take

$$\chi = \chi_0' + \chi_1 + \chi_2 + \chi_3 + \chi_4 \quad (42)$$

where χ_1 to χ_4 are given by equations (14) to (17) with

$$\left. \begin{aligned} \phi_1(x) &= \frac{P}{4\pi(1-\sigma)} \left[- \left\{ \frac{b_1 x^2}{(x^2 + b_1^2)^2} - \frac{b_2 x^2}{(x^2 + b_2^2)^2} \right\} \right. \\ &\quad \left. + \frac{3-2\sigma}{2} \left\{ \frac{b_1}{x^2 + b_1^2} - \frac{b_2}{x^2 + b_2^2} \right\} \right] \\ \phi_3(x) &= \frac{P}{4\pi(1-\sigma)} \left[- \left\{ \frac{b_1 x^2}{(x^2 + b_1^2)^2} + \frac{b_2 x^2}{(x^2 + b_2^2)^2} \right\} \right. \\ &\quad \left. + \frac{3-2\sigma}{2} \left\{ \frac{b_1}{x^2 + b_1^2} + \frac{b_2}{x^2 + b_2^2} \right\} \right] \\ \psi_2(x) &= \frac{Px}{4\pi(1-\sigma)} \left[\frac{b_1^2}{(x^2 + b_1^2)^2} - \frac{b_2^2}{(x^2 + b_2^2)^2} \right. \\ &\quad \left. + \frac{1-2\sigma}{2} \left\{ \frac{1}{x^2 + b_1^2} + \frac{1}{x^2 + b_2^2} \right\} \right] \\ \psi_4(x) &= \frac{Px}{4\pi(1-\sigma)} \left[\frac{b_1^2}{(x^2 + b_1^2)^2} + \frac{b_2^2}{(x^2 + b_2^2)^2} \right. \\ &\quad \left. + \frac{1-2\sigma}{2} \left\{ \frac{1}{x^2 + b_1^2} + \frac{1}{x^2 + b_2^2} \right\} \right] \end{aligned} \right\} \quad (43)$$

Again using the results of (33) to (36) we have

$$\left. \begin{aligned} \int_0^\infty \phi_1(u) \cos mu \cdot du &= \frac{P}{16(1-\sigma)} (\beta_1 - \beta_2) \\ \int_0^\infty \phi_3(u) \cos mu \cdot du &= \frac{P}{16(1-\sigma)} (\beta_1 + \beta_2) \\ \int_0^\infty \psi_2(u) \sin mu \cdot du &= \frac{P}{16(1-\sigma)} (\beta_1' - \beta_2') \\ \int_0^\infty \psi_4(u) \sin mu \cdot du &= \frac{P}{16(1-\sigma)} (\beta_1' + \beta_2') \end{aligned} \right\} \quad (44)$$

where

$$\left. \begin{aligned} \beta_1 &= \{2(1 - \sigma) + mb_1\} e^{-mb_1} \\ \beta_2 &= \{2(1 - \sigma) + mb_2\} e^{-mb_2} \\ \beta_1' &= \{(1 - 2\sigma) + mb_1\} e^{-mb_1} \\ \beta_2' &= \{(1 - 2\sigma) + mb_2\} e^{-mb_2} \end{aligned} \right\}. \quad (45)$$

Hence the four component stress functions are

$$\left. \begin{aligned} \chi_1 &= \frac{P}{4\pi(1 - \sigma)} \int_0^\infty \frac{mysS - (s + mbc)C}{m^2\Sigma} (\beta_1 - \beta_2) \cos mx \cdot dm \\ \chi_2 &= \frac{P}{4\pi(1 - \sigma)} \int_0^\infty \frac{ycS - bsC}{m\Sigma} (\beta_1' - \beta_2') \cos mx \cdot dm \\ \chi_3 &= \frac{P}{4\pi(1 - \sigma)} \int_0^\infty \frac{mycC - (c + mbs)S}{m^2\Sigma'} (\beta_1 + \beta_2) \cos mx \cdot dm \\ \chi_4 &= \frac{P}{4\pi(1 - \sigma)} \int_0^\infty \frac{ysC - bcS}{m\Sigma'} (\beta_1' + \beta_2') \cos mx \cdot dm. \end{aligned} \right\}. \quad (46)$$

Of these, χ_3 and χ_4 are not convergent at the lower limit; but convergence may be secured if further stresses are applied to the boundaries, so that the applied force is balanced. To make this clear, it is necessary to examine the divergent terms more closely. Those in the integrand of χ_3 will be found to be

$$\frac{y}{2b^3} (y^2 - 3b^2) \left\{ \frac{2(1 - \sigma)}{m^2} - \frac{b(1 - 2\sigma)}{m} \right\},$$

while in χ_4 there is the single divergent term

$$\frac{1 - 2\sigma}{2b^2m} y (y^2 - b^2).$$

When these are added the terms in $1/m$ combine to give a multiple of y . But such a term is trivial, as it gives nothing to the stresses. If we multiply it by a suitable exponential factor, such as e^{-mb} and subtract it from the integrand the convergence at the upper limit will be unaffected. To cancel the other term we now add a stress system

$$\chi_3' = \frac{4}{\pi} \int_0^\infty \frac{mycC - (c + mbs)S}{m^2\Sigma'} \cos mx \cdot dm \int_0^\infty \phi_3(u) \cos mu \cdot du,$$

where $\phi_3(u)$ is zero outside a finite range of values of u . We may then expand the $\cos mu$ and integrate term by term, obtaining

$$\chi_3' = \frac{4}{\pi} \int_0^\infty \left[\frac{3}{4m^2b^3} y \left(\frac{1}{2} y^2 - b^2 \right) \int_0^\infty \phi_3'(u) \cdot du + O(1) \right] dm.$$

It is now evident that the integral for $\chi_3 + \chi_4 + \chi_3'$ will contain no divergent term if

$$\int_0^\infty \phi_3'(u) du = -\frac{P}{4},$$

in which case the new stress system balances P .

Another method of securing convergence* is to subtract from the integrands of χ_3 and χ_4 terms which will cancel the divergence at the lower limit without affecting the convergence at the upper limit. Thus if we take

$$\left. \begin{aligned} \chi_3 &= \frac{P}{4\pi(1-\sigma)} \int_0^\infty \left\{ \frac{myC - (c + mb_s)S}{m^2\Sigma'} \cos mx - \frac{y(y^2 - 3b^2)}{4m^2b^3} \right\} \\ &\quad \times (\beta_1 + \beta_2) dm \\ \chi_4 &= \frac{P}{4\pi(1-\sigma)} \int_0^\infty \left\{ \frac{ysC - bcS}{m\Sigma'} \cos mx - \frac{y(y^2 - b^2)}{4mb^2} \right\} \\ &\quad (\beta_1' + \beta_2') dm, \end{aligned} \right\} \quad (47)$$

the integrals will converge at the lower limits, while the convergence at the upper limits is maintained by the exponential factors in $\beta_1, \beta_2, \beta_1', \beta_2'$.

The terms that have been subtracted are solutions of the bi-harmonic equation (2) and they do not affect the stresses on the boundaries. We have thus a solution valid for finite values of x . But the stresses tend to infinity with x . For we have

$$\chi_3 + \chi_4 = \frac{P}{4\pi} \int_0^\infty \left\{ \frac{y(y^2 - 3b^2)}{b^2m^2} (\cos mx - 1) + f(m) \cos mx \right\} dm,$$

where $f(m)$ is finite when $m = 0$, and when x is large

$$\chi_3 + \chi_4 \sim -\frac{Py(y^2 - 3b^2)}{4\pi b^3} \int_0^\infty \frac{1 - \cos mx}{m^2} dm.$$

But

$$\int_0^\infty \frac{1 - \cos mx}{m^2} dm = \frac{1}{2}\pi x,$$

and we have

$$\chi_3 + \chi_4 \sim -\frac{P}{8b^3} y(y^2 - 3b^2) x.$$

This corresponds to a stress-system

$$\widehat{xx} \sim -\frac{3Pxy}{4b^3}, \quad \widehat{yy} \sim 0, \quad \widehat{xy} \sim -\frac{3P}{8b^3} (y^2 - b^2).$$

* Cf. Filon, *loc. cit.*, § 15, pp. 88, *et seq.*

Integrating across the strip, we have at any section a total shear $-\frac{1}{2}P$ and a bending moment $-\frac{1}{2}Px$, which tends to infinity with x .

The physical meaning of this is plain. If we attempt to balance the applied force by transverse forces at infinity, these will produce an infinite bending moment in the finite part of the strip. This infinite bending moment corresponds to the divergent term in the solution. It can be removed, but only by placing an infinite bending moment at infinity. The resulting solution is not, however, as artificial as may at first appear. For if we suppose the strip to be cut at $x = \pm a$, where a is large compared with b , the solution will be that for a bar acted upon by a transverse force P at $(0, 0)$ and supported by shears and couples applied to its ends, the couples being so adjusted that the bending-moment vanishes at the middle of the bar. By adding further solutions of bending-moment type we may now adjust the conditions at the ends so that they correspond to one of usual types of fixing condition. We may, for example, make the bending moment vanish at the ends so that the conditions approximate to those of free support. There will, however, be small residual longitudinal forces on the ends, having a zero resultant. Alternatively, we may adjust the moments so that the middle line of the strip remains horizontal at the ends. We have then approximately the conditions for a clamped end.

By further introducing stress functions of the type $xy(b^2 - \frac{1}{3}y^2)$, which give both bending moment and shear, we may make the conditions at the two ends different obtaining, for example, the solution when one end is clamped and the other free.

Thus the solution for the transverse force may be regarded as complete. That for any distribution of transverse force is derivable as in the case of longitudinal forces and, by combining the two solutions, we have the solution for an arbitrary distribution of forces applied to the strip.

APPENDIX.

[*Added February 27, 1929.*]

It does not appear to be possible to express the integrals in (39) and (46) in terms of a finite number of elementary functions. These integrals, or their simpler components, must be regarded as defining new functions whose properties have to be independently investigated, and whose values should be tabulated. It will then be possible to enter upon a fuller discussion of stress distributions of this class.

It is, however, not difficult to find the values of the stresses at special points by direct computation. In what follows the results of such calculations are shown.

Stresses Due to a Central Longitudinal Force.

If the force acts in the middle of the strip, we have $b_1 = b_2 = b$, so that χ_7 and χ_8 vanish identically. In the remaining parts of χ it is convenient to make the substitutions

$$mb = u, \quad y = by', \quad x = bx', \quad (48)$$

so that x', y' are the co-ordinates measured in a unit equal to half the breadth of the strip. This leads to

$$\chi = \chi_0 + \chi_5 + \chi_6, \quad (49)$$

where

$$\left. \begin{aligned} \chi_0 &= \frac{Pb}{4\pi} \left[\frac{1-2\sigma}{1-\sigma} x' \log r' - 2y' \theta \right] \\ \chi_5 &= \frac{Pb}{2\pi(1-\sigma)} \int_0^\infty \frac{uy'sS - (s+uc)C}{u^2\Sigma} \{u - (1-2\sigma)\} e^{-u} \sin ux' du \\ \chi_6 &= \frac{Pb}{2\pi(1-\sigma)} \int_0^\infty \frac{sC - y'cS}{u\Sigma} \{2(1-\sigma) - u\} e^{-u} \sin ux' du \end{aligned} \right\}, \quad (50)$$

the symbols having now, in terms of the new variables, the meanings

$$\left. \begin{aligned} s &= \sinh u, & c &= \cosh u, \\ S &= \sinh uy', & C &= \cosh uy' \\ \Sigma &= \sinh 2u + 2u \end{aligned} \right\} \quad (51)$$

The longitudinal stress is now given by

$$\begin{aligned} \widehat{xx} &= \frac{1}{b^2} \frac{\partial^2 \chi}{\partial y'^2} \\ &= \frac{P}{4\pi b} \frac{x'}{r'^2} \left[\frac{2}{1-\sigma} \frac{y'^2}{r'^2} - \frac{3-2\sigma}{1-\sigma} \right] \\ &\quad + \frac{P}{2\pi(1-\sigma)b} \int_0^\infty \frac{uy'sS + (s-uc)C}{\Sigma} \{u - (1-2\sigma)\} e^{-u} \sin ux' du \\ &\quad + \frac{P}{2\pi(1-\sigma)b} \int_0^\infty \frac{(us-2c)C - uy'cS}{\Sigma} \{2(1-\sigma) - u\} e^{-u} \sin ux' du. \end{aligned}$$

We consider the values of this along the two lines $y' = 0$, $y' = 1$, i.e., along the central line and along one of the edges.

Putting $y' = 0$ and making a few easy reductions, we get for the stress on the axis

$$\left. \begin{aligned} \widehat{x}x_0 &= \frac{P}{4\pi(1-\sigma)b} \left[2X_1 - (3-2\sigma) \left(X_2 + \frac{1}{x'} \right) \right] \\ \text{where} \quad X_1 &= \int_0^\infty \frac{2-u^2}{\Sigma} \sin ux' \cdot du \\ X_2 &= \int_0^\infty \frac{3-2u+e^{-2u}}{\Sigma} \sin ux' \cdot du \end{aligned} \right\} \quad (52)$$

These integrals are very rapidly convergent at the upper limit and require no further treatment before computation.

The case of $y' = 1$ is a little different. The part of the stress due to χ_3 and χ_6 is

$$\frac{P}{2\pi(1-\sigma)b} \int_0^\infty \frac{(sc-u)(u+1) + 2c^2u - 2(1-\sigma)(sc-u+2c^2)}{\Sigma} e^{-u} \sin ux' \cdot du,$$

and this is not so rapidly convergent as the previous integrals. We therefore make the substitutions

$$\begin{aligned} sc - u &= \frac{1}{2}\Sigma - 2u \\ 2c^2 &= \cosh 2u + 1 \\ &= \sinh 2u + e^{-2u} + 1 \\ &= \Sigma - 2u + e^{-2u} + 1. \end{aligned}$$

The more slowly convergent terms now separate out to form an elementary integral and we get

$$\left. \begin{aligned} \widehat{x}x_1 &= \frac{P}{2\pi b(1-\sigma)} \left[\left\{ \frac{4x'}{(1+x'^2)^2} - X_3 \right\} - 2(1-\sigma) \left\{ \frac{2x'}{1+x'^2} - X_4 \right\} \right] \\ \text{where} \quad X_3 &= \int_0^\infty \frac{u(4u+1-e^{-2u})}{\Sigma} e^{-u} \cdot \sin ux' du \\ X_4 &= \int_0^\infty \frac{4u-1-e^{-2u}}{\Sigma} e^{-u} \cdot \sin ux' du \end{aligned} \right\} \quad (53)$$

The convergence is now extremely rapid.

Owing to the fluctuation in sign of the trigonometric factor, integrals of the type X_1 to X_4 are not conveniently calculated from ordinary quadrature formulæ except when x' is small. An analogue of Simpson's formula, adapted to use with trigonometric integrals, has been given by Filon in a recent paper.*

* L. N. G. Filon, "On a Quadrature Formula for Trigonometric Integrals," 'Proc. Roy. Soc. Edin.,' vol. 49, pp. 38-47 (1929).

By the aid of equation (20) of his paper, the integrals X_1 to X_4 have been calculated for $x' = \pi/9, \pi/3, \pi/2, 2\pi/3$ and π , using an interval for u of 0.5. For a special reason to be noted later, X_3 and X_4 have also been calculated for $x' = \pi/18$ and $\pi/30$.

Preliminary tests with Filon's equation (24) showed that the errors in the values of the integrals would be unlikely to affect the third decimal place.

The details of the calculation are not of much interest. Owing to the possibility that the final results might depend on small differences between relatively large numbers, eight decimal places were retained in the first stages, the tables of the exponential function by Newman and Glaisher being used.* But six places, with five in the final stages, would probably have been adequate. It is unnecessary to use values of u greater than 8 in the first two integrals, while the effective upper limits in X_3 and X_4 are 7 and 6 respectively.

It is easy to prove that the contributions from the infinite range above these limits are negligible. For, when u is large, we have

$$\frac{1}{\Sigma} = 2e^{-2u} (1 + \epsilon),$$

where ϵ is small and steadily decreases as u increases. When $u > 8$, ϵ is certainly less than 10^{-5} . Thus the remainder in X_1 may be written

$$2(1 + \epsilon) \int_8^\infty e^{-2u} (2 - u^2) \sin ux' du,$$

and the numerical value of this is less than

$$2(1 + \epsilon) \int_8^\infty (u^2 - 2) e^{-2u} du < 10^{-7}.$$

The remainders in the other integrals may be examined in the same way.

The values obtained for the integrals are shown in Tables I and II, the asymptotic values being added for comparison. The other columns in these tables give the values of the terms in \widehat{xx}_0 and \widehat{xx}_1 which contain parts additional to the integrals. With the aid of these columns the values of \widehat{xx} may be at once found, for any value of σ , from the formulæ

$$\left. \begin{aligned} \widehat{xx}_0 &= \frac{P}{4\pi(1-\sigma)b} [2X_1 - (3-2\sigma)X_2] \\ \widehat{xx}_1 &= \frac{P}{2\pi(1-\sigma)b} [X_3' - 2(1-\sigma)X_4] \end{aligned} \right\} \quad (54)$$

* Newman, 'Trans. Camb. Phil. Soc.', vol. 13, p. 145 (1883); Glaisher, *ibid.*, vol. 13, p. 243 (1883).

The values of the stresses for $\sigma = \frac{1}{2}$, i.e., for Poisson's ratio $= \frac{1}{2}$, are shown in Table III and graphically in fig. 2. They have been modified by the addition of $P/4b$ to each stress in order that the balancing forces at infinity may be in one direction only, and the signs have then been changed. The conditions then correspond to fig. 1, the force acting in the negative direction of the x -axis, and being balanced by forces at $+\infty$ only. Before these modifications are made, the value of the stress for any negative value of x is the same as for the corresponding positive value but of opposite sign. The values of the stresses for x negative in Table III are therefore obtainable without further calculation.

Table I.—Values of the Terms in the Equation for \widehat{xx}_0 .

x' .	X_1 .	X_2 .	X_3' .
$\pi/9 = 0.349$	0.066	0.069	2.934
$\pi/3 = 1.047$	0.380	0.533	1.488
$\pi/2 = 1.571$	0.604	0.799	1.436
$2\pi/3 = 2.094$	0.701	1.018	1.496
$\pi = 3.142$	0.785	1.250	1.568
∞	0.785	1.571	1.571

Table II.—Values of the Terms in the Equation for \widehat{xx}_1 .

x' .	X_3 .	X_4 .	X_3' .	X_4' .
$\pi/30 = 0.105$	0.055	0.017	0.355	0.190
$\pi/18 = 0.175$	0.090	0.028	0.567	0.311
$\pi/9 = 0.349$	0.174	0.054	0.935	0.568
$\pi/3 = 1.047$	0.363	0.095	0.590	0.904
$\pi/2 = 1.571$	0.341	0.050	0.182	0.856
$2\pi/3 = 2.094$	0.257	-0.034	0.032	0.812
$\pi = 3.142$	0.110	-0.208	-0.004	0.786
∞	0	-0.785	0	0.785

Table III.—Values of \widehat{xx}_0 , the Tension in the Middle Line, and \widehat{xx}_1 , the Tension in the Edge of a Strip Stressed as in fig. 1. ($\sigma = \frac{1}{2}$.)

x' .	$2b \cdot \widehat{xx}_0/P$.	$2b \cdot \widehat{xx}_1/P$.
$-\infty$	0	0
$-\pi$	0.002	-0.002
$-2\pi/3$	0.006	-0.004
$-\pi/2$	-0.002	0.027
$-\pi/3$	-0.118	0.159
$-\pi/9$	-0.992	0.511
$-\pi/18$	—	0.532
$-\pi/30$	—	0.521
0	∞	0.500
$\pi/30$	—	0.479
$\pi/18$	—	0.468
$\pi/9$	1.892	0.489
$\pi/3$	1.118	0.841
$\pi/2$	1.002	0.973
$2\pi/3$	0.994	1.004
π	0.998	1.002
∞	1.000	1.000

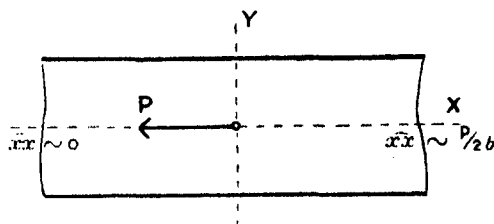


FIG. 1.

It will be seen that the stress across the strip is equalised at a distance from the force about equal to the width of the strip, the stresses at greater distances than this differing from their asymptotic values by less than 1 per cent.

It is interesting to notice that both stresses cross their asymptotic values at values of x' between 1.5 and 2 and then approach them from the other side. This phenomenon was observed by Filon* in his results for stresses produced by forces applied to the edges of a strip. The values of \widehat{xx}_1 in Table III show the additional interesting phenomenon of an initial decrease below the value at $x' = 0$. In order that the amount of this decrease might be estimated the tension in the edge of the strip has been calculated for the additional values $\pi/30$ and $\pi/18$ of x' . It will be seen that the decrease at $x' = \pi/18$ is about 3 per cent. of the asymptotic value of the stress or 6 per cent. of the stress at $x' = 0$. A rough graphical interpolation suggests that the

* 'Phil. Trans.,' A, vol. 201, pp. 115, 127 (1903).

stress has a least value when x' is about 0.24 and is then about 7 per cent. less than the value at $x' = 0$.

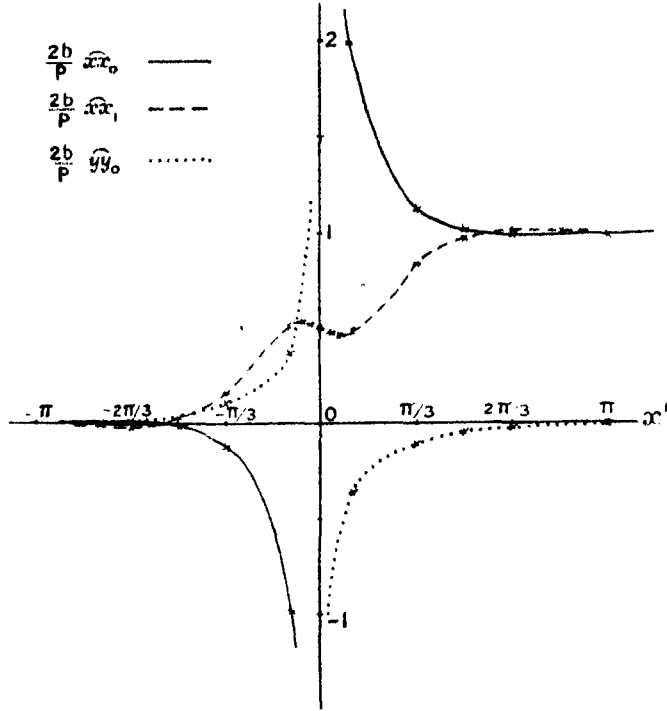


FIG. 2.—Stresses due to a force P acting at $(0, 0)$ in the negative direction of $0x$.

The value of the cross-stress $\hat{y}y$ on the middle line is now easily found. For, after a little reduction, we obtain

$$\left(\frac{\partial^2 \chi}{\partial x^2}\right)_{y=0} = \frac{P}{4\pi(1-\sigma)b} \left[\frac{1-2\sigma}{x'} + \int_0^\infty \frac{2u^2 + 2u + 1 - e^{-2u}}{\Sigma} \sin ux' du - 2(1-\sigma) \int_0^\infty \frac{1 + 2u - e^{-2u}}{\Sigma} \sin ux' du \right].$$

These integrals are easily expressible in terms of those already obtained, together with the additional integral

$$X_0 = \int_0^\infty \frac{\sin ux'}{\Sigma} du, \quad (55)$$

and we have finally

$$\hat{y}y_0 = \frac{P}{4\pi b} \left[\frac{1}{1-\sigma} X_5 - 2X_6 \right], \quad (56)$$

where

$$\left. \begin{aligned} X_5 &= 8X_0 - 2X_1 - X_2' \\ X_6 &= 4X_0 - X_2' \end{aligned} \right\} \quad (57)$$

The values of X_0 , X_3 , X_4 and \widehat{yy}_0 are shown in Table IV and the variation of \widehat{yy}_0 is also illustrated in fig. 2. The values have again been modified so as to conform to the configuration of fig. 1. It is of interest to observe that, although \widehat{yy}_0 is small when x' is greater than 1.5, yet it does not approach its asymptotic value as rapidly as do the tensions in the direction of the x -axis. There is a slight indication of a change of sign at $x' = \pi$, but the degree of accuracy of the figures is not sufficient for this to be asserted confidently. The values of \widehat{yy}_0 for negative values of x' may be found by a simple reversal of sign.

Table IV.—Values of \widehat{yy}_0 ($\sigma = \frac{1}{2}$) and its Component Integrals.

x' .	X_0 .	X_3 .	X_4 .	$2b \cdot \widehat{yy}_0/P$.
$\pi/9$	0.130	-2.026	-2.414	-0.364
$\pi/3$	0.312	0.248	-0.240	-0.110
$\pi/2$	0.369	0.308	0.040	-0.049
$2\pi/3$	0.389	0.214	0.060	-0.023
π	-0.002	0.000	-0.002	0.000
∞	0	0	0	0

Stresses Due to a Central Transverse Force.

For a transverse force P acting at the origin the stress function reduces to

$$\chi = \chi_0' + \chi_3 + \chi_4. \quad (58)$$

Modifying the values of χ_3 , χ_4 as in (47) and then making the same change of variables as before, we obtain

$$\left. \begin{aligned} \chi_0' &= \frac{Pb}{4\pi} \left[2x'\theta + \frac{1-2\sigma}{1-\sigma} y' \log r' \right], \\ \chi_3 &= \frac{Pb}{2\pi(1-\sigma)} \int_0^\infty \left\{ \frac{uy'cC - (c+us)S}{u^2\Sigma'} \cos ux' - \frac{y'(y'^2-3)}{4u^2} \right\} \\ &\quad \times \{2(1-\sigma) + u\} e^{-u} du, \\ \chi_4 &= \frac{Pb}{2\pi(1-\sigma)} \int_0^\infty \left\{ \frac{y'sC - cS}{u\Sigma'} \cos ux' - \frac{y'(y'^2-1)}{4u} \right\} \\ &\quad \times \{(1-2\sigma) + u\} e^{-u} du, \end{aligned} \right\} \quad (59)$$

where

$$\Sigma' = \sinh 2u - 2u, \quad (60)$$

and the other symbols are defined in (48) and (51).

We first consider the values of $\widehat{y}y$ on the line $x = 0$; denoting this stress by $\widehat{y}y_0'$ we have immediately

$$\widehat{y}y_0' = \frac{P}{4\pi b} \left[2Y_1 + \frac{1}{1-\sigma} \left(Y_2 - \frac{3-2\sigma}{y'} \right) \right], \quad (61)$$

where

$$\left. \begin{aligned} Y_1 &= \int_0^\infty \frac{(1-2u+e^{-2u})S - uy'C}{\Sigma'} du \\ Y_2 &= \int_0^\infty \frac{2u^2S - uy'(1-2u-e^{-2u})C}{\Sigma'} du \end{aligned} \right\}. \quad (62)$$

These integrals may be calculated from an ordinary quadrature formula. Their values for $y' = \frac{1}{3}$ and $\frac{2}{3}$, found by using Simpson's formula with an interval of 0.5, are shown in the first two columns of Table V. The corresponding values of $\widehat{y}y_0'$, taking $\sigma = \frac{1}{3}$ are given in the third column. The values for $y' = -\frac{1}{3}$ and $-\frac{2}{3}$ are found by a reversal of sign.

Table V.—Values of $\widehat{y}y$ on the Line $x' = 0$ due to a Transverse Force P acting at the Origin. ($\sigma = \frac{1}{3}$.)

y' .	Y_1 .	Y_2 .	$2b \cdot \widehat{y}y_0'/P$.
-1	—	—	0
$-\frac{2}{3}$	-0.971	-0.864	0.30
$-\frac{1}{3}$	-0.563	-0.445	1.28
0	—	—	∞
$\frac{1}{3}$	0.563	0.445	-1.28
$\frac{2}{3}$	0.971	0.864	-0.30
1	—	—	0

For the longitudinal stress we have

$$\widehat{x}x = \frac{P}{4\pi b} \left[2 \left(Y_3 + \frac{y'}{r'^2} \right) + \frac{1}{1-\sigma} \left(Y_4 - \frac{y'}{r'^2} - \frac{2x'^2y'}{r'^4} \right) \right], \quad (63)$$

where

$$\left. \begin{aligned} Y_3 &= \int_0^\infty \left\{ \frac{2uyC + (3-2u-e^{-2u})S}{\Sigma'} \cos ux' - \frac{3y'(u+1)}{u} e^{-u} \right\} du \\ Y_4 &= \int_0^\infty \left\{ \frac{uy'(2u-1+e^{-2u})C + 2(2u-u^2-1+e^{-2u})S}{\Sigma'} \cos ux' - 3y'e^{-u} \right\} du \end{aligned} \right\}. \quad (64)$$

In order that these integrals may be evaluated by Filon's method, it is necessary that the trigonometric functions should be multiplied by functions

of u which are finite when $u = 0$. This condition is satisfied in Y_4 but not in Y_3 . We therefore write

$$\begin{aligned} Y_3 &= Y_3' - 3y \int_0^\infty \frac{u+1}{u^2} e^{-u} (1 - \cos ux') du \\ &= Y_3' - 3xy \tan^{-1} x, \end{aligned} \quad (65)$$

where now

$$Y_3' = \int_0^\infty \left\{ \frac{2uyC + (3 - 2u - e^{-2u})S}{\Sigma'} - \frac{3y'(u+1)}{u} e^{-u} \right\} \cos ux' du. \quad (66)$$

It should also be noted that the final term in Y_4 may be omitted without loss, since it contributes only a finite constant bending-moment to the solution. The subsequent calculations were made after this term had been removed.

The calculation of Y_3' and Y_4' may now be carried out in a straightforward manner, using Filon's formula (22).^{*} This has been done for $y' = \frac{1}{3}$ and $\frac{2}{3}$ on each of the cross-sections $x' = 0, \pi/2$ and π . As y' increases, however, the convergence of the integrals at the upper limit becomes less rapid and, for calculations of the stress in the edge $y' = 1$, some further preliminary transformations are of value. To obtain the most convenient form of the integrals, it is best to return to the form in which they first appear after the differentiation of χ has been carried out. We have

$$\frac{\partial^2 \chi_3}{\partial y^2} + \frac{\partial^2 \chi_4}{\partial y^2} = \frac{P}{2\pi(1-\sigma)b} [I_1 + I_2],$$

where, putting $y' = 1$,

$$\begin{aligned} I_1 &= \int_0^\infty \left\{ \frac{cs+u}{\Sigma'} \cos ux' - \frac{3}{2u^2} \right\} \{2(1-\sigma) + u\} e^{-u} du \\ I_2 &= \int_0^\infty \left\{ \frac{2s^2}{\Sigma'} \cos ux' - \frac{3}{2u} \right\} \{(1-2\sigma) + u\} e^{-u} du. \end{aligned}$$

The least convergent terms may now be removed by using the substitutions

$$\begin{aligned} cs + u &= \frac{1}{2}\Sigma' + 2u, \\ 2s^2 &= \Sigma' + 2u - 1 + e^{-2u}. \end{aligned}$$

If, at the same time, we make the coefficient of $\cos ux'$ finite for $u = 0$ by the same method as before, we obtain

$$\begin{aligned} I_1 + I_2 &= (1-\sigma) \left\{ 2Y_5 - 3 \int_0^\infty \frac{1 - \cos ux'}{u^2} (u+1) e^{-u} du + 3 \int_0^\infty e^{-u} \cos ux' du \right\} \\ &\quad + \left\{ Y_6 + \frac{1}{2} \int_0^\infty (3u-2) e^{-u} \cos ux' du - \frac{3}{2} \int_0^\infty e^{-u} du \right\}, \end{aligned} \quad (67)$$

^{*} *Loc. cit. supra*, p. 107.

where

$$\left. \begin{aligned} Y_5 &= \int_0^\infty \left\{ \frac{e^{-2u} + 4u - 1}{\Sigma'} - \frac{3(u+1)}{2u^2} \right\} e^{-u} \cdot \cos ux' du \\ Y_6 &= \int_0^\infty \frac{4u^2 - 3u + 1 + (u-1)e^{-2u}}{\Sigma'} \cdot e^{-u} \cdot \cos ux' du \end{aligned} \right\}. \quad (68)$$

The last term in (67) corresponds to the bending-moment term which was disregarded above. When this is omitted and the values of the elementary integrals are inserted, the equation for the stress takes the form

$$\widehat{xx}_1' = \frac{P}{2\pi b} \left[Y_5' + \frac{1}{1-\sigma} Y_6' \right] \quad (69)$$

where

$$\left. \begin{aligned} Y_5' &= 2Y_5 + \frac{4}{1+x'^2} - 3x' \tan^{-1} x' \\ Y_6' &= Y_6 - \frac{3x'^2}{(1+x'^2)^2} \end{aligned} \right\}. \quad (70)$$

The convergence in Y_6 is now so rapid that the effective upper limit is 5. The same is true of the first term in Y_5 but the second term decreases more slowly. It is therefore best to write

$$Y_5 = \int_0^5 \phi(u) du + \int_5^\infty \frac{3(u+1)}{2u^2} e^{-u} \cos ux' du,$$

$\phi(u)$ being the complete integrand, and to find the value of the second integral from an asymptotic expansion. This is readily found by integrating $\frac{e^{-pu}}{u}$ and $\frac{e^{-pu}}{u^2}$ successively by parts and then putting $p = 1 - ix'$ and retaining only the real part. This leads to the expansions

$$\left. \begin{aligned} \int_v^\infty \frac{e^{-u} \cos ux'}{u} du &= e^{-v} \left[\frac{\cos(vx' + \theta)}{\lambda v} - \frac{\cos(vx' + 2\theta)}{\lambda^2 v^2} \right. \\ &\quad \left. + \dots + \frac{(-1)^{n-1} (n-1)!}{\lambda^n v^n} \cos(vx' + n\theta) \dots \right] \\ \int_v^\infty \frac{e^{-u} \cos ux'}{u^2} du &= e^{-v} \left[\frac{\cos(vx' + \theta)}{\lambda v^2} - \frac{2!}{\lambda^2 v^3} \cos(vx' + 2\theta) \right. \\ &\quad \left. + \dots + \frac{(-1)^{n-1} n!}{\lambda^n v^{n+1}} \cos(vx' + n\theta) \dots \right] \end{aligned} \right\}, \quad (71)$$

where

$$\left. \begin{aligned} \lambda &= \sqrt{1+x'^2} \\ \theta &= \tan^{-1} x' \end{aligned} \right\}. \quad (72)$$

With the aid of the equations (68) to (72) the value of \widehat{xx}' has been found for x' equal to 0, $\pi/9$, $\pi/3$, $\pi/2$, $2\pi/3$ and π . Combining (63) and (69) into a single equation, we may write

$$\widehat{xx} = \frac{P}{2\pi b} \left[Y_7 + \frac{1}{1-\sigma} Y_8 \right], \quad (73)$$

and the values of Y_7 and Y_8 are those shown in Table VI. The values of \widehat{xx} are those for $\sigma = \frac{1}{2}$. It will be seen that when $x' = \pi$ the values of \widehat{xx} are almost proportional to y' , so that the stress approximates to that due to a simple bending-moment. The asymptotic value of the tension in the edge $y' = 1$ is easily seen to be

$$\widehat{xx}_1 \sim \frac{P}{2b} \left(\frac{3}{2} x' - \frac{3}{\pi} \right),$$

and when $x' = \pi$ this has the value

$$- \frac{P}{2b} (3.757),$$

agreeing almost exactly with the calculated value. It would seem, then, that nothing is to be gained by extending the calculation to larger values of x .

In order to obtain a comparison with the elementary theory of bending we now add a stress system of simple bending-moment type expressed by

$$\widehat{xx} = 3.755 y',$$

and suppose the strip cut at $x' = \pm \pi$, while supported at these sections by the necessary shears. The modified values \widehat{xx}' of the stresses are shown in the last column of each section of Table VI. The conditions are now those shown in fig. 3, the residual tensions on the ends being extremely small. The elementary theory of bending would give for the stress in this case

$$\widehat{xx} = \frac{3P}{4b} (\pi - x') y'.$$

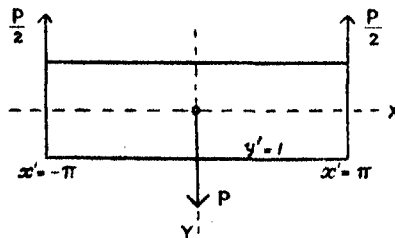


FIG. 3.

Table VI.—Values of Y_7 , Y_8 in Equation (73) and of \widehat{xx} when $\sigma = \frac{1}{b}$; \widehat{xx}' is the Stress when the Cross-sections $x' = \pm \pi$ are Freed from Bending-moment.

x'	$y' = \frac{1}{2}$				$y' = \frac{1}{3}$				$y' = 1$			
	Y_7	Y_8	$2b \cdot \widehat{xx}/P$	$2b \cdot \widehat{xx}'/P$	Y_7	Y_8	$2b \cdot \widehat{xx}/P$	$2b \cdot \widehat{xx}'/P$	Y_7	Y_8	$2b \cdot \widehat{xx}/P$	$2b \cdot \widehat{xx}'/P$
0	2.698	-1.129	0.410	1.862	1.281	0.136	0.462	2.965	1.848	1.534	1.198	4.963
$\pi/6$	—	—	—	—	—	—	—	—	1.005	1.192	0.794	4.549
$\pi/3$	—	—	—	—	—	—	—	—	-1.690	0.398	-0.380	3.375
$\pi/2$	-1.496	-0.005	-0.478	0.774	-2.963	-0.037	-0.925	1.578	-4.473	0.218	-1.313	2.442
$2\pi/3$	—	—	—	—	—	—	—	—	-6.774	0.114	-2.111	1.644
π	-3.936	0.014	-1.248	0.004	-7.874	0.028	-2.495	0.008	-11.814	-0.014	-3.755	0

The distribution of longitudinal stress over the sections $x' = 0$ and $x' = \pi/2$ as predicted by the exact theory and by the elementary theory are shown in fig. 4.

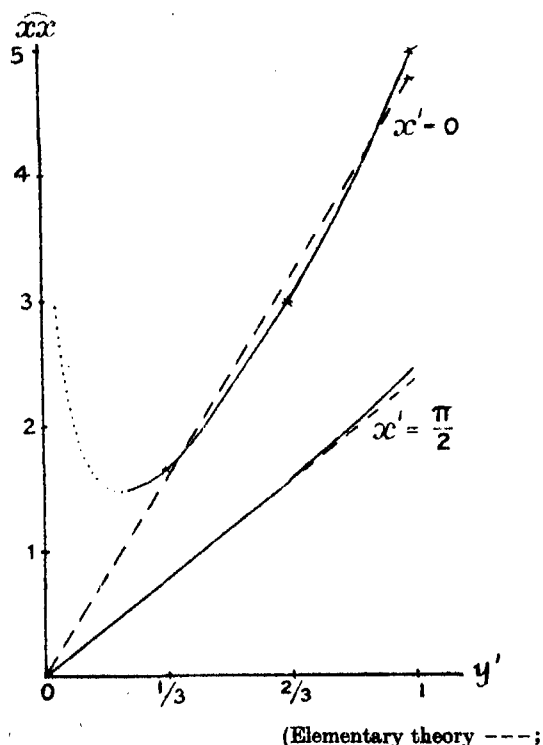


FIG. 4.—Distribution of stress over the sections $x' = 0$, $x' = \pi/2$, when $x' = \pm \pi$ are free from longitudinal stress.

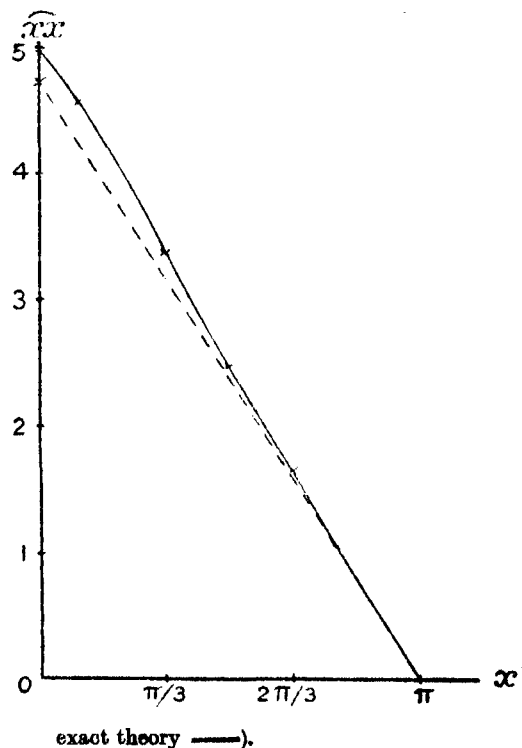


FIG. 5.—Distribution of stress on the edge $y' = 1$, when $x' = \pm \pi$ are free from longitudinal stress.

It is also of interest to compare the stresses in the edge $y' = 1$. Those given by the exact theory when $x' = \pm \pi$ are freed from longitudinal stress are shown in the last column of Table VI. The elementary theory gives the values in Table VII.

Table VII.—Stresses in the Edge $y' = 1$ as given by the Elementary Theory.

x'	σ_{xx}	x'	σ_{xx}
0	4.713	$\pi/2$	2.356
$\pi/2$	4.189	$2\pi/3$	1.571
$\pi/3$	3.142	π	0

Fig. 5 gives a comparison between the two theories.

To summarise the results obtained, we may say that the characteristic effects of an isolated force acting at the centre of the strip are not appreciable at a distance from the force equal to the width of the strip, when the force is longitudinal, or equal to $1\frac{1}{2}$ times the width of the strip when the force is transverse. The conditions at a "freely-supported" end may be closely imitated at any distance exceeding $1\frac{1}{2}$ times the width.

On the Intensity of Total Scattering of X-Rays.

By I. WALLER and D. R. HARTREE.

(Communicated by R. H. Fowler, F.R.S.—Received January 29, 1929.)

Introduction and Summary.

We shall here investigate theoretically the intensity of total scattering of X-rays by atoms distributed at random, *e.g.*, the scattering by the atoms of a monatomic gas. In the scattered radiation we shall not include the characteristic X-rays excited by the incident radiation. The scattered radiation consists then partly of radiation having the same frequency as the incident radiation (coherent scattered radiation) and partly of radiation having other frequencies (incoherent scattered radiation).† For sufficiently high frequency of the incident radiation the incoherent scattered radiation is then nearly monochromatic for a given scattering angle, and consists practically entirely of radiation whose wave-length and intensity is given by the formulæ for the Compton effect for the scattering by free electrons. Generally, however, it must be taken into account that several frequencies occur in the scattered radiation for each direction of scattering. The total intensity of the scattered radiation for a given direction has therefore to be taken as a sum of the intensities of the different components, each having a definite frequency.

General expressions for the scattered radiation are given by a scattering formula derived by one of us.‡ In this formula "relativity corrections" are

† Each of the frequencies in the incoherent scattered radiation corresponds to a transition from the initial state of the scattering atom. The energies of the final states of these transitions may lie in either the discrete or the continuous range of possible energy values.

‡ Waller, 'Z. Physik,' vol. 51, p. 213 (1928).

neglected; for the intensity of scattering in the Compton effect for free electrons, this approximation, and a further one which we also make, lead to the classical Thomson formula. This means that our intensity formula gives a useful approximation only if the incident radiation is not too hard (*e.g.*, has a wave-length not shorter than about 1 Å., in which case the error arising from the approximation just mentioned should not exceed a few per cent.).

In § 1 of this paper we deduce from the general scattering formula just mentioned an expression for the total scattering of the atoms in a gas, approximately valid if the frequency of the incident radiation is essentially higher than the K-absorption frequency of the atoms. In § 2 we apply this formula to the special case of the scattering by helium atoms, taking the wave functions which correspond to the case of vanishing interaction. In order to calculate the scattered radiation in practical cases it is necessary to find approximate wave functions for the initial state of the atom and the application to the simple case of helium makes evident the necessity for using wave functions of the right symmetry properties. This means a complication of the problem which does not arise when we are concerned only with the coherent scattering. In § 3 it is then shown how in most practical cases such wave functions can be formed from wave functions for the separate electrons corresponding to vanishing resonance interaction (neglect of "exchange processes"). These considerations can be directly applied to wave functions for the separate electrons calculated according to a method developed by one of us† which have been found to give results in close agreement with experiment for the coherent scattering.‡ Using these wave functions we get (§ 4) the scattering formula in a more explicit form. In § 5 we treat more generally the relation between our formula for the total scattering and an approximate one which may be derived from consideration concerning the scattering by each electron separately. In § 6 our formula for the total scattering is evaluated numerically for the case of argon, and compared with the experimental results of Barrett.§ Since the wave-lengths used by Barrett are rather short so that for the experimental results "relativity effects" are appreciable, we cannot make a strict comparison. We actually compare the theoretical scattered intensity, given by our formulæ in terms of the *classical* intensity of scattering by a free electron, with the scattered intensity observed by Barrett, expressed in terms

† Hartree, 'Proc. Camb. Phil. Soc.', vol. 24, pp. 89, 114 (1928).

‡ James, Waller and Hartree, 'Roy. Soc. Proc.,' A, vol. 118, p. 334 (1928); James and Brindley, 'Roy. Soc. Proc.,' A, vol. 121, p. 155 (1928).

§ 'Phys. Rev.', vol. 32, p. 22 (1928).

of the intensity of scattering of a free electron given by Dirac's formulæ.† The agreement seems to be satisfactory. The measurements of Barrett seem to be the only one suitable for a comparison with this theory.‡

§ 1. *Deduction of an Approximate Formula for the Total Scattering.*

We shall start from the general scattering formula published in a paper by one of us. The incident radiation may be assumed to consist of a monochromatic plane polarised X-ray wave, the electric vector of this wave being defined by the real part of

$$E_0 e^{2\pi i \nu (t - \mathbf{s} \cdot \mathbf{r}/c)}. \quad (1)$$

We will consider the time $t = 0$ chosen so that E_0 is real. \mathbf{r} is the vector distance from a fixed point, *e.g.*, the nucleus if the wave is scattered by an atom. \mathbf{s} is a unit vector in the direction of propagation of the incident wave.

It can formally be assumed that a state n of the scattering atomic system, atom or molecule, is represented by a single wave function Ψ_n , which is a function of the co-ordinates of the atomic system. The energy of the state n is denoted by E_n . The radiation scattered in any direction defined by the unit vector \mathbf{s}' consists of a number of components, each corresponding to a transition of the scattering system from its initial state n to a final state m . For any direction of scattering it is convenient to describe each component of the scattered radiation (at large distances from the scattering system) by a vector \mathbf{d} , which can be interpreted as the dipole moment which would give that radiation in that direction on the classical theory. The total radiation scattered in the direction \mathbf{s}' by atoms or molecules in the state n is then defined by two sums of such dipole moments

$$\sum_{E_m < E_n + h\nu} (\mathbf{d}_{nm} + \mathbf{d}_{nm}^*) + \sum_{E_m < E_n - h\nu} (\mathbf{d}_{mn} + \mathbf{d}_{mn}^*), \quad (2)$$

where the asterisk denotes the conjugate complex quantity. The frequencies of the components corresponding to the terms in the first and second of these sums are

$$\nu'_{nm} = (E_n - E_m)/h + \nu, \quad \nu'_{mn} = (E_n - E_m)/h - \nu \quad (2')$$

† Dirac, 'Roy. Soc. Proc., A, vol. 3, p. 405 (1926).

‡ Prof. P. Scherrer has kindly informed us about recent measurements made by him and A. Stäger on the total scattering of X-rays by mercury vapour, but there are difficulties in applying the theory to the scattering by such a heavy atom.

§ The final states m will usually include states in which an electron is free, and whose energies belong to the continuous range of possible energy values. In the formal presentation of the theory it is convenient to deal with discrete energy values only; this seems to be justified for the purposes of this paper.

respectively. In the first set of components we can have $m = n$, so that $\nu'_{nm} = \nu$. This component gives the coherent scattered radiation.

The electrons in the scattering system may be numbered $j = 1, 2, \dots, N$, and the position vector of the j th electron may be denoted by \mathbf{r}_j with components x_j, y_j, z_j . The co-ordinates of the nuclei may be denoted by $\mathbf{X}_l, \mathbf{Y}_l, \mathbf{Z}_l$ ($l = 1, 2, \dots, M$). In practice only the electrons will contribute appreciably to the scattered radiation. Taking this into account and making some formal alterations in the formulæ given in *loc. cit.*, we have the following formula for \mathbf{d}_{nm} ,

$$\mathbf{d}_{nm} = -\frac{e^2}{8\pi^2\mu\nu\nu'_{nm}} \left[E_0 D_{nm} + \frac{\hbar^2}{4\pi^2\mu} \sum_u \left\{ \frac{(E_0 \cdot \mathbf{A}_{nu}) \mathbf{A}'^*_{mu}}{\nu_{nu} + \nu} + \frac{(E_0 \cdot \mathbf{A}_{um}) \mathbf{A}'^*_{un}}{\nu_{mu} - \nu} \right\} \right] e^{2\pi i \nu'_{nm} t}, \quad (3)$$

where e and μ are the charge and mass of the electron. Writing dv for the volume element of the configuration space of all particles (electrons and nuclei),† we have

$$dv = \prod_{j=1}^N dx_j dy_j dz_j \prod_{l=1}^M dX_l dY_l dZ_l, \quad (4)$$

$$D_{nm} = \int \Psi_n^* \Psi_m \sum_{j=1}^N e^{\frac{2\pi i}{c}(\nu'_{nm} - \nu)\mathbf{r}_j} dv, \quad (5)$$

$$\left. \begin{aligned} \mathbf{A}_{un} &= \int \Psi_u^* \sum_{j=1}^N e^{-\frac{2\pi i}{c}\nu\mathbf{r}_j} \text{grad}_j \Psi_n dv \\ \mathbf{A}'_{un} &= \int \Psi_u^* \sum_{j=1}^N e^{-\frac{2\pi i}{c}\nu'_{un}\mathbf{r}_j} \text{grad}_j \Psi_n dv \end{aligned} \right\}, \quad (6)$$

We shall assume the initial state n of the atomic system to be its normal state. We are then concerned only with the first sum in (2). We shall further assume that the frequency ν of the incident wave is essentially higher than the K absorption frequency of the atoms in the system. Then the first term in the [] in (3) is the most important, and we shall calculate only that part of the scattered radiation which arises from this term in the expression for each \mathbf{d}_{nm} . This means that we put

$$\mathbf{d}_{nm} = -E_0 \frac{e^2}{8\pi^2\mu\nu\nu'_{nm}} D_{nm}. \quad (7)$$

† For systems more complicated than single atoms each wave function depends on the co-ordinates of the nuclei as well as on those of the electrons, and cannot in general be written as a product of a function of the co-ordinates of the nuclei and a function of the co-ordinates of the electrons. In the following we will be mainly concerned with atoms, for which the co-ordinates of the nucleus can be disregarded.

The intensity of the coherent scattered radiation is then given by

$$I_{\text{coh}} = I_{\text{cl}} |D_{nm}|^2, \quad (8)$$

I_{cl} being the intensity of the scattered radiation calculated according to the classical formula given by J. J. Thomson, and as far as the coherent scattering alone concerned, we get from this simple expression a satisfactory agreement with experimental results.†

It seems justifiable to assume that from (7) we can also get a proper approximation to the total scattering.‡ For the total intensity of all the components of the scattered radiation we get from (2) and (7)

$$I_{\text{tot}} = I_{\text{cl}} \sum_{E_m < E_n + h\nu} \left(\frac{\nu'_{nm}}{\nu} \right)^2 |D_{nm}|^2. \quad (9)$$

We shall now make the further assumption that all components giving an appreciable intensity have frequencies ν'_{nm} not very different from ν . This seems to be justified according to an earlier investigation of the scattering by an atom containing only one electron.§ We can then put $\nu'_{nm} = \nu$ in the right side of (9). For a similar reason we extend the summation over all states m . Writing D'_{nm} for the quantity obtained by putting $\nu'_{nm} = \nu$ in D_{nm} , that is

$$D'_{nm} = \int \Psi_n^* \Psi_m \sum_{j=1}^N e^{\frac{2\pi i \nu}{c} (\mathbf{s}' - \mathbf{s}) \cdot \mathbf{r}_j} dv, \quad (10)$$

we have to the approximation considered

$$I_{\text{tot}} = I_{\text{cl}} \sum_m |D'_{nm}|^2. \quad (11)$$

The quantities D'_{nm} defined by (10) can be interpreted as coefficients in an expansion in terms of wave functions; we have in fact

$$\Psi_n^* \sum_{j=1}^N e^{\frac{2\pi i \nu}{c} (\mathbf{s}' - \mathbf{s}) \cdot \mathbf{r}_j} = \sum_m D'_{nm} \Psi_m^*.$$

† See James, Waller and Hartree, *loc. cit.*

‡ A general discussion of the terms neglected in the approximation given by (7) is difficult, but for the one-electron problem it can be shown that they are small (a) for coherent scattering and $h\nu \gg$ ionisation energy, (b) for $h\nu/c \gg M_n$ where M_n is the mean momentum in the initial state (*cf.* Waller, 'Phil. Mag.', vol. 4, p. 1228 (1927)). It does not seem that there is likely to be any essential difference in order of magnitude of these terms for coherent scattering and incoherent scattering with ν'_{nm} nearly equal to ν .

§ Waller, 'Phil. Mag.', *loc. cit.*

Since the set of normal orthogonal functions Ψ_m^* must be assumed to be a complete set, we have

$$\begin{aligned}\sum_m |D'_{nm}|^2 &= \int \left| \Psi_m^* \sum_{j=1}^N e^{\frac{2\pi i \nu}{c}(\mathbf{s}' - \mathbf{s}) \cdot \mathbf{r}_j} \right|^2 dv \\ &= \int |\Psi_m^*|^2 \left| \sum_{j=1}^N e^{\frac{2\pi i \nu}{c}(\mathbf{s}' - \mathbf{s}) \cdot \mathbf{r}_j} \right|^2 dv.\end{aligned}\quad (12)$$

The total intensity of the scattered radiation is given by (11) and (12) to the approximation considered here.†

These formulæ are not necessarily restricted to the normal state of the atom (or molecule); they apply also to the scattering by an atomic system in any low state.

For an atom containing only one electron, it follows that

$$\sum_m |D'_{nm}|^2 = 1. \quad (13)$$

Thus to the approximation considered here, the total intensity of scattering by an atom containing a single electron is given by the Thomson formula for a free electron, which is a result found earlier. We will write R for the ratio of the intensity of total scattering by a many-electron atom to the classical intensity of scattering by a free electron. Then from (11) and (12) it follows that to this approximation where

$$R = I_{\text{tot}}/I_{\text{cl}} = \int |\Psi_m^*|^2 \left| \sum_{j=1}^N \exp(i\kappa \mathbf{r}_j) \right|^2 dv, \quad (14)$$

where

$$\kappa = 2\pi\nu(\mathbf{s}' - \mathbf{s})/c. \quad (14')$$

In the deduction of the general scattering formula a wave equation was used in which no account was taken of the spin of the electrons. In using this scattering formula we can therefore take the spin into account only as far as it is connected by Pauli's principle with the wave function in the co-ordinate space of the electrons. It seems justified to assume that we get in this way a proper approximation. The deduction just mentioned also rests on the assumption that we can represent each spectral term by one wave function. The validity of this assumption follows from the investigations on non-combining sets of wave functions, which we shall consider more closely in § 3.

† The possibility of devising a formula for the total scattering by a many-electron atom according to the same principle (use of "Vollständigkeits theorem") as had been used by Wentzel ('Z. Physik,' vol. 43, p. 1 (1927)) and one of us (J. Waller, 'Phil. Mag.,' *loc. cit.*) for a one-electron atom was first mentioned by Prof. W. Pauli in a discussion about this problem.

Further approximations have been made in that relativity effects have been neglected and in putting $v'_{nm} = v$. The results may, therefore, be expected to apply best to the scattering of radiation of not too short a wave-length by the lighter atoms.

§ 2. Discussion of a Special Case.

We will apply the formulæ (10) and (14) to the total scattering by a helium atom, as this simple case will illustrate the main points which arise in the treatment of a more general case.

We take the wave functions for the limit of vanishing interaction, when they can be written as sums of products of the wave functions of the two separate electrons, and consider first the scattering by a helium atom in an excited triplet state, for which the spins of the electrons are parallel, so the wave function must be antisymmetrical in the position co-ordinates of the two electrons.†

Thus for the initial state n we take

$$\Psi_n = \frac{1}{\sqrt{2}} [\psi_1(1) \psi_2(2) - \psi_2(1) \psi_1(2)], \quad (15)$$

and consider the scattering of the component of the radiation corresponding to a transition to state m with wave function

$$\Psi_m = \frac{1}{\sqrt{2}} [\psi_{m_1}(1) \psi_{m_2}(2) - \psi_{m_2}(1) \psi_{m_1}(2)]. \quad (16)$$

We will write

$$dx_j dy_j dz_j = dv_j.$$

$$\int \psi_a^*(j) \exp(i\mathbf{kr}_j) \psi_\beta(j) dv_j = f_{a\beta}. \quad (17)$$

All the ψ 's are orthogonal, as they are wave functions for one electron in the limit of vanishing interaction, so substituting (14'), (15), (16) in (10) and carrying out the integration we have

$$|D'_{nm}|^2 = 0 \quad \text{when } m_1, m_2 \text{ both different from 1 and 2} \quad (a)$$

$$= |f_{11} + f_{22}|^2 \quad \text{when } m_1 = 1, m_2 = 2 \text{ or } m_1 = 2, m_2 = 1 \quad (b)$$

$$\left. \begin{aligned} &= |f_{2, m_1}|^2, |f_{2, m_1}|^2 \quad \text{when } m_1 = 1, m_2 \neq 1, 2 \\ &\quad \text{or } m_2 = 1, m_1 \neq 1, 2 \text{ respectively} \\ &= |f_{1, m_1}|^2, |f_{1, m_1}|^2 \quad \text{when } m_1 = 2, m_2 \neq 1, 2 \\ &\quad \text{or } m_2 = 2, m_1 \neq 1, 2 \text{ respectively} \end{aligned} \right\} \quad (c)$$

$$= 0 \quad \text{when } m_1 = m_2 = 1 \text{ or } 2. \quad (d)$$

† Cf. Heisenberg, 'Z. Physik,' vol. 38, p. 411 (1926).

The result (a) indicates that the (to the approximation considered) incident radiation does not give rise to simultaneous transitions of both electrons; (b) gives the intensity of the coherent scattering, and (c) and (d) the intensities of components of the incoherent scattering. If only one electron were present, say with wave function ψ_1 , $|f_{11}|^2$ would be the intensity of coherent scattering [cf. (8)] and $|f_{1, m_1}|^2, |f_{1, m_2}|^2$ the intensities of two components of the incoherent scattering; the total intensity of incoherent scattering would be $1 - |f_{11}|^2$ by (13).

We see from (b) and (c) that for the scattering by a helium atom we must add the amplitudes of the coherent waves scattered by single electrons with the two wave functions ψ_1, ψ_2 present in the initial state of the atom, and must add the intensities of the incoherent waves scattered by these electrons, with one important exception. This exception is given by result (d), that (with anti-symmetrical wave functions) transitions to the states $m_1 = m_2 = 1$ or 2 cannot occur. For a single electron these transitions could occur, so if we wish to use the results for one electron to deduce the total scattering by a helium atom, we must take account of the fact that the corresponding component of the scattered radiation is absent. For one electron this component has the intensity $|f_{12}|^2$, so the total scattering by a helium atom is given by

$$\begin{aligned} R &= |f_{11} + f_{22}|^2 + 1 - |f_{11}|^2 + 1 - |f_{22}|^2 - 2|f_{12}|^2 \\ &= 2 + f_{11}f_{22}^* + f_{11}^*f_{22} - 2|f_{12}|^2. \end{aligned} \quad (18)$$

The same result follows by substituting (15) in (14); the object of the deduction here given is to show the origin of the term $-2|f_{12}|^2$. This term will in general be small when the frequency of the exchange of electrons 1 and 2 is small.

If the initial state has the symmetrical wave function

$$\Psi_* = \frac{1}{\sqrt{2}}[\psi_1(1)\psi_2(2) + \psi_2(1)\psi_1(2)],$$

we find similarly

$$R = 2 + f_{11}f_{22}^* + f_{11}^*f_{22} + 2|f_{12}|^2.$$

In this case it should be noted that the probability of a transition to a state in which both electrons have the same space wave function is different from the probability of the corresponding transition of one electron if the presence of the other is neglected.

If we had taken the wave function $\Psi = \psi_1(1)\psi_2(2)$ for the initial state, we would have found

$$R = 2 + f_{11}f_{22}^* + f_{11}^*f_{22}.$$

The difference between this and formula (18) shows that in calculating the total scattering by a many-electron atom it is necessary to consider carefully the question of the proper wave function by which to represent the initial state of the scattering atom. This question we now investigate.

§ 3. *On the Formation of Approximate Wave Functions of required Symmetry Properties for an Atom containing several Electrons.*

We consider an atom containing N electrons. The spin of the electrons is taken into account only as far as it is connected by Pauli's principle with the wave function in the co-ordinate space of the electrons.

Introducing external electric and magnetic fields as weak as we like, we may ensure that the system does not contain any degeneracy but that caused by the identity of the electrons. This means that from any wave function belonging to a characteristic of the Schrödinger equation (that is, to a spectral term) we can form by permutations of the electron numbers and linear combinations all wave functions belonging to the same term. All the wave functions of the atom can be grouped in a number of non-combining sets ("systems").†

We denote a wave function by $\Psi(1, 2, \dots N)$, j standing for x_j, y_j, z_j (the co-ordinates of one electron) ($1 \leq j \leq N$), and by $F(1, 2, \dots N)$ an arbitrary function or operator, symmetrical in all electron numbers $1, 2, \dots N$. Then, if Ψ' is a wave function belonging to another system, we have

$$\int \Psi'^* F \Psi dv = 0, \quad dv = \prod_{k=1}^N dx_k dy_k dz_k.$$

To each characteristic E_k in one of the systems belongs the same number f of linearly independent wave functions $\Psi_i^{(k)}(1, 2, \dots n)$, $i = 1, 2, \dots f$. According to Wigner (*loc. cit.*) these wave functions can be chosen in such a way that for any two terms E_k and $E_{k'}$ belonging to the same system

$$\int \Psi_i^{(k)*} F(1, 2, \dots n) \Psi_l^{(k')} dv = C \delta_{kl}, \quad \delta_{kl} = \begin{cases} 1 & l = k' \\ 0 & l \neq k' \end{cases},$$

the value of C being independent of l and l' but, of course, dependent on F and k, k' . This equation is valid also for $k = k'$ (i.e., $E_k = E_{k'}$). The normalisation condition means that $C = 1$ for $F = 1$. The expansion of $F(1, 2, \dots n) \Psi_i^{(k)}$

† Heisenberg, *loc. cit.*, and 'Z. Physik,' vol. 41, p. 239 (1927); Dirac, 'Roy. Soc. Proc.,' A, vol. 112, p. 661 (1926); Wigner, 'Z. Physik,' vol. 40, pp. 492, 883 (1926-7), and vol. 43, p. 624 (1927); Hund, 'Z. Physik,' vol. 43, p. 788 (1927); Delbrück, 'Z. Physik,' vol. 51, p. 181 (1928).

in terms of wave functions therefore involves only wave functions with the same suffix l , and has accordingly the form $F\Psi_i^{(k)} = \sum_k A_k \Psi_i^{(k)}$, so that an adequate representation of spectral terms by wave functions can be made by taking one of these wave functions $\Psi_i^{(k)}$ for each term, l being the same for all terms of the system. We can easily prove that for the evaluation of any matrix element $F_{kk'}$ of the symmetrical function $F(1, 2, \dots, n)$ we can just as well represent each term by the general wave function

$$\Psi_a^{(k)} = \sum_{l=1}^f a_l \psi_l^{(k)},$$

if the a_l 's are the same for all terms, and if, according to normalisation condition, $\sum_{l=1}^f |a_l|^2$ is equal to unity. We have in fact

$$\int \Psi_a^{(k)*} F \Psi_a^{(k)} dv = \sum_{ll'} a_l a_{l'} \int \Psi_l^{(k)*} F \Psi_{l'}^{(k)} dv = C.$$

In evaluating the integral (14) for the total intensity scattered, we can therefore use for the initial state n any wave function which has the right symmetry properties.

Each system is characterised by the symmetry properties of the wave functions belonging to it, and it follows from Pauli's principle that only certain types of symmetry are actually possible. Using the notation of symmetry characters introduced by Hund (*loc. cit.*) we can represent any system allowed by Pauli's principle by the symbol

$$A(N - q, q) \quad (q \leq N/2) \quad (19)$$

known as the antisymmetry character of the system. This symbol means that from any wave function belonging to this system we can form a wave function antisymmetrical in $N - q$ electrons, and in the other q electrons by permutation of electron numbers and linear combination. Using the notation that a bar under the electron numbers indicated that the wave function is antisymmetrical in these electrons, this wave function can be written

$$\Psi(\bar{1}, 2, \dots, \bar{N - q}, N - q + 1, N - q + 2, \dots, N) \quad (20)$$

The antisymmetry character (19) also means that by the procedure just mentioned we cannot form any wave function antisymmetrical in more than $N - q$ electron numbers, and the wave function (20) which is itself antisymmetrical in $N - q$ electrons and in the other q electrons, is known as the "antisymmetrical normal form" of the wave function of the system.†

† The "degree of degeneracy" of this system is $f = N! / (N - 2q + 1)! q! (N - q + 1)!$ (Wigner, *loc. cit.*). The multiplicity of each "term" due to the spins is $N - 2q + 1$ (Heisenberg, Wigner, *loc. cit.*).

The simplest interpretation of q is this ; if the electrons are divided into two groups of opposite spin, $N - q$ and q are the numbers in the larger and smaller groups respectively.

If the solution of the wave equation involves a degeneracy of any kind other than that caused by the identity of the particles, the considerations just mentioned can no longer be applied directly.

Since the many-electron problem cannot be solved exactly, it is necessary to use an approximate wave function. A suitable approximation is provided by considering each electron to be in a stationary state in the field of the nucleus and remaining electrons. In this approximation the interaction of the electrons is taken into account in so far as it can be expressed by a static field acting on each electron, but its essentially dynamical character, involving the interchange of electrons, is neglected. We will express this by saying that we neglect the "resonance interaction."

In this way approximate wave functions for the single electrons are found, and from them we have to form a wave function for the whole atom with definite symmetry properties. This problem is closely related to some investigations by Heisenberg, Wigner and Delbrück (*loc. cit.*), who have studied the wave functions of an atom by treating any interaction as a perturbation. We shall here treat the problem in a different way which makes it possible in cases of practical importance to find directly wave functions of zero order of approximation which have the required symmetry characters.

The use of a static field acting on each electron as an approximate expression of the interaction of the electrons provides deviations from a Coulomb field, and in order that the wave functions for the single electrons in the limit of vanishing resonance interaction shall be non-degenerate, we can assume a homogeneous magnetic field in addition.

The various wave functions for the individual electrons in the atomic state considered will be written

$$\psi_{\alpha_1}(j), \psi_{\alpha_2}(j) \dots \psi_{\alpha_N}(j), \quad (21)$$

j denoting the space co-ordinates of a single electron. These wave functions (*i.e.*, the suffixes $\alpha_1, \alpha_2, \dots \alpha_N$) need not all be different, but according to Pauli's principle each one can be identical with not more than one other, and any two which are identical must be wave functions of electrons of opposite spin. Two electrons having the same space wave function and opposite spins may be called a "closed pair" ; we will write s for the number of closed pairs ; clearly

$s \leq q$. If there are s closed pairs, we can suppose the wave functions so numbered that $\alpha_1 \dots \alpha_{N-s}$ are all different, and

$$\alpha_{N-s+1} = \alpha_1, \quad \alpha_{N-s+2} = \alpha_2, \dots, \quad \alpha_N = \alpha_s.$$

In the limit of vanishing interaction, any wave function for the whole system can be expressed in the form†

$$\sum_{(a)} C_{(a)} \psi_{a_1}(a_1) \psi_{a_2}(a_2) \dots \psi_{a_N}(a_N), \quad (21)$$

$(a) = (a_1, a_2, \dots, a_N)$ being any permutation of the electron numbers $1 \dots N$, and the $C_{(a)}$'s being constants. An expression of the form (21) will not generally have a definite symmetry character; on the other hand, if we take the resonance interaction of the electrons into account we must get perturbed wave functions of definite symmetry characters. We consider a set of perturbed wave functions belonging to a given term; these have a definite anti-symmetry character (19) and normal form (20); we wish to form wave functions of the type (21) which shall be the limit of these perturbed wave functions as the perturbation tends to zero; that is to say, we want to determine the coefficients $C_{(a)}$ in (21) so that this expression has the symmetry of this normal form.

Putting $N - q = p$ (we must have $p \geq q$, since $q \leq N/2$) we must have in the limit

$$\Psi(1, 2, \dots, p, p+1, p+2, \dots, p+q) = \sum_{(a)} C_{(a)} \psi_{a_1}(a_1) \psi_{a_2}(a_2) \dots \psi_{a_N}(a_N).$$

By arranging the factors in each product in the sum in such a way that the electron numbers have their natural order, we get

$$\begin{aligned} \Psi(1, 2, \dots, p, p+1, p+2, \dots, p+q) \\ = \sum_{(\beta)} C_{(\beta)} \psi_{\beta_1}(1) \psi_{\beta_2}(2) \dots \psi_{\beta_p}(p) \psi_{\beta_{p+1}}(p+1) \dots \psi_{\beta_{p+q}}(p+q) \end{aligned}$$

where $(\beta) = (\beta_1, \beta_2, \dots, \beta_{p+q})$ is a permutation of the suffixes $(\alpha_1, \alpha_2, \dots, \alpha_{p+q})$. We now permute $(1, 2, \dots, p)$ into $(b) = (b_1, b_2, \dots, b_p)$, multiply both sides of the equation by -1 if the permutation is an odd one, and sum for all permutations. This gives

$$\begin{aligned} p! \Psi(1, 2, \dots, p, p+1, p+2, \dots, p+q) \\ = \sum_{(\beta)} C_{(\beta)} \left[\sum_{(b)} (-)^{(b)} \psi_{\beta_1}(b_1) \dots \psi_{\beta_p}(b_p) \right] \psi_{\beta_{p+1}}(p+1) \dots \psi_{\beta_{p+q}}(p+q), \end{aligned}$$

† It is convenient to use Roman letters for the electrons and Greek letters as suffixes to distinguish the various wave functions for one electron.

where $(-)^{b_i}$ means $+1$ or -1 according as (b) is an even or odd permutation of $(1, 2, \dots, p)$. Then permuting $(p+1, p+2, \dots, p+q)$ into

$$(b') = (b_{p+1}, b_{p+2} \dots b_{p+q})$$

we get in the same way

$$\begin{aligned} p! q! \Psi(1, 2, \dots, p, p+1, p+2, \dots, p+q) \\ = \sum_{(\beta)} C_{(\beta)} \left[\sum_{(b)} (-)^{b_i} \psi_{\beta_1}(b_1) \dots \psi_{\beta_p}(b_p) \right] \left[\sum_{(b')} (-)^{b'_j} \psi_{\beta_{p+1}}(b_{p+1}) \dots \psi_{\beta_{p+q}}(b_{p+q}) \right] \\ = \sum_{(\beta)} C_{(\beta)} \begin{vmatrix} \psi_{\beta_1}(1) & \dots & \psi_{\beta_p}(1) \\ \vdots & & \vdots \\ \psi_{\beta_1}(p) & \dots & \psi_{\beta_p}(p) \end{vmatrix} \begin{vmatrix} \psi_{\beta_{p+1}}(p+1) & \dots & \psi_{\beta_{p+q}}(p+1) \\ \vdots & & \vdots \\ \psi_{\beta_{p+1}}(p+q) & \dots & \psi_{\beta_{p+q}}(p+q) \end{vmatrix}. \quad (22) \end{aligned}$$

The sum on the right side might contain terms corresponding to any permutation $(\beta) = (\beta_1 \dots \beta_{p+q})$ of $(\alpha_1 \dots \alpha_{p+q})$ (i.e., of the suffixes of the wave functions of the separate electrons), including interchanges of one or more wave functions between the two determinants.

If $s = q$ we can from (22) definitely find a unique expression for

$$\Psi(1, 2, \dots, p, p+1, p+2, \dots, p+q)$$

for vanishing resonance interaction. The number of suffixes $\alpha_1 \dots \alpha_N$ which are different is $N - s$, and in the case of $s = q$ this number is equal to p , these different suffixes being $\alpha_1 \dots \alpha_p$. In any non-vanishing term of the sum on the right-hand side of (22), $\beta_1 \dots \beta_p$ must be all different, and also $\beta_{p+1} \dots \beta_{p+q}$. In the case $s = q$, $\beta_1 \dots \beta_p$ must therefore be a permutation of $\alpha_1 \dots \alpha_p$ and $\beta_{p+1} \dots \beta_{p+q}$ a permutation of $\alpha_{p+1} \dots \alpha_{p+q}$. We therefore get from (22)

$$\begin{aligned} p! q! \Psi(1, 2, \dots, p, p+1, p+2, \dots, p+q) \\ = \left[\sum_{(\beta)} \pm C_{(\beta)} \right] \begin{vmatrix} \psi_{\alpha_1}(1) & \dots & \psi_{\alpha_p}(1) \\ \vdots & & \vdots \\ \psi_{\alpha_1}(p) & \dots & \psi_{\alpha_p}(p) \end{vmatrix} \begin{vmatrix} \psi_{\alpha_{p+1}}(p+1) & \dots & \psi_{\alpha_{p+q}}(p+1) \\ \vdots & & \vdots \\ \psi_{\alpha_{p+1}}(p+q) & \dots & \psi_{\alpha_{p+q}}(p+q) \end{vmatrix} \end{aligned}$$

which means that

$$\begin{aligned} \Psi(1, 2, \dots, p, p+1, p+2, \dots, p+q) \\ = A \begin{vmatrix} \psi_{\alpha_1}(1) & \dots & \psi_{\alpha_p}(1) \\ \vdots & & \vdots \\ \psi_{\alpha_1}(p) & \dots & \psi_{\alpha_p}(p) \end{vmatrix} \begin{vmatrix} \psi_{\alpha_{p+1}}(p+1) & \dots & \psi_{\alpha_{p+q}}(p+1) \\ \vdots & & \vdots \\ \psi_{\alpha_{p+1}}(p+q) & \dots & \psi_{\alpha_{p+q}}(p+q) \end{vmatrix} \quad (23) \end{aligned}$$

A being a constant.

If $s < q$, the number $N - s$ of different suffixes α is greater than p . We can by the method just mentioned get some information also in this case, i.e., that Ψ can be expressed as a sum of products of two determinants of orders p and q .

It appears that the condition $s = q$, for which the wave function can be expressed as a single product of two determinants, is usually, and perhaps always, satisfied for the normal state of an atom or ion. For we have the rule, at first stated empirically from the results of the analyses of complex spectra,[†] and later given a theoretical basis by Heisenberg,[‡] that of the different multiplet arising from a set of electrons with given space quantum numbers, the term of greatest multiplicity generally lies deepest and for the deepest terms no exceptions are known.|| But this term is just the one for which the spins of all electrons not in closed pairs are parallel, which is the case $s = q$.

If for homopolar molecules we form an approximate wave function in terms of the unperturbed wave functions of the component atoms after the method of Heitler and London,[¶] the condition $s = q$ does not hold for them, as each homopolar bond essentially involves two electrons, not members of closed pairs, with different spins and *different* wave functions, one from each atom. This can be seen already by considering the normal electronic state of the hydrogen molecule. But another approximation would be to consider each of the binding electrons as in a stationary state in the field of the nuclei and other electrons of *both* atoms, and it might be found that with this approximation, the two electrons have the same wave function, in which case the condition $s = q$ would apply here also.

§ 4. *Application of Approximate Wave Functions to Formula for Total Scattering.*

It is more convenient now to distinguish the different wave functions of a single electron by numerical suffixes, or generally by single Greek letter suffixes. Those in the first determinant in (23) will be written $\psi_1, \psi_2, \dots \psi_p$, and those in the second determinant will be written $\psi_{p+1}, \psi_{p+2}, \dots \psi_{p+q}$. Also we will write $1; p$ as an abbreviation for "the electrons 1 to p "; and $dv_{1;p}$ for

[†] See F. Hund, "Linienpektren," p. 124.

[‡] Heisenberg, 'Z. Physik,' vol. 41, p. 239, especially p. 257.

|| Hund, *op. cit.*

[¶] 'Z. Physik,' vol. 44, p. 455 (1927); London, 'Z. Physik,' vol. 46, p. 455 (1928).

the volume element of the co-ordinate space of these electrons, and will put

$$\Delta(1; p) = \begin{vmatrix} \psi_1(1) & \dots & \psi_p(1) \\ \vdots & \ddots & \vdots \\ \psi_1(p) & \dots & \psi_p(p) \end{vmatrix}, \quad \Delta'(p+1; p+q) = \begin{vmatrix} \psi_{p+1}(p+1) & \dots & \psi_{p+q}(p+1) \\ \vdots & \ddots & \vdots \\ \psi_{p+1}(p+q) & \dots & \psi_{p+q}(p+q) \end{vmatrix}, \quad (24)$$

so that the wave function (23) for an atom consisting of q closed pairs, and $p - q$ additional electrons all of the same spin, can be written

$$\psi = A \Delta(1; p) \Delta'(p+1; p+q). \quad (25)$$

If the wave functions $\psi_1 \dots \psi_p$ were different wave functions for a single electron in approximately the same field of force, they would be orthogonal; actually they are wave functions of a single electron in a field of force which is slightly different for different electrons, but it will be assumed for the present that they are exactly orthogonal, and departures from this will be considered later. In the case considered each of the wave functions in the second determinant is the same function of its arguments as a wave function in the first determinant, but in this section it will not be necessary to make use of this property.

In working with wave functions which involve such determinants, it is convenient to use the following notation. For a determinant of order p we write

$$\begin{aligned} \epsilon_{\alpha\beta\gamma\dots\pi} &= 0 \quad \text{unless } \alpha\beta\gamma\dots\pi \text{ are all different,} \\ &= 1 \quad \text{if } \alpha\beta\gamma\dots\pi \text{ is an even permutation of } 1, 2, 3, \dots, p, \\ &= -1 \quad \text{if } \alpha\beta\gamma\dots\pi \text{ is an odd permutation of } 1, 2, 3, \dots, p, \\ \delta_{\alpha\beta} &= 1 \quad \text{if } \alpha = \beta, \\ &= 0 \quad \text{if } \alpha \neq \beta. \end{aligned}$$

Further it is convenient to adopt the convention that in a product or in a single term a repeated Greek letter suffix indicates summation over all relevant values of that suffix (this notation is suggested by the "summation convention" of the calculus of tensors†). The determinant $\Delta(1; p)$ can then be written

$$\Delta(1; p) = \epsilon_{\alpha\beta\gamma\dots\pi} \psi_\alpha(1) \psi_\beta(2) \dots \psi_\pi(p), \quad (26)$$

the summations being over the values 1 to p for each of the repeated suffixes.

† Eddington, 'Mathematical Theory of Relativity,' p. 50.

The following properties of the coefficients $\varepsilon_{\alpha\beta\gamma\dots\pi}$ are required

$$\left. \begin{aligned} \varepsilon_{\alpha\beta\gamma\dots\pi} \varepsilon_{\alpha\beta\gamma\dots\pi} &= p! \\ \varepsilon_{\alpha\beta\gamma\dots\pi} \varepsilon_{\alpha'\beta\gamma\dots\pi} &= (p-1)! \delta_{\alpha\alpha'} \\ \varepsilon_{\alpha\beta\gamma\dots\pi} \varepsilon_{\alpha'\beta'\gamma\dots\pi} &= (p-2)! (\delta_{\alpha\alpha'} \delta_{\beta\beta'} - \delta_{\alpha\beta'} \delta_{\alpha'\beta}) \end{aligned} \right\}. \quad (27)$$

Since the wave functions $\psi_\alpha \dots \psi_\pi$ are taken to be orthogonal, we have

$$\int \psi_\alpha^*(j) \psi_\beta(j) dv_j = \delta_{\alpha\beta} \quad (28)$$

where $dv_j = dx_j dy_j dz_j$; and if F is a function of the co-ordinates of any one electron, we will write

$$\int \psi_\alpha^*(j) F(j) \psi_\beta(j) dv_j = F_{\alpha\beta}, \quad (29)$$

and will write $F_{\alpha\beta}^*$ for the conjugate of $F_{\alpha\beta}$, it is the $\beta\alpha$ component of $[F(j)]^*$.

From (26) to (29) it follows that

$$\int |\Delta(1; p)|^2 dv_1; p = p! \quad (30)$$

$$\int |\Delta(1; p)|^2 F(j) dv_1; p = (p-1)! F_{\alpha\alpha} \quad (1 \leq j \leq p), \quad (31)$$

$$\begin{aligned} \int |\Delta(1; p)|^2 F(j) [F(k)]^* dv_1; p &= (p-2)! [F_{\alpha\alpha} F_{\beta\beta}^* - F_{\alpha\beta} F_{\alpha\beta}^*] \\ &\quad (j \neq k; 1 \leq j \leq p, 1 \leq k \leq p). \end{aligned} \quad (32)$$

The first of these results gives directly the normalisation of the wave function (25), viz.

$$A^2 p! q! = 1. \quad (33)$$

The formula (14) for the intensity of total scattering can be written

$$R = p + q + \sum'_{j, k=1}^{p+q} \int |\Psi_\pi|^2 e^{i\mathbf{k} \cdot (\mathbf{r}_j - \mathbf{r}_k)} dv_1; p+q, \quad (34)$$

where Σ' denotes that the terms $j = k$ are omitted from the sum. There are two main types of terms in the sum according as the electrons j, k occur as arguments of wave functions in the same determinant or different determinants in (25) (i.e., according as these electrons have the same or different spin); in the former case the integral reduces to one of the type (32) and in the second to a product of two of type (31). We will write

$$\int \psi_\alpha^*(j) \exp(i\mathbf{k}\mathbf{r}_j) \psi_\beta(j) dv_j = f_{\alpha\beta},$$

(cf. (17)), and use suffixes without and with a dash to refer to wave functions in the first and second of the determinants (24) respectively. Then using (31), (32) the value of R found from (34) to be

$$R = p + q + (f_{aa} + f_{a'a'}) (f_{\beta\beta}^* + f_{\beta'\beta'}^*) - f_{a\beta} f_{a\beta}^* - f_{a'\beta'} f_{a'\beta'}^*. \quad (35)$$

We will require the result that the value of R given by (35) is invariant for certain orthogonal transformations of the wave functions ψ occurring in either determinant.

Suppose the coefficients $a_{\xi a}$ define an orthogonal transformation of $\psi_1 \dots \psi_p$

$$\phi_\xi = a_{\xi a} \psi_a. \quad (36)$$

We are taking the ψ 's as orthogonal, and the condition that the ϕ 's should be orthogonal is therefore

$$a_{\xi a} a_{\eta a}^* = \delta_{\xi\eta}$$

whence also

$$a_{\xi a} a_{\xi\beta}^* = \delta_{a\beta}. \quad (37)$$

Corresponding to (29) we define matrix elements R' involving the wave functions ϕ by

$$R'_{\xi\eta} = \int \phi_\xi^*(j) F(j) \phi_\eta(j) dv_j,$$

and from (36), we find

$$R'_{\xi\eta} = a_{\xi a}^* a_{\eta\beta} R_{a\beta},$$

so by (37)

$$\begin{aligned} R'_{\xi\xi} &= a_{\xi a}^* a_{\xi\beta} R_{a\beta} = \delta_{a\beta} R_{a\beta} = R_{aa} \\ R'_{\xi\eta} R'_{\xi\eta}^* &= a_{\xi a}^* a_{\eta\beta} R_{a\beta} a_{\xi\gamma}^* a_{\eta\epsilon}^* R_{\gamma\epsilon}^* \\ &= \delta_{a\gamma} \delta_{\beta\epsilon} R_{a\beta} R_{\gamma\epsilon}^* = R_{a\beta} R_{a\beta}^*, \end{aligned}$$

so that each term in (35) is invariant for an orthogonal transformation of the ψ 's occurring in either determinant separately.

It may be emphasised that in (35) the sums indicated by the repeated suffixes are to be taken over the *wave functions* occurring in one or other determinant, not over the separate electrons. Indeed, the contributions to R expressed by the sum in (34) are essentially from *pairs* of electrons, not from single electrons, and the contribution from all pairs of electrons occurring as arguments of the wave functions in a single determinant are the same, and so are the contributions from all pairs of electrons which occur as arguments of the wave functions in different determinants. This arises from the form (25) used for the wave function of the whole system, in which we cannot associate any particular electron with any particular wave function, and conforms to

the principles of the quantum-mechanical treatment of the many-body problem, in which the interchange of the electrons plays an essential part.

Nevertheless it is convenient as a conventional manner of speaking to describe the behaviour of an atom in a way which does appear to assign each electron to a single wave function, as when we speak of an atom having 2 K-electrons, 6 L-electrons, etc. We can do this by relating electrons to wave functions by a single term in the expansion of the determinant, say by the product of the elements of the principal diagonal.

Then indicating these electrons by ordinary letter suffixes, and retaining the summation sign for them, (35) becomes†

$$R_1 = p + q + \left[\sum_{j=1}^{p+q} f_{jj} \right]^2 - \sum_{j=1}^{p+q} |f_{jj}|^2 = \left[\sum_{j,k=1}^p + \sum_{j,k=p+1}^{p+q} \right] |f_{jk}|^2. \quad (38)$$

This formulæ gives the theoretical value of R_1 the ratio of the total intensity of scattering by a many electron atom to the classical intensity of scattering by a free electron, to the approximation explained in §2. If R_F is the value of R for scattering by the same number $p + q$ of free electrons, then to the same approximation, $R_F = p + q$. $R - R_F$ may be called the "excess scattering" due to the space distribution of the electrons, and $(R/R_F) - 1$ the "excess scattering per electron." It seems probable that R/R_F or $(R/R_F) - 1$ is the most suitable quantity in terms of which to make comparison with experiment, as the approximations made seem likely to have the same kind of effect on R and on R_F .

§ 5. *The Relation between the Scattering by a Many-electron Atom and that by a One-electron Atom.*

If we consider the j th electron alone, f_{jj} is the amplitude and $|f_{jj}|^2$ the intensity of the coherent scattering (cf. (8)) and since $R = 1$ for one electron (cf. (13)), $1 - |f_{jj}|^2$ is the intensity of the incoherent scattering.‡ If we tried to treat the scattering by a many-electron atom by adding the scattering by a number of independent single electrons, we would add the amplitudes of

† We have $f_{\alpha\alpha} + f_{\alpha'\alpha'} = f_{\beta\beta} + f_{\beta'\beta'} = f_{jj}$. The term $\Sigma |f_{jj}|^2$ arises from the terms $\alpha = \beta$ and $\alpha' = \beta'$ in $f_{\alpha\beta}f_{\alpha\beta}^*$ and $f_{\alpha'\beta'}f_{\alpha'\beta'}^*$, the terms $\Sigma' |f_{jk}|^2$ arise from the terms $\alpha \neq \beta$ and $\alpha' \neq \beta'$ in these product-sums.

‡ These amplitudes and intensities are in terms of the amplitude and intensity of classical scattering by a free electron.

the coherent waves scattered by the separate electrons, and the intensities of the incoherent waves, and obtain

$$R = \underbrace{\left| \sum_{j=1}^{p+q} f_{jj} \right|^2}_{\text{coherent}} + \underbrace{p + q - \sum_{j=1}^{p+q} |f_{jj}|^2}_{\text{incoherent.}} \quad (39)$$

This result is also obtained if the wave function of the many electron is taken as a single product of the separate wave function of the single electrons. The more exact formula (38) differs from this by including some negative terms involving all pairs of electrons with the same spin (or rather all pairs of wave functions in each determinant in (25)).

These terms arise because the incoherent radiation consists of components corresponding to different possible transitions of the atom from its initial state. When we express the many-electron problem as the sum of a number of one-electron problems, we allow each electron independently to have all the possible transitions of the one-electron problem, whereas actually in a many-electron atom some of these transitions of one electron cannot actually occur, as the final state would violate Pauli's exclusion principle. Thus some components of the incoherent scattered radiation which would be possible for a number of independent single electrons are missing from the radiation scattered from a many-electron atom, and it appears also that the intensities of other components may be altered.

This aspect of the negative terms in (38) which involve two wave functions has already been pointed out in § 2 in considering the simple case of He.

§ 6. *Approximate Wave Functions for the Single Electrons, Evaluation of Total Scattering in a Particular Case and Comparison with Experiment.*

We can make an approximation to the separate wave functions ψ by considering each as the wave function of an electron in a central non-Coulomb field of force (not necessarily the same for each electron). Taking spherical polar co-ordinates, origin at the nucleus, we have for the wave function of quantum numbers n, l, m

$$\psi = \gamma_{n,l}(r) P_l^m(\cos \theta) e^{im\phi} \quad (40)$$

where P_l^m is an associated Legendre polynomial.

No two wave functions in one determinant are the same, i.e., have all three quantum numbers n, l, m the same. If each of the $2(2l+1)$ wave functions of the same n, l but different m occurs in each determinant, we call the n, l group (conventionally, of electrons) "complete." It is convenient to have a

name for the $(2l + 1)$ wave functions in one determinant without those in the other (*i.e.*, for the $(2l + 1)$ electrons of the same n , l and same spin without those of the opposite spin), this will be called a "complete half group."

For a complete half-group, a change of the axis of the spherical harmonics corresponds to an orthogonal transformation of the ψ 's of this half-group† (such a transformation is in general impossible unless the half-group is complete), and since R is invariant for an orthogonal transformation of the ψ 's in either determinant, it follows that for an atom consisting of a number of complete half-groups the intensity of scattering in a given direction is independent of the orientation of the axis of the atom. This result would be expected as by a property of the spherical harmonics the charge distribution $\sum |\psi|^2$ is spherically symmetrical for a complete half-group, and so for an atom consisting of complete half-groups; but it does not hold in general if the wave function for the many-electron atom is taken as a single product of the wave functions for the different electrons. Its deduction here depends on the use of the wave function (25).

Since this result holds for atoms consisting of complete half groups, not only of complete groups, it applies to monatomic Na, K, ... vapours as well as to the inert gases and Hg vapour.

If we take the direction of $\mathbf{s}' \leftarrow \mathbf{s}$ as the direction $\theta = 0$ and choose the axis of the spherical harmonics in the wave functions in this direction also, as we may do if the atom consists of complete half-groups, and write $2\mathfrak{S}$ for the angle of scattering so that $|\mathbf{s}' - \mathbf{s}| = 2 \sin \mathfrak{S}$, and also write $\mu = \cos \theta$, $\sigma = 4\pi \sin \mathfrak{S}/\lambda$, then

$$\kappa \mathbf{r} = \sigma \mu \mathbf{r},$$

so that

$$f_{jk} = \int \psi_j^* \psi_k e^{i\sigma \mu r} r^2 dr d\mu d\phi. \quad (41)$$

For any particular wave functions ψ_j , ψ_k the integrations in ϕ , μ can be carried out exactly, leaving only that in r to be evaluated numerically.‡ It is clear from (41) that for different wave-lengths λ and angles of scattering $2\mathfrak{S}$, f_{jk} and so R should be a function of $\sin \mathfrak{S}/\lambda$ only.

† The product of two spherical harmonics of different order vanishes on integration over a sphere, so any surface spherical harmonic can be expanded in surface spherical harmonics of the same order with another axis. The wave functions forming a half-complete group involve the same $\chi(r)$ and $(2l + 1)$ independent surface spherical harmonics of degree l ; thus the wave functions for a given n , l and one axis can be found from those of a half-complete group with any other axis by an orthogonal transformation.

‡ For a complete half-group $\sum_j |\psi_j|^2$ is spherically symmetrical, so $\sum_j f_{jj}$ can be calculated as if $|\psi_j|^2$ is spherically symmetrical for each electron, but $\sum |f_{jj}|^2$ cannot be so calculated.

Since the wave functions involve the azimuth ϕ only through $e^{im\phi}$ the integration with respect to ϕ makes all f_{jk} zero except those for which ψ_j, ψ_k have the same m . Also the quantities f_{jk} ($j \neq k$) are likely to be most important when the electrons j and k have the same principal quantum number n , as then the principal maxima of ψ_j, ψ_k lie at approximately the same radius. So the chief terms involving two different wave functions are those for which n, m are the same and l different. Trial with the wave functions for a Coulomb field shows that the terms arising from wave functions with different principal quantum numbers are unlikely to contribute as much as 2 per cent. to R .

Values of $r\chi_{n,l}$ for any particular atom can be obtained by a method developed by one of us, of which the general idea is the solution of the wave equation of each electron in the field of the nucleus and of the charge distribution of the other electrons. The wave functions for which l and m are not both the same are orthogonal on account of the spherical harmonic factors, but two wave functions of the same l, m but different n are not exactly orthogonal as the functions $\chi_{n,l}$ for them are solutions of the wave equation in different central fields. This would bring in some additional terms both in the normalisation equation (33) and in the integrals occurring in the formula (34) for R . Estimation of these additional terms indicates that their effect on the calculated value of I is likely to be always small, probably less than 2 per cent.

In the calculated values of R which will be compared with experiment, these terms and the terms $|f_{jk}|^2$ where j and k refer to electrons with different principal quantum number n , will be omitted. It is possible that the total contribution to R from the terms so neglected would amount to 5 per cent., but it is probably much smaller.

Some numerical data for argon, calculated in this way, are given in the table, in such a form as to show the contributions to the total scattering from the various terms in (38) and from the various electron groups. It will be seen that in the range of values of $\sin \theta/\lambda$ covered by the calculations (and by the observations with which they will shortly be compared) the contribution from the M electrons to the excess scattering is very small; but they contribute to the term $p + q$ in (38), and so decrease the importance of the terms which depend on the atomic structure relative to the terms which would remain if all the electrons were free. The contribution from the term $|f_{jk}|^2$ ($j \neq k$), which arises from the use of the wave function (25) instead of the simple product of the wave functions of the single electrons, is of some interest. Its maximum value is about 1.4, and is probably about the same for any group of eight electrons consisting of two complete n, l groups with the same

n and $l = 0$ and 1. Its importance relative to the total scattering clearly decreases with the total number of electrons, and would be greater for neon than for argon.

Table.—Contributions to Total Scattering by Argon.

$\sin 3/\lambda$.		0.522.	0.783.	1.044.	1.566.	2.088.	2.610.
Σf_B	2 K	1.96	1.90	1.83	1.65	1.44	1.20
	8 L	5.52	3.60	2.04	0.46	0.02	0.02
	8 M	0.11	0.16	0.18	0.04	0.00	0.00
	Total	7.37	5.66	4.05	2.15	1.46	1.20
$(\Sigma f_B)^2$		54.2	32.0	16.4	4.6	2.1	1.4
$\Sigma (f_B^2)$	2 K	1.91	1.81	1.68	1.36	1.03	0.75
	8 L	3.95	1.97	1.03	0.39	0.15	0.04
	8 M	0.05	0.00	0.00	0.00	0.00	0.00
	Total	5.91	3.78	2.71	1.75	1.18	0.79
$\Sigma'' (f_{jk}^2)$	8 L	1.30	1.32	0.90	0.17	0.01	0.00
R/R _r		3.61	2.50	1.71	1.15	1.05	1.04

$$R = 18 + 1 \left[\left(\Sigma_j f_B \right)^2 - \Sigma_j (f_B^2) - \Sigma_{jk}'' (f_{jk}^2) \right], R_r = 18.$$

Σ''_{jk} = sum over all pairs of electrons with same spin and $j \neq k$.

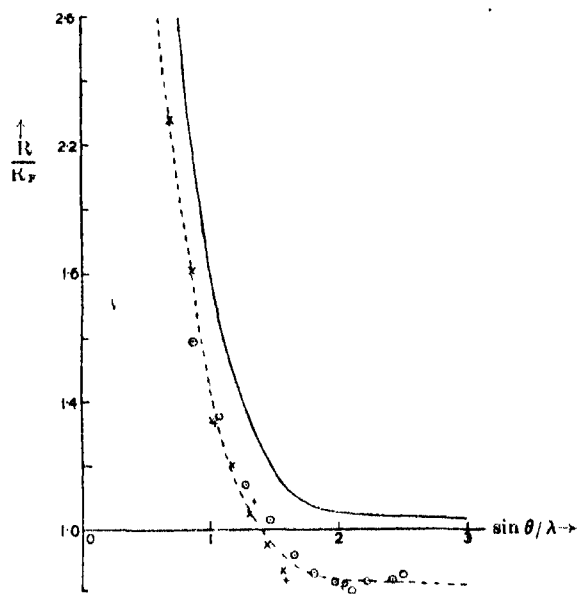
For a homopolar molecule the complete wave function is more complicated than a single product of two determinants, as has already been mentioned (see end of §3). Also the charge distribution of the electrons concerned in a homopolar band becomes concentrated to some extent between the atoms,† so may contribute appreciably to the excess scattering at angles of scattering at which for an atom the contribution from these electrons is negligible. There is also the possibility of an appreciable effect from the coupling of electronic and nuclear motions.

On account of the uncertainty of the effect of the binding electrons on the scattering by diatomic molecules, it is most satisfactory to compare theory and experiment for a monatomic gas or vapour, and moreover for one not too heavy, since for the heavier atoms the proportion of incoherent radiation is small, and it is known that, with the approximation to the wave functions ψ here

† See London, 'Z. Physik,' vol. 46, p. 455, fig. 3 (1928).

used, the theory leads to results in close agreement with experiment for the coherent scattering.†

The most suitable case for comparison of theory and experiment seems to be that of argon, for which Barrett‡ has recently obtained experimental results, and such a comparison is made in the figure. A strict comparison is not



Curves showing Theoretical and Observed Variation of R/R_F with $\sin \theta/\lambda$ for total scattering of X-rays by Argon.

Observed values : \odot , $\lambda = 0.39$. $+$, $\lambda = 0.48$. \times , $\lambda = 0.49$ Å.U.

possible, as for the short wave-lengths used by Barrett "relativity effects" are appreciable, whereas they are neglected in the derivation of the theoretical formula. We can try to allow for this by comparing theoretical and observed values of the ratio R/R_F , and such a comparison is made in the figure.

The values of R for the experimental points were taken from the figures in Barrett's paper, R_F was calculated from Dirac's formula (formula (1) and curves Q of Barrett's paper) and for different wave-lengths R/R_F is plotted

† James, Waller and Hartree, *loc. cit.*

‡ Barrett, *loc. cit.* Barrett mentions that He, the other monatomic gas for which he has made experiments, may have contained impurities; the probable impurities contain so many more electrons per molecule than He that a small amount of impurity would give quite a large excess scattering. The argon is mentioned as 95 per cent. pure, but the probable impurities have only a small effect on the excess scattering (5 per cent. Ne might make the observed value 3 per cent. low).

against $\sin \vartheta/\lambda$. The theoretical values of R have been calculated from formula (38), and for R_F the classical value 18 has been taken (cf. Table) corresponding to the fact that the approximations made in deriving (38) lead to classical scattering when applied to a free electron. As has been mentioned, it is probable that the effects of these approximations on R and on R_F should be of the same kind so that the effect on R/R_F should not be so large as the effect on either separately.

The experimental results agree closely with the theoretical result that R/R_F should be a function of $\sin \vartheta/\lambda$ only. Whether this should still be true when relativity effects are included is not certain; in the experimental results there is a suggestion of a small consistent difference between different wave-lengths at the larger angles of scattering which might be such a relativity effect.

Barrett's results give relative values of R/R_F for different angles of scattering and for different gases, but not absolute values, so it may be necessary to multiply them by a constant factor throughout. The broken curve in fig. 1 is the theoretical curve with all its ordinates multiplied by 0.80, and it will be seen that it agrees very well with the points plotted from Barrett's observed values; this suggests that these values should be multiplied by a factor about $1/0.80 = 1.25$ to convert them to absolute values. This, however, cannot be considered as certain, as the suggested correction is no greater than the relativity effect on R_F at large angles, and it is only an assumption, though it seems a reasonable one, that R/R_F is less affected by relativity effects than R_F itself.

The rapid increase of R/R_F with decreasing $\sin \vartheta/\lambda$ beginning about $\sin \vartheta/\lambda = 1.8$ is due to contributions from the L electrons, and it is satisfactory that theory and experiment agree about the place at which this increase starts.

This comparison of experiment with theory suggests firstly the desirability of making experiments for monatomic gases with longer wave-lengths, for which the uncertain relativity effects for the many electron atom would be smaller, and for which also the excess scattering would be larger at a given angle of scattering; and secondly the value of absolute measurements if the experimental difficulties could be overcome.

In conclusion one of us (D.R.H.) wishes to express his thanks to the International Education Board for a Fellowship during the tenure of which this work was done, and to Prof. Bohr for the privilege of working at the Institut for teoretisk Fysik at Copenhagen.

The First and Second Order Equations of the Quantum Theory.

By H. T. FLINT, D.Sc., King's College, London.

(Communicated by O. W. Richardson, F.R.S.—Received February 19, 1929.)

Introduction.

The form of the wave equation for a non-rotating electron suggests that it enters into the theory very much in the same way as the wave equation associated with electromagnetic theory. It would be expected to be derivable from equations of the first order corresponding to Maxwell's equations. It has been suggested* that the function ψ might enter by means of a relation such as

$$s = \text{grad } \psi \quad (1)$$

where s replaces the current four vector of the electromagnetic theory. The difficulty in connection with this procedure is to account for the phenomena associated with electronic rotation. Dirac has shown† how to overcome this difficulty and has derived first order equations which can be derived from generalisations of Maxwell's equations. There are certain difficulties with regard to the form of Dirac's results which have been much discussed and some of them have been removed.‡

There are two unsatisfactory points in the treatment of this question. One is the introduction of an operator $\left(\frac{h}{2\pi i} \frac{\partial}{\partial x^4} - e\phi_4\right)$ into the equations when it is desired to pass from a non-electromagnetic problem to one in which an electromagnetic field is present. The second difficulty lies in the occurrence of a term in mc . Darwin has pointed out this difficulty and considers that it is due to our inability to calculate electromagnetic mass in the quantum theory.

We shall discuss here a possible way out of both these difficulties and indicate the nature of the invariance to be associated with the first order equations.

The mode of procedure can be very concisely stated. We assume that the phenomena are five dimensional and that the invariance is of the type with which we are familiar in the theory of relativity but considered from the

* 'Roy. Soc. Proc.,' A, vol. 115, p. 213 (1927).

† 'Roy. Soc. Proc.,' A, vol. 117, p. 610 (1928).

‡ 'Roy. Soc. Proc.,' A, vol. 118, p. 604 (1928); vol. 121, pp. 524, 543 (1928); 'Z. Physik,' vol. 52, p. 356 (1928).

point of view of five dimensions. We assume that the phenomena are described by the introduction of two tensors which contain not only an antisymmetric but also a symmetric component and with the latter we associate the quantity mc , which enters through the occurrence of the symmetric component.

This procedure is unsatisfactory from the point of view of the theory of physical unity. We have by the introduction of a five dimensional continuum united into a geometrical theory both the laws of gravitation and electromagnetism, but we now place non-geometrical quantities into the continuum which play the part of mere actors upon the stage and do not occur as parts of the stage itself.

We come again to the state of affairs which existed with regard to electrodynamics just after the discovery of the relativity theory of gravitation.

At present it does not appear to be unduly optimistic to anticipate a complete theory based on the conception of unity in physics. Two ways seem to lie before us which lead to fields of research; the five dimensional and the new Einstein method. The link in each case is the wave equation which can, at least for the non-rotating electron, be introduced very simply into either. In the meanwhile we must content ourselves with a less satisfactory procedure.

Maxwell's Equations and their Generalisation.

In the theory of relativity electromagnetic phenomena are described by means of a tensor, F , and a four vector, s , and the first order equations, or Maxwell's equations, are written in the form :

$$\Sigma \frac{\partial F_{ab}}{\partial x^c} = 0, \quad (2)$$

$$\frac{1}{\sqrt{-g}} \frac{\partial}{\partial x^k} (\sqrt{-g} F^{jk}) = s. \quad (3)$$

In (2) the summation implied is taken over three of the numbers 1 to 4 in cyclic order, and eight equations are implied by (2) and (3).

In this theory F is an antisymmetric tensor.

We also note that (3) is written in the contravariant form. The importance of studying the wave equation by analogy with these equations has been recognised by J. M. Whittaker and J. Frenckel. These writers have shown that Dirac's equations in the form given by Darwin can be based on fundamental equations of this character. We shall refer to their work because our results can be most readily reduced to the form they give. Both show in detail that their results lead to the equations of Dirac so that we can save considerable repetition by referring to their papers instead of giving the reduction again

here. The references are to the last two papers mentioned in the introduction. Darwin's equations are obtained very readily by following Frenkel's procedure, while Whittaker's work leads to more equations on account of his relations (3') which we do not employ. We shall suppose that the five dimensional continuum is characterised by

$$d\sigma^2 = \gamma_{\mu\nu} dx^\mu dx^\nu, \quad (4)$$

where in accordance with the work of Kaluza, Klein and de Broglie we have :

$$\gamma_{mn} = g_{mn} - \xi \alpha^2 \phi_m \phi_n, \quad \gamma_{m5} = \gamma_{5m} = -\xi \alpha \phi_m, \quad \gamma_{55} = -\xi, \quad (5)$$

and for the contravariant components :

$$\gamma^{mn} = g^{mn}, \quad \gamma^{m5} = \gamma^{5m} = -\alpha \phi^m, \quad \gamma^{55} = \alpha^2 \phi_m \phi^m - \frac{1}{\xi}. \quad (6)$$

The Latin affixes denote that the possible values which may be assumed are : 1, 2, 3, or 4 and the Greek that the values range from 1 to 5. We assume that the value of ξ is unity and that $\alpha = e/mc$. (e in e.m. units.)

This differs from the interpretation of some writers but it introduces a remarkable simplicity into the five dimensional theory. Schrödinger's equation for a non-rotating electron becomes :

$$\text{div} (\text{grad } \psi) = 0, \quad (7)$$

and taken with the equation

$$d\sigma^2 = 0, \quad (8)$$

which results from our values of the constants, we find an exact analogy in the five dimensional theory of a particle with the wave theory of optics where a null-geodesic (8) is associated with a wave equation (7). This forms the subject of a paper to be published shortly by J. W. Fisher. The fifth co-ordinate does not occur in any of the functions of (5) or (6) where the g 's are the usual gravitational components and the ϕ 's the components of electromagnetic potential. Whenever the fifth co-ordinate occurs it does so in the factor $\exp (2\pi imc x^5 / \hbar)$ so that the operation $\partial / \partial x^5$ is equal to multiplication by $2\pi imc / \hbar$. This is equivalent to associating a fifth component of momentum with our particle of magnitude mc . Other writers have considered it to be e/α and we have simply written $e/\alpha = mc$ in determining the constant α . Recent work indicates that this is the correct value for the momentum.*

This simplicity with regard to the occurrence of x^5 is an example of the simple way in which the fifth dimension enters into our equations and we shall see that a similar simplicity occurs in the components of the tensors we introduce. Our assumption is that the phenomena are characterised by two covariant tensors, F and G , and by the introduction of two scalar quantities

* Eddington, 'Roy. Soc. Proc.,' A, vol. 121, p. 533 (1928).

ψ and θ . We shall suppose in accordance with (1) that two current vectors can be derived from these and we have :

$$J_\mu = \frac{\partial \psi}{\partial x^\mu}, \quad L_\mu = \frac{\partial \theta}{\partial x^\mu}. \quad (9)$$

Neither F nor G is antisymmetrical but they can, like any tensor, be expressed in two parts, one antisymmetrical and the other symmetrical.

Taking F as an example, we write :

$$F_{\mu\nu} = A_{\mu\nu} + S_{\mu\nu} \quad (10)$$

where $A_{\mu\nu}$ and $S_{\mu\nu}$ are antisymmetrical and symmetrical components respectively. Associated with this covariant tensor we have a contravariant, F , with components $F^{\mu\nu}$ and we write :

$$F^{\mu\nu} = A^{\mu\nu} + S^{\mu\nu}. \quad (11)$$

The covariant tensor appears to be endowed with a simplicity of structure characterised by the absence of any antisymmetric components with the suffix 5.

Thus all these components are of the form A_{mn} .

The simplicity with regard to the symmetrical components appears in the contravariant form, for S^{55} is zero and only components of the type S^{m5} exist.

The theory we give is, strictly, not limited in this way but the limitations imposed give a simplicity to our formulæ and are in accordance with the requirements of experiment, which means simply that our results lead to Dirac's equations for the rotating electron.

F and G are not entirely independent of one another. The relation between them calls to mind the relation between a six-vector and its reciprocal. The only parts of G which do not occur in F are those associated with its symmetrical components.

Comparison with (3) indicates that the fundamental equations are :—

$$\frac{1}{\sqrt{-\gamma}} \frac{\partial}{\partial x^\mu} (\sqrt{-\gamma} F^{\lambda\mu}) = J^\lambda, \quad (12)^*$$

$$\frac{1}{\sqrt{-\gamma}} \frac{\partial}{\partial x^\mu} (\sqrt{-\gamma} G^{\lambda\mu}) = L^\lambda. \quad (13)^*$$

* *Note added March 22, 1929.*—The equations (12) and (13) are not written in their invariant form. In the case of (12), for example, we require on the left the addition of $\left\{ \frac{\mu\nu}{\lambda} \right\} S^{\nu\mu}$ to make it invariant. But the simplicity in the form of S makes this easily calculable, and if we consider the case when $\lambda = 1$ we find that the contribution to the left hand side of (12) is $-\frac{e}{mc} H_{\mu}^1 S^{55}$ where H_{μ}^1 is a field component. The factor $\frac{e}{mc}$ makes this much smaller than the other terms of the equation, and we are perhaps justified in neglecting this term in practical cases. A similar observation applies to the second order equation.

The equation (2) is satisfied if the covariant F is of the form $\text{curl } u$ where u is a four-vector. We could, of course, introduce the corresponding form here for the antisymmetric component.

We proceed to show that (12) and (13) lead to the equations of Frenckel. We have begun with simplifications in the covariant tensor and we must examine how this affects the contravariant components.

We have :

$$\begin{aligned} F^{\lambda\mu} &= \gamma^{\lambda\alpha}\gamma^{\mu\beta}F_{\alpha\beta}, \\ &= \gamma^{\lambda\alpha}\gamma^{\mu\beta}A_{\alpha\beta} + \gamma^{\lambda\alpha}\gamma^{\mu\beta}S_{\alpha\beta}. \end{aligned}$$

Thus

$$A^{\lambda\mu} = \gamma^{\lambda\alpha}\gamma^{\mu\beta}A_{\alpha\beta}.$$

We have two cases to consider, represented as follows :

$$A^{im} = \gamma^{ia}\gamma^{mb}A_{ab} = g^{ia}g^{mb}A_{ab}, \quad (14)$$

$$A^{is} = \gamma^{ia}\gamma^{sb}A_{ab} = -\frac{e}{mc}g^{ia}\phi^bA_{ab}. \quad (15)$$

When the gravitational field is removed, the case we must consider in order to refer to the equations already obtained, all the g 's vanish except those of the form g^{mm} which are unity. In this case

$$A^{im} = A_{im}, \quad (16)$$

which simply means that the distinction between contravariance and covariance is lost for these components, and

$$A^{is} = -\frac{e}{mc}\phi^sA_s, \quad (17)$$

where a distinction remains.

We have also to obtain J^A for the contravariant components.

$$J^A = \gamma^{Aa}J_a = \gamma^{Aa}J_a + \gamma^{A5}J_5.$$

Note that

$$J_5 = \frac{\partial\psi}{\partial x_5} = \frac{2\pi imc}{h}\psi.$$

Thus

$$J^i = g^{ia}J_a - \frac{2\pi ic}{h}\phi^i\psi = \frac{\partial\psi}{\partial x^i} - \frac{2\pi ic}{h}\phi^i\psi.$$

The equation in which $\lambda = 1$ may be taken for comparison, and taking $\sqrt{-\gamma} = 1$ for convenience we find :

$$\frac{\partial}{\partial x^\mu} (F^{1\mu}) = J^1$$

or

$$\frac{\partial}{\partial x^\mu} (A^{1\mu}) = J^1 - \frac{\partial}{\partial x^\mu} (S^{1\mu}),$$

i.e.

$$\frac{\partial A^{12}}{\partial x^2} + \frac{\partial A^{13}}{\partial x^3} + \frac{\partial A^{14}}{\partial x^4} + \frac{\partial A^{15}}{\partial x^5} = J^1 - \frac{\partial S^{1\mu}}{\partial x^\mu}.$$

After insertion of the values in the absence of a gravitational field :

$$\begin{aligned} \frac{\partial A_{12}}{\partial x^2} + \frac{\partial A_{13}}{\partial x^3} + \frac{\partial A_{14}}{\partial x^4} - \frac{2\pi ic}{h} (\phi_2 A_{12} + \phi_3 A_{13} + \phi_4 A_{14}) \\ = \frac{\partial \psi}{\partial x^1} - \frac{2\pi ic}{h} \phi_1 \psi - \frac{\partial S^{1\mu}}{\partial x^\mu}. \end{aligned} \quad (18)$$

This equation is identical with the first of the equations (B) of Frenkel's paper, if we identify the quantities he introduces with ours.

We have, for example,

$$\begin{aligned} A_{12} = M_3, \quad A_{13} = M_2, \quad A_{14} = iN_1, \quad \psi = M_0, \\ \frac{\partial S^{1\mu}}{\partial x^\mu} = -\frac{2\pi imc}{h} N_1. \end{aligned}$$

The last relation suggests that the differentiation is with respect to x^5 , from which we are led to conclude that the contravariant components of S which occur are those of the form S^{15} . We then have :

$$S^{15} = -N_1.$$

A similar remark applies to the equations (13) which agree with Frenkel's equations (A).

The result may be summarised in the following way. The equations of Whittaker and Frenkel must be recognised as contravariant equations which possess their simplicity of form on account of the nature of the covariant tensor of the field. In investigating this question along these lines the attempt was at first made to introduce F and G as antisymmetric tensors. The treatment is then particularly simple and very satisfactory in form but in the end certain terms are missing. These are associated with the constant mc , and Darwin has pointed out, in the paper referred to, that this makes the analogy with the

electromagnetic equations rather a loose one. The only way in which it appears possible to introduce the missing terms, short of including them in an operator, as Darwin or Frenkel do, is to suppose that F is not antisymmetric. This appears to be a satisfactory way of filling in the gap and it is concluded that the occurrence of electromagnetic mass in the quantum theory is accounted for by the symmetric components.

The Second Order Equation.

A second order equation in ψ can be obtained from the relation

$$\text{grad } \psi = J,$$

or in terms of the components :

$$J_a = \frac{\partial \psi}{\partial x^a}.$$

We form the divergence of J which we write :

$$\frac{1}{\sqrt{-\gamma}} \frac{\partial}{\partial x^\mu} (\sqrt{-\gamma} J^\mu) \text{ or } \text{div} (\text{grad } \psi).$$

Hence from (12) :

$$\begin{aligned} \text{div} (\text{grad } \psi) &= \frac{1}{\sqrt{-\gamma}} \frac{\partial}{\partial x^\mu} \left\{ \frac{\partial}{\partial x^\nu} (\sqrt{-g} F^{\mu\nu}) \right\} \\ &= \frac{1}{\sqrt{-\gamma}} \frac{\partial}{\partial x^\mu} \left\{ \frac{\partial}{\partial x^\nu} (\sqrt{-g} S^{\mu\nu}) \right\}, \end{aligned} \quad (19)$$

since the antisymmetric part of F disappears on account of the summation over μ and ν .

The left side of (19) is a five dimensional expression and is sometimes written $\Diamond\psi$ while the corresponding four dimensional quantity is $\Box\psi$.

We have :

$$\Diamond\psi = \Box\psi - \frac{4\pi ic}{h} \phi^m \frac{\partial \psi}{\partial x^m} - \frac{4\pi^2}{h^2} (e^2 \phi_m \phi^m - m^2 c^2) \psi, \quad (20)$$

and when this is equated to zero we have the equation for the non-rotating electron. This is the equation which would be obtained if F were antisymmetrical. The presence of symmetrical components gives a term on the right and (19) appears in the form of a more general equation than (20). In order to examine the equation in a simple case such as occurs in experiment we take the example of a preponderating electromagnetic field, and therefore neglect the gravitational field.

Omitting the details of the calculation we obtain finally :

$$\square \psi - \frac{4\pi ic}{h} \phi_a \frac{\partial A_{ab}}{\partial x^b} + \frac{4\pi^2}{h^2} (c^2 \phi_a^2 - m^2 c^2) \psi = \frac{4\pi ic}{h} A_{ab} H_{ba},$$

where $H_{ba} = \frac{\partial \phi_a}{\partial x^b} - \frac{\partial \phi_b}{\partial x^a}$, an equation similar to that obtained by operational methods. The fifth equation of (12), which has not been used before, enters into this calculation. The equations (13) treated in the same way give a similar equation in θ .

Internal Friction in Certain Tidal Currents.

By S. F. GRACE, University of Liverpool.

(Communicated by J. Proudman, F.R.S.—Received February 20, 1929.)

§ 1. In the application of hydrodynamical theory to the motion of the water in the sea or ocean it has long been desirable to obtain some measure of the internal friction. Most writers on the subject have considered this to be equivalent to the determination of a "virtual kinematic coefficient of viscosity" (k), taken to represent the combined effect of molecular viscosity and eddy viscosity, and which was supposed to play a part in turbulent motion analogous to that of ordinary viscosity in non-turbulent motion, except that k might vary from place to place. The validity of this supposition has, however, recently been questioned.*

The importance of a knowledge of the internal friction was realised in 1902, when Nansen published the results of the Norwegian North Polar Expedition of 1893–96.† Subsequently methods for the determination of k were proposed,‡ the majority of which, however, involve the assumption that at a particular

* H. Jeffreys, 'Proc. Camb. Phil. Soc.,' vol. 25, No. 1 (1929).

† 'Oceanography of the North Polar Basin,' Kristiania.

‡ See, for example, Ekman, "On the Influence of the Earth's Rotation on Ocean-Currents," 'Ark. Matem.,' Stockholm, vol. 2, No. 11 (1905); Jacobsen, "Beitrag zur Hydrographie der Danischen Gewasser," 'Komm. Havundersø (Kjobenhavn), Ser. Hyd.,' vol. 2, No. 2 (1913); Schmidt, "Wirkungen der ungeordneten Bewegung im Wasser der Meere und Seen," 'Ann. Hyd.,' vol. 46, pp. 367, 431 (1917); Jeffreys, "On Turbulence in the Ocean," 'Phil. Mag.,' vol. 39, No. 233 (1920); Durst, "The Relationship between Current and Wind," 'Q.J.R. Met. Soc.,' vol. 50, p. 113 (1924).

place k may be considered to be independent of the depth. The only tidal work on the subject is due to J. Proudman* and J. H. Powell.† At the present time, however, no laws are known for the accurate prescription of the internal frictional forces, they are certainly not the simple viscous forces of non-turbulent motion.

It is proposed in the present paper to take up the tidal work. Powell's method is similar to much of the non-tidal work and determines an average value of k , independent of the depth. Proudman's method, however, does not depend upon the existence of k , it utilises observations of tidal currents and has been applied (*loc. cit.*) to observations extending over a fortnight, made in 1911 at four stations in the North Sea, viz., at Varne in the Straits of Dover, Smith's Knoll off the Norfolk coast, Horn's Reef and a point Da_1 off Denmark. Subsequently, however, observations extending over the two separate years 1922 and 1923 were made at Varne and Smith's Knoll, and were analysed at the Tidal Institute, University of Liverpool. It seemed desirable therefore to make use of these observations‡ and at the same time to modify Proudman's method slightly in order to take advantage of results which have been established for the frictional resistance of the sea-bottom. To make the discussion as comprehensive as possible observations made by Powell (*loc. cit.*) in the Sound of Jura and the Solent are also included, and those at Horn's Reef and Da_1 , already referred to, are re-examined.

The method of procedure, which is outlined in § 3, utilises data giving the velocities at different depths, and requires a knowledge of the friction at two definite depths. In this latter connection the friction at the bottom is taken to be $0.002\rho V^2$, ρ being the density and V the velocity there,§ and then two alternative assumptions are put forward, viz., (A) that a component of friction vanishes at the depth where the corresponding current component is stationary, (B) that the friction vanishes at the surface. The two assumptions (A) and (B) are distinct since a current component is found to be stationary with depth at some distance below the surface.

With these assumptions the method is quite definite, but difficulty was experienced in performing the actual numerical work on account of the roughness of the data. The current observations at the four North Sea stations

* See the "Discussion of Geophysical Subjects," 'The Observatory,' vol. 46 (1923).

† 'M.N.R. Ast. Soc., Geophys. Suppl.,' vol. 1, No. 6 (1925).

‡ The author is much indebted to the 'Conseil International pour l'exploration de la mer,' the body responsible for the observations, for permission to use, and to the authorities of the Liverpool Observatory and Tidal Institute, for access to these observations.

§ See Taylor, 'Phil. Trans.,' A, vol. 220, p. 1 (1920).

have been made with Jacobsen's current-meter, no observations are available at the surface or at the bottom, and the depths of the sea-bottom at Varne and Smith's Knoll were not noted at the time of observation. With regard to the last difficulty, however, it was decided that a value reliably representative of the depth at a station would be obtained by adding 5 metres to the lowest depth worked there, but that any further accuracy is unobtainable.*

Again, from the point of view of the present paper, the observations in the Sound of Jura and the Solent are incomplete, they appear to relate mainly to the motion in the direction of maximum flow ; by making certain assumptions, however, they can be used in conjunction with the method outlined later.

Before proceeding with the discussion a summary of the general conclusions, which become apparent in the sequel, will now be given ; the results refer to the principal lunar semi-diurnal tidal motions existing at the various stations. This tidal motion, although the main motion, does not constitute the whole motion of the water at a station ; the results therefore, while directly applicable to the semi-diurnal lunar tide, can only be regarded as approximate when the whole motion is to be considered.

(a) The results obtained for the years 1922 and 1923 at Varne and Smith's Knoll, under either of the assumptions (A) or (B), are separately consistent, thus showing that the conditions at a particular place persist with time and indicating that the results are representative of these conditions.

(b) When the maximum current is flowing at a station the frictional force, with which the water above a horizontal section acts on the water below, increases with the depth, the maximum friction being found at the bottom. Under assumption (A) the friction is negative at the surface and increases through zero (where the current is stationary with depth) to its value at the bottom ; under assumption (B) the friction increases from zero at the surface to its value at the bottom.

When the current is weak, the frictional force is small, and in general also increases with the depth.

(c) The actual values obtained for the friction vary from place to place, thus they are large for the Sound of Jura and very small in comparison for the station Da₁. At a particular station the numerical value obtained for the friction at any depth, other than at the bottom, depends upon which of the assumptions, (A) or (B), is made.

* The author here wishes to thank Dr. J. N. Carruthers, of the Ministry of Agriculture and Fisheries, for his advice and for the trouble he took in this connection.

(d) Under assumption (A) the average value of the frictional force at the surface at the instant of maximum flow, for the two North Sea stations, Varne and Smith's Knoll, is about 1.6 dynes/cm.². If the friction at the surface is of the same form as at the bottom and due to air-resistance, an average wind of, say, 40 m./sec., blowing in the direction of maximum flow, would be necessary. This wind velocity is much too large. Although, as explained later, the surface values are somewhat uncertain, it seems that the assumption (A) requires the existence of a surface drag which cannot be explained simply as being due to air-resistance, and for which at present no explanation is available.

(e) The variation of the current with depth at any station is such that the maximum current is found at some distance below the surface. Considering a horizontal section containing this maximum current, (A) assumes that the (turbulent) motion is such that the water passing down through the section carries with it as much forward momentum as is carried by the water passing up through the section. Under (B) however, the water passing down must carry more forward momentum than that passing up, but the mechanism by which this can be effected is unknown to the author. In rivers or channels it is assumed to be brought about by a transverse circulation, which has been attributed* to the effects of the sides; similar reasoning cannot, however, be applied to the motion of the water in the open sea.

The present paper is to be regarded as a preliminary survey on the subject of internal friction in tidal currents. During its preparation points have arisen which seem to call for further investigation, for example, it seems advisable to enquire further into the points at issue in (d) and (e) above. The work of the present paper was undertaken on the suggestion of Prof. J. Proudman, to whom the author is again greatly indebted for advice; the calculations under assumption (B), however, were suggested by Prof. G. I. Taylor.

General Equations.

§ 2. The discussion deals with motion in a restricted region of the earth's surface, and the mean surface of the sea may therefore be assumed to be a horizontal plane. A system of rectangular axes *Oxyz* is taken, with *Oxy* in the mean surface and *Oz* vertically upwards, so that for a point in the sea *z* will usually be negative.

The horizontal acceleration components for small motion take the form

$$\frac{\partial u}{\partial t} - 2\omega v, \quad \frac{\partial v}{\partial t} + 2\omega u, \quad (1)$$

* Gibson, 'Hydraulics,' 3rd ed., p. 331.

where u and v are the components of velocity parallel to Ox and Oy , t is the time and ω the component of the earth's rotation about the vertical.

Neglecting horizontal turbulence, the components of force per unit mass of the sea are

$$-\frac{1}{\rho} \frac{\partial p}{\partial x} + g \frac{\partial \bar{\zeta}}{\partial x} + \frac{\partial F}{\partial z}, \quad -\frac{1}{\rho} \frac{\partial p}{\partial y} + g \frac{\partial \bar{\zeta}}{\partial y} + \frac{\partial G}{\partial z}, \quad -\frac{1}{\rho} \frac{\partial p}{\partial z} - g.$$

where $-g\bar{\zeta}$ is the potential of the external disturbing forces, ρF and ρG are the components of frictional force per unit horizontal area with which the water above acts on the water below, and p , ρ , g have their usual significance.

Ignoring the vertical component of acceleration, it is seen that

$$\frac{1}{\rho} \frac{\partial p}{\partial z} = -g,$$

and, on integrating,

$$p = p_0 + g\rho(\zeta - z),$$

p_0 denoting the (uniform) atmospheric pressure-intensity and ζ the elevation of the free surface of the sea above mean sea-level.

The horizontal force components now take the form

$$-g \frac{\partial}{\partial x}(\zeta - \bar{\zeta}) + \frac{\partial F}{\partial z}, \quad -g \frac{\partial}{\partial y}(\zeta - \bar{\zeta}) + \frac{\partial G}{\partial z},$$

so that, writing $\zeta' = \zeta - \bar{\zeta}$, the equations of motion become

$$\frac{\partial u}{\partial t} - 2\omega v = -g \frac{\partial \zeta'}{\partial x} + \frac{\partial F}{\partial z}, \quad \frac{\partial v}{\partial t} + 2\omega u = -g \frac{\partial \zeta'}{\partial y} + \frac{\partial G}{\partial z}.$$

It may here be noted that the left-hand members of these equations are derivable from the observations whereas the quantities on the right are to be determined.

Now let σ be the speed of the principal lunar constituent of tidal elevation, i.e. $\sigma = 1.41 \times 10^{-4} \text{ sec.}^{-1}$, and let the terms of ζ' of period $2\pi/\sigma$ be written as

$$\zeta_1' \cos \sigma t + \zeta_2' \sin \sigma t.$$

Similarly, consider u , v , F , G analysed into their periodic terms, so that the constituents of period $2\pi/\sigma$ are

$$u_1 \cos \sigma t + u_2 \sin \sigma t, \dots \dots \dots, G_1 \cos \sigma t + G_2 \sin \sigma t,$$

and, finally, let the corresponding acceleration components (1) be written in the form

$$f_1 \cos \sigma t + f_2 \sin \sigma t, \quad g_1 \cos \sigma t + g_2 \sin \sigma t,$$

then

$$\left. \begin{aligned} f_1 &= \sigma u_2 - 2\omega v_1, & f_2 &= -\sigma u_1 - 2\omega v_2, \\ g_1 &= \sigma v_2 + 2\omega u_1, & g_2 &= -\sigma v_1 + 2\omega u_2, \end{aligned} \right\} \quad (2)$$

and the equations of motion become

$$\left. \begin{aligned} f_1 &= -g \frac{\partial \zeta_1'}{\partial x} + \frac{\partial F_1}{\partial z}, & f_2 &= -g \frac{\partial \zeta_2'}{\partial x} + \frac{\partial F_2}{\partial z}, \\ g_1 &= -g \frac{\partial \zeta_1'}{\partial y} + \frac{\partial G_1}{\partial z}, & g_2 &= -g \frac{\partial \zeta_2'}{\partial y} + \frac{\partial G_2}{\partial z}. \end{aligned} \right\} \quad (3)$$

On integrating from the bottom ($z = -h$) to a height z , it follows that

$$\bar{f}_1 = -g \frac{\partial \zeta_1'}{\partial x} + \frac{F_1 - F_1^h}{h + z}, \quad (4)$$

together with three similar equations, \bar{f}_1 being the mean value of f_1 over the interval and F_1^h the value of F_1 at the bottom.

Now it seems to be fairly generally accepted that the friction at the bottom of the sea is proportional to the square of the velocity there, the coefficient of proportionality being 0.002ρ , i.e., if V is the velocity at the bottom with components u and v , then

$$F^h = 0.002Vu, \quad G^h = 0.002Vv.$$

Hence by finding the constituents of F^h , G^h of period $2\pi/\sigma$, the values of F_1^h , F_2^h , G_1^h , G_2^h are determined.

Two alternative assumptions, (A) and (B), are now put forward:—

(A) Examining the variation of the current-component u_1 with depth, if at any point a well-defined maximum occurs, then it is assumed that at this point the corresponding component of internal friction F_1 vanishes. If this occurs at $z = -h'$, then $F_1^{h'} = 0$, and

$$\bar{f}_1^{h'} = -g \frac{\partial \zeta_1'}{\partial x} - \frac{F_1^h}{h - h'}, \quad (5A)$$

where $F_1^{h'}$, $\bar{f}_1^{h'}$ have been written for the values of F_1 , \bar{f}_1 corresponding to $z = -h'$. Similarly with the other components.

(B) The alternative assumption is made that, at the surface,

$$F_1 = F_2 = G_1 = G_2 = 0,$$

so that

$$\bar{f}_1^0 = -g \frac{\partial \zeta_1'}{\partial x} - \frac{F_1^h}{h}, \quad (5B)$$

together with three similar equations, \bar{f}_1^0 denoting the value of \bar{f}_1 for $z = 0$.

Method of Procedure.

§ 3. The observations at the North Sea stations give the currents at various depths, these have been analysed into their harmonic constituents and the

values at the surface and the bottom found by extrapolation. If the semi-diurnal lunar constituent is isolated, this constituent is such that the mean velocity for depth has a maximum and a minimum in directions at right angles and the hodograph is an ellipse. The horizontal axes Ox , Oy are taken parallel to the principal axes of this ellipse, Ox being the direction of maximum, Oy that of minimum flow.

In accordance with the notation of the previous section, the values of u_1 , u_2 , v_1 , v_2 at depths 0, 2.5, 5, 10, 15, ... metres and at the bottom are therefore determined from the observational data, and the time origin is so chosen that the mean values for depth of u_2 and v_1 are zero; the values, other than those obtained by extrapolation, are given in Table I. It may be noted that the

Table I.

Depth. Metres.	u_1 cm./sec.	u_2 cm./sec.	v_1 cm./sec.	v_2 cm./sec.	u_1 cm./sec.	u_2 cm./sec.	v_1 cm./sec.	v_2 cm./sec.
	Varne (1922).				Varne (1923).			
2.5	72.5	1.2	-1.5	-10.6	82.1	-0.1	-3.2	-10.8
5	76.2	-0.4	-1.4	-11.9	84.5	0.1	-2.5	-12.2
10	74.6	-1.7	0.0	-12.9	81.1	-0.4	0.7	-11.5
15	72.9	-0.4	0.0	-11.9	76.6	0.1	1.7	-12.5
20	70.6	0.7	1.7	-11.2	73.5	-0.6	1.9	-11.1
25	66.8	0.6	1.1	-10.3	70.5	0.2	0.7	-10.7
	Smith's Knoll (1922).				Smith's Knoll (1923).			
2.5	91.6	2.0	3.1	-15.0	88.6	1.0	3.0	-11.2
5	99.4	1.4	1.9	-16.9	98.9	0.7	0.2	-14.5
10	96.2	1.8	2.7	-15.9	94.9	1.5	0.3	-11.5
15	91.9	-0.2	0.9	-15.4	90.8	0.5	-0.6	-12.1
20	85.6	-1.5	-1.8	-10.8	85.6	0.8	-0.9	-8.1
25	80.4	-0.2	-1.1	-9.6	79.2	-0.7	-2.0	-9.7
30	71.8	-1.5	-2.7	-8.6	70.9	-2.3	-0.3	-8.4
	Horn's Reef.				Da ₁ .			
2.5	46.4	-1.5	0.4	-11.7	10.4	2.8	1.2	-5.0
5	51.0	-4.1	-1.2	-18.2	12.6	0.3	0.1	-6.5
10	53.0	-0.8	0.5	-19.0	15.2	1.3	0.3	-7.1
15	42.9	2.9	1.7	-9.5	13.9	1.2	1.2	-7.6
20	28.2	0.9	1.1	3.7	13.7	-0.1	1.5	-6.6
25	22.9	1.5	-1.4	12.9	14.9	0.6	-0.1	-6.1
30	18.7	-0.6	-0.8	14.9	13.1	0.7	0.0	-7.1
35					13.8	0.5	0.2	-5.6
40					12.5	-2.1	-0.4	-6.1
45					12.4	-1.6	-1.3	-6.5
50					12.5	-1.6	-1.9	-4.5

values at the surface and at the bottom are somewhat doubtful and estimates only can be given as to the probable values.

The observations for the Sound of Jura and the Solent may be considered to give the values of u_1 at the surface and at intervals of a quarter-depth, the values at the bottom being deduced from these; they are given in Table II.*

Table II.

	Total depth. Metres.	u_1 in cm./sec.				
		0.	$h/4$.	$h/2$.	$3h/4$.	h .
Jura	$h = 68$	180	178	169	152	126
Solent	$h = 45$	175	172	159	136	104

The values of f_1, f_2, g_1, g_2 are next evaluated by substituting in equations (2), and $\bar{f}_1, \bar{f}_2, \bar{g}_1, \bar{g}_2$, as defined in the previous section, are then obtained.

The quantities $F_1^h, F_2^h, G_1^h, G_2^h$ are rather troublesome to determine; for their evaluation use was made of the Tide-predicting Machine at the Liverpool Observatory and Tidal Institute.† The values of the harmonic constituents of the easterly and northerly components (V_E, V_N) of the velocity at the bottom are set separately on the machine, hourly values of V_E and V_N then read off over an interval of 15 days, and from these values those of $V = \sqrt{(V_E^2 + V_N^2)}$, VV_E and VV_N are obtained. The sets of values VV_E and VV_N are then separately analysed for the semi-diurnal lunar constituent.‡ A knowledge of this with reference to the axes Oxy leads to the determination of $F_1^h, F_2^h, G_1^h, G_2^h$ as explained at the end of the preceding section.

(A) Considering now the variation of u_1 with depth at any station, this quantity is found to exhibit a well-defined maximum value at some point below the surface, the position ($z = -h'$) of which can be determined approximately from a graphical representation of u_1 . Equation (5A) then provides the value of $g \cdot \partial \zeta_1' / \partial x$, and from equation (4) the values of F_1 at various

* The data in Table II are taken as being representative of the set of observations given in the original paper.

† The author here wishes to express his thanks to the authorities of the Liverpool Observatory and Tidal Institute for facilities offered in this connection and in particular to Dr. A. T. Doodson for advice regarding the use of the machine.

‡ See Doodson, 'Instructions for analysing tidal observations,' H.M. Stationery Office, London.

depths may be obtained. Similar work may also be performed using the equations involving respectively F_2 , G_1 and G_2 .

(B) When F_1^A is known, $g \cdot \partial \zeta_1' / \partial x$ is found from equation (5B), and equation (4) then provides the values of F_1 . The values of F_2 , G_1 and G_2 are similarly determined.

In order to adapt the observations for the Sound of Jura and the Solent to the discussion, it is assumed that

$$u_2 = v_1 = v_2 = 0.$$

There is some justification for this in that, in a narrow channel through which a rapid current flows, v_1 and v_2 will be small compared with u_1 , and u_2 will also be small.

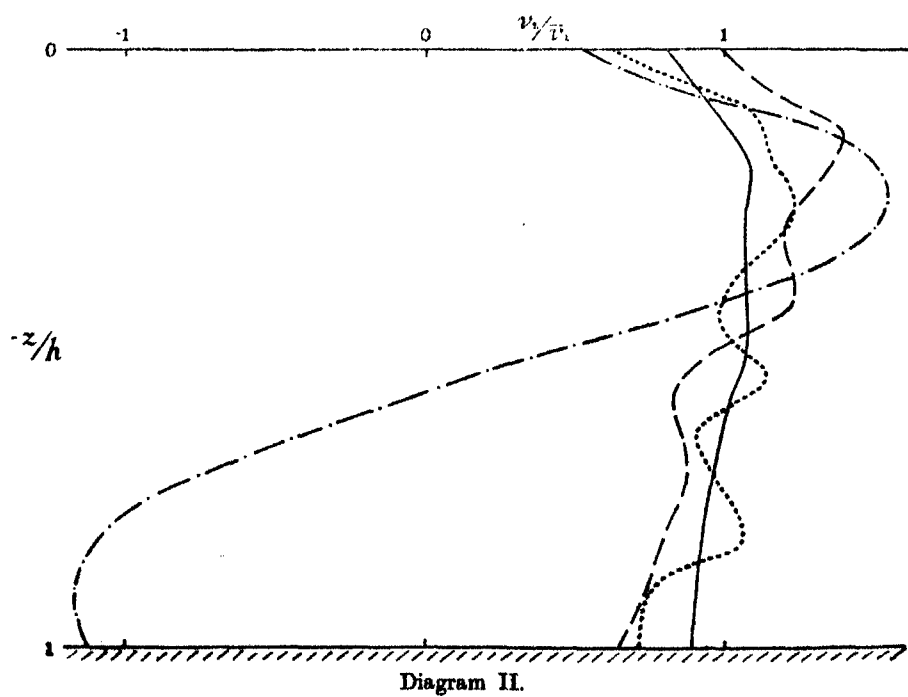
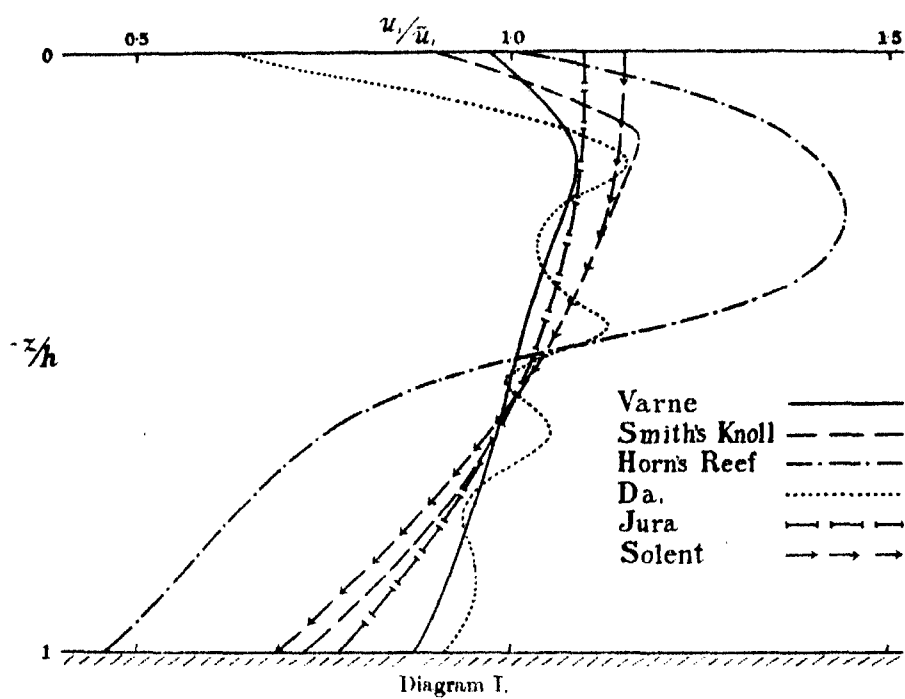
Results.

§ 4. The variations of u_1 and v_2 with depth at the different stations are shown in diagrams I and II. The curves in diagram I are obtained by plotting u_1/\bar{u}_1 against depth for the observations at the various stations; in order not to confuse the diagram, however, the curves for Varne and Smith's Knoll, which relate to different years, are replaced by their means. Diagram II is similarly constructed to exhibit the variations of v_2/\bar{v}_2 ; there are no curves on this diagram relating to the Sound of Jura or the Solent, since according to assumption v_2 is zero. The method of distinguishing between the various curves is explained on diagram I, and is followed in diagram II. Curves showing the variations of u_2 and v_1 with depth have not been drawn; these quantities are always small and oscillate about the value zero.

A point which arises from the forms of the curves in diagram I is that whereas the curves for the Sound of Jura and the Solent have their maxima very near the surface, those for the North Sea stations are well below, say at depths somewhere near $0.16h$. The latter result stands in good agreement with that obtained for the steady flow of water along a horizontal channel.*

No difficulty is experienced in applying the method of the previous section when assumption (B) is made. Under assumption (A) no outstanding difficulty occurs when use is made of the equations involving F_1 , but the roughness of the observations imposes a restriction on the application of the method to the equations involving F_2 , G_1 and G_2 . The quantities F_2 , G_1 , G_2 are all small compared with F_1 and, according to assumption (A), should vanish where the corresponding velocity components are stationary with depth. Now a glance at the diagrams I and II shows that whereas the u_1 curves, excepting that for Da_1 , each exhibit a single maximum, some of the v_2 curves appear to have two

* Cf. Gibson, 'Hydraulics,' 3rd ed., p. 330.



or more stationary values. The wavy appearance thus communicated to the v_2 curves is also a feature of those representing the variations of u_2 and v_1 , and of u_1 for the station Da₁.

This wavy appearance may be due to errors of observation and could be eliminated by smoothing processes. It was felt, however, that such processes are undesirable in that it is never certain whether they do or do not eliminate actual phenomena. It was decided therefore to work with actual rather than with smoothed values, so that in the results exhibited no attempt is made at smoothing.

In the case of the station Da₁ the values of u_1 are small. The graph of u_1/\bar{u}_1 exhibits a definite maximum at a depth of 10 metres, but maxima also appear at depths of 25 and 35 metres. The occurrence of these secondary maxima complicates the discussion under assumption (A); the work has, however, been included but the results cannot be regarded as entirely satisfactory.

It is interesting to note here that u_2 and v_1 being small, F_2 and G_1 should also be small, so that from the equations of motion it follows that f_2 and g_1 should be nearly constant. Since, however,

$$f_2 = -\sigma u_1 - 2\omega v_2, \quad g_1 = \sigma v_2 + 2\omega u_1,$$

this means that any large variation in u_1 should be balanced by a large variation in v_2 , since σ and 2ω are of the same order of magnitude. The diagrams I and II indicate that this is the case.

It will no doubt be conceded that there is general agreement between all the u_1 curves and also between all the v_2 curves, with the exception of those for Horn's Reef. At Horn's Reef the variation in u_1 is so large that v_2 has to change sign between the surface and the bottom.* Further v_2 exhibits a stationary value near the bottom, in addition to the one near the surface, which cannot be the result of an error of observation but seems to be necessary from considerations of the drag-effect of the bottom.

The occurrence of the two stationary values exhibited by the v_2 curve for Horn's Reef permits the direct calculation of G_2^h under assumption (A). The value thus obtained is not in good agreement with that obtained by the method outlined in § 3. To obtain agreement the motion at the bottom, which is obtained by extrapolation from the observations, must be slightly altered. The effect of this is to produce a motion, which although a possible deduction is not the obvious one from the observations, *i.e.*, the effect of the bottom at

* The curve in diagram II for Horn's Reef has been drawn by plotting $-v_2/\bar{v}_2$ against depth, since, on account of the positive and negative values of v_2 , \bar{v}_2 is small.

Horn's Reef on the motion of the water in the immediate neighbourhood may be one which would not be deduced from the observations. The consequence is that for this station the results may be somewhat unreliable. Otherwise since, as indicated by the forms of the u_1 and v_2 curves, the motion at Horn's Reef is in a way exceptional, it is possible that horizontal turbulent effects occur here, in which case the equations of § 2, obtained by neglecting horizontal turbulence, no longer hold. Observations for the years 1922 and 1923 for Horn's Reef have been made but have not yet been analysed; if the analysis becomes available it will be interesting to see if the observations utilised in this paper are at all exceptional.

Table III gives the variation of F_1 with depth at the various stations, obtained under assumption (A), while Table IV gives the variations of F_1 , F_2 , G_1 , G_2 under assumption (B). The values of F_2 , G_1 and G_2 under (A) are in general smaller than those under (B); the former tend to vanish at points where the corresponding velocity components are stationary with depth, while Table IV shows little tendency for the latter to vanish other than at the surface. The values of F_2 , G_1 and G_2 under (A) are not given since they are small, and also because there is not always good agreement between the depths at which they vanish and those at which the corresponding velocity components are stationary; this may however, as already pointed out, be due to the roughness of the data. On the other hand, under (B), there is no criterion to restrict the variation of the friction components, they are given as deduced from the observations.

The average value of F_1 at the surface for Varne and Smith's Knoll, under assumption (A), is $-1.6 \text{ cm.}^2/\text{sec.}^2$. In order to obtain some idea as to whether or not this surface-drag effect can be produced by air-resistance alone, it may be assumed that a constant wind of speed V blows in the direction of maximum flow. If the expression for the friction at the surface is of the same form as at the bottom, then the component of frictional force at the surface in the direction Ox is given by

$$\rho F = 0.002 \rho_a (V - u_1 \cos \sigma t)^2,$$

when the wind is in this direction, and by

$$\rho F = -0.002 \rho_a (V + u_1 \cos \sigma t)^2,$$

when the wind is in the opposite direction, ρ_a being the density of air. In either case

$$\rho F_1 = -0.002 \rho_a \cdot 2Vu_1,$$

giving $V = 40 \text{ m./sec.}$, a value, however, which is much too large.

Table III.—Values of F_1 (cm.²/sec.²) at Various Depths (A).

Depth. Metres.	Varne.		Smith's Knoll.		Horn's Reef.	Da ₁ .	Jura.	Solent.	Depth.
	(1922).	(1923).	(1922).	(1923).					
0	-1.78	-1.91	-1.35	-1.37	-0.6	0.0	-2.1	-1.1	0
5	-0.30	-0.21	0.00	0.00	-0.3	0.0	6.4	4.6	$h/4$
10	1.39	1.59	1.33	1.22	0.1	0.0	14.8	10.2	$h/2$
15	3.10	3.54	2.70	2.43	0.3	0.0	23.3	15.9	$3h/4$
20	4.78	5.53	4.06	3.63	0.4	0.1	31.8	21.6	h
25	6.47	7.52	5.35	4.82	0.5	0.1			
30	8.09	9.33	6.61	6.14	0.6	0.1			
32					0.7				
35			7.88	7.63		0.1			
40						0.2			
45						0.3			
50						0.3			
55						0.3			

Table IV.—Values of F_1 , F_2 , G_1 , G_2 (cm.²/sec.²) at Various Depths (B).

Depth. Metres.	Varne.								Horn's Reef.				Da ₁ .			
	(1922).				(1923).											
	F ₁ .	F ₂ .	G ₁ .	G ₂ .	F ₁ .	F ₂ .	G ₁ .	G ₂ .	F ₁ .	F ₂ .	G ₁ .	G ₂ .	F ₁ .	F ₂ .	G ₁ .	G ₂ .
5	1.18	-0.04	-0.12	-0.30	1.38	0.29	-0.36	-0.34	0.2	0.1	0.1	0.2	-0.1	-0.1	0.1	-0.1
10	2.58	0.05	-0.30	-0.40	2.87	0.63	-0.73	-0.55	0.5	0.2	0.3	0.4	-0.1	-0.1	0.1	-0.1
15	3.99	0.00	-0.38	-0.46	4.50	0.64	-0.86	-0.58	0.6	0.3	0.4	0.5	-0.1	-0.1	0.1	-0.1
20	5.38	-0.13	-0.41	-0.54	6.17	0.41	-0.77	-0.56	0.6	0.2	0.5	0.5	0.0	-0.1	0.1	-0.1
25	6.76	-0.43	-0.33	-0.60	7.84	0.03	-0.60	-0.55	0.7	0.1	0.4	0.5	0.1	-0.1	0.0	-0.1
30	8.09	-0.97	-0.07	-0.73	9.33	-0.60	-0.22	-0.73	0.6	0.0	0.1	0.5	0.0	0.0	0.0	-0.1
32									0.7	-0.1	0.1	0.5				
35													0.0	0.0	0.0	-0.1
40													0.1	0.0	0.0	-0.1
45													0.2	-0.1	0.0	0.0
50													0.3	-0.1	0.0	-0.1
55													0.3	-0.1	-0.1	-0.1

	Smith's Knoll.								Jura.	Solent.	Depth.
	(1922).				(1923).						
	F ₁ .	F ₂ .	G ₁ .	G ₂ .	F ₁ .	F ₂ .	G ₁ .	G ₂ .	F ₁ .	F ₁ .	
5	1.15	0.13	-0.18	0.02	1.18	0.06	-0.12	0.07	7.9	5.4	<i>h</i> /4
10	2.30	0.70	-0.67	0.03	2.20	0.69	-0.68	-0.04	15.9	10.8	<i>h</i> /2
15	3.47	1.01	-0.98	0.06	3.21	1.09	-1.08	-0.17	23.8	16.2	<i>3h</i> /4
20	4.64	1.11	-1.17	0.01	4.22	1.26	-1.31	-0.31	31.8	21.6	<i>h</i>
25	5.73	0.99	-1.24	-0.10	5.21	1.13	-1.34	-0.48			
30	6.80	0.44	-0.98	-0.25	6.34	0.42	-0.90	-0.55			
35	7.88	-0.69	-0.27	-0.41	7.63	-0.84	0.02	-0.43			

It should be noted that since the values of u_1 , u_2 , v_1 , v_2 for the North Sea stations at the surface and the bottom, and for the Sound of Jura and the Solent at the bottom, are obtained by extrapolation, a certain amount of latitude arises when fixing these values. The methods of the present paper require an accurate knowledge of the conditions in the neighbourhood of the bottom, thus the actual numerical values given to the components of friction may be slightly in error.

The Relativistic Theory of an Atom with Many Electrons.

By J. A. GAUNT, Trinity College, Cambridge.

(Communicated by R. H. Fowler, F.R.S.—Received March 8, 1929.)

§ 1. *Introduction.*

This paper derives the ordinary classification of multiplets, and the selection and summation rules, from Dirac's relativistic equation. The non-relativistic theory of the inner quantum number j and the magnetic quantum number u , and their selection rules, was worked out for an atom with any number of point-electrons by Born, Heisenberg and Jordan, using matrices, and by Dirac, using q -numbers.† The two methods are equivalent, and depend principally upon the properties of the total angular momentum. § 2 points out that the total angular momentum has the same properties in the new theory, so that the previous work can be taken over with scarcely any amendment.

§ 3 deals with a selection rule that has received little theoretical attention. The azimuthal quantum number for a single electron is denoted by k , and Σk is the sum for all the orbits involved in a given state. It is known empirically that Σk always changes by an odd number.‡ This is the basis of the distinction between S, P, D, ... and S', P', D', ... terms. The rule is proved rigorously in the absence of external fields. A practical consequence is that the O^{++} lines of nebular spectra, if rightly identified, can occur only in electric or non-uniform magnetic fields, for they have $\Delta \Sigma k = 0$.

A q -number theory of multiplets has not yet been developed, and we treat

† Born, Heisenberg and Jordan, 'Z. Physik,' vol. 35, p. 557 (1926); Dirac, 'Roy. Soc. Proc.,' A, vol. 111, p. 281 (1926).

‡ Hund, 'Linienpektren,' p. 132 (Berlin, 1927).

them by means of wave-mechanics in §§ 4 and 5. The azimuthal quantum number l is defined, although it cannot easily be expressed in terms of simple dynamical variables. The values of j appropriate to a multiplet of given l are deduced. They are generally derived by an argument about the composition of quantised vectors. This idea provides a very handy rule-of-thumb, but it is desirable to support it by a theoretical argument.

Finally, the summation rules for the intensities in a multiplet is proved to a first approximation. By "intensity" is meant a conventional intensity proportional to the square of the matrix-component of the electric moment; it is obtained from the Einstein A coefficient by dividing by the cube of the frequency. This part of the theory neglects quantities as small as the ratio of the spin separations to the total energy.

§ 2. *The Quantum Numbers j and u , and their Selection Rules.*

The atom consists of n electrons in a central electrostatic field of potential V . The electrons are formally distinguished by suffixes 1, 2, ... n ; and for this reason Dirac's matrices are denoted by $\sigma_x, \sigma_y, \sigma_z$ (forming a vector $\boldsymbol{\sigma}$), and ρ', ρ'', ρ''' . The spatial co-ordinates x, y, z form a vector \mathbf{r} of magnitude r ; and the momenta p_x, p_y, p_z form a vector \mathbf{p} . The distance between two electrons a and b is r_{ab} .

The wave-equation for a single electron is

$$[\mathbf{H} - E] \psi = 0, \quad (1)$$

where

$$\mathbf{H} \equiv -mc^2 - cV - c\rho'(\boldsymbol{\sigma} \cdot \mathbf{p}) - \rho'''mc^2.$$

Dirac defines the orbital and total angular momenta of an electron by

$$\mathbf{m} = \mathbf{r} \times \mathbf{p}, \quad \mathbf{M} = \mathbf{m} + \frac{1}{2}\hbar \boldsymbol{\sigma}. \quad (2)$$

(\times denotes a vector product). He shows that

$$\mathbf{M} \text{ commutes with } r \text{ and } H, \quad (3)$$

and proves formulæ such as

$$M_x x - x M_x = 0; \quad M_y x - x M_y = -i\hbar z; \quad M_z x - x M_z = i\hbar y, \quad (4)$$

and also

$$\mathbf{M} \times \mathbf{M} = i\hbar \mathbf{M}. \quad (5)$$

We define the total angular momentum of an atom with n electrons to be

$$\mathbf{G} = \sum_a \mathbf{M}_a. \quad (6)$$

Since variables belonging to different electrons always commute, (3) shows that

$$\mathbf{G} \text{ commutes with } r_a \text{ and } H_a. \quad (7)$$

Also from (4)

$$G_x x_a - x_a G_x = 0; \quad G_x y_a - y_a G_x = -ihz_a; \quad G_x z_a - z_a G_x = ihy_a, \quad (8)$$

and from (5)

$$\mathbf{G} \times \mathbf{G} = \sum_a \mathbf{M}_a \times \mathbf{M}_a = \sum_a i\hbar \mathbf{M}_a = i\hbar \mathbf{G}.$$

Thus \mathbf{G} has all the properties of the total angular momentum of a single electron, or of many point-electrons in the older theory, if it is a constant of the motion.

The wave-equation for the atom with n electrons is

$$[\mathbf{F} - E] \Psi = 0, \quad (9)$$

with the Hamiltonian

$$\mathbf{F} \equiv \sum_a H_a + \sum_{ab} P_{ab}. \quad (10)$$

The energy of interaction of two electrons is†

$$P_{ab} = [1 - \rho_a' \rho_b' (\boldsymbol{\sigma}_a \cdot \boldsymbol{\sigma}_b)] e^2 / r_{ab}.$$

We require to prove that \mathbf{G} commutes with P_{ab} . It evidently commutes with ρ_a', ρ_b' . Its relations with r_{ab} and $(\boldsymbol{\sigma}_a \cdot \boldsymbol{\sigma}_b)$ must be investigated.

We find from (8)

$$\begin{aligned} G_x x_a x_b - x_a x_b G_x &= 0, \\ G_x y_a y_b - y_a y_b G_x &= i\hbar (z_a y_b + y_a z_b), \\ G_x z_a z_b - z_a z_b G_x &= -i\hbar (y_a z_b + z_a y_b). \end{aligned}$$

Addition shows that G_x commutes with $(\mathbf{r}_a \cdot \mathbf{r}_b)$. By (7) it commutes with r_a^2 and r_b^2 . Therefore it commutes with r_{ab}^2 . Now

$$G_x r_{ab}^2 - r_{ab}^2 G_x = (G_x r_{ab} - r_{ab} G_x) r_{ab} + r_{ab} (G_x r_{ab} - r_{ab} G_x).$$

Since G_x is linear in the momenta, the bracket on the right is a function of the co-ordinates only, and commutes with r_{ab} . Hence it must vanish, to make the left-hand side vanish. That is,

$$G_x \text{ commutes with } r_{ab}.$$

Similarly for G_y and G_z .

By Dirac's formulæ (8)‡

$$\begin{aligned} \sigma_{ax} (\boldsymbol{\sigma}_a \cdot \boldsymbol{\sigma}_b) &= \sigma_{bx} + i\sigma_{ax}\sigma_{by} - i\sigma_{ay}\sigma_{bx}, \\ (\boldsymbol{\sigma}_a \cdot \boldsymbol{\sigma}_b) \sigma_{ax} &= \sigma_{bx} - i\sigma_{ax}\sigma_{by} + i\sigma_{ay}\sigma_{bx}. \end{aligned}$$

† Gaunt, 'Roy. Soc. Proc.,' A, vol. 122, p. 526 (1929).

‡ *Loc. cit.*, p. 615.

That is

$$\sigma_a(\sigma_a \cdot \sigma_b) = \sigma_b - i\sigma_a \times \sigma_b,$$

$$(\sigma_a \cdot \sigma_b)\sigma_a = \sigma_b + i\sigma_a \times \sigma_b,$$

so that

$$(\sigma_a + \sigma_b)(\sigma_a \cdot \sigma_b) = \sigma_b + \sigma_a + (\sigma_a \cdot \sigma_b)(\sigma_a + \sigma_b).$$

Hence \mathbf{G} commutes with $(\sigma_a \cdot \sigma_b)$.

This completes the proof that \mathbf{G} commutes with P_{ab} . Since it commutes with H_a also, it commutes with \mathbf{F} and is a constant of the motion. The total angular momentum now plays exactly the same part as in the older theory and in the theory of the hydrogen atom, and for proofs of the various formulæ the reader is referred to the papers cited above.† The argument is only outlined here.

G^2 commutes with \mathbf{G} , so we may write

$$G^2 = (g^2 - \frac{1}{4})\hbar^2; \quad G_z = u\hbar,$$

where g is a quantum number similar to Dirac's j , and u is the magnetic quantum number. The characteristic values of m_z are integral multiples of \hbar , and those of σ_z are ± 1 . So by (2) and (6) the values of u must be multiples of $\frac{1}{2}$ of the same parity as n .

Since by (8)

$$G_z z_a - z_a G_z = 0,$$

$$G_z(x_a + iy_a) = (x_a + iy_a)G_z = \hbar(x_a + iy_a),$$

$$G_z(x_a - iy_a) = (x_a - iy_a)G_z = -\hbar(x_a - iy_a),$$

we find for the matrix-components of the co-ordinates

$$\left. \begin{aligned} (u_1|z_a|u_2) &= 0 \quad \text{unless} \quad u_1 = u_2 \\ (u_1|x_a + iy_a|u_2) &= 0 \quad \text{unless} \quad u_1 = u_2 + 1 \\ (u_1|x_a - iy_a|u_2) &= 0 \quad \text{unless} \quad u_1 = u_2 - 1 \end{aligned} \right\}. \quad (11)$$

These give the usual polarisation rules, with $\Delta u = 0$ or ∓ 1 .

The rules (11) hold when G_x, G_y, G_z are substituted for x_a, y_a, z_a . Hence the equation

$$(G_x + iG_y)(G_x - iG_y) = G^2 - G_z^2 + \hbar G_z$$

has the diagonal component

$$(u|G_x + iG_y|u-1)(u-1|G_x - iG_y|u) = (g^2 - \frac{1}{4} - u^2 + u)\hbar^2.$$

† Or to Birtwistle, 'The New Quantum Mechanics' (Camb. Univ. Press, 1928), pp. 107-8, 119.

When u has its minimum value the left-hand side must be replaced by 0 ; therefore

$$u_{\min.} = -|g| + \frac{1}{2}.$$

By a similar argument

$$u_{\max.} = |g| - \frac{1}{2}.$$

Thus the range of u is indicated by

$$-j \leq u \leq j, \quad (12)$$

where

$$j = |g| - \frac{1}{2}. \quad (13)$$

(12) shows that j is the inner quantum number of spectroscopy.

By repeated application of (8) it is found that

$$G^2 G^2 x_a - 2G^2 x_a G^2 + x_a G^2 G^2 = 2h^2 \{G^2 x_a + x_a G^2 - 2(\mathbf{G} \cdot \mathbf{r}_a) x_a\}, \quad (14)$$

and also that $(\mathbf{G} \cdot \mathbf{r}_a)$ commutes with \mathbf{G} , and so with G^2 .

Define a vector \mathbf{s}_a by the equation

$$G^2 \mathbf{s}_a = (\mathbf{G} \cdot \mathbf{r}_a) \mathbf{G}.$$

Then G^2 commutes with \mathbf{s}_a , so that

$$(g_1 | \mathbf{s}_a | g_2) = 0 \quad \text{unless} \quad |g_1| = |g_2|. \quad (15)$$

By (14) we have

$$\begin{aligned} G^2 G^2 (\mathbf{r}_a - \mathbf{s}_a) &= 2G^2 (\mathbf{r}_a - \mathbf{s}_a) G^2 + (\mathbf{r}_a - \mathbf{s}_a) G^2 G^2 \\ &= 2h^2 G^2 (\mathbf{r}_a - \mathbf{s}_a) + 2h^2 (\mathbf{r}_a - \mathbf{s}_a) G^2. \end{aligned}$$

Hence $(g_1 | \mathbf{r}_a - \mathbf{s}_a | g_2)$ vanishes unless

$$(g_1^2 - \frac{1}{4})^2 - 2(g_1^2 - \frac{1}{4})(g_2^2 - \frac{1}{4}) + (g_2^2 - \frac{1}{4})^2 = 2(g_1^2 - \frac{1}{4}) + 2(g_2^2 - \frac{1}{4}),$$

that is

$$g_1 = \pm g_2 \pm 1,$$

with (15) this gives

$$(g_1 | \mathbf{r}_a | g_2) = 0 \quad \text{unless} \quad g_1 = \pm g_2 \text{ or } \pm g_2 \pm 1.$$

By (13) these conditions may be written

$$j_1 = j_2 \quad \text{or} \quad j_2 \pm 1,$$

which is the ordinary selection rule for j . It is rigorous for the dipole radiation. It shows that the values of j differ by integers ; they are, like the values of u , multiples of $\frac{1}{2}$ of the same parity as n .

The relative intensities of the Zeeman components in a weak magnetic field may also be calculated exactly as in previous theories.

§ 3. *The Selection Rule for Σk .*

In proving the selection rule that $\Delta \Sigma k$ is odd, we shall admit a magnetic field with a vector potential \mathbf{A} which is an odd function of the spatial co-ordinates. This treatment is both more general and more convenient, since degeneracy is removed. A special case is that of a uniform magnetic field. The Hamiltonian for a single electron is now

$$H \equiv -mc^2 - eV - \rho' (\boldsymbol{\sigma} \cdot c\mathbf{p} + e\mathbf{A}) - \rho''' mc^2. \quad (16)$$

Consider the effect of reversing the axes of co-ordinates, without, however, altering the spin co-ordinate. That is, x, y, z are to be replaced by $-x, -y, -z$, and \mathbf{p} by $-\mathbf{p}$. By hypothesis, \mathbf{A} becomes $-\mathbf{A}$, but V is unchanged. The new Hamiltonian is

$$H(-) \equiv -mc^2 - eV + \rho' (\boldsymbol{\sigma} \cdot c\mathbf{p} + e\mathbf{A}) - \rho''' mc^2. \quad (17)$$

Now multiply (16) by ρ''' in front and behind. This variable anticommutes with ρ' and commutes with the other variables in (16), and its square is unity. So (16) is changed into (17). That is

$$H(-) = \rho''' H \rho'''. \quad (18)$$

We define the product

$$\rho = (-)^n \rho_1''' \rho_2''' \dots \rho_n'''. \quad (19)$$

(The convenience of $(-)^n$ will appear later.) Then (18) may be written

$$H_a(-) = \rho H_a \rho. \quad (20)$$

for ρ_b''' commutes with H_a ($b \neq a$), and its square is unity. Also ρ commutes with $\rho_a' \rho_b'$, since ρ_a''' and ρ_b''' anticommute with ρ_a' and ρ_b' respectively and the other factors commute. Thus ρ commutes with P_{ab} , which also is unaltered by the change of sign. Therefore by (10) and (20)

$$F(-) = \rho F \rho.$$

We obtain, then, on changing the sign of the spatial co-ordinates in the wave-equation (9)

$$[\rho F \rho - E] \Psi(-) = 0,$$

or, after operating with ρ ,

$$[F - E] \rho \Psi(-) = 0.$$

Thus $\rho \Psi(-)$ satisfies the wave-equation (9) with the same characteristic energy E ; and it is bounded and vanishes at infinity. Therefore

$$\rho \Psi(-) = \lambda \Psi \quad (21)$$

where λ is a constant, which we will prove to be ± 1 .

At this point a lemma must be introduced. If α and β are two Hermitian spin-matrices, whose terms are denoted by $\alpha_{\mu\nu}$ and $\beta_{\mu\nu}$; and if components of the wave-function are similarly denoted by Ψ_μ ; then

$$\begin{aligned}\sum_{\mu} (\alpha \Psi)_\mu^* (\beta \Psi)_\mu &= \sum_{\mu, \nu, \tau} (\alpha_{\mu\nu} \Psi_\nu)^* \beta_{\mu\tau} \Psi_\tau \\ &= \sum_{\mu, \nu, \tau} \Psi_\nu^* \alpha_{\nu\mu} \beta_{\mu\tau} \Psi_\tau \\ &= \sum_{\nu} \Psi_\nu^* (\alpha \beta \Psi)_\nu.\end{aligned}\tag{22}$$

We can now find λ . The sign \int is used to denote an integration over the whole range of the spatial co-ordinates, and a sum over the values of the spin co-ordinates such as occurs in (22). By an obvious transformation

$$\begin{aligned}\lambda^2 \int \Psi'(-)^* \Psi'(-) &= \lambda^2 \int \Psi'^* \Psi' \\ &= \int (\rho \Psi'(-))^* \rho \Psi'(-) \\ &= \int \Psi'(-)^* \Psi'(-)\end{aligned}$$

by (22), since $\rho^2 = 1$. Thus $\lambda = \pm 1$, and after an operation by ρ on (21)

$$\Psi'(-) = \pm \rho \Psi'.\tag{23}$$

The states of the system fall into two sets, according to the sign that must be taken in (23). The state (or wave-function) is called "even" or "odd," according as the sign is + or -. The selection rule we are proving is that an ordinary emission or absorption involves one odd and one even state.

Suppose that the states m and n are both odd or both even; and let X be a component of the electric moment of the atom (or any odd function of the co-ordinates that commutes with ρ). Then

$$\begin{aligned}\int \Psi_m^* X \Psi_n &= - \int \Psi_m(-)^* X \Psi_n(-) \\ &= - \int (\rho \Psi_m)^* X \rho \Psi_n \\ &= - \int \Psi_m^* X \Psi_n\end{aligned}$$

by (22). Therefore the (mn) matrix-component of X must vanish, and the corresponding transition is forbidden.

Before we can express this rule in terms of Σk , we must be able to assign

to each state of the atom the appropriate electronic orbits. The idea of separate orbits is strictly applicable only to an atom in which there is no interaction between the electrons. We must therefore pick out the state of this simpler atom which is the first approximation to the given state of the more life-like atom, and which changes continuously into it as the interaction is increased from zero to its normal value. If this is done correctly, the general theory must hold for the first approximation, and can therefore be expressed in terms of the orbital quantum numbers.

The first approximation to the wave-function is

$$\Psi = \Sigma \pm \psi_a(1) \psi_b(2) \dots \psi_n(n) \quad (24)$$

where ψ_a, ψ_b, \dots are solutions of Dirac's equation (1); (a) summarises the co-ordinates of the a th electron; and the signs are chosen so as to make Ψ antisymmetrical. We have to determine the sign to be used in (23) when Ψ is given by (24).

For a single electron, (23) becomes

$$\psi(-) = -\lambda \rho''' \psi \quad (25)$$

where $\lambda = \pm 1$. ρ''' is a diagonal matrix whose final component is -1 ; so the fourth component of equation (25) is

$$\psi_4(-) = \lambda \psi_4. \quad (26)$$

If the azimuthal quantum number is k , Dirac's j is either k or $-k-1$, but in either case ψ_4 is a function of the radius alone multiplied by a tesseral harmonic P_k^u . Now

$$P_k^u(-) = (-)^k P_k^u$$

Therefore in (26)

$$\lambda = (-)^k.$$

Applying equations like (25) to the wave-function (24), we obtain

$$\Psi(-) = (-)^{\Sigma k} \rho \Psi,$$

where Σk is the sum of the azimuthal quantum numbers of the electronic orbits. Thus the sign in (23) is $+$ or $-$ according as Σk is even or odd; and the state has the same parity as Σk . (The $(-)^n$ is inserted in (19) in order to achieve this convenience.)

The selection rule may now be restated:

$$\Delta \Sigma k \text{ is odd.}$$

§ 4. Multiplets and the Summation Rule—Preliminaries.

In the next two sections we discuss the classification of multiplets from the point of view of wave-mechanics, and derive the summation rule for the intensities. We take over from q -number theory the fact that the angular momentum about the z -axis is a constant of the motion and defines the magnetic quantum number. In the absence of external fields the equations are spherically symmetrical, and there must be degeneracy in this quantum number. There are also degeneracies due to "resonance"; but in general the system is not otherwise degenerate. The problem of classification reduces to an enumeration of states with a given magnetic quantum number.†

Spin effects are treated as small perturbations. Each multiplet can be correlated with an energy-level of the atom with point-electrons of the older theory. Although the spin is inextricably woven into Dirac's equation, only the details of the perturbation theory are different, and not the general method.‡ The first step, therefore, is to solve the non-relativistic equation, and it is with wave-functions satisfying this equation that we are concerned in this section.

The atom with point-electrons has a magnetic quantum number, which we denote by m . Any energy-level has a range of values of m such as is indicated by

$$-l < m \leq l.$$

Thus the range of m serves to define a number l , which is a label belonging to the energy-level of the simplified atom, and so ultimately to the multiplet. Like m , it must be an integer; and we shall show later that it is the ordinary quantum number which distinguishes S, P, D, ..., terms. It is not easy to express it precisely in terms of the simple dynamical variables.

The wave-functions belonging to any energy-level all have the same symmetry-character; and upon it alone several properties depend. Apart from the degeneracy in m , there is a definite degree of degeneracy D , due to the formation of new wave-functions by permuting the electrons. By linear combinations of the wave-functions with a given energy and magnetic quantum number, it is possible to form a function ϕ^m , and $D - 1$ independent functions $\phi^m(P)$, $\phi^m(Q)$, ..., obtained from ϕ^m by permutations P , Q , ..., which have the following property.§ If T is any permutation operator

$$T\phi^m(P) = \omega\phi^m(Q), \quad (27)$$

† Cf. Pauli, 'Z. Physik,' vol. 31, p. 765 (1925).

‡ Gaunt, *loc. cit.*, § 3.

§ Heisenberg, 'Z. Physik,' vol. 41, p. 239 (1927).

where Q may or may not be the same as P , and $|\omega| = 1$. Also no function of the type $\phi^m(P)$ will combine with a function of different type $\phi^n(Q)$, the different types of function being distinguished by different values of ω in (27).

If two sets of wave-functions with the same symmetry-character are denoted by lower suffixes α and β , and if F is a symmetrical function of the co-ordinates of the electrons,

$$\int \phi_\alpha^m(P)^* F \phi_\beta^{m'}(P) d\tau = \int \phi_\alpha^m(Q)^* F \phi_\beta^{m'}(Q) d\tau. \quad (28)$$

This follows at once from (27) when we operate with a suitable permutation T . Each integral in (28) will be denoted by

$$(\alpha m | F | \beta m').$$

We must now prove a lemma, which will be used later. Let \mathbf{R} be the electric moment of the atom, and let

$$R(m, m') \equiv \sum_{m''} (\alpha m | \mathbf{R} | \beta m'') \cdot (\beta m'' | \mathbf{R} | \alpha m').$$

Then

$$\left. \begin{aligned} R(m, m') &= 0 && \text{if } m \neq m' \\ R(m, m) &= R' && (\text{independent of } m) \end{aligned} \right\}. \quad (29)$$

The selection rules obviously deal with the first statement, except when $m' = m \pm 2$; and they show that

$$\begin{aligned} R(m, m+2) &= (\alpha m | R_x | \beta m+1) (\beta m+1 | R_x | \alpha m+2) \\ &\quad + (\alpha m | R_y | \beta m+1) (\beta m+1 | R_y | \alpha m+2). \end{aligned} \quad (30)$$

But the equation

$$(\alpha m | R_x + iR_y | \beta m+1) = 0$$

shows that each matrix-component of R_y in (30) is $-i$ times the corresponding matrix-component of R_x ; so that the two terms on the right cancel. Similarly for $R(m, m-2)$.

To prove the second part of (29), rotate the axes of co-ordinates. The new wave-functions are linear combinations of the old wave-functions with the same energy but various m .

$$\left. \begin{aligned} \psi_\alpha^M &= \sum_m a(Mm) \phi_\alpha^m \\ \psi_\beta^M &= \sum_m b(Mm) \phi_\beta^m \end{aligned} \right\}, \quad (31)$$

$\psi(P)$, $\psi(Q)$, ..., are similarly connected with $\phi(P)$, $\phi(Q)$, ..., which do not

occur in (31) since they do not combine with ϕ . The conditions for orthogonality and normalisation are

$$\left. \begin{aligned} \sum_m a(Mm)^* a(M'm) &= 0 \text{ if } M \neq M' \\ &= 1 \text{ if } M = M' \end{aligned} \right\}. \quad (32)$$

Denoting matrix-components formed from the ψ 's by a dash,

$$(\alpha M | R | \beta M')' = \sum_{m, m'} a(Mm)^* b(M'm') (\alpha m | R | \beta m').$$

Hence, by use of (32),

$$\sum_{M'} (\alpha M | R | \beta M')' \cdot (\beta M'' | R | \alpha M')' = \sum_{m, m'} a(Mm)^* a(M'm') R(m, m').$$

Since a scalar product is invariant for a rotation of axes, the left hand side is $R(M, M')$. Multiply by $a(Mm)$ and sum for M , using (32)

$$\sum_M a(Mm) R(MM') = \sum_{m'} a(M'm') R(mm'),$$

or, by the first part of the lemma

$$a(M'm) R(M'M') = a(M'm) R(mm).$$

That is, $R(mm)$ is independent of m .

This expresses the rule that the (conventional) intensities in a weak Zeeman multiplet have the same sum for each initial (or final) state.† It may be verified by using the formulæ for the relative intensities of the Zeeman components. At present, however, our atom has only point-electrons, and the result is chiefly useful for proving the summation rule in a multiplet.

§ 5. Multiplets and the Summation Rule—Results.

The next step is to recognise the existence of the spin co-ordinates. The wave-functions satisfying Dirac's equation have their first two components negligible in comparison with the last two. It is therefore unnecessary to introduce more than two functions of the spin co-ordinate of an electron‡

$$\chi_a = 0, 0, 1, 0,$$

$$\chi_b = 0, 0, 0, 1.$$

Out of these are built up functions χ_i of all the spin co-ordinates having various symmetry-characters.

In order to form a function that is antisymmetrical in the positions and

† Cf. Neumann and Wigner, 'Z. Physik,' vol. 51, p. 844 (1928).

‡ Gaunt, *loc. cit.*, p. 527.

spins, ϕ 's of symmetry-character $A(\lambda_1 + \lambda_2)$ must be combined with χ 's of symmetry-character $S(\lambda_1 + \lambda_2)$. Corresponding to ϕ , $\phi(P)$, ..., we find functions χ , $\chi(P)$, ..., with properties similar to (27); and so we construct the antisymmetrical function

$$\Psi^{ui} \equiv D^{-i} \sum_P \phi^{u-i}(P) \chi_i(P). \quad (33)$$

The notation requires some explanation. The terms under the sum might have coefficients of modulus 1, but these can be absorbed in the ϕ 's. D^{-i} is a normalising factor, i denotes the contribution of χ to the magnetic quantum number, so that u is the total magnetic quantum number of Ψ . $\chi_i(P)$ is a sum of terms each containing χ_a 's and χ_b 's. Now

$$\sigma_z \chi_a = \chi_a; \quad \sigma_z \chi_b = -\chi_b,$$

so that each χ_a contribute $+\frac{1}{2}$ and each χ_b contributes $-\frac{1}{2}$ to the magnetic quantum number. Thus χ_i involves $\frac{1}{2}n + i$ χ_a 's and $\frac{1}{2}n - i$ χ_b 's. This shows that $2i$ has the same parity as n . Also if χ_i is to have the symmetry-character $S(\lambda_1 + \lambda_2)$ there must be at least λ_2 of each of the functions χ_a and χ_b . Hence

$$|i| \leq \frac{1}{2}n - \lambda_2 = \frac{1}{2}(\lambda_1 - \lambda_2) = s \quad (\text{say}).$$

There is now degeneracy of two kinds, in u and in s . The former must persist to the end, but the latter disappears when spin effects are no longer neglected. The single energy-level breaks up into a multiplet with various j 's. Since the range of u for any term of the multiplet is given by

$$-j \leq u \leq j,$$

the values of j may be found by counting the number of wave-functions for each value of u . This number is not altered by the perturbation, so the counting may be done with the wave-functions (33).

The restrictions upon i are $|i| \leq s$, $|u - i| \leq l$. Therefore the number of wave-functions for each value of u numerically less than $|l - s|$ is $2l + 1$ or $2s + 1$ (whichever is less), and for greater values decreases by one for each increase of u up to its maximum $l + s$. When j has one of its possible values, the number of functions with $u = j$ is one more than the number with $u = j + 1$. Therefore there is no value of j less than $|l - s|$, but j ranges from $|l - s|$ to $l + s$. This shows that the multiplicity is $2s + 1$ when $l \geq s$; and that l and s are the usual quantum numbers of spectroscopy.

The first effect of the spin perturbation is to form linear combinations of the functions (33) that have the same u . For each value of j , we may write

$$\begin{aligned}\Psi_{\alpha j}^u &= \sum_i a(uji) \Psi_{\alpha}^{ui}, \\ \Psi_{\beta j}^u &= \sum_i b(uji) \Psi_{\beta}^{ui}.\end{aligned}$$

The conditions for orthogonality and normalisation lead to

$$\begin{aligned}\sum_j a(uji)^* a(uji') &= 0 \quad \text{if } i \neq i' \\ &= 1 \quad \text{if } i = i'\end{aligned} \quad (34)$$

and similar equations for the b 's.

Since $\phi(P)$, $\phi(Q)$ are non-combining,

$$\begin{aligned}\int \Psi_{\alpha}^{u*} \mathbf{R} \Psi_{\beta}^{u'} &= D^{-1} \sum_p \int \phi_{\alpha}^{u-i}(P)^* \mathbf{R} \phi_{\beta}^{u'-i}(P) d\tau. \\ &= (\alpha u - i | \mathbf{R} | \beta u' - i),\end{aligned}$$

and since $\chi_i \chi_{i'}$ vanishes unless $i = i'$,

$$\begin{aligned}\{\alpha j u | \mathbf{R} | \beta j' u'\} &\equiv \int \Psi_{\alpha j}^{u*} \mathbf{R} \Psi_{\beta j'}^{u'} \\ &= \sum_i \int a(uji)^* \Psi_{\alpha}^{ui*} \mathbf{R} b(u'j'i) \Psi_{\beta}^{ui} \\ &= \sum_i a(uji)^* b(u'j'i) (\alpha u - i | \mathbf{R} | \beta u' - i).\end{aligned}$$

The intensity of the line $\alpha j u - \beta j' u'$ is proportional to

$$\{\alpha j u | \mathbf{R} | \beta j' u'\} \cdot \{\alpha j u | \mathbf{R} | \beta j' u'\}^* = \{\alpha j u | \mathbf{R} | \beta j' u'\} \cdot \{\beta j' u' | \mathbf{R} | \alpha j u\}.$$

Summing these intensities over all states of the multiplet β , and using (34), we have

$$\begin{aligned}\sum_{j'u'} \{\alpha j u | \mathbf{R} | \beta j' u'\} \cdot \{\beta j' u' | \mathbf{R} | \alpha j u\} \\ &= \sum_{u'i} a(uji)^* (\alpha u - i | \mathbf{R} | \beta u' - i) \cdot a(uji) (\beta u' - i | \mathbf{R} | \alpha u - i) \\ &= \sum_i a(uji)^* a(uji) R' \quad \text{by (29)} \\ &= R'.\end{aligned}$$

This is independent of j and u . Thus the sum of the intensities of lines from the term αj to all terms of the multiplet β is proportional to the weight $2j + 1$ of that term. A similar summation rule applies to the terms of the multiplet β . In finding these summation rules, intensities of the order of the spin energy have been neglected. Therefore the question whether inter-combination

lines should be included in the sums does not arise, as their intensities are here assumed to be negligible.

Conclusions.

1. The selection rules are rigorous if there are no external fields.
2. The rule " $\Delta\Sigma k$ is odd" is equally rigorous, even in a uniform magnetic field.
3. The summation rule holds if magnitudes of the order of the spin energy are neglected.

I should like to thank Dr. P. A. M. Dirac for his criticisms of this paper.

Perturbation Theory in Quantum Mechanics—II.

By A. H. WILSON, Emmanuel College, Cambridge.

(Communicated by R. H. Fowler, F.R.S.—Received March 8, 1929.)

1. Introduction.

In a previous paper* the theory of perturbations was discussed for systems which possess only discrete spectra. The theory is now extended to systems with both discrete and continuous spectra, and in addition a slightly more general method of perturbation is considered. The Hamiltonian H of the perturbed system is split up into three parts H_0 , H_1 , $H_2(t)$, two of which can be chosen arbitrarily. The solutions of the perturbed problem can then be worked out in terms of the characteristic functions corresponding to the Hamiltonian $H_0 + H_2(T)$, where T is any arbitrary fixed time. In general, however, the series of perturbations does not converge, and different modes of splitting up the Hamiltonian will lead to different formal results. The perturbation theory does usually give the correct physical results, and it is therefore necessary to give some explanation of how this happens. In (I) the asymptotic nature of certain solutions was emphasised, but this does not extend to the more general systems treated here. It is suggested that the usual boundary conditions do not give an adequate description of any but the simplest atomic problems, and that more detailed restrictions, determined by

* 'Roy. Soc. Proc.,' A, vol. 122, p. 589 (1929). Referred to hereafter as (I).

the experimental conditions, ought to be substituted. As this is impossible in practice, an alternative method is to regard the motion as a perturbation on that Hamiltonian $H_0 + H_2(T)$ which most nearly corresponds to the experimental conditions. (For example, we may regard an electron as free or bound according as the experiment determines the number of free or bound electrons respectively, whereas in the usual theory the initial Hamiltonian is taken as fundamental.) This criterion, together with the initial conditions, suffices to fix the division of H into the three parts $H_0, H_1, H_2(t)$ which at first were chosen arbitrarily. The formal solution can be worked out on this basis, and it is then assumed that this solution is asymptotic to the one which would be obtained if the full boundary conditions were used. This suggestion is in accordance with the fact that a hydrogen atom in an electric field gives rise not only to the usual Stark effect, but also to an ionisation effect.

In § 2 the perturbation equations are derived in a slightly more general form than has previously been given. The theories of Born,* Dirac† and Oppenheimer‡ are particular cases of that given here, and are obtained by particular choices of $H_0, H_1, H_2(t)$. To obtain Born's theory we take $H_1 = 0$, and for Oppenheimer's we take $H_2(t) = H_2(T)$ and $T = 0$. In Dirac's theory we have $H_1 = 0, H_2(0) = 0$ and $T = 0$. Each of these theories is appropriate for the solution of special problems, but the more general method of this paper is required for the full discussion of the perturbation theory.

In § 3 the necessary existence theorems are proved, and in § 4 the validity of the perturbation theory is discussed.

2. The Perturbation Equations. §

2.1. We consider an atomic system which is subjected to an arbitrary perturbation from outside. The unperturbed system is characterised by a Schrödinger equation

$$\left(H_0 + H_1 - i \frac{\hbar}{2\pi} \frac{\partial}{\partial t} \right) \psi^0 = 0, \quad (1)$$

where H_0 and H_1 are independent of the time. The differential equation (1) will involve several independent variables, but, as we are not interested in the difference between degenerate and non-degenerate systems, the theory will be the same as for only one independent variable. We suppose that equation

* 'Z. Physik,' vol. 40, p. 167 (1926).

† 'Roy. Soc. Proc.,' A, vol. 112, p. 661 (1926).

‡ 'Phys. Rev.,' vol. 31, p. 66 (1928).

§ I am indebted to Mr. L. C. Young for verifying the details of this section.

(1) is separable, and that, with given boundary conditions, one of the resulting ordinary differential equations possesses a continuous set of characteristics as well as a discrete set, while the other equations only have discrete characteristics. The equations will be written in terms of the space variable which gives rise to the continuous characteristics, the other variables not appearing explicitly.

We put

$$\psi^{(1)} = \phi^{(1)}(x, W) e^{-2\pi i W t / \hbar},$$

where $\phi^{(1)}(x, W)$ is independent of the time, and W is a real parameter to be determined by the boundary conditions. Equation (1) takes the form

$$L\{\phi^{(1)}\} - W\phi^{(1)} \equiv (H_0 + H_1 - W)\phi^{(1)} = 0. \quad (1A)$$

Since the boundary points are always singularities of this differential equation the condition that $|\phi^{(1)}|^2$ should be integrable over the whole of the configuration space is a sufficient boundary condition. In practice, this is nearly equivalent to the more usual condition that $\phi^{(1)}$ must be finite and continuous.

If $\int |\phi^{(1)}|^2 dx$ taken over the whole of the configuration space is finite, the corresponding value of W is a discrete characteristic, and the totality of such values of W constitutes the discrete spectrum.

The theory of continuous spectra has been studied by Weyl,* and has been applied to quantum mechanics by various writers. As there seems to be some obscurity in the applications, the theory is given briefly here for reference.

$X(x, W)$ is a continuous function of the two variables x and W , and $X(x, 0) = 0$. Also,

$$\int \{X(x, W)\}^2 dx = \omega(W)$$

exists and is a continuous function of W . Then $X(x, W)$ is called a permissible solution of (1A) if it satisfies the equation

$$L\{X(x, W)\} - WX(x, W) + \int_0^W X(x, \lambda) d\lambda = 0.$$

W_1 belongs to the continuous spectrum if and only if $X(x, W_1)$ is a permissible solution of (1A) and the function $\omega(W)$ is not constant in the neighbourhood of W_1 .

* 'Math. Ann.', vol. 68, p. 220 (1910).

The fundamental theorem is that any permissible solution can be expressed in the form

$$X(x, W) = \int_0^W \phi^{(1)}(x, \lambda) \xi(\lambda) d\lambda,$$

where $\xi(\lambda)$ is the indefinite integral of a function of integrable square.†

In future the characteristic functions belonging to the discrete spectrum will be denoted by $\phi_n^{(1)}(x)$, while those belonging to the continuous spectrum will be written as $\phi^{(1)}(x, W)$. The functions must be normalised as follows.

For the discrete set,

$$\int \phi_n^{(1)}(x) \phi_m^{(1)}(x)^* dx = \delta_{nm},$$

where the integral is taken over the whole of the configuration space, $\phi_m^{(1)}(x)^*$ is the conjugate of $\phi_m^{(1)}(x)$, and δ_{nm} is the usual Kronecker δ .

For the continuous set we define

$$\Delta_n F = \int_W^{W + \Delta_n W} \phi^{(1)}(x, W) dW/h,$$

where the range of integration $\Delta_n W$ is a finite interval of the continuous spectrum of W . The normalisation required in the quantum theory is then given by‡

$$\int \Delta_n F \cdot \Delta_m F^* dx = \Delta_{nm} W/h,$$

where $\Delta_{nm} W$ is the common part of the intervals $\Delta_n W$ and $\Delta_m W$. We also have the orthogonal relation

$$\int \phi_n^{(1)}(x) \Delta_m F^* dx = 0.$$

If Ψ_0 is a function of integrable square satisfying the same boundary conditions as the characteristic functions and for which $L(\Psi_0)$ is continuous and quadratically integrable, then Ψ_0 can be expanded in the absolutely and uniformly convergent representation§

$$\Psi_0(x) = \sum_n c_n \phi_n^{(1)}(x) + \int_{-\infty}^{\infty} \phi^{(1)}(x, W) c(W) dW \quad (2)$$

where

$$c_n = \int \Psi_0(x) \phi_n^{(1)}(x)^* dx$$

and

$$c(W) = \frac{1}{h} \frac{d}{dW} \int_0^{\infty} dx \Psi_0(x) \int_0^W \phi^{(1)}(x, \lambda)^* d\lambda.$$

† Weyl, *loc. cit.* See also Hobson, 'Functions of a real Variable,' vol. 1, 2nd ed., p. 613.

‡ Oppenheimer, *loc. cit.*

§ Weyl, *loc. cit.*, theorem 7.

In quantum problems the spectrum falls into one of three classes. In the first class the spectrum is entirely discrete and the integral does not appear in (2). In the second class the discrete characteristics range from $W = -\infty$ to $W = 0$, and the continuous ones from $W = 0$ to $W = \infty$. The integral is then taken between 0 and ∞ . In the third class there is no discrete spectrum, and the sum disappears from (2). The general formula includes all these particular cases, which are obtained by making $\phi_n^{(1)}$ or $\phi^{(1)}(W)$ identically zero when the corresponding part of the spectrum does not exist. Since the representation (2) is uniformly convergent we may multiply by Ψ_0^* , integrate with respect to x and invert the order of integration or integrate term by term. This gives

$$\int |\Psi_0|^2 dx = \sum_n |c_n|^2 + \int_{-\infty}^{\infty} |c(W)|^2 dW,$$

showing that $\sum_n |c_n|^2$ and $\int_{-\infty}^{\infty} |c(W)|^2 dW$ are finite. Whether the Riesz-Fischer theorem holds in general for Sturm-Liouville functions involving continuous spectra, does not seem to be known, but it seems to be true for all cases of physical importance. For c_n and $c(W)$ to be the coefficients of a function of integrable square, it is necessary that $\sum_n |c_n|^2$ and $\int_{-\infty}^{\infty} |c(W)|^2 dW$ should be finite, and we shall assume it is sufficient in all cases which occur in the quantum theory.

2.2. If Ψ_0 is the wave function of the system at time $t = 0$, and if the system is isolated and subject to no external perturbations, then the wave function at any subsequent time is

$$\Psi = \sum_n c_n \psi_n^{(1)} + \int_{-\infty}^{\infty} \psi^{(1)}(W) c(W) dW. \quad (3)$$

Now suppose that at a given time, say $t = 0$, a perturbation $H_2(t)$ is added, giving a Schrödinger equation

$$\left(H_0 + H_1 + H_2(t) - i \frac{\hbar}{2\pi} \frac{\partial}{\partial t} \right) \psi = 0. \quad (4)$$

Also suppose that we can solve the equation

$$\left(H_0 + H_2(T) - \frac{i\hbar}{2\pi} \frac{\partial}{\partial t} \right) \psi^{(2)} = 0, \quad (5)$$

where T is any fixed time. The characteristic functions of (5) will, in general, consist of a discrete set and a continuous set, which will satisfy the same

orthogonal conditions as $\psi^{(1)}$. We denote the continuous characteristics by μ , and take the range of values to be $(-\infty, \infty)$.

We assume a solution of equation (4) in the form

$$\begin{aligned} \psi = & \sum_n c_n \psi_n^{(1)} + \int_{-\infty}^{\infty} \psi^{(1)}(W) c(W) dW \\ & + \sum_m a_m(t) \psi_m^{(2)} + \int_{-\infty}^{\infty} \psi^{(2)}(\mu) \gamma(\mu, t) d\mu. \end{aligned} \quad (6)$$

The first line is merely the wave function Ψ of the undisturbed system, the coefficients c_n and $c(W)$ being determined by the initial conditions as in equation (2). $a_m(t)$ is a function of the time only, and $\gamma(\mu, t)$ is a function of μ and t . These coefficients have to be determined so that (6) gives a solution of equation (4) satisfying the condition that $\int |\psi|^2 dx$ is finite. After substituting (6) in the differential equation (4), we expand all the non-vanishing terms of the resulting expression in the form $\sum_n \alpha_n \psi_n^{(2)} + \int_{-\infty}^{\infty} \psi^{(2)}(\mu) \beta(\mu) d\mu$. Assuming that the unknown coefficients can subsequently be determined so as to allow the necessary inversion of the order of integration, we obtain, by equating to zero the coefficients of $\psi_n^{(2)}$ and of $\psi^{(2)}(\mu)$, the following set of differential equations for the quantities $a_n(t)$ and $\gamma(\mu, t)$

$$i\hbar/2\pi \cdot \dot{a}_n(t) = g_n(t) + \sum_m H_{nm} a_m(t) + \int_{-\infty}^{\infty} H_n(\mu)^* \gamma(\mu, t) d\mu. \quad (7)$$

$$i\hbar/2\pi \cdot \dot{\gamma}(\mu, t) = g(\mu, t) + \sum_m H_m(\mu) a_m(t) + \int_{-\infty}^{\infty} H(\mu, \lambda) \gamma(\lambda, t) d\lambda. \quad (8)$$

The coefficients in (7) and (8) are given by the formal expansions

$$H_2(t) \Psi = \sum_m g_m(t) \psi_m^{(2)} + \int_{-\infty}^{\infty} \psi^{(2)}(\mu) g(\mu, t) d\mu$$

$$\{H_1 + H_2(t) - H_2(T)\} \psi_m^{(2)} = \sum_n H_{nm} \psi_n^{(2)} + \int_{-\infty}^{\infty} \psi^{(2)}(\mu) H_m(\mu) d\mu$$

and

$$H(\mu, \lambda) = \frac{1}{\hbar^2} \frac{d}{d\mu} \frac{d}{d\lambda} \int \{H_1 + H_2(t) - H_2(T)\} dx \int_0^\lambda \psi^{(2)}(\lambda) d\lambda \int_0^\mu \psi^{(2)}(\mu)^* d\mu.$$

In the next section we shall examine under what conditions it is possible to obtain a solution of the perturbation equations (7) and (8) satisfying $\sum_n |a_n(t)|^2$ finite and $\int_{-\infty}^{\infty} |\gamma(\mu, t)|^2 d\mu$ finite, which is a necessary condition for $\int |\psi|^2 dx$ to be finite. Whether this is a sufficient condition does not, as it

happens, arise, since the restrictions imposed are already too heavy for most quantum problems, and we conclude that in general the perturbation theory does not give a solution satisfying the boundary conditions.

3. The Existence Theorems.

3.1. Simplifying the notation, we have the following equations,

$$\frac{dw_i}{dz} = a_i(z) + \sum_j u_{ij} w_j + \int_{-\infty}^{\infty} u_i(\mu) v(\mu, z) d\mu \quad (i = 1, 2, \dots) \quad (9)$$

$$\frac{dv(\mu, z)}{dz} = b(\mu, z) + \sum_j u(\mu)_j w_j + \int_{-\infty}^{\infty} u(\mu, \lambda) v(\lambda, z) d\lambda. \quad (10)$$

In (I) the solution of the corresponding equations was obtained as a matrix. This is not possible here, since in addition to the matrix of the coefficients u_{ij} , there is also the nucleus $u(\mu, \lambda)$ and the two sets of functions $u_i(\mu)$, $u(\mu)_j$, which we may call "mixed nuclei." We have therefore to introduce the idea of limited nuclei, corresponding to limited matrices.

3.2. A nucleus $G(\lambda, \mu)$ is said to be limited with bound M provided

$$\left| \int_{-X}^X \int_{-X}^X G(\lambda, \mu) x(\lambda) y(\mu) d\lambda d\mu \right| \leq M$$

for all X , $x(\lambda)$, $y(\mu)$, where $x(\lambda)$, $y(\mu)$ are complex functions of the real variables λ , μ , satisfying

$$\int_{-\infty}^{\infty} |x(\lambda)|^2 d\lambda \leq 1, \quad \int_{-\infty}^{\infty} |y(\mu)|^2 d\mu \leq 1.$$

Similarly a mixed nucleus $G(\lambda)$ is limited with bound M provided

$$\left| \sum_{i=1}^N \int_{-X}^X G_i(\lambda) x_i y(\lambda) d\lambda \right| \leq M$$

for all N , X , x_i , $y(\lambda)$, subject to

$$\sum_{i=1}^N |x_i|^2 \leq 1, \quad \int_{-\infty}^{\infty} |y(\lambda)|^2 d\lambda \leq 1.$$

Most of the properties of limited matrices extend at once to limited nuclei. Those that are used in the sequel are given below without proof, the proofs being trivial extensions of those given by Hellinger and Toeplitz* for matrices.

We define the product of two nuclei $G_1(\lambda, \mu)$, $G_2(\lambda, \mu)$ to be the nucleus $\int_{-\infty}^{\infty} G_1(\lambda, \nu) G_2(\nu, \mu) d\nu$. There are also obvious definitions of the product of a nucleus with a mixed nucleus, of two mixed nuclei, and of a mixed nucleus with a matrix.

* 'Math. Ann.', vol. 69, p. 289 (1910).

1. The product of two limited nuclei with bounds M, M' is limited with bound MM' .

2. If $G(\lambda, \mu)$ is limited with bound M , then

$$\int_{-\infty}^{\infty} \left| \int_{-\infty}^{\infty} G(\lambda, \mu) y(\mu) d\mu \right|^2 d\lambda \leq M$$

and

$$\int_{-\infty}^{\infty} \left| \int_{-\infty}^{\infty} G(\lambda, \mu) x(\lambda) d\lambda \right|^2 d\mu \leq M$$

where

$$\int_{-\infty}^{\infty} |x(\lambda)|^2 d\lambda \leq 1, \quad \int_{-\infty}^{\infty} |y(\mu)|^2 d\mu \leq 1;$$

and conversely.

3. With the same hypothesis,

$$\int_{-\infty}^{\infty} |G(\lambda, \mu)|^2 d\lambda \leq M, \quad \int_{-\infty}^{\infty} |G(\lambda, \mu)|^2 d\mu \leq M.$$

3.3. We now proceed to solve the differential equations. We assume that the point z_0 is not a singularity of any of the equations, and that it is possible to surround z_0 by a finite domain D free from singularities. We have then to find solutions of (9) and (10) reducing to given values w_0 and $v(\mu, z_0)$ at z_0 , and satisfying $\sum_i |w_i|^2$ finite and $\int_{-\infty}^{\infty} |v(\mu, z)|^2 d\mu$ finite. We also assume that $\sum_i |a_i(z)|^2$ and $\int_{-\infty}^{\infty} |b(\mu, z)|^2 d\mu$ are bounded, and that $u_i, u_i(\mu), u(\mu)_j, u(\mu, \lambda)$ are all limited throughout the whole of D . The coefficients are functions of z , but it is convenient not to show the dependence on z explicitly. The method adopted is to solve the equations (9) formally, leaving $v(\mu, z)$ arbitrary. The value of w_i is then substituted in (10) giving rise to an integro-differential equation for $v(\mu, z)$ only, which can be solved for $v(\mu, z)$.

We therefore first solve the non-homogeneous system

$$\frac{dw_i}{dz} = \sum_j u_{ij} w_j + c_i.$$

The corresponding homogeneous system was treated in (I), and it was shown that the necessary and sufficient condition for the existence of a solution of the required type is that a certain matrix $\Omega(u)$ is limited. It is sufficient that the matrix (u_{ij}) is limited, and the solution is given by $w = \Omega(u) w_0$. We now make the further assumption that the inverse matrix Ω^{-1} exists, such that $\Omega(u) \Omega^{-1}(u) = 1$. To solve the non-homogeneous system we make the substitution

$$w = \Omega(u) W,$$

where W denotes the set (W_1, W_2, \dots) . We then have

$$\begin{aligned}\frac{dw}{dz} &= uw + \Omega(u) \frac{dW}{dz} \\ &= uw + c,\end{aligned}$$

where c is the set (c_1, c_2, \dots) . Denoting as usual the operator $\int_{z_0}^z dz$ by Q , we obtain on integration

$$w = \Omega(u) w_0 + \Omega(u) Q \Omega^{-1}(u) c. \quad (11)$$

Also

$$\begin{aligned}\sum_i |w_i|^2 &= \sum_i \left| \sum_j \Omega_{ij} w_j^0 + \sum_{rj} \Omega_{ir} Q \Omega_{rj}^{-1} c_j \right|^2 \\ &\leq A \left\{ \sum_i \left| \sum_j \Omega_{ij} w_j^0 \right|^2 + \sum_i \left| \sum_{rj} \Omega_{ir} Q \Omega_{rj}^{-1} c_j \right|^2 \right\},\end{aligned}$$

where A is a constant. Since both Ω and $\Omega Q \Omega^{-1}$ are limited, this last expression is finite provided $\sum_j |c_j|^2$ is bounded in D . It was proved in (I) that $\Omega(u)$ is majorised by $\exp(sM)$, where M is the bound of the matrix (u_{ij}) , and s is the length of the curve from z_0 to z . The series (11) for w_i is therefore majorised by an exponential series, and the differentiation is justified.

Applying this to equation (9), we can obtain a solution in the form (11) provided $\sum_i \left| a_i + \int u_i(\mu) v(\mu, z) d\mu \right|^2$ is bounded in D . This will certainly be satisfied if both $\sum_i |a_i|^2$ and $\sum_i \left| \int u_i(\mu) v(\mu, z) d\mu \right|^2$ bounded in D , which is true since $u_i(\mu)$ is limited throughout D .

Thus, provided we can subsequently determine $v(\mu, z)$ such that $\int |v(\mu, z)|^2 d\mu$ is finite, the above solution for w_i satisfies all the conditions.

3.4. We have now to obtain a solution of equation (10). On substituting the expression for w_i in (10) we obtain an integro-differential equation of the following form

$$\frac{dv(\mu, z)}{dz} = f(\mu, z) + \int_{-\infty}^{\infty} K(\mu, \lambda; z) v(\lambda, z) d\lambda. \quad (12)$$

Provided $\int_{-\infty}^{\infty} |f(\mu, z)|^2 d\mu$ is bounded and the nucleus $K(\mu, \lambda; z)$ is limited

with bound N throughout D , we can solve this equation by successive approximations.

Defining

$$K_1(\mu, \lambda; z) = K(\mu, \lambda; z)$$

$$K_n(\mu, \lambda; z) = \int_{-\infty}^{\infty} K(\mu, \nu; z) d\nu QK_{n-1}(\nu, \lambda; z) \quad (n \geq 2),$$

it is easily seen that $K_n(\mu, \lambda; z)$ is limited with bound $s^{n-1} N^n / (n-1)!$

The nucleus

$$F(\mu, \lambda; z) = K_1(\mu, \lambda; z) + K_2(\mu, \lambda; z) + \dots$$

therefore exists and is limited with bound

$$N \left(1 + sN + \frac{1}{2!} s^2 N^2 + \dots \right) = N \exp(sN)$$

and is uniformly limited in D.

Now put $v(\mu, z_0) + Qf(\mu, z) = v_0(\mu, z)$ and consider the expression

$$v(\mu, z) = v_0(\mu, z) + Q \int_{-\infty}^{\infty} F(\mu, \lambda; z) v_0(\lambda, z) d\lambda. \quad (13)$$

It satisfies equation (12) formally. Also

$$\begin{aligned} |v(\mu, z) - v_0(\mu, z)| &\leq Q \left\{ \int_{-\infty}^{\infty} |F(\mu, \lambda; z)|^2 d\lambda \cdot \int_{-\infty}^{\infty} |v_0(\lambda)|^2 d\lambda \right\}^{\frac{1}{2}} \\ &\leq \exp(sN) \left\{ \int_{-\infty}^{\infty} |v_0(\lambda)|^2 d\lambda \right\}^{\frac{1}{2}}, \end{aligned}$$

where $v_0(\lambda)$ is the upper bound of $v_0(\lambda, z)$ in D. Since $\int_{-\infty}^{\infty} |v_0(\lambda, z)|^2 d\lambda$ is bounded in D, and therefore $\int_{-\infty}^{\infty} |v_0(\lambda)|^2 d\lambda$ is finite, the series (13) has an exponential series as its majorant, and the differentiation is justified.

Further

$$\begin{aligned} \int_{-\infty}^{\infty} |v(\mu, z)|^2 d\mu &= \int_{-\infty}^{\infty} \left| v_0(\mu, z) + Q \int_{-\infty}^{\infty} \{ F(\mu, \lambda; z) v_0(\lambda, z) d\lambda \}^2 d\mu \right. \\ &\leq A \left\{ \int_{-\infty}^{\infty} |v_0(\mu, z)|^2 d\mu + \int_{-\infty}^{\infty} \left| Q \int_{-\infty}^{\infty} F(\mu, \lambda; z) v_0(\lambda, z) d\lambda \right|^2 d\mu \right\} \end{aligned}$$

where A is a constant, and since $F(\mu, \lambda; z)$ is limited $\int_{-\infty}^{\infty} |v(\mu, z)|^2 d\mu$ is finite.

We have therefore to show that $f(\mu, z)$ and $K(\mu, \lambda; z)$ satisfy the conditions specified above.

Now

$$f(\mu, z) = b(\mu, z) + \sum_{ij} u(\mu)_i \{ \Omega_{ij} w_j^0 + \sum_r \Omega_{ir} Q \Omega_{rj}^{-1} a_j \}$$

and $\int_{-\infty}^{\infty} |f(\mu, z)|^2 d\mu$ will be finite provided both $\int_{-\infty}^{\infty} |b(\mu, z)|^2 d\mu$ and

$$\int_{-\infty}^{\infty} \sum_{ij} |u(\mu)_i \{ \Omega_{ij} w_j^0 + \sum_r \Omega_{ir} Q \Omega_{rj}^{-1} a_j \}|^2 d\mu$$

are finite. The first condition is true by hypothesis, and since $u_i(\mu)$ is limited the second is satisfied if

$$\sum_i | \sum_j \Omega_{ij} w_j^0 + \sum_{rj} \Omega_{ir} Q \Omega_{rj}^{-1} a_j |^2$$

is finite. This is true as Ω and $Q \Omega^{-1}$ are limited and $\sum_j |a_j|^2$ is bounded in D .

We next have

$$K(\mu, \lambda; z) = u(\mu, \lambda) + \sum_{irj} u(\mu)_i \Omega_{ir} Q \Omega_{rj}^{-1} u_j(\lambda)$$

and is limited by § 3.2 theorem 1.

This completes the proof of the existence of solutions of equation (10).

4. *Perturbations in Atomic Problems.*

We now revert to the notation of § 2, and consider the perturbation theory in the light of the existence theorems just proved. In the first place, consider the ordinary theory when only discrete characteristics occur. Equation (7) then becomes

$$i\hbar/2\pi \cdot \dot{a}_m(t) = \sum H_{mn} a_n(t)$$

which was fully treated in (I). The necessary and sufficient condition for the existence of a solution was shown to be that the matrix $\Omega(H)$ is limited. In general this means that the matrix (H_{mn}) must be limited, as only a very singular type of unlimited matrix (H_{mn}) could give rise to a limited $\Omega(H)$. The perturbation theory was originally given for the case when a small parameter occurs in the perturbing term, and it is usually stated that the series of perturbations is convergent for sufficiently small values of the parameter. This is now seen to be irrelevant, as the convergence is that of an exponential series if (H_{mn}) is limited, and otherwise the series probably does not converge at all. The smallness of the parameter is of importance in that, as was shown in (I), it sometimes allows an asymptotic solution to exist when no exact solution is possible.

When we come to deal with the more general case of systems with continuous as well as discrete spectra the interpretation is not quite so simple. In the

first place the perturbations do not usually lead to limited matrices, and secondly there seem to be no solutions corresponding to the asymptotic ones of the simpler case. The question as to when the conditions laid down in § 3 will be satisfied is a difficult one, and no general rule can be given. It would seem probable, however, that they will be satisfied if and only if the perturbing term in the differential equation for ψ is not the leading term at any of the singularities of the equation. For in this case the introduction of the new term will not affect the nature of the solution in the neighbourhood of the boundary points. When this is not so, we shall obtain entirely different results corresponding to the different divisions of the Hamiltonian H into the parts H_0, H_1, H_2 , two of which can be chosen arbitrarily. Of course these formal solutions will not be convergent, but some of them will have a physical meaning. As there is no *a priori* reason for preferring one divergent series to another, the question arises as to which solutions we are to accept and which we are to reject.

Oppenheimer bases his theory on what he calls "nearly orthogonal functions." The property that he demands of these functions has nothing to do with the convergence of the series of perturbations, and can only affect the rate of convergence. It is therefore on the same footing as the parameter which occurs in the other perturbation theories. An alternative suggestion is that the boundary conditions are inadequate to deal with problems in which there is any ambiguity in the interpretation of the results. In the simple case of an isolated hydrogen atom the attraction of the nucleus is the only force acting on the electron, and there can be no ambiguity. When we come to consider the effect of a constant electric force on a hydrogen atom the conditions are entirely altered. At a large distance from the nucleus the constant field is greater than that due to the nucleus, and it is impossible to tell which part of the field the electron is in. If initially the electron is near the nucleus in a state of given energy, there is a probability that it will escape into a state of equal energy in that part of the field where the external force predominates, and the atom will be ionised. To observe this ionisation of atoms by an electric field we would not be concerned with the number of atoms possessing electrons in a given stationary state but with the number of free electrons moving under the action of the field, and we should have to arrange our experimental conditions accordingly. This would introduce boundary conditions of which we cannot take account in the mathematical solution of the problem. On the other hand, if we were interested in the effect of the electric field on the spectrum of the atom we should have to deal with the number of electrons

in given stationary states of the atoms, or alternatively in the stationary states as modified by the external field. This would require an entirely different set of experimental conditions which would introduce entirely new boundary conditions into the complete mathematical solution. When we neglect these boundary conditions and substitute idealised ones we can scarcely expect our mathematical treatment to be complete. One way of turning the difficulty without introducing the explicit boundary conditions is to work out a formal solution in that system of orthogonal functions which most nearly satisfies the experimental conditions, and to assume that this is asymptotic to the real solution. Thus for the hydrogen atom in an electric field we may work out the solution in terms of the functions corresponding to a free electron in an electric field. This will give the dissociation phenomena, and is just Oppenheimer's result. If, however, we use the functions corresponding to the stationary states of the unperturbed atom we obtain the ordinary Stark effect. The suggestion put forward above does therefore offer a not unreasonable explanation of the apparent inconsistencies of the perturbation theory.

The Emission of Soft X-Rays by Different Elements at Higher Voltages.

By O. W. RICHARDSON, F.R.S., Yarrow Research Professor of the Royal Society, and F. S. ROBERTSON, M.I.E.E., Senior Lecturer in Electrical Engineering, King's College, London.

(Received March 18, 1929.)

In a former paper* we investigated, by the photoelectric method, the efficiency of 14 elements as emitters of soft X-rays under various exciting voltages up to 500. We found that the efficiency had only an extreme variation by a factor of about 2 among all the elements tried which had a range of atomic number from 6 (carbon) to 79 (gold). It was also found to be a periodic function of the atomic number having for the elements tested a maximum about the middle of the periods falling away to a minimum value at the end. This is in contrast to the behaviour of ordinary X-rays for which the efficiency is proportional to the atomic number. It is to be remembered that the efficiencies

* 'Roy. Soc. Proc.,' A, vol. 115, p. 280 (1927).

in the two cases are measured under different conditions and by different methods ; but even when due allowance is made for this it is obvious that there is a radical difference between them. However, there must be an intermediate region in which there is a transition between the properties which characterise soft X-rays and those which characterise ordinary X-rays, and this fact makes experiments at higher voltages interesting.

The former experiments terminated at 500 volts because we had no convenient means available for obtaining much higher voltages, but after some delay we succeeded in getting a 6000 volt direct current generator made by Messrs. Evershed and Vignoles. This really consisted of three 2000-volt machines in series, and was provided with terminals at the junctions so that the full voltage could be subdivided into three approximately equal sections. With this apparatus it is very convenient to take observations at about 2000, 4000 and 6000 volts respectively. At first we had some trouble with gas effects and electron field currents at the higher voltages, but these were overcome eventually and steady and reliable readings were obtained.

The 14 targets which had previously been prepared were again employed, in an apparatus identical with that already described. The X-radiation was recorded by means of the photoelectric current produced when it fell upon a nickel plate connected to the insulated quadrants of a Dolezalek electrometer, the beam of X-radiation as before being made to pass between two condenser plates before impinging on the nickel plate. Arrangements were made at these higher potential differences to have one of the condenser plates at earth potential and the other at any potential down to 1075 volts negative to earth, so that no measurable current due to electrons or positively or negatively charged ions could pass through the condenser to the photoelectric plate. As the apparatus was otherwise unaltered it will be sufficient to refer to the former paper for a description of the details of it.

The elements examined and their atomic numbers are : carbon (6), silicon (14), chromium (24), manganese (25), iron (26), cobalt (27), nickel (28), copper (29), molybdenum (42), palladium (46), silver (47), tungsten (74), platinum (78), and gold (79). Six of these elements could be mounted in the tube at any one time and as before they were grouped so that two elements in each group were always present in some other group. In this way it is possible to check all the elements against each other, and also to eliminate the results of any changes in the absolute value of the effect caused, for example, by an alteration of the surfaces of the targets or the photoelectric plate. Such changes may be appreciable as a result of opening up the tube to interchange

the targets but are negligible in the course of a set of observations under satisfactory working conditions. When such changes have occurred they appear to affect the results from all the targets in the tube in nearly the same proportion.

In the previous paper it was pointed out that up to potential differences of 500 volts the ratio $\frac{\text{Photoelectric current}}{\text{Thermionic current}}$ (i_p/i_t) is highest in any given period

of the periodic table near the centre of the period and falls fairly steadily as the beginning of the next period is approached. Fig. 1 shows a plot of the average values of i_p/i_t which we finally found at 2068, 4000 and 5920 volts respectively, as ordinates against atomic number as abscissæ. In the lower part indicated by \blacktriangle are also shown the similar data for 300 and 500 volts, which were plotted in figs. 4 and 6 of the former paper. Considering the 14 elements as a whole the changes are perhaps not so great as might have been expected. Over the whole range from 300 to 6000 volts molybdenum maintains its position as the most efficient element. There is, however, a very remarkable change in the group of elements from chromium to copper both within the group and for the group as a whole in relation to the other elements. At 300 volts the most efficient of these elements was chromium (24) and the least efficient copper (29). The line joining the points for the intervening elements zigzagged about but had a distinct declining tendency with increasing atomic number. This was shown to hold down to 100 volts in fig. 7 of the former paper. At 2068 volts the zigzagging is as marked as ever but the trend is now upward with increasing atomic number, manganese (25) being the least and nickel (28) being the most efficient member. At 4000 volts the same tendency is still more pronounced, the two first members chromium (24) and manganese (25) sharing equally the position of least efficiency and copper (29) that of greatest. At 5920 volts the zigzagging has disappeared, the efficiency drops a little at first from Cr (24) to Mn (25) and Fe (26), and then rises slowly at first and then more rapidly in passing through Co (27) and Ni (28) to a much higher value at Cu (29). The same kind of thing is happening also in the middle of the fifth and sixth long periods. At the low voltages gold is much less efficient than Pt. The disparity, which should be measured not by the difference of the ordinates but by the proportion this bears to one of them, is much reduced at 2068, still further reduced at 4000 and at 5920 volts gold actually exceeds platinum. Silver does not succeed in reaching a higher value than palladium, but the disparity between them falls from about 6 per cent. at 300 volts to 1.5 per cent. at 5920 volts. These facts are brought out more clearly by the detailed values shown in Table I.

Table I.

Volts ↓	Change in the value of i_p/i_t expressed as a percentage of its value for the first-named element in each case.	
	Pd to Ag.	Pt to Au.
300	5.94 per cent. decrease	17.16 per cent. decrease
400	3.42 per cent. „	20.64 per cent. „
500	4.64 per cent. „	28.79 per cent. „
2068	7.6 per cent. „	14.62 per cent. „
4000	1.78 per cent. „	12.96 per cent. „
5920	1.57 per cent. „	0.389 per cent. increase

The behaviour of the group Cr to Cu as a whole compared with the remaining 8 elements is also very noteworthy. At the low voltages chromium has the highest efficiency of all the 14 elements with the exception of molybdenum, and the group as a whole has about the average efficiency of all the elements. At 5920 volts Cr, Mn, Fe and Co are much below all the other elements, and the group as a whole has an efficiency well below the average. How this comes about will now be made clearer by considering the behaviour of the elements more individually.

In figs. 2, 3, 4 and 5 the values of i_p/i_t for each of the elements tested are plotted against the exciting voltage, figures from 500 volts downwards have been taken from the previous paper and multiplied by a factor 0.666 to allow for the correction necessary on account of the difference between the dimensions and the relative positions of the condenser plates, targets and photoelectric plates in the two tubes. In the case of C, Si, Mo and Pd the three points at 2068, 4000 and 5920 lie in each case on a straight line to the accuracy of our measurements. These lines are, however, not pointing to the origin but to points on the ordinate axis at a considerable positive distance from it. Moreover the slopes are all less than the average slopes of the approximately straight portions previously found near the origin. It is evident that there must be an intervening portion with some curvature, probably convex upward. Silver and gold have curves at the high potentials which are very slightly convex upwards. They probably run into the former low voltage values in roughly the manner indicated by the broken line. This is, of course, a long extrapolation and may not be right.

In the case of W and Pt and the group Cr, Mn, Fe, Co, Ni, Cu the curves at the high voltages are distinctly convex upwards. In fact with Mn, Fe, Co and Ni i_p/i_t has practically reached a saturation value independent of the

voltage at these voltages. These curves may extrapolate on to the low voltage values in a similar manner to that shown for Au in fig. 5.

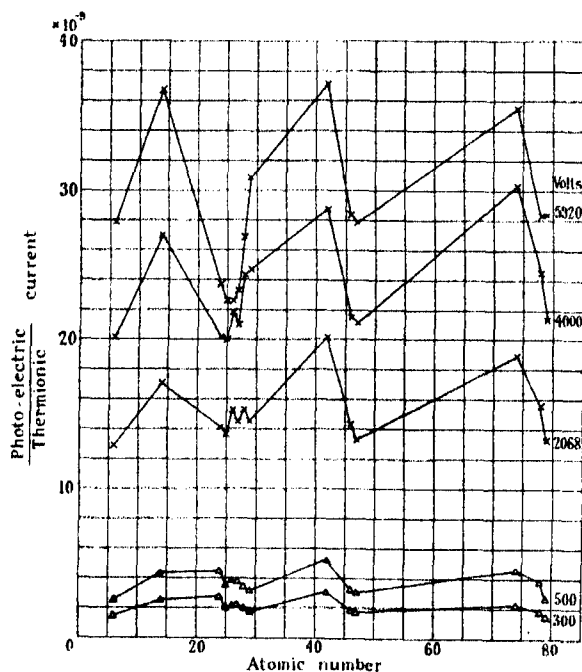


FIG. 1.

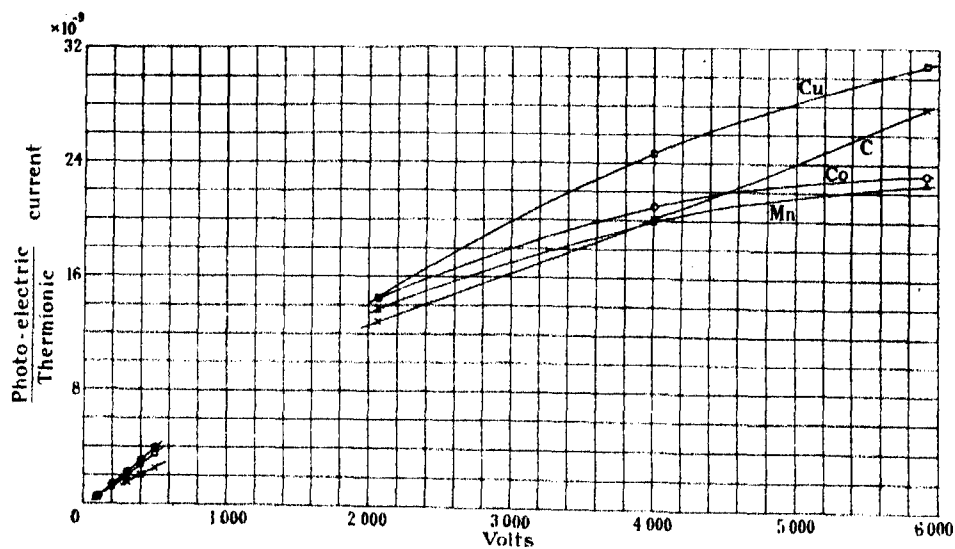


FIG. 2.

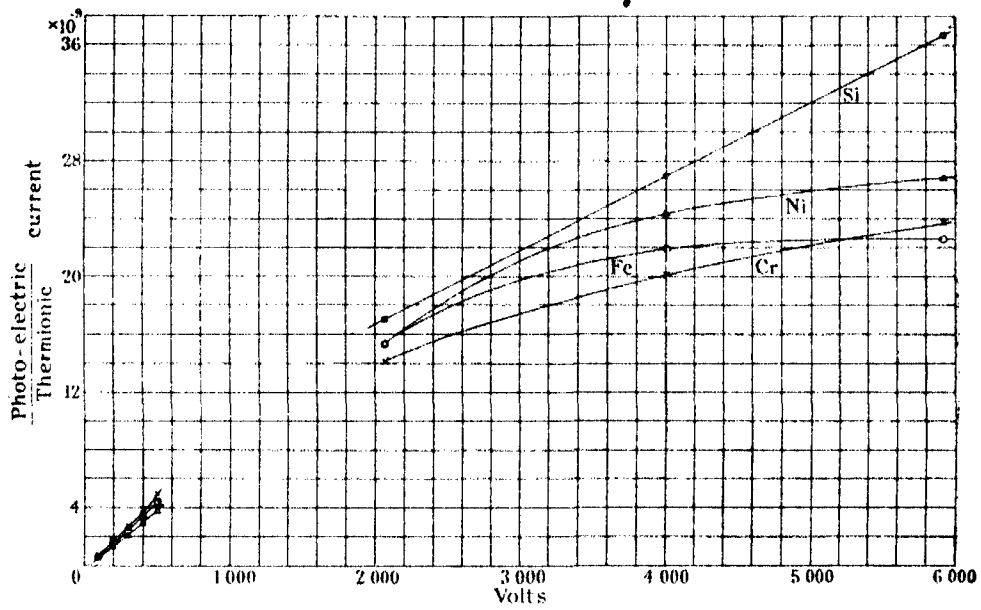


FIG. 3.

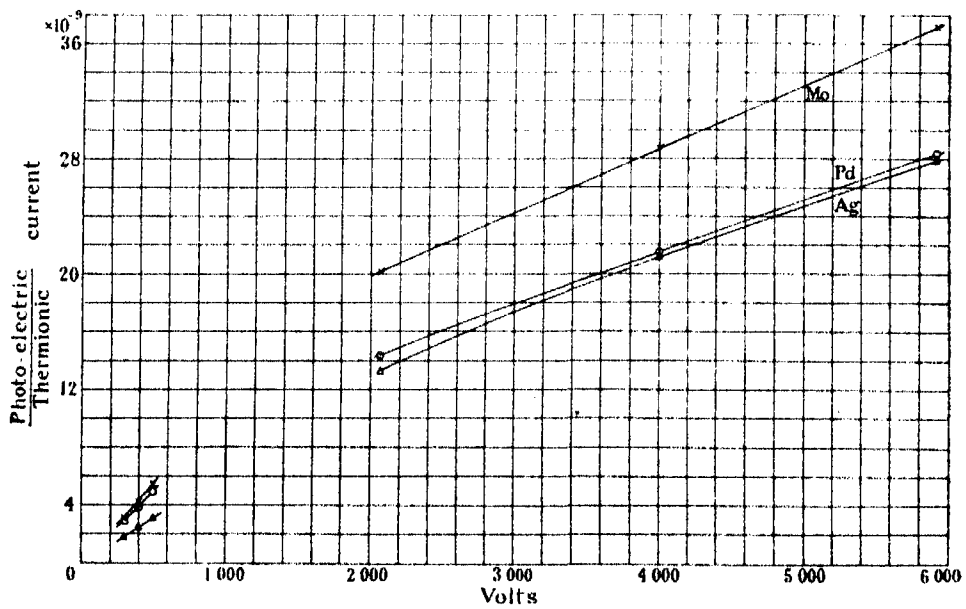


FIG. 4.

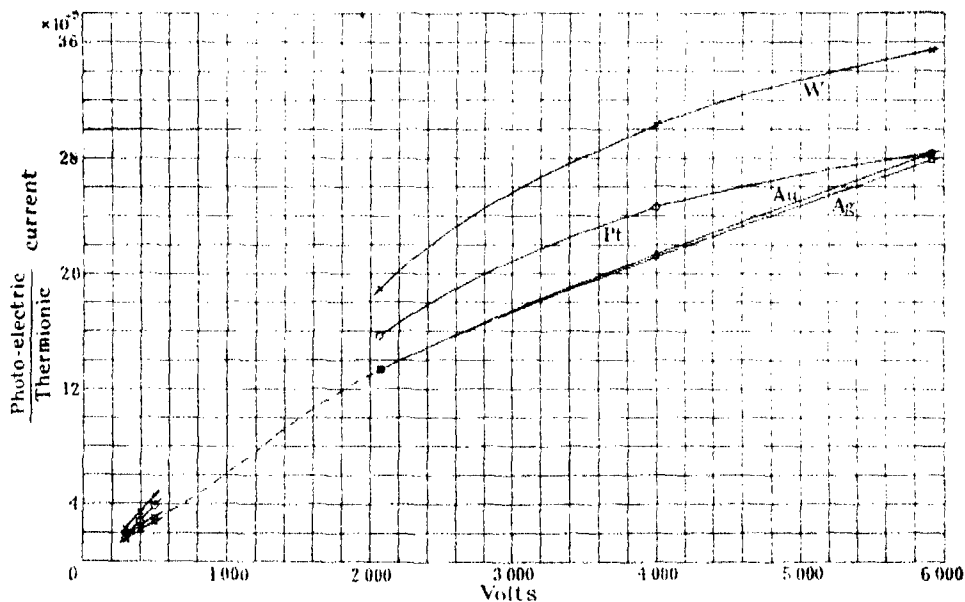


FIG. 5.

All the high voltage data shown in figs. 1 to 5 are the means of the results of a considerable number of consistent experiments except in the case of Fe, Co and Ni at 4000 volts. These points are each the result of a single observation. They are, however, believed to be reliable as the readings for the other elements present in the tube in this experiment agreed with the results of other experiments. In the other cases the number of observations varied up to a maximum of 10 for copper at 5920 volts.

After the high voltage experiments had been completed the targets remaining in the tube were the six for the Cr to Cu group. These were then tested at four lower voltages, 1527, 923, 500 and 300 volts, partly to investigate the intervening gap and partly to see how the values which were being got would check with those found in the former experiments. Only one observation was taken at 923 volts. This and the means of two each taken at 1527, 500 and 300 volts are plotted on the right-hand side of fig. 6. On the left-hand side are shown the data from the former paper for these elements corrected by the factor $2/3$ for the change in the dimensions of the apparatus already referred to. The values at 500 volts are about 15 per cent. lower and those at 300 volts about 8 per cent. higher than those recorded in the previous paper. Why the 500-volt results should be higher than those at 300 volts lower we do not know, but fluctuations in the absolute magnitude of this kind which we

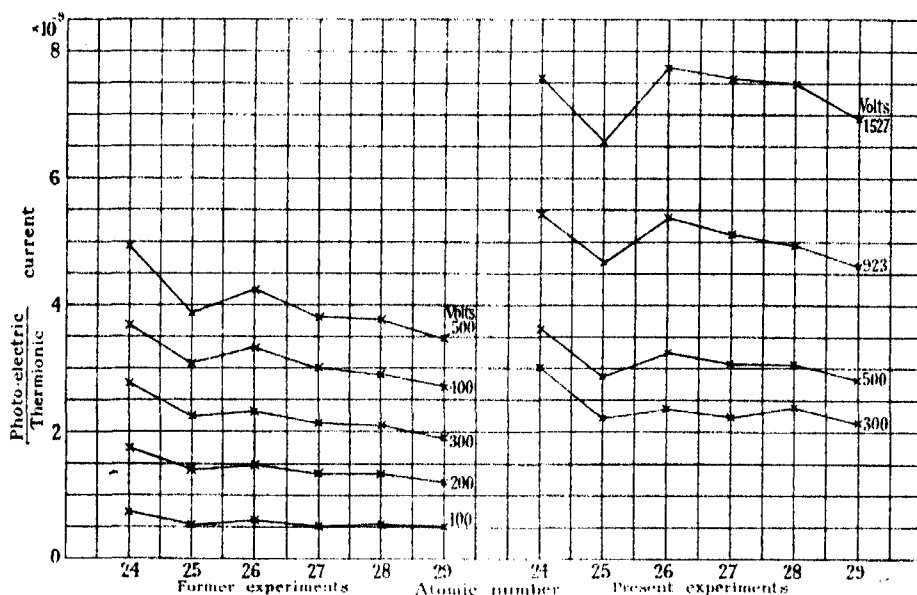


FIG. 6.

are not able to control do occur between different experiments. At any rate it is clear that no change had taken place in the sensitivity of the apparatus and that the present data are quite comparable with the former to the accuracy with which we can repeat absolute values. The relative values for the different elements at 500 and 300 volts respectively are the same as before to the accuracy of the observations.

When we turn to the higher voltages 923 and 1527 we find that the results show a transition from the behaviour at 500 volts towards that shown for 2068 volts in fig. 1. Thus the relative strength of chromium is diminishing and that of iron increasing so that at 1527 volts iron has the highest value of i_p/i_t for all the elements in the group. The absolute values at 923 and 1527 would fall below the curves such as those shown for Mn, Co and Cu in fig. 2 if these were joined by a curve similar to the broken line for Au in fig. 5. On account of the small number of observations and of the possibility of something having affected the absolute values this may not be of much significance.

The agreement at the lower voltages must be considered very satisfactory when it is remembered that the ratio i_p/i_t is susceptible to any change in the condition of the surface both of the target and of the photoelectric plate, and that some of these effects are not yet properly understood or completely under control. Fortunately such changes do not seem to affect appreciably the

relative values given by the different elements in the same tube at any one time.

We realise fully that this investigation is in many respects very incomplete, but we had to interrupt it temporarily at this stage and it was arranged that it should be continued by Mr. U. Nakaya of the Imperial Research Institute of Tokyo, who was at the time at King's College, London. His observations will be presented in a later communication.

The Suspension of Sand in Water.

By H. E. HURST, M.A., D.Sc., F.Inst.P.

(Communicated by G. C. Simpson, F.R.S.—Received March 14, 1929.)

(1) Description of Apparatus and Experiments.

The following experiments were undertaken to find the laws governing the suspension in water of fairly large particles such as river sand.

It is obvious that stream-line motion in horizontal layers cannot support particles heavier than water, and that their suspension must be due to turbulent motion. An apparatus was designed to give, as far as possible, turbulent motion uniformly distributed without any steady flow. This was similar to the paddle wheel apparatus used by Joule in determining the mechanical equivalent of heat.

It consists of a vertical cylinder of length 70 cm. and diameter 25 cm. to contain the mixture of water and sand. In this is a vertical shaft provided with nine vanes with intervals of 6·5 cm. between centres. The vanes extend 5 cm. from the shaft, and are 2·5 cm. wide. Attached to the circumference of the cylinder are four sets of baffles, through gaps in which the vanes of the propeller rotate with a clearance of 0·6 cm. The propeller is rotated by a motor connected to it by pulleys, which allow of a variety of speeds. The motion in the vessel is turbulent, but the turbulence is not strictly haphazard inasmuch as some parts of the motion must be repeated at regular intervals.

It is probable also that the turbulence is not uniformly distributed, but is to some extent symmetrical about the axis of rotation. At vertical intervals of $3\frac{1}{2}$ cm. are 12 taps.

An experiment consists of putting suitable quantities of sand and water into the apparatus, rotating the propeller at a steady speed and taking samples from the various taps.

The relative proportions of sand and water are obtained by collecting the sample in a graduated vessel and allowing the sand to settle. This method is accurate enough, as samples are variable and several must be taken to give a representative result.

Experiments have been carried out on three different sizes of sand sifted out through sieves of 20 and 30, 30 and 60, 60 and 90 meshes to the inch. These are here called coarse, medium and fine sand, and the average diameter of the particles sifted by them was 0.9 mm., 0.4 mm. and 0.2 mm. For the greater part of the experiments the sand used was from the desert and rounded by being wind-blown. Any fine particles are eliminated by rotating the propeller, stopping it, allowing the sand to settle, and as quickly as possible running off the water. After this has been done a few times a moderately uniform sample is left.

(2) *Theory of Suspension.*

Consider the mass of water in turbulent motion. Solid particles are suspended and are in similar motion to that of the water. For the sake of simplicity the particles are assumed to be uniform in mass and shape. The motion of the water and particles is assumed to be haphazard without any general movement of translation or rotation. The velocities of the particles are assumed to be randomly distributed if taken over sufficiently large volumes and time-intervals.

Suppose that in the liquid a cylinder with its axis vertical and ends horizontal is isolated by a membrane, permeable to the liquid but not to the solid particles. Let the cylinder have unit area of cross-section and height dh and be situated at a vertical height h from some horizontal plane of reference.

Let there be n particles per cubic centimetre at height h , and let

ρ be the density of the material of the particles.

m the mass of a particle.

ρ_1 the density of the liquid.

u the velocity of a particle.

$\overline{u^2}$ the mean-square velocity of agitation of a particle.

If the distribution of particles is in a steady state the condition of the cylinder will not be affected by the insertion of the membrane.

The external pressures on the membrane due to the impact of particles will be balanced by the effective weight of the particles inside the cylinder. Assuming, as we are entitled to do, that the collisions with the imaginary membrane are perfectly elastic we have for equilibrium, equating the forces acting on the ends,

$$\frac{1}{2}mn\bar{u}^2 = \frac{1}{2}m(n + dn)\bar{u}^2 - nm dh \frac{\rho - \rho_1}{\rho} g = 0,$$

the solution of which is

$$n = n_0 e^{\frac{-3g(\rho - \rho_1)h}{\rho\bar{u}^2}}.$$

where n_0 is the concentration of particles at the level $h = 0$.

This distribution of density is similar to that found by Perrin for colloidal particles in Brownian Movement, and also to the density of the free atmosphere.

(3) *Experimental Results.*

Experiments have been carried out with three kinds of sand and many different speeds of the propeller. The results have always been to show that for a given sample of sand and propeller speed the concentration of sand n at height h is given by

$$n = n_0 e^{-\alpha h},$$

where α is a function of the speed of the propeller and varies with the kind of sand.

Fig. 1 shows the distribution of sand with height for a particular sample, the speed of the propeller being constant. Three results are given relating to different values of n_0 . In this diagram $\log n$ is plotted against h .

It will be seen that the curves are parallel straight lines. A point to be noted is that the samples from even-numbered taps always show relatively greater concentrations than those from odd numbered taps, though the taps are approximately symmetrically placed with regard to the propeller and baffles.

Seven sets of experiments have been actually plotted and all give straight lines. In all, excluding preliminary experiments, about 80 experiments have been made, so the law of distribution is well established.

Assuming that

$$\alpha = 3g(\rho - \rho_1)/\rho\bar{u}^2,$$

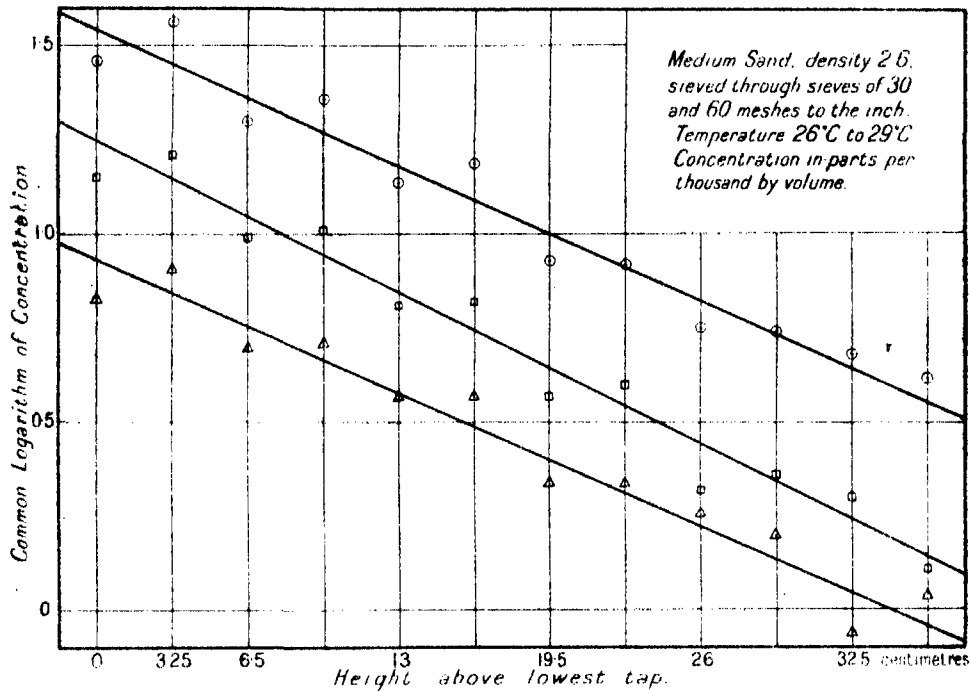


FIG. 1.—Relation of Concentration of Sand to Height.

\bar{u}^2 has been calculated for each experiment and plotted against the square of the revolutions of the propeller. The results for the different samples of sand are given in fig. 2. Only very general conclusions can be drawn from these curves. These are :—

- (1) For the same velocity of the water fine sand acquires a greater velocity of agitation than coarse.
- (2) The velocity of agitation of the sand increases less rapidly than the velocity of the propeller.
- (3) The shape of the sand particles must exert considerable influence as two samples of the fine sand from different sources although sieved in the same way gave different results.

Owing to the irregular shape of the sand particles it is not worth while to make any detailed mathematical investigations, until more experimental work has been done.

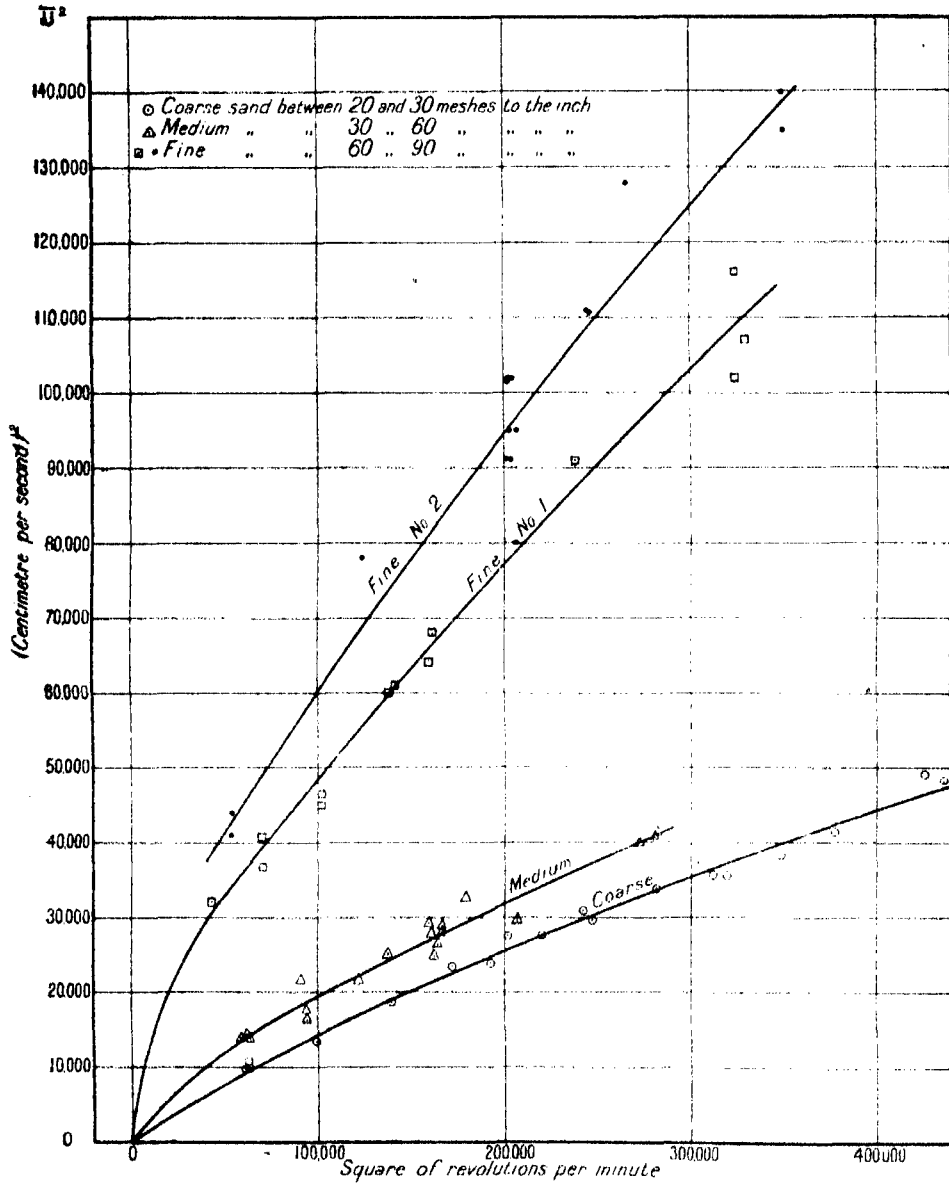


FIG. 2.—Relation between Mean Square Velocity of Sand Particles and Square of Revolutions of Propeller.

Conclusion.

The investigation shows that the particles in suspension due to turbulent motion in a liquid, when the turbulence is uniformly distributed behave like

the molecules in a gas. It is hoped that this analogy will be fruitful when applied to the practical problems arising out of the suspension of solid particles in the water of streams. These problems are often of considerable economic importance. It is suggested that the analogy may also be made use of to illustrate some of the laws dealt with in the kinetic theory of gases, since a suspension may be looked upon as a model of a gas.

*The Transfer of Heat by Radiation and Turbulence in the
Lower Atmosphere.*

By D. BRUNT, M.A., B.Sc.

(Communicated by G. C. Simpson, F.R.S.—Received March 18, 1929.)

I.—*Introduction.*

The air within any element of volume may gain or lose heat by (1) absorption or emission of radiation, (2) transport of heat in the vertical by turbulence, (3) ascent of saturated air producing condensation and liberating latent heat, (4) arrival of warmer or colder air in a horizontal direction. There are not available any data in a suitable form to permit our discussing the last of these factors, but it is fairly easy to detect occasions when rapid changes are taking place by an examination of records of wind velocity and direction. The third is not operative at levels below the lowest cloud layer, and for that reason it is proposed in the present paper to restrict the discussion to the lowest layers of the atmosphere, where radiation and turbulence are the controlling factors. An endeavour will be made in a subsequent paper to extend the discussion to higher levels, taking account of the third factor mentioned above.

II.—*Absorption and Emission in the Atmosphere.*

It is generally accepted that the simple gases in the atmosphere do not absorb appreciably either the shortwaved radiation from the sun or the long-waved radiation from the earth's surface and the water vapour in the atmosphere. There is some absorption by carbon dioxide, but most of the absorption in the atmosphere is produced by water vapour. There is available a series of measurements of the absorbing power of water-vapour, carried out

by Hettner,* and summarised by Simpson† in a recent memoir. The main results of Hettner's observations may be summarised as follows: A column of air containing 0.3 mm. of precipitable water in the form of vapour will absorb completely all radiation of wave-lengths between $5.5\ \mu$ and $7\ \mu$, and greater than about $14\ \mu$, and will absorb some, but not all, of the radiation between $4\ \mu$ and $5.5\ \mu$, between $7\ \mu$ and $8\ \mu$, and between $11\ \mu$ and $14\ \mu$. There is a band from $8\ \mu$ to $11\ \mu$ within which the vapour is transparent to radiation. This band is of considerable meteorological importance on account of the fact that the wave-length at which maximum intensity occurs in the spectrum of terrestrial radiation, or $10\ \mu$, falls within it. The main absorption band of CO_2 is centred about $15\ \mu$. Simpson states (*loc. cit.*, p. 12), that the essential facts can be represented by assuming that *within the restricted regions of wave-lengths concerned* the emission of radiation from water-vapour is equal to black body radiation at the same temperature, and that the radiation of these wave-lengths is completely absorbed by a layer of air containing 0.3 mm. of precipitable water. By the adoption of this very simple basis, Simpson was able to explain satisfactorily a number of phenomena, and it is therefore proposed to adopt the same basis in the present paper.

Thus it will be assumed that a layer of air containing 0.3 mm. of precipitable water absorbs completely all radiation between $5.5\ \mu$ and $7\ \mu$, and above $14\ \mu$, and that absorption and radiation by water-vapour outside these limits may be neglected.

The physical limitations of this assumption can be readily stated. The absorbing power of water-vapour increases with wave-length, and for wave-lengths greater than about $30\ \mu$, effectively complete absorption takes place with much less than 0.3 mm. of precipitable water, but only a relatively small part of the energy is contained within the range of wave-lengths beyond $30\ \mu$. This is partially compensated for by the assumption that 0.3 mm. of precipitable water can absorb all radiation of wave-lengths between $14\ \mu$ and about $17\ \mu$, and by the effect of the absorption band of CO_2 , which is centred at $15\ \mu$. In the earth's atmosphere the amount of CO_2 is 0.045 per cent. by weight and 1 c.c. will contain about 6×10^{-7} grammes of CO_2 . Simpson states (*loc. cit.*, p. 4) that at the centre of the CO_2 absorption band at $15\ \mu$ a column containing 0.06 grammes per square centimetre of cross-section will absorb about 88 per cent. of the incident radiation. In the lower atmosphere, therefore, a column of 10^5 cm. or 1 km. will contain sufficient CO_2 to absorb 88 per cent. of the

* 'Ann. Physik,' vol. 55, p. 476 (1918).

† 'Mem. R. Met. Soc.,' No. 21 (1928).

incident radiation at $15\ \mu$. Thus the amount of absorption by CO_2 is small within a layer of thickness of about 40 metres, such as we shall consider below, but it will help in sharpening the limit of $14\ \mu$ which we have assumed. The tables of intensity of radiation from a black body at a temperature of 280° on the absolute scale, show that rather more than 80 per cent. of the energy which can be absorbed by water-vapour is contained within the limits $5.5\ \mu$ to $7\ \mu$, and above $14\ \mu$, and we may therefore expect that the assumption made above will yield results which are substantially in agreement with the observed phenomena. This assumption is largely justified by the success with which it has been used by Simpson in explaining a variety of phenomena in the atmosphere.

The maximum intensity of black body radiation from the earth's surface at normal temperature is at about $10\ \mu$, and that of radiation from a black body at a temperature of 220° absolute, which is approximately the temperature of the stratosphere, is at about $12\frac{1}{2}\ \mu$.

Thus of the radiation emitted by the earth's surface, the part within the band from $8\ \mu$ to $11\ \mu$, which passes through the atmosphere unabsorbed, is of considerable magnitude. As soon as the radiation within this band leaves the earth's surface, it ceases to be available for terrestrial purposes, unless there is a cloud layer above, capable of reflecting it back to the earth's surface. If we therefore restrict our attention for the time being to clear skies, which permit the radiation between $8\ \mu$ and $11\ \mu$ to escape into space, we can restrict our attention entirely to those wave-lengths within which water-vapour radiates and absorbs. The present paper is almost entirely concerned with radiation within these limits of wave-length, and in order to save continual re-statement the name W-radiation is used to denote radiation restricted to the wave-lengths within which water-vapour amounting to $0.3\ \text{mm.}$ of precipitable water radiates like a black body.

The W-radiation coming up from the earth's surface is completely absorbed in a relatively thin layer of air, which in turn re-emits radiation appropriate to its own temperature. Thus while the radiation between $8\ \mu$ and $11\ \mu$ passes out through the atmosphere unchanged, the W-radiation is absorbed and re-emitted many times over, if Hettner's figures for absorption can be accepted.† It is customary to speak of water-vapour as endowing the air with a power of absorption or emission, but it would be more logical to regard the presence of "dry air" as endowing the water-vapour with an enhanced specific heat. For the dry air, though it takes no part in absorption or emission (except for CO_2), shares with the water-vapour any gain or loss of heat, and so its presence weights the water-vapour with an added specific heat.

The length of the column of air which contains 0.3 mm. of precipitable water is readily deduced as follows. Call this length l . Then a cylinder of volume 1 c.c. will contain 0.03 cm. or 0.03 gramme of water. Let $p_w mb$ be the vapour pressure, ρ_w the density of water-vapour, T the absolute temperature and R the gas constant for water-vapour. The

$$p_w = R\rho_w T \quad \text{and} \quad R = 4.62 \times 10^3$$

and

$$l\rho_w = 0.03$$

$$l = 0.03/\rho_w = 0.03 \times 4.62 \times 10^3 \times T/p_w = 139T/p_w \text{ centimetres.}$$

If we take $T = 275a$, the length l is equal to about 380 metres; and with such values of the vapour pressure as occur in the lower atmosphere, where p_w is normally of the order of 10 mb and is often much greater than this, l is a length of the order of 40 metres. With such small values of l it is legitimate to treat the layer of thickness l as having uniform temperature equal to the mean temperature of the layer, so far as computing the radiation from the layer is concerned. This method is adopted below in order to compute the amount of radiation moving upward or downward through the atmosphere.

III.—An Equation for Radiative Transfer.

Beginning at the ground we divide the whole atmosphere into layers of varying thickness such that each contains 0.3 mm. of precipitable water. The

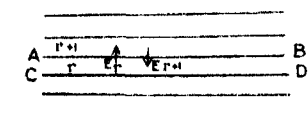


FIG. 1.

thickness of each layer is bT/p_w where b is a numerical constant equal to 139 in c.g.s. units, while T and p_w represent the mean absolute temperature and the mean vapour pressure in millibars, within each layer. The thickness of each layer is thus proportional to the appropriate value of T/p_w .

Let AB in fig. 1 be the upper boundary of the r th layer. The amount of W-radiation moving upward across AB is equal to E_r , the radiation from the r th layer, since no radiation reaching AB can by hypothesis have originated below CD , the lower boundary of the r th layer. Similarly the amount of W-radiation moving downward across AB is equal to E_{r+1} , the radiation from the $(r+1)$ th layer. The net upward flux of radiation across AB , which we call F_r , is given by

$$F_r = E_r - E_{r+1} \quad (1)$$

If T_r be the mean temperature of the r th layer, then with the usual notation

$$\begin{aligned} F_r &= E_r - E_{r+1} = -\Delta E_r = -\frac{\Delta E}{\Delta T}(T_{r+1} - T_r) \\ &= -\frac{\Delta E}{\Delta T} \cdot \left\{ \frac{1}{2} \left(\frac{\Delta T}{\Delta z} l \right)_{r+1} + \frac{1}{2} \left(\frac{\Delta T}{\Delta z} l \right)_r \right\}, \end{aligned} \quad (2)$$

$$= -\frac{\partial E}{\partial T} \cdot \frac{\partial T}{\partial z} l = -\frac{\partial E}{\partial T} \frac{\partial T}{\partial z} \frac{bT}{p_w} = -k \frac{\partial T}{\partial z}. \quad (3)$$

The use of the differential coefficient $\partial E/\partial T$ in place of the corresponding finite-difference ratio is justified by the slow rate of change of this quantity with T , as shown in the next paragraph. The use of the differential coefficient $\partial T/\partial z$ in place of the corresponding finite-difference ratio is justified if we neglect small quantities of the first order, and also by the fact that in practice $\partial T/\partial z$ is determined by the measurement of the difference of temperature at points separated by a finite difference of level. In this way we obtain the expression $-k \frac{\partial T}{\partial z}$ for the net upward flux of heat, k being a quantity which normally changes only very slowly with height, as is seen from a consideration of the factors involved in it.

The value of b depends upon the assumption that 0.3 mm. of precipitable water absorbs completely the W-radiation passing through it. Should the estimate of 0.3 mm. be too small, the value of b is proportionately too small. Thus any uncertainty as to the true value of b is due only to uncertainty as to the truth of the estimate of 0.3 mm. for the quantity of precipitable water which will completely absorb W-radiation. The value of $\partial E/\partial T$ can be readily deduced from a table given by Simpson (*loc. cit.*, p. 8). The following small table is sufficient to show the nature of its variation :—

Temperature.	200a	220a	270a	295a
$\frac{\partial E}{\partial T} \times 10^3$	1.6	2.0	3.0	3.5

Within these limits of temperature $\partial E/\partial T$ appears to be almost accurately a linear function of temperature

$$\frac{\partial E}{\partial T} \times 10^3 = 3.0 + 0.2 (T - 270).$$

The vapour pressure p_w varies from day to day at a given place, but shows no marked diurnal variation. It varies to some extent with height. According

to Hann* the relative values of p_w at the ground, at 0.5 km. and at 1 km. are 1.0, 0.83 and 0.68. But observations frequently show a much slower decrease with height than this. Thus Steiner† found in his discussion of kite ascents made at Rostock, that vapour pressure showed extremely little variation with height up to 600 metres.

If we assume a temperature of 275a and a vapour pressure of 5 mb., corresponding to relative humidity of about 70 per cent., the value of k in equation (3) is found to be

$$3 \times 10^{-3} \times 139 \times 275 \div 5 = 23, \text{ the units being the gramme-calorie and minute.}$$

We can use this figure to compute the upward flux of radiation corresponding to any given value of $\partial T/\partial z$. Let us assume the lapse rate of temperature to be adiabatic, so that $\partial T/\partial z = -10^{-4}$. Then the vertical flow of radiation is 2.3×10^{-3} gramme calories per minute. To compare this with the average amount of radiation coming in from the sun, we take the solar constant to be 2 gramme calories per square centimetre per minute. Allowing for averaging over day and night, and over all latitudes, and assuming Aldrich's value of the albedo 0.43, we find that the amount of incoming energy which has to be transported out again by radiation, turbulence, or otherwise, is about 0.275 gramme calories per square centimetre per minute. Thus with the assumptions made above in evaluating k , and assuming an adiabatic lapse-rate, except for the radiation contained within the transparent band from $8\frac{1}{2} \mu$ to 11μ , which passes out through the atmosphere without absorption, less than one-hundredth of the incoming energy can be disposed of by passing outward as W-radiation through the lowest layers. While it is true that the lapse-rate may from time to time exceed many times the adiabatic, this only occurs during a part of the day, and moreover the value of k deduced above is based on a low figure for vapour pressure. With larger vapour pressures k is diminished. It can therefore be accepted that under normal conditions only a very small fraction of the incoming solar radiation passes back through the lowest layers of the atmosphere as W-radiation.

It will be noted that the flow of energy by radiation is always from high temperature to low temperature, so that radiation tends to produce isothermal conditions. There is a resemblance between the results here derived and the equations for conduction of heat in solids.

* 'Lehrbuch der Meteorologie,' p. 243.

† 'Wiss. Abhandl. Luftwarte Rostock,' Heft 1 (1926).

The net flux of heat across unit area of a horizontal surface at height $z + dz$ is

$$-k \frac{\partial T}{\partial z} - \frac{\partial}{\partial z} \left(k \frac{\partial T}{\partial z} \right) dz.$$

A disc of air of unit horizontal area and thickness dz will therefore gain a quantity of heat $-\frac{\partial}{\partial z} \left(k \frac{\partial T}{\partial z} \right) dz$ per minute. If c_p be the specific heat of air at constant pressure, and the unit of time t be 1 second, this gain of heat must be equal to $60\rho c_p \frac{\partial T}{\partial t} dz$. Thus the equation of radiative transfer of heat may be written :—

$$\rho c_p \frac{\partial T}{\partial t} = \frac{1}{60} \frac{\partial}{\partial z} \left(k \frac{\partial T}{\partial z} \right) = \frac{b}{60} \frac{\partial}{\partial z} \left(\frac{T}{p_w} \frac{\partial E}{\partial T} \frac{\partial T}{\partial z} \right). \quad (4)$$

We have seen that in the lowest layers of the atmosphere k will vary slowly with height, while $\partial T/\partial z$ is shown by observation to be subject to variation within wide limits, a lapse rate 10 times the dry adiabatic lapse rate being by no means uncommon near the ground. Thus in an investigation of the transfer of heat by radiation in the lowest layers we may treat k as constant in equation (4), giving T and p_w the values corresponding to the level under discussion. Equation (4) then reduces to

$$\frac{\partial T}{\partial t} = \frac{b}{60\rho c_p} \frac{T}{p_w} \frac{\partial E}{\partial T} \frac{\partial^2 T}{\partial z^2} = K_R \frac{\partial^2 T}{\partial z^2}. \quad (5)$$

This equation is similar to that for conduction of heat in a solid with a constant K_R replacing the thermometric conductivity κ . The quantity K_R is equal to $k/60\rho c_p$ where k is defined in equation (3). Again, taking $T = 275a$, $p_w = 5$ mb. we find

$$K_R = \frac{23}{60\rho c_p} = \frac{23}{60 \times 0.00125 \times 0.24} = 1.3 \times 10^3.$$

For the reasons given above, in discussing k , this estimate of K_R is likely to be rather higher than the normal values, on account of the low value assumed for p_w . For larger values of p_w , K_R is reduced in inverse proportion. The constant K_R might, on the analogy with the conduction of heat in solids, be called the *radiative diffusivity*. Even allowing for the fact that the value of 1.3×10^3 is likely to be rather high, it is very much in excess of the corresponding coefficient for the molecular conduction of heat, whose value is about 0.16 in the same units.

The derivation of equation (3) is based on the assumption that there is a complete layer of air whose water-vapour content is equivalent to 0.3 mm. of precipitable water, above and below the level across which the flux of radiation is to be stated. It cannot therefore be applied without further consideration to heights above the ground of less than l as defined above.

If in fig. 1 the surface AB is only just above the ground, whose temperature is T_s , the W-radiation moving upward across AB is $E(T_s)$, while the downward moving W-radiation is of intensity $E(T_1)$, where T_1 is the mean temperature of the first complete layer of thickness l . The upward flux across AB

$$\begin{aligned} &= E(T_s) - E(T_1) = -\Delta E = -\frac{\Delta E}{\Delta T} \Delta T \\ &= -\frac{\Delta E}{\Delta T} \cdot \frac{\Delta T}{\Delta z} \Delta z = -\frac{\partial E}{\partial T} \cdot \frac{\partial T}{\partial z} \Delta z \end{aligned}$$

where $\Delta z = \frac{l}{2} = \frac{bT}{2p_w}$. Hence the net upward flux across AB

$$= -\frac{\partial E}{\partial T} \cdot \frac{\partial T}{\partial z} \cdot \frac{bT}{2p_w} = \frac{1}{2}k \frac{\partial T}{\partial z}, \quad (6)$$

where k is derived from the mean values of T and p_w for the lowest layer of thickness l .

For heights $z < l$, the upward radiation will be the same as though the missing fraction $(l - z)/l$ of the complete black body layer, were concentrated into an infinitesimally thin layer at the surface. If the temperature of the surface is T_s , and temperature at height z is T , the mean temperature of this black body layer is

$$\frac{T + T_s \frac{z}{l}}{2} + T_s \frac{l - z}{l} = T + \frac{\partial T}{\partial z} \left(z - \frac{z^2}{2l} \right), \quad (7)$$

where

$$\frac{\partial T}{\partial z} = \frac{T - T_s}{z}.$$

Hence we find from equation (2) that the net upward flux at height z is

$$-\frac{\partial E}{\partial T} \frac{\partial T}{\partial z} \left\{ \frac{l}{2} + \left(z - \frac{z^2}{2l} \right) \right\} = -\frac{\partial E}{\partial T} \frac{\partial T}{\partial z} \cdot \frac{l^2 + 2lz - z^2}{2l}. \quad (8)$$

This expression reduces to $-\frac{\partial E}{\partial T} \frac{\partial T}{\partial z} \frac{l}{2}$ when $z = 0$, agreeing with (6), and reduces to $-\frac{\partial E}{\partial T} \frac{\partial T}{\partial z} l$ when $z = l$ agreeing with the standard form of the equation. Thus in the lowest layer l the value of k decreases steadily from its value at $z = l$ to half that value at the ground. If conditions approach a

steady state so that the upward flux becomes the same at all heights, then the lapse-rate $\partial T/\partial z$ at height l must be half its value at the ground. The required condition of steadiness is possibly reached in inversions on clear nights, but there are no observations available in sufficient detail to test this possibility.

IV.—*The Upward Transmission of Heat by Turbulence.*

An expression for the rate at which heat is conveyed upward or downward by eddies has been given by G. I. Taylor,* who found that the upward flow of heat due to eddies could be represented as $-k\rho c_p \frac{\partial \theta}{\partial z}$, where ρ is the density, c_p the specific heat of air, θ is the potential temperature at a height z , and K an essentially positive quantity, which measures the activity of the eddies at height z . Taylor's derivation of this expression suffers from the disability that it only applies to an incompressible atmosphere. If T is the absolute temperature, θ the potential temperature, and p the pressure at height z , and if P be the standard pressure to which the potential temperature is referred, then

$$\theta = T (p/P)^{-\gamma} \quad (9)$$

where γ is a constant whose value for air is 0.29. Hence $\partial \theta/\partial z$ involves the arbitrary standard pressure P , and so cannot be regarded as a suitable factor for expressing the vertical flux of heat. It was the presence of P in the expression for the vertical flux which first suggested the desirability of re-considering the whole question. It turns out that a very slight re-arrangement of Taylor's original analysis makes it possible to allow for the compressibility of the air. Also it is found that the flux of heat by turbulence should be expressed in terms of the absolute temperature.

It is shown in any text-book of heat that the quantity of heat necessary to raise the temperature of 1 gramme of atmospheric air by an amount dT at constant pressure is $c_p dT$. Of this a part $c_v dT$ is used in increasing the internal energy of the air, and the remaining part $(c_p - c_v) dT$ is used in expanding against the pressure of the surrounding air. Atmospheric air thus behaves as though its specific heat were c_p in any change of state which does not involve changes of pressure.†

We now require to evaluate the flux of heat across a large horizontal area A forming part of the isobaric surface of pressure p , which is at height z at time t .

* 'Phil. Trans. Roy. Soc.,' A, vol. 215, p. 1 (1915).

† *Vide* W. H. Dines, 'Q. J. Roy. Met. Soc.,' vol. 37, p. 188 (1913), or V. Bjerknes, 'Met. Zeit.,' Heft 4/5 (1917).

We shall regard p as the vertical co-ordinate. The potential temperature at any point will therefore be represented by $\theta(p, t)$. Following Taylor's method we assume that an eddy, which is originally a normal specimen of the air at its level, breaks away from the level p_0 at time t_0 , and reaches the level of p at time t carrying with it its original potential temperature, and that after crossing the isobaric surface p it mixes with its new surroundings. Let m be the mass of this eddy. Provided $p_0 - p$ is small, and that $t_0 - t$ is small, we may write

$$\theta(p_0, t_0) = \theta(p, t) + (p_0 - p) \frac{\partial \theta}{\partial p} + (t_0 - t) \frac{\partial \theta}{\partial t}, \quad (10)$$

where $\frac{\partial \theta}{\partial p}$ may now be interpreted as $\frac{\partial \theta}{\partial z} \cdot \frac{\partial z}{\partial p}$. The absolute temperature of the moving eddy at the time when it reaches the level of p is therefore given by

$$\left(\frac{p}{P}\right)^{\gamma} \left\{ \theta(p, t) + (p_0 - p) \frac{\partial \theta}{\partial p} + (t_0 - t) \frac{\partial \theta}{\partial t} \right\} \quad (11)$$

For at each stage of its motion the moving eddy takes up the pressure of its surroundings. It follows from this that the mixing takes place "at constant pressure," and that in mixing with its surroundings the eddy shares out its excess or defect of thermal energy, which we have seen is to be measured by

$$\text{mass of eddy} \times \text{specific heat } c_p \times \text{absolute temperature.} \quad (12)$$

The motion of the eddy across the isobaric surface p is therefore equivalent to a flow of heat

$$mc_p \left(\frac{p}{P}\right)^{\gamma} \left\{ \theta(p, t) + (p_0 - p) \frac{\partial \theta}{\partial p} + (t_0 - t) \frac{\partial \theta}{\partial t} \right\}. \quad (13)$$

But this is always positive, and we require an expression which shall take account of the fact that the upward moving eddies are equivalent to a flow of heat upwards, and the downward moving eddies to a flow of heat downwards. This is most simply done by taking m positive for upward moving eddies, and negative for downward moving eddies. With this proviso we find that the net upward eddy-flux of heat is

$$\begin{aligned} \Sigma c_p m \left(\frac{p}{P}\right)^{\gamma} \left\{ \theta(p, t) + (p_0 - p) \frac{\partial \theta}{\partial p} + (t_0 - t) \frac{\partial \theta}{\partial t} \right\} &= c_p \left(\frac{p}{P}\right)^{\gamma} \theta(p, t) \Sigma m \\ &+ c_p \left(\frac{p}{P}\right)^{\gamma} \frac{\partial \theta}{\partial p} \cdot \Sigma m (p_0 - p) + c_p \left(\frac{p}{P}\right)^{\gamma} \frac{\partial \theta}{\partial t} \cdot \Sigma m (t_0 - t). \end{aligned} \quad (14)$$

But there can be no resultant flow of mass across the isobaric surface, otherwise its pressure would change. It follows that

$$\Sigma m = 0. \quad (15)$$

Also in $\Sigma m(t_0 - t)$, $t_0 - t$ is always negative, and any given value of $t_0 - t$ is equally likely to be associated with positive and negative values of m . Hence

$$\Sigma m(t_0 - t) = 0.$$

In the expression (14) above only the middle term remains. Further in $\Sigma m(p_0 - p)$, $p_0 - p$ is positive for positive values of m , and negative for negative values of m , and so each term in the summation is positive. The resultant upward flow of heat is

$$c_p \left(\frac{p}{P}\right)^\gamma \frac{\partial \theta}{\partial z} \cdot \frac{\partial z}{\partial p} \Sigma m(p_0 - p). \quad (16)$$

But if T is the absolute temperature at height z , it follows from equation (9) above that

$$\frac{1}{\theta} \frac{\partial \theta}{\partial z} = \frac{1}{T} \frac{\partial T}{\partial z} - \frac{\gamma}{p} \frac{\partial p}{\partial z}.$$

Hence

$$\left(\frac{p}{P}\right)^\gamma \frac{\partial \theta}{\partial z} = \frac{T}{\theta} \frac{\partial \theta}{\partial z} = \frac{\partial T}{\partial z} + \frac{\gamma g}{R},$$

since

$$\frac{\partial p}{\partial z} = -g\rho.$$

But $\gamma g/R$ is equal to the dry adiabatic lapse rate. Denoting this by α , we may write

$$\left(\frac{p}{P}\right)^\gamma \frac{\partial \theta}{\partial z} = \frac{\partial T}{\partial z} + \alpha. \quad (17)$$

We define K by the relation

$$K = \frac{\Sigma m(p_0 - p)}{g\rho^2}, \quad (18)$$

which is equivalent to Taylor's expression for K . Then the resultant upward eddy flow of heat across the isobar p is seen to be

$$-K\rho c_p \left(\frac{\partial T}{\partial z} + \alpha\right). \quad (19)$$

The corresponding expression derived by Taylor is

$$-K\rho c_p \frac{\partial \theta}{\partial z}. \quad (19^1)$$

The difference between (19) and (19¹) arises from the difference in the expressions used for the flow of heat due to an eddy in Taylor's paper and in equation (13) above. Taylor assumed the flow of heat to be proportional to the potential temperature, and not to the absolute temperature.

The factor $\frac{\partial T}{\partial z} + \alpha$ is the difference between the lapse rate and the adiabatic.

The net eddy flow of heat is upward, downward, or zero, according as the lapse rate is greater than, less than, or equal to the adiabatic lapse rate. The expression (19) gives the upward flow across unit area of the isobaric surface p . The upward flow across unit area of the isobaric surface $p + dp$ is

$$- K\rho c_p \left(\frac{\partial T}{\partial z} + \alpha \right) - c_p \frac{\partial}{\partial p} \left(K\rho \left(\frac{\partial T}{\partial z} + \alpha \right) \right) dp.$$

The net gain of heat between these two isobars

$$= c_p \frac{\partial}{\partial z} \left(K\rho \left(\frac{\partial T}{\partial z} + \alpha \right) \right) \frac{dp}{g\rho} = \frac{dp}{g} c_p \frac{\partial T}{\partial t}, \quad (20)$$

since the mass between the two isobaric surfaces p and $p + dp$ is dp/g . Thus we finally deduce the diffusion equation,

$$\rho \frac{\partial T}{\partial t} = \frac{\partial}{\partial z} \left(K\rho \left(\frac{\partial T}{\partial z} + \alpha \right) \right). \quad (21)$$

This equation gives the rate of change of temperature produced by eddies at the level of a particular isobaric surface at whose instantaneous level K , ρ , and $\partial T/\partial z$ have been evaluated. At a subsequent time the height of this isobar may have varied. This limitation of the equation may appear troublesome and is readily removed. The rate of change of temperature at a particular height z may be written

$$\left(\frac{\partial T}{\partial t} \right)_z = \frac{\partial T}{\partial t} + \frac{\partial T}{\partial p} \frac{\partial p}{\partial t} = \frac{\partial T}{\partial t} - \frac{1}{g\rho} \frac{\partial T}{\partial z} \frac{\partial p}{\partial t} = \frac{\partial T}{\partial t} - \frac{R}{g\rho} \frac{\partial T}{\partial z} \frac{\partial}{\partial t} (\rho T)$$

or

$$\rho \frac{\partial T}{\partial t} = \rho \left(\frac{\partial T}{\partial t} \right)_z + \frac{R}{g} \frac{\partial T}{\partial z} \frac{\partial}{\partial t} (\rho T). \quad (22)$$

Now the changes of density are due to the expansion or contraction produced by changes in temperature. Therefore $\frac{\partial}{\partial t} (\rho T) = \rho \frac{\partial T}{\partial t} + T \frac{\partial \rho}{\partial t}$ is of the same order of magnitude as $\rho \frac{\partial T}{\partial t}$. In the last expression in (22) above, $\frac{R}{g} \frac{\partial T}{\partial z}$ is of the order of $\frac{3 \times 10^8 \times 10^{-4}}{10^8}$ or 3×10^{-4} , and so neglecting a small quantity

of this order by comparison with unity, we may reduce the expression to $\rho \left(\frac{\partial T}{\partial t} \right)_z$, and the equation (21) above may be applied without correction to give the changes of temperature at a particular height z .

This equation can be further simplified in certain cases. In the atmosphere the density varies only relatively slowly with height, and if we neglect these variations the equation becomes

$$\frac{\partial T}{\partial t} = \frac{\partial}{\partial z} K \left(\frac{\partial T}{\partial z} + \alpha \right). \quad (23)$$

If further we assume that K does not vary with height it can be further reduced to

$$\frac{\partial T}{\partial t} = K \frac{\partial^2 T}{\partial z^2}, \quad (24)$$

This equation is directly comparable with that for conduction of heat in a solid. A similar equation was given by Taylor with θ in place of T .

It may be noted in passing that equation (21) as applied to a particular height z could have been derived directly, with the term $\frac{R}{g} \frac{\partial T}{\partial z} \frac{\partial}{\partial t} (\rho T)$ added on the left-hand side, by much the same analysis as we used above. The only difference in procedure is that the Σm would not be zero, but $\frac{1}{g} \frac{\partial p}{\partial t}$, since the rate of transport of mass $\times g$ across a surface measures the rate of increase of pressure at that surface.

A somewhat different treatment of eddy diffusion has been given by L. F. Richardson.* He defines Z as any one of certain entities such as horizontal momentum in a given azimuth, weight of water in unit mass of atmosphere, or any other quantity which has its total unchanged by (a) re-arrangement of that portion, or (b) by delay. If χ be defined as the amount of Z per unit mass of atmosphere, the upward flux of Z is expressed by $-c \frac{\partial \chi}{\partial z}$, where it is stipulated that c must not become infinite when $\partial \chi / \partial z = 0$. Beyond this restriction no assumption is made as to the way in which c may depend upon z , χ or $\partial \chi / \partial z$. The one restriction mentioned is imposed in order to provide that the upward flux of Z shall vanish when $\partial \chi / \partial h = 0$, and this implies that χ must be unchanged by the simple transportation of air to a different level. In a later paper†

* 'Roy. Soc. Proc.,' A, vol. 96, p. 9 (1919).

† 'Phil. Trans. Roy. Soc.,' A, vol. 221, p. 1 (1920); 'Weather Prediction by Numerical Process' (Camb. Univ. Press), 1922.

Richardson suggests that χ may be potential temperature, or mass of water or smoke per unit mass at atmosphere. Exception may be taken to this suggestion in so far as it concerns potential temperature. Though Richardson does not explicitly state it, it is presumed that when χ is potential temperature, Z is available heat content. But we have already seen that the available heat content is not completely specified by potential temperature alone, so that in this case a given value of χ does not correspond to a definite value of Z . Richardson's deduction of his diffusion equation may be summarised by the equations,

$$\frac{\partial}{\partial t}(\rho\chi) = -\frac{\partial}{\partial z}(\text{upward flux}) = \frac{\partial}{\partial z}\left(c\frac{\partial\chi}{\partial z}\right). \quad (25)$$

It is difficult to assign a definite meaning to the left-hand side of this equation since there is no clearly defined physical entity which corresponds to potential temperature. The latter is a mathematical abstraction rather than a physical concept. Moreover this equation is not consistent with the assumption on

which it appears to be based. For if the flux of potential temperature $c\frac{\partial\chi}{\partial z}$ is independent of height, then $\frac{\partial}{\partial z}\left(c\frac{\partial\chi}{\partial z}\right) = 0$, and χ should not vary with time.

But as Richardson has pointed out* the flux of heat across unit area of a horizontal surface is $c\frac{\partial\chi}{\partial z}\left(\frac{p}{P}\right)^\gamma$, and hence a layer of air of thickness dz will gain per unit time an amount of heat $\left(c\frac{\partial\chi}{\partial z}\right)\frac{\gamma\delta p}{\delta z}\frac{p^{\gamma-1}}{P^\gamma}.dz$ and the absolute temperature cannot remain constant. Hence the potential temperature will also vary—a result which is inconsistent with the diffusion equation (25) above.

V.—*The Combined Effects of Radiation and Turbulence.*

The equations which determine the changes of temperature produced by turbulence (21), (23) and (24) above, should be compared with equations (4) and (5), which give the changes produced by radiation. The equation (4) may be written in the form

$$\rho\frac{\partial T}{\partial t} = \frac{\partial}{\partial z}\left(\rho K_R\frac{\partial T}{\partial z}\right), \quad (26)$$

which corresponds in form with equation (21), except that $\partial T/\partial z$ appears instead of $\frac{\partial T}{\partial z} + \alpha$.

* 'Weather Prediction,' p. 70.

Reasons have been adduced to show that a reasonably good first approximation to the variations produced by radiation and turbulence respectively can be obtained by the use of equations (5) and (24). Adding these two equations, we find that the combined effects of radiation and turbulence are represented in the equation

$$\frac{\partial T}{\partial t} = (K + K_R) \frac{\partial^2 T}{\partial z^2}. \quad (27)$$

Both K and K_R are positive, and their sum is accordingly positive. It is however probable that K and K_R will be found to vary very differently with height and time of day. The variations of K_R are affected more by vapour pressure than by any other factor, and K_R will not vary within very wide limits with time of day, as vapour pressure has no very marked diurnal variation. K , on the other hand, is likely to vary within wide limits as the lapse rate changes, being smaller under stable than under unstable conditions in the vertical.

In a first analysis of the phenomena we shall treat both K and K_R as remaining constant through small ranges of height z . It is then seen from equation (27) that the condition that the temperature should rise is that $\partial^2 T / \partial z^2$ should be positive, and the condition that temperature should fall is that $\partial^2 T / \partial z^2$ should be negative, whether we consider the effects of radiation or of turbulence, or of both.

If it is desired to evaluate the net outward flow of radiation across a horizontal plane, care must be taken to allow for the functional difference between equations (3) and (19). The flow of heat by radiation is upward or downward according as the temperature decreases or increases with height, but the flow of heat by turbulence is upward or downward according as the lapse rate is greater or less than the adiabatic. Some examples are shown in fig. 2, where the line AB indicates the adiabatic lapse rate, and the line CDE represents actual distribution of temperature. The small diagrams on the right indicate by arrows the direction of flow of heat by radiation and turbulence, a doubly feathered arrow indicating a larger amount of flow than a single feathered arrow. Thus in fig. 2a, though the general transfer by radiation is upward, and the general transfer by turbulence is downward, the air at D is gaining heat from both. In fig. 2b the transfer of heat is upward both by radiation and turbulence in CD, and the air at D is being warmed. In fig. 2c radiation and turbulence work together in causing a downward flow of heat in CD, and produce a cooling of the air at D. The effect may be summarised

in a few words. Where there is a bend in the temperature height diagram the effect of both radiation and turbulence is to smooth out the bend. If

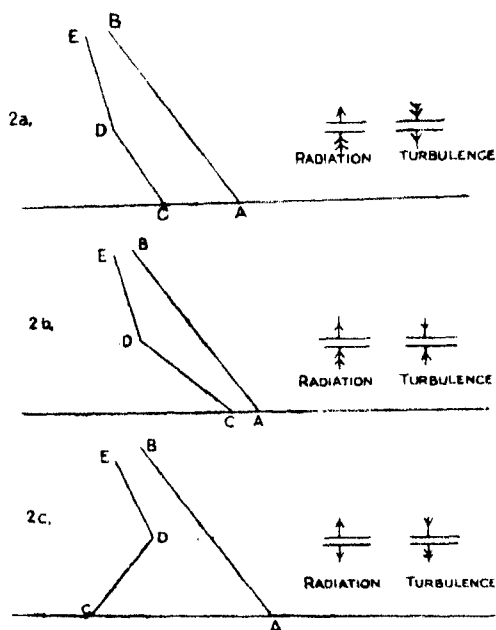


FIG. 2.

the lapse rate is constant at all heights, then provided K and K_R do not vary with height, both radiation and absorption will give rise to a steady stream of heat which will pass through the atmosphere without producing any changes of temperature.

It will have been noted that the flow of heat by turbulence is only directed upward when the lapse rate exceeds the adiabatic. Observations of temperature in the free air indicate that at heights of a few hundred metres and less, the temperature begins to rise in the mornings before the lapse rate has reached the adiabatic, and several writers have regarded this as an indication of the action of some powerful agent other than turbulence, in causing a flow of heat upwards.* Equation (27) shows, however, that the temperature at, say, 200 metres, should begin to rise as soon as the lapse rate immediately below 200 metres has surpassed the value of the lapse rate above 200 metres. Or in the more general case, using equation (23), and neglecting the small

* S. Chapman, 'Q. J. R. Met. Soc.', vol. 51, p. 101 (1925); Schmidt, 'Sitz. Akad. Wiss. Wien,' vol. 127, No. IIa (1918).

variation of ρ with height, turbulence should cause an increase of temperature at 200 metres as soon as $K \left(\frac{\partial T}{\partial z} + \alpha \right)$ has a lower value below 200 metres than above it. It has frequently been remarked that the temperature at the top of the Eiffel Tower begins to rise in the morning before the lapse rate has attained the adiabatic. But it has never been conclusively shown that the early rise of temperature at the top of the tower is not due to the effects of sunshine on the instrument or its housing, or on the tower itself. It is extremely difficult to measure the temperature of the air at a height of more than a few metres above the ground. Even with electrically recording instruments difficulties arise as to the exact position of the zero of the trace. There are therefore no observations available which can be used to determine with accuracy whether the phenomena observed can be accounted for by the use of equation (27) above.

The analysis of Section IV above does not take account of large scale convection, since it tacitly assumes that both the area A across which the flux of heat is measured, and the time over which conditions are averaged are both sufficiently great to include the effect of a large number of eddies. It does not appear legitimate to assume that the time over which conditions must be averaged to yield a reasonable estimate of the effects of large scale convection currents, is sufficiently short to permit us to neglect changes in external conditions during this interval. Further discussion of this point is postponed until detailed observations of temperature at different heights above the ground are available.

Values of K have been estimated by numerous observers from observations of temperature or wind at different heights, and it has been found that K varies within very wide limits. Taylor obtained values of K of the order of $3 \cdot 10^3$ in inversions over the Great Banks of Newfoundland, and on sunny afternoons K has been found to attain values of over 10^5 . Thus while K_R is comparable with K in inversions, it is much smaller than K under conditions when there is vigorous turbulence. When observations of temperature at different heights above the ground are available, $K + K_R$ can be readily deduced by the use of equation (27), and this value may be taken as giving the value of K alone when it is considerably in excess of 10^3 .

The fact that K is considerably greater than K_R except in inversions has an important bearing on the question of the persistence of superadiabatic lapse rates. The late Lord Rayleigh showed* for an incompressible fluid that it

* 'Phil. Mag.,' vol. 32, p. 529 (1916).

is possible for the fluid to remain stable with a heavy layer of density ρ_2 above a lighter layer of density ρ_1 , provided

$$\frac{\rho_2 - \rho_1}{\rho_1} < \frac{27\pi^4 \kappa \nu}{4gh^3},$$

where h is the depth of the fluid, κ its molecular thermal conductivity, and ν its kinematic coefficient of viscosity. In the atmosphere, however, giving κ and ν their appropriate values for air, this inequality leads to the result that except possibly for a layer whose thickness is a few inches only, any slight increase of the lapse rate beyond the adiabatic limit should be unstable. In discussing this result the present writer suggested* that ν should be replaced by an eddy frictional coefficient and that molecular conductivity could be neglected by comparison with the effects of radiation. It now appears, however, that except in very still air, both κ and ν should be replaced by K , while in very still air κ should be replaced by K_R . Rayleigh's results and their extension by Jeffreys,† are only applicable to incompressible fluid, and further discussion of the stability of superadiabatic lapse rates must be postponed until the corresponding formulæ for a compressible fluid have been derived.

VI.—Summary.

A simplifying assumption as to the nature and extent of the effects of radiation and absorption by water-vapour in the atmosphere, based on Hettner's measurements of absorption by water-vapour, makes it possible to reduce the problem of the transfer of heat by radiation and absorption to a tractable form. This transfer is found to be analogous to the conducting of heat in a solid, the ordinary coefficient of molecular conductivity being replaced by a much larger coefficient, the radiative diffusivity K_R .

The transfer of heat by eddies in a turbulent atmosphere is evaluated for a compressible atmosphere, and it is shown that the eddy flux of heat is proportional to the difference between the lapse rate and the adiabatic, and to the eddy-diffusivity K , defined by Taylor.

The relative magnitudes of K_R and K are considered. K is normally of the order of 10^3 in inversions but is usually greater than 10^5 when the atmosphere is fairly turbulent. Both radiation and turbulence tend to smooth out any bends in a temperature height curve.

* 'Nature,' vol. 115, p. 299 (1925).

† 'Phil. Mag.,' vol. 2, p. 833 (1926); 'Roy. Soc. Proc.,' A, vol. 118, p. 195 (1928).

*The Influence of Nitrogen Peroxide on the Combination
of Hydrogen and Oxygen.*

By H. W. THOMPSON and C. N. HINSHELWOOD.

(Communicated by Sir Harold Hartley, F.R.S.—Received February 18, 1929.)

It has recently been shown that small traces of nitrogen peroxide exert a remarkable influence on the combination of hydrogen and oxygen, even at temperatures far below that at which the normal reaction has an appreciable velocity.* At any such temperature there exist two sharply defined critical concentrations of nitrogen peroxide, between which there is instantaneous inflammation of the hydrogen and oxygen, but above or below which there is only an extremely slow reaction.† The transition at each of these nitrogen peroxide pressures is very abrupt.

An analogous phenomenon can be observed in the union of oxygen and hydrogen alone. Between certain limiting concentrations there is immediate explosion, but above and below these a reaction with a measurable velocity takes place.

In a previous paper‡ an explanation of these results was suggested, based upon the theory of "reaction chains." If in such a chain one active molecule can give rise, after a sequence of changes, to more than one, the reaction velocity will increase indefinitely, and explosion ensue, except in so far as various deactivation processes keep the effect of the branching chains in check.§ The balancing of these various influences determines the critical limits of concentration. According to the previous results, the chains are initiated by molecules of hydrogen peroxide in mixtures of hydrogen and oxygen when these react in the absence of nitrogen peroxide, but when nitrogen peroxide is present the chains are very readily initiated by a reaction between molecules of this gas and hydrogen.

For hydrogen and oxygen mixtures without nitrogen peroxide, the effect of various factors, such as temperature, and nature and size of the vessel was examined, and the results enabled a definite theory of the mechanism of the reaction to be constructed. A similar detailed investigation has now been made of the phenomena observed in presence of nitrogen peroxide, which had previously only been studied at one pressure of hydrogen and oxygen. The

* H. B. Dixon, private communication.

† Gibson and Hinshelwood, 'Trans. Faraday Soc.,' vol. 24, p. 559 (1928).

‡ Thompson and Hinshelwood, 'Roy. Soc. Proc.,' A, vol. 122, p. 610 (1929).

§ Semenov, 'Z. Physik,' vol. 46, p. 109 (1927).

results allow the theory outlined in the previous paper to be elaborated and completed.

The experimental methods employed were in general essentially the same as those previously described.

The Critical Concentrations of Nitrogen Peroxide for various Pressures of Hydrogen and Oxygen.

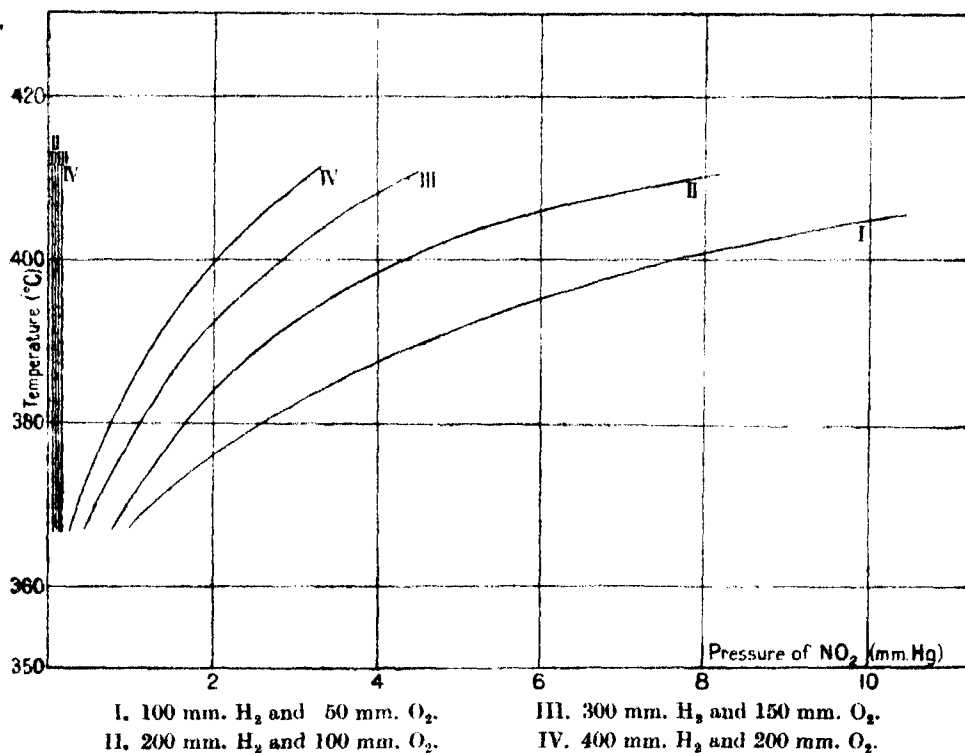
For equivalent proportions of hydrogen and oxygen the critical concentrations of nitrogen peroxide move nearer together as the total pressure is increased, the lower one being raised and the upper one lowered.

Preliminary experiments were made as follows. The concentrations of nitrogen peroxide between which ignition occurred in a porcelain bulb at 390° C. were first determined with 200 mm. H_2 and 100 mm. O_2 . Then various concentrations of the peroxide greater than the upper limit were mixed with 200 mm. H_2 and 100 mm. O_2 , and the mixture was slowly drawn out of the apparatus by the pump. The pressure at which explosion occurred was observed, and from this the partial pressures of all three gases could be calculated. The results indicated that the smaller the pressure of hydrogen and oxygen the greater was the concentration of nitrogen peroxide required to stop the explosion. The results obtained by this method, which we may call the withdrawal method, were not very regular. It was therefore necessary to employ the original method, in which the critical pressures of nitrogen peroxide for each pressure of hydrogen and oxygen were determined by repeated trial. The experiments were made at various temperatures. The results are tabulated below, and shown in the figure.

Temperature, ° C.	Pressure of NO_2 in mm. mercury.							
	Lower limit				Upper limit.			
	100 mm. H_2 .	200 mm. H_2 .	300 mm. H_2 .	400 mm. H_2 .	100 mm. H_2 .	200 mm. H_2 .	300 mm. H_2 .	400 mm. H_2 .
410	0.053	0.076	0.107	0.144	>9.9	7.9	4.4	3.1
390	0.068	0.09	0.122	0.160	4.6 (3.2)	2.7 (2.5)	1.8 (2.1)	1.3 (1.4)
370	0.09	0.12	—	0.15	1.47	0.98	0.59	0.39

NOTES.-(a) The figures in brackets were obtained in a much earlier series of experiments and in a different bulb.

(b) During the series of experiments it was necessary to replace the porcelain bulb by another similar one. The results obtained with the two bulbs showed no noticeable discrepancy.

*Influence of Nitrogen.*

In the presence of nitrogen the upper critical concentration of nitrogen peroxide for a particular pressure of hydrogen and oxygen is lowered; the lower limit is probably but little affected. Whereas, for example, the upper limit for 200 mm. H_2 and 100 mm. O_2 at $396^\circ C.$ is > 3.3 mm. NO_2 , for 200 mm. H_2 and 478 mm. air, i.e., 100 mm. O_2 and 378 mm. N_2 , it becomes 1.47 mm. NO_2 . Other results are:—

(a) 200 mm. H_2 , 100 mm. O_2 , 378 mm. N_2 —

Upper limit: 406° , 1.45 mm. NO_2 ; 390° , 0.66 mm.; 375° , 0.45 mm.

Lower limit: 395° , 0.075 mm. NO_2 .

(b) 100 mm. H_2 , 50 mm. O_2 , 189 mm. N_2 —

Upper limit: 395° , 1.20 mm. NO_2 ; 382° , 0.84 mm.

These experiments were repeated in a silica bulb. Although the results obtained were somewhat variable and differed slightly from those obtained with the porcelain bulb, they were qualitatively in agreement with them.

Influence of the Ratio of Oxygen to Hydrogen on the Critical Nitrogen Peroxide Concentrations.

Some experiments by the "withdrawal" method, previously described, were carried out to discover the effect on the upper critical nitrogen peroxide concentration of the ratio of oxygen to hydrogen in the gas. In order to obtain the results in the most convenient form it would be desirable so to arrange matters that the total pressure of hydrogen and oxygen at the actual point of ignition is the same in each experiment, thereby allowing the effect of their ratio alone on the nitrogen peroxide concentration to be seen by direct inspection. This could be attained by a tedious process of trial and error in the choice of the initial concentrations. The information required can, however, be obtained in a simpler manner as follows.

Silica Reaction Vessel. Total Initial Pressure 600 mm. Gases mixed and then Pressure lowered until Explosion occurred.

	Initial pressure of NO ₂ .	Ratio O ₂ /H ₂ .	Total pressure at ignition point.	Mean.	Pressure of NO ₂ at ignition point.
	mm.				
Series I—					
400° C.	3.27	{ 0.50 0.70 1.00 2.00	312, 259, 281, 270 262, 282 200 112	281 275 200 112	1.53 1.49 1.09 0.61
Series II—					
405° C.	2.70	{ 0.50 1.00 2.00	334, 325 303, 305 233, 223	330 304 228	1.48 1.37 1.03
Series III—					
405° C.	2.70	{ 0.50 0.70 1.00	343 335 329	343 335 329	1.54 1.51 1.48
Series IV—					
410° C.	3.27	{ 0.50 2.00	330, 307 293, 276, 238	318 269	1.43 1.21

In spite of some variability in the results it is seen that in all the experiments the critical pressure of nitrogen peroxide decreases as the proportion of oxygen increases; but, from the way in which the experiments were carried out, the total pressure at the ignition point decreases simultaneously. It has, however, already been found that as the total pressure of hydrogen and oxygen is

increased, so the upper critical concentration of nitrogen peroxide is lowered. Thus if the total pressures given in the above table for the experiments with high oxygen ratios had been increased and made equal to those for the low oxygen ratios, the critical nitrogen peroxide pressures would have become still smaller. The upper critical concentration of nitrogen peroxide does, therefore, really decrease as the ratio O_2/H_2 increases; and the decrease as we pass from the ratio 0.5 to 2.0 is even greater than that indicated by the figures recorded in the table.

Further experiments were made using a porcelain vessel in the hope that data of greater accuracy would be obtained, but irregularities were still noticed. In this series the rate of withdrawal was varied, and also the time during which the mixture was allowed to remain in the reaction vessel before withdrawal. But the results were essentially the same as those previously obtained. It seems therefore that "time-lag" phenomena are not involved.

Porcelain Reaction Vessel. Total Initial Pressure 600 mm. Temperature
396° C.

Ratio O_2/H_2 .	Total pressure at ignition point.	Pressure of NO_2 at ignition point.
0.50	mm. 321	mm. 1.76
1.00	272	1.50
2.00	210	1.15

Discussion.

The facts may be summarised as follows :—

- (a) In presence of nitrogen peroxide the explosion takes place at temperatures where hydrogen and oxygen alone are almost completely inert to one another.
- (b) There are two critical concentrations of nitrogen peroxide for each pressure of hydrogen and oxygen between which only is the explosion possible.
- (c) Of these critical concentrations the lower is raised and the upper lowered as the total pressure of hydrogen and oxygen is increased.
- (d) For a given total pressure the upper limit is lowered by an increase in the proportion of oxygen to hydrogen.
- (e) The upper limit is lowered by the presence of nitrogen, the lower limit not being much affected.

- (f) The upper limit is much the same in silica vessels as in porcelain vessels ; the lower limit tends to drift in a rather indefinite way, but the difference in the two kinds of vessel is not very great.

(a) shows that the process initiating the chain must be a reaction involving nitrogen peroxide ; it will appear that it is not necessary to specify its nature more exactly. (b) shows that the chains are controlled by two kinds of deactivating mechanism, one of which becomes less effective and the other more effective as the concentration of the nitrogen peroxide increases. In accordance with the theory discussed in the previous paper we assume the upper limit to be reached when the deactivating influence of nitrogen peroxide on the hydrogen peroxide formed in the course of the chains becomes great enough. The existence of the lower limit has not quite such an obvious explanation. With hydrogen and oxygen in the absence of nitrogen peroxide there is a lower critical pressure, conditioned by the circumstance that at higher pressures diffusion to the surface becomes less easy and deactivation at the surface less important. But in the reaction now under consideration the amount of nitrogen peroxide is too small a fraction of the total gas appreciably to affect the diffusion of molecules to the wall of the vessels ; thus we assume it to act rather as a catalytic poison for a wall reaction which would normally break the chains. This reaction we may suppose to be the interaction of H_2O_2 and H_2 , which in the gas phase propagates the chain, but at the surface terminates it, because the energy is given up to the wall.

The whole process may be thought of in the following way, which, however, is only intended to give an approximate picture of the sort of mechanism which probably underlies the observed effects.

(1) Reaction of NO_2 with H_2 yielding activated H_2O_2 either directly or by intermediate stages. (2) The active H_2O_2 reacts with H_2 in the gas phase giving rise to a cycle of processes whereby ultimately α molecules of active H_2O_2 arise from each of the original ones. We assume for simplicity that this cycle is not broken by deactivating mechanisms, which are supposed to act rather by destroying the H_2O_2 itself. Thus α is probably two. (If we represent an active molecule by an asterisk, we have $\text{H}_2\text{O}_2^* + \text{H}_2 \rightarrow 2\text{H}_2\text{O}^* \rightarrow 2\text{H}_2^*$ or $2\text{O}_2^* \rightarrow 2\text{H}_2\text{O}_2^*$.) (3) Some of the active H_2O_2 , however, reacts with hydrogen at the surface, uselessly as far as chain propagation is concerned. We must assume that there is a competition between NO_2 and H_2 for occupation of the surface, and further that the amount of each adsorbed on the surface is inversely proportional to a function of the pressure of the other.

(4) Active H_2O_2^* may also be deactivated by collision with NO_2 in the gas phase. (This process might give activated oxygen, which could then re-form active H_2O_2 at a later stage; but we may regard this merely as an increase in the rate of 2 relative to 4.) (5) A similar process may occur at the surface with the adsorbed NO_2 , but this does not appear to play any essential part. (6) Active H_2O_2 is decomposed also by collision with the normal hydrogen peroxide molecules existing in the gas at a concentration $K[\text{H}_2][\text{O}_2]$. (7) Active H_2O_2 is decomposed at the surface spontaneously. (8) Deactivation of H_2O_2 by molecules of oxygen in the gas phase may occur. (9) Deactivation by nitrogen may also occur.

Writing the essential results of these processes in symbols we have :—

- (1) $x\text{NO}_2 + y\text{H}_2 \rightarrow \text{H}_2\text{O}_2^*$.
- (2) $\text{H}_2\text{O}_2^* + \text{H}_2 \rightarrow \alpha\text{H}_2\text{O}_2^* \text{ (gas)}$.
- (3) $\text{H}_2\text{O}_2^* + \text{H}_2 \rightarrow \text{inactive molecules (surface)}$.
- (4) $\text{H}_2\text{O}_2^* + \text{NO}_2 \rightarrow \text{inactive molecules (gas)}$.
- (5) $\text{H}_2\text{O}_2^* + \text{NO}_2 \rightarrow \text{inactive molecules (surface)}$.
- (6) $\text{H}_2\text{O}_2^* + \text{H}_2\text{O}_2 \rightarrow \text{inactive molecules (gas)}$.
- (7) $\text{H}_2\text{O}_2^* \rightarrow \text{inactive molecules (surface)}$.
- (8) $\text{H}_2\text{O}_2^* + \text{O}_2 \rightarrow \text{inactive molecules (gas)}$.
- (9) $\text{H}_2\text{O}_2^* + \text{N}_2 \rightarrow \text{inactive molecules (gas)}$.

Processes (1), (2), (3) and (4) are assumed to be the controlling ones, the balance of which gives rise to the critical limits; the others have a greater or smaller influence on the exact position of the limits.

Writing down the condition for a stationary state we have

$$\begin{aligned} \frac{d[\text{H}_2\text{O}_2^*]}{dt} = & k_1 f \{ [\text{NO}_2] [\text{H}_2] \} + \alpha k_2 [\text{H}_2\text{O}_2^*] [\text{H}_2] - k_3 [\text{H}_2\text{O}_2^*] [\text{H}_2] \\ & - k_3 [\text{H}_2\text{O}_2^*] \frac{[\text{H}_2]^x}{[\text{NO}_2]^y} - k_4 [\text{H}_2\text{O}_2^*] [\text{NO}_2] \\ & - k_5 [\text{H}_2\text{O}_2^*] \frac{[\text{NO}_2]^y}{[\text{H}_2]^x} - k_6 [\text{H}_2\text{O}_2^*] K [\text{H}_2] [\text{O}_2] \\ & - k_7 [\text{H}_2\text{O}_2^*] - k_8 [\text{H}_2\text{O}_2^*] [\text{O}_2] - k_9 [\text{H}_2\text{O}_2^*] [\text{N}_2] = 0. \end{aligned}$$

Thus

$$[\text{H}_2\text{O}_2^*] = \left[\frac{k_1 f \{ [\text{NO}_2], [\text{H}_2] \}}{(1 - \alpha) k_2 [\text{H}_2] + k_3 \frac{[\text{H}_2]^x}{[\text{NO}_2]^y} + k_4 [\text{NO}_2] + k_5 \frac{[\text{NO}_2]^y}{[\text{H}_2]^x} + k_6 K [\text{H}_2] [\text{O}_2] + k_7 + k_8 [\text{O}_2] + k_9 [\text{N}_2]} \right].$$

The rate of reaction is proportional to this and becomes explosive when the denominator ceases to be positive. The terms in heavier type are the most important. $(1 - \alpha) k_2 [H_2]$ is essentially negative. For small values of $[NO_2]$ the only important positive term is $k_3 \frac{[H_2]^p}{[NO_2]^v}$; at first this is large enough to make the whole expression positive; as $[NO_2]$ increases it diminishes. When the term becomes too small to keep the whole denominator positive the lower critical limit is reached. Then there is a region of unstable chains and explosive reaction until $k_4 [NO_2]$ becomes great enough, when the upper limit is reached. (a) and (b) of the facts summarised above have now been taken into account. (c) is accounted for by the fact that if $[H_2]$ is increased $[NO_2]$ must also be increased to give the same value of $k_3 \frac{[H_2]^p}{[NO_2]^v}$. Thus the lower limit is raised. The terms $k_6 K [H_2][O_2] + k_8 [O_2]$ give the displacement of the upper limit in the right sense with increasing pressure. (d) is accounted for by the fact that if for a given total pressure $[O_2]/[H_2]$ is increased, $k_8 [O_2]$ is increased and $(1 - \alpha) k_2 [H_2]$ decreased; thus the upper limit can be reached for a smaller value of $k_4 [NO_2]$. (e) is expressed by the term $k_9 [N_2]$; it is to be remarked in this and in other connections that the k_3 term can become very large as $[NO_2]$ decreases, and outweigh the effect of the other terms more easily than the k_4 term can. Thus $k_9 [N_2]$ does not affect the lower limit much.

There is an alternative theory of the lower limit which should perhaps be considered. If we dispense with the assumption that nitrogen peroxide acts as a catalytic poison for the deactivating process 3, the denominator of the expression above will not be positive at all until the value of $[NO_2]$ reaches that corresponding to the upper limit. In other words, the smallest trace of nitrogen peroxide should initiate the explosion. But it is also evident that if $[NO_2]$ is actually zero there is no explosion. Now the first traces of nitrogen peroxide added may be rendered ineffectual by adsorption on the walls. Thus a finite concentration would be necessary to raise the effective value of $k_1 f\{[NO_2], [H_2]\}$, the numerator, above zero. This would correspond to the critical lower limit.

We do not suggest that the above explanations are exact in detail, for the whole process is evidently one of great complexity. But it seemed to be a definite advantage if the principal facts could be fitted into some simple hypothetical scheme, which should at least represent the kind of mechanism underlying this remarkable reaction. Moreover taking the results of the present

with those of the previous investigation, it may be said that the theory which has been suggested has a considerable degree of coherence. In presence of nitrogen peroxide unstable reaction chains are set up between certain sharply defined limits of concentration. In the absence of nitrogen peroxide, but at a higher temperature, unstable chains make their appearance between certain limits of hydrogen and oxygen concentration in a way so similar that it is satisfactory to be able to attribute their initiation to another peroxide, namely, hydrogen peroxide. The interruption of these chains is attributed to the action of the walls of the vessel, and to the mutual destruction of peroxide molecules; the latter mechanism is analogous to that which recent studies in combustion have indicated for the action of "anti-knocks." The hypothesis that hydrogen peroxide is involved in the chains is a simple and natural one, since this substance would be formed by the simplest kind of bimolecular encounter between hydrogen and oxygen, and its formation in flames has indeed been demonstrated by several observers.

Summary.

Small amounts of nitrogen peroxide between certain sharply defined limits of concentration are able to cause explosion in mixtures of hydrogen and oxygen, which in the absence of the nitrogen peroxide would react with extreme slowness. At the critical concentrations of nitrogen peroxide the transition from very slow reaction to explosion is abrupt. The influence of temperature, pressure, proportion of oxygen to hydrogen, presence of nitrogen, and nature of the reaction vessel on the critical concentrations has been investigated, and the results have been interpreted in terms of a theory of reaction chains. In presence of nitrogen peroxide a reaction takes place whereby activated hydrogen peroxide is produced; this undergoes a cycle of changes in which the energy of activation and heat of reaction are handed on to the molecules formed, and ultimately two activated hydrogen peroxide molecules appear for one originally formed by the action of the nitrogen peroxide. The reaction chain thus "branches," and the reaction velocity would increase indefinitely, i.e., the reaction become explosive, unless some deactivating mechanism destroyed the hydrogen peroxide. Several such mechanisms exist; decomposition or reaction with hydrogen at the wall of the vessel, deactivation by mutual destruction of two hydrogen peroxide molecules, or by destruction of hydrogen peroxide by nitrogen peroxide ("anti-knock" action). The balancing of these deactivating mechanisms and the tendency of the chains to branch determines the various critical limits between explosion and slow reaction.

The Action of Metastable Atoms of Helium on a Metal Surface.

By M. L. E. OLIPHANT, B.Sc., 1851 Exhibition Research Student, University of Adelaide.

(Communicated by Sir Ernest Rutherford, P.R.S.—Received March 21, 1929.)

[PLATE I.]

In the course of a series of experiments on the action of positive ions of helium on a metal surface with which they collided, it was observed that neutral excited atoms of the gas were able to set free large numbers of electrons from the surface. Under appropriate conditions the recombination of helium ions and electrons is able to give very large numbers of these excited atoms, and a process has been developed by which it is possible to obtain an intense beam and study its behaviour under different conditions.

The recognition of the existence of metastable states of excited atoms has led to the explanation of many anomalous effects in gaseous discharges, and of some photo-synthesised reactions involving a mixture of gases. However, our knowledge of the state is very meagre,* and it is still possible to fall into considerable error and uncertainty in measurements which, unknown to the experimenter, involve the formation of excited neutral atoms. Examples of this will be given in the discussion at the end of this paper. Although it has long been recognised† that a collision between an excited atom and a metal might well lead to the ejection of an electron from the conductor by a sort of collision of the second kind, yet the magnitude of the effect under appropriate conditions has not been fully appreciated. The part which this type of collision plays in the cathode phenomena of the arc and glow discharges, and the effect which it may have on the characteristics of "probe" collectors, has yet to be determined.

Recently J. H. Coulliette,‡ following up the work of Webb and Messenger,§ has shown that metastable atoms are able to travel considerable distances across a discharge tube and set free electrons from a metal surface. Uyt-

* *Vide* Franck and Jordan, "Anregung von Quantensprungen durch Stösse"; Springer, 1926, pp. 6, 119 and 232.

† *E.g.* Webb, 'Phys. Rev.', vol. 24, p. 113 (1924); Messenger, 'Phys. Rev.', vol. 28, p. 962 (1926).

‡ 'Phys. Rev.', vol. 32, p. 636 (1928).

§ *Loc. cit.*

hoeven* has found it necessary to assume such an action of metastable atoms on a Langmuir collector in the positive column of the discharge in rare gases. The conditions under which experiments are carried out have not allowed, however, of any quantitative estimate of the efficiency of the process, though the results of the latter investigation suggest that it is high.

Apparatus.—Helium gas was admitted to the chamber O, fig. 1, through a fine leak, passing on the way over activated charcoal cooled in liquid air. An

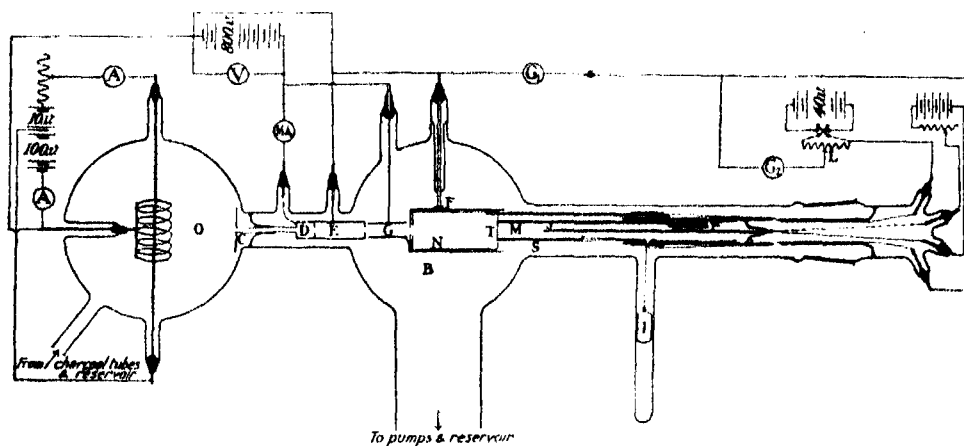


FIG. 1.

arc of 50 to 400 milliamperes at about 100 volts was maintained in O between the coiled tungsten filament and the surrounding grid. The gas in O was thus highly ionised and the plate C, when charged negatively, attracted positive ions, some of which entered the hole in the centre. Of these the larger portion collided with the walls of the canal, 3 mm. in diameter and 5 cm. long, but a few travelled right through and were then stopped by a reverse field between D and E. Any electrons set free from the walls of the canal, or from the electrodes, were bent out of the way and removed between the condenser plates G. The pressure in the portion B of the apparatus, was kept at a very low value (about 4×10^{-5} mm.), by a large four-stage Gaede diffusion pump, operating through a short length of 5 cm. tubing and a very large mercury trap of low resistance. In this way an atomic beam streamed in from O where the pressure was about 0.01 mm. and the gas was then pumped back to the reservoir.

After passing between G the neutral beam entered the shielding box F and

* 'Proc. Nat. Acad. Sci.,' vol. 15, p. 32 (1929); 'Phys. Rev.,' vol. 31, p. 913 (1928); 'Phys. Rev.,' vol. 31, p. 827 (1928).

struck a target of molybdenum T. The target was surrounded by a cylinder N, insulated from it and from F, which served to collect any charge arriving from T.

The target was fastened over the end of a nickel cylinder M which itself could slide within an external cylinder S. It normally rested so that the plane of the target coincided with the opening in the collector N, but could be drawn back against the pull of a tungsten spring P by using an electromagnet to move the piece of soft iron I. This was attached to M by a fine tungsten wire passing through the coned hole in the glass supporting tube. A filament J, inside the cylinder M, but insulated from it, could be used to heat the target by radiation to a bright red heat, or by electron bombardment to a white heat.

The accelerating potentials were supplied by a battery of small accumulators (up to 800 volts), or by an Evershed direct current generator giving up to 5500 volts. The current to the target plus the collector N, *i.e.*, any current entering the system as a whole, could be detected by a galvanometer G_1 . The current to the collector alone was measured by the galvanometer G_2 , of sensitivity 2×10^{-10} amps./mm., which sensitivity could be varied by a universal shunt. A potentiometer L enabled potentials from $+40$ to -40 volts relative to the plate to be applied to the collector N.

The helium used was fractionated 10 times from charcoal in liquid air, and traces of hydrogen were removed by electrolysing a trace of oxygen from the glass wall of a discharge tube into the glowing gas, after a method described by Taylor.* The pump and the apparatus formed a closed system, so that the gas removed from B was returned to the reservoir and purified by passing over charcoal in liquid air before returning to the discharge tube A. The apparatus was of pyrex glass, the metal parts molybdenum or nickel, with the exception of the canal which was of platinum. The ground joint at L, and those on the steel pump, were greased with a grease of very low vapour pressure (10^{-7} mm.).† The whole of the glass portion was baked out for several hours at 500° C. each time the apparatus was opened, and the metal parts were thoroughly glowed out in the best available vacuum. Before admitting gas to the system the pressure was reduced to 10^{-6} mm. as measured by an ionisation gauge. The system was separated from the exhausting pump and the gas inlet by mercury cut-offs barometrically operated, and no stop-cocks were used on this portion of the apparatus. That the apparatus was perfectly vacuum tight

* 'Nature,' vol. 121, p. 708 (1928); 'Roy. Soc. Proc.,' A, vol. 123, p. 252 (1929).

† Burch, 'Roy. Soc. Proc.,' A, vol. 123, p. 271 (1929).

was shown by the fact that the pressure did not rise above 10^{-4} mm. of mercury after standing for 7 weeks.

Operation of the Tube.—The apparatus was originally designed to study the effect of positive ions on the target T, but after the tube had been operated for some time and the helium used had been intensively purified, it became evident that the electron emissions observed were abnormally large, often, indeed, larger than the positive ion current itself. Also the secondary emission did not increase proportionally with the positive ion current, but much more rapidly. Finally, on preventing ions from reaching the system by reversing the field between D and E, and by applying a potential across G, the electron current from T to N still persisted almost unchanged. The emission was clearly electronic, for a moderate magnetic field parallel to the target completely stopped it, and it came from T, for on drawing the target right back into the sleeve S the current fell almost to zero. The emission increased rapidly with the arc current in O, but decreased as the potential applied to C was increased. The first caused a shrinking of the non-luminous sheath of positive ions surrounding C and an increase of the positive ion current flowing to it. The second caused a slight increase of the positive ion current to C and an increase in the thickness of the sheath.

Since the galvanometer G_1 indicated no current whatever, the emission of electrons from T could not have been caused by the impact of charged particles. The emission ceased when the arc was switched off, or when the accelerating potential applied to C was removed. The conclusion reached is therefore that radiation or excited atoms were being produced *in the canal and diaphragm system, or in the sheath in front of C*, and that the impact of this radiation or of the excited atoms on the target caused the emission of electrons.

Radiation Hypothesis.—In the positive ion sheath and canal there is a mixture of positive ions with normal and excited atoms. The excited atoms can emit radiation spontaneously or, if they be in the metastable state, after an impact with an electron or fast moving neutral atom or ion. Radiation produced in this way can have little effect, for the electron current from the target disappears when the potential of C is reduced to that of the grid and the positive ion current thereby cut off. The positive ions could emit radiation when neutralised by an electron at the wall of the canal. The possibility of any considerable excitation in the neutral gas atoms by impact with the positive ions is ruled out for several reasons. Firstly, the efficiency of the process is low, especially at the velocities used*; secondly, the probability of collision is

* Franck and Jordan, *loc. cit.*, p. 188; Hooper, 'Phys. Rev.', vol. 27, p. 109 (1928); Gurney, 'Phys. Rev.', vol. 32, p. 795 (1928).

small, owing to the low pressure ; and thirdly, the very homogeneous velocity experimentally found for the beam of ions issuing from the canal, which agrees within 1 per cent. with the energy corresponding to the potential applied to C, means that little energy could have been lost by impact.*

Only a very small fraction of the radiation produced in the canal system could possibly reach the target ; a rough estimate from the geometry of this apparatus and allowing generously for reflection from the walls of the canal, gives less than 10^{-3} . The total number of ions which could have entered the canal in one particular experiment corresponded to a current of $< 10^{-5}$ amperes. The electron current set free from the target was 2.3×10^{-7} amperes, 2.3 per cent. of the ion current. If each ion gave rise somewhere in the canal to a quantum of radiation which travelled to the target, the overall efficiency of the photo-electric process which gave the electrons would be 2.3 per cent., which is prohibitively large. When the factor of 10^{-3} is introduced for the fraction of the radiation reaching the target, the possibility that the effect is photo-electric is ruled out altogether.

Neutral Particle Hypothesis.—When a positive ion is neutralised the probability is greatest that the electron will be recaptured into one of the outer high energy levels of the atom, a theoretical deduction which has been verified by Mohler† for recombination in the glow discharge. Presumably the electron can gain the ground level by a single jump, or by a series of quantum jumps involving radiation, provided a metastable level is not encountered on the way. Thus in the case of helium, if the electron is absorbed into one of the outer triplet levels of the atom it must finally come to rest in the metastable 2^3S ground-level for the triplet system,‡ for combination between the triplet and singlet systems is not permitted. The probability of recombination into a triplet level must be at least as high as into a singlet level. Indeed there is evidence that it is considerably greater, so that large numbers of metastable atoms must be produced during recombination.

Capture of electrons by positive ions at the surface of a conductor differs from recombination between ions and free electrons in two respects. The ion has to do work in order to extract the electron from the metal, and the chance of a three-body collision, by which the excess of energy goes off as kinetic energy of a second electron, must be very much greater. This chance will be

* Cf. Kennard, 'Phys. Rev.', vol. 31, p. 423 (1928) ; Harnwell, 'Phys. Rev.', vol. 31, p. 634 (1928) ; Dempster, 'Phil. Mag.', vol. 3, p. 115 (1927).

† 'Phys. Rev.', vol. 31, p. 187 (1928).

‡ Franck and Jordan, *loc. cit.*, p. 119.

increased by the degree of penetration of the ion into the metal surface, i.e., by the velocity of the ion perpendicular to the surface. For glancing angles of incidence of a beam of ions the amount of "specular" reflection without neutralisation or much loss of energy, is known to be very large,* and for the same reasons the number of ions which are neutralised, but which then leave the surface as excited atoms, might also be large.† Experimental evidence will be given that this is indeed the case, but a discussion from the point of view of the mechanism of the neutralisation of positive ions at metal surfaces will be given in a later paper.

The above considerations serve to show that in the glancing impacts of positive ions upon the walls of the canal there exists a mechanism for producing a stream of excited atoms, which are capable of setting free electrons when they collide with the target, by a process analogous to a collision of the second kind. Owing to the random velocity of the ions crossing the boundary of the sheath surrounding the electrode, and the distortion of the field by the edges of the hole in the centre, especially when the sheath thickness is small, the probability is large that an ion which enters the canal will collide with the wall. The number of metastable atoms, indicated by the electron emission from the target, increases very rapidly as the sheath thickness is decreased, passing through a maximum when it becomes about twice the diameter of the orifice. For sheath thicknesses less than this some of the positive ions collide with the walls of the canal at angles too far from glancing for metastable atoms to be formed so readily.

Velocity Distribution of the Electrons.—By applying varying retarding potentials between the collecting cylinder N and the target, the velocity distribution of the electrons from T has been investigated. Such a retarding potential curve, for a Mo target, is given in fig. 2. A differentiated form of the same curve is shown dotted in the same figure. There is an abrupt maximum velocity at about 15 volts. For the maximum energy V of the electrons ejected from a surface whose work function is ϕ -volts, by a metastable atom whose energy is M volts, we have the relation

$$V + \phi = M.$$

* Gurney, 'Phys. Rev.', vol. 32, p. 467 (1928); Read, 'Phys. Rev.', vol. 31, p. 629 (1928).

† Gerthsen, 'Ann. Physik,' vol. 85, p. 881 (1928), has shown that a great part of what has been interpreted as a photoelectric effect due to radiation produced by impact of positive ions on a metal surface, is in reality an emission of electrons produced by excited atoms resulting from ions which have been neutralised and scattered from the surface.

For He the energy of the metastable level is 19.7 volts,* and the work function of Mo is 4.3 volts.† so that $V = 15.4$ volts. The difference of 0.4 volt between

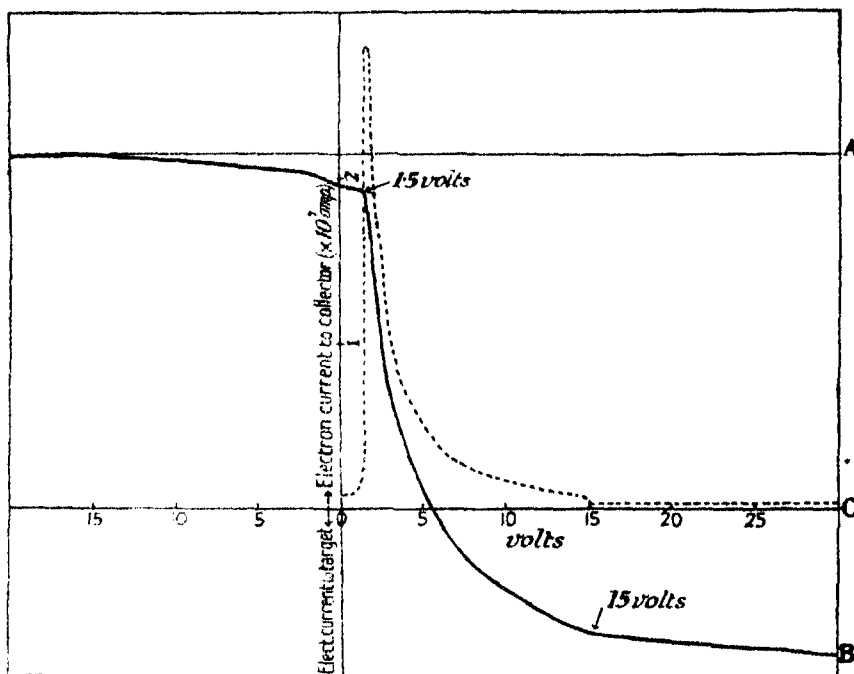


FIG. 2.—Velocity Distribution of Electrons ejected from hot Molybdenum by Metastable Ions of Helium.

the calculated and the observed values arises from the contact p.d. between the target and the collecting cylinder, for though both of the same metal, the target had been heated much more rigorously than the latter. This difference due to contact potential changes from day to day, varying for the same surfaces from 0.1 to 0.8 volt. A sharp limit is also found for the lower velocity of the electrons at about 1.9 volts, corrected for contact potential.

It will be seen that the retarding potential curve falls below the volt axis, the direction of the current reversing at about 5.5 volts, and this must mean that electrons are there being collected by the target from the collector. These electrons arise from the collision with the collector of excited atoms scattered

* Franek and Jordan, *loc. cit.*, p. 121.

† 'Handb. Physik,' vol. 14, p. 69.

from the target unchanged. Owing to the small size of the target relative to the collector this electron current does not show saturation as readily as the current from the target, which is saturated completely when the potential applied is greater than 15 volts, that is when electrons from the cylinder are prevented from reaching it. At the same time the large relative surface of the collecting cylinder ensures that there is very little chance of reflection of excited atoms back to the target, all metastable atoms coming from the target being multiplied reflected so many times at the collector surface that they must assume their normal state before escaping. Assuming that the same fraction of the metastable atoms which undergo transformation results in the ejection of electrons at the target and the collector, the ratio of the electron current from the collector to the sum of the electron currents from target plus collector is a measure of the fraction of the atoms scattered in an excited state. From the graph it is evident that the fraction so scattered, *i.e.*, BC/AB , is about 40 per cent.

The amount of reflection varies markedly with the gas condition of the surface. It is as large as 50 per cent. for a red hot surface, while it sinks to about 10 per cent. or less for a freshly introduced target, or for one which has been cold for some hours. The reflected fraction also decreases with the velocity of the original positive ions, *i.e.*, with the velocity of the metastable atoms. For instance, for a Mo surface at a red heat, the following reflection coefficients were found :—

Velocity of ions.	Percentage of metastable atoms reflected.
volts.	per cent.
2100	< 5
800	10 to 20
400	40 to 50
120	> 50

The probability that a collision will result in a return to the ground orbit evidently increases with the depth of penetration into the metal. The fraction reflected increases rapidly as the angle of incidence of the beam on the target decreases, the increase being most marked for velocities greater than those corresponding to an ion velocity of 400 volts. In the present apparatus the angle could be changed only by demolishing the target and the surrounding collecting system, so that the measurements were confined to two angles other

than the normal, 45° and 15° with the surface. For "600 volt" metastable atoms the reflected fractions were :—

Angle of incidence.	Fraction reflected.
°	per cent.
90	10 to 30
45	15 to 40
15	40 to 60
For 200 volt atoms :	
°	per cent.
90	40
45	40 to 70
15	60 to 90

A few measurements have been made for targets of Ni and Mg. The results for Ni were almost identical with those for Mo, as might be expected from the value of 4.4 volts for the work function.* The Mg was deposited in a thick layer over the target and the inside walls of the collecting cylinder by evaporation in the apparatus itself. For a freshly deposited surface the maximum velocity of the electrons set free was found to be 16.8 volts. The work function of Mg is 3.01 volts,† so that here, where the contact p.d. is eliminated by identity of the two surfaces, the agreement with the theoretical value is excellent. The fraction of metastable atoms reflected unchanged from fresh Mg was never larger than 30 per cent., but for older surfaces tended to become considerably larger. Retarding potential curves for a Mg surface are given in fig. 3.

The total number of electrons set free at the target plus the collecting cylinder does not vary very much with the surface, *i.e.*, with the fraction scattered. Thus of the metastable atoms which are transformed to the normal condition at a metal surface, a definite fraction appears to set free an electron from the surface. It is remarkable that surfaces as different in work function and other properties as Mo and Mg should agree as to the total number of electrons set free, and it is difficult to formulate any explanation other than that every metastable atom gives rise to an electron.

Significance of the Sharp Lower Limit to the Velocity.—The existence of a lower limit to the velocity of the electrons ejected from a clean metal surface by metastable atoms of helium gives strong support to the hypothesis that ejection

* 'Handb. Physik,' vol. 14, p. 69.

† 'Handb. Physik,' vol. 14, p. 73.

always takes place outwards from the metal. If any of the electrons received an impulse in the direction of the surface they would undergo scattering and

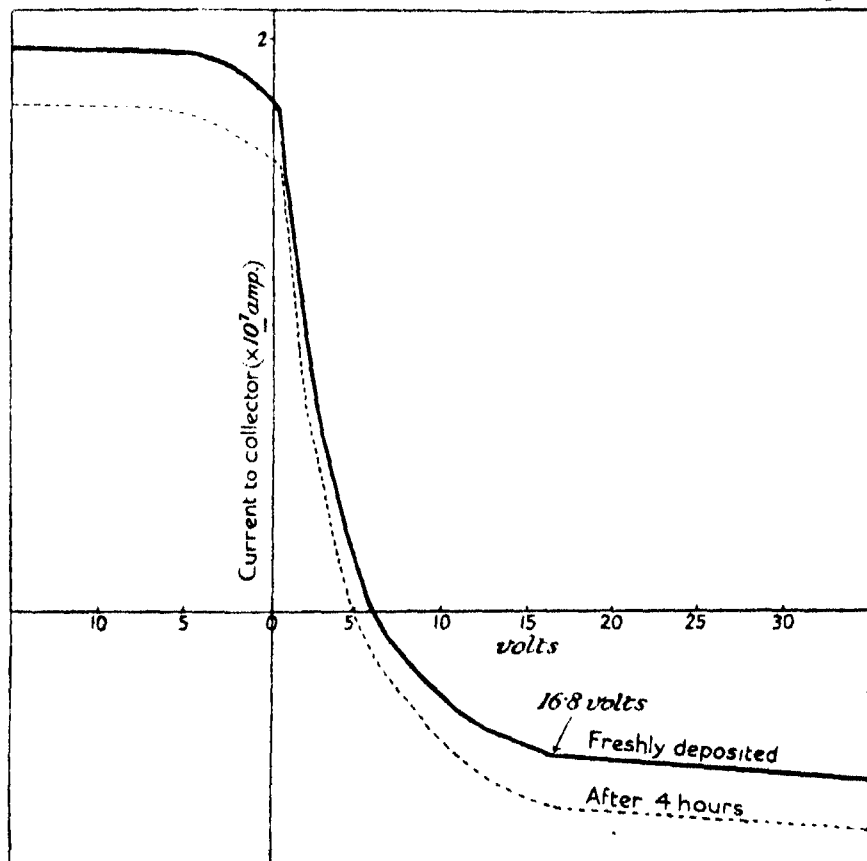


FIG. 3.—Retarding Potential Curves for fresh and aged surfaces of Magnesium. The total emission from target and cylinder does not vary with the state of the surface.

absorption, and an appreciable number would emerge with considerably decreased velocities, so that a sharp cut-off would no longer appear. We may assume then that the velocities which the electrons possess outside the metal are determined only by the work which has to be done in order to bring them through the surface, and as has been pointed out to me by Mr. R. H. Fowler this leads to a natural explanation of the low velocity limit.

At ordinary temperatures electrons in a metal form a "degenerate" gas, and are almost wholly condensed and in the same average state of energy as at the absolute zero of temperature.* The energy distribution curve is para-

* For a concise statement of the essentials of Sommerfeld's electron theory of metals see R. H. Fowler, 'Statistical Mechanics' (Camb. Univ. Press, 1929), p. 543, *et seq.*

bolic,† so that there are no electrons with zero energy in the conductor, but the number at first increases rapidly with energy and then more slowly, and is finally cut off sharply at ordinary temperatures at a characteristic maximum energy ϵ^* . This maximum energy can be calculated if the number n_0 of free electrons per unit volume is known for the particular conductor, from the formula of Sommerfeld's theory

$$\epsilon^* = \frac{h^2}{8m} \left(\frac{3n_0}{\pi} \right)^{2/3}.$$

The total height of the potential barrier through which the electrons have to escape is $\epsilon^* + \phi$, where ϕ is the ordinary thermionic work function of the surface. For an electron of energy ϵ , less than ϵ^* , to escape, energy equal to $\epsilon^* + \phi - \epsilon$ must be given it from some external source. If this energy is provided by a metastable atom the condition of escape becomes

$$M \geq \epsilon^* + \phi - \epsilon.$$

For $\epsilon = 0$ the metastable energy M must be greater than the total potential jump at the surface.

For clean Mo the following table has been prepared from the calculated values of ϵ^* (assuming various numbers N of free electrons for each metal atom in the solid), for the velocity V_0 with which electrons of zero energy in the metal would be ejected.

N.	ϵ^* .	$\epsilon^* + \phi$.	V_0 .
	volts.	volts.	volts.
1	5.4	9.7	10
2	8.6	12.9	6.8
3	11.2	15.5	4.2
4	13.6	17.9	1.8

$$\begin{aligned}\phi \text{ for Mo} &= 4.3 \text{ volts.} \\ M \text{ for He} &= 19.7 \text{ volts.}\end{aligned}$$

The actually observed minimum velocity is about 1.9 volts, so that if Mo possesses about four free electrons for each atom the agreement with experiment is excellent.

In the case of Ni the experiments of Davison and Germer‡ show that an electron on entering a surface is accelerated by about 18 volts, while the calcu-

† R. H. Fowler, 'Roy. Soc. Proc.,' A, vol. 118, p. 229 (1928).

‡ 'Proc. Nat. Acad. Sci.,' vol. 14, p. 317 (1928).

lated value of the potential jump is 16.2 volts.* The minimum velocity should lie therefore between 1.7 and 2.5 volts. Actually it occurs at 2.1 volts. For magnesium the minimum is too variable to attempt any correlation with theory.

Although this accounts satisfactorily for the position of the minimum velocity, it does not account for the appearance of a maximum number of electrons with velocities very near this value. It must be remembered, however, that there are two factors to be considered. The probability that an electron will undergo a transition from the interior of the metal to the outside, under the influence of a metastable atom, will probably decrease as the difference between the energy of the metastable state and the negative potential energy of the electron in the metal increases, and this probability may well overbalance the preponderance of electrons in the metal in energy states far removed from zero.

Experiments on the "Reflection" of Positive Ions as Metastable Atoms at a Metal Surface.—The process outlined above for the formation of the metastable atoms from positive ions at the walls of the canal tube, was tested by modifying the apparatus slightly, as schematically indicated in fig. 4. A beam of positive

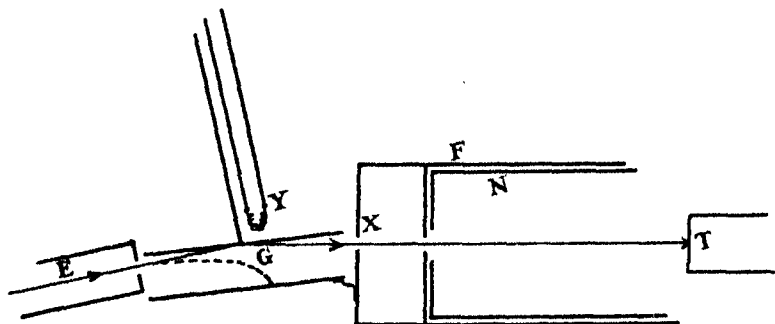


FIG. 4.

ions or of metastable atoms from the canal could be fired on to a metal surface, the upper plate of the condenser G, and anything "specularly" reflected collected in the same system as previously, with the addition of the diaphragm X to define the reflected beam. A filament Y was fastened above the reflecting plate to heat it by radiation and by electron bombardment.

With E, fig. 1, at the same potential as C, a beam of ions with metastable and excited atoms hit the plate; some of these were scattered into the collector system and struck the target. The galvanometer G_1 measured then the total

* See R. H. Fowler, 'Statistical Mechanics,' *loc. cit.*

positive ion current collected. The fraction of the ions reflected increased with the degassing of the plate, and with decrease of the velocity down to 120 volts, the lowest practicable potential which would give a well defined beam. A few volts were applied across the plates of G to prevent electrons set free from the plates from entering the collector. The electron emission from the target was then found to be more than three times the positive ion current striking it (1.2×10^{-9} amps.). From other experiments which will be described in a later paper, it is known that emissions of this order are not produced by the beam of positive ions alone, so that the metastable atoms were also scattered at the plate. A field was now applied between the condenser plates sufficiently large to prevent any ions from reaching the upper plate or entering the collector, so that the ions now followed instead the dotted curve in fig. 4. Ions scattered from this lower plate could not reach the collecting system. This bending away of the positive ions could not have altered the composition of the neutral beam hitting the reflecting plate. The electron emission was decreased by 40 per cent. This difference must be due to the electrons set free from the target by the positive ions and by neutral excited atoms formed from the ions on scattering from G. The known ion current given by the galvanometer G_1 could not possibly account for more than a 15 per cent. decrease. The remainder must then have been due to the neutral metastable atoms formed by scattering of the positive ions at G. These results are in complete agreement with the assumptions made earlier as to the origin of the excited atoms in the beam issuing from the canal, and they also supply direct proof of the scattering of metastable atoms at a metal surface.

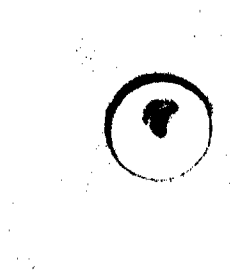
The conclusions reached can be applied to other experiments which have been carried out which have also involved the formation of metastable atoms of high energy. For instance Penning* has investigated the electron emission produced by positive ions of Ne which pass down a fine metal canal, so that his results must be influenced by spurious emissions due to the neutral atoms. Taylor† has used an electrical discharge, electrically screened from a nickel plate in the same space, to investigate the photoelectric effect due to radiation from the glowing rare gas. Metastable atoms were almost certainly able to diffuse to the plate and there set free electrons. Relatively very few of the excited atoms can produce an effect larger than a photoelectric effect, owing to the very high efficiency of the process by which they set free electrons.

* 'Vers. K. Ak. Wet. Amsterdam,' vol. 36 (1927); 'Physica,' vol. 8, p. 13 (1928).

† 'Roy. Soc. Proc., A,' vol. 117, p. 508 (1928).



Mo surface "sputtered" by metastable H_2 atoms.



Mo surface "sputtered" by H_2^+ atoms.

FIG. 5. (The stained spot on each target defines the portion eroded by the beam.)

Mohler* has also used an electrically screened discharge to investigate photo-ionisation produced by the radiation in the same gas, and his results must also be influenced by the diffusion of excited atoms. These examples will serve to indicate how electron emission from metal surfaces produced by metastable atoms can be a source of great uncertainty unless rigorously guarded against or allowed for.

"Sputtering" of the Target.—The spot on a target bombarded by the beam of metastable and of normal atoms shows a discoloration and disintegration similar to that produced by the impact of positive ions,† but of a much smaller intensity. A photograph of a Mo target bombarded with such a beam for 6 hours is reproduced in fig. 5 (Plate 1), and for comparison a similar target bombarded by positive helium ions of the same energy for 2 hours.

The kinetic energy of the metastable atoms is probably of the same order as that of the original beam of positive ions, in this case 800 volts, for it is known from experiments on positive ion reflection from clean metal surfaces at glancing angles, that the "reflected" ions retain 80 per cent. or more of their original energy.‡ If this were so the heating effect at the target should be much greater than could be produced by a beam of atoms at the temperature of the discharge. A copper-constantin thermocouple, welded to the surface of the target, indicated a temperature of 94° C. where struck by a beam of neutral atoms which set free 2×10^{-7} amps. of electrons. A super-imposed positive ion current of 10^{-7} amps. caused an additional rise to 110° C. Without excited atoms or positive ions the temperature was only 7° C. above the room temperature. The heating effect of the metastable atoms is therefore of the same order as that produced by positive ions, and the assumption that they possess about the same energy is justified.

If the sputtering produced by positive ions were due entirely to local heating and vaporisation at the point of impact of each ion, as suggested by Hippel§ in the most comprehensive theory of cathode sputtering yet produced, then the impact of neutral atoms with similar kinetic energy should produce identically the same effects. Actually it is found that while some disintegration is produced it is far less intense than that produced by positive ions. The charged condition of the ion must therefore play a part in the process of cathode disintegration.

* 'Phya. Rev.,' vol. 28, p. 46 (1926).

† Oliphant, 'Proc. Camb. Phil. Soc.,' vol. 24, p. 451 (1928).

‡ Gurney, *loc. cit.*; Read, *loc. cit.*

§ 'Ann. Physik,' vol. 81, p. 1043 (1926), and vol. 86, p. 1006 (1928).

Summary.

(a) A method is developed for producing a beam of metastable atoms of helium by the impact of positive ions at glancing incidence on the walls of a gas-free platinum canal which serves to define the beam.

(b) The metastable atoms so produced set free electrons from a metal surface with which they collide, the maximum velocity of the electrons corresponding to the difference between the energy of the metastable state and the work function of the surface.

(c) A fraction of the metastable atoms can be reflected from a metal surface, the number so reflected varying with the gas condition of the surface.

(d) Experiments are described which prove directly the production of metastable atoms by glancing impact of positive ions on a metal surface.

(e) It is shown that some sputtering is produced by the impact of the fast moving neutral atoms, which possess a large fraction of the original energy of the positive ions from which they originated. The intensity of such disintegration is far less than that produced by positive ions, and suggests that the charge of the ion is a factor in the process.

I wish to express my thanks to Sir Ernest Rutherford and to Dr. Chadwick for their interest and advice in this work, and in particular to Mr. R. H. Fowler for his many suggestions.

The Criterion for Turbulence in Curved Pipes.

By G. I. TAYLOR, F.R.S., Yarrow Research Professor of the Royal Society.

(Received March 19, 1929.)

Summary.—Experiments are described in which coloured fluid is introduced through a small hole in the side of a glass helix through which water is running. The conclusion reached by Mr. C. M. White, as a result of resistance measurements, that a higher speed of flow is necessary to maintain turbulence in a curved pipe than in a straight one, is verified directly. In a pipe bent into a helix the diameter of which was 18 times that of the cross-section, steady stream-line motion persisted up to a Reynolds number, 5830, *i.e.*, 2·8 times Reynolds' criterion for a straight pipe. This occurred in spite of the fact that the flow was highly turbulent on entering the helix.

When fluid flows through a pipe, the resistance ceases to be proportional to the velocity of flow at a lower speed when the pipe is curved than it does when it is straight. It has usually been considered that this indicates that turbulence appears at a lower speed in curved pipes than it does in straight ones, but it has been pointed out by Prof. Dean* that the circulation in the cross section of the pipe which causes the increase in resistance at low speeds is a steady motion. The speed at which the flow ceases to be steady and becomes turbulent cannot be found from resistance measurements in the simple way that it can for straight pipes. Prof. Eustice† states indeed that there appears to be no marked critical velocity for flow in coiled pipes, and Prof. Dean‡ seems to accept this view. Recently, however, Mr. C. M. White§ has given reasons for believing that a definite critical velocity exists for curved pipes. He finds that the effect of curvature in the pipe is to increase the critical velocity very considerably above the value applicable to straight pipes.

He made a number of experiments on the resistance offered by helical pipes to fluids flowing through them. The results were represented on a diagram|| in which the ordinates were C , the ratio of the resistance of a curved pipe to that of a straight pipe of the same length and cross section. The abscissæ represented the non-dimensional number $\frac{dvp}{\mu} \left(\frac{d}{D}\right)^{\frac{1}{2}}$ which he calls Dean's criterion. In this expression, d is the diameter of cross section of the

* 'Phil. Mag.' vol. 5, p. 684 (1928).

† 'Roy. Soc. Proc.,' A, vol. 84, p. 114 (1910).

‡ *Loc. cit.*, p. 695.

§ 'Roy. Soc. Proc.,' A, vol. 123, p. 645 (1929).

|| 'Roy. Soc. Proc.,' A, vol. 123, p. 660 (1929).

pipe, D is the diameter of the helix into which it is wound, v is the mean velocity of flow, μ is the viscosity and ρ the density of the fluid. $dv\rho/\mu$ is the well-known Reynold's number. This curve is reproduced in fig. 1.

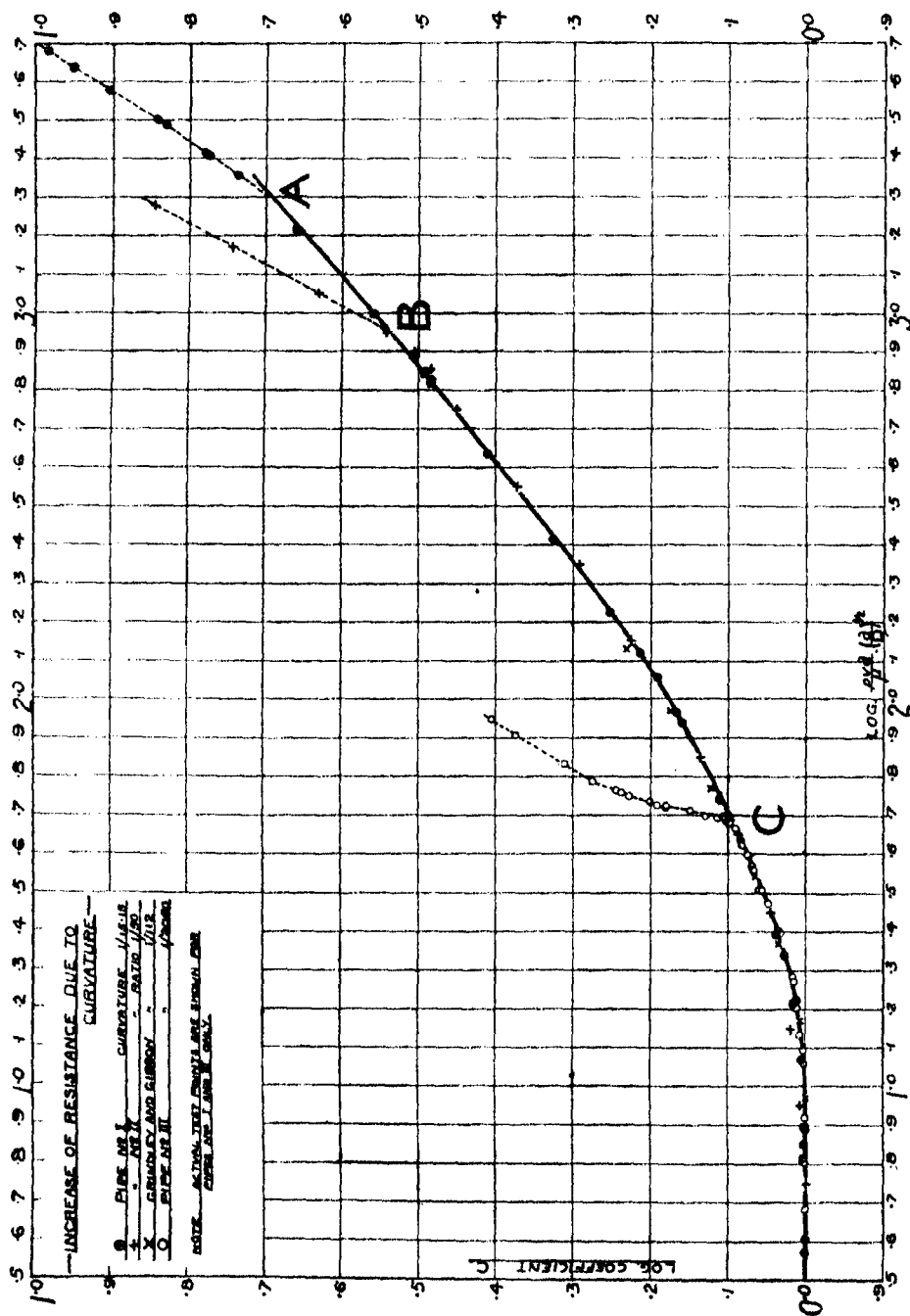


FIG. 1.—Fluid initially highly turbulent, but long stilling length interposed between entrance and gauging length.

Experiments were made with three pipes whose values of d/D were respectively $1/2050$, $1/50$ and $1/15 \cdot 15$. It was found that when the results of experiments covering a large range of speeds of flow were set on the diagram of fig. 1, the points obtained from all three pipes lay on the same curve at low speeds. When the velocity reached a certain value, however, the representative points suddenly left the curve and lay on a steeper one corresponding with a greater rate of increase in resistance with speed.

This is shown in the three dotted curves, corresponding with the three helices used, which branch off at the points A, B and C (fig. 1) from the curve common to all helical pipes. Mr. White inferred that these points mark the speeds at which the flow ceased to be steady and became turbulent. He pointed out that they correspond with speeds which are much higher than those at which turbulence persists in a straight pipe.

As has been mentioned this conclusion is opposed to views of previous workers on the subject. In these circumstances it seemed highly desirable to obtain some direct information by means of colour bands as to the state of turbulence or steadiness of flow in helical glass pipes.

Experiments of this type have already been carried out by Prof. Eustice* but they were not capable of detecting a rise in Reynolds' criterion due to curvature because the colour was led into the curved pipe at its entrance, *i.e.*, before Dean's circulation had had a chance of establishing itself. If the effect of curvature in the pipe had been to decrease the speed at which turbulence appears, then by adjusting the speed of flow Prof. Eustice might have expected to get stream-line flow in the entrance, or straight "leading in" portion of his pipe, followed by turbulence in the curved part. On the other hand, if Mr. White's interpretation of his experiments is correct, turbulence which had already appeared in the entrance or straight portion of the pipe, owing to the speed of flow exceeding Reynolds critical speed, might disappear in the curved part of the pipe. This disappearance could not have been detected in Prof. Eustice's experiments because his colour bands would have lost their identity in the initial turbulent part of the stream before reaching the part where the effect of curvature had made the flow steady.

For this reason I decided to repeat some of Prof. Eustice's experiments, using helical glass tubes and introducing the coloured band into the stream only after it had traversed at least one whole turn of the helix. In order that the flow might not be disturbed the colour band was introduced through a small hole bored through the glass.

* 'Roy Soc. Proc.,' A, vol. 85, p. 119 (1911).

Three glass tubes with uniform bore of about 6 mm. were chosen from a large stock. Two of these were bent into the form of helices with the coils spaced as closely as the glass blower could bend them. Small holes $\frac{1}{2}$ mm. in diameter were bored in them at a few points and a concentrated solution of fluorescein was allowed to flow slowly through them. Water was made to flow through the glass helices and the speed of flow was found by measuring the time taken to fill a 500 c.c. measuring glass.

Two helices were made with the following dimensions :—

Helix I. $d = 0.610$ cm., $D = 11.4$ cm., so that $D/d = 18.7$ and $(d/D)^{\frac{1}{4}} = 0.232$.

Helix II. $d = 0.568$ cm., $D = 18.1$ cm., $D/d = 31.9$, $(d/D)^{\frac{1}{4}} = 0.177$.

In each case the same phenomenon was observed. At low speeds the flow was steady. The circulation in the plane of the cross section indicated by Dean's theory was very clearly shown by the fluorescent band of fluid.

Dean's circulation is indicated in fig. 2, which shows a section of the pipe with the stream lines of the component of flow in the cross section. The helix is supposed to lie with its axis horizontal and fig. 2 is the upper section of one of the coils by a vertical axial plane. The flow is towards the axis of the helix near the wall of the tube and away from it in the centre. The hole for admitting the fluorescein was bored at the side of the section as shown in fig. 2. The

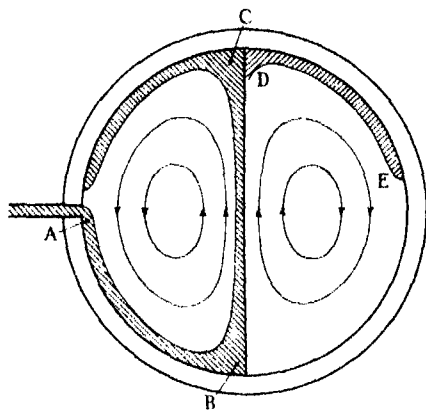


FIG. 2.—Circulation in the cross-section of a curved pipe.

course which the colour band would be expected to pursue in the plane of the cross section is shown as the shaded band ABC (fig. 2). It will be seen that the colour band first flows inwards along the wall till it reaches the innermost point B of the cross section. It then leaves the wall and moves across the middle of the section to the outermost point C. It then moves inwards again along the wall.

In my experiments the course pursued by the colour band was always identical with that just indicated

up to the point C. At this point most of the colour always followed the course indicated, and sometimes all of it did so; but sometimes some of the colour would pursue the course shown by the line DE

(fig. 2). This was no doubt due to imperfections in the uniformity of the helix. When the colour did not divide at C the way in which it kept to one half of the cross section was very striking. It was found that over a great part of the range of speeds used the band seemed to make one complete circuit of the semicircle ABC in about one half a turn of the helix.

As in Reynolds' experiments with a straight pipe, it was found that the flow was steady up to a certain speed. At this speed the colour band began to vibrate in an irregular manner, but it still seemed to retain its identity through at least one whole turn of the helix. This indicates that the unsteadiness was not at first of a type which gives rise to diffusion of momentum by eddies and hence to a rapid rise in resistance. In fig. 3, which shows graphically the results

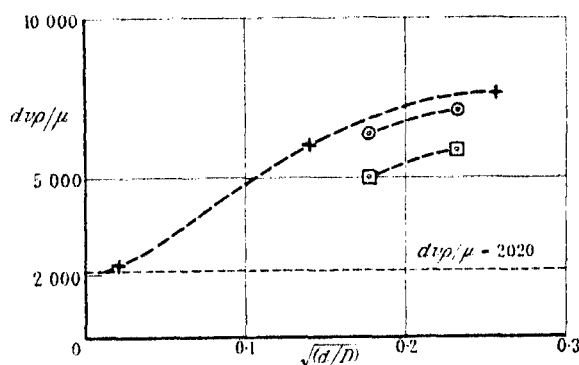


FIG. 3.

- + Speed at which White's curve indicates first appearance of turbulence.
- ⊙ Lowest speed at which flow appears completely turbulent in a helical glass tube.
- ◻ Highest speed at which flow is quite steady.

of these measurements, the point where this irregular vibration first made its appearance is indicated by a square, thus ◻.

On increasing the speed this irregular vibration increased in violence till, at a point which could be measured with some accuracy, the stream became completely turbulent so that the identity of the colour band was lost in a distance of a few millimetres from its source. The speeds at which the flow became completely turbulent in this sense are shown as circles, ⊙, in fig. 3.

Fig. 3 shows the results in a non-dimensional form, the ordinates being the Reynolds' number, dvp/μ , at which the turbulence appears. The abscissæ are $(d/D)^{1/2}$. The data from which the fig. 3 was constructed are given in Table I. In that table T_1 is the time taken by the water to fill a 500 c.c. measure when the flow first ceased to be truly steady. T_2 is the corresponding time

when the speed of flow was increased so that the water appeared completely turbulent. The temperature of the water was 11° C. throughout and its viscosity was taken as $\mu = 0.01277$.

Table I.

Glass Helix I. $(d/D)^{\frac{1}{2}} = 0.232$, $T_1 = 14$ seconds, $T_2 = 11\frac{1}{2}$ seconds.

Highest Reynolds number for which motion is steady is $dv\rho/\mu = 5830$.

Lowest Reynolds number for complete turbulence is $dv\rho/\mu = 7100$.

Glass Helix II. $(d/D)^{\frac{1}{2}} = 0.177$, $T_1 = 19$ seconds, $T_2 = 15$ seconds.

Highest Reynolds number for which motion is steady is $dv\rho/\mu = 5010$.

Lowest Reynolds number for complete turbulence is $dv\rho/\mu = 6350$.

Mr. White's Data.

Pipe No. I. $(d/D)^{\frac{1}{2}} = 0.257$. Reynolds number corresponding with point A, fig. 1, is $dv\rho/\mu = 7590$.

Pipe No. II. $(d/D)^{\frac{1}{2}} = 0.141$. Reynolds number corresponding with point B, fig. 1, is $dv\rho/\mu = 6020$.

Pipe No. III. $(d/D)^{\frac{1}{2}} = 0.0221$. Reynolds number corresponding with point C, fig. 1, is $dv\rho/\mu = 2270$.

Reynolds' criterion for a straight pipe is taken as $dv\rho/\mu = 2020$.

Comparison with Mr. White's Experiment.

At the bottom of Table I are given Mr. White's data taken from his curve (see fig. 1). The values of Reynolds number, corresponding with points A, B and C, on that curve are 7590, 6020 and 2270* respectively. These are shown as crosses, +, in fig. 3.

The value of Reynolds' criterion for a straight pipe, which is taken as 2020, is shown as a dotted line in fig. 3.

Inspection of fig. 3 shows that Mr. White's conclusion is amply verified in experiments with colour bands. The flow was completely turbulent on entering the helix. This was demonstrated by passing the water first through a straight glass tube containing a $\frac{1}{2}$ -mm. hole of the same type as that in the glass helix.

At approximately the speed indicated by Reynolds' criterion, $dv\rho/\mu = 2020$, the flow became turbulent in the straight pipe. It then entered the helix in this state but after passing through only one coil in the case of glass helix No. 1, or $2\frac{1}{2}$ † coils in the case of glass helix No. 2, it had become steady again.

* Mr. White gives slightly different figures in his paper, but the figures here given seem to me the more consistent with his curves.

† These happened to be the distances of the $\frac{1}{2}$ mm. holes from the ends of the helices.

This steadiness persisted up to a value $dv\rho/\mu = 5830$ in the case of helix No. 1, *i.e.*, up to 2.8 times the speed at which turbulence persists in a straight pipe. It will be noticed in fig. 3 that Mr. White's measurements correspond far more closely with the speed at which the flow first appears completely turbulent than with the speed at which it first begins to fluctuate. This might be expected because a fluctuation which does not cause the colour band to become diffused is not likely to cause any considerable increase in resistance.

This work was carried out in the Cavendish Laboratory through the kindness of Sir Ernest Rutherford, to whom the author wishes to express his thanks.

Analysis by X-ray Spectroscopy.

By C. E. EDDY, M.Sc., International Education Board Fellow, Prof. T. H. LABY, M.A., Sc.D., and A. H. TURNER, M.Sc., Research Physicist, University of Melbourne.

(Communicated by Sir Ernest Rutherford, P.R.S.—Received January 31, 1929.)

[PLATE 2.]

Summary.

The possibilities of chemical analysis by X-ray emission spectra have been tested. As compared with other methods of spectral analysis the K and L spectra have the advantages.

- (1) The number of lines in the spectra is small.
- (2) Moseley's law greatly simplifies the identification of a line.
- (3) Generally the four K or about six L lines are sufficient to identify an element; the known relative intensities of the lines are an additional aid to identification.
- (4) The fact that a minimum potential is required to excite a group of X-ray lines is a further aid to the identification, as the second or higher order lines can be excluded when necessary.

The technique of the construction of the X-ray tube and a spectrometer in order to eliminate lines of elements not in the sample under examination, and the identification of the spectral lines, is described.

In spite of these advantages, owing to lines in certain X-ray spectra obtained during the search for elements of atomic number 43, 61, 72, 75 and 85 being wrongly identified, suspicion has fallen on the method, which we believe is unjustified, as the errors referred to can be avoided.

The X-ray analysis method is found to be much more sensitive than was indicated by previous workers who showed that amounts of 0.1 per cent. could be detected; we find that the spectra of elements present to three parts in a million can be readily observed. The optical method is capable of detecting as little as one part in one hundred thousand. Suitable control experiments were made to prove that the lines observed were correctly identified and came from the alloy under investigation.

The X-ray spectra of seven samples of zinc and one of manganese have been examined. One zinc sample was spectroscopically pure; the others were alloys of composition known by analysis or by synthesis. No impurities were found in the zinc, which was pure by optical spectroscopy.

In comparison with analysis by optical spectroscopy, the X-ray method has the advantages:—

- (1) It is apparently more sensitive.
- (2) The sensitivity is independent of the element sought and of the elements with which it is mixed.
- (3) There is greater certainty in identifying the lines observed.

The optical method has the disadvantages:—

- (1) It is only quantitative for elements present up to about 0.5 to 1 per cent.
- (2) The number of raies ultimes tends to diminish as the element giving rise to them diminishes until sometimes three, two, one or no lines remain.
- (3) The raies ultimes generally are present in a spectrum crowded with lines—resolution and therefore identification is more difficult than for X-ray spectra.

The X-ray method has the disadvantages:—

- (1) Elements of low atomic weight require a vacuum spectrometer.
- (2) Excitation of the K spectra of the elements of high atomic number requires high potentials and highly evacuated X-ray tubes.
- (3) The technique at present is difficult and the equipment is elaborate and costly. We believe these difficulties can be very considerably diminished.

X-ray spectral analysis is valuable in searching for rare, including the recently discovered, elements, in the analysis of metals for which the physical

properties are considerably changed by small quantities of impurities, in the analysis of elements difficult to separate by chemical methods (*e.g.*, rare earths, platinum metals), and of materials such as those used for atomic weight determinations, where the highest purity is essential.

A partly completed investigation shows that the X-ray method is capable of giving results of a quantitative nature.

Introduction.

In principle, any spectrum can be used as a means of revealing the presence of an element, such as the K, L, and M high frequency, the arc, flame, spark and molecular emission spectra as well as the corresponding absorption spectra, since all these spectra are characteristic of the element or elements giving rise to them. In certain cases, chemical methods of analysis have been considerably supplemented by spectral methods, particularly (*a*) when elements of very similar chemical properties occur together, as in the case of the rare earths,* or of metals of the platinum group, and (*b*) when it is required to detect a very small proportion of certain elements in the presence of other elements, as, for example, traces of silver, copper, and iron in gold, of cadmium in zinc, and of bismuth in copper. In these cases, detection of the elements by chemical means is difficult.

Analysis by Optical Spectroscopy.—The work of Fraunhofer, and of Kirchhoff and Bunsen in 1859, in demonstrating that many elements when heated in a flame produced emission spectra, each of which was characteristic of the emitting element, gave rise to the hopes that the spectroscope could be used to a great extent in chemical analysis, but very little advance was made for many years. The main reason for the disuse of the spectroscope appears to have been the fact that, in some cases, it was extraordinarily sensitive (Roscoe showed that strong spectra could be obtained with as little as one three-millionth of a milligram of sodium), while on the other hand, particularly with elements of high melting point, the method was very insensitive. This lack of proportionality between the intensity of the spectra and the amount of an element present tended to prejudice the use of spectroscopic methods generally.

The revival of the spectrum analysis is mainly due to the work of Lockyer, Hartley, and his colleagues, and de Gramont. Lockyer† found that the lengths of some lines in arc or spark spectra were sensitive to the percentage of

* Crookes, 'Brit. Assoc. Rep.', p. 558 (1886).

† Lockyer, 'Phil. Trans.,' A, vol. 164, p. 479 (1874).

the element present, but many difficulties arise in an application of this property, however, as the lengths of the lines are dependent upon the length of arc or spark, the current strength, and other experimental conditions as well as on the amount of the element present. Hartley* found that, in the spark spectra of solutions, certain lines persisted even when the element occurred as a mere trace, and Pollok and Leonard† continued his work to show that good qualitative results could be obtained in certain cases, but the method was too restricted in application to be useful generally.

The methods introduced in 1895 by de Gramont,‡ who used the condensed spark method of obtaining spectra and found that certain lines disappear as the proportion of the element decreases, has, however, been much more successful. Since these sensitive lines, or *raies ultimes*, of de Gramont persist even when very small traces of an element are present, and their number increases definitely with increase in the percentage of an element, they have been of great use§ in detecting small quantities of an impurity and in giving reasonably reliable quantitative information as to the amount of it present.

Although analysis by spectroscopy utilising the *raies ultimes* has proved the most effective of the optical methods, having the practical advantages (1) only a comparatively simple apparatus is required; (2) visual observation of the spectrum is possible in some cases; (3) a photographic record is not difficult to obtain; (4) the operative technique is comparatively simple and rapid, there are, however, certain disadvantages which limit its application. The great complexity and the overlapping of the lines of the arc and spark spectra when several elements are present give rise to considerable difficulty in the interpretation of the lines observed. The application of the *raies ultimes* method is also limited to cases in which the element occurs in small proportions, and as it increases to more than a small percentage (possibly about 1 per cent.) the number of lines increases until the whole spectrum of the element is emitted. Further, the results obtained are only approximately quantitative, whereas many problems in the study of the physical properties

* Hartley, 'Phil. Trans.,' A, vol. 175, pp. 49, 325 (1884).

† Pollok and Leonard, 'Proc. Roy. Soc. Dub.,' vol. 11, pp. 217, 229, 257 (1908).

‡ De Gramont, 'Ann. Chem. Physique,' vol. 17, p. 437 (1909); 'Ann. Chem.,' vol. 3, p. 269 (1915); 'C. R.,' vol. 171, p. 1106 (1920).

§ Meggers, Kiess and Stimson, 'Sci. Pap. Bur. Stand.,' No. 444 (1922); Twyman, 'Two lectures on the development and present position of chemical analysis by emission spectra' (A. Hilger, Ltd., London, 1925); Twyman and Smith, 'Tech. Pub. Amer. Inst. Min. and Met. Engineers,' No. 79 (1928).

of metals require a very accurate knowledge of the amounts of impurities present !*

Analysis by X-ray Spectroscopy.—The use of X-ray spectra in detecting the presence of elements was responsible for the discovery of hafnium,† masurium,‡ rhenium,§ and illinium,|| elements which had not been detected by chemical methods. Urbain speaks of X-ray analysis as the most significant and crucial test of an element, and Rutherford of its sensitiveness and infallibility as a guide in fixing the atomic number of an element. The lines in certain X-ray spectra obtained during the search for elements of atomic number 43, 61, 72, 75 and 85, however, were wrongly identified, and this brought suspicion on the method which we believe is unfounded, as existing theory and technique enable such errors to be avoided.

X-ray spectral analysis has the great advantage that it uses a very simple spectra, the interpretation of which is greatly facilitated by the Moseley relationship; the simplicity of the spectra is illustrated in fig. 1, where a portion of the optical spectrum is shown for comparison. There are disadvantages, on the other hand, for a complicated and expensive apparatus is required, the technique is difficult, and results cannot be obtained with rapidity, but in the light of our experience we believed these difficulties could be very considerably diminished. It was thought advisable to investigate the possibilities of the method, and the results obtained in a systematic analysis of the impurities occurring in several samples of zinc are described in what follows.

In the X-ray method, the material to be investigated is placed on the target of an X-ray tube, and the radiations analysed with a crystal spectrometer. In order that the X-ray beam will contain only radiations from the target itself, special care is required in the tube design to ensure that secondary

* Vide Smithells, 'Impurities in Metals' (Chapman & Hall, London, 1928).

† Coster and Hevesy, 'Nature,' vol. 111, pp. 79, 182 (1923); Coster, 'Phil. Mag.' vol. 46, p. 956 (1923); Zaceks, 'Z. Physik,' vol. 15, p. 31 (1923); De Broglie and Carbrera, 'C. R.,' vol. 176, p. 433 (1923); Coster, 'Z. Electrochemie,' vol. 29, p. 334 (1923).

‡ Noddack and Tacke, 'Nature,' vol. 116, p. 54 (1925); 'Naturw.,' vol. 13, p. 567 (1925).

§ Pollard, 'C. R.,' vol. 183, p. 737 (1926); Berg, 'Phys. Z.,' vol. 28, p. 864 (1927); Noddack, 'Naturw.,' vol. 15, p. 333 (1927).

|| Lapp, Rogers and Hopkins, 'Phys. Rev.,' vol. 25, p. 106 (1925); Cork, James and Fogg, 'Proc. Nat. Acad. Sci.,' vol. 12, p. 696 (1926); Harris, Yntema and Hopkins, 'J. Amer. Chem. Soc.,' vol. 48, p. 1594 (1926); Meyer, Schumacher and Kotowski, 'Naturw.,' vol. 14, p. 771 (1926); Rolla and Fernandes, 'Z. anorg. Chem.,' vol. 160, p. 190 (1927); Herszfinkiel, 'C. R.,' vol. 184, p. 968 (1927); Brunetti, 'Accad. Lincei Atti,' vol. 4, p. 515 (1926).

radiations from other parts of the tube cannot enter the slit system, and for the same reason the slit jaws should be constructed of the material to be investigated. The characteristic X-ray spectra differ from those in the optical region in that the lines due to different elements are produced with widely different excitation voltages, and also in that all the lines in one series of an

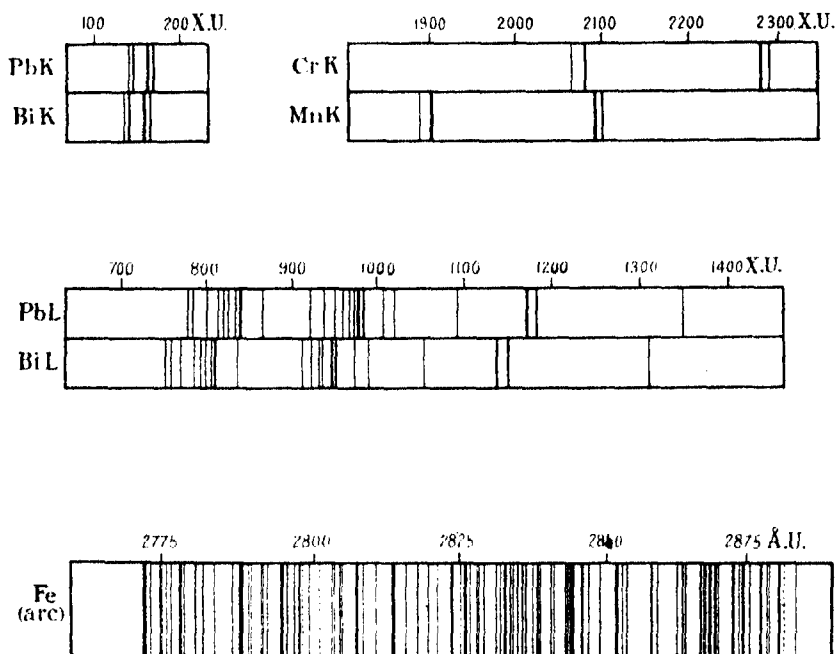


FIG. 1.—The spectra are shown as they would appear when photographed with the dispersion given by (A) an X-ray spectrometer, radius 10 cm., with calcite crystal; (B) a Rowland grating of 14,400 lines to the inch, with Eagle mounting at 3 metres.

element fall within a comparatively narrow range of wave-lengths. In fig. 2 are shown the variation with atomic number of excitation voltage, and of the wave-lengths of the principal lines, for the K and L series respectively. The dotted lines indicate approximately the region outside which certain practical difficulties arise; the short wave-length limit is set by the highest potential the tube will stand, as well as by the difficulty of working with very small reflection angles; the long wave-length limit is determined by absorption by the tube window, by the air in the spectrometer system, and by the film wrapping, any extension into the longer wave-lengths necessitating the use of a vacuum spectrometer.

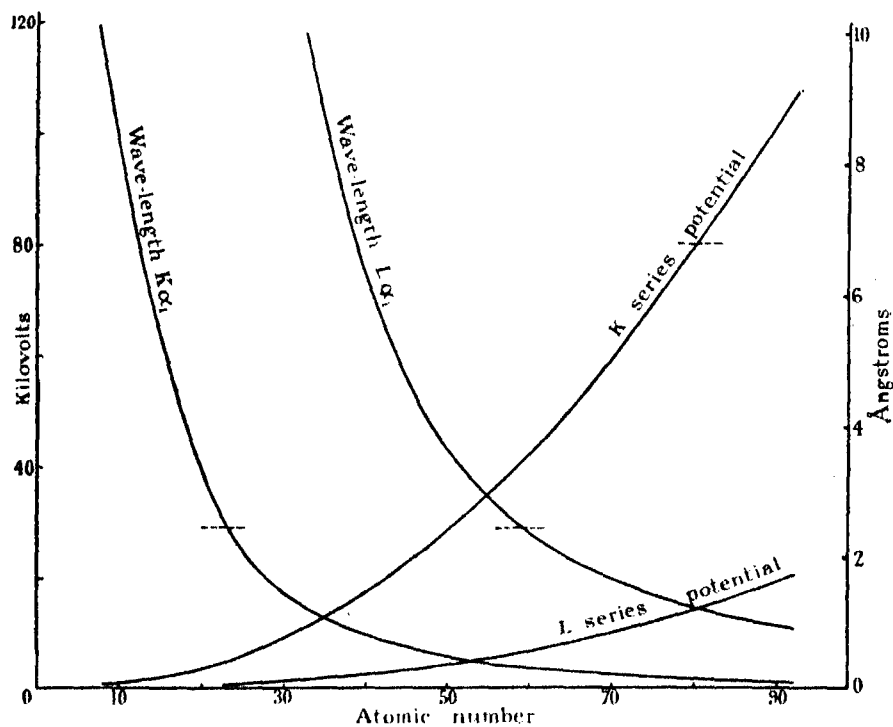


FIG. 2.

Experiment.

The X-ray Tube.—Two different tubes of the glass-metal type with hot cathodes and readily removable targets were used, the first being shown to scale in fig. 3. The anode and cathode portions were each insulated from the

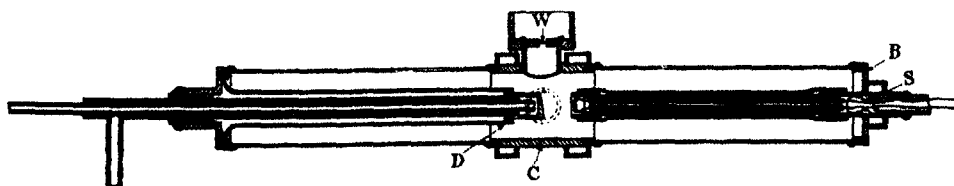


FIG. 3.

central portion C carrying the window W by means of pyrex tubes, the glass-metal joints being made with sealing wax. The window was supported between two slotted discs made of the same material as the target, and was waxed into C. The tungsten filament was supported by long leads passing through the lamp seal S waxed into the end plate B and was surrounded by an adjustable

focussing hood. The target was soldered at the back to the cooling tubes at D, and could be easily removed by breaking a wax joint. Both anode and cathode stems were enclosed in pyrex sheaths to prevent sputtering of the metal at high voltages. The metal portions were constructed of brass plated with specially pure silver to a thickness of 0.002 mm. Water jackets were provided for cooling all the wax joints. This tube was found to run satisfactorily with potentials up to 60 k.v. and currents up to 15 m.a. The window material at first used was very thin mica, but this was discarded later owing to the small amounts of iron which it contained, and one of cellophane of 0.02 mm. substituted; such a window was found to be satisfactory for tube potentials up to 35 k.v., but with potentials in excess of this the cellophane window rapidly punctured and aluminium foil 0.03 mm. thick was used.

The second tube is shown to scale in fig. 4. This tube was constructed

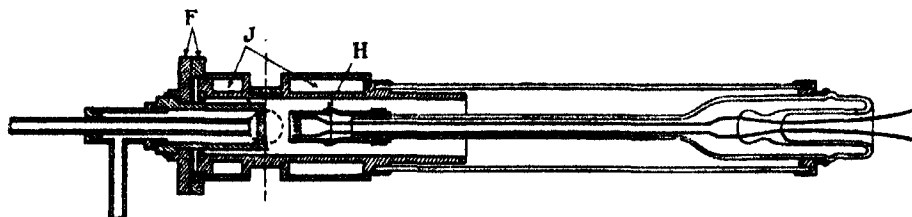


FIG. 4.

entirely of zinc with the exception of the outside brass water jackets JJ, the case hardened steel flanges F, and the hood and its supports H, which were made of pure silver. This tube was designed so that only the metal to be analysed was exposed to the discharge (except for the silver hood and the tungsten filament), thus eliminating any possibility of unknown contamination of the target face by sputtering. The zinc ingots used for the tube walls were cast in pyrex tubes *in vacuo* and proved quite gastight. No solder was used, all joints being made of wax. This tube ran satisfactorily with potentials of 40 k.v. and currents up to 10 m.a. In order that the times of exposure should be as short as possible, the windows used were the thinnest that would withstand the atmospheric pressure, and careful attention was paid to the focussing of the cathode rays to obtain a maximum intensity of X-rays through the slit system; to this end, a line focus parallel to the slit was adopted, and the target face inclined so that the rays utilised left it at nearly grazing angle. With these arrangements, a complete K spectrum of zinc could be obtained with an exposure of 150 m.a.-seconds.

Mr. B. S. Gosling, of the Research Laboratories of the General Electric

Company, Wembley, designed to suggestions made by one of the authors a demountable experimental X-ray tube for exciting the spectra of elements which require a high potential. This tube was of the metal-glass type, with joints of copper to glass, or of copper to copper by electroplating (*e.g.*, the window of copper foil was plated on to the main body of the tube). The tube was successfully tested at Wembley at 130 kilovolt A.C., and 140 kilovolt rectified. Unfortunately the tube was broken while being transported to Australia.

Preparation of Targets.—The targets were prepared in the following way. Ingots of a suitable size of the material to be analysed were cast in pyrex tubes *in vacuo*, and cooled rapidly, so that the crystals formed were small, it being probable that many of the impurities present would be confined in the inter-crystal spaces. The targets were then turned to size, and a further cut taken off the face and sides with a quartz tool, to remove any iron contamination; the use of very fine emery paper was impossible as this was shown to introduce iron, and a glass tool was unsatisfactory for similar reasons. The target was then thoroughly etched in pure dilute hydrochloric acid, washed (with rubbing to remove any metal which may have been deposited from the acid) in distilled water, dried, and inserted in the tube. A similar procedure was followed in preparing the zinc portions of the second tube.

For some of the preliminary work, zinc targets containing known amounts of copper were prepared; these elements were chosen because they form a solid solution. The copper was added to the zinc in the form of short pieces of fine wire, and the whole melted *in vacuo*, being kept molten for about 2 hours and thoroughly agitated at frequent intervals. On cooling, samples were taken from the top and bottom of the ingot, and colorimetric tests for the copper showed a homogeneous alloy had been obtained. Chemical analysis showed that the three alloys prepared contained respectively 1.12, 0.112, and 0.011 per cent. of copper. The other targets used were taken from various samples of zinc, and were prepared in the manner indicated above.

Pumping System.—The tube was pumped continuously during operation by a Gaede diffusion pump backed by a Hyvac, while a potassium trap to absorb mercury vapour was placed between the pumps and the tube.

Spectrometer.—The radiation was analysed photographically using a rotating crystal spectrometer. The wave-length range conveniently covered by the apparatus was from about 2300 X.U. to 450 X.U., *i.e.*, reflection angles from 23° to 4° for the calcite crystal used, the crystal being rocked uniformly over any required angle by means of a heart-shaped cam and a small electric motor.

Within this range occurred either the K or L series lines of all the elements from chromium (24) to uranium (92), with the exception of six elements from iodine (53) to cerium (58). Unless otherwise stated, the slit width was 0.1 mm., the resolving power of the spectrometer then being such that the $K\alpha$ lines were well separated for all elements.

Exposures and Development of Films.—To cover the whole range, several exposures were made, the crystal being rocked over a degree for each. The applied voltage was regulated to be at least twice that necessary to excite the lines sought, in order that intense characteristic radiation would be produced. So that very faint lines could be detected, exposures were made sufficiently long to clearly define the continuous background, and it was found that from 5 to 20 milliampere-hours were required per degree. It was found necessary to take out the target after about 8 hours' running to remove the thin film of tungsten which was deposited from the filament and which tended to absorb the softer rays and interfere with the attempts at quantitative analysis.

To enable faint lines to be detected, a suitable photographic emulsion and developer should be selected. The plate should have a high gamma (or contrast) value, and the time of development should be such as to give a maximum contrast. The developer should be one which keeps the grain size as small as possible, gives a minimum chemical fog, a large value for gamma, and for which the time of development is reasonably slow to allow for ease in timing. Kodak "Superspeed Duplitised" X-ray film was used with a rear intensifying screen, and was developed with a Wratten hydroquinone mixture at a temperature of 20° C. for 4 minutes. The wave-lengths of the lines were determined by a method previously described,* the K series lines of zinc being used as reference lines.

Results of Qualitative Experiments.

1. *The Sensitivity of the Method.*—It appeared desirable first to discover the sensitiveness of the method in detecting impurities present in known amounts, and for this the three alloys of copper and zinc previously mentioned were used in the tube first described. It was found that very strong lines appeared after quite short exposures, and it was quite evident that the lowest concentration (0.011 per cent. of copper) was well within the limits of the method. A sample of commercially pure zinc was then used, the chemical analysis of which (carried out by chemists with long experience in the analysis of zinc) revealed the presence of copper, iron, and lead in the amounts shown below.

* Eddy and Turner, 'Roy. Soc. Proc.,' A, vol. 111, p. 117 (1926).

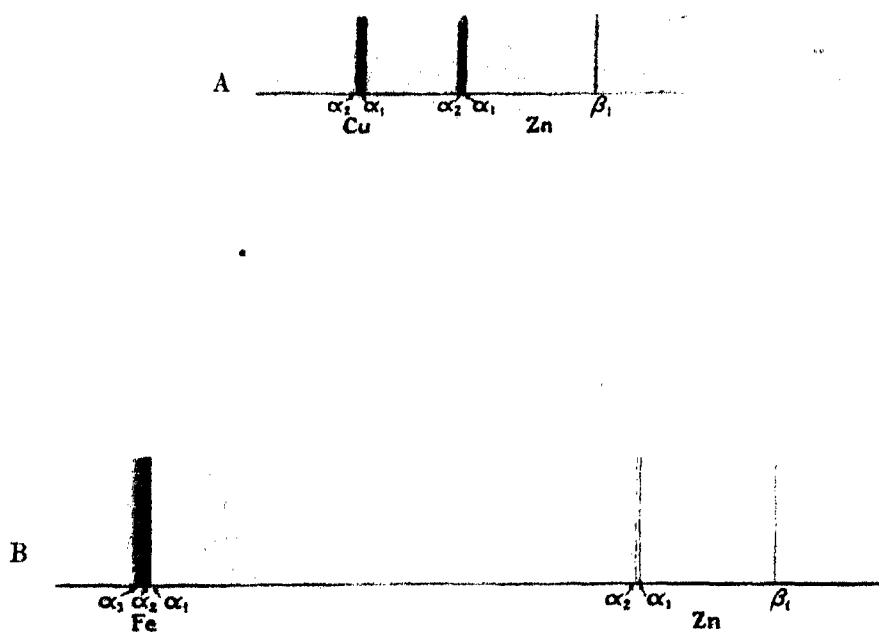


FIG. 5.—The zinc $K\alpha$ and β lines together with (A) copper $K\alpha$ lines due to 0·0007 per cent. ; (B) iron $K\alpha$ lines due to 0·0003 per cent. In the original the weak α_3 line of iron is clearly visible as well as the stronger α_1 , α_2 doublet.

A spectral analysis of this showed the $K\alpha$ doublets of copper and iron and the $L\alpha$ doublet of lead quite strongly defined upon the continuous background. Table I shows the exposures necessary to strongly register the lines stated. It will be noticed that smaller percentages require shorter exposures than would be expected from a comparison with those necessary for the larger percentages. This is due to the fact that, with short exposures, no continuous background is obtained, but with the longer exposures the continuous spectrum is registered on the film, and faint lines have a greater density through being superimposed upon it. On first consideration, it might be thought that the background of continuous radiation would diminish the contrast between the line and its background. A consideration, however, of the Hurter and Driffield curve of photographic density against the logarithm of the exposure appears to explain why the smaller percentages do not require correspondingly increased exposures. No continuous background is present for the larger percentages, and the density of the spectral line lies on the initial part of the curve, but with the smaller percentages the increased exposure produces a background of continuous radiation to the line, and the sum of their densities falls on the steep part of the curve, where a small increment in the intensity gives a larger increment in density than in the initial part of the curve.

It will also be noticed that larger exposures are required to register the L series lines of an impurity than the K series lines of another impurity, even although the wave-lengths concerned are practically the same.

Table I.

(The applied voltage was 25 k.v., and the tube current 10 m.a. in each case.)

Element.	Percentage present.	Series used.	Exposure time.
Copper	1.12	K	1 minute
"	0.112	K	3 minutes
"	0.011	K	5 "
"	0.0007	K	12 "
Iron	0.0003	K	15 "
Lead	0.0002	L	15 "

Control Experiments.—It is essential that there should have been no possibility of contamination of the target with these metals during its manufacture and that the lines recorded on the films were not due to secondary radiations from portions of the tube or slit system. Some suspicion was aroused from the fact

that the iron lines were stronger than was expected from the intensity of the lines due to the copper which was present in more than twice the amount. The targets had first been turned up with a steel tool and may have been contaminated with iron in this way. The substitution of another target which had been prepared with a quartz tool and etched as described previously did not result in any diminution in the intensity of the iron lines. As the mica window would contain some traces of iron, it was thought that this might be contributing some radiation. This was shown to be the case when a target of very pure silver was substituted, and iron lines were still found with a much reduced intensity, but no traces of copper or lead lines. With the substitution of a cellophane window, no iron lines were obtained with the silver target. Therefore the iron radiation from the window accounted to only a small extent for the lines recorded on the earlier films, and these were still obtained with the zinc target.

That the small amount of iron present in the mica window could give rise to easily recognisable lines is of special interest. Unfortunately, there was not sufficient of this mica available to permit of a chemical determination of its iron content. The largest amount which could have been present is the iron in 10 mm. by 0.1 mm. by 0.02 mm. (*i.e.*, the volume in front of the slit) of mica, of mass 6×10^{-5} gms. As the mica was a clear, transparent sample, its iron content was at most 5 per cent. each of Fe_2O_3 and FeO ,* giving the mass of iron producing the lines to be about 3×10^{-6} gms.

The iron lines could have been excited either as fluorescent radiation due to some absorption of the main X-ray beam—a very inefficient process—or by the direct action of a few cathode rays which struck the window. These possibilities were examined in the following way; a sheet of copper foil was placed in the path of the X-ray beam outside the aluminium window (which was sufficiently thick to absorb all the cathode rays), but very long exposures failed to produce any copper lines, the silver target being used; with the foil attached to the internal surface of the window, however, the lines were obtained quite strongly. This showed clearly that the radiations from the iron in the mica were due to cathode rays, and not to the absorption of X-rays. The failure to obtain the K absorption edge of copper in both positions of the foil was further evidence that there was no appreciable selective absorption of the X-rays by the window material which would give rise to secondary characteristic radiations. The mass of copper giving rise to these radiations, with a foil thickness of 0.00034 mm., was about 3×10^{-6} gm. Since the number

* See Dana, 'System of Mineralogy,' p. 618.

of cathode rays striking the window would be very small compared with those striking the target, it is evident that a smaller amount of an element than this in the focal spot will produce detectable spectral lines.

This suggested to one of the authors the possibility of using the window of a cathode ray tube as the source of X-rays for spectroscopic analysis. The material to be analysed could either be the actual window or be placed on the external surface of the window, thereby avoiding the necessity of evacuating the X-ray tube each time a sample is to be examined. Tests are being made to verify the apparent advantages of this method of exciting the emission spectra.

A test was made to discover whether secondary radiations from the tube walls could give rise to any lines. The interior of the tube was heavily silver-plated, so exposures were made for silver lines using a target of spectroscopically pure zinc, but no trace of them could be found, showing that the tube design was satisfactory in preventing X-rays from the tube walls gaining admission to the spectroscope.

In fig. 5A are shown the copper $K\alpha$ lines obtained from a target containing 0.0007 per cent. of that element, together with the $K\alpha$ and β lines of the main material, zinc; in fig. 5B, the iron $K\alpha$ lines corresponding to an amount of 0.0003 per cent. are similarly shown. The bands of continuous radiation are due to the very much longer exposures necessary for the impurities than for the zinc. It will be seen that an impurity present to only three parts in a million can readily be recognised by its X-ray spectrum, and an examination of the photographs will show that it is quite reasonable to expect that amounts of one in a million, and perhaps even less, can be detected. The X-ray spectral analysis method is therefore seen to be extremely sensitive.

2. *Spectral Analysis of a Sample of Commercial Electrolytic Zinc No. 1.*—The sample of zinc previously used, for which chemical analysis revealed as impurities only copper, iron, and lead, was then investigated to find whether evidences of other elements could be obtained spectroscopically. The crystal was rotated to reflect wave-lengths between the limits of 950 and 2000 X.U.; within this range would fall the K series of elements from manganese (25) to bromine (35), and the L series of elements from neodymium (60) to bismuth (83). The exposures were made sufficiently long to ensure that radiations from impurities present to one or two parts in a million would be recognised. Some lines belonging to the L series of tungsten (from the deposits on the target from the filament) and of mercury (from the diffusion pump) were identified. In addition to these, other lines were identified as belonging to the elements

given below. The observed values of the wave-lengths of these lines, and the elements to which they are attributed, as well as the accepted wave-lengths (shown in brackets) are given in Table II. As all these lines were fairly faint,

Table II.

Element.	K series.		
	α_2 .	α_1 .	β_1 .
Fe	1938 (1937)	1932 (1932)	1753 (1753)
Cu	1542 (1541)	1538 (1537)	1388 (1389)
Ge	1255 (1254)	1251 (1251)	1127 (1126)
Co	1791 (1790)	1784 (1785)	1616 (1616)
Ni	1658 (1659)	1655 (1655)	—
As	1178 (1177)	1173 (1173)	—

Element.	L series.		
	α_2 .	α_1 .	β_1 .
Pb	1183 (1183)	1173 (1172)	979 (980)
Bi	1153 (1153)	1142 (1141)	950 (949)

it was difficult to measure their distances from a reference line with a great degree of accuracy, and for this reason the wave-lengths have been given only to the nearest X.U. (10^{-11} cm.). It will be seen that the three elements known to be present by chemical analysis (iron, copper, and lead) are identified by the three strongest lines of either the K or L series. The relative intensities of the K series lines (α_2 , α_1 , β_1 , β_2) are approximately in the ratio 5 : 10 : 3·5 : 1·5 so that the β_2 lines cannot be expected in cases where the α lines are faint. In addition, good evidence was obtained for the presence of germanium and cobalt with three lines in the K series, and for bismuth with a similar number in the L series. Two lines only could be found belonging to nickel, but as these were very faint the β lines could not be expected. In the case of arsenic, there is really only the evidence of the α_2 line, as the $K\alpha_1$ line is coincident with the $L\alpha_1$ line of lead. No lines other than those enumerated above were found on the films.

By comparing the intensity of the lines of the elements undetected by chemical means with those from the copper, it appeared evident that the amounts of each present could scarcely be more than 0·0001 per cent., and might probably

be considerably less. Bismuth, germanium, and arsenic are frequent impurities in zinc ores, while there is good reason to expect the presence of cobalt and nickel in the sample examined. A careful chemical analysis of a similar sample of zinc showed that arsenic was present to less than 0.00001 per cent.

3. *Analysis of Sample of Commercial Electrolytic Zinc No. 2.*—The spectrum of this sample was investigated very carefully in the region from 2300 X.U. to 400 X.U. Within this range lie either the K or L series lines of all elements from chromium (24) to uranium (92) with the exception of five elements from caesium (55) to praseodymium (59). To permit of reasonable exposures, a slit width of 0.2 mm. was used; this produced a small broadening of the already faint lines, making it impossible to determine the wave-lengths very accurately, but the error so introduced did not cause any ambiguity in interpretation. Evidences of 17 elements out of the 64 in the above range were obtained. To prove that none of the lines were due to radiations from parts of the tube other than the target, the second tube described, constructed with the interior metal parts of the zinc under investigation, was used, and with one exception,* the presence of these elements was confirmed. Table III

Table III.

Element. (K series) λ_{a_2}	Values of Observed wave-length \sim true wave-length.				Intensity of a lines.
	a_2	a_1	β_1	β_2	
Cr 2289 X.U.	1 X.U.	1 X.U.	0 X.U.	3 X.U.	Moderate.
Mn 2102	2	0	2	4	Moderate.
Fe 1937	1	0	0	3	Strong.
Co 1790	1	1	2	2	Faint.
Cu 1541	0	0	2	3	Strong.
Zn 1436	Used as reference lines				Very strong.
Ga 1342	2	3	—	—	Very faint.
Ge 1255	0	0	2	1	Faint.
Sr 877	1	3	—	—	Very faint.
Mo 712	2	0	1	2	Faint.
Ag 563	1	2	2	2	Very faint.
Cd 538	0	0	2	1	Faint.
Sn 494	2	2	3	1	Faint.
Sb 474	2	1	2	—	Faint.

(L series)	l	a_2	a_1	η	β_1	β_2	β_3	β_4	β_5	β_6	γ_1	γ_2	γ_3	γ_4	γ_5	γ_6
W 1484	1	1	1	—	—	—	1	—	—	2	1	0	1	0	2	1
Hg 1250	—	2	2	—	1	0	—	—	—	—	1	—	—	2	—	—
Pb 1183	1	0	0	2	1	—	2	1	4	0	4	3	—	—	—	—
Bi 1153	0	0	1	0	4	—	5	—	—	—	—	—	—	—	—	—

* This exception was strontium; the first target gave two very faint strontium K lines which were not given by the second. In addition, the second target gave molybdenum lines, which we attribute to the association of this element with the tungsten in the filament.

contains the lines obtained from the two tubes ; for the sake of brevity the wave-lengths of the lines measured are not given, but the difference between the measured value and the true value of the wave-length as obtained from spectroscopic tables is shown for each line.

In most cases, an element is identified by its four K series lines, or by at least six of its L series lines and therefore the identification of the element is complete. The case of antimony, with three lines, and of gallium, with two, indicates a smaller percentage of these elements than of the others. The tungsten lines can be attributed to deposition from the filament, and the mercury to traces of vapour from the pump passing the potassium trap ; the silver may be due to sputtering from the hood and filament leads.

Some few ambiguities arose in the interpretation of the spectra in allotting certain lines to the correct element, but satisfactory identifications were possible. The bismuth line $L\beta_1$ (949 X.U.) would be very close to the second order antimony $K\alpha_2$ (948) and cadmium β_1 (948), but the presence of five other bismuth lines identified this element. It should be noted that since second order lines are much weaker than first order lines, and since the latter, for impurities present in small amount, are weak, the former will be very weak and should not be observed. When it is necessary to determine whether a line is a second order line or a first order line of double the wave-length, the question can be decided by taking an exposure with an applied potential lower than that necessary to excite the second order line. The $K\alpha_2$ line of tin (494) lies close to the silver $K\beta_1$ (496), and the tin $K\alpha_1$ (489) close to the reversed silver absorption edge at 485 ; the two tin β lines, however, were well defined in the photographs, and, since the absorption edge was a reversed one, the α_1 line could be readily distinguished from it. The antimony $K\alpha_2$ line coincided with cadmium $K\beta_1$ at 474, but the presence of three other cadmium lines and of two others of antimony identified both elements. It must be pointed out that no real difficulty arose from these ambiguities, and that all of the 85 lines recorded on the films were found to correspond well with the complete spectra of the elements concerned. From the intensities of the lines of the various impurities detected in this sample, it is probable that no element was present in an amount greater than 0.0005 per cent., and that many were in much smaller amounts than this.

4. *Analysis of Sample of Zinc in which Bismuth was found absent by Chemical Tests.*—Four spectra were observed with exposures sufficient to record one part in a million of bismuth ; other than tungsten and mercury lines, only two very faint lines corresponding in wave-length to the $L\alpha$ doublet of

bismuth were observed. These lines would be explained by the presence of less than 1 in 10^6 of bismuth.

5. *Analysis of a Sample of "Spectroscopically Pure" Zinc.*—This sample, prepared by fractional distillation,* was obtained from the New Jersey Zinc Co., and was used as a rigorous control test of the method. With the exception of zinc and of faint mercury and tungsten lines, no lines could be detected over the entire spectrum range permitted by the apparatus.

6. *Analysis of Manganese for Masurium and Rhenium.* This sample was the "mud" deposit from an electrolytic cell, in the form of a fine black powder. As rubbing the powder into the roughened copper anode proved unsatisfactory, a "glass" was prepared by fusing some of it with borax on to the surface of the copper. The $K\alpha$ doublet of manganese was obtained from this target, but owing to its low thermal conductivity the glass fused and disappeared from the focal spot. Prof. Hartung was good enough to reduce, by the thermit method, the manganese oxide (and presumably the oxides of masurium and rhenium, if present) to the metallic form. The resulting metal was remelted in a vacuum arc and the button resulting used as a target. The melting points of masurium and rhenium have been deduced by Swinne† to be about 2300° and 3300° C.; since manganese melts at about 1250° , we assumed (but with some doubt) that the former elements were not volatilised during the reduction and remelting processes. Five exposures for the L series of rhenium and the K series of masurium gave none of the lines of these elements. As the $L\alpha$ doublet of rhenium is close to the $K\alpha$ doublet of zinc, lead spectrometer slits and an iron window support were used for these photographs.

Comparison of Merits of X-ray and Optical Methods.

The previous work of Noddack, Tacke, and Berg‡ showed that X-ray spectra of impurities amounting to about 0.1 per cent. could be detected. The experiments described above show that the X-ray method is sensitive to amounts as small as 0.0001 per cent. Since Meggers, Kiess and Stimson have detected impurities down to 0.001 per cent. using the method of the raies ultimes, it is seen that the X-ray is more sensitive than the optical method.

A general comparison of the merits of the two methods becomes of importance. Our observations show that an element present in only 3 in 10^6 parts emits all the lines of both its K and L spectra, and these can be recorded photo-

* Singmaster, 'Metal Ind.,' vol. 31, p. 31 (1927).

† Swinne, 'Z. techn. Phys.,' vol. 6, p. 464 (1925).

‡ Noddack, Tacke and Berg., 'Preuss. Akad. Wiss. Berlin,' vol. 19, p. 399 (1925).

graphically if a sufficient exposure is given. It is sufficient for the identification of an element to record the α_2 , α_1 and β_1 lines of its K spectrum, or about five lines of its L spectrum. In the optical method (raies ultimes) the number of observable lines from an element tends to diminish as the proportion of an element diminishes, in fact the identification of an element may depend on observations on a couple of lines or even one line in a crowded spectrum. Table IV illustrates this statement.

Table IV.

Mixture of elements.	Percentage.	Number and intensity of sensitive lines.
Bi in Cu	0.005	1 faint line.
Ca in Mg	0.2 to 0.1	3 faint.
As in Cu	0.11	2 faint and 3 barely visible.*
	0.03	2 barely visible.
Pb in Zn	0.009	3 (1 of which is faint).
Fe in Zn	0.008	3 barely visible.
	0.003	1 barely visible.
Cd in Zn	0.75	6 lines.
	0.25	5 (1 just visible).
	0.10	4 faint.
	0.010	3 faint.
	0.001	1 very faint.

* This description of the intensity of the lines is that used by Twyman.

The above information has been obtained by Twyman and his co-workers in the investigation of mixtures in which the occurrence of the impurities mentioned is of technical importance.† (The presence of bismuth in copper to 0.005 per cent. makes the copper excessively brittle; calcium to assist the casting of magnesium is added to between 0.1 to 0.2 per cent., and in excess of the latter amount is objectionable; very small amounts of arsenic in copper greatly reduce the electrical conductivity of the copper.‡ Other examples of the large changes in mechanical and electrical properties, and in the power of a metal to resist corrosion, due to traces of metallic impurities, are discussed by Smithells.) In comparison with the above figures for the sensitivity of the optical method in detecting iron in zinc, it is to be remembered that 0.0003 per cent. of iron gave a quite strong and complete K spectrum with the X-ray method.

A further limit to the optical method arises when the "most persistent" line (i.e., that sensitive line which disappears last, and therefore which determines the lowest amount detectable) of one element coincides actually (or

† Twyman and Smith, *loc. cit.*, p. 17.

‡ Smithells, *loc. cit.*, p. 112.

nearly) with a sensitive line of another element ; in such a case, this line gives little definite information, and the lower limit of the optical method for a particular element is thus seen to depend on the other elements which may also be present. For example, the following pairs of persistent lines are of practically the same wave-length and therefore difficult to distinguish between :—

Ba	4554·2* A.U.	Cs	4555·4* A.U.
Mg	2852·1*	Na	2852·8
Li	6707·87*	Ca	6707·95.

The lines marked with an asterisk are the most persistent for the elements mentioned. In general, the resolution available in spectroscopic analysis would not be sufficient to enable the Li and Ca lines to be separated, and there might be difficulty with the others. This close proximity of sensitive lines is a serious disadvantage of the optical method. This limitation does not apply to the X-ray method, since the whole spectrum persists for small amounts, and there is no difficulty in distinguishing between the spectra of different elements.

Because of their great sensitivity, spectral analysis methods should have considerable applications, particularly in cases where chemical methods are handicapped. They can be used to give information as to the purity of precipitates in various stages of chemical analyses, and of materials for use in atomic weight determinations, as well as in the preparation of samples of pure elements. The application of the optical method has already met with considerable success, and the X-ray method has been shown to compare very favourably, both with regard to sensitivity and to the certainty of the results. For work wherein great accuracy is required (for which suitable apparatus and skilled workers would be available) the X-ray method would have greater opportunities than in factory routine.

Experiments have been carried out to determine the degree of accuracy with which quantitative analyses can be made by the X-ray method, and it is found that a fairly correct idea of the amount of an impurity present can be obtained. These results will shortly be published.

This investigation was undertaken in order to solve certain problems brought to our attention by Dr. Ian Wark, to whom we are indebted for the chemical analyses of the samples of zinc used. We are indebted to Mr. Gilbert Rigg for advice on the metallurgical questions which arose during the experiments, and for the spectroscopically pure zinc which he obtained for us from the New

Jersey Zinc Co. We are also grateful to Mr. B. S. Gosling for designing and testing, and to Mr. C. C. Patterson and the General Electric Company for constructing, an experimental X-ray tube. Part of the cost of the investigation was met by the gift of the Victorian Chamber of Manufactures to the University of Melbourne.

The Soft X-Ray Emission from Various Elements after Oxidation.

By L. P. DAVIES, King's College, London.

(Communicated by O. W. Richardson, F.R.S.—Received March 18, 1929.)

In 1927, Richardson and Robertson* published the results of some experiments on the soft X-ray efficiencies of 14 different elements. They found that there was no very great difference in the efficiencies, the highest, that of molybdenum, being roughly twice that of carbon, which was the lowest. The results show that in any group of the periodic table, the efficiency is high towards the middle of the group and lower at the end of it.

In the present experiments, the efficiencies of various elements after oxidation have been studied. The apparatus used was the same as that used before by the writer† for investigating the photoelectric properties of metals in the soft X-ray region. The last photoelectric plate to be tested was of cobalt, and as this was found to be as satisfactory as any of the others, it was left in the tube.

The following elements have been tested to find the effect of oxidation on the total soft X-ray emission: silicon, manganese, iron, cobalt, nickel, copper, molybdenum, palladium and tungsten. Four elements could be examined at once, and they were placed in a four-sided holder as described before. The elements were oxidised in the following way: The plates were placed in a quartz tube and this tube was suspended inside an electric furnace. The elements were raised to a temperature of 500°–600° C., and kept at that temperature for various times. The time of heating depended on how easily the element oxidised.

* 'Roy. Soc. Proc.,' A, vol. 115, p. 280 (1927).

† 'Roy. Soc. Proc.,' A, vol. 119, p. 543 (1928).

The first set of metals was iron, cobalt, nickel and copper. These targets had been used before (unoxidised) and had been bombarded to red heat for the purpose of degassing. The oxidised targets were carefully placed in the target-holder and the apparatus mounted up. The usual processes for ensuring a good vacuum were gone through. Before taking any readings the anticathode was gently bombarded with electrons from the inner filament under a potential difference of 600 volts. The bombarding current was only of the order of a milliampere so that some of the gas in the surface of the targets might be removed, without the reduction of the oxides.

After several sets of readings had been taken, the bombarding current was increased to the order of 1/10 ampere, the targets becoming red-hot. More readings were then taken.

The next group of metals used was iron, molybdenum, tungsten and platinum. The metals were first put into the apparatus unoxidised and were bombarded at red heat to free them from gas. Some readings were taken with the targets unoxidised ; and, as in the previous set of elements, the emission from the oxidised targets was studied before and after bombardment at red heat.

The last four elements to be investigated were silicon, manganese, palladium and gold. Targets of manganese and silicon are very difficult to cut and so the targets and target-holder used by Richardson and Robertson for their experiments on the soft X-ray emission from pure elements were very kindly lent. The only difference was that Richardson and Robertson's framework was six-sided, the sides being 2×1 cm., whereas the one previously used in these experiments was four-sided, each side being 2×1.4 cm. Six elements, silicon, chromium, manganese, palladium, platinum and gold, were fitted into the framework, but unfortunately after the apparatus was set up it was found that the anticathode could only be turned through about 280° , and thus it was not possible to use two of the faces, platinum and chromium. Owing to lack of time, the anticathode could not be adjusted and replaced so as to use these two targets. Readings before and after bombardment to red heat were taken, as before.

After all the observations had been made, the various sets of elements were removed and examined. They all still possessed the appearance of oxidation. The targets also showed signs of tungsten sputtering from the working filament.

Results.

Curves are drawn plotting the ratio i_p/i_t (photoelectric to thermionic current) against the atomic number of the element, at the voltages 600, 500, 400 and 300 volts. The solid angle of the effective beam of soft X-rays was exactly the same as in the previous experiment and had the value $0.03047 \times 0.743/4\pi$, so that readings of i_p must be multiplied by $4\pi/0.03047 \times 0.743$ to give their absolute value.

A typical set of curves obtained with unoxidised iron, cobalt, nickel and copper is shown in fig. 1. Fig. 2 shows the curves obtained when these metals

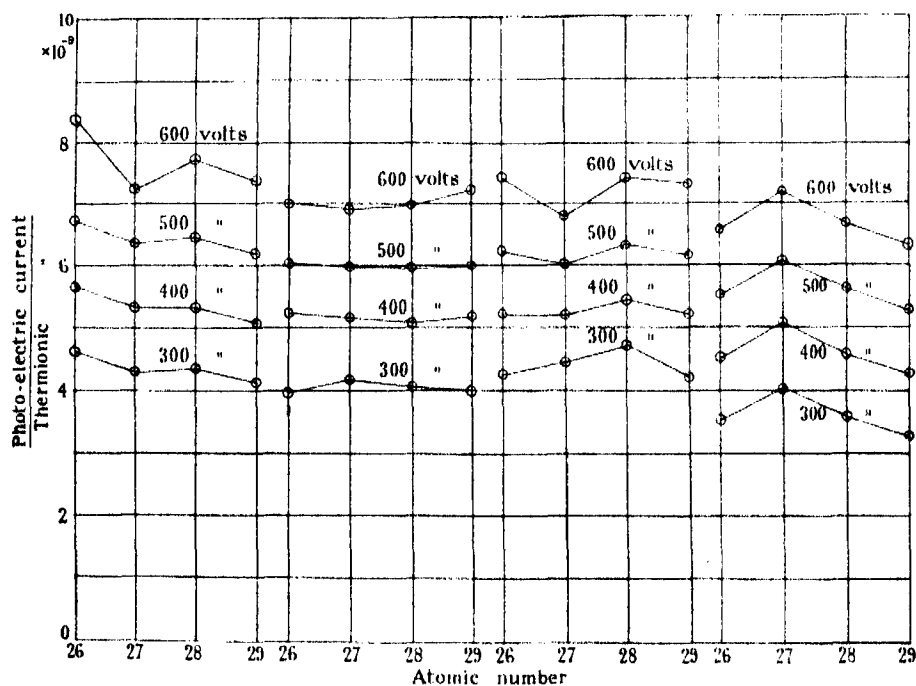


FIG. 1.

FIG. 2.

FIG. 3.

FIG. 4.

have been oxidised. After several sets of similar readings (*i.e.*, with the values of i_p/i_t for all the metals approximately the same) the curves suddenly reverted to a shape approximating to that obtained with clean metals, at the higher voltages. At 300 volts the value for iron is too low. These curves are shown in fig. 3. After bombardment at red heat the curves shown in fig. 4 were obtained. It will be noticed that i_p/i_t has increased for cobalt and decreased for the other three metals. After more bombardment at red heat and throughout several sets of results, this shape of curve still persisted.

After cleaning and re-oxidising the metals, further readings were taken. These gave curves similar to those of fig. 1. By an error, a somewhat larger thermionic current (from the loop filament) than before was used in the first degassing process.

The next set of metals is iron, tungsten, platinum and molybdenum. Some readings were taken with these metals unoxidised; the values agree very well

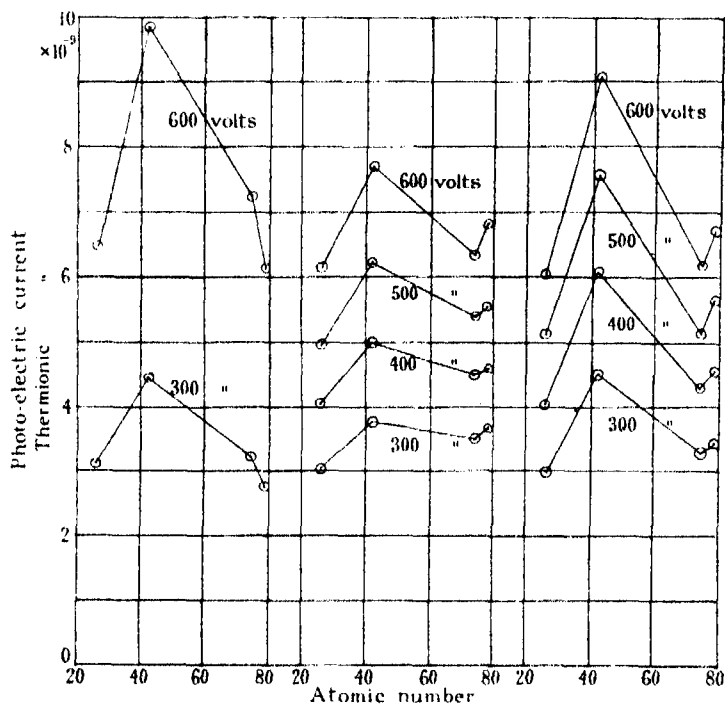


FIG. 5.

FIG. 6.

FIG. 7.

with those obtained by Richardson and Robertson. The curves are shown in fig. 5. The values for the oxidised metals are shown in fig. 6. Molybdenum, which previously had a value roughly 50 per cent. higher than the others, is now only 20 per cent. higher. The values for tungsten and iron are also lowered. After bombardment at red heat, the curves in fig. 7 were obtained. Molybdenum has returned to its high value, while tungsten and iron are still about 10 per cent. lower than platinum. The efficiency of platinum remains fairly steady, which is to be expected, as it is not oxidised.

The results obtained by Richardson and Robertson for unoxidised manganese, palladium, gold and silicon are shown in fig. 8. The curves for the oxidised elements are given in fig. 9. It will be seen that the value for silicon has fallen

slightly, the values for manganese, palladium and gold have all increased, manganese slightly and palladium and gold considerably. After bombard-

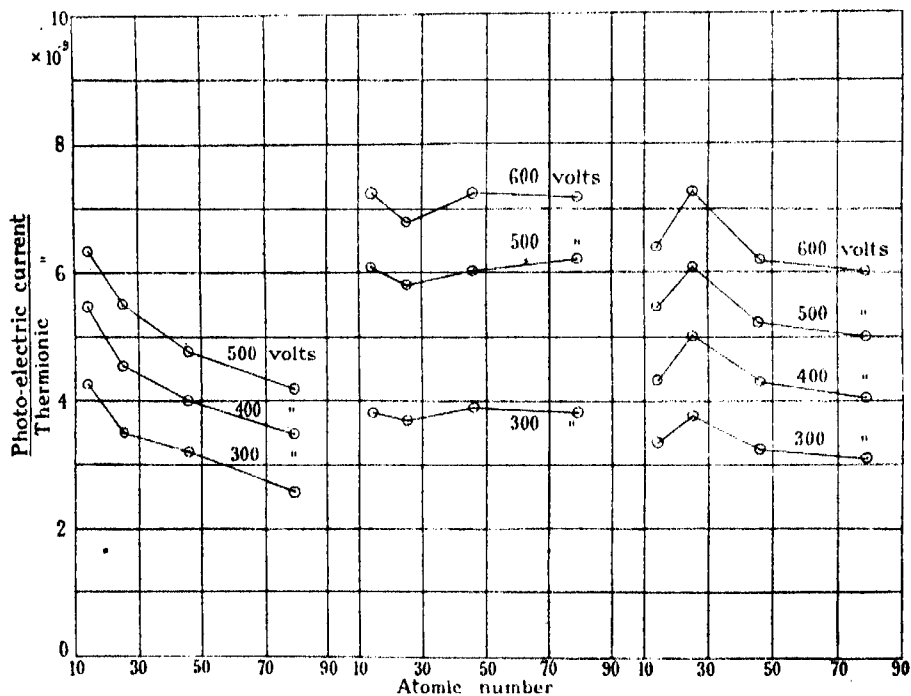


FIG. 8.

FIG. 9.

FIG. 10.

ment at red heat the results obtained are shown in fig. 10. Manganese has risen a little more, while silicon, palladium and gold have all decreased. After continued bombardment at red heat no change in these values was found. This last set of elements, owing to lack of time, was not investigated so thoroughly as the first two sets, and therefore too much stress should not be laid on the results.

TABULATION OF RESULTS.

Set I.—Iron, Cobalt, Nickel, Copper.

Effect of Oxidation.—The curves become nearly flat at first, later approximating to those of the unoxidised metals.

Effect of Bombardment to Red Heat.—The efficiency of cobalt rises to a high value. This may perhaps be explained by the fact that tungsten sputtering was found on the cobalt target.

Set II.—Molybdenum, Tungsten, Iron and Platinum.

Effect of Oxidation.—The molybdenum, tungsten and iron efficiencies are lowered, while platinum remains approximately constant.

Effect of Bombardment to Red Heat.—Molybdenum regains its high value but tungsten and iron are unchanged.

Set III.—Palladium, Gold, Silicon and Manganese.

Effect of Oxidation.—(1) Palladium: the efficiency has risen about 20 per cent. The oxidation of this target appeared to be very slight. (2) Manganese: the value is about 3 per cent. higher. (3) Silicon: this has a value about 4 per cent. higher.

Effect of Bombardment to Red Heat.—Manganese increases a little, while palladium and silicon decrease.

Gold appears to increase after being heated in air, decreasing again after being bombarded to red heat.

The outstanding feature of the results is the levelling up of the efficiencies of the elements after oxidation. This suggests that the oxygen atoms simply introduce a common factor into the emitting targets. If this is the case the efficiency of each anticathode will be the average efficiency of the oxygen and element present. On this basis, knowing i_p/i_t for the element and for its oxide, we may calculate what i_p/i_t would be for oxygen. For example, when molybdenum is heated in air, MoO_3 is obtained. Let i_p/i_t for the oxygen atom be x . That of unoxidised molybdenum at 600 volts is 9.91×10^{-9} , and of oxidised molybdenum is 7.62×10^{-9} . Then if the summation effect is the one obtained, we shall have

$$\frac{9.91 \times 10^{-9} + 3x}{4} = 7.62 \times 10^{-9},$$

i.e., $x = 6.99 \times 10^{-9}$, at 600 volts.

If this view is the correct one, the value of i_p/i_t for oxygen should be approximately the same when calculated from the data for the other oxides. That this is the case is seen from the following table. The oxide given is, as far as could be ascertained, the most probable one obtained when the element is heated in air.

Table I.

Element.	Oxide.	Value of i_p/i_t for oxygen.			
		600 volts.	500 volts.	400 volts.	300 volts.
Mo	MoO ₃	6.99	—	—	3.53
W	WO ₃	6.09	—	—	3.58
Co	Co ₃ O ₄	6.66	5.82	5.05	4.17
Fe	Fe ₃ O ₄	6.02	5.62	4.98	3.43
Ni	NiO	6.25	5.52	4.95	3.77
Cu	Cu ₂ O*	7.04	5.75	5.45	3.86
Mean value		6.51	5.68	5.09	3.72

* This is taken as the average of Cu₂O and CuO.

In comparing the values for oxidised and unoxidised silicon, manganese and palladium, the values given by Richardson and Robertson for the pure elements have been used. The value of i_p/i_t for platinum at 300 volts is given by Richardson and Robertson as 2.962×10^{-9} , and the value obtained by the writer is 3.29×10^{-9} . The difference between the two values is accounted for by the fact that the solid angle is not the same in the two tubes, and also by the fact that Richardson and Robertson used a nickel photoelectric detector. Taking the value of platinum as standard, the values of i_p/i_t at 300 volts for silicon, manganese and palladium can be calculated for the present apparatus. Similarly, the values can be calculated at 500 volts. When this has been done, i_p/i_t for oxygen can be deduced as before. The results of the calculation are given in Table II.

Table II.

Element.	Oxide.	Value of i_p/i_t for oxygen.			
		600 volts.	500 volts.	400 volts.	300 volts.
Mn	Mn ₂ O ₃ *	—	5.99	—	3.78
Pd	PdO	—	7.29	—	4.54
Si	SiO ₂	—	5.95	—	3.56
Mean value for Mn, Pd, Si		—	6.41	—	3.96

* This is taken as the average of MnO₂, Mn₂O₃ and Mn₃O₄.

The values agree fairly well with those of Table I.

The results given in the tables seem in accordance with the hypothesis that

the soft X-ray efficiency of an atom is not greatly changed when it enters into chemical combination.

To convert the values of i_p/i_t into absolute efficiencies it is necessary to multiply by $4\pi/0.03047 \times 0.743$, in order to allow for the solid angle.

The absolute efficiency of oxygen (from the mean values in Table I) therefore becomes at 600 volts, 3.61×10^{-6} , at 500 volts, 3.15×10^{-6} , at 400 volts, 2.82×10^{-6} , and at 300 volts, 2.06×10^{-6} .

In figs. 11, 12 and 13 the values of i_p/i_t for the oxidised elements, at 500, 400 and 300 volts respectively, are compared with the values given by Richardson and Robertson for the pure elements. i_p/i_t for the oxidised elements has been calculated for Richardson and Robertson's apparatus taking platinum as standard. The values for oxygen are also shown in these graphs.

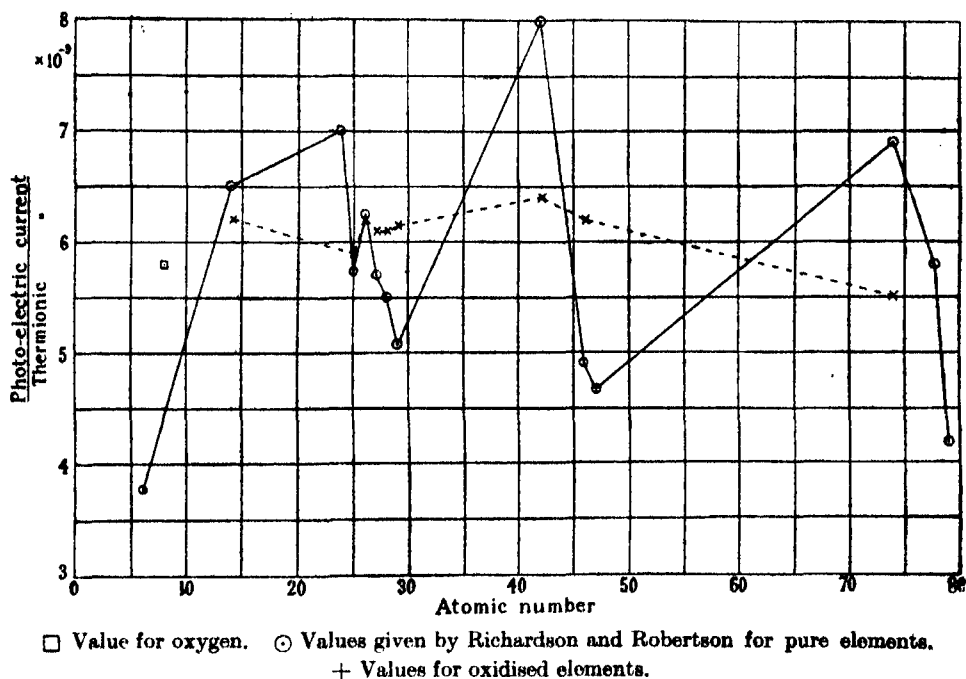


FIG. 11.

In order to compare the numbers at 300 volts with those given in Table I of Richardson and Robertson, the product $\alpha Ne/2\beta^*$ must be evaluated. This for oxygen is 5.26.

* For details, see L. P. Davies, *loc. cit.*, p. 550.

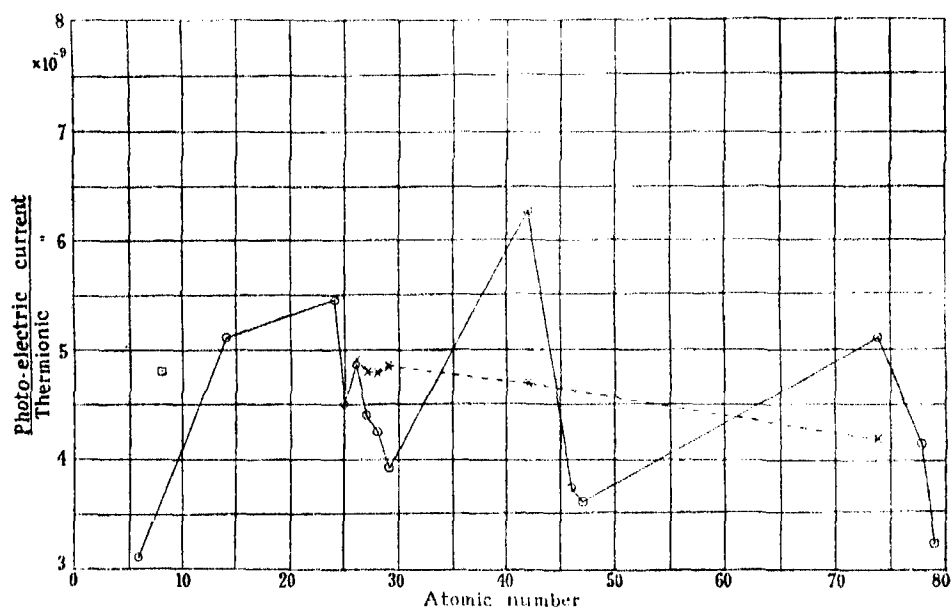


FIG. 12.

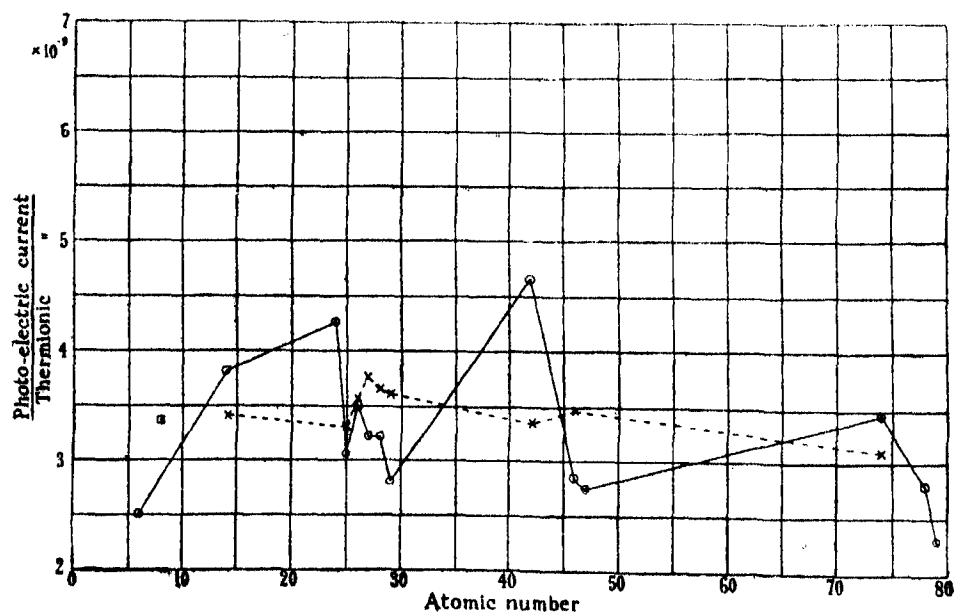


FIG. 13.

In conclusion, the writer would like to express her gratitude to Prof. Richardson for suggesting this problem and for interest and advice during the experiments.

Summary.

The effect of oxidation on the total soft X-ray emission from the following elements has been studied: Silicon, manganese, iron, cobalt, nickel, copper, molybdenum, palladium and tungsten. The efficiencies are levelled up after oxidation, and this suggests that the efficiency of the oxide is the average efficiency of the oxygen and element present. On this assumption, the efficiency for oxygen is calculated and its mean value is at 600 volts, 3.61×10^{-6} at 500 volts, 3.15×10^{-6} , at 400 volts, 2.82×10^{-6} , at 300 volts, 2.06×10^{-6} .

The Third Positive Carbon and Associated Bands.

By R. K. ASUNDI, B.A., M.Sc., Research Scholar of the University of Bombay,
King's College, London.

(Communicated by O. W. Richardson, F.R.S.—Received March 18, 1929.)

[PLATE 3.]

Introduction.

The band spectra associated with carbon are numerous and many of them were known to the earliest workers in spectroscopy.* They divided the bands into two main divisions, the positive and the negative bands. Thus they recognised the first positive carbon bands which are now called the Swan bands, the second positive bands which we now call the Ångström bands, the third positive and the fourth positive carbon bands. Among the negative bands known to them were the first negative or Deslandres' bands which are now known to be due to the ionised CO (CO^+) molecule. With the exception of the first positive bands or Swan bands, all the positive bands are now attributed to the neutral CO molecule. In recent years several new band systems have been added to the positive list,† and two, the comet-tail bands or low pressure

* Kayser, 'Handbuch der Spectroscopie,' vol. 5, pp. 226-234.

† Cameron, 'Phil. Mag.,' vol. 1, p. 405 (1926); Hopfield and Birge, 'Phys. Rev.,' vol. 29, p. 922 (1927); Asundi, 'Nature,' vol. 123, p. 47 (1929); Johnson and Asundi, 'Roy. Soc. Proc.,' A, vol. 123, p. 560 (1929); Herzberg, 'Z. Physik,' vol. 52, p. 825 (1929).

carbon bands,* and the Baldet-Johnson combination bands,† to the negative band systems. The history of the correlation of all these band systems is an interesting one and is adequate proof of the extraordinary usefulness of the quantum theory in the interpretation of molecular spectra. In this paper we are mainly concerned with the third positive carbon bands and such other bands as are usually associated with them.

These bands‡ were originally measured by Deslandres. Wolter could not obtain some of them which therefore were considered as spurious. Johnson and Birge gave the quantum interpretation of these bands, which fell into three n'' progressions, viz., $n' = 0, 1$ and 4 , the last two being spurious according to Wolter. Duffendack and Fox proved that the bands forming the $n' = 4$ progression belong to a new system of bands which they called 3A, with an initial electronic level higher than that of the third positive bands. All these bands have been obtained on all the plates taken in the first order of a 21-foot Rowland grating, by the present writer. The superficial structure of all the bands forming the same n'' progression is the same but differs from the structure of the rest of the bands. It is therefore suggested that the bands forming the $n'' = 1$ progression also arise from an initial electronic level different from that of the third positive bands. These may be called the 5B bands. It is scarcely necessary to say that all these band systems have the same final electronic level.

By the discovery due to Cameron (*loc. cit.*) in 1926 of some new bands in the ultra-violet, in a tube containing CO in high pressure neon, and their quantum interpretation by Johnson (*loc. cit.*), who showed that the initial and the final electronic levels of these bands were respectively identical with the final of the third positive and the final of the fourth positive carbon bands, the emitter of all these bands has been conclusively proved to be the CO molecule. Related to these bands has been discovered a new band system described later in this paper, which has the same final state as all these bands and an initial state which is identical with the new level at $\nu = 58927$, found by Hopfield and Birge (*loc. cit.*).

The final electronic level which is common to all these band-systems of the CO molecule is generally believed to be a 3P level. The Cameron bands are

* Pluvinet and Baldet, 'Astrophys. J.,' vol. 34, p. 89 (1911); Fowler, 'Monthly Notices, R.A.S.,' vol. 70, p. 484 (1910); Johnson, 'Roy. Soc. Proc.,' A, vol. 108, p. 343 (1925).

† Johnson, *loc. cit.*; Baldet, 'C. R.,' vol. 178, p. 1525 (1924).

‡ Deslandres, 'C. R.,' vol. 106, p. 842 (1888); Wolter, 'Z. Wiss. Phot.,' vol. 9, p. 361 (1911); Johnson, 'Nature,' vol. 117, p. 376 (1926); Birge, 'Phys. Rev.,' vol. 28, p. 1175 (1926); Duffendack and Fox, 'Nature,' vol. 118, p. 12 (1926).

five-headed and Johnson (*loc. cit.*) found that the electronic separations between successive heads are almost the same as the separations between corresponding heads of the third positive bands, if the second head of the latter bands is disregarded. This indicated that the level in question might be a quintet level. Birge (*loc. cit.*), however, took exception to this view. He believed that the level was a triple level; that the six heads of the third positive bands were due to three P and three Q branches; that in the Cameron bands the first Q head was missing; and that the equality of electronic separations indicated by Johnson was fortuitous. On Birge's assumption that the second, fourth and sixth heads of the third positive bands are Q heads, it is necessary that the electronic separation between the fourth and second heads should be the same for all bands of the third positive carbon and Cameron systems, as also the separation between the sixth and the fourth heads. These separations are tabulated below:—

Band.	Third positive.				Cameron.
	4-2.		6-4.		6-4.
	Wolter.	Asundi.	Wolter.	Asundi.	
0-0	43.7	42.5	48.4	48.5	—
0-1	40.2	39.7	49.2	48.3	—
0-2	37.8	37.6	47.1	46.8	—
0-3	34.2	34.8	46.6	45.9	48.1*
0-4	32.8	32.7	47.0	45.2	48.1*

* Mean value from five bands of the same sequence.

The table shows that whereas the difference 6-4 is fairly constant throughout all the bands, the maximum difference between two values being 3.3 v, the difference 4-2 is far from being constant, changing as it does by about 10 v. Moreover, the distance of each band head from its origin should ordinarily be roughly constant in all the bands of the same system. This will hardly be the case on this interpretation. Birge has entered into a detailed consideration of this point (*loc. cit.*) and concludes that this need not be taken as a serious objection since a similar discrepancy is said to be observed in the case of red CN bands by Mulliken. The fine structure analysis of the third positive bands given in this paper, however, points to the level being a quintet one, so that the five heads of the Cameron bands are all R heads, and the rough equality of the electronic separations observed by Johnson is what one would expect on this

view, if the distance of heads from origins is fairly constant. The following table gives the unweighted mean values from all bands, of the electronic separations between successive heads on this basis, and the mean value of the true electronic separations between successive origins of the quintet level, as determined from the analysis of the 0-0 and 0-1 third positive bands.

Heads.	Cameron.	Third positive.		True mean value from origins.
		Wolter.	Asundi.	
1-2	37.3*	29.6	30.6	29.5
2-3	18.9	20.0	20.0	19.9
3-4	18.0	19.9	18.8	20.8
4-5	29.2	27.7	28.4	29.8

* This value is likely to be much in error since the first two heads of these bands are very faint.

This table shows the rough equality of intervals in the Cameron and third positive bands. It also shows that the distance of each band head from its origin is roughly constant. As a matter of fact, if the second and third heads in the 0-0 and 0-1 bands, where, as the fine structure analysis also indicates, there is much crowding together of unresolved lines, are not taken into consideration, this distance is about 8.6 v, comparable with the value 7.7 v from Ångström* or the new bands† ($3^1S \rightarrow 2^1P$). In the third positive bands, therefore, only the second head is a Q head all the rest being P heads. It is just a matter of chance that this Q branch alone out of the five Q branches forms a head; for it is a surprising fact that in the spectra of the neutral CO molecule no other Q branch forms a head. The Ångström bands, the new $3^1S \rightarrow 2^1P$ bands, the fourth positive bands, all contain strong Q branches but in none of them do they form heads.

Production of the Bands.

The production of these bands is exceedingly simple. Any ordinary discharge tube containing CO or CO₂, when excited by an uncondensed discharge will show these bands. In these experiments a H type tube having a small capillary was used. It has carbon electrodes, a mirror on one end and a quartz window at the other. A small bulb containing magnesite was attached to the tube and this was gently heated to give the necessary CO₂ in the tube whenever required. The tube was arranged in an end-on position and the light was

* Huithen, 'Ann. Physik,' vol. 71, p. 41 (1923).

† Johnson and Asundi, *loc. cit.*

focussed by a quartz lens on to the slit of the instrument. The third positive and the associated bands were photographed in the first order of a 21-foot Rowland grating. This grating has a dispersion of 2.6 Å. per millimetre in the first order. Wolter has photographed the 0-1 band in the second order of a similar grating. On comparing the present measurements of this band taken in the first order, with those recorded by him, it was found that there is very good agreement among them and that no line measured by him up to about 35 Å. from the first head has been missed in these plates. Measurements were made on two independent plates and they agreed to 0.02 Å. The exposures necessary were about 7 hours for all except some 3 A bands. The temperature of the sub-basement room in which the grating is mounted in a suitable case, did not alter by more than 0.1° C. during the exposure. For comparison the international standards of the iron arc spectrum were used. The new bands previously mentioned lie in the near infra-red and the visible region. These were photographed on a glass c.d. instrument having a dispersion of about 150 Å. per millimetre in the region 7000-9000 $\lambda\lambda$, and of about 60 Å. between 5000-7000 $\lambda\lambda$. Neocyanine and kryptocyanine plates hypersensitised by ammonia before use were employed.

Third Positive Carbon Bands.

These bands extend from λ 2825 to λ 3493 and consist of only one n'' progression. The bands are apparently six-headed the overall multiplet width being 102.5 ν for the 0-0 band with a marked tendency to decrease with higher vibrational states, so that for the 0-4 band this value is 91 ν . The bands are very intense and apart from the complexity of structure due to the many heads, are just as simple to resolve as the Ångström bands. Wolter's observation that there is a repeated alternation of intensity in the structure of the bands is not exactly correct. A repeated rise and fall of intensity is no doubt observable in the reproduction of the 0-1 band given by Wolter. It is due to the fact that just where the structure lines of this band fade away, the 5 B band beginning at λ 2930 starts and the three or four heads of this band give an impression of such intensity distribution. The 5 B band at λ 2930 is comparatively weak but its heads are stronger than the fading structure lines of the third positive band. Such sort of repeated rise and fall of intensity due to proximity of complicated bands is more striking when one tries to photograph the new bands described in this paper on a high dispersion instrument like the grating used in these experiments. There is, however, one peculiarity associated with the third positive bands which does not seem to have been

observed by previous workers. These bands as is well known are degraded to the violet, but outside the first head there are a number of structure lines which decrease in spacing towards the higher wave-lengths forming ultimately a faint diffuse head, after which they continue further with gradual increase in spacing. These are very faint but they seem to accompany all the third positive bands. We cannot at present say whether they form part of these bands. No attempt has been made in the present paper to explain them. The fine structure analysis of only the 0-0 and 0-1 bands has been done, and therefore it has not been possible to give a vibrational equation representing the origins. The following equation is based on the values of the heads, ω_0 and $\omega_0 x$ being deduced from the mean values of the five intervals from band to band :—

$$\nu = \left. \begin{array}{r} 35287.0 \\ 323.4 \\ 341.4 \\ 359.2 \\ 389.5 \end{array} \right\} - (1726.5 n'' - 14.4 n''^2).$$

The following table gives the heads arranged according to vibrational analysis :—

$\begin{array}{c} n'' \\ \backslash \\ n' \end{array}$	0.		1.	
	λ (air).	ν (vac.).	λ (air).	ν (vac.).
0	2833.08 (7)	35287.0	2977.38 (7)	33576.8
	30.15 (10)	323.4	74.49 (10)	609.5
	28.73 (9)	341.4	72.86 (9)	628.1
	27.28 (8)	359.2	71.16 (5)	647.1
	24.86 (8)	389.5	68.57 (7)	676.5
	2.		3.	
0	3134.35 (7)	31895.3	3305.66 (7)	30242.5
	31.47 (10)	924.6	02.76 (8)	269.7
	29.51 (9)	944.6	00.51 (6)	289.7
	27.68 (5)	963.3	3298.43 (5)	308.7
	24.94 (5)	991.4	95.52 (5)	335.0
	4.			
0	3493.31 (5)	28618.0		
	90.44 (4)	641.6		
	87.73 (9)	663.8		
	85.36 (3)	683.2		
	82.23 (5)	709.0		

The figures in brackets indicate estimated intensity.

3 A Bands.

These bands are five-headed. But they are very faint and could be photographed only after long exposures. Moreover, the absorption of rays by air becomes pronounced in these bands so that the 0-0 band could only be photographed with an exposure of 30 hours on the grating. The fifth head is the strongest with estimated intensity 5 and the first head has an intensity 2. Therefore under low dispersion they appear to be double-headed.* The electronic separation between the two extreme heads is 70 ν for the 0-0 band with a tendency, as in the third positive bands, to decrease with higher vibration states, the 0-4 band having a value 65 ν . The quantum analysis of the gross structure of these bands is tabulated below :—

$n'' \searrow n'$	0.		1.	
	λ (air).	ν (vac.).	λ (air).	ν (vac.).
0	2295.9 (0)	43542.5	2389.75 (2)	41832.6
	—	—	88.95 (1)	846.7
	—	—	88.51 (1)	854.3
	—	—	86.95 (2)	881.7
	2292.22 (3)	43612.4	85.89 (5)	900.3
		2.	3.	
0	2489.94 (2)	40149.6	2596.93 (2)	38495.5
	89.07 (0)	163.7	95.94 (1)	510.2
	88.69 (0)	169.7	—	—
	87.11 (1)	195.1	93.84 (0)	541.4
	85.81 (5)	216.2	92.56 (5)	560.4
		4.		
0	2711.40 (2)	36871.0		
	10.25 (2)	886.0		
	—	—		
	2708.09 (0)	36915.0		
	06.59 (5)	935.9		

The equation representing the heads is :—

$$\nu = \left. \begin{array}{l} 43542.5 \\ \text{---} \\ \text{---} \\ \text{---} \\ 43612.4 \end{array} \right\} - (1726.5 n'' - 14.4 n''^2).$$

* Duffendaek and Fox, 'Astrophys. Journ.', vol. 65, p. 220 (1927).

The final state is thus identical with that of the third positive bands. The overall electronic separation for the 0-0 band is 69.9 ν , while the corresponding separation in the third positive band is 102.5 ν . There is thus a shrinkage of 32.6 ν , which can be explained on the assumption that the transition involved is $^5P \rightarrow ^5P$. On this basis the overall $\Delta\nu$ for the higher 5P level will be 32.6. Just as in the case of $^2P \rightarrow ^2P$ or $^3P \rightarrow ^3P$ transitions the Hund selection rule $\Delta\sigma s = 0$ is obeyed here also, as a result of which there are only five heads.

5 B Bands.

These bands also degrade towards the violet and are more intense than the 3 A bands. They are also undoubtedly five-headed but in each of the bands one or other of the heads is missing, probably being confused with other lines and therefore not prominently observed. Outside the third head, which is the first observed of the 0-0 band, there is a double-headed band, probably due to CO_2 , degraded towards the red and it is likely that the first two heads of the 5 B band are masked by the structure work of this extraneous band. The following table gives the vibrational analysis of these bands:—

$\begin{smallmatrix} n'' \\ \backslash \\ n \end{smallmatrix}$	0.		1.	
	λ (air).	ν (vac.).	λ (air).	ν (vac.).
0	—	—	2793.07 (6)	35792.9
	2661.87 (8)	37556.4	2789.11 (6)	843.3
	60.42 (8)	577.0	87.37 (8)	865.5
	58.80 (6)	599.8	85.80 (6)	885.8
2			3.	
0	2930.76 (3)	34110.9	3079.90 (8)	32459.2
	29.25 (3)	128.5	78.40 (2)	475.0
	—	—	75.73 (4)	503.2
	24.86 (2)	179.7	73.49 (6)	526.9
4.			5.	
0	3242.14 (8)	30835.0	3419.17 (6)	29238.5
	40.69 (6)	848.8	17.49 (6)	252.9
	37.74 (6)	876.9	14.65 (4)	277.2
	35.18 (8)	901.3	11.52 (3)	304.1

Figures in brackets indicate estimated intensity.

The following equation represents the heads satisfactorily :—

$$\nu = \begin{array}{r} \text{---} \\ \text{---} \\ 37556.4 \\ 577.0 \\ 599.8 \end{array} \left. \vphantom{\begin{array}{r} \text{---} \\ \text{---} \\ 37556.4 \\ 577.0 \\ 599.8 \end{array}} \right\} - (1726.5 n'' - 14.4 n''^2).$$

The electronic separation between the first and fourth heads is about 67ν very nearly the same as in the third positive bands (68.3). The final state is the same as that of these latter bands. It seems likely from this equality of electronic separation that the upper level is either a D or S level. Of course it may be argued that these bands really constitute the $n' = 1$ progression of the third positive bands. But though their fine structure analysis has not been attempted by the writer, still he is inclined to the view that because their superficial structure is different from that of the third positive bands, they form a new system by themselves.

New Bands.

A number of bands degraded towards the red have been photographed under small dispersion, and their wave-lengths determined by the measurement of three independent plates. These bands are of a complex structure probably having five heads; but under the low dispersion used it has been possible to measure only the two extreme heads with any certainty. Some of these bands could be identified with the triplet carbon bands of Merton and Johnson.* It was therefore thought that the rest of the bands also belonged to the triplet system. But they could not be arranged on that basis. The intensity of the triplet bands as produced here is very weak as compared to their intensity when produced in helium or argon. The triplet band at $\lambda 6464.6$ which has an intensity 10 in helium, has an intensity of only 2 as produced here. Other triplet bands were so mixed up with the rest of the bands that it has not been possible to effect a complete separation of the bands of the two systems below $\lambda 5700$. The bands of wave-lengths higher than $\lambda 5700$ have been separated and it has been possible to give the following vibrational analysis, assuming the band at $\lambda 8592$ to be the 1-0 band.

* 'Roy. Soc. Proc.,' A, vol. 103, p. 383 (1923).

n'' n'	0.		1.		2.		3.	
	λ (air).	ν (vac.).	λ (air).	ν (vac.).	λ (air).	ν (vac.).	λ (air).	ν (vac.).
1	8592	11636						
2	7833.9 88.0	12761.8 674.0						
3	7210.4 57.0	13864.5 776.0	8222.5 81.0	12158.5 072.5				
4	6685.7 6726.3	14953.2 862.9	7552.5 98.0	13237.0 157.7				
5	6244.0 75.0	16011.0 15931.8	6990.2 ---	14301.8 ---				
6	5861.0 89.0	17057.2 16976.1	6513.5 51.0	15348.5 260.6	7314.0 59.0	13668.4 13585.1		
7			6105.2 ---	16375.0 ---	6804.0 41.5	14693.2 612.7		
8			5749.1 75.9	17389.2 17308.5	6366.9 ---	15702.0 ---	7116.5 ---	14048.0 ---

The equation representing these band heads is :—

$$\nu = 10491 + (1154.4 n' - 9.5 n'^2) - (1721.5 n'' - 13.7 n''^2).$$

Hopfield and Birge (*loc. cit.*) have discovered a new level at 58927 ν , for the CO molecule. Assuming a transition to exist between this as the initial level and the final level (48438 ν) of the third positive carbon bands as the final level it will give rise to bands whose heads can be represented by

$$\nu = 10489 + (1155 n' - 9 n'^2) - (1726.5 n'' - 14.4 n''^2).$$

The equation representing the new bands is very close to this. There is a possibility of considerable error in the measurement of the bands of higher wave-lengths because the dispersion of the instrument falls rapidly in that region. Therefore the discrepancy between the two equations may be taken to be within the limits of experimental error. Experiments are in progress using instruments of higher dispersion and a detailed account of this band system must therefore be reserved for a future communication.

Fine Structure of the Third Positive Carbon Bands at $\lambda\lambda$ 2833 and 2977.

The structure of these bands is very complicated there being no obvious

regularity such as we find in less complicated bands. This arises from the fact that each band consists of five P, five Q and five R branches. At first sight it seemed almost a hopeless task to analyse the bands from plates taken in the first order of the grating, but subsequent measurements of the plates showed that in the case of the band at λ 2977, even the second order measurements recorded by Wolter in no way simplify the task. This indicated that the complexity of structure may not be avoided even if the third order of the grating was used. This, coupled with the fact that no line recorded by Wolter was missed in the λ 2977 band, on the first order plates, led me to attempt an analysis of the bands on the data of the first order plates. Measurements were taken on two independent plates and they agreed to 0.02 Å. This introduces an error of 0.2 to 0.3 cm^{-1} in the absolute measurements.

Each band consists of five sub-bands. The first high frequency band will be called the 5P_1 band, the second 5P_2 band and so on. Each of these consists of a P, a Q and R branch, the intensity distribution being $Q > P > R$, thus indicating that the transition involved is an $S \rightarrow P$.* On account of the complexity of structure and the crowding together of lines in all except the 5P_3 bands, it is not possible to say with certainty how many lines are missing in each sub-band. Therefore an evaluation of σ on this basis is out of the question and consequently the theoretical significance which arises out of a knowledge of the values of σ accompanying a transition, is unfortunately not forthcoming.

Table I gives the wave-number data of all the 15 branches and the initial term differences in each of the two bands analysed. The initial term differences should be the same for the same sub-band in the two bands analysed, though theoretically they may differ in values from the initial term differences for the other sub-bands. But this change in the value of the term differences both in the initial and final states is so small for the different sub-bands, that we have assumed it to be negligible. So that in Table II are collected the initial term differences for all the 10 sub-bands and their weighted mean. Table III similarly gives the final term differences and their weighted means for the two bands.

* Mulliken, 'Phys. Rev.', vol. 29, p. 410 (1927).

Table I.

Note.—The letter D before a line indicates that the line is a close double, *d* a diffused line, and *b* a blend with another line.

Band at λ 2833.					
j'' .	P.		Q.		R.
³ P ₆ .					
1.5	35295.6	2.8	35298.4 <i>d</i>	—	—
2.5	292.9	7.6	300.5	12.3	35312.8
3.5	290.9	11.9	302.8	16.6	319.4
4.5	289.3	15.8	305.1 <i>d</i>	21.0	326.1
5.5	287.8	20.9	308.7	24.6	333.3
6.5	287.0 <i>d</i>	25.8	312.8	30.1	342.9D
7.5	287.0	30.1	317.1	34.3	351.4 <i>b</i>
8.5	287.0	34.5	321.5	38.8	360.3 <i>b</i>
9.5	287.8	39.0	326.8	43.8	370.6 <i>d</i>
10.5	289.3	44.0	333.3D	—	—
11.5	290.9	47.1	338.0	52.2	390.2 <i>b</i>
12.5	292.9	52.4	345.3	56.5	401.8D
13.5	295.6	57.0	352.6	60.5	413.1
³ P ₄ .					
1.5	35325.3	3.2	35328.5	7.8	35336.3
2.5	324.2	6.8	331.0	13.1	344.1D
3.5	323.4	—	—	—	—
4.5	323.4	16.8	340.2	20.1	360.3 <i>b</i>
5.5	323.4	20.7	344.1 <i>b</i>	26.5	370.6 <i>d</i>
6.5	323.4	25.4	348.8	30.3	379.1D
7.5	324.2	29.6	353.8 <i>b</i>	—	—
8.5	325.3	33.9	359.2 <i>b</i>	38.9	398.1 <i>b</i>
9.5	326.8	38.4	365.2D	—	—
³ P ₂ .					
2.5	35342.9D	6.9	35349.8	—	—
3.5	341.4	12.4	353.8 <i>b</i>	16.8	35370.6 <i>d</i>
4.5	341.4	16.3	357.7	21.4	379.1D
5.5	343.7	21.5	365.2D	26.0	391.2 <i>b</i>
6.5	344.1D	26.5	370.6 <i>d</i>	30.5	401.1
7.5	346.5	29.7	376.2	34.4	410.6D
8.5	348.8	35.2	384.0 <i>b</i>	39.0	423.0
9.5	351.4 <i>b</i>	39.8	391.2 <i>b</i>	—	—
10.5	354.4	43.7	398.1 <i>b</i>	—	—

Table I—(continued).

Band at λ 2833.					
j'' .	P.		Q.		R.
	5P_1 .				
6.5	35359.2b	24.8	35384.0b	30.9	35414.9b
7.5	360.3b	29.9	390.2b	34.9	425.1D
8.5	361.8	35.1	396.9	38.8	435.7b
9.5	—	—	—	—	—
10.5	365.2D	—	—	—	—
11.5	367.5	48.8	416.3	51.6	467.9
12.5	370.6d	—	—	—	480.6
13.5	374.4	57.1	431.5b	61.5	493.0
	5P_1 .				
4.5	35391.2b	16.1	35407.3	20.2	35427.5
5.5	390.2b	20.4	410.6	25.1	435.7b
6.5	389.5	25.4	414.9b	—	—
7.5	389.5	29.9	419.4	34.9	454.3
8.5	391.2	33.9	425.1D	38.9	464.0
9.5	392.7	38.8	431.5b	43.7	475.2
10.5	394.9	43.6	438.5	—	—
11.5	398.1b	47.9	446.0	52.9	498.9
12.5	401.8D	52.6	454.4	—	—
13.5	406.3	56.4	462.7	—	—
14.5	410.6D	61.3	471.9	—	—
	Band at λ 2977.				
j'' .	P.		Q.		R.
	5P_1 .				
1.5	33585.3	3.0	33588.3	—	33602.4
2.5	582.7	7.7	590.4	12.0	609.5b
3.5	580.6	11.9	592.5	17.0	616.6b
4.5	578.9	16.2	595.1	21.5	624.1b
5.5	577.6	20.9	598.5	25.6	632.7D
6.5	576.8	25.6	602.4	30.3	641.3b
7.5	—	—	606.5	34.8	—
8.5	576.8	34.5	611.3b	—	—
9.5	577.6	39.0	616.6b	43.8	660.4b
10.5	578.9	43.5	622.4D	48.0	670.4b
11.5	580.6	47.5	628.1	—	—
12.5	582.7	52.2	634.9D	57.2	692.1
13.5	585.3	56.8	642.1	—	—

Table I—(continued).

Band at λ 2977.					
j'' .	P.		Q.		R.
	³ P ₄ .				
1.5	—	—	33616.6 <i>b</i>	7.5	33624.1 <i>b</i>
2.5	33611.3	8.0	619.3	—	—
3.5	610.5	11.9	622.4D	16.0	638.4D
4.5	609.5 <i>b</i>	16.4	625.9	20.8	646.7
5.5	609.5	20.4	629.9	24.5	654.4
6.5	610.5	24.4	634.9D	30.0	664.9
7.5	611.3 <i>b</i>	30.0	641.3 <i>b</i>	34.0	675.3
8.5	612.9	34.2	647.1	38.9	686.0 <i>b</i>
9.5	614.6	39.1	653.7 <i>b</i>	43.4	697.1D
10.5	616.6	43.8	660.4 <i>b</i>	—	—
11.5	619.3	—	—	—	—
12.5	622.4D	—	—	—	—
	³ P ₃ .				
2.5	33630.8	7.6	33638.4D	—	—
3.5	629.2	12.1	641.3 <i>b</i>	16.8	33658.1
4.5	628.1	16.9	645.0	21.5	666.5
5.5	—	—	649.1 <i>d</i>	26.1	675.2
6.5	—	—	653.7 <i>b</i>	30.0	683.7
7.5	628.1	30.0	658.1	34.9	693.0
8.5	629.2	34.3	663.5	39.6	704.1D
9.5	630.8	39.6	670.4 <i>b</i>	43.6	714.0 <i>b</i>
10.5	632.7	43.8	676.5	48.0	724.5 <i>b</i>
11.5	634.9D	47.7	682.6 <i>b</i>	52.7	735.3
	³ P ₂ .				
6.5	33647.1	24.8	33671.9	29.3	33701.2 <i>b</i>
7.5	649.1 <i>d</i>	30.7	679.8 <i>d</i>	34.2	714.0 <i>b</i>
8.5	652.2	33.8	686.0 <i>b</i>	38.5	724.5 <i>b</i>
9.5	656.3	38.6	694.9 <i>b</i>	42.6	737.5
10.5	660.4 <i>b</i>	43.7	704.1D	47.9	752.0D
11.5	665.0	47.1	712.1 <i>d</i>	—	—
12.5	670.4 <i>b</i>	52.1	722.5	—	—
13.5	676.5	—	—	—	—
	³ P ₁ .				
4.5	33677.6	15.9	33693.5	20.5	33714.0 <i>b</i>
5.5	676.5	20.6	697.1D	25.4	722.5
6.5	676.0	25.2	701.2 <i>b</i>	28.9	730.1
7.5	676.5	29.5	706.0	33.7	739.7
8.5	677.6	34.5	712.1 <i>d</i>	39.9	752.0D
9.5	679.8 <i>d</i>	39.0	718.8	42.8	761.6
10.5	682.6 <i>b</i>	43.7	726.3	—	—
11.5	686.0 <i>b</i>	48.1	734.1	52.7	786.8
12.5	690.2	52.6	742.8	—	—
13.5	694.9 <i>b</i>	57.1	752.0	61.2	813.2
14.5	700.1	61.5	761.6	65.2	826.8

Table II.—Initial Term Differences. $\Delta F'j$.

j'	0-0 band.										0-1 band.	Weighted mean.
0.5	2.8	3.2	7.8	6.9								3.0
1.5	7.6	6.8	13.1	12.4								7.6
2.5	11.9	12.3										12.1
3.5	15.8	16.6										16.5
4.5	20.9	21.0	20.7	21.5	16.8							20.9
5.5	25.8	24.6	25.4	26.5	21.4	16.1						20.5
6.5	30.1	29.6	30.3	29.7	30.5	25.4	20.4	20.2	20.9	16.9	15.9	25.3
7.5	34.5	34.3	33.9	35.2	34.4	24.8	20.4	25.1	25.6	24.5	21.5	25.4
8.5	39.0	38.8	38.4	39.8	39.0	35.1	34.9	33.9	34.5	34.2	30.0	29.9
9.5	44.0	43.8		43.7		38.8	38.8	38.9	39.0	39.1	38.6	38.5
10.5	47.1					48.8	51.6	52.6	52.2	47.5	47.1	47.9
11.5	52.4	52.2				57.1	61.5	56.4	56.8	57.2	52.7	52.4
12.5	57.0	60.5										57.1
13.5												61.3
												56.8
												52.2
												47.9
												43.8
												39.0
												34.5
												30.0
												25.3
												20.5
												16.5
												12.1
												7.6
												3.0

VOL. CXXIV.—A.

Table III.—Final Term Differences. $\Delta F''j$.

j''	0-0 band.										0-1 band.	Weighted mean.
1.5	5.5	4.3	5.3	8.4								5.3
2.5	9.6	10.0	7.6	12.4	12.9							9.2
3.5	13.5	14.3										13.2
4.5	17.3	17.4	16.8									17.1
5.5	21.7	20.5	21.8	21.1	20.8	17.1	16.9	17.1	17.5	18.1	13.2	21.1
6.5	25.8	25.8	25.3	24.1	24.9	21.1	20.8	21.1	21.7	21.7	21.5	25.0
7.5	30.1	29.9	28.5	27.4	26.6	28.2	28.2	29.2	29.0	28.4	25.6	28.9
8.5	33.7	33.5	32.4	32.6	31.8	32.4	32.5	32.5	33.7	33.0	29.7	33.0
9.5	37.5	37.3		36.8		36.6	36.7	36.9	37.7	38.0	33.4	36.9
10.5	42.4					40.4		41.0	41.8	42.3	37.7	41.0
11.5	45.1	44.9				45.7	44.2	44.9	45.4	50.0	41.6	44.7
12.5	49.7	49.2				49.1	48.1	49.0	49.6		47.9	48.6
13.5												
												5.3
												9.2
												13.2
												17.1
												21.1
												25.0
												28.9
												33.0
												36.9
												41.0
												44.7
												48.6

M

Application of the Combination Principle and Term Formulation.

According to the quantum theory of molecular spectra the lines of the P, Q and R branches are given, as is well-known, by the following expressions :—

$$R(j) = \nu_0 + F'(j+1) - F''(j), \quad (1)$$

$$Q(j) = \nu_0 + F'(j) - F''(j), \quad (2)$$

$$P(j) = \nu_0 + F'(j-1) - F''(j). \quad (3)$$

The following combination relations deduced from these, give us the spacing of the rotational levels in the initial and final states :—

$$Q(j+1) - P(j+1) = R(j) - Q(j) = \Delta F'(j), \quad (4)$$

$$Q(j) - P(j+1) = R(j) - Q(j+1) = \Delta F''(j). \quad (5)$$

Using old quantum mechanics, the rotational energy can be expressed in the simplest case by

$$F(j) = Bm^2 = B(j - \rho)^2,$$

where j takes half-integral values for the even electron molecule CO.

Now

$$\Delta F(j) = F(j+1) - F(j) = (B - 2B\rho) + 2B(j). \quad (6)$$

If therefore the set of spacing of rotational levels obtained from observational data by relations given in (4) and (5) are expressed by an equation

$$\Delta F(j) = a + bj,$$

then

$$a = B - 2B\rho \quad \text{and} \quad b = 2B,$$

or

$$B = b/2 \quad \text{and} \quad \rho = -\frac{a - (b/2)}{2}.$$

In this way one can calculate B and ρ for the initial and the final states. The $\Delta F'j$ and $\Delta F''j$ values were fitted to a linear equation because the experimental accuracy did not warrant the use of a higher degree polynomial. Moreover, the linear equations derived, represented the data sufficiently well and within the limits of experimental error. Table IV gives the equations derived and the observed and calculated $\Delta F(j)$ values.

Table IV.

0-0 band. $\Delta F'j = 4.485j - 3.673.$			0-0 band. $\Delta F''j = 3.985j - 0.895.$			0-1 band. $\Delta F''j = 3.948j - 0.636.$		
Calc.	Obs.	O - C.	Calc.	Obs.	O - C.	Calc.	Obs.	O - C.
3.06	3.0	-0.06	5.08	5.0	-0.08	5.29	5.3	+0.01
7.54	7.6	+0.06	9.07	9.0	-0.07	9.23	9.2	-0.03
12.03	12.1	+0.07	13.05	13.2	+0.15	13.18	13.2	+0.02
16.51	16.5	-0.01	17.04	17.1	+0.06	17.13	17.1	-0.03
21.00	20.9	-0.10	21.02	21.1	+0.08	21.08	21.1	+0.02
25.48	25.3	-0.18	25.01	25.0	-0.01	25.03	25.0	-0.03
29.97	30.0	+0.03	28.99	29.0	+0.01	28.97	28.9	-0.07
34.45	34.5	+0.05	32.98	32.8	-0.18	32.92	33.0	+0.08
38.94	39.0	+0.06	36.96	36.9	-0.06	36.87	36.9	+0.03
43.42	43.6	+0.18	40.95	41.0	+0.05	40.82	41.0	+0.18
47.91	47.9	-0.01	44.93	44.9	-0.03	44.77	44.7	-0.07
52.39	52.4	+0.01	48.92	49.0	+0.08	48.71	48.6	-0.11
56.88	56.8	-0.08						
61.36	61.3	-0.06						

The initial and final states are represented by the following equations :—

$$\begin{aligned}
 F_0'(j) &= 2.243(j - 0.32)^2 && \text{(initial)} \\
 F_0''(j) &= 1.993(j - 0.72)^2 && \text{(final for 0-0)} \\
 F_1''(j) &= 1.974(j - 0.68)^2 && \text{(final for 0-1).}
 \end{aligned}$$

The existence of large values of ρ is genuine. Their theoretical significance is not clear, we having no definite information about such higher multiplet levels. It is clear, however, that they are characteristic of the quintet level in both states. The same values for ρ persist if a higher degree polynomial is used to represent the data and also if the rotational energy function is derived from the new quantum mechanics.

Band Origins.

These were calculated by using equation (3) on the lines of the P branches and sometimes by equation (2) on Q lines. The values deduced from the various chosen lines did not differ among themselves by more than 0.5 cm.^{-1} . The following table gives the five origins of the two bands :—

	0-0.	0-1.
P ₅	35296.3	33586.2
P ₄	326.3	615.2
P ₃	346.3	635.0
P ₂	367.4	655.5
P ₁	397.9	684.6

It will be seen that there is a marked contraction in the electronic separations of the 0-1 band. While this may partly be due to experimental errors, the systematic manner in which the contraction proceeds from level to level indicates that perhaps it is genuine. The contraction appears to be more pronounced in the two extreme levels where it is 1.1 and 1.4 v. Similar contraction of electronic levels with higher vibration states is also observed in the case of the β bands of NO.* The theory of the rotational distortion of electronic multiplets has been developed by Kemble and others.† It would be very desirable to have also a theory of the vibrational distortion of electronic multiplets.

Molecular Constants.

The following table gives the molecular constants of CO for this band system. As previously noted it has not been possible to evaluate ω_0 and $\omega_0 x$. The latest values of the fundamental units have been used.

Initial state.	Final state.
$B_0' = 2.243$ $I_0' = 12.33 \times 10^{-40} \text{ g. cm.}^2$ $r_0' = 1.10 \times 10^{-8} \text{ cm.}$	$B_0'' = 1.993, B_1'' = 1.974$ $I_0'' = 13.91 \times 10^{-40} \text{ g. cm.}^2$ $r_0'' = 1.24 \times 10^{-8} \text{ cm.}$

The moment of inertia for the final state is thus $13.91 \times 10^{-40} \text{ g. cm.}^2$. The Cameron bands which have this level for their initial state and the final level of the fourth positive carbon bands for their final state are degraded towards the red, thus indicating that I_0'' for this latter level must be smaller than this value. The value now commonly accepted is 14.9×10^{-40} .‡ This value has been indirectly obtained by measurements of the infra-red absorption doublet band by Lowry§ using the Kemble equation, $\Delta\nu = \frac{1}{\pi} \sqrt{\frac{KT}{I}}$. Burmeister's values by the same method|| give 14.7×10^{-40} . Unfortunately this band has not been resolved into its fine-structure. But in cases where the moments of inertia calculated by measurements on the doublet using the above equation are compared with those obtained by fine structure analysis using the equation $\nu_e = mh/4\pi^2 I$, the agreement is qualitative,¶ the values

* 'Phys. Rev.,' vol. 30, p. 150 (1927).

† 'Phys. Rev.,' vol. 30, p. 387 (1927); *ibid.*, vol. 32, p. 250 (1928).

‡ 'Report on Molecular Spectra,' p. 225.

§ 'J. Opt. Soc. Am.,' vol. 8, p. 647 (1924).

|| 'Report on Molecular Spectra,' p. 12.

¶ *Vide*, International Critical Tables.

obtained by fine structure analysis being lower than those obtained by the Kemble equation. Another indirect qualitative method has also been used for computing the I_0 for this level from the relation between ω_0 and I_0 .^{*} This relation observed by Mecke† and others which indicates that for similar electronic states the product $\omega_0 \times I_0$ is constant, is only qualitatively true. On the other hand, the I_0 associated with the initial state of the Ångström bands which is a 2^1S level is 14.26×10^{-40} , and the final level of the fourth positive carbon bands and the Cameron bands being a 1^1S level, one would expect a much lower value than this for its moment of inertia. It thus appears that the value now accepted is very high. It would be very valuable to have a fine structure analysis of the fourth positive carbon bands. But since most of these bands lie in the far ultra-violet, the prospect of a complete analysis appears to be remote. The present writer has, however, analysed some of the bands in the near ultra-violet taken in the first order of the 21-foot grating. The bands are not resolved near the head and the P branch is very weak. A preliminary analysis, however, gives $B_{18}'' = 1.60$ with $\alpha = 0.023$. Assuming a linear change in the values of B'' , we get by extrapolation $B_0'' = 2.01$, which gives $I_0'' = 13.8 \times 10^{-40}$. This value is lower than the value of I_0'' for the final of the third positive carbon bands, and thus fits in with the observed red degradation of the Cameron bands.

Mention must also be made of some recent remarks of Mulliken‡ on the electronic levels of CO. While theoretically he finds that CO can possess quintet levels, he rules out the possibility of such levels on energy considerations. But the foregoing experimental evidence shows that the levels of the third positive carbon bands are certainly quintet.

In conclusion, I should like to express my indebtedness to Dr. R. C. Johnson, for the unceasing kindness with which he has guided me throughout the investigation.

Summary.

1. The third positive carbon bands, the 3 A bands and the so-called Wolter spurious bands, have been photographed in the first order of a 21-foot grating.

2. The Wolter spurious bands are regarded as forming a new system of bands.

3. A complete vibrational analysis of these three systems is given, which shows that they have all got the same final electronic state.

* 'Report on Molecular Spectra,' p. 225.

† 'Z. Physik,' vol. 32, p. 823 (1925).

‡ 'Phys. Rev.,' vol. 32, p. 769 (1928).

4. A new band system, photographed under low dispersion, has been described. A vibrational analysis of these bands is given, which shows that their initial level is identical with the new level at $\nu = 58927$ found by Hopfield and Birge, and their final level is the same as the final level of the above three band systems of the CO molecule.

5. The fine structure analysis of the 0-0 and 0-1 bands of the third positive system is given and the usual molecular constants evaluated. This analysis shows that the final level of these bands is a quintet P level, the transition being $^5S \rightarrow ^5P$. The 3 A bands are probably due to the transition $^5P \rightarrow ^5P$.

DESCRIPTION OF PLATE 3.

1. Third positive Carbon bands, 0-4, 0-3, and 0-2, enlarged 3.5 times. 2. Third positive Carbon bands, 0-1 and 0-0, enlarged 4.5 times. 3. New bands, enlarged three times.

Hydrodynamic Forces acting on a Cylinder in Motion, and the Idea of a "Hydrodynamic Centre."

By W. G. BICKLEY, M.Sc., Lecturer in Mathematics, Battersea Polytechnic.

(Communicated by G. I. TAYLOR, F.R.S.—Received March 19, 1929.)

There are two general methods of determining the forces acting on a cylinder due to the two-dimensional motion of a surrounding liquid. One is applicable to the case of a stationary cylinder in a stream, in the form*

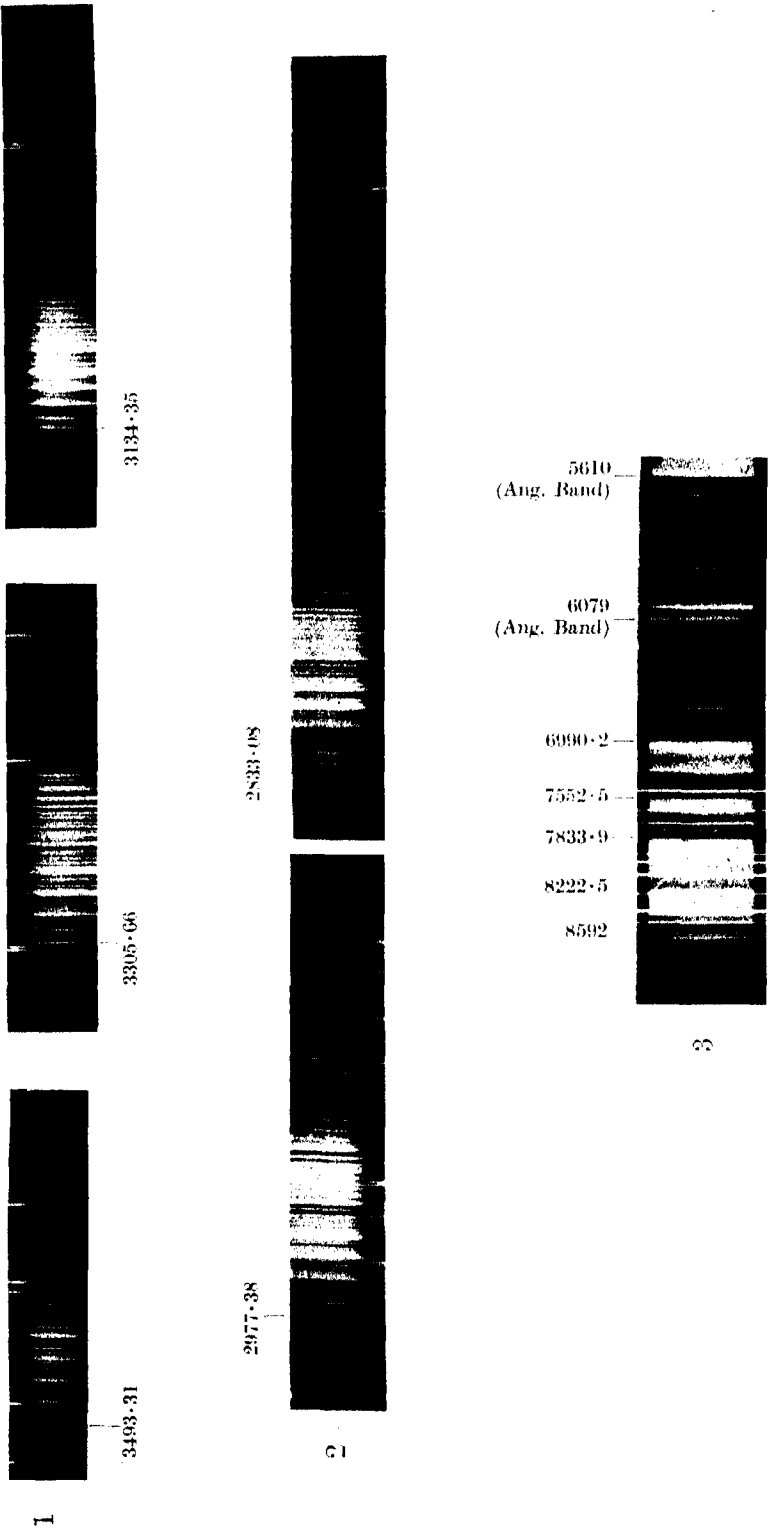
$$X - iY = \frac{1}{2}\rho \int \left(\frac{dw}{dz}\right)^2 dz. \quad (1.1)$$

$$M = -\frac{1}{2}\rho \Re \int \left(\frac{dw}{dz}\right)^2 z \cdot dz, \quad (1.2)$$

where X and Y are the components of the resultant force, parallel to the x and y axes, and M is its moment about the origin; ρ is the density of the fluid, and w is the velocity potential-stream-function for the fluid motion; z is as usual the complex variable $x + iy$. The other is that obtained from the general theory of the "impulse."† The first of these is unable to deal

* Cf. Glauert, 'Aerofoil and Airscrew Theory,' p. 81 (Cambridge, 1926).

† Cf. Lamb, 'Hydrodynamics' (4th ed.), ch. 6, especially p. 165 (Cambridge, 1916).



with a rotating cylinder, and the second is unable to include "circulation." In the course of an investigation of the effects of rotation upon the circulation round, and the forces acting upon, a Joukowski aerofoil, to which problem neither method applies, since the combined effect of rotation and circulation is needed, a quite general result was obtained, which it is thought worth while to publish separately.

Imagine a cylinder moving with a velocity whose components are U and V (relative to axes in the plane of a section, and fixed relative to the section) and with angular velocity ω about the origin; let there, moreover, be a circulation Γ round the body. Then the complex velocity-potential-stream-function, w , and the velocity potential, ϕ , may be written

$$w = \Gamma w_1 + U w_2 + V w_3 + \omega w_4 = \Gamma w_1 + w', \quad (2.1)$$

$$\phi = \Gamma \phi_1 + U \phi_2 + V \phi_3 + \omega \phi_4 = \Gamma \phi_1 + \phi', \quad (2.2)$$

where w_1 and ϕ_1 are cyclic, ϕ_1 having cyclic constant -1 , and $w_2, w_3, w_4, \phi_2, \phi_3$ and ϕ_4 are single-valued. These can all be determined by the usual methods if the appropriate conformal transformation is known. Also, if dn be an element of the outward drawn normal, the condition that the velocity of the fluid at the boundary should have its normal component equal to the normal component of that of the body gives

$$\partial \phi_1 / \partial n = 0 \quad (2.3)$$

$$-\frac{\partial \phi}{\partial n} = (U - \omega y) \frac{dy}{ds} - (V + \omega x) \frac{dx}{ds} \quad (2.41)$$

or

$$\frac{\partial \phi}{\partial n} \cdot ds = V dx - U dy + \omega (x dx + y dy), \quad (2.42)$$

ds being an element of the boundary. At infinity, if it be assumed that the fluid is at rest there, $w_1 \sim 1/2\pi \cdot \log z$, and w_2, w_3 and w_4 are of order $1/z$.

Now if p be the pressure at any point,

$$\frac{p}{\rho} = \frac{\partial \phi}{\partial t} - \frac{1}{2} \left\{ \left(\frac{\partial \phi}{\partial x} \right)^2 + \left(\frac{\partial \phi}{\partial y} \right)^2 \right\}. \quad (3.1)$$

The value of $\partial \phi / \partial t$ needs careful consideration. The variation of ϕ at any fixed point is due to two causes: (1) the motion of the axes of reference, and (2) changes in the values of U, V and ω (possible changes of Γ being left out of account for the present), *i.e.*, the acceleration of the body. The contribution due to the first of these is

$$-U \frac{\partial \phi}{\partial x} - V \frac{\partial \phi}{\partial y} - \omega \frac{\partial \phi}{\partial \theta} = -U \frac{\partial \phi}{\partial x} - V \frac{\partial \phi}{\partial y} + \omega \left(y \frac{\partial \phi}{\partial x} - x \frac{\partial \phi}{\partial y} \right), \quad (3.2)$$

and that due to the second (using dots to denote t -derivatives) is

$$\dot{\phi}' = \dot{U}\phi_2 + \dot{V}\phi_3 + \dot{\omega}\phi_4. \quad (3.3)$$

If dz is an element of the boundary, the force due to p acting on dz is given in magnitude and direction by $\iota p \cdot dz$. Thus if X and Y are the components of the resultant force due to fluid pressure acting on the cylinder,

$$X + \iota Y = \oint \iota p \cdot dz = \oint p(dx - dy). \quad (3.4)$$

Taking first the velocity terms in (3.1), and using the suffix 1 to denote the boundary, and 2 to denote any closed curve surrounding it, we have

$$\begin{aligned} & \left(\oint_1 - \oint_2 \right) \frac{1}{2} \left\{ \left(\frac{\partial \phi}{\partial x} \right)^2 + \left(\frac{\partial \phi}{\partial y} \right)^2 \right\} (\iota dx - dy) \\ &= \iint \frac{1}{2} \left(\frac{\partial}{\partial x} + \iota \frac{\partial}{\partial y} \right) \left\{ \left(\frac{\partial \phi}{\partial x} \right)^2 + \left(\frac{\partial \phi}{\partial y} \right)^2 \right\} \cdot dx \cdot dy \\ &= \iint \left\{ \frac{\partial \phi}{\partial x} \cdot \frac{\partial}{\partial x} \left(\frac{\partial \phi}{\partial x} + \iota \frac{\partial \phi}{\partial y} \right) + \frac{\partial \phi}{\partial y} \cdot \frac{\partial}{\partial y} \left(\frac{\partial \phi}{\partial x} + \iota \frac{\partial \phi}{\partial y} \right) \right\} dx \cdot dy \\ &= - \left(\oint_1 - \oint_2 \right) \frac{\partial \phi}{\partial n} \left(\frac{\partial \phi}{\partial x} + \iota \frac{\partial \phi}{\partial y} \right) ds - \iint \left(\frac{\partial \phi}{\partial x} + \iota \frac{\partial \phi}{\partial y} \right) \nabla^2 \phi \, dx \cdot dy, \end{aligned}$$

where the double integrals are taken over the area between 1 and 2, and where also the double integral last written vanishes if ϕ has no singularities in this region. (By excluding small circles in their neighbourhood, the effects of vortices and sources could be included; the results have been obtained elsewhere by another method.)* In our case, if we take 2 to be the circle at infinity, the integrals over it vanish, since $\partial \phi / \partial x$ and $\partial \phi / \partial y$ are at most of order $1/r$ at a large distance, r . Thus

$$\begin{aligned} X + \iota Y = \rho \oint_1 \left[\left\{ -U \frac{\partial \phi}{\partial x} - V \frac{\partial \phi}{\partial y} + \omega \left(y \frac{\partial \phi}{\partial x} - x \frac{\partial \phi}{\partial y} \right) + \dot{\phi}' \right\} (\iota dx - dy) \right. \\ \left. + \frac{\partial \phi}{\partial n} \left(\frac{\partial \phi}{\partial x} + \iota \frac{\partial \phi}{\partial y} \right) ds \right]. \end{aligned}$$

Using the value of $\partial \phi / \partial n \cdot ds$ from (2.42), we obtain, after some reduction,

$$\begin{aligned} X + \iota Y &= \rho \oint_1 \left[\left\{ -\iota U + V + \omega(x + \iota y) \right\} \left(\frac{\partial \phi}{\partial x} dx + \frac{\partial \phi}{\partial y} dy \right) + \dot{\phi}' (\iota dx - dy) \right] \\ &= \rho \oint_1 [(-\iota U + V + \omega z) d\phi + \iota \dot{\phi}' dz] \\ &= -\iota \rho (U + \iota V) [\phi] + \rho \omega \oint_1 z d\phi + \iota \rho \oint_1 \dot{\phi}' dz. \end{aligned} \quad (4.1)$$

* 'Phil. Trans.,' A, vol. 228 (in the press).

The cyclic constant of ϕ is $-\Gamma$, so the first term gives $\iota\rho\Gamma(U + \iota V)$, the known effect of circulation and translation. The second term can be split up into

$$\begin{aligned} \rho\omega\Gamma\oint_1 z d\phi_1 + \rho\omega\oint_1 z d\phi' \\ = \rho\Gamma\omega\oint_1 z d\phi_1 + \rho\omega[z\phi'] - \rho\omega\oint_1 \phi' dz, \end{aligned} \quad (4.11)$$

after integration by parts—and the integrated part vanishes since ϕ' is single-valued. Now the impulse of the motion causing, ϕ' , *i.e.*, of the motion of the fluid with the circulation annulled, is given by a pressure $\rho\phi'$ applied to the fluid at the boundary, so that, if I denote this impulse,

$$I = -\rho\oint_1 \phi' \cdot \iota dz.$$

Thus the last integral in (4.11) is $-\iota\omega I$ —and the last in (4.1) is $-\dot{I}$. There remains the first integral in (4.11). Since $\partial\phi_1/\partial n$ is zero on the boundary the corresponding stream function is constant there, and so we may replace ϕ_1 by w_1 in this integral, and have

$$\oint_1 z dw_1 = \oint_1 z \frac{dw_1}{dz} dz,$$

and by Cauchy's theorem the value of this integral is the same along any closed curve enclosing the boundary, since w_1 has no singularities between the boundary and infinity. Now near infinity we can write

$$w_1 = \frac{\iota}{2\pi} \log(z - a) + O(z^{-2}), \quad (4.12)$$

whence

$$\frac{dw_1}{dz} = \frac{\iota}{2\pi} \left(\frac{1}{z} + \frac{a}{z^2} \right) + O(z^{-3}), \quad (4.13)$$

so that the integral round the circle at infinity gives $-a$. Thus

$$\rho\oint_1 z d\phi = -\rho\Gamma a - \iota I. \quad (4.14)$$

Collecting the results, and inserting them in (4.1), we get,

$$X + \iota Y = \iota\rho\Gamma(U + \iota V + \iota\omega a) - \iota\omega I - \dot{I}. \quad (4.2)$$

We notice here that $(U + \iota V + \iota\omega a)$ is the velocity of the point given by

$z = a$, and we shall denote this by $U_a + iV_a$. (4.12) enables us to interpret this point as the limit to which the centre of the approximately circular streamlines due to circulation *only* tends as they tend to infinity; it is therefore fixed relative to the section, and we propose to term it the "hydrodynamic centre" of the section. If we take it as origin, then, the term in a in (4.2) disappears. The remaining terms of (4.2) are well known from the theory of the impulse, and may be termed the "relativity terms," as they are due to the motion of the axes of reference. Referring to the "hydrodynamic centre" as origin

$$X + iY = i\Gamma(U_a + iV_a) - i\omega I - \dot{I}. \quad (4.3)$$

which gives the resultant force in a very compact form.

Next for the moment of the forces due to the fluid pressures, about the origin. The moment of the force on an element dz is $p(x \cdot dx + y \cdot dy)$, so that the total moment, M , is given by

$$M = \oint_1 p(x \cdot dx + y \cdot dy). \quad (5.11)$$

Now $(x \cdot dx + y \cdot dy)$ is the real part of $(x + iy)(dx - idy)$ so that M is the real part of

$$M' = \oint_1 p(x + iy)(dx - idy). \quad (5.12)$$

Dealing with the velocity terms first, in the same manner as before, we find

$$\begin{aligned} & \left(\oint_1 - \oint_2 \right) \left[\frac{1}{2} \left\{ \left(\frac{\partial \phi}{\partial x} \right)^2 + \left(\frac{\partial \phi}{\partial y} \right)^2 \right\} (x + iy) \right] (dx - idy) \\ &= \iint \left(i \frac{\partial}{\partial x} + \frac{\partial}{\partial y} \right) \left[\frac{1}{2} \left\{ \left(\frac{\partial \phi}{\partial x} \right)^2 + \left(\frac{\partial \phi}{\partial y} \right)^2 \right\} (x + iy) \right] \cdot dx dy \\ &= \iint \frac{1}{2} \left[2i \left\{ \left(\frac{\partial \phi}{\partial x} \right)^2 + \left(\frac{\partial \phi}{\partial y} \right)^2 \right\} + 2i(x + iy) \left\{ \frac{\partial^2 \phi}{\partial x^2} \cdot \frac{\partial \phi}{\partial x} + \frac{\partial^2 \phi}{\partial x \partial y} \cdot \frac{\partial \phi}{\partial y} \right\} \right. \\ &\quad \left. + 2(x + iy) \left\{ \frac{\partial^2 \phi}{\partial x \partial y} \cdot \frac{\partial \phi}{\partial x} + \frac{\partial^2 \phi}{\partial y^2} \cdot \frac{\partial \phi}{\partial y} \right\} \right] dx dy, \\ &= \iint i \left(\frac{\partial \phi}{\partial x} \frac{\partial \chi}{\partial x} + \frac{\partial \phi}{\partial y} \frac{\partial \chi}{\partial y} \right) dx dy, \end{aligned}$$

where

$$\chi = (x + iy) \left(\frac{\partial \phi}{\partial x} - i \frac{\partial \phi}{\partial y} \right).$$

By Green's theorem, and because $\nabla^2\phi = 0$, the integral last written is equal to

$$- \imath \left(\oint_1 - \oint_2 \right) \frac{\partial \phi}{\partial n} \cdot \left(\frac{\partial \phi}{\partial x} - \imath \frac{\partial \phi}{\partial y} \right) (x + \imath y) ds.$$

Thus

$$\begin{aligned} M' &= \imath \rho \left(\oint_1 - \oint_2 \right) \frac{\partial \phi}{\partial n} \left(\frac{\partial \phi}{\partial x} - \imath \frac{\partial \phi}{\partial y} \right) (x + \imath y) ds \\ &\quad - \frac{1}{2} \rho \oint_2 \left\{ \left(\frac{\partial \phi}{\partial x} \right)^2 + \left(\frac{\partial \phi}{\partial y} \right)^2 \right\} (x + \imath y) (dx - \imath dy) \\ &\quad + \rho \oint_1 \left\{ -U \frac{\partial \phi}{\partial x} - V \frac{\partial \phi}{\partial y} + \omega \left(y \frac{\partial \phi}{\partial x} - x \frac{\partial \phi}{\partial y} \right) + \dot{\phi}' \right\} (x + \imath y) (dx - \imath dy). \end{aligned}$$

Using the value of $\partial \phi / \partial n \cdot ds$ from (2.42), the integrals over the boundary reduce to

$$\begin{aligned} &\rho \oint_1 \left[\imath (x + \imath y) \{V + \imath U + \omega (x - \imath y)\} \left(\frac{\partial \phi}{\partial x} dx + \frac{\partial \phi}{\partial y} dy \right) \right. \\ &\quad \left. + \dot{\phi}' (x + \imath y) (dx - \imath dy) \right] \\ &= \imath \rho (V + \imath U) \oint_1 z d\phi + \imath \omega \rho \oint_1 (x^2 + y^2) d\phi \\ &\quad + \rho \oint_1 \dot{\phi}' (x + \imath y) (dx - \imath dy) \quad (5.21) \end{aligned}$$

The middle term is purely imaginary, and so may be omitted as contributing nothing to M . By (4.14),

$$\rho \oint_1 z d\phi = -\rho \Gamma a - \imath I.$$

Again, the real part of the last term of (5.21) is

$$\rho \oint_1 \dot{\phi}' (x \cdot dx + y \cdot dy) = -\dot{L}, \quad (5.22)$$

where L is the moment about the origin of the impulse, I . Consequently the contribution of the inner integrals to M is

$$\Re (V + \imath U) (I - \imath \rho \Gamma a) - \dot{L}, \quad (5.23)$$

We have still to consider the outer integrals. It will be found, upon a little reduction, that they give

$$- \frac{1}{2} \rho \oint_2 \left(\frac{\partial \phi}{\partial x} - \imath \frac{\partial \phi}{\partial y} \right)^2 z \cdot dz = - \frac{1}{2} \rho \oint_2 \left(\frac{dw}{dz} \right)^2 z \cdot dz.$$

302 *Hydrodynamic Forces acting on Cylinder in Motion.*

Now when z is large,

$$\frac{dw}{dz} = \frac{i\Gamma}{2\pi z} + O(z^{-2}),$$

and so

$$z \left(\frac{dw}{dz} \right)^2 = -\frac{\Gamma^2}{4\pi^2 z} + O(z^{-2}),$$

and consequently the integral is $2\pi i \times \frac{1}{2}\rho \times \Gamma^2/4\pi^2$, which is purely imaginary, and so contributes nothing to M . Finally then

$$M = \Re (V + iU)(1 - i\rho\Gamma a) - \dot{L}. \quad (5.31)$$

Again the result can be simplified by using the "hydrodynamic centre" as origin, and taking moments about it, for then the term in a disappears, and we have

$$M_a = \Re (V_a + iU_a)I - \dot{L}_a, \quad (5.32)$$

the suffix a denoting, as before, the use of the "hydrodynamic centre" as origin. If U_a and V_a are parallel to the principal axes of inertia of the section, and A and B are the corresponding inertia coefficients, we have

$$I = AU_a + iBV_a,$$

so that

$$M_a = (A - B)U_aV_a - \dot{L}_a. \quad (5.4)$$

Equations (4.3) and (5.4) are the results it was set out to demonstrate. They show that, provided we take the "velocity" to be that of the "hydrodynamic centre," the well-known formulæ for the force and moment of the fluid pressures still hold when the body has rotation, as well as translation and circulation. It is particularly to be noted that ω does not occur explicitly in the force equation—except, of course, in the "relativity" terms; and that neither ω nor Γ appear explicitly in the moment formula. Of course in the case of an aerofoil, Γ is determined by a *further* condition in terms of U , V and ω . The application to this problem has given results which it is hoped to publish.

[*Note added in proof.*—Since the above was written, two other treatments of this problem have appeared. Glauert* expresses the force and moment in terms of the velocity of the fluid relative to the cylinder, at its surface, and his formulæ are equivalent to the above. Lamb† uses analysis similar to

* Aeronautical Research Committee, R. and M. 1215 (1929).

† " " " " R. and M. 1218 (1929).

the above, but fails to note the simple interpretation in terms of what I have called the "hydrodynamic centre."]

In conclusion it remains to thank Prof. G. I. Taylor, F.R.S., for his suggestion of the problem of the rotation of the Joukowski aerofoil, the solution of which necessitated the obtaining of these results, and for his interest in, and helpful comments upon, my work.

Gaseous Combustion in Electric Discharges. Part III.—The Cathodic Combustion of Dry Carbonic Oxide Detonating Gas.

By G. I. FINCH and D. L. HODGE, Imperial College of Science.

(Communicated by Prof. W. A. Bone, F.R.S.—Received March 20, 1929.)

Introduction.

In Parts I and II* of the present series an account was given of an investigation of the ignition and slow non-self-propellant combustion of electrolytic gas in direct current discharges. In those experiments a smooth direct current discharge was maintained between cooled platinum or copper electrodes in pure electrolytic gas, confined over sulphuric acid, at pressures between 30 and 180 mm. in such a manner as to eliminate, as far as possible, any chemical combination other than that caused only by the ionisation of the gases. The proportionality between the rate of chemical change and the current was then studied.

It was shown that (i) an electric discharge can be passed through electrolytic gas in such a manner that combination takes place at a rate which is determined only by the discharge; (ii) up to a certain limiting current, which depends upon (a) the nature of the cathode material, (b) the gas pressure, and (c) the gap width, combustion is confined to the cathode zone, its rate being directly proportional to the current, *i.e.*, to the number of ions arriving at the cathode in a given time; (iii) after a certain limiting current has been exceeded, combustion commences abruptly in the inter-electrode zone and is thereafter superposed upon the cathodic combustion, the two then continuing as independent simultaneous effects; (iv) this inter-electrode combustion, like the cathodic,

* 'Roy. Soc. Proc.,' A, vol 111, p. 257 (1926), and vol. 116, p. 529 (1927).

is also proportional to the current passing; unlike the cathodic, however, it is independent of the material of the electrodes, but dependent upon (a) the gas pressure, and (b) the gap width.

Finally it was shown that when electrolytic gas is ignited by such a direct current discharge (v) ignition occurs without lag on attainment of the igniting current; (vi) the gas pressure and igniting current are connected by a hyperbolic relation over a considerable range of conditions; and (vii) the value of the igniting current is raised by either a deficiency or an excess of water vapour in the gas within the ignition zone.

From these facts it was concluded that the non-explosive combustion was primarily determined by the ionisation of the gaseous medium through which the current passed, and that ignition was determined by the attainment in some portion of the gas traversed by the discharge of a certain definite concentration of suitable ions or electrically charged particles, in the building up of which moisture materially assisted.

Electrolytic gas was employed in the above experiments because it is a comparatively simple mixture which can be prepared in a high degree of purity and whose product of combustion is easily and rapidly removable; it has, however, the disadvantage that the moisture contents of the gas immediately in contact with the discharge can neither be estimated nor accurately controlled, and in view of the profound effect which moisture is known to have upon combustion generally, it was decided to extend the investigation to a simple case of gaseous combustion in which the moisture contents of the reacting gases could be rigidly controlled. A suitable gas for this purpose is a mixture of carbonic oxide and oxygen in equivalent proportions, which for the sake of brevity will be hereinafter called the "detonating gas."

The effect of moisture upon the combustion of carbonic oxide has been the subject of much experimental study by Dixon, Bone and others,* who have found that water in general actively promotes it. Bone and his co-workers† have, however, shown that carbonic oxide and oxygen can and do combine without the intervention of moisture, and that the influence of moisture diminishes with increasing pressure of the gaseous medium.

EXPERIMENTAL.

In Part I‡ it has been shown that the simplest form of combustion of electrolytic gas in direct current discharges is that occurring at the cathode, since

* See Bone and Townend, "Flame and Combustion in Gases" (Longmans, 1927).

† 'Roy. Soc. Proc.' A, vol. 110, p. 615 (1926).

‡ *Loc. cit.*

such cathodic combustion is proportional to the current passed by the discharge and is independent of the gas pressure, gap width and potential fall between the electrodes, but depends upon the nature of the cathode material. It was decided, therefore, to limit the scope of the present investigation to an examination of the cathodic combustion of dry "detonating gas" at a variety of different electrode materials, and then later to study the influence of moisture upon such combustion.

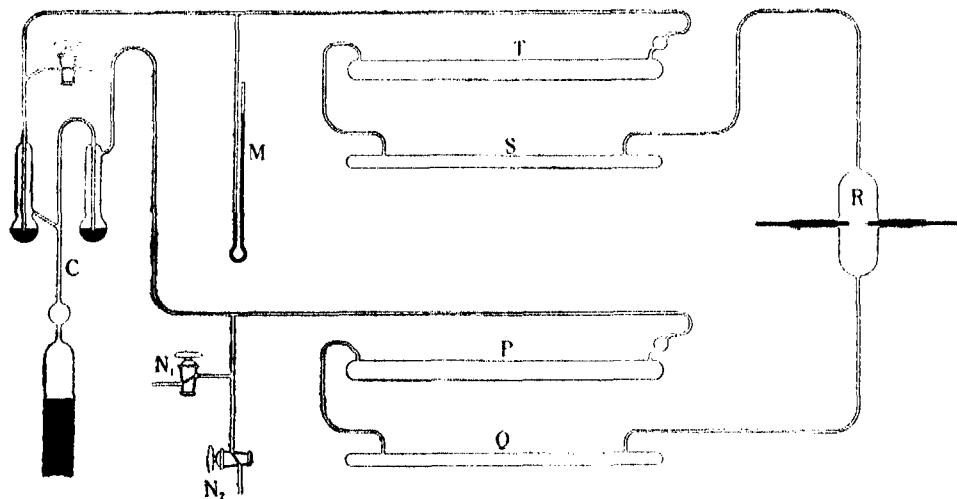
The results of our experiments have shown that in the cathodic region carbonic oxide can be and is burnt directly by oxygen in the absence, and therefore without the intervention of, either moisture or metal atoms sputtered from the cathode by the passage of the discharge; but that metal atoms (and also electrically charged moisture as will be shown in a further communication) actively promote such combustion by the overcoming of the electrostatic forces of repulsion existing between similarly charged ions of carbonic oxide and oxygen.

It is our intention, in conjunction with Prof. Bone, in a future paper to develop this view and show in detail how it affords a reasonable explanation of the facts concerning the combustion of carbonic oxide which have recently been established in his and our researches. Meanwhile, it will suffice to say that we are all agreed that the combustion of carbonic oxide is conditioned by a prior ionisation of both combustible and oxygen molecules; and that as the majority of such ionisation will naturally be positive, an electrostatic repulsion will be set up between the positively charged molecules of carbonic oxide and oxygen whose effect may be likened to that of a reduction in pressure and which can be counteracted by the presence of suitably charged water or metal atoms, or by an increase in pressure either upon the gas as a whole or exerted selectively upon the charged gaseous molecules alone.

Description of Apparatus.

In order to ensure the passage of a dry gaseous mixture past the electrodes and also to absorb sufficiently rapidly the products of combustion, it was found necessary to employ a gas circulation system. The apparatus is shown in the figure. The vertical reaction vessel R, was fitted with two electrodes consisting each of a 2 cm. length of 18 S.W.G. wire, pointed and polished to a cone of 1 mm. height, and pressed into stout brass rods which were, in turn, sealed with sealing wax into the side tubes of the reaction vessel. Gas leaving this vessel first passed through a 60 cm. long tube, S, containing purified

phosphoric anhydride, then over a 60 per cent. caustic potash solution contained in a 60 cm. long tube, T, and thence to the intake side of the circulating pump C.* From the output side of the circulator the gas flowed over concentrated



sulphuric acid contained in the 60 cm. long tube and thence over the phosphoric anhydride in the 60 cm. long tube, Q, from which it finally re-entered the reaction vessel, R. The mercurial manometer, M, enabled pressure changes, and hence the velocity of the reaction to be observed.

Preparation of the Carbonic Oxide Detonating Gas.

Oxygen was prepared from recrystallised potassium permanganate, washed through spiral washers containing caustic potash solution and then stored over a 50 per cent. glycerine and boiled out, distilled water solution. Prior to mixing, the purity was checked by analysis in a Bone and Wheeler gas analysis apparatus. Impurities amounted to less than 0.1 per cent. and consisted wholly of adventitious nitrogen.

Carbonic oxide was prepared from formic acid in the well-known manner, care being taken, however, to add the formic acid to the sulphuric acid sufficiently slowly. The gas was passed through spiral washers containing caustic potash solution and stored over glycerine-water.

As soon as convenient after preparation, the individual gases were dried over concentrated sulphuric acid and mixed in their proper proportions ($2\text{CO} + \text{O}_2$) and the mixture stored in a 10-litre steel gas holder over mercury. Its com-

* 'J. Chem. Soc.,' vol. 127, p. 2464 (1925).

position was then checked, and adjusted to the correct proportions as and when found necessary. The final composition of the mixture did not vary from that represented by $2\text{CO} + \text{O}_2$ by more than 0.2 per cent.

The detonating gas was admitted through the stopcock, N_1 , to the apparatus, which had been previously evacuated through the stopcock, N_2 , by means of a "Hyvac" oil pump. Owing to the change with pressure in the mercury level of the manometer, M, and of the mercury piston column of the circulator pump, the actual working volume of the apparatus varied with the pressure of the gas contained in the apparatus and with the barometric pressure. By suitably adjusting the amount of mercury in the piston column prior to each experiment, the volume change due to daily fluctuations in the barometric pressure was eliminated. By determining the volume of the apparatus by means of a standard gas burette, with the circulator pump in action, a curve was constructed relating the volume of the apparatus to pressure as read on the manometer M. At 90 mm. Hg. the apparatus under working conditions contained 50.9 c.cm. at N.T.P. and 16.7 c.cm. at 30 mm.

The electrical circuit was essentially as described in Part II of this series. To enable the potential drop between the electrodes to be determined, however, a tapped 40 megohm, non-inductive, potential-dividing resistance was shunted across the electrodes, and an electrostatic voltmeter connected to suitableappings adjacent to the centre point of the resistance.

Experimental Procedure.

The electrodes were first sealed into the vessel and set at a definite gap width and the surface of the cathode point was then brought to a uniform condition by "running in" in the manner previously outlined (Part I, p. 263). The apparatus was now exhausted, whereupon the "detonating gas" mixture stored in the steel gas holder was admitted to a pressure of approximately 120 mm. After commencing circulation, the direct current generator was started, the discharge current being controlled as required by means of the variable water resistance. Readings of the gas pressure, room temperature and potential drop between the electrodes were taken synchronously at suitable intervals. The discharge current was maintained at a constant value throughout each individual experiment.

From the resulting experimental data the value of c/i , *i.e.*, the ratio of the rate of combustion in cubic centimetres at N.T.P. per minute to the current in milliamperes, was determined for each set of experimental conditions.

As above stated, the experiments were confined to those current ranges

within which combustion occurred solely in the cathode zone. A two-fold check of the combustion being entirely cathodic was afforded by visual observation (absence of bright positive column) and by the constancy of the value of the c/i ratio for any given set of conditions in which either current or gap width was varied.

Experimental Results.

A preliminary series of experiments was carried out with the object of determining within what range of conditions the combustion of dry detonating gas was purely cathodic. The results showed that, provided the gap width did not exceed 3 mm., the upper current limit was about 4 and 5 milliamperes with platinum and copper cathodes respectively. In the case of platinum, slow catalytic combustion commenced when the current exceeded 4 milliamperes. Below about 1.2 milliamperes the character of the discharge underwent a sudden change and combustion was no longer confined to the cathode zone but also took place in the positive column, *i.e.*, in the inter-electrode zone. Such inter-electrode combustion could also be obtained with currents between 2 and 5 milliamperes by suitably increasing the gap width and gas pressure. Thus these observations established the important fact that not only cathodic but also inter-electrode combustion can occur in dry "detonating gas."

Series A.—In Part I it was shown that the ratio of the rate of cathodic combustion of electrolytic gas to current was constant and independent of the gas pressure, the degree of separation of the electrodes and of the nature of the anode material, but dependent upon the nature of the cathode material, the value of the c/i ratio at a platinum cathode greatly exceeding that obtained with a copper cathode. The experiments of the present series were carried out with the object of determining to what extent, if any, the cathodic combustion of dry detonating gas resembles that of electrolytic gas. The results of these experiments are recorded below in Table I. The gap width was varied between 0.5 and 3 mm.

A preliminary series of experiments showed that the rate of combustion was independent of the rate of circulation when the latter was varied between 6 and 25 strokes of the mercury piston per minute. In all experiments the results of which are recorded below, however, the rate of circulation was maintained at between 23 and 25 strokes per minute. Each c/i ratio value recorded in Table I is the mean value of a number of determinations, not less than 8, but sometimes as many as 15, the two variables being gap width (between 0.5 and 3 mm.) and current within the range given in the table.

The cathode potential drop was determined by plotting the total potential

drops between the electrodes against different gap widths for a series of currents. On extrapolation to zero gap width, the potential drop—gap width curves converged and intersected at or near the ordinate. The mean of the zero gap width—potential drop values thus obtained was taken as being equal to the sum of the individual electrode potential drops. Of this value it was assumed that 20 volts was due to the anode, and that the remainder represented the cathode fall of potential. c/i is the ratio of detonating gas in cubic centimetres at N.T.P. per minute burnt at the cathode to the current in milliamperes passed by the discharge.

Table I.—Series A. Cathodic Combustion of Dry $2\text{CO} + \text{O}_2$.

Electrodes.		Cu \pm .	Cu — ; Pt +.	Pr — ; Cu +.	Pt \pm .
c/i {	at 90 mm.	0.07	0.07	0.24	0.24
	at 75 mm.	0.07	0.07	0.24	0.24
	at 60 mm.	0.07	0.07	0.23	0.23
	at 45 mm.	0.06	0.06	0.22	0.22
	at 30 mm.	0.06	0.06	0.21	0.21
Cathode potential fall in volts		355	355	375	375
Current range in milliamperes		1.5 to 5.0	1.5 to 5.0	1.5 to 3.65*	1.5 to 3.65*

* Above about 4 milliamperes vigorous catalytic combustion set in abruptly.

These results showed that the ratio of the rate of cathodic combustion of "detonating gas" to current was less than that obtained with electrolytic gas and, unlike that of the latter, was dependent upon the gas pressure, though only to a slight extent. While we are unable at the moment to offer an explanation of this last fact, it is, nevertheless, clear that the pressure effect recorded, was, for reasons previously given in Part I, pp. 275–6, far too small to be accounted for on catalytic grounds. In all other respects cathodic combustion is similar in the two gaseous mixtures under consideration. Thus, in both cases, cathodic combustion was found to be proportional to the current and independent of the gap width and anode material, but differed with the nature of the cathode material, combustion being far more vigorous at a platinum than at a copper cathode. Indeed, in the case of the "detonating gas" the c/i ratio found with a platinum cathode is more than three times that obtained with a copper cathode. Such a marked increase cannot be accounted for by the comparatively slight difference in the cathode potential falls at platinum and copper. This phenomenon clearly has an important bearing upon the mechanism of cathodic combustion. It was decided therefore to extend our

experiments to a systematic examination of the cathodic combustion of dry "detonating gas" at different metals. In addition to platinum and copper, the metals chosen for the purpose of these experiments were silver, gold, palladium, tungsten, tantalum, aluminium and magnesium; thus covering a wide range from strongly electronegative to strongly electropositive metals. The results of these experiments are recorded in the following Table II. The c/i values were determined at a mean gas pressure of 90 mm.

Table II.

Cathode material.	c/i .	Cathodic potential fall.
Ag	0.29	345
Au	0.25	330
Pt	0.24	375
Pd	0.23	Not determined
Mg	0.10	Not determined
Al	0.09	320
Cu	0.07	355
W	0.045	Not determined
Ta	0.045	Not determined

Discussion of the Results.

It has been previously suggested (Part I, p. 276) that the variation in the value of the c/i ratio with the nature of the cathode material might, in some way, be connected with the ease of electron emission exhibited by the different cathode materials. The cathode potential fall values tabulated in Table II, however, at once invalidate any such explanation.

If, on the other hand, the different metals used as cathodes be arranged in descending order of their corresponding c/i values, a striking similarity with the well-known series into which Crookes ordered various metals from the point of view of their ease of sputtering cathodically will at once be noticed. This phenomenon has recently been systematically studied by Güntherschulze* at the Reichsanstalt in Charlottenberg, and by Von Hippel and Blechschmidt† in Jena, and their results, taken in conjunction with those established in the course of this investigation, enable us to put forward an explanation of the mechanism of the cathodic combustion of dry "detonating gas."

* 'Z. Physik,' vol. 36, p. 563 (1926), and vol. 38, p. 575 (1926); 'Z. Technische Physik,' vol. 8, p. 169 (1927); 'Chem. Zentralblatt,' vol. 2, p. 385 (1927).

† 'Ann. Physik,' vol. 81, p. 1001 (1926).

The main facts relating to the cathodic sputtering of metals established by the above investigators, are as follows :—

- (i) The rate of such sputtering is proportional to the current.
- (ii) The sputtered metal is projected away from the cathode into the cathode zone in the atomic state.*
- (iii) By far the greater proportion of the atoms sputtered into the cathode zone return thence back to the cathode, the amount of such returned metal increasing with the gas pressure. At pressures above about 15 mm. no sputtered metal escapes beyond the cathode glow, all being returned to the cathode. The total amount of sputtering, *i.e.*, the sum of the metal returned to the cathode together with the metal completely escaping beyond the discharge, depends upon the gas and nature of the cathode material, but is independent of the gas pressure. It is probable that the sputtered metal atoms are negatively charged.
- (iv) The formation of an oxide film decreases or practically suppresses sputtering, even from metals which, in an inert atmosphere, otherwise sputter freely.
- (v) Sputtering is independent of the temperature of the cathode.
- (vi) Sputtering is due to the bombardment of the cathode by ions, and increases with the atomic weight of the gas.

The various cathode materials used by us can be sharply divided into two classes according to whether they sputter freely or otherwise in an atmosphere containing oxygen. Silver, platinum, gold, and palladium, with which metals the c/i values are 0.29, 0.24, 0.25 and 0.23 respectively, sputter freely; magnesium, aluminium, copper, tantalum and tungsten, which give c/i values of 0.10, 0.09, 0.07, 0.045 and 0.045 respectively, are poor or practically non-sputterers. Copper, it is true, sputters in an inert atmosphere, but under the conditions of our experiments the copper cathode was coated with oxide, with the result (as has been shown by Güntherschulze and v. Hippel and Blechschmidt) that sputtering was greatly reduced. The formation of oxide films were, indeed, observed by us in the case of all metals giving low c/i values.

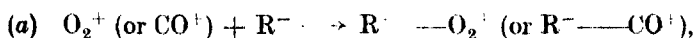
In the light of these facts it is now possible to put forward the following

* This fact had been previously independently established by one of us (G.I.F.) during a spectroscopic examination of the glow surrounding a cool copper cathode in electrolytic gas, in the course of which a line spectrum of that metal was obtained.

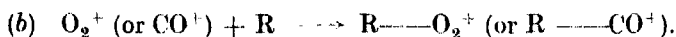
explanation of the mechanism of the cathodic combustion of dry carbonic oxide "detonating gas" :—

Under the conditions of our experiments, such combustion is primarily determined by the ionisation of the gases in the cathode zone. Such ionisation is, however, by itself not sufficient to enable combination to take place, the formation of carbon dioxide requiring the sufficiently close approach of suitable ions. In the cathode zone both oxygen and carbonic oxide gas molecules are ionised, whereby the majority become positively charged. A small proportion of the molecules, however, acquire a negative charge by picking up electrons. In the cathodic region the electrostatic repulsion between similarly charged ions greatly reduces the frequency of, or prevents effective collisions, with the result that the rate of combustion is slow, combustion being practically limited to ions of dissimilar charge. But where combustion occurs at a freely sputtering cathode, the cathode zone contains an abundance of metal atoms,* which are probably negatively charged, in addition to gaseous ions and free electrons. The mechanism of combustion at such a freely sputtering cathode proceeds then as follows :—

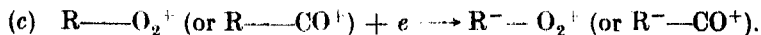
(i) In addition to oppositely charged ions combining directly to form carbon dioxide positive oxygen and carbonic oxide ions separately combine with negatively charged or neutral metal atoms to form neutral or positively charged loose complexes : thus—



or



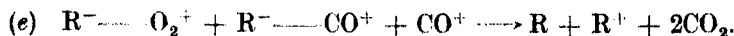
(ii) in the event of (b) the resulting metal-gas complex is virtually neutralised on impact with a free electron : thus—



(iii) The resulting electrically neutral metal-gas complexes combine with each other or with suitable ions to form neutral carbon dioxide and neutral or both neutral and positively charged metal atoms, thus :—

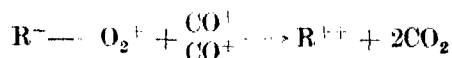


or



* According to Güntherschulze (*loc. cit.*) in the case of silver, for example, one ionic impact with the cathode results in the sputtering of some 30 to 40 silver atoms.

According to the above explanation a reaction of the type



is precluded on the grounds of electrostatic repulsion. Further, it may be concluded from the fact that the c/i value is so low in the case of non-sputtering cathodes that similarly charged oxygen and carbonic oxide ions do not combine directly, and further that combustion does not take place between, say, oxygen ions and neutral carbonic oxide molecules, or between neutral metal-gas complexes and neutral gaseous molecules.

The return to the cathode of by far the greater proportion, indeed, under the conditions of our experiments (relatively high gas pressures, *i.e.*, above 30 mm.) the whole of the sputtered metal, is readily explained. Metal atoms, which become positively charged in the cathode zone as a result of bringing about the union of positive carbonic oxide and oxygen ions, will be drawn back to the cathode under the influence of the intense electrical field, assisted by the powerful drift towards the cathode of positive gaseous ions, which also accounts sufficiently for the return of uncharged metal atoms. Thus, whilst combustion in the electric discharge is primarily determined by a prior ionisation of both gases, the union of suitable ions of like charge requires that the electrostatic repulsion between such ions be overcome or counteracted by some other force or agency producing an opposite effect. This is the rôle played by sputtered metal atoms when they virtually neutralise the charges on ions with which they form loose complexes. Other such forces or agencies producing a similar effect are, as has been shown in Part II, moisture, the presence of which reduces the least igniting current of electrolytic gas, and pressure which we have shown to be hyperbolically related with the least igniting current.

At a meeting of the Royal Society in March, 1926, Sir Ernest Rutherford suggested that an attempt might be made to relate cathodic combustion with current in terms of fundamental units. Since, however, such combustion is not confined to a surface but takes place throughout a body of gas within the confines of the cathode zone, such a calculation necessarily involves the making of certain assumptions.

Thus, if it be assumed that (i) the current as measured by the milliammeter be wholly due to electrons leaving the cathode and traversing the cathode zone; (ii) the number of oxygen and carbonic oxide positive ions, in the proportion of 1 to 2, formed in the cathode zone as a result of the passage of each electron be given by the cathode potential fall (say, 350 volts) divided by the

mean ionisation potential of oxygen and carbonic oxide (say, 13.5 volts); and (iii) all ions thus generated combine to form carbon dioxide, then, since a current of 1 milliampere maintained during 1 minute corresponds to the passage through the cathode zone of $3.77 \cdot 10^{17}$ electrons which should, in accordance with the above assumptions, produce $97.76 \cdot 10^{17}$ ions of oxygen and carbonic oxide, the calculated value of the c/i ratio is 0.36. The fact that this calculated value is of the same order, though somewhat greater than that experimentally obtained at cathodes of the freely sputtering class of metals, lends considerable additional support to the view put forward above in explanation of the mechanism of the cathodic combustion of dry carbonic oxide.

Further, by taking into account the rôle played in cathodic combustion by sputtered metal particles as previously outlined, a similar result can be arrived at independently of the above assumptions. Thus, Güntherschulze found that, under the most favourable conditions for the complete loss of metal by sputtering, the maximum complete loss amounted to only 7 per cent. of the total metal sputtered, the remaining 93 per cent. being returned to the cathode. We have carried out the following experiments on the sputtering of silver:—

A weighed silver wire, No. 18 S.W.G. and 2.5 cm. long was suspended axially in a 4 cm. diameter glass vessel, fitted with an anode of copper gauze and evacuated to between 0.01 and 0.001 mm. A steady direct current discharge was then passed for definite periods after each of which the loss in weight of the silver wire was determined. According to Güntherschulze (*loc. cit.*) the conditions of these experiments were extremely favourable to complete loss of silver by sputtering. The results of these experiments are given below in Table III.

Table III.

Time in minutes.	Current in milliamperes.	Weight loss in gram.
60	2.18	0.0131
60	2.18	0.0133
30	1.46	0.0049

The mean of these results shows that the complete loss to the silver cathode by sputtering due to the passage of 1 milliampere during 1 minute amounted to 0.000106 gr. According to Güntherschulze the total amount sputtered must have been 0.00151 gr., of which 93 per cent. was returned to the cathodes the net loss of silver from the cathode being 7 per cent. (0.000106 gr.). If, in

accordance with the explanation of the mechanism of cathodic combustion advanced above, it be now assumed that (i) a surplus of oxygen and carbonic oxide ions are generated within the cathode zone ; (ii) the formation of two molecules of carbon dioxide requires the presence of either (a) two or (b) three sputtered metal particles ; and (iii) each such metal particle, having fulfilled its rôle of bringing about combustion by overcoming electrostatic repulsion between ions of similar charge, returns to the cathode without further assisting combustion, then, since 0.00151 gr. silver, corresponding to $8.48 \cdot 10^{18}$ atoms, are sputtered by 1 milliampere flowing during 1 minute, in the event of (a) $8.48 \cdot 10^{18}$ molecules or 0.313 c.c.m. of carbon dioxide at N.T.P. are formed. Hence $c/i = 0.313 \cdot \frac{3}{2} = 0.47$; or, (b) in the event of 3 atoms of silver being necessary to form 2 molecules of carbon dioxide, then the calculated value of $c/i = 0.313$, which is in fairly close agreement with the value of $c/i = 0.29$ experimentally obtained at a silver cathode.

Finally, by taking into consideration another fact established by Güntherschulze and von Hippel and Blechschmidt a similar result can be arrived at independently in another way. These observers showed that between 30 and 40 silver atoms were sputtered as a result of a single impact of a positive ion upon the cathode. Taking the mean of these two values, and assuming that (i) the cathode zone contains an excess of positive ions ; (ii) the current as measured by the milliammeter be absolutely given by the number of positive ions arriving at the cathode ; and (iii) either (a) 2 or (b) 3 sputtered metal atoms are required for the formation of 2 molecules of carbon dioxide, then, since a current of 1 milliampere maintained throughout 1 minute records the arrival of $3.77 \cdot 10^{17}$ positive ions at the cathode, and hence the sputtering of $35 \cdot 3.77 \cdot 10^{17}$ silver atoms, the calculated value of c/i in the event of (a) is 0.731, and (b) 0.487 if three sputtered silver atoms act in the formation of 2 molecules of carbon dioxide.

The fact that the above three independent methods of calculating the c/i ratio for the cathodic combustion of carbonic oxide all give results which are of the same order as those experimentally obtained must be regarded as strong support of the views on cathodic combustion which we have put forward and outlined above. Indeed, the calculated results enable the conclusions previously arrived at to be extended in so far as the following probable conclusions may be drawn therefrom, namely, that (i) only a proportion of the ions formed within the cathode zone combine ; (ii) some of the sputtered metal atoms are returned to the cathode without having assisted in promoting combustion ; and finally (iii) the formation within the cathode zone of two molecules

of carbon dioxide from positive ions of carbonic oxide and oxygen requires the assistance of three atoms of sputtered metal.

Summary.

In the foregoing experiments it has been shown that :—

(i) An electric discharge can be passed through dry carbonic oxide “detonating gas” in such a manner that combustion takes place at a rate which is determined solely by the current passed by the discharge.

(ii) Over a considerable range of gas pressure, gap width and current, combustion is purely cathodic, *i.e.*, confined to the cathode zone.

(iii) The rate of such cathodic combustion is directly proportional to the current.

(iv) Such cathodic combustion is nearly independent of the gas pressure, but depends upon the cathode material.

(v) Under suitable conditions of gas pressure, gap width and current, combustion of the dry “detonating gas” occurs in the interelectrode zone, such combustion being proportional to the current and superposed upon the aforesaid cathodic combustion.

(vi) Combustion at cathodes consisting of freely sputtering metals is more vigorous than at poorly or non-sputtering metals.

(vii) The cathodic potential falls in dry “detonating gas” at the different metals examined vary between 320 and 375 volts, and are practically independent of the gas pressure.

From these facts it may be concluded that (i) the combustion of dry “detonating gas” in a direct current discharge is primarily determined by the ionisation of both the constituent molecules of the gas ; (ii) in the cathode zone both negative and positive ions are formed, but mainly the latter ; (iii) suitable ions of opposite sign combine directly to form carbon dioxide ; (iv) electrostatic forces of repulsion keep apart and prevent combination of ions of like charge, unless they are counteracted by some other force or agency producing an opposite effect ; (v) one of these are negatively charged metal atoms sputtered from the cathode which, by forming electrically neutral metal-gas complexes with positive ions, overcome the aforesaid electrostatic repulsion, whereby sufficiently close approach of ions of like charge is rendered possible and combustion takes place. Another such agency is, as we have found, pressure or the presence of moisture.

The results of three calculations on independent lines of the ratio of the rate

of cathodic combustion of dry detonating gas to current, based upon certain simple assumptions and the facts hitherto established by us in regard to such combustion, and by others relating to the cathodic sputtering of metals, are in such close agreement with the values experimentally determined and set forth above that they afford strong support of the conclusions arrived at.

One of us (D.L.H.) wishes to thank the London County Council for a grant which has enabled him to devote his full time to this research.

The Connection between the Zig-Zag Structure of the Hydrocarbon Chain and the Alternations in the Properties of Odd and Even Numbered Chain Compounds.

By ALEX MÜLLER.

(Communicated by Sir William Bragg, F.R.S.—Received April 3, 1929.)

X-ray investigation* of a single crystal of $n\text{-C}_{20}\text{H}_{42}$ has shown that the CH_2 -groups of the chain molecule lie equally spaced on two parallel rows, the lines between successive centres thus forming a zig-zag. Analysis of X-ray photographs of similar substances leaves no doubt that the same chain persists not only through a whole series of hydrocarbons, but is also present in a large number of other carbon chain compounds. The object of this paper is to show how a number of observations on their physical properties are connected with the zig-zag structure of the chain molecule.

The following fig. 1 represents a section through a crystal. X-rays show that

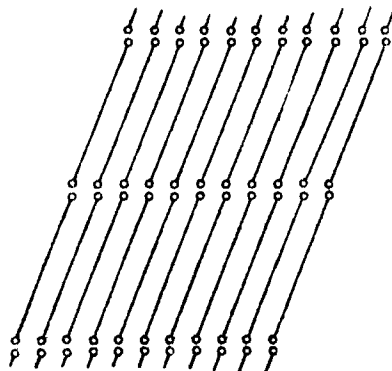


FIG. 1.

* 'Roy. Soc. Proc.,' A, vol. 120, p. 437 (1928).

the chains lie side by side, the parallel lines in the drawing being the chain axes. The ends of the molecules, marked by small circles, arrange themselves in equidistant parallel layers. In the following deductions we consider molecules in which the two end groups are chemically identical, such as hydrocarbons, dibasic acids, etc.

It is impossible to see from this simple model why the odd and even numbered substances should have alternating physical properties. The difficulty, however, disappears when the zig-zag chain structure is introduced into the model.

The following fig. 2 shows the two types of an odd and an even numbered

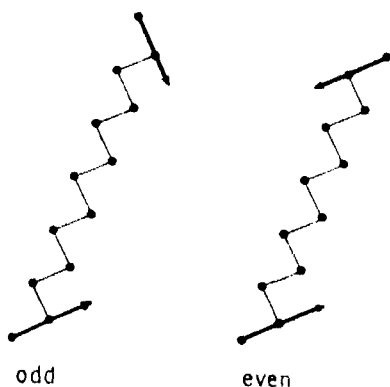


FIG. 2.

chain molecule. The CH₂-groups are marked by black circles. The lines connecting the two last groups in each drawing (marked by arrows) are parallel in the even, and not parallel in the odd numbered chain. This is an important point to remember.

How the molecules link together at their ends is the question which next arises. X-ray investigation of the hydrocarbon C₂₉H₆₀ has shown that the two nearest molecules join so as to have a centre of symmetry. It is assumed here that this type of linkage exists in all chain compounds both odd and even. This must be correct provided the crystals have chains of such length that there is no appreciable interaction between the end groups of each molecule, and provided moreover the chain axes are at right angles to the end layers. For short chains and inclined axes we no longer expect to find a strictly centrosymmetrical linkage, but at least something approaching it.

It is interesting to see that this centrosymmetrical linkage is to be expected if the end groups are electric—or magnetic dipoles. If two dipoles join as shown in fig. 3, the arrangement has centrosymmetry.

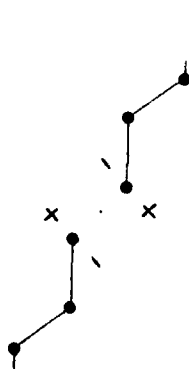


FIG. 3.

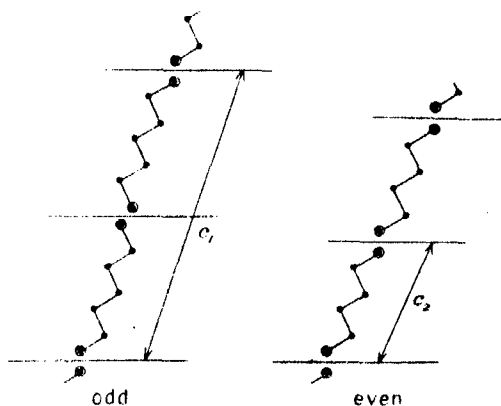


FIG. 4.

Fig. 4 shows the arrangement of even and odd numbered molecules according to the principles given above. The horizontal lines indicate the positions of the successive end layers.

The rings at the ends of each chain represent the end groups. The drawing shows that there is an essential difference between the odd and even numbered arrangements. The first pattern repeats itself every second molecule as we move in the direction "*c*." In the second pattern all the successive molecules are identically situated. The period of repetition is marked by the long arrows c_1 and c_2 . In the actual crystal one expects therefore to find two molecules to lie along the "*c*" axis in those crystals which are built of odd numbered chains, and only one molecule in crystals containing even numbered molecules.

This conclusion agrees with the results of a recent investigation on the dibasic acid series by Dr. Caspari.*

Certain features of the crystal habit of these long chain compounds will next be discussed with the aid of the model. The following fig. 5 shows the arrangement of the molecules in the two types of crystals.

The chain axes are here represented by fine straight lines, the arrows at the ends of the chains are end groups. The diagram shows again the essential difference between the odd and even substances. In the even series all the end layers are identically situated, *i.e.*, they can be brought into coincidence by a parallel shift in the direction B_2B_3 . This no longer holds for the odd number series. Here there are two types of layers. The first layer I in the diagram is identical with III; V ... and the second layer II is identical with

* 'J. Chem. Soc.,' p. 3235 (1928).

IV; VI I and II cannot be made to coincide by a parallel shift. Therefore all the odd members of a series and all the even members of a series are

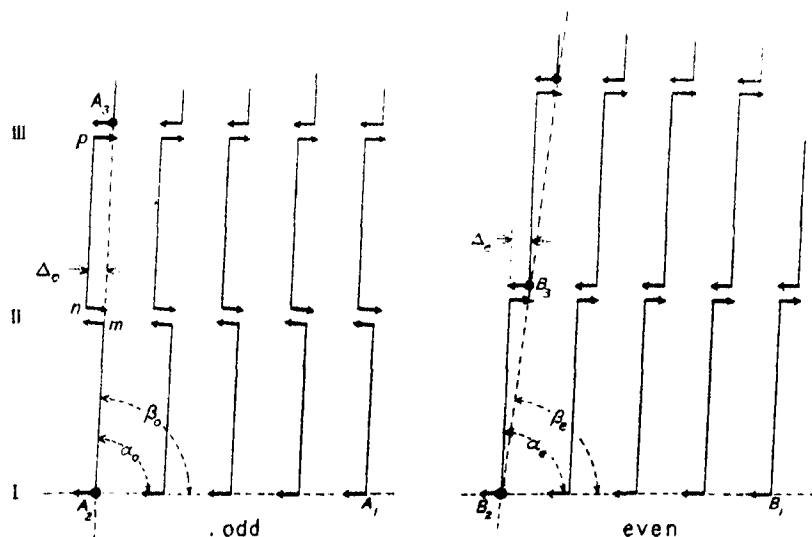


FIG. 5.

similar amongst themselves. Between the odd and the even members, however, there exists a distinct structural difference which has its origin in the peculiar structure of the chain. This difference must be responsible for the alternations of the properties between the odd and the even numbered substances.

An explanation of the behaviour of the β -angles can now be suggested.

In fig. 5 the angles β_o and β_e are quantities which can actually be observed, and measured either directly with a crystalgoniometer, or indirectly by using X-ray data. Supposing we deal first with substances whose chains are so long that the mutual influence of the end groups at each end of the molecules is negligible, and whose β -angles are nearly 90° . The angles α_o and α_e between the chain axes and the basal planes A_1A_2 , B_1B_2 are then no longer dependent upon the chain length, and according to the diagram we expect to find that the β_o angle in the odd number series to be constant, *i.e.*, independent of the chain length. This does, however, not hold for the even series, and the reason for this can be seen in the diagram. The chain axes are separated by an amount Δ_o or Δ_e as shown in the drawing. Supposing we start from A_2 and follow the line A_2mnpA_3 . A_2 and A_3 are identical points in the lattice, and the angle β_o measures therefore directly the inclination of the chain axes relative to the basal plane, *i.e.*, it is identical with α_o . In the second drawing which refers

to the even numbers β_e is no longer identical with α_e and depends both upon the chain length and the quantity Δ_e . The β -angles must therefore behave differently in the odd and the even series. As the chains become shorter we expect to find a gradual change in both α_o and α_e to take place. Superposed on this will be the effect which has just been discussed. We expect that the β -angles in both the odd and the even series will undergo a gradual change as we ascend the series but they will alternate, *i.e.*, they must lie on two separate smooth curves.

This conclusion again describes exactly the observations in the dicarboxylic acid series (*loc. cit.*).

It has been known for a long time that the melting points of chain compounds alternate as shown in the following fig. 6. It is now quite easy to give a reason for this.

If the structures of the odd and the even substances differ from each other as has been shown in this paper, then their corresponding lattice energies will also be different, and their melting points will behave as indicated in the above diagram. Similar things will happen for other physical constants. The molecular volumes and the heat of crystallisation

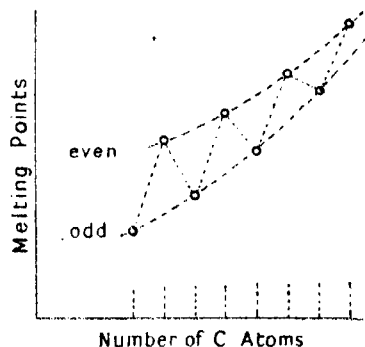


FIG. 6.

alternate in the fatty acid series. This has been shown by W. E. Garner* in his very interesting work on the properties of chain compounds.

A numerical calculation of the lattice energies is at present not possible. Too little is known about the forces which hold these substances together. A more detailed experimental study will perhaps help to see deeper into the nature of the forces. An account of some new observations will appear shortly.

In conclusion, the writer wishes to thank Sir W. Bragg for taking a friendly and encouraging interest in this work.

* 'J. Chem. Soc.,' vol. 125, p. 881 (1923) and vol. 127, p. 720 (1925).

On the Stability of Unimolecular Films. Part I.—The Conditions of Equilibrium.

C. G. LYONS and ERIC K. RIDEAL, Laboratory of Physical Chemistry, Cambridge.

(Communicated by Sir William Hardy, F.R.S.—Received March 12, 1929.)

Of the factors which determine the state of equilibrium of a unimolecular film on the surface of water the two which have been subjected to the most exhaustive examination are the effects of changes in temperature and pressure. In previous communications a generalisation of the effects of kinetic agitation on the state of a film,* and the conditions of equilibrium imposed by the phase rule on the various states of such films† have been described. As pointed out originally by Hardy,‡ in film formation the magnitude and direction of the adhesional forces between the surface and the polar "heads" of the spreading molecules is one of primary importance. The effects of replacement of one type of polar head by another have been examined in detail by numerous investigators; but the effect on the state of a film of one substance of changing the magnitude of this adhesion, a factor clearly as important as the conditions of temperature and pressure, has not hitherto been considered. In these communications the results of an investigation on the effects of such a change are described.

Unimolecular films of long chain fatty acids on the surface of water can exist in three well-defined states, the highly dispersed or vaporous, the expanded and the condensed. The expanded state, first noted by Labrouste, was considered originally by Adam to be vaporous in character. Schofield and Rideal (*loc. cit.*), however, from an examination of the isothermals of the force area curves for a series of acids concluded that expanded films behaved as liquids rather than as vapours, and further, calculated that the true vapour pressure of a film of myristic acid at ordinary temperatures should be about 0.2 dynes per centimetre. A similar suggestion was made independently by Langmuir and later accepted by Adam,§ when with a sensitive apparatus he effected the measurement of the vapour pressure of expanded films, which

* Cf. Schofield and Rideal, 'Roy. Soc. Proc.,' A, vol. 110, p. 167 (1926).

† Cf. Cary and Rideal, 'Roy. Soc. Proc.,' A, vol. 109, p. 301 (1925).

‡ 'Roy. Soc. Proc.,' A, vol. 88, p. 303 (1913).

§ Langmuir, "Third Colloid Symp. Monog.," p. 48 (1925); Adam and Jessop, 'Roy. Soc. Proc.,' A, vol. 110, p. 423 (1926).

proved to be in good agreement with that predicted by Schofield and Rideal. It seemed probable that expanded films consist of some arrangement of tilted molecules with the chains still enmeshed and the heads free, as suggested by Schofield and Rideal and Langmuir. Adam*, however, has concluded that the heads adhere to one another with sufficient tenacity to render this view improbable.

In addition to this difference of view in respect to the nature of the expanded film, there is likewise no unanimity of opinion as to the structure of the condensed state.

Langmuir and Adam† noted that on acid solutions the force area curve of a condensed film of palmitic acid differed from that on an alkaline solution. The latter observer found that on solutions more alkaline than P_H 5.5 a force area curve consisting of only one straight line was obtained. On solutions more acid than P_H 5.0 the force area curve consisted, however, of two straight lines (fig. 1), the film at low pressures being more compressible and occupying larger areas than at higher pressures. Langmuir attributed this increased compressibility and area at low pressures to an increase in size of the head group, by adsorption of hydrogen ions from the underlying solution, accompanied by an increase in mobility of the film. Adam concluded that the two states of the film corresponded to the packing of the heads and chains respectively, and evaluated the areas of different "head" groups. Hartridge and Peters and later Egner and Hägg‡ suggested that the two forms of film corresponded to the unionised and ionised states of the head group. We may note, however, that these two forms of film are obtained with substances for which a similar explanation is impossible.

Both Langmuir and Adam observed that films on weakly acid solutions are much less stable, and tend to contract spontaneously. Görter and Grendel§ have repeated this work, but the behaviour of the films and the limiting areas described by these authors differ in almost every respect from those of the other workers in this field.

Finally we may note that Müller|| in his analysis of crystals of fatty acids by means of X-rays, suggested that in a condensed film the molecules might

* 'Roy. Soc. Proc.,' A, vol. 117, p. 533 (1928).

† Langmuir, 'J. Amer. Chem. Soc.,' vol. 39, p. 1848 (1917); Adam, 'Roy. Soc. Proc.,' A, vol. 99, p. 33 (1921).

‡ Hartridge and Peters, 'Roy. Soc. Proc.,' A, vol. 101, p. 348 (1922); Egner and Hägg, 'Phil. Mag.,' vol. 4, p. 667 (1927).

§ 'Proc. K. Akad. Wet. Amsterdam,' vol. 29, p. 1062 (1926).

|| 'Roy. Soc. Proc.,' A, vol. 114, p. 542 (1927).

be inclined at a constant angle to the surface, and not vertically orientated ; and that the cross section of the molecule as defined by Langmuir and Adam was the projected cross sectional area of the tilted molecule. Müller could find no significant cross section corresponding to the head area as defined by Adam.

One of the most convenient materials for the purpose of this investigation was found in palmitic acid, for which substance the adhesion of the polar carboxylic group for the underlying solution can readily be altered by a change in the hydron concentration of the solution. Such alterations are found to affect the crystal equilibrium spreading pressures, and the states of the film at different temperatures and pressures are found to be determined by the magnitude of this adhesion. An examination of these changes is found to lead to a more detailed picture of the structure of the films than is possible from a consideration of the effects of variation in temperature and pressure alone.

The Force/Area Curves of Palmitic Acid.

Experimental.—For the study of the force area curves of palmitic acid on the surface of solutions of different acidity a trough apparatus of the type described by Adam and Jessop and sensitive to 0.25 dyne per centimetre was employed.

Kahlbaum's palmitic acid recrystallised from hot alcohol and melting sharply at 62.5° C. was employed. The buffer solutions were made up with grease-free water from the directions given by Clark.

The results of these determinations are shown in the following diagram, in

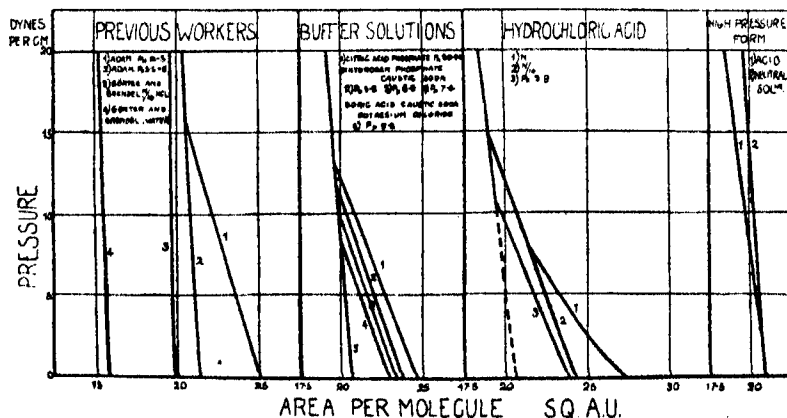


FIG. 1.—The Force/Area Curves for Palmitic Acid.

which are included for comparison the curves previously obtained by Adam and Görter and Grendel (*loc. cit.*).

It will be noted that the results of Görter and Grendel could not be reproduced, but that the few data previously published by Adam are substantiated. In the table are given the values of the limiting areas per molecule of the condensed film of palmitic acid as found by different observers.

Table I.—Molecular Area in A.U.² Extrapolated to Zero Compression.

Author.	State I.	State II on N/10 HCl.	
Adam	21.1 20.4	25.0 —	Early values. Later corrected value.
Görter and Grendel	15.0 on water 21.0 on acids	None None	
Müller	20.5	—	X-ray investigation on crystals.
This investigation	20.6	24.4	

The value obtained for the limiting area in the compressed state is in good agreement with Adam's later and corrected value. The existence of the two states of the film noted by Langmuir and Adam has been confirmed, but the very sudden change in type of curve noticed by Adam between P_H 5.0 and P_H 5.5 was probably fortuitous, since these curves reveal a gradual transition between one form and the other.

The high pressure state of the film is obtained on all solutions provided the pressure is high enough, and under ordinary conditions is definitely solid, transition to the liquid form taking place either at pressures coincident with or very close to the point of intersection of the force/area curves of the two states of the film.

The high pressure region of the force/area curves is practically independent of the nature of the underlying solution. It, however, increases very slightly in steepness as the solution becomes more alkaline, though the area at zero compression remains unaltered. The resistance to compression is a direct measure of the magnitude of the cohesive forces between the molecules; and the slight increase in compressibility on the more alkaline solutions shows that the strength of these cohesive forces is increased if the attraction of the polar head-group of the molecule for the surface be increased by increasing its alkalinity. It is to this increase in cohesion when the forces of attraction are increased, that we may attribute the much greater tendency

of the molecules to orientate themselves parallel to one another on alkaline solutions.

It will be noted that the properties of the film are influenced by the composition of the surface layers of the solution rather than by the bulk composition. Thus a capillary active citric acid-sodium phosphate buffer solution over a range P_H 3.2-7.6 gives force/area curves identical with those obtained on 0.1 N hydrochloric acid, whilst a potassium hydrogen phosphate caustic soda buffer solution gives a series of transitional stages between P_H 5.8- P_H 7.4.

The more easily compressible form of the film is only obtained at low pressures and on solutions whose surface layers are definitely acid. On such surfaces the acid is practically unionised and it seems that the ionised acid has little tendency to form this liquid condensed film. The significance of this observation will be discussed in Part II in the light of the results of equilibrium spreading pressure measurements obtained on similar solutions.

The Collapse of the Film on Acid Solutions.

The equilibrium pressures between the collapsed film and the residual unimolecular film have been measured on several solutions. These values were obtained by passing round gradually narrowing hysteresis cycles with long waiting before pressure readings were taken. Owing to the slowness of the transition between the two states they are, however, subjected to an error of about 1 dyne per centimetre. The following values were obtained (Table II).

Table II.—Equilibrium Pressures between the Unimolecular Film and the Collapsed Film.

Solution.	P_H .	Collapsed film equilibrium pressure.	State of the unimolecular film in equilibrium with collapsed film.
		dynes per cm.	
Hydrochloric acid	1.4	11.0	Liquid
Citric acid	3.1	10.0	"
Phosphate	4.8	12.0	"
Buffer	6.1	16.3	Solid
Water	7.0	Much higher	"

On the more acid solutions these equilibrium pressures are below the pressure at the intersection of the two force/area curves, and therefore the transition may be represented, following Langmuir, by the equilibrium.

Liquid unimolecular film \rightleftharpoons solid multimolecular film. The pressure at which collapse commences is, owing to hysteresis, above this equilibrium pressure but is not constant as was thought by Langmuir. The film sometimes solidifies before collapse commences, but always liquefies as the pressure falls to the equilibrium value.

On more alkaline solutions, however, the unimolecular film in equilibrium with the collapsed film is definitely solid. The equilibrium pressures are here very much higher, which is in agreement with the conclusions drawn above that the solid condensed film is associated with a strong adhesion for the surface.

These equilibrium pressures owing to the small size of the nuclei of the collapsed film are much larger than the equilibrium pressures between macro-crystals of palmitic acid and the unimolecular film (*v. infra*), a phenomenon analogous to the increased vapour pressure exerted by small drops.

The Equilibrium Spreading Pressures.

As was shown by Cary and Rideal (*loc. cit.*), surface spreading from a crystal proceeds to form a unimolecular film until an equilibrium spreading pressure is reached, by measurement of which a direct measure of the attraction of the molecule for the surface is obtained.

The equilibrium spreading pressures of palmitic acid have been measured on a number of buffer solutions, utilising the ring method and chain balance apparatus described by Cary and Rideal. The difference between the surface tension of the solution before and after a film of palmitic acid had attained equilibrium with a few crystals placed on the surface, is taken as the equilibrium spreading pressure, for this equilibrium pressure was independent of the amount placed on the surface. This established the purity of the acid. The apparatus was enclosed in a box with glass windows, and maintained at constant temperature.

On acid solutions spreading proceeds but slowly, in some cases 24 hours being necessary for equilibrium to be attained. The rate of spreading increases rapidly as the alkalinity of the solution rises. Equilibrium is reached practically instantaneously on very alkaline solutions. Thus, the rate of spreading as well as the equilibrium pressure depends to a large degree on the attraction of the polar head group of the acid for the surface of the solution.

The values obtained for the equilibrium spreading pressures are shown in the following curves (fig. 2).

The value obtained at P_H 2.0, viz., 5.5 dynes per centimetre at 21° C., is

in close agreement with the one previously recorded value of Cary and Rideal., viz., 5.7 dynes per centimetre on N/100 HCl.

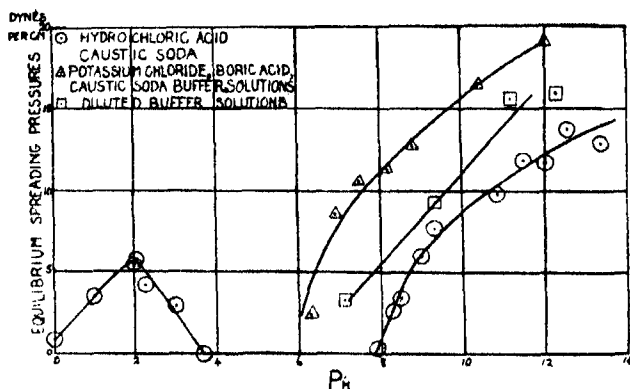


FIG. 2.—The Equilibrium Spreading Pressures of Palmitic Acid at 21° C.

It is seen that there is little tendency for palmitic acid to spread as a condensed film on acid solutions, the maximum pressure recorded (6.0 dynes per centimetre) being very low compared with the pressures reached on alkaline solutions. On acid solutions the film is liquid and of the more easily compressible type possessing a limiting area of 24.4 sq. A.U.

There seems, as a result of observation over 24 hours, to be no measurable tendency for palmitic acid to spread at ordinary temperatures over the surface of buffer solutions of P_H 3.5 to P_H 6.5. Films obtained on these solutions by spreading with the aid of a volatile solvent are therefore unstable, and as was shown above, they tend to collapse with great ease.

On solutions of hydrochloric acid there is a small tendency to spread with a maximum in the spreading pressure at P_H 2.0. This is consistent with Frumkin's* observation that the anion is preferentially adsorbed at the surface of dilute acid solutions, but becomes displaced by the hydrogen ion as the bulk concentration increases.

On alkaline solution the spreading proceeds rapidly, the surface tension falling to a minimum and then rising again to a definite value. The first minimum corresponds to the formation of a solid unimolecular film in the less compressible form of limiting area 20.6 A.U., dissolution then occurs to form, as will be shown later (Part III), a stable bimolecular film. This dissolution gives rise to the later fall in the spreading pressure after the initial spreading is

* 'Z. Phys. Chem.,' vol. 109, p. 34 and vol. 111, p. 190 (1924).

completed. The final equilibrium spreading pressures of these bimolecular films formed on alkaline solutions are very small.

From the curves it will be observed that just as on acid solutions the capillary active citric acid affects the superficial film, so do buffer solutions containing borates yield spreading pressures different from those given by caustic soda of identical P_H . The borate ion is adsorbed at the surface and increases its apparent alkalinity. The effect of dilution of the buffer solution whilst maintaining the P_H constant confirms this view.

We may conclude from these changes of spreading pressure with the P_H of the solution, that the attraction of the molecule for the surface is greatly influenced by the acidity or alkalinity of the medium, and is very low for surfaces of an acidic character.

The Latent Heats of Spreading.

This variation in the force of attraction with the P_H of the medium should be accompanied by a parallel change in the latent heat of spreading from a crystal to a unimolecular film. The decrease in free energy on spreading over an alkaline surface should be greater than that accompanying spreading over an acid surface.

The equilibrium pressures have accordingly been determined on potassium chloride, caustic soda, borate buffers at two different temperatures, and compared with those obtained above at 21° C. The latent heats of spreading were then calculated therefrom with the aid of the modified Clapeyron equation

$$\frac{dF}{dT} = \frac{\lambda}{T(A_2 - A_1)}$$

where λ is the latent heat of spreading, F the equilibrium of spreading pressure, and A_2 and A_1 the molecular area in film and crystal respectively. The equilibrium spreading pressures are given in the following table.

Table III.

P_H .	Temperature ° C.	Equilibrium spreading pressures in dynes per centimetre on the surfaces of buffer solutions containing boric acid potassium chloride and caustic soda.
8.2	27	18.0
8.9	27	18.2
9.0	27	18.2
9.9	26	22.4
8.8	38	29.7
9.5	37	30.6
9.6	39	29.7
11.4	40	30.6

On the very alkaline solutions at high temperature the rate of solution of the film is so rapid that the errors introduced into these readings are of the order of 1-2 dynes per centimetre and they must consequently be regarded as less accurate than those obtained at lower temperatures and on less alkaline solutions.

From these data the spreading pressure increases by ca. 10.8 dynes per centimetre for a 10° C. rise in temperature, a value to be compared with 5.8 dynes per centimetre per 10° C. obtained by Cary and Rideal on N/100 hydrochloric acid where the spreading is slow. Taking the experimentally determined values of the areas on these two solutions we obtain :—

Solution.	Area per molecule.	λ calories per gram molecule.
Borate buffer P_H 9	A.U. 20.0	9100
N/100 HCl	24.4	5650

On alkaline solutions the film is solid, while on the acid solution the film is in the liquid condensed state. These values are therefore not strictly comparable. We can, however, determine the latent heats of spreading from crystals into films of different forms, by correlating the equilibrium spreading pressures obtained by Cary and Rideal, with the areas per molecule obtained by a study of the force/area curves for the film at the corresponding temperatures. The values obtained are shown in Table IV.

It will be seen that on acid solutions spreading to form an expanded film requires 8000 calories, for a liquid condensed film 5620 calories and for a solid condensed film 4640 calories. The latent heat of spreading on alkaline surfaces to form a solid condensed film is 9100 calories, a value much larger than the corresponding value on acid solutions. The increased attraction of the molecule for an alkaline surface is therefore, as was expected, paralleled by an increase in the latent heat of spreading over that surface.

These values indicate that a solid condensed film tends to expand first into a liquid condensed and then into an expanded film not only as the temperature increases, but also as the underlying surface becomes increasingly acid. This has been confirmed by indirect observation on the films themselves.

Table IV.

Temperature.	Equilibrium pressure.	Area/molecule.	λ crystal film calories per gram molecule.	State of film.
<i>Myristic Acid on Dilute Acid.*</i>				
° C.	dyne.	sq. Å.U.		
1	0.6	26.3	5910	Slightly expanded from liquid condensed.
5	2.84	26.5	6040	"
10	5.68	28	6490	Partially expanded."
15	8.52	34	8040	Fully expanded.
20	11.36	33	7930	"
25	14.2	32.5	7940	"
30	17.04	32.5	8070	"
<i>Pentadecylic Acid on Dilute Acid.†</i>				
17	13.7	20.2	4660	Solid condensed.
21	16.0	19.8	4610	"
28	19.0	19.5	4660	"
<i>Palmitic Acid on Dilute Acid.†</i>				
18	0.6	24.2	5620	Liquid condensed.
<i>Palmitic Acid on Alkaline Solutions.†</i>				
18	7-18	19.5-20.0	9100	Solid condensed.

* Area measurements given by Adam and Jessop, 'Roy. Soc. Proc.,' A, vol. 112, p. 362 (1926).

† Area measurements given below.

The Transition into the Expanded Film.

It will be noticed (fig. 1) that on N hydrochloric acid the area of the film at zero compression is slightly increased (27.6 sq. Å.U.) compared with the typical area (24.4 sq. Å.U. on N/10 hydrochloric acid) of the liquid condensed film. The film is showing signs of expansion on a surface, which on account of its high acidity exerts but little attraction for the carboxylic head group.

The study of the effect of the attraction for the surface on the expansion of the film has been studied using pentadecylic acid instead of palmitic acid, to avoid the inconvenience of working at high temperatures. The effect of decreasing the number of carbon atoms in the chain is similar to that of increasing the temperature for the original substance.

The force/area curves for pentadecylic acid on hydrochloric acid solutions of varying acidities are shown in fig. 3, while Table V gives the corresponding areas per molecule extrapolated to zero compression.

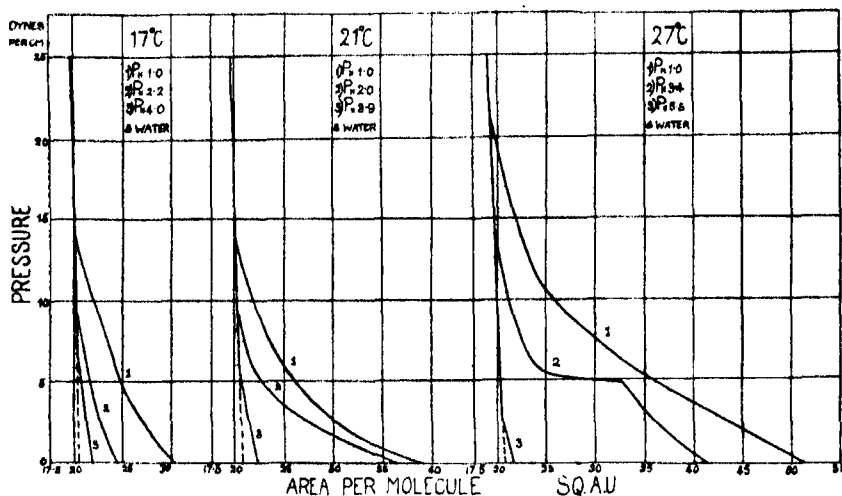


FIG. 3.—The Force/Area Curves for Pentadecylic Acid.

Table V.

Temperature.	P _H .	Area/molecule.	Nature of film.
° C.		sq. Å.U.	
17	1.0	30.2	Partially expanded.
	2.2	24.3	Low pressure form condensed.
	4.0	21.8	Condensed.
	Water	21.8	"
21	1.0	39.5	Nearly completely expanded.
	2.0	37.5	" "
	3.9	22.0	Condensed.
	Water	22.0	"
27	1.0	51.5	Completely expanded.
	3.4	41.6	Nearly completely expanded.
	5.5	21.6	Condensed.
	Water	21.6	"

Inspection of the curves and the table of areas immediately reveals that there is a gradual transition from the expanded state of the film through the liquid condensed form to the solid condensed film, both as the temperature is lowered and as the attraction for the surface is increased. These curves therefore confirm the conclusions which have been drawn above from the latent heats of spreading from a crystal to form each state of the film.

It has been shown that the strength of the cohesive forces between neighbouring molecules runs parallel with the strength of the forces of attraction between the polar head group and the underlying surface. It seems probable that the

transition into the expanded from the solid condensed film is due to the diminution in both these forces. This diminution may be caused either by weakening primarily the cohesive forces, *i.e.*, by raising the temperature, or by weakening primarily the attractive forces, *i.e.*, by increasing the acidity of the surface. That these two methods are substantially identical, has been demonstrated both from the study of the films themselves and from the thermal data for the formation of the films.

Summary.

The force/area curves and the equilibrium spreading pressures of unimolecular films of palmitic acid have been examined on a series of acid and alkaline solutions. It is shown that the tendency to spread into the expanded state is increased by an increase in the acidity of the solution. The latent heats of spreading on acid and alkaline surfaces confirm this view. The conversion of condensed to expanded films by alteration of the hydrogen ion concentration alone has been achieved in the case of pentadecylic acid.

On the Stability of Unimolecular Films. Part II.—The Mechanism of Film Expansion.

By C. G. LYONS and ERIC K. RIDEAL.

(Communicated by Sir William Hardy, F.R.S.—Received March 12, 1929.)

In Part I it was shown that the adhesion of a unimolecular film of a fatty acid to an underlying aqueous solution could be varied by alteration of the hydron concentration of the solution. Increasing the alkalinity effected an increase in the adhesional force of the polar heads, and under isothermal conditions a film could be converted from the expanded to the liquid condensed and even to the solid condensed state, by causing an increase in these adhesional forces, this process being perfectly reversible. Whilst ionisation of the acid occurs over a limited range of P_H , the alteration in adhesional forces by a change in P_H and the effects of such change on the state of the film extend, contrary to the conclusions of Egner and Hägg,* over a much wider range of P_H .

Since contraction and expansion of the film coincide with an increase and

* 'Phil. Mag.,' vol. 4, p. 667 (1927).

decrease respectively in the adhesional forces holding the polar heads to the surface, we may infer that expansion is effected by a gradual tilting of the molecules from the close packed formation existing in the solid condensed state. We have noted that Müller* from X-ray determinations on crystals of fatty acids suggested that it seemed possible that even in a film in the solid condensed state the molecules were already tilted. Objections to this view were raised by Adam,† since he found but one characteristic area for long chain molecules in the solid condensed state, which was, with few exceptions, independent of the nature of the head group. He further found that the area in the liquid condensed state was dependent on the nature of the head group.

Since we conclude from the experiments in Part I that film expansion is due to increase in the angle of tilt, it is necessary to make a more detailed analysis of the structure of a film composed of parallel but not necessarily vertically orientated molecules, to examine how far the objections of Adam to the hypothesis of tilting molecules in a film in the condensed state are valid.

The Solid Condensed Film.

The limiting area of 20·6 A.U. for the solid condensed film has been shown by Adam‡ to be characteristic of a number of substances consisting of hydrocarbon chains and different types of head groups. Two consecutive molecules in a unimolecular film may be represented as in the diagrammatical sketch, fig. 1. Müller§ has shown that the chain consists of a zig-zag arrangement of carbon atoms, the distance between two scattering centres on either side of the molecule being 2·54 A.U.

We will consider stearic acid for which accurate X-ray data exist. The data for the unit cell, which contains four molecules, are given by Müller (*loc. cit.*) as $a = 3·546$ A.U., $b = 7·381$ A.U., $\beta = 63^\circ 38'$. From this we can calculate that the area occupied by two molecules perpendicular to the lengths of the molecule has the dimensions

$$a' = 5·546 \sin 63^\circ 38' = 4·97 \text{ A.U. } b' = 7·381 \text{ A.U.}$$

Applying these results to the sketch in fig. 2 we obtain

$$AB = 4·97 \text{ A.U. and } BC = 2·54 \text{ A.U.}$$

On calculation of the area occupied by one molecule if it stands on the

* 'Roy. Soc. Proc.,' A, vol. 114, p. 542 (1927).

† 'Roy. Soc. Proc.,' A, vol. 117, p. 533 (1928).

‡ 'Roy. Soc. Proc.,' A, vol. 101, p. 452 (1922).

§ 'Roy. Soc. Proc.,' A, vol. 120, p. 437 (1928).

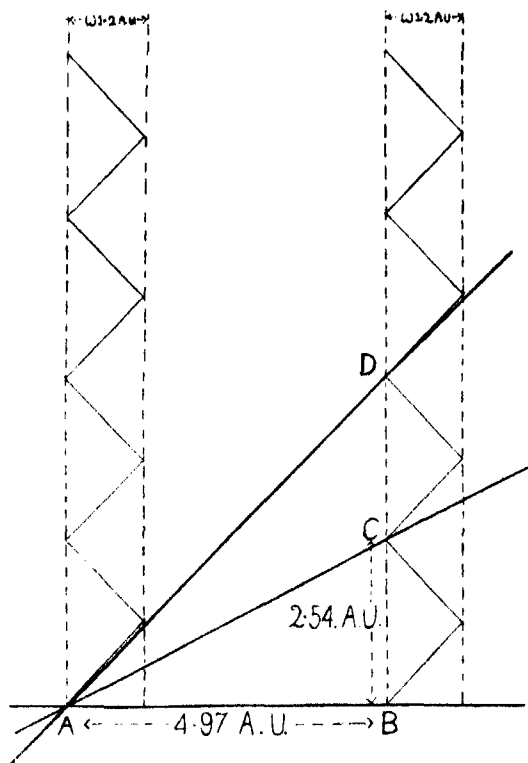


FIG. 1.

plane through BC and parallel to the b axis of the crystal (*i.e.*, perpendicular to the plane of the paper), it is seen that $AC = (AB^2 + BC^2)^{\frac{1}{2}} = (2.54^2 \times 4.97^2)^{\frac{1}{2}} = 5.58$ A.U., which is in good agreement with the 5.546 A.U. of the observed unit cell. The area occupied by two molecules on this plane is $7.381 \times 5.58 = 41.2$ sq. A.U., and the area occupied by one molecule on this plane is therefore 20.6 sq. A.U., which is in very good agreement with the actual area occupied by one molecule in a unimolecular film.

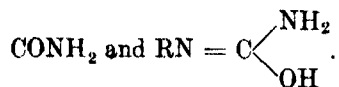
In other words the molecule occupies on the surface of water the area it would occupy on a plane through AC, which is a plane such that relative to the neighbouring chain each chain has moved up a distance equal to two carbon atoms (one whole zig-zag).

It is now possible to explain why there is only one stable position of tilt, which is identical for a large number of molecules with different head-groups. These head-groups are all small in size so that they are unlikely to force the molecules further apart from one another, and they are all asymmetric in

character or asymmetrically attached to the chain. This asymmetry will give rise to a tendency of the molecule to tilt, and in practice tilting occurs such that one chain is moved up relative to the next by one whole zig-zag. This position will be of great stability, for the chains will then once more interlock with one another, for, although the chains are not in contact, their fields of force will vary in a zig-zag manner like the chains themselves. Thus every head-group which has sufficient asymmetry and adhesional force to cause the molecule to tilt at all, will cause it to tilt to this angle at which the chains again interlock, and it would need considerably more force to cause it to tilt to the next stable state, *i.e.*, in the plane AD (fig. 1), in which each chain would have moved relative to its neighbour by a distance of four carbon atoms (two whole zig-zags).

The solid condensed film is therefore pictured as composed of molecules possessing asymmetrically attached head-groups, which are all tilted to such an angle that the zig-zag chains interlock. As this angle depends solely on the structure of the chain, it will be independent of the nature of the head-group unless this is either symmetrical to the chain length or so highly asymmetric that the molecule tilts to the next interlocking position with a relative displacement of *two* whole zig-zags, when the limiting area on the plane AD (fig. 1) will be 26.1 sq. A.U.

Examples of molecules tilted two whole zig-zags of carbon atoms by very asymmetric heads, and thus presenting in the solid condensed film an area of 26.1 sq. A.U. per molecule, are already known; thus Adam* has shown that the long chain ureas give two types of stable and solid films in the high pressure less compressible form having areas at zero compression of 20.8 sq. A.U. and 26.3 sq. A.U. per molecule respectively (values obtained by extrapolation of Adam's curves), the form having the larger area being stable below a certain critical temperature. The areas obtained for these two forms agree well with those calculated, *viz.*, 20.6 and 26.1 A.U. respectively for molecules tilted in the two interlocking positions. The two forms may be ascribed to the different asymmetries of the tautomeric forms of the urea head groups $R - NH -$



Inspection of the drawing (fig. 1) reveals the fact that when the molecule is tilted so that the relative displacement of neighbouring molecules is two zig-zags of the carbon chain, then the first carbon atom in the chain is very close

* 'Roy. Soc. Proc.,' A, vol. 101, p. 452 (1922).

to if not actually in the water surface. It is therefore to be anticipated that compounds possessing a polar substituent in the α position will act as extremely asymmetric molecules, and acquire the tilt corresponding to the relative displacement of two zig-zags of the chain. Adam* gives areas of 26.3 ± 0.5 A.U. for the films of monomyristin and monopalmitin in the high pressure incompressible form. He states that the films are "very viscous liquids," but that "dust on the surface obviously does not move very easily." It is possible, since the compression curves are very steep, that the films are in reality solids of weak rigidity. If this be the case, the observed areas are in excellent agreement with those calculated.

A further search for molecules tilted in this second position has revealed the fact that a long chain amine heptadecylamine gives forms definitely rigid and strong solid films with an area at zero compression of 26.2 sq. A.U., a value again in good agreement with that calculated above.

The force/area curves for heptadecylamine on solutions of various hydrogen ion concentrations are shown in fig. 2.

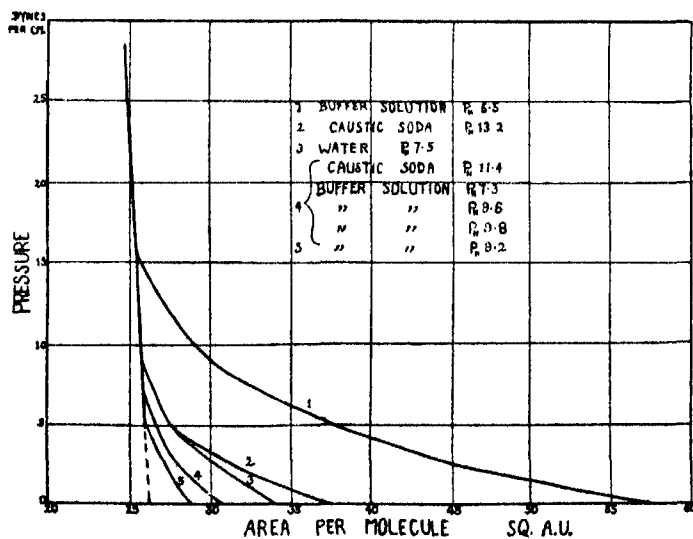


FIG. 2.—The Force/Area Curves for Heptadecylamine at 15° C.

It will be observed that the low pressure form of the film decreases from 37 sq. A.U. on strong alkalis to 28.7 sq. A.U. on moderately weak alkalis, and then expands again on more acid solutions. Solution takes place too readily to obtain force/area curves on solutions more acid than $P_H = 6.5$, but the area

* 'Roy. Soc. Proc.,' A, vol. 106, p. 694 (1924).

per molecule at zero compression is very large on these solutions. The area of the film at zero compression in the liquid condensed state is 30.6 A.U., an area obtained over a considerable range of temperature and alkalinity.

The isohydric point of the amine was found by indicators to be ca. $P_H = 10$, thus it is the undissociated base which yields the most stable condensed films. On very alkaline solutions these films tend to expand in a manner similar to the behaviour of palmitic acid on very acid solutions (*cf.* Part I). Hydroxide and salt formation by the amine, however, causes an expansion, and in this respect it differs from palmitic acid. This may be ascribed to an alteration in the character of the head-group on conversion of the nitrogen from the tri-valent to the pentavalent state. Although experiments were carried out over a very considerable range of temperature (5° C. to 40° C.), no sign of a transition to a solid film of limiting area 20.6 sq. A.U. was obtained. In this respect the amine differs from the ureas, confirming the view that the two areas given by the latter substances correspond to two different tautomeric forms of their head-group.

We may observe that such an arrangement of interlocking chains as has been postulated above is found in the crystal structure of the diamond. The fact that, apart from the two limiting areas of 20.6 sq. A.U. and 26.1 sq. A.U. respectively, corresponding to a relative displacement of the hydrocarbon chains by one and two completed zig-zags respectively, no other areas have been assigned to solid condensed films formed by substances with hydrocarbon and various polar head-groups, present strong evidence for the hypothesis that solid films are obtained only when the molecules have interlocked chains. This interlocking may occur when the displacement of one molecule relative to its neighbour is either one or two whole zig-zags.

It may be noted that the usual picture of a uniform sheet of vertically orientated molecules as constituting a solid film of palmitic acid must on this view be replaced by a sheet of molecules inclined at an angle of 63° 38' to the horizontal. In general these sheets on a large surface will not all be inclined in one direction, so that the sheet will in fact consist of a mottled surface of small patches, the molecules all inclined at the same angle to the vertical, but the direction of the inclination of each patch not necessarily being identical. It can readily be shown that, provided the areas of individual patches are greater than 0.3 μ square, the apparent increase in superficial area per molecule, due to the mutual inclination of two patches at angles of 63° 38', will not exceed 0.1 A.U. per molecule.

The very slow rate of attainment of mechanical rigidity of films of palmitic

acid observed by Mouquin and Rideal* may then be due to a process of re-orientation of these patches to form a uniform surface of like inclined and like orientated molecules.

The Liquid Condensed Film.

It has been shown in Part I that this type like the expanded film is formed from the solid condensed film by successive weakening of the cohesive and attractive forces. The first effect of the weakening of these forces will be that the molecules will lose their crystal-like orientation which they possess in the solid condensed film. This conclusion is confirmed not only by the liquid nature of these films, but also from the X-ray examination of the behaviour of fatty acids on various surfaces. In this way Trillatt† has shown that on an alkaline glass surface the orientation of the molecules all parallel to one another was very strong, while on acid glass surfaces it was more feeble, though still present.

In a solid condensed film, the molecules are caused to tilt by an asymmetry of the head-group, but this tilt is restricted to a certain value at which neighbouring chains interlock with one another. When, however, the forces of orientation between two molecules are diminished, the restriction by interlocking will vanish, and each molecule will be able to tilt at the angle set up naturally by the asymmetry of the head-group.

It is therefore reasonable to suppose that the low-pressure type of condensed film consists of these "freely" tilted molecules. Increase in pressure on these freely tilted molecules will, by increasing the forces between neighbouring molecules, gradually force them into such a tilt that the chains of adjacent molecules again interlock. The transitional stages observed in Part I on almost neutral solutions consist of such a compromise between freely tilted and interlocking molecules. The film will contain molecules in both states and possibly also molecules tilted at an incompletely freed angle.

The observed properties of the liquid condensed film are in close accordance with this hypothesis. It explains the variation in degree of development of this state of the film with the attraction for the surface, which has deprived the so-called "head areas" of Adam of a considerable portion of their significance. For, the degree of free tilting of the molecules depends on the strength of the orientating forces, and these in turn depend on the strength of the attraction of the molecule for the surface.

Further, the absence of an area in the crystalline state corresponding to the

* 'Roy. Soc. Proc.,' A, vol. 114, p. 690 (1927).

† 'Ann. Physique,' vol. 6, p. 5 (1920).

liquid condensed film is now explained, for "freely tilted" molecules could not exist in the solid state which is composed only of completely interlocked molecules.

As has been mentioned above, X-rays reveal that the orientation of fatty acids on acid surfaces, although diffuse, is certainly present. This observation leads directly to the view that in the liquid condensed state the molecules are all freely tilted, but in the main orientated parallel to one another. Such a structure is the two dimensional analogue of the smectic state of liquid crystals, and it is noteworthy that such a state is obtained in long chain compounds, *e.g.*, ammonium oleate. The concept of the liquid expanded state as a two dimensional liquid crystal is in agreement with the properties of such films, and furthermore offers a ready interpretation for their limiting areas.

Our knowledge of the spatial structure of the polar heads of these film-forming materials when immersed in water is extremely scanty. But if it be assumed that in the condition of free tilting the polar head tends to become as deeply immersed in the solution as possible, the direction of the valency bond between the group and the last carbon atom of the chain will be perpendicular to the water surface. We can calculate from the "head areas" determined by Adam the following angles between the valency direction and the chain:—

Head group.	Area per molecule in liquid condensed film.	Angle between long axis of chain and valency direction of polar head.
	A.U.	°
—COOH	24.4*	137.5
—NH ₂	30.6*	127
—OH	21.0	149
—COOR	22.0	147.5
—OCOCH ₃	23.0	144

* Areas of the liquid condensed state obtained in these investigations.

Muller finds that the angle of each zig-zag in the chain lies between 78° and 92°, and the angle between the valency bond uniting two carbon atoms in the chain and the long axis of the chain lies between 129° and 136°. These values are shown in the following diagram (fig. 3).

This speculation suggests that the amino group $\text{C} - \text{N} \begin{matrix} \nearrow \text{H} \\ \searrow \text{H} \end{matrix}$ and the carboxyl group $\text{C} - \text{C} \begin{matrix} \nearrow \text{O} \\ \searrow \text{O} \end{matrix} \text{H}$ are relatively symmetrical, lying almost within the

limits given by Müller for the angle which the $\text{CH}_2\text{-CH}_2$ linkage in the hydrocarbon chain itself, would make with the long axis of the chain; whilst the

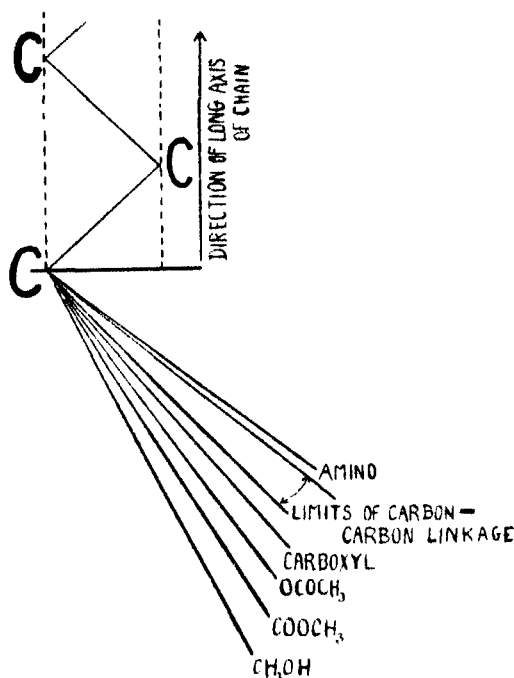


FIG. 3.

long chain acetates and esters lie, as is to be expected, intermediate between the acids and the alcohols; the $\text{-CH}_2\text{-OH}$ group containing an unbalanced hydroxyl group appears to be relatively asymmetric.

It is interesting to compare the above series of increasing asymmetry with the magnitudes of the electric moments of these groups, determined by Williams* from measurements of the dielectric constants:—

Head group.	Angle of tilt, in degrees.	Electric moment, E.S.U. 10^{18} .
C — NH_2	127	+1.5
C — CH_3	129-136	0
C — COOH	137.5	-0.9
C — OCH_3	144	-1.2
C — OH	149	-1.7

* 'J. Amer. Chem. Soc.' vol. 50, p. 2350 (1928).

The parallelism both in sign and in extent of the tilting of the hydrocarbon chain effected by different head groups, as determined from the areas at the position of free tilting with the values of the electric moments of these groups determined from their dielectric constants is extremely close. It will be noted that, as the electric moment increases and becomes increasingly positive in sign, the molecule tends to tilt lower on to the surface of the water.

Ionisation of the amine increases the moment, thus causing the molecule to tilt lower, whilst ionisation of the acid causes a relative decrease in the electric moment, and thus tends to render the molecule more erect.

It is hoped to investigate in more detail the relationship between the magnitude and sign of the electric moment and the state of the film in a subsequent communication.

The Expanded Film.

The two condensed states of films have been shown to correspond to the crystalline and smectic states in three dimensional systems. Further, the transitions between the condensed states through the expanded to the vaporous films has been shown to be a continuous process dependent on the angle of tilt of the molecules on the surface. We must regard this process as the two dimensional analogue of passage from the crystalline through the smectic to the liquid and finally to the vapour state, as the intra molecular cohesion is weakened. The expanded state is therefore to be regarded as a two dimensional liquid in agreement with conclusions drawn from a consideration of the character of FA/F curves. No definite conclusions can be drawn as to orientation of the head group of the molecules or the molecules themselves in this state, since it is probable that the straight chain character of the molecule will be relaxed by free rotation when partial separation and increased tilting takes place.

It seems therefore that we must recognise the existence of two types of forces acting on the molecules, firstly, the attractive forces between the chain and the surface which tend to make the molecule lie flat on the surface, and secondly, the orientating forces tending to make the molecules arrange themselves with parallel chains. The latter forces result from cohesion between neighbouring molecules and the attraction of the polar head-group for the surface.

The properties of the film under any given set of conditions will depend on the relative strength of these forces. If the forces of orientation are strong, the molecules will all be arranged parallel to one another with interlocking chains. If, as is usual, the attractive forces between the head-group and the

surface are sufficiently asymmetric, the molecules will tilt to such an angle that the chains again interlock. This is the arrangement of the molecule in the solid condensed film. As the orientating forces become weakened the asymmetry of the head-group will cause the molecules to tilt freely with the chains no longer interlocking, but still to a large extent parallel to one another. The liquid condensed film is then obtained. If the orientating forces are still further weakened the attraction between the chain and the water surface becomes apparent, and the molecules become more and more free, and tilt lower and lower, the film changing through the truly liquid expanded film eventually into the vaporous film, in which the orientating forces are practically negligible and the molecules are lying flat on the surface.

The gradual transition from the solid condensed film through the liquid condensed and expanded films to the vapour film is thus due to the gradual increase in the angle of tilt of the molecules of the film as their mutual interactions become weakened compared with the attraction of the chain for the surface.

Summary.

The view is advanced that the transition from a solid condensed film through the stages of liquid condensed and expanded to the vaporous state is due to an increasing tilt of the molecules. Factors affecting this tilting of the molecules are the adhesion of the polar head and hydrocarbon chain for the water and the hydrocarbon chains for one another.

It is shown that the two limiting areas of 20.6 and 26.1 A.U. obtained for long chain compounds in the solid condensed state are determined by the interlocking of the chains after relative displacements between neighbouring molecules of two and four carbon atoms respectively, which displacements determine the limits of tilt imposed by this restriction by interlocking in the solid condensed state. The state of the liquid condensed films is compared with the smectic state of three dimensional liquid crystals, and the molecules in the film are considered to be freely tilted in this state. An approximate measure of the asymmetry of various head-groups is made from the limiting areas observed.

The expanded state is considered as definitely liquid in character. The force-area curves of heptadecylamine have been measured and shown to conform with these hypotheses.

On the Stability of Unimolecular Films. Part III.—Dissolution in Alkaline Solutions.

By C. G. LYONS and ERIC K. RIDEAL.

(Communicated by Sir William Hardy, F.R.S.—Received March 12, 1929.)

Introduction.

In the previous communications (Parts I and II) it was shown that the conditions of equilibrium of a unimolecular film of palmitic acid were influenced both by the temperature and the attraction of the polar head-group for the underlying solution, which in the case of the carboxyl group could be altered by changing the acidity or alkalinity of the surface layers of the solution. On alkaline surfaces this attraction increases to such an extent that not only does an expanded film tend to contract to form a condensed film, but actual dissolution may occur. Adam* noticed that condensed films of palmitic acid showed a small slow decrease in area on a solution of P_H 8.5, while on a solution of P_H 10.0 this decrease in area took place so rapidly that he could not obtain force/area curves.

An attempt has been made to examine the mechanism of the dissolution process and to investigate the relationship between the rate of solution and the alkalinity of the underlying solution. The experiments were carried out on an apparatus designed so that the pressure of the film was maintained constant as the film dissolved. As the molecules left the film for the underlying solution the gaps in the film are closed by the pressure, and the area of the film gradually decreases. The factors influencing this rate of decrease in area at constant pressure have been studied.

Experimental.

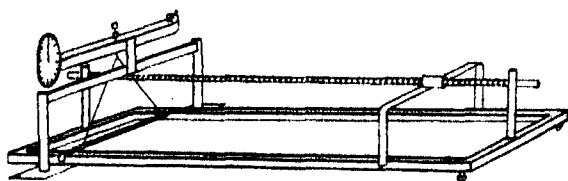
The apparatus consisted essentially of a trough of the type described by Langmuir and Adam and improved by Adam and Jessop. The pressure on the film was measured by a torsion wire apparatus similar to that described by the latter authors.†

The early trial stages of the work were carried out on an iron trough 22 inches long by 6 inches wide by $\frac{3}{8}$ inch deep. To prevent rusting, this trough was covered with a thin coating of paraffin wax by painting with a benzene solution of the wax.

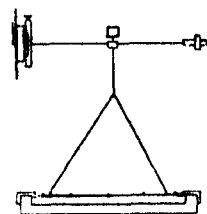
* 'Roy. Soc. Proc.,' A, vol. 99, p. 336 (1919).

† 'Roy. Soc. Proc.,' A, vol. 110, p. 423 (1926).

The later work, however, was carried out in a nickel trough of similar surface dimensions but rather deeper. This was made out of a sheet of soft nickel



General View of Trough Apparatus.



Section through Torsion Head.

FIG. 1.

$\frac{3}{16}$ inch thick, by bending it into the form of the trough and soldering the corners. A rim $\frac{3}{8}$ inch wide was then soldered on to the trough and ground perfectly flat. For some purposes this trough proved rather deep, and it was therefore fitted with a tightly-fitting hollow brass box, occupying about three-quarters of its volume, the small gaps between the brass box and the edges of the trough being sealed with paraffin wax.

The film was placed on the surface of the solution in this trough, and confined between a movable float and waxed glass barriers, resting on the waxed edges of the trough in the manner of the previous workers. The movable float was made of strip copper coated with collodion, and had small vertical pieces of copper attached to its ends, to which the ends of narrow strips of platinum foil ($1/100$ mm. thick) were soldered (fig. 1). The other ends of the platinum foil were soldered to brass Γ shaped strips soldered to the sides of the trough. The platinum foils standing vertically in the surface of the solution acted as effective seals and prevented the film leaking past the float.

The movable copper float was attached to a torsion wire apparatus by a very light triangle made from thin glass capillary tube. This was rigidly fixed by means of metal loops and a little sealing wax to the copper float along the base of the triangle, and by hard wax to a small brass rod along its vertical portion. This small brass rod carried a mirror and was attached to the centre of a fine steel torsion wire whose elastic limit was considerably above any torsion developed in these experiments. By means of the mirror on the rod, a lamp, a vertical scale and a suitable optical system, the position of the float could easily be kept adjusted in its neutral position.

The pressure on the film was measured by the torsion which had to be exerted by the wire to keep the float in its neutral position against the pressure

of the film, which was then read off directly on the torsion head. The apparatus was calibrated as described by Adam and Jessop by a small scale pan attached to an arm, which could, when required, be attached to the brass rod in the middle of the torsion wire.

To study the dissolution process it was necessary to design some method of reducing the film area at constant pressure. For this purpose a long worm gear was arranged horizontally over the centre of the trough and supported by posts at each end (fig. 1). This screw was turned by a wheel attached to its end which was connected by a suitable gearing to an electric motor. A rider travelling on the worm gear carried arms which fitted just over the side of the trough. As the screw was turned the rider moved, pushing along before it the waxed glass barrier which confined the film. By this means the area of the film could be slowly reduced while its pressure was maintained constant.

The whole trough apparatus was contained in a large air thermostat which could be heated to a constant temperature by electrically-controlled heating lamps. The gear moving the barrier confining the film was operated and controlled by an electric motor outside the thermostat which was fitted with glass windows so that the speed of movement of the barrier was easily controlled and read from outside.

The film was spread over the surface in petroleum ether, and its area read by means of a pointer, attached to the moving rider, which travelled over a scale arranged parallel to the length of the trough; and its pressure read directly from the torsion head, being the torsion required to hold the float in its neutral position against the pressure of the film.

When studying the dissolution process, the film was spread over the surface and the torsion head was adjusted to a certain pressure, and the area of the film was then decreased mechanically as described above, keeping the float in its neutral position. The area of the film was then read at small time intervals, and from these readings the rate of decrease in area/area curves were drawn for constant film pressure.

In this way the dissolution process has been followed on solutions of various alkalinities, buffer solutions, especially that containing boric acid potassium chloride caustic soda for solutions less alkaline than $P_H 10.3$ being employed. Typical curves showing the rate of decrease in area for unit area of film with the time are shown in fig. 2 whilst Table I contains a brief summary of the more significant results obtained.

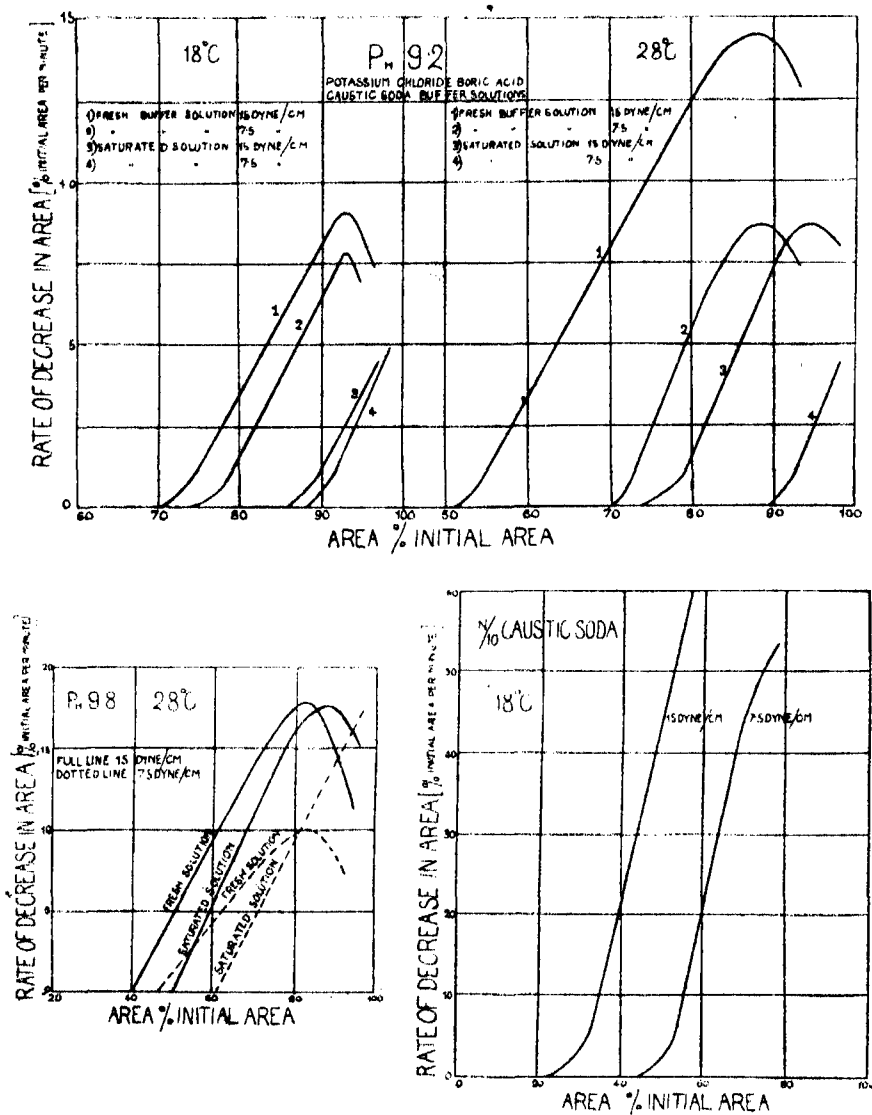


Fig. 2.

It will be seen that the rate of decrease in area is appreciably enhanced by increasing the alkalinity of the solution and the temperature. It is also slightly increased by increasing the pressure.

Inspection of the experimental curves for the rates of solution reveal several interesting features, firstly, that if the film pressure be maintained constant, complete dissolution of the film does not take place but that some form of

Table I.

Boric acid caustic soda potassium chloride buffer solutions.			Maximum rate of decrease in area (per cent. initial area per minute).	
P _H .	Pressure.	Temperature.	Fresh Solutions.	Saturated Solutions.
	dyne/cm ² .	° C.		
9.2	7.5	18	7.8	5.3
9.2	15.0		8.7	4.4
9.5	7.5		8.1	8.2
10.3	7.5		11.6	16.0
9.2	7.5	28	8.7	4.4
9.8	7.5		10.0	17.3
10.3	7.5		> 30.0	> 30.0
8.8	15.0		2.1	1.9
9.2	15.0		14.0	8.5
9.8	15.0		17.9	17.6
10.3	15.0		> 30.0	> 30.0
N/10 caustic soda	7.5	18	> 50.0	
	15.0	18	> 60.0	

relatively insoluble film is left; secondly, that on a fresh buffer solution the dissolution process is initially autocatalytic in nature but that the curves become constant and reproducible after a certain number of experiments have been carried out on the liquid contained in the trough.

The Constitution of the Residual Film.

It is observed that on solutions of alkalinity between P_H 8.5 and 13.0 complete solution of the film does not occur but that some type of insoluble film remains on the surface, the limiting area being dependent both on the P_H of the underlying liquid and on the pressure of the film. Under any given set of experimental conditions these limiting areas are reproducible to within 3 to 4 per cent.

In the following diagrams are shown these limiting areas on fresh buffer solutions and on those which after the solution process has been carried out several times have attained constant and reproducible rates of solution.

These limiting areas are not the product of a collapse phenomenon as observed on acid solutions, for such collapse proceeds invariably to a small and variable area with the production of numerous strain lines. On these alkaline solutions the residual areas are large and definite and can be maintained at constant pressure for several hours, and further, no strain lines can be observed in the film.

It appears that when solution of the film proceeds at various places in the film surface, the molecules of sodium palmitate entering the underlying solution

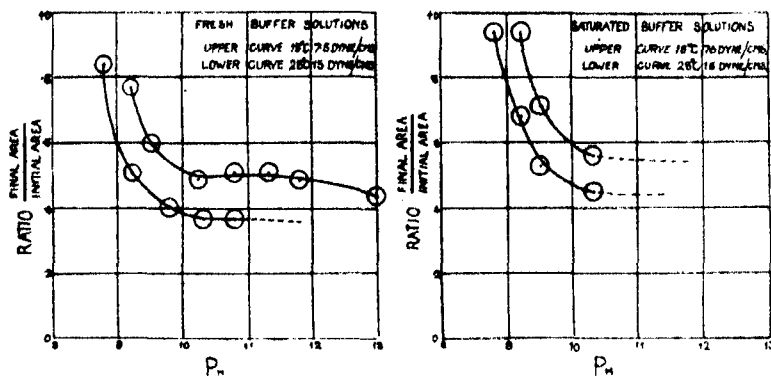
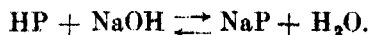


FIG. 3.

protect the residual film from solution. This protection is effected by adsorption of the dissolved molecules at the surface, thus giving rise to a double layer of orientated molecules. We may therefore regard the residual film as a double film of orientated molecules of palmitic acid and sodium palmitate with their polar heads orientated together in such a way that inert hydrocarbon chains are exposed both to the air surface and to the underlying solution. Such a film will show little tendency to dissolve.

If this conception of the mechanism of the dissolution process be correct and if both the top and bottom layers of this bimolecular layer consist of molecules in contact and under the same pressure, the area of the film should be exactly half that of the original film. It is found that the residual film does possess this area within narrow limits over a wide range of P_H 9.5–12 as well as over a considerable range of pressures and temperatures (fig. 3). Buffer solutions more alkaline than P_H 10.3 could not be maintained at constant alkalinity for a sufficient time for them to become saturated. The form of the final area/ P_H curves for these solutions must therefore be obtained from the final areas on fresh solutions.

On relatively acid solutions, however, the limiting area is larger than that corresponding to a bimolecular film, and on alkaline solutions somewhat less. It is clear that the stability of the film is not dependent only on the existence of a close-packed double layer, but must depend on the existence of an equilibrium on the surface of the solution.



On acid and neutral solutions a unimolecular layer of free acid is quite stable. As the alkalinity of the surface layers of the solution increases the equilibrium residual bimolecular film will contain in the underlying layer increasing quantities of sodium palmitate until the complete double layer is formed. This will then be stable towards a relatively great increase in alkalinity of the solution as it is completely protected from the solution by the hydrocarbon chains. This hypothesis as to the nature of the residual film formed on alkaline solutions is supported not only by the well-known fact that the surface excess of soap calculated with the aid of the Gibbs equation $\Gamma = d\sigma/d\mu$ yields value for Γ some twice that of a unimolecular packed film (McBain*) but also by examination of the structure of films of soap bubbles and the composition of froth on soap solutions.

Perrin† concluded from a study of the interference colours on soap films that such films were made up of elementary leaflets, which were composed of a double layer of fatty acid molecules with their polar groups orientated towards one another as they are in a crystal of the acid. This was confirmed by Wells.‡ These authors concluded that the bimolecular layer was composed entirely of fatty acid molecules formed by the hydrolysis of the soap, but Miss Laing,§ from analysis of soap foam, showed that both acid and soap are present, and concluded that the bimolecular layer consisted of an acid sodium soap $\text{NaP} \cdot \text{HP}$, an arrangement more stable than a bimolecular film composed of fatty acid alone.

That an acid soap has greater stability than a soap of any other composition has been demonstrated by studies of soap solutions themselves, *e.g.*, for the palmitate by McBain and Buckingham, for the laurate by McBain and Eaton, and for the oleate by McBain and Stewart.|| Similarly, Ekwall,¶ in an extended study of soap solutions, has shown that a solution of an acid soap of the composition $\text{NaX} \cdot \text{HX}$ has a lower surface tension than a solution of a soap of any other composition. Films of acid soap at the surface of a solution will therefore be of great stability. Harkins** has also concluded by observations on the

* 'J. Amer. Chem. Soc.,' vol. 45, p. 2230 (1927).

† 'Ann. Physique,' vol. 10, p. 160 (1918).

‡ 'Ann. Physique,' vol. 10, p. 69 (1921).

§ 'Roy. Soc. Proc.,' A, vol. 109, p. 28 (1925).

|| 'J. Chem. Soc.,' vol. 131, p. 2679 (1927), vol. 133, p. 2166 (1928), and vol. 131, p. 1392 (1927).

¶ 'Acta Acad. Abo. Math. Phys.,' vol. 6, p. 3 (1927).

** 'J. Amer. Chem. Soc.,' vol. 47, p. 1854 (1925).

surface tension of sodium nonylate solutions that the surface layer consists of both free fatty acid and neutral soap molecules.

The evidence, both from the study of soap films and soap solutions is, therefore, in agreement with the view that the residual film consists of an elementary bimolecular leaflet containing both palmitic acid and sodium palmitate.

The Free Energy of Formation of Bimolecular Films.

In Part I it was observed that when dissolution commenced the spreading of palmitic acid from a crystal involved two distinct phases, the formation of a transitory film of high spreading pressure, followed by a rise in the surface tension to a small but constant spreading pressure. This phenomenon is now readily understood since the unimolecular layers formed initially are not stable, but as we have noted above, go partly into solution to form a stable bimolecular layer.

The equilibrium spreading pressures of these bimolecular films have been determined and are included in the following table.

Table II.—Equilibrium Pressures in Dynes per Centimetre.

Temperature ° C.	P_H .	Unimolecular.	Bimolecular.	Change in equilibrium pressure of the bimolecular film for a 10° C. rise.	
				P_H .	Dynes per cm. per 10° C.
21	8.2	11.6	4.8	—	—
21	8.8	13.1	3.6	—	—
21	9.4	14.5	3.6	—	—
21	9.5	14.7	3.6	8.2	8.5
21	11.4	18.3	3.0	8.8	6.3
27	8.2	18.0	9.7	9.4	4.6
40	8.8	29.7	15.6	9.5	4.2
39	9.4	29.7	11.9	11.4	4.5
40	9.5	30.6	11.5	—	—
40	11.4	36.0	11.7	—	—

The higher values obtained between P_H 8 and 9 for the change in the equilibrium pressure with the temperature of the bimolecular film are due to the fact that on these solutions at low temperatures complete closely-packed bimolecular film is not present in the equilibrium state.

With a mean temperature coefficient for the spreading pressure of the complete bimolecular film of 0.44 dynes per centimetre per ° C. the latent heat

of spreading from a crystal to a bimolecular film may be calculated from the Clapeyron equation

$$\frac{\partial F}{\partial T} = \frac{\lambda}{T(A_{\text{film}} - A_{\text{crystal}})}.$$

Inserting the values $A_{\text{film}} = 10.3$ A.U., $dF/dT = 0.44$ we obtain $= 1870$ calories per gm. molecule, a value considerably smaller than the latent heats of spreading into the various forms of unimolecular film obtained in Part I. The decrease in free energy of spreading accompanying the change from a solid unimolecular film to a bimolecular film on a solution of constant P_H is therefore $9100 - 1870 = 7230$ cal. per gm. molecule.

The Effect of Saturation of the Underlying Solution.

Examination of the curves (fig. 3) shows that the final areas obtained on any one solution increases with the number of films which have been placed on the surface and allowed to dissolve. This increase in area is not indefinite but proceeds until after a certain number of runs, the final area remains constant. Simultaneously corresponding changes in the rate of decrease in area take place, and the curves with successive films are only reproducible when the final area remains constant.

This effect is not due to change in alkalinity of the solution, for the alkalinity as measured by the hydrogen electrode is not detectably different from that of the same solution before any film is placed on the surface. It has been shown to be due to the effect of saturation of the underlying solution with the molecules of the dissolved film. In early runs not all the molecules which are dissolved by the solution will be adsorbed at the surface, but until saturation is reached some will remain in the interior of the solution. The change in area of the early runs is therefore caused not only by the transition of the unimolecular into the more stable bimolecular film, but is also in part due to the passage of molecules from the film into true solution in the bulk of the underlying solution. It is therefore only when the bulk of the solution is saturated that the conversion into a bimolecular film proceeds alone, and not until this saturation is reached will the experimental curves become reproducible.

The Nature of the Autocatalytic Effect.

On fresh buffer solutions the process of dissolution is initially autocatalytic, the rate of decrease in area of the film at constant pressure being determined by an equation of the form

$$dx/dt = K_1 (K_2 - x)x,$$

where x is the amount of bimolecular film formed and K_1 and K_2 are constants.

This equation leads to the parabolic form for the rate of decrease in area/area curves, which is obtained experimentally, as shown in fig. 4 from the

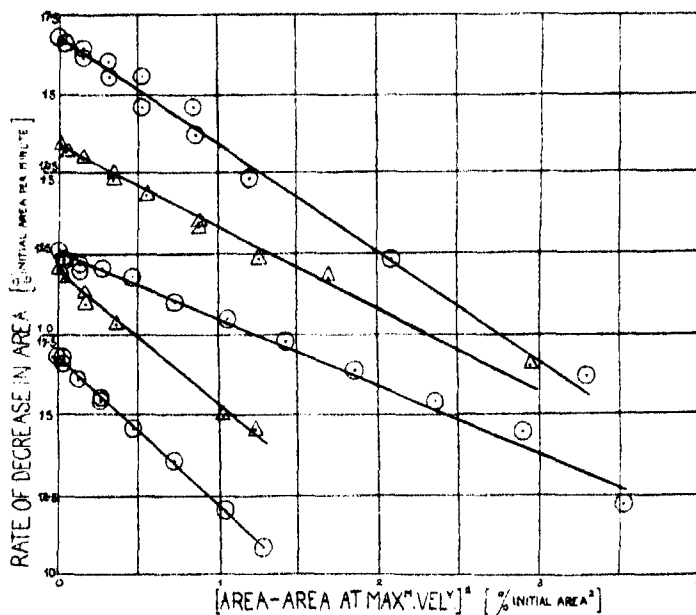


FIG. 4.

straight lines which are obtained by plotting the initial rate of decrease in area against the square of the difference between the area at any instant and the area for the maximum velocity.

In accordance with this equation the rate of transition of the unimolecular to the bimolecular film rises to a maximum. For solutions for which the final area approximates to half the initial area, this maximum is attained when the area is 82 per cent. of the original value, the fraction being independent both of the velocity of dissolution and the final area, as will be seen from Table III which contains details of a few typical runs.

Table III.

Maximum rate of decrease in area, percentage initial area per minute.	Final area, percentage initial area.	Area of maximum velocity, percentage initial area.
1.25	64	83
1.36	50	82
0.71	43	81
1.67	52	82
1.78	51	82
1.75	45	83
0.88	41	81

On the less alkaline solution on which the decrease in area is small the maximum velocity is attained when the area is greater than this value.

During the later stages of the transition, the rate of change decreases in a linear manner with the decrease in area, and the rate at any time is determined by an equation for a unimolecular reaction

$$dx/dt = K (A - x).$$

On saturated solutions, the autocatalytic dissolution tends to decrease, and the linear form predominates, the initial rates increasing considerably.

Solid unimolecular films of the acid, when placed on alkaline solutions with the aid of petrol ether, exist in a metastable state, and solution does not take place until a nucleus is formed. Such nuclei for solution are produced by soap molecules arriving underneath the film forming the eventual lower layer of the double film which is the stable modification. The rate of dissolution thus increases with an increase in concentration of the lower layer, and since on fresh solutions all the molecules in the lower layer must have been derived from the upper film the reaction is autocatalytic. The maximum rate of solution is attained when all the molecules in the top film are within range of contact of molecules in the lower film. The minimum ratio of molecules on the lower film to those in the upper necessary to establish these conditions is one to four, thus giving a maximum rate of solution after 20 per cent. of the top film has entered into solution in agreement with the experimental results. On soap containing solutions the lower film is partly completed with the aid of molecules derived from the solution and the rate of solution accordingly loses its autocatalytic character. Under such circumstances the rate of transition of the unimolecular to the bimolecular layer follows a simple unimolecular law.

Summary.

The rates of solution of unimolecular films of palmitic acid on alkaline solutions have been examined. It is found that over a wide range of alkalinity a new form of film is stable, and it is suggested that this form consists of a bimolecular leaflet, analogous to the elementary leaflet in a soap bubble. On weakly alkaline solutions the lower layer of the bimolecular film is less closely packed than the upper layer, the closeness of packing, however, increases with increasing alkalinity. The process of solution of a unimolecular film commences at nuclei formed by adsorption of soap molecules underneath the surface, and, consequently, when there is initially no soap in the bulk of the solution the dissolution process is autocatalytic in character; with increasing quantities of soap in solution the process loses its autocatalytic character until finally the rate of solution is proportional to the area of unimolecular film left exposed on the surface.

We wish to thank the London County Council and the Department of Scientific and Industrial Research for grants which have enabled one of us (C. G. L.) to take part in these investigations.

The Electrical Condition of Hot Surfaces during the Adsorption of Gases. Part III.—A Platinum Surface at Temperatures up to 850° C.

By G. I. FINCH and J. C. STIMSON.

(Communicated by Prof. W. A. Bone, F.R.S.—Received March 29, 1929.)

Introduction.

The experimental results on the electrical charging of gold, silver and nickel surfaces, as set forth in Parts I and II* of the present series, have led to the conclusion that there are at least five different types of adsorption of a gas on a hot metallic surface, each of which can be clearly defined in terms of the nature of the charge on, and the tenacity with which such charge is retained by, the surface. In three such cases the adsorbed gaseous molecules are in an active, electrically charged condition. Before the full significance of these observations in their bearing upon the nature and mechanism of heterogeneous catalysis can be properly appreciated it will be necessary to accumulate systematically further facts relating to the electrical condition of hot surfaces; and with this object the investigation is being extended to a variety of different surfaces. An account is given below of the experimental results obtained with a platinum surface at temperatures up to 850° C.

Experimental.

The apparatus used and the experimental procedure followed was as previously described.† Platinum specially supplied by Messrs. Johnson and Matthey, and stated by them to contain over 99·5 per cent. Pt and to be free from non-platinum metals, in the form of a 22 S.W.G., 6 by 10 cm. sheet, to which was fused a 25 S.W.G. similar platinum wire, was employed and will be referred to in what follows for the sake of brevity as the surface. The charges were measured by means of a Lindemann quadrant electrometer.

* 'Roy. Soc. Proc.,' A, vol. 116, p. 379 (1927); vol. 120, p. 235 (1928).

† *Loc. cit.* (The surface under investigation occupied a comparatively small section of the furnace, the whole length of which had been previously explored in the usual manner by a thermocouple for uniformity of temperature. The temperature of the zone actually occupied by the platinum sheet in these experiments would not vary from the maximum experimental temperature of 850° C. by more than $\pm 15^\circ$ C.)

Experimental Results.

As found previously in the case of gold, silver and nickel, the charge acquired by the hot surface in contact with any of the gases employed was found to be independent of the gas pressure within wide limits (between 1 and 760 mm.).

In the cases of gold and silver, the surfaces on heating soon settled down to such a condition that the charges on the surface, whether *in vacuo* or in contact with gases, were readily reproducible in successive experiments. On the other hand, the nickel surface at first exhibited certain apparent irregularities in this respect which, however, as described in Part II, disappeared after the surface had been "normalised" by a series of successive oxidations and reductions. The results obtained with the platinum sheet were such as to show that the condition of this metal was even more influenced by its previous history of heat treatment than was nickel. While the full significance of the behaviour of the platinum sheet in our experiments is as yet not clear, nevertheless in what follows the results obtained are set forth in detail because it is highly probable that these observations may help in the future to throw light upon the reason for the frequently observed pronounced differences in the catalysing powers of various platinum surfaces.

Series A.—Preliminary Experiments with the Platinum Sheet up to 500° C.

The platinum sheet and wire were treated with boiling fuming nitric acid and then washed with distilled water, after which treatment the surface was suspended in the vertical quartz vessel, the necessary handling being effected with quartz-tipped pliers. The surface was heated *in vacuo* (below 10^{-5} mm.) at 500° during 7 days. No charge was exhibited by the surface at any time during this period. This unexpected result was repeatedly confirmed in the following manner:—With the insulated surface connected to the electrometer and exhibiting no charge at room temperature a charge of +1.019 volt above the earth potential was impressed upon it by means of a standard cell. The surface-electrometer system was found to preserve the impressed charge practically unimpaired during 1 hour. On earthing and reinsulating the system the charge fell to 0.00 volt and remained at this value. This test was repeated with -1.019 volt impressed on the surface-electrometer system at both room temperature and at 500° with a similar result, showing that the insulation of the system was above suspicion.

At 500°, on admission of hydrogen* to the apparatus, a constant hydrogen

* To a pressure of, in this case, approximately 200 mm. It has been previously shown, however, and repeatedly confirmed in this investigation, that the rate of attainment and magnitude of the charges due to the contact of the hot surfaces with a gas are wholly independent of the pressure of the gas within the range of 1 and 760 mm.

charge of -1.36 volt was acquired by the surface within 60 minutes. The corresponding charge temperature curve, recorded in fig. 1, curve $H_2(1)$,

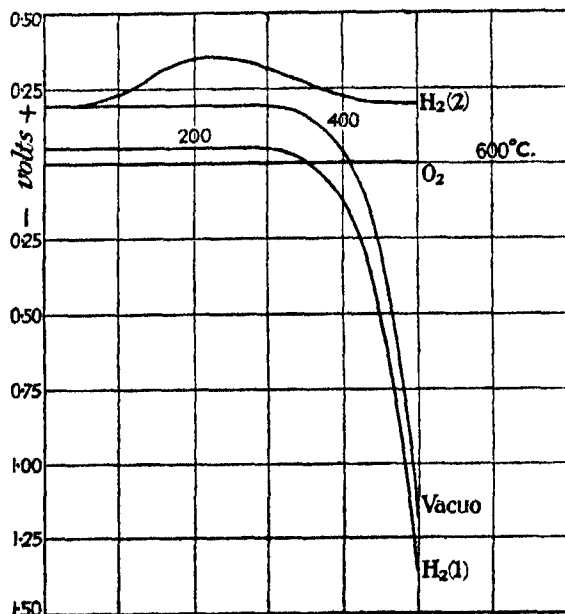


FIG. 1.

was confirmed several times, both with rising and falling temperature. A remarkable feature of this curve is that, whilst above 360° the surface exhibits the usual negative hydrogen charge, below 360° the charge becomes slightly positive ($+0.05$ volt) and persists as such even at room temperature. It was at first thought that this slight but distinct positive charge might be a spurious one and due to a possible shift in the zero of the electrometer, but this supposition was disproved by repeated earthings of the surface-electrometer system followed by reinsulation, whereupon the positive charge of 0.05 volt was slowly restored.

On evacuation to below 10^{-5} mm. at 500° the hydrogen charge of -1.36 volt at first rose within 5 minutes to -1.81 volt and then fell slowly in the course of 5 hours to -1.61 volt, at which value the charge remained unchanged during three full days' further evacuation at 500° . Oxygen was now admitted to the apparatus, whereupon the charge fell slowly, attaining a constant value of 0.00 volt at 500° within 3 hours. After 24 hours further heating at this temperature, during which the charge remained unchanged and the insulation and shielding of the electrical circuit were frequently checked, the apparatus

was evacuated, whereupon the surface began to charge up negatively, a constant value of -1.36 volt being attained within 3 hours. The results of further experiments of this series during which the temperature was maintained at 500°C . may be conveniently summarised in the order in which they were carried out as follows, the respective charges being in all cases constant values:—Hydrogen, $+0.38$ volt; *in vacuo*, -1.10 ; oxygen, $+0.05$; *in vacuo*, -1.01 ; oxygen, 0.00 ; *in vacuo*, -1.13 ; oxygen, 0.00 ; *in vacuo*, -1.13 ; oxygen, 0.00 ; *in vacuo*, -1.13 ; hydrogen, $+0.04$; *in vacuo*, -1.11 ; hydrogen, $+0.04$; *in vacuo*, -1.11 ; oxygen, 0.00 ; hydrogen, $+0.20$; *in vacuo*, -1.19 ; oxygen, 0.00 ; hydrogen, $+0.20$; *in vacuo*, -1.19 ; oxygen, 0.00 ; *in vacuo*, -1.19 ; hydrogen, $+0.20$; *in vacuo*, -1.19 ; oxygen, 0.00 ; *in vacuo*, -1.19 ; hydrogen, $+0.20$; oxygen, 0.00 ; *in vacuo*, -1.19 .

The time of evacuation to below 10^{-5} mm. at 500° necessary to remove the constant oxygen or hydrogen charge and to restore the *in vacuo* charge was in each case about 60 minutes. With hydrogen the oxygen charge could be burnt off and the hydrogen charge established within 5 minutes. Similarly, the hydrogen charge could be completely replaced by the oxygen charge, or the *in vacuo* charge by either hydrogen or oxygen, within 5 minutes.

Thus after the treatment outlined above the *in vacuo*, hydrogen and oxygen charges at 500°C . on the platinum surface had settled down to constant and reproducible values of -1.19 , $+0.20$ and 0.00 volt respectively. With the surface thus "normalised" at 500° the corresponding charge-temperature curves were determined and are recorded in fig. 1 curves *vacuo*, $\text{H}_2(2)$ and O_2 .

In view of the fact that the surface was now in such a condition that it exhibited a charge at room temperature, whether *in vacuo* or in contact with hydrogen, electrolytic gas was admitted to the apparatus with the object of seeing whether the surface was in such a condition as to be capable of promoting the combustion of this gas at room temperature. The result of this experiment was negative, no contraction in the volume of the electrolytic gas being noted during 24 hours. It is true that the gas in contact with the surface was stagnant, no provision having been made for adequate circulation; furthermore, since the ratio of surface to weight of the platinum sheet was low, heat evolved as a result of any possible catalytic action would have been rapidly dissipated, thus preventing any marked rise in the temperature of the actual surface itself of the platinum sheet. We hope in the near future to repeat this experiment in a more suitable apparatus, in which provision will be made for adequate

circulation of the gases, together with removal of the product of combustion, and also for suitable temperature control.

Series B.—Experiments with the Platinum Sheet up to 660° C.

The temperature of the surface *in vacuo* was now raised from 500° (-1.19 volt) to 660°, whereupon the charge became constant at -1.00 volt. The corresponding charge-temperature curve was then determined and is recorded in fig. 2, curve *vacuo* (1).

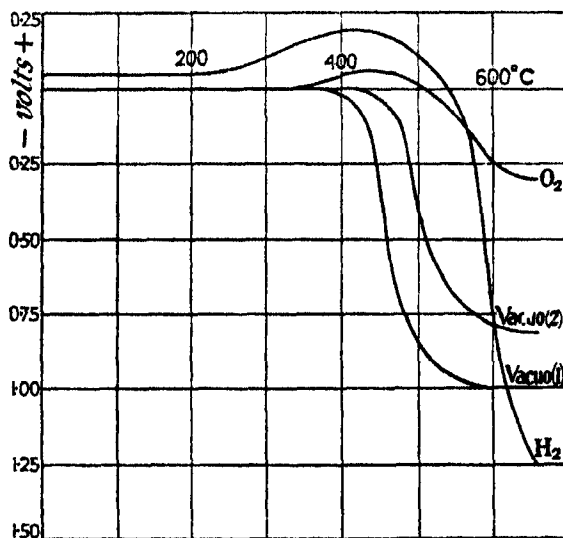


FIG. 2.

In the next experiment the hydrogen charge-temperature curve was determined and is recorded in fig. 2, curve H_2 . On evacuation at 660° the *in vacuo* charge (-1.00 volt) was restored within 5 minutes. The oxygen charge-temperature curve was now determined and is recorded in fig. 2, curve O_2 . The apparatus was then evacuated and the charge gradually became more negative, a constant value of -0.82 volt being attained in about 40 hours. Thus, the treatment of the surface with oxygen had resulted in a change of the value of the *in vacuo* charge from -1.00 to -0.82 volt. The new *in vacuo* charge-temperature curve is recorded in fig. 2, curve *vacuo* (2), and it will be seen that it is similar to the curve *vacuo* (1) but shifted somewhat to the right, *i.e.*, towards the region of higher temperatures. Repeated experiments were now carried out with hydrogen, oxygen and *in vacuo*, the results of which

confirmed those recorded in fig. 2, curves H_2 , O_2 , and *vacuo* (2), thus showing that the surface was now "normalised" at 660° .

Series C.—Experiments with the Platinum Sheet at Temperatures up to $850^\circ C$.

The temperature of the surface *in vacuo* was now raised from 660° (-0.82 volt) to 850° . The charge gradually changed in the course of 2 days to -0.48 volt at which value it remained constant. The corresponding charge-temperature curve was then determined and is recorded in fig. 3, curve *vacuo*. The

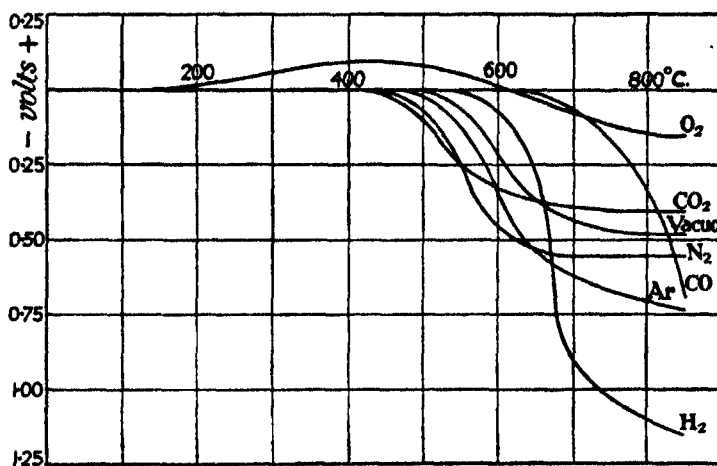


FIG. 3.

further experiments and results of this series may be conveniently summarised in the order in which they were carried out as follows, the charges recorded being those observed at 850° :—Oxygen, -0.15 volt; *vacuo*, -0.48 ; Hydrogen, -1.16 ; oxygen, -0.15 ; hydrogen, -1.16 ; *vacuo*, -0.48 ; argon, -0.74 ; *vacuo*, -0.48 ; nitrogen, -0.55 ; *vacuo*, -0.48 ; carbonic oxide, -0.69 ; *vacuo*, -0.48 ; carbonic oxide, -0.69 ; oxygen, -0.15 ; carbonic oxide, -0.69 ; *vacuo*, -0.48 ; carbon dioxide, -0.40 ; *vacuo*, -0.48 .

It will be seen from these results that the surface was now fully "normalised," the results being reproducible at will, irrespective of the nature of the gas with which the surface had been previously in contact. The corresponding charge-temperature curves are recorded in fig. 3, curves *vacuo*, O_2 , H_2 , Ar, N_2 , CO, and CO_2 . The charge due to any of the gases examined could be removed and the *in vacuo* charge restored by evacuation at $850^\circ C$. within 60 minutes. When the surface, previously exhibiting the *in vacuo* charge, was brought into contact with any of the above gases at 850° the corresponding charge was

fully established within 5 minutes. Likewise the hydrogen or carbonic oxide charge at 850° could be completely removed and the oxygen charge fully established, or *vice versa*, within 5 minutes after admission of oxygen to the surface.

Series D.—Experiments with Mixtures of Non-reacting Gases at 850° C.

In order to obtain a comparison between the relative charging effects upon the surface of different non-reacting gases experiments were carried out in which mixtures of two such gases in varying proportions were admitted to the apparatus. The results are given in Table I.

Table I.—Charges on a Platinum Surface at 850° C.

Gas.	Charge (volts).
<i>In vacuo</i>	—0.48
Oxygen	—0.15
Hydrogen	—1.16
Carbonic oxide	—0.69
Argon	—0.74
Nitrogen	—0.55
Argon + 2 per cent. O ₂	—0.15
Argon + 2 per cent. H ₂	—1.16
Nitrogen + 2 per cent. O ₂	—0.15
Nitrogen + 2 per cent. H ₂	—1.16
Argon + 50 per cent. N ₂	—0.63
Hydrogen + 50 per cent. CO	—1.16

Discussion of the Results.

The results recorded in Series A show clearly that the surface of a freshly rolled sheet of the platinum employed is in an unstable or “un-normalised” condition until it has been heated alternatively in contact with hydrogen and oxygen. A similar effect had not been noted in the case of either gold or silver. This does not, however, by itself justify the conclusion being drawn that the latter metals differ as regards “normalisation” in the sense previously used by us from platinum; because the previous history of the gold gauze used for the purpose of the experiments described in Part I included several oxidations and reductions at temperatures up to 600°, and the gold and silver sheets were first heated to 850° C. before being brought into contact with gases. It is possible, therefore, that in the case of the gold and silver surfaces hitherto examined that these had been fully “normalised” by the heating *in vacuo* to which they had been subjected before the actual charge-temperature measurements with gases were carried out. It must not be overlooked, however,

that the results obtained with nickel (Part II) show that heating alone to 850° C. did not suffice to "normalise" this surface. In connection with this we are carrying out with a fresh gold sheet further experiments at low temperatures, and the results so far to hand show no evidence of the gold behaving otherwise than normally. Thus it would appear that of the four metals so far examined by us, two, viz., platinum and nickel require alternate oxygen and hydrogen treatments before they become "normalised," i.e., exhibit constant and reproducible charge-temperature relationships. In connection with this attention may be drawn to the results obtained by Smith* in his studies on the sintering of metals. Smith found that the sintering temperature, i.e., the temperature at which the rate of conversion of the microcrystalline and amorphous arrangements of the atoms on the surface begins to change rapidly into the macroscopic variety, of gold and silver were 200 and 180° C. respectively; but that nickel and platinum only commenced to sinter at temperatures in the neighbourhood of 700° C. It would seem highly probable, therefore, that "normalisation" of a metal surface in the sense employed above involves a structural change in the arrangement of the surface atoms of the metal sheet. Further, in connection with this, reference might here be made to the observations of Bone and Andrew† who found that the subsequent activity of a gold surface in promoting the union of "detonating gas" ($2\text{CO} + \text{O}_2$) at 320° was greatly reduced if the surface was kept over a prolonged period *in vacuo* at room temperature, a fact which is indicative of structural changes having been brought about as a result of such cooling.

The final charge-temperature results of Series A which are recorded in fig. 1, and were obtained after the surface had been normalised at 500° C. by repeated oxidations and reductions, are specially significant in that the surface exhibited a definite positive charge of 0.19 volt either in contact with hydrogen or *in vacuo* at room temperature. As has been stated above, a preliminary experiment carried out with the object of seeing whether the surface in this condition was in a specially active condition catalytically was carried out with a negative result. In connection with this we are, however, carrying out further experiments, and the results so far to hand afford considerable support to the view that the platinum surface was, at the close of the experiments of Series A, in a catalytically active condition, and that such condition is associated with a positive *in vacuo* or hydrogen charge at room temperature.

"Normalisation" of the surface by reduction followed by oxidation at

* 'J. Chem. Soc.,' vol. 123, p. 2008 (1923).

† 'Roy. Soc. Proc.,' A, vol. 109, p. 459 (1925).

660° left the surface at room temperature uncharged *in vacuo* but still exhibiting a positive charge in contact with hydrogen. A similar process carried out repeatedly at 850° completely removed all trace of such super-activity of the surface, which no longer showed a charge at room temperature; the results obtained with platinum "normalised" at 850° C., resembling in character those obtained with the metals previously examined, and thus supporting the hypothesis put forward in Parts I and II to account for the charging up of a hot metal *in vacuo* or in contact with gases.

The fact that the charge due to any of the gases examined in contact with platinum were readily removed (within 45 minutes) solely by evacuation at 850°, shows that only types I and II of the five possible types of adsorption* which we have so far been able to distinguish are met with in the case of platinum.

Results of experiments upon the charging up of hot nickel and platinum surfaces in contact with non-reacting gaseous mixtures are given in Part II (p. 240) and in the present paper (Table I). Although this particular experimental field has not as yet been systematically explored, nevertheless the results so far obtained enable the gases examined to be arranged into an order of increasing activity with which they charge up a hot metal surface. Thus at 850° the *in vacuo* charge is displaced, and the respective gas charge wholly established by a partial pressure of only 1 mm. of any of the gases so far examined by us. Argon (—0·74 volt) and nitrogen (—0·55 volt) are practically equal in their effect, since a mixture of the two gases in equal proportions gives a surface charge (on platinum) of —0·63 volt, whilst argon or nitrogen with 2 per cent. of oxygen or hydrogen imparts to the surface the oxygen or hydrogen charge respectively. The charge due to an equivalent mixture of carbonic oxide or hydrogen and oxygen is always nearer to the oxygen charge, from which it may be concluded that of all gases oxygen is the most active in charging up the surface. Thus the above gases may be placed as follows in order of increasing activity in charging up a hot metal surface:—*In vacuo* : $\left\{ \begin{array}{l} \text{argon} \\ \text{nitrogen} \end{array} \right\}$; carbonic oxide; hydrogen; oxygen.

It will be noticed that when the temperature of the platinum surface, "normalised" at 500°, was raised for the first time to 660° *in vacuo*, the corresponding charge was only established after about 48 hours. On first heating to 850° a similar period elapsed before the *in vacuo* charge at this temperature was exhibited by the surface. On subsequent occasions, however, the *in*

* Part II, p. 244.

vacuo charge was always rapidly established (within 60 minutes). These facts strongly support the view put forward in Part II (p. 241) that the *in vacuo* charge is probably a result of structural changes of a permanent nature in the arrangement of the surface atoms of the metal sheet.

Summary.

The electrical charging of a platinum sheet in contact with various gases and *in vacuo* has been studied at temperatures up to 850° C. The following facts have been established :—

- (i) The platinum sheet becomes electrically charged in contact with a gas or *in vacuo*, the temperature at which the charge is first exhibited depending upon its previous treatment.
- (ii) Oxidation, followed by reduction with hydrogen at 500° “normalises” the surface which then exhibits a positive charge at room temperature in contact with hydrogen or *in vacuo*.
- (iii) When heated to 660°, “normalisation” is again necessary whereafter the surface still exhibits a positive charge at room temperature when in contact with hydrogen but not *in vacuo*.
- (iv) After “normalisation” at 850° the surface no longer gives a charge at room temperature.
- (v) The charge on the “normalised” platinum sheet due to a gas is characteristic of the latter, and dependent on the temperature, but is independent of the gas pressure between 1 and 760 mm.
- (vi) The charge due to any of the gases examined can be rapidly removed by evacuation at 850°.
- (vii) The experimental results obtained with non-combining mixtures enable the gases examined to be placed in an order of their increasing activity in charging up the surface.

From these facts, in conjunction with those previously established and set forth in Parts I and II of this series, it is concluded (i) that the “normalising” of a metal surface involves a rearrangement of the surface atoms by a process akin to sintering, and (ii) that platinum does not combine directly and form chemical compounds with any of the gases examined, some adsorbed gaseous molecules being condensed and forming an electrically neutral layer on the surface, and others held thereon by weak electrical attraction whereby one bond between the constituent atoms of each molecule is weakened.

One of us (J.C.S.) wishes to thank the Department of Scientific and Industrial Research for a personal grant which enabled him to devote his full time to this work.

On Einstein's Unified Field Theory.

By G. C. McVITTIE, M.A. (Edin.), Christ's College, Cambridge.

(Communicated by A. S. Eddington, F.R.S.—Received May 6, 1929.)

I.—*Introduction.*

In a recent paper* Prof. A. Einstein has proposed equations determining a field containing both gravitational and electromagnetic phenomena, the underlying geometry being of a type which admits the possibility of giving any arbitrary vector in the field a displacement which conserves parallelism at a distance. The purpose of the present paper is to try and obtain light on the new theory by applying it to a special case in which an exact solution of the usual gravitational and electromagnetic equations of the relativity theory is known.

In § II we obtain this solution, that is to say, we determine a set of values of the $g_{\mu\nu}$ and ϕ_μ which exactly satisfies the recognised relativity equations. It is found that this solution corresponds to an electrostatic field uniform in direction and nearly constant but with a slight exponential change of strength as we go along the field.

In § III we deduce the explicit values of Einstein's 16 quantities $^*h_\mu$ which link the $g_{\mu\nu}$ and ϕ_μ to the variables employed in his new equations.

In § IV we test whether the new equations proposed by Einstein are satisfied. It is shown that the new equations are satisfied to the first order but not exactly. That is to say the new equations are not equivalent to the old beyond the first order. We here consider the electrical quantities as of the first order whilst the gravitational effects are of the second order. (Einstein himself always speaks of the agreement between the old and new equations being to the first approximation, but it was not very clear from his paper, whether this implied that they differed in terms of higher order, or merely that the investigation had not been carried beyond the first order.) We have also examined the law $\mathfrak{B}_{ke/e}^* = 0$, suggested but not actually developed as a likely field law by Einstein. This is also only found to be true to a first approximation.

* 'Berlin Akad. Sitzb.,' vol. 1, p. 2 (1929).

II.—The Gravitational Field of an Electrostatic Field of Uniform Direction.

The metric is taken to be $ds^2 = g_{44} dx_4^2 - g_{11} dx_1^2 - g_{22} dx_2^2 - g_{33} dx_3^2$ where the $g_{\mu\nu}$ are all positive. It is assumed that the $g_{\mu\nu}$ are functions of x_1 alone and that $g_{22} = g_{33}$. The electromagnetic potential vector

$$(\phi_4, \phi_1, \phi_2, \phi_3) \equiv (\phi_4, 0, 0, 0)$$

and ϕ_4 is assumed to be a function of x_1 alone.

If $F_{\mu\nu}$ denotes the electric and magnetic force vector, all its components vanish in this case except

$$F_{41} = -F_{14} = \phi_4'$$

where a dash denotes differentiation with respect to x_1 . The condition for no electric charge or current in the field is

$$\frac{\partial \tilde{F}^{\mu\nu}}{\partial x_\nu} = 0,$$

where

$$\tilde{F}^{\mu\nu} = F^{\mu\nu} \sqrt{-g}.$$

In our case this equation reduces to

$$\frac{d}{dx_1} (g^{44} g^{11} \phi_4' \sqrt{g_{44} g_{11} g_{22} g_{33}}) = 0,$$

whence

$$\phi_4' = \frac{\alpha}{4\sqrt{\pi}} \sqrt{\frac{g_{44} g_{11}}{g_{22} g_{33}}}.$$

where $\alpha/4\sqrt{\pi}$ is a constant of integration.

The general expression for the electromagnetic energy tensor is

$$E^\nu_\mu = -F^{\nu\alpha} F_{\mu\alpha} + \frac{1}{4} F^{\alpha\beta} F_{\alpha\beta} g^\nu_\mu.$$

Hence in this case the non-zero components of this tensor are

$$E^1_1 = -E^2_2 = -E^3_3 = E^4_4 = \frac{\alpha^2}{32\pi} \frac{1}{g_{22} g_{33}}.$$

The gravitational equations are now

$$G_{\mu\nu} = -8\pi E_{\mu\nu}, \tag{1}$$

where $G_{\mu\nu}$ is the contracted Riemann-Christoffel tensor. The surviving Christoffel symbols for this metric are :—

$$\begin{aligned}\{11, 1\} &= \frac{1}{2} \frac{1}{g_{11}} \frac{dg_{11}}{dx_1}, & \{22, 1\} &= -\frac{1}{2} \frac{1}{g_{11}} \frac{dg_{22}}{dx_1}, \\ \{12, 2\} &= \frac{1}{2} \frac{1}{g_{22}} \frac{dg_{22}}{dx_1}, & \{33, 1\} &= -\frac{1}{2} \frac{1}{g_{11}} \frac{dg_{33}}{dx_1}, \\ \{13, 3\} &= \frac{1}{2} \frac{1}{g_{33}} \frac{dg_{33}}{dx_1}, & \{44, 1\} &= \frac{1}{2} \frac{1}{g_{11}} \frac{dg_{44}}{dx_1}, \\ \{14, 4\} &= \frac{1}{2} \frac{1}{g_{44}} \frac{dg_{44}}{dx_1},\end{aligned}$$

In virtue of the assumption $g_{22} = g_{33}$ the equations (1) reduce to three, viz. :—

$$\begin{aligned}\frac{1}{4} \frac{1}{g_{11}} \frac{1}{g_{44}^2} \left(\frac{dg_{44}}{dx_1} \right)^2 - \frac{1}{2} \frac{1}{g_{11}} \frac{1}{g_{44}} \frac{d^2 g_{44}}{dx_1^2} + \frac{1}{4} \frac{1}{g_{11}^2} \frac{1}{g_{44}} \frac{dg_{11}}{dx_1} \frac{dg_{44}}{dx_1} \\ - \frac{1}{g_{11}} \left\{ \frac{1}{g_{22}} \frac{d^2 g_{22}}{dx_1^2} - \frac{1}{2} \frac{1}{g_{22}^2} \left(\frac{dg_{22}}{dx_1} \right)^2 - \frac{1}{2} \frac{1}{g_{11}} \frac{1}{g_{22}} \frac{dg_{11}}{dx_1} \frac{dg_{22}}{dx_1} \right\} = -\frac{\alpha^2}{4g_{22}^2}, \quad (1.1)\end{aligned}$$

$$\begin{aligned}\frac{1}{4} \frac{1}{g_{44}} \frac{1}{g_{11}^2} \frac{dg_{44}}{dx_1} \frac{dg_{11}}{dx_1} - \frac{1}{2} \frac{1}{g_{11}} \frac{1}{g_{44}} \frac{d^2 g_{44}}{dx_1^2} + \frac{1}{4} \frac{1}{g_{11}} \frac{1}{g_{44}^2} \left(\frac{dg_{44}}{dx_1} \right)^2 \\ - \frac{1}{2} \frac{1}{g_{44}} \frac{1}{g_{11}} \frac{1}{g_{22}} \frac{dg_{44}}{dx_1} \frac{dg_{22}}{dx_1} = -\frac{\alpha^2}{4g_{22}^2}, \quad (1.2)\end{aligned}$$

$$\frac{1}{2} \frac{1}{g_{11}} \frac{d^2 g_{22}}{dx_1^2} - \left\{ \frac{1}{4} \frac{1}{g_{11}^2} \frac{dg_{11}}{dx_1} - \frac{1}{4} \frac{1}{g_{11}} \frac{1}{g_{44}} \frac{dg_{44}}{dx_1} \right\} \frac{dg_{22}}{dx_1} = -\frac{\alpha^2}{4g_{22}}. \quad (1.3)$$

The equations (1.1) and (1.2) are identical if

$$\frac{1}{g_{22}} \frac{d^2 g_{22}}{dx_1^2} - \frac{1}{2} \frac{1}{g_{22}^2} \left(\frac{dg_{22}}{dx_1} \right)^2 - \frac{1}{2} \frac{1}{g_{11}} \frac{1}{g_{22}} \frac{dg_{11}}{dx_1} \frac{dg_{22}}{dx_1} = \frac{1}{2} \frac{1}{g_{22}} \frac{1}{g_{44}} \frac{dg_{44}}{dx_1} \frac{dg_{22}}{dx_1}, \quad (1.4)$$

whence

$$\frac{dg_{22}}{dx_1} = A \sqrt{g_{22} g_{11} g_{44}}, \quad (1.5)$$

where A is a constant of integration.

Again (1.4) and (1.3) are identical if

$$\left\{ \frac{1}{4} \frac{1}{g_{11}} \frac{1}{g_{44}} \frac{dg_{44}}{dx_1} + \frac{1}{4} \frac{1}{g_{11}} \frac{1}{g_{22}} \frac{dg_{22}}{dx_1} + \frac{1}{4} \frac{1}{g_{11}} \frac{1}{g_{44}} \frac{dg_{44}}{dx_1} \right\} \frac{dg_{22}}{dx_1} = -\frac{\alpha^2}{4g_{22}},$$

or

$$\frac{1}{g_{11}} \frac{d}{dx_1} (\log g_{22} g_{44}^2) \cdot \frac{dg_{22}}{dx_1} = -\frac{\alpha^2}{g_{22}}. \quad (1.6)$$

Hence we may replace the three equations (1.1), (1.2), (1.3) by the equivalent ones (1.1), (1.5), (1.6).

If now

$$g_{22} = e^{-ax_1},$$

we have, by (1.5), if $A = -\alpha$, that

$$g_{11} g_{44} = e^{-ax_1},$$

and (1.6) now becomes

$$\frac{dg_{44}}{dx_1} - \frac{1}{2} \alpha g_{44} = \frac{\alpha}{2} e^{ax_1},$$

whence

$$g_{44} = e^{ax_1}.$$

Hence

$$g_{11} = e^{-2ax_1},$$

and it is found on substitution that these values of the $g_{\mu\nu}$ now satisfy (1.1).

Hence finally a rigorous solution of the gravitational and electrical field equations is

$$ds^2 = e^{ax_1} dx_1^2 - e^{-2ax_1} dx_1^2 - e^{-ax_1} dx_2^2 - e^{-ax_1} dx_3^2,$$

$$\phi_4 = \frac{1}{2\sqrt{\pi}} e^{\frac{1}{2}ax_1}, \quad \phi_1 = 0, \quad \phi_2 = 0, \quad \phi_3 = 0.$$

To show that this represents an electrostatic field uniform in direction and nearly constant but with an exponential increase of strength as we proceed down the field, we determine the electric force which would be measured by an observer at an arbitrary point $P \equiv (\tau, a, b, c)$ in this field. We first transfer the origin to P by means of the transformation

$$X_4 = e^{iaa} (x_4 - \tau), \quad X_1 = e^{-aa} (x_1 - a),$$

$$X_2 = e^{-iaa} (x_2 - b), \quad X_3 = e^{-iaa} (x_3 - c),$$

which leaves the expression for the line element unchanged in form, viz. :—

$$ds^2 = e^{a'X_1} dX_4^2 - e^{-2a'X_1} dX_1^2 - e^{-a'X_1} dX_2^2 - e^{-a'X_1} dX_3^2$$

where

$$\alpha' = \alpha e^{aa}.$$

We now transform to natural co-ordinates $(\bar{X}_4, \bar{X}_1, \bar{X}_2, \bar{X}_3)$ at P by means of the transformation*

$$X_i = \bar{X}_i - \frac{1}{2} \{pq, i\}_P \bar{X}_p \bar{X}_q \quad (i, p, q = 1, 2, 3, 4),$$

where $\{pq, i\}_P$ denotes that the value of the Christoffel symbol at P has been taken.

* A. S. Eddington, 'Math. Theory of Relat.,' chap. III.

This transformation is

$$\begin{aligned} X_4 &= \bar{X}_4 - \frac{1}{4}\alpha'\bar{X}_1\bar{X}_4, & X_1 &= \bar{X}_1 + \frac{1}{2}\alpha'\bar{X}_1^2 - \frac{1}{4}\alpha'\bar{X}_4^2 - \frac{1}{4}\alpha'\bar{X}_3^2 - \frac{1}{4}\alpha'\bar{X}_2^2, \\ X_2 &= \bar{X}_2 + \frac{1}{4}\alpha'\bar{X}_1\bar{X}_2, & X_3 &= \bar{X}_3 + \frac{1}{4}\alpha'\bar{X}_1\bar{X}_3. \end{aligned}$$

The electromagnetic potential vector $(\phi_4, 0, 0, 0)$ at the point P in the x co-ordinates now becomes $(\bar{\phi}_4, \bar{\phi}_1, \bar{\phi}_2, \bar{\phi}_3)$ in the \bar{X} -co-ordinates where

$$\bar{\phi}_4 = \left(\frac{\partial x_4}{\partial \bar{X}_4} \phi_4 \right)_P, \quad \bar{\phi}_1 = \left(\frac{\partial x_4}{\partial \bar{X}_1} \phi_4 \right)_P, \quad \bar{\phi}_2 = 0, \quad \bar{\phi}_3 = 0.$$

The corresponding electric and magnetic force vector at P is given by

$$(\bar{F}_{41})_P = -(\bar{F}_{14})_P = -\left(\frac{\partial \bar{\phi}_1}{\partial \bar{X}_4} - \frac{\partial \bar{\phi}_4}{\partial \bar{X}_1} \right)_P = \frac{\alpha'}{4\sqrt{\pi}} = \frac{\alpha e^{ax}}{4\sqrt{\pi}},$$

all the other components of this tensor being zero.

Hence the electromagnetic force measured at P is an electric force in the direction of the x -axis, constant at any given point, but increasing in magnitude exponentially as we travel down the field.

III.—The Values of Einstein's Sixteen ${}^s h_\mu$.

We take the line element and the electromagnetic vector potential to be respectively.

$$\begin{aligned} ds^2 &= e^{ax} dx_4^2 - e^{-2ax} dx_1^2 - e^{-ax} dx_2^2 - e^{-ax} dx_3^2, \\ \phi_4 &= \frac{1}{2\sqrt{\pi}} (e^{4ax} - 1), \quad \phi_1 = \frac{1}{2}\alpha, \quad \phi_2 = 0, \quad \phi_3 = 0, \end{aligned}$$

where we have added the constants $-\frac{1}{2\sqrt{\pi}}$ and $\frac{1}{2}\alpha$ to the previously obtained values of ϕ_4 and ϕ_1 respectively, as may always be done.

Prof. A. Einstein describes the field by means of 16 variables, ${}^s h_\mu$, which he connects with the $g_{\mu\nu}$ and ϕ_μ by means of the equations

$$g_{\mu\nu} = {}^s h_\mu {}^s h_\nu \quad (s, \mu, \nu = 1, 2, 3, 4), \quad (2)$$

$$\phi_\mu = \Lambda^a_{\mu\alpha} = {}^s h^a \left(\frac{\partial {}^s h_\mu}{\partial x_a} - \frac{\partial {}^s h_a}{\partial x_\mu} \right), \quad (3)$$

$$(s, \alpha, \mu = 1, 2, 3, 4)$$

where

$${}^s h^a = \frac{\text{minor of } {}^s h_a \text{ in } | {}^s h_a |}{| {}^s h_a |}.$$

In our case the equations (2) are

$$\begin{aligned} e^{ax_1} &= \sum_{s=1}^4 {}^s h_4^2, & -e^{-2ax_1} &= \sum_{s=1}^4 {}^s h_1^2, & -e^{-ax_1} &= \sum_{s=1}^4 {}^s h_2^2, \\ -e^{-ax_1} &= \sum_{s=1}^4 {}^s h_3^2, & 0 &= \sum_{s=1}^4 {}^s h_\mu {}^s h_\nu \quad (\mu \neq \nu = 1, 2, 3, 4). \end{aligned}$$

We obtain a particular solution of these equations if we put all the ${}^s h_\mu$ except ${}^4 h_4$, ${}^3 h_3$, ${}^2 h_2$, ${}^1 h_1$, ${}^4 h_1$, ${}^1 h_4$ equal to zero so that these 10 equations reduce to 5, viz. :—

$$-e^{-2ax_1} = {}^4 h_1^2 + {}^1 h_1^2, \quad (2.1)$$

$$-e^{-ax_1} = {}^2 h_2^2, \quad (2.2)$$

$$-e^{-ax_1} = {}^3 h_3^2, \quad (2.3)$$

$$e^{ax_1} = {}^4 h_4^2 + {}^1 h_4^2, \quad (2.4)$$

$$0 = {}^4 h_4 {}^4 h_1 + {}^1 h_4 {}^1 h_1. \quad (2.5)$$

These equations are satisfied by

$$\left. \begin{aligned} {}^4 h_4 &= e^{\frac{1}{2}ax_1} \cosh v, & {}^1 h_1 &= i e^{-ax_1} \cosh v \\ {}^4 h_1 &= e^{-ax_1} \sinh v, & {}^1 h_4 &= i e^{\frac{1}{2}ax_1} \sinh v \\ {}^3 h_3 &= i e^{-\frac{1}{2}ax_1}, & {}^2 h_2 &= i e^{-\frac{1}{2}ax_1} \end{aligned} \right\} \quad (2.6)$$

where $i = \sqrt{-1}$ and v is an undetermined function of x_1 . To determine v we use the equations (3).

We first calculate the sh^μ .

We have

$$h = |{}^s h_\mu| = {}^3 h_3 {}^2 h_2 ({}^4 h_4 {}^1 h_1 - {}^1 h_4 {}^4 h_1) = -i e^{-\frac{1}{2}ax_1}.$$

Hence

$$\left. \begin{aligned} {}^4 h^4 &= e^{-\frac{1}{2}ax_1} \cosh v, & {}^1 h^1 &= -i e^{ax_1} \cosh v \\ {}^1 h^4 &= i e^{-\frac{1}{2}ax_1} \sinh v, & {}^4 h^1 &= -e^{ax_1} \sinh v \\ {}^3 h^3 &= -i e^{\frac{1}{2}ax_1}, & {}^2 h^2 &= -i e^{\frac{1}{2}ax_1} \end{aligned} \right\}. \quad (2.7)$$

The four equations (3) now reduce to the two, viz. :—

$$\frac{1}{2}\alpha = -{}^4 h^4 \frac{d^4 h_4}{dx_1} - {}^2 h^2 \frac{d^2 h_2}{dx_1} - {}^3 h^3 \frac{d^3 h_3}{dx_1} - {}^1 h^4 \frac{d^1 h_4}{dx_1}, \quad (3.1)$$

$$\frac{1}{2\sqrt{\pi}}(e^{iax_1} - 1) = {}^1 h^1 \frac{d^1 h_4}{dx_1} + {}^4 h^1 \frac{d^4 h_4}{dx_1}. \quad (3.2)$$

On substituting the value (2.6) and (2.7) of the ${}^*h_\mu$ and ${}_jh^\mu$ respectively, we find that the equation (3.1) reduces to an identity whilst the equation (3.2) becomes

$$\frac{1}{2\sqrt{\pi}}(e^{i\alpha x_1} - 1) = e^{i\alpha x_1} \frac{dv}{dx_1},$$

whence

$$v = \frac{1}{2\sqrt{\pi}} \left(\frac{1}{3\alpha} + \frac{2}{3\alpha} e^{-i\alpha x_1} - \frac{1}{\alpha} e^{-\alpha x_1} \right), \quad (3.3)$$

the constant of integration being determined so that $v = 0$ when $\alpha = 0$.

Hence the ${}^*h_\mu$ and ${}_jh^\mu$ given by the equations (2.6), (2.7) and (3.3) are a solution of the equations (2) and (3).

IV.—Einstein's Field Equations.

We now examine whether or not the set of ${}_jh^\mu$, ${}^*h_\mu$ and ϕ_μ , given in the previous paragraph, satisfy (to a first approximation) the field laws given for them by Prof. A. Einstein.*

These equations are

$$\mathfrak{B}^a_{ke/e} - \mathfrak{B}^\sigma_{kr} \Lambda^a_{\sigma r} = 0, \quad (4)$$

$$[h(\phi_{\underline{k}; \underline{a}} - \phi_{\underline{a}; \underline{k}})]_{/a} = 0, \quad (5)$$

where

$$\Lambda^a_{\sigma r} = \Delta^a_{\sigma r} - \Delta^a_{r\sigma} \quad \text{and} \quad \Delta^a_{\sigma r} = {}_jh^a \frac{\partial^2 h_\sigma}{\partial x_r^2}.$$

Underlining a suffix means raising or lowering it.

$$\mathfrak{B}^a_{ke} = h(\Lambda^a_{ke} + \phi_e \delta^a_k - \phi_k \delta^a_e).$$

A semicolon denotes the "affine derivative," *e.g.*,

$$A_\mu;_\sigma \equiv \frac{\partial A_\mu}{\partial x_\sigma} - A_\alpha \Delta^a_{\mu\sigma},$$

$$A^\mu;_\sigma \equiv \frac{\partial A^\mu}{\partial x_\sigma} + A^a \Delta^a_{\sigma\mu}.$$

A solidus denotes the "affine divergence" of a tensor, *e.g.*,

$$\mathfrak{I}^{p\sigma}_{/r} = \frac{\partial \mathfrak{I}^{p\sigma}}{\partial x_r} + \Delta^p_{tr} \mathfrak{I}^{t\sigma} + \Delta^{\sigma}_{tr} \mathfrak{I}^{p/r},$$

where

$$\mathfrak{I}^{t\sigma} = hT^{t\sigma}$$

and

$$\phi_k = \Lambda^a_{ka}.$$

* *Loc. cit.*, equations (10a) and (11).

The $\Delta^a_{\mu\nu}$ which do not vanish are

$$\begin{aligned}\Delta^4_{11} &= \frac{1}{2\sqrt{\pi}} e^{-\frac{1}{2}\alpha x_1} (e^{\frac{1}{2}\alpha x_1} - 1) & \Delta^3_{21} &= \Delta^3_{31} = -\frac{1}{2}\alpha, \\ \Delta^1_{11} &= -\alpha, & \Delta^1_{41} &= \frac{1}{2\sqrt{\pi}} (e^{\frac{1}{2}\alpha x_1} - 1), \\ \Delta^4_{41} &= \frac{1}{2}\alpha.\end{aligned}$$

On substitution of these values for the $\Delta^a_{\mu\nu}$ and the known values of $(\phi_4, \phi_1, \phi_2, \phi_3)$ we find that the only \mathfrak{B}^a_{ke} which do not vanish are

$$\begin{aligned}\mathfrak{B}^4_{41} &= -\mathfrak{B}^4_{14} = -i\alpha e^{-\frac{1}{2}\alpha x_1}, \\ \mathfrak{B}^3_{34} &= -\mathfrak{B}^3_{43} = -\frac{i}{2\sqrt{\pi}} e^{-\frac{1}{2}\alpha x_1} (e^{\frac{1}{2}\alpha x_1} - 1), \\ \mathfrak{B}^2_{24} &= -\mathfrak{B}^2_{42} = -\frac{i}{2\sqrt{\pi}} e^{-\frac{1}{2}\alpha x_1} (e^{\frac{1}{2}\alpha x_1} - 1),\end{aligned}$$

and, of course, $\mathfrak{B}^a_{ke} = g^{kk} g^{ee} \mathfrak{B}^a_{ke}$ in our case. The \mathfrak{B}^a_{ke} should satisfy the fundamental identity

$$\mathfrak{B}^a_{ke/a} = \frac{\partial \mathfrak{B}^a_{ke}}{\partial x_a} - \Delta^t_{ka} \mathfrak{B}^a_{te} - \Delta^t_{ea} \mathfrak{B}^a_{kt} = 0,$$

and it is verified that our values satisfy it.

If we examine the vanishing of the other divergence, i.e., $\mathfrak{B}^a_{ke/e} = 0$, which Prof. A. Einstein seems to consider as a possible field law, we find that it is satisfied by our values except in the case of the following components:—

$$\begin{aligned}\mathfrak{B}^4_{4e/e} &= \frac{\partial \mathfrak{B}^4_{41}}{\partial x_1} + 2\Delta^4_{41} \mathfrak{B}^4_{41} = \frac{1}{2}\alpha^2 e^{-\frac{1}{2}\alpha x_1}, \\ \mathfrak{B}^4_{1e/e} &= \mathfrak{B}^4_{1e/e} = \frac{i\alpha e^{-\frac{1}{2}\alpha x_1}}{2\sqrt{\pi}} (e^{\frac{1}{2}\alpha x_1} - 1),\end{aligned}$$

which, it is observed, can vanish only to a first approximation, i.e., provided we neglect the second and higher powers of α .

We now examine the field law actually given by Prof. A. Einstein, i.e., the equations (4) and (5). Since all the \mathfrak{B}^a_{ke} are zero in our case except those of the forms \mathfrak{B}^a_{ae} , \mathfrak{B}^a_{ea} , the equations (4) become (the summation convention being suspended)

$$\sum_{e=1}^4 \frac{\partial \mathfrak{B}^a_{ae}}{\partial x_e} + \sum_{e=1}^4 \{\Delta^a_{ae} \mathfrak{B}^e_{ae} + \Delta^a_{ee} \mathfrak{B}^a_{ae}\} = 0 \quad (\alpha = 1, 2, 3, 4), \quad (4.1)$$

and

$$\frac{\partial \mathfrak{B}^a_{ka}}{\partial x_a} + \sum_{e=1}^4 \{\Delta^a_{ae} \mathfrak{B}^e_{ke} + \Delta^a_{ek} \mathfrak{B}^k_{ae} + \mathfrak{B}^a_{ea} (\Delta^k_{ea} - \Delta^k_{ae})\} = 0$$

$$(\alpha \neq k = 1, 2, 3, 4). \quad (4.2)$$

On substitution, we find that the set of equations (4.1) reduce to one, viz.

$$\frac{d\mathfrak{B}_{41}^4}{dx_1} + \Delta_{41}^4 \mathfrak{B}_{41}^4 = 0, \quad (4.3)$$

and the set (4.2) to one, viz.,

$$\Delta_{41}^1 \mathfrak{B}_{14}^4 = 0, \quad (4.4)$$

the rest being identities.

On substituting our values of \mathfrak{B}_{41}^4 , Δ_{41}^1 , Δ_{41}^4 into (4.3) and (4.4) we find that the former is rigorously satisfied whilst the latter reduces to

$$\frac{i\alpha}{2\sqrt{\pi}} (e^{i\alpha x_1} - 1) e^{-i\alpha x_1} = 0,$$

which is satisfied to a first approximation only, *i.e.*, if the second and higher powers of α are neglected.

The equations (5) are

$$\sum_{a=1}^4 \frac{\partial}{\partial x_a} [h(\phi_{k;\underline{a}} - \phi_{\underline{a};k})] + \sum_{t,a=1}^4 \Delta_{ta}^k [h(\phi_{t;\underline{a}} - \phi_{\underline{a};t})] = 0,$$

where

$$\phi_{k;\underline{a}} - \phi_{\underline{a};k} = g^{aa} \frac{\partial \phi_k}{\partial x_a} - g^{kk} \frac{\partial \phi_a}{\partial x_k} + \sum_{e=1}^4 (g^{ae} \Delta_{ea}^k - g^{ke} \Delta_{ek}^a) \phi_{\underline{e}}.$$

All the $(\phi_{k;\underline{a}} - \phi_{\underline{a};k})$ are zero in our case except

$$(\phi_{4;\underline{1}} - \phi_{\underline{1};4}) = -(\phi_{1;\underline{4}} - \phi_{\underline{4};1}) = \frac{\alpha}{4\sqrt{\pi}} e^{\alpha x_1} (e^{i\alpha x_1} - 1).$$

On substitution the equations (5) reduce to the two :

$$\frac{d}{dx_1} [h(\phi_{4;\underline{1}} - \phi_{\underline{1};4})] + \Delta_{41}^4 [h(\phi_{4;\underline{1}} - \phi_{\underline{1};4})] = 0.$$

$$\Delta_{41}^1 [h(\phi_{4;\underline{1}} - \phi_{\underline{1};4})] = 0,$$

whence it is found that the first equation is satisfied rigorously but that the second becomes

$$\frac{\alpha}{8\pi} e^{-i\alpha x_1} (e^{i\alpha x_1} - 1)^2 = 0,$$

which again is only satisfied approximately, *i.e.*, if the third and higher powers of α are neglected.

In conclusion, I should like to thank Prof. A. S. Eddington, F.R.S., at whose suggestion the investigation was undertaken, for his interest throughout the progress of the work and his help during its preparation for publication.

A Collision Problem in the Wave Mechanics.

By C. G. DARWIN, F.R.S.

(Received March 28, 1929.)

In the present work the wave mechanics are applied to the discussion of a collision problem of a more complicated type than has, I think, hitherto been done. Though there is nothing very new in the process it is rather interesting to see how a wave function behaves which involves two bodies, and is therefore outside our ordinary space intuitions. But the work had a much more general aim, as an attempt to see whether a sharper line of demarcation could be drawn between the particle-like and the wave-like properties of matter. Put briefly, I take a problem which would be regarded at first sight as irreconcilable with a pure wave theory, but thoroughly typical of the behaviour of particles, and show how in fact the correct result arises naturally from the consideration of waves alone. I have been led in this way to certain not very original speculations on the basis of the quantum theory and these are given at the end of the paper. These are not in the least intended to be a general formulation of the theory, but rather as an examination of a particular type of attempted formulation. I fear that the views expressed will be found partly obvious and perhaps partly inconsistent or even erroneous. My excuse for giving them is that the quantum theory seems already sufficiently developed for us to attempt something more than a mathematical formulation of it, and that a generally accepted physical understanding will be more quickly reached by agreement or disagreement with expressed opinions, than by waiting for the arrival of a full-grown theory. It has been an extraordinarily difficult task to express the ideas I intended, and I wish to thank Prof. D. R. Hartree for many valuable criticisms of my first attempts to do so, though he must be exonerated from all blame if the final result is unintelligible or erroneous.

1. The quantum mechanics have been expressed in a variety of ways, which place the emphasis differently, but it has been shown that they are all exactly equivalent, so that we may choose which we will. I shall use the following description, limiting myself to the simpler cases which do not involve considerations of relativity. We take a partial differential equation of the wave type, set down according to certain rules depending on the particular system considered. We solve this subject to certain boundary conditions, expressive of all the limitations imposed by slits, mirrors, diffraction gratings, moving

shutters, etc., that may occur in the proposed system, and obtain as result the wave function ψ , a function of all the co-ordinates of the system and of the time.* From this we form a set of functions, of which the simplest is $|\psi|^2$; this process may be called taking the intensities. We next have to prepare for the particle aspect, by applying certain rules so as to normalise the intensities, a process entirely foreign to the idea of waves. Finally, we make the *interpretation*, in which we say that the normalised intensities measure the probability of the particles having such and such positions, momenta, energies, etc., and these are the results verified by observation.

This procedure needs supplementing in one particular which is important for our present purpose; without this extension it is limited to occurrences in which the conservation theorems hold. If for example we want to apply it to such a process as the passage of β -rays through an absorbing foil, the method will only work if we include the atoms and electrons of the foil as variables in our equation, for only thus can the equation of energy hold. We are then forced to work out not only the motion of the β -rays, but also the ionisation of the atoms of the foil, which is not observed and usually does not interest us. At the end, therefore, we estimate the probability for the β -particle being in any given position, etc., by taking an average over all types of ionisation which could be associated with that position. This is a most discouragingly complicated procedure, but still it is conceivably possible, and by its means we can extend the general method to occurrences which involve such processes as absorption.

2. One of the most important points in the whole quantum theory, due to Heisenberg,† is that the *observation* of the particles may only be made once, as it itself disturbs the system in a way that is unknowable. Now in a great many experiments we observe a succession of events, and in order to conform to Heisenberg's principle we have to regard the process as a sequence of experiments, each observation ending one and starting the next. Loosely speaking, at each observation we imagine the wave turned into a particle, and then for the passage to the next we turn it back into a wave. It was the main object of the present work to gain a clearer understanding of what happens if we refrain from making one of the observations which our instrument would

* There is no hard and fast distinction between the conditions imposed by the boundary and by the form of the differential equation. Thus to represent a mirror we may either take the condition that ψ vanishes on its face, or we may include the other side of the mirror in the dynamical system, by taking a discontinuous potential field in the differential equation.

† 'Z. Physik,' vol. 43, p. 172 (1927).

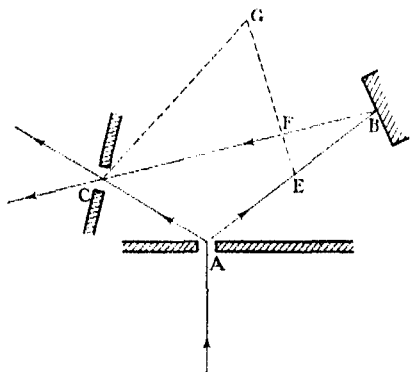
allow, for we must then be able to carry the ψ calculation through this stage of the experiment, without applying the process which I have called turning the wave into a particle and then back again.

To make the matter more definite we had better have an example. Suppose that we are observing the passage of β -rays by means of Wilson clouds. We imagine the rays to be passing from a source through any system of slits, electric or magnetic fields, absorbing foils, crystals to produce interference, moving shutters, etc. Interposed at three places in their path are three cloud chambers which record their passage, and of course in doing so influence their motion, but we shall suppose not so as to stop it completely. The chambers are so disposed that all the rays that enter the second or third will have gone through the first. We observe the cloud tracks of the individual β -rays in all three chambers, and the experiment consists in working out statistical relations between them—say that for every 10 particles in the first chamber there are 5 in the second and 3 in the third. Now the ratio 5 : 3 for the last two chambers will be obtained whether we observe the first chamber or not ; but if we do not look at it, it must be legitimate to regard this chamber as one of the obstacles in the path of the β -rays, on the same footing as the slits and absorbing foils. As it entails absorption, we must include its atoms in our wave equation in the manner described above. There is little doubt that the existing quantum theory would verify that the observations in the second and third chambers are the same whether we regard them as produced by a highly complicated “interference pattern” produced by the first, or whether we observe the actual passage of a particle through the first and regard the wave as restarted there. It would require almost the philosophy of the solipsist to believe that the first chamber gives a cloud track when it is watched and an interference pattern when unwatched ; we have to suppose that the two descriptions are only different aspects of the same thing. This shows that what appears at first sight to be an effect which can only be attributed to particles may, on closer examination, and including more interactions in the system, prove to be explicable without going outside the consideration of continuous solutions of partial differential equations.

The problem which I propose to discuss was dictated by these considerations. It was intended to represent what we may call an unwatched experiment, and to show how a discussion only involving the wave function ψ would give spontaneously the results which simple intuition would suggest could only be due to particles.

3. We shall first describe our ideal experiment in terms of particles, and then

consider how it will appear for waves. On a small hole A in a screen (see figure) there is placed a film of matter composed of atoms of mass m . Incident on



this film is a continuous stream of atoms of mass M and velocity V . The two types each carry an electric charge e , so as to repel one another—the general result would be the same for any law of force, but this one has the advantage that the exact solution is known. In consequence of the collision both types of particle will be scattered away, each type giving rays in all directions, or at any rate in all forward directions.

But that is not all, for the elementary principles of energy and momentum show that if M goes along AB , then m must go along a certain definite direction AC , and both particles must have prescribed velocities. We shall call such a pair of particles a coherent pair. If two observers watch for scintillations in the appropriately related places, they will always see them simultaneously.* The discussion of this coherence by the methods of the wave mechanics is the first half of our problem.

Our object is next so to modify the experiment as to bring the coherence into evidence without directly observing it. Suppose that a mirror is put at any place B , so as to reflect regularly any particles which impinge on it. Somewhere on the line of the reflected beam, at C , we place a screen with a small hole, and at some distance beyond we observe the scintillations of the particles that come through according to their directions. In general we shall have two pencils emerging along the lines AC and BC respectively, each composed of both M and m . This will also be true even when the directions AB and AC correspond to a coherent pair, but with one exception. Suppose that the velocity of M along AB is greater than that of m along AC , then for one particular setting of the mirror the time taken by M to go along ABC will be exactly equal to the time taken by m to go straight from A to C , and the two particles will collide again, and will be scattered at C . The emerging atoms are now composed of a beam of M along AC and of m along BC (which do not interest us) but there will also be atoms of both types completely scattered in all

* In addition to the scintillations of M at B , which are coherent with m at C , there will be scintillations of m at B , of which the partners do not in general fall at C . These do not interest us.

forward directions by the second collision. The scintillations produced by these scattered atoms constitute the second part of our experiment.*

We next consider the experiment from the point of view of waves, and shall see how hard it is to explain the second collision by a direct intuitive argument. If the incident M is a steady stream, there will be a plane sine-wave falling on A and on the further side there will be two sets of spherical waves, one of type M and the other m , each with wave-length varying with the inclination to the direction of the incident wave. In the neighbourhood of the line AB the M wave can be represented as a certain sine-wave with amplitude varying inversely as the distance from A , and the reflexion will not alter its character as it goes along BC . When it comes to C it is in some way capable of acting on the m wave which has come straight from A ; for any other setting of B there is no interaction. Now in wave theory we are quite familiar with cases where one special position produces an interaction far greater than any other, and find that such effects are due to interference. This cannot be invoked here, for a little consideration will show that the effect is totally unlike interference. Suppose that we replace the mirror at B by two at E and F , arranged so as to reflect the beam on to the line BC in exactly the same phase, but by a shorter path. This wave will have the same wave-length and phase as that reflected at B , and yet we know by the particle theory that there will be no interaction at C . The only apparent difference is that the amplitude is larger, but it would be contrary to all experience to suppose that the amplitudes of two waves would affect their interference qualitatively. Moreover it may be noticed that there will be a second collision with mirrors placed at E and G , provided that the path $AEGC$ is equal to ABC ; the angle between the two waves will now be changed, and yet they will interact, which again is quite unlike interference. The same sort of argument suggests that, whatever interaction there may be, it will have the wrong intensity, for we should expect the intensity of the scattered waves to be proportional to the product of the intensities of the two "interfering" waves, and so to the inverse fourth power of the distance AC , whereas with particles it is only proportional to the square.

All this seems to show that the wave theory will find it hard to explain the

* I cannot guarantee that the experiment is practicable, but a rough calculation shows that there is nothing in the orders of magnitude to prevent it. The holes at A and C must be so large that they do not themselves produce much diffraction, and yet so small that a large *proportion* of the pairs emergent at C have been close enough together to be markedly deflected by their collision. The first condition requires the incident velocity to be large, the second small; but taking the particles as electrons, there is a range over which it should be possible to satisfy both conditions.

second collision, but the argument is full of fallacies. We have been thinking of two superposed waves in three dimensional space, whereas it is really a single wave in six dimensions. We shall see that when the problem is properly worked out, the condition for the second collision is that there should be a considerable intensity in the wave function at a point at which the co-ordinates of M and m have the same value. We shall be able to show that this condition is only satisfied at C .

4. In solving the problem I propose to use the method which I developed a year ago in connection with a number of problems of free motion.* In this method a wave function is constructed which itself fulfils all the conditions of the problem, by the device of building up "wave packets" by Fourier integrals out of the standard solutions of the differential equation. It is perhaps worth pointing out that the packets do *not* represent the separate atoms, they are merely a mathematical device for giving the macroscopic conditions of the problem. It is true that the conception was used by Heisenberg† in his discussion of the Uncertainty Principle; but this was because he was there concerned with such questions as the greatest precision with which a particle could be located, and a wave packet represents the nearest approximation to a point that is possible. Here the purpose is different, as we are not concerned with locating *individual* particles. We use the method merely as a way of putting down an expression which satisfies the differential equation for ψ and conforms to the suitable boundary conditions. In this way we can constrict a stream of particles laterally to represent a slit, and if we want to know their velocity directly and without applying the formal quantum rules for the momentum, we can find it by a longitudinal restriction of the train of waves, because this train will be propagated with the group velocity.

To the present writer it seems that the methods of the quantum theory now prevalent lay a very undue stress on the solutions of the ψ equation of the type called proper functions (or eigenfunctions). These functions have enormous practical advantages in that they are the only ones at all easy to discover mathematically, and being the simplest they are those we are apt to look for both theoretically and experimentally; but if we are to accept the full implications of the validity of the ψ equation, we must admit that all its solutions are to be regarded as on an equal footing. This is, of course, nothing but a new aspect of two very old controversies, the first as to whether the general vibration of a string is represented by a function $f(x - \alpha t)$ or by an

* 'Roy. Soc. Proc.,' A, vol. 117, p. 258 (1927).

† *Loc. cit.*

infinite series of harmonic terms, and the second as to whether red light is contained in white or is created by the spectroscopist. These controversies were happily settled by the decision that both parties were right, and my point is that the present methods of the quantum theory show some tendency to deny this, by maintaining that the infinite series of harmonic terms is a more fundamentally correct aspect than the other. However that may be, there can be no question that by taking more general solutions of the ψ equation, we can reproduce the actual physical conditions of many experiments in a much more complete manner, often so much so that the evaluation of the intensities and the final interpretation become almost trivial.

It should be quite possible to work out the solution with packets represented by any form of "peak function," but there is a practical convenience in using the Gaussian function $e^{-x^2/2\sigma^2}$, because the integrals that occur can then usually be evaluated explicitly at every stage, and the parameter σ can be made to represent roughly the breadth of a slit, etc. The assumption of this particular function is, of course, a specialisation, and makes the process unsuitable for general theorems, but that does not matter, since we are here concerned with illustration, not generalisation.

5. By virtue of the property of centres of gravity the solution for the collision of two free charged particles can be reduced to that of the motion of a single particle past a centre of force, and this has been discussed by Gordon,* Mott† and Temple‡. I shall use a solution which is essentially the same as one described by Gordon and as Temple's, but is perhaps simpler, and can be conveniently adapted for the present purpose. This consists in substituting

$$\psi = F(r - z) \cdot \exp \frac{i}{\hbar} \left(pz - \frac{p^2}{2m} t \right)$$

in the wave equation, for it then appears that F obeys an ordinary differential equation, which is easily discussed. We shall use this method, adapting it at once to our own problem.

If the co-ordinates of M and m are respectively \mathbf{X} and \mathbf{x} (three for each) the wave equation for their interaction is

$$\left(-\frac{\hbar^2}{2M} \nabla_{\mathbf{X}}^2 - \frac{\hbar^2}{2m} \nabla_{\mathbf{x}}^2 + \frac{e^2}{r} \right) \psi = i\hbar \frac{\partial \psi}{\partial t} \quad (5.1)$$

* 'Z. Physik,' vol. 48, p. 180 (1928).

† 'Roy. Soc. Proc.,' A, vol. 118, p. 542 (1928).

‡ 'Roy. Soc. Proc.,' A, vol. 121, p. 673 (1928).

where ∇_X^2 , ∇_x^2 are the usual operators associated with X and x , and $r = |X - x|$. We take two velocity vectors, U , u , and write

$$\zeta = r - (U - u, X - x)/|U - u| \quad (5.2)$$

and substitute

$$\psi = F(\zeta) \exp(i/h) \{M(U, X) + m(u, x) - \frac{1}{2}(MU^2 + mu^2)t\}. \quad (5.3)$$

This will satisfy the equation (5.1), provided that F satisfies

$$\zeta \frac{d^2 F}{d\zeta^2} + \frac{dF}{d\zeta} - \frac{i}{h} \frac{|U - u| Mm}{M + m} \zeta \frac{dF}{d\zeta} - \frac{e^2}{h^2} \frac{Mm}{M + m} F = 0,$$

and we are thus led to discuss the equation

$$\zeta \frac{d^2 F}{d\zeta^2} + \frac{dF}{d\zeta} - \frac{i}{b} \zeta \frac{dF}{d\zeta} - \frac{\beta}{b} F = 0, \quad (5.4)$$

where

$$b = h(M + m)/Mm|U - u|$$

and

$$\beta = e^2/h|U - u|. \quad (5.5)$$

The equation is of hypergeometric type and its solution follows the usual lines so that we need only give the results. There are two asymptotic series

$$\left. \begin{aligned} F_1(\zeta) &\sim (\zeta/b)^{i\beta} \{1 + (ib/\zeta)(i\beta)^2 + (ib/\zeta)^2[i\beta(i\beta - 1)^2]/2! + \dots\} \\ F_2(\zeta) &\sim e^{i\zeta/b} (\zeta/b)^{-1-i\beta} \{1 - (ib/\zeta)(i\beta + 1)^2 + \\ &\quad + (ib/\zeta)^2[(i\beta + 1)(i\beta + 2)]^2/2! - \dots\} \end{aligned} \right\}, \quad (5.6)$$

and the particular combination of them which is finite at the origin is

$$F(\zeta) = F_1(\zeta) + F_2(\zeta) \cdot \beta \Gamma(i\beta)/\Gamma(-i\beta). \quad (5.7)$$

If we substitute the leading terms in (5.3), then the term from F_1 has exponential factor

$$\exp i \{M(U, X) + m(u, x)\}/h, \quad (5.8)$$

and the other, after substituting for ζ and b , has

$$\exp i \{rMm|U - u| + (MX + mx, MU + mu)\}/h(M + m). \quad (5.9)$$

Evidently the first corresponds somehow to plane waves and the second to emerging spherical waves, but as it stands the waves are spread all over space, so that the actual solution has little definite meaning. We must give it a meaning by clothing it with the details of our experiment.

6. We first consider the problem without the mirror at B , so as to show that two suitably placed observers will always see scintillations simultaneously.

We have to represent m at rest near the origin, and M advancing towards it with velocity V , but on account of the *uncertainty principle* there is no such thing as a free particle exactly at rest in the wave theory. In nature the difficulty does not arise, because the particles of the film are held together by forces, but it would be troublesome to apply this method, since it would introduce a quantisation that is quite irrelevant to our problem. The alternative is to concentrate the wave at a certain instant of time and then let it spread; if the concentration is over a fairly large area the spreading will not be rapid. We shall suppose that the initial value of the part of the wave function concerned with m is $\psi_m = e^{-x^2/2\sigma^2}$, which implies a concentration roughly within a sphere* of radius σ . By applying Fourier's theorem we then take

$$\psi_m = \int^{(3)} \exp - \frac{\sigma^2 m^2}{2\hbar^2} u^2 + i \frac{m}{\hbar} \{ (u, x) - \frac{1}{2} u^2 t \} du_1 du_2 du_3. \quad (6.1)$$

This can now be evaluated for any later time and (rejecting an unimportant outside factor) gives† $e^{-x^2/2\sigma'^2}$ where $\sigma'^2 = \sigma^2 + i\hbar t/m$.

Since m is now restricted to the neighbourhood of the origin it would be quite legitimate to take an infinite wave to represent the incident wave of M , but it will be convenient to be able to display the velocities of the two particles after the collision, and in order to do this we provide a "time marker," by limiting the length of the incident train. It is hardly an extra complication to limit the breadth as well, and makes the treatment more uniform, but we can conveniently mark the distinction between the forward and crosswise directions by shaping the packet as a spheroid instead of a sphere. We therefore take

$$\begin{aligned} \psi_M = \int^{(3)} \exp - \frac{\tau^2 M^2}{2\hbar^2} (U_1^2 + U_2^2) - \frac{\nu^2 M^2}{2\hbar^2} (U_3 - V)^2 \\ + i \frac{M}{\hbar} \{ (U, X) - \frac{1}{2} U^2 t \} dU_1 dU_2 dU_3. \end{aligned} \quad (6.2)$$

This represents a wave, roughly concentrated inside a spheroid of axes τ, τ, ν , advancing towards the origin along X_3 with velocity V . Like the m wave it will spread with the time, and we have supposed it so adjusted that it will come to a "focus" at time zero round the origin.‡

* It would be just as easy to work with an ellipsoid instead of a sphere, but would make no essential difference, and would unnecessarily increase the number of our symbols.

† For details see my paper, *loc. cit.*

‡ If τ, ν are complex it would be focussed at some other time, but still on the axis of X_3 ; if a factor $\exp - iMU_1 A/\hbar$ is included in the integrand, it will focus at the point A, O, O . Any modifications of this kind are easily inserted, but nothing is gained by the generality.

It is now clear what the solution of the wave equation must be, for part of it must represent the product $\psi_M \psi_m$ asymptotically. We therefore take

$$\psi = \int^{(6)} dU_1 \dots du_3 \exp - \frac{\tau^2 M^2}{2\hbar^2} (U_1^2 + U_2^2) - \frac{v^2 M^2}{2\hbar^2} (U_3 - V)^2 - \frac{\sigma^2 m^2}{2\hbar^2} u^2 \\ \exp (i/\hbar) \{M(U, X) + m(u, x) - \frac{1}{2}(MU^2 + mu^2)t\} F(\zeta), \quad (6.3)$$

where ζ is given by (5.2) and F by (5.7). This will be the sum of two terms corresponding to the two asymptotic series of F . These series are valid as long as ζ is not small, that is to say, excluding from the six-space those regions round the forward direction, where $X_1 = x_1$, $X_2 = x_2$ and X_3 has any value greater than x_3 .

The function F contains factors which are not amenable to direct integration, but it is easy to see how they may be removed. The chief contribution to the integral is derived from the range determined by the quadratic exponentials; it is roughly speaking the range for all three components of u between $\pm \hbar/\sigma m$, for U_1 and U_2 between $\pm \hbar/\tau M$ and for U_3 between $V \pm \hbar/vM$. These ranges represent the velocities implied by the uncertainty principle, and it is evidently one of the conditions of the experiment that the uncertainties of velocity should be much less than V . We conclude that in the slowly varying factors it will be legitimate to replace $|U - u|$ by V . This applies not only to the factor $\beta \Gamma(i\beta)/\Gamma(-i\beta)$ in F , but also to the factors $(\zeta/b)^{i\beta}$ and $(\zeta/b)^{-i\beta}$ in F_1 and F_2 . They represent changes of phase of the approaching and receding waves, and will have no effect on intensity, so that (though they are strictly necessary to make the solution valid) we may omit them. We are not concerned in the present work with the absolute amount of scattering and shall therefore replace $(\zeta/b)^{-1}$ and the other outside factors of F_2 by $(r - X_3 + x_3)^{-1}$. These modifications and omissions are equivalent to replacing F_1 by unity and F_2 by $e^{i\phi}/(r - X_3 + x_3)$, and we see that the F_1 term in (6.3) correctly gives the incident wave. It only remains to work out the scattered wave which depends on F_2 . In substituting (5.9) we must replace $|U - u|$ not by V , as in the slowly varying terms, but by $U_3 - u_3$ which is a better and sufficient approximation, since U_3 is of the magnitude of V . Then the scattered wave is

$$\psi = \int^{(6)} \frac{dU_1 \dots du_3}{r - X_3 + x_3} \exp - \frac{\tau^2 M^2}{2\hbar^2} (U_1^2 + U_2^2) - \frac{v^2 M^2}{2\hbar^2} (U_3 - V)^2 - \frac{\sigma^2 m^2}{2\hbar^2} u^2, \\ \exp \frac{i}{\hbar} \left\{ \frac{Mm}{M+m} r (U_3 - u_3) + \frac{(MX + mx, MU + mu)}{M+m} - \frac{1}{2}(MU^2 + mu^2)t \right\}.$$

This can now be integrated for all six variables. We omit certain factors outside the exponential and write

$$\sigma'^2 = \sigma^2 + i\hbar t/m, \quad \tau'^2 = \tau^2 + i\hbar t/M, \quad v'^2 = v^2 + i\hbar t/M,$$

and find

$$\begin{aligned} \psi = & \frac{1}{r - X_3 + x_3} \exp - \frac{1}{2} \left(\frac{1}{\sigma'^2} + \frac{1}{\tau'^2} \right) \left\{ \left(\frac{MX_1 + mx_1}{M + m} \right)^2 + \left(\frac{MX_2 + mx_2}{M + m} \right)^2 \right\} \\ & - \frac{1}{2\sigma'^2} \left(\frac{MX_3 + mx_3 - Mr}{M + m} \right)^2 - \frac{1}{2v'^2} \left(\frac{MX_3 + mx_3 + mr - Vt}{M + m} \right)^2 \\ & + \frac{iMV}{\hbar} \left\{ \frac{MX_3 + mx_3 + mr}{M + m} - \frac{1}{2} Vt \right\}. \end{aligned} \quad (6.4)$$

This is the asymptotic form of the scattered wave. Observe that, as we should expect, it only exists sensibly for positive time, because when t is negative the fourth quadratic factor makes ψ negligible.

Though it is quite easy to write down the intensity from (6.4), we can see what it is like without doing so. In the first place the growing quantities σ'^2 , etc. (or rather the growth of the corresponding real expressions $\sigma^2 + (\hbar t/cm)^2$, etc., which occur in the intensity) express the fact that with the lapse of time the initial uncertainty of velocity will lead to a great uncertainty of position; but there will be an interval of time during which this can be disregarded. During this interval we may say that we should expect to find the two particles near the places described by

$$\left. \begin{aligned} MX_1 + mx_1 &= 0 \\ MX_2 + mx_2 &= 0 \\ MX_3 + mx_3 - Mr &= 0 \\ MX_3 + mx_3 + mr - (M + m)Vt &= 0. \end{aligned} \right\} \quad (6.5)$$

These equations present the facts of collision, but in a rather unusual way; they are easily brought into a more familiar form. From the last two we derive $r = Vt$, and if we substitute this value in the third equation, we can derive the three equations of momentum by differentiating with regard to the time. For the equation of energy we have to make use of the value of r in terms of X and x . Since

$$Mm(X_1 - x_1)^2 = (M + m)(MX_1^2 + mx_1^2) - (MX_1 + mx_1)^2, \text{ etc.,}$$

we deduce that

$$Mmr^2 = (M + m)(MX^2 + mx^2) - M^2r^2.$$

Also X , x , and r are all proportional to the time, so that we may set $X = \dot{X}t$, $x = \dot{x}t$, $r = Vt$ and hence we find the energy equation

$$M\dot{X}^2 + m\dot{x}^2 = MV^2.$$

It is unnecessary to discuss the details further; two observers at places indicated by the elementary particle theory, will always see scintillations simultaneously.

7. It is perhaps worth considering how we could have worked out the general characters of (6.4) without solving the wave equation in detail; for with a different law for the force of interaction the equation may not be soluble, and yet we can express the results of the collision qualitatively. Since we know all about the velocity of each particle for every direction, we might be tempted to construct a three dimensional wave for each separately and then bind them together by taking four quadratic exponentials of the types given by (6.5). This method breaks down at the very beginning, because there is no expression for a radially emergent wave of wave-length varying with the direction. We must proceed as follows. Assume as phase factor an arbitrary linear function of X, x, r, t . From this we can derive seven expressions, of the type $\frac{h}{2i} \left(\psi^* \frac{\partial \psi}{\partial x} - \psi \frac{\partial \psi^*}{\partial x} \right)$, for the momenta of the two particles and their joint energy. Now elementary considerations enable us to express the positions of the particles in terms of the time and the direction of motion of one of them, and a comparison of the two sets of equations fixes the form of the phase factor as the same as the last line of (6.4). On this phase we must impose four quadratic exponentials (or some form of peak function) determined by linear combinations of (6.5). It is not very clear what particular choice should be made for these four, and probably it is in general immaterial, but by considering the case where the train of incident M waves is of infinite length, we can see that three of the four must not involve the time, and so must be the first three of (6.5); for the fourth it would seem that $r - Vt$ is just as valid as the one we obtained.

The method of solution by wave packets makes it very easy to show a feature of general theory, which is by no means so easy when only proper functions are used. The passage of a particle past a fixed centre of force is clearly a limiting case of the collision of two free particles, and it should be possible to discuss it by taking one of the two particles as of very large mass. If we try to use only proper functions, the wave is spread uniformly over the whole six-space, and so the first step in the discussion must be equivalent to what we have done for all values of the masses—to concentrate the heavy mass in a packet. With our method we merely need to make m large in (6.4). Then the first three terms show that x_1, x_2, x_3 stay near zero, the fourth gives V for the velocity of recession of M, and the phase

factor expresses the fact that the wave velocity is as usual half the group velocity.

8. We now come to our second problem, where the coherence of the pairs of particles is observed indirectly by means of the second collision. It will be convenient to take the mirror at B as infinite in area, so that we must restate the problem. We keep the mirror in a fixed position and consider all the reflexion from it; then we have to show that associated with the fixed mirror there is a certain definite point C where second collisions occur. There will as a fact be also another place C', where reflected m collides with direct M instead of the converse, but this adds nothing new. It is not practically possible to carry out what would be the most satisfactory method of solution. This would consist in solving the wave equation (5.1) subject to the usual conditions of finiteness for ψ , but now with the added condition that it should vanish over the plane of the mirror in both X and x . If this could be done, the two collisions would appear as a single effect; we should build up the wave packets as in the last problem, and ought to find that in the field of six-fold integration there were secondary parts giving perceptible contributions, which would correspond to the regions round C and C'. Since this method is impracticable, we must be content with an adaptation of (6.4).

In § 6 the incident wave of M was taken as of limited length. With this limitation the scattered wave groups have velocities appropriate to particles, and so cannot possibly come to a second collision except in the region round C. Now our whole object is to show that the second collision does not in the least depend on this particle-like property of wave groups, but will occur even when the incident wave is a uniform train of infinite length. We must therefore now take v as infinite, and it will make no further change in the form of (6.4) to take τ as infinite also, that is to say to have the incident M-wave infinite in breadth as well as length. If we had chosen to do this in the first problem, we should have started simply with $\psi_M = \exp iMV(X_3 - \frac{1}{2}Vt)/h$ and there would have been only three-fold, instead of six-fold integrations. We therefore replace (6.4) by

$$\begin{aligned} \psi = \frac{1}{r - X_2 + x_3} \exp - \frac{1}{2\sigma'^2(M+m)^2} \{ & (MX_1 + mx_1)^2 \\ & + (MX_2 + mx_2)^2 + (MX_3 + mx_3 - Mr)^2 \} \\ & + i \frac{MV}{h(M+m)} \{ MX_3 + mx_3 + mr - \frac{1}{2}(M+m)Vt \}, \quad (8.1) \end{aligned}$$

and this is now a steady wave (apart from the slowly increasing σ') and contains no direct indication of the velocities of the particles after the first collision.

We next have to represent the reflexion. In each of the three-spaces X and x of which the six-space is composed, there is a plane, expressed by the same numerical coefficients in both cases, and the condition is that ψ will vanish when X is on this plane, whatever x may be, and vice versa. Now for values of X near the mirror, the wave function practically vanishes except for values of x far from it, and so r is large and in this region the wave equation is practically satisfied with the term in c^2/r omitted. If we subtract from this ψ an expression of the same form but with X replaced by X' , its image point in the mirror, we shall satisfy the wave equation to the same approximation while making ψ vanish on the surface. It is not, of course, an accurate solution, because the factor outside the exponential now involves $r' = |X' - x|$, instead of $r = |X - x|$; but it represents the reflexion of M with sufficient accuracy. That the error is quite negligible can be easiest seen from the analogy of particles; we are neglecting the force exerted between the coherent pair m and M , when M has reached the mirror. There will also be a reflexion of m , and the whole system of waves will be

$$\psi(X, x) - \psi(X', x) - \psi(X, x') + \psi(X', x') \quad (8.2)$$

where $\psi(X, x)$ is given by (8.1), and X', x' are respectively the image points of X, x in the mirror.

We need only discuss the term $\psi(X', x)$ which represents the interaction of reflected M with m , since $\psi(X, x')$ will merely give the similar effect with the rôles of M and m interchanged. We have

$$\begin{aligned} \psi(X', x) = & \frac{1}{r' - X_3' + x_3} \exp - \frac{1}{2\sigma'^2(M + m)^2} \{ (MX_1' + mx_1)^2 \\ & + (MX_2' + mx_2)^2 + (MX_3' + mx_3 - Mr')^2 \} \\ & + \frac{i}{h(M + m)} \{ MX_3' + mx_3 + mr' - \frac{1}{2}(M + m)Vt \}. \end{aligned} \quad (8.3)$$

If we needed actually to work out in detail the scattering produced by the second collision, it would be necessary to expand this in the form

$$\int^{(6)} dU_1 \dots du_3 \exp i \{ M(U, X) + m(u, x) - \frac{1}{2}(MU^2 + mu^2)t \} / h \cdot \phi(U, u),$$

which is possible since (8.3) satisfies the wave equation approximately without the terms in c^2/r , and then introduce $F_2(\zeta)$ a second time to give the result of the second collision. But we only really want to find where the collision will occur, and all this is unnecessary. For we may say that the region of collision

is that part of the six-space where the force e^2/r is important, and this is determined by the three equations $X = x$. Now there is only a small part of the six-space where the wave function does not vanish; it is given by the quadratic terms in (8.3). We therefore conclude that there will be a second scattering of the waves at the place* where

$$\left. \begin{aligned} MX_1' + mx_1 &= 0 \\ MX_2' + mx_2 &= 0 \\ MX_3' + mx_3 - Mr' &= 0 \\ X_1 = x_1, \quad X_2 = x_2, \quad X_3 = x_3 \end{aligned} \right\} \quad (8.4)$$

In order to see that this corresponds with the result of the particle theory, it is only necessary to introduce an auxiliary variable, conveniently called Vt , and defined by the equation

$$MX_3' + mx_3 + mr' = (M + m)Vt.$$

It is then obvious that we have exactly the equations that we should have in the particle theory, but there with t signifying the time, and so shall determine exactly the same place for the second collision. A simple calculation shows that if

$$X_1 \sin \eta + X_3 \cos \eta = p$$

is the plane of the mirror, the point C is at

$$\begin{aligned} X_1 = x_1 &= -2pM \sin \eta / \{M(2 \cos \eta - 1) + m\} \\ X_2 = x_2 &= 0 \\ X_3 = x_3 &= 2pM(1 - \cos \eta) / \{M(2 \cos \eta - 1) + m\}. \end{aligned}$$

9. We have seen by the discussion of our problem that whereas crude intuition would suggest that the occurrence of the second collision must be a definite property of particles, yet it can be fully explained without the invocation of particle properties. There is of course no suggestion that we can dispense with the idea of particles altogether, but only that we can *postpone* thinking about them until the next stage of the experiment when they produce scintillations. Though for practical reasons the example was chosen in a specially simple way, yet it does not seem to have any very specialised features which would make it exceptional, and so we are led to speculate that the possibility of this postponement is general. We will then assume that the ψ equation

* The same argument applied in § 6 of course gives the origin as the place of first scattering.

is competent to yield all particle-like properties, whenever we infer them indirectly without actual observation. This is entirely in accordance with the present state of the mathematical theory, but is equally contrary to our habits of thought about quantum problems, and so it may be well to illustrate it further.

Consider for example one of the most striking manifestations of particle characters, the ray tracks of α -particles in a Wilson cloud chamber. We have to connect this in some way with the theory of radioactive disintegration as presented by Gamow. In that theory the radium nucleus contains what we may call an α -wave which is slowly and continuously leaking out as a spherical wave. It would seem at first sight that we *must* regard Gamow's calculation as determining only the probability of disintegration, and that when this has taken place, we start the next stage by assigning a definite direction for the motion of the α -particle; after which we reconvert it into a wave, but now on a narrow front, so as to find its subsequent history. Before seeing why this assumption is unnecessary in explaining the track, we may notice that it introduces severe difficulty in another aspect of the matter. It should certainly be possible to make α -rays exhibit diffraction (though it has not been verified experimentally), say, by sending them through a crystal and observing scintillations beyond—the appropriate distance is about a kilometre, but that does not affect the argument. This shows that we have got to be prepared to consider the spherical wave of Gamow as having an existence outside the nucleus. Turning now to the cloud track, what we have to explain is this. Suppose that we are looking at the track, but with its earlier half covered up. We see the later part, and our principle of postponement tells us that it must be possible to represent the earlier part by means of ψ without a mention of the track, though we know that if we took away the cover we should see it; the ψ has got to be spherically symmetrical about the radium, and so it seems impossible that it can represent the anisotropy of the track. In view of what has gone before we can see how the answer is to be given. The wave ψ is not a spherical wave, because it must contain factors corresponding to all the ionisable atoms in the unseen part of the chamber. Before the very first collision it can be represented as the product of a spherical wave for the α -particle, by a set of more or less stationary waves for the atoms. But the first collision changes this product into a function in which the two types of co-ordinate are inextricably mixed, and every subsequent collision makes it worse. In the multiple space the exponent of the phase factor, as indicated by (6.4), will be a sum of linear terms composed partly of the co-ordinates

associated with the particles, and partly of their mutual distances. Without in the least seeing the details, it looks quite natural to expect that this phase factor will have some special character, such as vanishing, when the various co-ordinates satisfy a condition of collinearity. So without pretending to have mastered the details, we can understand how it is possible for the ψ function, so to speak, not to know in what direction the track is to be, but yet to insist that it shall be a straight line. The decision as to the actual track can be postponed until the wave reaches the uncovered part, where the observations are made.

In some such way as this we can see how it is possible to postpone speaking of particles, in cases where intuition indicated that it was unavoidable to invoke them. The important question arises as to whether this is always so; for if there are cases of failure, there is some defect in our mathematical theory, and it must be one of our chief objects to delimit when and where it occurs. There is no indication of any such failure at present, though perhaps a slight doubt may attach to the relationship between matter and radiation, because Dirac's theory* presents the ψ equation in a rather different form from that used for material particles; but it would seem legitimate to dismiss this doubt in view of the great general similarity of radiation and matter. It thus seems legitimate to suppose that it is always admissible to postpone the stage, at which we are forced to think of particles, right up to the point at which they are actually observed.

10. In the present section I propose to discuss certain fundamental questions of the quantum theory. One of the most unexpected things about the new discoveries was that it is possible to present the theory so that some of its main features are very nearly identical with those of the classical theory of sound. Of course the analogy must not be pushed too far, but as our habits of thought are always much dependent on analogies, it seemed to me that it would be of interest to examine in more detail the form the theory would take when this aspect is emphasised at the expense of the customary dynamical one.

We shall therefore take the wave function ψ as the central feature of the quantum theory, recognising that this is in some respects a retrograde step to make, for it is a chief doctrine of the philosophy of modern physics that our theories should only contain observable quantities. Against this objection it may be urged that it is doubtful whether we should ever have had a theory of relativity or a statistical theory of thermodynamics, if the condition of observability had been imposed when scientists first began to study

* 'Roy. Soc. Proc.,' A, vol. 114, p. 243 (1927).

dynamics or the theory of gases. Underlying all the earlier developments of the statistical theory was the idea that we could, if only we had the patience, work out in detail the motions of all the molecules; no one ever pretended that it was possible to do so, but the ideal possibility gave confidence in those consequences of the theory that were attainable. If we had been required to dispense with this underlying assumption, we should have had to develop thermodynamics without a fundamental absolute basis of dynamics, a task that no one has attempted. In a final formulation of the quantum theory, we should have to acknowledge the failure of the analogy between the practically unknowable motions of molecules, and the theoretically unknowable ψ , but it may help to harden the outline of our *incomplete* theory to imagine that there is a definite quantity ψ , even though a second postulate immediately asserts that it is unknowable. From the practical point of view the great advantage of thinking in terms of ψ is that it forces on our attention the diffractive effects of matter and treats them as an even more fundamental property than the ray-like properties which suffice for the description of most ordinary events. Our method of thought will be analogous to the principle that geometrical optics is a special case of physical optics, not that the framework of geometrical optics is to be extended so as to include physical as an exceptional case. I shall omit altogether from consideration some of the most interesting aspects of the quantum theory, in particular the relativity conception of time, and also all questions connected with the individuality of particles as typified by the Exclusion Principle.

The preceding sections go to show how it comes about that there is no need to invoke particle-like properties in the unobserved parts of any occurrence, since the wave function ψ will give all the necessary effects. It must therefore also be possible to divide the component parts of an observing chamber into two halves, of which one half is included under ψ , and the observed result is given by *interpreting* the effect of the original system and this half together on the other. For example if we are observing the scintillations of α -particles, we usually think of the stopping of the α -particle as the observation. The scintillation is due to the bursting of a small zinc sulphide crystal, and we might include the atoms of this crystal in our ψ along with the α -wave. We might go further by including the emitted radiation and take as the observation the intensity of light in the retina of the eye. Even this is not all, for we might include the photoelectrons emitted from the retina, and the optic nerve also, but somewhere in the brain we are absolutely compelled to stop. We can say that all the occurrences right up to the brain are non-committal, in that they

contain no definite implication of where and when the α -particle came ; it is only after our consciousness has animated the proceedings that it is possible to infer back and describe what actually happened in the familiar language of particles. If these ideas are admissible, we can put the inexplicable feature of the quantum theory, the irreconcilability of wave and particle, in exactly the place where we have got in any case to have an inexplicability, in the transfer from objective to subjective.

Following this line of argument, we are led to the conception of a sub-world which contains no mention of observation at all. In this sub-world ψ is an unthinkable complicated function of all the variables associated with all the particles of the world ; nothing definite is happening at all, but it expresses simultaneously everything that could possibly happen. The form of ψ may be pictured as like the strains of a many-dimensioned continuum. It bears a rather close resemblance to the Gibbsian *ensemble* of a set of systems, though it is composed not of an infinite set of "representative points" but of a single "representative continuum." In this last respect it is a more complicated conception than that of Gibbs, but in another it is simpler, for Gibbs had to consider a large number of systems all at once, whereas here we only have a single system which describes the whole world, embodying in itself the whole of the *ensemble*.* It is troublesome to have to think about a "representative continuum," and for some purposes we shall find it useful to replace the idea. The function ψ has a definite value for all the values of all the variables which correspond to all the particles of the world. We split up each variable by taking each of the infinite number of values in its range as a co-ordinate in a new space, and in this space we mark a single point so that it records the magnitude of ψ for all the new co-ordinates. In this "multi-infinite" space a single point then represents the state of the world and a single line its history. It is interesting to observe that the quantum itself plays no part at all in the sub-world, except as a dimensional constant which can be incorporated with the other dimensional constants of the system. It should also be noted that there is no need to allow for the phase factors introduced by each particle of the assembly, for they merely contribute to a general arbitrary constant affecting ψ .

The sub-world of ψ expresses in its own way everything that happens ; but it is a dead world, not involving definite events, but instead the potentiality for all possible events. It becomes animated by our consciousness, which so

* Quite apart from the special point of view discussed here, it is a good characterisation of the quantum theory to say that every assembly is its own *ensemble*.

to speak cuts sections of it when it makes observations. These observations are described in a language and by means of a set of rules which are quite foreign to the sub-world ; the quantum itself enters for the first time, and the characteristic feature is the normalisation of $|\psi|^2$, etc., whereby we can talk of atoms, electrons and light-quanta. Provided that we retain the accurate form of ψ , the mathematical rules of the interpretation suffice for a complete verification of the theorems of conservation of energy, etc. ; the trouble with them in the quantum theory has only arisen through attempts to work with an incomplete ψ . Every observation enables us to obtain information about ψ , but it is partial information, because something, if it is only ourselves, has been omitted from the observation. Observations can never tell us all about the position of the world-point in the " multi-infinite " space, but merely indicate a region near which it must lie. In many cases the courses of all the possible world-lines in the region are so similar that we can forecast the future with great certainty, as in macroscopic dynamics ; but in atomic motions we should regard the successive observations as strung out in the neighbourhood of the line, all correlated with it but not directly with one another. Their irregular positions round the line give rise to the apparent discontinuities which are bound to occur when we use the language of particles. We see why all the theorems about observed particles have the validity of thermodynamics, and not the absolute validity which we have imputed to the sub-world of ψ .

To conclude, it was not intended that these speculations should represent anything more than a description of what one possible formulation of the quantum theory would yield. The result is perhaps not very favourable to it ; but I think that, if the matter is considered critically, it will be seen that at any rate some of its difficulties are not to be attributed to the particular formulation adopted here, but are inherent in the nature of things.

Summary.

In the quantum theory one method of procedure is to regard the motion of matter as a wave motion, but this motion must be *interpreted* in terms of particles in order to describe what is observed. Motions can be imagined which seem to imply particles in cases where they are not directly observed. An ideal experiment of this kind is devised, depending on collisions between two free bodies, and it is shown that the particle-like behaviour is given just as successfully by the wave theory. This implies that the interpretation can sometimes be postponed, and there follow speculations as to the consequences of this postponement in the general theory.

*A Photoelectric Method of Measuring the Light of the Night Sky
with Studies of the Course of Variation through the Night.*

By Lord RAYLEIGH, F.R.S.

(Received April 3, 1929.)

The investigations already published on the intensity of the light of the night sky* have been made by means of visual photometry, using a convenient instrument with a self-contained luminous source of radioactive origin. Nothing could rival this for simplicity and portability; it is always ready and requires no attention. On the other hand visual photometry is not a very satisfactory process even for ordinary light, and with this faint light it is far from giving the desirable degree of accuracy. I have therefore spent much effort in trying to replace it by some photoelectric method of measurement. A satisfactory method has now been evolved, and will be described, together with the results.

A preliminary notice of the earlier results was given in a paper written at the request of Prof. S. Chapman, F.R.S., Chairman of the International Committee on Terrestrial and Solar Relationships, the receipt of which was acknowledged by him on June 19, 1928.† The relevant passage is :—

“ Most of the difficulties have been overcome and preliminary observations have been in progress for some months past. I have been able to follow the changes of intensity from hour to hour on clear nights. Some evidence has been found suggesting diurnal periodicity. The observed intensity nearly always increases between nightfall and midnight, beyond which the observations have not usually been carried.”

The first efforts were made with selenium cells of various patterns. The necessary deflection could be obtained, but only with long exposures to the

* ‘ Roy. Soc. Proc.,’ A, vol. 106, p. 117 (1924) ; *ibid.*, vol. 109, p. 428 (1925) ; *ibid.*, vol. 119, p. 11 (1928).

† The paper was afterwards published in ‘ Nature,’ September 8, 1928. I have thought it well to emphasise the date at which it was sent in to Prof. Chapman, because it was before the date of McLennan’s Bakerian lecture of June 28th (abstract circulated June 27). Prof. McLennan was, of course, unaware of this ; nor is it important, except to show that the conclusions were formulated independently for publication. At the same time it is not strictly correct to say, as he does, that the experiments made by him and by H. J. C. Ireton in April, 1928, were the first to give evidence of the existence of a diurnal variation.

light. After trials (in more senses than one) lasting over some weeks, this method was abandoned.

A thalofide cell was tried, using a sensitive D'Arsonval galvanometer. The deflections, though detectable, were insufficient.

Much time was spent in attempting to amplify the continuous current of a photoelectric cell with a three or four electrode valve. Some experimenters have reported great photometric sensitivity obtained in this way, but I was not successful in getting the sensitivity quite up to the necessary standard for the present purpose. I then fell back on the use of electrometer and photoelectric cell. My experience of electrometers dated from many years ago, when no convenient patterns were available, so that I had wished to avoid this method, but on trying a Lindemann quartz fibre electrometer, success was at once obtained.

The electrometer was used as a highly sensitive galvanometer by means of an alcohol-xytol resistance tube establishing a leak to earth. The resistance of the tube was probably about 10^{10} ohms, though its value was not determined.

The method of measurement was, in brief, to equalise the controlled artificial illumination of a white screen to the brightness of the sky. The whole apparatus was set up in a dark room, and the sky was seen through a small aperture measuring 90×150 mm. This aperture faced nearly to the north. It was approximately focussed onto the photoelectric cell by means of a lantern condenser of the ordinary pattern, 4 inches in diameter and about 3 inches equivalent focal length. The optic axis of the condenser was elevated at 45° , and the photoelectric cell took in a cone of sky of about 24° (12° either side of axis). The patch of sky was seen through an oblong aperture in a broad black velvet frame, placed vertically in a shutter and therefore oblique to the optic axis of the condenser but capable of transmitting the full beam. At the option of the observer this aperture could be opened, or closed, with a white card which entirely filled it (see fig. 1). The card was carried on a light arm of bamboo, 50 cm. in length, and capable of rotation about a fixed axis. The arm was, in fact, attached to the rotating part of a bicycle hub, the fixed axle of the latter coming out perpendicular from the wall. The rotating hub which carried the arm was prolonged axially into a handle which came convenient to the observer's hand. By a turn of the wrist the wooden arm could be rotated, between fixed stops, which caused the white card either to come into view and fill the aperture, or to retreat behind the black velvet frame, leaving the aperture open to the sky. Owing to the small moment of inertia, and the easy rotation, this change could be carried out instantaneously.

Small pieces of rubber sponge served as convenient shock absorbers, and prevented any shaking of the electrometer.

A small incandescent lamp with a ground glass diffusing screen was placed high up on the wall behind the observer, at a distance of about 5.5 metres from the white card, which was illuminated by it, the rays passing just over

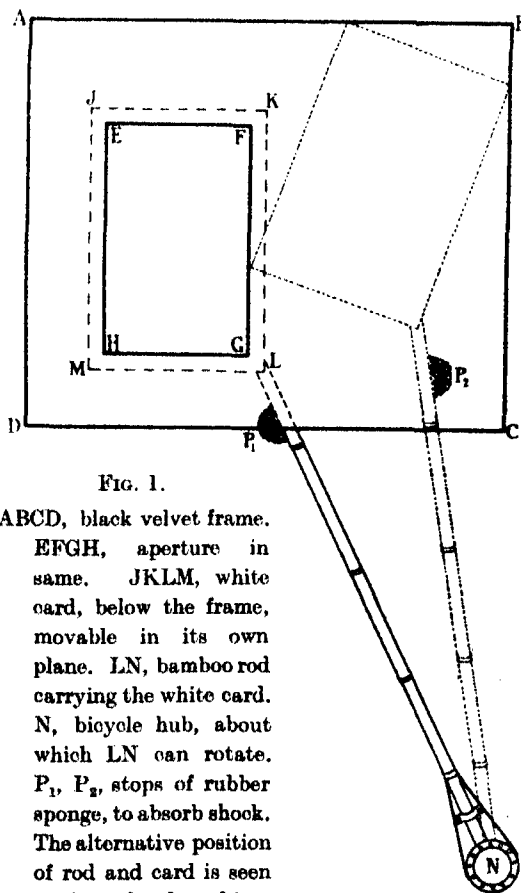


FIG. 1.

ABCD, black velvet frame.
EFGH, aperture in same. JKLM, white card, below the frame, movable in its own plane. LN, bamboo rod carrying the white card. N, bicycle hub, about which LN can rotate. P₁, P₂, stops of rubber sponge, to absorb shock. The alternative position of rod and card is seen to the right, dotted in.

the observer's head. The mutual arrangement of the parts is shown in fig. 2, which is not, of course, to scale. The brightness was controlled by a resistance in the lamp circuit, which was placed conveniently to the observer's hand, and the measurement consisted in equalising the electrometer deflection with (1) the aperture open to the sky, (2) the aperture closed by the illuminated card. When this adjustment was satisfactory, the voltage across the lamp was read and recorded. This voltage was a measure of the intensity of the sky

illumination. The definiteness and reproducibility of this measure depends, of course, for one thing upon the constancy of behaviour of the lamp under a

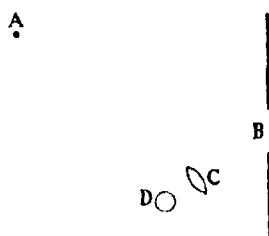


FIG. 2.—A, incandescent lamp.

B, aperture in shutter, backed by the sky, or alternatively filled in by a white screen.

C, condensing lens. D, photo-electric cell.

given voltage. The lamp was "aged" by running it at normal voltage (4 volts) for a considerable number of hours before taking it into use. In use it was run very much below this voltage at values not more than about 2.2 volts, which was enough to give the faint light required. As an additional precaution, it was not left on longer than necessary. Under these circumstances, and in view of known photometric experience, it was thought safe to rely on the constancy of illumination under given voltage.*

It will be observed that this method of measurement does not require that the zero of the electrometer or its sensibility should remain constant over long periods. All that is required is that its behaviour should be satisfactory for a minute or so while the equalisation is being obtained. When the needle is unsteady, this usually arises from failure of the dry batteries used to maintain the potential of the electrometer quadrants, or those used on the photoelectric cell. If even one cell in either of these batteries is beginning to fail, unsteadiness is introduced.

The method does not require that the photoelectric cell should be of constant sensitivity, but *does* require that the spectral distribution of sensitivity should not change. This is necessary, because the incandescent lamp, run much below its rated voltage, is far redder than the night sky† and the relative values will be altered if the quality of the cell alters. This is liable to occur if a discharge passes through the cell, for such treatment does not in general affect the yellow and blue sensitivities to the same extent. I have reason to believe that, in fact, this did occur, owing to the cell being accidentally exposed to the daylight while a voltage, quite safe under night conditions but unsafe for day ones, was left on it. This probably happened more than once, before its importance was realised. Owing to this I cannot regard the series of definitive experiments,

* It was found unsatisfactory to rely on the usual lamp sockets with spring contacts. The voltmeter contacts were soldered to the wires coming through the lamp bulb.

† Former experiments made visually showed that a gas-filled lamp at its normal voltage is nearly comparable with the night sky, 'Roy. Soc. Proc.,' A, vol. 106, p. 134 (1924).

presently to be described, as being of any value for comparing month with month, or determining the annual periodicity. They can only be fully relied on for determining the diurnal variation. In designing future work it will be important to bear this source of error in mind.

The photoelectric cell was used near its maximum voltage, which is conditioned to some extent by the intensity of the light. As is well known, excessive voltage leads to intermittent passage of a current, causing jerks of the electrometer needle.

The voltage on the lamp was read to 0.01 volt on a medium sized Weston voltmeter. It is in general possible to rely on the reading as really giving the sky intensity (as modified by the prevailing atmospheric conditions) to the accuracy aimed at, *i.e.*, ± 0.005 volt. It would probably not be difficult with a little further elaboration of detail to reduce the error to half this amount. But the advance already made on the visual method is very great, since the error of reading has been reduced about ten times. This improvement makes it possible to record the hourly changes of intensity, and opens up a wide field of investigation.

The photoelectric cells used have been various. They were all gas-filled. In the visual photometric work already published and in progress, three spectral regions are contemplated, *viz.*, the region of the green auroral line ($\lambda 5577$) and the red and blue regions on either side of this line, *not* including the line itself. The red and auroral regions have shown the largest variation visually, and are therefore of most interest; but, unfortunately, the ordinary potassium or rubidium photoelectric cells which have been most readily obtainable are not sensitive to these regions. For them we must have recourse either to caesium cells or to the special red sensitive cells described by N. R. Campbell* and supplied by the Research Laboratory of the General Electric Company, Wembley, Middlesex.

I was furnished with caesium cells by the kindness of Prof. F. A. Lindemann, F.R.S., and also of the Wembley laboratories. They were tried under a deep yellow screen (Wratten 21), such as to transmit the auroral green line, but to cut off the blue. Unfortunately, however, the sensitiveness proved insufficient to allow of satisfactory measurements of sky intensity.

Using one of Campbell's red sensitive cells with a Wratten No. 21 filter, a number of preliminary measurements were made. The results are shown on the graph, fig. 3. They established definitely the feasibility of the method, and showed that the course of change could be followed from hour to hour.

* 'Phil. Mag.', vol. 6, p. 633 (1928).

Moreover, all of the four graphs give an indication of the general tendency to rise towards midnight. Owing to the failure of the cell, this series could

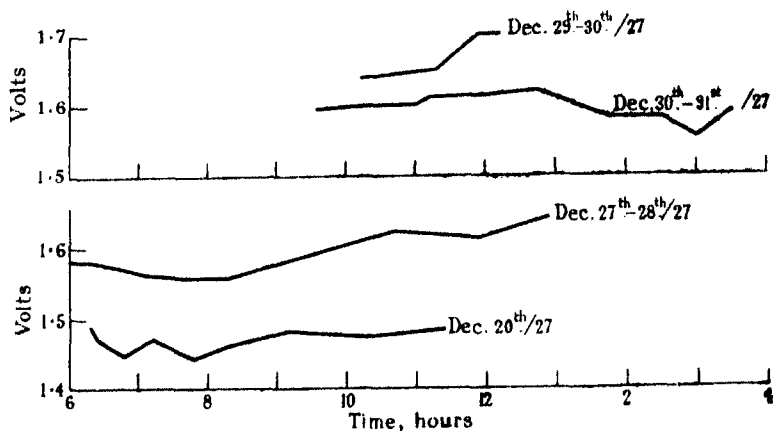


FIG. 3.

not be continued long enough to establish definitely the reality of this tendency.*

I then had recourse to a rubidium cell, also made by the Wembley Laboratories. This has remained in use for the definitive work so far accomplished. The sensitivity is practically nil for the green auroral line, and is limited to shorter waves than this. It was possible, however, to use it either with a Wratten pale yellow screen No. 9, or a blue screen No. 47, dividing, what in the visual work I have called the blue region, into two portions. In all cases the variation of intensity in these subdivisions of the blue region were found to proceed *pari passu*. For further work, therefore, the filters were discarded, and the cell used without them.

It has been thought best to give the results in full (Table I), omitting only a few readings taken shortly before or after those which are recorded, and showing no change. The intensities are recorded in volts, and vary over a range of 1.80 to 2.14 volts.

To determine the ratio of intensities corresponding to this, the voltage was set at 1.80 volts, and the electrometer reading taken. A neutral glass of known opacity, selected from the series used for visual photometric work,

* This failure was due to gradual absorption of the hydrogen filling by the alkali metal as described by Campbell. Later a cell was supplied fitted with a palladium tube for admitting hydrogen. But its arrival was delayed by various circumstances and at that stage it appeared undesirable to interrupt the routine work in progress.

was then placed in front of the lamp. The glass found suitable by a preliminary trial was No. 4 on the scale, having a density of 0·4, and an opacity equal to the antilogarithm of this, or 2·51. It was found in a series of concordant experiments that to compensate for the interposition of this glass it was necessary to increase the voltage from 1·80 to 2·14, which, by a coincidence, is exactly the range over which the lamp has been used in measuring the night sky intensity.

The effective intensity varies therefore as $(V)^{4.7}$, where V is the voltage on the lamp. One step on the (geometric) scale used in the visual work is equivalent to 0·085 volts. $\pm 0\cdot005$ volts (the limit of accuracy to which the readings were recorded) is equal to 0·059 on the visual scale.

This standardisation applies to the condition of the cell at the end of the series of readings. As already emphasised it probably does not apply to the earlier part of the series owing to the change in the condition of the cell due to the accidental passage of a discharge. Unfortunately I have no record of the exact date when this was suspected to have occurred, as its importance was not realised until much later.

Table I.

Date.	Hour.	Volts.	Sky.
1928.			
Wednesday, February 22	11.29 p.m.	1·86	Fairly clear.
Saturday, February 25	11.12 "	1·82	Very clear.
Monday, April 9	10.3 "	1·82	Fairly clear.
	11.30 "	1·89	Clear.
	11.40 "	—	Moon rises.
Wednesday, April 18	11.5 "	1·80	Fairly clear.
	11.8 "	1·81	"
	11.13 "	1·82	"
Thursday, October 11	7.0 "	1·92	Clear.
	7.20 "	1·87	"
	9.22 "	1·86	"
Friday, October 12	7.10 "	1·88	"
	7.35 "	1·88	"
	10.51 "	1·89	"
Saturday, October 13	8.26 "	1·84	"
	11.0 "	1·86	"
Wednesday, October 17	7.50 "	1·93	"
	10.15 "	1·93	"
	11.20 "	1·93	"
Thursday, October 18	9.25 "	1·96	"
	11.12 "	2·03	"
	11.22 "	2·06	"
Saturday, October 20	9.15 "	1·97	"
	10.33 "	2·01	"
	11.37 "	2·03	"
	12.10 "	2·06	"
	12.55 "	2·07	"

Table I—(continued).

Date.	Hour.	Volts.	Sky.
1928.			
Sunday, October 21	1.3 a.m.	2.08	Clear.
	10.7 p.m.	2.05	Very clear after rain.
	10.22 "	2.05	" "
	10.25 "	2.04	" "
	11.25 "	2.05	" "
	11.57 "	2.04	" "
Monday, October 22	1.50 a.m.	2.05	" "
	1.52 "	2.06	" "
Tuesday, November 6	11.10 p.m.	1.92	Clear.
Wednesday, November 7	6.18 "	1.95	"
	7.9 "	1.92	"
	9.14 "	1.91	"
Thursday, November 8	7.54 "	1.91	"
Friday, November 9	6.55 "	1.89	"
	8.4 "	1.89	"
	10.6 "	1.90	"
	12.0 "	1.94	"
Saturday, November 10	3.50 a.m.	1.94	Fairly clear.
Thursday, November 15	6.12 p.m.	1.90	"
	9.50 "	1.97	"
	11.59 "	2.04	Very clear.
Friday, November 16	3.22 a.m.	2.00	Very clear indeed.
Monday, November 19	10.2 p.m.	1.98	Very clear.
	10.47 "	1.98	"
	11.55 "	2.06	"
Tuesday, November 20	11.52 "	1.94	Clear.
Wednesday, December 5	11.26 "	1.98	"
Thursday, December 6	9.8 "	1.87	Fairly clear.
	9.20 "	1.89	Clear.
	10.49 "	1.93	Fairly clear.
	11.9 "	1.93	Clear.
	11.55 "	1.95	Very clear.
Friday, December 7	1.40 a.m.	1.96	"
	2.10 "	1.96	Clear.
Friday, December 14	6.12 p.m.	1.97	"
	6.28 "	1.97	"
	7.17 "	2.00	"
	8.3 "	2.05	"
	9.45 "	2.12	"
	10.58 "	2.14	"
	11.57 "	2.12	"
Saturday, December 15	2.55 a.m.	2.09	Fairly clear.
Monday, December 17	11.15 p.m.	1.98	Clear.
Saturday, December 29	6.24 "	1.91	Fairly clear.
1929.			
Monday, January 1	6.55 p.m.	1.93	Clear.
Saturday, January 12	7.12 "	1.91	Very clear.
	7.19 "	1.92	"
	7.34 "	1.93	"
	8.11 "	1.93	"
	9.21 "	1.92	"
	10.15 "	1.93	"
	11.8 "	1.96	"

Table I—(continued).

Date.	Hour.	Volts.	Sky.
1920.			
Sunday, January 13	0.2 a.m.	1.97	Clear.
	1.13 "	1.94	Fairly clear.
	2.45 "	1.94	Very clear.
Tuesday, January 15	9.27 p.m.	2.02	Fairly clear.
Wednesday, January 16	10.33 "	1.94	Very clear.
	10.53 "	1.94	"
	11.40 "	1.98	"
Thursday, January 17	0.6 a.m.	1.98	"
	2.16 "	1.92	"
Sunday, February 3	8.10 p.m.	1.87	"
	9.16 "	1.85	"
	10.20 "	1.84	"
	11.40 "	1.88	"
Monday, February 4	12.0 "	1.88	"
	0.55 a.m.	1.88	"
	1.28 "	1.88	"
	2.5 "	1.87	"
	2.30 "	1.87	"
	6.37 p.m.	1.90	Clear.
	6.45 "	1.88	"
	6.57 "	1.87	"
	7.55 "	1.84	"
	9.20 "	1.86	Very clear.
Friday, February 8	10.17 "	1.87	"
	11.15 "	1.85	Fairly clear.
	7.0 "	1.89	Very clear.
	7.32 "	1.88	"
	8.7 "	1.90	"
Monday, February 11	11.25 "	1.84	Fairly clear.
	7.55 "	1.91	Very clear.
	9.38 "	1.93	"
Tuesday, February 12	11.31 "	1.93	Fairly clear.
Wednesday, February 13	10.21 "	1.99	Very clear.
	9.51 "	2.01	Very clear (frosty).
	10.4 "	2.03	" "
	10.37 "	2.04	" "
Thursday, February 14	11.57 "	2.11	" "
	1.50 a.m.	2.01	" "
	11.1 p.m.	2.00	" "
	11.14 "	2.01	" "
	11.56 "	2.02	" "
Friday, February 15	3.20 a.m.	2.02	Very clear.
Saturday, March 2	7.33 p.m.	1.96	Very clear (frosty).
	8.0 "	1.96	" "
	9.15 "	1.96	" "
	10.20 "	1.98	" "
	11.12 "	1.97	" "
Sunday, March 3	0.5 a.m.	1.97	" "
	0.45 "	1.97	" "
Monday, March 4	7.35 p.m.	1.94	" "
	8.15 "	1.93	" "
	9.5 "	1.93	" "
	10.3 "	1.93	" "
	11.12 "	1.92	" "
	12.0 "	1.93	" "
Tuesday, March 5	1.34 a.m.	1.89	" "

Table I—(continued).

Date.	Hours.	Volts.	Sky.
1929.			
Thursday, March 7.....	8.2 p.m.	1.96	Very clear.
	9.10 "	1.95	"
	10.7 "	1.94	"
	11.3 "	1.94	"
	12.0 "	1.93	"
Friday, March 8.....	9.43 "	1.94	"
	10.18 "	1.94	"
	11.13 "	1.92	"
	11.57 "	1.96	"
Saturday, March 9.....	2.32 a.m.	1.90	"
	7.39 p.m.	1.97	"
	7.55 "	1.96	"
	8.56 "	1.97	"
	10.3 "	1.96	"
	11.11 "	1.93	Clear.
	12.2 "	1.92	Very clear.
	1.26 a.m.	1.91	"
Sunday, March 10.....	8.3 p.m.	1.92	Very clear.
	8.58 "	1.88	Clear.
	9.58 "	1.88	Very clear.
	11.4 "	1.92	"
Monday, March 11.....	12.0 "	1.94	"
	2.32 a.m.	1.91	"

The observations above tabulated show the same kind of variability as is observed in visual photometry.

They do not indicate very distinctly the annual periodicity which I have observed for several years in the visual intensities. This is attributed to the changes in colour sensitivity of the cell which occurred owing to the accidental passage of discharges on one or two occasions, which prevent the readings being comparable with one another throughout the entire series.

Table II refers only to those nights of the final series on which a midnight measurement was obtained. The value at midnight is taken as zero, and the departure from this value at other hours is tabulated. The unit is 0.01 volt on the incandescent lamp. When the observations actually taken did not fall near enough to the hour, interpolations over fractions of an hour are made, though the adjustments thus introduced are insignificant.

If the variation were quite irregular, then departures at hours other than midnight would be as often positive as negative. On the other hand, with an undisturbed regular periodicity culminating at midnight, only negative values would occur at other hours. The actual case is intermediate. Negative

Table II.

Date.	Hour.												
	6	7	8	9	10	11	12	1	2	3	4	5	6
Oct. 20-21.....				-9		-4	0	+1					
21-22.....					+1	+½	0		+1½				
Nov. 9-10.....		-5	-5		-4		0				0		
15-16.....	-14				-7		0			-4			
19-20.....					-8	-8	0						
Dec. 6-7.....				-6		-2	0		+1				
14-15.....	-15	-12	-7		0	+2	0			-3			
Jan. 12-13.....		-6	-4	-5	-4	-2	0	-3		-3			
16-17.....						-4	0		-6				
Feb. 3-4.....			-1	-3	-4		0	0	-1				
13-14.....					-9	-6	0		-10				
14-15.....						-2	0			0			
March 2-3.....			-1	-1	+1	0	0	0					
4-5.....			0	0	-1	-1	0		-4				
7-8.....			+3	+2	+1	+1	0						
8-9.....				-2	-2	-4	0			-6			
9-10.....			+4	+5	+4	+4	0	-1					
10-11.....			-2	-6	-6	-2	0		-3				
Mean	-14	-7.7	-1.4	-2.5	-2.7	-2	0	-0.6	-3.1	-3.2	0		

and positive values occur, but the former preponderate greatly. Of all departures—

48 are negative,

15 are positive,

8 are undetermined sign (nearly zero).

Disregarding the departures which are appreciably zero, the ratio of the number of negative to the number of positive departures is—

3.1 before midnight,

3.7 after midnight.

It is pretty evident even without calculation that this great preponderance of negative values could hardly be the result of chance. But, to put the matter on a more definite basis, we may calculate the probability that the preponderance of negative departures would be at least as high as this if positive departures were as likely as negative ones.

If in n trials negative departures occur r times, the required probability is (see Todhunter's Algebra, § 728) the sum of $n - r + 1$ terms of the series

$$\left(\frac{1}{2}\right)^n \left[1 + n + \frac{n(n-1)}{1 \cdot 2} + \frac{n(n-1)(n-2)}{1 \cdot 2 \cdot 3} + \dots \right].$$

For the present case $n = 63$, and 16 terms are to be taken.

The numerical result is that the probability is 2×10^{-5} or 1 in 50,000.

This method of calculation is possibly open to objection, in that the "trials," unlike separate tossings of a coin, are not all independent of one another. To avoid this objection, we may take the sign of the departure of the first observation after dark, and of the last before dawn (midnight = 0). We find that of 30 cases which gave a definite result—

24 are negative,

6 are positive.

Calculating as before, we find the chance of so high a result being accidental is only about 7×10^{-4} , or 1 in 1300.

It appears then that the reality of the midnight maximum is well established. This naturally raises the question of what is the normal course of the variation during the 24 hours. But here we are met with the impossibility of tracing what happens during daylight. From this point of view it is evidently important to examine closely what happens as night conditions set in. Table III gives the observations of intensity on three favourable occasions, with the distances of the sun below the horizon.* Night values are attained when the

Table III.

† Date.	G.M.T.	Sun below horizon.	Intensity.
1929.	hr. min.	° ' "	volts.
March 2	7 6	—	2.32
	7 16	—	2.07
	7 21	16 33	2.01
	7 25	17 10	1.98
	7 28	17 37	1.97
	7 33	18 22	1.96
	9 15	—	1.96
March 4	7 21	16 1	2.04
	7 23	16 19	2.02
	7 26	16 47	2.00
	7 27	16 56	1.98
	7 35	18 9	1.94
	7 40	19 26	1.94
March 9	7 22	—	2.17
	7 28	15 43	2.14
	7 33	16 10	2.01
	7 35	16 46	2.00
	7 38	17 13	1.98
	7 39	17 22	1.97
	7 42	17 49	1.96
	7 44	18 7	1.97
	7 55	—	1.96

* The Astronomer Royal kindly had these calculated for me by Mr. W. H. M. Greaves. I have interpolated for intermediate times with sufficient accuracy.

sun is more than 17° but less than 18° below the horizon. 18° is usually taken as marking the disappearance of all daylight in the west. According to Table III night conditions observed at a greater altitude in the northern sky set in perceptibly before this. There can be no lag amounting to more than a few minutes between the disappearance of daylight and the night sky illumination attaining its normal value.

The observations which I have been able to secure are not enough to give statistical regularity. The mean for each hour has been given at the bottom of Table II, but it is premature at this stage to attempt to fit them to a periodic function. All that can well be said is that the lowest values generally tend to occur immediately after dark, and probably also immediately before dawn. The evidence on the latter point is less complete, the reason being that I have been obliged to carry out the observing work single handed, and that having observed up till midnight, and with other occupations in the daytime, I could hardly undertake more than one observation in the small hours.

The greatest range of variation has been observed at midwinter, when observation can be begun about 6 p.m., given favourable weather near the time of new moon. Unfortunately this condition was not often fulfilled, and one or two favourable chances were missed by absence. From the general trend of the means for successive hours given at the bottom of Table II we may estimate the mean value at 6 p.m. to be from 0.1 to 0.14 volts lower than at midnight. This would make the mean intensity at 6 p.m. 0.8 or 0.7 of the mean intensity at midnight.

All the definitive work given in Table I applies to the region on the blue side of the auroral line, carried out as it was with a photoelectric cell only sensitive in this region. As already mentioned, to select part of this region by means of pale yellow or blue colour filters makes no difference to the character of the variations observed. They are the same as when we make no such selection.

The preliminary work using the red and yellow sensitive cell under a deep yellow filter suggest a similar variation for the region including the auroral line, though, owing to the failure of the cell, it could not be sufficiently completed. The results of McLennan and Ireton* by the photographic method are much more definite on this point. Their method differs from that here used not only in being photographic but also in using the radiation of the entire hemisphere. Owing to the poor transmission near the horizon, such a

* 'Roy. Soc. Proc.,' A, vol. 120, p. 353.

method would rarely be satisfactory under the atmospheric conditions of this country.

So far as comparison is at present possible, the results of the two investigations seem to be in general harmony.

Further and more regular observing work throughout the night can hardly be undertaken except at a regular observatory with assistants on night duty at all times.

It would be very desirable to make observations in a high northern latitude, so as to cover a much larger fraction or even the whole of the 24 hours. An estimate should also be made of the minimum brightness of the sky during total eclipse of the sun.

Summary.

A method of observing the intensity of the night sky is described, using a photoelectric cell and an electrometer with leakage resistance. The intensity of a patch of sky is matched with the intensity of a white screen illuminated by an incandescent lamp. The latter is controlled by a resistance, and measured by the voltage across the lamp.

The work refers chiefly to that part of the light of the night sky which lies on the blue side of the auroral line. Part of the observed variation is irregular. Superposed upon this there is a regular diurnal variation with maximum at midnight. The evidence is discussed statistically and is found to be ample to warrant these conclusions. Aside from irregular variations, the value at 6 p.m. in winter is believed to be 0.7 or 0.8 of the value at midnight.

Night conditions are observed immediately within a very small number of minutes, on the disappearance of daylight in the west. In all probability the two phenomena are simply superposed—like daylight and moonlight.

The Quantum Theory of Dispersion in Metallic Conductors.

By R. DE L. KRONIG, Physisch Laboratorium der Rijks-Universiteit,
Utrecht.

(Communicated by R. H. Fowler, F.R.S.—Received April 12, 1929.)

1. *Formulation of the Problem.*—The propagation of electromagnetic waves in a homogeneous isotropic medium showing metallic conductivity has been treated phenomenologically on the basis of classical electrodynamics.* If in Maxwell's equations for the electromagnetic field

$$\begin{aligned}\text{curl } \mathbf{E} &= -\frac{1}{c} \frac{\partial \mathbf{B}}{\partial t}, & \text{curl } \mathbf{H} &= \frac{1}{c} \left(\frac{\partial \mathbf{D}}{\partial t} + 4\pi \mathbf{I} \right), \\ \text{div } \mathbf{D} &= 4\pi \rho, & \text{div } \mathbf{B} &= 0,\end{aligned}$$

we assume that

$$\mathbf{D} = \epsilon \mathbf{E}, \quad \mathbf{B} = \mu \mathbf{H}, \quad \mathbf{I} = \sigma \mathbf{E}, \quad (1)$$

where ϵ is the dielectric constant, μ the permeability and σ the electrical conductivity, we get

$$\begin{aligned}\text{curl } \mathbf{E} &= -\frac{\mu}{c} \frac{\partial \mathbf{H}}{\partial t}, & \text{curl } \mathbf{H} &= \frac{1}{c} \left(\epsilon \frac{\partial \mathbf{E}}{\partial t} + 4\pi \sigma \mathbf{E} \right), \\ \text{div } \mathbf{E} &= \frac{4\pi \rho}{\epsilon}, & \text{div } \mathbf{H} &= 0.\end{aligned}$$

These equations are satisfied by

$$\left. \begin{aligned} E_x &= F e^{-\frac{2\pi\nu\kappa z}{\sigma}} \cos \left[2\pi\nu \left(t - \frac{nz}{c} \right) + \gamma \right], \\ H_y &= F' e^{-\frac{2\pi\nu\kappa z}{\sigma}} \cos \left[2\pi\nu \left(t - \frac{nz}{c} \right) + \gamma' \right] \end{aligned} \right\}, \quad (2)$$

and all the other components of \mathbf{E} and \mathbf{H} as well as ρ equal to zero, provided $n, \kappa, F, F', \gamma, \gamma'$, obey the relations

$$n^2 = \mu/2 (\sqrt{\epsilon^2 + 4\sigma^2/\nu^2} + \epsilon), \quad (3)$$

$$\kappa^2 = \mu/2 (\sqrt{\epsilon^2 + 4\sigma^2/\nu^2} - \epsilon), \quad (4)$$

$$F' = \frac{F}{\mu} \sqrt{n^2 + \kappa^2}, \quad \tan(\gamma - \gamma') = \kappa/n,$$

* See e.g. Drude, 'Lehrbuch der Optik'; Abraham und Föppl, 'Theorie der Elektrizität,' I.

where ν , ϵ and γ are arbitrary real constants. (2) represents a plane electromagnetic wave of frequency ν , linearly polarised in the direction x and travelling in the direction z with a phase velocity corresponding to an index of refraction n and a decrease in its amplitude corresponding to an extinction coefficient κ . By considering the boundary conditions at a plane surface of the medium adjacent to vacuum one finds for the coefficient of reflection in the case of perpendicular incidence

$$R = \frac{(n - \mu)^2 + \kappa^2}{(n + \mu)^2 + \kappa^2}. \quad (5)$$

For non-ferromagnetic substances μ can be put equal to unity without appreciable error. For ferromagnetic substances in the region of long Hertzian waves μ is not a constant so that the preceding considerations do not apply, while for higher frequencies it seems to approach unity. Throughout what follows we shall hence put $\mu = 1$ so that (3), (4), (5) now become

$$n^2 = \frac{1}{2}(\sqrt{\epsilon^2 + 4\sigma^2/\nu^2} + \epsilon), \quad (6)$$

$$\kappa^2 = \frac{1}{2}(\sqrt{\epsilon^2 + 4\sigma^2/\nu^2} - \epsilon), \quad (7)$$

$$R = \frac{(n - 1)^2 + \kappa^2}{(n + 1)^2 + \kappa^2}. \quad (8)$$

If further $\frac{4\sigma^2}{\nu^2} \gg \epsilon$ and also $\frac{\sigma}{\nu} \gg 1$, we obtain by developing

$$n = \kappa = \sqrt{\sigma/\nu}, \quad (9)$$

$$R = 1 - 2\sqrt{\nu/\sigma}. \quad (10)$$

The experiments of Hagen and Rubens* in the far infra-red have confirmed (10) for various metals at room temperature up to frequencies of about 3.10^{12} , corresponding to a wave-length of 10μ . For higher frequencies deviations become noticeable, and in the optical region (10) fails entirely. Evidently the indiscriminate use at high frequencies of the constants ϵ and σ in (1) giving the displacement current $\frac{\epsilon - 1}{4\pi} \frac{\partial \mathbf{E}}{\partial t}$ and the conduction current $\sigma \mathbf{E}$ for slowly varying fields, is to be blamed for this.

Until recently it appeared difficult to improve the theory, no satisfactory interpretation of metallic conduction being available. This gap has now been

* 'Ann. Physik,' vol. 11, p. 873 (1903).

filled through the work of Bloch,* who shows how the conducting properties of a crystal lattice under a constant electric field can be understood by considering the simultaneous influence of the field and the thermal vibrations of the lattice on the distribution of the electrons in the crystal over their various stationary states. The ideas which he has developed we shall use as a basis of the subsequent discussion, in which for simplicity we confine ourselves to studying the propagation in a cubic lattice of a plane monochromatic wave travelling in the direction of one of the crystallographic axes and linearly polarised parallel to one of the other two. The principal objects of our investigation will be :—

- (1) A determination of the accuracy with which the phenomenological theory can be expected to hold for different frequencies and temperatures.
- (2) The nature of the deviations from the phenomenological theory and their connection with the properties of the crystal.

2. *The General Properties of the System.*—In studying the influence of an electromagnetic wave on a crystal lattice it seems at first that we are confronted with the same difficulties which stand in the way of a satisfactory formulation of quantum electrodynamics. Nevertheless it is possible to proceed if it be remembered that in order to compute the coherent radiation scattered by a system of charged particles, which alone is of importance in determining the refraction and extinction of the incident wave, the quantization of the electromagnetic field may be disregarded. Correct results are obtained in this case by calculating that part of the current distribution induced in the system which vibrates with the same frequency as the incident wave, and in considering it as giving rise to the coherent scattered radiation according to the laws of classical electrodynamics.†

We shall later consider the current flowing inside a cube in the crystal lattice, the basic cube, whose edges, of length L , are parallel to the co-ordinate axes, if a plane electromagnetic wave of frequency ν , polarised in the direction x and travelling in the direction z , is falling on it. If L be chosen small compared to the wave-length and to the distance in which the amplitude of the wave decreases appreciably on account of absorption, then the vector potential A

* 'Z. Physik,' vol. 52, p. 555 (1928).

† Gordon, 'Z. Physik,' vol. 40, p. 117 (1927); Klein, *ibid.*, vol. 41, p. 407 (1927); Waller, 'Phil. Mag.,' vol. 4, p. 1228 (1927). For a rigorous justification of the results obtained see Dirac, 'Roy. Soc. Proc.,' A, vol. 114, p. 243, 710 (1927).

of the wave at every instant may be considered the same for all points of the cube and given by

$$A_x = -\frac{cF}{2\pi\nu} \sin 2\pi\nu t, \quad A_y = A_z = 0, \quad (11)$$

while its scalar potential vanishes. The electric field in the cube due to the radiation will then be

$$E_x = F \cos 2\pi\nu t, \quad E_y = E_z = 0. \quad (12)$$

We must further discuss the stationary states of the crystal. Following Bloch we shall regard the lattice in its action on one of the conduction electrons in first approximation as an electric field in which the potential energy V of the electron is periodic with a period a , the lattice constant, in the direction of each of the three co-ordinate axes. We shall assume that the edge L of the basic cube is a large integral multiple Ga of a , which for radiation whose wave-length is sufficiently long, as in the optical and infra-red region, is not in conflict with the restrictions previously imposed upon the value of L . Then according to Bloch (see his equation (6a)) the eigenfunctions of the electron, obeying the wave equation

$$\Delta\psi + \frac{8\pi^2m}{h^2} (W - V) \psi = 0,$$

are given by

$$\psi_{l_1, l_2, l_3}(xyz) = e^{2\pi i(l_1 x/L + l_2 y/L + l_3 z/L)} u_{l_1, l_2, l_3}(xyz), \quad (13)$$

if we restrict ourselves to those which are periodic in the directions x, y, z with a period L . l_1, l_2, l_3 are integers, while u is a function periodic with a period a in each of the directions of the three co-ordinate axes. The ψ 's we assume normalised.

The energy of the stationary state belonging to the eigenfunction ψ_{l_1, l_2, l_3} we shall denote by $W(l_1, l_2, l_3)$. In case its explicit value is required, we shall, just as Bloch in his calculation of the conductivity (see his equation (63c)) assume it given by

$$W(l_1, l_2, l_3) = \omega [(2\pi l_1/G)^2 + (2\pi l_2/G)^2 + (2\pi l_3/G)^2]. \quad (14)$$

For free electrons this formula is exact with

$$\omega = h^2/8\pi^2ma^2,$$

a quantity of the order of magnitude 5.10^{-12} , but even if the binding effect of

the lattice makes itself felt, it has still an approximate validity with a smaller value of ω . Introducing in place of l_1, l_2, l_3 the new variables

$$\xi = 2\pi l_1/G, \quad \eta = 2\pi l_2/G, \quad \zeta = 2\pi l_3/G, \quad (15)$$

and the quantity

$$\rho = \sqrt{\xi^2 + \eta^2 + \zeta^2}, \quad (16)$$

we can write (14)

$$W(\xi\eta\zeta) = \omega\rho^2. \quad (17)$$

When there is temperature equilibrium, the distribution of the electrons over the various stationary states will be governed by the statistics of Dirac and Fermi,* the number in the state l_1, l_2, l_3 being equal to

$$f_0(l_1l_2l_3) = 2/\{\alpha e^{W(l_1l_2l_3)/kT} + 1\}, \quad (18)$$

since for each combination $l_1l_2l_3$ there will be two possible orientations of the electron in a magnetic field. If $W(l_1l_2l_3)$ is given by (14), then for large G the stationary states will lie close together. Inside a parallelepipedon $d\xi d\eta d\zeta$ there will be $\frac{G^3}{8\pi^3} d\xi d\eta d\zeta$ combinations $l_1l_2l_3$, and therefore

$$f_0(l_1l_2l_3) \frac{G^3}{8\pi^3} d\xi d\eta d\zeta \text{ electrons.} \quad (19)$$

If the electron gas is almost degenerate, which will be the case at ordinary temperatures, then (see Bloch, *loc. cit.*) the constant α in (18) is given by

$$\alpha = e^{-\omega\rho_0^2/kT},$$

where

$$\rho_0 = \sqrt[3]{6\pi^2K}, \quad (20)$$

and $2K$ is the number of conduction electrons per cell and also per atom if for simplicity we assume that there is one atom in each cell of the cubic lattice. With (17) and the abbreviation

$$\delta = \omega(\rho^2 - \rho_0^2)/kT \quad (21)$$

we get hence

$$f_0(\xi\eta\zeta) = f_0(\rho) = 2/(e^\delta + 1). \quad (22)$$

3. The Validity of the Phenomenological Theory.—If a constant electric field is applied to the crystal lattice considered in the previous section, it will cause an electron in a given state $l_1l_2l_3$ to make transitions to other states $l_1l_2l_3$ and disturb the distribution (22). A current will begin to flow and would increase beyond limits if there were no other influences coming into

* Dirac, 'Roy. Soc. Proc.,' A, vol. 112, p. 661 (1926); Fermi, 'Z. Physik,' vol. 36, p. 902 (1926).

play. Already in the absence of an electric field, however, an electron will not stay in its state $l_1 l_2 l_3$ indefinitely, but will undergo transitions to other states on account of its interaction with the thermal vibrations of the lattice. It is just this agency which establishes the equilibrium distribution (22) in the absence of a field, and which sees to it that a new equilibrium distribution is finally reached if an electric field is present.

As Bloch has shown (see his equation (70)) this new equilibrium distribution will have the form

$$f(\xi\eta\zeta) = f_0(\rho) + \xi\chi(\rho), \quad (23)$$

and the total current per cubic centimetre corresponding to it is then given by

$$I_x = \frac{e}{mL^3} \iiint \tau \xi^2 \chi(\rho) \frac{G^3}{8\pi^3} d\xi d\eta d\zeta \quad (24)$$

if it is assumed that the momentum associated with a state $l_1 l_2 l_3$ has the components $\tau\xi$, $\tau\eta$, $\tau\zeta$. This is rigorously true for free electrons with

$$\tau = \hbar/2\pi a,$$

which is about 10^{-10} , and will still have approximate validity with a smaller value of τ for electrons not too firmly bound. But $\chi(\rho)$ according to Bloch (see his equation (83)) is given by

$$\chi(\rho) = -\frac{4FeMa^2\rho^2\omega v}{G^3\pi^3C^2\hbar} \left(\frac{8\pi^2m}{\hbar^2}\right)^2 \left(\frac{\hbar v}{ak\Theta}\right)^3 \frac{\partial f_0}{\partial \rho} \frac{\Theta}{T}, \quad (25)$$

F denoting the strength of the field, M the mass of the basic cube, v the velocity of propagation of elastic waves in the lattice, which is assumed to be the same for longitudinal and transversal waves, C a constant determined by the firmness of binding and Θ the characteristic temperature entering in Debye's theory of the specific heat of solids. It is also presupposed in the derivation of (25) that $T \gg \Theta$. By dividing the current calculated from (24) and (25) by the field strength Bloch obtains the conductivity (see his equation (85)) which in our notation has the value

$$\sigma = \frac{4(6\pi^2K)^2}{3\pi^5} \frac{e^2 M \tau \omega v}{G^3 a m C^2 \hbar} \left(\frac{8\pi^2m}{\hbar^2}\right)^3 \left(\frac{\hbar v}{ak\Theta}\right)^5 \frac{\Theta}{T}. \quad (26)$$

The relation (24), giving the current for constant fields, will not apply accurately for variable fields since it takes some time before the equilibrium distribution (23) is attained when the strength of the electric field is changed. To get an estimate of this time of relaxation we inquire for the rate of change of the current when the electric field which has established the distribution

(23) is suddenly turned off. For this purpose it is only necessary to know how many more electrons are leaving a state $l_1 l_2 l_3$ than are entering per second on account of the impacts with the lattice if the distribution is given by (23). Calling this number $n(\xi\eta\zeta)$ we get

$$\dot{I}_x = -\frac{e}{mL^3} \iiint \tau \xi n(\xi\eta\zeta) \frac{G^3}{8\pi^3} d\xi d\eta d\zeta. \quad (27)$$

But according to Bloch (see the equation following his equation (76))

$$n(\xi\eta\zeta) = -\frac{2\pi eFa}{h} \frac{\partial f_0}{\partial \rho} \frac{\xi}{\rho}. \quad (28)$$

Substituting (25) in (24) and (28) in (27) and remembering that according to (21) and (22) $\partial f_0 / \partial \rho$ is different from zero only in the immediate neighbourhood of $\rho = \rho_0$ so that ρ may be replaced by ρ_0 in the factors with which $\partial f_0 / \partial \rho$ is multiplied, we find with the help of (26)

$$\dot{I}_x = -\beta I_x$$

with

$$\beta = 4\pi K e^2 \tau / h m a^2 \sigma. \quad (29)$$

K is of the order of magnitude 1, a about 10^{-8} , while for good conductors the value of τ may be put equal to 1/10 the value of τ for free electrons, *i.e.*, 10^{-20} , and σ is of the order 10^{18} at room temperature. Then β lies between 10^{13} and 10^{14} , and $1/\beta$ will have to be regarded as the time of relaxation.*

One must expect hence that the phenomenological theory of dispersion in metallic conductors, using in the relation (1) the value of σ for constant fields, will for an alternating field given by (12) be in error by amounts of the order $e^{-\beta/\nu}$. These errors become serious at ordinary temperatures for frequencies between 10^{13} and 10^{14} in agreement with experiment. For increasing temperatures the region of validity extends towards larger frequencies, since β changes proportional to T on account of the factor $1/\sigma$. Unfortunately no experimental data are available showing the influence of temperature on the applicability of the formulæ (9) and (10), and new material with the above predictions in mind would be very desirable.†

* The time of relaxation thus calculated is solely due to the finite intervals between the impacts of the electrons with the lattice and distinct from the effects of self-induction. These become negligible for systems of small dimensions, as our basic cube, and are implicitly contained in Maxwell's equations when we consider the distribution of current for the lattice as a whole.

† [Note added in proof.—It is of interest to compare our result with that which can be obtained by an analogous consideration on the basis of the older picture where the electrons were regarded as forming an ideal gas (see Lorentz, 'The Theory of Electrons,'

4. *The Region of High Frequencies.*—When the frequency ν of the incident wave becomes large compared to β , the impacts of the electrons with the lattice will cease to play an important part. We may then apply the dispersion theory to the system whose eigenfunctions and energy values are given by (13) and (14) respectively.† If the electron is in the state $l_1 l_2 l_3$, which for brevity we denote by r , while s is any of the other states, then that part of the current density due to it which vibrates with frequency ν is

$$I_x(r) = \frac{e^2 F}{2\pi m \nu L^3} \left[1 + \frac{2}{hm} \sum_s \frac{\nu_{rs} |p_x(rs)|^2}{\nu_{rs}^2 - \nu^2} \right] \sin 2\pi \nu t \quad (30)$$

if the vector potential of the wave is given by (11)/ p_x is the x -component of the momentum and $p_x(rs)$ hence given by

$$p_x(rs) = \frac{h}{2\pi i} \int \psi^*_r \frac{\partial \psi_s}{\partial x} dx dy dz, \quad (31)$$

the integration extending over the basic cube.

The integrand in (31) for two states $l_1 l_2 l_3$ and $l'_1 l'_2 l'_3$ will be according to (13)

$$e^{2\pi i \left[\frac{(l'_1 - l_1)x}{L} + \frac{(l'_2 - l_2)y}{L} + \frac{(l'_3 - l_3)z}{L} \right]} u^*_{l_1 l_2 l_3} \left(\frac{2\pi i l'_1}{L} u_{l_1 l_2 l_3} + \frac{\partial u_{l_1 l_2 l_3}}{\partial x} \right).$$

Integration over the first of the two terms gives zero on account of the orthogonality of the eigenfunctions. Furthermore the u 's have the period a in the direction of each of the co-ordinate axes so that we may write them as Fourier's series

$$u_{l_1 l_2 l_3} = \sum_{g_1 g_2 g_3 = -\infty}^{\infty} b_{g_1 g_2 g_3} e^{2\pi i \left(\frac{g_1 x}{a} + \frac{g_2 y}{a} + \frac{g_3 z}{a} \right)}.$$

For free electrons only the constant term b_{000} is present, while for weakly bound electrons also the higher terms will occur with coefficients $b_{g_1 g_2 g_3}$ small

2nd edition, p. 267, *et seq.*). By treating the interaction of the electrons and the atoms or ions of the metal as impacts between perfectly elastic spheres one finds

$$\beta = \frac{3}{2\Lambda} \sqrt{\frac{\pi kT}{2m}},$$

where Λ is the mean free path of an electron between two impacts with an atom. With the experimental value of β one gets for Λ at room temperature about 10^{-8} cm. Note also that here β is proportional to \sqrt{T} , while the new theory gives proportionality with T on account of the factor $1/\sigma$.

† Klein, *loc. cit.*; Waller, *loc. cit.*

compared to b_{000} , of which again b_{100} , b_{010} and b_{001} will in general be the biggest. We will hence have with good approximation

$$u_{l_1 l_2 l_3}^* \frac{\partial u_{l_1' l_2' l_3'}}{\partial x} = \frac{2\pi i}{a} b_{000}^* \sum_{g_1 g_2 g_3 = -\infty}^{\infty} g_1 b_{g_1 g_2 g_3}' e^{2\pi i \left(\frac{g_1 x}{a} + \frac{g_2 y}{a} + \frac{g_3 z}{a} \right)}.$$

Substituting this in the integrand of (31) we see that $p_x(rs)$ will be different from zero only if,

$$l_1' = l_1 \pm G, \quad l_2' = l_2, \quad l_3' = l_3, \quad (32)$$

$$l_1' = l_1 \pm 2G, \quad l_2' = l_2, \quad l_3' = l_3, \quad (33)$$

$$l_1' = l_1 \pm G, \quad l_2' = l_2 \pm G, \quad l_3' = l_3, \quad (34)$$

.

and will in general be largest for the transitions (32). Moreover since according to (21) and (22) practically all the electrons in the crystal have values ξ , η , ζ which lie within a sphere of radius ρ_0 , given by (20), in the $\xi\eta\zeta$ -space, it is easily seen with the help of (17) that the frequencies of the transitions (33), (34), etc., will for most electrons be much bigger than the frequencies of the transitions (32). For frequencies adjacent to the region in which the phenomenological theory holds the latter will be predominant, and in the following discussion we shall hence consider only them. If we presuppose that $u_{l_1 l_2 l_3}$ does not depend essentially on l_1 , l_2 , l_3 , an assumption which Bloch justifies and uses in his paper (see the equation preceding his equation (64)), we find

$$|p_x(l_1, l_2, l_3; l_1 \pm G, l_2, l_3)|^2 = P^2,$$

a constant independent of l_1 , l_2 , l_3 . Introducing ξ , η , ζ from (15) we may write this

$$|p_x(\xi, \eta, \zeta; \xi \pm 2\pi, \eta, \zeta)|^2 = P^2. \quad (35)$$

The associated frequencies are according to (16) and (17)

$$\nu(\xi, \eta, \zeta; \xi \pm 2\pi, \eta, \zeta) = -\frac{4\pi\omega}{h}(\pi \pm \xi). \quad (36)$$

The classical analogue of these frequencies is the fundamental in the oscillatory motion which is superimposed upon the uniform motion of a sufficiently swift particle travelling through the field with the periodic potential V . Assuming complete degeneracy of the electron gas so that according to (22) we have a uniform density of electrons corresponding to $f_0 = 2$ within a sphere of radius ρ_0 in the $\xi\eta\zeta$ -space, there will be according to (19)

$$\frac{G^3}{4\pi^2} (\rho_0^3 - \xi^3) d\xi \quad (37)$$

electrons between ξ and $\xi + d\xi$.

Using (35), (36) and (37) we get from (30) the total current density*

$$I = \frac{e^2 F}{8\pi^3 m v a^3} \int_{-\rho_0}^{\rho_0} d\xi (\rho_0^2 - \xi^2) \\ \times \left[1 - \frac{16\pi\omega (\pi + \xi) P^2}{h^2 m} \frac{1}{\left[\frac{4\pi\omega}{h} (\pi + \xi) \right]^2 - v^2} \right] \sin 2\pi v t.$$

In the frequency region

$$\frac{4\pi\omega}{h} (\pi - \rho_0) < v < \frac{4\pi\omega}{h} (\pi + \rho_0)$$

the integral has no definite value, the denominator in the second term becoming zero for a certain ξ . As is well known, however,† we get that part of the current which is 90° out of phase with the electric field of the incident wave, the displacement current, by taking the principal value of the integral:

$$\frac{\epsilon - 1}{4\pi} \frac{\partial E_x}{\partial t} = - \frac{(\epsilon - 1) v F}{2} \sin 2\pi v t = \frac{e^2 F \sin 2\pi v t}{8\pi^3 m v a^3} \int_{-\rho_0}^{\rho_0} d\xi (\rho_0^2 - \xi^2) \\ \times \left[1 - \frac{16\pi\omega (\pi + \xi) P^2}{h^2 m} \frac{1}{\left[\frac{4\pi\omega}{h} (\pi + \xi) \right]^2 - v^2} \right],$$

from which we obtain

$$\epsilon = 1 - \frac{e^2 \rho_0^3}{3\pi^3 m a^3} \frac{1}{v^2} + \Omega \frac{1}{v^2} \left[v_2^2 - v_1^2 + \frac{1}{2} (v + v_1) (v + v_2) \log \left(\frac{v + v_1}{v + v_2} \right)^2 \right. \\ \left. + \frac{1}{2} (v - v_1) (v - v_2) \log \left(\frac{v - v_1}{v - v_2} \right)^2 \right] \quad (38)$$

with

$$\Omega = \frac{e^2 P^2}{2\pi^3 h m^2 a^3} \left(\frac{h}{4\pi\omega} \right)^3, \quad v_1 = \frac{4\pi\omega}{h} (\pi - \rho_0), \quad v_2 = \frac{4\pi\omega}{h} (\pi + \rho_0). \quad (39)$$

Also from the connection between absorption and dispersion‡ we get the part

* In this expression no account has been taken of the exclusion principle of Pauli in case a transition of a certain electron considered leads to a state already occupied by another electron. That this omission does not introduce an error has been shown in a paper by H. Kramers and the author, 'Z. Physik,' vol. 48, p. 174 (1928).

† Kramers, 'Proceedings of the Volta Congress, 1927,' vol. 2.

‡ Kramers, *loc. cit.*

of the current in phase with the electric field, the conduction current. If both ν_1 and ν_2 are positive

$$\sigma E_x = \sigma F \cos 2\pi \nu t = \frac{e^2 P^2 F}{4\pi^2 \hbar m^2 \nu a^3} \left(\frac{\hbar}{4\pi \omega} \right)^2 (\nu_2 - \nu)(\nu - \nu_1) \cos 2\pi \nu t,$$

from which

$$\sigma = \frac{\pi}{2} \Omega \frac{1}{\nu} (\nu_2 - \nu)(\nu - \nu_1) \quad (\nu_1 < \nu < \nu_2), \quad (40)$$

while $\sigma = 0$ for all other values of ν . The values (38) and (40) of ϵ and σ must then be substituted in (6), (7) and (8) to get the optical constants n , κ and R .*

Although on account of the simplifying assumptions made in the course of our derivations the results thus obtained cannot be expected to check quantitatively with the experimental data, a number of features of the dispersion of light in metallic conductors can be qualitatively understood. Since ν must be large compared to β , given by (29), in order that the considerations of this paragraph may apply, and since β , as we have seen, lies between 10^{13} and 10^{14} at ordinary temperatures, we must confine ourselves here to the optical behaviour of metals in the visible and ultra-violet region of the spectrum. At lower temperatures the limit of validity of the theory will lie further toward low frequencies. It may be mentioned in this connection that according to measurements of de Sélincourt† lowering the temperature has only a small effect on the coefficient of reflection of silver in the ultra-violet region, probably entirely due to the change in the lattice constant resulting from temperature contraction. From this we may conclude that already at ordinary temperatures the impacts of the electrons with the lattice play a negligible rôle in this

* [Note added in proof:—At the point of the preceding considerations where ϵ and σ are first introduced, the question arises if a correction should not be made analogous to the replacing of $(n^2 - 1)$ by $3(n^2 - 1)/(n^2 + 2)$ in the classical theory of dispersion in transparent media. There the reason for this change is the appearance in the electromagnetic field of an oscillating dipole of terms decreasing as $1/r^2$ and $1/r^3$ besides those decreasing as $1/r$, which alone are of importance at large distances r (in the wave zone). In the classical theory a very general investigation of the problem by Darwin ('Trans. Camb. Phil. Soc.', vol. 23, p. 137 (1924)) makes the substitution plausible for absorbing media too. In the quantum theory the terms in $1/r^2$ and $1/r^3$ have never been considered, and it appears that it will not be possible to fit them into the theory before the artificial distinction between static and wave fields has been removed. For that reason we have decided not to make the correction at present (which would be quite considerable), and it may hence become necessary later to revise the comparison with the experiment given below.]

† 'Roy. Soc. Proc.' A, vol. 107, p. 247 (1925).

region, while marked changes in the reflection at higher temperatures indicate that the influence of the impacts becomes noticeable.

In fig. 1 we have given a graphical representation of ε and σ as calculated from (38) and (40) with

$$\frac{e^2 \rho_0^3}{3\pi^3 m a^3} = 5.10^{30}, \quad \nu_1 = 5.10^{14}, \quad \nu_2 = 2.10^{15}.$$

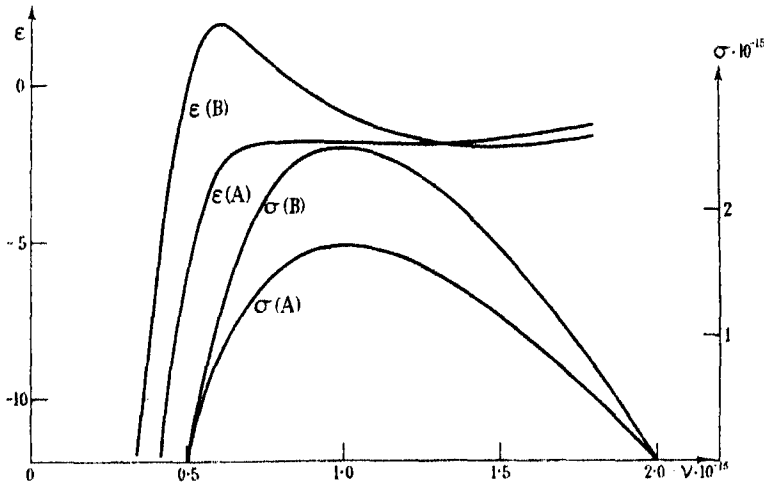


FIG. 1.

That these values are reasonable we see as follows: $\rho_0^3/3\pi^2$ is of the order of magnitude 1 according to (20). $1/a^3$, the number of atoms per cubic centimetre, is for metals like Ag and Au, which we later shall use for comparison, about 6.10^{22} . From this we get a justification of the first equation above. The assumption for ν_1 and ν_2 gives us ω , since according to (39) $4\pi^2\omega/h$ is the arithmetic mean of ν_1 and ν_2 , ω becoming thus $2 \cdot 10^{-13}$, a value as we should expect according to a previous remark. For Ω we have chosen two values, $\Omega = 2.2$ (curves A) and $\Omega = 3.2$ (curves B). According to the definition (39) of Ω this signifies that P^2/m is of the same order of magnitude as ω , which is sensible, since P is an element of the matrix representing the momentum and ω is of the order of magnitude of the mean energy of an electron. Fig. 2 shows the values of ε and σ for Ag and Au obtained from (6) and (7) by using for n and κ the values determined by Minor* and Meier.† One sees that the theory accounts satisfactorily for the empirical type of curves and the order of

* 'Ann. Physik,' vol. 10, p. 581 (1903); Diss. Göttingen, 1903.

† 'Ann. d. Physik,' vol. 31, p. 1017 (1910); Diss. Göttingen, 1910.

magnitude of ϵ and σ with one kind of electrons only, no distinction being made for them any more between free and bound electrons.

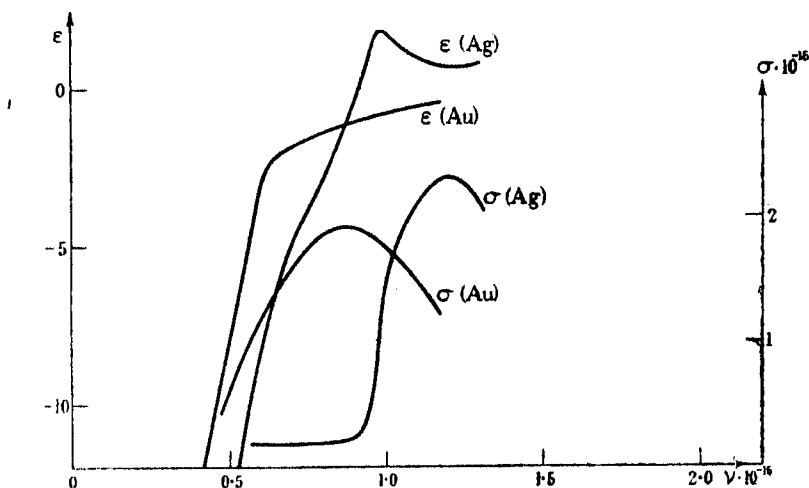


FIG. 2.

It may be mentioned here that it seems difficult to set up a theory of dispersion in metallic conductors in the frequency region where ν is neither small nor large compared to β .

Summary.

1. On the basis of the notions developed by Bloch in order to interpret metallic conduction and under certain simplifying assumptions it is shown that the equilibrium distribution of the conduction electrons in a crystal over their various stationary states, established by the joint influence of the applied electric field and the impacts with the lattice due to thermal agitation, has a time of relaxation $1/\beta$, where β is given by (29).

2. The classical phenomenological theory of the dispersion of light in metallic conductors, in which it is presupposed that current density and electric field are connected in the same way for variable and for constant fields, will fail when the frequency ν of the light becomes comparable to β , a measure of the accuracy being $e^{-\beta/\nu}$. For ordinary temperatures β lies between 10^{13} and 10^{14} , in agreement with experiment, and changes proportional to the absolute temperature.

3. A dispersion theory is developed for the region of high frequencies, $\nu \ll \beta$,

which gives a satisfactory qualitative account of the optical behaviour of metals in the visible and ultra-violet part of the spectrum.

I wish to take this opportunity of acknowledging my indebtedness to the Lorentz Fonds, at whose invitation I have been conducting research at the University of Utrecht.

On the Interpretation of the Relativity Wave Equation for Two Electrons.

By N. F. MOTT, B.A., St. John's College.

(Communicated by R. H. Fowler, F.R.S.—Received April 12, 1929.)

In the general non-relativity quantum dynamics that has been developed by Dirac and others, the motion of a dynamical system is described by a wave function $\psi(\xi_1 \dots \xi_n; t)$; and one interprets this wave function by postulating that

$$|\psi(\xi'_1 \xi'_2 \dots \xi'_n; t)|^2 d\xi'_1 \dots d\xi'_n$$

is the probability that, at time t

$$\xi_r' \leq \xi_r \leq \xi_r' + d\xi_r' \quad (r = 1 \dots n).$$

The relativity wave function for a single electron can be interpreted in a similar manner. If* $\psi(xyzt)$ be the wave function, and ϕ the conjugate function, then $\phi\psi(xyzt) dx dy dz$ is the probability that the electron will be found, at time t , in the volume element $dx dy dz$.

It is, of course, necessary that the wave function should be normalised, i.e., that

$$\int \phi\psi dx dy dz = 1,$$

because the probability that the electron is to be found somewhere in the whole of space is unity. It is also necessary for the consistency of the theory that the normalisation should persist through time, i.e., that

$$\frac{\partial}{\partial t} \int \phi\psi dx dy dz = 0. \quad (1)$$

* ψ has of course four components ψ_λ . $\phi\psi$ is to be taken as an abbreviation for $\sum_{\lambda=1}^4 \phi_\lambda \psi_\lambda$.

This, as is well known, follows at once from the so-called equations of motion of the quantum theory. We use the symbolic matrix notation of Dirac, where $\phi\psi$ is written for $\int \phi\psi \, dx \, dy \, dz$. The wave equations of motion are

$$\begin{aligned} ih \frac{\partial}{\partial t} \psi &= H\psi, \\ -ih \frac{\partial}{\partial t} \phi &= \phi H. \end{aligned}$$

We have to prove that,

$$\frac{\partial}{\partial t} (\phi\psi) = 0,$$

that is, that

$$\frac{\partial \phi}{\partial t} \psi + \phi \frac{\partial \psi}{\partial t} = 0,$$

a result which follows at once from the wave equation, whether relativistic or not.

Now, in the relativity wave equation for two electrons,* there occur two times, one for each electron. The wave function ψ is a function of eight variables—as well as the spin variables; we have

$$\psi = \psi(x_1 y_1 z_1 t_1, x_2 y_2 z_2 t_2).$$

The two times must refer to two separate experiments. To fix our ideas, let us consider a definite occurrence, the collision between two electrons. Two wave packets are moving towards each other, and they are going to hit “dead on” in such a way that they get mixed up. Then after the collision, the probability that we shall find one electron in the volume element $dx_1 \, dy_1 \, dz_1$ at time t_1 , and the other in the volume element $dx_2 \, dy_2 \, dz_2$ at time t_2 is

$$\phi\psi(x_1 y_1 z_1 t_1; x_2 y_2 z_2 t_2) \, dx_1 \, dy_1 \, dz_1 \, dx_2 \, dy_2 \, dz_2.$$

Now, in order that this interpretation may be consistent we need something more than a mere normalisation of ψ . For suppose we only wish to observe *one* electron. Suppose we have, say, a Geiger counter at the point $x_1 y_1 z_1$, and we wish to know the probability that an electron will be found there in a volume element $dx_1 \, dy_1 \, dz_1$ at the time t_1 . This probability must clearly be†

$$dx_1 \int \phi\psi(x_1 t_1; x_2 t_2) \, dx_2.$$

* Eddington, ‘Roy. Soc. Proc.’, vol. 122, p. 358 (1929), Gaunt, ‘Roy. Soc. Proc.’, vol. 122, p. 513 (1929).

† Writing \mathbf{x} for x, y, z .
 $d\mathbf{x}$ for $dx \, dy \, dz$.

We have integrated over all possible places where the second electron might be found, should we, at time t_2 , make an experiment to find it. But the probability of an electron entering our Geiger counter at time t_1 must clearly be independent of the time t_2 at which our second experiment might be made—seeing that it never is or need be made. Therefore, if our interpretation of the wave equation is to make sense, we must have

$$\frac{\partial}{\partial t_2} \int \phi \psi (\mathbf{x}_1 t_1; \mathbf{x}_2 t_2) d\mathbf{x}_2 = 0. \quad (2)$$

The equality (2) is not, as far as one can see, a general property of the wave functions, but it is true in the only case in which it seems possible to give any physical meaning to a wave function with two times. Let us consider first the value of (2) when t_1 is equal to t_2 . Then the equality (2) is true if, at the moment t_1 , there is no appreciable probability that *both* electrons are in the neighbourhood of \mathbf{x}_1 . By “neighbourhood” we mean, within a distance r such that ϵ^2/r is comparable with the kinetic energy of the electrons. In other words, (2) is satisfied as long as the experimental conditions are such that we may be sure that no collision is taking place at the point \mathbf{x}_1 at the time t_1 . This would be the case in almost any actual experiment; and also we should probably expect the interpretation to go wrong if the electrons might be engaged in a collision at the moment of the experiment, because it would be impossible to do an experiment on the one electron, without some risk of upsetting the other.

If t_2 is not equal to t_1 , but some later time, then (2) is true if ψ vanishes in the “neighbourhood” of the set of points for which

$$c^2(t_2 - t_1)^2 = (\mathbf{x}_2 - \mathbf{x}_1)^2.$$

That is to say that, if (2) is to be satisfied, we must be sure not only that no collision is taking place at \mathbf{x}_1 at time t_1 , but also that the second electron is so far away from \mathbf{x}_1 that it could not be disturbed, at time t_2 , by a disturbance that has started out from \mathbf{x}_1 at time t_1 , and which travelled with the velocity of light. This, I think, also, is what we might expect. The detection of the first electron at \mathbf{x}_1 at time t_1 might very well set up an electromagnetic disturbance, which would affect the (imaginary) second experiment at $\mathbf{x}_2 t_2$, if it got there in time.

The proof that equation (2) is satisfied under these conditions is almost obvious. If

$$R_{12} = \sqrt{(x_2 - x_1)^2 - c^2(t_2 - t_1)^2}$$

then the conditions imply that ψ shall vanish unless

$$\frac{\epsilon^2}{R_{12}} \ll [\text{Kinetic energy of the electrons}].$$

It is clear, therefore, that over all that part of \mathbf{x}_2 space which contributes anything to the integral in (2), ψ must satisfy the wave equation for two electrons in free space *with no interaction*. The equation (2) follows in the same way as the equation (1) for one electron.

It appears, therefore, that the interpretation of the two-electron equation is consistent, and further that all results of physical importance can be obtained by using one time only, putting $t_1 = t_2$ in the wave equation. It would, however, be of interest to obtain a solution of the wave equation containing the two times, so that we could see what happens in the case excluded above, when one experiment is in the absolute future of the other, and so may be affected by it.

The Scattering of Fast Electrons by Atomic Nuclei.

By N. F. MOTT, B.A., St. John's College, Cambridge.

(Communicated by N. Bohr, For. Mem. R.S.—Received April 25, 1929.)

Section 1.—The hypothesis that the electron has a magnetic moment was, as is well known, first introduced to account for the duplexity phenomena of atomic spectra. More recently, however, Dirac has succeeded in accounting for these same phenomena by the introduction of a modified wave equation, which conforms both to the principle of relativity and to the general transformation theory. Formally, at least, on the new theory also, the electron has a magnetic moment of eh/mc , but when the electron is in an atom we cannot observe this magnetic moment directly; we can only observe the moment of the whole atom, or, of course, the splitting of the spectral lines, which we may say is “caused” by this moment. The question arises, has the *free* electron “really” got a magnetic moment, a magnetic moment that we can by any conceivable experiment observe? The question is not so simple as it might seem, because a magnetic moment eh/mc can never be observed directly, *e.g.*, with a magnetometer; there is always an uncertainty in the external electromagnetic field; due to the uncertainty in the position and

velocity of the electron, and this uncertainty is greater than the effect of the electron magnet which we are trying to observe.* Our only hope of observing the moment of a free electron is to obtain a "polarised" beam, in which all the spin axes are pointing in the same direction, or at any rate more in one direction than another. The obvious method of obtaining such a polarised beam is a Stern-Gerlach experiment, but here again the Uncertainty Principle shows that this is impossible*; in fact, it appears certain that no experiment based on the classical idea of an electron magnet can ever detect the magnetic moment of the electron.

We are, however, unwilling to give up altogether the idea of the direction of the spin axis of the free electron, because of the form that the solution of the wave equation has for this case. Whether we consider an infinite plane wave, or a wave packet, there are, in the solution, two arbitrary constants A , B , which are just enough to determine a "spin" direction. Further, it has been shown by Darwin† that the electromagnetic field due to a wave packet can be separated formally into two parts, the one due to the charge and current, and the other due to the magnetic moment of the electron, which points in a definite direction and is determined by A , B . As we have pointed out, this second part cannot be observed, because it is less than the uncertainty in the first; but nevertheless, we can associate formally a direction of the spin axis with any given solution of the wave equation.

Now, have these constants A , B , this direction of the spin axis, any physical meaning? Suppose, for example, a wave packet were to fall on a nucleus; would the scattered intensity depend on the A and B of the initial wave packet? This can only be decided by a mathematical investigation, to which the greater part of this paper is devoted. If the scattered intensity does not depend on A , B , that would be very satisfactory; we should consider A and B to be constants used in the mathematics, but with no physical meaning, and the spin of a free electron to be something non-existent. However, we shall find that the scattered intensity does depend on A and B , so that the spin direction has some meaning after all. Suppose an electron, about whose spin direction we know nothing, falls on a nucleus and is scattered through a given angle; we now know that its spin axis is more likely to be in one direction than another. Suppose an unpolarised beam, in which the spin axes are pointing in all directions at random, falls on a target and is scattered; the scattered beam is partly polarised; more spin axes point in one direction than another; and this

* These arguments are due to Prof. Niels Bohr, and are discussed further in an appendix.

† C. G. Darwin, 'Roy. Soc. Proc.,' A, vol. 120, p. 631 (1928).

polarisation could be detected by letting the scattered beam fall on a second target. Since the beam is polarised it will not be scattered in the same way as an unpolarised beam; actually we shall find that the scattering is asymmetrical about the direction in which the beam falls on the second target, and this could be detected experimentally.

In this paper we shall investigate the scattering of fast electrons by atomic nuclei, using the wave equation of Dirac. As well as investigating the polarisation, we shall obtain a formula* for the scattering of an unpolarised beam, which is to replace the Rutherford formula for fast electrons. In Section 2 we shall obtain certain general results for scattering by a field of force $V(r)$. In Section 3 we shall investigate the scattering by a Coulombian field of force, and determine the scattering law and the polarisation to be expected. The mathematics can be interpreted without difficulty, since the energy is an integral of the equations of motion, and we are not troubled by transitions to negative energy. We may emphasise once again that we do not want to know how the spin axis is turned when the electron is deflected, so much as how the direction of the spin axis affects the probability of the electron being scattered in a given direction, as it is this last that will be observable experimentally.

Section 2.—We consider the scattering of an infinite plane wave by a centre of force $V(r)$. If we were working with Schrödinger electrons, the wave equation would be

$$\nabla^2\psi + \frac{8\pi^2m}{h^2}(W + V)\psi = 0, \quad (1)$$

and we should have to find a solution ψ , such that for large r

$$\psi \sim I + S \cdot u(\theta, \phi), \quad (1.1)$$

where I is written for $\exp(2\pi ipz/h)$ and represents the incident wave, and S for $\exp(2\pi ipr/h)/r$ to represent the scattered wave. Then, if a beam of electrons were to fall on a foil, say, of thickness t and containing n nuclei per unit volume, the proportion of the original beam scattered in a given solid angle will be

$$nt |u(\theta, \phi)|^2 \sin \theta \, d\theta \, d\phi.$$

With Dirac electrons, we have, of course, four components of the wave function, $\psi_1, \psi_2, \psi_3, \psi_4$. The wave equation is the familiar wave equation of Dirac.†

$$[p_0 + V(r)/c - 2\pi i\hbar(\sigma, \text{grad}) + \rho_3 mc] \psi = 0, \quad (2)$$

* This formula, of course, includes "Relativity correction" as well as "spin correction," but does not include the effect of radiative forces.

† 'Roy. Soc. Proc.,' A, vol. 117, p. 610 (1928).

and, as before, we want a solution representing an incident plane wave falling on the nucleus and a scattered wave—a solution ψ therefore, such that, for large r

$$\psi \sim a_\lambda I + S u_\lambda(0\phi). \quad (3)$$

The a_λ are constants, but not all arbitrary constants, for if any two are given, the other two are known.† We set

$$a_3 = A, \quad a_4 = B,$$

where A and B are arbitrary complex constants. Then we have

$$a_1 = -Ap/(p_0 + mc), \quad a_2 = Bp/(p_0 + mc).$$

The current represented by the incident wave is equal to $\sum_{\lambda=1}^4 |a_\lambda|^2$, which is proportional to $AA^* + BB^*$. In the same way, the current scattered depends on u_3, u_4 only.

To interpret our formulae, therefore, we choose A, B in such a way that

$$AA^* + BB^* = 1.$$

Then, if $n P \sin \theta d\theta d\phi$ is the proportion of the original beam scattered in a given solid angle, we have

$$P = |u_3(0\phi)|^2 + |u_4(0\phi)|^2. \quad (4)$$

The constants A, B determine also the polarisation, or direction of the spin axis, of the incident electrons. When we speak of the direction of the spin, we shall mean the direction referred to axes with respect to which the electron is at rest; it is this that will be distributed equally in all directions in an unpolarised beam. If χ, ω are the spherical polar angles of the spin direction, then‡

$$-\frac{B}{A} = \cot \frac{1}{2}\chi \cdot e^{i\omega}. \quad (5)$$

In the same way, u_4/u_3 will determine the polarisation of the electrons scattered in any direction. To determine the proportion scattered from an unpolarised beam, we must average P of equation (4) over all values of χ, ω .

If we find ψ_3 and ψ_4 for the two cases $A = 1, B = 0$ and $A = 0, B = 1$,

† Darwin, 'Roy. Soc. Proc.,' A, vol. 118, p. 654 (1928).

‡ Darwin, 'Roy. Soc. Proc.,' A, vol. 120, p. 631 (1928).

then we can form the general solution (3) by superposition of these two. We shall show in the next section that these two solutions are of the form

$$\left. \begin{aligned} \psi_3 &\sim I + Sf(\theta) \\ \psi_4 &\sim Sg(\theta)e^{i\phi} \end{aligned} \right\}, \quad (6.1)$$

and

$$\left. \begin{aligned} \psi_3 &\sim -Sg(\theta)e^{-i\phi} \\ \psi_4 &\sim I + Sf(\theta) \end{aligned} \right\}, \quad (6.2)$$

where $f(\theta)$, $g(\theta)$ are functions of θ (not ϕ) which depend on the form of $V(r)$.

By superposition of these two, we have at once the general solution of the form (3), with

$$\begin{aligned} u_3(\theta\phi) &= Af - Bge^{-i\phi}, \\ u_4(\theta\phi) &= Bf + Age^{i\phi}. \end{aligned}$$

Hence we have

$$\begin{aligned} |u_3|^2 + |u_4|^2 &= (|A|^2 + |B|^2)(|f|^2 + |g|^2) \\ &\quad + (fg^* - f^*g)(-AB^*e^{i\phi} + A^*Be^{-i\phi}), \end{aligned} \quad (7)$$

so, if $nP \sin \theta d\theta d\phi$ is the proportion of the beam scattered in the solid angle $\sin \theta d\theta d\phi$, then we see from (4), (5) that

$$P = |f|^2 + |g|^2 + D \sin \chi \sin(\omega - \phi), \quad (8)$$

where

$$D(\theta) = i(fg^* - f^*g)$$

and χ , ω determine the direction of the spin axis of the incident electrons.

To obtain the number \bar{P} scattered from an unpolarised beam, we must average over all directions of the spin axis: we obtain

$$\bar{P} = |f|^2 + |g|^2. \quad (9)$$

Unless, however, $D(\theta) = 0$ for the angle of scattering considered, the function P will depend on the polarisation of the incident beam; and if the incident beam is unpolarised, the scattered beam will not be. We shall be able to detect this polarisation by scattering the beam again by a second nucleus.

Before considering this double scattering in detail, it will be well to point out an obvious trap. On the old Quantum Theory, one used to say that a magnet, such as an electron magnet, must orientate itself either parallel or anti-parallel to a magnetic field. Such an assumption would in our case lead to inconsistent results. For from equation (8) we see that electrons whose spin axes lie parallel and anti-parallel to the direction of motion are scattered

in the same way as an unpolarised beam. Suppose then we always had a weak magnetic field in the direction of motion, before and after scattering; then the scattering would always be normal, and the double scattering experiment would give a null result, which is contrary to the result of the following calculation. The fallacy is probably this, that we must not think of the axes of the electron magnets as lying parallel and anti-parallel to the field, but as precessing round it.

We shall now consider the double scattering experiment. A beam of

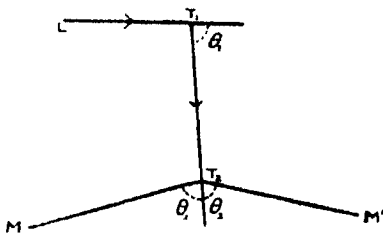


FIG. 1.

electrons LT_1 falls on a target T_1 and is scattered. A second target is placed at T_2 so that the electrons scattered through an angle θ_1 in the plane of the paper (for which $\phi = 0$) undergo a second scattering. We observe the number of electrons scattered by T_2 at a given angle θ_2 . If the beam T_1T_2 is polarised, the second scattering will not be

symmetrical about T_1T_2 ; the number scattered in the directions T_2M , T_2M' will not be the same.

Suppose we represent the initial beam LT_1 by

$$\psi_3 = AI \quad \psi_4 = BI.$$

We shall, of course, have to average over all spin directions later. The direction of the spin axis of the scattered beam T_1T_2 is determined, according to (5), by the ratio of the amplitudes of the two components of the wave function of the scattered beam, namely*

$$Af_1 - Bg_1, \quad Ag_1 + Bf_1.$$

We now rotate our axes through an angle θ_1 so that T_1T_2 becomes the axis of z and we can represent the beam of electrons T_1T_2 by

$$\psi_3 = A_1I \quad \psi_4 = B_1I$$

with†

$$A_1 = (Af_1 - Bg_1) \cos \frac{1}{2}\theta_1 + (Ag_1 + Bf_1) \sin \frac{1}{2}\theta_1$$

$$B_1 = (Ag_1 + Bf_1) \cos \frac{1}{2}\theta_1 - (Af_1 - Bg_1) \sin \frac{1}{2}\theta_1.$$

We can now obtain the number of electrons scattered by the second target T_2 in a given direction $\theta_2\phi_2$; we must insert these values of A_1 , B_1 for A , B ,

* f_1 is written for $f(\theta_1)$, etc.

† Darwin, 'Roy. Soc. Proc.,' A, vol. 118, p. 654 (1928).

in (7) and average over all directions of the spin axis of the initial beam LT_1 . We are interested primarily in the asymmetry in the scattering about the line T_1T_2 . For given θ_1, θ_2 , therefore, but variable ϕ_2 , a straightforward calculation shows that the number scattered per unit solid angle is proportional to

$$1 - \delta \cos \phi_2, \quad (10)$$

where

$$\delta = 2 \frac{(f_1 g_1^* - f_1^* g_1)(f_2 g_2^* - f_2^* g_2)}{(f_1 f_1^* + g_1 g_1^*)(f_2 f_2^* + g_2 g_2^*)}.$$

The greatest asymmetry, therefore, will be found in the directions TM, TM', in the plane of the paper. In the plane through T_1T_2 perpendicular to the plane of the paper, the scattering is symmetrical about T_1T_2 . It was in this plane that asymmetry was looked for by Cox, McIlwraith and Kurrelmeyer,[†] and the asymmetry found by them must be due to some other cause.

We must now show that we can obtain solutions of the wave equation of the form (6.1), (6.2), and obtain expressions for f and g . We shall first consider Schrödinger electrons.[§] The general solution of (1) is

$$\sum a_k P_k(\cos \theta) L_k(r)$$

where L_k is the bounded solution of

$$\frac{d^2 L}{dr^2} + \frac{2}{r} \frac{dL}{dr} + \left[\frac{8\pi^2 m}{h^2} (E + V) - \frac{k(k+1)}{r^2} \right] L = 0. \quad (11)$$

For large r , L_k has the form

$$L_k \sim r^{-1} \cos(2\pi pr/h + \eta_k^0).$$

Remembering that

$$e^{i\theta \cos \theta} = \left(\frac{\pi}{2r}\right)^{\frac{1}{2}} \sum_{k=0}^{\infty} (2k+1) i^k P_k(\cos \theta) J_{k+\frac{1}{2}}(r)$$

we see that the solution of (1) of the form (2) is

$$i \sum_{k=0}^{\infty} (2k+1) e^{i\eta_k^0 + ik\pi} P_k(\cos \theta) L_k(r)$$

with

$$u(\theta, \phi) = \frac{h}{2\pi p} \sum_{k=0}^{\infty} \left(k + \frac{1}{2}\right) \left[e^{2i\eta_k^0 + \frac{2k+1}{2}\pi i} + 1 \right] P_k(\cos \theta).$$

The general solution in spherical harmonics of Dirac's wave equation (2)

[†] 'Proc. Nat. Ac. Sci.,' vol. 14, p. 545 (1928).

[§] Cf. Faxen and Holtmark, 'Z. Physik,' vol. 45, p. 307 (1927); Mott, 'Roy. Soc. Proc.,' A, vol. 118, p. 542 (1928); Gordon, 'Z. Physik,' vol. 48, p. 187 (1928).

has been given by Darwin for the case of discrete energy values, and his analysis is immediately applicable to our case. A set of solutions are:—

$$\begin{array}{ll}
 (\alpha) & \psi_3 = (k+1) P_k G_k & \psi_4 = -G_k P_k^1 \\
 (\beta) & \psi_3 = k P_k G_{-k-1} & \psi_4 = G_{-k-1} P_k^1 \\
 (\gamma) & \psi_3 = P_k^1 G_k & \psi_4 = (k+1) G_k P_k \\
 (\delta) & \psi_3 = -G_{-k-1} P_k^1 & \psi_4 = G_{-k-1} P_k
 \end{array}$$

Here P_k is the ordinary Legendre-coefficient $P_k(\cos \theta)$ (not Darwin's notation) and P_k^1 is $\sin \theta \frac{d}{d(\cos \theta)} P_k(\cos \theta) e^{i\phi}$. $G_k(r)$ is the bounded solution of the pair of equations

$$\left. \begin{aligned}
 \frac{2\pi}{h} \left(p_0 + \frac{\epsilon V}{c} + mc \right) F + \frac{dG}{dr} - \frac{k}{r} G &= 0, \\
 -\frac{2\pi}{h} \left(p_0 + \frac{\epsilon V}{c} - mc \right) G + \frac{dF}{dr} + \frac{k+2}{r} G &= 0.
 \end{aligned} \right\} \quad (13)$$

Now, G_k has the asymptotic form

$$G_k \sim r^{-1} \cos(2\pi pr/h + \eta_k) \quad (14)$$

Hence, in the same way as for Schrödinger electrons, we can form a solution representing an incident wave and a scattered wave. From (α) and (β) we see that a solution with the asymptotic form (6.1) is

$$\left. \begin{aligned}
 \psi_3 &= i \sum_{k=0}^{\infty} \{ (k+1) e^{i\eta_k} G_k + k e^{i\eta_{-k-1}} G_{-k-1} \} (-)^k P_k(\cos \theta) \\
 \psi_4 &= i \sum_{k=0}^{\infty} \{ -e^{i\eta_k} G_k + e^{i\eta_{-k-1}} G_{-k-1} \} (-)^k P_k^1(\cos \theta) e^{i\phi},
 \end{aligned} \right\} \quad (15)$$

and that

$$\left. \begin{aligned}
 f(\theta) &= \frac{h}{2\pi p} \cdot \frac{1}{2} \sum_0^{\infty} i \{ (k+1) (e^{2i\eta_k + k i\pi} + 1) + k (e^{2i\eta_{-k-1} + k i\pi} + 1) \} P_k(\cos \theta) \\
 g(\theta) &= \frac{h}{2\pi p} \cdot \frac{1}{2} \sum_0^{\infty} i \{ - (e^{2i\eta_k + k i\pi} - 1) + (e^{2i\eta_{-k-1} + k i\pi} - 1) \} P_k^1(\cos \theta)
 \end{aligned} \right\} \quad (16)$$

In an exactly similar way from (γ) and (δ), we can construct a solution of the form (6.2), with the same f and g .

There is no difficulty in justifying these processes mathematically, provided that the series (12), (16) converge absolutely. And they do converge absolutely, if $V(r) \rightarrow 0$ faster than $1/r^2$, as may be seen by solving equation (11) for very

large k , when V may be considered as a perturbation. We shall consider the case of a Coulombian field in the next section.

Section 3.—We shall now consider the case that is of greatest interest, namely, the scattering by an atomic nucleus with inverse square law field, such that

$$V(r) = Ze^2/r.$$

We know that, for Schrödinger electrons, with neglect of relativity and spin, the scattering obeys the Rutherford law. It is interesting to compare the second order wave equation for Dirac electrons* with the Schrödinger equation, and to see what are the order of the deviations to be expected from Rutherford scattering. This second order equation is

$$\left[-\left(p_0 + \frac{Ze^2}{cr} \right)^2 - 4\pi^2 \hbar^2 \nabla^2 + m^2 c^2 + \frac{2\pi i e^2 \hbar}{cr^3} \rho_1(\sigma r) \right] \psi = 0,$$

where cp_0 is equal to the energy E of the electron, including the rest mass.

The order of magnitude of the various terms is best seen if we take for our unit of length $1/2\pi$ times the de Broglie wave-length in free space, namely

$$\hbar/2\pi p = \hbar/2\pi (p_0^2 - m^2 c^2)^{1/2} = \frac{\hbar}{2\pi m V} \left(1 - \frac{v^2}{c^2} \right)^{1/2}.$$

The wave equation then becomes

$$\left[\nabla^2 + 1 + \frac{2\mu\alpha}{r} + \frac{\alpha^2}{r^2} - i \frac{\alpha}{r^3} \rho_1(\sigma r) \right] \psi = 0, \quad (17)$$

where

$$\alpha = \frac{2\pi Ze^2}{\hbar c} = \frac{Z}{137}, \quad \mu = \frac{p_0}{\sqrt{p_0^2 - m^2 c^2}} = \frac{c}{v}.$$

The last three terms inside the square bracket may be said to "cause" the scattering. For small velocities of the incident electron, it is clear that the term $2\mu\alpha/r$ is much larger than the other terms, and therefore the scattering is approximately inverse square. But for velocities comparable with the velocity of light, μ tend to unity, and so the effect of the "spin" term, $i\alpha/r^3 \cdot \rho_1(\sigma r)$, will be of the same order as the effect of the inverse square law term. For light nuclei, α is very much smaller than unity, and therefore the "relativity" term α^2/r^2 , which is "responsible" for the fine structure of atomic spectral lines, has only a small effect on the scattering.

We can obtain a solution of equation (17) of the form (6.1) by the method of Born† and Wentzel.‡ The method yields a solution of the form

$$\psi^{(0)} + \alpha \psi^{(1)} + \alpha^2 \psi^{(2)} + \dots,$$

* Dirac, 'Roy. Soc. Proc.' vol. 117, p. 610 (1928).

† 'Z. Physik,' vol. 38, p. 803 (1926).

‡ 'Z. Physik,' vol. 40, p. 590 (1927). We should have to use an 'Abschirmungsfeld.'

with $\psi^{(0)}$ representing the incident wave, and the other terms the scattered wave. Such a method is only convenient for the evaluation of $\psi^{(1)}$; the author has actually evaluated $\psi^{(1)}$ by this method, and the calculation provides a useful check upon the subsequent work. For light nuclei, for which α is small, this first approximation would probably be sufficient; but the interest of $\psi^{(2)}$ lies in this, that to the first order of approximation f and g turn out to be real, and there is therefore no polarisation to this order. We shall therefore return to formula (15) and from it evaluate ψ as far as $\psi^{(2)}$.

In our subsequent work we shall take the unit of length to be $h/2\pi p$.

The equations (13) have been solved for F_k and G_k by Darwin, and by Gordon*; for continuous energy values Gordon's solution is more suitable. We introduce the following notation

$$q = \frac{\alpha E/mc^2}{\sqrt{(E/mc^2)^2 - 1}} = \frac{2\pi\epsilon^2}{hv},$$

$$q' = \frac{\alpha}{\sqrt{(E/mc^2)^2 - 1}} = \frac{2\pi\epsilon^2}{hv} \left(1 - \frac{v^2}{c^2}\right)^{\frac{1}{2}}$$

$$\rho = \sqrt{k^2 - \alpha^2}, \quad \alpha = \frac{2\pi Z\epsilon^2}{hc},$$

v is the classical "velocity" of the particle defined by

$$E = mc^2 \left(1 - \frac{v^2}{c^2}\right)^{-\frac{1}{2}}. \quad (18)$$

With the usual notation for generalised hypergeometric series, we write

$$F(\alpha; \beta; x) = 1 + \frac{\alpha}{1! \beta} x + \frac{\alpha(\alpha+1)}{2! \beta(\beta+1)} x^2 + \dots$$

The asymptotic expansion of this function for large x is well known.† We require the first term only; for pure imaginary x we have

$$\left. \begin{aligned} F(\alpha; \beta; x) &\sim \frac{\Gamma(\beta)}{\Gamma(\beta-\alpha)} (-x)^{-\alpha}, \\ \text{or} \quad F(\alpha; \beta; x) &\sim \frac{\Gamma(\beta)}{\Gamma(\alpha)} e^x x^{\alpha-\beta} \\ &\quad | \arg(-x) | < \pi \quad | \arg x | < \pi \end{aligned} \right\}, \quad (19)$$

according as the real part of $-2\alpha + \beta$ is greater or less than zero.

* Darwin, 'Roy. Soc. Proc.,' A, vol. 118, p. 654 (1928); Gordon, 'Z. Physik,' vol. 48, p. 11 (1928).

† Cf. for example, Gordon, 'Z. Physik,' vol. 48, p. 187 (1928).

With this notation we have* for G_k ,

$$G_{-k-1} = N \left[\frac{e^{-i\pi\rho} c_k \zeta_k}{\Gamma(\rho + 1 + iq)} + \frac{e^{+i\pi\rho} c_k' \zeta_k'}{\Gamma(\rho + 1 - iq)} \right],$$

where

$$\zeta_k = \frac{\Gamma(\rho + 1 + iq)}{\Gamma(2\rho + 1)} e^{+\frac{\pi i \rho}{2} + \frac{q}{2}} F(\rho + 1 + iq; 2\rho + 1; 2ir) \frac{1}{2} (2r)^\rho e^{-ir}/r,$$

$$\zeta_k' = \frac{\Gamma(\rho + 1 - iq)}{\Gamma(2\rho + 1)} e^{-\frac{\pi i \rho}{2} + \frac{q}{2}} F(\rho + iq; 2\rho + 1; 2ir) \frac{1}{2} (2r)^\rho e^{-ir}/r,$$

and

$$c_k/c_k' = -(k - iq')/(\rho - iq)$$

and N is a normalising factor.

From formulæ (19) we have at once

$$\zeta_k \sim \frac{1}{2} (2r)^{iq} \cdot e^{ir}/r,$$

$$\zeta_k' \sim \frac{1}{2} (2r)^{-iq} \cdot e^{-ir}/r,$$

and

$$G_{-k-1} \sim r^{-1} \cos(r + q \log 2r + \eta_{-k-1})$$

with η_k given by

$$e^{2i\eta_{-k-1}} = - \frac{k - iq'}{\rho - iq} e^{-i\pi\rho} \frac{\Gamma(\rho + 1 - iq)}{\Gamma(\rho + 1 + iq)} \\ = B_k \text{ say.}$$

The asymptotic expansion of G_k is not quite of the form (14), differing from it by the logarithmic term; as has been pointed out by various authors, for an inverse square law field the incident wave is not quite plane. We can, however, construct the solution of the form (6.1) without difficulty. This solution is

$$\left. \begin{aligned} \psi_3 &= i \sum_{k=0}^{\infty} [(2k+1) \zeta_k' + \{kB_k + (k+1) B_{-k-1}\} \zeta_k] (-)^k P_k(\cos \theta) \\ \psi_4 &= i \sum_{k=0}^{\infty} [B_k - B_{-k-1}] \zeta_k (-)^k P_k^1(\cos \theta) e^{i\phi} \end{aligned} \right\} \quad (21)$$

These series converge absolutely for given r . A method previously given by the present author† can be used to prove that, for large r

$$i \sum_{k=0}^{\infty} (2k+1) \zeta_k'(r) (-)^k P_k(\cos \theta) \sim e^{ir \cos \theta - iq \log r (1 - \cos \theta)}.$$

This represents the incident wave. The remaining terms represent outgoing

* Gordon, *loc. cit.*, p. 13, equation (10). If we put Gordon's j' equal to our k , then his ψ_3 is equal to our $r G_{-k-1}$.

† Mott, 'Roy. Soc. Proc.,' A, vol. 118, p. 543.

waves only. We cannot, however, obtain the form of the wave for large r by inserting the asymptotic solution (20) for ζ_k , because the series so obtained do not converge. They can, however, be summed as the limit of a power series on its radius of convergence.* If we express the functions ζ_k as the contour integrals from which the asymptotic expansion is obtained, it is easy to see that these sums do in fact give the asymptotic form of (21). The method is the same as that used in the author's previous paper. We see, therefore, that (21) is a solution of the wave equation with the asymptotic form (6.1) with

$$I = e^{ir \cos \theta - iq \log r (1 - \cos \theta)},$$

$$S = e^{ir + iq \log 2r/r},$$

and

$$f(\theta) = \frac{1}{2}i \sum [kB_k + (k+1)B_{-k-1}](-)^k P_k(\cos \theta)$$

$$g(\theta) = \frac{1}{2}i \sum [B_k - B_{-k-1}](-)^k P_k^1(\cos \theta),$$

the summation of each series being carried out as the limit of a power series on its radius of convergence.

We can express f and g in terms of series which do not contain q' . If we write

$$c_k = -e^{-iq\rho} \Gamma(\rho - iq)/\Gamma(1 + \rho + iq)$$

and

$$F(\theta) = \frac{1}{2}i \sum_0^\infty (-)^k \{kC_k + (k+1)C_{k+1}\} P_k(\cos \theta),$$

$$G(\theta) = \frac{1}{2}i \sum_0^\infty (-)^k \{k^2C_k - (k+1)^2C_{k+1}\} P_k(\cos \theta),$$

we obtain

$$\left. \begin{aligned} f &= -iq'F + G \\ g &= [iq'(1 + \cos \theta)F + (1 - \cos \theta)G]/\sin \theta \end{aligned} \right\}. \quad (23)$$

F and G are functions of θ , α^2 and q . It has not been found possible to sum the series in terms of known functions; we can, however, write $q = \alpha\mu$ and expand F and G as power series in α . We shall obtain the first two terms of the expansion. α has, of course, any value from $1/137$ for hydrogen up to about $3/4$ for the heavy nuclei; and for fast electrons μ will be about 3, though for slow electrons it will be greater. *Our approximation is best, therefore, for fast electrons and for light nuclei.*

* Whittaker and Watson, 'Modern Analysis,' p. 155.

If we refer to the series (22), and put $q = q'$ and $\alpha^2 = 0$, we obtain

$$\left. \begin{aligned} f(\theta) &= -\frac{1}{2}i \Sigma (2k+1) \frac{\Gamma(k+1-iq)}{\Gamma(k+1+iq)} P_k(\cos \theta) \\ g(\theta) &= 0 \end{aligned} \right\}. \quad (24)$$

This corresponds to a neglect of relativity and spin. Since $g = 0$ we see that the direction of the spin axis is unchanged on collision. The series (24) occurs in the investigation of the scattering of Schrödinger electrons; it can be summed by the method of the author's previous paper,* the sum being

$$R \operatorname{cosec}^2 \frac{\theta}{2},$$

where

$$R = \frac{1}{2}q \exp \left[2iq \log \sin \frac{\theta}{2} + \frac{\Gamma(1-iq)}{\Gamma(1+iq)} + i\pi \right].$$

The scattering is therefore classical, as it should be.

Now, α occurs in F and G only as α^2 , so that as a first approximation we can neglect α altogether. Let F_0, G_0 be the values of F and G to this approximation. Since we know f_0 and g_0 when $q = q'$, and q' does not occur in F and G , we have at once from (23)

$$\begin{aligned} iq F_0 &= -R, \\ G_0 &= R \cot^2 \frac{\theta}{2}. \end{aligned}$$

Hence

$$\left. \begin{aligned} f_0 &= \left(\frac{q'}{q} - 1 + \operatorname{cosec}^2 \frac{\theta}{2} \right) R \\ g_0 &= - \left(\frac{q'}{q} - 1 \right) R \cot^2 \frac{\theta}{2} \end{aligned} \right\}. \quad (24)$$

These are the first order scattering formula that we should obtain by the Born method. The ratio of f_0 and g_0 is real; it follows that to this order there is no polarisation. It is therefore of interest to evaluate f and g to the next power of α, q .

Expanding C_k in powers of α we have

$$\begin{aligned} C_k &= \frac{(-)^k \Gamma(k-iq)}{\Gamma(1+k+iq)} + \frac{\alpha^2}{2k^2} (-)^k \left[i\pi + \frac{1}{k} \right]. \quad k \neq 0 \\ &\quad + \text{terms } \alpha^2 q, \text{ etc.} \end{aligned}$$

* Mott, 'Roy. Soc. Proc.,' vol. 118, p. 543 (1928). The result given there can be simplified to that given above. Cf. Whittaker and Watson, p. 240.

Neglecting terms of the order $\alpha^2 q$ we obtain†

$$iqF = iqF_0,$$

$$G = G_0 + \frac{\alpha^2}{4} \left[\pi \operatorname{cosec}^2 \frac{\theta}{2} - i \log \operatorname{cosec}^2 \frac{\theta}{2} \right],$$

whence from (23), (24) we can obtain at once formulæ for f and g .

To this order, we find that f/g is not real; we have therefore some polarisation on a collision; the constant that determines the polarisation is

$$fg^* - f^*g = \frac{i\alpha^2 q'}{4} \operatorname{cosec} \theta \log \operatorname{cosec} \frac{\theta}{2} + \text{terms of order } \alpha^4.$$

To the same order

$$|f|^2 + |g|^2 = \frac{1}{4} \left[q^2 \operatorname{cosec}^4 \frac{\theta}{2} + \frac{q'^2 - q^2}{4} \operatorname{cosec}^2 \frac{\theta}{2} + \frac{\pi q \alpha^2}{4} \frac{\cos^2 \frac{\theta}{2}}{\sin^3 \frac{\theta}{2}} + \text{terms of order } \alpha^4 \right].$$

We shall now return to the ordinary unit of length; our formulæ are most conveniently expressed in terms of v , the velocity of the electron, defined by (18). We have then

$$|f|^2 + |g|^2 = \frac{Z^2 e^4}{4m^2 v^4} \left(1 - \frac{v^2}{c^2} \right) \left[\operatorname{cosec}^4 \frac{\theta}{2} - \frac{v^2}{c^2} \operatorname{cosec}^2 \frac{\theta}{2} + \frac{v}{c} \pi \frac{2\pi Z e^2}{hc} \frac{\cos^2 \frac{\theta}{2}}{\sin^3 \frac{\theta}{2}} + \text{terms of order } \alpha^2 \right], \quad (25)$$

and

$$fg^* - f^*g = \frac{Z^2 e^4}{4m^2 v^4} \left(1 - \frac{v^2}{c^2} \right)^{3/2} \frac{v}{c} 4i\alpha \operatorname{cosec} \theta \log \operatorname{cosec} \frac{\theta}{2}. \quad (26)$$

The formulæ (25) and (26) determine the total scattering and the polarisation of the scattered beam. They are, of course, calculated with neglect of radiative

† We use the formulæ

$$\sum_0^\infty \frac{P_k(\cos \theta)}{k+1} = \int_0^1 \frac{dx}{\sqrt{1-2x \cos \theta + x^2}} = \log \left(1 + \operatorname{cosec} \frac{\theta}{2} \right)$$

$$\sum_1^\infty \frac{P_k(\cos \theta)}{k} = \int_0^1 \left(\frac{1}{x \sqrt{1-2x \cos \theta + x^2}} - \frac{1}{x} \right) dx = \log \frac{\operatorname{cosec}^2 \frac{\theta}{2}}{1 + \operatorname{cosec} \frac{\theta}{2}}.$$

forces, which, for fast electrons, is a serious matter. An electron deflected through 90° by a nucleus of charge Ze would, on the classical theory, lose an amount of energy equal to *

$$\frac{1}{Z} \frac{4}{3} (2\pi + 3) \frac{1}{2} m v^2 \frac{v^3}{c^3}.$$

This formula is calculated with neglect of relativity, but it shows that for light nuclei, an electron with a velocity approaching that of light is acted on by forces comparable with the electrostatic field of the nucleus. For heavy nuclei, however, the radiative forces are less important, but for heavy nuclei our approximations are less good—though there would be no difficulty in pushing them to any degree of accuracy required. The author hopes, in a later paper, to consider in greater detail the effect of radiative forces on the scattering.

From (25) and (26) we can see the order of magnitude of the effect that may be expected in the double scattering experiment considered in Section 2. In equation (10), we suppose that both θ_1 and θ_2 are 90° ; then we have approximately

$$\delta = 11.2 \times \frac{(1 - v^2/c^2) v^2/c^2}{2 - v^2/c^2} \alpha^2,$$

δ has a maximum when $v/c = 0.764$ so there is an optimum value of the velocity of the incident electrons. With this value of v/c we have

$$\delta = (Z/96)^2,$$

Z being the atomic number of scattering nucleus.

For light elements, therefore, the effect is very small, and, indeed, may not exist, since the radiative forces are so considerable. For heavy elements, however, the effect of the radiative forces falls off inversely as the atomic number, whereas the polarisation effect increases with Z^2 , and so it seems certain that the Dirac theory of the electron does predict a polarisation on collision. Whether the effect could be observed experimentally is more doubtful; the K electrons of heavy atoms have themselves velocities of the order of $0.7c$, and would interfere with the nuclear scattering.

The proportion of an unpolarised beam scattered in a given solid angle is given by (9), so that for the scattering of fast electrons (25) is to replace Rutherford's formula $Z^2 e^4 / 4m^2 v^2 \csc^4 \frac{\theta}{2}$. Our formula bears no resemblance

* Kramers, 'Phil. Mag.', vol. 46, p. 845 (1923).

to Darwin's* classical relativity correction; this is not surprising in view of the fact that we are dealing with a case where the wave-length is long compared to the classical distance of closest approach. There is therefore no possibility of forming a wave packet that must follow the classical orbit.

Nothing occurs in the wave mechanics at all analogous to the spiral orbits of the classical theory.

The formula does not agree very well with the available experimental evidence, giving in all cases too little scattering. Chadwick and Mercier, for instance, have investigated the scattering of β particles from Ra C by aluminium. At angles from 10° – 20° our formula gives $2/3$ of the observed scattering. It is possible that the radiative forces may be sufficient to account for this divergence. Without a fuller investigation nothing can be said on this point.

In conclusion, the author would like to express his thanks to Prof. Niels Bohr for the opportunity to work at his Institute, and for constant help and discussion.

Summary.

The scattering of a beam of fast electrons by an atomic nucleus is investigated, using the wave equation of Dirac. A scattering formula is obtained, and it is found that the scattered beam is polarised. A method by which this polarisation could be detected is discussed.

APPENDIX.

Suppose we wish to observe the spin of a free electron directly, with a magnetometer. We will suppose the electron to be at a distance R from the magnetometer, so that the order of magnitude of the magnetic field due to the spin is

$$\frac{eh}{mc} \cdot \frac{1}{R^3}. \quad (1)$$

Now, there may also be a magnetic field due to the motion of the electron; the order of magnitude of this field is

$$\frac{ev}{c} \cdot \frac{1}{R^2}. \quad (2)$$

Now, by the Uncertainty Principle, R and v cannot both be known at the same time; if ΔR , Δv are the uncertainties in our knowledge of R and v , then

$$\Delta R \cdot \Delta v > h/m. \quad (3)$$

* C. G. Darwin, 'Phil. Mag.' vol. 25, p. 201 (1925).

Now, in order that (1), the effect of the spin, shall be observable, it must be greater than the uncertainty in (2). That is to say

$$\frac{h}{m} \cdot \frac{1}{R} > \Delta v.$$

Hence from (3)

$$\Delta R > R.$$

The experiment will therefore be impossible, since the uncertainty in the position of the electron would have to be greater than the distance of the electron from the magnetometer; the uncertainty in (1) would be greater than the field (1) that we want to measure.

Stern Gerlach Experiment.—A beam of electrons travels along the z axis with velocity v_z in an unhomogeneous magnetic field \mathbf{H} . We shall suppose that H_z is everywhere zero, and that in the plane Oyz H_x is also zero. The force on the electron magnets tending to split the beam is

$$\frac{eh}{mc} \frac{\partial H_y}{\partial y},$$

and in the plane Oyz this is the only force in y direction. However, the beam must be of finite breadth, and since

$$\frac{\partial H_y}{\partial y} = - \frac{\partial H_x}{\partial x}, \quad (2)$$

it is clear that H_x is only zero in the plane Oyz . In general

$$\begin{aligned} H_x &= \int_0^x \frac{\partial H_x}{\partial x} dx \\ &= \int_0^x \frac{\partial H_y}{\partial y} dx. \end{aligned} \quad \text{by (2)}$$

Electrons, therefore, travelling at a distance Δx from the plane Oyz will be subject to a force

$$\frac{ev_z H_x}{c} \quad (3)$$

in the direction Oy due to their motion through the field, and we see that (3) is equal to

$$\frac{ev_z}{c} \frac{\partial H_y}{\partial y} \Delta x. \quad (4)$$

This force is in different directions according as Δx is positive or negative,

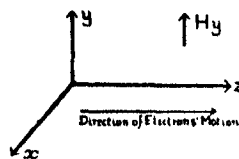


FIG. 2.

and will therefore cause a spreading of the beam, which will mask the Stern-Gerlach splitting, unless (4) is less than (1), *i.e.*, unless

$$mv_x \Delta x < h. \quad (5)$$

Now the uncertainty principle states that

$$\Delta v_x \cdot m \Delta x \sim h. \quad (6)$$

That is to say, that the slit that we use to limit our beam to the dimensions of Δx will introduce an uncertainty in the velocity Δv_x , given by (6). Inequality (5) therefore leads to the inequality

$$\Delta v_x > v_x.$$

That is to say, the slit must be so narrow (of the order of the de Broglie wavelength) that we have not got a beam at all, but a cylindrical wave emerging from it.

Infra-Red Investigations of Molecular Structure.—Part I.*
Apparatus and Technique.

By C. P. SNOW (Keddey Fletcher-Warr Student) and A. M. TAYLOR
(Ramsay Memorial Research Fellow).

(Communicated by T. M. Lowry, F.R.S.—Received March 14, 1929.)

In what is by far the most exhaustive description of practical work in the infra-red, Robertson and Fox† have deplored the lack of detail given in most

* It is the aim of this series of papers to extend knowledge of the structure of molecules by work in the infra-red. There are three obvious lines of development. The first is the study of the spectra of diatomic gases and the deductions which follow according to the classical quantum theory; this has already been done with success by Imes (Sleator, 'Astrophys. J.', vol. 48, p. 125 (1918); Imes, *ibid.*, vol. 50, p. 251 (1919)) for the hydrogen halides. Comparisons will be made of the molecular constants from the infra-red bands with those obtained from electronic band spectra.

As a second development there is the use of the infra-red results in the light of the newer quantum theory. Dennison's prediction ('Phys. Rev.', vol. 31, p. 503 (1928)) of the shape of absorption bands needs confirmation by experiment; and, if absolute intensities of absorption bands can be measured, the wave-mechanics is ready with an interpretation. Thirdly, the problems offered by triatomic molecules will be attempted.

—E. K. Rideal, C. P. Snow, F. I. G. Rawlins, A. M. Taylor.

† 'Roy. Soc. Proc.,' A, vol. 120, p. 128 (1928).

papers on the subject. Their work has removed most of the uncertainty which hinders such researches as this; but since they do not discuss the use of gratings, and since we have found by experience that it is impossible to make a technique too clear, it has seemed desirable that the construction and use of an instrument should be described.

The objects of the investigation determined the type of instrument to be made. It was to be designed to give dispersion and resolution sufficient to analyse a fine structure with a frequency difference of one or two wave numbers; it was to be efficient from $2\ \mu$ to $6\ \mu$ and it was to be used for the determination of absolute coefficients of absorption.

There were the alternatives of a grating or a prism instrument. The dispersion of a prism is given by

$$\frac{d\theta}{d\lambda} = 2 \frac{d\mu}{d\lambda} \sec \frac{1}{2} (A + \theta).$$

For rock salt with an angle A of 60° the quantity is of the numerical order of 100. For a reflection grating used at angles of incidence and diffraction both equal to θ

$$\frac{d\theta}{d\lambda} = \frac{n}{2a} \sec \theta = \frac{n}{\sqrt{4a^2 - \lambda^2 n^2}} \quad \left(\sin \theta = \frac{n\lambda}{2a} \right)$$

where n is the order of the spectrum and a the grating constant. If a is $1/945$ cm. and $n = 1$, $d\theta/d\lambda$ is of the order of 500. Accordingly, we were led to the choice of a grating spectrometer similar to that used by Sleator and Imes (*loc. cit.*) but modified in plan in order to give greater spectral intensity. This was made necessary by the small separations in the fine structure with which we planned to deal. Small separations make necessary narrow spectrometer slits, and hence for reasonably large deflections of the galvanometer great intensity of the spectral image is essential.

The Optical System.

The use of a combination of a grating and a rock salt prism in series depends upon the selection by the prism of radiation consisting of a band of frequencies less than one octave in length, and the analysis of this band by the grating. The first order spectrum is convenient. The rock salt prism is of the nature of a filter, and need only be of large enough dispersion to restrict the band within the limits of an octave. Like Sleator and Imes, we used an 18° prism backed by a plane silver mirror. The effective angle is of course doubled.

The method of using prism and grating in order to obtain the shortest air path is shown in fig. 1.

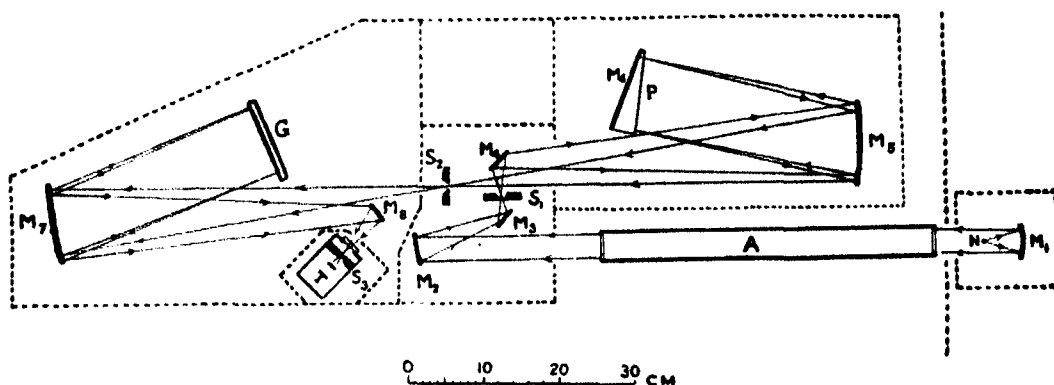


FIG. 1.—Scale Plan of Apparatus.

- | | |
|--|---|
| N = Source (Nernst glower). | $s_1 s_2 s_3$ = slits. |
| A = Gas absorption tubes. | P = Rock-salt prism. |
| M ₁ M ₂ M ₅ M ₇ = Concave mirrors. | G = Grating. |
| M ₃ M ₄ M ₆ M ₈ = Plane mirrors. | T = Thermopile. |
| Position of screens shown thus - - - - - | Path of rays shown thus \longleftrightarrow |

The Base Plate.

The apparatus was set up on a plane slab of slate, 180 cm. \times 76 cm., which was supported on brick piers built directly into the earth. Each part of the spectrometer was mounted on a stand with the appropriate motions, in every case with an adjustment for height. The greatest care was taken that the centre of each mirror was at exactly the same height, and that the axis of the mirror (whether plane or concave) was accurately horizontal. If these precautions were not exactly observed the images of the slit were found to be slanted, and it was impossible to obtain a pure spectrum. When the optical system was in adjustment the stands were securely waxed down to the slate slab.

The Source of Radiation.

The source of radiation was a Nernst glower N, run off a 220-volt constant supply battery; a 100-volt lamp, an iron wire resistance lamp, and a small rheostat were used in series. The current was read by an ammeter, and was maintained constant throughout any series of readings. It was usually about 0.8 amperes.

In order to have parallel rays through the tubes we made use of a device

mentioned by Robertson and Fox (*loc. cit.*). The Nernst filament was placed at the principal focus of a concave mirror M_1 of 5 cm. focal length and 3 cm. aperture. The mirror was of glass, silvered and polished on the front surface, and held in a circular mount by a small wire spring. This holder was adjustable in any direction by means of three screws at the back. The Nernst glower had vertical and horizontal movements so that its middle point could be accurately brought to the principal focus of M_1 . The whole system had a mounting which permitted of rotation about a vertical axis.

The Absorption of the Radiation.

The parallel beam of radiation so produced was directed axially through the gas absorption tubes, which were 45 cm. long and which had rock salt end plates of 2.5 cm. aperture. The gas tubes were mounted on a rotating holder, so that first one and then the other tube could be put in the path of the beam. The radiation energy from the gas tubes was collected by a second concave mirror M_2 of 15 cm. focal length and directed into the first slit S_1 off a small plane mirror M_3 .

In setting this up there were three essentials. The angles of incidence and reflection had to be small in order to minimise the astigmatism of the image produced at S_1 . The focal length of M_2 had to be short enough to enable the radiation diverging from the slit S_1 to fill the large mirror M_5 . The diameter of the end plates of the gas tubes was 2.5 cm. The diameter of M_5 was 10 cm., and its focal length 52.5 cm. Consideration of vertically opposite angles showed that the focal length of M_2 had to be about 15 cm. The third requirement was the filling of the whole length of the slit S_1 by the image, in order to get the maximum amount of energy into the spectrometer. This meant that rays proceeding from opposite ends of the Nernst glower, after crossing each other at the mid-point of the tubes, must fall upon the edge of the mirror M_2 and be reflected on to the ends of the slit. The aperture of M_2 must be at least great enough, therefore, to deal with the cone of radiation AOB in fig. 2. This necessitates a mirror of 5.0 cm. aperture.

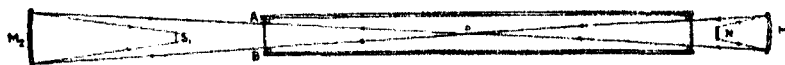


FIG. 2.

The Selection of the Required Portion of the Spectrum.

The mirror M_5 was so placed as to be at a distance equal to its focal length from the image of S_1 in M_4 . The height of the pole of M_5 was made the same

as the standard height of the centres of the other members of the optical system, and the axis was made horizontal. When the slit S_2 had been set at the standard height, the prism, backed with a plane silvered mirror M_5 and with its mid-point similarly set to the same height, was placed in the path of the parallel beam from M_5 . It was rotated about horizontal and vertical axes until the spectrum formed was accurately focussed upon the slit S_1 . The prism was then removed, and the white light from the mirror M_5 was made to pass between M_4 and S_1 by slight rotation of the prism table.

The second slit S_2 was placed at the sharply focussed image of S_1 and was set to the standard height. If all the adjustments were accurately made the image of S_1 falling upon S_2 was truly vertical.

The prism was gripped upon a brass plate having three legs which registered with three grooves cut in the face of a plane horizontal turntable. The brass plate bore an upright carrying a small mirror, the mirror was centred over the centre of rotation of the turntable. By means of a telescope and illuminated scale, this mirror could be used for determining the rotation of the prism. The prism was 12 cm. \times 11.5 cm., had an angle of 18° , and was 5 mm. thick at the thin edge.

It may be noted that the position of the second slit S_2 is somewhat unusual, for the radiation crosses its own path. This arrangement enables the angles of incidence and reflection at the mirrors M_5 and M_6 to be as small as possible, and minimises astigmatism of the image.

The Analysis of the Radiation.

The mirror M_7 was a duplicate of M_5 , was similarly adjusted, and was placed so as to be filled by radiation proceeding from the latter through the slit S_2 . S_2 was itself at the principal focus of both mirrors. The beam, which was made parallel after reflection from M_7 , was allowed to fall upon the grating G. The angle GM_7S_2 was as small as possible to minimise astigmatism.

The grating was held in a frame which had three levelling screws (with locking nuts) which registered with three radial grooves cut in the face of a horizontal turntable. The turntable was provided with verniers which travelled upon a graduated circle, the plane of which was accurately parallel to the face of the turntable.

The circle was of brass, graduated on an inlaid band of gold, and by its use the rotation of the table could be read to 10 seconds of arc with an error of less than 5 seconds. A fine adjustment screw was provided for rotating the table.

The grating was ruled on a gold blank welded to a brass block 10 cm. \times 10 cm. \times 1 cm. The number of lines to the centimetre was 945. It was ruled by the N.P.L. with a special form of tool to give maximum intensity at angles of diffraction which correspond to wave-lengths 2.7 μ and 4.4 μ .

In setting up the grating the first care was to arrange its centre at the standard height. The next was to alter the levelling screws of the turntable until an accurate level gauge showed it to be horizontal. This ensured that the axis of rotation was vertical.

The grating frame had three levelling screws; the heads of two lay on a line parallel to the grating. The next step was to set these screws in such a way that the lines of ruling were truly vertical. Finally, by the use of the third levelling screw, the grating was set perpendicular to the incident radiation coming from M_7 . When this had been done, the beam was reflected back along its own path and the geometrical image of the slit S_2 was sharply focussed on the slit itself. The small mirror M_8 was placed with its axis of rotation vertical, and it was arranged so that radiation falling on it from the grating was reflected into the thermopile slit S_3 . To make the geometrical image of the slit S_2 to fall upon S_3 , the grating had to be rotated through a small angle ϕ . By further rotation the spectral images could be made to pass in succession over the slit S_3 . The thermopile T was carried on a slotted arm in order that the slit could be placed at the sharpest focus of the image of S_2 .

Detection and Measurement of Intensity of the Spectral Image.

The thermopile T was a Moll linear pile mounted in a brass container with polished rock salt window; the leads were taken through ebonite plugs and the vessel was absolutely airtight. It was necessary to work the pile in an airtight casing in order to eliminate unsteadiness due to minute changes of pressure in the atmosphere. As these changes are adiabatic, they cause unequal heating and cooling of the two sets of thermo-junctions.* Measurement showed that an increase of sensitivity of only 20 per cent. was obtained by evacuation of the thermopile container. In view of the extra complication involved in having a vacuum pump always connected to the vessel, it was not considered advisable to utilise this increase. The pile was worked at atmospheric pressure.

The thermopile had a resistance of 20 ohms and was in series with a Super-Paschen galvanometer made by the Cambridge Instrument Company. This had a figure of merit of 25000, a resistance of 12 ohms, and at a period of swing

* Taylor, 'Nature,' vol. 117, p. 892 (1926).

of 10 seconds a current sensitivity of 1 mm. deflection at 1 metre scale distance for a current of 2×10^{-11} amperes. The relation between current and deflection was for reasonable deflections approximately linear.

The magnetic shielding of the galvanometer was by a closed Mu-metal cylinder, and a surrounding soft iron sheath also closed top and bottom. The shielding was tolerably efficient. The magnetic system was controlled by two small magnets mounted inside the shield and adjusted from outside by two milled wheels. The galvanometer had to be protected from mechanical disturbance; after trial of many different methods, the one finally adopted was of the crudest, but it has proved nevertheless most effective. A wooden shelf was screwed to iron brackets fixed into the corner formed between two solid brick walls which were virtually the main structural walls of the building. The galvanometer was placed directly upon this shelf and it was found that, when the period of swing of the suspended magnetic system was long, the mechanical disturbances were inappreciable. The galvanometer was surrounded by thick layers of cotton wool in order to minimise drifting of the zero caused by temperature variations of the controlling magnets.

Despite precautions, all accurate work had to be done at night or, at the best, after the University Electrical Power Station, which was only 20 yards distant from the apparatus, had closed down for the evening. No particular care was taken with the leads from the thermopile and galvanometer, however, save that copper terminals were used. A single piece of ordinary double wire, multistrand copper, silk covered electric lighting flex was used. No thermoelectric effects were observed to arise either in the flex or the terminals.

Thermal Shielding.

The whole spectrometer was enclosed in shields made of galvanised sheet iron; the system of shields made a complete case. The Nernst glower was enclosed in a small case of asbestos board; a large shield of asbestos, with a hole for the transmission of the parallel beam from M_1 , separated the Nernst glower case from the spectrometer case. The spectrometer was further divided into parts by internal walls of sheet iron. The rock salt prism and mirror M_5 was in one part, the grating and mirror M_7 was in another; the arrangement of mirrors M_2 , M_3 , M_4 and the two slits S_1 and S_2 were in a third, and the thermopile contained was in a separate sheet iron case which was packed with cotton wool. Holes for transmission of the radiation were of the smallest possible size in order to cut out all stray radiation effects. Fig. 1 gives a sketch of the shields.

The Experimental Procedure.

The Prism.—The first step was to calibrate the prism. The angle was 18° and as the ray traversed the prism twice the effective angle was 36° . The total effective deviation was twice the angle made by the incident beam with the back surface of the prism. The change in effective deviation was equal to twice the angle through which the prism was turned. From the formula for minimum deviation, $\mu = \sin A + D/2/\sin \frac{1}{2}A$, the deviation corresponding to any value of μ could be found. With μ plotted as a function of the wave-length λ from the tables of Coblentz,* it was possible to calculate the change in deviation, and hence the angle through which it was necessary to turn the prism in order to pass from the yellow light of sodium $\lambda = 0.589 \mu$ to any other wave-length. For example, when the prism was set so that the slit S_2 was illuminated by yellow light, and was then further rotated through $31'$ of arc, the slit was then filled with radiation of which the mean wave-length was 5.3μ . Actually the dispersion was so small that quite a large range of wave-length was thrown upon the slit S_2 . This was a great advantage. It was not necessary to re-set the prism frequently during progress along the spectrum, and no errors were introduced by rapid variations of intensity with wave-length of the radiation transmitted through S_2 . A variation of this kind would have been brought about if the slit had been filled with radiation of a narrow band of wave-length.

The Grating.

From the method the grating equation was

$$a \{ \sin \theta + \sin (\theta + 2\phi) \} = n\lambda,$$

where n is the order of the spectrum, λ the wave-length of the radiation, a the grating constant, θ the angle of incidence and $(\theta + 2\phi)$ the angle of diffraction. Rewritten, this becomes

$$2a \sin (\theta + \phi) \cos \phi = n\lambda,$$

2ϕ is the angle between the incident and diffracted beams, and is found by setting the grating so that the reflected geometrical image fell upon the slit S_2 , and by measuring the angle through which the grating had to be turned in order to cause the image to fall up the thermopile slit S_3 . This angle is ϕ , and was found to be $23' 40''$, so that $\cos \phi = 0.99998$ and could be neglected.

The equation then became for the first order spectrum

$$\lambda = 2a \sin \alpha$$

* 'Dict. Applied Physics,' vol. 4, p. 136 (1923).

where $\alpha = \theta + \phi$. Here α is the angle through which the grating has been turned in order to cause, firstly, the geometrical image, and, secondly, the diffracted image to fall upon the thermopile slit S_3 . The zero position when the geometrical image fell upon S_3 was determined visually; and this was checked by plotting galvanometer deflections in the infra-red region of the spectrum, and by taking the zero point as the position of maximum deflection. The results agreed within 5 seconds of arc. As a second check the position of maximum absorption of CO_2 in the atmosphere was measured and found to agree with that found by E. F. Barker* at 4.23μ (the doublet is unsymmetrical and has its centre at 4.25μ).

The Gas Tubes.

The gas tubes were tested carefully for equality of transmission in the spectral region in which work was to be done. When the rock-salt end plates were well polished (upon an almost dry pitch-plate slightly rough) and with accurate centring of the axes of the tubes along the path of the parallel beam, no difficulty was experienced in obtaining exact equality of transmission of both tubes in the region $4.3\text{--}6 \mu$. Of course, it was necessary to ensure that each of the tubes occupied identical positions in the path of the radiation, and that they returned accurately to this position.

The tubes were vacuum tight; the rock salt plates were held in contact by screw caps with rubber rings carried in grooved recesses at the ends of the tubes. The tube to be filled with the gas under examination was evacuated and washed out three or four times with dry nitrogen before the gas was admitted. After the tube had been again evacuated the gas was admitted slowly, and the tube again evacuated. This was repeated twice, and finally the gas was reduced to a suitable pressure, usually less than 10 cm. of mercury.† The gases were dried with phosphoric oxide before admission.

Observations.

With sufficiently narrow slits the galvanometer deflections usually obtained were of the order of 10 to 40 mm. Readings were taken, the radiation passing through each gas tube alternately, until a constant value for I_t/I_0 , the ratio of the transmitted intensity to incident intensity, was obtained. So great a number of readings was always taken that deviations from the mean could

* 'Astrophys. J.,' vol. 55, p. 391 (1908).

† It has been found that, with strongly absorbing gases, sharp fine structure bands are obtained at a pressure of 7–15 cm. The optimum percentage absorption is 20–50 per cent.

be discarded, and only those results used which were concordant. This method, though very laborious, reduced experimental error to a minimum. The angular settings of the grating were converted into wave numbers, and the percentage absorption was plotted against the wave number. The fact that the curves so obtained (see Part II of the paper) were not in any way smoothed out, but show the actual experimental results untouched, is a good criterion of the accuracy of the technique. It must be remembered that most other curves shown for absorption measurements are subjected to idealisation in the preparation of the illustrations. Such idealisation is unnecessary in the case of measurements with an apparatus sufficiently accurate for the work.

The reproducibility of the observations was particularly remarkable. It was usually impossible to detect any break in the curves between readings on successive nights, the value for the measured absorption at any point being quite independent of external factors. The temperature of the room was sufficiently constant to make unnecessary any correction of the grating-constant with temperature. It is fair to interpret the results obtained with the apparatus as giving a measure of the absolute coefficients of absorption. The curves shown in Part II are, however, drawn without correction for slit width.

The most important detail of all was that concerning density of points of observation and the slit widths. The slits S_2 and S_3 were kept equal, and their width had to be calculated. The angular size of the slit is measured by the fraction, width of slit/length of optical path from the grating. Half the angle is then the angle through which it is necessary to turn the grating in order that the diffracted image shall be displaced through a distance equal to 1 slit width. Half this angle therefore substituted in the formula for dispersion of a grating $d\theta/d\lambda = n/\sqrt{4a^2 - n^2\lambda^2}$ gives the minimum wave-length separation of two sharp lines which should theoretically be capable of resolution by the instrument.

The angular width of the slits (whose mechanical width was 0.3–0.4 mm.) used in Part II of this paper was about 0.0005 radian or about 100 seconds of arc. The wave-length was about 5.3 μ , so the minimum distance between two lines in the fine structure which could have been resolved was $d\lambda = 0.005 \mu$ or 1.7 wave numbers. This is then the actual width of the slit. The broadening of the spectral image due to diffraction has been neglected. For infinitely narrow slits the broadening of a sharp line is given by $d\lambda = 2\lambda/Nn$, where N is the total number of lines in the grating and n the order of the spectrum. As $N = 7560$, then for $n = 1$ the broadening is of the order of 0.0014 μ or 0.50 wave numbers. This increases the effective slit width to 0.0064 μ or 2.2 wave numbers, with a corresponding increase of the limit of resolution in

this region of the spectrum. As the angular range through which the grating must be turned in order to displace the spectral image by a distance equal to a slit width is half the angular size of the slit, this sets a limit to the useful density of points of observation. Four or at most six readings per slit width is the maximum. In the experiments to be described in Part II the angular size of the slit was 100 seconds of arc and readings were taken every 10 seconds of rotation of the grating. That is to say, five readings were taken per slit width.

Reduction of slit width to this size meant reducing the galvanometer deflection to 20 mm. at most in the region of 5.3μ , and it was only by the exercise of scrupulous care that the necessary accuracy has been achieved.

In the diatomic molecules resolved before this, the separations have been of the order of $10\text{--}20 \text{ cm.}^{-1}$. With the instrument described the wave-number separation of the fine structure of the NO band at 5.3μ has been measured and found to be 3.35 cm.^{-1} , 0.05 cm.^{-1} error. With this work the second part of the paper has to deal. One wave-number is probably the smallest separation which could be resolved by the spectrometer in its present form.

Since the writing of the second part, one of us (C.P.S.) has begun measurement of the band of carbon monoxide at 4.66μ . A fine structure has been revealed. This is gratifying when it is remembered that E. F. Lowry* was unable to find any trace of structure in the band, a result contrary to all theoretical expectations. This point is referred to in the introduction to Part II; the work on carbon monoxide will form Part III of the series.

This paper would not be complete without a number of acknowledgments. We owe much to Mr. F. I. G. Rawlins, whose knowledge of the literature of the subject has been a great help; to Sir Robert Robertson, for encouragement and advice; to the Imperial Chemical Industries, who have provided much of the money necessary for the apparatus; to the Ramsay Memorial Research Trust and the Keddey Fletcher-Warr Studentship Board, who have made it possible for us to carry out the work. Finally, we are glad to pay a special tribute to Dr. E. K. Rideal, for his vision, unfailing interest and encouragement.

* 'J. Opt. Sci. Ann.,' vol. 8, p. 647 (1924).

Infra-Red Investigations of Molecular Structure. Part II.—The Molecule of Nitric Oxide.

By C. P. SNOW (Keddey Fletcher-Warr Student), F. I. G. RAWLINS, and
E. K. RIDEAL.

(Communicated by T. M. Lowry, F.R.S.—Received March 10, 1929.)

Introduction.

There have been few attempts at the resolution of the vibration-rotation bands of a diatomic molecule. In 1919 Imes was successful with the bands of three of the hydrogen halides, work which was later extended by Colby and Meyer; Czerny proved the existence of a doublet due to HI, but the weakness of the absorption prevented more detailed study; E. F. Lowry in 1924 failed to analyse the structureless doublets of carbon monoxide, although his apparatus was similar to that used by Imes.* It does not seem possible that the carbon monoxide bands are really continuous, and it is suggested that the fine-structure would reveal itself if a lower pressure of the gas were used† (E. F. Lowry worked at one atmosphere pressure). The molecule of CO, like those of the hydrogen halides, has a permanent electric moment, and its bands must be similar in kind.

Apart from HF, HCl, HBr, HI and CO, NO is the only other diatomic molecule with a permanent electric moment, and its choice as the subject of this research was natural. It is more definitely homopolar than the hydrogen halides, although the distinction is almost certainly one of degree; there was the interest of establishing the self-evident proposition that there is no fundamental difference in the bands of NO and the bands of HCl. There was also the advantage of knowledge of the electronic band spectrum of the molecule acquired by Guillery, Jenkins, Barton and Mulliken, and summarised by Mulliken.‡ The thoroughness of this work makes NO one of the best-known of molecules to the spectroscopist. It has been mentioned in the introduction

* Imes, 'Astrophys. J.,' vol. 50, p. 251 (1919); Colby and Meyer, *ibid.*, vol. 53, p. 300 (1921); Czerny, 'Z. Physik,' vol. 44, p. 235 (1927); Lowry, 'J. Opt. Sci. Am.,' vol. 8, p. 647 (1924).

† Indications of the fine-structure of the band at $4.66\ \mu$ have now been obtained. It is hoped to publish this work shortly.

‡ Guillery, 'Z. Physik,' vol. 42, p. 121 (1927); Jenkins, Barton and Mulliken, 'Phys. Rev.,' vol. 30, p. 180 (1927); Mulliken, 'Phys. Rev.,' vol. 32, pp. 186, 761 (1928).

to Part I that throughout this series of papers there will be maintained the deal of correlation between infra-red and electronic band spectra. Accordingly, it became our aim to compare the constants of the molecule in the normal state as derived from electronic band spectra and as obtained from the direct measurements of the infra-red. The unexcited electronic state of the molecule is, of course, the only one with which infra-red observations are concerned.

Another reason lay in a peculiarity of the molecule itself. It is the only common diatomic molecule which has an odd number of electrons. This made it probable that it would be the most favourable, if not the only, case for the detection of a gyroscopic motion in a diatomic molecule. The full argument is developed later, and here it is enough to say that a Q branch was predicted and observed.

History.

There has been one study before this of the infra-red spectrum of nitric oxide. In 1908, Warburg and Leithauser* gave the coarse structure of the bands of four oxides of nitrogen. They plotted one band due to NO, with its centre at 5.302μ , and resolved it into a structureless doublet. The value of this knowledge as a guide was considerable, and we have been able to confirm the main features of their outline.

Experimental.

The general methods for the use of the instruments have already been discussed in Part I, and it remains to describe those details which concern nitric oxide specifically.

Preparation and Storage.

The nitric oxide was prepared from a mixture of saturated solutions of ferrous sulphate and sodium nitrite by acidification with dilute sulphuric acid. It was washed through water and sodium hydrate solution.

The gas was stored over distilled water which had been made air-free by boiling, and was led to the observation tube through a series of tubes filled with phosphoric oxide. The stream of gas was made to pass very slowly.

There was no sign of bands due to nitrogen peroxide or water at any time during the work. The absence of nitrogen peroxide bands, which were carefully looked for, was taken as a proof of the purity of the gas and the adequacy of the vacuum circuit.

* 'Ber. D. Chem. Ges.,' vol. 1, p. 148 (1908).

Observations.

The observations fell naturally into three divisions:—

(1) An exploration of the band found by Warburg and Leithauser. The effective slit-width was fairly wide, and readings were taken every minute of the divided circle. The general outlines of the band were established and conclusive evidence of fine-structure obtained. For this survey, the gas was kept at a pressure of $\frac{1}{4}$ atmosphere.

(2) A general semi-detailed study of the whole band was next achieved. It was found by trial and error that the optimum pressure was $\frac{1}{8}$ atmosphere, and this was used in all subsequent work. At this pressure the percentage of absorption is reasonable (10–40 per cent.) and the bands have their greatest sharpness. Readings were taken at intervals of 30 seconds of arc (corresponding approximately to a reading each wave number).

A satisfactory idea of the fine-structure was obtained, but the separation is so small that many of the bands were misshapen, and some appeared to be missing.

(3) From (2) it was clear that it was necessary to narrow the slits so much that readings could profitably be taken every 10 seconds of arc. This meant a mechanical slit-width of 0.3–0.4 mm. The unavoidable reduction in intensity was met by working at night with the galvanometer at its maximum useful sensibility.

The whole central portion of the band was mapped in the course of this refined analysis.

Graphs corresponding to stages (2) and (3) show how far it has been found possible to improve the precision of the observations.

Before we began the work described under (1) and again before that under (3), the tubes were carefully compared in order to ensure that relative readings of intensity were not vitiated by inequalities in the rock-salt plates. For (2) a linear correction was needed, but for (3), after repolishing and re-setting of the plates, the tubes transmitted equally.

Accuracy of Reading.

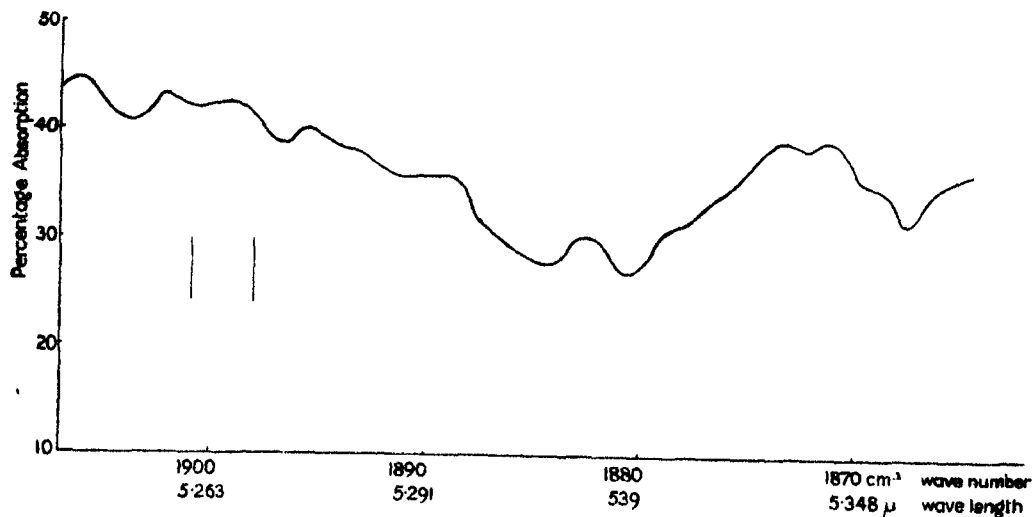
Each reading involves (a) a setting of the circle, and (b) the reading of the galvanometer deflection.

The error in (a) probably amounts to not more than ± 2 seconds of arc, or $\pm 0.0002 \mu$ or ± 0.06 of a wave number. Taken in conjunction with (b), this is practically negligible; the difference in wave-lengths measured are therefore taken as accurate.

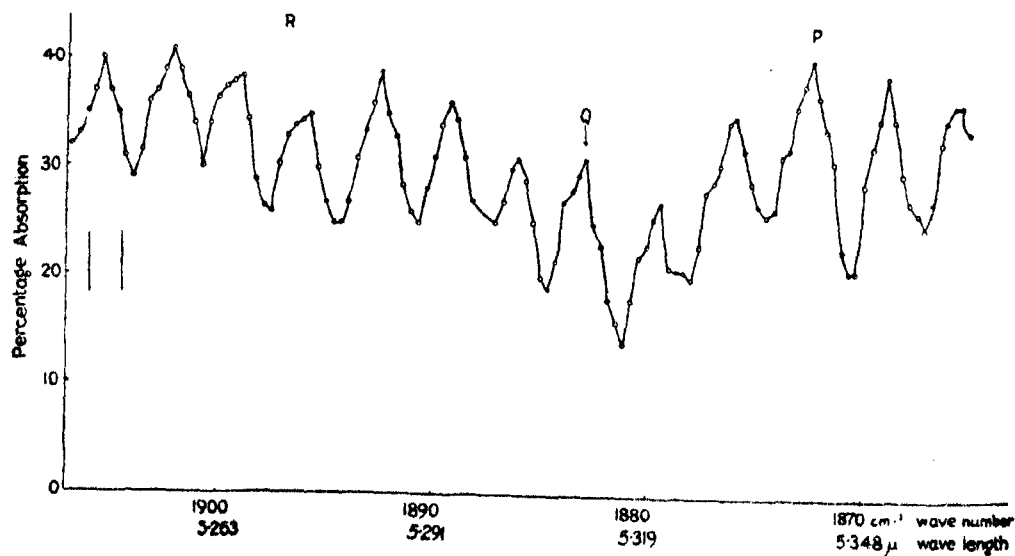
Upon (b) the whole accuracy depends.

During the stage (2), the slit-widths were such as to give galvanometer throws of 40 mm. at 1 metre scale distance. Although it is not claimed that any one deflection was read to greater accuracy than 1.0 mm., yet the taking of a number of throws showed the possibility of making a final judgment to a considerably higher accuracy than this.

On graph (A), [stage (2)], a curve rounded off between the actual observations is given.



Graph A.



Graph B.

For stage (3), it was obvious that small deflections would have to be faced if the slit-widths were to be reduced to less than six times the finest interval between readings. Since stage (2) showed that the fine-structure bands were of the order 3 wave numbers apart, readings at 0.3 wave numbers (*i.e.*, 10 seconds of arc) were a theoretical and practical necessity.

The very narrow slit-width corresponding to this wave number difference brought the deflections down to the order of 16 mm. (at 1 metre scale distance). Working entirely at night, and taking a large number of throws for each observed point (often as many as 8 or 10 for each tube, and repeating until satisfactory constancy was obtained), we were able greatly to reduce the actual error of 0.5 mm. in any one reading. If it is borne in mind that the readings were separated by very small intervals, it will be seen that it was possible to detect changes in the percentage absorption which would have been outside the limit of accuracy for any one point, even though taken with the above precautions. The pragmatic test is the smoothness of the curves [graph B]: these are part of the refined analysis, and represent actual observed points connected by straight lines.

Finally, the following considerations satisfied us of the soundness of the results :—

- (i) A comparison of the curves (A) and (B), which were obtained at an interval of six weeks from each other, shows the chief features preserved unchanged. The coarseness of wave number settings in (A) meant less sharpness and occasionally the missing of a head; but the characteristics of the fine-structure can be recognised.
- (ii) On starting work each night for stage (3), we found almost without exception no difficulty in recapturing the intensity and gradient of the curve under analysis. As the alteration in sensibility of the galvanometer is apt to be appreciable from night to night, this gave a final confidence.
- (iii) The constancy of wave number separation of the band heads (see below) in both R and P branches was remarkable.

We give a small specimen table of actual readings obtained in the course of stage (3).

Circle reading.	Air tube (mm. throw).	Gas tube (mm. throw).	Percentage transmission.	Notes.
182 50 10	13.5 (5 throws)	8.6 (average of 8)	64	These readings are towards higher wave-lengths, and the deflection tends to get smaller.
20	13.5 (4 throws)	8.25 (average of 8)	61	
30	13.5 (7 throws)	8.0 (5 identical throws)	59	
182 50 40	13.5 (3 throws)	8.5 (3 throws)	63	The large number of air throws was made necessary by an anomalous one which was at length discarded.
50	13.5 (4 throws)	8.75 (average of 8)	66	
51 0	17.0 (7 throws)	11.75 (average of 8)	69	Air deflection was so constant that 3 good throws established it. Great care necessary to obtain head of band.
10	12.75 (average of 8)	9.75 (average of 8)	77	
20	12.75 (average of 8)	9.9 (average of 10)	79	
30	12.75 (average of 6)	9.9 (average of 8)	79	Sensibility of galvanometer altered. Good readings but period so slow that the night's work was finished on the lowered sensibility shown in the next three points.
				The drop is sudden, and the galvanometer changes make it sharper than is really the case.
				—
				The flattening after the sudden drop is noteworthy.

Results.

There are 42 bands on each side of the Q branch. Intensity of absorption is so small beyond about the 30th member that it was not profitable to explore further. There is a definite Q branch with its head at the wave number 1882.9. The wave number separations of the six bands on each side of this were averaged as below in order to obtain values for the molecular constants.

R.	cm. ⁻¹ .	P.	cm. ⁻¹ .	Average.
*Q → 1	3.15	*Q → 1'	3.50	3.32
1 → 2	3.32	1' → 2'	3.50	3.37
2 → 3	3.20	2' → 3'	3.50	3.35
3 → 4	3.25	3' → 4'	3.50	3.37
4 → 5	3.20	4' → 5'	3.45	3.33
5 → 6	3.25	5' → 6'	3.50	3.37
= $\frac{\text{sum of average}}{6} = 3.35$				

* There are irregularities in intensity of absorption near the centre of the band, and these figures have not the accuracy of the other. Further theoretical treatment of the central lines will be given later.

We take the value $\delta\nu = 3.35 \text{ cm.}^{-1}$.

From this it follows that $I = h/4\pi^2\delta\nu = 1.64 \times 10^{-39}$ gm. cm.², where I is the moment of inertia; it is doubtful whether the second place is significant. The inter-nuclear distance $r = 1.15 \times 10^{-8}$.

It may be mentioned that the separations with which stage (3) is concerned are much smaller than those which have previously been resolved in the spectra of diatomic molecules. Consequently, there would have been no justification for an averaging process over the separations of the bands of the P or R branches, for any error—even of our smallest reading (0.3 wave number)—would have made a serious disturbance. The regularity in both branches was so great that the average taken as above was the obvious course.

Electronic Bands of NO.

From the research of M. Guillery (*loc. cit.*) on the γ bands, and Jenkins, Barton and Mulliken on the β bands of nitric oxide, the electronic band spectrum has become among the best known of molecular spectra. The early formal analogy to Al, suggested by Mulliken* at the beginning of his analysis proved the clue to the assignment of the following energy levels:—

X	² P normal
A	² S
B	² P
C	² S
D	—

The state X occurs in all the known bands of NO ($X \leftrightarrow A$, $X \leftrightarrow B$, $X \leftrightarrow C$, $X \leftrightarrow D$), and is consequently regarded as the normal state. It may be represented, according to Mulliken's nomenclature, as:

$$(\text{outer electrons only}) \quad (2s^*)^2 (3s^p)^2 (2p^p)^4 (3s^*)^2 3p^p.$$

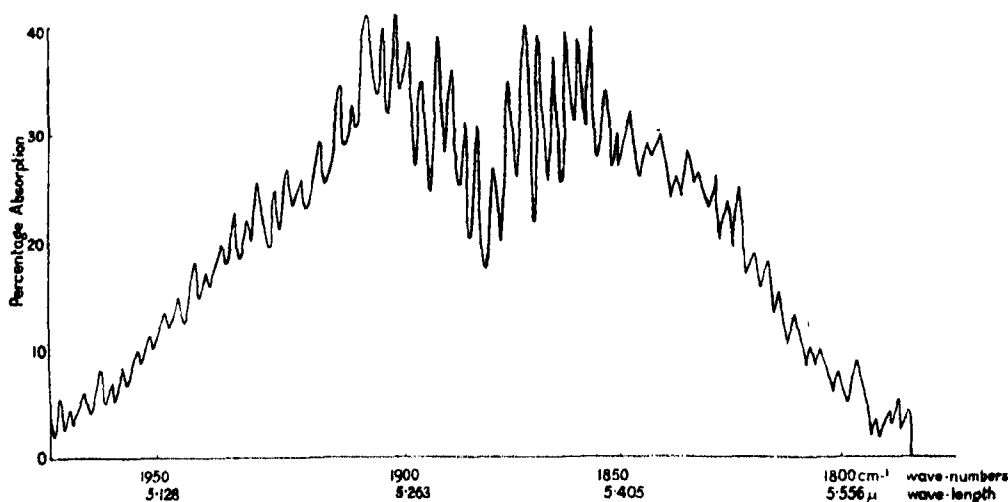
The presence of the $3p^p$ electron with large promotion energy explains the fact that the first excited state has r_0 smaller than in the normal ²P state. All the excited levels correspond to excitations of the $3p^p$ electron. The molecular constants for some of the electronic states, and the corresponding data from the infra-red measurements, are given in the table:—

	Infra-red normal state.	² P R.S.M.	² S (first excited) R.S.M.	² P (second excited) R.S.M.
Vibration frequency	1883	1892	2352	1030
r_0	1.15×10^{-8}	1.15×10^{-8}	1.07×10^{-8}	1.42×10^{-8}
I_0	1.64×10^{-39}	1.63×10^{-39}	—	—

* 'Phys. Rev.', vol. 26, p. 561 (1925).

The agreement with the figures of the normal state derived from the electronic bands is more than satisfactory. The only point of difference is the vibration frequency, and the explanation of this is obvious. The electronic data give a frequency ω_0 which can only apply if the displacements of the nuclei are infinitely small; the infra-red band is caused by an oscillator which is slightly but perceptibly anharmonic, and whose vibration frequency is $\omega_0(1 - x)$ to a first approximation—where x is a small constant.

The molecular constants of the normal state of NO would appear to be established definitely.



THE FUNDAMENTAL OF NO.

The Q branch.

As was mentioned in the introduction to this paper, the molecule of NO stands in a class by itself as the only common diatomic molecule with an odd number of electrons. Many of its uncommon physical properties—its paramagnetism, for instance—are directly due to the odd electron; it has already been mentioned that spectroscopic evidence describes the state of this electron. The presence of a Q branch is another eccentricity imposed by an unshared electron.

For an infra-red band, these are the three possible branches:—

$$R(m) = \nu_0 + f(m+1) - f(m)$$

$$Q(m) = \nu_0 + f(m) - f(m)$$

$$P(m) = \nu_0 + f(m-1) - f(m).$$

The Q branch was noticed first in the methane and ammonia spectra, and was attributed to a gyroscopic motion of the molecule, although Kratzer* pointed out that the condition was not rigid. It can be said that a vector σ (representing an angular momentum) parallel to the nuclear axis, and accordingly perpendicular to the vector m (nuclear rotation), permits the $m \rightarrow m$ transition and the Q branch resulting from it. Now it is well known that odd-electron molecules have a resultant electronic angular momentum which can be represented by a vector σ parallel to the nuclear axis and a vector ϵ perpendicular to it. It is also known that σ is large compared to ϵ . Hence in NO there is the condition for the presence of a Q branch satisfied; and, if any diatomic molecule shows a Q branch, it would be expected to be NO.

[The mechanical picture of the NO molecule is a gyroscope or symmetrical top.† Rotation is no longer in an invariable plane, and should strictly be represented by j , equal to the vector sum of m and σ . Quantisation should then be applied to j and not m . However, the effect is so small as to be experimentally undetectable except in the Q branch and in the suppression of convergence (see later).]

The Q branch is definitely present in the NO band, at 1882.9 cm^{-1} . Compared with known Q branches, it is small (reference should be made to Robertson and Fox,‡ whose work shows the larger Q branches of NH_3 and PH_3). This is expected from the difference in size of the causes. Translating the vector scheme mechanically in order to reach the gyroscopic picture, we may regard the determining cause as an electronic angular momentum about the axis of figure. In NH_3 the cause is almost certainly an angular momentum due to a nuclear rotation, which is of the same order as that responsible for the R and P branches.

From the observed fact that the head of the Q branch falls at wave number 1882.9 , and that Mulliken§ found the vibration frequency of the normal molecule ω_0 at wave number 1892 , it may fairly be concluded that we are dealing in the present work with the fundamental of the NO molecule. This we may represent as the transition $n'' = 0 \rightarrow n' = 1$, where n'' is the initial vibrational state of the molecule and n' the excited, or, according to the new mechanics, $n'' = \frac{1}{2} \rightarrow n' = \frac{3}{2}$.

It was natural, therefore, to search for the overtone, which should fall in the

* 'Naturw.', vol. 11, p. 577 (1923).

† 'Phys. Rev.', vol. 30, p. 31 (1927).

‡ 'Roy. Soc. Proc.', A, vol. 120, p. 128 (1928).

§ 'Phys. Rev.', vol. 30, p. 150 (1927).

region of 2.7μ . No sign of absorption between 2.2μ and 4μ has yet been detected. As the vibration has been shown to be anharmonic, the absence of the overtone is difficult to explain. If it is present, its intensity is smaller than theory requires. On the other hand, the small amount of convergence (see below) also suggests that the potential function of the molecule should be represented by a near approach to that of the harmonic oscillator. It is possible that this apparent simplification would be achieved if the energy state of the molecule were expressed in terms of j instead of m ; the problem is being attacked by a comparison with the behaviour of CO.

Convergence.

A slight convergence has been noticed in the R branch; in it the separation of the bands is 0.3 wave numbers less than the separation in the P branch. The convergence of the bands within the R branch itself is small to the thirtieth member.

Early theory, particularly that due to Kratzer,* introduced a coupling term between the equations describing the rotational and vibrational states, and the treatment was remarkably successful in its description of the HCl bands.

The wave mechanics as already established has not fully described the coupling effect; Sommerfeld† points out that this can be accomplished by the addition of perturbation terms. But Kratzer's theory must hold approximately for an ordinary (1S) diatomic molecule, and it seems to be the odd-electron (2P) character of the NO molecule which is the determining influence.

The contrast between the unsymmetrical hydrogen compounds and the evenly balanced dumb-bell of NO is a marked one. Apart from its gyroscopic abnormality, NO appears the much more rigid rotator.

Alternating Intensities.

Our results show no appreciable alternations of intensity either in the P or R branch, when m is small. This is in accordance with the remarks of Van Vleck‡ on gyroscopic molecules. He points out that a rotation through 360° rather than through 180° is necessary to restore the molecule to a position indistinguishable from that initially assumed, for the motion is not confined to a single plane. This results in the presence of changes of angular momentum by units both of $h/2\pi$ and h/π . An expansion in Fourier series of the second

* 'Z. Physik,' vol. 3, p. 289 (1920).

† 'Atombau und Spektrallinien,' pp. 24 et seq. (1928).

‡ 'Phys. Rev.,' vol. 28, p. 980 (1926).

order term of the energy radiation contains terms in both $2\pi\omega_mt$ and $4\pi\omega_mt$, and of amplitude of the same order for low values of m . Hence there should be no alternation of intensity in the immediate neighbourhood of the Q branch, and this indeed is what is actually observed.

Further out from the centre, corresponding to larger values of m , changes in angular momentum of h/π become more probable, and consequently some indication of alternating intensity might be expected. Our graphs do in fact give a hint of this effect. With increase of temperature, the invariable axis becomes nearly normal to the inter-nuclear axis, and alternating intensities should become now pronounced. Also the Q branch should diminish in intensity. It is hoped to devise a method for investigating these points experimentally, although the alternative is very small and irregular.

It must be remarked that Loomis and Wood* find no evidence of alternating intensities in the electronic band system of Na_2 . In this case the Van Vleck explanation is not adequate; a much more complete theory is now generally accepted, and according to this no alternation in NO would be expected.

Ordinary Intensities.

As the curves of the refined analysis are regarded as a quantitative statement, it is proposed that a theoretical analysis of absolute intensities upon the lines of Dennison and Bourgin† may be conducted by two of the present authors. This should lead to a value of the electric moment of the molecule, as suggested by Schrödinger‡ and others.

Summary.

1. The vibration-rotation band-spectrum of nitric oxide proves to be a fundamental, with its centre at 1882.9 cm.^{-1} , $n'' = \frac{1}{2} \rightarrow n' = \frac{3}{2}$, with the fine-structure consisting of P, Q and R branches with at least 42 rotation bands in each of the P and R branches. No overtone ($n'' = \frac{1}{2} \rightarrow n' = \frac{5}{2}$) has been found.

2. The molecular constants derived from the separation of the fine-structure bands (3.35 cms.^{-1}) corresponds almost exactly with those obtained from electronic band spectral data.

* 'Phys. Rev.', vol. 32, p. 223 (1928).

† Dennison, 'Phys. Rev.', vol. 31, p. 503 (1928); Bourgin, *ibid.*, vol. 32, p. 237 (1928).

‡ 'Wave Mechanics' (R. Inst. Lecture, 1928), p. 18.

3. Table of data :—

Infra-red.	Electronic (Jenkins, Barton and Mulliken).
$I = 1.64 \times 10^{-39} \text{ gm./cm.}^2$ $\nu_0 = 1.15 \text{ \AA.}$ $\omega = 1882.9$ $[\omega = \omega_0 (1-x)]$	$I = 1.63 \times 10^{-39} \text{ gm./cm.}^2$ $\nu_0 = 1.15 \text{ \AA.}$ $\omega_0 = 1892$

4. The presence of a Q branch is in accordance with the gyroscopic character of an odd-electron molecule.

The absence of alternating intensities in bands of low rotational quantum number agrees with theoretical predictions for the gyroscopic diatomic molecule.

5. The facts relating to the ground state of nitric oxide, its physical magnitudes, and its electronic angular momentum about the nuclear axis, form a consistent whole.

Acknowledgments.

It is a pleasure to thank the Keddey Fletcher-Warr Board for a research studentship to one of us (C. P. S.); Dr. A. M. Taylor for invaluable help throughout the work; and Mr. Geoffrey Smith of the Laboratory of Physical Chemistry for able assistance in the preparation of the gas.

The Arc Spectrum of Germanium.

By K. R. RAO, D.Sc., Government of Madras Research Scholar, Imperial College of Science, London.

(Communicated by A. Fowler, F.R.S.—Received April 18, 1929.)

Introductory.

In a former communication* an account was given of an investigation on the analysis of the Spark Spectra of Germanium (Ge II, Ge III, Ge IV) made by the writer in collaboration with Prof. A. L. Narayan. The present paper is an attempt at the elucidation of the arc spectrum of germanium.

The investigations of this spectrum made up to 1912 are summarised in Kayser's 'Handbuch,' vol. 5. With the aid of the existing measures and the recurring frequency differences pointed out by Paulson, McLennan and McLay† have indicated a few combinations arising from the deep terms of Ge I. Richter‡ has measured the arc spectrum to λ 2417 with a 6-metre concave grating and arrived at some of the groups identified by McLennan and McLay. The most important contribution is that of Gartlein§ who has extended the spectrum to λ 1873 and classified most of these lines.

In a recent paper|| Prof. A. Fowler has extended the analysis of the arc spectrum of silicon, the most important feature of which is the identification of a group of $3p'$, 1^3D , P terms arising from a configuration of one s electron and three p electrons. Such terms have been found also in C I, N II, O III and in P II. While the spark spectra of germanium are exactly analogous to those of silicon, the published analysis of Ge I by Gartlein did not, at first sight, seem to be entirely in consonance with that of Si I. A further investigation of the spectrum was therefore taken up by the writer at the suggestion of Prof. Fowler.

Observations of the arc spectrum have been extended to λ 1630. Gartlein's analysis has been slightly modified in the present work and extended to the region of small wave-lengths. About 50 new lines have been added, most of which have been classified.

Observational Data.

The region λ 2500– λ 1900 has been photographed with a small quartz spectrograph made by Bellingham and Stanley, giving an average dispersion

* Rao and Narayan, 'Roy. Soc. Proc.,' A, vol. 119, p. 607 (1928).

† 'Trans. Roy. Soc. Canada,' vol. 20, sec. 3, p. 355 (1926).

‡ 'Z. Wiss. Phot.,' vol. 25, p. 380 (1928).

§ 'Phys. Rev.,' vol. 31, p. 782 (1928).

|| 'Roy. Soc. Proc.,' A, vol. 123, p. 422 (1929).

of about 6 Å. per millimetre between λ 2100 and λ 1900. The arc between pure graphite electrodes, containing a small piece of metallic germanium,* served as the source. The region below λ 2020 has been investigated by a vacuum spectrograph with a metre grating having 30,000 lines per inch and giving a dispersion of about 8.6 Å. per millimetre. The instrument gave lines of excellent definition. The arc was situated a few centimetres from the fluorite window covering the slit and between the arc and the window a slow stream of nitrogen was passed through the side tube of a water-cooled annular chamber attached to the instrument, as devised by Mr. E. W. H. Selwyn for Prof. Fowler's work on silicon. The method is peculiarly suitable for the study of arc spectra in the region λ 2050– λ 1550, where it is often difficult by the usual methods (*e.g.*, the spark between metallic poles) to differentiate the arc lines from those of the spark.

A comparison spectrum was taken at first without germanium in the graphite electrodes in order to eliminate any lines due to possible impurities in the graphite. The spectrum contains bands of CO but the lines of germanium are characteristically sharp and could be easily distinguished from those of the bands. The plate was measured five times by a Hilger comparator reading to 0.001 mm., the standards at first used being the carbon lines 1931.027 and 1656.27 (Bowen's measures) and the nitrogen pair 1745.26 and 1742.74. But the wave-lengths so obtained were found to be consistently about 0.08 Å. too high when compared with the calculated wave-lengths in the case of some lines. The error was found to be in the adoption of the carbon standard 1931.027. In the final determinations, the calculated wave-length λ 1970.89 of Ge was used as a standard instead of the carbon line, for which the interpolated value now got is λ 1930.94, in close agreement with λ 1930.95 adopted by Prof. Fowler in his paper on silicon. It is expected that the error in the wave-lengths tabulated does not generally exceed 0.03 Å.

Results.

The notation used is the one adopted by Prof. Fowler, the prefix to each term denotes the orbit of the "series electron" and at the same time indicates the possible combinations with other terms. The terms which are to be expected in the spectrum of Ge I, according to Hund's Theory are listed in Table I.

* A small quantity of Ge (H.S. brand) was supplied by Adam Hilger, Ltd., and reported to be of a high degree of purity.

Table I.

1_1	2_1 2_2	3_1 3_2 3_3	4_1 4_2 4_3	5_1 5_2 5_3	6_1 6_2	Term prefix.	Terms.
2	2 6	2 6 10	2 2	1		$4p$	3P 1D 1S
2	2 6	2 6 10	2 1			$5s$	3P 1P
2	2 6	2 6 10	2 1 1			$4d$	3F 3D 3P 1F 1D 1P
2	2 6	2 6 10	2 1	1	1	$5p$	3D 3P 3S 1D 1P 1S
2	2 6	2 6 10	2 1	$6s$		3P 1P	
2	2 6	2 6 10	1 3	$4p'$		3S 3S 3D 3P 1D 1P	

The combinations arising from these terms are shown in Table II which is self-explanatory.

Table II.

	$4p$ 3P_0 567.11 65558.0	3P_1 852.80 65000.89	3P_2 5715.31 64148.09	1D_2 9241.91 58432.78	1S_0 49190.87
$5s$ 3P_0 = 28106.43	36894.46 (40)				
3P_1 = 27855.84 ^{250.59}	37702.15 (20)	37145.05 (30)	36292.26 (50)	30576.90 (40)	21334.93 (20)
3P_2 = 26440.33 ^{1416.61}	38560.56 (30) 37707.79 (30)			31992.49 (20)	
$6s$ 3P_0 = 13387.7	51613.2 (6)				
3P_1 = 13409.8 ^{-22.1}	52147.9 (5)	51591.0 (6)	50738.4 (6)	45023.1 (4)	35781.29 (10)
3P_2 = 11647.5 ^{1762.3}	53353.0 (4) 52500.3 (5)			46786.1 (1)	
$7s$ 3P_0 = 8391.5	56609.4 (3)				
3P_1 = 8637.4 ^{-245.9}	56921.0 (0)	56363.1 (3)	55510.4 (3)	49795.8 (1)	
3P_2 = 6826.6 ^{2010.8}	58374.0 (1) 57521.8 (1)			—	
$5s$ 1P_1 = 25537.65	40020.37 (15)	39463.26 (15)	38610.41 (12)	32895.09 (60)	23653.24 (50)
$6s$ 1P_1 = 11383.4	54173.8 (3)	53616.4 (2)	52763.5 (3)	47049.2 (5)	37807.63 (8)
$7s$ 1P_1 = 6444.3				51988.4 (5)	42746.55 (4)
$8s$ 1P_1 = 4215.2				54217.5 (3)	44975.7 (2)
$4d$ 3D_1 = 16595.7	48962.2 (8R)	48405.5 (6R)	47552.7 (3)	41837.4 (5)	32594.24 (10)
3D_2 = 16676.1 ^{-80.4}	48325.0 (9R) 47472.1 (5)			41756.53 (4)	
3D_3 = 16413.9 ^{263.2}	47734.1 (10R)			42018.92 (12)	
$5d$ 3D_1 = 10088.3	55470.2 (2)	54912.0 (0)	—	—	
3D_2 = 10185.6 ^{-97.3}	54814.8 (4) 53962.5 (3)			48247.6 (0)	
3D_3 = 9872.4 ^{313.2}	54275.0 (4)			48561.1 (2)	

Table II—(continued).

	$4p\ ^3P_0$ 567.11 65558.0	3P_1 568.80 65000.89	3P_2 5715.31 64148.09	1D_2 5941.91 58432.78	1S_0 49190.87
$4d\ ^3F_2 = 15489.3$ $^3F_2 = 15235.2$ 264.1		49511.5 (6R)	48658.9 (5) 48912.9 (7R)	42943.35 (15) 43197.71 (10)	
$5d\ ^3F_3 = 8729.7$			55418.9 (2)	49702.7 (4R)	
$4d\ ^3P_0 = 13578.2$ $^3P_1 = 13853.4$ -275.2 $^3P_2 = 14120.6$ -267.2	51704.2 (4)	51422.7 (5) 51147.2 (5) 50880.4 (4)	50294.7 (5) 50027.2 (5)	44579.8 (2) 44312.5 (5)	35337.66 (9)
$5d\ ^3P_0 = 7861.9$ $^3P_1 = 8127.3$ -265.4 $^3P_2 = 8379.5$ -252.2	57432.3 (1)	57139.0 (3) 56873.4 (3) 56620.7 (3)	56019.9 (3) 55769.3 (3)	50305.0 (2) 50054.0 (1)	
$4d\ ^1D_2 = 17078.3$ $5d\ ^1D_2 = 9840.4$ $6d\ ^1D_2 = 4672.8$		47922.6 (5) — —	47069.8 (3) 54307.1 (3) —	41354.61 (20) 48593.0 (5R) 53760.0 (6)	
$4d\ ^1P_1 = 12711.0$ $5d\ ^1P_1 = 7501.4$ $6d\ ^1P_1 = 4406.1$	— —	52290.6 (2) ? 57502.6 (1)	51437.0 (3) 56646.6 (3)	45721.7 (5) 50931.8 (3) 54028.0 (1)	36479.77 (20) 41090.12 (6) 44783.5 (0)
$4d\ ^1F_3 = 12966.0$ $5d\ ^1F_3 = 6616.4$ $6d\ ^1F_3 = 4291.2$			51182.3 (00)	45466.6 (15R) 51816.4 (9) 54141.6 (5)	
$4p\ ^1P_1 = 10084.4$ $4p\ ^3P_0 = 7882.9$ $^3P_1 = 8160.9$ -278.0 $^3P_2 = 8903.1$ -742.2	— 57397.3 (2)	— — —	54062.0 (1) 57118.0 (1) 55985.7 (3) 55245.0 (1)	48349.1 (3) —	39107.5 (10) 50271.5 (3) 41031.5 (5)
$4p\ ^1D_2 = 7466.7$ $4p\ ^3D_1 = 5833.3$ $^3D_2 = 5869.9$ -36.6 $^3D_3 = 5902.9$ -33.0	— 59725.0 (2)	— 59167.4 (2) 59131.4 (3)	56682.0 (3) — 58277.8 (2) 58245.2 (4)	50965.5 (7)	
$^1X_1 = 6035.5$ $^3X_2 = 4307.1$				52396.3 (2)	43156.4 (0)
		60692.9 (0)	59841.9 (1)		

Table III gives details of the wave-lengths, intensities, wave-numbers and the classification of the lines of the Ge arc from the visible region to λ 1600. Wave-lengths given to three places of decimals are from Richter, except those marked *, which are corrected values from Rowland and Tatnall (*cf.* Kayser, 'Handbuch'). The rest down to λ 2000 are from Gartlein and the remainder are measurements by the writer. The intensities of the lines below λ 2000 are visual estimates by the writer and are on a different scale from those of the remaining lines.

Table III.

λ I.A. air (int.).	ν (vac.).	Classification.		
		Triplets.	Inter-combination.	Singlets.
4685.841 (20)	21334.93		$4p^1S_0-5s^3P_1$	
4226.565 (50)	23653.24			$4p^1S_0-5s^1P_1$
3269.503 (40)	30576.90		$4p^1D_2-5s^3P_1$	
3124.831 (20)	31992.49		$4p^1D_2-5s^3P_2$	
3067.138* (10)	32594.24		$4p^1S_0-4d^3D_1$	
3039.086 (60)	32895.09			$4p^1D_2-5s^1P_1$
2829.012 (9)	35337.66		$4p^1S_0-4d^3P_1$	
2793.935 (10)	35781.29		$4p^1S_0-6s^3P_1$	
2754.596 (50)	36292.26	$4p^3P_2-5s^3P_1$		
2740.436 (20)	36479.77			$4p^1S_0-4d^1P_1$
2709.631 (40)	36894.46	$4p^3P_1-5s^3P_0$		
2691.351 (30)	37145.05	$4p^3P_1-5s^3P_1$		
2651.580 (20)	37702.15	$4p^3P_0-5s^3P_1$		
2651.184 (30)	37707.79	$4p^3P_2-5s^3P_2$		
2644.182 (8)	37807.63			$4p^1S_0-6s^1P_1$
2592.548 (30)	38560.56	$4p^3P_1-5s^3P_2$		
2589.201 (12)	38610.41		$4p^3P_2-5s^1P_1$	
2556.288 (10)	39107.50			$4p^1S_0-4p'^1P_1$
2533.241 (15)	39463.26		$4p^3P_1-5s^1P_1$	
2497.974 (15)	40020.37		$4p^3P_0-5s^1P_1$	
2436.41 (5)	41031.5		$4p^1S_0-4p'^3P_1$	
2417.375 (20)	41354.61			$4p^1D_2-4d^1D_2$
2397.919* (6)	41690.12			$4p^1S_0-5d^1P_1$
2394.105* (4)	41756.53		$4p^1D_2-4d^3D_2$	
2389.48 (5)	41837.4		$4p^1D_2-4d^3D_1$	
2379.154* (12)	42018.92		$4p^1D_2-4d^3D_3$	
2359.22 (4)	42373.9			
2338.652* (4)	42746.55			$4p^1S_0-7s^1P_1$
2327.934* (15)	42943.35		$4p^1D_2-4d^3F_2$	
2316.44 (0)	43156.4			$4p^1S_0-1X_1$
2314.225* (10)	43197.71		$4p^1D_2-4d^3F_3$	
2305.59 (1)	43359.5			
2282.71 (00)	44181.2			
2256.00 (5)	44312.5		$4p^1D_2-4d^3P_2$	
2252.76 (00) ?	44376.2			
2252.43 (1)	44382.7			
2247.03 (2)	44489.4			
2242.47 (2)	44579.8		$4p^1D_2-4d^3P_1$	
2232.27 (0)	44783.5			$4p^1S_0-6d^1P_1$
2222.73 (2)	44975.7			$4p^1S_0-8s^1P_1$
2220.39 (4)	45023.1		$4p^1D_2-6s^3P_1$	

Table III--(continued).

λ I.A. air (int.).	ν (vac.).	Classification.		
		Triplets.	Inter-combination.	Singlets.
2198.73 (15R)	45466.6			$4p^1D_2-4d^1F_3$
2186.46 (5)	45721.7			$4p^1D_2-4d^1P_1$
2136.71 (1)	46786.1		$4p^1D_2-6s^1P_2$	
2124.76 (58)	47049.2			$4p^1D_2-6s^1P_1$
2123.83 (3)	47069.8		$4p^1P_2-4d^1D_2$	
2105.83 (5)	47472.1	$4p^1P_2-4d^1D_2$		
2102.26 (3)	47552.7	$4p^1P_2-4d^1D_1$		
2094.27 (10R)	47734.1	$4p^1P_2-4d^1D_3$		
2086.03 (5)	47922.6		$4p^1P_1-4d^1D_2$	
2071.98 (0)	48247.6		$4p^1D_2-5d^1D_2$	
2068.66 (9R)	48325.0	$4p^1P_1-4d^1D_2$		
2067.63 (3)	48349.1			$4p^1D_2-4p'^1P_1$
2065.22 (6R)	48405.5	$4p^1P_1-4d^1D_1$		
2058.59 (2)	48561.1		$4p^1D_2-5d^1D_3$	
2057.25 (5R)	48593.0			$4p^1D_2-5d^1D_1$
2054.46 (5)	48658.9	$4p^1P_2-4d^1F_3$		
2043.79 (7R)	48912.9	$4p^1P_2-4d^1F_3$		
2041.72 (8R)	48962.2	$4p^1P_2-4d^1D_1$		
2019.08 (6R)	49511.5	$4p^1P_1-4d^1F_2$		
2011.31 (4R)	49702.7		$4p^1D_2-5d^1F_3$	
2007.55 (1)	49795.8		$4p^1D_2-7s^1P_1$	
λ (vac.).				
1998.91 (5)	50027.2	$4p^1P_2-4d^1P_2$		
1997.84 (1)	50054.0		$4p^1D_2-5d^1P_2$	
1989.20 (3)	50271.5		$4p^1D_2-4p'^1P_1$	
1988.28 (5)	50294.7	$4p^1P_2-4d^1P_1$		
1987.87 (2)	50305.0		$4p^1D_2-5d^1P_1$	
1970.89 (6)	50738.4	$4p^1P_2-6s^1P_1$		
1965.39 (4)	50880.4	$4p^1P_1-4d^1P_2$		
1963.41 (3)	50931.8			$4p^1D_2-5d^1P_1$
1962.11 (7)	50965.5			$4p^1D_2-4p'^1D_2$
1955.14 (5)	51147.2	$4p^1P_1-4d^1P_1$		
1953.80 (00)	51182.3		$4p^1P_2-4d^1F_3$	
1950.15 (00)	51278.1			
1944.66 (5)	51422.7	$4p^1P_1-4d^1P_0$		
1944.09 (3)	51437.0		$4p^1P_2-4d^1P_1$	
1938.32 (6)	51591.0	$4p^1P_1-6s^1P_1$		
1937.49 (6)	51613.2	$4p^1P_1-6s^1P_0$		
1934.08 (4)	51704.2	$4p^1P_0-4d^1P_1$		
1929.89 (9)	51816.4			$4p^1D_2-5d^1F_3$
1923.52 (5)	51988.4			$4p^1D_2-7s^1P_1$
1917.62 (5)	52147.9	$4p^1P_0-6s^1P_1$		
1912.39 (2)	52290.6		$4p^1P_1-4d^1P_1$	
1908.53 (2)	52396.3			$4p^1D_2-X_1$
1906.78 (0)	52445.0			
1904.75 (5)	52500.3	$4p^1P_2-6s^1P_2$		
1895.25 (3)	52763.5		$4p^1P_2-6s^1P_1$	
1874.31 (4)	53353.0	$4p^1P_1-6s^1P_2$		
1865.10 (2)	53616.4		$4p^1P_1-6s^1P_1$	
1860.12 (6)	53760.0			$4p^1D_2-6d^1D_2$
1853.14 (3)	53962.5	$4p^1P_2-5d^1D_2$		
1850.90 (1)	54028.0			$4p^1D_2-6d^1P_1$

Table III—(continued).

λ (vac.).	ν (vac.).	Classification.		
		Triplets.	Inter-combination.	Singlets.
1849.73 (1)	54062.0		$4p\ ^3P_2-4p'\ ^1P_1$	
1847.01 (5)	54141.6			$4p\ ^1D_2-6d\ ^1F_3$
1845.91 (3)	54173.8		$4p\ ^3P_0-6s\ ^1P_1$	
1845.04 (0)	54199.4			
1844.42 (3)	54217.5			$4p\ ^1D_2-8s\ ^1P_1$
1843.61 (0)	54241.4			
1842.47 (4)	54275.0	$4p\ ^3P_2-5d\ ^3D_2$		
1841.38 (3)	54307.1		$4p\ ^3P_2-5d\ ^1D_2$	
1824.34 (4)	54814.8	$4p\ ^3P_1-5d\ ^3D_2$		
1821.10 (0)	54912.0	$4p\ ^3P_1-5d\ ^3D_1$		
1810.12 (1)	55245.0	$4p\ ^3P_2-4p'\ ^3P_2$		
1804.44 (2)	55418.9	$4p\ ^3P_2-5d\ ^3F_3$		
1802.77 (2)	55470.2	$4p\ ^3P_0-5d\ ^3D_1$		
1801.46 (3)	55510.4	$4p\ ^3P_2-7s\ ^3P_1$		
1793.10 (3)	55769.3	$4p\ ^3P_2-5d\ ^3P_2$		
1786.17 (3)	55985.7	$4p\ ^3P_2-4p'\ ^3P_1$		
1785.08 (3)	56019.9	$4p\ ^3P_2-5d\ ^3P_1$		
1774.21 (3)	56363.1	$4p\ ^3P_1-7s\ ^3P_1$		
1766.49 (3)	56609.4	$4p\ ^3P_1-7s\ ^3P_0$		
1766.14 (3)	56620.7	$4p\ ^3P_1-5d\ ^3P_2$		
1765.33 (3)	56646.6		$4p\ ^3P_2-5d\ ^1P_1$	
1764.23 (3)	56682.0		$4p\ ^3P_2-4p'\ ^1D_2$	
1758.29 (3)	56873.4	$4p\ ^3P_1-5d\ ^3P_1$		
1750.82 (0)	56921.0	$4p\ ^3P_0-7s\ ^3P_1$		
1750.76 (1)	57118.0	$4p\ ^3P_1-4p'\ ^3P_0$		
1750.12 (3)	57139.0	$4p\ ^3P_1-5d\ ^3P_0$		
1746.10 (3)	57270.5			
1742.24 (2)	57397.3	$4p\ ^3P_0-4p'\ ^3P_1$		
1741.18 (1)	57432.3	$4p\ ^3P_0-5d\ ^3P_1$		
1739.05 (1)	57502.6		$4p\ ^3P_1-5d\ ^3P_1?$	
1738.47 (1)	57521.8	$4p\ ^3P_2-7s\ ^3P_2$		
1718.54 (2)	58188.9			
1716.88 (4)	58245.2	$4p\ ^3P_2-4p'\ ^3D_3$		
1715.92 (2)	58277.8	$4p\ ^3P_2-4p'\ ^3D_2$		
1713.09 (1)	58374.0	$4p\ ^3P_1-7s\ ^3P_2$		
1712.32 (1)	58400.3			
1691.15 (3)	59131.4	$4p\ ^3P_1-4p'\ ^3D_2$		
1690.12 (2)	59167.4	$4p\ ^3P_1-4p'\ ^3D_1$		
1681.61 (1)	59470.4			
1675.72 (1)	59675.8			
1674.34 (2)	59725.0	$4p\ ^3P_0-4p'\ ^3D_1$		
1671.07 (1)	59841.9	$4p\ ^3P_2-^3X_2$		
1670.50 (1)	59862.3			
1663.52 (1)	60113.5			
1649.29† (2)	60632.5			
1647.64 (0)	60692.9	$4p\ ^3P_1-^3X_2$		
1639.73 (1)	60985.6			

† Line of Ge II (more intense at the pole).

Classification.

The most easily excited lines in the arc spectrum of germanium should result from the combination of $5s\ ^3P\ ^1P$ with the deepest $4p\ ^3P\ ^1D\ ^1S$. These groups

were arrived at independently by McLennan and McLay, Richter and Gartlein, and agree well with corresponding groups of similar elements in the periodic table.

The series of $ms\ ^3P$ terms may first be considered. In four electron systems, such as the neutral atom of germanium, it is known according to Hund's theory that while $ms\ ^3P_0\ ^3P_1$ tend to the limit 2P_1 of the next ionised three electron system, $ms\ ^3P_2\ ^1P_1$ converge to the level 2P_2 . This is illustrated well in the following Table IV where obviously the difference $ms\ (^3P_0 - ^3P_2)$ gradually increases to the limiting difference $^2P_1 - ^2P_2$.

Table IV.*

	C I.	N II.	O III.	Si I.	P II.	S III.	Ge I.	As II.	Se III.	Sn I.
$ms\ (^3P_0 - ^3P_2)$	60.1	167.96	375.30	271.93	528.1	451.0	1666.10	2512.6	—	3988
$(m+1)s\ (^3P_0 - ^2P_2)$	—	170.70	373	282.9	546.8	—	1740.2	—	—	—
$(m+2)s\ (^3P_0 - ^3P_2)$	—	173.4	—	284.2	—	—	1764.9	—	—	—
	C II.	N III.	O IV.	Si II.	P III.	S IV.	Ge II.	As III.	Se IV.	Sn II.
Limit: $(^2P_1 - ^2P_2)$	64.0	174.4	387	287	566	—	1768	2943	—	4245

* The data have been taken from papers mostly in 'Roy. Soc. Proc.,' and 'Phys. Rev.' The difference for As II is from the following probable multiplet in the visible region.

	$5s\ ^3P_2$	1586.6	3P_1	926.1	3P_0
$5p\ ^3P_0$			17089.3 (9)		
3P_1	16597.0 (6)		^{494.1} 18183.4 (7)		19109.6 (7)
3P_2	17986.0 (8)		^{1389.0} 19572.4 (8)		
3S_1	18751.4 (8)		20338.2 (7)		21264.1 (3)

If a similar feature occurs in Ge I, the difference $ms\ (^3P_0 - ^3P_2)$ should increase gradually to the limit $^2P_1 - ^2P_2 = 1768$ of Ge II. But according to Gartlein's analysis the differences are :—

$$5s\ (^3P_0 - ^3P_2) = 1666,$$

$$6s\ (^3P_0 - ^3P_2) = 1931,$$

$$\dots\dots\dots$$

$$\text{limit } ^2P_1 - ^2P_2 = 1768.$$

Several attempts were made to modify the group $4p\ ^3P - 6s\ ^3P$ to bring it into consonance with the above considerations. But the levels $6s\ ^3P_1$ and $6s\ ^3P_2$ could not be altered, as the possible alternatives were quite unsatisfactory. So the line $\nu 51613$ was taken to be $4p\ ^3P_1 - 6s\ ^3P_0$ instead of $\nu 51423$, adopted by Gartlein. The detection of a similar third member of the series supports the modification that has been made. The differences $ms\ (^3P_0 - ^3P_2)$ thus obtained are given in the above Table IV and seem to be satisfactory. An interesting feature which these terms show, if correct, is the partial inversion of the higher members. This may perhaps be due to the very large ratio (1415 : 250) between the intervals of the first member $5s\ ^3P$ of Ge I, while in Si I this ratio is roughly 2 (195 : 77).

The group of $4d$ terms may next be considered. According to Gartlein the differences $4d\ (^3D_1 - ^3D_2)$ and $4d\ (^3D_2 - ^3D_3)$ are 1106 and 254. They are too large and apparently do not agree with the corresponding differences in C I, Si I or Sn I. The differences in the group $4p\ ^3P - 4d\ ^3D$, adopted in the present work, are - 80 and 262. McLennan and McLay have come to the same conclusion. The partial inversion of the $4d\ ^3D$ term is a feature which occurs also in Sn I where the group has been established by observations of the Zeeman effect of the lines, independently by Back and by Green and Loring.*

The group $4p\ ^3P - 4d\ ^3P$ has also to be slightly altered, since the lines $\nu 51423$ and $\nu 51613$ are interchanged.

For some time, in the early stages of the work, considerations of analogy with Si I led the writer to think that these two $4d$ triplet groups might perhaps be the $4p \rightarrow 4p'$ combinations and that the $4p \rightarrow 4d$ groups were still to be discovered in or about the same region; that the terms $4d\ ^3F_3, ^3F_2$ may really be $4d\ ^3D_3, ^3D_2$ with an undiscovered $4d\ ^3D_1$ level in the vicinity of these. For the values of $4d\ ^3D$ terms here adopted are about 5000 units larger than their usual value in arc spectra, and, further, in Si I the levels $4d\ ^3F_3, ^3F_2$ have not been found to give strong combination lines as in Ge with $4p\ ^3P$. But failure to detect a suitable 3D_1 level close to $4d\ ^3F_2$ and the discovery of higher Rydberg members $5d\ ^3D, 5d\ ^3P$ which are closely analogous to the $4d$ terms, have led to the present assignment.

The identification of the singlet terms was found somewhat difficult. The location of $ms\ ^1P_1$ and $md\ ^1P_1$ levels is supported by the existence of satisfactory intercombination lines. The series of lines $4p\ ^1D_2 - md\ ^1F_3$ and

* Back, 'Z. Physik,' vol. 43, p. 309 (1927); Green and Loring, 'Phys. Rev.,' vol. 30, p. 574 (1927).

$4p^1D_2 - md^1D_2$ are, however, suggested only by examination of the appearance of the lines and the probable term values that are to be expected. The choice was among the lines which have not entered into any of the triplet levels.

Probable combinations arising from the transition $4p \rightarrow 4p'$ are also given in Table II. Of these the group $4p^3P - 4p'^3D$ appears isolated and fairly strong on the plate; all the lines of this group are of the same slightly diffuse appearance. From the intensity of the lines and 3D differences which they give it was considered that it cannot be a third member of the series $4p^3P - md^3D$. Hence the present assignment. The suggested structure of the $4p^3P - 4p'^3P$ group is only tentative. It is expected that further light on this group of terms will be thrown by an extension of the arc spectrum of Sn and also by the analysis of singly-ionised As, which is now under investigation by the author.

Term Values.

Three members of the triplet series $4p^3P - ms^3P$ and of some of the singlet series are available for the determination of the absolute values of the terms with reasonable accuracy. Considering the triplet series we find:—

$$(1) \left. \begin{aligned} 4p^3P_1 - 5s^3P_0 &= 36894.5 \\ -6s^3P_0 &= 51613.2 \\ -7s^3P_0 &= 56609.4 \end{aligned} \right\} \nu = 63139 - \frac{R}{\left[m + 1.126369 - \frac{0.0815}{m} \right]^2}$$

$$4p^3P_1 = 63139; 4p^3P_0 = 63696.$$

$$(2) \left. \begin{aligned} 4p^3P_1 - 5s^3P_1 &= 37145.1 \\ -6s^3P_1 &= 51591.0 \\ -7s^3P_1 &= 53363.1 \end{aligned} \right\} \nu = 62667 - \frac{R}{\left[m + 1.221756 - \frac{0.148143}{m} \right]^2}$$

$$4p^3P_1 = 62667; 4p^3P_0 = 63224.$$

$$(3) \left. \begin{aligned} 4p^3P_1 - 5s^3P_2 &= 38560.6 \\ -6s^3P_2 &= 53353.0 \\ -7s^3P_2 &= 58374.0 \end{aligned} \right\} \nu = 64927 - \frac{R}{\left[m + 1.118361 - \frac{0.078219}{m} \right]^2}$$

$$4p^3P_1 = 64927; 4p^3P_0 = 65484.$$

Thus while ms^3P_0 and ms^3P_1 terms tend approximately to the same limit ms^3P_2 terms approach a definitely higher limit, in keeping with Hund's

theoretical considerations. The difference ${}^{\infty}P_0 - {}^{\infty}P_2 = 65484 - 63696 = 1788$ agrees well with ${}^3P_1 - {}^3P_2 = 1768$ of Ge II.

The singlets $4p\,{}^1D_2 - ms\,{}^1P_1$ give the following formula :—

$$\left. \begin{aligned} 4p\,{}^1D_2 - 5s\,{}^1P_1 &= 32895.1 \\ -6s\,{}^1P_1 &= 47049.2 \\ -7s\,{}^1P_1 &= 51988.4 \\ -8s\,{}^1P_1 &= 54217.5 \end{aligned} \right\} \nu = 58506 - \frac{R}{\left[m + 1.119789 - \frac{0.049813}{m} \right]^2}$$

$$4p\,{}^1D_2 = 58506; \quad 4p\,{}^3P_0 = 65631.$$

These converge, therefore, to the same limit as $ms\,{}^3P_2$ terms. The (obs.-calc.) for the last line is -81 .

The term values shown in the table have been calculated by adopting the value $4p\,{}^3P_0 = 65558.0$, the mean of the limits derived from the $ms\,{}^1P_1$ and $ms\,{}^3P_2$ terms.

The largest term $4p\,{}^3P_0$ in the spectrum of Ge I is therefore found to be equal to 65558.0, giving the ionisation potential of Ge I as 8.09 volts approximately.

Comparison of Terms.

In the following table the term values of C I, Si I, Ge I and Sn I are brought together. It is interesting to notice that the $d\,{}^3D$ terms have a value of about 12000 in C I and Si I, while in Ge I and Sn I they are much higher and range about 16000. Again, if the identification of the group of $4p'$ terms of Ge I prove correct, they are seen to be very small compared with those of Si I and C I, the singlets being deeper than the triplets.

Table showing Term Values.

	C I.	$\Delta\nu$.	Si I.	$\Delta\nu$.	Ge I.	$\Delta\nu$.	Sn I.	$\Delta\nu$.
$mp\,{}^3P_0$	91017.3		65765		65558.0		59690	
3P_1	91002.5	14.8	65688	77.1	65000.9	557.1	57998	1692
3P_2	90975.0	27.5	65542	146.1	64148.1	852.8	56262	1736
1D_2	81312		59466		58432.8		51077	
1S_0	69860		50371		49190.9		42527	
$ms\,P_0$	30686.0		26082		28106.4		25049	
3P_1	30666.0	20.0	26005	77.1	27855.8	250.6	24775	374
3P_2	30625.9	40.1	25810	194.8	26440.3	1415.5	21061	3714
1P_1	29626		24773		25537.7		20433	

Term Values—(continued).

	C I.	Δv .	Si I.	Δv .	Ge I.	Δv .	Sn I.	Δv .
$(m+1)s^3P_0$			11521		13387.7		—	
3P_1			11452	68.8	13409.8	-22.1	11467	
3P_2			11238	214.0	11647.5	1762.3	7271 ?	4196 ?
1P_1			10894		11383.4			
$(m+2)s^3P_0$			6544		8391.5			
3P_1			6492	52.7	8637.4	-246.9		
3P_2			6260	231.5	6626.6	2010.8		
1P_1			6130		6444.3			
$(m+3)s^1P_1$			3885		4215.2			
md^1F_3	12979 ?		12404		12966.0		9795	
md^3F_3					15489.3		15545	
3F_3					15235.2	254.1	15114	431
md^3P_1	11709				14120.6		11009	
3P_1	-10.0				13853.4	-267.2	10706	-303
3P_0	-5.0				13578.2	-275.2	10193	-518
1P_1	12779		12378		12711.0		9562	
md^1D_3	11414 ?		11506		17078.3		12544	
3D_1	[12715]		11580		16595.7		16007	
3D_2	5.0		11560	19.9	16676.1	-80.4	15181	-226
3D_3	10.0		11508	52.0	16413.9	262.2	12202	3805
$(m+1)d^1F_3$			6873		6616.4			
$(m+1)d^1P_1$			6963		7501.4			
3P_2					8379.5			
3P_1					8127.3	-252.2		
3P_0					7861.9	-265.4		
$(m+1)d^1D_3$			6647		9840.4			
3D_1			6789		10088.3			
3D_2			6733	55.5	10185.6	-97.3		
3D_3			6646	87.0	9872.4	313.2		

Term Values—(continued).

	C I.	$\Delta\nu$.	Si I.	$\Delta\nu$.	Ge I.	$\Delta\nu$.	Sn I.	$\Delta\nu$.
$(n+2) d^1 F_3$			4342		4291.2			
1P_1			4429 ?		4406.1			
1D_2			4189		4672.8			
$mp' ^3D_1$			20489		5833.3			
3D_2			20472	17.1	5869.9	-36.6		
3D_3	26731		20443	28.4	5902.9	-33.0		
1D_2			18414		7466.7			
$mp' ^3P_2$	15565		15266		8903.1			
3P_1			15199	-66.3	8160.9	-742.2		
3P_0			15163	-36.0	7882.9	-278.0		
1P_1			—		10084.4			

Summary.

Observations of the arc spectrum of germanium have been extended to λ 1630 and about 50 new lines have been added, most of which have been classified.

The analysis published by Gartlein has been slightly modified to bring it into better agreement with that of the spectra of related elements. The detection of the higher members of some of the series made possible the calculation of the absolute values of the terms. The largest term, $4p\ ^3P_0 = 65558.0$, gives the ionisation potential of Ge I a value of 8.09 volts approximately.

It is a pleasure to acknowledge my great indebtedness to Prof. A. Fowler, F.R.S., for suggesting the present investigation, for permitting me the use of his results on Si I prior to publication, and for his continual interest and encouragement. My thanks are due also to the Andhra University and the Government of Madras for the award of a scholarship which has enabled me to undertake this work at the Imperial College of Science.

A Study of the Catalysis by Silver of the Union of Hydrogen and Oxygen.

By D. L. CHAPMAN, M.A., F.R.S., Fellow of Jesus College, Oxford, and
W. K. HALL, B.A., Jesus College, Oxford.

(Received April 11, 1919.)

D. R. Hughes and R. C. Bevan* discovered a simple and delicate method of testing whether a metallic nickel surface is covered with a layer of oxide. The investigation was conducted with metal drawn into the form of a wire. It was found, that when the wire was heated electrically at a temperature of $164^{\circ}\text{C}.$, hydrogen molecules (temperature $14^{\circ}\text{C}.$ and pressure $12910 \times 10^{-6}\text{ mm.}$) removed nearly twice as much heat from a surface known to be oxidised, as from one completely reduced to the metallic state on reflection from the surfaces under similar conditions. Consequently, in an atmosphere of hydrogen, a given current raised the wire to a higher temperature when all oxide had been previously removed from the surface. The accommodation coefficient (*i.e.*, the ratio of the energy actually removed from the wire by an escaping hydrogen molecule to that which would have been removed if the molecule had attained the temperature of the metal) was found to be 0.25 for a metallic surface, and 0.48 for an oxidised surface. Invisible films of oxide, only a few molecules deep, could thus with certainty be detected.

They were thereby enabled to show that a nickel surface was immediately oxidised by exposure to oxygen at the temperature of the laboratory. The invisible oxide thus formed and the black oxide produced by continued heating in an atmosphere of oxygen catalysed the combination of hydrogen and oxygen at the same temperature, a temperature not below that at which reduction by hydrogen occurred. Concerning the catalysis by nickel of the reaction between hydrogen and oxygen, they came to the inevitable conclusion that, during the combination of the gases the metal was completely covered by a layer of oxide, and the mechanism of the catalysis was similar to that of other readily oxidisable metals like copper, and was merely alternate oxidation and reduction of the surface.

The method of procedure adopted by Hughes and Bevan has been applied by us in an investigation of the catalysis by silver of the same reaction. In

* 'Roy. Soc. Proc.,' A, vol. 117, p. 100 (1927).

this case the phenomenon has interesting peculiarities* of which we have endeavoured to discover the cause.

D. L. Chapman, J. E. Ramsbottom, and C. G. Trotman† showed that silver from which all oxygen has been removed, either by its prolonged heating *in vacuo*, or by its reduction with hydrogen, was very much more effective in promoting the union of hydrogen and oxygen than silver which had been heated to dull redness in oxygen. Furthermore, it was found that indefinite amounts of water could be synthesised both with an active metallic wire and with an inactive oxidised wire without changing in the least their respective activities. These facts appeared to the authors to be most simply explained by the assumption that the wire which had been heated to dull redness in oxygen was completely covered with a film of oxide, which was less effective as a catalyst than the metal surface.

Determinations, made by us, of the accommodation coefficients of hydrogen at the surfaces in question support the assumption of Chapman, Ramsbottom and Trotman that silver which has been heated in oxygen is covered with a film of oxide. At the same temperature and pressure hydrogen molecules removed less heat from a hot metallic silver surface than from a surface of the metal which has been subjected to the action of oxygen at a high temperature.‡ When both were heated in hydrogen at the same pressure and with the same current the metallic wire assumed a higher temperature. Nevertheless the assumption of Chapman, Ramsbottom and Trotman that a metallic silver surface remains unoxidised when it is acting as a catalyst for the union of hydrogen and oxygen must be abandoned. Silver when it is brought into contact with oxygen or with a mixture of oxygen and hydrogen is almost immediately covered with a film of oxide; but this oxide, formed at a low temperature, is a much more effective catalyst than the oxide formed at a high temperature. There is a notable difference in the reducibility of the two varieties of the oxide films, the active oxide being much more easily reduced to silver by hydrogen than the inactive form. There appear, in fact, to be two forms of silver oxide, an easily reducible form, a very active catalyst for the combination of hydrogen and oxygen, and a less active form which is correspondingly more resistant to reduction. The temperature of reduction of either variety of the oxide film is certainly not above that at which the film will

* Bone and Wheeler, 'Phil. Trans.,' A, vol. 206, p. 1 (1906).

† 'Roy. Soc. Proc.,' A, vol. 107, p. 92 (1925).

‡ The temperature at which such experiments are performed must, of course, be below that at which the oxide is reduced.

catalyse the union of hydrogen and oxygen at a measurable rate. This latter fact is in agreement with the hypothesis that the mechanism of the catalysis is in both cases one of alternate oxidation and reduction. However, the following objection can be raised against this theory in the case of the inactive oxide film. The first stage of the process is *ex hypothesi* a reduction of the oxide to silver, and this silver would during the second stage be reoxidised ; but the oxide thus produced ought to be the active variety since the temperature of catalysis has been observed to be below that at which the inactive film is formed from silver and pure oxygen. The objection would be fatal to the hypothesis if it were not for the circumstance that the silver formed from a solid oxide in the early stages of the reduction cannot have the properties of the normal metal existing as a separate phase, but must in fact be looked upon as isolated atoms which on reoxidation furnish molecules of oxide having approximately the same position and orientation as the original molecules of oxide from which they were formed.

A similar assumption affords an explanation of the fact that the oxide film formed by the action of oxygen on the cold metal is so much more active and easily reducible than a film which has been formed at a high temperature. The immediate action of the molecules of oxygen on the surface atoms of silver is to form molecules of silver oxide of which the configuration is unstable. Such instability would clearly confer on the oxide the properties of increased catalytic activity and easier reducibility. On raising the temperature of the unstable oxide the molecules would be sufficiently released to enable them to take up the most stable arrangement, and the oxide would then become inactive.

Experimental.

The apparatus and procedure were very similar to those of D. R. Hughes and R. C. Bevan. Silver wires, 0.0254 cm. in diameter, and of lengths varying between 38 cm. and 99 cm., were heated electrically. The reaction vessel was a vertical glass tube of 3 cm. internal diameter, and of such a length as to correspond with the wire it contained, and the gases were separately admitted to the reaction vessel from two containers—the oxygen from one and the hydrogen from the other—the ratio of the volume of the container of the oxygen to the sum of the volumes of the reaction chamber, the McLeod gauge, and the connecting tubes being approximately 1 : 10.

Fortunately the thin film of silver, which during the course of the experiments volatilised on to the inner surface of the reaction vessel, caused the gases

to combine at a negligible rate only at 16° C., the temperature at which the reaction chamber was maintained by means of a thermostat.

The temperature of the catalyst was calculated from its electrical resistance.

In determining the temperature coefficient of electrical resistance of a cold drawn silver wire we encountered a difficulty ; for, on heating the wire to about 90° C. a certain amount of strain was gradually removed, and its electrical resistance diminished. On the wire being cooled again to 0° C. its conductivity was found to have increased. The wire had therefore to be annealed at a dull red heat, before its constants of resistance were determined.

Within the limits of experimental error, it was found that resistance of silver between 0° C. and 300° C. could be represented by the equation

$$R_t = R_0 (1 + 0.004 t)$$

where R_t is the resistance at t° C., and R_0 the resistance at 0° C.*

The resistance at 16° C. of a wire was, as explained later, estimated by extrapolation from curves drawn by plotting the energy lost per second (amperes \times volts) against the resistance, when the wire was heated under standard conditions by currents of varying magnitudes, and the result was confirmed by direct measurement using a very small current with the wire surrounded by gas at atmospheric pressure. The resistance at 0° C. and at any other temperature could then be calculated.

Although the relative cooling of the heated wire by conduction of heat to the leads was greatly reduced by the use of a long wire, the error from this cause was not inconsiderable at higher temperatures. A correction was therefore applied by subtracting the resistance of a wire 38 cm. long from that of a wire 99 cm. long when both were heated by the same current in gas at the same pressure. The result was to a sufficient degree of accuracy the resistance of the central portion of the longer wire, and since this central portion was fairly evenly heated—provided the reaction vessel contained gas—the resistance thus obtained could be used to estimate its temperature. In a good vacuum the temperature gradient even of the central portion of the long wire was not negligible.

The state of the surface of the wire can be most conveniently inferred from curves obtained by plotting the energy lost per second by the wire against its electrical resistance when heated by currents of varying magnitudes in gas at a given pressure. The curves thus obtained approximate to straight lines.

* *Vide* Matthiesen, 'Phil. Mag.,' vol. 21, p. 107 (1861); Somerville, 'Phys. Rev.,' vol. 31, p. 261 (1910).

The exact temperature of reduction of an oxide film may be readily deduced from the curve showing the behaviour of the oxidised wire heated in hydrogen. The temperature at which the curve deviates from a straight line is the temperature at which reduction of the oxide begins.

Before any experiments were performed the wire was cleaned by its being heated at dull redness, first in oxygen, then in a vacuum, and finally in hydrogen, the operations of heating being repeated in the same order until the results obtained with it were exactly reproducible. Poisoning of the catalyst by volatile impurities was prevented by inserting between the reaction vessel and the rest of the apparatus U-tubes surrounded by liquid air. The poisons are probably organic impurities; mercury although not actually a poison in the case of silver must be excluded, since if the surface of the silver becomes covered with an amalgam the original results are not reproducible until all the mercury has been removed from the surface.*

Experiment I A demonstrates that hydrogen molecules remove less heat from a hot metallic silver wire than from a wire previously heated to dull redness in oxygen :—

- (a) The wire was heated to dull redness in hydrogen (pressure 48810×10^{-6} mm.) for half-an-hour, and then in a vacuum for a quarter-of-an-hour. Finally, it was heated in hydrogen (pressure 48810×10^{-6} mm.) with a gradually increasing current, the corresponding differences in potential being observed.
- (b) The wire was heated to dull redness in oxygen (pressure 516500×10^{-6} mm.). The oxygen was pumped out, the apparatus washed out with hydrogen, and finally filled with hydrogen at a pressure of 48810×10^{-6} mm. The wire was then heated by a gradually increasing current, the corresponding differences in potential being observed.

The results of the experiment are shown on the graphs of the accompanying figure.

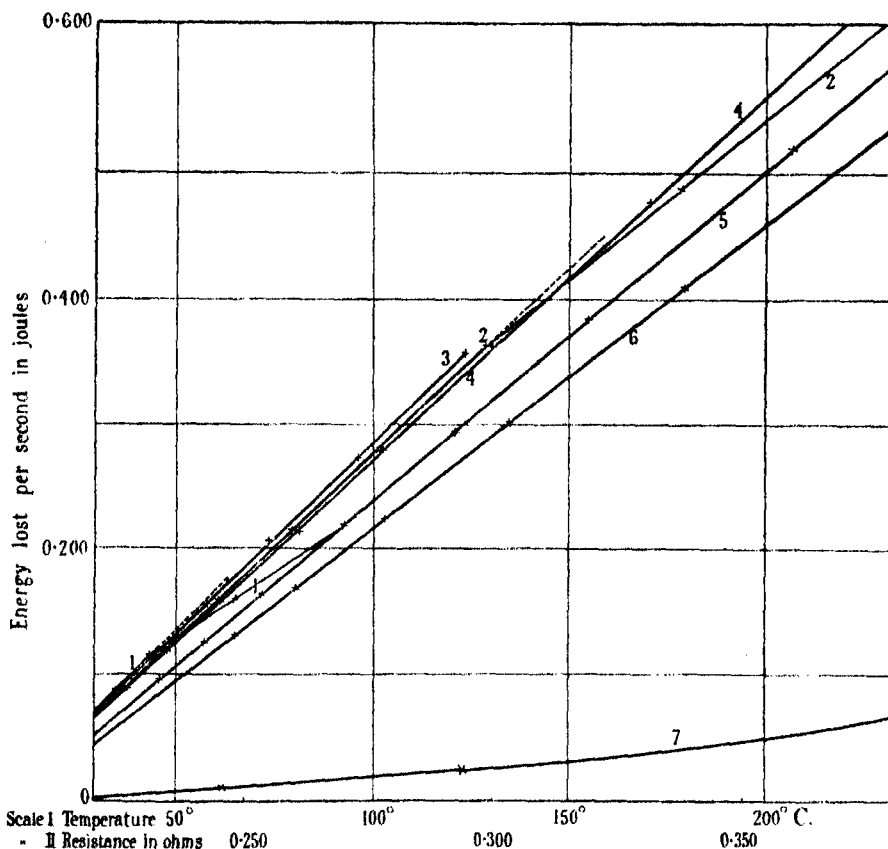
Curve (5) metallic wire.

Curve (2), wire oxidised at high temperature.

It will be observed that reduction of the oxide starts at a temperature of about 130° C.

Experiment II A demonstrates that when a wire with a metallic surface and a wire oxidised at a high temperature are heated in a mixture of hydrogen and oxygen in the ratio of 10 : 1 at the total pressure of 48810×10^{-6} mm.,

* In the case of platinum mercury is a powerful poison.



- Curve 1.—Wire, covered with active oxide, heated in hydrogen. (Oxide was reduced about 40° C.)
 Curve 2.—Wire, covered with inactive oxide, heated in hydrogen. (Oxide was reduced about 130° C.)
 Curve 3.—Wire, covered with active oxide, heated in mixture of hydrogen and oxygen. (Combination occurred at measurable rate at 128° C.)
 Curve 4.—Wire, covered with inactive oxide, heated in mixture of hydrogen and oxygen. (Combination occurred at measurable rate at 447° C.)
 Curve 5.—Metallic wire heated in hydrogen.
 Curve 6.—Wire heated in oxygen.
 Curve 7.—Wire heated *in vacuo*.

the heat lost per second is very nearly identical for both surfaces. In the case of short wires the difference was too small to be measurable.

The results are shown by the curves (3) and (4).

The experiment compels us to conclude that when it is exposed to a mixture of hydrogen and oxygen a metallic silver surface becomes almost completely

covered with a layer of oxide. If anything, the oxide formed at a low temperature can communicate heat to the gas molecules more readily than the stable oxide formed at a high temperature, but the difference is slight. That the curves (3) and (4) fall respectively a little below the curves (1) and (2) is, of course, accounted for by the fact that oxygen molecules remove less heat from a hot surface than the same number of hydrogen molecules.

Combination of hydrogen and oxygen began to take place at an appreciable rate on the active wire at a temperature of $128^{\circ}\text{C}.$; but was not taking place at the same rate on the inactive wire until a temperature of $447^{\circ}\text{C}.$ had been reached. This accounts for curve (3) being much shorter than curve (4).

After being employed as a catalyst the inactive wire gave with hydrogen the same accommodation coefficient as that determined with it before being put to such use. Moreover the accommodation coefficient of hydrogen determined with an active wire, after it had been employed as a catalyst, was almost identical with that determined with an inactive wire provided that the former determination was carried out rapidly and the common temperature of the determinations was sufficiently low. The more active oxide was, however, reduced at a very much lower temperature than the inactive variety. In both cases the temperature at which the oxide was reduced was much lower than that at which it promoted combination of hydrogen and oxygen at a measurable rate.

Experiment III A is a comparison of the reducibilities and the activities of the two varieties of the oxide.

The temperature of the oxidised wire surrounded by hydrogen at a pressure of 48810×10^{-6} mm. was raised in stages of equal intervals of temperature. The wire was heated at each temperature for half an hour and then tested for reduction by repeating a determination of the heat loss per second at a lower temperature. Alternatively, the temperature at which reduction of the oxide starts can be determined with equal accuracy from the curve obtained by plotting the heat lost per second in hydrogen against the resistance. The curve deviates from an approximate straight line at the temperature of reduction.

The temperatures of reduction by hydrogen of the active and inactive oxides are shown by curves (1) and (2), and the results are tabulated below.

	Temperature of reduction.	Temperature of combination.
	$^{\circ}\text{C}.$	$^{\circ}\text{C}.$
Active oxide.....	about 40	128
Inactive oxide.....	.. 130	447

The temperature of combination signifies that temperature at which one twentieth of the total oxygen present disappears in 5 minutes.

Experiment IV A demonstrates that during the combination of hydrogen and oxygen on an active wire, the surface is covered with oxide.

The metallic wire was heated in hydrogen (pressure 48810×10^{-6} mm.) by a current of 1.1 amperes. An equilibrium temperature of 157° C. was thereby attained. Oxygen enclosed in its container at the same pressure was then admitted to the reaction vessel, the heating current being maintained constant. At the low pressure at which we were working the mixing of the hydrogen and oxygen was complete after a few seconds. The resulting mixture contained 1 molecule of oxygen to 10 molecules of hydrogen, and the total pressure was, of course, the same as the original common pressure of the unmixed hydrogen and oxygen. The admission of the oxygen caused the temperature of the wire, as measured by its electrical resistance, to fall immediately to 128° C. As combination of the gases occurs at this temperature there was thereafter a gradual fall in pressure and a consequent rise in temperature.*

In a second experiment conducted in the same manner with a current of 1.0 ampere the temperature fall was from 119° C. to 98° C., but in this case no combination of the gases could be measured.

Now the sudden fall in temperature of the wire observed immediately after the admission of the oxygen to the reaction chamber could not have been due to the replacement of hydrogen molecules by an equal number of oxygen molecules since oxygen removes less heat from a hot surface than hydrogen at the same pressure. In fact, when the wire was heated by a current of 1.1 amperes in oxygen at a pressure of 48810×10^{-6} mm., its equilibrium temperature was as high as 167° C.

It is obvious, therefore, that the admitted oxygen rendered the surface of the wire more capable of communicating heat to hydrogen molecules, and as it is known that the accommodation coefficient between an oxide and hydrogen is greater than the accommodation coefficient between the corresponding metal and hydrogen, we may legitimately conclude that in the presence of the mixture of oxygen and hydrogen the silver was oxidised on its surface. The results are tabulated below.

* The heat generated by the formation of water at the surface of the wire is comparatively small, and could not appreciably alter the temperature of the wire.

Before admitting oxygen :—

Pressure of hydrogen.	Current.	Resistance of wire.	Temperature.	Energy lost per second.
48810×10^{-6} mm.	1.1 amps.	0.3194 ohm	157° C.	0.3865 joule

After admitting oxygen :—

Pressure of mixture.	Current.	Resistance of wire.	Temperature.	Energy lost per second.
48810×10^{-6} mm.	1.1 amps.	0.2942 ohm	128° C.	0.3561 joule

Inactive wire heated in a similar mixture :—

Pressure of mixture.	Current.	Resistance of wire.	Temperature.	Energy lost per second.
48810×10^{-6} mm.	1.1 amps.	0.2902 ohm	131° C.	0.3620 joule

A series of experiments, of which it is unnecessary to give the details here, were next performed. These established the following facts :—

- (a) The oxide film can be removed from an inactive wire by heating it in a vacuum to dull redness for 90 minutes. After this treatment the accommodation coefficient between the surface and hydrogen was identical with that given by thoroughly reduced silver, and the wire became active.*
- (b) An inactive wire cannot be rendered active by its being heated in a mixture of hydrogen and oxygen at any temperature.
- (c) That to render a wire inactive it must be heated to a temperature of at least 440° C. either in oxygen or in a mixture of hydrogen and oxygen, provided that the pressure of the oxygen does not considerably exceed 0.5 mm. Hydrogen mixed with the oxygen does not prevent the wire from becoming inactive.

We have assumed above—probably without sufficient explicit justification—that the films of inactive and active oxide almost completely cover the surface of the silver. An estimate of the upper limit of the proportion of

* Chapman, Ramsbottom and Trotman, *loc. cit.*

uncovered silver at the surface of an inactive wire can be obtained from the following considerations. Assume for this purpose that water cannot be formed at all at the surface of the inactive oxide. The rate of combination of hydrogen and oxygen would then be equal to the product of the rate of combination under the same conditions at the surface of a similar active wire and the proportion of uncovered silver at the surface of the inactive wire. But under the same conditions of temperature and pressure the rate of combination of hydrogen and oxygen is at least 100 times greater at the surface of an active wire than at the surface of an inactive wire. This proves that under the assumption made the proportion of uncovered silver at the surface of the inactive wire cannot exceed one hundredth. If, however, we may assume that water can be formed at the surface of the inactive oxide, we should have to conclude that the proportion of uncovered silver was still less.

The fact, that the accommodation coefficient with hydrogen of a surface covered with inactive oxide is almost identical with that of a surface covered with active oxide, supports the view, that the active oxide almost completely covers the surface of the silver. The conclusions also receive support from the following experiment.

F. G. Keyes and R. Hara* have determined the equilibrium pressure of oxygen over silver and silver oxide, and have obtained the following results :—

Temperature (° C.)	200	300	400
Equilibrium pressure (atmospheres)	1.75	19.8	109.2

Extrapolation from these results gives the dissociation pressure of silver oxide at 181° C. as 1 atmosphere. Therefore a silver wire heated at a temperature below 181° C. in oxygen at atmospheric pressure ought to become completely covered with silver oxide.

A metallic silver wire was heated in oxygen at a pressure of 1 atmosphere to 300° C., and during a period of 24 hours the temperature was gradually reduced to 150° C. After cooling the oxygen was removed, the apparatus washed out with hydrogen, and the accommodation coefficient between the wire and hydrogen determined. No difference could be detected between the amount of heat removed by hydrogen molecules from a wire treated in this way, and that, from the wire oxidised by the various methods already described. In fact a metallic silver wire, which had been exposed to oxygen at a pressure as low as 100×10^{-6} mm. at 16° C. was tested in a similar way, and found to communicate to molecules of hydrogen nearly an identical amount of heat.

* 'J. Amer. Chem. Soc.,' vol. 44, p. 479 (1922).

It therefore seems possible to cover the surface of silver almost completely with oxide at all temperatures below 400°C. , although the pressure of oxygen used may be far smaller than the equilibrium pressure over silver oxide and silver at that temperature. Theoretically this is possible and to be expected, although, of course, the formation of a separate oxide phase could not occur in oxygen at a pressure below the equilibrium pressure. Below this pressure the depth of the film could not much exceed the order of molecular diameters.

Oxygen taken up by silver cannot be removed by exhaustion at 16°C. and is therefore not adsorbed oxygen. It is certainly combined chemically with the silver in the form of a surface compound, whose dissociation pressure is very small at 16°C.

Making corrections for the heat loss due to metallic conduction and direct radiation, we have determined the accommodation coefficient of hydrogen (temperature 16°C. and pressure $48810 \times 10^{-6}\text{ mm.}$) at a silver surface heated to 100°C. and found it to be 0.25.* The corresponding accommodation coefficient of an oxidised silver surface was found to be 0.28.

Second Series of Experiments performed with a large Surface of Silver.

In this series of experiments the effective surface of the silver was two hundred times greater than in the experiments described above. The direct measurement of the oxygen in the surface films of oxide was thereby made possible, and the results thus obtained have confirmed the conclusions drawn from the first series of experiments. Obviously as under the same conditions, the rate of formation of water from its elements was so very much more rapid the determinations of catalytic activities had to be made at much lower temperatures. Although the results confirmed generally those obtained with the short electrically heated wire there was one difference to which attention must be drawn. After long use, i.e., after its surface had been oxidised and reduced a great number of times, both the active and inactive oxide films were reducible at lower temperatures, and were also catalytically more active. This effect was probably due to the fact that the fused quartz reaction chamber, which had been substituted for one made of glass, could be more effectively cleaned by heating. The same effect was observed with the short wire, but it was not so pronounced.

One hundred and nine metres of silver wire were cut into lengths of 5 metres each. These were folded and introduced into a quartz tube of 100 c.c. capacity. The wide quartz tube terminated in a long narrow neck at the end of which

* *Vide* Soddy and Berry, 'Roy. Soc. Proc.,' A, vol. 84, p. 576 (1911).

was a ground joint used for connecting it with the rest of the apparatus. The ground joint was lubricated with metaphosphoric acid. As before the catalyst was protected from impurities and mercury vapour by U-tubes immersed in liquid air. The heating of the silver to temperatures below 150° C. was accomplished by immersing the quartz tube in a thermostat, and to higher temperatures by surrounding the tube with a furnace.

Experiment I B. showed that silver which had been completely outgassed in a vacuum at a red heat did not absorb a measurable amount of hydrogen at moderate temperatures, but dissolved an appreciable quantity of the gas at a red heat. The dissolved hydrogen could not be removed in a vacuum at a temperature below a red heat.

Experiment II B established the following facts :—

At 16° C. metallic silver will adsorb enough oxygen to cover its entire surface with a layer of silver oxide. The oxidation was initially very rapid even at the lowest pressures, and practically ceased after 5 minutes. The pressure of oxygen in equilibrium with the oxide could not be measured, and no oxygen could be removed by exhaustion. The oxide was readily reduced by hydrogen at 16° C., and nearly all of it could be removed by this means in 12 hours. After reduction it was possible to reform the oxide layer and to synthesise indefinite amounts of water by repeating the alternate oxidation and reduction.

There seems, therefore, to be no reason why a mixture of hydrogen and oxygen should not by alternate oxidation and reduction of the silver at 16° C. be completely converted into water. Since the oxidation is much faster than the reduction, the silver is during the synthesis almost completely covered with oxide. Furthermore, the rate of formation of water must be the same as the rate of reduction of this oxide and therefore proportional to the partial pressure of the hydrogen. That the rate is proportional to the partial pressure of the hydrogen and independent of that of the oxygen has been shown to be the case by W. A. Bone and R. V. Wheeler* and by A. F. Benton and J. C. Elgin.†

The mass of silver used was 58.265 grm. Its volume was 5.554 c.c., and its total surface 872.545 sq. cm.

The number of gram atoms of oxygen required to oxidise the surface atoms of the silver completely (assuming that the faces (100), (110) and (111) are present at the surface in equal proportions) is 0.833×10^{-6} .

The silver was heated to redness in hydrogen, and the occluded hydrogen

* *Loc. cit.*

† 'J. Amer. Chem. Soc.,' vol. 48, p. 3027 (1928).

subsequently removed at a red heat in a vacuum. The results are tabulated below :—

	Duration of treatment.	Temperature.	Oxidation.	Reduction.
			Number of gram molecules of Ag_2O formed.	Number of gram molecules of Ag_2O removed.
		° C.		
1st oxidation	5 minutes	16	1.38×10^{-6}	
1st reduction	90 minutes	16		1.19×10^{-6}
2nd oxidation	5 minutes	16	1.10×10^{-6}	
2nd reduction	90 minutes	16		1.14×10^{-6}
3rd oxidation	5 minutes	16	1.12×10^{-6}	
3rd reduction	90 minutes	16		1.14×10^{-6}
4th oxidation	5 minutes	16	1.11×10^{-6}	
4th reduction	12 hours	16		1.29×10^{-6}
5th oxidation	5 minutes	16	1.18×10^{-6}	
5th reduction	4 hours	16		1.19×10^{-6}
6th oxidation	5 minutes	16	1.12×10^{-6}	

After this treatment the catalyst was shown to be quite active. At 16°C . a mixture of hydrogen and oxygen in the ratio 4 : 1 and at a pressure of 131600×10^{-6} mm. combined to completion upon it in 60 minutes. The excess of hydrogen in the mixture afterwards reduced the surface oxide in the usual way.

Experiment III B showed that a metallic surface can be formed by long heating of silver containing dissolved oxygen to redness in a vacuum. Dissolved oxygen is removed much more slowly by this method than by reduction with hydrogen, so that the process lasts many days, and even then is probably not quite complete. Tested as above the wire furnished the results recorded below.

	Duration of treatment.	Temperature.	Oxidation.	Reduction.
			Number of gram molecules of Ag_2O formed.	Number of gram molecules of Ag_2O removed.
		° C.		
1st oxidation	5 minutes	16	1.00×10^{-6}	
1st reduction	12 hours	16		0.93×10^{-6}

Experiment IV B.—An inactive film of silver was formed on the surface of the catalyst by heating the quartz vessel, previously filled with oxygen, at a

pressure of 2 mm. to redness with a furnace. By this treatment the surface was rendered inactive. Its temperature had to be raised to 100° C., before the rate of combination of hydrogen and oxygen in contact with it equalled the rate of formation of water from an identical mixture in contact with the activated surface at 16° C. Furthermore the oxide was not reduced by hydrogen at a measurable rate below 100° C. At 150° C., however, the reduction proceeded readily until approximately a unimolecular layer of oxide had been removed. By this treatment the efficiency of the metal as a catalyst had been considerably increased—despite the large quantity of dissolved oxygen which it still contained—as the following results show.

	Duration of treatment.	Temperature.	Oxidation.	Reduction.
			Number of gram atoms of oxygen taken up.	Number of gram atoms of oxygen removed.
1st reduction	1½ hours	150		1.15 × 10 ⁻⁶
oxidation	5 minutes	16	0.56 × 10 ⁻⁶	
reduction	12 hours	16		0.47 × 10 ⁻⁶
oxidation	5 minutes	16	0.46 × 10 ⁻⁶	
reduction	12 hours	16		0.43 × 10 ⁻⁶
oxidation	5 minutes	16	0.46 × 10 ⁻⁶	

In the presence of the wire, a mixture of hydrogen and oxygen in the ratio 4 : 1 and at a pressure of 99810×10^{-6} mm. combined to completion at 16° C. in 3 hours.

Experiments V B, VI B and VII B confirm the view that the dissolved oxygen contained in the less active form of silver is not the direct cause of its inactivity.

Experiment V B.—Silver was heated at 150° C. in oxygen ; and an appreciable amount of the gas was dissolved. Yet the catalytic activity of the metal was not thereby diminished. Of the oxygen taken up by the silver only that portion was removed by hydrogen at 16° C. which existed as oxide on its surface. The results of the examination of the properties of the catalyst are shown below on p. 492.

The reaction between hydrogen and oxygen in a mixture containing four volumes of the former to one volume of the latter gas at a total pressure of 91240×10^{-6} mm. was complete after 50 minutes at a temperature of 16° C.

	Duration of treatment	Temperature.	Oxidation.	Reduction.
			Number of gram atoms of oxygen taken up.	Number of gram atoms of oxygen removed.
		° C.		
1st oxidation	20 hours	150	5.69×10^{-6}	
reduction	12 hours	16		1.40×10^{-6}
oxidation	5 minutes	16	0.78×10^{-6}	
reduction	12 hours	16		0.97×10^{-6}
oxidation	5 minutes	16	0.65×10^{-6}	

Experiment VI B.—Silver was heated in oxygen at a pressure of 2.23 mm. to saturation at 400° C. At this temperature oxygen was rapidly occluded by the metal, and a large volume of gas went into solution. Nevertheless the rate of combination of hydrogen and oxygen at 16° C. at the surface of the metal after this treatment was not less than one half of that observed when the combination occurred under the same conditions at the surface previously oxidised at a low temperature. To reduce the catalytic activity of the oxide film appreciably the metal must be heated in oxygen at a temperature not below 440° C.; but at these temperatures the solubility of oxygen in silver, for the pressures of gas employed, is considerably less than at 400° C.

Experiment VII B.—Silver was saturated with oxygen at a red heat and after cooling shown to be an inactive catalyst. Reduction of the surface oxide on this catalyst by hydrogen at 150° C. followed by complete replacement of the oxide by treatment with oxygen at the same temperature rendered the surface catalytically active.

Conclusions.

1. When a surface of metallic silver is brought into contact with gaseous oxygen in sufficient quantity to form more than a complete unimolecular layer of oxide at the temperature of the laboratory, it becomes coated almost immediately with a film of silver oxide, and very little, if any, of the surface is left unoxidised.

2. When metallic silver is heated to redness in oxygen and allowed to cool in the gas a film of oxide is also formed at the surface.

3. The film of oxide formed at a low temperature catalyses the combination of hydrogen and oxygen much more readily than the film formed at a high temperature, and is also more easily reducible by hydrogen.

4. It is assumed as a working hypothesis that in the active film, formed at a low temperature, some of the molecules of silver oxide are in relatively unstable positions, but that on raising the temperature, the arrangement of these molecules becomes a more stable one, and the film in consequence becomes less chemically active.

5. The mechanism of the catalysis of the union of hydrogen and oxygen by the film is one of alternate reduction and reoxidation of the film.

Experiments are now being conducted with a view to determining more precisely the character of the change which takes place when an unstable oxide film becomes stable.

A Detailed Study of the "Radioactive Decay" of, and the Penetration of α -Particles into, a Simplified One-Dimensional Nucleus.

By R. H. FOWLER, F.R.S., and A. H. WILSON.

(Received April 20, 1929.)

§ 1. *Introduction.*—Gamow's* elegant deduction by general arguments of the law of radioactive decay by α -particle emission and his subsequent investigations on artificial disintegration suggested to us the desirability of investigating as closely as possible any simple model of a decaying nucleus as a verification of his general approximations. For the model chosen the exact investigation of the decay process is almost trivial. Since we obtained this, now some time ago, Dr. Gamow informed us that he had also obtained equivalent detailed results. Still more recently such results have been published by Kudar.† We shall not therefore dwell upon them here. The application of the same ideas, however, to the reverse process of penetration presents points of very definite interest, which we think are well worth discussion. The main point that arises is that the chance of penetration depends (or appears to depend) on whether the energy of the incident α -particle is or is not equal to a characteristic energy of the nucleus itself. This is a point which is not dealt with by

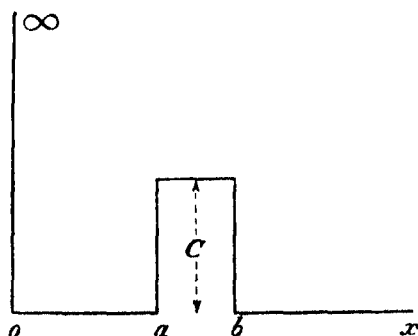
* Gamow, 'Z. Physik,' vol. 51, p. 204 (1928); Gamow and Houtermans, 'Z. Physik,' vol. 52, p. 496 (1928); Gamow, 'Z. Physik,' vol. 52, p. 510 (1928).

† Kudar, 'Z. Physik,' vol. 53, pp. 61, 95, 134 (1929).

Gamow in his paper. We have discussed it with him, and now put forward the results we have obtained.*

Since the solution of the decay problem is required in the main discussion of the penetration of α -particles into the nucleus it is included here in § 2 for reference. We must emphasise that we claim no novelty, except of detail, for the work of § 2; the general lines by now are a matter of fairly common knowledge.

§ 2. *Exact Solution of a Simple Problem of Radioactive Decay.*—We consider a one-dimensional problem with the potential energy U shown in the figure.



The solution we require is to represent at $t = 0$ as nearly as possible a standing wave confined to the "nucleus" between 0 and a , of energy E_0 ($< C$) representing one α -particle of this energy. To the right it is to contain waves travelling to the right only, representing the possibly escaping α -particle. All the wave-functions may be affected by a decay factor $e^{-\lambda' t}$, $\lambda' > 0$. We proceed to verify by construction that such solutions exist.

The wave function satisfies the equation

$$\frac{\partial^2 \Psi}{\partial x^2} - \kappa^2 \left\{ U + \frac{\hbar}{2\pi i} \frac{\partial}{\partial t} \right\} \Psi = 0 \quad \left(\kappa^2 = \frac{8\pi^2 m}{\hbar^2} \right), \quad (1)$$

where m is the mass of the α -particle. We assume a time factor of the usual form, so that

$$\Psi = \psi e^{-2\pi i E t / \hbar}, \quad (2)$$

but allow that

$$E = E_0 - i\lambda'. \quad (3)$$

* We should like to record here that Mr. R. W. Gurney has also observed in a letter to us that the difference between α -particles with energies equal or unequal to a characteristic of the nucleus had been overlooked by Gamow in his original paper on penetration.

For $0 < x < a$, since $\psi(0) = 0$ on the rigid boundary,

$$\Psi = A \sin \kappa \sqrt{E} x e^{-2\pi i E t / \hbar}. \quad (4)$$

For $a < x < b$,

$$\Psi = [B e^{-\kappa \sqrt{(C-E)}(x-a)} + B' e^{\kappa \sqrt{(C-E)}(x-a)}] e^{-2\pi i E t / \hbar}. \quad (5)$$

For $x > b$,

$$\Psi = D e^{i\kappa \sqrt{E}(x-b) - 2\pi i E t / \hbar}. \quad (6)$$

The conditions of continuity at $x = a$ and $x = b$ are

$$\begin{aligned} A \sin \kappa \sqrt{E} a &= B + B', \\ A \cos \kappa \sqrt{E} a &= (-B + B') \sqrt{\frac{C-E}{E}}, \\ D &= B/\vartheta + B'\vartheta, \\ iD \sqrt{\frac{E}{C-E}} &= -B/\vartheta + B'\vartheta, \end{aligned}$$

where

$$\vartheta = e^{\kappa \sqrt{(C-E)}(b-a)}.$$

These conditions can all be satisfied if and only if

$$\begin{aligned} 0 &= \sin \kappa \sqrt{E} a + \sqrt{\frac{E}{C-E}} \cos \kappa \sqrt{E} a \\ &\quad - \frac{1}{\vartheta^2 C} [C - 2E + 2i \sqrt{E(C-E)}] \left[\sin \kappa \sqrt{E} a - \sqrt{\frac{E}{C-E}} \cos \kappa \sqrt{E} a \right]. \end{aligned} \quad (7)$$

The condition that the solution shall be nearly a standing wave confined to the "nucleus" $0 < x < a$ is that ϑ is very large. The characteristics of the problem—the roots of (7)—are therefore to be obtained on that basis. To a first approximation, $\vartheta = \infty$, the values of E are the roots of

$$\tan \kappa \sqrt{E} a = -\sqrt{\frac{E}{C-E}}, \quad (8)$$

or

$$\kappa \sqrt{E} a = n\pi - \arctan \sqrt{\frac{E}{C-E}}, \quad (9)$$

the arc tan being taken between 0 and $\frac{1}{2}\pi$. We denote any one of these by E_0 . Then very roughly

$$E_0 = \frac{n^2 \pi^2}{a^2 \kappa^2} = \frac{n^2 \hbar^2}{8a^2 m}. \quad (10)$$

In the next approximation ϑ is so large that the new real term is trivial and

one may retain only the new imaginary term. Putting $E = E_0$ in the small part and using (8), the equation (7) becomes

$$\tan \kappa \sqrt{E}a = -\sqrt{\frac{E}{C-E}} - \frac{4iE_0}{9^2C}, \quad (11)$$

which to this approximation is equivalent to

$$\begin{aligned} \kappa \sqrt{E}a &= n\pi - \arctan \left\{ \sqrt{\frac{E}{C-E}} + \frac{4iE_0}{9^2C} \right\}, \\ &= n\pi - \arctan \sqrt{\frac{E}{C-E}} - \frac{4i(C-E_0)E_0}{9^2C^2}. \end{aligned} \quad (12)$$

Hence $E = E_0 - i\lambda'$ where

$$\lambda' = \frac{8(C-E_0)E_0^2}{9^2C^2} \frac{1}{\kappa \sqrt{E_0}a + \sqrt{\frac{E_0}{C-E_0}}}. \quad (13)$$

In order that ϑ should be large it is not necessary that $C \gg E_0$, but obviously we may assume that it is not true that $C - E_0 \ll E_0$. Thus the last denominator in (13) is nearly $n\pi$.

We now return to the conditions of continuity, which reduce with sufficient accuracy to

$$B = \frac{1}{2}A \left(\sin \kappa \sqrt{E}a - \sqrt{\frac{E}{C-E}} \cos \kappa \sqrt{E}a \right) = (-)^{n-1} A \sqrt{\frac{E_0}{C}}, \quad (14)$$

$$B' = \frac{B}{9^2C} [C - 2E_0 + 2i\sqrt{E_0(C-E_0)}], \quad (15)$$

$$D = (-)^{n-1} \frac{2A}{9^2C} [C - E_0 + i\sqrt{E_0(C-E_0)}] \sqrt{\frac{E_0}{C}}. \quad (16)$$

The absolute values must be fixed by a normalising condition at $t = 0$, which is necessarily partly arbitrary. If we take it to be

$$\int_0^b \psi \psi^* dx = 1,$$

and neglect terms of order 9^2 compared with the leading terms we find

$$|A|^2 = \frac{2}{a} \frac{1}{1 + 1/(\kappa \sqrt{C-E_0})a}. \quad (17)$$

This is the same result as we should find from the natural normalising condition

$$\int_0^\infty \psi \psi^* dx = 1$$

for a potential barrier of height C extending from $x = a$ to $+\infty$. We can only obtain (17) by integrating far enough past $x = a$ for the wave-functions to have become negligible. The result (17) is certainly right. Of course ψ^* is determined by an equation whose characteristics are $E^* (= E_0 + i\lambda')$ but the differences between E , E^* and E_0 do not give significant terms in the normalisation at $t = 0$.

We can now check up Gamow's interpretation of λ' and its connection with the outward flux of particles. On account of λ' , $\Psi^*\Psi^*$ contains the time factor

$$e^{-2\pi i(E-E^*)t/\hbar} = e^{-4\pi\lambda' t/\hbar}.$$

The solution normalised to unity in the nucleus at $t = 0$ decays thereafter at a rate $e^{-\lambda t}$, where

$$\lambda = \frac{4\pi\lambda'}{\hbar} = \frac{16(C-E_0)E_0^2}{\sqrt{(2m)a^3C^2}} \frac{1}{1 + 1/\{\kappa\sqrt{(C-E_0)a}\}}. \quad (18)$$

On the other hand the outward flux in particles per second is given by the well known formula

$$\frac{\hbar}{4\pi m i} \{\Psi^* \text{grad } \Psi - \Psi \text{grad } \Psi^*\}.$$

To evaluate this we have

$$\Psi = D e^{i\kappa\sqrt{E}(x-b) - 2\pi i E t/\hbar}, \quad \Psi^* = D^* e^{-i\kappa\sqrt{E^*}(x-b) + 2\pi i E^* t/\hbar},$$

so that the flux is equal to

$$2\sqrt{\frac{E_0}{2m}} |D|^2 e^{-\lambda t + \lambda \sqrt{\frac{m}{2E_0}}(x-b)}. \quad (19)$$

The flux past a given plane must, of course, decay at rate $e^{-\lambda t}$ and must depend on the position of the plane as shown by (19), since, as Gamow has pointed out, particles reaching that plane at a given time correspond to a state of affairs at a previous time in the nucleus. Near the nucleus and near $t = 0$ the flux is therefore

$$2\sqrt{\frac{E_0}{2m}} \cdot \frac{4E_0(C-E_0)}{a^3C^2} \cdot \frac{2}{a} \frac{1}{1 + 1/\{\kappa\sqrt{(C-E_0)a}\}} = \lambda.$$

This completes the verification in detail of Gamow's theory for this example, correct at every stage to terms of order \mathfrak{S}^{-2} .

§ 3. *The Converse Problem. The Penetration of α -particles into the Nucleus.*—So far we have merely put down, possibly with new details, results due to Gamow in a form convenient for our purpose. We will now try to study more

thoroughly than he has yet done, the converse problem of the penetration of an α -particle into a previously empty "nucleus." We observe at once that when ϑ is large the only possible solutions of the type studied in the last section are those for which the energy is almost exactly a characteristic of the completely isolated nucleus ($\vartheta = \infty$).

We will now investigate a problem in which there is a steady stream of α -particles incident on the nucleus from the right, which are reflected at the nucleus, and at the same time, of course, maintain a standing wave in the nucleus itself. This problem, one finds at once, is really steady, has real E but no characteristics. Solutions exist for all real E . With the potential energy of the figure we may take

$$\Psi = A_1 \sin \kappa \sqrt{Ex} e^{-2\pi i Et/h} \quad (0 < x < a), \quad (20)$$

$$\Psi = [B_1 e^{-\kappa \sqrt{(C-E)(x-a)} + B_1' e^{\kappa \sqrt{(C-E)(x-a)}}] e^{-2\pi i Et/h} \quad (a < x < b), \quad (21)$$

$$\Psi = [D_1 e^{-i\kappa \sqrt{E}(x-b)} + D_1' e^{i\kappa \sqrt{E}(x-b)}] e^{-2\pi i Et/h} \quad (b < x). \quad (22)$$

The conditions of continuity at $x = a$ and $x = b$ are

$$A_1 \sin \kappa \sqrt{Ea} = B_1 + B_1',$$

$$A_1 \cos \kappa \sqrt{Ea} = (-B_1 + B_1') \sqrt{\frac{C-E}{E}},$$

$$D_1 + D_1' = B_1/\vartheta + B_1'\vartheta,$$

$$i(D_1 - D_1') \sqrt{\frac{E}{C-E}} = B_1/\vartheta - B_1'\vartheta.$$

The equations have solutions for all E , and on solving them we find that D_1 and D_1' are conjugate complex quantities,

$$|D_1| = |D_1'|, \quad (23)$$

$$D_1 = \frac{1}{4} A_1 \left[\vartheta \left\{ 1 + i \sqrt{\frac{C-E}{E}} \right\} \left\{ \sin \kappa \sqrt{Ea} + \sqrt{\frac{E}{C-E}} \cos \kappa \sqrt{Ea} \right\} \right. \\ \left. + \frac{1}{\vartheta} \left\{ 1 - i \sqrt{\frac{C-E}{E}} \right\} \left\{ \sin \kappa \sqrt{Ea} - \sqrt{\frac{E}{C-E}} \cos \kappa \sqrt{Ea} \right\} \right]. \quad (24)$$

Equation (23) characterises a steady state in which the flux of particles in the incident and reflected beams are equal. Equation (24) shows that in general $|A_1/D_1|^2$ is proportional to ϑ^{-2} , but that if E happens to be equal to E_0 , the real part of one of the characteristics of the first problem, then

$$D_1 = (-)^{n-1} \frac{A_1}{2\vartheta} \left\{ 1 - i \sqrt{\frac{C-E_0}{E_0}} \right\} \sqrt{\frac{E_0}{C}}. \quad (25)$$

In this case $|A_1/D_1|^2$ is of the order ϑ^2 instead of ϑ^{-2} . Thus the wave function inside the nucleus is negligible when $E \neq E_0$ compared with its value when $E = E_0$, and so the α -particles practically only penetrate into the nucleus (or at least only penetrate and stay in the nucleus, one cannot here determine which) when their energy is almost exactly that of a characteristic of the nucleus—that is, an energy capable of producing a type of resonance. Of course the agreement need not be absolutely exact—in order that $|A_1/D_1|^2$ should be of order ϑ^2 it is necessary that

$$E = E_0 \left\{ 1 + O\left(\frac{1}{\vartheta^2}\right) \right\}. \quad (26)$$

§ 4. *Chance of Entry of an α -particle into an Empty Nucleus.*—We can now determine the rate at which the α -particle enters the nucleus when (26) is satisfied or more correctly the chance of entry of the α -particle, by fitting together the solutions of §§ 2, 3 so as to give a negligible wave-function in $0 < x < b$ at time $t = 0$. To do this we have only to take $A_1 = -A$ and add the two Ψ 's. We then find, to a sufficient approximation,

$$\Psi = A_1 \sin \kappa \sqrt{E_0} x e^{-2\pi i E_0 t / h} (1 - e^{-\lambda t}) \quad (0 < x < a), \quad (27)$$

with a corresponding wave-function in $a < x < b$. Inside the nucleus $\Psi \Psi^*$ varies like $(1 - e^{-\lambda t})^2$, which gives the variation with time of the number of particles inside, or rather the chance that the α -particle has entered between the times 0, t . It will be noticed that this number or chance increases initially as t^2 , whereas a variation like t rather than t^2 might have been expected. But this is a usual feature of a resonance problem. The proper quantum theory interpretation will appear shortly.

The corresponding incident and reflected beams of α -particles are of intensities controlled by $|D_1|^2$ and $|D + D_1'|^2$ respectively, and it is easily verified after reduction that

$$|D + D_1'|^2 = |D_1|^2 \left\{ 1 - \frac{16(C - E_0)E_0}{C^2} (e^{-\lambda t} - e^{-\lambda t}) \right\}.$$

The total number of α -particles incident in the interval 0, t_0 is $\sqrt{\frac{2E_0}{m}} |D_1|^2 t_0$, and the number reflected is therefore

$$\begin{aligned} & \sqrt{\frac{2E_0}{m}} \int_0^{t_0} |D + D_1'|^2 dt \\ &= \sqrt{\frac{2E_0}{m}} |D_1|^2 t_0 - \sqrt{\frac{2E_0}{m}} |D_1|^2 \frac{16(C - E_0)E_0}{\lambda C^2} (1 - e^{-\lambda t_0}). \end{aligned} \quad (28)$$

It is easily verified that the last term is equal to

$$\left[\int_0^b \psi \psi^* dx \right]_{t_0}$$

so that there is the necessary conservation theorem, the excess of the incident over the reflected particles being equal to the "number" retained in the nucleus.

We have thus obtained a consistent set of formulæ which involve a hitherto unspecified time t_0 , and it is now necessary to attempt a proper interpretation. In the first place one observes that the occurrence of t_0 is a necessary consequence of Heisenberg's uncertainty principle and equation (26). Our formulæ only hold on the assumption that we know the energy of the α -particle with an error ΔE of order given by

$$\Delta E = E_0/\vartheta^2.$$

Such α -particles can only be associated with wave trains of length Δt , of order

$$\frac{\hbar \vartheta^2}{2\pi E_0}. \quad (29)$$

and this Δt may therefore be taken to be the t_0 which occurs in our formulæ. The chance that such an incident α -particle stays in the nucleus is then represented after (28) by

$$\frac{8(C - E_0) E_0}{C^2} \frac{(1 - e^{-\frac{1}{2}\lambda t_0})^2}{\frac{1}{2}\lambda t_0}.$$

Using (29) we find that

$$\frac{1}{2}\lambda t_0 = \frac{8(C - E_0) E_0^{\frac{1}{2}}}{C^2} \frac{1}{\kappa a + (C - E)^{-\frac{1}{2}}}.$$

This is very rough and a sufficiently accurate value when the hump is high is

$$\frac{1}{2}\lambda t_0 = \frac{8(C - E_0) E_0}{C^2} \frac{1}{\kappa a \sqrt{E_0}}.$$

With reasonable numerical values this is moderately large and $\kappa a \sqrt{E_0}$ moderately small. The chance of capture then approximates to

$$\kappa a \sqrt{E_0}.$$

For other values of E than E_0 we should conclude that the chance of capture is negligible.

After having drawn this distinction between $E = E_0$ and $E \neq E_0$ we have to ask if it has any significant application to any conceivable experiment. We

must confess at once that it cannot be of practical importance. The length of wave-train required by (29) is so long that our investigation cannot refer to the conditions of any conceivable experiment. We must be content therefore in this investigation in having found and discussed certain interesting theoretical features of the problem of artificial disintegration which were overlooked in earlier investigations.

Summary.

In this note we solve exactly for a simplified nucleus the problem of α -particle disintegration (determination of the *complex* characteristics of the wave-equation with the proper boundary conditions). We then proceed to discuss the converse problem of the penetration of an α -particle into the nucleus from without—a problem which is the basis of Gamow’s theory of *artificial* disintegration. We find that the problem *formally* depends very much on whether the energy of the incident α -particle is or is not equal to the real part of a characteristic of the nucleus bombarded. We show that this type of penetration has features characteristic of a resonance effect as one should expect. We show finally, however, that our solutions are not of *practical* importance as they do not correspond to the conditions of any conceivable experiment. Further progress has been made in a forthcoming paper by Gamow and Houtermans.

The Process of Coagulation in Smokes.

By H. S. PATTERSON, R. WHYTLAW-GRAY, F.R.S., and W. CAWOOD, Leeds University.

(Received February 1, 1929.)

It has been shown experimentally* for a variety of smokes that the process of coagulation follows to a first approximation the simple linear relation

$$\sigma = \sigma_0 + Kt$$

where σ is the particulate volume of the smoke at time t and σ_0 is the initial particulate volume obtained by extrapolation, K being a constant for a given cloud. In the smokes studied K was found to vary within fairly wide limits for the same substance, even when the conditions were apparently closely reproduced. At the time it seemed unlikely that these variations could be attributed to experimental error; and the evidence suggested that some important factors affecting the process had not been recognised. It was therefore decided to carry out further experiments on smokes and to study the possible influence of the degree of heterogeneity and of electrification, as well as the effect of size on the rate of coagulation. Before embarking on this programme, the process of counting was scrutinised, errors eliminated and the method improved.

A large mass of data has now been collected and certain definite results emerge which it is the object of this paper to present.

Method of Counting.

Prolonged experience with the method of counting has shown that the accuracy of individual points is largely determined by various subsidiary factors, the importance of which was not realised earlier. It is absolutely essential that the particles should be stationary in the microscope field during the short period in which a count is made. Originally it was believed that two taps rotating in phase, and thus giving a closed system, were necessary. We have since found that steadiness depends on other factors such as the rigidity of the mechanism, amount of the dead space, and perfection of the rotating tap, and that the large tap by which smoke entered the cell from the chamber is quite unnecessary. A considerable time was spent in tracing the sources of the irregular movements of the particles in the cell.

* 'Roy. Soc. Proc.,' A, vol. 116, p. 540 (1927).

The essential conditions for satisfactory working have been found to be perfect rigidity of the apparatus, reduction of the dead space on the exit side of the cell to a minimum, and perfection in the finish of the bore of the rotating tap so as to interrupt the stream sharply.

A new apparatus embodying these improvements has been made and used for a considerable period. With this the counting can be carried out more quickly and with greater accuracy. We find it possible with practice to count 60 to 80 fields per minute, the diaphragms being chosen of such a size that an average of 3 or 4 particles is seen. Under these conditions the particles are stationary in the field for about one-fifth of a second.

Experimental Results.

The first experiments were carried out with ammonium chloride, the smokes being produced as described before.*

Special precautions were always taken to ensure that the air in the chamber before dispersal was free from particulate matter, the test adopted being the practical absence of a visible Tyndall cone when the beam from an external arc lamp was focussed in the chamber. This is an extremely rigid test and with the filtering apparatus at our disposal there was always a slight indication of the path of the beam. This degree of purity corresponds in the cell to about 1000 visible particles per cubic centimetre.

The first series of experiments was carried out with different weight concentrations with the object of tracing the influence of size on the rate of coagulation. The weights volatilised were 60, 30, 15, 7.5, 3, 1 mg. per cubic metre. Contrary to previous experience the graphs obtained for the lower weight concentrations exhibited a well-marked curvature. Those above 15 mg., however, approximated to straight lines, the slopes of which tended to increase as the weight dispersed diminished. Moreover, the initial numbers decreased in the case of the smaller weight concentrations. These effects are well marked and are on the average quite outside any experimental error. The progressive change in the curves is best followed from the accompanying diagram drawn from the experimental results (fig. 1). It will be noted that the curvature which is great at first, diminishes rapidly and approximates later to straightness. Above a concentration of about 15 mg., curvature is as a rule imperceptible. This statement summarises the general results, but occasionally distinct exceptions were obtained. For example, there have been

* *Loc. cit.*, p. 546, methods 1 and 3.

observed sometimes 7.5 mg. clouds possessing all the characteristics of 3 mg. clouds, both as to number and curvature.

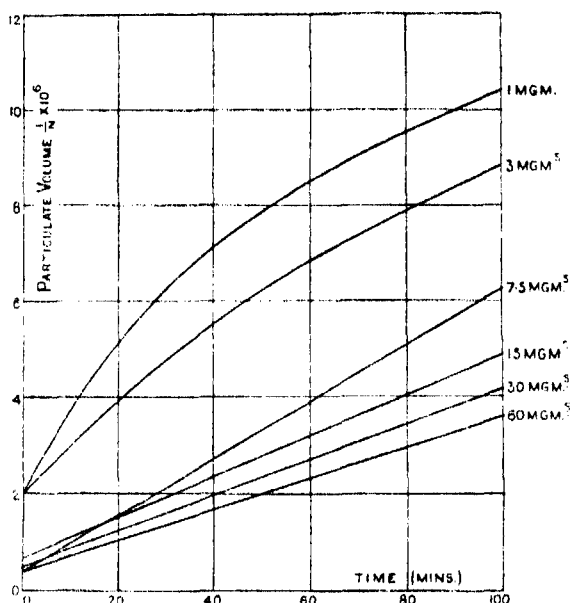


FIG. 1.—Typical Particulate Volume Curves of Ammonium Chloride Smokes, examined Dry.

Some of the particles in dilute clouds were exceedingly difficult to see and impossible to count accurately, and the question therefore arose as to whether microscopic particles were not also present. Experiments with other optical systems supported this possibility. It had previously been noticed that when precautions were not taken to dry the air in which the cloud was dispersed, the ammonium chloride particles appeared brighter in the cell. This observation led to an attempt to brighten them by condensing moisture around them. After some trouble it was found that the simple device of introducing a small roll of damped filter paper into the leading tube between the chamber and the cell was very effective in brightening the particles. Even in 1 mg. clouds in which previously the particles had been on the limit of visibility, no faint particles were to be seen. The cause of this condensation of moisture has been investigated and has been found to be due to traces of hydrogen chloride adsorbed on the particles. Since ammonium chloride dissociates on volatilisation, there is likely to be a slight loss of ammonia owing to its more rapid rate of diffusion, leaving an excess of hydrogen chloride which

condenses on the particles. It has been found that a smoke formed in the presence of a trace of ammonia does not show the brightening effect. Moreover it has been found possible to make the particles in smokes composed of non-hygroscopic materials such as alizarin, fluorescein, mercuric chloride and sodium chloride, brighten in moisture by the previous addition of traces of diluted hydrogen chloride gas to the air in the smoke chamber. Counting experiments with fine clouds showed a large increase in numbers by this procedure which could not be attributed to hydrogen chloride droplets, since in the absence of particulate matter, the same concentration of diluted hydrogen chloride gas gave no particles whatever.

Using this modification in the procedure, a new series of clouds of varying weight concentration was studied. The particulate volume curves are shown in fig. 2. In the first place it will be noted that for the small concentrations

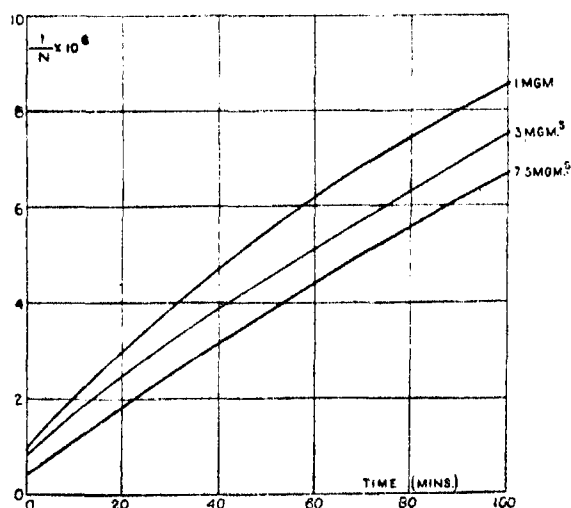


FIG. 2.—Typical Particulate Volume Curves of Ammonium Chloride Smokes, examined Wet.

the initial numbers are much greater, showing that in the previous experiments the finest particles were missed. Further, the curvature even at the lowest concentration is much slighter, which again is not incompatible with this idea. If it be assumed that all the particles in these clouds were counted, and there is every reason to suppose that very few particles were missed, we must conclude that the process of coagulation in dilute clouds is not a simple linear function of the time, and that the average value of K increases definitely with fall of weight concentration. Of course, these results do not explain why any given

cloud should be difficult to reproduce, or why occasionally marked deviations from these typical forms are encountered.

It seemed possible that the lack of reproducibility might in part be due to the weight concentration or the smoke differing on successive occasions from the actual amount volatilised. It seemed desirable to estimate the amount of solid matter present in the dispersed state. The estimation of small quantities of materials at these low concentrations presents difficulties. It was necessary to devise a method by which the particulate matter in a few litres of air could be determined. In the case of the more dilute clouds, the weight per litre was of the order of $5 \cdot 10^{-6}$ gms., that is, the method must detect at least 10^{-7} gm.

This can readily be estimated by the Nessler reaction, provided that all the ammonium chloride can be caught and dissolved in a relatively small volume of water. This might have been accomplished by using the microfiltration method employed in earlier investigations* but there was always the possibility that particles of a certain size range might pass through the filter. Since,

however, ammonium chloride is easily vaporised and in this state can be condensed quantitatively on a cooled surface, we decided to use this principle rather than that of filtration. Accordingly, an apparatus was devised in which the ammonium chloride smoke was first converted into vapour by passing through a heated glass spiral and then condensed out on a cooled surface. The apparatus is shown in fig. 3.

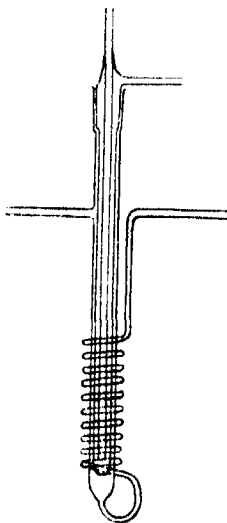


FIG. 3.

One or more litres of the cloud is sucked in slowly through the spiral, which is heated by an air bath to 400° – 500° C., when the vapour condenses on the surface of the water cooled inner tube. The inner tube is then removed and washed, and the ammonium chloride in a given volume of liquid determined by comparison in a colorimeter after addition of Nessler's reagent. Careful tests have been made to see whether

any ammonium chloride escapes precipitation or is carried through as particulate matter, but these all gave negative results. We have made a practice of always determining the weight concentration in duplicate, and the data for a given cloud generally agree as closely as can be expected. The amount is invariably smaller than the weights dis-

* 'Roy. Soc. Proc.,' A, vol. 102, p. 616 (1923).

persed from the heated boat, but there is no constant proportion between them, and obviously, the weight concentration in the cloud is difficult to reproduce by the present method. The appended table contains some of the results we have obtained.

Weight dispersed.	Weight concentration of cloud.
7.5	5.3
7.5	7.1
7.5	5.7
15.0	6.6
15.0	11.5
30.0	19.4
30.0	10.4
30.0	24.4

It is evident from these figures that the actual weight concentration of the smoke is invariably smaller than the weight volatilised ; moreover, there is no constant proportionality between the two. This has been found to be the case not only in the experiments cited, but in many other instances. Chance variations in the distribution of the ammonium chloride in the heated boat, and in the conditions during dispersal are probably the explanation of these anomalies.

The next step was to carry out another series of counting experiments with smokes of different concentrations in which the actual mass present in the particulate state was determined experimentally and not inferred from the weight volatilised from the boat. When this was done the previous haphazard variations were found to disappear, and in all cases the change in form of the curves was found to run parallel to the mass of material in the smoke. We do not wish to lay too much stress on the importance of this weight factor in determining the behaviour of a smoke, but other conditions being constant it is undoubtedly of considerable moment.

Ten smoke clouds produced on different occasions were investigated, and when the data were examined it was found that the results could be expressed by a comparatively simple formula. In all the ten clouds a similar degree of agreement between the experimental and calculated curves was obtained. Later on it will be shown that other factors have to be taken into account.

In figs. 4 and 5 are reproduced two of the ten smoke clouds, together with the curves calculated from the formula. The experimental points and the formula used for calculations are given in the appended tables.

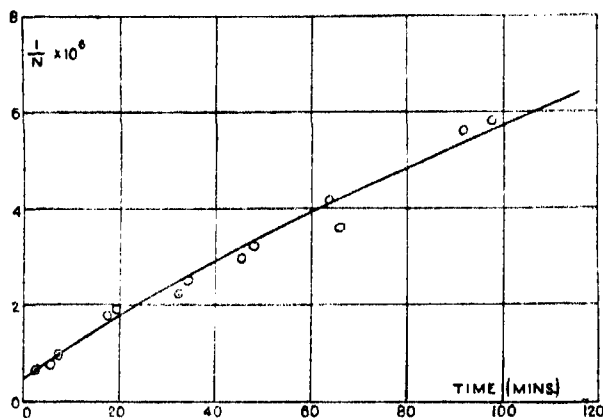


FIG. 4.—Particulate Volume Curve of Ammonium Chloride Smoke, examined Wet.
Concentration 5.7 mg./cu.m.

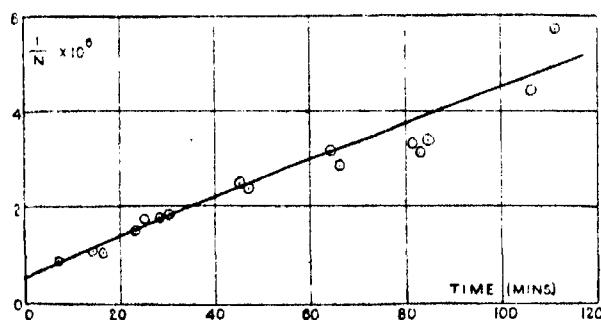


FIG. 5.—Particulate Volume Curve of Ammonium Chloride Smoke, examined Wet.
Concentration 24.4 mg./cu.m.

Table I.—Weight Concentration of Smoke 5.7 mg. per cubic metre.

Time from start. <i>t</i> minutes.	Number per c.c. $\times 10^{-6}$.	Particulate volume $\sigma \times 10^6$.
3½	1.52	0.66
6½	1.29	0.78
8	1.05	0.95
18	0.556	1.80
19½	0.520	1.92
33	0.451	2.22
35	0.401	2.50
46	0.339	2.95
48	0.311	3.21
64	0.239	4.18
66	0.280	3.57
92	0.179	5.58
98	0.173	5.78

The curve is drawn from the equation

$$t = \frac{\sigma - 0.4 \cdot 10^{-6}}{2.2 \cdot 10^{-8} \left[1 + \frac{9 \cdot 10^{-6}}{9.68 \cdot 10^{-4} \sigma^{\frac{1}{2}}} \right]^2}.$$

Table II.—Weight Concentration of Smoke 24.4 mg. per cubic metre.

Time from start, <i>t</i> minutes.	Number per c.c. $\times 10^{-6}$.	Particulate volume $\sigma \times 10^4$.
7½	1.18	0.85
14	0.923	1.08
16	0.930	1.08
23	0.694	1.44
25	0.613	1.63
28	0.580	1.72
30	0.560	1.79
45	0.394	2.54
47	0.418	2.39
64	0.314	3.18
66	0.361	2.77
81	0.310	3.22
83	0.315	3.17
85	0.305	3.28
108	0.226	4.42
113	0.175	5.72

The curve is drawn from the equation

$$t = \frac{\sigma - 0.4 \cdot 10^{-6}}{2.2 \cdot 10^{-8} \left[1 + \frac{9 \cdot 10^{-6}}{15.71 \cdot 10^{-4} \sigma^{\frac{1}{2}}} \right]^2}.$$

There is one noteworthy point which emerges when the experimental evidence presented so far is considered, viz., that many of the graphs are definitely curved, and that usually this curvature is most pronounced in the early stages of the smoke. Consequently the extrapolated values for σ_0 given previously (*loc. cit.*) are probably too high. Therefore it seemed important to explore the early stages of coagulation. Even with the improved counting method, however, it was not possible to obtain points earlier than some minutes after dispersal, and as at this stage coagulation is very rapid, little reliance can be placed on the extrapolated initial number. Extrapolation of the formula just mentioned which fitted the results pointed to the possibility that the true initial number might be indefinitely large. Were this the case we would have to conclude that the smoke was formed initially by molecular collision in contradistinction to the idea of condensation around nuclei already present.

This latter theory would set a limit to the initial number of particles determined by the number of nuclei, whilst no such limitation is imposed by the former.

In order to investigate this point it seemed only to be necessary to dilute the cloud as soon after formation as possible. In the first case a very large number of particles per cubic centimetre should be found, whilst if condensation had taken place on a limited number of nuclei, no large increase should be apparent. Accordingly it was arranged to blow a rapid stream of air over the volatilising material so that the smoke was diluted immediately after formation. When this was done it was at once evident that the number present in the chamber as soon as observation was possible had been very greatly augmented. Moreover, these blown smokes exhibited, when examined in the ultramicroscope, a greater uniformity in size. Whereas in the ordinary smokes the particles after coagulation has proceeded for an hour or so are markedly heterogeneous and fall past each other in the field, in the blown clouds all the particles appear to fall at more or less the same rate. The same disparity can be detected in the early stages, but it is not so apparent as the particles fall more slowly and exhibit rapid Brownian motion.

The exact degree of uniformity obtained depends largely on experimental conditions, such as rapidity of air stream, temperature of volatilisation, etc.

The arrangement used for the production of this type of smoke was to blow a stream of carefully-filtered and dust-free air at a known rate over the material heated in a metal boat to a definite temperature. The boat was placed in a cylinder and heated electrically by a spiral of nichrome ribbon enclosed in a silica tube. The blast emerged into the cubic metre chamber, the contents of which were briskly agitated by means of a revolving fan.

Normally on examining the smoke as soon as it was possible to count, the numbers were of the order of 5×10^6 per cubic centimetre. From the known rate of coagulation the numbers immediately after dispersal must have been considerably greater than 10^7 per cubic centimetre. Now the air blown over the boat had a volume of about 20 litres, whilst the chamber had a volume of 1000 litres. Consequently the number of particles per cubic centimetre in the blast was about 5×10^8 . But the blast was used to dilute the actual smoke formed by volatilisation. The volume of this cannot be estimated with certainty, but it is unlikely to exceed the volume of the saturated vapour at the temperature of volatilisation. For a cloud of 10 mg. of ammonium chloride we can suppose a maximum estimate of 10 c.c. so that in the instant before the first dilution, the number per cubic centimetre must have been at

least 10^{12} . It is obvious that if a small fraction of a second elapsed before the highly concentrated smoke was diluted by the blast the time would have been sufficient for aggregation from the molecular state to have taken place. If we were to assume that condensation took place on nuclei already present a number of the order of 10^9 per cubic centimetre would have to be postulated in carefully filtered air. This seems very unlikely, and we may therefore suppose that the process of coagulation is a continuous one from the molecular state. This view affords a simple explanation of the difference in type between the blown smokes and those dispersed in the usual way. In the latter the condensed vapour or concentrated smoke arising from the heated boat is not immediately diluted, and on account of the high number concentration and the temperature, coagulation takes place with great rapidity so that by the time dilution has been accomplished the smoke has become markedly heterogeneous. The effect of the blast is to arrest coagulation at a much earlier stage and so produce a more nearly homogeneous smoke containing a relatively large number of particles. Thus the graphs obtained in the former case express the later stages of the coagulation process, whilst the latter apply to the earlier stages of more homogeneous smokes.

It is easy too, in the light of these ideas, to see why it is so difficult to obtain smokes of the same behaviour on different occasions. Reproducibility depends not only on the same procedure for dispersal being followed, *i.e.*, temperature, weight concentration, etc., but also is conditioned by the time at which the very rapid initial coagulation is slowed down by dilution. It is clear that a fraction of a second may produce a large difference in the smoke. The difference between ammonium chloride smokes put up in the old way and those formed in the air stream is exemplified by the two curves shown in fig. 6 which are typical of a large number of results. It will be seen that in the blown curve not only are the numbers very much greater, but also the rate of coagulation tends to be slower. This at first sight is surprising, since it might be thought that the larger number of particles would correspond to a smaller average size; for we have shown (*loc. cit.*, p. 551) that theory indicates an increase in the rate of coagulation with decrease in average size. In reality, the average size, that is the size of the average particle in the blown cloud, is larger since, owing to the extreme heterogeneity of the other type, most of the mass is concentrated in a small number of large particles. As a result the most numerous particles which determine mainly the rate of coagulation are much smaller than would be anticipated from the weight concentration.

So far we have dealt only with ammonium chloride smokes, but the same

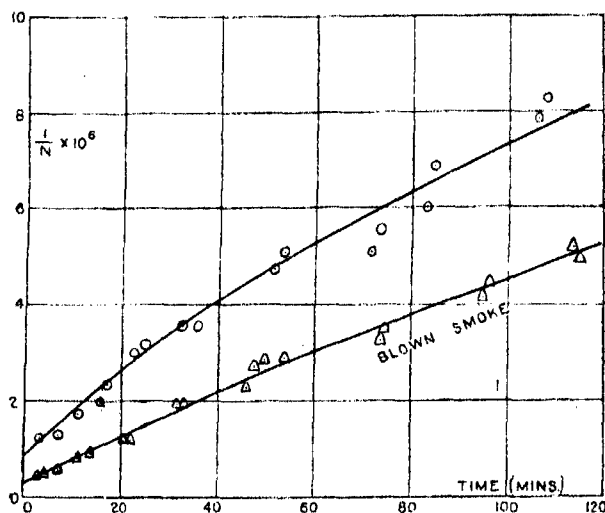


FIG. 6.—Particulate Volume Curves of Ammonium Chloride Smoke. Blown Smoke (lower curve) compared with smoke formed by the old method (upper curve).

difference in type has been found with other substances by varying the conditions of dispersal in this fashion. Characteristic results obtained with resin are reproduced in fig. 7. The actual experimental points are given and it will

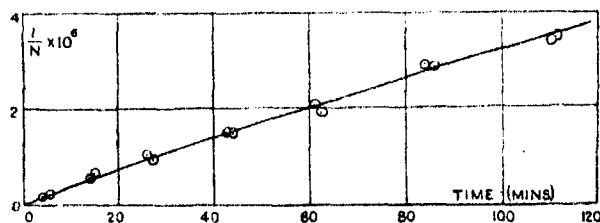


FIG. 7.—Particulate Volume Curves of Resin Smoke.

be noted that readings obtained with the blown clouds fall closer to the mean curve. This is due to the greater ease in counting when the particles are all approximately of the same brightness.

It is clear that the fresh experimental evidence furnished by this investigation shows that the simple linear relationship is not always followed, and, moreover, the rate at which coagulation takes place varies with the size of the average particle and the degree of heterogeneity of the smoke. The effect of size was foreseen theoretically, but the influence of differing degrees of heterogeneity was not recognised.

Collision Theory of Coagulation.

It is obvious that the theory previously advanced (*loc. cit.*) must be extended to embrace the experimental facts just described. Since the Smoluchowski theory was worked out only for the case of systems originally homogeneous, many simplifying assumptions were introduced. The underlying postulates of this theory and the modifications necessary to make it generally valid will now be considered.

Smoluchowski shows that the probability of encounter between a particle and others in its neighbourhood is $4\pi DS n$, where n is the number of particles per cubic centimetre, whilst D is the relative diffusion coefficient for any two particles, and S is the radius of the sphere of attraction between two particles for each collision considered separately. The total number of collisions is clearly $\frac{1}{2} (4\pi DS) n^2$, so that $2\pi DS$ is the coagulation constant.

In order to find an average value for the coagulation constant Smoluchowski proceeds as follows:—

Considering the collision between two unequal particles, it is clear that $D = D_1 + D_2$ where D_1 and D_2 are the respective diffusion coefficients, whilst for S , in conformity with collisions for molecules of gases, the value $S = \frac{1}{2} (S_1 + S_2)$ is assumed, S_1 and S_2 being the respective radii of the spheres of attraction.

Now Einstein has shown that the diffusion coefficient

$$D = RT/N.B,$$

where N is the Avogadro number, and B is the mobility. Assuming Stokes' equation for the mobility

$$D = D_1 + D_2 = \frac{RT}{6\pi\eta N} \left(\frac{1}{r_1} + \frac{1}{r_2} \right),$$

where η is the viscosity.

If now we assume that

$$S_1 = sr_1 \quad \text{and} \quad S_2 = sr_2$$

we find that

$$2\pi DS = \frac{2\pi RT (r_1 + r_2)}{6\pi\eta N (r_1 r_2)} \cdot \frac{S_1 + S_2}{2} = \frac{1}{6} \frac{RT}{\eta N} \left[\frac{(r_1 + r_2)^2}{r_1 r_2} \right] s.$$

If the colliding particles are of equal radii $r_1 = r_2$, and

$$2\pi DS = \frac{2}{3} \frac{RT}{\eta N} s.$$

When $s = 2$ the particles unite only when they come into contact, and

$$2\pi DS = \frac{4}{3} \frac{RT}{\eta N} = K,$$

where K is the ordinary Smoluchowski coagulation constant.

Suppose now that two particles of equal radius aggregate. The radius of the complex is proportional to $(2r^3)^{\frac{1}{3}} = 1.26r$, that is, approximately equal to r . Now even in the case in which a particle of radius 1 collides with a particle of radius 2, the value of the factor $(r_1 + r_2)^2/r_1 r_2$ is only increased in the ratio of 1.125 to 1, as compared with the collision of two unit or equal particles. Now it will be shown later that in a smoke originally homogeneous, collisions between particles with as great a difference in size as this are comparatively rare compared with the collisions between particles of nearly equal size. Consequently if we were to start from a cloud of homogeneous particles, provided that the degree of coagulation is not great, we might assume the same value $\frac{4}{3}RT/N$ for all the collisions, since the average value of $(r_1 + r_2)^2/r_1 r_2$ will not change appreciably. These are the assumptions on which the constancy of the Smoluchowski coagulation factor is based.

Now the measurements of Tuorila* for fairly homogeneous sols show a satisfactory agreement with the Smoluchowski constant as calculated above, indicating that $s = 2$, as assumed in calculating the constant. For dilute smokes, dispersed in a gentle stream of air, on the other hand, values of s of 4 or 5 may easily be obtained. Since there is no reason for supposing that the sphere of influence in the case of smoke particles is greater than that obtaining in sols, it is necessary to investigate how far smokes would be expected to have the same coagulation constant as sols.

Now in the case of many smokes, three of the assumptions made by Smoluchowski for sols do not hold good. In the first place the mobility is not given by Stokes' equation; in the second, smokes are so inhomogeneous initially that we cannot assume the simple value for $(r_1 + r_2)^2/r_1 r_2$; and, thirdly, the particles are not in general spherical.

In a previous communication† we have noted that in considering the coagulation of smokes, the Cunningham value for the mobility, namely $(1 + A\lambda/r)/6\pi\eta r$ should be used, in which A is a constant, and λ is the mean free path of the air molecules. Inserting this value into the equation for the diffusion we obtain

$$D = D_1 + D_2 = \frac{RT}{6\pi\eta N} \left[\frac{1 + A\lambda/r_1}{r_1} + \frac{1 + A\lambda/r_2}{r_2} \right].$$

* 'Koll. Chem. Beihefte,' vol. 24, p. 1 (1927).

† 'Roy. Soc. Proc., A,' vol. 116, p. 540 (1927).

If we assume a mean value r for r_1 and r_2 in the correction terms $A\lambda/r_1$ and $A\lambda/r_2$, we find

$$D = \frac{RT}{6\pi\eta} \left(1 + A\lambda/r\right) \left[\frac{1}{r_1} + \frac{1}{r_2}\right].$$

The error introduced by this procedure is not great provided we assign the proper mean value for r . Consequently the Smoluchowski coagulation factor becomes

$$K = \frac{1}{2} \frac{RT}{\eta N} \left[\frac{(r_1 + r_2)^2}{r_1 r_2} \right] (1 + A\lambda/r) s,$$

where r is the mean value of the radius for the particles in a cloud as a whole. For a homogeneous cloud this becomes

$$K = \frac{2}{3} \frac{RT}{\eta N} (1 + A\lambda/r) s.$$

From this equation, which we gave in the above-mentioned paper, it follows that the coagulation factor is not a constant for all clouds, but will vary from smoke to smoke depending on the average radius of the particles, and will also vary slightly during the coagulation of a given smoke. This latter variation gives rise to a slight curvature in the coagulation curve, but it is so small as to be outside the limit of experimental error, except for smokes in which the average size of particle is very small.

It is very difficult to assign practically the correct value to r . Strictly speaking, r is the radius of the average particle; that is, the weighted mean radius taking account of size and number. To calculate this requires a knowledge of the size distribution for each smoke, and this at present it is not practicable to obtain. The value which we have hitherto assigned, namely, the radius calculated from the average mass of a particle, is clearly incorrect, since if, as frequently happens, the smoke consists of a few large particles in which is concentrated most of the mass, and a large number of fine particles, a totally wrong radius will be obtained.

It may be noted that for a fairly coarse smoke, that is, one in which the radius of the average particle is greater than, say, $2 \cdot 10^{-5}$ cm., the term $(1 + A\lambda/r)$ does not differ greatly from unity and is in the nature of a correction term. For fine smokes, however, the term becomes large, and any error in the assignment of the correct value for r will cause an appreciable difference in the value of the coagulation factor. In the earliest stages of a smoke, soon after condensation it may approximate to a value of 100, and from this, in conjunction with the high concentration of particles obtaining at this time, it

follows that a high degree of complexity will be reached in a very short time interval.

We will now proceed to the consideration of the term $(r_1 + r_2)^2/r_1r_2$ in the Smoluchowski coagulation factor. This term has a minimum value of 4 for the collision of two particles of equal size. For the collision of different sized particles, the term may increase considerably, if there is a larger divergence of size. In the following table are given values of the factor divided by 4 for the collisions of particles of various sizes with one of unit size.

Size of particles colliding with unit particle.	$\frac{(r_1 + r_2)^2}{4r_1r_2}$
1	1.00
2	1.13
3	1.33
4	1.56
5	1.80
10	3.02
25	6.76
50	12.74
100	25.50

It is obvious from this table that particles differing greatly in size will unite very much more rapidly than those of equal size. In other words, if a smoke contains initially a number of large and fine particles, the fine particles will tend rapidly to become less numerous. The actual velocity with which this occurs will depend upon the mobility of the particles, that is, on their size. For a coarse smoke even if there is a considerable divergence of size, the term $(1 + A\lambda/r)$ will not differ greatly from unity, and consequently, though there is a tendency for the finer particles to disappear more rapidly than those of moderate size, this will take place slowly. For very fine particles, on the other hand, the term $(1 + A\lambda/r)$ may become 10 or 100, and in this case there will be a very rapid disappearance of the finest particles.

This furnishes an explanation of the very noticeable disappearance of the particles from many volatilised smokes after the lapse of a few minutes, and generally of the type of system which is formed. For a very short period, probably a small fraction of a second, after condensation, a considerable size range is present, but owing to the great mobility of these very fine particles, the finest tend to disappear almost instantly and leave a fairly homogeneous smoke. If now this smoke is rapidly diluted before coagulation to large particles of small mobility has taken place, a fairly homogeneous smoke will result, since any remaining fine particles will soon coagulate with the larger

ones. This case applies to the blown smokes. If, however, coagulation is allowed to proceed for a short period longer, a considerable size range comprising large particles of low mobility will be formed, and under these conditions the inhomogeneity with respect to the larger particles will tend to remain, and the ordinary type of smoke will be obtained. On further coagulation a homogeneous smoke will, of course, tend towards heterogeneity, but an inhomogeneous smoke may tend to become more homogeneous, since the rate of increase of size range due to coagulation may well be less than the decrease due to the disappearance of the smaller particles.

Now microscopic examination indicates that in a heterogeneous smoke, numbers of particles of the same order of magnitude are found for ranges of radius of 1 to 4 or 1 to 5, whilst the finest particles seen on the slide probably consist of more than one size range grouped together. In addition, the finest particles visible in the cell are almost certainly invisible on a slide examined by direct light. We may therefore assume that for an ordinary inhomogeneous cloud the range of radius to be taken into account is about 1 to 7. The effect of the presence of various size ranges on the average value of the factor $(r_1 + r_2)^2/4r_1r_2$, assuming that equal numbers of particles of the various radii are present, is indicated in the following table:—

Range of radius.	Average value of $\frac{(r_1 + r_2)^2}{4r_1r_2}$.
1	1.00
1 to 2	1.06
1 to 3	1.11
1 to 4	1.15
1 to 5	1.19
1 to 6	1.21
1 to 7	1.24
1 to 8	1.27

It will be seen that even a considerable size range has a comparatively small effect on the average value of the factor, that is, on the coagulation constant. This is due to the fact that by far the greater number of collisions take place between particles of approximately equal size, so that the large increase in the factor, due to divergence in size, is counterbalanced by the comparative rarity of such collisions. It may be noted that in calculating this table, it has been assumed that the factor $(1 + A\lambda/r)$ has the same value for each size of particles. Very little error is introduced by this assumption provided the particles are

not very small, as collisions in which the error would be appreciable are relatively few.

It might be supposed that, owing to the variation of the size range during coagulation, the average value of the factor $(r_1 + r_2)^2/4r_1r_2$ might change appreciably with time. In the case of a homogeneous cloud, the size distribution at any period has been calculated by Smoluchowski. From his size distribution it is easy to find the percentage of particles of various radii present at any period, and hence the average value of $(r_1 + r_2)^2/4r_1r_2$. In the following table are given the average values of the factor for a smoke originally homogeneous, when the number of particles has decreased owing to coagulation to 0.50, 0.25, 0.125 of the number originally present :—

Fraction of initial number of particles present.	Average value of $\frac{(r_1 + r_2)^2}{4r_1r_2}$.
1.00	1.00
0.50	1.01
0.25	1.09
0.125	1.16

It appears from this table that this factor, and so the coagulation constant, tends to increase slightly with time, especially in the later stages of the smoke, and that consequently a curvature opposite in sense to that produced by the factor $(1 + A\lambda/r)$ is introduced into the coagulation curves. Actually the effect is rather smaller than that calculated, since the more rapid combination of particles of divergent sizes tends to keep the smoke more uniform.

In the case of heterogeneous smokes the corresponding distribution equations have been worked out, but the labour involved in the arithmetical calculations is so great that numerical results have not been obtained. It seems clear, however, that the alteration of the factor with time should be less for a heterogeneous smoke owing to the greater influence of the above-mentioned tendency.

The opposed action of the two factors $(1 + A\lambda/r)$ and $(r_1 + r_2)^2/4r_1r_2$ has interesting consequences in the case of fine smokes, *e.g.*, 1 mg. For these smokes the coagulation graphs should exhibit an appreciable curvature, but actually it is sometimes found that they approximate closely to a straight line. It may be assumed that, in this case, the variation of the two factors compensates. In the case of coarse smokes it might be thought that an upward curvature should be obtained. Actually such smokes coagulate much more slowly owing to the smaller value of the factor $(1 + A\lambda/r)$. The range is

more restricted therefore after a given time, and so a marked curvature would not be expected. In practice an upward tendency is often noticeable, but owing to the rapid rate of fall of the larger particles in such smokes, the curvature would tend to be exaggerated by experimental error. It may be noted that whereas the effect of the factor $(1 + A\lambda/r)$ would be most marked in the early stages of the smoke, that of the factor $(r_1 + r_2)^2/4r_1r_2$ would appear mainly in the later stages. A sigmoid coagulation curve might thus be obtained, the coagulation being more rapid at first and latterly, whilst in the intermediate period it would be slower. Indications of such curves have, in fact, been obtained experimentally, but as the variations are small they almost fall within the limit of the error of experiment.

In addition to the factors hitherto considered which may exert an influence on the rate of coagulation, another assumption is made by Smoluchowski, which for many smokes does not hold good. In the deduction it is assumed that coagulation takes place between spherical particles, and since this applies to all stages of the coagulation process, it follows that the new particles formed by collision must also be spherical, that is, that the particles must be liquid. Now in the case of solids, even if we suppose the original particles to be spherical, those formed by coagulation will be irregular. This irregularity is unlikely to be pronounced unless chain formation takes place. Chain-like structures are, however, chiefly found in the highly-electrified smokes produced by volatilisation from an arc, and are not at all common in those made by the methods we have described. In the absence of such structures the rapid initial coagulation should tend, by the time that counts are possible, to have formed approximately spherical particles, and visual observation gives a general confirmation of this view. Now it has been shown by Millikan* that slight irregularities in the shape make very little difference to the rate of fall of a particle, so that in our case the mobility, and consequently the rate of coagulation, should be little affected. Actually, of the two substances used for producing the smokes discussed in this communication, resin forms particles which seem to be fluid when examined microscopically, whilst owing to the rapid absorption of water by the particles in volatilised ammonium chloride smokes, it seems likely that even in the comparatively dry air of the chamber irregularities would tend to be removed by solution. We may therefore assume that for the materials here considered, the error introduced by deviation of the shape from the spherical is small, if not entirely negligible.

From these considerations, it will be understood that it is a matter of extreme

* 'Physical Review,' vol. 22, p. 1 (1923).

difficulty to deduce an equation to represent the course of coagulation of smokes of varying weight concentration, even when all other factors are kept as constant as possible. We have not yet succeeded in finding a satisfactory method for determining the complete size distribution, and consequently it is impossible either to assign an accurate value for the size range or to take account of its variation with time. We can therefore only evaluate the factor $(r_1 + r_2)^2/4r_1r_2$ approximately, whilst even an approximate valuation of the average radius is open to grave errors.

These difficulties are, of course, most accentuated for the very heterogeneous smokes produced without an air blast. We have, however, found that the course of coagulation of all the smokes formed in this way for which we have measured the weight concentration, may be reproduced by the semi-empirical coagulation factor :—

$$K = \frac{2}{3} \frac{RT}{\eta N} \cdot 1.25 \left(1 + A \frac{\lambda}{r}\right)^2.$$

where r in this case is the average radius calculated from weight concentration and number. In this equation, the value 1.25 has been inserted for the factor $(r_1 + r_2)^2/4r_1r_2$ since experimentally it is probable that a range of radius from 1 to 7 is present with approximately equal numbers of each size. The square of the factor $(1 + A\lambda/r)$ has been introduced in order to endeavour to take account of the fact that the error in estimating the average radius from weight and number is much greater in the early stages of a smoke than in the later. This is apparent when we consider that in the early stages, whereas by far the greater part of the mass of the cloud may be concentrated in a comparatively few particles, the greater number may be very fine. On the other hand, in the later stages, the size of the average particle will be much greater owing to the tendency of the fine particles to disappear, and will be much nearer to the radius given from weight and number. It will, of course, be understood that this is a purely empirical way of introducing this correction, and that the index of the term might well be some number other than 2 for smokes of different heterogeneity. At the same time, the formula has the practical advantage of enabling the behaviour of these smokes to be closely reproduced.

Now we have previously shown that

$$\frac{2}{3} \frac{RT}{\eta N} = 1.76 \cdot 10^{-9} \text{ cm.}^2/\text{min.}$$

$$A\lambda = 9 \cdot 10^{-6}.$$

The coagulation equation therefore becomes

$$\sigma = \sigma_0 + 2 \cdot 20 \cdot 10^{-8} (1 + 9 \cdot 10^{-6} r^{-1}) t.$$

Since r is the average radius of the particles at any time estimated for the weight concentration and number, it follows that it will have different values at different times. For the purpose of calculation, it is convenient to express r in terms of σ , which may be done in the following way.

If M is the mass in grams per cubic metre of the cloud, n is the number of particles per cubic centimetre, and σ the particulate volume, the mass of each particle is $M \cdot 10^{-6}/n = M\sigma \cdot 10^{-6} = \frac{4}{3}\pi r^3 \rho$, where r is the average radius and ρ the density of the particles. Considering the particles as spheres, the average radius is therefore given by

$$r = (3M\sigma \cdot 10^{-6}/4\pi\rho)^{\frac{1}{3}} = (2 \cdot 39 \cdot 10^{-7} M\sigma/\rho)^{\frac{1}{3}}.$$

Inserting this value for r in the coagulation equation we have

$$\sigma = \sigma_0 + 2 \cdot 20 \cdot 10^{-8} [1 + 9 \cdot 10^{-6} (2 \cdot 39 M\sigma \cdot 10^{-7}/\rho)^{-\frac{1}{3}}]^2.$$

This equation cannot be easily solved for σ . The times corresponding to varying values of σ are therefore calculated from the equation in the form:—

$$t = \frac{\sigma - \sigma_0}{2 \cdot 20 \cdot 10^{-8} [1 + 9 \cdot 10^{-6} (2 \cdot 39 M\sigma \cdot 10^{-7}/\rho)^{-\frac{1}{3}}]^2}.$$

If we assume the density of the ammonium chloride particles to be normal, $\rho = 1 \cdot 5$, and the equation becomes

$$t = \frac{\sigma - \sigma_0}{2 \cdot 20 \cdot 10^{-8} [1 + 9 \cdot 10^{-6}/5 \cdot 42 \cdot 10^{-4} m^{\frac{1}{3}} \sigma^{\frac{1}{3}}]^2}$$

where m is the concentration of the smoke in *milligrams per cubic metre*. This equation was used for the calculation of the curves given in figs. 5 and 6. It will be seen that the agreement with the experimental points is as close as can be expected considering the assumption made in the deduction of the equation.

In the case of many of the blown smokes, the problem is considerably simplified. For these the size range seems to be sufficiently small for the factor to approximate to unity. Also, since large particles are to a great extent absent in the early stages, the value of r calculated from the weight concentration and number gives a fairly accurate measure of the radius of the average particle. Consequently, in these cases the coagulation process is very nearly in conformity with the simple formula previously given (*loc. cit.*, 551), viz.,

$$\sigma = \sigma_0 + 1 \cdot 76 \cdot 10^{-8} (1 + 9 \cdot 10^{-6}/r) t.$$

In this equation also it is, of course, necessary to take into account the variation of the average radius with time so that, as explained above, the formula becomes

$$\sigma = \sigma_0 + 1.76 \cdot 10^{-8} [1 + 9 \cdot 10^{-8} (2.39 M \sigma \cdot 10^{-7} / \rho)^{-1}]$$

or

$$t = \frac{\sigma - \sigma_0}{1.76 \cdot 10^{-8} [1 + 9 \cdot 10^{-8} (2.39 M \sigma \cdot 10^{-7} / \rho)^{-1}]}$$

The lower dotted curve given in fig. 8 is calculated from the formula for a blown resin smoke having a concentration of 15 mg. per cubic metre. It will be seen that this is in close agreement with the curve drawn through the experimental points. It must, however, be noted that the agreement is not so good

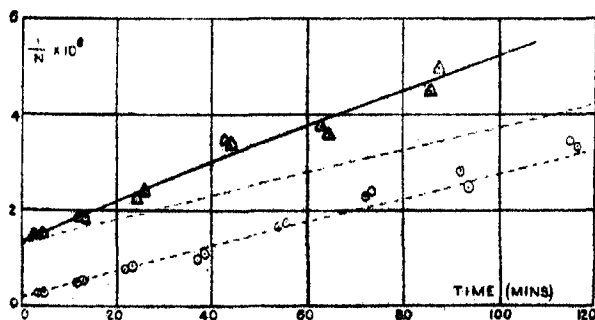


FIG. 8.—Particulate Volume Curves of Resin Smoke.

for all blown smokes. It is only when the conditions are such that the smoke produced is fairly uniform in the early stages that the simple coagulation formula is satisfactory. The upper curve refers to a 15 mg. resin smoke which was produced in the old way, that is, to a very heterogeneous smoke. The corresponding dotted curve is calculated from the simple formula, assuming that $\sigma_0 = 1.2 \times 10^{-6}$. It will be seen that in this case, which is typical of unblown clouds, there is a wide divergence between the theoretical and the practical curves.

The Structure and Electrification of Smoke Particles.

By H. S. PATTERSON, R. WHYTLAW-GRAY, F.R.S., and W. CAWOOD, Leeds University.

(Received April 25, 1929.)

[PLATES 4, 5.]

The experiments described in the previous paper refer to coagulating systems in which the particles are approximately spherical in form, and in which Brownian movement is mainly the cause of collision. It is evident that a simple theoretical treatment is applicable to this type only.

Before ammonium chloride and resin were selected for producing the smokes suitable for our purpose, a large amount of preliminary work was carried out on various systems in order to determine the form and structure of the particles, and also to discover whether electrification was a factor influencing the coagulation process to any marked extent. This work brought to light interesting facts which are of some consequence when attempting a general survey of aerial disperse systems.

STRUCTURE.

As regards structure the microscopic methods employed previously for large aggregates have been refined and improved so as to allow of the examination of the so-called ultra-microscopic particles present in these dilute smokes. The deposits were collected on microscopic cover-glasses and examined by means of a 2 mm. Leitz apochromatic objective in conjunction with a Koristka achromatic substage condenser. This combination was used dry (for contact with oil immediately alters the structure of the aggregates) but it gives approximately a two-thirds cone of illumination. For visual work a 58 or an H. Wratten light filter was used and for photography a C or a C + D. Sometimes it was advantageous to use dark ground illumination and then a Beck oil immersion dark ground focussing illuminator in conjunction with a 4 mm. Zeiss apochromatic objective was found to give the best results.

In general it has been found that the type of particle depends mainly on the method by which the smoke is produced. High temperature reactions and the arc discharge favour the formation of loose aggregates and a high degree of complexity whilst volatilisation at a lower temperature gives rise to larger particles of a more compact structure composed of relatively few units. Of

the first type we have studied the smokes of CdO, MgO, Ag and Au formed by the arc discharge in air and of the second As_2O_3 , HgCl_2 and a number of organic materials which can be volatilised at comparatively low temperatures.

Results.

(a) Arc Smokes.

Cadmium Oxide.—The complexes consist very largely of chains. The larger chains may be 10^{-8} cm. long and consist of hundreds of fine particles of the order of 10^{-5} cm. radius. The particles as photographed by transmitted light do not all appear to be in contact, but are separated by quite a definite space (Plate 4, fig. 1). Observation shows that this appearance is mainly due to the particles in the strings not all lying in the same plane, and consequently not all being simultaneously in focus, though it is possible that amicroscopic particles may be present. Some evidence for this has been advanced by Walmsley* as the result of an X-ray examination of similar material. With dark ground illumination the diffraction discs tend to fill up the gaps in the chain, but no greater degree of complexity is revealed. It is perhaps surprising that with particles of this small magnitude no Brownian motion is detectable in the chains, even when these project in free air.

Silver.—The chains for the dilute silver smokes studied are very much shorter and the packing is apparently closer.

Gold.—The greater number of particles in a gold smoke consist of chains and loose aggregates. Occasionally, as in the case of silver, large spheres are present, and these often have attached to them fine hair-like chains of particles.

Magnesium Oxide.—The particles in a smoke dispersed from an arc show a close resemblance to those of cadmium oxide. Intermingled with the fine particles forming the chains are, however, a few larger units, whilst occasionally single spheres of much larger size may be noticed. There is little indication of crystalline structure in the units of large size which can be resolved clearly; they produce the impression of somewhat irregular vitreous spheres (Plate 4, fig. 2).

A totally different type of particle is produced by burning magnesium ribbon in air. In this case the aggregates are built up of minute cubic crystals frequently united by their corners into systems of considerable complexity. Some of the larger consist of a single cube with a few smaller cubes attached at various points. The greater number of the particles are made up of minute apparent spheres, doubtless in reality cubes beyond the limit of resolution

* 'Proc. Phys. Soc.,' vol. 40, p. 7 (1927).

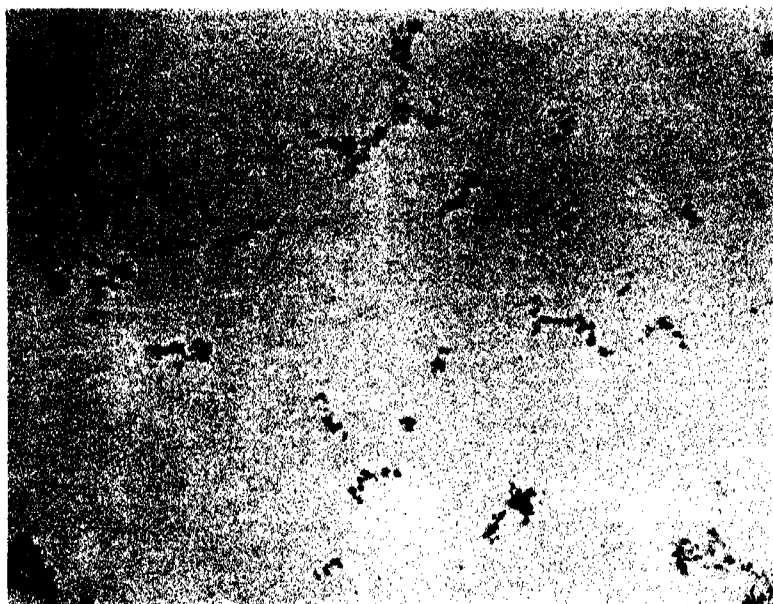


FIG. 1.—Cadmium Oxide ; Arc Smoke. ($\times 1500$.)

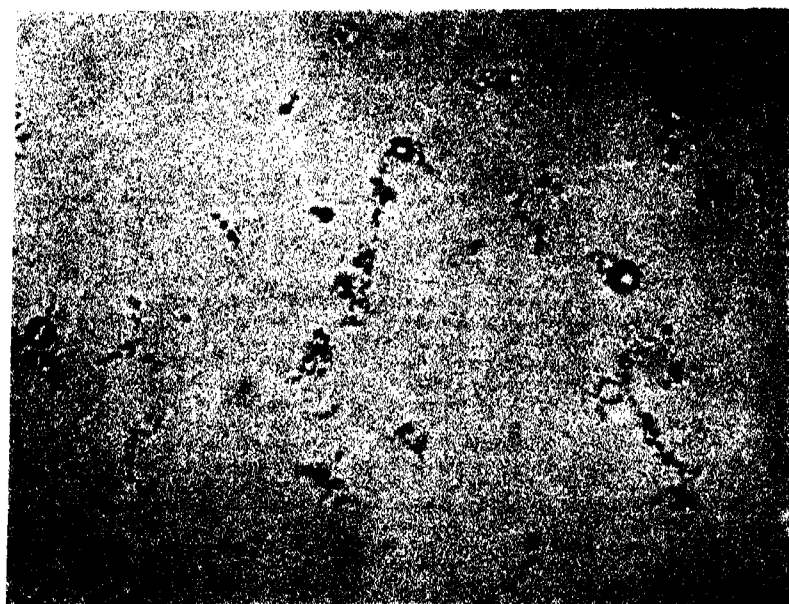


FIG. 2.—Magnesium Oxide ; Arc Smoke. ($\times 1500$.)

(Facing p. 524.)



FIG. 3. —Meta-xylene-azo- β -naphthol; Volatilised Smoke. ($\times 750$.)

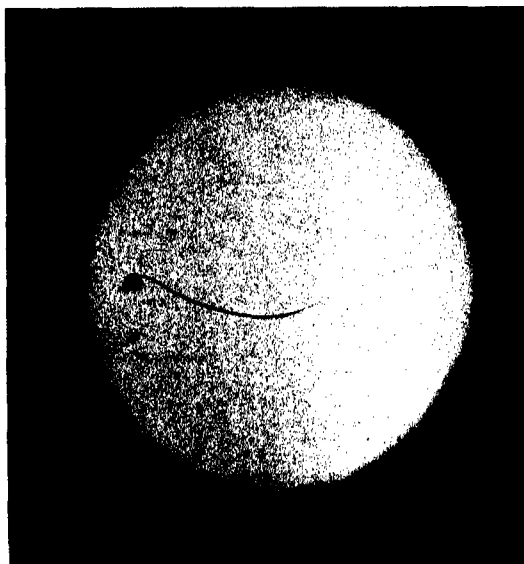


FIG. 4. —Meta-xylene-azo- β -naphthol; Volatilised Smoke. ($\times 750$.)

of the microscope. A typical photograph of this smoke has been reproduced already.* It should be noted that in this and in all other cases collection by sedimentation tends to exaggerate the proportion of the larger and more complex particles.

(b) *Volatilised Smokes.*

Arsenic Trioxide.—Particles of this substance show only a slight degree of aggregation and consist almost entirely of octahedral crystals, which are very much larger than the primary particles in arc smokes.

Mercuric Chloride.—The greater number of the particles are irregularly spherical in form and consist of tightly-packed crystalline aggregates similar in size to those of arsenic trioxide. Sometimes transparent spheres may be noticed which suggests that the original particles were supercooled liquid which subsequently crystallised. Occasionally needles of the usual crystalline form are observed.

Organic Substances.

We have examined smokes produced by volatilising fluorescein, acetanilide, salol, resin, *m*-xylene-azo- β -naphthol, α - and β -naphthalene-azo- β -naphthol and other organic materials. Of these, acetanilide forms a mixture of needle-shaped crystals and small spherical particles. Fluorescein and resin give non-crystalline spheres, the absence of aggregates being very noticeable in the latter, indicating that coalescence rather than aggregation takes place. The salol particles consist mainly of supercooled liquid droplets, which do not easily wet the slide, but on standing crystallisation appears to take place. At the same time either condensation of vapour or the spreading of a thin film forms remarkable ring-like structures round the central particle. Experiments were also tried with various dye-stuffs. Prof. Rowe, of the Department of Colour Chemistry, very kindly suggested and prepared for us various azo-dyes, which he considered might be stable on volatilisation. Of these α - and β -naphthalene-azo- β -naphthol formed spheres or short prismatic crystals, which on the slide gave little indication of secondary change. *M*-xylene-azo- β -naphthol gave rise to the most remarkable effects after the particles had been deposited by sedimentation. At first a mixture of red supercooled spherical droplets, together with some closely packed crystal aggregates, were formed. On standing some of the crystalline particles developed hair-like tails of remarkable length and extreme tenuity. As the tail grew, not only did the crystal aggregate tend to diminish in size, but the surrounding droplets

* 'Roy. Soc. Proc.,' A, vol. 113, p. 310 (1926).

evaporated. In the final stages, in many cases, merely very long hairs only were left (Plate 5, fig. 3); in others the original nucleus formed the head of a tadpole-like structure (Plate 5, fig. 4). In the larger particles the dimension of the crystalline nucleus was of the order of 10^{-4} cm., whilst the tail was sometimes as long as 0.15 mm. The tail decreased in thickness from the nucleus outwards, the order of thickness being 10^{-5} cm.; this can only be estimated as the true thickness may be well beyond the limit of microscopic resolution. The tails did not lie wholly in the plane of the slide and were in consequence difficult to photograph. In view of the remarkable structure of these particles, experiments were made with other substances of similar chemical constitution to see whether similar effects would occur. The materials used were benzene-azo- β -naphthol, and two of the toluene β -naphthols. The effect in all these materials was very much less marked and the only approximation to tails observed was the formation in some cases of hair-like crystals growing from a central nucleus.

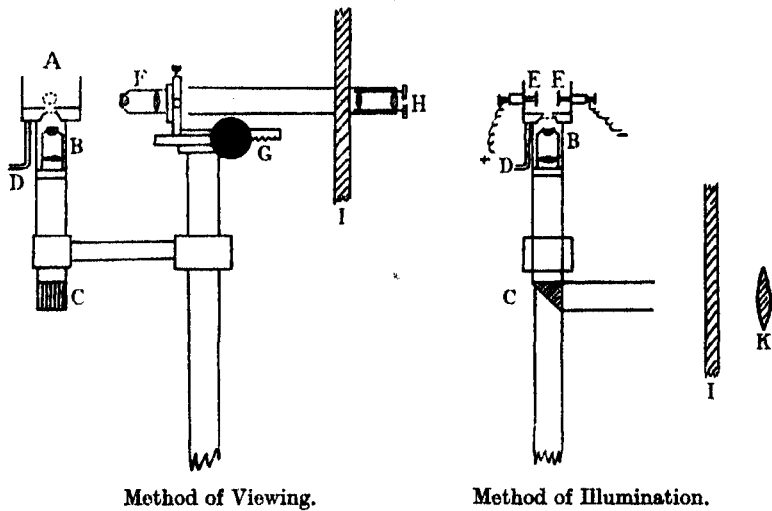
ELECTRIFICATION.

Before the possible effect of electrification on coagulation could be considered it was necessary to obtain reliable data. The literature contains many observations on the charged particles in smokes, but no quantitative data on the variation of number with time or on the relative proportions of opposite sign are available.

The most direct method of obtaining the proportion of electrified particles at different periods during the life of the smoke is by direct counting. Methods based on the transport of electricity in an electric field are both difficult to carry out and to interpret.

The method we have used consists essentially in observing the particles in a special ultramicroscope cell and then applying a horizontal electric field. The particles then sort themselves into three classes according to whether they are positively or negatively charged, or whether they are neutral. The general arrangement of the apparatus will be clear from the diagram. A is an observation cell open at the top, placed inside the cubic metre chamber containing the smoke. It is illuminated by a vertical focussed beam of light from an arc, the lens system and prism being shown at B and C. The smoke contents of the cell could be changed by applying a gentle suction at D. Two electrodes at EE were arranged to give a horizontal electric field. Observations were made with a microscope FF projecting through the wall of the chamber and carrying a diaphragm in the eyepiece. In working, a count was first made of the total particles, the electric field was then applied, when the charged

particles moving horizontally in opposite directions were enumerated. It will be noted that in this apparatus all frictional effects have been eliminated



A, observation cell ; B, illuminating objective ; C, glass prism ; D, lead from suction ; E, electrified plates ; F, viewing objective ; G, rack for focussing ; H, eyepiece ; I, side of chamber ; K, condenser for arc beam.

since the smoke does not pass through connecting tubes, but simply drifts gently into the cell. Earlier experiments showed that erroneous results were often caused by this source of error. About 300 particles were investigated for each point in order to obtain a good statistical average. It may be noted that with practice a large number of particles can be counted in this way very quickly, so that the average obtained applies only to a short time interval. Counts with this cell gave the proportions of the three types of particles present in the smoke at anytime, but these numbers are purely relative, since the volume in which the count was made is indeterminate. The total number of particles was determined independently by making alternate counts by the method described in a previous paper.* By combining the two sets of results it was possible to obtain the actual number of the three types present per cubic centimetre of cloud at definite time intervals.

Another point also calls for comment. It is not possible to obtain such intense illumination in the electrical cell as in the cell used for counting the total. Consequently a certain fraction of the smaller particles may not be enumerated. This might lead to entirely wrong percentages of the total

* 'Roy. Soc. Proc.,' A, vol. 116, p. 540 (1927).

if the percentages of the larger particles carrying charges were different from those of the smaller. We have endeavoured to investigate this (a) by examining smokes differing widely in weight concentration, that is to say, differing in average size of particle, and (b) by confining our observations in alternate counts to bright and faint particles. The results indicate no appreciable difference between the percentage of electrified particles of different sizes.

Experimental Results.

Preliminary experiments showed, as might be expected, that the electrical character of smokes depends very largely on the method used for their formation. In conformity with the experience of others* we find that violent chemical reactions, such as the combustion of magnesium ribbon, give rise to highly electrified smokes, the individual particles appearing to carry a considerable number of unit charges. Smokes formed in this way are closely analogous in their electrical condition. On the other hand, smokes volatilised at a comparatively low temperature contain as a rule very few electrified particles initially, but these particles rapidly acquire charges as the cloud ages.

Ammonium Chloride.—A series of smokes of different weight concentration produced in the usual way from a closed heater were studied. Some of the results are shown in the appended tables.

7.5 mg. clouds.

(a).			(b).			(c).		
Time from start, min.	Fraction of particles charged.	Number per c.c. charged $\times 10^{-4}$.	Time from start, min.	Fraction of particles charged.	Number per c.c. charged $\times 10^{-4}$.	Time from start, min.	Fraction of particles charged.	Number per c.c. charged $\times 10^{-4}$.
7½	0.05	0.045	9½	0.07	0.047	8½	0.08	0.090
31	0.25	0.086	25	0.18	0.071	28	0.19	0.096
47½	0.42	0.117	41	0.32	0.095	47	0.36	0.115
66	0.51	0.125	64	0.49	0.119	69½	0.46	0.105
83½	0.60	0.134	92	0.62	0.132	108½	0.60	0.089
106	0.65	0.133	124	0.71	0.134	137	0.69	0.084

* De Broglie, 'Ann. Chim. Phys.,' vol. 16, p. 5 (1909); De Broglie and Brizard, 'C. R.,' vol. 148, p. 1457, and vol. 149, pp. 923, 924 (1909).

15 mg. clouds.

(a).			(b).		
Time from start, min.	Fraction of particles charged.	Number per c.c. charged $\times 10^{-6}$.	Time from start, min.	Fraction of particles charged.	Number per c.c. charged $\times 10^{-6}$.
9½	0.07	0.051	8	0.04	0.035
24½	0.20	0.104	22	0.20	0.120
41	0.28	0.111	39	0.34	0.144
74½	0.50	0.136	59	0.42	0.132
97½	0.60	0.133	78	0.55	0.154
119½	0.59	0.113	97	0.64	0.134
143½	0.77	0.125			

30 mg. clouds.

(a).			(b).			(c).		
Time from start, min.	Fraction of particles charged.	Number per c.c. charged $\times 10^{-6}$.	Time from start, min.	Fraction of particles charged.	Number per c.c. charged $\times 10^{-6}$.	Time from start, min.	Fraction of particles charged.	Number per c.c. charged $\times 10^{-6}$.
6½	0.03	0.034	7	0.06	0.089	9½	0.05	0.062
22	0.13	0.089	25½	0.20	0.143	22	0.08	0.051
52	0.35	0.155	56	0.34	0.135	38½	0.22	0.100
72	0.46	0.163	74	0.41	0.127	58	0.33	0.117
104	0.56	0.150	128	0.66	0.139	75½	0.54	0.160
127	0.64	0.159				101	0.55	0.135
						119	0.66	0.145

60 mg. clouds.

(a).			(b).		
Time from start, min.	Fraction of particles charged.	Number per c.c. charged $\times 10^{-6}$.	Time from start, min.	Fraction of particles charged.	Number per c.c. charged $\times 10^{-6}$.
8	0.03	0.040	11½	0.08	0.073
36½	0.16	0.106	35	0.24	0.152
67	0.41	0.164	53	0.41	0.194
102	0.53	0.143	76½	0.47	0.102
127½	0.66	0.148	115½	0.67	0.168
			162	0.70	0.129

It will be seen that at the start the number of electrified particles is small but increases rapidly at first, apparently tending towards a limit of about 70 per cent. in the later stages. Beyond this point we have obtained some indication that the percentage slowly increases. It will be noted also from these figures that the particles in the clouds of higher concentration appear not to become electrified quite so rapidly.

In these tables we have given merely the values for the total number of electrified particles per cubic centimetre, but since each sign was counted separately we have also data for estimating whether the smoke as a whole is charged. Though, as could be expected, considerable variations occur in the individual points, the numbers of positively and negatively electrified particles are, within the limits of error, equal when a number of points is considered. The smokes, therefore, as a whole are electrically neutral.

The effect of X-rays on the electrification of these smokes has also been investigated by placing a Coolidge tube inside the chamber during the dispersal of the smoke. In this case, apparently, a high percentage of charged particles is immediately formed, and this percentage persists practically unchanged for long periods. This is shown in the results below :—

Time from start, min.....	5	7	23	25	49	52	64	67	84	87	104	106	122	124
Fraction of particles charged	0.76	0.77	0.83	0.79	0.73	0.75	0.85	0.75	0.79	0.81	0.76	0.81	0.76	0.79

On the average, then, about 78 per cent. of the particles are charged.

Magnesium Oxide.

The smokes were made by burning about 6 inches of magnesium ribbon inside the chamber. The results of two experiments chosen at random from a series of experiments are given below.

A.

Time from start, min.	Fraction of particles charged.	Fraction positive.	Fraction negative.
7	0.89	0.38	0.51
28	0.90	0.47	0.44
49	0.88	0.47	0.41
74	0.88	0.40	0.47
89	0.95	0.46	0.45
97	0.91	0.45	0.46

B.

Time from start, min.	Fraction of particles charged.	Fraction positive.	Fraction negative.
5	0·91	0·48	0·43
22	0·92	0·44	0·48
39	0·89	0·45	0·45
58	0·91	0·49	0·42
75	0·93	0·45	0·48
91	0·86	0·42	0·45
108	0·87	0·47	0·40

It will be seen that, as in the case of clouds charged by X-rays, the fraction of electrified particles remains constant. In each of the experiments quoted on the average 90 per cent. of the particles are charged, whilst the positives are respectively 44 per cent. and 46 per cent., and the negatives 46 per cent. and 44 per cent. It is clear that equal numbers of opposite sign are present, and since there is no experimental reason whatever for doubting that the positive and negative charges carried by the particles are on the average equal, it follows that the clouds as a whole must be electrically neutral.

Silver.—Smoke produced from the arc gave results closely parallel to those just described. This is another example of a highly charged smoke.

Discussion of the Results.

From these results it is clear that the electrification of a smoke depends largely on the way in which it is produced. The particles in smokes volatilised from a heater are initially but slightly charged, whilst those made by the arc or by burning magnesium ribbon are highly charged. The latter call for little comment; the ionisation around an arc or in the neighbourhood of burning magnesium is likely to be so great that heavy charges would be caught by the particles. That this is the case is evidenced by the high percentage of charged particles persisting for some hours. For it is obvious that a charge will only be neutralised and an uncharged particle produced when the particles carrying equal and opposite charges coagulate. The chance of this taking place depends on the range of charge present in the smoke, and this must be considerable if a high percentage of charged particles is to endure.

The electrification of smokes volatilised from a heater is more difficult to explain. It might be thought that the catching of ions from the air by particles would afford a full explanation of the results, but when the matter is considered in detail a difficulty arises. We are much indebted to Mr. Ewles of the Physics

Department for kindly measuring the ionisation of the air in our chamber. This was found to correspond to a rate production of 30 ions per second, or 1800 per minute. Now our results show that in the first 10 minutes or so after a smoke is dispersed, the rate of increase of charged particles is about 5000 per minute. Immediately after dispersal the ionisation in the chamber may be entirely altered owing to emission from the heater, so that these results are not surprising. In the second quarter of an hour, and probably also in the later stages, the same difficulty occurs. For this second period, the rate of increase of charged particles is between 2000 and 3000 per minute, but since charges are being neutralised simultaneously by collision, the number of ions involved must be greater than this. It therefore seems likely that the rate at which charges are caught is about twice as great as the measured rate of production of ions in the chamber. Although we are not in a position definitely to explain this anomaly, it seems likely that the rate of ionisation measured in dust-free air may be different from that when smoke is present, or indeed the smoke particles themselves may be directly electrified by the radiation which ionises the air. Until a wider investigation has been made, however, it would be premature to attempt any further interpretation of the facts.

In conclusion we should like to say that our experiments have brought to light no marked difference in the coagulation rates of comparable smokes which differ greatly in electrical character. The difference between the rate of coagulation of comparable smokes of MgO and ammonium chloride indicate that electrification exercises little, if any, effect. Moreover, we have as yet detected no appreciable difference in the coagulation of ammonium chloride smokes of the same weight concentration, dispersed either normally or in the presence of X-rays.

Ionisation by Collision in Monatomic Gases.

By J. S. TOWNSEND, F.R.S., Wykeham Professor of Physics, Oxford, and
S. P. MACCALLUM, D.Phil., Fellow of New College, Oxford.

(Received May 6, 1929.)

1. Two papers by Dr. R. Atkinson on the development of currents in gases have recently appeared in the 'Proceedings of the Royal Society' where he refers to some work which has been done in the Electrical Laboratory, Oxford.

We wish to make some remarks on the theories of ionisation which he advocates and to draw attention to some contradictions.

In his first paper Atkinson describes a theory of ionisation which may be called the "Stosse zweiter Art" theory. It is stated that the principles on which this theory is based are not *ad hoc* assumptions but are well known and generally accepted. "Thus if they succeed in accounting for Prof. Townsend's results they must be accepted as the only assumptions that cover the whole experimental field."

We are unable to share the general and complete confidence placed in these views, and we are unable to find definite experimental evidence in support of the principles on which the theory is based. We find that if these principles be accepted it would be impossible to obtain a consistent explanation of many simple phenomena which are observed in electric discharges in monatomic gases.

2. There are two principal processes involved in the assumptions which make up the complete "Stosse zweiter Art" theory. The first action takes place in the collisions between electrons and atoms of a monatomic gas, when the electrons move in a field of force and acquire amounts of energy which are equal to or slightly greater than that corresponding to a certain critical potential. In one of these collisions an electron loses all its energy and the normal atom is converted into a metastable atom. There are several critical potentials but in gases at high pressures "it is only the first critical potential together with any others which may lie close to it that can be operative."* Very few electrons ever reach an energy much above that of the first critical potential. The first critical potential may not be a radiation potential; that is, in this

* It would appear that these effects are obtained at pressures of a few millimetres such as are used in our experiments.

metastable state the atom does not radiate energy. The metastable atoms, being electrically neutral, move by diffusion throughout the gas.

3. The second process, which accounts for the increase of conductivity, consists in the ionisation of molecules of gases which are "always" present as traces of impurity. These molecules are ionised by the transference of energy from the metastable atoms with which they collide. The number of atoms ionised in this way is said to be independent of the amount of impurity within wide limits, and multiplying or dividing the amount of impurity by 10 would have very little effect on the increase of the current. Large increases in current are thus obtained when the partial pressure of the impurity is as low as 10^{-6} mm. where no appreciable effect would be obtained due to direct collisions between electrons and molecules of the impurity. For example, it is stated that the results of the experiments* which we obtained with neon at 37 mm. pressure in no way invalidate these contentions. In fact if the "well known" and "generally accepted" principles on which the "Stosse zweiter Art" theory depends were true, large increases of conductivity, due to impurity, would be obtained in monatomic gases at 40 mm. pressure, unless the gas were purified to such an extent that the pressure due to impurities were less than one part in 40 million of the pressure of the gas. It would be difficult to establish a claim to have obtained this degree of purity so that from this point of view the Stosse zweiter Art theory may be supposed to cover the whole experimental field.

4. The experiments with helium which are supposed to be explained by this theory are very numerous. In this gas the first critical potential is given as 19.77 volts, so that when electrons acquire energy in amounts corresponding to this voltage they become operative and convert the normal atoms of the gas into metastable atoms. Increases of conductivity should therefore be obtained when the electrons attain this amount of energy. It is interesting to consider Bazzoni's experiments† with helium, which are also quoted as examples of experiments, which may be explained by the Stosse zweiter Art. In these experiments the currents flow from a heated filament to a co-axial cylindrical electrode. The apparatus, which was very simple, was contained in a quartz envelope and was heated strongly to drive off impurities. The gas was found by spectroscopic examination to be free from mercury vapour or any other impurity. Large increases in current were obtained when the potential difference between the electrodes was increased above the value 20.4

* Townsend and MacCallum, 'Phil. Mag.', vol. 5, p. 695 (1928).

† Bazzoni, 'Phil. Mag.', vol. 32, p. 566 (1916).

volts. There was no marked increase in the current when the potential between the filament and the cylinder was 25 volts which is near the ionisation potential usually given for helium.

Bazzoni attributed the increase in conductivity observed in this experiment to ionisation of the gas by the direct collisions of electrons with atoms, when the energy of the electron was 20.4 volts.

5. The principal difficulty in arriving at any definite conclusion about helium is that experimenters have obtained widely different results, although the well-known methods of purifying the gas and testing it spectroscopically were adopted.

In order to discover the cause of these discrepancies we undertook a more complete investigation of helium and neon, a few years ago; and after various attempts we have obtained quite consistent results and made measurements of the conductivity in which experimental errors are very small. In the course of these investigations we found that the ordinary spectroscopic method of detecting impurities is not an adequate test. We found it necessary to adopt a much more sensitive test depending on the sparking potential, which indicates to what extent currents may be affected by impurities.

Some of the results which have been obtained with these gases have already been published, but the investigations are not yet completed.

6. We have already pointed out that there are many phenomena which show that any hypotheses such as those involved in the theory of the *Stosse zweiter Art* are untenable. In order to make this quite clear it is necessary to take numerical examples to show what results would follow from the first hypothesis which states that very few electrons attain energy above that corresponding to the first critical potential. The conditions with regard to force and pressure, for which the theory was adopted, were those usually obtained in experiments with photoelectric currents between parallel plates where large increases in conductivity are obtained by increasing the electric force. The ratio of the force to the pressure is of the order of the value of X/p for the minimum sparking potential. In neon the minimum sparking potential is obtained when the ratio X/p is 62. Thus the first hypothesis may be supposed to hold in experiments where X/p is less than 30.

Let us consider the energy acquired by the electrons in photoelectric currents between parallel plates with a constant force of 100 volts per centimetre, neglecting losses of energy in small amounts, and taking the first critical potential to be 16 volts and the ionising potential to be 21 volts in neon. The electrons acquire the energy corresponding to the first critical potential in

passing through the plane 1.6 mm. from the negative electrode and those that lose no energy in collisions acquire the energy of 21 volts when they reach the plane, 2.1 mm. from the negative electrode.

The number of electrons that traverse the distance between the planes without colliding with atoms is a maximum when the direction of motion of the electrons is normal to the planes, and for the purpose of this calculation it may be assumed that all the electrons are moving in the direction of the electric force with the velocity of 16 volts in passing through the first plane. Thus if n be the number of electrons passing through the first plane the number that do not collide with atoms in traversing the space between the two planes is $n e^{-x/l}$, x being the distance between the planes and l the main free path of the electrons. The others which collide with atoms have their direction of motion changed, and it may be supposed that most of them lose energy in amounts corresponding to critical potentials since they make several collisions with atoms in the space between the planes.

Since there are many critical potentials, and very few electrons attain energies much above the first critical potential, it may be supposed that with the gas at 5 mm. pressure ($X/p = 20$) less than 10 per cent. of the electrons attain the ionising potential.

The number that attain the ionising potential may be taken to be of the order $n e^{-x/l}$ and this number diminishes rapidly as the pressure increases since l is inversely proportional to the pressure. With a pressure of 20 mm. ($X/p = 5$) the number of electrons that attain the ionising potential would be of the order $n \times 10^{-4}$ and with a pressure of 50 mm. ($X/p = 2$) the number would be of the order $n \times 10^{-10}$. Under these conditions there would be no appreciable increase of current due to ionisation of atoms of a monatomic gas by the direct collisions with electrons in any experiments where X/p was small (of the order $X/p = 2$), whether the gas be pure or impure.

7. In the experiments on photoelectric currents the increases in the current with the distance between the plates are much greater than the rate of increase indicated by the above figures, and it would be necessary to attribute the increases to impurities (or to some other process of ionisation) if the above hypothesis were approximately correct. The photoelectric current being small, very small traces of impurities would suffice to provide the additional electrons and positive ions generated in the gas, and it might be impossible to detect impurities in such small quantities with a spectroscope. But when the large currents which are maintained in gases with small electric forces are considered, it becomes immediately evident that the hypotheses involved in the Stosse zweiter Art theory are untenable.

In the ordinary long discharge tubes the electric force is very small in the uniform luminous column, which for certain pressures of the gas extends from the positive electrode to within a short distance of the negative electrode, and the conductivity is maintained by ions generated in the gas. In the well-known neon tubes which emit the neon red light large currents of the order of 10^{-2} amperes are obtained in wide tubes with the gas at a few millimetres pressure the value of X/p being about 2 or $2\cdot5$ in the uniform positive column. According to the above hypothesis all the positive ions in the gas must under these conditions be derived from impurities and the gas would not conduct (when X/p is small), unless it contained impurities in amounts sufficient to provide the positive ions in a current of the order of 10^{-2} amperes. And since the positive ions move under the electric force toward the cathode, it would be necessary to suppose that near the positive electrode there is some continuous supply of impurities to provide positive ions to take the place of those that move to the negative electrode.

It is not necessary to make any observations with a spectroscope in order to see that the current is not maintained by impurities. With a gas, slightly impure, the positive column is discoloured but the discoloration is moved by the current towards the negative electrode. The characteristic red colour of pure neon is thus obtained at first in the part of the tube near the positive electrode, and subsequently throughout the whole tube except at the end of the positive column adjacent to the cathode.

In order to obtain any rational explanation of the conductivity of the positive column of a neon tube it is necessary to suppose that the greater part of the positive ions are derived from ionisation of the atoms of neon. And we are led to the conclusion that ionisation of atoms of neon can be obtained with values of X/p in the range from $X/p = 1$ to $X/p = 2$.

8. It is interesting to examine these theories by considering the light emitted by the gas as well as the conductivity. The accepted theory of the light in the visible spectrum, indicates that in order to obtain a large number of lines it is necessary that the atoms should acquire energy in amounts corresponding to many critical potentials, so that it must be supposed that in many collisions with atoms the electrons have energies which are practically the same as the ionising potential. Thus any hypotheses, such as the first hypothesis involved in the Stosse zweiter Art theory, which imposes a limit to the energy which the electrons may attain is not in agreement with the fact that the number of lines in the spectrum of the positive column is very large when the gas is at a high pressure and the conductivity is maintained with a small force (X/p of the order 2).

So long as the lines in the spectrum of the light emitted from the positive column are those which are universally attributed to neon, we feel that it is unreasonable to suppose that the conductivity is principally due to impurities.

9. In his second paper Atkinson continues his comments on our experiments and gives another theory of conductivity where the ionisation of monatomic gases at high pressures is attributed to the direct collisions of electrons with atoms of the gas, which is quite contrary in principle to the theory he advocated in his first paper. The reason for this inconsistency is not explained except that he states we have *now* shown that spectroscopic purity is essential.

In his first paper it was maintained that the Stosse zweiter Art embodied the only assumptions which cover the whole experimental field, and it was made quite clear that it applied to experiments such as those made by Bazzoni, who stated very definitely that the gas he used was spectroscopically pure. It may be mentioned here that in our earlier experiments with helium the gas was tested by the ordinary spectroscopic method and it was found to contain no impurities as far as could be observed, and it may be presumed that other experimenters who said they used pure gases also tested the gases spectroscopically although they may not have considered it necessary to mention such an ordinary precaution.

In a note at the foot of his first paper it is stated that the contentions there set forth are in no way invalidated by the results of the experiments we made with neon at 37 mm. pressure, and it is these very experiments which he uses to illustrate his second theory.

10. The second theory includes many of the principal hypotheses which form the basis of the original theory of ionisation by collision known as Townsend's theory. It is now assumed that electrons produced in the gas are due to collisions of the electrons with atoms, and that there is a steady state in which the increase in current, due to this process, is continuous and may be represented by the formula $n = n_0 e^{\alpha x}$ where the coefficient α is connected with the force and the pressure by the relation $\alpha/p = f(X/p)$. The new theory differs from the original theory of ionisation by collision by the introduction of the hypothesis that an electron ionises an atom of a monatomic gas in the first or second collision immediately after it has acquired an amount of energy corresponding to the ionising potential. This additional hypothesis indicates large increases in photoelectric or thermionic currents when the potential difference between the electrodes is just above the ionising potential whether the gas be pure or impure.

The greater part of Atkinson's second paper is devoted to showing that the

probability of losses of energy of electrons in critical amounts, less than the ionising potential, is small, a conclusion from our experiments which we have found it necessary to emphasise on many occasions for many years past.

Many physicists have accepted the hypotheses that the probability of losses of energy in critical amounts is large, and we have frequently indicated that such hypotheses cannot be reconciled with many ordinary phenomena. We may take this opportunity here of pointing out errors of this kind made by Atkinson himself. In his first paper, referring to collisions of electrons (with energies from 0 to 20 volts) which occur with molecules of impurities, he says that "practically in every such case the electron will lose all its energy."

The high probability of ionisation in the collisions of electrons with atoms of monatomic gases, which is a characteristic feature of his second theory is another example of the same kind of error.

11. This theory bears a strong resemblance to the theory given by Franck and Hertz* to explain their experiments where recurring maxima were observed in the rate of increase of current with potential, at points where the potentials of the accelerating field was a multiple of the ionising potential, a theory which may also be said to have been "universally accepted" for some years. In this theory the electrons are supposed to ionise atoms of the gas when they attain the energy corresponding to the ionising potential, and the loss of energy in collisions with atoms that are not ionised is supposed to be negligible. It is remarkable that in the experiments where recurring maxima have been observed the potentials are multiples of 20·5 volts in helium and 16 volts in neon. The theory of recurring maxima has been adopted by Holst and Oosterhuis,† and objections to the conclusions they have drawn from the theory have already been pointed out.‡

12. Atkinson is wrong when he states that we appear to have assumed that the quantum theory predicts a high probability of loss of energy in collisions. We have made no statement to this effect. We do not consider that the quantum theory gives any indication of the probability of transfer of energy from electrons to atoms or molecules of the gas. All that the quantum theory indicates is that when energy is transferred in large amounts these amounts should be proportional to the frequency of certain spectral lines (in those collisions where there is no permanent change of structure of the atom or molecule such

* Franck and Hertz, 'Phys. Z.', vol. 17, p. 411 (1916).

† Holst and Oosterhuis, 'C. R.', vol. 174, p. 577 (1922), and 'Phil. Mag.' vol. 46, p. 1117 (1923).

‡ Townsend, 'Phil. Mag.', vol. 45, p. 444 (1923).

as ionisation or dissociation). This does not conflict with any theory of conductivity.

Atkinson is also wrong when he states that the only definite statement of the authors with regard to the distribution of energy in the steady state has been that it might approach a Maxwellian one. We have frequently pointed out that there is no case where the actual distribution of the energy in a stream of electrons is known. The distribution of the velocities has been discussed in a paper* published in the 'Philosophical Magazine.'

It was there stated that it was of importance not to introduce any hypothesis as to the distribution of energy in investigating ionisation by collision. Referring to the distribution of energy in a stream at various distances x from the cathode it was stated (p. 1073) that for small values of x "the mean kinetic energy of the electrons and the distribution of the energy about the mean value changes with the distance." In the steady state for larger values of x , where the current is given by the formula $n = n_0 e^{-ax}$ the mean kinetic energy \bar{U} "and the distribution about the mean is independent of x ."

It was also stated (p. 1076) that in the initial stages where x is small "the mean energy of the group may attain the value \bar{U} before ionisation by collision begins to have any appreciable effect on the current." The reason being "that comparatively few of the electrons have energies much different from the mean energy of the group in the earlier stages of motion through the gas." It was not suggested that any of these various distributions resembled the Maxwellian distribution.

13. In order to indicate the most rational conclusions which may be drawn from the simplest experiments on the conductivity of monatomic gases it is sufficient to consider the photoelectric currents between parallel plates when increases in conductivity are obtained by the process of ionisation by collision. For this purpose we may refer to the experiments which we have published in a recent paper on the Electrical Properties of Neon.†

We shall assume that the gas was pure so that the increases in the current above the saturation current are due to the ionisation of atoms of the gas, and that in neon the first critical potential is 16 volts and the ionisation potential is 21 volts. As there are several critical potentials between 16 and 21 volts, the average potential of the group may be taken as 18 volts. These figures may not be exactly correct but they serve to illustrate the principles on which definite conclusions may be obtained from the experiments. The unit of

* Townsend, 'Phil. Mag.', vol. 45, p. 1071 (1923).

† Townsend and MacCallum, 'Phil. Mag.', vol. 6, p. 857 (1928).

energy of an electron may be taken as that corresponding to 1 volt so that if E be the energy of an electron the velocity of agitation is $5.8 \times 10^7 \times \sqrt{E}$ cm. per second.

14. The curve (fig. 4, *loc. cit.*) gives the relation between the current and the distance x between the plates when there is a constant force of 100 volts per centimetre and a constant gas pressure of 3.3 mm. for the initial stages of the development of the currents. If n_0 be the constant current obtained with distances x between the plates of less than 2 mm., the current $2n_0$ is obtained when the distance is 7 mm., the potential difference between the plates at this point being 70 volts. The following are the values of the currents at intermediate distances :—

x .	n/n_0 .	x .	n/n_0 .
0.3	1.08	0.5	1.46
0.4	1.27	0.6	1.71

The loss of energy of an electron due to small losses in ordinary collisions (of the order of $6 \times 10^{-5} E$) may be neglected in this experiment (where $X/p = 30$), compared with a loss of 18 volts. If an electron loses this amount of energy it cannot subsequently acquire a sufficient amount of energy to ionise an atom in the space between the negative electrode and a plane at 3.9 mm. from this electrode. The experiments show that the current is increased from n_0 to $1.25n_0$ by the electrons which are generated within this space. Thus the energy E of the electrons in the collisions with the atoms which are ionised varies from 21 to 39 volts and the average energy \bar{E} in these collisions is about 32 volts, which is the potential at a plane 1.1 mm. from the plane where the energy of the electrons is 21 volts. Thus while the electrons are moving in the gas with energies above that corresponding to the ionisation potential they make several collisions with atoms without losing energy in large amounts (of 18 volts).

15. The average number of such collisions which are made by electrons at distances less than 3.9 mm. from the negative electrode may be taken as the number of collisions made by an electron in moving the distance 1.1 mm. This number depends on the velocity of agitation U of the electron, the velocity W in the direction of the electric force and the mean free path l .*

* Townsend, 'Electricity in Gases,' p. 286.

The number of collisions made by an electron in moving the distance δx in the direction of the electric force is

$$U \cdot \delta x / W \cdot l \quad \text{or} \quad \frac{m \cdot U^2 \cdot \delta x}{0.82 \cdot e \cdot X \cdot l^2}, \quad (1)$$

taking the usual formula for W ,

$$\left(W = \frac{X \cdot e \cdot l \cdot 0.82}{m \cdot U} \right).$$

It will be observed that the number of collisions is proportioned to the kinetic energy of the electron $\frac{1}{2}mU^2$ and when no energy is lost in collisions this energy is $x \cdot e \cdot X$, where X is the electric force, and x the distance of the electron from the negative electrode. The number of collisions made by electrons in the space between the planes at distances 2.1 and 3.2 mm. from the negative electrode is therefore obtained by simple integration. The value to be attributed to l depends upon the specification of a collision and for the purposes of this calculation the mean free path of an electron in neon at 1 mm. pressure will be taken as 0.1 cm.

The number of collisions made by an electron in traversing the distance between the planes $x = 0.21$ and $x = 0.32$ is thus found to be 80.

Thus an electron after it has attained the ionising potential makes, on the average, 80 collisions without loss of energy, before it ionises an atom in the space between the planes $x = 0.21$ and $x = 0.39$. The average energy in the collisions with atoms that are ionised is 32 volts.

16. The proportion of the number of collisions with atoms that are ionised to the number in which the losses of energy are 18 volts may be found by considering the coefficients of ionisation α for the steady state where the increase of current due to the collisions of electrons with atoms is given by the formula $n = n_0 e^{\alpha x}$. In this case the mean energy \bar{E} of a group n does not change as the stream moves in the direction of the electric force. The number of electrons in the group increases from n_1 to $2n_1$ in traversing the space between two planes when the distance b between the planes is given by the formula $e^{\alpha b} = 2$. Hence $\alpha b = 0.693$ and the potential difference between the planes $X \cdot b$ is $0.693 \cdot X/a$.

In neon at 3.3 mm. pressure, and with an electric force of 100 volts per centimetre ($X/p = 30$), the value of α/p is 0.43, so that the potential $X \cdot b$ is 48 volts. Thus when the group has the mean energy \bar{E} , corresponding to the steady state, the number in the group is increased from n to $2n$ when the group moves through the distance 4.8 mm. in the direction of the electric force, but

when the group starts with zero velocity from the negative electrode the number is not increased from n to $2n$ until the electrons arrive at a plane 7 mm. from the negative electrode. This shows that the group must attain the energy of approximately 22 volts before the number is increased from n to $2n$ in moving through 4.8 mm. Hence in the steady state (where $n = n_0 e^{ax}$) the average energy \bar{E} is approximately 22 volts (when $X/p = 30$).

17. In the steady state the number of electrons that pass through any plane at a distance x from the negative electrode has been found experimentally to be given by the formula $n = n_0 e^{ax}$. The energy gained by a stream of electrons in passing through the space between the two planes at distances x_1 and x_2 from the negative electrode is

$$n_0 X \int_{x_1}^{x_2} e^{ax} \cdot dx = \frac{X}{a} \cdot (n_2 - n_1),$$

where X is the electric force, n_1 the number entering the space through the first plane and n_2 the number passing out through the second plane. The energy of the electrons entering the space is $n_1 \cdot \bar{E}$ and the energy of those passing out is $n_2 \bar{E}$. If c be the kinetic energy lost in ionising an atom the total energy lost by ionisation is $(n_2 - n_1) c$. Hence

$$X \cdot (n_2 - n_1)/a = (n_2 - n_1)(c + \bar{E}) + F, \quad (2)$$

where F is the energy lost in the space between the planes in the collisions with atoms which are not ionised.*

Let C_2 be the number of collisions in which electrons lose energy in large amounts and let the average of these amounts be 18 volts. With values of X/p greater than 15 the loss of energy of electrons in small amounts of the order of 6×10^{-6} E may be neglected, and the following equation is obtained

$$18C_2 = \left(\frac{X}{a} - c - \bar{E} \right) C_1, \quad (3)$$

where C_1 is the number of collisions in which atoms are ionised ($C_1 = n_2 - n_1$).

In order to show how the ratio C_2/C_1 depends on the electric force and pressure of the gas, it is convenient to have $(n_2 - n_1)$ a simple multiple of n_1 . The distance between the planes may be taken so that

$$e^{a(x_2 - x_1)} = 11, \quad \text{or} \quad (x_2 - x_1)p = 2.4p/a.$$

This gives $C_1 = 10n_1$.

It has been found that, in some collisions, atoms of neon are ionised by electrons having an energy of about 21 volts. The electrons may have some

* Townsend, 'Phil. Mag.', vol. 45, p. 1071 (1923).

kinetic energy after the collision in which an atom is ionised, and if v be the energy of the two electrons after the collision, the loss of energy to the stream when an atom is ionised would therefore be $(21 - v)$ volts, and this is the energy represented by c . Thus 21 volts may be taken as an upper limit to the value of c .

18. The total number of collisions (C_3) between electrons and atoms in the space between the planes depends on the mean free path and on the distribution of the velocities of the electrons. As these are uncertain the ratio C_3/n_1 cannot be determined accurately, but in order to indicate a probable value of the total number of collisions the ratios C_3/n_1 have been calculated on the supposition that the energy of agitation is equal to \bar{E} . The formula thus obtained is

$$C_3/n_1 = 2300 : \bar{E} \cdot p^2/X\alpha, \quad \{(n_2 - n_1) = 10n\},$$

where X is expressed in volts per centimetre. In the following table the values of α/p , C_2/n_1 and C_3/n_1 , are given for different values of X/p , the corresponding values of C_1 being $10n_1$ in each case (c being taken as 21 volts in equation (3) to determine the ratio C_2/n_1).

Values of C_2/n_1 and C_3/n_1 , C_1 being $10n_1$.

X/p .	α/p .	\bar{E} .	C_2/n_1 .	$C_3/n_1 \times 10^{-2}$.
160	2.19	37	8	2.4
100	1.57	31	7	4.5
60	0.99	25	8	9.6
30	0.43	22	15	39
20	0.24	19	24	92
10	0.053	16	80	690
2.5	0.01 ?	12	80	1.1×10^4

With the values of X/p , 10 and 2.5 the total number of collisions C_3 is large and the total loss of energy in small amounts is appreciable. In these cases it is necessary to add a term $(5.5 \cdot 10^{-5} \cdot \bar{E} \cdot C_3)$ representing this loss on the left of equation (3) to find C_2/n_1 .

The probable error in the determination of α/p is about 2 or 3 per cent. when X/p is greater than 10, the error in \bar{E} is about 5 or 6 per cent., and in the smaller values of C_2/n_1 the error may be 10 or 12 per cent.

The ratio C_2/C_1 diminishes as X/p increases, thus with $X/p = 10$ there are 80 collisions in which the electrons lose energy in amounts of 18 volts to every 10 in which atoms are ionised, with $X/p = 60$ there are 8 collisions in which the loss is 18 volts to every 10 in which atoms are ionised.

The proportion of the number of collisions in which atoms are ionised or losses occur in amounts of 18 volts to the total number of collisions C_2 increases with the value of X/p . With the larger values of X/p the energy of the electrons exceeds 18 volts in most of the collisions. With $X/p = 160$, 10 atoms are ionised out of a total of 240 collisions, with $X/p = 100$, 10 are ionised out of a total of 450. Thus the probability of an atom being ionised increases with the energy of the electron in the collisions with the atoms. The probability of losses of energy occurring in amounts of 18 volts also increases with the energy of the electrons.

The above figures show that it would be quite impossible to form a theory of conductivity on the hypothesis that electrons, when they acquire energies above certain critical amounts, lose energy in these amounts in collisions with atoms without taking into consideration the fact that the probability of any such losses occurring is small.

The Magnetic Anisotropy of Naphthalene Crystals.

By S. BHAGAVANTAM.

(Communicated by Sir C. V. Raman, F.R.S.— Received March 4, 1929.)

1. *Introduction.*

In a recent paper Raman and Krishnan* have shown how the phenomenon of birefringence exhibited by liquids in a magnetic field can be utilised to determine the degree of magnetic anisotropy of the molecules concerned. Since magnetic double refraction is an effect arising from the molecules being both magnetically and optically anisotropic, and the optical anisotropy is known from studies on light scattering, the magnetic anisotropy can be evaluated from the known value of the Cotton-Mouton constant.† In this way, they showed that the benzene molecule has a high degree of magnetic anisotropy, the susceptibility in a direction perpendicular to the benzene ring being about twice as great as that in any direction parallel to the ring. In another paper‡ they showed how this magnetic anisotropy may reasonably be explained in terms of the special

* 'Roy. Soc. Proc.,' A, vol. 113, p. 511 (1927).

† 'Roy. Soc. Proc.,' A, vol. 117, p. 1 (1927); see also 'Phil. Mag.,' vol. 5, p. 498 (1928).

‡ 'Comptes Rendus,' vol. 184, p. 449 (1927).

structure of the benzene molecule. Considerations of the same kind suggest that the higher members of the aromatic series (*e.g.*, naphthalene and anthracene) should exhibit an even more striking degree of anisotropy. Some calculations, as yet unpublished, by Krishnan indicate that the naphthalene molecule should have, in directions perpendicular to the ring, a susceptibility about four times as large as in directions parallel to the ring.

It is known that diamagnetism of crystals is in general anisotropic. In a recent paper Raman and Krishnan* have discussed the case of nitrates and carbonates and shown how the anisotropy of the crystals is in each case connected with the structure of the individual ions. If, as stated above, the naphthalene molecule possesses a large magnetic anisotropy in the liquid state, it is reasonable to expect that naphthalene crystals in the solid state should also exhibit a very pronounced magnetic anisotropy. In fact, Bragg† and Oxley‡ have made some qualitative observations on the magnetic behaviour of naphthalene crystals which support this inference, but no quantitative results are available. The present work was undertaken with a view to obtain some measurements of the susceptibility of the crystals in different directions and with the hope that such data would be of assistance in determining the orientation of the molecules in the crystal lattice.

2. *Its Crystalline Form.*

It is necessary to use extra pure naphthalene in the investigation. It is carefully tested for freedom from impurities containing iron. The substance readily crystallises from alcohol solution, the crystals being formed as thin flakes. According to Groth§ the crystals take the shape given below in fig. 1, the flakes being parallel to the *ab* plane. They belong to the monoclinic prismatic class :

$$a : b : c :: 1.3777 : 1 : 1.4364. \quad \beta = 122^\circ 49',$$

c is the (001) face and there is a perfect cleavage along that plane. *r* is the (201) face and *p* is the (110) face.

It may be noted that according to Groth the crystals formed from alcoholic solution are often elongated along the *b* axis, thus taking the hexagonal form shown in fig. 1 in which BD and GF are the longest sides. Actually, however, in the course of this investigation it is often found that the reverse is the case,

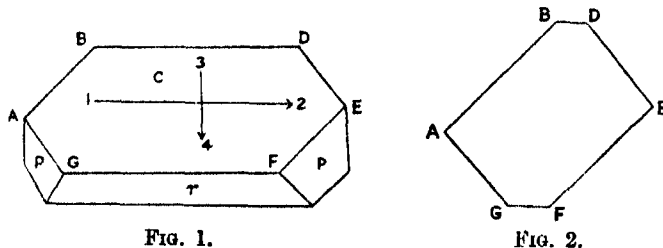
* 'Roy. Soc. Proc.,' A, vol. 115, p. 549 (1927).

† Sir William Bragg, 'Proc. Roy. Inst.' (1927).

‡ 'Roy. Soc. Proc.,' A, vol. 98, p. 267 (1921).

§ 'Chem. Krist.,' vol. 5, p. 364 (1919).

so much so that the lines GF and BD practically disappear, thus giving rise to a form approximating to a four-sided figure as shown in fig. 2, the other two



sides being rarely visible. Both forms of the crystal, however, have the same interfacial angles. It is found possible to obtain crystals of both habits in the same dish, *i.e.*, under the same conditions of concentration and temperature. These forms are the only ones observed, the type indicated in fig. 2 always preponderating.

Coming back to the crystal faces as marked in fig. 1 it is evident that the line that is common to the "c" face and "r" face, both of which contain the "b" axis, will be parallel to the "b" axis. In order to identify this axis, the six angles between the lines enclosing the "c" face have been calculated and the observed values are compared with the calculated values. The angles can be easily measured under a microscope with a cross wire in the eyepiece and a graduated rotating stage.

Angle as marked in fig. 1.	A.		B.		D.		E.		F.		G.	
Calculated	71	58	54	1	54	1	71	58	54	1	54	1
Observed	70	0	58	0	50	0	74	0	58	0	54	0

Only the acute angles have been given, in the actual case the angles being their supplements. It is seen that they roughly agree and the "b" axis is at once identified as the one that is bounded by the two equal angles each $54^{\circ} 1'$, that is, in fig. 1, with the lines BD or GF.

3. Behaviour in a Uniform Field.

Since in the monoclinic prismatic class of crystals, the *b* axis is an axis of symmetry, it must coincide with one of the axes of the magnetic ellipsoid, the other two lying in the *ac* plane. We may infer, therefore, that when the plate is

hung with (3-4) vertical in a homogeneous field, the " *b* " axis, *i.e.*, the line (1-2) should move into either an equatorial or an axial position. Actually it is found that the crystal plate, when suspended with the line (3-4) vertical, swings into an equatorial position.

To find the two other magnetic axes which will necessarily lie in a plane perpendicular to the " *b* " axis but need not coincide with the crystallographic ones, the deportment of the crystal in a homogeneous field is studied. For this purpose it is suspended in the field by means of a fine silk fibre, attached to it by the smallest possible amount of Canada balsam. Referring to fig. 1, when the crystal hangs with the " *b* " axis (line 1-2 in fig. 1) vertical, the cleavage plane sets at about 60° with the field. When the crystal is turned over and suspended with the line (2-1) vertical, it again makes an angle of about 60° with the field on the opposite side. It is clear, therefore, that the magnetic axis in the *ac* plane which sets itself along the lines of force makes an angle of about 60° with the " *a* " axis. The crystallographic data show that the supplement of the angle between the *a* and *c* axes is $57^\circ 11'$ which differs little from 60° . Hence it follows that the second magnetic axis practically coincides with the *c* axis and that the third axis is a line perpendicular to both the " *b* " and " *c* " axes. Numerous crystals of naphthalene have been examined and the foregoing results are obtained in every case. It is evident, therefore, that OM, Ob, Oc, the axes of the magnetic ellipsoid are situated in relation to Oa, Ob, Oc, the crystallographic axes in the manner represented in fig. 3.

4. Measurement of Susceptibility.

(a) *Tractive Forces in a Non-Uniform Field.*—A suspension of glass fibre about $1\frac{1}{2}$ metres long is attached at the upper end to an index rotating on a graduated circle. The crystal is fixed at its lower end with the smallest possible amount of Canada balsam and hangs in a non-uniform field with a large gradient. The glass fibre is sufficiently thick to prevent rotation of the crystal and is viewed in focus through a microscope. When the field is put on, the crystal moves into a weaker part of the field and the deflections produced are observed. Since they are small, we may, as a first approximation, assume that the deflection in each case is proportional to the mechanical force acting on the crystal and hence to the susceptibility in the direction of the field. The crystal may be placed in different orientations relatively to the field by rotating the index and the deflections noted. The results with a particular crystal are tabulated below :—

Orientation.	Deflection.	Calculated susceptibility.
<i>b</i> axis along the field	10 divisions	-700×10^{-7}
<i>Oc</i>	6 "	-420×10^{-7}
<i>OM</i>	22 "	-1540×10^{-7}

The figures given in column 3 are obtained by taking the mean of the three principal susceptibilities to be equal to that obtained by Pascal for naphthalene from the additive values. They represent the gramme-molecular susceptibility.

(*b*) *The Null Method.*—The method of Rabi* has also been followed with some modifications. The crystal is suspended in the same manner as previously but is surrounded by an aqueous solution of MnCl_2 of suitable concentration. The particular concentration for which there is no motion of the crystal along the direction of the gradient is hit off after a few trials. The principle applied is that, under these conditions, the force acting on the crystal in the direction of the gradient is zero, if the volume susceptibility of the crystal (in the direction of the field) is the same as that of the surrounding solution. If the concentration of the solution is known, its volume susceptibility can at once be calculated and hence that of the crystal in the particular direction. The value obtained for the gramme-molecular susceptibility along the *b* axis was -710×10^{-7} and along the *c* axis -390×10^{-7} . Taking the mean susceptibility calculated from Pascal's data as -897×10^{-7} , the third value along the line perpendicular to *b* and *c* works out as -1590×10^{-7} . The value is numerically so high that it is not easy to find an immersion liquid with which it can be directly compared by the null method. Even a saturated solution of potassium iodide is found to have far too low a value when compared to the susceptibility in this direction. These values noted above coincide in their order of magnitude with the values directly obtained and noted previously.

5. *The Optical Anisotropy of Naphthalene.*

Groth mentions that naphthalene crystals exhibit a high degree of birefringence. It was thought that it would be of interest to study this quantitatively and find whether there is any analogy between the magnetic and optical characters of the substance. He states that naphthalene exhibits in the polariscope an axial figure lying in the *ac* plane. This has been confirmed. It may be noted that in order to observe the figures successfully, monochromatic light should be used and the crystals chosen should be very thin. These facts

* 'Phys. Rev.,' vol. 29, p. 174 (1927).

themselves indicate that the birefringence of the crystal is very large. The thin flakes of the crystal exhibit in the polariscope the rings surrounding only one of the optic axes, the other axis lying outside the field of vision. It is clear from the observations that the *ac* plane contains the optic axes.

The inclination of the visible optic axis to the normal to the surface has been obtained by comparing the interference figure with that of borax of known axial angle. The apparent inclination of the optic axis to the normal comes out to be $48^{\circ} 18'$. The obtuse bisectrix appears to emerge just beyond the field of vision on the other side of the normal. Its distance from the centre of the field corresponds roughly to an angle of about 33° . Since the *c* axis is also inclined to the normal at an angle of $32^{\circ} 49'$, it can be inferred that the obtuse bisectrix coincides roughly with it. This is checked independently by calculation and the deviation is found to be only 3° . Further the maximum birefringence for sodium light has also been estimated, by measuring the thickness and counting the number of complete rings in a particular case.

Thickness of the plate = 0.0033 cm.

Number of complete rings = 28 ; λ for sodium light = 0.000589 cm.

Maximum birefringence = 0.499.

By the method of immersion* the two principal values of the refractive index in the cleavage plane have been obtained, one of them being 1.775 along the *b* axis and the other 1.570 along the *a* axis. A rotation apparatus fixed to the stage of a microscope has also been used to find the inclination of the optic axis to the normal. The apparent angle found by this method is 48° , which is very nearly the same as the one obtained by means of the interference figure. The principal indices in the *ac* plane calculated from the above data work out as 1.932 along the obtuse bisectrix which is inclined at 3° to the *c* axis and 1.442 along the other principal axis in the plane. The results can be tabulated as below.

Axis as marked in fig. 3.	Susceptibility.	Refractive index.
OM	-1590×10^{-7}	1.442
Ob	-710×10^{-7}	1.775
Oc	-390×10^{-7}	1.932

This gives a maximum birefringence of 0.490, which agrees with the foregoing value. It is to be noted that the axes of the optical and the magnetic

* See Johannsen, 'Manual of Petrographic Methods,' p. 253.

ellipsoids roughly coincide and the magnitudes of the numerical values follow the reverse order in the two cases.

The density of the crystal is 1.152 and the refractive index of the liquid naphthalene at 99.6° is 1.583 and its density at the same temperature is 0.9634. If the crystal were an isotropic solid to which the Lorentz formula is applicable, its calculated refractive index would be 1.721, whereas the mean of the three observed indices is 1.716. Thus there appears to be a diminution of 1.6 per cent. in the Lorentz constant as the substance passes from the liquid into the solid state. Such a diminution in the Lorentz constant with increasing density is to be expected from theoretical considerations.*

6. *A Discussion of the Results.*

A glance at the table given in the previous page shows that the optical and the magnetic susceptibilities along the three axes follow a reverse order in their magnitudes, the direction of the maximum diamagnetic susceptibility coinciding with the direction of the minimum refractive index. This result enables us to explain the experimental fact that the naphthalene derivatives in the liquid state show a strong positive birefringence in a magnetic field. The expression for the Cotton-Mouton constant C_m is

$$\frac{3(n_0^2 - 1)}{80\pi n_0 \lambda k T v} \cdot \frac{[(A - B)(A' - B') + (B - C)(B' - C') + (C - A)(C' - A')]}{(A + B + C)^2},$$

where A, B, C are the moments induced along the three principal axes of the molecule by unit electric force in the incident light waves, acting respectively along those three axes and A', B', C' are the magnetic moments induced in the molecule by unit magnetic field acting in the same three directions. It is clear that if the optical moments follow the order A, B, C and the magnetic ones follow the reverse order C', B', A', then the expression takes a positive value. It is to be remembered in this connection that the magnetic moments are negative as the crystal is diamagnetic. The magnitude of the effect depends upon the difference of the magnetic susceptibilities in the three directions. In a case like that of naphthalene, where we have pronounced differences, the effect must be positive and very large.

It now remains to be seen how far the data will assist us in fixing the plane of the molecule in the crystal lattice. The dimensions of the unit cell as determined by the X-ray data are, in A.U. :—

$$a = 8.34; \quad b = 6.05; \quad c = 8.69,$$

and the unit cell is of the form shown in fig. 4.

* Raman and Krishnan, 'Roy. Soc. Proc.,' A, vol. 117, p. 549 (1928).

Bragg* places one molecule at each corner of the cell and two at the centres of the faces OO' and cc' as shown in fig. 4. Thus each cell contains two molecules,

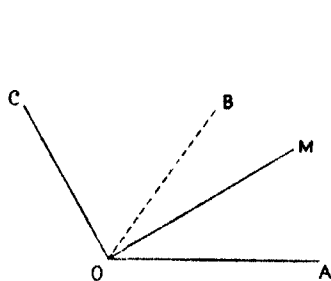


FIG. 3.

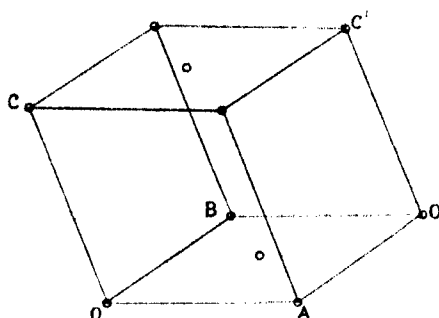


FIG. 4.

both of them being similarly orientated. Further, by comparing it with the dimensions of the unit cell of anthracene, he concludes that the length of the molecule is along the line oc , *i.e.*, the c axis. In fixing the plane of the molecule, he remarks, "on making up a model, however, it is seen that it is much more likely that the plane of the molecule lies nearer to the ac plane than the bc plane. The molecules lock together much better if that is so. Moreover, if the molecules lie in the bc plane they would be close neighbours in that plane, and at the same time there would be wide gaps between consecutive planes." However, it is found very difficult to reconcile this placing of the molecule with the magnetic and the optical data given above.

In this connection the work of Owen and Honda and Také Soné on graphite and diamond is very significant.† They have found that graphite shows a large diamagnetic anisotropy, the susceptibility in a direction perpendicular to the hexagonal ring being nearly seven times as large as in directions parallel to the ring, whereas diamond is practically isotropic. There is a similar contrast when we compare the magnetic behaviour of the aromatic and the aliphatic series of carbon compounds. The aromatics show a large magnetic anisotropy, whereas the aliphatics show a comparatively feeble anisotropy. This parallelism can be explained by the well-known fact that the structure of graphite resembles that of aromatics whereas the structure of diamond is analogous to that of aliphatics. The arrangement of the carbon atoms in naphthalene closely resembles that in graphite. Hence we are led to conclude that the

* 'X-rays and Crystal Structure,' p. 233 (1925).

† Owen, 'Ann. Physik,' vol. 37, p. 657 (1912); Honda and Také Soné, 'Sci. Rep. Tohoku Univ.,' vol. 2, p. 25 (1913).

direction of maximum diamagnetic susceptibility is perpendicular to the plane of the ring. This at once suggests that the plane of the molecule should be the *bc* plane (figs. 3 and 4), as OM has the largest susceptibility.

Independent evidence is also available from observations on light scattering in liquids. Ramanathan* calculated the moments induced in the benzene molecule when the incident electric field in the light wave acts along the three principal axes of the molecule. He concluded that the molecule has an axis of optical symmetry, perpendicular to the plane of the ring. When the incident field is parallel to this axis, the optical moment induced is much smaller than when the field acts along directions perpendicular to it. Similar considerations indicate that in naphthalene, the optical moment induced when the incident field is in a direction perpendicular to the plane of the molecule is much less in comparison with the moments induced when the incident field acts in directions parallel to the ring. This again suggests that the plane of the molecule is to coincide with the *bc* plane (figs. 3 and 4), for along the line OM we have the minimum refractive index. This conclusion is in accordance with the one arrived at from the magnetic data.

7. Summary of the Results.

Quantitative studies show that naphthalene crystals exhibit a remarkable degree of magnetic and optical anisotropy. Two of the magnetic axes of the naphthalene crystal are found to coincide with two of the crystallographic axes, namely, *b* and *c*, and the third is a line perpendicular to both of them. The principal susceptibilities were found to be as follows:—

χ_m , along the *b* axis -710×10^{-7} ; along the *c* axis -390×10^{-7} ; and along a line perpendicular to both these -1590×10^{-7} .

Two of the axes of the optical ellipsoid are found to similarly coincide with *b* and *c* axes to within about 3° and the data for the refractive indices for the D-line are as follows:—

Along the *b* axis, 1.775; along the *c* axis, 1.932; and along a line perpendicular to both these, 1.442.

Bragg supposes that the two molecules in the cell are similarly orientated with their planes parallel to the *ac* plane. Contrary to this, the foregoing results suggest that the molecules are so orientated as to have their planes parallel to the *bc* plane of the unit cell in the crystal.

The maximum axis of the magnetic ellipsoid is found to roughly coincide

* 'Roy. Soc. Proc.,' A, vol. 110, p. 123 (1926).

with the minimum axis of the optical ellipsoid and vice versa. This leads us to a simple explanation of the strong positive birefringence exhibited by aromatic liquids in a magnetic field.

I have much pleasure in acknowledging the great help rendered by Mr. Krishnan during the progress of this work and the kind encouragement of Prof. C. V. Raman. I take this opportunity of expressing my gratefulness to both of them. The investigation was carried out in the laboratory of the Indian Association for the Cultivation of Science, Calcutta.

The Influence of Hydrogen Ion Concentration on the Adsorption of Weak Electrolytes by Pure Charcoals.

By HAROLD JOHN PHELPS and RUDOLPH ALBERT PETERS, Department of Biochemistry, Oxford.

(Communicated by Sir Harold Hartley, F.R.S.—Received February 18, 1929.)

Recent progress in enzyme chemistry has been largely due to the use of adsorbents. In vitamin studies also, adsorbents such as Fuller's earth have been introduced with marked success.* A prominent feature of such work is the influence of hydrogen ion concentration upon the efficiency of the adsorption. A technique recently introduced by Kinnersley and Peters† for concentrating the antineuritic vitamin (B 1) involves at one stage the adsorption of the vitamin by acid-treated Norite charcoal. In this case also it has been found that the hydrogen ion concentration influences considerably the degree of adsorption.

Adsorbents which are themselves of acidic or basic character might be expected to be influenced in their behaviour by hydrogen ion concentration, but in the case of charcoal the reason for the change in adsorptive power is more obscure. Bartell and Miller‡ have stressed the importance of using pure charcoals in the study of adsorption phenomena. It is probable indeed that many of the anomalous results obtained by workers in this subject have been due to the use of various impure charcoals. The acid-treated charcoal

* Seidell, 'U.S. Public Health Rep.,' vol. 31, p. 314 (1916).

† 'Biochem. J.,' vol. 21, p. 777 (1927).

‡ 'J. Amer. Chem. Soc.,' vol. 54, p. 1866 (1932).

used in the vitamin work contained about 1 per cent. of mineral impurity. It was important therefore to discover whether the effect of hydrogen ion concentration on the adsorption by pure charcoals was equally marked, and if so whether these effects could be correlated with the recognised chemical properties of various adsorbates.

In this paper we propose to show that the adsorption of simple weak organic acids and bases by pure charcoal is much influenced by hydrogen ion concentration. The experiments upon these substances are described in the first part of the paper while the results obtained with histidine and histamine and some of the simpler amino acids are described in the second part.

Previous Work.

It is beyond the scope of this paper to review all the work which has been done upon charcoal adsorption. The elaborate studies of Miller and his associates have shown the importance of obtaining a pure charcoal. They have further demonstrated that provided a pure charcoal be used the results obtained with charcoals from different sources do not differ fundamentally. Bartell and Miller* have found evidence for the belief that the adsorption of salts is predominantly hydrolytic. This view is not confirmed by Kolthoff† or by Schilow and Lepin‡.

The effect of hydrogen ion concentration on adsorption by charcoal seems to have been little studied. Michaelis and Rona§ appear to have been the first to note variations that could be ascribed to this cause. In their paper, which was qualitative rather than quantitative in character, they distinguish three types of adsorption, typified by albumin, amylase and trypsin. More recently Fromageot and Wurmser|| found that in the case of formic, acetic, propionic, oxalic, citric, succinic and pyruvic acids the adsorption of the acids was much greater than that of the corresponding sodium salts. In many cases the latter seemed not to be adsorbed at all. These workers further found that the curve relating hydrogen ion concentration with the adsorption of citric and oxalic acids followed in a general way their dissociation curves. There were, however, marked deviations from which they concluded that there was no simple relation between the adsorption of different radicles and their dissociation

* 'J. Amer. Chem. Soc.,' vol. 54, p. 1866 (1922), and vol. 56, p. 1150 (1924).

† 'Z. Electrochem.,' vol. 33, p. 497 (1927).

‡ 'Z. Phys. Chem.,' vol. 94, p. 25 (1920).

§ 'Biochem. Z.,' vol. 25, p. 359 (1910).

|| 'C. R.,' vol. 179, p. 972 (1924).

constants. These results were obtained with what was described as a highly purified charcoal, but the actual ash content was not stated.

Rather later Skumburdis* showed that the sodium salt of iso-valerianic acid was less adsorbed than the acid itself. The latter worker seems to have been in ignorance of the results obtained by the French workers, which indeed have escaped attention in the literature.

Experimental.

The following details of technique are generally applicable to the experiments performed in the course of this investigation. Commercial Norite charcoal was purified by extraction with mixed hydrochloric and hydrofluoric acids as described by Miller.† After this treatment its activity as an adsorbent for hydrochloric acid was about one-third that of the untreated charcoal. The charcoal used in the research came from one 12-lb. sample of Norite charcoal. It was extracted in quantities of about 30 gm. at a time in platinum basins. After extraction, the charcoal underwent a thorough washing with hot water, first by decantation and finally on a Buchner funnel until the washings were chloride free. The charcoal was finally ignited to a bright red heat *in vacuo* to remove small traces of volatile matter and irreversibly adsorbed acids. It was not found that the results differed with different samples of extracted charcoal. The ash content of the charcoal so purified was less than 0.07 per cent.

In view of the difficulty of purifying large amounts of charcoal and in order to facilitate manipulation, the experiments were performed upon a small scale. The solutions were diluted to 0.2 per cent. in order to eliminate effects other than true surface effects as far as possible; for histidine and histamine even more dilute solutions were used. In the case of the simple acids and bases, various hydrogen ion concentrations were obtained by partial neutralisation with strong acids and bases. The resulting mixtures of the weak acids and bases with their salts were to some extent self-buffering. In the case of other substances small amounts of buffer solutions were added. A total volume of 22 or 23 c.c. was shaken with charcoal in a shaking machine placed in a room maintained at $20^{\circ}\text{C.} \pm 0.1$. Unless otherwise stated the solutions were shaken with charcoal in the proportion of 10 mg. of charcoal to 1 c.c. Twelve hours were usually allowed for equilibrium to be attained. This, however, was purely a matter of convenience as experiments with hydrochloric acid showed

* 'Koll. Z.,' vol. 44, p. 127 (1928).

† 'J. Phys. Chem.,' vol. 30, p. 1031 (1926).

that equilibrium was established in less than 4 hours ; this substance, moreover, was found by Miller to be one of the slowest adsorbates to come into equilibrium. As many of the substances employed formed good media for the growth of micro-organisms, it was found necessary in certain cases to shake for periods much less than 12 hours to minimise the destructive effect of growing bacteria. At the end of each experiment the mixture was centrifuged and the clear solution decanted from the charcoal. The equilibrium values of the hydrogen ion concentration were determined by the bubbling hydrogen electrode except in the case of the very dilute histidine and histamine solutions, where colorimetric estimations were made. In all cases in which samples of the centrifugate could not be analysed immediately, the solutions were stored in the laboratory cold store to reduce errors caused by the growth of bacteria. That an error from this source might be serious was shown by the fact that a 0.01 per cent. histidine solution was found to have lost about 30 per cent. of its histidine after standing for less than 24 hours at room temperature.

The substances used were with one exception either B.D.H. or Kahlbaum products. The simple acids and bases were further purified by distillation. Succinic acid was used as its crystalline sodium salt, while histidine and histamine were used as the hydrochloride and acid phosphate respectively. The glutamic acid was prepared by us from gluten flour and recrystallised from aqueous alcohol.

Methods of Estimation.

(a) *Propionic and Caproic Acids.*—The simple acids were estimated by titrating between the limits of pH 3 and 10, using brom-phenol-blue and thymol-phthalein as indicators. For each analysis a 5-c.c. sample was titrated with standard acid to pH 3 and a similar sample with standard alkali to pH 10. A control sample of the solution before adsorption was similarly titrated. The range pH 3 to pH 10 covers the ionisation of the weak acid and not those of the strong acid or base with which it is associated, so that within the limits of accuracy required only the weaker acid is titrated. This method is essentially similar to that used by van Slyke and Palmer* and by Harris.†

(b) *Succinic Acid.*—The method employed for the estimation of succinic acid was essentially the same as that used by Moyle.‡ The test samples were all made exactly neutral to brom-cresol-purple. Excess silver nitrate was then added. The precipitated silver succinate was allowed to coagulate for an

* 'J. Biol. Chem.,' vol. 41, p. 567 (1920).

† 'Roy. Soc. Proc.,' B, vol. 95, p. 440 (1924).

‡ 'Biochem. J.,' vol. 18, p. 351 (1924).

hour or so. It was then filtered off on a black filter. Instead of washing with dilute ammonium nitrate, however, the washing was done with three changes of distilled water. Correction was made for the solubility of silver succinate by analysing two proofs from the original solution with each series of experiments. If the two proofs did not agree, the series was neglected. Care was taken that approximately the same volume of water was washed through each sample in any one series. The precipitates were then dissolved in 2-N nitric acid and the papers well washed with hot water. The silver was then estimated by thiocyanate.

(c) *n-propylamine and n-butylamine*.—The amines were estimated by distilling in steam from a strongly alkaline solution into N/70 sulphuric acid and titrating with N/70 caustic soda. Methyl red was used as an indicator. The distillations were carried out in an apparatus identical with that usually employed for micro-Kjeldahl analyses.

(d) *The Amino Acids*.—Glycine, alanine, glutamic and aspartic acids were estimated by the "van Slyke" micro analysis apparatus for determining amino nitrogen. Histidine presented more difficulty. It was finally estimated by the micro-colorimetric method described by Koeassler and Hanke.* Very dilute solutions (0.01 per cent.) could be employed for the estimation and duplicate experiments agreed within 5 per cent. The results obtained were sufficiently accurate for the purposes required, *i.e.*, to demonstrate any large change in adsorption with hydron concentration. In the experiments 0.01 per cent. solutions of histidine hydrochloride were used, these being treated in this case with 5 mg. of charcoal for each cubic centimetre of solution, the total volumes being 10 or 11 c.c. Histamine was estimated in a similar way, using, however, 0.02 per cent. solutions of the acid phosphate which gives a colour reaction of intensity comparable with that given by a 0.01 per cent. solution of histidine hydrochloride.

It was found that experiments with histidine and histamine had to be conducted especially quickly to avoid errors due to bacterial action. Estimations were therefore carried out as soon as possible after the completion of shaking with charcoal, and the whole experiment finished in a day. Owing to the difficulties of excluding carbon dioxide from these dilute solutions, the *pH* values were determined colorimetrically to an accuracy of 0.1 *pH*.

Experimental Results.

Section I. Monocarboxylic Acids.—The results are plotted in figs. 1 and 2. It will be seen that between *pH* 3.5 and 5.5 the adsorption of propionic acid

* 'J. Biol. Chem.,' vol. 39, p. 497 (1919).

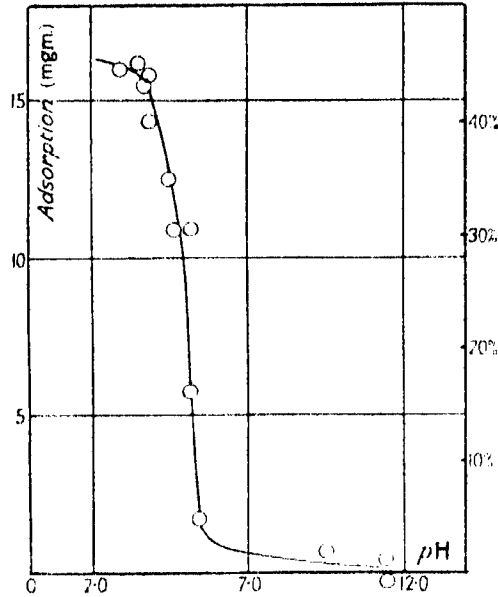


FIG. 1.*—Showing the influence of hydrogen ion concentration on the adsorption of propionic acid. The adsorption is expressed in milligrams per 200 mg. of charcoal from 20 c.c. of solution containing originally 1.8 mg. per cubic centimetre. The hydrogen ion concentration is expressed in pH units.

* The scale on the right-hand side of figs. 1 to 5 inclusive represents the adsorption as a percentage of the total amount of adsorbate originally present.

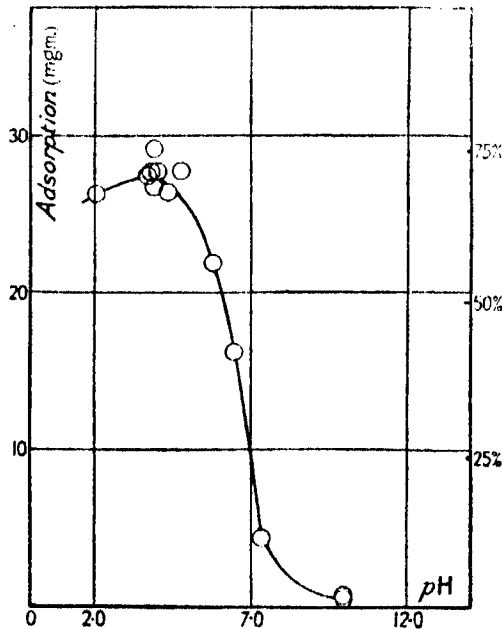


FIG. 2.—Showing the influence of hydrogen ion concentration on the adsorption of caproic acid. The adsorption is expressed in milligrams per 200 mg. of charcoal from 20 c.c. of solution containing originally 1.94 mg. of the acid per cubic centimetre. The hydrogen ion concentration is expressed in pH units.

falls almost to zero. As the dissociation constant of propionic acid given by Ostwald* is 1.34×10^{-5} , this region covers almost exactly the ionisation range of propionic acid. The adsorption of caproic acid falls off equally suddenly and rapidly between pH 4.8 and 7.5. This range is rather more alkaline than would correspond with the ionisation range of caproic acid, K_a is given by Ostwald (*loc. cit.*) as 1.45×10^{-5} . There is, however, no doubt of the general relation between adsorption and ionisation.

Dicarboxylic Acids.—The only member of this series that has been investigated is succinic acid. The results are shown graphically in fig. 3. In solutions

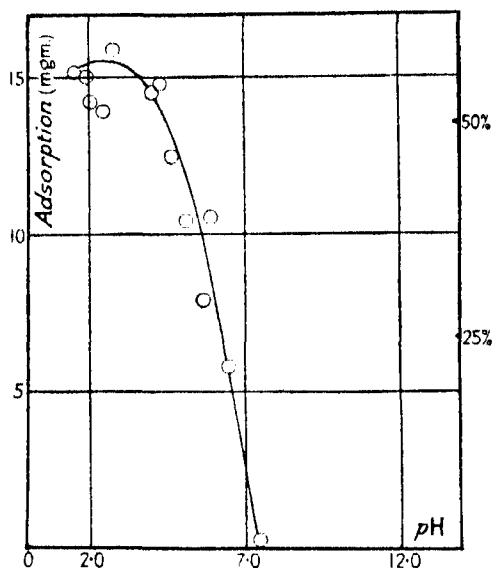


FIG. 3.—Showing the influence of hydrogen ion concentration on the adsorption of succinic acid. The adsorption is expressed in milligrams per 200 mg. of charcoal from 20 c.c. of solution containing originally 1.28 to 1.40 mg. of acid per cubic centimetre.

more alkaline than pH 7.0, the adsorption is nil. From pH 7.0 to pH 4.0, the adsorption rises rapidly until it is about 16 mg. per 200 mg. of charcoal. In solutions more acid than pH 3.0, there is some indication that the adsorption falls off. It is at once obvious that the adsorption is greatest under conditions in which the ionisation of succinic acid is virtually nil. The value given by Ostwald (*loc. cit.*) for K_{a_1} is 6.65×10^{-5} and that given by Chandler† for K_{a_2} is 2.7×10^{-6} . Assuming these figures, which were determined at $25^\circ C.$, to be approximately true at $20^\circ C.$ the degree of adsorption of succinic

* 'Z. Phys. Chem.,' vol. 3, pp. 170, 241 (1889).

† 'J. Amer. Chem. Soc.,' vol. 30, p. 694 (1908).

acid is in almost exact proportion to the degree of ionisation as plotted from the dissociation curve. The coincidence of these two phenomena in all three cases points strongly to the conclusion that adsorption proceeds predominately through the unionised molecules.

It may be concluded that for the acids studied, which may be regarded as typical of the series, the decrease in adsorption with increasing acidity of the solution may be correlated almost quantitatively with the percentage of unionised molecules present. Ionisation is therefore a large factor in determining adsorption, and it is the unionised molecule that is adsorbed. This conclusion confirms and extends that reached by Fromageot and Wurmser (*loc. cit.*).

If the conclusion put forward as a result of a study of the adsorption of acids is correct, it should be possible to demonstrate a similar relation in the case of the bases. Bases should tend to be most adsorbed in alkaline solution. The following experiments show that this is so.

The Adsorption of Normal Amines.—The results for the two amines investigated, *n*-propylamine and *n*-butylamine are shown in figs. 4 and 5. In the

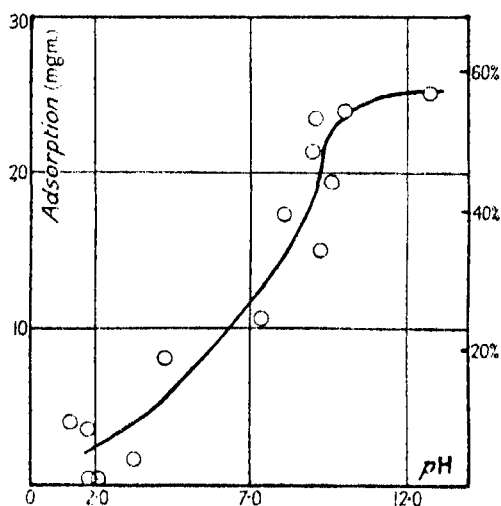


FIG. 4.—Showing the influence of hydrogen ion on the adsorption of *n*-propylamine. The adsorption is expressed in milligrams per 200 mg. of charcoal from 20 c.c. of solution containing originally from 1.89 to 1.92 mg. per cubic centimetre.

case of the bases the adsorption increases progressively with increasing alkalinity of the solutions, and therefore with decreasing ionisation of the bases. In these cases, however, the curve does not rise abruptly like those of

the carboxylic acids and cannot therefore be correlated directly with the ionisation curve. Several possible explanations of this phenomenon may be given,

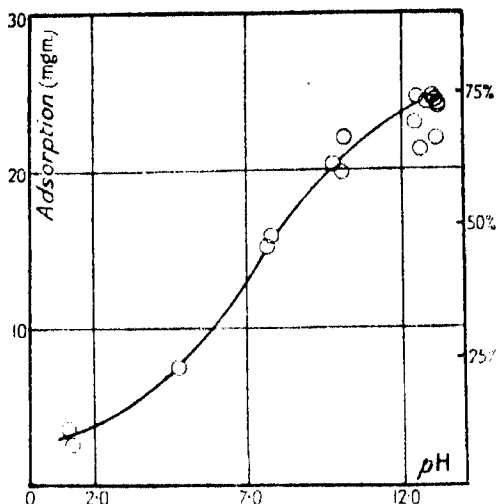


FIG. 5.—Showing the influence of hydrogen ion on the adsorption of *n*-butylamine. The adsorption is expressed in milligrams per 200 mg. of charcoal from 20 c.c. of solution containing originally from 1.66 to 1.71 mg. per cubic centimetre. The hydrogen ion concentration is expressed in *pH* units.

but it is thought better to leave the question until more work has been done. The results obtained with the amines support the general view that adsorption increases with decreasing ionisation.

It must not be forgotten in this connection that the purified charcoals had been treated with acid. Subsequent to this, they had been heated to a high temperature. Experiment has shown that these charcoals give a neutral extract with water and that a current of air in which a sample of the charcoal has been ignited is free from hydrogen chloride; but the possibility that very minute traces of acid are still present in the charcoal and are influencing the adsorption of the bases cannot be entirely ignored.

Section II. The Adsorption of Amino Acids.—In Section I it has been shown that ionised substances tend not to be adsorbed, so that it would be expected upon the classical view of the ionisation of the amino acids that there would be a maximum adsorption at the iso-electric point, the region of least dissociation. It has been stated, especially by Michaelis, that the simple amino acids such as glycine are not adsorbed by charcoal at any *pH*. We doubted this statement at the outset of the research upon theoretical grounds, but it

has been completely confirmed for the mono-amino-mono-carboxylic acids studied. Both glycine and alanine showed no adsorption at any pH. The experimental results for alanine are shown in the table. It would seem therefore that the adsorption of the mono-amino-mono-carboxylic acids ($\text{R-CH}_2\text{-NH}_2\text{-COOH}$) cannot be predicted by supposing them to behave as a

Table.—The Adsorption of Alanine.

The "nitrogen volumes" are those determined by analysis in the van Slyke apparatus.

Solutions.	Nitrogen volumes corrected for dilution by buffers and blank.	Adsorption in mg. of amino nitrogen per 200 mg. of charcoal.
	c.c.	mg.
Proofs	2.70	—
Dilute HCl, pH 2	2.70	0.00
Acetate buffer, pH 3	2.68	0.01
Phosphate buffer, pH 4	2.70	0.00
Alanine solution, unbuffered, pH 4	2.66	0.02
Acetate buffer, pH 6	2.69	0.00
Phosphate buffer, pH 9	2.68	0.01

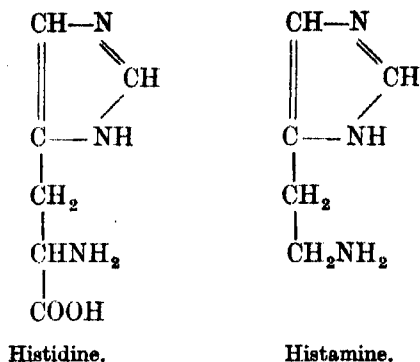
mixture of a weak acid and a weak base. Experiments upon the di-carboxylic mono-amino acids, aspartic and glutamic acids, showed that they were slightly adsorbed with a tendency to a minimum at pH 5. This effect was, however, slight. The maximum adsorption was in fact never more than 10 per cent., so that more experimental work is needed to establish it with certainty. It may be concluded that the simple amino acids *per se* do not show the profound changes in adsorption shown by the normal weak acids and bases.

In view of the work of Warburg* upon the oxidation of the amino acids upon the surface of charcoal, it was necessary to establish that the effects described in this paper could not be due to the oxidation of the substances concerned on the surface of the charcoal. A consideration of the variety of the effects alone is sufficient to exclude such a possibility, but in order to make certain we carried out a few experiments in a Barcroft apparatus upon the oxygen uptake of the charcoal used in the presence of aspartic acid. The results of these convinced us that the effects of catalytic oxidation could be ignored in this connection.

Histidine and Histamine.—It was considered of interest to study the

* 'Biochem. Z.,' vol. 119, p. 134 (1921).

adsorption of a ring amino acid. Histidine was therefore studied, and also the base histamine in order to provide an interesting comparison.



Both of these are of biochemical interest. Whereas histidine is a normal constituent of proteins and is one of the amino acids especially needed in nutrition, histamine is a powerful excitant of smooth muscle tissue, and generally has marked pharmacological properties. Any striking difference in adsorption is likely to be significant in interpreting the differences of action between these two substances.

Fig. 6 gives the results obtained. These show that histidine and histamine follow a similar curve form pH 3 to pH 7.3 approximately, their adsorption rising rapidly between pH 4.5 and pH 6.5. To the alkaline side of pH 7.3 the curves deviate. Whereas the curve for histamine rises rapidly to completion (within the limits of experimental error), that of histidine tends to fall. It is interesting to find out whether the curves obtained can be correlated with the known dissociation constants for histidine. According to Harris (*loc. cit.*) the curve for K_b lies between the limits of pH 4 to 7 approximately, and that for K_a between 7 and 10. The point at which these curves cross is about pH 7. That is to say, the percentage of unionised molecules is maximal at pH 7 which is sufficiently near the turning-point of the histidine curve to suggest that the two phenomena are closely related. The marked deviation of histamine from histidine to the alkaline side of pH 7.5 can only be attributed to the absence of the carboxyl grouping from the former; further, as the simpler amino acids showed no adsorption, the rise from pH 4 to pH 7 must be correlated with the ionisation of a basic grouping. Hence these results are quite consistent with the classical view of the dissociation of the amino acids, according to which in the case of histidine the change in ionisation to the alkaline side is due to the ionisation of the carboxyl group. On the other hand, the results

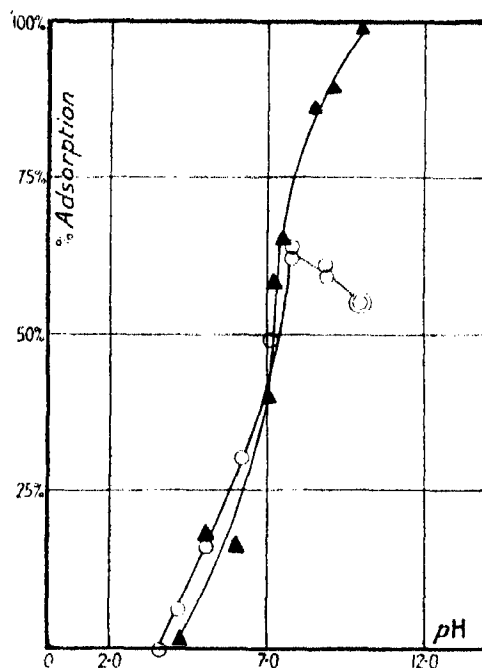


FIG. 6.—Showing the influence of hydrogen ion concentration on the adsorption of histidine (circles), and histamine (triangles). The adsorptions are expressed as percentages of the total amounts originally present in solution which are adsorbed by 50 mg. of charcoal. The hydrogen ion concentrations are expressed in pH units.

for alanine and glycine cannot readily be reconciled with such a view. Whether they are explicable by the newer views of the constitution of amino acids,* it remains for further work to determine.

Discussion of Results.†

In the cases of the acids and bases studied there is a pronounced decrease in adsorption with increasing ionisation. For the acids the fall in the adsorption may be correlated almost quantitatively with the percentage of unionised molecules present. For the amines the adsorption is maximal in alkaline solutions in which the ionisation of the bases is virtually nil, and the adsorption is virtually nil in acid solutions in which the ionisation is maximal. The

* Bjerrum, 'Z. Phys. Chem.,' vol. 104, p. 147 (1923).

† We have assumed for the purposes of this research that the effects obtained have taken place at a carbon-water interface. It is likely, however, that conditions at any interface are rendered very complex (Hardy, 1928) in view of the profound effect of small traces of impurities. No special attempt was made to remove adsorbed gases from the charcoals used in our work.

decrease in adsorption with decreasing pH is in these cases too gradual to be compared quantitatively with the ionisation curve of the base. These results confirm, amplify and extend the conclusions of Fromageot and Wurmser.

From these results it is reasonable to conclude that adsorption proceeds through the medium of unionised molecules. This conclusion has also been reached by Schilow (*loc. cit.*) and others. Hydrolytic adsorption of the sodium salts of the simple acids such as that observed by Miller (*loc. cit.*) has not been noticed, nor has there been found molecular adsorption of these salts such as that described by Kolthoff (*loc. cit.*). With the charcoals used in this work the adsorption of succinic, propionic, and caproic acids is nil in solutions of acidity corresponding with the existence of their sodium salts. As Miller and Kolthoff used sugar charcoals this difference in the properties of two different forms of pure carbon is of interest.

The theory advanced by Bartell and Miller* seems to be untenable for the weak acids and bases, as it assumes that adsorption takes place through the medium of the ion, although the final result may be the adsorption of the molecule.

The results described here are consistent with Langmuir's theory of adsorption from solution,† if the charcoal is pictured as an uncharged surface. According to this theory there is a kinetic equilibrium between molecules arriving at the surface from the interior of the solution, and those passing from the surface to the interior. Hence adsorbed molecules are continually being displaced by solvent or solute molecules. It is possible that entry into the surface by the ions is largely prevented by surrounding water sheaths (hydration). In the case of charcoal, it is likely that the kinetic equilibria are complicated by capillary effects (as has been suggested by Langmuir).

Some Biological Considerations.

The predominance of surface in the reactions of the living cell makes a discussion of these findings of interest in this connection. Charcoal is perhaps the nearest approach which we have to a neutral surface. Though it is certain that many of the cell surfaces are charged, adsorption effects due to this might be expected to be superimposed upon any which would take place in its absence. Some idea as to such underlying events can be obtained from these results with charcoal. In the absence of specially charged surfaces, we learn

* 'J. Phys. Chem.,' vol. 28, p. 992 (1924).

† Langmuir, 'J. Amer. Chem. Soc.,' vol. 39, p. 1848 (1917); Henry, 'Phil. Mag.,' vol. 44, p. 689 (1922).

that at the reaction of the living cells (say pH 6·6 to 7·4), simple weak aliphatic acids will not be adsorbed. The simpler weak bases will be slightly but definitely adsorbed. Hence there will be no accumulation at the interfaces of the cell of such substances as lactic acid or of β -hydroxy-butyric acid, unless such acids become attached to basic portions of protein or to other surfaces which may happen to have some basic dissociating group. Doubtless the considerable adsorption of the bases, which rises especially to the alkaline side of the true neutral point is of real significance in regard to their physiological activity. It can be imagined for instance that if the slightly adsorbed histidine becomes converted by some enzyme system in the cell into the strongly adsorbed histamine, in the course of which the solution immediately adjacent to the surface is made more alkaline, then ideal conditions for action of the base at a surface would be reached. The case of the amino acids is peculiar. A neutral surface does not apparently adsorb the simpler amino acids. Why is it then that such acids upon injection into the blood stream leave it again so rapidly for the tissues? To quote a definite instance, Seth and Luck* have shown that 1 gm. of glycine injected intravenously into the dog, disappears from the circulation almost completely in a matter of 17 minutes. Similar results were obtained for alanine. Mere distribution will not explain these results. They may possibly be partly due to ready synthesis to peptide in the tissue, but it seems to be likely also that they indicate the presence of some charged surface able to retain the acids. There would seem to be little doubt that the facts described here must be taken into general account, even if they require to be modified in detail to suit the particulars of specialised structures.

Summary.

The influence of hydrogen ion concentration upon the adsorption of various substances by purified charcoal has been studied.

In the case of propionic, caproic and succinic acids, adsorption decreases with increasing alkalinity between the limits of C_H $10^{-3.0}$ – $10^{-7.0}$ (pH 3·0–7·0). This change follows approximately the ionisation curves of the acids.

In the case of the bases *n*-propylamine and *n*-butylamine, adsorption increases with increasing alkalinity, becoming maximal at C_H $10^{-11.0}$ (pH 11·0). The effect is not so directly correlated with ionisation.

The amino acids glycine, alanine and aspartic acid, show no pronounced adsorption at any C_H . The adsorption of the amino acid histidine has been

* 'Biochem. J.,' vol. 19, p. 366 (1925).

compared with that of the corresponding base histamine. The adsorption of these substances follow a similar curve from C_H $10^{-4.0}$ – $10^{-7.3}$ (pH 4.0–7.3). After this they deviate. The adsorption of histamine rising to completion at C_H $10^{-10.0}$ (pH 10.0) whereas the adsorption of histidine slightly decreases with increasing alkalinity.

The results with histidine are explicable upon the classical view of the dissociation of the amino acids, whereas those with glycine, alanine and aspartic acid seem to require further explanation.

It is concluded that adsorption in the case of the substances studied proceeds predominately through the unionised molecule.

We wish to express our gratitude to Sir Harold Hartley for the loan of apparatus.

The Effect of a Nuclear Spin on the Optical Spectra.

By J. HARGREAVES, B.A., Clare College, Cambridge.

(Communicated by R. H. Fowler, F.R.S.—Received April 3, 1929.)

Introduction.

Some recent work has been done by Back and Goudsmidt on the "hyperfine" structure of the optical spectrum of bismuth,* and more recently similar work has been carried out for caesium by Jackson.† In each of these investigations the fine structure was examined closely with a view to revealing a still finer structure, and it was found in both cases that the lines attributed to electronic spin were themselves composed of several distinct lines. In fact, for caesium, each of the fine (electron spin) lines of the principal series was found to split up into two; for bismuth the hyperfine structure was more complicated. Back and Goudsmidt attributed the structure to a nuclear spin, and working out the consequences of this on the lines of the old quantum mechanics they found that a nuclear spin of $4\frac{1}{2}$ quanta is necessary to account for the facts; a spin of a $\frac{1}{2}$ quantum is similarly attributed by Jackson to the nucleus of caesium. The hypothesis explains very satisfactorily in a qualitative way the results of observation. In the work described in the present paper the methods

* 'Z. Physik,' vol. 43, p. 321 (1927), and vol. 47, p. 174 (1928).

† 'Roy. Soc. Proc.,' A, vol. 121, p. 432 (1928).

of the new quantum mechanics have been applied to the problem. More precisely, we consider the motion of a single electron in a Coulombian field due to a nucleus possessing a $\frac{1}{2}$ quantum of spin. It will be seen that the results can easily be extended to the case of any central field, and the principle could also be extended to the case of an atom with a nuclear spin of $\frac{1}{2}(nh/2\pi)$, but the detailed working out would be very heavy for $n > 1$ (at any rate, using the methods explained in this paper), owing to the large number of wave functions which would be necessary to specify any state of the atom.

It will be seen that the results we obtain are substantially the same as Jackson's so far as the energy levels are concerned, but the calculated intensities are not consistent with the observed transitions, and we deduce a combination rule which is radically different from Jackson's.

In the following section we explain briefly the results obtained by an application of the old quantum theory.

§ 1. We suppose that the electron has a total angular momentum $j\hbar$ (\hbar will be used throughout to denote Planck's constant divided by 2π), where j is half an integer (the electron spin is included in j), and that the nucleus has a spin of amount $i\hbar$. Consider the way in which the two angular momenta combine, supposing the result to be quantised, and equal in magnitude to $f\hbar$. Then

$$|j - i| \leq f \leq |j + i|,$$

so that f can take integral or half-integral values (according as $|j \pm i|$ are integers or half-integers) between the limits indicated. Hence the total number of possible values of f is $2q + 1$, where q is the lesser of the two numbers j and i . Accordingly, if we define the total electronic angular momentum properly (viz., $j = |k \pm \frac{1}{2}|$, where $k = 0, 1, 2$, etc., for the S, P, D, etc., levels) we find at once the number of separate levels into which the S, P, D, ... levels split up, when we give i any particular value.

For caesium $i = \frac{1}{2}$, and for the S levels $j = \frac{1}{2}$ so that $f = 0, 1$. For the P levels $f = 0, 1, 1$ or 2 . Each of the spin doublets splits up into two, and there are therefore two S levels, and four components for each of the higher levels. The case of bismuth is not so simple: $i = 4\frac{1}{2}$ and so the maximum number of levels is 10. The number of levels for the S, P, D terms are 2, 6, 10 respectively.

The above analysis gives us no clue as to the possible transitions. Any state of the atom is labelled by four quantum numbers n, k, j, f . The rules of combination for the k and j are of course unchanged, since the total intensity of the spin fine-structure lines must remain the same, but we do not know the

rule for f . Jackson's results indicate (as we should expect) that f can only change by ± 1 , or 0. Further rules are given which will be explained later.

In fig. 1 are shown the multiplet S and P levels, with the appropriate quantum numbers, and the corresponding spin configuration. Thus $\uparrow\downarrow$ and $\downarrow\uparrow$

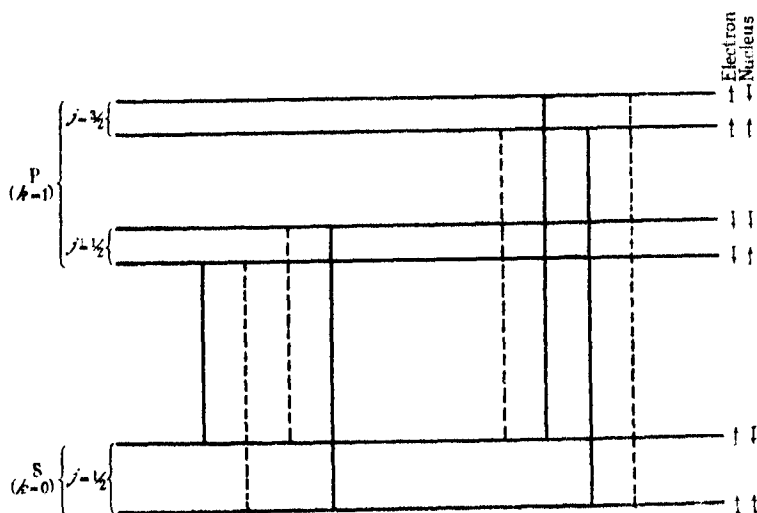


FIG. 1.—The dotted lines represent unobserved transitions.

indicate states in which the electron spin and nuclear spin are parallel but of opposite signs (called antiparallel states), while $\uparrow\uparrow$ and $\downarrow\downarrow$ indicate states in which they are parallel and of the same sign (parallel states). (We shall see that the assumption that in any state the spin axes are either parallel or antiparallel is justified.) The first arrow will always indicate the electron. Further, owing to the difference in sign between electron and nuclear charges, the magnetic moments are of opposite sign. Accordingly the parallel configuration leads to opposite signs in the increments of energy due to the two spins. Bearing these considerations in mind it is easy to construct the levels shown in the figure. The transitions observed by Jackson are also shown. Other transitions were either absent, too weak to observe, or else possibly they were too close to those indicated to be separated from them. The figure indicates that there are no transitions (or only weak ones) between parallel and antiparallel states.

We might notice before proceeding that a comparison of the observed and calculated values of the increment of energy suggests (as indicated by Jackson) that the ratio of magnetic to mechanical moment in the nucleus is not given

by $e/m'c$ (where m' is the nuclear mass), as we might expect by comparison with the electronic spin, but by (approx.) $2e/m'c$. It is suggested that this is due to the nuclear charge being situated chiefly in the outer part of the nucleus. It would seem that this question, as well as the actual amount of mechanical moment, is connected very closely with the actual structure of the nucleus and its relativistic motion.

§ 2. The question of the fine structure due to electronic spin has been dealt with in the new mechanics by Pauli,* Darwin,† and more recently Dirac‡ has shown that the electronic spin itself is a relativity effect. We shall deal with the present problem on the lines of Pauli's treatment, introducing, in addition to the electronic spin variables, similar ones for the nuclear spin. It would appear difficult to introduce the necessary modification into Dirac's relativity equation, and anyhow such a procedure would introduce two similar effects in different ways. Pauli's treatment was found to yield very good approximate results for the electron spin, failing only in the determination of the S levels, and so we should expect a similar treatment in the present problem to yield useful results, though we shall find that the S levels are not given correctly. We shall, however, show that empirical equations can be constructed which give the correct S levels.

We have to choose a number of dynamical variables which will be sufficient to describe the motion of the system. In addition to the variables x , p_x , etc., we shall suppose the electron and nuclear spins to be represented by two vectors $\mathbf{S}' = S'_x, S'_y, S'_z$ and $\mathbf{S}'' = S''_x, S''_y, S''_z$, respectively. For convenience we write

$$\mathbf{S}' = \frac{1}{2}h\boldsymbol{\sigma}, \quad \mathbf{S}'' = \frac{1}{2}h\boldsymbol{\rho}. \quad (1)$$

x , y , z , p_x , p_y , p_z , satisfy the usual quantum conditions and in addition the quantities S'_x, S'_y, S'_z , etc., satisfy the "Vertauschungs" relations for angular momentum variables, e.g.,

$$S'_y S'_z - S'_z S'_y = i\hbar S'_x$$

or

$$\left. \begin{aligned} \sigma_y \sigma_z - \sigma_z \sigma_y &= 2i\sigma_x \\ \text{and similarly} \quad \rho_y \rho_z - \rho_z \rho_y &= 2i\rho_x \end{aligned} \right\} \quad (2)$$

with similar relations obtained by cyclic interchange of the suffixes. Further

* 'Z. Physik,' vol. 43, p. 601 (1927).

† 'Roy. Soc. Proc.,' A, vol. 115, p. 1 (1927), and vol. 116, p. 227 (1927); quoted as *loc. cit.* I and II respectively.

‡ 'Roy. Soc. Proc.,' A, vol. 117, p. 610 (1928), and vol. 118, p. 351 (1928). Also Darwin, 'Roy. Soc. Proc.,' A, vol. 118, p. 654 (1928).

any one of the σ 's commutes with any one of the ρ 's, and a σ or ρ commutes with any other variable such as x or p_x , *e.g.*,

$$\left. \begin{aligned} \sigma_x p_x - p_x \sigma_x &= 0 \\ \sigma_x x - x \sigma_x &= 0 \end{aligned} \right\}, \quad (3)$$

The characteristic values of the σ 's and ρ 's must be ± 1 . The maximum number of variables which commute among themselves is five, and therefore we can express five appropriate variables as diagonal matrices at any given instant of time. We choose $x, y, z, \sigma_x, \rho_x$, and hence require to find the wave functions

$$\psi(x, y, z, \sigma_x, \rho_x).$$

Since σ_x and ρ_x may each have only two discrete characteristic values, *viz.*, ± 1 , the wave function ψ splits up into four distinct wave functions which we shall write as:—

$$\left. \begin{aligned} \psi(x, y, z, 1, 1) &= \psi_\alpha(x, y, z) \\ \psi(x, y, z, -1, 1) &= \psi_\beta(x, y, z) \\ \psi(x, y, z, 1, -1) &= \psi_\gamma(x, y, z) \\ \psi(x, y, z, -1, -1) &= \psi_\delta(x, y, z) \end{aligned} \right\}. \quad (4)$$

We must in addition introduce the normalising condition:

$$\sum_{\alpha, \beta, \gamma, \delta} \int \bar{\psi}_\alpha \psi_\alpha d\tau = 1, \quad (5)$$

the integral being extended over all space ($d\tau = dx dy dz$). We choose then the matrix scheme in which $x, y, z, \sigma_x, \rho_x$ are diagonal, and the wave functions ψ are then the eigenfunctions of the Hamiltonian. The conditions expressed in (2) and (3), together with the fact that the σ 's and ρ 's have ± 1 for their characteristic values, are exactly the conditions to be satisfied by similar matrices in Dirac's paper,* and therefore we can, by a canonical transformation which leaves all diagonal matrices unchanged, bring them to the forms:

$$\left. \begin{aligned} \sigma_x &= \begin{pmatrix} 0 & 1 & 0 & 0 \\ 1 & 0 & 0 & 0 \\ 0 & 0 & 0 & 1 \\ 0 & 0 & 1 & 0 \end{pmatrix} & \sigma_y &= \begin{pmatrix} 0 & -i & 0 & 0 \\ i & 0 & 0 & 0 \\ 0 & 0 & 0 & -i \\ 0 & 0 & i & 0 \end{pmatrix} & \sigma_z &= \begin{pmatrix} 1 & 0 & 0 & 0 \\ 0 & -1 & 0 & 0 \\ 0 & 0 & 1 & 0 \\ 0 & 0 & 0 & -1 \end{pmatrix} \\ \rho_x &= \begin{pmatrix} 0 & 0 & 1 & 0 \\ 0 & 0 & 0 & 1 \\ 1 & 0 & 0 & 0 \\ 0 & 1 & 0 & 0 \end{pmatrix} & \rho_y &= \begin{pmatrix} 0 & 0 & -i & 0 \\ 0 & 0 & 0 & -i \\ i & 0 & 0 & 0 \\ 0 & i & 0 & 0 \end{pmatrix} & \rho_z &= \begin{pmatrix} 1 & 0 & 0 & 0 \\ 0 & 1 & 0 & 0 \\ 0 & 0 & -1 & 0 \\ 0 & 0 & 0 & -1 \end{pmatrix} \end{aligned} \right\}. \quad (6)$$

* 'Roy. Soc. Proc.,' A, vol. 117, p. 610 (1928).

This is not a unique solution, but it is the simplest that we can construct, and 4-rowed square matrices are the simplest ones we can use, just as Pauli's 2-rowed matrices were the simplest in his problem. Larger matrices only lead to the repetition of the solutions, and give the same physical results.

The quantities σ , ρ satisfy in addition to (2) the equations

$$\sigma_x \sigma_y = -\sigma_y \sigma_x = i\sigma_z, \text{ etc.} \quad (7)$$

We now treat the σ 's and ρ 's as operators and find the α , β , γ , δ components which are the result of operating on ψ by polynomial functions of the σ 's and ρ 's. We therefore consider $(g\psi)_\alpha$ where g is any polynomial in the σ 's and ρ 's, and contains no other dynamical variable, so that g commutes with x , y , z , p_x , p_y , p_z . Our matrix scheme being that defined above we have,

$$(x', y', z', \sigma_x', \rho_x' | g | x'', \dots, \rho_z'') \\ = g(\sigma_x', \rho_x', \sigma_z'', \rho_z'') \delta(x' - x'') \delta(y' - y'') \delta(z' - z''), \quad (8)$$

and so

$$g\psi(x' \dots \rho_x') = \sum_{\sigma_x'', \rho_x''} \int (x' \dots \rho_x' | g | x'' \dots \rho_z'') dx'' dy'' dz'' \psi(x'' \dots \rho_z'') \\ = \sum_{\sigma_x'', \rho_x''} g(\sigma_x'' \dots \rho_z'') \psi(x' \dots \rho_x''). \quad (9)$$

The α , β , γ , δ components are obtained by giving σ_x' , ρ_x' their appropriate characteristic values, and are derived from the elements of g in the first, second, third and fourth rows respectively of its matrix (as is easily seen by inspecting the matrices for σ_x , ρ_x in (6)). Thus if g (obtained by substitution of the values for σ , ρ from (6) in the algebraic expression for g) is the matrix

$$g \equiv \left. \begin{pmatrix} a_{1,1} & a_{1,2} & a_{1,3} & a_{1,4} \\ a_{2,1} & a_{2,2} & a_{2,3} & a_{2,4} \\ a_{3,1} & a_{3,2} & a_{3,3} & a_{3,4} \\ a_{4,1} & a_{4,2} & a_{4,3} & a_{4,4} \end{pmatrix} \right\}, \quad (10)$$

then

$$(g\psi)_\alpha = a_{1,1} \psi_\alpha + a_{1,2} \psi_\beta + a_{1,3} \psi_\gamma + a_{1,4} \psi_\delta$$

and similar expressions for $(g\psi)_\beta$, $(g\psi)_\gamma$, $(g\psi)_\delta$. This simple rule is used in calculating the results of all such operations in the subsequent work, and it seems unnecessary to write down the explicit expressions required.

Since the σ 's and ρ 's commute, the characteristic values of $\sigma_x + \rho_x$, etc., are the sums and differences of the characteristic values of σ_x , ρ_x separately, i.e. ± 2 , 0. This means that the spin axes of the nucleus and electron must be parallel or antiparallel, and it will be seen later that in any particular state the spin configuration is definitely fixed, being as indicated in fig. 1.

§ 3. We now come to the specific problem, being the motion of an electron of mass m and charge e in a Coulomb field of intensity Ze/r^2 , due to a heavy nucleus of mass m' , which has a mechanical moment $\frac{1}{2}h$. We suppose that a uniform magnetic field of intensity H is superposed in the direction Oz , as in Darwin's earlier problem, in order to make the system non-degenerate. This procedure simplifies the work considerably and by making $H \rightarrow 0$ we obtain the required results.

There will be an increment of energy in the system due to the presence of the nuclear moment. If μ , μ_0 are the magnetic moments of the nucleus and electron respectively, μ_0 is given by

$$\mu_0 = eh/2mc,$$

while μ will be of the order of $-Zeh/2m'c$ (Jackson's investigation shows that for caesium this must be multiplied by a factor which is approximately 2). Since $\mu_0 \gg \mu$ the problem is really one of a perturbation on the electron spin problem. We shall neglect quantities of the order of $\mu_0\mu$, or, in other words, we shall neglect the mutual energy of the two spins, and take into account only the interaction energy of the nuclear moment and the orbital momentum, which is of a much greater order. It should be noticed that we neglect μ_0^2 although $\mu_0^2 \gg \mu$. This is quite legitimate for our purpose, since the inclusion of μ^2 would merely lead to a shift in the levels, and not to a splitting up into several levels, which is the object of our investigation.

The components of nuclear magnetic moment are $\mu\rho_x$, $\mu\rho_y$, $\mu\rho_z$, and give rise to a vector potential A , ($= A_x, A_y, A_z$), where

$$A_x = \left(\mu\rho_z \frac{\partial}{\partial y} - \mu\rho_y \frac{\partial}{\partial z} \right) \left(\frac{1}{r} \right) = \frac{\mu}{r^3} (z\rho_y - y\rho_z),$$

etc. The additional term in the Hamiltonian is therefore

$$\begin{aligned} \frac{e}{mc} (\mathbf{p} \cdot \mathbf{A}) &= \frac{e\mu}{mcr^3} \{ p_x (z\rho_y - y\rho_z) + \dots + \dots \} \\ &= \frac{e\mu}{mcr^3} (\mathbf{p} \cdot \mathbf{M}), \end{aligned} \quad (11)$$

where \mathbf{M} is the orbital angular momentum of the electron. The term due to electron spin is*

$$\frac{Z\mu_0 e}{2mcr^3} (\boldsymbol{\sigma} \cdot \mathbf{M}), \quad (12)$$

and we see therefore that qualitatively a nuclear spin has the same effect as an electron spin. The complete Hamiltonian for the case in which electron

spin is included has been given by Darwin.* We have therefore to add to this just the term in (11), and doing this the Hamiltonian may be written :—

$$H = \sum_{r=0}^6 H_r,$$

where

$$\left. \begin{aligned} H_0 &= \frac{1}{2m} (p_x^2 + p_y^2 + p_z^2) + V; & H_1 &= -\frac{1}{2mc^2} (W_0 + V)^2; \\ H_2 &= \frac{-Z\mu_0 e}{2mcr^3} (\boldsymbol{\sigma} \cdot \mathbf{M}); & H_3 &= \frac{e\mathbf{H}}{2mc} (xp_y - yp_x); \\ H_4 &= \mu_0 \mathbf{H} \sigma_z; & H_5 &= \frac{\mu e}{mcr^3} (\boldsymbol{\rho} \cdot \mathbf{M}); & H_6 &= \mu \mathbf{H} \rho_z. \end{aligned} \right\} \quad (13)$$

H_0 is the non-relativistic, non-spin Hamiltonian; H_1 is the relativity correction, where W_0 is an eigenwert of H_0 ; H_2 is the electron spin correction and H_3 the nuclear spin correction; while H_3 , H_4 , H_6 are the energies of the orbital momentum, electron magnet, and nuclear magnet respectively in the magnetic field \mathbf{H} .

The Schrödinger wave-equation is then

$$W\psi = H\psi \quad (14)$$

in which $W = i\hbar \partial/\partial t$; $p_x = -i\hbar \partial/\partial x$, etc., while the σ and ρ operators are interpreted according to (10). Calculating the results of these operations (14) may be written as four equations in ψ_a , ψ_b , ψ_γ and ψ_δ and we find immediately

$$\begin{aligned} W\psi_a &= (H_0 + H_1) \psi_a - \frac{i\hbar\mu_0 Ze}{2mcr^3} \{(\kappa_x - i\kappa_y) \psi_b + \kappa_z \psi_a\} + \mu_0 \mathbf{H} \psi_a \\ &\quad - \frac{i\hbar e \mathbf{H}}{2mc} \kappa_z \psi_a - \frac{i\hbar\mu e}{mcr^3} \{(\kappa_x - i\kappa_y) \psi_\gamma + \kappa_z \psi_a\} + \mu \mathbf{H} \psi_a, \end{aligned} \quad (15.1)$$

$$\begin{aligned} W\psi_b &= (H_0 + H_1) \psi_b - \frac{i\hbar\mu_0 Ze}{2mcr^3} \{(\kappa_x + i\kappa_y) \psi_a - \kappa_z \psi_b\} - \mu_0 \mathbf{H} \psi_b \\ &\quad - \frac{i\hbar e \mathbf{H}}{2mc} \kappa_z \psi_b - \frac{i\hbar\mu e}{mcr^3} \{(\kappa_x - i\kappa_y) \psi_\delta + \kappa_z \psi_b\} + \mu \mathbf{H} \psi_b, \end{aligned} \quad (15.2)$$

$$\begin{aligned} W\psi_\gamma &= (H_0 + H_1) \psi_\gamma - \frac{i\hbar\mu_0 Ze}{2mcr^3} \{(\kappa_x - i\kappa_y) \psi_b + \kappa_z \psi_\gamma\} + \mu_0 \mathbf{H} \psi_\gamma \\ &\quad - \frac{i\hbar e \mathbf{H}}{2mc} \kappa_z \psi_\gamma - \frac{i\hbar\mu e}{mcr^3} \{(\kappa_x + i\kappa_y) \psi_a - \kappa_z \psi_\gamma\} - \mu \mathbf{H} \psi_\gamma, \end{aligned} \quad (15.3)$$

* *Loc. cit.* II.

$$\begin{aligned}
W\psi_\delta = (H_0 + H_1) \psi_\delta - \frac{ih\mu_0 Z e}{2mcr^3} \{(\kappa_x + i\kappa_y) \psi_\gamma - \kappa_z \psi_\delta\} - \mu_0 H \psi_\delta \\
- \frac{ihcH}{2mc} \kappa_z \psi_\delta - \frac{ih\mu e}{mcr^3} \{(\kappa_x + i\kappa_y) \psi_\beta - \kappa_z \psi_\delta\} - \mu H \psi_\delta,
\end{aligned} \quad (15.4)$$

where

$$\kappa_x = y \frac{\partial}{\partial z} - z \frac{\partial}{\partial y}, \text{ etc.} \quad (16)$$

The last two terms in each equation are due to the nuclear moment. The equations without these extra terms are equivalent to Darwin's equations twice over (with $\psi_\alpha = \psi_\gamma$, and $\psi_\beta = \psi_\delta$).

The solution of the equation

$$W\psi = H_0\psi$$

is

$$\psi = P_{n,k,u} e^{-iW_0 t/\hbar} = \frac{1}{r} W_{n,k+1} \left(\frac{2Zr}{na} \right) P_k^u(\cos \theta) e^{iu\phi} e^{-iW_0 t/\hbar}, \quad (17)$$

where

$$P_k^u(x) = (k-u)! (1-x^2)^{1/2} \left(\frac{d}{dx} \right)^{k+u} \frac{(x^2-1)^k}{2^k \cdot k!}, \quad (18)$$

and a is the radius of Bohr's one-quantum orbit of hydrogen. The following relations are taken from Darwin* and will be required later:

$$\left. \begin{aligned}
\kappa_z P_{n,k,u} &= iu P_{n,k,u} \\
(\kappa_x + i\kappa_y) P_{n,k,u} &= -i(k-u) P_{n,k,u+1} \\
(\kappa_x - i\kappa_y) P_{n,k,u} &= -i(k+u) P_{n,k,u-1}
\end{aligned} \right\} \quad (19)$$

$$\left. \begin{aligned}
\int_0^\pi \int_0^{2\pi} \sin \theta d\theta d\phi |P_k^u(\cos \theta) e^{iu\phi}|^2 &= \frac{4\pi}{2k+1} (k+u)! (k-u)! \\
\int_0^\pi \int_0^{2\pi} \sin \theta d\theta d\phi P_k^u(\cos \theta) P_{k'}^{u'}(\cos \theta) e^{i(u-u')\phi} X &= 0 \\
\text{unless } k' = k \pm 1, \text{ where} \\
X = \sin \theta e^{-i\phi}, \cos \theta, \text{ or } \sin \theta e^{i\phi}; \\
\int_0^\pi \int_0^{2\pi} \sin \theta d\theta d\phi P_k^u(\cos \theta) e^{iu\phi} Y &= \frac{4\pi (k+u)! (k-u)!}{(2k+1)(2k-1)}, \\
\text{where} \\
Y = P_{k-1}^{u-1}(\cos \theta) e^{-i(u-1)\phi} \sin \theta e^{-i\phi}, \\
P_{k-1}^u(\cos \theta) e^{-iu\phi} \cos \theta, \text{ or } P_{k-1}^{u+1}(\cos \theta) e^{-i(u+1)\phi} \sin \theta e^{i\phi}.
\end{aligned} \right\} \quad (20)$$

Regarding the problem as one of a perturbation on the relativity problem we write $(H_0 + H_1)\psi = (W_0 + W_1)\psi$. The unperturbed system is degenerate,

* *Loc. cit.*, I, p. 5; *loc. cit.* II, p. 234.

and, therefore, using Schrödinger's perturbation method* we try to find a solution of the form

$$\left. \begin{aligned} \psi_a &= \sum_{k,u} a_{k,u} P_{n,k,u} \exp \{-i(W_0 + W_1 + \Delta W_a(k,u))t/\hbar\} \\ \psi_b &= \sum_{k,u} b_{k,u} P_{n,k,u} \exp \{-i(W_0 + W_1 + \Delta W_b(k,u))t/\hbar\} \\ \psi_\gamma &= \sum_{k,u} c_{k,u} P_{n,k,u} \exp \{-i(W_0 + W_1 + \Delta W_\gamma(k,u))t/\hbar\} \\ \psi_\delta &= \sum_{k,u} d_{k,u} P_{n,k,u} \exp \{-i(W_0 + W_1 + \Delta W_\delta(k,u))t/\hbar\} \end{aligned} \right\}, \quad (21)$$

where the a 's, ..., d 's are constants, and $\Delta W_a(k,u)$, etc., are constants depending on k, u . Therefore

$$(W - W_0 - W_1) \psi_a = \sum \Delta W_a(k,u) a_{k,u} P_{n,k,u} \exp \{-i(W_0 + W_1 + \Delta W_a(k,u))t/\hbar\}, \quad (22)$$

etc., since $W = i\hbar \partial / \partial t$. Substitute from (21), (22) in equations (15), multiply each equation by $\bar{P}_{n,k,u}$ and integrate over all space, noting that (the orthogonality relation) $\int \bar{P}_{n,k,u} P_{n,k,u} d\tau = 0$, unless $u' = u$. Using (19) we obtain from (15.1) :—

$$\begin{aligned} \Delta W_a(k,u) a_{k,u} \int P_{n,k,u} \bar{P}_{n,k,u} d\tau &= \frac{Ze\mu_0\hbar}{2mc} \{-(k+u+1)b_{k,u+1} + ua_{k,u}\} \int \frac{1}{r^3} P_{n,k,u} \bar{P}_{n,k,u} d\tau \\ &+ (u+1)a_{k,u} \omega \int P_{n,k,u} \bar{P}_{n,k,u} d\tau \\ &+ \frac{\mu e\hbar}{mc} \{-(k+u+1)c_{k,u+1} + ua_{k,u}\} \int \frac{1}{r^3} P_{n,k,u} \bar{P}_{n,k,u} d\tau \\ &+ \omega' a_{k,u} \int P_{n,k,u} \bar{P}_{n,k,u} d\tau, \end{aligned} \quad (23)$$

where

$$\omega = \mu_0 H, \quad \omega' = \mu H.$$

Writing†

$$\left. \begin{aligned} \beta_1 &= \frac{Ze\mu_0\hbar}{2mc} \int \frac{1}{r^3} P_{n,k,u} \bar{P}_{n,k,u} d\tau / \int P_{n,k,u} \bar{P}_{n,k,u} d\tau \\ &= \frac{4Z^4 m^2 e^7 \mu_0}{ch^5 n^3} \cdot \frac{1}{2k(2k+1)(2k+2)} \\ \text{and} \\ \beta_2 &= \frac{eh\mu}{mc} \int \frac{1}{r^3} P_{n,k,u} \bar{P}_{n,k,u} d\tau / \int P_{n,k,u} \bar{P}_{n,k,u} d\tau \\ &= \frac{8Z^4 m^2 e^7 \mu}{ch^5 n^3} \cdot \frac{1}{2k(2k+1)(2k+2)} \end{aligned} \right\} \quad (24)$$

* 'Ann. Physik,' vol. 81, p. 109 (1926).

† Darwin, loc. cit. II, and Waller, 'Z. Physik,' vol. 38, p. 635 (1926).

(23) may be written

$$\Delta W_a(k, u) a_{k,u} = \beta_1 \{ua_{k,u} - (k+u+1)b_{k,u+1}\} + (u+1)\omega a_{k,u} \\ + \beta_2 \{ua_{k,u} - (k+u+1)c_{k,u+1}\} + \omega' a_{k,u} \quad (25.1)$$

with similar equations from (15.2), (15.3), (15.4), viz.,

$$\Delta W_b(k, u) b_{k,u} = \beta_1 \{-ub_{k,u} - (k-u+1)a_{k,u-1}\} + (u-1)\omega b_{k,u} \\ + \beta_2 \{ub_{k,u} - (k+u+1)d_{k,u+1}\} + \omega' b_{k,u} \quad (25.2)$$

$$\Delta W_\gamma(k, u) c_{k,u} = \beta_1 \{+uc_{k,u} - (k+u+1)d_{k,u+1}\} + (u+1)\omega c_{k,u} \\ + \beta_2 \{-uc_{k,u} - (k-u+1)a_{k,u-1}\} - \omega' c_{k,u} \quad (25.3)$$

$$\Delta W_\delta(k, u) d_{k,u} = \beta_1 \{-ud_{k,u} - (k-u+1)c_{k,u-1}\} + (u-1)\omega d_{k,u} \\ + \beta_2 \{-ud_{k,u} - (k-u+1)b_{k,u-1}\} - \omega' d_{k,u} \quad (25.4)$$

If we now suppose that $\Delta W_a(k, u) = \Delta W_b(k, u+1) = \Delta W_\gamma(k, u+1) = \Delta W_\delta(k, u+2) = \Delta W$, and in (25.1) to (25.4) write $u, u+1, u+1, u+2$ respectively for u , we can eliminate the constants $a_{k,u}, b_{k,u+1}, c_{k,u+1}, d_{k,u+2}$, and obtain a quartic equation for ΔW . The equations for (25) become

$$\{\Delta W - (\beta_1 + \beta_2)u - (u+1)\omega - \omega'\} a_{k,u} + \beta_1(k+u+1)b_{k,u+1} \\ + \beta_2(k+u+1)c_{k,u+1} = 0, \quad (26.1)$$

$$\{\Delta W + (\beta_1 - \beta_2)(u+1) - u\omega - \omega'\} b_{k,u+1} + \beta_1(k-u)a_{k,u} \\ + \beta_2(k+u+2)d_{k,u+2} = 0, \quad (26.2)$$

$$\{\Delta W - (\beta_1 - \beta_2)(u+1) - (u+2)\omega + \omega'\} c_{k,u+1} + \beta_2(k-u)a_{k,u} \\ + \beta_1(k+u+2)d_{k,u+2} = 0, \quad (26.3)$$

$$\{\Delta W + (\beta_1 + \beta_2)(u+2) - (u+1)\omega + \omega'\} d_{k,u+2} + \beta_2(k-u-1)b_{k,u+1} \\ + \beta_1(k-u-1)c_{k,u+1} = 0. \quad (26.4).$$

In this way we obtain solutions of our equations in which $a_{k,u}, b_{k,u+1}, c_{k,u+1}, d_{k,u+2}$ are finite, other terms being small, the finite terms containing the same time factor.

In the particular case where $\beta_2 = \omega' = 0$ equations (26.1) and (26.2) reduce to Darwin's pair of equations, and (26.3), (26.4) give the same pair with c, d substituted for a, b . This provides a useful check on the algebra. The quartic equation in ΔW in this case has two pairs of equal roots.

§ 4. So far we have treated the nuclear and electron spin moments on an equal footing, but in order to solve the equations (26) we shall treat the nuclear spin as a perturbation on the electron spin, since $\beta_2 \ll \beta_1$. We may now take

$H = 0$ and therefore $\omega = \omega' = 0$, since we are not interested in the Zeeman effect. The superposed field has served its purpose of giving us non-degenerate solutions in which the ΔW 's are all different. If we neglect β_2 we obtain the double quadratic equation

$$\{\Delta W^2 + \beta_1 \Delta W - \beta_1^2 k(k+1)\}^2 = 0 \quad (27)$$

giving two levels twice over

$$\Delta W = \beta_1 k \quad \text{or} \quad \Delta W = -\beta_1(k+1). \quad (28)$$

If, further,

$$a'_{k,u}, \quad b'_{k,u+1}, \quad c'_{k,u+1}, \quad d'_{k,u+2};$$

and

$$a''_{k,u}, \quad b''_{k,u+1}, \quad c''_{k,u+1}, \quad d''_{k,u+2},$$

are the values of the constants in the two solutions respectively we have

$$\left. \begin{aligned} (k-u)a'_{k,u} + (k+u+1)b'_{k,u+1} &= 0 \\ (k-u-1)c'_{k,u+1} + (k+u+2)d'_{k,u+2} &= 0 \end{aligned} \right\} \quad (29)$$

and

$$\left. \begin{aligned} a''_{k,u} &= b''_{k,u+1} \\ c''_{k,u+1} &= d''_{k,u+2} \end{aligned} \right\}. \quad (30)$$

We therefore assume solutions (for $\beta_2 \neq 0$) of the form (1) $\Delta W = \beta_1 k + \delta_1$ with increments $\epsilon_1', \epsilon_2', \epsilon_3', \epsilon_4'$ in the corresponding a, b, c, d , or (2) $\Delta W = -\beta_1(k+1) + \delta_2$ with similar increments $\epsilon_1'', \dots, \epsilon_4''$. Substituting in the equations (26) and eliminating the ϵ 's we get quadratics for δ_1, δ_2 , giving to a sufficiently good approximation the roots in ΔW . It will be sufficient in our subsequent work to neglect the ϵ 's, but we shall need to find the three ratios $a:b:c:d$ in each of the four solutions (only two of these ratios being given in (29) or (30)).

Carrying out the first substitution indicated and neglecting products of $\delta_1, \epsilon_1', \dots, \epsilon_4'$, we obtain with the help of (29)

$$\{(2k+1)\delta_1 + \beta_2 k(2k+3)\} \{\delta_1 - \beta_2 k\} = 0,$$

giving roots

$$\delta_1 = -\frac{k(2k+3)}{2k+1} \beta_2 \quad \text{or} \quad k\beta_2.$$

We can similarly solve for δ_2 and the results we obtain finally are

$$\begin{aligned} \Delta W &= \beta_1 k - \beta_2 k(2k+3)/(2k+1), \quad \beta_1 k + \beta_2 k, \\ &-\beta_1(k+1) - \beta_2(k+1), \quad \text{or} \quad -\beta_1(k+1) + \beta_2(k+1)(2k-1)/(2k+1), \end{aligned} \quad (31)$$

β_1 and β_2 being of opposite sign (due to the difference in sign of μ, μ_0) the roots

as written are in descending order of magnitude. The ratio $a_{k,u} : c_{k,u+1}$ can now be found for each root, the other ratios being given by (29) or (30).

The second and third roots in (31) are exact, as may easily be verified, and we could, knowing this, solve the equations for the other roots exactly, but this is unnecessary, and anyhow we should have to derive the above approximations in order to make them manageable. The complete solutions are given in the following section.

§ 5. Using (5), the normalising condition is

$$a_{k,u}^2 \int P_{n,k,u} \bar{P}_{n,k,u} d\tau + (b_{k,u+1}^2 + c_{k,u+1}^2) \int P_{n,k,u+1} \bar{P}_{n,k,u+1} d\tau + d_{k,u+2}^2 \int P_{n,k,u+2} \bar{P}_{n,k,u+2} d\tau = 1. \quad (32)$$

Since all the integrands contain the same function $f_{n,k}(r)$ of r , we shall suppose this normalised, and, therefore, using the relations (20), (32) gives

$$a_{k,u}^2 (k+u)! (k-u)! + (b_{k,u+1}^2 + c_{k,u+1}^2) (k+u+1)! (k-u-1)! + d_{k,u+2}^2 (k+u+2)! (k-u-2)! = 1. \quad (33)$$

The common factor in the integrals (see equations (20)), viz.,

$$4\pi/(2k+1)(2k-1),$$

can be absorbed in the normalisation of $f_{n,k}(r)$. The complete normalised solutions are:—

$$\left. \begin{aligned} \text{I. } \Delta W &= \beta_1 k - \beta_2 k(2k+3)/(2k+1) \\ a_{k,u}^2 &= (k+u+1)(k-u)/\{(k+u)!(k-u)!2(2k+1)(k+1)\}; \\ b_{k,u+1} &= -\frac{k-u}{k+u+1} a_{k,u}; \quad c_{k,u+1} = \frac{k+u+2}{k+u+1} a_{k,u}; \\ d_{k,u+2} &= -\frac{k-u-1}{k+u+1} a_{k,u} \end{aligned} \right\} \quad (34.1)$$

$$\left. \begin{aligned} \text{II. } \Delta W &= \beta_1 k + \beta_2 k \\ a_{k,u}^2 &= (k+u+1)(k+u+2)/\{(k+u)!(k-u)!2(2k+1)(k+1)\}; \\ b_{k,u+1} &= -\frac{k-u}{k+u+1} a_{k,u}; \quad c_{k,u+1} = -\frac{k-u}{k+u+1} a_{k,u}; \\ d_{k,u+2} &= \frac{(k-u-1)(k-u)}{(k+u+2)(k+u+1)} a_{k,u} \end{aligned} \right\} \quad (34.2)$$

$$\text{III. } \left. \begin{aligned} \Delta W &= -\beta_1(k+1) - \beta_2(k+1) \\ a_{k,u}^2 &= (k-u)(k-u-1)/\{(k+u)!(k-u)!2k(2k+1)\}; \\ b_{k,u+1} &= c_{k,u+1} = d_{k,u+2} = a_{k,u} \end{aligned} \right\} \quad (34.3)$$

$$\text{IV. } \left. \begin{aligned} \Delta W &= -\beta_1(k+1) + \beta_2(k+1)(2k-1)/(2k+1) \\ a_{k,u}^2 &= (k-u)(k+u+1)/\{(k+u)!(k-u)!2k(2k+1)\}; \\ b_{k,u+1} &= a_{k,u}; \quad c_{k,u+1} = d_{k,u+2} = -\frac{(k-u-1)}{(k+u+1)}a_{k,u} \end{aligned} \right\} \quad (34.4)$$

u can take all integral values between $-(k+2)$ and k , since for these values at least one of $P_{n,k,u}$, $P_{n,k,u+1}$, $P_{n,k,u+2}$ exists, but there are certain special cases in which the relations I-IV do not hold as they stand.

(i) For $u = k$, only $a_{k,u}$ is different from zero. If we repeated the work with this assumption we should find that only the root II exists for this value of u . However, this is automatically accounted for in the relations between the constants, since in I, III and IV $a_{k,u}$ contains a factor $(k-u)$ which is zero for $u = k$.

(ii) For $u = k-1$, $d_{k,u+2} = 0$. Here the root III is missing, and this also is accounted for, since in III $a_{k,u}^2$ contains a factor $(k-u-1)$.

(iii) For $u = -(k+1)$, $a_{k,u} = 0$. The root III is again missing. $(k+u)!$ does not now exist, and we therefore express the constants in terms of $b_{k,u+1}$ or $c_{k,u+1}$. Further in III

$$a_{k,u}^2 = (k-u)(k-u-1)(k+u+1)/\{(k-u)!(k+u+1)!2k(2k+1)\} = 0,$$

the corresponding root being therefore excluded.

(iv) For $u = -(k+2)$, only the root II exists. $d_{k,u+2}$ is now the only non-zero constant, and we therefore express the other constants in relations I-IV in terms of it. It is then found that these relations give $d_{k,u+2} = 0$, except for the root II, as required.

All these exceptional cases are therefore contained in the general relations I-IV, and need therefore no longer concern us. It is important to notice the range of u for the different roots, viz. :—

$$\left. \begin{aligned} \text{For I,} \quad & -(k+1) \leq u \leq (k+1) \\ \text{For II,} \quad & -(k+2) \leq u \leq k \\ \text{For III,} \quad & -k \leq u \leq k-2 \\ \text{For IV,} \quad & -(k+1) \leq u \leq k-1 \end{aligned} \right\} \quad (35)$$

§ 6. The method employed has given a wrong result for $k = 0$, since $\int \frac{1}{r^3} P_{n,k,u} \bar{P}_{n,k,u} d\tau$ is divergent for $k = 0$. The nature of the failure is, of course, the same as in the case of electron spin alone. In order to make this investigation complete in itself we shall assume a solution, showing that empirical equations can be constructed which give this solution, and further do not alter the solutions for $k > 0$. In the case of electron spin alone the solutions of ΔW are $\beta_1 k$, $-\beta_1(k+1)$, and (for a Coulomb field) β_1 contains $[2k(2k+1)(2k+2)]^{-1}$ as a factor. Therefore although β_1 is divergent at $k = 0$ we may attach a meaning to $\lim_{k \rightarrow 0} (\beta_1 k)$; on the other hand $-\beta_1(k+1)$ is divergent at $k = 0$. The assumption of the single solution $(\beta_1 k)_{k=0}$ is justified by Darwin's later work, using the Dirac relativity equation. Further, it may easily be verified by a comparison of the two papers that the values of the constants a , b on this assumption are exactly those found by the more accurate treatment of the problem. The difficulties in the present problem are quite analogous to those of the earlier one, and therefore we shall, without any mathematical justification but encouraged by the success of making similar assumptions in the earlier problem, assume two solutions of the form

$$[(\beta_1 + \beta_2)k]_{k=0} \quad \text{and} \quad [\beta_1 k - \beta_2 k(2k+3)/(2k+1)]_{k=0},$$

discarding the other two expressions for ΔW which are divergent for $k = 0$. We shall moreover assume the values of the constants given in I and II with $k = 0$.

In the electron-spin problem the effect of Dirac's relativity equation is to add a term to each of the equations for ψ_α , ψ_β . This is equivalent to the addition of a term $-ir \partial \psi_\alpha / \partial r$ inside the first bracket $\{ \}$ on the right-hand side of (15.1), with similar additions in the other equations (15). These extra terms, as shown by Darwin, have the effect of leaving the P, D, and higher levels unchanged, while they give the correct levels for the S terms. This additional term is equivalent to the addition of an operator to the Hamiltonian

$$-\frac{\hbar \mu_0 Z e}{2mc r^3} r \frac{\partial}{\partial r}. \quad \text{This is equal to}$$

$$-\frac{\hbar \mu_0 Z e}{2mc r^3} \left(x \frac{\partial}{\partial x} + y \frac{\partial}{\partial y} + z \frac{\partial}{\partial z} \right) = -\frac{i \mu_0}{mc} (\mathbf{E} \mathbf{p}),$$

where \mathbf{E} is the electric intensity. This additional term in equations (15) with $\beta_2 \neq 0$ gives one root corresponding to $\Delta W = (\beta_1 k)_{k=0}$. If we add a similar term $-\frac{i \mu}{mc} (\mathbf{E} \mathbf{p})$ for the nuclear moment we get the one root

$\{(\beta_1 + \beta_2)k\}_{k=0}$. This simple addition is therefore insufficient to give the two necessary S levels. It is found by trial that the modifications indicated in the following equations give the required results,—

$$(W - W_0 - W_1) \psi_a = -\frac{i\hbar\mu_0 Ze}{2mcr^3} \left\{ (\kappa_x - i\kappa_y) \psi_\beta + \kappa_z \psi_a - ir \frac{\partial}{\partial r} \psi_a \right\} \\ - \frac{i\hbar\mu_e}{mcr^3} \left\{ (\kappa_x - i\kappa_y) \psi_\gamma + \kappa_z \psi_a - ir \frac{\partial}{\partial r} \psi_a \right\}, \quad (36.1)$$

$$(W - W_0 - W_1) \psi_\beta = -\frac{i\hbar\mu_0 Ze}{2mcr^3} \left\{ (\kappa_x + i\kappa_y) \psi_a - \kappa_z \psi_\beta - ir \frac{\partial}{\partial r} \psi_\beta \right\} \\ - \frac{i\hbar\mu_e}{mcr^3} \left\{ (\kappa_x - i\kappa_y) \psi_\delta + \kappa_z \psi_\beta + ir \frac{\partial}{\partial r} \psi_\beta - 2ir \frac{\partial}{\partial r} \psi_\gamma \right\}, \quad (36.2)$$

$$(W - W_0 - W_1) \psi_\gamma = -\frac{i\hbar\mu_0 Ze}{2mcr^3} \left\{ (\kappa_x - i\kappa_y) \psi_\delta + \kappa_z \psi_\gamma - ir \frac{\partial}{\partial r} \psi_\gamma \right\} \\ - \frac{i\hbar\mu_e}{mcr^3} \left\{ (\kappa_x + i\kappa_y) \psi_a - \kappa_z \psi_\gamma + ir \frac{\partial}{\partial r} \psi_\gamma - 2ir \frac{\partial}{\partial r} \psi_\beta \right\}, \quad (36.3)$$

$$(W - W_0 - W_1) \psi_\delta = -\frac{i\hbar\mu_0 Ze}{2mcr^3} \left\{ (\kappa_x + i\kappa_y) \psi_\gamma - \kappa_z \psi_\delta - ir \frac{\partial}{\partial r} \psi_\delta \right\} \\ - \frac{i\hbar\mu_e}{mcr^3} \left\{ (\kappa_x + i\kappa_y) \psi_\beta - \kappa_z \psi_\delta - ir \frac{\partial}{\partial r} \psi_\delta \right\}. \quad (36.4)$$

It is easily seen that these equations give the same P, D levels as before, for after substitution from (21) the additional terms in (36) lead to integrals containing

$$\int_0^\infty \frac{1}{r^3} \left\{ \frac{1}{r} W_{n,k+\frac{1}{2}}(r) \right\} r \frac{d}{dr} \left\{ \frac{1}{r} W_{n,k+\frac{1}{2}}(r) \right\} r^2 dr \\ = \frac{1}{2} \left[\left\{ \frac{1}{r} W_{n,k+\frac{1}{2}}(r) \right\}^2 \right]_0^\infty \\ = 0 \text{ for } k \neq 0,$$

since $W_{n,k+\frac{1}{2}}(r) = 0 (r^{k+1})$ at the origin and approaches zero exponentially at ∞ . To find the solution for $k=0$ we suppose (neglecting second order quantities as usual) that, either

$$(i) \quad \psi_a = a_0 P_{n,0,0} = \frac{a_0}{r} W_{n,\frac{1}{2}} \left(\frac{2Zr}{an} \right); \quad \psi_\beta = \psi_\gamma = \psi_\delta = 0,$$

or

$$(ii) \quad \psi_a = \psi_\delta = 0, \quad \psi_\beta = b_0 P_{n,0,0}, \quad \psi_\gamma = c_0 P_{n,0,0},$$

or

$$(iii) \quad \psi_a = \psi_\beta = \psi_\gamma = 0, \quad \psi_\delta = d_0 P_{n,0,0}.$$

We substitute in equations (36), multiply by $r^{-1}W_{n,l}(\frac{2Zr}{an})$ and integrate over all space. In (i)

$$a_0 \Delta W = - \left(\frac{\hbar \mu_0 Z e}{2mc} + \frac{\hbar \mu e}{mc} \right) a_0 \int \frac{1}{r^4} W_{n,l} \left(\frac{2Zr}{an} \right) r \frac{d}{dr} \left\{ \frac{1}{r} W_{n,l} \left(\frac{2Zr}{an} \right) \right\} r^2 dr,$$

$$\Delta W = \beta_{1,0} + \beta_{2,0}$$

say. Case (iii) gives the same solution for ΔW . In case (ii),

$$b_0 \Delta W = \beta_{1,0} b_0 - \beta_{2,0} (b_0 - 2c_0),$$

$$c_0 \Delta W = \beta_{1,0} c_0 - \beta_{2,0} (c_0 - 2b_0),$$

therefore,

$$[\Delta W - (\beta_{1,0} + \beta_{2,0})][\Delta W - (\beta_{1,0} - 3\beta_{2,0})] = 0,$$

giving the desired solutions. Further the relations between the constant a_0 , b_0 , c_0 , d_0 in case (i), (ii) (with $\Delta W = \beta_{1,0} + \beta_{2,0}$), and (iii) are exactly those obtained from II in § 5, putting $k = 0$, and $u = 0, -1, -2$, respectively. Also the values of the constants in case (ii) with $\Delta W = \beta_{1,0} - 3\beta_{2,0}$ are exactly those obtained from I, § 5, with $k = 0$, $u = -1$. These four solutions are, moreover, the only ones we can obtain from I and II with $k = 0$.

§ 7. Before proceeding to find the intensities of the various transitions we shall consider the assignment of appropriate quantum numbers to the levels I-IV. In order to do this we shall find the value of the total angular momentum. The orbital angular momentum has been shown to be equal to $\sqrt{k(k+1)}\hbar$. We shall try to find the total angular momentum of the system in the form $\sqrt{f(f+1)}\hbar$, and take f as the new quantum number, so that we shall then have five quantum numbers to describe a state of the atom, viz., n, k, m^* ($= u+1$), j, f .

If \mathcal{M}^2 is the matrix which represents the square of the total angular momentum we have

$$\begin{aligned} \mathcal{M}^2 &= (yp_x - zp_y + \tfrac{1}{2}\hbar\sigma_x + \tfrac{1}{2}\hbar\rho_x)^2 + \dots + \dots \\ &= \{(yp_x - zp_y)^2 + \dots + \dots\} + \hbar\{(\sigma_x + \rho_x)(yp_x - zp_y) + \dots + \dots\} \\ &\quad + \frac{\hbar^2}{4}\{\sigma_x^2 + \rho_x^2 + 2\sigma_x\rho_x + \dots + \dots\} \end{aligned} \quad (37)$$

We have to find the diagonal elements of \mathcal{M}^2 in the matrix scheme in which the Hamiltonian is a diagonal matrix, so that if M^2 is a typical element

$$M^2 = \sum_{n, k, \gamma, l} \int \bar{\psi}_n \mathcal{M}^2 \psi_n d\tau. \quad (38)$$

The first term in \mathcal{M}^2 is due to the orbital angular momentum and therefore gives a term $k(k+1)\hbar^2$ in M^2 . The second term in \mathcal{M}^2 written as an operator is :

$$-i\hbar^2 \left\{ \left(y \frac{\partial}{\partial z} - z \frac{\partial}{\partial y} \right) (\sigma_x + \rho_x) + \text{etc.} \right\} = -i\hbar^2 \{ \kappa_x (\sigma_x + \rho_x) + \text{etc.} \},$$

and the corresponding part of M^2 is

$$\begin{aligned} & -i\hbar^2 \int \bar{\psi}_\alpha \{ \kappa_x (\psi_\beta + \psi_\gamma) - i\kappa_y (\psi_\beta + \psi_\gamma) + 2\kappa_z \psi_\alpha \} d\tau \\ & -i\hbar^2 \int \bar{\psi}_\beta \{ \kappa_x (\psi_\alpha + \psi_\delta) + i\kappa_y (\psi_\alpha - \psi_\delta) \} d\tau \\ & -i\hbar^2 \int \bar{\psi}_\gamma \{ \kappa_x (\psi_\delta + \psi_\alpha) + i\kappa_y (\psi_\alpha - \psi_\delta) \} d\tau \\ & -i\hbar^2 \int \bar{\psi}_\delta \{ \kappa_x (\psi_\beta + \psi_\gamma) + i\kappa_y (\psi_\beta + \psi_\gamma) - 2\kappa_z \psi_\delta \} d\tau. \end{aligned} \quad (39)$$

The third term in \mathcal{M}^2 is, since $\sigma_x^2 = 1$, etc.,

$$\frac{3}{4}\hbar^2 + \frac{1}{2}\hbar^2 (\sigma_x \rho_x + \dots + \dots),$$

giving a term in M^2 which is

$$\frac{3}{4}\hbar^2 + \frac{1}{2}\hbar^2 \int [\bar{\psi}_\alpha \psi_\alpha + \bar{\psi}_\beta (2\psi_\gamma - \psi_\rho) + \bar{\psi}_\gamma (2\psi_\beta - \psi_\gamma) + \bar{\psi}_\delta \psi_\delta] d\tau, \quad (40)$$

Using (19) and (20) the terms in (39) and (40) can be shown to give

$$\begin{aligned} & \frac{3}{4}\hbar^2 + 2u\hbar^2 a_{k,u}^2 (k+u)! (k-u)! \\ & - 2(u+2) d_{k,u+2}^2 (k+u+2)! (k-u-2)! \\ & - 2\hbar^2 (k+u+1)! (k-u)! a_{k,u} (b_{k,u+1} + c_{k,u+1}) \\ & - 2\hbar^2 (k-u-1)! (k+u+2)! d_{k,u+2} (b_{k,u+1} + c_{k,u+1}) \\ & + \frac{1}{2}\hbar^2 [a_{k,u}^2 (k+u)! (k-u)! + d_{k,u+2}^2 (k+u+2)! (k-u-2)! \\ & + (4b_{k,u+1} c_{k,u+1} - b_{k,u+1}^2 - c_{k,u+1}^2) (k+u+1)! (k-u-1)!]. \end{aligned}$$

Using the relations I-IV, § 5, we can show at once that the different values of M^2 are,

$$\left. \begin{aligned} \text{for I, } M^2 &= k(k+1)\hbar^2, & \text{so that } f &= k \\ \text{II, } M^2 &= (k+1)(k+2)\hbar^2, & f &= k+1 \\ \text{III, } M^2 &= (k-1)k\hbar^2 & f &= k-1 \\ \text{IV, } M^2 &= k(k+1)\hbar^2 & f &= k \end{aligned} \right\}. \quad (41)$$

This provides a justification for the quantum numbers assigned by Jackson to the four levels. It is clear that states I and IV have zero for their characteristic values of $\sigma_x + \rho_x$, etc., while II and III have $+2$ and -2 respectively.

We can show in a similar way that the magnetic quantum number $m^* = u + 1$, or that the total angular momentum round an axis parallel to an imposed uniform magnetic field is $(u + 1)h$. For if \mathcal{M}_z is the dynamical variable for this quantity

$$\begin{aligned}\mathcal{M}_z &= (xp_y - yp_x) + \frac{1}{2}h\sigma_z + \frac{1}{2}h\rho_z \\ &= -i\hbar \left(x \frac{\partial}{\partial y} - y \frac{\partial}{\partial x} \right) + \frac{1}{2}h\sigma_z + \frac{1}{2}h\rho_z \\ &= -i\hbar \frac{\partial}{\partial \phi} + \frac{1}{2}h\sigma_z + \frac{1}{2}h\rho_z\end{aligned}$$

(ϕ being the azimuthal angle), so that the diagonal elements M_z are given by

$$\begin{aligned}M_z &= \sum_{\alpha, \beta, \gamma, \delta} \int \bar{\psi}_\alpha \left[\left(-i\hbar \frac{\partial}{\partial \phi} + \frac{1}{2}h\sigma_z + \frac{1}{2}h\rho_z \right) \psi \right]_\alpha d\tau \\ &= -i\hbar \sum \int \bar{\psi}_\alpha \frac{\partial \psi_\alpha}{\partial \phi} d\tau + \frac{1}{2}h \int (2\bar{\psi}_\alpha \psi_\alpha - 2\bar{\psi}_\beta \psi_\beta) d\tau \\ &= u\hbar \int \bar{\psi}_\alpha \psi_\alpha d\tau + (u + 1)h \int (\bar{\psi}_\beta \psi_\beta + \bar{\psi}_\gamma \psi_\gamma) d\tau \\ &\quad + (u + 2)h \int \bar{\psi}_\delta \psi_\delta d\tau + h \int (\bar{\psi}_\alpha \psi_\alpha - \bar{\psi}_\beta \psi_\beta) d\tau \\ &= (u + 1)h \int (\sum \bar{\psi}_\alpha \psi_\alpha) d\tau \\ &= (u + 1)h.\end{aligned}\tag{42}$$

Since u can take all integral values between $-(k + 2)$ and k , m^* can take values between $\pm(k + 1)$, as we should expect on the grounds of the old quantum theory.

§ 8. The algebraic formulæ for the intensities are easily obtained. We already know that the possible changes in k, j are $\Delta k = \pm 1$, $\Delta j = \pm 1, 0$. The fact that our investigation leads to the formerly known results when we put $\beta_2 = 0$ is sufficient verification of this, though it may be easily verified algebraically. Therefore, the only lines whose intensities we shall calculate will be those shown in fig. 2, between states with quantum number k , and states with quantum number $k - 1$. It is easily found by the formulæ obtained below that the only changes in f are $\Delta f = \pm 1, 0$, the transition for $\Delta f = 2$ being forbidden (these are shown dotted in fig. 2).

Simple formulæ for the intensities of the transitions $(k, u) \rightarrow (k-1, u-1)$, $(k, u) \rightarrow (k-1, u)$, $(k, u) \rightarrow (k-1, u+1)$ (Zeeman effect), have been given

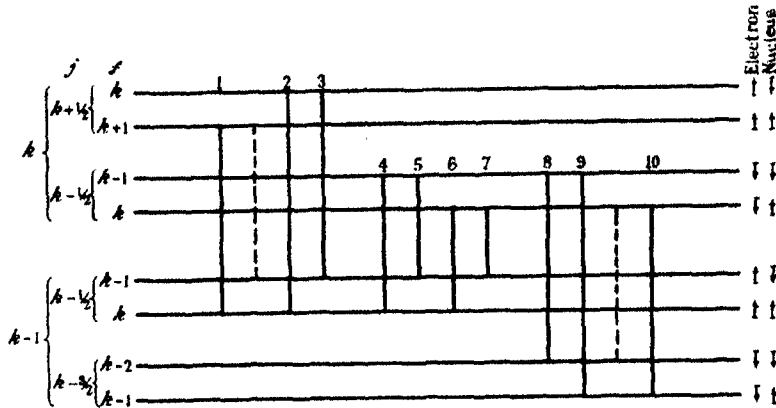


FIG. 2.

by Darwin* for the electron spin doublets, and we shall merely require an extension of these. In finding the relative intensities of the lines of the multiplet structure we may neglect the part of ψ depending on r , since this is exactly the same in all the components. The total intensity of a transition from a state with wave functions ψ to another with functions ψ' (the ψ 's and ψ' 's being normalised) is given by

$$\sum_{x, y, z} \left| \int x \sum_{a, \beta, \gamma, \delta} \psi_a \overline{\psi'_a} d\tau \right|^2. \quad (43)$$

Using the formulæ given in (20) we obtain formulæ exactly analogous to those of Darwin,

$$\begin{aligned} & \left(\begin{matrix} k \rightarrow k-1 \\ u \rightarrow u-1 \end{matrix} \right) \\ &= [(k+u)! (k-u)!]^2 \left[a_{k,u} a'_{k-1,u-1} + \frac{k+u+1}{k-u} (b_{k,u+1} b'_{k-1,u} \right. \\ & \quad \left. + c_{k,u+1} c'_{k-1,u}) + \frac{(k+u+1)(k+u+2)}{(k-u-1)(k-u)} d_{k,u+2} d'_{k-1,u+1} \right]^2 \end{aligned} \quad (44.1)$$

$$\begin{aligned} & \left(\begin{matrix} k \rightarrow k-1 \\ u \rightarrow u \end{matrix} \right) = 4 [(k+u)! (k-u)!]^2 \left[a_{k,u} a'_{k-1,u} \right. \\ & \quad \left. + \frac{k+u+1}{k-u} (b_{k,u+1} b'_{k-1,u+1} + c_{k,u+1} c'_{k-1,u+1}) \right. \\ & \quad \left. + \frac{(k+u+1)(k+u+2)}{(k-u)(k-u-1)} d_{k,u+2} d'_{k-1,u+2} \right]^2 \end{aligned} \quad (44.2)$$

* Loc. cit. II, p. 242.

$$\begin{aligned}
 \binom{k}{u} \rightarrow \binom{k-1}{u+1} &= [(k+u)! (k-u)!]^{-2} \left[a_{k,u} a'_{k-1,u+1} \right. \\
 &+ \frac{k+u+1}{k-u} (b_{k,u+1} b'_{k-1,u+2} + c_{k,u+1} c'_{k-1,u+2}) \\
 &\left. + \frac{(k+u+1)(k+u+2)}{(k-u)(k-u-1)} d_{k,u+2} d'_{k-1,u+3} \right]^2. \quad (44.3)
 \end{aligned}$$

These formulæ give the intensities of the Zeeman components, and we obtain the total intensities by summing over all the possible values of u , as given in (35). We have simply to substitute in (44) the values of the constants a, b, c, d given in I-IV, § 5. The intensities thus calculated of the Zeeman components of the lines marked 1-10 in fig. 2 are given as follows:—

- (1) $\frac{(k+1)(2k-1)}{k(2k+1)} (6k^2 - 2k - 2 - 4u - 2u^2);$
- (2) $\frac{2k-1}{k(k+1)(2k+1)} (2k^2 + 2k + 2 + 4u + 2u^2);$
- (3) $\frac{k(2k-1)}{(k+1)(2k+1)} (6k^2 + 10k + 2 - 4u - 2u^2);$
- (4) $\frac{1}{k^2(2k+1)(2k-1)} (6k^2 + 2k - 2 - 4u - 2u^2);$
- (5) $\frac{2k+1}{k^2(2k-1)} (k - k - 2 - 3u - u^2);$
- (6) $\frac{2k-1}{k(2k+1)} (2k^2 + 2k + 2 + 4u + 2u^2);$
- (7) $\frac{1}{k^2(2k+1)(2k-1)} (k^2 - 3k + 2 - (2k-3)u + u^2);$
- (8) $\frac{k(2k+1)}{(k-1)(2k-1)} (6k^2 - 14k + 6 - 2u^2 - 4u);$
- (9) $\frac{2k+1}{k(k+1)(2k-1)} (2k^2 - 2k + 2 + 4u + 2u^2)$
- (10) $\frac{(2k+1)(k-1)}{k(2k-1)} (6k^2 - 2k - 2 - 4u - 2u^2).$

In the first place, to our order of approximation the relative intensities are independent of the amount of separation. It appears that of the first three lines (2) is weak compared with (1) and (3) owing to the comparative smallness of the factor $(2k-1)/[k(k+1)(2k+1)]$. For a similar reason (7) is weak compared with (8) and (10). For the rest we can say little as to the com-

parative strengths, as u can in all cases take positive and negative values. The intensities could be summed for all values of u , but instead of carrying out this laborious calculation the numerical intensity ratios of the D series and P series have been determined. For these we simply sum the intensities of the lines (1)–(10) over the appropriate ranges of u for $k = 2, 1$ respectively. The results are shown in fig. 3, together with the spin axes configuration.

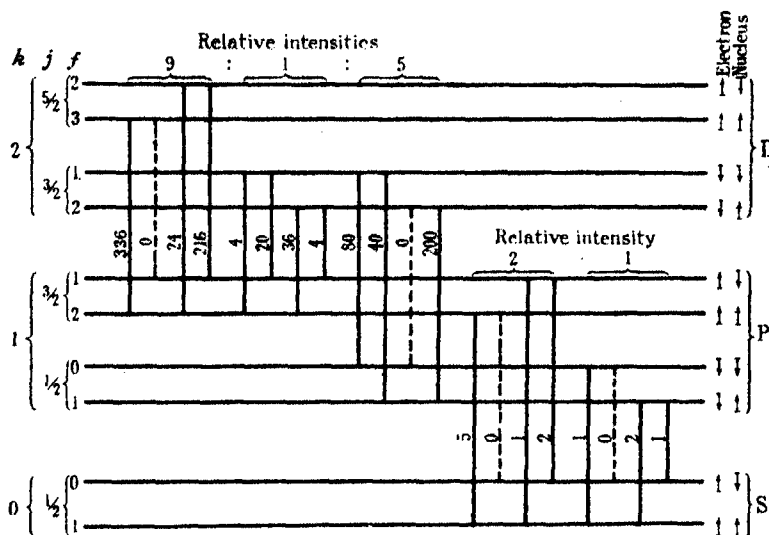


FIG. 3.

It appears that the strongest lines are those in which there is no change in the spin configuration, while the next strongest are those in which there is one change, either that of the nucleus or that of the electron. The weakest are those in which both directions are reversed. The line $f = 0 \rightarrow f = 0$ in the P series is accidentally zero (as is commonly the case for $\Delta j = 0$). The ratios of the total intensities for transitions $j = \frac{5}{2} \rightarrow j = \frac{3}{2}$, $j = \frac{3}{2} \rightarrow j = \frac{3}{2}$, $j = \frac{3}{2} \rightarrow j = \frac{1}{2}$, for the D series are 9 : 5 : 1 which agrees with the previous well known results for electron spin fine structure. Further the ratio of the total intensities for the lines $j = \frac{3}{2} \rightarrow j = \frac{1}{2}$ and $j = \frac{1}{2} \rightarrow j = \frac{1}{2}$ in the P series is 2 : 1. These results provide a useful check on the numerical work.

Jackson has only observed the P series, and the lines which he observed are shown in fig. 1. A comparison with fig. 3 shows a divergence of results in the transitions $j = \frac{1}{2} \rightarrow j = \frac{1}{2}$. Whereas we have found a strong line and two equal lines of half the strength, Jackson has found two distinct lines only. It should

be noticed that the rule we have deduced for the relative intensities is quite consistent and holds good for the D series as well as the P series.

The separations of the electron spin doublet levels due to nuclear spin are given by

$$-\beta_2 k(2k+3)/(2k+1) - \beta_2 k = -4\beta_2 k(k+1)/(2k+1)$$

and

$$-\beta_2(k+1) + \beta_2(k+1)(2k-1)/(2k+1) = -4\beta_2 k(k+1)/(2k+1),$$

so that the separation is the same for each doublet. The ratio of this to the electron spin separation is

$$\frac{-4k(k+1)}{(2k+1)^2} \cdot \frac{\beta_2}{\beta_1}.$$

This differs from the ratio given by the old mechanics by a factor

$$-4k(k+1)/(2k+1)^2$$

(or, in the case of the P levels 8/9). This does not affect appreciably Jackson's conclusions as to the magnetic moment of the nucleus.

Summary.

Using six dynamical variables for the spins of the nucleus and electron, the effect is calculated of a nuclear mechanical moment $\frac{1}{2}h$ on the optical spectrum of an atom with a central field, and the results compared with Jackson's recent observations for caesium. It is found that each of the electron spin fine structure levels splits up into two. The method employed gives the wrong result for the S levels, but empirical equations are constructed which give two levels (as required by experiment and elementary quantum theory considerations). The total angular momentum for each level is calculated in the form $\sqrt{[f(f+1)]}h$ and a new quantum number f accordingly assigned. The angular momentum round an axis parallel to the direction of a superposed uniform magnetic field is also calculated, thus fixing the magnetic quantum number. The intensities of the Zeeman components of the transitions are calculated and are found to be independent of the central field, while the rule $\Delta f = \pm 1, 0$ is found. In particular the numerical values of the relative intensities of the lines of the P and D series are calculated. It is found that those transitions are strongest in which neither the spin axis of the electron nor that of the nucleus is reversed, the next strongest being those in which one is reversed. This does not agree with Jackson's results, from which he deduced that there are only weak transitions (if any)

between states in which the spin axes are parallel and antiparallel respectively. The separation of the electron spin fine structure levels differs from Jackson's estimation by a numerical factor which for the P levels is 8/9.

I desire to express my best thanks to Mr. R. H. Fowler, F.R.S., and to Dr. P. A. M. Dirac for their invaluable advice and criticism.

A Comparison between the Behaviour at the Ac₃ Point of Single Crystal Iron and Polycrystal Iron, both in the Strained and Unstrained State.

By H. QUINNEY, M.A.

(Communicated by G. I. Taylor, F.R.S.—Received April 10, 1929.)

The experiments described here were undertaken with the object of investigating the effect of the initial crystal size on the behaviour of pure iron, during its passage through the Ac₃ point, when the iron changes its allotropic form, and the crystalline structure changes from the body centred cubic lattice arrangement to the face centred cubic lattice.

The energy of a crystal may be considered as consisting of the energy stored in the substance of the crystal itself and the energy stored in the surface, this surface energy being similar to the energy due to surface tension in a liquid. The energy per unit mass should be less in a specimen cut from a single crystal than in a specimen consisting of a number of crystals. Also, if a specimen is overstrained, it will contain additional energy due to the strain, and the strain will produce a greater surface energy.

It seemed probable that the difference in internal energy would affect the behaviour of the iron at the Ac₃ point. There might be a difference in the temperature at which the allotropic change occurred, and there would probably be a difference in the heat evolution.

Single crystals were prepared about 1 inch by $\frac{1}{2}$ inch by $\frac{1}{4}$ inch and for each crystal a temperature time chart was taken. The crystal was contained in a silica tube which was heated in a suitable resistance furnace with a fixed steady current sufficient to raise the temperature of the furnace to well over 1000° C.*

* Actually the highest temperature attained was never allowed to exceed 980° C. owing to fear of a change in the calibration of the thermocouples used, which were of the Pt-Pt Rh type.

The silica tube was connected to a hyvac pump, and the pump was kept running continuously throughout the test so that oxidation was prevented during the process of heating.

The thermocouple was bedded in the centre of the crystal. A small hole was drilled of sufficient diameter to insert the thermocouple, which was previously insulated with a very thin layer of pyruma putty burnt hard before attaching to the crystal. The leads (which unavoidably were partly included in the furnace) from the crystal to the cold junction were protected by a heavy porcelain tube, and the junction of this tube to the crystal was likewise sealed with pyruma putty. Actually, the specimen was placed in the hottest part of the furnace, so that the temperature of the thermocouple wires fell off as the distance from the crystal increased. Readings of temperature were taken on a galvanometer (fitted with antireep suspension) at intervals of a quarter of a minute.

The results of these tests indicate that there is no difference in the temperature of the Ac_3 point, whether the iron on being heated the first time passes from the single crystal to the polycrystal state on passing through the Ac_3 point, or, as is the case on heating a second time, passes from the β to the γ state in the polycrystal state. There is, however, a marked difference in the form of the temperature-time curve at Ac_3 according as the transformation takes place on first passing through the Ac_3 point when the single crystal is converted into the polycrystal state, or, as is the case on second heating, when the change is from β to γ , but in the latter both the β and γ states are of the polycrystal type.

In fig. 1 three curves are shown. Curve 2 shows the temperature-time relation when the single crystal passes through the Ac_3 point, and curve 3 shows the temperature-time relation when the resulting polycrystal iron on being again heated passes through the Ac_3 point.

Curve 1, fig. 1, shows the two curves 2 and 3 superimposed. It will be seen that the portion of the curve beyond the critical point is continuously lower in the case of the single crystal than is the case when the change from β to γ occurs with the small crystals. It may be assumed that the rate of supply of heat to the furnace is identical in the two cases. If one knew the exact form which the temperature-time curve would assume if there were no absorption of heat at the Ac_3 point, one could estimate the amount of heat absorbed at this point by measuring the distance AB, fig. 1, by which the observed curve drops below the hypothetical curve. Actually we do not know exactly what this curve is, because it is not exactly a straight line, and any change in the specific

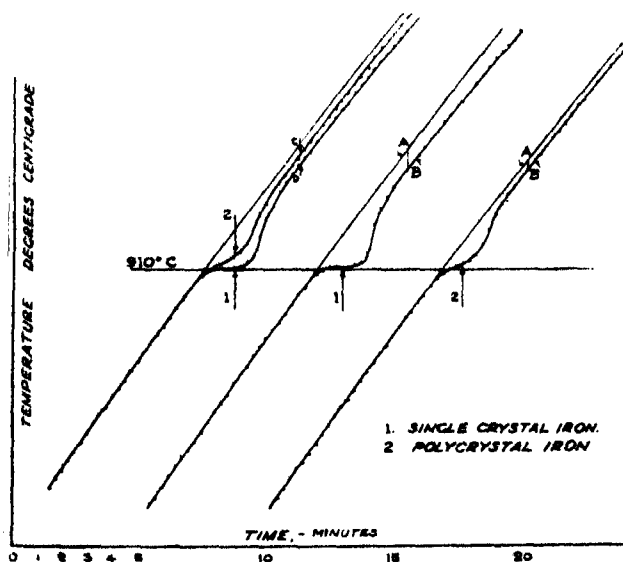


FIG. 1.

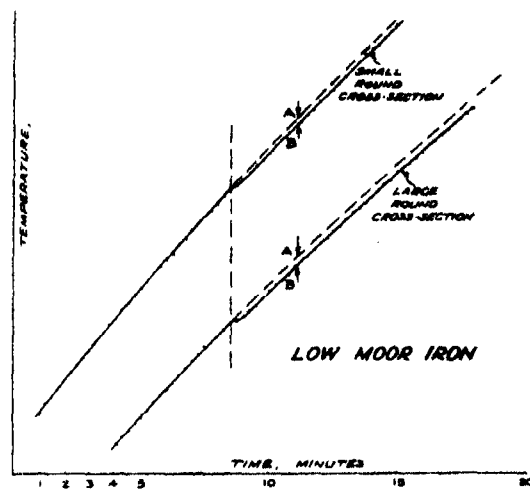


FIG. 1A.

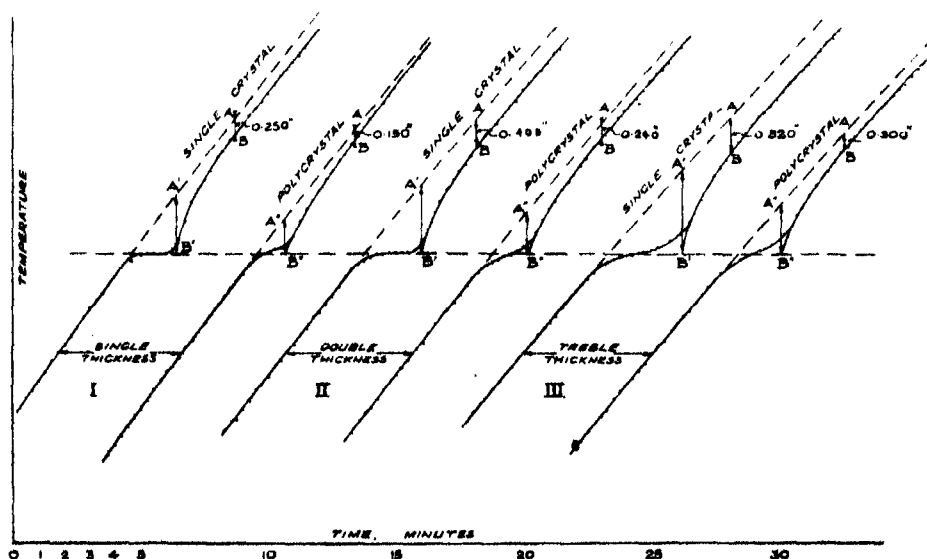


FIG. 1B.

This scale for temperature is $1'' = 27^\circ \text{C}$.

heat of the metal at the Ac_3 point would alter the slope. On the other hand changes in specific heat, if they occur, might be expected to affect both curves 1 and 2 equally, hence the difference shown as CD in curve 1, fig. 1, is a measure

of the heat absorbed. It was found, however, that if the temperature-time curve below the Ac_3 point was produced as a curve with uniform curvature it is approximately parallel to the observed curve above the Ac_3 point. This indicates that the change in specific heat is small.

The fact, that when the curve is produced in this way it is approximately parallel to the actual observed curve after the Ac_3 point, enables us to estimate the true drop of temperature due to the heat absorption in any particular case.

This temperature drop AB is not that of the specimen only, but that of the specimen and a certain proportion of the furnace. The heat of the furnace cannot be determined directly.

It is possible, however, to arrive at an estimate of what would be the drop in temperature if the heat absorbed were confined to the specimen only by making experiments with specimens of different cross section, and for this purpose observations were made with a round specimen of Lowmoor iron nearly filling the cross section of the tube, and of length rather more than a third that of the furnace. This specimen was then turned down until its cross section was only 0.312 of its original section, and observations again taken in the same way. The results are shown in fig. 1A.

The temperature lag AB was 1.12°C . for the large specimen and 0.67°C . for the small one.

If C_{r1} is the heat capacity per unit length of the large specimen and C_{r2} of the small one

$$C_{r1} : C_{r2} = \text{ratio of cross sections} = 3.2 : 1.$$

This ratio is also the ratio of the total amounts of heat absorbed at the Ac_3 point, for these two specimens. If the heat capacity of the furnace per unit length is K_r , then the ratio of the temperature lag in the first case to that in the second is $(K_r + C_{r2}) \times C_{r1} / (K_r + C_{r1}) \times C_{r2}$. This is measured by $1.12/0.67$; and since $C_{r2} = 0.312 C_{r1}$ we have

$$0.312 \frac{0.312 + K_r/C_{r1}}{1 + K_r/C_{r1}} = \frac{1.12}{0.67} \text{ or } \frac{K_r}{C_{r1}} = 0.445.$$

If the heat could be prevented from escaping from the furnace the drop in temperature would be greater than 1.12°C . in the ratio $(C_{r1} + K_r) : C_{r1}$, we have therefore

$$D_r = 1.12 (C_{r1} + K_r)/C_{r1} = 1.12 \times (1 + 0.445) = 1.62^\circ \text{C}.,$$

where D_r implies the drop in temperature in absence of heat capacity of furnace.

The same method that was applied to determine the heat capacity of the furnace in the case of round specimens was applicable to the rectangular specimens. It is not possible to use directly the value of K_f obtained from the experiment with round specimens because the rectangular specimens were not long compared with the diameter of the furnace. On the other hand it is to be expected that the same value for the effective heat capacity of the furnace would approximately be applicable to experiments with one, two, or three thicknesses of material, provided the length and breadth of the pieces were the same in all cases. Accordingly, separate heating curves were obtained with the furnace containing a single flat specimen, rather longer than those used in fig. 1, and these were compared with corresponding curves obtained from testing double and treble thicknesses of metal. The separate pairs of curves are shown in fig. 1B.

In the case of the single crystal specimen* the distance AB was found to be 0.25 inch, whence the temperature lag = 0.25 inch \times 9 = 2.25° C. for single thickness, 3.7° C. for double thickness, and 4.68° for treble thickness.

Calling K the effective heat capacity of the furnace for these rectangular specimens, we then have as before in the case of the round specimen :

$$\frac{K_f + C_{f1}}{K_f + C_{f2}} \times \frac{C_{f2}}{C_{f1}} = \frac{3.67}{2.25} \text{ and } C_{f2} = 2C_{f1},$$

where C_{f1} = heat capacity per unit length of single specimen and C_{f2} = heat capacity per unit length of double specimen.

Hence

$$\frac{1 + K_f/C_{f1}}{2 + K_f/C_{f1}} = \frac{3.67}{2.25} \times \frac{1}{2} = 0.815.$$

$$\begin{aligned} 1 + K_f/C_{f1} &= 0.815 (2 + K_f/C_{f1}) = 1.6 + 0.815 K_f/C_{f1} \\ &= 1.63 - 1 = 0.63 \quad \text{or} \quad K_f/C_{f1} = 3.41, \end{aligned}$$

and again we have for flat specimen

$$D_f = 2.25 (1 + K_f/C_{f1}) = 10^\circ \text{C.},$$

where D_f = drop of temperature in absence of heat transfer from furnace.

* The heat absorption for pure iron such as is obtained by decarburizing mild steel is much greater than that obtained for ordinary commercial iron such as Lowmoor iron. The steel employed for decarburizing was kindly provided by Sir William Larke, Chairman of The National Federation of Iron and Steel Manufacturers, and the composition was according to the manufacturers, Messrs. David Colville & Sons, Ltd., C, 0.15; Si, 0.07; S, 0.046; P, 0.024; Mn, 0.47 per cent.

Again, taking single and treble thickness, we have in the same way

$$\frac{K_f + C_n}{K_f + C_n} \times \frac{C_n}{C_n} = \frac{5.2}{2.5} \quad \text{and} \quad C_n = 3C_n.$$

hence

$$\frac{1 + K_f/C_n}{3 + K_f/C_n} = \frac{5.2}{2.5} \times \frac{1}{3},$$

or

$$2.5 + 2.5 K_f/C_n = 5.2 + 1.733 K_f/C_n,$$

i.e.,

$$K_f/C_n = 2.7/0.767 = 3.52,$$

as against 3.42 obtained for curves I and II. This gives

$$D_f = 2.25 (1 + K_f/C_n) = 2.25 (1 + 3.5) = 10.2^\circ \text{C.}$$

It will be noticed that the agreement between this value and the value 10°C. obtained from experiments with I and II thicknesses, is very good, which shows that the method employed is correct.

Examining curves for polycrystal iron in the same way we have :—

Temperature lag obtained from curves fig. 1B marked also AB gives for

single specimen	$1.35^\circ \text{C.},$
double specimen	$2.16^\circ \text{C.},$
treble specimen	$2.7^\circ \text{C.},$

using the same symbols as before we have :—

$$\frac{K_f + C_{f1}}{K_f + C_{f2}} \times \frac{C_{f2}}{C_{f1}} = \frac{2.16}{1.35},$$

and since $C_{f2} = 2C_{f1}$, we have

$$\frac{1 + K_f/C_{f1}}{2 + K_f/C_{f1}} = \frac{2.16}{1.35} \times \frac{1}{2} = \frac{1.08}{1.35},$$

or

$$1 + \frac{K_f}{C_{f1}} = \frac{1.08}{1.35} \left(2 + \frac{K_f}{C_{f1}} \right),$$

$$1.35 + 1.35 K_f/C_{f1} = 2.16 + 1.08 K_f/C_{f1},$$

$$0.27 K_f/C_{f1} = 0.81, \text{ i.e., } K_f/C_n = 3.00.$$

Using the curves I and III another estimate for D_f is obtained.

$$\frac{K_f + C_{f1}}{K_f + C_{f3}} \times \frac{C_{f3}}{C_{f1}} = \frac{2.7}{1.35} \quad \text{and} \quad C_{f3} = 3 C_{f1},$$

so that

$$\frac{1 + K_f/C_f}{3 + K_f/C_f} = \frac{2.7}{1.35} \times \frac{1}{3} = \frac{0.1}{0.15} = 0.666,$$

$$\frac{1 + K_f/C_{f1}}{3 + K_f/C_{f1}} = 0.66,$$

$$1 + K_f/C_{f1} = 1.98 + 0.66 K_f/C_{f1},$$

therefore

$$0.34 K_f/C_{f1} = 0.98,$$

$$K_f/C_{f1} = 0.98/0.34 = 2.90.$$

This gives $D_f = (1 + 2.9) \times 1.35 = 5.26^\circ \text{C}$. The values of K_f/C_{f1} for polycrystal iron are not in such good agreement as those obtained for a single crystal iron.

The heat capacity for polycrystal iron cannot be appreciably different from that of the same specimen when converted into a single crystal, so that K_f/C_{f1} should have been the same in all cases. For the single crystals the values were 3.41 and 3.50 for the polycrystal they are 2.90 and 3.0.

Comparison of K_f and K_r .

It is of some interest to compare the effective heat capacities of the furnace in the two cases. A small difference might be expected because the flat specimens were not long compared with the diameter of the furnace.

We found $K_r/C_{r1} = 0.445$ and $K_f/C_{f1} = 3.47$ (mean value for large crystals) and the heat capacities per unit length of the round and flat specimens should be proportional, to their cross section.

These were 0.562 square inch and 0.09 square inch respectively hence

$$C_{r1} = C_{f1} = 0.562/0.09.$$

Hence we have

$$\frac{\text{Effective heat capacity per unit length with long round specimen}}{\text{Effective heat capacity per unit length with short rectangular specimen}}$$

$$= \frac{0.445}{3.47} \times \frac{0.562}{0.09} = 0.80.$$

This shows, that the effect of length is not great but the difference is in the right direction, because one might expect in the case of the short specimen an increase in effective heat capacity of the furnace due to the portion of it just beyond the ends of the specimen.

The point on the curve, where the temperature is again approaching a steady

rate of rise, is an indication of the rate at which the temperature is equalised between the furnace and the specimen.

After a time of absorption of heat the equalising of temperature, as between specimen and furnace, to its final steady rate of increase will probably follow a law which is likely to be roughly exponential, though the details of the heat transfer are much too complicated to calculate. It seems therefore that there is some justification for producing the observed curve as though it were an exponential until it meets the line representing the Ac_3 change at 910°C . This has been done in all cases represented in fig. 1b. In that diagram B' is the point where the best fitting exponential curve meets the 910°C . line on being produced backwards, and A' is the point on the extrapolation of the first part of the heating curve immediately above B'. The value A'B' should agree roughly with the estimated value D_f calculated from the value AB.

The values of D_f previously calculated for single crystal were (10°C . and 10.2°C .).

The values of A'B' measured from fig. 1b in the three cases for single crystal specimens were---

Single thickness	9°C .
Double thickness	9.9°C .
Treble thickness	11.52°C .

It appears that the temperature drop estimated in this way is in very good agreement with that found previously.

In the same way the points A''B'' on curves fig. 1b for polycrystal iron should agree roughly with the estimated values for the heat drop for polycrystal iron.

The values of D_f for polycrystal iron were $D_f = 5.4^\circ\text{C}$. and 5.25°C .

The values of A''B'' were---

Single thickness	5.52°C .
Double thickness	5.58°C .
Treble thickness	7.20°C .

Again, it is seen that there is good agreement between the calculated temperature drop and the values A''B''.

Estimate of Difference between Single Crystal Heat Absorption and Polycrystal Heat Absorption at the Ac_3 Point.

The mean value of K_f/C_{f1} was found to be about 3.25 and to estimate the fall of temperature at Ac_3 in absence of heat capacity of furnace the observed

drop in temperature AB has to be multiplied by $(C_{f1} + K_f)/C_{f1} = 4.25$ in the case of single thickness and by $(2C_{f1} + K_f)/2C_{f1} = 2.625$ in the case of double thickness and by $(3C_{f1} + K_f)/3C_{f1} = 2.08$ in the case of treble thickness.

Taking the difference in the values of AB (fig. 1b) for single and polycrystal iron for these three cases the estimated drop of temperature in each case will be :—

$$\text{Single thickness} \quad \dots \quad 0.9 \times 4.25^\circ \text{C.} = 3.83^\circ \text{C.}$$

$$\text{Double thickness} \quad \dots \quad 1.35 \times 2.62^\circ \text{C.} = 3.54^\circ \text{C.}$$

$$\text{Treble thickness} \quad \dots \quad 2.7 \times 2.08^\circ \text{C.} = 5.60^\circ \text{C.}$$

$$\text{Mean value } 4.32^\circ \text{C.}$$

We can compare the value 4.32°C. with the difference between A'B' and A''B''—

$$\text{Mean value for A'B'} = 10.1^\circ \text{C.}$$

$$\text{Mean value for A''B''} = 6.1^\circ \text{C.}$$

difference of mean values = 4°C.

It appears therefore that with the iron employed in these experiments the difference in heat drop between single crystal and polycrystal states, at the Ac₃ point, is about 4°C.

Change in Heat Absorption due to Plastic Strain.

The writer owes a great debt of gratitude to Mr. S. Lees, M.A., Hopkinson Lecturer in Thermodynamics and Fellow of St. John's College, Cambridge, for his help and advice. He suggested, that the difference between the single crystal and polycrystal iron at the Ac₃ point could be accounted for, as already stated, by the existence of surface energy at the crystal faces of the polycrystal iron. It was further considered, that, if this be the true explanation of the difference between single crystal and polycrystal iron on passing through the Ac₃ point, then mechanical overstrain, which leads to a breaking up of the crystals of the metal might reduce the heat absorption at the critical point in question owing to the increase in crystal surface area.

A number of temperature-time curves of overstrained iron are shown in figs. 2 and 3. The overstrain was intentionally of a very severe character with a view to producing the largest possible degree of breaking up of the crystals before examining their behaviour at the Ac₃ point.

Fig. 2 shows in the upper part a comparison between the temperature-time curve for a heavily overstrained single crystal and an unstrained single crystal. The two curves are superimposed, 1 being the overstrained single crystal and

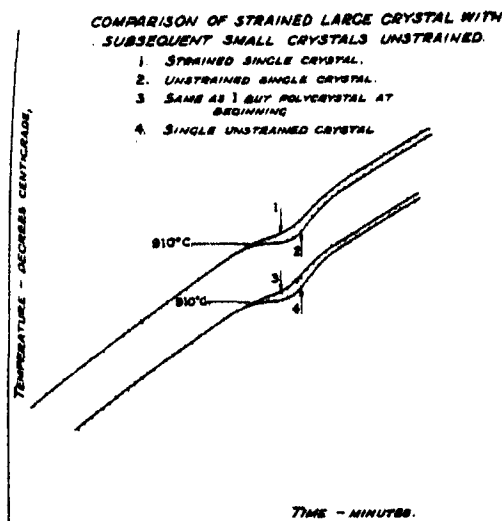


FIG. 2.

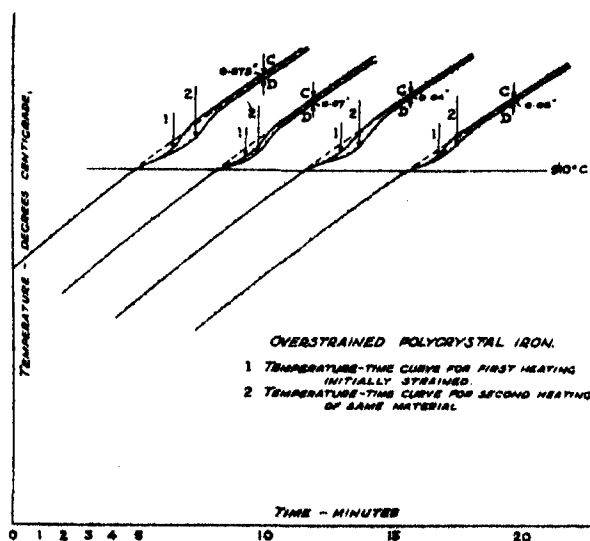


FIG. 3.

The scale for Temperature is $1'' = 48^\circ \text{C}$.

2 the results obtained from a similar unstrained single crystal. In the lower part a comparison is shown between the temperature-time curve for the resulting polycrystal iron and a corresponding temperature-time curve for unstrained single crystal iron, these curves are marked 3 and 4.

It will be seen from fig. 2 that the heat absorption is considerably reduced

at the Ac_3 point when the single crystal is heavily overstrained and the heat absorption for the overstrained single crystal is more nearly equal to that obtained when unstrained polycrystal iron passes through the Ac_3 point.

A further comparison is shown in fig. 3 between the temperature-time curves obtained for strained and unstrained polycrystal iron marked I and II respectively. It will be seen that the curve for strained material actually ends above the dotted curve, which is a continuation of the first heating curve. This indicates that the ordinary absorption of heat at the Ac_3 point is associated with an evolution of heat due to release of strain energy at the critical point Ac_3 , and that the net result may be an actual evolution of heat.

As already stated the precise determination of whether this is so or not depends upon a knowledge of the specific heats of the metal before and after the critical point Ac_3 .*

The parallelism between the extrapolation of the heating curve before the Ac_3 point and the observed curve after heating is again observed, and the difference in heat absorption, between the strained and unstrained metal can again be deduced from a knowledge of the value CD . A mean value† for CD from a number of experiments gave $CD = 0.055$ which represents $0.88^\circ C$.

The specimens were of rectangular cross section and similar to those previously examined so that the heat absorption in the absence of heat capacity of furnace is obtained from CD in the manner already described.

Using the conversion factor 4.25 previously found for specimens of the same size the difference between the temperature drop in the two cases, in the absence of heat capacity of the furnace, is found to be equal to $0.055 \times 16 \times 4.25 = 3.74^\circ C$.

This indicates that the surface energy is largely released at the critical point Ac_3 when the allotropic change for β and γ iron proceeds in the case of pure iron at a temperature of $910^\circ C$.

Farren and Taylor‡ observed an increase in the internal energy of metal in the overstrained state. They recorded for mild steel an increase in internal

* Experiments so far conducted by various investigators into the question of variation of specific heat of iron and steel by the method of mixture calorimetry appear to overlook a possible change of state consequent on cooling in the calorimeter. In the case of steel this may render the values so obtained at fault in so far as heating is concerned. Even in the case of pure iron it may well be true that the changes in internal energy consequent on variation in grain size above and below the critical point Ac_3 may also introduce errors of the same kind.

† Fig. 3 contains only a selection of the results from which this mean is taken.

‡ 'Roy. Soc. Proc.' A, vol. 107 (1925).

energy equal to 14 per cent. of the work done. The calculated rise of temperature due to the heat equivalent of the work done was about $1\frac{1}{2}^{\circ}$ C. higher than the actual rise in temperature.

The degree of overstrain was less than that required to produce rupture in tension, and as the extent of the overstrain possible in tension is limited by the formation of a neck, the majority of the specimen is much less overstrained than that which occurs in the neighbourhood of breakdown.

On the other hand, where temperature-time curves of overstrained iron are shown in figs. 2 and 3, the overstrain was of a very severe character. The specimens were first compressed, then twisted in torsion and again compressed to a rectangular cross section, in order to break up the crystals to the fullest extent.

Although the value 3.75° C. determined from the temperature-time curves is in excess of the $1\frac{1}{2}^{\circ}$ C. referred to above, it is possible, however, that 3.75° C. represents less than 14 per cent. of the heat equivalent of the work done. Moreover the determination of the value 3.75° C. from the temperature-time curve could not be measured to the same degree of accuracy as the experiments described by Farren and Taylor.

Further the overstrained material used in these experiments was pure iron whereas in the experiments of Farren and Taylor the material was mild steel.

Comparison between the Dilatation of Single Crystal and Polycrystal Iron.

An estimate of the relative contraction of single crystal and polycrystal iron is shown in fig. 4.

AB gives the contraction at Ac_3 for single crystal iron and A'B' gives the corresponding contraction for polycrystal iron. A'B' is roughly half AB. It appears therefore that the change from a single crystal to a polycrystal state reduces the contraction at the Ac_3 point in the same ratio as the corresponding reduction in heat absorption. The accuracy of these values for dilatation are open to question owing, in the first place, to the high temperature reached in the case of pure iron at the critical point Ac_3 and the consequent softness of the metal, and, further, owing to rapid oxidation, but a comparison is justifiable. It would be an advantage to be able to record dilatation *in vacuo* as was the case in taking the heating curves, because the results indicate that the precise form of the dilatation curve depends upon the initial state of the metal due to either thermal or mechanical treatment.



FIG. 4.

In conclusion, I should like to thank Prof. C. E. Inglis for the opportunity and encouragement to do this work at the Engineering Laboratory, Cambridge.

It is owing to the very kind interest taken in these observations by Prof. G. I. Taylor, F.R.S., that the results obtained were analysed in the manner described. The experiments necessary for determining the equivalent heat capacity of the furnace and the method of applying them, were done under his direction.

*The Absorption Spectra of Halogens and Inter-halogen Compounds
in Solution in Carbon Tetrachloride.*

By A. E. GILLAM and R. A. MORTON.

(Communicated by Prof. E. C. C. Baly, C.B.E., F.R.S., Liverpool University.
—Received April 18, 1929.)

When two solutions are mixed the absorption spectrum of the new solution will be the mean of those of the separate solutions provided that no chemical interaction occurs. The mere fact of a departure from additivity does not, however, necessarily denote the formation of true chemical compounds. The solute or solutes may undergo solvation, loosely bound aggregates may occur, and even when marked deviations from the simple law of mixtures are observed it is rarely possible to prove the quantitative formation of a given chemical compound from spectroscopic data alone.

The above considerations apply with some force to the problem of the absorption spectra of halogens and inter-halogen compounds in an inert solvent. The three elements show perfectly characteristic absorption bands, they are known to interact with the formation of some quite stable compounds, some relatively stable compounds, and some apparently very unstable compounds.

There is, for instance, no doubt whatever that iodine monochloride, iodine trichloride, and iodine monobromide are definite compounds, whereas until very recently there was no convincing physiochemical evidence for the existence of bromine chloride BrCl . The present investigation was planned as follows :—

- (a) The absorption curves for solutions of the halogens, chlorine, bromine and iodine, in an inert solvent were to be determined.
- (b) Summation curves were to be constructed on the assumption that solutions containing different halogens in stoichiometric proportions would obey the simple mixture law.
- (c) Experimental absorption curves were to be obtained with solutions of definite inter-halogen compounds.
- (d) Experimental curves for mixtures in proportions corresponding with known compounds, and with compounds the existence of which remained doubtful, were to be measured.

It will be seen at once that if the absorption spectrum of iodine chloride in relation to iodine and chlorine is comparable with the absorption spectrum of iodine bromide in relation to iodine and bromine, then bromine chloride, if it exists, should exhibit precisely the same relationship to bromine and chlorine.

Experimental.

Solvent.—The solvent chosen for the work needs to be transparent to visible and ultra-violet light and must not interact with the solutes. Carbon tetrachloride, if free from carbon bisulphide, the commonest impurity, transmits freely as far as $265\ \mu\mu$, and is completely inert towards the halogens.*

Technique of Absorption Spectra Measurements.—Two Hilger E3 quartz spectrographs were used in conjunction with sector photometers. In one case the light source was an iron-nickel arc (line spectrum), whilst in the other, a high-tension under-water spark between tungsten electrodes was used (continuous spectrum). Fiduciary lines in the work with a continuous light source, were obtained by photographing the aluminium spark in air at the top and bottom of each plate. Match points were usually determined visually as it

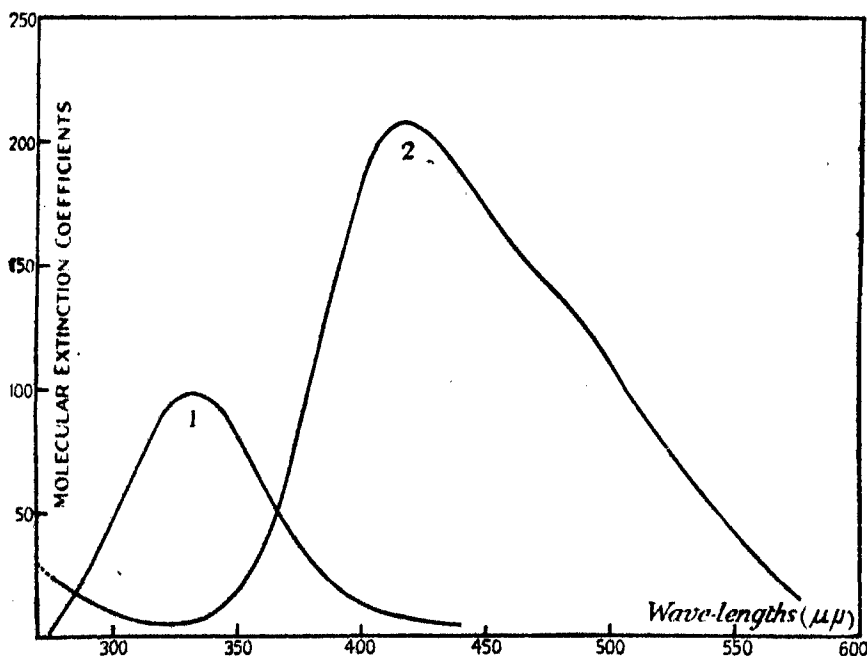


FIG. 1.—Absorption Spectra of Chlorine and Bromine in Carbon Tetrachloride.
Curve 1—Chlorine solution. Curve 2—Bromine solution.

* Medicinal carbon tetrachloride made by Messrs. Albright and Wilson is quite suitable.

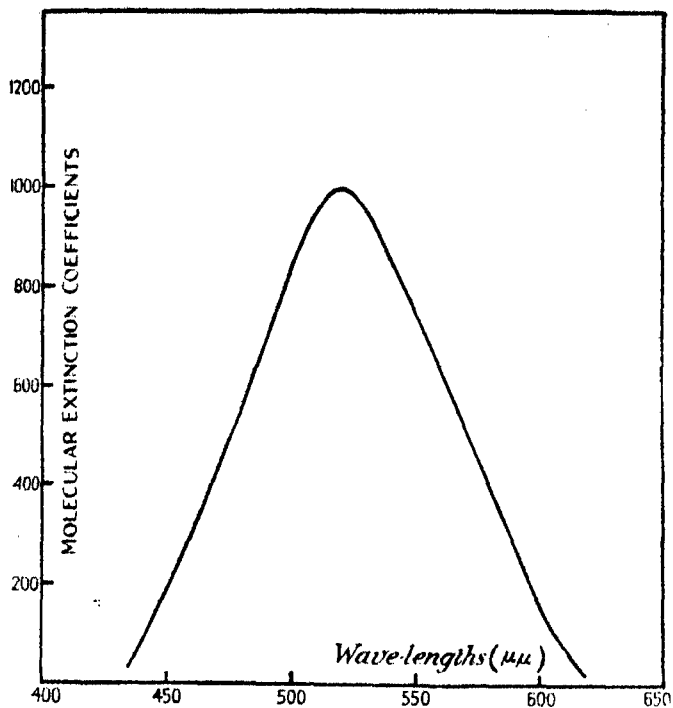


FIG. 2.—Absorption Spectrum of Iodine in Carbon Tetrachloride.

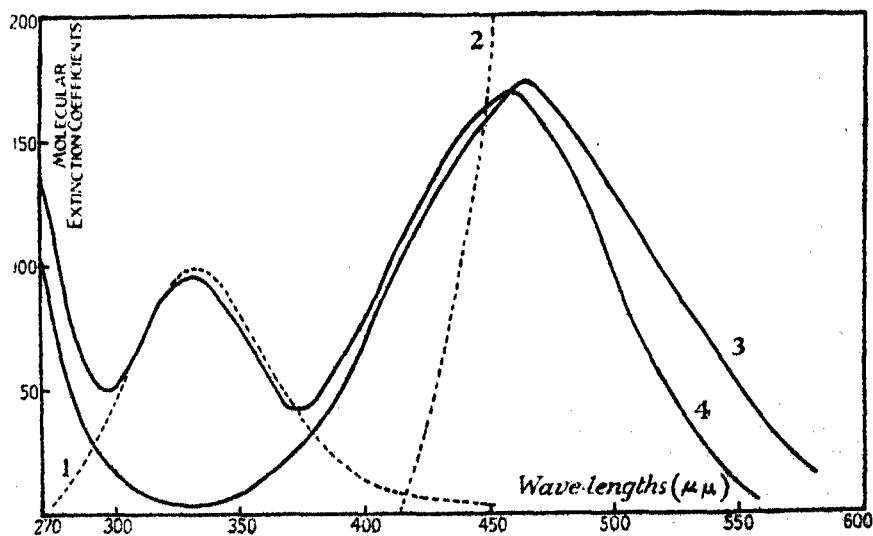


FIG. 3.—Absorption Spectra of Solutions in the system Iodine-Chlorine. Curve 1 (dotted)—Chlorine. Curve 2 (dotted)—Iodine. Curve 3 (continuous)—Iodine monochloride observed. Curve 4 (continuous)—Iodine trichloride observed.

was found that the use of a registering microphotometer did not increase the accuracy of measurement for the broad continuous bands shown by the halogens under the conditions of experiment. Whenever a solution showed absorption in the visible region, an entirely independent set of measurements was

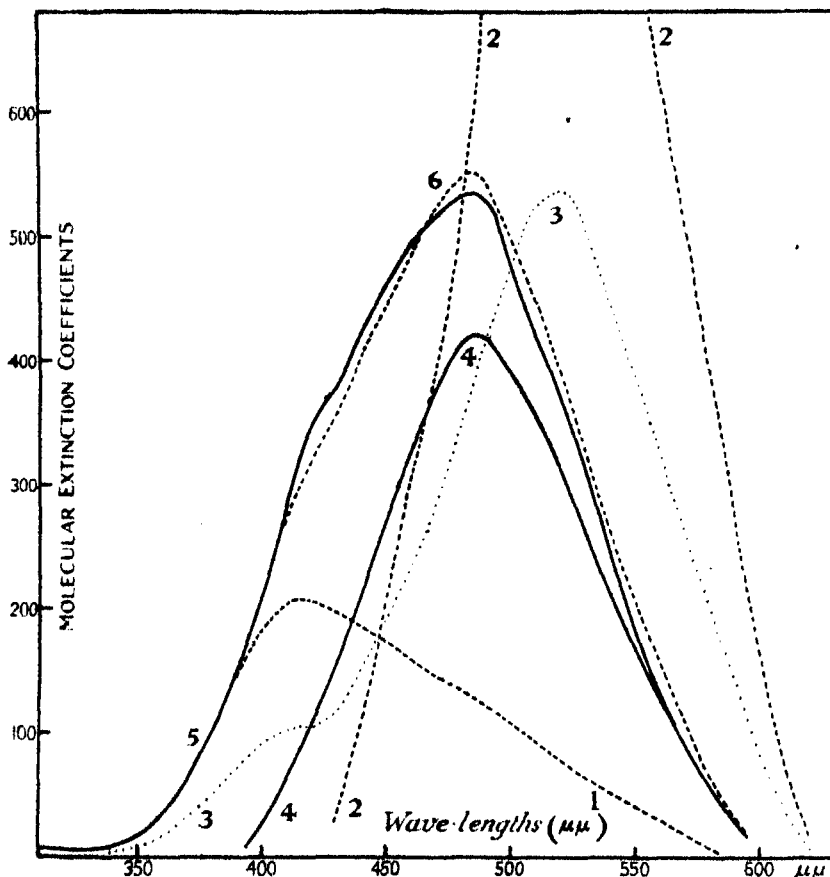


FIG. 4.—Absorption Spectra of Solutions in the system Iodine-Bromine. Curve 1 (dotted line)—Bromine in carbon tetrachloride. Curve 2 (dotted line)—Iodine in carbon tetrachloride. Curve 3 (dotted line)—Mean of iodine + bromine curves. Curve 4 (continuous line)—Iodine monobromide observed. Curve 5 (continuous line)—Iodine tribromide observed. Curve 6 (dotted line)—Summation of observed $\text{IBr} + \text{Br}_2$ curves.

carried out in duplicate by two observers working on a new model of the Hilger-Nutting visual spectrophotometer. The majority of the curves shown in figs. 1 to 5 are the result of concordant photographic and visual determinations.

In the preliminary work absorption cells of the ordinary type were used,

but it was found that the solute, particularly if it were chlorine, was liable to escape from the solution during the period necessary for the completion of the measurements. All the preliminary data were therefore rejected and fresh determinations carried out using a different type of cell. The new cells were of fused quartz, constructed in one piece with flat fused-on end plates. The cells were filled by means of a side tube, the solution reaching well into the tube,

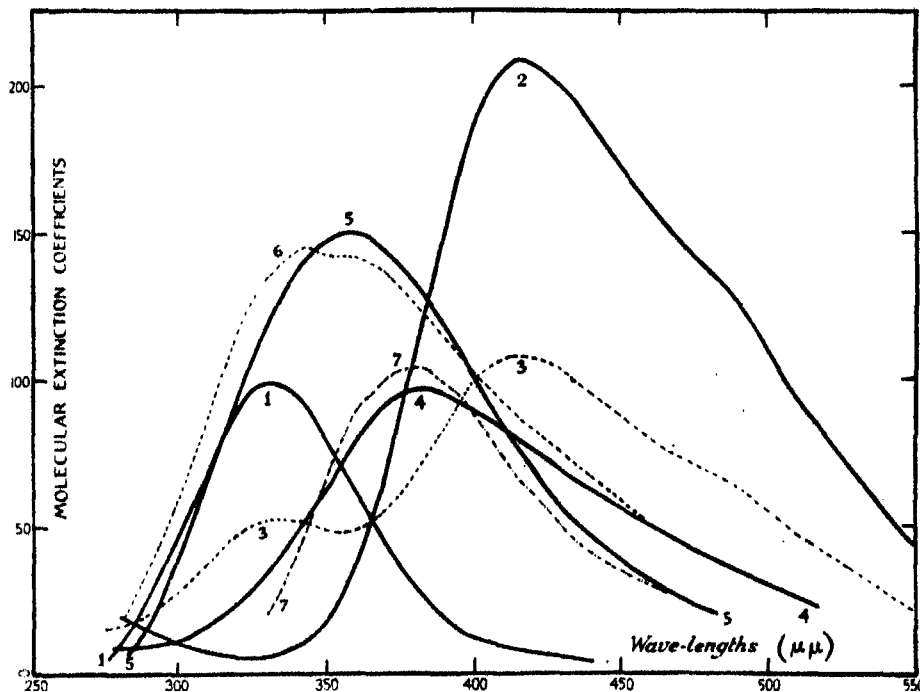


FIG. 5.—Absorption Spectra of Solutions in the system Chlorine-Bromine. Curve 1—(continuous line)—Chlorine. Curve 2 (continuous line)—Bromine. Curve 3 (dotted line)—Mean of chlorine and bromine curves. Curve 4 (continuous line)—Bromine monochloride, observed. Curve 5 (continuous line)—Bromine trichloride, observed. Curve 6 (dotted line)—Summation of observed $\text{BrCl} + \text{Cl}_2$ curves. Curve 7 (dotted line)—Observed BrCl_2 curve minus Cl_2 curve.

which could then be closed so as to eliminate the escape of gas. Comparison cells were used throughout to correct for the absorption and reflexion losses, due to the solvent and the cell materials.

Statement of Results.—The molecular extinction coefficient ϵ has been plotted against wave-length, ϵ being defined by the well-known equation $\log I_0/I = \epsilon cd$, c being the molar concentration and d the thickness in centimetres. It is usual to describe an absorption band as showing ϵ maximum, at a certain wave-

length, the maximum being fixed by the two parameters, wave-length and extinction coefficient. Now that the study of absorption spectra of solutions is becoming more and more quantitative, a more precise notation seems to be called for.

In order to reproduce a given measurement it is necessary to know the cell thickness, the concentration, and the photometer setting at the maximum. Unless a substance is perfectly stable, and obeys Beer's law strictly, the statement that the wave-length of maximum absorption occurs at $x \mu\mu$ with e maximum $= y$, is a very incomplete description of the observation. As v. Halban and Eisenbrand* have made clear, the accuracy, *i.e.*, the relative error of e , depends, other things being equal, on the magnitude of $\log I_0/I$ (E). It is therefore important that E should be specified, directly or indirectly. By analogy with other notations in physical chemistry one might write $E_d^c(350 \mu\mu) = 1 \cdot 0_{1\text{cm.}}^{0 \cdot 1\text{M}}$. This would constitute a complete description of the datum. It would, however, make it necessary for the molecular extinction coefficient to be specified separately, or left for the reader to calculate. Perhaps a better notation would be

$$e_d^c(350 \mu\mu) = 10,$$

i.e., in an actual case

$$e \text{ max. } (350 \mu\mu) = 10_{1\text{cm.}}^{0 \cdot 1\text{M}}.$$

If such a notation were generally accepted, the problem of reproducibility in absorption spectra would be reduced to a question of manipulation only.

Results.—The results of the investigation are to be seen in the curves in figs. 1 to 5. The following tabular summary has the advantage of emphasising the quantitative side.

Table I.

	Chlorine.	Bromine.	Iodine.
λ maximum $\mu\mu$	332	417	520
e max. _d ^c	$[99]_{\text{d}}^{0 \cdot 0085}$	$[208]_{\text{d}}^{0 \cdot 00187}$	$[985]_{\text{d}}^{0 \cdot 000718}$
Atomic weight	35.5	80	127

It will be noticed that the extinction coefficients and the positions of the maxima show the periodicity usually associated with the properties of the halogens.

* 'Roy. Soc. Proc.,' A, vol. 116, p. 153 (1927).

Table II.

	Bromine chloride (BrCl).	Iodine chloride (ICl).	Iodine bromide (IBr).
λ maximum $\mu\mu$	380	464	487
ϵ max. $\frac{\epsilon}{d}$	$[97]^{.006}_1$	$[173]^{.00426}_2$	$[420]^{.00174}_3$

Discussion.—As regards the halogens it is only necessary to state that our materials were carefully purified by standard methods and the concentration determined by means of potassium iodide-thiosulphate titrations immediately before the absorption was studied. The results are in good agreement with earlier work as will be seen from the following summary.

Liveing and Dewar* described an absorption in chlorine vapour at 302–356 $\mu\mu$, whilst v. Halban and Siedentopf† recorded a maximum in the vapour at 334 $\mu\mu$, as against our determination of 332 $\mu\mu$ in carbon tetrachloride. The very recent data of Barratt and Stein‡ are in agreement.

Plotnikow§ has measured the absorption of bromine in various solvents for four mercury lines. He found that Beer's law was obeyed, and also concluded that the visible absorption consists of two super-imposed absorption bands. Ribaud|| recorded a maximum in bromine vapour at 419–422 $\mu\mu$, whilst Dobbie and Fox¶ gave the maximum as 417 $\mu\mu$. Bovis** finds that liquid bromine in very thin films shows a band at λ maximum 417–421 $\mu\mu$, λ minimum 348 $\mu\mu$. In carbon tetrachloride he found two maxima at 258 and 415 $\mu\mu$ respectively.

The colour of iodine solutions has been much studied. Some solvents yield brown solutions, others violet; the differences being generally ascribed to differences in solvation. The violet solutions such as are formed in carbon tetrachloride are regarded as normal and the solutes are not, it would appear, appreciably solvated. The absorption of the violet solutions indicates a maximum very near to that shown by the vapour, namely, at 520 $\mu\mu$ or

* 'Proc. R. Inst.,' vol. 10, p. 245 (1883).

† 'Z. Phys. Chem.,' vol. 103, p. 71 (1922); 'Z. Elektrochem.,' vol. 28, p. 496 (1922).

‡ 'Roy. Soc. Proc.,' A, vol. 122, p. 582 (1929).

§ 'Z. Phys. Chem.,' vol. 79, p. 357 (1912).

|| 'Ann. Physik,' vol. 12, p. 107 (1919).

¶ 'Roy. Soc. Proc.,' A, vol. 99, p. 456 (1921).

** 'C. R.,' vol. 178, p. 1964 (1924), *ibid.*, vol. 185, p. 57 (1927); 'Ann. Physique,' vol. 10, p. 232 (1928).

thereabouts, whereas the brown solutions show a maximum at $447\ \mu\mu$, cf. Batley.*

For solutions in chloroform, carbon tetrachloride and carbon bisulphide, Rigollot† gives the maximum as $520\ \mu\mu$; Carelli‡ records a maximum at $515\ \mu\mu$ in the latter solvent, whilst Brode§ finds the head of the band in carbon tetrachloride to be at $518\ \mu\mu$. Getman,|| on the other hand, in a very recent paper, records measurements with a Nutting photometer showing the maximum to be at $540\ \mu\mu$ in all three solvents. In our data the band occurs at $520\ \mu\mu$.

The compounds iodine monochloride and iodine trichloride form a convenient starting point for the discussion of the absorption spectra of the inter-halogen compounds. Discovered in 1814 by Gay-Lussac, their real existence as chemical compounds was definitely established by the work of Stortenbeker¶ on the freezing point curves of mixtures of iodine and chlorine. It was shown by Trapp** that iodine chloride exists in two forms differing in melting point and designated as the α and β forms. Little work appears to have been published on the absorption spectrum of iodine monochloride, except that Roscoe and Thorpe†† pointed out the resemblance between the spectrum of iodine chloride and bromine, and that Gernez‡‡ noticed that the spectrum of the vapour differs from that of either chlorine or iodine.

In the present work standardised solutions of iodine and chlorine were mixed so that the halogens were present in exactly equimolecular proportions, and allowed to stand for an hour until the violet colour of the free iodine had disappeared. The concentrations used varied between 0.004 and 0.01 molar with respect to iodine chloride. Measurements were made both by the visual and photographic methods. The absorption curve showed a maximum at $464\ \mu\mu$ and a minimum at $334\ \mu\mu$, and differed completely from the curves for chlorine and iodine. As a control, two different specimens of commercial iodine chloride labelled "pure" were dissolved in carbon tetrachloride and the absorption spectra determined. The curves obtained in this way agreed

* 'Trans. Faraday Soc.,' vol. 24, p. 438 (1928).

† 'C. R.,' vol. 112, p. 38 (1891).

‡ 'Rend. Accad. Sci. Fis. Mat. Napoli,' vol. 27, p. 274 (1921).

§ 'J. Amer. Chem. Soc.,' vol. 48, p. 1877 (1926).

|| 'J. Amer. Chem. Soc.,' vol. 50, p. 2883 (1928).

¶ 'Z. Phys. Chem.,' vol. 3, p. 11 (1889); 'Rec. Trav. Chim., Pays-Bas,' vol. 7, p. 152 (1889).

** 'J. Prakt. Chem.,' vol. 63, p. 108 (1854).

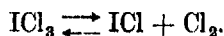
†† 'Phil. Trans.,' vol. 167, p. 207 (1876).

‡‡ 'C. R.,' vol. 74, p. 660 (1872).

exceedingly well with those obtained with equimolecular mixtures. The results so far indicated that it was highly probable that the solutions contained a large amount of iodine chloride. It was, however, quite possible that some dissociation should occur in accordance with the expression



In order to test the possibility of dissociation, solutions 10 times as concentrated as those already used were examined in the ultra-violet and also in the visible to ascertain whether any trace of free chlorine or free iodine could be detected. The results were completely negative, so that it must be concluded that iodine chloride is quite stable under the conditions of the experiments. It must, however, be understood that this only applies to freshly prepared, cold, carbon tetrachloride solutions, as it is noticed that solutions of iodine monochloride in this solvent appear to decompose on standing in glass vessels exposed to daylight, when the characteristic violet colour of iodine solutions makes its appearance. The next step was to examine the absorption spectra of solutions containing three equivalents of chlorine to one of iodine, corresponding with ICl_3 . As will be seen from fig. 3 this mixture exhibits two maxima corresponding quite closely with those characterising chlorine and iodine monochloride. It would therefore seem as if iodine trichloride is not stable in dilute carbon tetrachloride solutions, but rather dissociates according to the equation



It will be noticed from fig. 3 that there is a slight discrepancy between the experimental iodine monochloride band and the similar "iodine trichloride" band. Any dissociation of iodine monochloride will be hindered by the presence of excess chlorine, and as iodine absorbs much more intensely than any other constituent of the solutions a very small proportion of free iodine would broaden the "ICl" band on the long wave side. The fact that the solutions containing three equivalents of chlorine to one of iodine are less absorbent on the long wave side of $464 \mu\mu$ than the equimolecular solutions, is consistent with a very small degree of dissociation of iodine chloride. A sample of commercial iodine trichloride was then examined under the same conditions. The absorption curve showed exactly the same maxima as before, but the $464 \mu\mu$ band was a little more intense and the chlorine band a little less intense. Probably, the material had lost some chlorine as a result of dissociation.

Iodine monobromide was first prepared by Balard in 1826 as a solid melting

at 42°. Terwogt* studied the freezing points, boiling points, vapour pressures and specific gravities of iodine—bromine mixtures. The freezing point curves indicate the presence of a compound which is in all probability IBr, but the boiling point curves show that such a compound must dissociate very readily. There seems to be no evidence of the existence of iodine tribromide. The only reference we have been able to find to the absorption spectrum of iodine bromide is in a general paper by Ruff† dealing with the use of the spectroscope as a means of detecting compound formation in mixtures. It is stated that there is no evidence of compound formation in a highly diluted mixture of iodine and bromine in carbon tetrachloride.

Reference to fig. 4 will show that the absorption spectrum of an equimolecular solution of bromine and iodine shows very considerable deviation from the simple mixture law. Whether the observed curve differs greatly from the true curve for IBr will depend naturally on the degree of dissociation



When solutions containing three equivalents of bromine for one of iodine are examined, it is found that the observed curve is made up almost quantitatively of a summation of the observed "IBr" curve and the observed curve for bromine. It therefore seems reasonable to conclude that iodine tribromide, if it exists at all, must be almost completely dissociated into iodine bromide and bromine at the dilutions used. The difference between the summation curve for iodine and bromine and the observed curve for the equimolecular mixture is moreover so great that the IBr molecule must be regarded as the main constituent of the solute.

There seems to be considerable doubt concerning the existence of bromine chloride. Balard,‡ in 1826, followed by Loewig§ in 1829 and Schonbein|| in 1863, recorded the formation of a highly refracting yellow liquid when chlorine was passed into bromine cooled in a freezing mixture. There is, however, no proof that such a liquid is bromine monochloride. Loewig also claimed to have isolated a bromine chloride pentahydrate. In 1877, Borneman¶ described bromine chloride as a red brown liquid stable only at temperatures below 10°, but came to the conclusion that Loewig's pentahydrate was really a mixture of

* 'Z. Anorg. Chem.,' vol. 47, p. 203 (1905).

† 'Z. Phys. Chem.,' vol. 76, p. 21 (1911).

‡ 'Ann. Chim. Phys.,' vol. 32, p. 337 (1826).

§ 'Dissertation,' Heidelberg (1829).

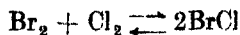
|| 'J. Prakt. Chem.,' vol. 88, p. 483 (1863).

¶ 'Liebig's Annalen,' vol. 180, p. 183 (1877).

the hydrates of bromine and chlorine. Berthelot* cast doubt on the early claims to have isolated bromine chloride because of the very small amount of heat which is developed when chlorine gas is led into liquid bromine. In more recent times Thomas and Dupois† have claimed that bromine chloride may be prepared by the action of bromine on liquid chlorine.

Lebeau,‡ in an important investigation, studied the freezing point curves for the system bromine-chlorine, only to find no evidence of compound formation in the liquid or solid states, although mixed crystals of varying composition were deposited. On the other hand, Andrews and Carlton§ discovered a marked contraction in volume when liquid chlorine and liquid bromine were mixed, a result not inconsistent with at least some compound formation. Karsten|| confirmed the work of Lebeau and concluded that the investigation of freezing points afforded no evidence for the existence of bromine chloride or bromine trichloride either in the solid or the liquid phase. Investigation of the boiling points for the system bromine-chlorine gave similar results.

The evidence for compound formation under these conditions would therefore appear to be extremely slender. When, however, the conditions are considerably different as in the work of Forbes and Fuoss¶ on the oxidation potentials of chlorine-bromine mixtures in dilute hydrochloric acid, evidence is forthcoming that the reaction



does in fact correspond with the experimental data.

There can be no doubt that the work of Simpson,** James, Walden, Delepine and Ville,†† and also of Hanson and James‡‡ in the field of organic chemistry is best interpreted on the assumption that bromine chloride can occur in solution. It was as a result of the recent work of Hanson and James (*loc. cit.*), that we decided to investigate this problem. These authors observed that an equimolecular mixture of chlorine and bromine, dissolved in carbon tetrachloride, reacted with cinnamic acid as bromine chloride were such a compound

* 'Ann. Chim. Phys.,' vol. 21, p. 375 (1880).

† 'C. R.,' vol. 143, p. 282 (1906).

‡ 'C. R.,' vol. 143, p. 580 (1906).

§ 'J. Amer. Chem. Soc.,' vol. 29, p. 688 (1907).

|| 'Z. Anorg. Chem.,' vol. 53, p. 365 (1907).

¶ 'J. Amer. Chem. Soc.,' vol. 49, p. 143 (1927).

** Simpson, 'Roy. Soc. Proc.,' A, vol. 27, pp. 118, 424 (1879).

†† James, 'J. Chem. Soc.,' vol. 43, p. 37 (1883); Walden, 'Berlin Acad. Ber.,' vol. 30, p. 2883 (1897); Delepine and Ville, 'C. R.,' vol. 170, p. 1390 (1920).

‡‡ 'J. Chem. Soc.,' p. 1955 (1928).

existent, the products of addition being the two stereoisomeric β -chloro- α -bromo- β -phenyl-propionic acids. The whole of the experimental work recorded in the present communication had been completed when the work of Barrett and Stein (*loc. cit.*) appeared, on the bromine-chlorine system and anticipated our conclusions with regard to the existence of bromine chloride. These authors were the first to provide definite physicochemical evidence for the existence of this compound, and the present work provides ample confirmation of their conclusions especially since the data on iodine chloride and iodine bromide furnish a useful check on the validity of the reasoning.

Examination of the curves recorded in fig. 5 shows that for equimolecular solutions of chlorine and bromine, the observed curve is widely different from the summation curve obtained on the assumption of no interaction. The head of the band is now at $380\ \mu\mu$ and the wave-length shift together with the absence of any marked inflexion near $330\ \mu\mu$ shows definitely that a new absorbing entity must be present. When the curve for solutions containing three equivalents of chlorine to one of bromine is examined, it will be seen that it corresponds quite closely with the summation of chlorine and the "BrCl" curves. It is clear that bromine trichloride cannot exist at the dilutions we have used, and that its absorption is roughly that of chlorine plus that of the equimolecular mixture of chlorine and bromine. When, however, the chlorine curve is subtracted from the curve obtained with the Cl : Br = 3 : 1 mixture, it is found that the new curve, whilst agreeing as regards the wave-length of maximum absorption with the 1 : 1 curve, differs from it in that the "BrCl" portion of the curve shows a definitely narrower band in the 1 : 3 mixture than in the 1 : 1 solution. This can only mean that bromine chloride is dissociated appreciably into chlorine and bromine at the dilution used. Free chlorine would throw back the dissociation so that the BrCl portion of the 3 : 1 solution is nearer to the true absorption spectrum of bromine chloride, than the curve for the equimolecular solution.

Summary.

1. The absorption spectra of chlorine, bromine and iodine in carbon tetrachloride have been studied.

2. It is shown that iodine chloride, iodine bromide and bromine chloride possess absorption bands, the maxima of which are accurately measurable. At the dilutions necessary for the investigation of absorption spectra all three compounds are dissociated to some extent, with iodine chloride the dissociation is barely detectable, with iodine bromide it remains small, whilst

with bromine chloride it is much greater, but still remains probably less than 50 per cent.

3. Solutions containing halogens in the proportions necessary for the formation of iodine trichloride, iodine tribromide and bromine trichloride, were found to contain the monohalide and free halogen only.

*On the Emission of Soft X-Rays by Different Elements, with
Reference to the Effect of Adsorbed Gas.*

By U. NAKAYA, Research Scholar of the Government of Japan, King's
College, London.

(Communicated by O. W. Richardson, F.R.S.—Received April 23, 1929.)

[PLATE 6.]

1. *Introduction.*

The ejection of photoelectrons from a metal surface exposed to soft X-rays has been commonly used as the method for measuring the intensity of these rays. However, the relation between the intensity of soft X-rays and the photoelectric current as a function of the nature of the surface of the photoelectric detector seems to have received comparatively little attention. In the present work, the effect of adsorbed gas molecules on the photoelectric plate has been given special consideration. The investigation is an extension of the work of Richardson and Robertson* who measured the relative soft X-ray emissivities of 14 elements. The special conditions of the experiment like the polishing of the surface, the state of degassing of the photoelectric plate and the conditions of oxidation of the target faces, have been investigated more thoroughly. Having ascertained the conditions necessary for reliable values, the emission of soft X-rays has been compared for 11 elements, Si, Cr, Mn, Fe, Co, Ni, Cu, Pd, W, Pt, and Au.

2. *Apparatus and Connections.*

The apparatus used consisted of a quartz containing vessel, the details of which are shown in fig. 1. The part of the tube where soft X-rays are excited

* Richardson and Robertson, 'Roy. Soc. Proc.,' A, vol. 115, p. 280 (1927), *ibid.*, vol. 124, p. 188 (1929).

is similar to the one used by Richardson and Robertson, and the part containing the photoelectric detectors resembles the one used by Bandopadhyaya.*

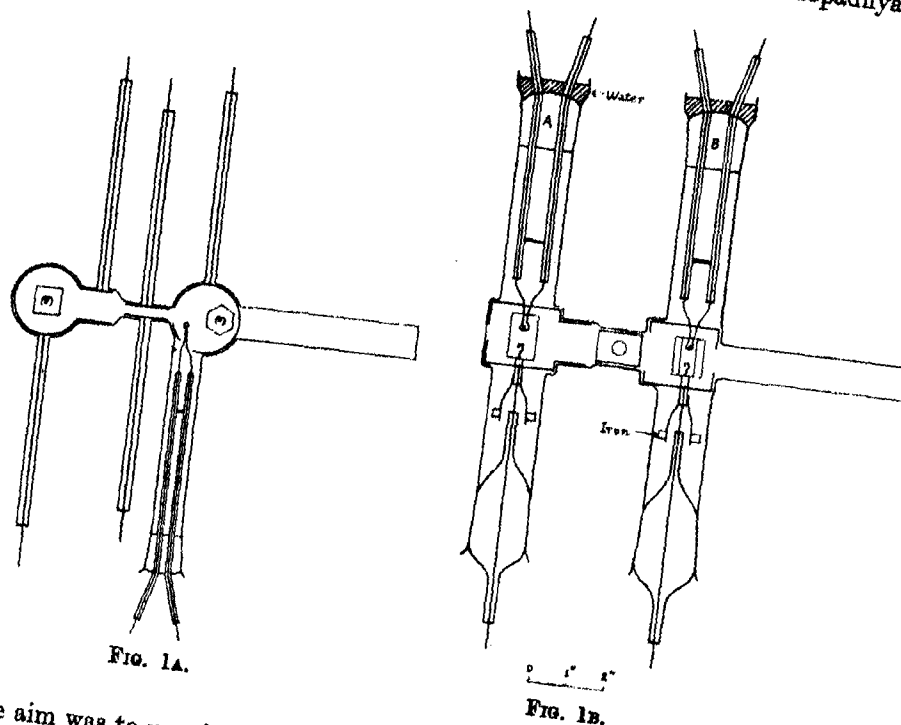


Fig. 1A.

Fig. 1B.

The aim was to use six elements for generating soft X-rays and four elements as photoelectric detectors at a time. The details of using the elements could be understood by reference to fig. 1, and to the papers of Richardson and Robertson and Bandopadhyaya. The targets and detectors could be separately degassed by electronic bombardment from inside the hexagonal and rectangular structures. The main changes in the apparatus from those used by the above-mentioned workers consisted in the following two points:—

- (1) The lantern-like structures rotated on brass rods supported from the bottom. The structures contained small hooks by which they could be removed out of the tube or put in through the openings at the top, A and B. In this manner the supporting rods were never moved out of position, thus ensuring geometrical constancy for different sets of experiments.

* G. B. Bandopadhyaya, 'Roy. Soc. Proc.,' A, vol. 120, p. 46 (1928).

- (2) The part of the tube surrounding the photoelectric detector was made fairly wide and in the inside was a shield covering the whole space around the detectors. In this manner the undesirable effect of the charging up of the quartz wall was avoided.

A Gaede three-stage mercury pump suitably backed was used to exhaust the tube. The usual precautions for degassing the quartz walls and the metal parts were taken. The shields were thoroughly degassed by bombarding with electrons to red heat before the targets and the detectors were introduced. The baking of the quartz wall was done by a hand blow-pipe flame. Two liquid air traps and a McLeod gauge were suitably connected and the reading was taken at the highest vacuum obtainable which was decidedly below 10^{-6} mm.

The electrical connection used is similar to that used by Richardson and Robertson (see fig. 2). Up to 1050 volts a storage battery was used. Above

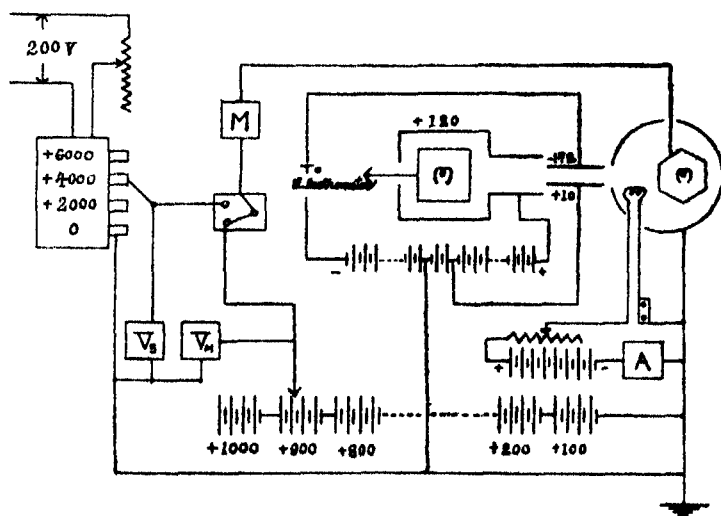


FIG. 2.

this and up to 4500 volts a motor-generator (output 15 milliamp. at 5000 volts) was employed. Below 750 volts a Weston D.C. voltmeter gave the applied potential, while values above this were read from two Hartmann-Braun electrostatic voltmeters of ranges 500 to 2000 and 1500 to 5000 volts. The photoelectric current i_p was measured by a Dolezalek electrometer (sensitivity 1190 divisions per volt and capacity 0.0000797 mfd.) by the method of scale and stop-watch. This direct method was considered suitable for these experi-

ments, in which, as will be shown presently, there are so many uncertainties of conditions. The thermionic current i_t was measured by a microammeter M in fig. 2.

3. Effect of Adsorbed Gas Molecules on the Photoelectric Detector.

In all the experiments, the ratio i_p/i_t was taken as a measure of the efficiency of soft X-ray excitation for different targets, keeping the photoelectric detector the same. It is known that a change of the photoelectric plate alters the value of i_p/i_t for the same intensity of the soft X-ray in accordance with the photoelectric efficiency of the detectors. Now considering the same photoelectric plate, it is found that the presence of adsorbed gas molecules affects considerably the value of i_p/i_t .

As a preliminary test, six targets of W, Fe, Co, Ni, Cu and C were examined with a photoelectric plate of nickel. In fig. 3 is shown the variation of i_p/i_t caused by the presence of gas molecules on the photoelectric plate. As a

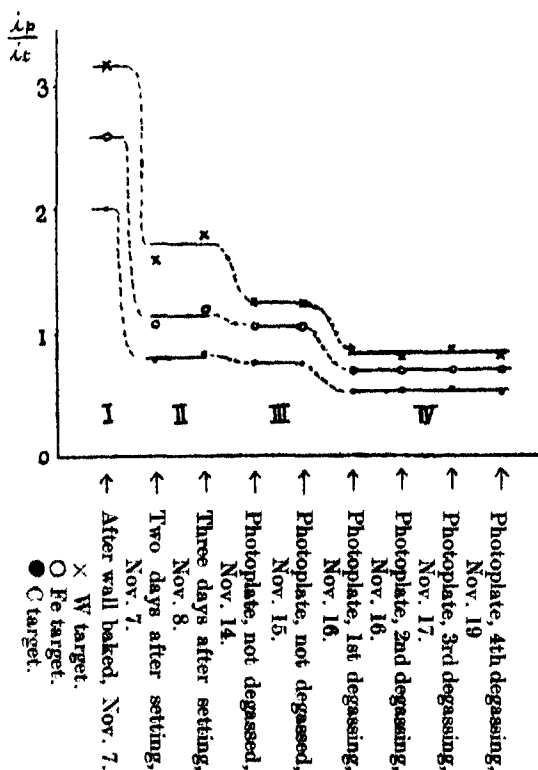


FIG. 3.

result we are led to classify roughly the state of the surface of the detector into four states. In all these states the target is degassed to the same extent by being kept red hot by bombarding for about 40 minutes in the morning at a pressure of about 10^{-5} mm.

State I.—The quartz wall surrounding the photoelectric plate is baked, keeping the plate cool, and readings were taken after the wall cooled down. This state is supposed to be one in which there is adsorbed on the photoelectric plate an amount of gas molecules much greater than that necessary for a state of equilibrium at that pressure, as the process of recovery is slow at ordinary temperature.

State II.—Here we have the state of the photoelectric plate two or three days after it is sealed into the tube and maintained in equilibrium with a pressure of 10^{-6} mm. We can suppose that the amount of adsorbed gas molecules is less than in State I, but slightly in excess of the amount necessary for equilibrium at ordinary temperature and pressure.

State III.—Readings were also taken about a week after the setting up of the tube during which time the photoelectric plate was kept in vacuum (pressure 10^{-5} to 10^{-6} mm.). Here we can assume the state of equilibrium between the adsorbed gas molecules and those in the surrounding space.

State IV.—The photoelectric plate is now heavily bombarded and raised to red heat, until the equilibrium pressure becomes about 0.5×10^{-5} mm., the target being raised to red heat at the same time. At this stage all the adsorbed gas molecules would have come out.

In fig. 3 are shown the results of experiments with W, Fe and C in all the four states. It will be seen that the values of i_p/i_t in State I are nearly four times the values in State IV, and that there is a regular decrease as we proceed from State I to State IV. It will be clear that with gradual removal of adsorbed gas molecules there is a fall in the value of i_p/i_t .

A closer examination of this phenomenon was conducted with a different set of targets, Cr, Mn, Fe, Co, Ni and Cu, keeping the same photoelectric detector of nickel. The results are given in Table I. It will be seen that the values for the same states taken on different days are fairly consistent. Also the ratio of i_p/i_t in State II to that in State IV is very nearly constant, being independent of the intensity of the same X-ray beam.

This leads us to the important point, that for measurements of the relative soft X-ray emissivities of different elements the photoelectric detector must be kept in the same state of degassing, and also that for the comparison of the photoelectric activity of different elements for any soft X-ray beam they should

Table I.—Nickel Photoelectric Plate, 550 volts.

State of detector.	Target.					
	Cr.*	Mn.	Fe.	Co.	Ni.	Cu.
II November 23	9.75	6.91	7.84	7.25	8.10	7.80
II November 23	8.99	6.69	7.76	7.06	7.80	7.69
II November 24	10.59	7.06	7.89	7.25	8.70	7.84
Mean of II	9.78	6.89	7.83	7.19	8.20	7.78
IV November 26	3.92	2.81	3.30	2.76	3.59	3.31
IV November 28	3.99	2.68	3.14	2.74	3.57	3.15
IV November 29	4.34	2.64	3.25	2.74	3.77	3.16
Mean of IV	4.08	2.71	3.23	2.75	3.64	3.21
Ratio of two means	2.39	2.54	2.42	2.61	2.25	2.42

* This specimen is broken into two and the larger piece is placed on top.

all be in the same state of degassing. Failure to observe this point would lead to unreliable results as could be seen by reference to Table I and fig. 3.

In the later experiments all measurements of soft X-ray emissivities were taken with the State IV of the detector. It was observed that even after thorough degassing there were variations of about 5 per cent. in the absolute values of i_p/i_t as measured from day to day, but the relative values remained nearly the same. It appears, however, as will be shown later, that during the process of bombarding the degassing is thoroughly done, but as the detector cools down, some gas molecules will be re-adsorbed by it, probably, in a stoichiometric relation with the surface atoms of the detector, because readings are taken 2 or 3 hours after the bombarding.

Some facts supporting this idea were observed. After State IV, the McLeod gauge was usually sticking. But on certain occasions when the readings were being taken, the pressure inside the tube rose suddenly to about 10^{-6} mm. and showed no evidence of sticking. In such cases the pump used was enough to reduce it to sticking pressure in several minutes, but the value of i_p/i_t could not be reduced to the proper value at once. Fig. 4 represents two such examples measured and shows the gradual recovery of the condition of the surface. The value of i_p/i_t was measured every 3 minutes after getting sticking pressure, and it is observed that it takes about 20 or 30 minutes to get to the value proper to that pressure. This shows that even after sticking pressure

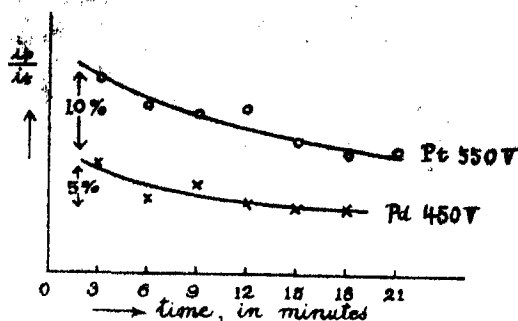


FIG. 4.

is obtained, it takes some time for the surface density of gas molecules to attain the proper equilibrium value.

4. Effect of Heavy Bombarding on the Target Face.

So far we considered the effect of heavy bombarding as the liberation of adsorbed gas molecules from the photoelectric metal surface. This will be undoubtedly the main effect but there appears to be another effect. In all cases when we opened the tube and examined the surfaces of the metal pieces, we noticed that the surface has lost the brilliancy of polish which it had before being sealed into the tube. Since bombarding was always carried on the back side of the targets, there is little possibility of contamination due to the sublimation of tungsten. So far, the surfaces had been polished with emery paper No. 0 and were not suitable for metallurgical examination. The targets were therefore polished in the proper manner, that is, in four stages with emery papers, then selvyt and alumina powder, and finally with magnesium oxide. The microphotograph of the surface of iron polished in this manner is shown in fig. 5 (Plate 6). Targets polished in this manner were then sealed into the tube and bombarded for 3 days, gradually increasing the bombarding current as the degassing process proceeded. The equilibrium pressure became about 0.5×10^{-5} mm., the temperature of the targets being maintained at about 900°C . After this treatment the surfaces were examined as before, and the microphotograph of the same face of iron is shown in fig. 6 (Plate 6). It was observed that the metal surface was etched by this process and no etching was necessary to bring out the crystal faces. The same was true in the case of Cr, Mn, Co, Ni and Cu, the amount of etching being different for the different metals. Probably this is partly due to the oxidation of the surface and partly due to the sublimation of metal. Thus the effect of bombarding is not only to liberate



FIG. 5.—Polished iron, before bombardment. ($\times 100$.)



FIG. 6.—The same specimen, after bombardment, not etched at all. ($\times 100$.)

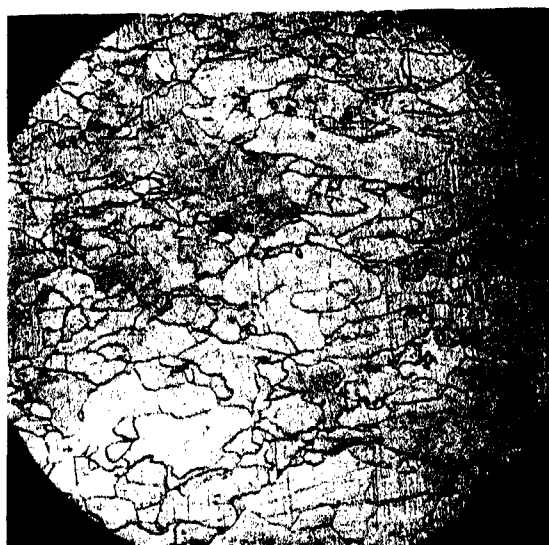


FIG. 7.—Pure electrolytic iron, etched in the ordinary way. ($\times 100$.)

adsorbed gas molecules but also to bring out the crystal faces. Experiment was not carried further in this line, but all targets were heated to this condition throughout this investigation.

The iron target used was found to be wrought iron and full of slags as could be seen from figs. 5 and 6. This target was replaced by one of pure electrolytic iron in later experiments (Plate 6, fig. 7). All the other targets were also examined metallurgically and found to be pure enough for the present work except Mn. This sample showed some slags and some characteristics of alloys due to impurities. Since a purer specimen could not be obtained this specimen was used. Amongst the photoelectric plates Co was found purer than Ni and was more fine-grained. In later experiments Co was used chiefly as the detector.

In order to get some idea regarding this alteration of surface, the value of i_p/i_i was measured for six elements, W, Au, Pd, C, Si and Pt in two modes of bombarding. The one is at low temperature and long bombarding, the other is at high temperature and short bombarding. In the former, targets were kept just below dull red heat for 24 hours spread about equally over 4 days, and in the latter at bright red heat for 5 hours spread over 2 days, the photoelectric plate being kept at red heat in both cases. The results are given in Table II.

Table II.—Cobalt Photoelectric Detector.

		C.	Si*.	Pd.	W.	Pt.	Au.	
Low temperature	volts. 450	1.44	2.55	2.05	2.12	1.81	1.73	Mean of 2 sets.
High temperature		1.51	2.66	2.17	2.38	1.99	1.91	One set.
Ratio		1.05	1.04	1.06	1.12	1.10	1.10	1.08 (mean).
Low temperature	550	1.91	3.22	2.67	2.90	2.46	2.35	Mean of 2 sets.
High temperature		2.12	3.75	2.80	3.25	2.70	2.62	Mean of 2 sets.
Ratio		1.11	1.16	1.05	1.12	1.10	1.11	1.11 (mean).
Low temperature	740	2.96	5.25	4.06	4.59	3.65	3.56	Mean of 2 sets.
High temperature		3.50	5.90	4.41	5.19	4.40	4.30	One set.
Ratio		1.18	1.13	1.08	1.13	1.20	1.21	1.15 (mean).

* This specimen is broken into two and smaller piece is placed on top.

As is seen from the table the values of i_p/i_i are always about 10 per cent. higher for the target which was heated to higher temperature. It is difficult to state whether this is due to the alteration of surface in the latter case or to

insufficient degassing of gas molecules adsorbed on the target in the former. But if we define this state of the surface (which was heated to such extent that the small crystals on the surface come out visibly) as well degassed state, the value of i_p/i_t is higher for that state. It is also noticed that the ratio of the values in two states, as a mean for six elements, is larger for higher voltage on target. Therefore, if we plot the value of i_p/i_t against voltage, the curve for well degassed state of target is not only higher than the other, but also steeper.

If the heavy bombarding of the target gives a higher value of the emissivity for soft X-rays, detector being supposed to be in the same condition, it is of primary importance to bombard all targets to the same condition for the comparison of their relative emissivities. This is the case for almost all targets, because they are bombarded at the same time to the same degree. But two specimens, Cr and Si, were too difficult to be cut into suitable form, and were broken into two pieces during preparation. Unexpected phenomena were observed with these specimens. When we put them into the supporting frame in such a manner that the larger piece (about three-quarters of the whole dimension for Si and two-thirds for Cr) came on top, that is nearer to the bombarding filament, the value of i_p/i_t was much larger compared with the case when we put the smaller piece on top. At 450 volts the value of Si for the former was 1.55 taking W unity (Table V), while for the latter the corresponding value was 1.12 (Table II). Similarly for Cr, the value with larger piece on top gave 1.48 taking Co unity (Table I), while the one with the small piece on top gave only 1.03 (Table V), both at 550 volts. These specimens were observed through a window during the process of heavy bombarding, and it was found that the upper piece, which was nearer the bombarding filament, became bright red hot, while the lower piece remained at dull red heat. Now it will be clear that when the larger portion of these targets was heavily bombarded the value of i_p/i_t became much larger. If this is the case, we must consider that the effect of the presence of gas molecules on target is opposite to that in the case of the photoelectric plate. Investigations in this line analogous to those shown in fig. 3 could not be done in the case of targets, because an excess of adsorbed gas molecules on the targets gave plenty of gas when the thermionic current was put on:

5. Notes on Experimental Details.

After heavy bombarding of the photoelectric plate, if we take the reading in 2 or 3 hours, we always notice that the motion of the electrometer spot on the scale is not uniform, showing that some additional charge is irregularly super-

posed. This irregular phenomenon was observed to vanish gradually, and after 3 or 4 hours the motion of the electrometer spot became steady. As we must bombard the target and photoelectric plates every day before taking readings, it is not possible to take the readings over a wide range in one day. As mentioned above, since it is difficult to reproduce exactly the same condition of adsorbed gas molecules on the surface of the photoelectric plate as well as of the target, it is desirable to take readings over a complete range in one day and compare them with another set taken on another day. In order to see the cause of this phenomenon we observed the motion of the electrometer spot just after the bombarding of the photoelectric plate, without any thermionic current. It was noticed that the velocity of the motion of the electrometer spot without any radiation was of the same order of magnitude as the velocity with incidence of soft X-radiation. Its direction was always first positive, and after some time, say 1 hour, became negative and gradually vanished, the spot oscillating at times. The current i_d due to this disturbance was measured in the same manner as i_p every 5 or 10 minutes after finishing bombarding and is shown in fig. 8, curve *a*. The irregular nature of the curve

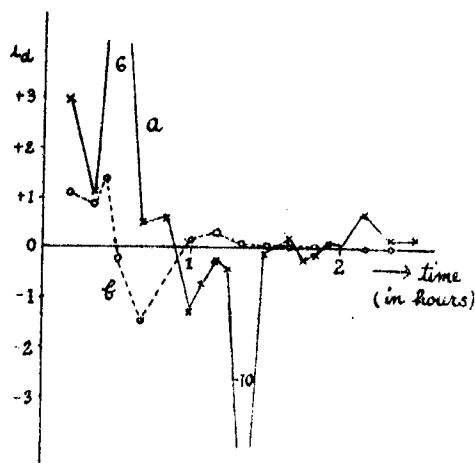


FIG. 8.

and specially the change of sign* will be due to the charge of the quartz wall and sealing wax at that point where the leading rod supporting the photoelectric plates touches them, because this rod was kept at high voltage while bombarding. Then the bombarding potential was reduced from 550 volts, which was used up to this stage, to 400 volts, increasing at the same time the bombarding

* Eguchi, 'Phil. Mag.', vol. 49, p. 178 (1925).

current. Just before stopping bombarding, the bombarding current was increased by about 20 per cent. which made the photoelectric plate bright red hot ; by this the rod was also warmed up but not to such an extent as to soften the sealing-wax. Then the supporting rod was connected to earth as soon as the high voltage was cut off. By this method we could get the steady spot in 1 hour after bombarding, as shown by curve *b* in fig. 8.

Next the effect of polishing the surface was examined. Three specimens of Co and Fe, respectively, were cut from the same materials. Of these I was metallurgically polished as described above, II was polished with emery paper No. 000, and III was polished with rough emery paper No. 1. The results are given in Table III. They show a regular, though slight, difference for different targets. This difference cannot be due to any error in the measurements, nor can it be due to the difference in the degree of polishing, for the order of variation is not the same for Co and Fe. The cause of the variation may be the difference in the geometrical disposition of the targets with respect to the filament and the condenser.

For taking the data (ii) and (iii), the targets and the photoelectric plates were well bombarded during the night, and the pressure inside kept at 10^{-6} mm. by keeping the charcoal trap in liquid air overnight. The readings were taken on the next morning without bombarding again. The results are not much different, and this method was employed whenever continuous reading over 10 hours was required.

6. *Effect of Bombarding in a Hydrogen Atmosphere.*

As all the experiments hitherto made showed that the presence of gas molecules on the photoelectric plate and target plays an important part in the excitation and absorption of soft X-radiation, we must consider the process of degassing still further. Now heating of a metallic surface means expulsion of adsorbed gas molecules and at the same time absorption of them by chemical combination. Although the pressure at which they are bombarded is of the order of 10^{-6} mm., the rise of temperature accelerates the velocity of chemical combination. Further the surface density of the gas will be much greater than the space density measured. It is difficult to differentiate between the adsorbed and chemically combined molecules, but if we define the adsorbed molecules as those which obey the expression,

$$q = ap_n^{\frac{1}{2}},$$

bombarding to red heat at the pressure of 10^{-5} mm. will be enough to expel all adsorbed gas molecules. On the contrary sometimes the amount of gas

molecules on the metal surface is increased with temperature, as observed by Langmuir* in case of platinum.

In order to see this effect all the targets and photoelectric plates were heated in a hydrogen atmosphere to reduce the surface film of oxide, after the surfaces were well bombarded. Hydrogen was put in, by heating a palladium tube with a hydrogen flame. As we could not introduce the palladium tube on the high vacuum side, it was put in the low vacuum side with the arrangement of taps as shown in fig. 9. First, all the taps, except No. 3, were opened,

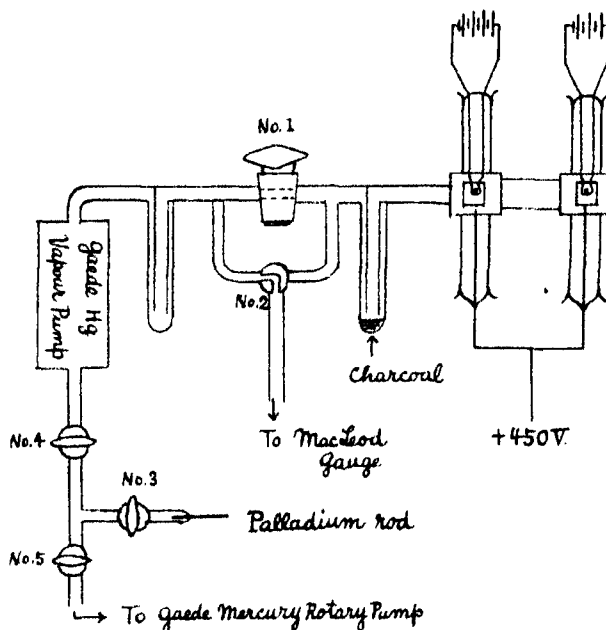


FIG. 9.

and the system was evacuated to about 10^{-4} mm. by the Gaede mercury rotary pump, the mercury vapour pump not having been operated and liquid air taken off from the charcoal trap. Then hydrogen of 10^{-1} mm. was introduced and the tube was again evacuated. This washing process was usually repeated twice. After that about 40×10^{-3} mm. of hydrogen was put in and all taps except Nos. 1 and 2 were stopped. Then bombarding was begun at 450 volts under red heat. After 10 minutes the bombarding was stopped and when the tube was cooled down the pressure was found to be reduced to $30\text{--}35 \times 10^{-3}$ mm., showing that hydrogen was consumed during this treatment. This process

* 'J. Amer. Chem. Soc.,' vol. 40, p. 1361 (1918).

was repeated usually three times. Then the pressure was reduced to the order of 10^{-6} , and $15-20 \times 10^{-3}$ mm. of hydrogen was put in and red hot bombardment was begun. This was the highest pressure at which we can bombard the target to red heat without glow discharge through hydrogen. This process was repeated three or four times, each bombarding being continued for 15 to 20 minutes. After that the mercury vapour pump was started to evacuate the residual hydrogen, and the procedure for getting high vacuum was repeated as in the case of air.

The first hydrogen treatment was carried out on the same setting which was intended to see the effect of polishing. The results are tabulated in Table III.

Table III.—Cobalt Photoelectric Plate, 450 volts.

	Co I.	Co II.	Co III.	Fe I.	Fe II.	Fe III.
(i) After initial bombardment, January 17	2.25	2.22	2.18	2.40	2.45	2.44
(ii) „ second „ „ 18	2.19	2.13	2.17	2.35	2.48	2.38
(iii) „ third „ „ 19	2.18	2.14	2.16	2.33	2.47	2.36

Hydrogen treatment was carried out.

(iv) After initial bombardment, January 23	2.48	2.39	2.38	2.63	2.78	2.59
(v) „ „ „ „ 23	2.46	2.39	2.40	2.63	2.72	2.61
(vi) „ second „ „ 24	2.50	2.41	2.42	2.66	2.73	2.59
(vii) „ third „ „ 25	2.66	2.55	2.60	2.81	2.88	2.74
Ratio of (iii) and (iv)	1.138	1.118	1.101	1.129	1.125	1.097
Ratio of (vi) and (vii)	1.065	1.058	1.078	1.056	1.055	1.056

As is seen from the table, the value of i_p/i_t becomes about 10 per cent. higher after bombarding in the hydrogen atmosphere for all the targets. The important point for our present purpose is that the values become very consistent after this treatment. For example, the values of two sets (vi) and (vii) appear a little deviated, but if one takes the ratio between the two values they become identical within an error of 2 per cent.

The variation of i_p/i_t as a function of i_t , which is of primary importance, was examined in this state at three stages of voltages, and found to be constant within the range of the experiment. The values were measured in a relatively wide range at 450 volts and are tabulated in Table IV. As our method of measurement is not accurate to more than 1 per cent., this result leads us to conclude that i_p/i_t is independent of the thermionic current at least within the range of 15 to 60 microamperes.

Table IV.—Co II Target, Co Photoelectric Plate, 450 volts.

i_t (microamperes).	i_p/i_t .	i_t (microamperes).	i_p/i_t .
57.9	2.515	37.2	2.498
54.1	2.500	35.3	2.508
49.0	2.520	32.5	2.512
44.1	2.500	28.6	2.508
42.5	2.510	24.2	2.490
41.3	2.515	21.6	2.510
39.5	2.518	18.15	2.530
39.0	2.515	15.51	2.525

This hydrogen treatment was carried out on two other settings for 11 elements. One set is composed of Si, W, Co, Au, Pd, Pt and another set is Cr, Mn, Fe, Co, Ni, Cu, the same Co specimen was used for both settings. Fig. 10 shows the variation of i_p/i_t with successive bombarding. In both cases the value of

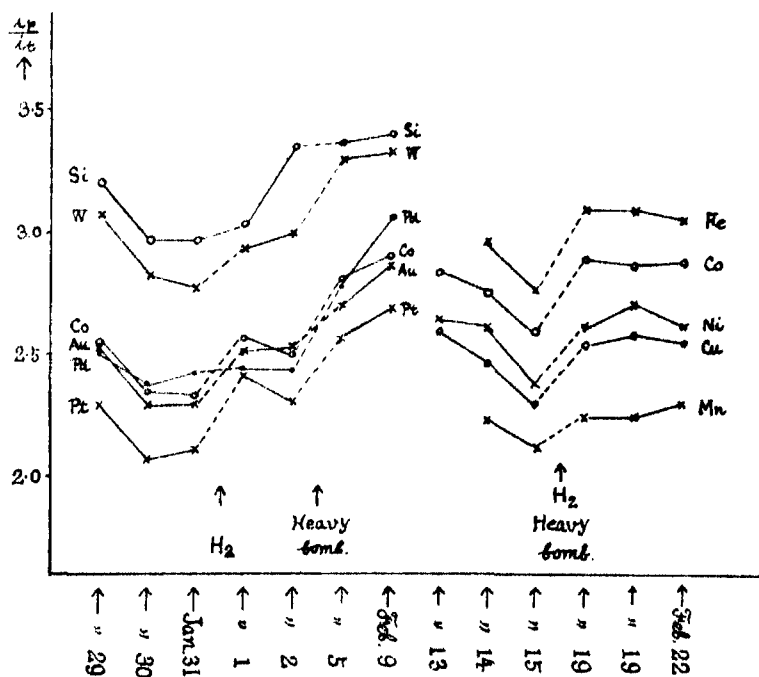


Fig. 10.—Cobalt Photoelectric Detector, 450 volts.

i_p/i_t gradually decreases as degassing goes on before hydrogen treatment, which corresponds to the small variations in region IV of fig. 3. After this, bombarding in hydrogen gives about a 10 per cent. increase in values as in the

case of the first setting given in Table III. This increase may be partly due to the adsorbed hydrogen molecules on the photoelectric plate, but mainly it will be due to the taking off of the oxide film on the target, because in the first set the values of W, Au, Co and Pt increase more or less in parallel, but the values of Si and Pd remain almost unchanged. This may be due to the special affinity of these elements for hydrogen to form the compounds SiH_4 and PdH_2 , owing to which hydride films will replace the oxide ones. Si showed an increase in value after the second bombarding, but Pd did not show the expected increase until we bombarded it to cherry red heat for 3 hours. It is also noticed that the value of Co is in good agreement for two settings after being bombarded in hydrogen followed by heavy bombarding in hydrogen vacuum.

7. Measurements of Relative Soft X-ray Emissivities of Eleven Elements in Final Conditions.

The experiments hitherto made are of a more or less preliminary nature for obtaining a condition in which consistent data can be obtained. Now the measurement of efficiencies of exciting soft X-radiations were carried out under the final conditions, for 11 elements in two settings. The conditions are as follows: The surface of the target was polished with emery paper No. 000 and put into the tube without being touched by the fingers.* All the metallic parts were degassed by bombarding to red heat for 2 or 3 days, and after that the bombarding in hydrogen was carried out in the manner described in the preceding chapter, and then the bombarding of the target and photoelectric plate was continued in the hydrogen vacuum until the equilibrium pressure at cherry red heat came down to about 0.5×10^{-5} mm. A Co plate, polished metallurgically, was used as a photoelectric detector. As it is desirable to keep the thermionic current more or less constant all over the ranges, we cut down the sensitivity of the electrometer for higher voltages, by putting a condenser in parallel with the electrometer. For this purpose a condenser of capacity 0.0002513 mfd., specially insulated with quartz rods, was used, which was kindly lent by Mr. Robertson to whom the writer expresses his deep sense of gratitude.

The results obtained with the storage battery up to 1050 volts are described in this section; they are summarised in Table V and also in fig. 11. The specimens were arranged and tested in two groups having Co in common.

* In the preliminary course of experiments we sometimes noticed slight mark of finger prints on the edge of the target after opening the tube.

Table V—Cobalt Photoelectric Plate.

Voltage.	Date.	Si.*	Co.	Pd.	W.	Pt.	Au.	Cr*.	Mn.	Fe.	Co.	Ni.	Cu.	Date.
150		(0.96)	—	—	(0.860)	—	(0.586)	0.765	0.488	0.715	0.663	0.561	0.542	Feb. 20
250	Feb. 9	(2.00)	(1.385)	—	(1.475)	—	(1.129)	1.460 1.432	1.028 1.028	1.411 1.351	1.261 1.249	1.139 1.128	1.121 1.101	Feb. 20 ,, 22
350	Feb. 9	3.31 (3.37)	1.99 (2.03)	2.03 (2.06)	2.33 (2.30)	1.82 (1.79)	1.85 (1.82)	2.19 2.24	1.635 1.625	2.215 2.22	2.02 2.01	1.86 1.81	1.81 1.78	Feb. 20 ,, 22
450	Feb. 9	5.11 (5.17)	2.91 (2.86)	3.09 (2.82)	3.34 (3.32)	2.68 (2.52)	2.87 (2.86)	2.91 2.92	2.28 2.27	3.01 3.04	2.78 2.75	2.55 2.55	2.51 2.53	Feb. 20 ,, 22
550	Feb. 9	7.15 (7.14)	3.69 (3.77)	4.11 (3.87)	4.23 (4.34)	3.50 (3.64)	3.76 (3.95)	3.79 3.79	2.84 2.79	4.03 3.96	3.74 3.66	3.36 3.31	3.39 3.34	Feb. 20 ,, 22
650	Feb. 9	9.29 (9.30)	4.59 —	5.26 —	5.48 (5.58)	4.58 —	5.05 (5.06)	4.84 4.79	3.54 3.51	5.04 5.06	4.70 4.65	4.27 4.26	4.30 4.39	Feb. 20 ,, 22
750	Feb. 9	11.72 —	5.85 —	6.37 —	6.95 —	5.92 —	6.32 (6.50)	5.70 5.90	4.23 4.30	6.16 6.17	5.69 5.61	5.10 5.08	5.25 5.38	Feb. 20 ,, 22
1040	Feb. 9	—	9.25	10.70	12.00	9.81	12.20	10.30	6.39	10.35	8.75	8.02	9.05	Feb. 22

* Si well bombarded, Cr not well bombarded; both are not so reliable for the reason described in section 4.

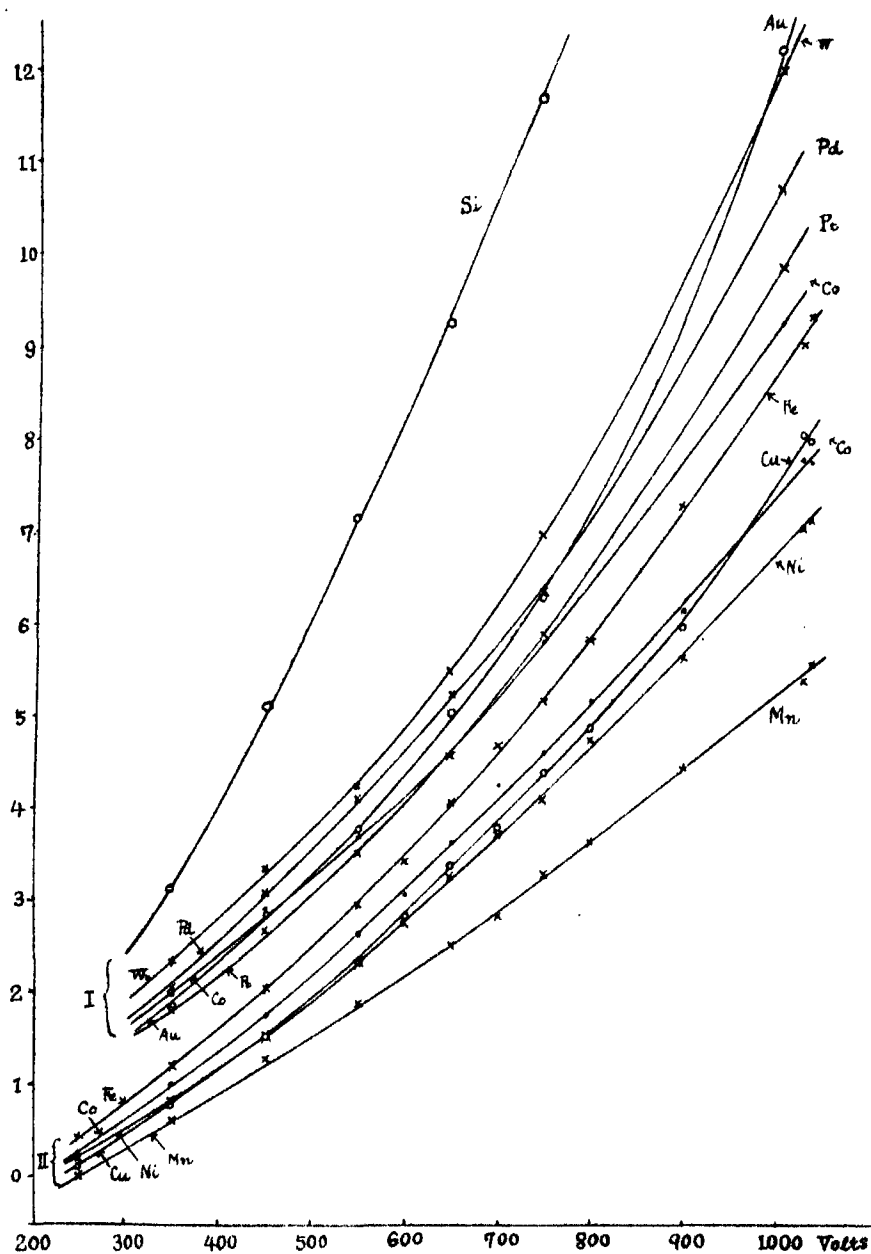


FIG. 11.—Ordinates of Group II are reduced by 1.0.

From these data we can see that the values are, at least for a given specimen, reliable within a range of 2 per cent. of error in the final condition described

above. For different settings Co shows a maximum difference of value of about 5 per cent.

Plotting these values against voltage, fig. 11, it is noticed that i_p/i_t does not vary proportionally with voltage, as hitherto assumed by many authors as a first approximation, but always shows slight but regular curvature.* These data were taken as follows:—At a given voltage readings were taken for each of six targets in succession and then the voltage was changed to get another set of readings. In order to make sure of this point, we kept the target fixed and measured the value of i_p/i_t for four elements, Si, Co, W and Au, at every 50 volts from 150 volts to 650 or 750 volts. The values are plotted in fig. 12 with

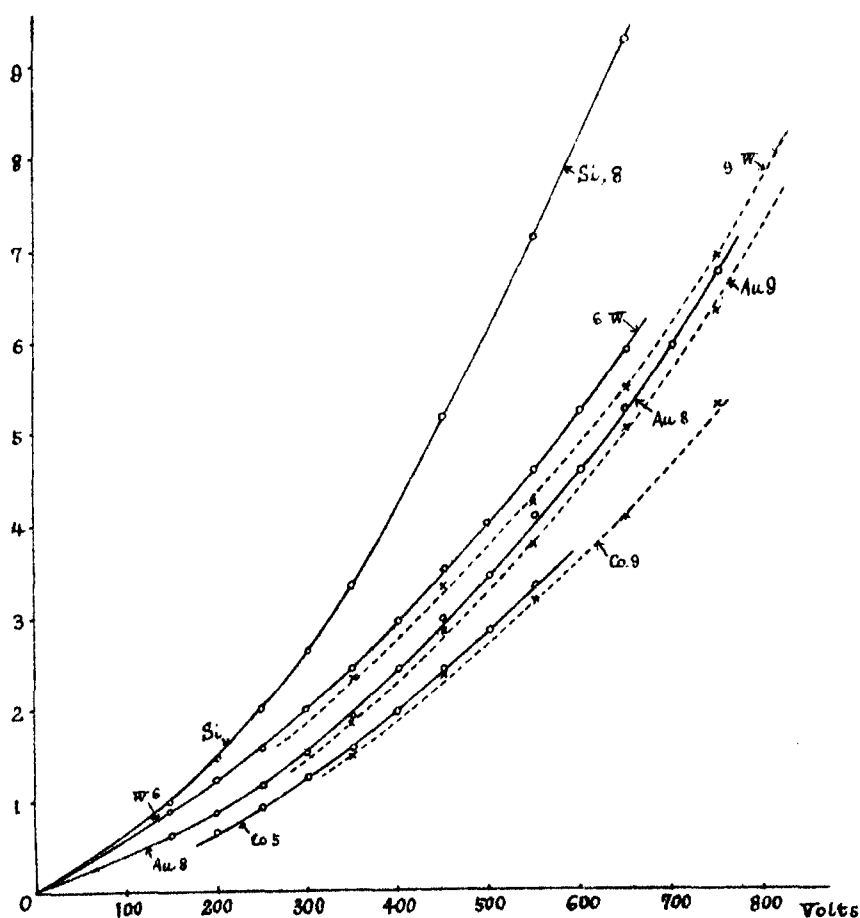


FIG. 12.—Ordinates of Cobalt reduced by 0.5.

* The breaks due to critical potentials can be ignored in this curve, because of the difference in scale.

small circles. The curves drawn in dotted lines are the same as the corresponding ones in fig. 11. In all cases these corresponding curves show good agreement in the character of the curvature. The differences in absolute values are also quite consistent, and if we allow for the appropriate corrections, which are different for different days within the range of 6 per cent., these two curves become identical. In Table V the values in brackets are the ones corrected in this manner.

Further, we can see in both the figures that the curvature is not the same for all elements. As is seen in fig. 11 the curvature of Au is largest, W and Pt and Cu next, and Mn is almost a straight line. The reversal of order in relative magnitude of two elements at different voltages is not a matter of chance, as we can see the gradual approaching of the two curves, resulting in crossing. Thus, for example, the curve of Au crosses the curves of W, Pd and Co in this range, and that of Cu crosses those of Co and Ni.

As the range of the Weston voltmeter was limited to 750 volts, above that up to 1050 volts an electrostatic voltmeter was employed. This range was measured for the second group only and the results are tabulated below. These values are also plotted in fig. 11 and agree well with the range measured with the Weston voltmeter.

Table VI*.—Cobalt Photoelectric Plate, Electrostatic Voltmeter and Storage Battery.

Voltage.	Cr.	Mn.	Fe.	Co.	Ni.	Cu.	Date.
600	4.00	3.01	4.40	4.05	3.76	3.83	February 23
			4.58	4.08	3.73	3.89	" 25
700	5.07	3.83	5.70	5.25	4.73	4.78	" 23
			5.56	5.05	4.68	4.84	" 25
800	6.20	4.64	6.83	6.16	5.76	5.86	" 23
			6.86	6.14	5.69	6.05	" 25
900	7.46	5.44	8.29	7.15	6.64	6.97	" 23
			8.19	7.24	6.72	7.14	" 25
1030		6.60	10.04	8.77	8.15	8.96	" 23
			10.03	8.68	7.96	8.85	" 25

* All data of February 25 were taken, keeping one target fixed, and all values of four elements are multiplied by 1.056.

8. Measurements in Higher Voltage Region.

As the relative emissivities of soft X-radiations was found to be different for different voltages, we felt it important to see the state of affairs at higher

voltages. The measurements were carried out for six elements of the Cr group from 1500 volts to 2000 volts. A gap between 1000 volts and 1500 volts could not be filled with our motor-generator. The motor-generator used could give a fairly steady voltage, but fluctuation within 20 volts had to be allowed. All the conditions were the same as described in the preceding chapter.

The constancy of i_p/i_t as a function of i_t was examined with respect to the Mn target and it was found to be fairly constant. The mean of two data gave 13.4 at 1500 volts with i_t nearly 45 microamperes, while the corresponding value was 13.7 with i_t nearly 15 microamperes. All the data in this chapter were taken in the range of 15 to 8 microamperes of thermionic current, whereas the data up to 1050 volts which were described in the preceding chapter were taken in the range of 35 to 45 microamperes of thermionic current.

The results are tabulated in Table VII.

Table VII.—Cobalt Photoelectric Plate, Electrostatic Voltmeter and Motor-generator.

Voltage.	Date.	Cr.	Mn.	Fe.	Co.	Ni.	Cu.	Voltage.	Cu.
1500	February 26	36.7	13.52	33.3	28.9	22.7	40.2	1500	39.2
	" 28	34.8	13.78	32.7	30.4	22.2	39.2		
	March 5	36.1	17.05	34.2	26.7	21.4	40.7		
1750	February 26	75.8	21.1	63.7	56.1	36.3	96.9	1600	65.9
	" 28	63.5	21.6	66.5	57.4	30.5	—	1700	87.7
2000	" 26	94.6	26.9	96.9	82.1	46.3	—	1800	116.0
	" 28	92.5	27.3	95.8	78.7	38.0	—		

As is seen from this table the consistency of the values taken on different days in this range is not so satisfactory as in the case of the voltages under 1000 volts, the maximum difference being about 20 per cent. But it should be noted that this range is the one in which the value of i_p/i_t increases rapidly with slight variation of voltage.

In this range the emissivity of Cu became the highest among the six elements. The value above 1800 volts was too large to be measured with our apparatus. The range above 2000 volts could be studied with only two targets, viz., Ni and Mn, because the value of i_p/i_t for other targets became too large. As for the Co target, it was just beyond our range if we use the Co photoelectric detector but could be measured by using a carbon detector.

It was observed in this region that when we increase the voltage beyond 2000 volts the value of i_p/i_t increases up to about 2500 volts with nearly the same rate as in the region of 1500 to 2000 volts (Table VII). But this rate of increase in the value of i_p/i_t gradually decreases when we proceed above 2500 volts and in the region between 3500 to 4500 volts the increase of the value becomes very small. Then if we plot the value of i_p/i_t against voltage, the curve takes the form of a saturation curve.

Experiments were carried on to verify this point, but the discrepancy of the data became more enhanced in this region than that in the region of 1500 to 2000 volts. Then we tried to take readings in two ways by increasing and decreasing the voltage, and it was found that the curves always showed some hysteresis effect. Two examples are shown in fig. 13, in which curves drawn

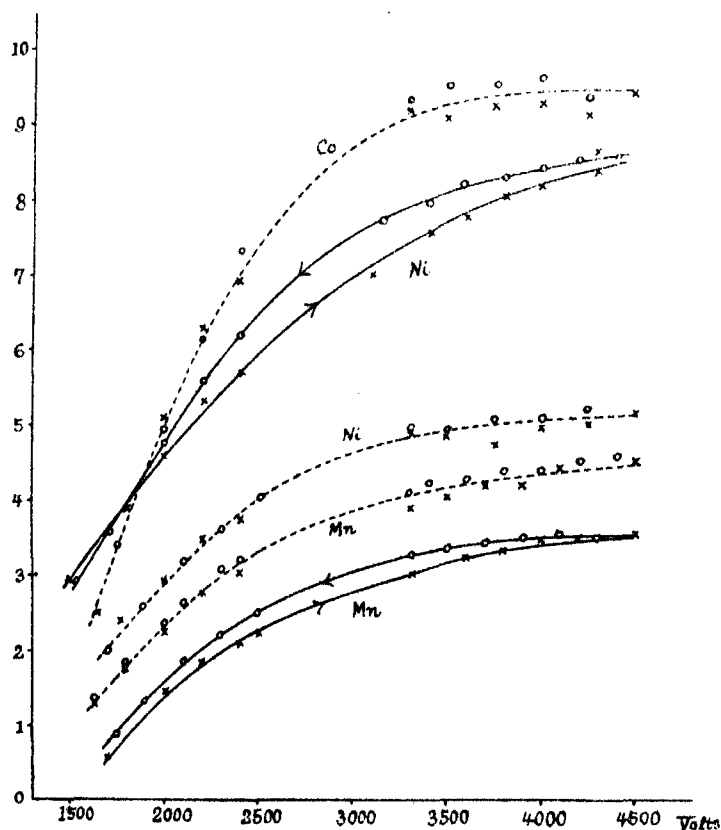


FIG. 13.—Full line : Co photoelectric detector, ordinate of Ni is increased 1.0, that of Mn is reduced 1.0. Broken line : C photoelectric detector. \times always shows ascending voltage, \circ always shows descending voltage.

in full lines are those obtained with Co photoelectric detector, and the values marked with crosses represent increasing voltage, the small circles showing decreasing voltage. This hysteresis effect is also observed when we use a carbon detector, but to a less extent. In the figure, curves drawn in dotted lines show the mean curves obtained with the carbon photoelectric detector.

As one of the causes of this phenomenon we can consider some fatigue or reverse effect which may occur on the target or photoelectric plate. In order to test this point, we kept the voltage and thermionic current constant and measured the value of i_p/i_t at every 3 or 5 minutes. It was found that the value does not remain constant but varies regularly with time. In fig. 14 are

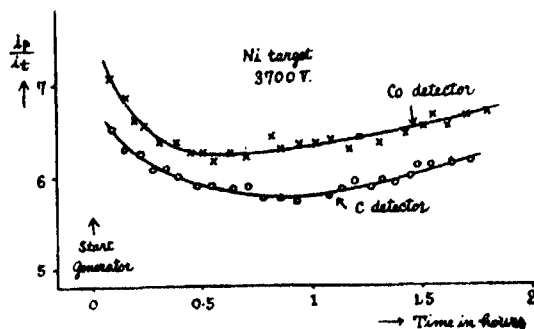


FIG. 14.

shown two such examples each taken over 2 hours continuously. The radiation from the Ni target at 3700 volts was received on Co and C photoelectric plates, and in both cases it was observed that the value of i_p/i_t first gradually decreases and becomes steady for some time, say, 20 minutes, and then gradually increases. The amount of variation is of the order of 15 per cent. and just enough to explain the amount of hysteresis observed above. This phenomenon cannot be explained with the insufficient experimental data available at present. But it appears very probable that in the high voltage region the variation of the value of i_p/i_t is more sensitive to the presence of gas molecules on the target or photoelectric plate or both than in the low voltage region. A slight variation in the equilibrium state of adsorbed gas molecules, which is caused by applying a thermionic current to the target for a long time, can give rise to this amount of variation in the value of i_p/i_t . If this is the case, the first part of the curve will be explained by the analogy of the photoelectric fatigue of the detecting plate, which has been studied by many workers in the ultra-violet region. The final gradual increase may be explained by the liberation of adsorbed gas molecules from the target, which is considered to increase the value of i_p/i_t .

because in this region of voltage the target must have been warmed up appreciably by the thermionic current. Though these two reverse effects are superposed, the fatigue effect of the photoelectric plate becomes steady as can be expected with the analogy of ultra-violet radiation, while the liberation of gas molecules from the target will increase proportionately with time.

From these considerations, by taking the mean value for increasing and decreasing voltage, the discrepancy of data could be lessened by about 10 per cent. These mean values are summarised in Table VIII. As is seen from the table, even if we take the mean value for increasing and decreasing voltage, the values taken on different days show a considerable variation. But if we take the ratio of the two values taken on different days we find the ratio constant. The data taken on March 4 are higher than those taken on March 1 by about 15 per cent. for Ni and 23 per cent. for Mn all over the range, and the latter coincides fairly well with those given in Table VII at 2000 volts. The difference of 8 per cent. in the ratio of variation for Ni and Mn, may be due to the difference in the conditions for two metals, which were studied at different times, though on the same day. This shows that the variation of i_p/i_i is very sensitive in this high voltage region. At any rate, by this method of arranging the data, we can determine the shape of curve with fairly good accuracy, in spite of the large amount of discrepancy between individual absolute readings.

Table VIII.—Cobalt Photoelectric Detector.

Voltage.	Ni.			Mn.		
	March 1.	March 4.	Ratio.	March 1.	March 4.	Ratio.
1500	—	22.5	—	—	21.7	—
2000	39.3	43.6	1.11	29.8	36.6	1.23
2500	54.3	62.7	1.15	39.9	49.0	1.23
3500	71.3	81.6	1.14	50.2	61.4	1.22
4000	74.2	86.3	1.16	53.1	65.3	1.23
4500	75.1	88.5	1.18	54.4	67.3	1.24

Next the range from 1000 to 1500 volts was examined with increasing and decreasing voltage, because this is important to connect the ranges of the storage battery and the motor-generator. The results are given in Table IX, which shows that the apparent hysteresis effect is negligible in this range with a well degassed target and photoelectric plate.

Table IX.—Cobalt Photoelectric Detector, March 5.

	Cr.	Mn.	Fe.	Co.	Ni.	Cu.
1st 1020-volt storage battery	9.68	6.95	10.34	9.25	8.91	9.25
2nd 1500-volt motor generator	36.1	17.05	34.2	26.7	21.4	40.7
3rd 1020-volt storage battery	9.85	6.90	10.68	9.08	9.05	9.36

Referring to Tables V, VI, VII, VIII and IX, the curves of i_p/i_s were plotted against voltage all over the range from 0 to 4500 volts in fig. 15. The values up to 1500 volts are plotted according to Table V and IX, and those in the

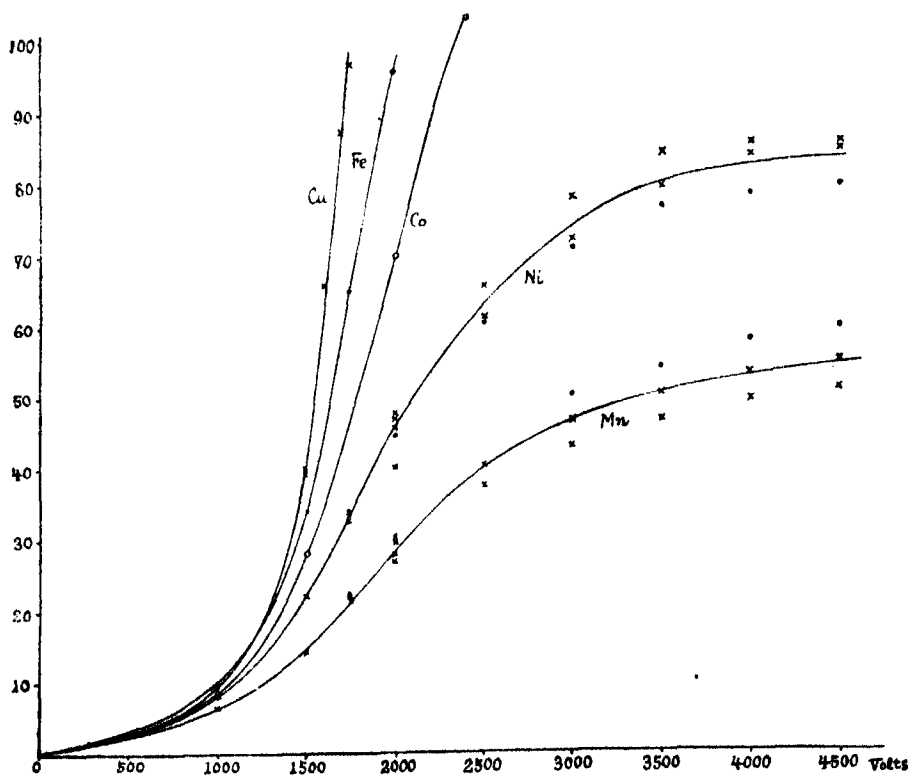


FIG. 15.

region 1500 to 2000 volts from Table VII. Above 2000 to 4500 volts they are only plotted for Ni and Mn. For this range the data in Table VIII are employed but these values were divided by a certain constant, proper to each set, so that the values at 1500 volts coincide, for each element, with the mean value at that point which was determined from the data in Table VII. This correction

was of the order of 25 per cent. Black dots represent the values received with the carbon detector, a similar correction being also made. The degree of accuracy of the curve in this region will be seen from the range over which the various sets of values lie.

As is seen from this figure, the value for Cu becomes highest above 1500 volts and its rate of increase becomes very large, being almost vertical. Now it will be clear that the larger curvature for Cu (fig. 11) as compared with the other elements of this group, is not a matter of chance but a preparatory stage for getting this steep portion of the curve.

9. *Summary of Results.*

All the experiments carried out in this investigation showed that the presence of adsorbed gas molecules on the photoelectric plate and target play an important rôle in the absorption and excitation of soft X-radiation. This is probable when we consider that all the phenomena concerned are to be taken as surface phenomena. As for the absorption of these rays, the effect of adsorbed gas molecules increases the efficiency of liberation of photoelectrons, which is clear from the experiments described in section 3. The amount of increase is larger the more adsorbed gas molecules there are on the surface. The relative change in the values of i_p/i_t for different states of the adsorbed gas molecules on the photoelectric plate, is the same for the radiations produced by the different targets. This suggests that the proportionality will also hold for the degassed state of a metal between the true intensity of soft X-rays, which cannot be known from this experiment, and the photoelectric current produced by them.

Next as for the excitation of soft X-rays, the effect of the presence of gas molecules on the target could not be studied with the same certainty as in the case of the photoelectric plate. But it appears very probable that the effect is reversed in this case and the excitation of soft X-rays for a given amount of thermionic current decreased with the presence of gas molecules on the target. The increase in the value of i_p/i_t with a heavy bombarding of the target compared with the case of a long bombarding at low temperature, the peculiar phenomenon observed with the broken targets, the increase in the value with the reduction of oxide films on the targets with hydrogen, the variation of the value of i_p/i_t with time observed at high voltages; all support this idea that the excitation of soft X-radiation is increased with the liberation of gas molecules from the target.

In the final condition in which all targets and photoelectric plates are well

degassed and the oxide films on these surfaces are reduced with hydrogen, the value of i_p/i_t became very consistent and could be measured within an error of 2 or 3 per cent. to 1000 volts. These results showed that the curve of i_p/i_t as a function of voltage is not a straight line, but rises upwards, showing a regular deviation from the assumption that Kramer's theory applies to this region. This may be partly explained by assuming that the specific photoelectric activity of the photoelectric detector is greater for larger values of ν . This receives support from a similar phenomenon known in the region of ultra-violet radiation. This curvature, however, is not the same for different targets, and shows that it must be chiefly due to some other phenomenon taking place on the target. Accordingly the relative emissivities for different elements are not the same for different voltages. The rate of variation of the different curves differs to such an extent that some of them cross one another in the region of 0 to 1000 volts.

In the high voltage region, six elements of the Cr group were studied up to 2000 volts. Among them Co, Ni and Mn were examined up to 4500 volts, and it was found that the value of i_p/i_t increases at first and then gradually approaches a constant value, giving an appearance similar to a saturation curve. This was the case also when we received the radiation on the carbon photoelectric detector. The general nature of the curves in the high voltage region is in good agreement with that of curves under 1000 volts, this point being most clearly seen in the case of the Cu target. The question why this curve takes the form similar to a saturation curve is an interesting problem, but it cannot be explained by any theory hitherto proposed. Accordingly in this paper no attempt has been made to explain the relative emissivities for different elements in connection with the atomic theory.

In conclusion, I want to thank Prof. O. W. Richardson for suggesting this investigation and for his kind interest in the work which was carried out in the Wheatstone Laboratory, and also Prof. H. C. H. Carpenter for having kindly placed at my disposal his metallurgical apparatus.

*On the Criteria for the Stability of Small Motions.**

By R. A. FRAZER, B.A., B.Sc., and W. J. DUNCAN, B.Sc., A.M.I.Mech.E.

(Communicated by H. Lamb, F.R.S.—Received April 25, 1929.)

1. *Introduction.*

When a dynamical system receives a small disturbance from a state of rest or steady motion, the ensuing small motion is governed by a system of linear differential equations. In order to determine the stability, the conventional procedure is to examine the signs of certain "test functions," which can be constructed in succession from the coefficients of the determinantal equation by Routh's well-known rules (see Routh's "Rigid Dynamics," vol. 2, 6th ed., p. 228). However, the series of test functions for a determinantal equation of general degree are not stated by Routh in an explicit form; and the expressions would, in fact, be exceedingly cumbersome. An alternative is to use for the stability criteria the signs of certain "test determinants." This method, which is very convenient in practice, is not described in works on dynamics known to the writers, and may be novel. The present paper contains a brief account of these determinants and of certain other simple forms of test function.

The stability of a system is usually dependent upon so many factors that the exact influence of individual factors may be extremely difficult to trace in a purely algebraic discussion of the test functions; but such obscurities can often be avoided by a graphical representation of the criteria. A suitable graphical treatment for problems of a certain wide class will be described. For a detailed illustration of the application of the method to the stability of aeroplane wings, the reader is referred to R. and M. 1155.*

2. *Test Determinants for Equations of General Degree.†*

The dynamical system under consideration will be assumed to possess m

* The writers are indebted to the Aeronautical Research Committee for permission to publish in the present amplified form certain sections of Reports and Memoranda No. 1155 'The Flutter of Aeroplane Wings.'

† The determinantal forms of the test functions given in § 2 originally appeared in Appendix I to Technical Paper No. 2336 of the Aeronautical Research Committee, entitled 'Interim Report upon Flutter Theory,' by R. A. Frazer (November, 1926).

degrees of freedom. The generalised co-ordinates will be taken as x_1, x_2, \dots, x_m , and the dynamical equations will be written

$$\left. \begin{aligned} a_{11}\ddot{x}_1 + b_{11}\dot{x}_1 + c_{11}x_1 + a_{12}\ddot{x}_2 + b_{12}\dot{x}_2 + c_{12}x_2 + \dots \\ \quad + a_{1m}\ddot{x}_m + b_{1m}\dot{x}_m + c_{1m}x_m = 0 \\ a_{21}\ddot{x}_1 + b_{21}\dot{x}_1 + c_{21}x_1 + a_{22}\ddot{x}_2 + b_{22}\dot{x}_2 + c_{22}x_2 + \dots \\ \quad + a_{2m}\ddot{x}_m + b_{2m}\dot{x}_m + c_{2m}x_m = 0 \\ \vdots \\ a_{m1}\ddot{x}_1 + b_{m1}\dot{x}_1 + c_{m1}x_1 + a_{m2}\ddot{x}_2 + b_{m2}\dot{x}_2 + c_{m2}x_2 + \dots \\ \quad + a_{mm}\ddot{x}_m + b_{mm}\dot{x}_m + c_{mm}x_m = 0 \end{aligned} \right\}. \quad (1)$$

If D be used to represent differentiation with respect to time t , and if the typical operator, $a_{11}D^2 + b_{11}D + c_{11}$ be abbreviated as $a_{11}(D)$, then the foregoing equations can be expressed in the form

$$\left. \begin{aligned} a_{11}(D)x_1 + a_{12}(D)x_2 + \dots + a_{1m}(D)x_m &= 0 \\ a_{21}(D)x_1 + a_{22}(D)x_2 + \dots + a_{2m}(D)x_m &= 0 \\ \vdots \\ a_{m1}(D)x_1 + a_{m2}(D)x_2 + \dots + a_{mm}(D)x_m &= 0. \end{aligned} \right\} \quad (2)$$

In accordance with the standard treatment of such equations, a typical solution will be taken as

$$x_1 = X_1 e^{\lambda t}, \quad x_2 = X_2 e^{\lambda t}, \quad \dots \quad x_m = X_m e^{\lambda t}, \quad (3)$$

where the quantities X are independent of t , and determine the amplitude and phase relationships; and where λ is any root of the determinantal equation

$$\Delta(\lambda) \equiv \begin{vmatrix} a_{11}(\lambda), a_{12}(\lambda), \dots, a_{1m}(\lambda) \\ a_{21}(\lambda), a_{22}(\lambda), \dots, a_{2m}(\lambda) \\ \vdots \\ a_{m1}(\lambda), a_{m2}(\lambda), \dots, a_{mm}(\lambda) \end{vmatrix} = 0. \quad (4)$$

The stability of the system depends upon the nature of the roots of (4). This equation will be of degree not higher than $2m$ in λ and will be written for conciseness

$$\Delta(\lambda) \equiv p_0 \lambda^n + p_1 \lambda^{n-1} + p_2 \lambda^{n-2} + \dots + p_{n-1} \lambda + p_n = 0, \quad (5)$$

where $n \geq 2m$, and all the coefficients are assumed real. Routh's rule for the construction of test functions appropriate to (5), is as follows:—

The first two test functions are p_1 and $p_1 p_2 - p_0 p_3$ subject to the assumption

that p_0 is made positive. The remaining test functions may be constructed consecutively by writing

$$\begin{array}{l} \text{for} \\ \text{the values} \end{array} \begin{array}{c|c|c|c|c|c|c} p_0 & p_1 & p_2 & p_3 & p_4 & p_5 & \text{etc.} \\ p_1 & \frac{p_1 p_2 - p_0 p_3}{p_1} & p_3 & \frac{p_1 p_4 - p_0 p_5}{p_1} & p_5 & \frac{p_1 p_6 - p_0 p_7}{p_1} & \text{etc.} \end{array}$$

An objection to this procedure is that with equations of high degree the test functions, when written explicitly in terms of the coefficient p , become increasingly cumbersome as the process of construction is continued. It will now be shown that equivalent functions can be found very simply as a group of determinants.

Consider the following sequence, whose law of formation will be obvious

$$\begin{aligned} T_1 &\equiv p_1; & T_2 &\equiv \begin{vmatrix} p_1 & p_0 \\ p_3 & p_2 \end{vmatrix}; & T_3 &\equiv \begin{vmatrix} p_1 & p_0 & 0 \\ p_3 & p_2 & p_1 \\ p_5 & p_4 & p_3 \end{vmatrix} \\ T_4 &\equiv \begin{vmatrix} p_1 & p_0 & 0 & 0 \\ p_3 & p_2 & p_1 & p_0 \\ p_5 & p_4 & p_3 & p_2 \\ p_7 & p_6 & p_5 & p_4 \end{vmatrix}; & T_5 &\equiv \begin{vmatrix} p_1 & p_0 & 0 & 0 & 0 \\ p_3 & p_2 & p_1 & p_0 & 0 \\ p_5 & p_4 & p_3 & p_2 & p_1 \\ p_7 & p_6 & p_5 & p_4 & p_3 \\ p_9 & p_8 & p_7 & p_6 & p_5 \end{vmatrix} \quad \text{etc.} \end{aligned}$$

Then it can readily be shown that Routh's substitution will convert T_r into T_{r+1}/p_1 . The method of proof is general, but it will be sufficiently illustrated by reference to one determinant of the series, e.g., T_5 . Apply the substitution, and write the new value of the determinant as T_5' ; then

$$T_5' = 1/p_1^5 \begin{vmatrix} p_1 p_2 - p_0 p_3 & p_1 & 0 & 0 & 0 \\ p_1 p_4 - p_0 p_5 & p_3 & p_1 p_2 - p_0 p_3 & p_1 & 0 \\ p_1 p_6 - p_0 p_7 & p_5 & p_1 p_4 - p_0 p_5 & p_3 & p_1 p_2 - p_0 p_3 \\ p_1 p_8 - p_0 p_9 & p_7 & p_1 p_6 - p_0 p_7 & p_5 & p_1 p_4 - p_0 p_5 \\ p_1 p_{10} - p_0 p_{11} & p_9 & p_1 p_8 - p_0 p_9 & p_7 & p_1 p_6 - p_0 p_7 \end{vmatrix}$$

Multiply columns (2) and (4) by p_0 , and add to columns (3) and (5), respectively; then

$$T_5' = 1/p_1 \begin{vmatrix} p_1 p_2 - p_0 p_3 & p_1 & p_0 & 0 & 0 \\ p_1 p_4 - p_0 p_5 & p_3 & p_2 & p_1 & p_0 \\ p_1 p_6 - p_0 p_7 & p_5 & p_4 & p_3 & p_2 \\ p_1 p_8 - p_0 p_9 & p_7 & p_6 & p_5 & p_4 \\ p_1 p_{10} - p_0 p_{11} & p_9 & p_8 & p_7 & p_6 \end{vmatrix}$$

which determinant will at once be identified as T_6 , on development of the latter in terms of the minors comprised by its first two columns.

Since p_1 and T_2 are already known to be test-functions, the remaining determinants of the set appear as the higher test-functions. In the application to an equation of a specified degree n , a cipher should be substituted for the coefficients p whose suffixes exceed the value n . The process then terminates automatically with T_n , which in point of fact is merely $p_n T_{n-1}$. The necessary and sufficient conditions for complete stability of the system are that all the determinants, T_1, T_2, \dots, T_{n-1} , and p_0, p_n shall be positive.

3. Test Functions for the Quartic and the Sextic.

(a) *The Quartic.*—The full set of necessary and sufficient conditions for stability are here

- (i) All coefficients p positive ;
- (ii) T_3 positive.

These can be shown to be equivalent to the conditions that all the test determinants should be positive.

(b) *The Sextic.*—In this case the necessary and sufficient criteria are

- (i) Coefficients p_0, p_1 , and p_6 positive ;
- (ii) T_2, T_3, T_4 , and T_5 positive.

It does not appear that these can be replaced by any much simpler equivalent set. The condition that *all* the coefficients p and T_5 should be positive is necessary, but not in general sufficient.

4. Criteria for the First Onset of Instability in a Previously Stable System.

In the further discussion of the stability criteria, attention will be restricted to a particular class of problem which is commonly met with in mathematical physics. Information is often required as to the influence of a continuous variation of particular parameters on the stability of a dynamical system. It will be supposed that the system is known to be definitely stable for one datum set of values of the parameters, and that these parameters are continuously varied until an instability makes its appearance. The problem for solution is the determination of the critical values of the parameters corresponding to this first instability.

In accordance with the conditions of the problem, it will be assumed that some, or all, of the coefficients a, b, c , in the dynamical equations—and therefore

some, or all, of the coefficients p in (5)—are functions of a set of real parameters ξ, η, ζ , etc. In the datum condition, with $\xi = \xi_0$; $\eta = \eta_0$; $\zeta = \zeta_0$, etc., the system is known to be stable: thus, for this set of values of ξ, η, ζ , etc., the real parts of all the roots of (5) are negative, and no root is purely imaginary. Now suppose the parameters to be varied continuously until the first instability appears. The change from stability to instability can occur under one of the following circumstances only:—

- (a) The real part ρ of a complex root $\rho + i\sigma$ changes sign from negative to positive, and accordingly vanishes at the critical condition.* In this case, a previously damped *oscillation* changes into an unstable *oscillation*—the critical condition being where the oscillation is neutral (*i.e.*, simple harmonic). Since all the coefficients p are assumed real, the equation (5) will now possess two equal and opposite pure imaginary roots $\pm i\sigma$. The critical parameters for this case will, accordingly, be such that any eliminant of the equations $\Delta(\lambda) = 0$ and $\Delta(-\lambda) = 0$ vanishes.
- (b) A real root changes sign from negative to positive. In this case a previous subsidence becomes a divergence, the critical change being indicated by

$$p_n = 0. \quad (6)$$

The eliminant referred to under the heading (a) can be expressed in a variety of different forms, certain of which will be discussed later in § 6. For immediate purposes it will suffice to obtain merely that form which may be regarded as the standard. Suppose, firstly, n to be even (*i.e.*, $n = 2r$). Then since (5) is to be consistent with $\Delta(-\lambda) = 0$, the critical root will also necessarily satisfy

$$p_0 y^r + p_2 y^{r-1} + p_4 y^{r-2} + \dots + p_{2r-2} y + p_{2r} = 0, \quad (7A)$$

$$p_1 y^{r-1} + p_3 y^{r-2} + \dots + p_{2r-3} y + p_{2r-1} = 0, \quad (7B)$$

in which y has been written in place of the original λ^2 .

When n is odd (*i.e.*, $n = 2r + 1$) the corresponding pair is

$$p_0 y^r + p_2 y^{r-1} + p_4 y^{r-2} + \dots + p_{2r-2} y + p_{2r} = 0, \quad (8A)$$

$$p_1 y^r + p_3 y^{r-1} + p_5 y^{r-2} + \dots + p_{2r-1} y + p_{2r+1} = 0. \quad (8B)$$

* The possibility of infinite roots will be disallowed. An infinite root would imply that p_0 can vanish; normally, p_0 represents the discriminant of the kinetic energy of the system, and is therefore essentially positive.

Elimination of y by Sylvester's method leads, in the case $n = 2r$, to the relation :—

$$\begin{vmatrix} p_0 & p_2 & p_4 & p_6 & \dots & p_{2r-4} & p_{2r-2} & p_{2r} & 0 & 0 & 0 & \dots & 0 & 0 \\ 0 & p_0 & p_2 & p_4 & \dots & p_{2r-6} & p_{2r-4} & p_{2r-2} & p_{2r} & 0 & 0 & \dots & 0 & 0 \\ \vdots & \vdots & \vdots & \vdots & & \vdots & \vdots & \vdots & \vdots & \vdots & \vdots & & \vdots & \vdots \\ 0 & 0 & 0 & 0 & \dots & p_0 & p_2 & p_4 & p_6 & p_8 & p_{10} & \dots & p_{2r-2} & p_{2r} \\ p_1 & p_3 & p_5 & p_7 & \dots & p_{2r-3} & p_{2r-1} & 0 & 0 & 0 & 0 & \dots & 0 & 0 \\ 0 & p_1 & p_3 & p_5 & \dots & p_{2r-5} & p_{2r-3} & p_{2r-1} & 0 & 0 & 0 & \dots & 0 & 0 \\ \vdots & \vdots & \vdots & \vdots & & \vdots & \vdots & \vdots & \vdots & \vdots & \vdots & & \vdots & \vdots \\ 0 & 0 & 0 & 0 & \dots & 0 & p_1 & p_3 & p_5 & p_7 & p_9 & \dots & p_{2r-2} & p_{2r-1} \end{vmatrix} = 0.$$

The determinant is of order $2r - 1$, and on rearrangement of its columns and rows, it will be identified as the $(2r - 1)$ th member of the sequence of test determinants T defined on p. 644. Thus, one form of the eliminant of (7A) and (7B) is

$$T_{n-1} = 0. \quad (9)$$

It will readily be seen that this result is also valid in the case where n is odd.

The relations (6) and (9) jointly determine all possible values of the parameters, ξ , η , ζ , etc., for which the dynamical system undergoes a critical transition from stability to instability. Those values which correspond to the inception of a divergence will necessarily satisfy (6), whereas the values appropriate to the inception of oscillatory instability will necessarily satisfy (9).

For simplicity, suppose that there are merely two variable parameters concerned, *e.g.*, ξ and η . If these parameters be treated as co-ordinates in a plane, then (6) and (9) determine a pair of curves, which may for brevity be referred to as the "divergence curve D ," and "the unstable oscillation curve U ," respectively. Now it has been assumed as an essential condition of the problem that the system is known to be completely stable for the datum values $\xi = \xi_0$, $\eta = \eta_0$. Let P_0 denote the corresponding datum point in the diagram, and P the point appropriate to current values of ξ and η . The

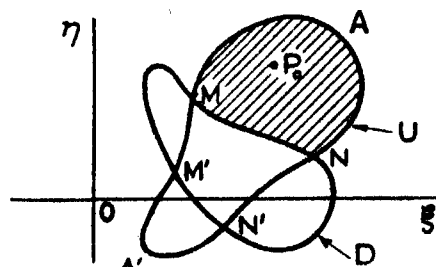


FIG. 1.

(Stable area shaded.)

system will be completely stable for the values of ξ and η provided that we can travel from P_0 to P without crossing either of the curves D , U .

Since (9) has been derived as the eliminant of $\Delta(\lambda) = 0$ and $\Delta(-\lambda) = 0$, it determines not only groups of values of ξ and η which provide equal and opposite imaginary roots $\pm i\sigma$ (i.e., simple harmonic oscillations), but also all groups which provide equal and opposite *real* roots $\pm\rho$. It follows that the whole of the curve U does not necessarily correspond to the inception of oscillatory instability. On the other hand, the existence of a pair of real roots $\pm\rho$ implies that a divergence must already have been established; so that all such branches of the curve U as can be reached from P_0 continuously without passage across D necessarily correspond to the condition of incipient oscillatory instability.

In the diagram fig. 1, both U and D are shown for simplicity as single oval curves with four real intersections $MM'NN'$. The stable area surrounding P_0 is MNA , but other completely stable areas may, of course, exist. A judicious interpretation of the diagram will often suffice to indicate the remaining stable area, if any. For instance, in the diagram actually shown, no point exterior to the oval curve U can correspond to stability, since T_{n-1} would then necessarily be negative. Moreover, no point interior to D can lead to stability, since p_n would then be negative. Thus, the only possible stable area, other than MNA , is the area $M'N'A'$. In this region, although both p_n and T_{n-1} are necessarily positive, some lower order test determinant may yet be negative. In practice, the most convenient procedure would be to calculate the stability for some one representative point within the suspected area $M'N'A'$. If the system is stable for this one point, it is necessarily stable throughout the whole area.

5. Illustrative Case of System with Two Degrees of Freedom.

The dynamical equations are here most conveniently written

$$a_1\ddot{x} + b_1\dot{x} + c_1x + d_1\ddot{y} + e_1\dot{y} + f_1y = 0 \quad (10A)$$

$$a_2\ddot{x} + b_2\dot{x} + c_2x + d_2\ddot{y} + e_2\dot{y} + f_2y = 0. \quad (10B)$$

It will be assumed that these equations are in the form given by Lagrange's method, or some equivalent. In this case the coefficients d_1 , a_2 are equal, and the common value may be denoted by P .

Let determinants be written in the abbreviated form

$$|ad| \equiv \begin{vmatrix} a_1 & d_1 \\ a_2 & d_2 \end{vmatrix}, \text{ etc.}$$

Then, the determinantal biquadratic corresponding to (10A) and (10B) will be

$$p_0\lambda^4 + p_1\lambda^3 + p_2\lambda^2 + p_3\lambda + p_4 = 0 \quad (11)$$

where

$$p_0 = |ad| \quad (12A)$$

$$p_1 = |ae| + |bd| \quad (12B)$$

$$p_2 = |af| + |be| + |cd| \quad (12C)$$

$$p_3 = |bf| + |ce| \quad (12D)$$

$$p_4 = |cf|. \quad (12E)$$

The curves D and U defined in § 4 will be, respectively,

$$p_4 \equiv |cf| = 0 \quad (13)$$

and

$$T_3 \equiv \begin{vmatrix} p_1 & p_0 & 0 \\ p_3 & p_2 & p_1 \\ 0 & p_4 & p_3 \end{vmatrix} = p_1 p_2 p_3 - p_0 p_3^2 - p_4 p_1^2 = 0. \quad (14)$$

The influence on the stability of a simultaneous variation of any two of the coefficients a, b, c , etc., may now readily be traced graphically by adoption of the two selected coefficients as co-ordinates ξ, η in a plane. An illustrative case is where the selected coefficients are $c_1 \equiv \xi, f_2 \equiv \eta$; these measure the direct forces of restitution. Then the curves D and U will obviously both be conic sections. The conic D will be a rectangular hyperbola whose asymptotes are the co-ordinate axes; whereas the curve U will be a conic of the general form

$$A\xi^2 + 2H\xi\eta + B\eta^2 + 2G\xi + 2F\eta + C = 0. \quad (15)$$

It will be found, after some reduction, that

$$4(AB - H^2) = p_1^2 P^2 [4e_2 b_1 - (e_1 + b_2)^2]. \quad (16)$$

Thus, U will be an ellipse or a hyperbola according as

$$4e_2 b_1 - (e_1 + b_2)^2 > 0 \quad \text{or} \quad < 0, \quad (16A)$$

and when $P = 0$ it will be a parabola.

It is interesting to note that the result (16A) is dependent merely upon the coefficients b and e , which represent the dissipative forces in the system. The expression on the left of (16A) is, in fact, the discriminant of the dissipation function

$$2F \equiv b_1 \dot{x}_1^2 + e_2 \dot{x}_2^2 + (e_1 + b_2) \dot{x}_1 \dot{x}_2. \quad (17)$$

Thus, on the assumption that b_1 and e_2 are positive, the condition of ellipticity is that F shall be positive for all values of the velocities \dot{x}_1, \dot{x}_2 .

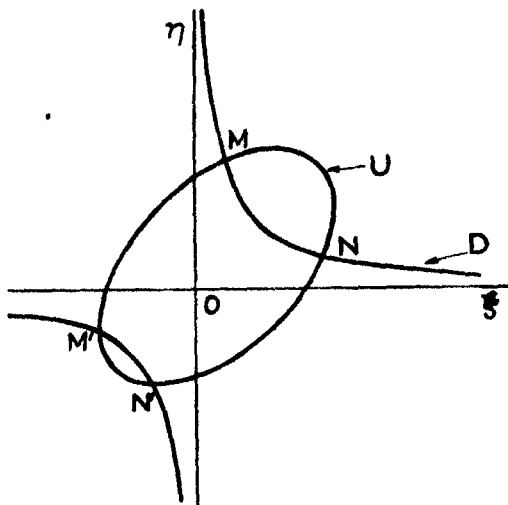


FIG. 2.

From the form of (14) it will be seen that of the four points common to D and U , one pair (M, N) lie on the straight line $p_3 = 0$. Since the expressions for p_4 and p_3 do not involve the coefficients a and d , it follows that the two points M, N will be common to all the conics U which are obtainable by a variation of these inertial coefficients. It can, further, be shown that when merely one or other of the two coefficients a_1 or d_2 is varied, the family of conics U will pass through the two fixed points M, N , and touch two fixed parallel straight lines.

The geometry of the diagram, for the foregoing special case where the variable parameters are c_1 and f_2 , has been developed in considerable detail by the writers in relation to the problem of the stability of aeroplane wings. For a detailed account of the results reference should be made to R. & M. 1155.*

6. *Alternative Forms for the Penultimate Test Determinant T_{n-1} .*

From the foregoing discussion it will be clear that the penultimate test function T_{n-1} is normally the most useful of the group. However, for numerical work, the determinantal form of this function is apt to be laborious in use, and other forms are preferable. Now it follows from the argument of §4 that any eliminant of $\Delta(\lambda) = 0$ and $\Delta(-\lambda) = 0$ can be adopted as a test function

* *Loc. cit.*

equivalent to T_{n-1} . Some alternative forms of this eliminant will now be exemplified by the case where the determinantal equation is a sextic.

Here, the equations whose eliminant is required, are

$$p_0 y^3 + p_2 y^2 + p_4 y + p_6 = 0 \quad (18A)$$

$$p_1 y^2 + p_3 y + p_5 = 0. \quad (18B)$$

Probably the simplest form for the eliminant is merely

$$-R \equiv (p_0 y_1^3 + p_2 y_1^2 + p_4 y_1 + p_6)(p_0 y_2^3 + p_2 y_2^2 + p_4 y_2 + p_6) \quad (19)$$

where y_1 and y_2 are the calculated roots of (18B).

The expression R differs from the determinant

$$T_5 \equiv \begin{vmatrix} p_1 & p_0 & 0 & 0 & 0 \\ p_3 & p_2 & p_1 & p_0 & 0 \\ p_5 & p_4 & p_3 & p_2 & p_1 \\ 0 & p_6 & p_5 & p_4 & p_3 \\ 0 & 0 & 0 & p_6 & p_5 \end{vmatrix} \quad (20)$$

merely by a factor, which can be found by a comparison of the coefficients of p_6^3 . In T_5 the coefficient of p_6^3 is $-p_1^3$; whence the identity

$$T_5 \equiv p_1^3 R.$$

Since p_1 is necessarily positive for stability, the method for the sextic can be summarised as follows:—

Solve the quadratic

$$p_1 y^2 + p_3 y + p_5 = 0$$

and let the roots be y_1 and y_2 .

Then the penultimate test function can be taken as

$$R_5 = -(p_0 y_1^3 + p_2 y_1^2 + p_4 y_1 + p_6)(p_0 y_2^3 + p_2 y_2^2 + p_4 y_2 + p_6)$$

and must be positive for stability.

It should be noted that in the critical condition one of the factors of R_5 necessarily vanishes, that involving y_1 for example. The critical frequency f of the corresponding oscillation is then given by

$$y_1 = -4\pi^2 f^2. \quad (21)$$

The advantage of this method is that the numerical work involved is more concise and less laborious than the direct calculation of the determinant T_5 . Moreover, fewer differences of sign occur in the expression of the function.

It may also be noted that for stability both the roots y_1 and y_2 must be real

and negative. For, if the roots were complex, the factors in R_5 would be conjugate imaginaries and R_5 would be necessarily negative. Moreover, real roots of opposite sign would imply that p_1 and p_5 were of opposite sign, a condition incompatible with stability*; and two real positive roots are immediately prohibited by the form of R_5 .

Another treatment of the equations (18A) and (18B) leads to a form of the test function involving only third-order determinants. If a third equation obtained by multiplying (18B) by y be used with (18A) and (18B), the set can be solved at once for y (the powers of y being regarded for the moment as independent variables) with the result

$$y \begin{vmatrix} p_1 & p_0 & 0 \\ p_3 & p_2 & p_1 \\ p_5 & p_4 & p_3 \end{vmatrix} + \begin{vmatrix} p_1 & p_0 & 0 \\ p_3 & p_2 & p_1 \\ 0 & p_5 & p_3 \end{vmatrix} = 0. \quad (22A)$$

Next, divide the same set of equations by y , and again solve for y . Then

$$y \begin{vmatrix} p_1 & p_0 & 0 \\ p_3 & p_2 & p_1 \\ 0 & p_5 & p_3 \end{vmatrix} + \begin{vmatrix} p_1 & p_0 & 0 \\ p_5 & p_4 & p_3 \\ 0 & p_5 & p_3 \end{vmatrix} = 0. \quad (22B)$$

Whence the eliminant, which can readily be identified with $p_1 T_5$, is

$$p_1 T_5 \equiv \begin{vmatrix} p_1 & p_0 & 0 \\ p_3 & p_2 & p_1 \\ p_5 & p_4 & p_3 \end{vmatrix} \times \begin{vmatrix} p_1 & p_0 & 0 \\ p_5 & p_4 & p_3 \\ 0 & p_5 & p_3 \end{vmatrix} - \begin{vmatrix} p_1 & p_0 & 0 \\ p_3 & p_2 & p_1 \\ 0 & p_5 & p_3 \end{vmatrix}^2 = 0. \quad (23A)$$

This may be written for brevity

$$p_1 T_5 \equiv \Delta_0 \Delta_2 - \Delta_1^2. \quad (23B)$$

The critical frequency $f (= \sqrt{-y}/2\pi)$ is then given directly by (22A) or (22B).

The alternative treatments of the test-function T_5 as given above can be generalised to apply to equations of any degree. In order to obtain the forms corresponding to (22) and (23) it will be necessary to add to the original pair of equations corresponding to (18A) and (18B) a further set obtained by multiplication by appropriate powers of y (e.g., for an even degree $n = 2m$, the multipliers are $1, y, \dots, y^{m-2}$ and $1, y, \dots, y^{m-2}$, respectively). The equations as they then stand, when solved for y , give

$$y \Delta_0 + \Delta_1 = 0 \quad (24A)$$

* See remarks on sextic, § 3.

and, when divided throughout by y , give

$$y\Delta_1 + \Delta_2 = 0 \quad (24B)$$

in which the determinants Δ are of order two less than the determinant T_{n-1} .

Then the eliminant is

$$R_{n-1} \equiv \Delta_0\Delta_2 - \Delta_1^2 = 0 \quad (25)$$

and at a critical condition

$$4\pi^2 f^2 = \Delta_1/\Delta_0 = \Delta_2/\Delta_1. \quad (26)$$

The eliminant R_{n-1} can be expressed in terms of the standard test determinants as follows :—

$$R_{n-1} = T_{n-5} T_{n-1}. \quad (27)$$

If the coefficients be varied continuously from an initial set compatible with complete stability, the first oscillatory instability is indicated by the vanishing of T_{n-1} ; and provided that p_n is still positive, all the subsidiary test functions must be positive. Hence the first critical condition occurs when R_{n-1} vanishes.

A general form of the test function corresponding to (19) is

$$R_{n-1} = \pm (p_0 y_1^r + p_2 y_1^{r-1} + \dots + p_{2r}) (p_0 y_2^r + p_2 y_2^{r-1} + \dots + p_{2r}) \quad (28)$$

where y_1 and y_2 are the roots of

$$Q(y) = 0 \quad (29)$$

and $Q(y)$ is any quadratic partial eliminant of the equations (7) or (8). The correct sign in (28) for stability could be decided most readily in practice by a numerical calculation of R_{n-1} for a known stable condition of the system.

Partial eliminants of any degree can be very readily obtained by Sylvester's method, and an example will make the general process clear. Let the original equation be an octic, so that equations (7) become

$$p_0 y^4 + p_2 y^3 + p_4 y^2 + p_6 y + p_8 = 0, \quad (30A)$$

$$p_1 y^3 + p_3 y^2 + p_5 y + p_7 = 0. \quad (30B)$$

Multiply (30B) by y . In the set of three equations now available treat any two of the powers of y as independent variables and the remainder as constants, and eliminate. For example, the three equations can be written

$$p_1 y^4 + y(p_3 y^2 + p_5 y + p_7) = 0.$$

$$p_0 y^4 + y(p_2 y^2 + p_4 y + p_6) + p_8 = 0.$$

$$y(p_1 y^2 + p_3 y + p_5) + p_7 = 0.$$

Upon elimination of y^4 and y the result is

$$\begin{vmatrix} p_1 & p_3y^2 + p_5y + p_7 & 0 \\ p_0 & p_2y^2 + p_4y + p_6 & p_8 \\ 0 & p_1y^2 + p_3y + p_5 & p_7 \end{vmatrix} = 0. \quad (31)$$

Many alternative forms of quadratic eliminant exist, corresponding to the different possible methods of performing the elimination. It may be noted that when equations (30) have two roots in common, these roots are necessarily the roots of (31); under this condition the coefficients satisfy a number of identical relations, and all the forms of the quadratic eliminant become identical.

The general rule in partial elimination can be stated as follows:—Let the equations be of the m th and n th degrees, respectively. To obtain a partial eliminant of degree r , multiply the first by $y^0, y^1, \dots, y^{n-r-1}$ and the second by $y^0, y^1, \dots, y^{m-r-1}$. There are then $(m+n-2r)$ equations, from which $(m+n-2r-1)$ powers of y can be eliminated; the eliminant is clearly of degree r in y , and is a determinant of order $(m+n-2r)$.

Further Investigations of the Spectrum of Ionised Nitrogen (N II).

By L. J. FREEMAN, B.Sc., D.I.C., Imperial College of Science and Technology,
South Kensington.

(Communicated by A. Fowler, F.R.S.—Received May 3, 1929.)

In a previous paper* on the spectrum of ionised nitrogen (N II), the triplet and singlet terms based on the $2p\ ^3P$ term of N III were dealt with. Mention was also made of a second group of terms based on the $2p'$ terms of N III. This group contains singlet, triplet, and quintet terms. Three of the deepest of these triplet terms were found by Bowen,† namely, $2p'\ ^3S$, $2p'\ ^3P$ and $2p'\ ^3D$ in the notation here adopted. The first part of the present paper deals with the identification of some of the quintet terms of this second group. The second part refers to some additional combinations arising from triplet terms of the first group. For completeness, a brief account of some singlet identifications by W. E. Pretty has been included.

* Fowler and Freeman, 'Roy. Soc. Proc.,' A, vol. 114, p. 662 (1927).

† 'Phys. Rev.,' vol. 29, p. 231 (1927).

Quintets.

Three multiplets, previously suggested as being due to double electron transitions in the triplet system, have now been found (following a suggestion by Prof. H. N. Russell) to belong to the quintet system.

The predicted quintet terms based on $2p' \ ^4P$ of N III are as follows : —

1_1	$2_1 \ 2_2$	$3_1 \ 3_2 \ 3_3$	4_1	Term prefix.	Terms.
2	1 3			$2p'$	5S
2	1 2	1		$3s'$	5P
2	1 2	1		$3p'$	$^5S \ ^5P \ ^5D$
2	1 2	1		$3d'$	$^5P \ ^5D \ ^5F$
2	1 2		1	$4s'$	5P

There is a similar set of triplet terms based on $2p' \ ^4P$ and several other singlet and triplet terms based on the doublet terms of the $2p'$ row of N III, namely, $2p' \ ^3S$, $2p' \ ^3P$, and $2p' \ ^3D$.* None of these triplet or singlet terms, however, has been found.

Nine quintet multiplets have been observed altogether, resulting in the identification of all the $3s'$, $3p'$ and $3d'$ terms. The deepest term, $2p' \ ^5S$, has not been found. The similarity between quintet and triplet terms, which is mentioned later, suggests that the quintet combination $2p' \ ^5S - 3s' \ ^5P$ should occur in the extreme ultra-violet close to the triplet combination $2p \ ^3P - 3s \ ^3P$ † at λ 671.

Quintet Term Values.

The absolute values of the quintet terms have not been determined, as no intercombinations with the triplet system have been observed. It is probable, however, that any given quintet term (say $3s' \ ^5P$) is about 100,000 units smaller than the corresponding triplet term ($3s \ ^3P$), since the triplet limit ($2p \ ^2P$ in N III) is roughly 100,000 units deeper than the quintet limit ($2p' \ ^4P$ in N III).‡ For purposes of reference, however, and to avoid negative term values, $3s' \ ^5P_3$ has been given an arbitrary value of 90,000, near to the value of $3s \ ^3P_2$ (89769).

* L. J. Freeman, 'Roy. Soc. Proc.,' A, vol. 121, p. 324 (1928).

† $1 \ ^5P - 1 \ ^3P$ in the notation of the previous paper.

‡ *Loc. cit.*

The nine quintet multiplets are given in Table I. (Numbers enclosed in brackets are calculated values for lines which have not been observed.)

Table I.—Quintet Combinations of N II.

	$3s' {}^3P_3$		$3s' {}^3P_2$		$3s' {}^3P_1$
	90000.0	70.6	90070.6	56.0	90126.6
$3p' {}^5S_2 = 65885.7$	24114.3 (3)	70.6	24184.9 (2)	56.0	24240.9 (1)
$3p' {}^5D_4 = 71939.4$ 53.9	*18080.6 (5) 53.9				
$3p' {}^5D_3 = 71903.3$ 43.1	18006.7 (3)	70.6	18077.3 (4)		
$3p' {}^5D_2 = 72036.4$ 29.4	17963.6 (0)	70.6	18034.2 (3)	56.2	18080.4 (2)
$3p' {}^5D_1 = 72065.8$ 15.8			18004.8 (00)	55.8	*18060.6 (5) 15.8
$3p' {}^5D_0 = 72081.6$					18045.0 (1)
$3p' {}^5P_3 = 70053.5$ 44.0	19946.5 (2)	70.5	†20017.0 (6) 43.1		
$3p' {}^5P_2 = 70097.5$ 24.1	19902.5 (2)	71.4	†19973.9 (10)	55.7	20029.6 (2)
$3p' {}^5P_1 = 70121.6$			24.3 19949.6 (1)	55.9	20005.6 (0) 24.1

* Used twice.

† Coincident with $3p {}^3S_1 - 3d {}^3P_1$

‡ Coincident with $3p {}^3D_3 - 3d {}^3F_4$

Table I—(continued).

	$3p^1D_4$	$3p^1D_3$	$3p^1D_2$	$3p^1D_1$	$3p^1D_0$				
	71939.4	53.9	71993.3	43.1	72036.4	29.4	72065.8	15.8	72081.6
$3d^1F_5 = 52637.9$	19301.5 (5)								
$3d^1F_4 = 52678.5$	40.6								
$3d^1F_3 = 52678.5$	19290.9 (2)	54.0	19314.9 (3)						
$3d^1F_2 = 52712.1$	33.6		33.7						
$3d^1F_1 = 52737.5$	19227.3 (00)	53.9	19281.2 (2)	43.2	19324.4 (2)				
$3d^1F_0 = 52737.5$	26.4				26.0				
$3d^1F_4 = 52753.2$	15.7		(19255.9)		19298.4 (1)	29.9	*19328.3 (1)		
					(19283.2)		15.7		
							19312.6 (1)	15.7	*19328.3 (1)
$3d^1D_4 = 50751.8$	21187.6 (2)	54.1	21241.7 (0)						
$3d^1D_3 = 50765.8$	14.2		13.7						
$3d^1D_2 = 50777.4$	21173.4 (0)	54.6	21238.0 (1)	42.1	21270.1 (0)				
$3d^1D_1 = 50785.3$			12.1		11.1				
$3d^1D_0 = 50788.9$			21215.9 (0)	43.1	21259.0 (0)	30.2	21289.2 (1)		
					7.9		(21280.5)		(21296.3)
					21251.1 (0)		21276.9 (0)		

* Used twice.

Table I—(continued).

	$3d' {}^4P_2$		$3d' {}^4P_1$		$3d' {}^4P_0$
	51371.3	—38.5	51332.8	—26.1	51306.7
$3p' {}^4P_2 = 70053.5$ 44.0	18682.2 (4)	—38.5	18720.7 (1)		
$3p' {}^4P_2 = 70097.5$ 24.1	18726.1 (2)	—39.4	18765.5 (0)	—22.9	*18788.4 (3)
$3p' {}^4P_1 = 70121.6$			22.9	—26.6	18815.0 (0)
			*18788.4 (3)		
$3p' {}^4S_2 = 65885.7$	14512.6 (2)	—37.8	14550.4 (1)	—27.9	14578.3 (1)
$3p' {}^4D_2 = 71939.4$ 53.9	20568.9 (2)				
$3p' {}^4D_2 = 71993.3$ 43.1	(20622.0)		(20660.5)		
$3p' {}^4D_2 = 72036.4$ 29.4	(20665.1)		(20703.6)		(20729.7)
$3p' {}^4D_1 = 72065.8$ 15.8			(20733.0)		(20759.1)
$3p' {}^4D_0 = 72081.6$					(20774.9)
* Used twice.					
	$3p' {}^4P_2$		$3p' {}^4P_1$		$3p' {}^4P_0$
	70053.5	44.0	70097.5	24.1	70121.6
$3d' {}^4D_2 = 50751.8$ 14.0	19301.5 (5)				
$3d' {}^4D_2 = 50785.8$ 11.6	19287.7 (2)	43.8	19331.5 (1)		
$3d' {}^4D_2 = 50777.4$ 7.9	19276.7 (0)	43.6	19320.3 (1)	23.3	19343.6 (1)
$3d' {}^4D_1 = 50785.3$ 3.6			(19312.2)		19336.6 (1)
$3d' {}^4D_0 = 50788.9$					(19332.7)

The quintet term values and separations are collected in Table II together with those for O III.† In neither spectrum have the absolute values of the terms been determined so that no true comparison of the values given can be made. An examination of the term separations, however, shows that those for O III are all about 2.3 times as great as those for N II. This ratio does not vary much, the highest and lowest values being 2.46 and 2.20.

† Mihul, 'C. R.', vol. 184, p. 89 (1926) and Thesis, University of Nancy, Paris (1927).

Table II.—Comparison of *N II* Quintets with *O III* Quintets.

Term.	<i>O III</i>	$\Delta\nu$	<i>N II</i>	$\Delta\nu$	$\frac{\Delta\nu \text{ } O \text{ III}}{\Delta\nu \text{ } N \text{ II}}$
$3s' \text{ } ^5P_1$	76285.6		90126.6		
P_2	76161.2	124.5	90070.6	56.0	2.22
P_3	76000.0	161.2	90000.0	70.6	2.28
$3p' \text{ } ^5D_0$	49335.7		72081.6		
D_1	49300.9	34.8	72065.8	15.8	2.20
D_2	49232.4	68.5	72036.4	29.4	2.33
D_3	49132.3	100.0	71993.3	43.1	2.32
D_4	49005.0	127.3	71939.4	53.9	2.36
$3p' \text{ } ^5P_1$	46325.1		70053.5		
P_2	46267.9	57.3	70097.5	24.0	2.39
P_3	46166.8	101.1	70121.6	44.1	2.29
$3p' \text{ } ^5S_2$	38783.8		65885.7		
$3d' \text{ } ^5F_1$	20335.1		52753.2		
F_2	20296.4	38.7	52737.5	15.7	2.46
F_3	20238.8	57.6	52712.1	25.4	2.27
F_4	20163.1	75.7	52678.5	33.6	2.25
F_5	20071.0	92.0	52637.9	40.6	2.27
$3d' \text{ } ^5P_1$			51306.7		
P_2			51332.8	—26.1	
P_3			51371.3	—38.5	
$3d' \text{ } ^5D_0$				
D_1			50785.3		
D_2			50777.4	7.9	
D_3			50765.8	11.6	
D_4			50751.8	14.0	

Comparison of N II Quintets with N II Triplets.

The quintet terms are set out in Table III alongside the corresponding triplet terms. For converting the notation used in the previous paper to the present notation, the old and the new designations of each term are given side by side in Table VI.

Table III.

Quintets.				Triplets.			
	Term values.	$\Delta\nu$	$\Sigma\Delta\nu$		Term values.	$\Delta\nu$	$\Sigma\Delta\nu$
$3s' {}^5P$	90000	70 56	126	$3s {}^3P$	89769	136 31	167
$3p' {}^5D$	71939	53 43 29 15	140	$3p {}^3D$	72167	96 60	156
$3p' {}^5S$	65885			$3p {}^3S$	69953		
$3p' {}^3P$	70122	44 24	68	$3p {}^3P$	68179	58 35	93
$3d' {}^5F$	52637	40 33 25 15	113	$3d {}^3F$	52193	81 59	140
$3d' {}^5D$	50751	14 11 7 —	32+	$3d {}^3D$	51353	30 24	54
$3d' {}^3P$	51371	-38 -26	-64	$3d {}^3P$	49988	-51 -28	-79

The two systems of terms are seen to run nearly parallel, both in relative magnitudes and in relative separations. This has the effect of making corresponding quintet and triplet combinations occur close to each other in the spectrum, and resemble each other in general appearance. Thus $3s' {}^5P - 3p' {}^5D$ is at $\lambda 5535$ and $3s {}^3P - 3p {}^3D$ is at $\lambda 5679$; $3p' {}^5D - 3d' {}^5D$ is at $\lambda 4718$, and $3p {}^3D - 3d {}^3D$ is at $\lambda 4803$.

Such a similarity was also observed between the doublets and quartets of N III* and of C II.†

The differences in the energy levels when the series electron occupies various orbits is obviously not much affected by the disposition of the inner electrons.

* *Loc. cit.*

† Fowler and Selwyn, 'Roy. Soc. Proc.,' A, vol. 120, p. 312 (1928).

Triplets.

Six new triplet combinations have been found, resulting in the identification of two new terms. In the notation of the previous paper on *N II* these are 3^3P and $2^3F'$, which in the notation adopted here become $4p^3P$ and $4d^3F$. The identification of triplet terms is now complete as far as the $4d$ row. The new multiplets are set out below. The measures of the two groups beyond $\lambda 7000$ are rather unsatisfactory owing to the faintness and diffuseness of the lines which tend to become lost in the continuous background.

	$4d^3F_4$		$4d^3F_3$		$4d^3F_2$
	29021.4	85.8	29107.2	64.2	29171.4
$3p^3D_3 = 72167.3$ 96.2	43145.8 (5)	85.7	43060.1 (1) 96.1		(42995.9)
$3p^3D_2 = 72263.4$ 60.8			43150.0 (4)	64.0	43092.0 (1) 60.5
$3p^3D_1 = 72324.2$					43152.5 (3)
	$4p^3P_1$		$4p^3P_1$		$4p^3P_0$
	35587.0	70.9	35657.0	24.1	35682.0
$3d^3D_3 = 51353.9$ 30.3	15766.9 (4) 30.0				
$3d^3D_2 = 51384.3$ 24.0	15796.9 (1)	70.5	*15726.4 (3) 24.5		
$3d^3D_1 = 51408.4$	(15821.4)		15750.9 (1)	24.5	*15726.4 (3)
$3s^3P_2 = 89769.4$ 136.4	54180 (5) 136	69	54111 (0) 135		
$3s^3P_1 = 89905.7$ 31.6	54316 (1)	70	54246 (0) 31	27	54219 (0)
$3s^3P_0 = 89937.3$			54277 (0)		
$3s^1P_1 = 89658.0$	54072 (1)		(54000)		(53976)
$3d^3P_2 = 49988.6$ —51.8	14399.2 (3) —51.0	69.9	14329.3 (2) —53.7		
$3d^3P_1 = 49936.8$ —28.0	14348.2 (1)	72.8	14275.6 (0 π) —25.0	25.0	*14250.6 (1)
$3d^3P_0 = 49908.8$			*14250.6 (1)		
	$4p^3D_3$		$4p^3D_2$		$4p^3D_1$
	35984.6	96.2	36080.8	60.9	36131.8
$3d^3P_2 = 49988.6$ —51.8	14002.1 (3)	95.1	13907.0 (0) —54.7		(13856.9)
$3d^3P_1 = 49936.8$ —28.0			13852.3 (2)		(13805.0)
$3d^3P_0 = 49908.8$					13771.0 (2)

* Used twice.

Comparison of N II Triplets with N III Quartets.

In Table IV, the triplet term separations for N II are compared with the quartet term separations for N III. It is seen that for corresponding terms (*i.e.*, terms for which the "series" electron occupies the same orbit in both spectra) the separations are very similar in the two systems. This similarity is well shown in the figure, where the two sets of term separations are plotted to scale. For the triplets, the total separation has been plotted; for the quartets, the separation between the first and third components.

Table IV.—Term Separations for N II Triplets and N III Quartets.

Triplets (N II).			Quartets (N III).		
	$\Delta\nu$	$\Sigma\Delta\nu$		$\Delta\nu$	$\Sigma\Delta\nu$
$3s\ ^3P$	$\left. \begin{matrix} 136 \\ 31 \end{matrix} \right\}$	167	$3s'\ ^4P$	$\left. \begin{matrix} 116 \\ 62 \end{matrix} \right\}$	178
$3p\ ^4D$	$\left. \begin{matrix} 96 \\ 60 \end{matrix} \right\}$	156	$3p'\ ^4D$	$\left. \begin{matrix} 96 \\ 62 \\ 35 \end{matrix} \right\}$	158
$3p\ ^3P$	$\left. \begin{matrix} 58 \\ 35 \end{matrix} \right\}$	93	$3p'\ ^4P$	$\left. \begin{matrix} 58 \\ 43 \end{matrix} \right\}$	101
$3d\ ^3F$	$\left. \begin{matrix} 81 \\ 59 \end{matrix} \right\}$	140	$3d'\ ^4F$	$\left. \begin{matrix} 71 \\ 51 \\ 35 \end{matrix} \right\}$	122
$3d\ ^3D$	$\left. \begin{matrix} 30 \\ 24 \end{matrix} \right\}$	54	$3d'\ ^4D$	$\left. \begin{matrix} 28 \\ 22 \\ 13 \end{matrix} \right\}$	50
$3d\ ^3P$	$\left. \begin{matrix} -51 \\ -28 \end{matrix} \right\}$	-79	$3d'\ ^4P$	$\left. \begin{matrix} -54 \\ -35 \end{matrix} \right\}$	-89
$4s\ ^3P$	$\left. \begin{matrix} 119 \\ 51 \end{matrix} \right\}$	170	$4s'\ ^4P$	$\left. \begin{matrix} 116 \\ 62 \end{matrix} \right\}$	178
$4p\ ^3D$	$\left. \begin{matrix} 96 \\ 50 \end{matrix} \right\}$	146	$4p'\ ^4D$	$\left. \begin{matrix} 89 \\ 60 \\ 46 \end{matrix} \right\}$	149
$4p\ ^3P$	$\left. \begin{matrix} 70 \\ 24 \end{matrix} \right\}$	94	$4p'\ ^4P$	$\left. \begin{matrix} 52 \\ 44 \end{matrix} \right\}$	96
$4d\ ^3F$	$\left. \begin{matrix} 85 \\ 64 \end{matrix} \right\}$	149	$4d'\ ^4F$	$\left. \begin{matrix} 74 \\ 49 \\ - \end{matrix} \right\}$	123
$4d\ ^3D$	$\left. \begin{matrix} 35 \\ 26 \end{matrix} \right\}$	61	$4d'\ ^4D$	$\left. \begin{matrix} 29 \\ 27 \\ - \end{matrix} \right\}$	56

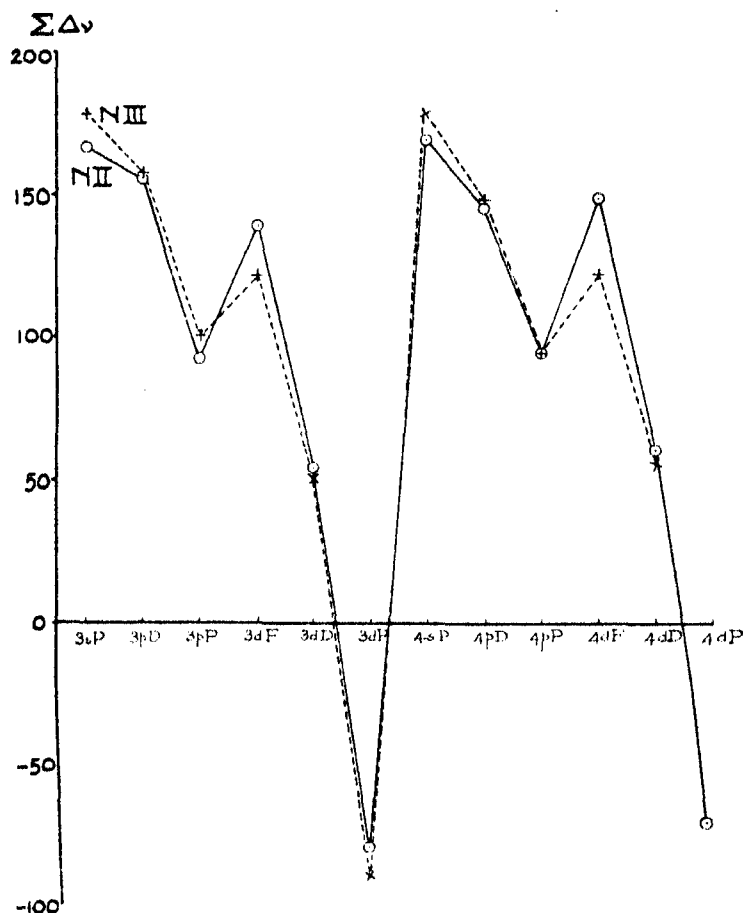
Term Component Separations for *N II* Triplets and *N III* Quartets.

Table VII is a list of *N II* lines newly classified in this paper. Those marked with an asterisk were not recorded in the previous paper. In a few cases the wave-lengths have been revised as better plates have been obtained.

Singlets.

W. E. Pretty,* by an application of his work on shifts in spectral lines, has identified three singlet terms belonging to the main family, namely, $4p^1D$, $4p^1S$, and $4d^1D$. The identification of each term is supported by two combinations with previously known singlet terms, with the addition, in the case of $4p^1S$, of an intercombination with a triplet term. With the object of

* 'Proc. Phys. Soc.' (*in the press*).

collecting all the new data for N II in one paper, these results of Pretty's are given below :—

	$4p^1D_2$ 36153.27
$3s^1P_1 = 89657.96$ $3d^1F_3 = 52168.02$	53500.8 (1) 16014.75 (5)
	$4p^1S_0$ 36676.8
$3s^1P_1 = 89657.96$ $3s^3P_1 = 89905.73$ $3d^1P_1 = 51754.50$	52981.5 (4) 53231.1 (2) 15077.7 (2)
	$4d^1D_2$ 28919.78
$3p^1P_1 = 64633.77$ $3p^1D_2 = 74235.10$	35713.89 (4) 45314.7 (3)

It should be noted that the interchange of the values of $3d^1P$ and $3d^1D$, suggested by Prof. Fowler,* is confirmed by the existence of the combination $3d^1P - 4p^1S$, which would be forbidden if the first term were $3d^1D$ instead of $3d^1P$.

In previous comparisons of the terms of N II with those of O III† and C I,‡ the value of $4p^1D$ for N II was suggested as 37045, this value resulting from taking the line at 15123 as $3d^1F - 4p^1D$. From the small magnitude of the shift of this line, however, Pretty considers this identification to be wrong. His value of 36153 for $4p^1D$ is supported by two combinations, both giving lines which have the appropriate shift.

No further light has been thrown on the apparent abnormality of the p^1S terms. The value of $4p^1S$ appears to fit in better than those of $3p^1S$ and $2p^1S$ when compared with O III and C I, although it is more than 4000 units larger than the expected value obtained by extrapolation with a Hicks' formula calculated from $2p^1S$ and $3p^1S$.

All the observed combinations involving singlet terms are collected in Table V.

* 'Roy. Soc. Proc.,' A, vol. 117, p. 329 (1928).

† *Loc. cit.*

‡ Fowler and Selwyn, 'Roy. Soc. Proc.,' A, vol. 118, p. 43 (1928).

Table V.—Summary of Singlet Combinations observed in *N II*.

	$2p^1S_0$ 147118.8	$3p^1D_1$ 74235.1	$3p^1P_1$ 64633.8	$3p^1S_0$ 60572.5	$4p^1D_1$ 36153.3	$4p^1S_0$ 36676.8
$3s^1P_1 = 89905.7$	*57313.0 (7)	15670.6 (5)	25271.9 (6)	29333.2 (3)		53231.1 (2)
$3s^1P_1 = 89668.0$	57460.9 (5)	15422.9 (6)	25024.3 (10)	29085.5 (6)	53500.8 (1)	52981.5 (4)
$3d^1F_3 = 52334.3$		21900.7 (1)				
$F_3 = 52374.9$		21959.8 (4)				
$3d^1F_3 = 52168.0$		22067.1 (5)			16014.9 (5)	15077.7 (2)
$3d^1P_1 = 51754.5†$		22480.6 (10)				
$3d^1D_2 = 51384.3$		22850.7 (0)				
$3d^1D_2 = 48725.6†$		25509.5 (6)	15908.3 (3)			
$4s^1P_1 = 40867.4$		33247.7 (7)	23646.2 (3 π)	19585.3 (3)		
$4d^1D_2 = 28919.8$		45314.7 (3)	35714.0 (4)			
$5s^1P_1 = 24018.7$			40616.6 (3)	36552.3 (1 π)		
	$3s^1P_1$ 89658.0					
$3p^1D_1 = 72324.2$	17334.0 (3)					
$D_2 = 72363.4$	17394.7 (4)					
$3p^1P_0 = 68273.3$	21384.5 (2)					
$P_1 = 68238.1$	21419.8 (2)					
$P_2 = 68179.7$	21478.3 (2)					
$3p^1S_0 = 69953.7$	19704.4 (3)					

* There is also a strong *N III* line here.† The values for $3d^1D_2$ and $3d^1P_1$, given in the previous paper, are interchanged here.

Table VI.—Term Designations in N II.

Old.	New.	Old.	New.
1^3P	$2p^3P$	$1^1S'$	$2p^1S$
$1^3P'$	$3s^3P$	$1^1D'$	$2p^1D$
$1^3S'$	$3p^3S$	$1^1P'$	$3s^1P$
2^3P	$3p^3P$	$2^1S'$	$3p^1S$
$1^1D'$	$3p^1D$	1^1P	$3p^1P$
$1^3P'''$	$3d^3P$	$2^1D'$	$3p^1D$
1^1D	$3d^1D$	$1^1P'''$	$3d^1P$
$1^1F'$	$3d^1F$	1^1D	$3d^1D$
$2^3P'$	$4s^3P$	$1^1F'$	$3d^1F$
$2^3S'$	$4p^3S$	$2^1P'$	$4s^1P$
3^3P	$4p^3P$	$3^1S'$	$4p^1S$
$2^1D'$	$4p^1D$	2^1P	$4p^1P$
$2^3P'''$	$4d^3P$	$3^1D'$	$4p^1D$
2^1D	$4d^1D$	$2^1P'''$	$4d^1P$
$2^1F'$	$4d^1F$	2^1D	$4d^1D$
$1^1D'''$	$4f^1D$	$2^1F'$	$4d^1F$
1^1F	$4f^1F$	$1^1D'''$	$4f^1D$
$1^1G'$	$4f^1G$	1^1F	$4f^1F$
$3^3P'$	$5s^3P$	1^1G	$4f^1G$
β^3S	$2p'^3S$	$3^1P'$	$5s^1P$
β^3P'	$2p'^3P$		
β^1D	$2p'^1D$		

Table VII.—Newly Classified Lines of N II.

λ .	ν .	Classification.	λ .	ν .	Classification.
*7259.3 (2)	13771.0	$3d^3P_0-4p^3D_1$	5565.30 (0)	17963.5	$3s'^3P_0-3p'^3D_1$
(7241.8)	(13805.0)	$P_1 \quad D_1$	*5552.54 (00)	18004.8	$P_1 \quad D_1$
*7217.0 (2)	13852.3	$P_1 \quad D_2$	5551.95 (3)	18006.7	$P_1 \quad D_2$
(7214.6)	(13856.9)	$P_2 \quad D_1$	5543.49 (3)	18034.2	$P_1 \quad D_2$
*7188.7 (0)	13907.0	$P_2 \quad D_2$	5540.16 (1)	18045.0	$P_1 \quad D_0$
*7139.8 (3)	14002.1	$P_2 \quad D_2$	5535.39 (5)	18000.6	$P_1 \quad D_2$
			5530.27 (4)	18077.3	$P_1 \quad D_2$
*7015.3 (1)	14250.6	$\left\{ \begin{array}{l} 3d^3P_1-4p^3P_0 \\ P_0 \quad P_1 \end{array} \right.$	5526.26 (2)	18090.4	$P_1 \quad D_2$
*7003.0 (0n)	14275.6	$P_1 \quad P_1$			$P_1 \quad D_2$
*6976.8 (2)	14329.3	$P_2 \quad P_1$	5351.21 (4)	18682.2	$3p'^3P_0-3d'^3P_2$
*6967.6 (1)	14348.2	$P_1 \quad P_2$	5340.20 (1)	18720.7	$P_2 \quad P_2$
*6942.9 (3)	14399.2	$P_2 \quad P_2$	5338.66 (2)	18726.1	$P_2 \quad P_2$
			*5327.45 (0)	18765.5	$P_2 \quad P_2$
*6888.7 (2)	14512.6	$3p'^3S_2-3d'^3P_2$	5320.96 (3)	18788.4	$\left\{ \begin{array}{l} P_2 \quad P_1 \\ P_1 \quad P_2 \end{array} \right.$
*6870.8 (1)	14550.4	$S_2 \quad P_2$	5313.43 (0)	18815.0	$P_1 \quad P_1$
*6857.6 (1)	14578.3	$S_2 \quad P_1$			$P_1 \quad P_1$
†6030.5 (2)	15077.7	$3d^1P_1-4p^1S_0$	5199.50 (00)	19227.3	$3p'^3D_2-3d'^3F_2$
			5190.42 (2)	19260.9	$D_2 \quad F_2$
6357.0 (3)	15726.4	$\left\{ \begin{array}{l} 3d^3D_2-4p^3P_1 \\ D_1 \quad P_0 \end{array} \right.$	*5186.17 (0)	19276.7	$3p'^3P_2-3d'^3D_2$
6347.1 (1)	15750.9	$D_1 \quad P_0$	5184.97 (2)	19281.2	$D_2 \quad F_2$
6340.67 (4)	15766.9	$D_1 \quad P_1$	5183.21 (2)	19287.7	$P_2 \quad D_2$
6328.6 (1)	15796.9	$D_2 \quad P_2$	*5180.34 (1)	19298.4	$D_2 \quad F_2$
(6318.8)	(15821.4)	$D_1 \quad P_2$	5179.50 (5)	19301.5	$\left\{ \begin{array}{l} D_2 \quad F_2 \\ D_1 \quad P_2 \end{array} \right.$
†6242.52 (5)	16014.75	$3d^1F_2-4p^1D_2$			$D_1 \quad P_2$

* Not recorded in previous paper.

† Identified by W. E. Pretty.

Table VII—(continued).

λ .	ν .	Classification.	λ	ν .	Classification.
5175.89 (3)	19314.9	D_3 F_4	4145.76 (3)	24114.3	$3s' {}^4P_3 - 3p' {}^4S_3$
5174.46 (1)	19320.3	P_3 D_3	4138.65 (2)	24184.9	P_3 S_3
5173.37 (2)	19324.4	D_3 F_3	4124.10 (1)	24240.9	P_1 S_3
5172.32 (1)	19328.3	$\left\{ \begin{array}{l} D_1 \\ D_0 \end{array} \right.$ F_3	†2799.20 (4)	35713.99	$3p {}^1P_1 - 4d {}^1D_2$
5171.46 (1)	19331.5	P_3 D_3	(2325.08)	(42995.9)	$3p {}^3D_3 - 4d {}^3F_3$
5170.08 (1)	19336.6	P_1 D_1	*2321.62 (1)	43060.1	D_3 F_3
5168.24 (1)	19343.6	P_1 D_2	*2319.90 (1)	43092.0	D_3 F_3
5023.11 (2)	19902.5	$3s' {}^4P_3 - 3p' {}^4P_3$	2317.01 (5)	43145.8	D_3 F_4
5012.03 (2)	19946.5	P_3 P_3	2316.65 (3)	43152.5	D_1 F_3
*5011.24 (1)	19949.6	P_3 P_1	2316.46 (4)	43156.0	D_2 F_3
5005.14 (10)	19973.9	P_3 P_3	†2206.10 (3)	45314.7	$\int 3p {}^1D_2 - 4d {}^1D_3$
4997.23 (0)	20005.5	P_1 P_1			$\{ 3p {}^3S_1 - 5s {}^3P_0$
4994.36 (6)	20017.0	P_3 P_3	†1886.82 (4)	52981.5	$3s {}^1P_1 - 4p {}^1S_0$
4991.22 (2)	20029.6	P_1 P_3	†1877.97 (2)	53231.1	$3s {}^3P_1 - 4p {}^1S_0$
4860.35 (2)	20568.9	$3p' {}^4D_4 - 3d' {}^4P_3$	†1868.50 (1)	53500.8	$3d {}^1P_1 - 4p {}^1S_0$
4721.59 (0)	21173.4	$3p' {}^4D_4 - 3d' {}^4D_3$	*1849.4 (1)	54072	$3s {}^1P_1 - 4p {}^3P_3$
4718.43 (2)	21187.6	D_3 D_3	*1848.1 (0)	54111	$3s {}^3P_3 - 4p {}^3P_1$
4712.13 (0)	21215.9	D_3 D_3	*1845.7 (5)	54180	P_3 P_3
4709.45 (1)	21228.0	D_3 D_3	*1844.4 (0)	54219	P_1 P_0
4706.41 (0)	21241.7	D_3 D_3	*1843.5 (0)	54246	P_1 P_1
4704.33 (0)	21251.1	D_3 D_1	*1842.4 (0)	54277	P_0 P_1
4702.57 (0)	21259.0	D_3 D_3	*1841.1 (1)	54316	P_1 P_3
4700.12 (0)	21270.1	D_3 D_3			
*4698.62 (0)	21276.9	D_1 D_0			
(4697.83)	(21280.5)	D_1 D_1			
4695.91 (1)	21289.2	D_1 D_3			
(4694.34)	(21296.3)	D_0 D_1			

* Not recorded in previous paper.

† Identified by W. E. Pretty.

Summary.

In further investigating the spectrum of ionised nitrogen, nine terms belonging to a quintet system have been identified and two new terms of the triplet system. Some 75 lines have been newly classified.

The author wishes to thank Prof. Fowler for the kindly help and advice which he has always given.

The Structure of the High Pressure Carbon Bands and the Swan System.

By R. C. JOHNSON, M.A., D.Sc., and R. K. ASUNDI, B.A., M.Sc., University of London, King's College.

(Communicated by T. R. Merton, F.R.S.—Received May 8, 1929.)

Introduction.

The so-called high pressure "CO" bands—or high pressure carbon bands, as they are better called—were first found by Fowler* in 1910 in tubes containing carbon monoxide at relatively high pressures. The system was described as consisting of some six apparently double-headed bands degraded to the violet, their wave-lengths being approximately at—

$$\begin{array}{cccccc} 6441 \} & 5897 \} & 5431 \} & 5030 \} & 4679 \} & 4365 \} \\ 6420 \} & 5878 \} & 5413 \} & 5015 \} & 4663 \} & 4353 \} \end{array} \text{ A.U.}$$

In 1923 the conditions of production of this spectrum were further investigated by Merton and Johnson† who obtained the bands with considerable strength by condensed discharges in capillary tubes fitted with carbon electrodes, and containing CO at pressures of 5 mm. and more. It was found that while the high pressure bands and the Swan bands were mingled in the light from the capillary of the tube, the former bands were isolated in bluish jets where the two ends of the capillary merged into the wider parts of the tube. Further observations indicated that the introduction of a little CO₂ destroyed the bands, but that the system re-appeared after a few minutes, in which time presumably the carbon dioxide had been reduced to monoxide by the carbon electrodes. A reproduction of these bands photographed under low dispersion is given in the above-mentioned paper.

No further experimental work appears to have been done on this system, and it has not been correlated with any other band system or assigned any place in the system of electronic levels of the CO molecule. We have therefore made an attempt to photograph the system under high dispersion with a view to fine structure analysis and identification of the molecular emitter. For this purpose large discharge tubes having a bore of about 15 to 20 mm. and a length of 60 or 70 cm. were used. These had at least one of the electrodes

* 'M.N.R.A.S.' vol. 70, p. 484 (1910).

† 'Roy. Soc. Proc.,' A, vol. 103, p. 386 (1923).

made of carbon and were fitted with side bulbs containing caustic potash and phosphorus pentoxide and a palladium regulator. The tubes were filled with carbon monoxide to such a pressure (probably 20–40 mm.) that a condensed discharge could just be forced through by the $\frac{1}{4}$ kilowatt 15,000 volt transformer used. Some of the tubes had large side flasks attached to them, increasing thereby the volume of gas in the tube, and giving the tubes a life of 4 to 6 hours during which the high pressure bands were emitted strongly. After some such period the pressure fell below the optimum value, and deposits of carbon had accumulated on the walls of the tube. Impurities such as hydrogen, carbon dioxide, and water-vapour were found to inhibit formation of the high pressure bands, and the tube always attained its best condition after running for about an hour (removing meanwhile any little hydrogen present through the regulator). Under these conditions the wide bore is practically filled with light, and presents a remarkable appearance, as of dense pale blue puffs of smoke (showing the high pressure system), threaded by a narrow green ribbon (showing the Swan system). If side tubes having a fair capacity (*e.g.*, flasks) are attached to the discharge tube the high pressure glow is capable of diffusion into these. The appearance is suggestive of an afterglow emitter, but if this is its true nature it is of very short duration. Photographs of the H.P. bands were taken in times varying from 4 to 10 hours in the first order of a 21-foot grating. The green band in the neighbourhood of λ 5000 is exceedingly faint and was not attempted. Before considering the results obtained it will be an advantage to summarise our present knowledge of the Swan spectrum and its emitter, with which it will subsequently be shown that the high pressure carbon system is intimately related.

The Swan System.

The origin of this system has been the object of much controversy, although recently general agreement appears to have been reached that the emitter is a C_2 molecule. In 1926 an investigation of the system was made by one of the writers* who arrived at the conclusion that a HC-CH molecule was responsible. Since that time the definite recognition of band spectra from the molecule BeO^\dagger (which has the same number of electrons as C_2), and more especially the rapid theoretical developments due to the work of Mulliken‡ and others, have not only removed any intrinsic objection to a C_2 emitter but have given it

* 'Phil. Trans.,' A, vol. 226, p. 157 (1927).

† 'Roy. Soc. Proc.,' A, vol. 122, p. 211 (1929); 'Phys. Rev.,' vol. 33, p. 163 (1929).

‡ 'Phys. Rev.,' vol. 29, p. 637 (1927).

strong support. In addition, experimental work such as that of Pretty,* has shown that the Swan bands can be produced by a condensed discharge through CO, free as far as possible from hydrogen and water-vapour, and with an intensity apparently independent of the amount of hydrogen which may be introduced. Mention may also be made in passing of a paper by Shea,† who has published detail of a fine-structure analysis of five bands of the Swan system, in which a correction has been made to the author's previously assigned j -values. Shea has also derived accurate values of the molecular constants.

In the next section of this communication it will be shown that the Swan system and the H.P. carbon system have a common final state, and this furnishes entirely new and reliable evidence that the emitter responsible for both systems is certainly not a hydrocarbon and must indeed be a C_2 molecule. The inhibiting effect of hydrogen on the H.P. carbon system is definitely against a hydrocarbon emitter on the one hand, while on the other hand there is convincing evidence against an oxycarbon emitter for the Swan system (*vide* 'Phil. Trans.,' vol. 226, pp. 186-190). On the basis of a C_2 emitter much, if not all, of the experimental data described in that paper find a favourable explanation in the light of more recent developments. We take a few examples of this. The similarity between the Swan spectrum and the Second Positive Nitrogen spectrum—while a close one—is by no means as complete as was previously supposed. Both systems arise from $^3P \rightarrow ^3P$ transitions and the band structure in both cases exhibits σ -type rotational doubling. In the Swan molecule, however, rotational levels of one of the electronic states are *completely* suppressed (giving rise to the recorded staggering effect in the band structure), while in the Nitrogen molecule there is only a *partial* suppression. It may also be mentioned that while the two 3P states of the N_2 molecule are *normal* those of the Swan emitter are probably *inverted*. Such differences are intelligible if the emitters are C_2 and N_2 . Other experimental observations such as the association of the Swan bands with the CH bands λ 4315, etc., are to be expected under the experimental conditions described in the above-mentioned paper in which both carbon and hydrogen were present. Equally it is to be noted, Pretty's experiments produced the Swan bands in CO when no trace of the CH bands or H α was observed. These facts are consistent with a C_2 emitter and the present writers endorse this view.

* 'Phys. Soc. Proc.,' vol. 40, p. 71 (1928).

† 'Phys. Rev.,' vol. 30, p. 825 (1927).

Correlation of the H.P. Carbon Bands and the Swan System.

The six recorded H.P. bands belong to a single n'' progression ($n' = 0$). The proximity of the coefficient of n'' to that of the Swan system first suggested the possibility of a relationship between these systems. A careful search was subsequently made in the near ultra-violet and four comparatively faint bands were recorded. These therefore become the (0, 0), (0, 1), (0, 2), and (0, 3) bands of the system, and the correct n'' values of the six previously known bands are given by (0, 4) to (0, 9). By the use of neo-cyanine plates we have also identified two additional bands (0, 10) and (0, 11) in the near infra-red. These data are given in Table I and have been expressed by the formula :

$$\nu = 29212 - (1627n'' - 11.7n''^2) \quad (1)$$

Table I.—High Pressure Carbon Bands.

n'' ($n' = 0$).	Int.	λ (air) I.A.	$\nu_{\text{vac.}}$	$\Delta\nu$ O.—C.
0	1	3419	29241	+29
1	1	3619.5	27620	+23
2	1	(Conf.)	—	—
3	2	4093	24426	—10
4	7	4368.82	22883	— 8
5	15	4680.17	21361	— 8
6	1	(V. Faint)	—	—
7	5	5434.93	18394	— 2
8	10	5899.27	16946	+ 2
9	8	6442.27	15518	+ 1
10	6	7083.2	14114	+ 2
11	4	7852.5	12731	0

The (Obs.—Calc.) values of column 5 are satisfactory when it is recalled that the bands (0, 0) to (0, 3) are particularly faint and settings were made on the apparent centre of the unresolved band-work. The other data refer to the band *heads*, all of which are degraded to the violet. The intensities of column 2 are approximate photographic intensities only, and are to be regarded as descriptive rather than quantitative. They illustrate, however, the main features of the peculiar intensity distribution, which has a notable minimum at about the (0, 6) band. The same oscillating intensity phenomenon is also found in the β bands of NO ($^2P \rightarrow ^2P$),* and as far as we know it has received no theoretical explanation. Equation (1) may be compared with the expression for the origins of the Swan system :

$$\nu = 19379.20 + (1773.42n' - 19.35n'^2) - (1629.88n'' - 11.67n''^2). \quad (2)$$

* 'Phil. Mag.,' vol. 2, p. 631 (1926).

It is at once apparent that the two-band systems have a common final electronic state, which is almost certainly the normal state of the C_2 molecule. The small difference between $f(n'')$ as deduced from the H.P. carbon system and the Swan system is accounted for by the fact that in the former case the wave-numbers relate to band heads, and in the latter case to band origins.

It may perhaps be mentioned at this point that the apparent doublet character of the H.P. bands as seen under low dispersion is due merely to condensations which constitute the P and R branches.

Fine-Structure of the H.P. Carbon Bands.

As previously mentioned, photographs of the H.P. carbon bands have been obtained in the first order of a 21-foot grating of the bands (0, 4), (0, 5), (0, 7), (0, 8) and (0, 9). Except in the case of the (0, 5) band these were not sufficiently strong to permit of satisfactory reproduction. The H.P. bands bear an exceptionally close resemblance in their fine-structure to the Swan bands as developed under low temperature conditions, and the Swan band λ 4737 of spectrum 3 ('Phil. Trans.,' vol. 226, opp. p. 230, 1927) may be taken as typical of the appearance of the H.P. carbon bands.

The H.P. bands consist of P and R branches only, and they undoubtedly represent a transition $^3P \rightarrow ^3P$. In the absence of fine-structure data Mulliken* had speculated that they might possibly arise from a $^1P \rightarrow ^1P$ transition of the molecule C_2 . This is now, however, seen to be impossible. We thus have knowledge at present of three levels of the C_2 molecule and these are all 3P levels. As in the case of the Swan bands, the first 16 to 18 members of the P branch (which goes to the head) either are not of sufficient strength or are insufficiently resolved to make identification possible. Under low temperature conditions, these constitute almost the whole of the P branch, and thus no analysis of the data by means of the combination principle has been possible. We have, however, been able to distinguish many of the triplets of the R branches of the bands, and to trace these, in part or whole, back to the band origins. The data for the (0, 7) yellow-green band proved somewhat fragmentary in this respect, and have therefore not been included in this paper. The data in the case of the violet (0, 4), blue (0, 5), yellow (0, 8) and red (0, 9) R branches are of sufficient reliability and interest to justify their inclusion. Tables II, III, IV and V contain these data. It was at first intended to make calculations of the moment of inertia of the molecule in several of the final vibrational states, by analysis of the data of the R branches only, but the

* 'Phys. Rev.,' vol. 32, p. 214 (1928).

existence of perturbations led to the abandonment of this project. Nevertheless, the application of approximate graphical methods to the data, indicated for the moments of inertia of the vibrational states $n'' = 5, 8$ and 9 , values of the same order as those which are deducible from analysis of the Swan system.

Table II.— (ν_{vac}) R-branch Data of H.P. Band λ 4368.82.

j_1	R_2	Δ_{21}	R_1	Δ_{10}	R_0
$3\frac{1}{2}$			22936.4		
$4\frac{1}{2}$			38.3		
$5\frac{1}{2}$			40.0		
$6\frac{1}{2}$			42.8	(6.4)	22936.4
$7\frac{1}{2}$			45.2	(5.2)	40.0
$8\frac{1}{2}$			47.4d	(4.6)	42.8
$9\frac{1}{2}$			50.3d	(4.3)	46.0d
$10\frac{1}{2}$			53.7d	(3.4)	50.3d
$11\frac{1}{2}$	22957.6d	(0.4)	57.2d	(2.5)	54.73d
$12\frac{1}{2}$	61.7	(1.0)	60.7	(2.3)	58.4
$13\frac{1}{2}$	67.31	(1.57)	65.74	(1.33)	64.41
$14\frac{1}{2}$	72.60	(1.39)	71.21	(1.69)	69.52
$15\frac{1}{2}$	76.20	(1.13)	75.07	(1.05)	74.02
$16\frac{1}{2}$	80.65	(1.11)	79.54	(1.22)	78.32
$17\frac{1}{2}$	84.27	(0.94)	83.33	(0.81)	82.52
$18\frac{1}{2}$	89.22	(1.08)	88.14	(1.08)	87.06
$19\frac{1}{2}$	92.40	(0.54)	91.86	(0.66)	91.20
$20\frac{1}{2}$	98.02	(0.81)	97.21	—	—
$21\frac{1}{2}$	—	—	99.40	(0.39)	99.01
			A \rightarrow A.		
			B \rightarrow B.		

Table III.—(ν_{vac}) R-branch Data of the H.P. Band λ 4680.17.

j_1	R_2	Δ_{21}	R_1	Δ_{10}	R_0
$1\frac{1}{2}$			21410.2	(12.4)	21397.8
$2\frac{1}{2}$			12.1	(10.1)	21402.0
$3\frac{1}{2}$			14.0	(8.7)	05.3
$4\frac{1}{2}$			15.74	(6.3)	09.4
$5\frac{1}{2}$			18.7d	(5.7)	13.0
$6\frac{1}{2}$			21.1	(5.4)	15.7
$7\frac{1}{2}$			23.5	(4.8)	18.7d
$8\frac{1}{2}$	21427.3	(0.7)	26.6	(4.5)	22.1
$9\frac{1}{2}$	31.3	(1.2)	30.1	(3.53)	26.57
$10\frac{1}{2}$	35.23	(1.5)	33.74	(3.61)	30.13
$11\frac{1}{2}$	38.97d	(1.5)	37.48	(3.0)	34.50
$12\frac{1}{2}$	43.15	(1.61)	41.54	(2.8)	38.77d
$13\frac{1}{2}$	46.99	(2.21)	44.78	(1.63)	43.15
$14\frac{1}{2}$	50.52	(1.45)	49.07	(1.53)	47.54
$15\frac{1}{2}$	54.49	(1.12)	53.37	(1.10)	52.27
$16\frac{1}{2}$	59.41	(1.13)	58.28	(1.18)	57.10
$17\frac{1}{2}$	63.40	(0.79)	62.61	(0.94)	61.67
$18\frac{1}{2}$	68.98	(1.07)	67.91	(1.12)	66.79
$19\frac{1}{2}$	72.55d	(0.48)	72.07d	(0.70)	71.37
			A \rightarrow A.		
			B \rightarrow B.		

Table IV.—(ν_{vac}) R-branch Data of the H.P. band λ 5899.27.

j_1	R_1	Δ_{11}	R_1	Δ_{10}	R_0
$1\frac{1}{2}$			16976.4d		
$2\frac{1}{2}$			78.3d		
$3\frac{1}{2}$			80.3d		
$4\frac{1}{2}$			82.4		
$5\frac{1}{2}$			85.55		
$6\frac{1}{2}$			87.8	(5.4)	16982.4
$7\frac{1}{2}$			90.76	(5.2)	85.55
$8\frac{1}{2}$	16995.45	(1.05)	94.4	(4.8)	89.6
$9\frac{1}{2}$	17000.11	(1.8)	98.33	(3.95)	94.38
$10\frac{1}{2}$	04.93	(2.1)	17002.81	(3.9)	98.92
$11\frac{1}{2}$	09.68	(2.42)	07.26	(3.11)	17004.15
$12\frac{1}{2}$	14.76	(2.4)	12.37	(3.17)	09.20
$13\frac{1}{2}$	18.59	(2.14)	16.45	(1.71)	14.74
$14\frac{1}{2}$	23.46	(1.62)	21.84	(1.52)	20.32
$15\frac{1}{2}$	28.44	(1.13)	27.31	(1.13)	26.18
$16\frac{1}{2}$	34.94	(1.36)	33.58	(1.29)	32.29
$17\frac{1}{2}$	40.18	(0.90)	39.28	(0.91)	38.37
$18\frac{1}{2}$	47.49	(1.22)	46.27	(1.22)	45.05
$19\frac{1}{2}$	52.53	(0.59)	51.94	(0.82)	51.12
$20\frac{1}{2}$	60.88d	—	59.59	—	—
$21\frac{1}{2}$	—	—	—	—	—
$22\frac{1}{2}$	75.16	(0.74)	74.42	(1.05)	73.37
			A \rightarrow A.		
			B \rightarrow B.		

Table V.—(ν_{vac}) R-branch Data of the H.P. Band λ 6442.27.

j_1	R_0	Δ_{11}	R_1	Δ_{10}	R_0
$1\frac{1}{2}$			15545.15		
$2\frac{1}{2}$			47.17		
$3\frac{1}{2}$			49.1d		
$4\frac{1}{2}$			51.28		
$5\frac{1}{2}$			55.3		
$6\frac{1}{2}$			56.6		
$7\frac{1}{2}$			59.7		
$8\frac{1}{2}$	15564.8	(1.12)	63.68	(4.94)	15558.74
$9\frac{1}{2}$	69.65	(2.0)	67.68	(4.24)	63.44
$10\frac{1}{2}$	74.8	(2.5)	72.29	(3.76)	68.53
$11\frac{1}{2}$	79.78	(2.63)	77.15	(3.14)	74.01
$12\frac{1}{2}$	85.18	(2.84)	82.34	(3.10)	79.25
$13\frac{1}{2}$	89.10	(2.22)	86.92	(1.74)	85.18
$14\frac{1}{2}$	94.08	(1.52)	92.56	(1.53)	91.03
$15\frac{1}{2}$	99.77	(1.23)	98.54	(1.13)	97.41
$16\frac{1}{2}$	15606.30	(1.23)	15605.07	(1.24)	15603.83
$17\frac{1}{2}$	12.39	(0.94)	11.45	(0.93)	10.52
$18\frac{1}{2}$	19.76	(1.12)	18.64	(1.18)	17.46
$19\frac{1}{2}$	25.78	(0.67)	25.11	(0.73)	24.38
			A ↑	B ↑	

Perturbations.—The existence of perturbations in the R branches is exhibited by plotting the second differences (using the central component of each triplet) against j_1 values. Instead of being constant, these exhibit a violent oscillation. In fig. 1 are plotted such data derived from Tables III, IV and V (the violet band includes a few somewhat uncertain identifications and is therefore not used). It is, of course, true, that if a line has been incorrectly identified, then an oscillation of the $\Delta^2 R(j_1) : j_1$ curve will result. It will be observed, however, that there is a very precise correspondence of the deviations in all three bands. It is certain that perturbations are largely responsible for the curves of fig. 1

since otherwise (a) the close correspondence of the curves would require that a similar error (in both magnitude and direction) must have been made for

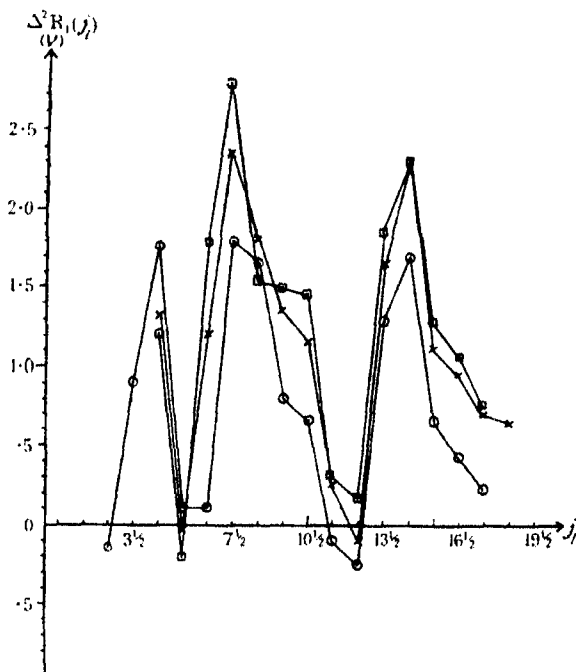


FIG. 1.—Perturbations in the R Branches of the H.P. Carbon Bands.
 ○ Blue Band. × Yellow Band. □ Red Band.

the corresponding member of each band, and (b) the fact that the second differences derived from the two alternate-missing-line series fall in the case of each band on to a fairly smooth oscillating curve will be unexplained. It is difficult with the present available data to say precisely which members are perturbed. There certainly appears to be a range of considerable disturbance between R ($12\frac{1}{2}$) and R ($7\frac{1}{2}$). It is clear that the perturbations are associated with the initial (excited) level of the H.P. bands since (a) they are common to all of the bands examined of the $n' = 0$ progression, and (b) there is no perturbation of the fine-structure of the Swan bands for these j_i values.

Attention may be drawn at this point to a feature which will be mentioned later, and which is shown in fig. 4. This is of the nature of a perturbation but appears to affect in this special way only the less refrangible components of the triplets. We refer to the discontinuity of about 1 v which occurs between $j_i = 12\frac{1}{2}$ and $13\frac{1}{2}$.

General Fine-Structure Interpretation.—From the close similarity of the Swan system and the high pressure carbon system, arising as they do in $^3P \rightarrow ^3P$ transitions in the C_2 molecule, it follows that within certain limitations to be discussed in the next section, the general interpretation of Swan structure given by Mulliken* is equally applicable to the H.P. bands. Fig. 2 illustrates

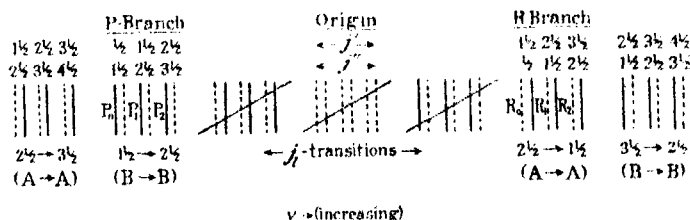


FIG. 2.—Fine-Structure near the Origin of typical H.P. and Swan Bands.

diagrammatically the structure of a typical Swan or H.P. band in the neighbourhood of the origin (except that to avoid confusion the rapid diminution in triplet width as we proceed outwards from the origin has not been indicated). Fig. 3

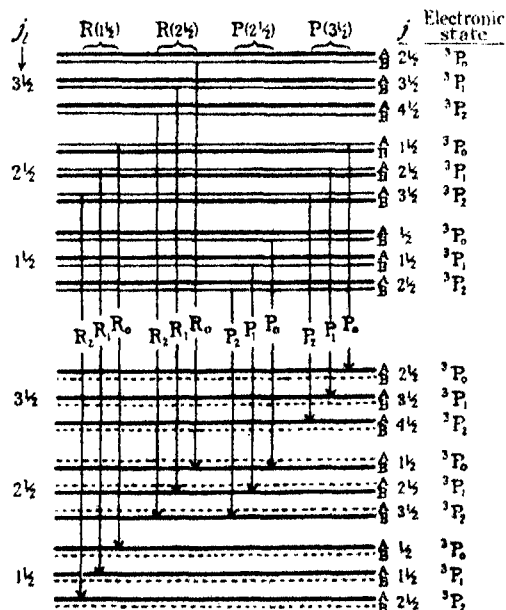


FIG. 3.—Rotational Transitions in a typical Swan Band.

has been constructed to show the precise transitions which are responsible for the band structure of fig. 2 in the case of the Swan bands. A slightly different

* 'Phys. Rev.', vol. 29, p. 644 (1927).

diagram appropriate to the H.P. bands is given later in fig. 5. In fig. 3 three rotational levels corresponding to values of $j_i^* = 1\frac{1}{2}, 2\frac{1}{2}, 3\frac{1}{2}, \dots$, have been drawn for each electronic state. Each rotational level is triple due to the presence of a resultant electronic spin momentum $s = 1$. Each component level is thus characterised by $j = j_i + s, j_i, j_i - s$, which is the vector sum of j_i and s . Each component of the triple levels is again double, the sub-states being denoted A and B (this is the so-called σ -type doubling). Transitions between sub-states $A \rightarrow A$ and $B \rightarrow B$ are permitted in the formation of P and R branches, and of the type $A \rightarrow B$ and $B \rightarrow A$ in the formation of Q branches. This particular hypothesis is at present accepted as a convention only, inasmuch as the reverse limitation may really be the true one.

The phenomenon of alternating intensities in band lines which occurs in all symmetrical molecules is manifest here in the case of C_2 . Analysis of the He_2 bands originally showed that the particular suppressed levels for the A and B sub-states were given by

$$\left. \begin{array}{lll} j_i = \sigma_i + \frac{1}{2}, & \sigma_i + 2\frac{1}{2}, & \sigma_i + 4\frac{1}{2} \dots\dots \text{B type} \\ j_i = \sigma_i + 1\frac{1}{2}, & \sigma_i + 3\frac{1}{2}, & \sigma_i + 5\frac{1}{2} \dots\dots \text{A type} \end{array} \right\} \quad (3)$$

and in the absence of evidence to the contrary it may be assumed that this is generally true for homo-polar molecules. Here, as we are dealing with P states we have $\sigma_i = 1$. In He_2 we appear to have an extreme type of symmetry in which *complete* suppression takes place for *all* electronic levels in accordance with equation (3). It will therefore be clear from fig. 3 that in He_2 , transitions between like electronic states, e.g., $^1S \rightarrow ^1S$, $^3P \rightarrow ^3P$ will be impossible. In the Second Positive Nitrogen bands ($^3P \rightarrow ^3P$) there is but partial suppression of the sub-states given by equation (3) for the various electronic levels. This means of course merely a reduction of intensity. All the six components corresponding to a single rotational transition $\Delta j_i = \pm 1, 0$, are thus present. The Swan triplets indicate total suppression in one of the electronic states only, although in the absence of further information from other spectra of the C_2 molecule it would remain an open question whether this was in the initial or final state. The similar triplet structure of the H.P. carbon bands suggests—though it is not conclusive—that total suppression probably takes place in the common final state. It is not possible with the available experimental evidence to say whether partial suppression takes place in the initial electronic state as well, since, as fig. 3 will show, successive triplets would be reduced in

* j_i replaces the j_k of Mulliken's earlier papers, and σ_i replaces σ_k . For the latest notation vide 'Phys. Rev.', vol. 32, p. 186 (1928).

intensity to the same extent. The intensities of the initial levels in fig. 3 have been drawn to indicate how partial suppression would operate, on the assumption that it does so. It will be clear from the figure how the joint action of the two effects: σ -type doubling and suppression of alternate rotational levels, results in the so-called "staggering" in position of the triplets of fig. 2. This phenomenon occurs in both the Swan and the H.P. carbon bands.

In regard to the number of missing lines near the origin, the minimum value of j_i is limited by $j_i > \sigma_i$, and σ_i for both initial and final states is 1. As we are dealing with a molecule having an even number of electrons j_i takes half-integral values (using the old quantum theory), and its minimum value in both initial and final states is $1\frac{1}{2}$. The first observable triplets of the two branches $R(j_i)$, $P(j_i)$ are therefore $R(1\frac{1}{2})$ and $P(2\frac{1}{2})$.

There remains one further remark to make in explanation of the labelling of the three components of any triplet as R_2 , R_1 , R_0 or P_2 , P_1 , P_0 . A somewhat different, and purely arbitrary numbering has been used by Mulliken* to distinguish the three components in the case of the Swan system. The designation employed in figs. 2 and 3 has the advantage of representing in the subscript a definite physical quantity σ , which on account of the selection principle $\Delta\sigma = 0$ is the same in the initial and final states.

The Triplet Intervals in the H.P. System.—The variation in triplet width from large values near the band origin to vanishingly small values for j_i large, is attributable to a change of the condition of the molecule from Hund's case (a) to Hund's case (b).† The facts briefly stated are these. In a diatomic molecule the total orbital angular momentum of the electrons, represented by the quantum number l (the group quantum number of atomic spectra), is in precession about the strong electric field along the inter-nuclear axis. The quantised component of l along this axis, viz., σ_l , is therefore responsible for a magnetic field in this direction, which, under the conditions of case (a) is the dominating magnetic field of the molecule. The resultant electronic spin momentum s (the algebraic sum of the several electronic spins $s_i = \pm \frac{1}{2}$) which is orientated by the internal magnetic field of the molecule is thus quantised with respect to the inter-nuclear axis, about which it precesses. Its quantised component σ_s along this axis may therefore take any one of the values lying between s and $-s$. In the case of a 3P molecular state we thus have $\sigma_l = 1$, $s = 1$, and hence $\sigma_s = 1, 0, -1$. This gives three values for

* 'Phys. Rev.', vol. 29, p. 644 (1927).

† 'Z. Physik,' vol. 36, p. 657 (1926).

$\sigma (= \sigma_i + \sigma_s)$, viz., 2, 1, and 0, which distinguish the three components of each rotational level. The vector sum of σ and m gives j the total angular momentum of the whole molecule. The rotational terms in Hund's case (a) are therefore given by

$$F(j) = f(\sigma) + B(j^2 - \sigma^2) \quad (4)$$

giving the triple structure when for σ its three values 0, 1 and 2 are substituted.

Case (b) arises when σ_i no longer gives rise to the dominating magnetic field in the molecule, and when as a result, it is no longer in exclusive control of the orientation of s . When, for example, rotation of the molecule takes place, there is a magnetic field along the m -axis, and s will then be quantised with respect to the resultant field, i.e., along the j_i axis. This quantum number may appropriately be described as j_s , and may take values lying between s and $-s$, (precisely as did σ_i above). The resultant momentum of the whole molecule is here given by $j = j_i + j_s$. The structure of the rotational terms is then given by

$$F(j) = f(j, j_s) + B(j^2 - \sigma_i^2) \quad (5)$$

corresponding to triplets of constant separation when case (b) is fully attained. In practice between low and high values of j there is a transition stage in which we pass from conditions of approximately case (a) to case (b). This variable element in the triple separation is represented by the term $f(j, j_s)$ which for large j values will, of course, attain a constant value dependent on the particular value of j_s .

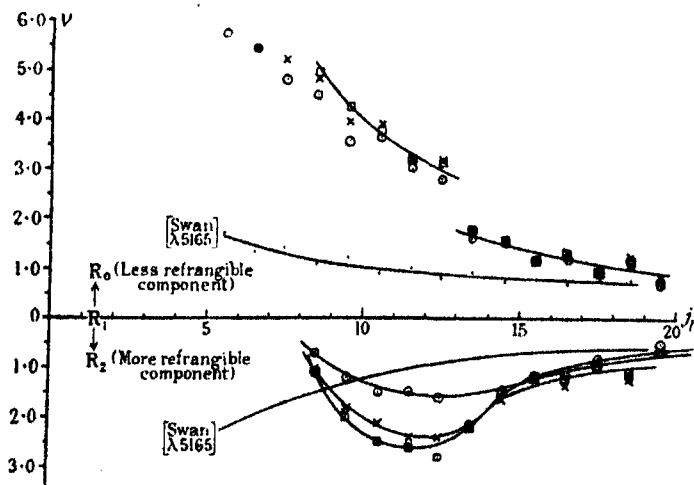


FIG. 4.—Triplet Intervals in the R Branches of the H.P. Carbon Bands.
 ○ Blue Band. × Yellow Band. □ Red Band.

We proceed now to consider the special case of the triplet intervals in the H.P. carbon bands. The data for the R branches of the red, yellow and blue bands have been plotted in fig. 4, and for comparison the triplet intervals of the Swan band λ 5165 have been plotted on the same diagram. The j_i axis represents the position of the central component R_1 , and the separations of the less refrangible and more refrangible components R_0 and R_2 respectively, are plotted above and below the line. There are several remarkable features.

(1) There is a notable discontinuity in the disposition of the R_0 branch at $j_i = 12\frac{1}{2} : 13\frac{1}{2}$. (To avoid undue complication of the R_0 branch below this point a smooth line has been drawn in the case of the red band only.) The effect is very remarkable and occurs in the case of all the bands at precisely this value of j_i .

(2) The R_2 branch presents an anomaly of a different character, which appears to begin at about the same value of j_i as the above and may be related to it. The R_1R_2 interval gradually ceases to increase as j_i diminishes, and ultimately a coalescence of the R_1R_2 components takes place at about $j_i = 7\frac{1}{2}$. The deflection of the R_2 component in fig. 4 appears the most marked in the case of the blue band, and it would be of considerable interest to have information of the magnitude of this effect in the bands of still lower final vibrational quantum number.

(3) As in the case of the Swan bands for high j values, there is a more rapid approach of R_2 to R_1 than of R_0 to R_1 , ultimately, we may presume, resulting in a coalescence of the two components. In the Swan band λ 5165 this takes place at about $j_i = 50$. We may perhaps summarise this anomaly and the preceding one described in (2) by remarking that there appears to be much less permanency about the component branch which has j_i in the same sense as j_i .

(4) The variation of triplet width with vibrational quantum number is comparatively small, especially for the higher j_i values (excepting of course, the anomalous region below $13\frac{1}{2}$ of the R_2 branch). The graph of triplet width for the (0, 0) Swan band in fig. 4 would thus be but little different for the (0, 1), (0, 2), etc., bands. It will be observed that the triplet width in the H.P. carbon bands is greater than that of the Swan bands. These observed triplet widths represent, as we see from fig. 3, the difference between the triplet separations of the initial and final electronic states. We should anticipate this feature as a consequence of the regular diminution in triplet width for the higher excited 3P levels. Now there is good reason to believe, as Mulliken* has

* 'Phys. Rev.', vol. 32, p. 186 (1926).

indicated, that both the normal and the initial Swan states of the molecule are *inverted* 3P states. This is discussed fully in the concluding part of the present paper. It is not, however, possible to draw any conclusion from the previous observation of the relative triplet widths in the two band systems as to the character (normal or inverted) of the initial 3P level of the H.P. system. On either hypothesis plausible values of the triplet separations can be constructed for the three known electronic states. We mention here, however, that other considerations based on the construction of the C_2 molecule have led us to the conclusion that the initial H.P. level is a *normal* state, and contrasts in this respect with the other two. The rotational transitions giving rise to the H.P. bands are thus of the type shown in fig. 5.

(5) In fig. 4 in the unperturbed parts of the R branches (between about $j_1 = 13\frac{1}{2}$ and $19\frac{1}{2}$) it is of interest to compare the magnitude of the stagger in *triplet width*, in the case of the H.P. bands and the Swan bands. Although this is not, as far as we can see, directly correlated with the positional staggering of the triplets, nevertheless its magnitude is probably an indirect indication of the magnitude of the σ -type doubling (*i.e.*, of the A-B sub-state separation) in the three electronic levels. The observed stagger represents

the difference of these two separations for the initial and final states of that particular system. As the magnitude of the effect is greater in the H.P. bands than in the Swan bands (*vide* fig. 4), it follows that the AB sub-state separation is considerably less for the initial state of the H.P. system than for the initial state of the Swan system. It is therefore probable that the latter is also smaller than the separation in the ground state.

The Structure of the C_2 Molecule.

In an important new series of papers by Mulliken* (based on the previous fundamental work of Hund†) we have laid for us the foundations of a detailed

* 'Phys. Rev.', vol. 32, p. 186 (1928), and vol. 32, p. 761 (1928).

† 'Z. Physik,' vol. 36, p. 657 (1926); vol. 37, p. 742 (1927); vol. 42, p. 93 (1927), and vol. 43, p. 805 (1927).

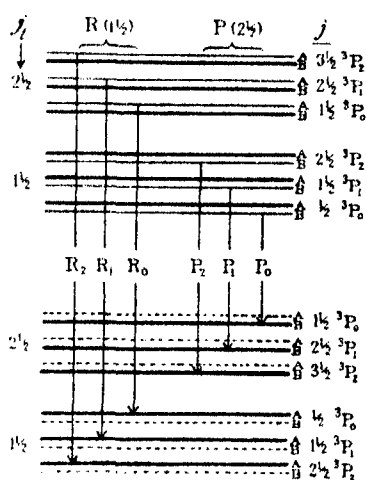


FIG. 5.—Rotational Transitions in a typical H.P. Carbon Band.

knowledge of the structure of diatomic molecules. By such detailed knowledge we mean the values of n , l , σ , and s , ($= \frac{1}{2}$) for each electron of the molecule, together with the resultant l , σ , and s of the molecule as a whole. The methods which have been developed by Hund and Mulliken make use of band spectra data such as the evidence of fine-structure analysis, energy of dissociation, multiplet widths, and excitation potentials, and involve the important basic principles applied by Hund to line spectra, and an extended application of the Pauli principle to the "united atom." This work is difficult to summarise and reference should be made to the original papers. We proceed here to deal specifically with the C_2 molecule. We must derive three different electronic structures which all give 3P states and for which the two known transitions are possible and in accordance with the selection rule $\Delta l = \pm 1$. Our knowledge of adjacent molecules CN , N_2 , and CO , must lead us to anticipate that these particular transitions will be of the right energy order. It must be shown that the molecule can be synthesised from two carbon atoms in low-lying states, and conversely, the vibrational energy of dissociation of the molecule in these three electronic states must be consistent with the states of the two carbon atoms from which it can be built. Finally, we should be able to account for the peculiar experimental conditions (high pressure carbon monoxide) which seem to be necessary for the formation of one of the 3P states of the C_2 molecule.

Table VI.—States of the Carbon Atom.

(1) State without field.	(2) State with field.	(3) Detailed configuration with field.	(4) Component states in each configuration.	(5) Configura- tion summary.
3P	$\begin{cases} ^3S^P \\ ^3P_{2,1} \end{cases}$	$\begin{cases} (1s)^2(2s)^2(2p^2)^2 \\ (1s)^2(2s)^2(2s^2)(2p^2) \end{cases}$	$\begin{cases} (3) \quad \sigma_z = 0, \sigma_x = 1, 0, -1 \\ (6) \quad \sigma_z = \pm 1, \sigma_x = 1, 0, -1 \end{cases}$	$\begin{cases} s^4p^2 \\ s^2p^4 \end{cases}$
1D	$\begin{cases} ^1S^D \\ ^1P^D \\ ^1D^D \end{cases}$	$\begin{cases} (1s)^2(2s)^2(2s^2)^2 \\ (1s)^2(2s)^2(2s^2)(2p^2) \\ (1s)^2(2s^2)^2(2p^2)^2 \end{cases}$	$\begin{cases} (1) \quad \sigma_z = 0, \sigma_x = 0 \\ (2) \quad \sigma_z = \pm 1, \sigma_x = 0 \\ (2) \quad \sigma_z = \pm 2, \sigma_x = 0 \end{cases}$	$\begin{cases} s^4 \\ s^2p^2 \\ s^4p^2 \end{cases}$
1S	$^1S^S$	$(1s)^2(2s)^2(2p^2)^2$	$(1) \quad \sigma_z = 0, \sigma_x = 0$	s^4p^2

In Table VI are given some data of the carbon atom. The three lowest states of the atom are known to be 3P , 1D , and 1S , rising in the order given. These arise from the carbon atom $(1s)^2(2s)^2(2p)^2$. In column 2 are given the incipient states of the molecular type which are inherent in the atom when

placed in an electric field. From these can be inferred the detailed electronic configurations which give rise to them, by using the data of Table I in Mulliken's paper. Details of these configurations are given in column 3. Column 4 gives the number of component states for each configuration class. In column 5 is Mulliken's brief and convenient summary of the configuration data of column 3. This latter description of the quasi-molecular state of the "atom in the field" is adequate for many purposes, inasmuch as when the molecule is formed by bringing close together two such atoms (the strong inter-nuclear field then replacing the artificial electric field) the molecular configuration class is simply obtained by addition of these data. This is the σ_l conservation rule. We cannot, however, deduce the *detailed* structure of the molecule by merely adding the two appropriate rows of column 3. The Pauli restriction principle limits the number of electrons in the molecule of any given type, and to form the molecule, "promotion" of some of the electrons is necessary. This convenient term is employed by Mulliken to indicate a forced increase of the principal quantum number of an electron (accompanied, of course, by an appropriate change $\Delta l_r = \pm 1$ in l).

Mulliken's view of the structure of the C_2 molecule in its ground state and in the initial Swan state is as follows :—

$$\left. \begin{array}{l} \text{Ground State : } (1s^s)^2 (2s^p)^2 (2s^s)^2 (3s^p)^2 (2p^p)^3 (3s^s) : {}^3P_1^P \\ \text{Initial Swan State : } (1s^s)^2 (2s^p)^2 (2s^s)^2 (3s^p) (2p^p)^3 (3s^s)^2 : {}^3P_1^D \end{array} \right\} \quad (6)$$

The electron types are given in the order which experimental evidence shows to be that of diminishing energy of binding. The characteristic $(2p^p)^3$ group, which requires one more electron to complete the shell, is responsible for the inverted character of the triplet level. The molecule is assumed to be of the s^0p^3 type since this would give inverted 3P levels, rather than, for example, of the s^7p^5 type which would have normal 3P levels. This is because in the adjacent molecule CN there is definite evidence that (in contrast to the united atom) the 3P levels *are* inverted, and therefore must contain the group $(2p^p)^3$. The C_2 molecule given above in (6) can be constructed from carbon atoms in several different states. We have selected from Table VI those pairs of atomic states which will give a s^0p^3 molecule in 3P molecule states, and have listed these in Table VII. (The molecular states are derived by compounding each pair of states of column 2.) Table VII is by no means a complete list of the pairs of atomic states which will provide a 3P molecular state. A considerable number of others can be derived from carbon atoms in excited states such as 3S , 1P , 3D , etc. The three states, ${}^3P_{0.1.2}$, 1D_2 and 1S_0 ,

Table VII.—Synthesis of States of the C_2 Molecule.

Atom states without field.	Atom states with field.	Molecular states.
$^3P + ^3P$	$^3P_{\pi} + ^3S^P$	$^1P, ^3P, ^1D, ^3P_i$
$^3P + ^1D$	$^3S^P + ^1P^D$	$^3P, ^1D, ^1P$
$^3P + ^1D$	$^3P_{\pi} + ^1D^D$	$^3P, ^1D, ^1P, ^3P$
$^3P + ^1S$	$^3P_{\pi} + ^1S^S$	$^3P^P$

are, however, the lowest states, and according to Fowler and Selwyn* their term values (below the ionisation level) are $\left\{ \begin{array}{l} 91017.3 \\ 91002.5 \\ 90975.0 \end{array} \right\}$, 81312 and 69860 v.

All such pairs of atomic states from which the known 3P molecular states can be synthesised, are theoretically possible products of dissociation. The actual products can only be determined if the energy of dissociation (D) of the molecule is known for that particular state. The values of D are known for the ground state and the initial (Swan) state of the C_2 molecule. For the ground state $D_0 = D = 7.02$ volts, and as Mulliken suggests, it is reasonable to suppose that the products are two 3P atoms. For the initial (Swan) state the data are less reliable. D_0 has been given as 5.0 volts,† and from this $D = 5.0 + 2.4 = 7.4$ volts. Mulliken gives $D_0 = 6.4$ volts and from this $D = 8.8$ volts. It seems probable, however, as Mulliken suggests, that the dissociation products of the molecule in this state are a 3P and 1D atom. From Fowler and Selwyn's data the 1D state corresponds to an excitation of about $\nu 9690$ ($= 1.2$ volts) above the normal. In this case the best value of D for the initial (Swan) state is probably $7.0 + 1.2 = 8.2$ volts, and hence D_0 should be 5.8 volts.

We shall now discuss the structure of the molecule in the initial H.P. state. We can theoretically derive an excited inverted 3P state of the C_2 molecule by displacing one of the ($2s^2$) electrons to the ($3s'$) shell, but the energy to do this is probably far in excess of the excitation potential (3.61 volts) of the H.P. bands. Alternatively, we might imagine the outermost electron ($3s'$) excited to ($4s''$), but if so this type of transition is of the "optical" type rather than of the "X-ray" type (to which the Swan bands belong).

Incidentally, we may remark that most of the molecular electronic transitions

* 'Roy. Soc. Proc.,' A, vol. 118, p. 34 (1928).

† 'Phil. Trans.,' A, vol. 226, p. 181 (1927).

discussed by Mulliken are described by him as of this "X-ray" type. This valuable conception seems to us to throw light on a puzzling feature associated with the terms of many molecules. If the ionisation potential v_i of the molecule is available, it is well known that the effective principal quantum numbers of the various terms can be deduced from $\sqrt{R/(v_i - v)}$. Now for molecular terms of the same type these quantum numbers are seldom found to differ by unity—as they should do if, as in atoms, the electronic terms are expressible by a Rydberg formula. We can thus say that if the effective principal quantum numbers of molecular terms increase by unity (as in He_2 , for example), this is evidence that the electronic transitions are of the atomic or "optical" type. But if, as is frequently the case, there is no simple relationship between the effective quantum numbers, it is evidence of the "X-ray" type of transition. There is, in fact, no simple meaning to be attached to the effective principal quantum number of the molecular term in these cases. The electronic transition giving the Swan bands, for example, is $(3s') \rightarrow (3s'')$ involving a change in l , only.

We are of the opinion that the structure of the C_2 molecule in the initial (H.P.) state is :

$$(1s')^2 (2s'')^2 (2s'')^2 (3s'')^2 (2p'')^2 (3s') (3p'') : {}^3P_n'' \quad (7)$$

This produces a *normal* 3P state, and the electronic transition giving the H.P. bands is $(3p'') \rightarrow (2p'')$. Details of the typical rotational transitions have already been given in fig. 5. Unfortunately the H.P. bands consist of one ($n' = 0$) progression only, and the vibrational energy of dissociation of the molecule in this state is not known. We suggest, however, that the dissociation products are possibly a 3P and a 1S atom, in which case we predict $D = 9.63$ volts, and hence $D_0 = 9.63 - 3.61 = 6.02$ volts.

The experimental conditions under which the H.P. bands are produced call for some discussion. We should be disposed at first sight to imagine that a C_2 molecule loaded with 3.61 volts energy could be produced in such gases as CO_2 , C_2N_2 , C_2H_2 , etc., as well as in CO . We incline to the opinion that the difference is found in the comparatively low resonance potentials of these gases. That of CH is 2.86 volts; that of CN is 3.18 volts. C_2 molecules of 3.61 volts energy would be unlikely in the presence of a large excess of such molecules as these which have lower excitation potentials. The inhibiting effect of traces of hydrogen, water-vapour, carbon dioxide, etc., in CO is explicable along these lines also. On the other hand the resonance potential of CO is 5.98 volts,* and C_2 molecules of 3.61 volts energy will be capable of

* Corresponding to the excitation of the Cameron bands.

existence among these, inasmuch as collisions will be possible without loss of energy. The rôle of pressure in the production of the spectrum is more obscure.

The absence of a combination system between the initial H.P. level and the initial Swan level is in harmony with Hund's selection principle $\Delta l_r = \pm 1$ for symmetrical molecules. On this basis the ground state and two excited states have been classed as $^3P_i^P$, $^3P_i^D$, and $^3P_n^D$.

It is scarcely necessary to add in conclusion that there remain a vast number of problems to which theory at present gives no answer. It is, for example, remarkable that of the theoretically possible C_2 molecules which may be constructed from the data of Table VI: s^8p^4 , s^9p^3 , $s^{10}p^2$, etc., we should only have spectroscopic evidence of one of these, and that in this molecule (s^9p^3) only the 3P state is found out of the possibilities 3P , 3S , 3F , 1P , 1F , 5P . Such problems as these will require a fuller understanding of molecular structure.

Summary.

(1) The conditions of production of the high pressure carbon system and the Swan system are discussed. Both these systems are due to a C_2 molecule.

(2) Four new H.P. bands have been found in the near ultra-violet, and two more in the near infra-red. These, with the known bands, form a single vibrational progression ($n' = 0$), and the H.P. system and the Swan system are found both to represent transitions to a common final state.

(3) The fine-structure of the H.P. bands (0, 4), (0, 5), (0, 8) and (0, 9) has been investigated. The bands consist of P and R branches only, and the electronic transition involved is $^3P_n^D \rightarrow ^3P_i^P$.

(4) Detailed examination of the structure of the R branches of these bands has revealed several anomalies and perturbations of an unusual type.

(5) The methods employed by Hund and Mulliken for the elucidation of molecular structure are summarised, and Mulliken's application to the C_2 molecule has been extended to cover the initial state of the H.P. system. This is believed to be a *normal* 3P level and different in this respect from the two lower 3P levels which are believed to be inverted.

On the Direct Determination of the Electrostatic Moments of Molecules.

By R. J. CLARK, Carnegie Teaching Fellow in the University of Edinburgh.

(Communicated by Sir Ernest Rutherford, P.R.S.—Received May 13, 1929.)

Introduction.

According to Faraday's ideas, the specific inductive capacity of a substance is due to the polarisation of the molecules as wholes. This is the basis of the old Clausius-Mosotti theory of dielectrics, on which it is shown first that the polarisation P is proportional to the polarising field, *i.e.*,

$$P = kE,$$

k being the dielectric constant, and second that δ being the density of the dielectric,

$$\frac{k-1}{k+2} \cdot \frac{1}{\delta} = \text{constant}.$$

Now it is known that some substances have large negative temperature coefficients for their dielectric constants which cannot thus be accounted for. To provide for this Debye proposed the theory that the molecules were permanently polarised and that they were systematically orientated in the field. This leads to the equation

$$\frac{k-1}{k+2} = aT^{-1} + bT^{-2},$$

to represent the change of specific inductive capacity with temperature. This theory has been developed by Gans and others, and a number of measurements have been made by Smyth and others, who have found the molecular moments of many substances by measuring the dielectric constants at different temperatures.

An account will now be given of some measurements made by a direct method of determination of moments, with the object of showing that the moments were permanent, were developed in chemically polar substances and were directly measurable.

As some preliminary experiments were made, it may be of interest to give an account of them first.

Preliminary Experiments.

The first experiment intended to show whether the molecule of potassium vapour had any large electric moment, was done with the simple apparatus shown in fig. 1. A glass tube is provided at D and E, with two diaphragms, having in them circular holes 1.5 and 0.5 mm. in diameter respectively. At F, 74 mm. from E, is a knife-edge set 1 mm. from a plate parallel to it, a potential difference of 1000 volts was maintained between them. The distance from F to G is 314 mm. and from D to E 250 mm. When looked at through the hole in the diaphragm D, the knife-edge covers half the field of view through

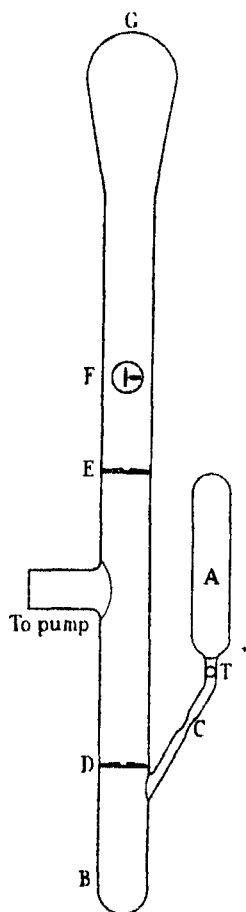


FIG. 1.

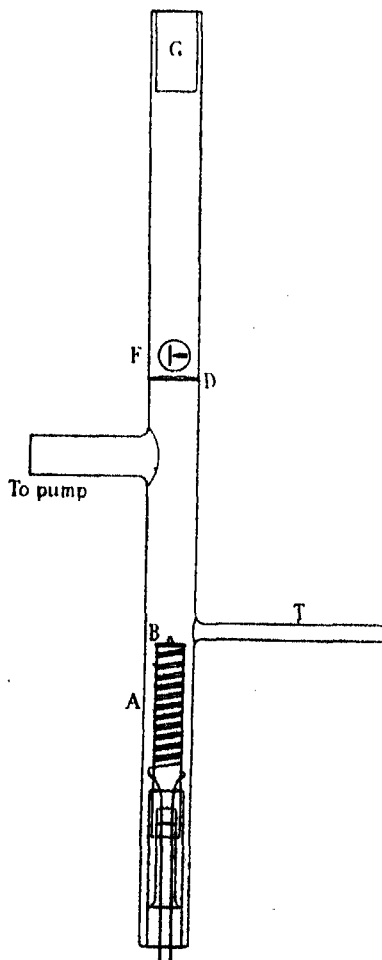


FIG. 2.

the hole in E. The knife-edge was a piece of razor blade and was sharpened. At A is a device for introducing potassium, essentially by breaking the neck of a small bottle containing some metal which had previously been purified and freed from gas. The evacuation being finished, the neck of this bottle was broken off by a piece of iron moved along the tube T by a magnet, and when the metal had run into B, this device was sealed off at C.

On warming the tube B, a molecular stream passed first through the diaphragms, then between the electrodes and was condensed on the end G of the tube by cooling that with liquid air. Some observations on potassium and some on sodium were made with this apparatus, or with others differing from it in no essential detail. No deflection of any part of the molecular stream could be found, and it was concluded therefore, that the electric moment was too small to detect if it was permanent, and that if it was induced by the field, that the potential gradient was too small to show it.

The next preliminary experiments were made with a salt, mercuric chloride, which was chosen for convenience. The apparatus was very like that used before; it is shown diagrammatically in fig. 2. The end G of the tube was made re-entrant to hold liquid air. The knife-edge was 0.3 mm. from the plate and was distant 7 mm. from the hole in the diaphragm D. The other diaphragm is omitted. The source of the molecular stream was a small bottle with a narrow neck, rigidly wedged with mica strips into a small electric heater inserted through the end of the tube. The neck of this bottle is broken off to open it—a scratch being made on it before it is put in the apparatus. The portion remaining is about 1.5 cm. long and 0.5 mm. in diameter, and the molecular stream issues from this. The purpose of this long neck is to increase the intensity of the stream along the axis of the tube. It is easy to show that if the diameter of the neck is less than the mean free path, then the concentration along the axis increases with the length of the neck, and if the length is also greater than the mean free path, that the concentration along the axis increases still more rapidly.

To prevent dissociation as far as possible, the salt HgCl_2 used in this experiment, and the others used later on, were first dried and then distilled *in vacuo* several times. After the bottles were filled they were heated at 100°C . for some hours, a good vacuum being maintained in them meanwhile, and then finally they were sealed off.

After setting up the apparatus and exhausting it, the bottle was opened, and on heating it, a molecular stream passed across the knife-edge and was condensed on the cold surface at the other end of the tube. When the knife-

edge was maintained at a potential 1000 volts greater than the plate opposite it, the shape of the deposit was not the same as it was when there was no potential difference. There seemed to be a distinct deposit in the shadow of the knife-edge. It was observed that a large amount of HgCl_2 in this case had diffused all over the cold surface. This is almost certainly due to dissociation of the salt.

These experiments showed that the salts could be distilled with reasonable rapidity, without an excessive amount of dissociation, and one of them indicated the presence of an electric moment, though there is the possibility of the reflection from the knife-edge, being altered by the electric field. It is therefore necessary to make a quantitative measurement to obtain further information.

Quantitative Determination of an Electric Moment.

To make a numerical estimate of the moment, one might proceed as in the Stern and Gerlach experiment, and perform the electrical analogue to the magnetic deviation of atomic rays. This experiment requires very fine adjustment, and makes great demands on the experimenter's skill, and for that reason an easy method had to be found, as that experiment is beyond the capacity of the present writer.

Suppose a narrow stream of molecules, moving along a path AB (fig. 3). If we put in this stream a wire, W, at right angles to the direction of the stream,

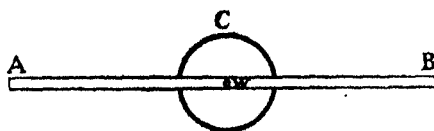


FIG. 3.

and maintained by a battery at a potential considerably greater than that of a coaxial cylinder C surrounding it, then there will be a very rapidly changing electric field surrounding the wire, and if the electrodes are properly made, the field outside the wire will agree in its actual value with that which can be calculated from elementary electrostatics. It is therefore necessary only to measure the potential between the two electrodes, and their diameters; no determination of the field experimentally is required other than these measurements. Further, and this is most important, it is unnecessary to have all the parts exactly aligned, but only to have the mouth of the bottle, the slits in the cylinder and some part of the cold plate in a straight line, and this is very easy to do.

As the wire is in the beam, some molecules will pass on either side of it, just outside its surface. As they are moving initially in straight lines which are in planes perpendicular, or very nearly perpendicular to the axis of the wire, they will move through a field of force with the centre of attraction on the axis of the wire, and will describe central orbits, in planes perpendicular to the wire. The only calculation required is to find the deflection.

If C be the capacity per centimetre length of the electrode system then

$$C = 1/2 \log (b/a)$$

where b is the radius of the outer cylinder and a the radius of the wire.

The potential gradient is $E = -dV/dr = 2VC/r$ and the gradient of the field is $-2VC/r^2 = 2Q/r^2$, Q being the charge per centimetre on the wire.

A particle whose mass is m and whose electrostatic moment is μ , if it is r cm. from the axis of the wire, will have an acceleration in the direction of r decreasing given by

$$-\frac{d^2r}{dt^2} = \frac{\mu}{m} \cdot \frac{dE}{dr} \cos \theta = \frac{\mu}{m} \cdot \frac{2Q \cos \theta}{r^2},$$

where θ is the angle which its axis makes with the gradient of the field. There will be no component at right angles to this. It will be assumed that the molecules are orientated by the field and that $\cos \theta = \pm 1$. This assumption seems for various reasons to be the most probable representation of what happens. With this assumption, the case reduces to that of motion in a central orbit.

It can be shown in the ordinary way, first that the orbits are hyperbolic for such velocities as are met with—these velocities are about 2×10^4 cm. per second, and second, that if a be the semi-major axis of an orbit, $\xi = \mu \cdot 2VC/m$, the acceleration at unit distance from the centre, V_0 the initial velocity of projection, and R the distance of the point of projection, then since the orbits are hyperbolic

$$1/a = V_0^2/\xi - 2/R.$$

Now $R = 0.5$ so that $2/R = 4$ under the conditions of the experiment, and it can be neglected, since, as it will appear later on, V_0^2/ξ is of the order of 10^6 . The semi-major axis is then to a sufficient approximation, given by $1/a = V_0^2/\xi$.

For those particles which pass just outside the wire, the apsidal distance is ρ , the radius of the wire. In fig. 4, let $CA = a$ the semi-major axis,

$AS = a(e - 1) = \rho$ the apsidal distance, b = the conjugate axis, ψ = the angle between the asymptotes CX , CX' , then since

$$b/a = \tan \frac{1}{2}\psi = \sqrt{e^2 - 1},$$

and consequently $e = \pm \sec \frac{1}{2}\psi$,

$$a = \rho/(e - 1) = \rho/(\sec \frac{1}{2}\psi - 1).$$

Again $\xi = aV_0^2 = V_0^2\rho/(\operatorname{cosec} \frac{1}{2}\phi - 1)$, since the measured angle of deflection, ϕ , is the supplement of the angle between the asymptotes. Since $\xi = 2Q\mu/m$,

$$\mu = V_0^2\rho m/2Q(\operatorname{cosec} \frac{1}{2}\phi - 1).$$

As molecules can move along both the positive and the negative branch of the hyperbola, there will be two such sets of hyperbolic orbits, one on each side of the

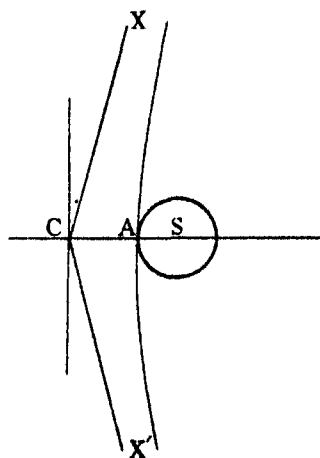


FIG. 4.

wire, and there will therefore be two deposits parallel to the wire appearing on the cold plate. If $2d$ be the distance between the inner edges of the deposits, and D the distance of the wire from the plate, then $\tan \phi = (d + \rho)/D$. For since the deflections are small, the distance between the apses of the two sets of orbits is very nearly the diameter of the wire. Without sensible error therefore

$$\operatorname{cosec} \frac{1}{2}\phi = 2D/(d + \rho).$$

The velocities of the molecules are not all of the same magnitude; the root mean square velocity is $\bar{v} = \sqrt{3kT/m}$. The velocities are grouped quite closely around this value, and it will be taken as the velocity of projection; with this assumption we have

$$\mu = \frac{3kT}{2Q} \cdot \frac{\rho}{D/(d + \rho) - 1},$$

which is the equation used in reducing the experimental measurements. It will be noticed that the mass of the molecule does not appear, and all that is required is the temperature of distillation. There is, in general, a difference between the actual average velocity in a molecular stream, and the average velocity calculated from the temperature. The difference is not very great unless there is a considerable pressure in the vessel producing the stream. As the present experiments are not very accurate, this difference will be ignored.

To put this idea into practice the apparatus shown in fig. 5 was constructed.

A small heater A has, inside it, the bottle B containing the salt. This bottle has an inserted tube in which is put one junction of a thermocouple. The thermocouple leads are brought out through a pinch seal C. At D there is a diaphragm with a hole 6 mm. in diameter and just above it the electrodes.

The slit above the diaphragm is 6.0 mm. long and 0.6 mm. wide.

The electrodes are mounted on mica and the leads are brought out through pinch seals as before. The smaller electrode is 0.00125 cm. in diameter. It is led over guides with V notches and is held under tension by a spring, which will stand a temperature of 500° C. without losing its elasticity. The electrodes are wedged in a slot in the glass work and thus held rigidly. At the top of the whole apparatus there is a vessel E with a flat bottom which can be filled with liquid air, or other refrigerant; the bottom of this vessel serves as a surface on which the spots are deposited. The distance from the wire to the cold plate is 21.5 cm., and the distance from the mouth of the bottle to the wire is 24 cm. approximately, though it varies slightly from experiment to experiment as the apparatus is cut in two to clean it, and refill the heater after an

experiment. The whole apparatus was mounted on a stand in a vertical position, the heater at the lower end, and was exhausted by a pump in the usual way.

The potential difference applied to the electrodes was measured by means of a milliammeter in series with a wire-wound megohm resistance-box. The source

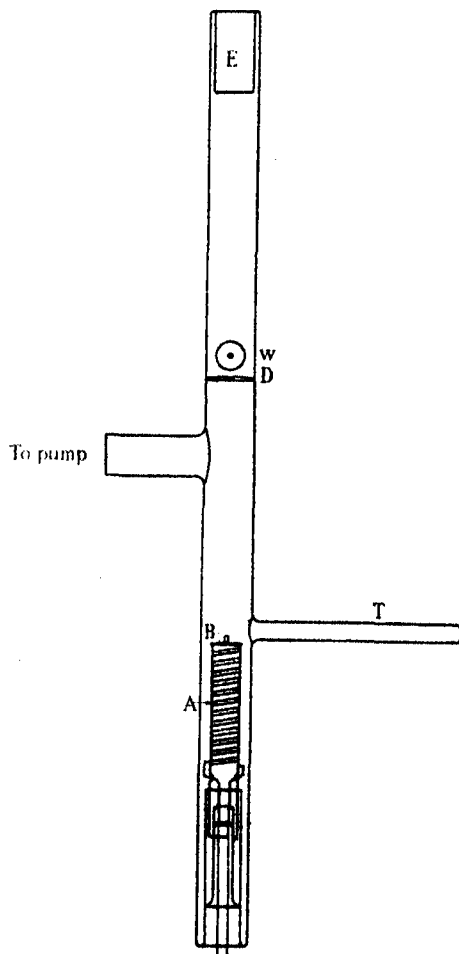


FIG. 5.

of potential was a battery of accumulators. The temperature of the bottle was measured by an iron-constantan thermocouple whose e.m.f. was measured by a potentiometer. The thermocouple was calibrated by using some of the following fixed points—ice, M.P.; water, B.P.; naphthaline, B.P., benzo-phenone, B.P., and sulphur, B.P. The determination was made to the nearest degree.

The measurement of the deposited spots was done by taking a photograph of them by means of a camera with a fixed extension and a lens of short focus. This camera gives a magnification of 2.65 to 1 and the measurements then made on the photographs were reduced by dividing them by this number. Very faint lines can be brought out by proper lighting, and a suitable plate and development.

With this apparatus, the first compound tried was arsenic trioxide As_2O_3 . Chemically, this is not a very polar substance, and one would expect that it would have a rather small molecular moment, and this turns out to be the case. The substance was chosen for this reason, and also because it is easy to work with. Three experiments were made altogether, one experiment with no field, two experiments with a potential difference of 1000 volts between the electrodes, and two with 600 volts between the electrodes. The details of an experiment are given below.

The diameter of the wire = 0.00050 inches, so that $\rho = 0.000625$ cm. The other radius of the electrodes = 1.2 mm. The capacity is

$$\frac{1}{2 \log (0.12/0.000625)} = \frac{1}{10.52} \text{ e.s.u. per centimetre,}$$

and since the potential difference is 1000 volts, the charge per centimetre on the wire is $Q = 0.316$ e.s.u.

On the corresponding photographic plate, the distance between the lines is 1.5 mm. and the magnification is 2.65 to 1, so that the actual distance is 0.56 mm.

The deflection d is half this or 0.28 mm. The distance to the cold plate from the wire = 21.5 cm.

The temperature of distillation increased 5°C. between the beginning and the end of the experiment. The average was $252^\circ \text{C.} = 525^\circ$ absolute.

The calculation then is

$$\mu = \frac{3 \times 525 \times 6.25 \times 10^{-4} \times 1.37 \times 10^{-16}}{6.32 \times 10^{-1} \times 430/0.27 - 1} = 1.3 \times 10^{-19} \text{ e.s.u. cm.}$$

With no field on the electrodes there are no lines on the plates, and with

600 volts on the plates the measured value of the moment is unchanged, being 1.4×10^{-19} e.s.u. cm. which is the same within the experimental error.

Discussion.

Taking the results of these experiments at their face value they would seem to indicate that the moments of As_2O_3 is of the right order of magnitude to agree with the theory of permanent dipoles put forward by Debye. Further, it appears that the moment is not influenced by the strength of the field and is therefore a permanent characteristic of the molecule. There was no definite indication on any of the plates of more than two lines, so that there seems to be no definite orientation of the molecules, save parallel or antiparallel to the field. The preliminary experiments made showed very little, save that there was a very small moment if any, in a potassium or sodium atom. This is what one would expect. The moment of an atom should be of the order of its volume or 10^{-26} e.s.u. cm. which could not be detected in an experiment of this kind, or rather one of this order of accuracy.

It is clear that this method of experiment must be further developed before a number of observations on different substances can be profitably undertaken. It will be necessary to decrease the width of the slit to about 0.05 to 0.10 mm. and to increase the potential difference between the electrodes to about 10,000 volts. For a substance like As_2O_3 this should give a central spot about $\frac{1}{2}$ mm. broad and a deflection of about 2.5 mm. The deflected lines will then be about 5.5 mm. apart, and if they are sharp, as they appear to be, it will be possible to resolve them if they are multiple, due to definite paths such as occur in the Stern and Gerlach experiment.

It has been assumed that the molecules orientate themselves with their axes along the field. From the result of the experiment this may quite possibly be the case, though from the lack of proper resolution in these experiments, it would be rash to hazard an opinion. It is true that if the axes set themselves parallel and antiparallel to the field that such a particular orientation cannot be shown by this method, for the line due to the antiparallel molecules on one side of the wire will fall, since the diameter of the wire is so small, on top of the line due to the parallel molecules on the other side of the wire.

If any other definite orientations occur it will be possible to detect them, subject to the same restriction that each line will be a double one being a deposit of molecules passing, some on each side of the wire.

This assumption raises the same difficulty as in the Stern and Gerlach experiment. There is no available system of collisions to bring about the gain and

loss of energy; the only possible mechanism seems to be radiation. The wave-length of this radiation would be far in the infra-red, about $\lambda = 300 \mu$ as is easily calculated. This question was discussed by Einstein and Ehrenfest in 1922. It is, however, possible for the molecules to change their velocity on going into the field, the magnitude of the change being given by

$$\delta (\frac{1}{2}mv^2) = \int \mu \cos \theta \frac{dE}{ds} ds.$$

Now it will never be possible on going into the field in an actual experiment to make $dE/ds = 0$ exactly, so that in general there must be a change of velocity on entering the field for all molecules but those whose electric axes remain permanently at right angles to the field. Such molecules would not be deflected so that those which are deflected will have their velocities changed. The molecules in this experiment entered the field along the direction of the lines of force, and there was certainly a finite value of dE/ds over the distance that they travelled, from a point outside where $E = 0$ to a point well inside where E is large. The molecules therefore changed their velocity. The change in velocity is not easy to calculate, but a maximum possible value can be found. We have for this

$$\frac{1}{2}m (V_1^2 - V_2^2) = \int \mu \cos \theta \frac{dE}{ds} ds = \pm (E_1 - E_2) \mu.$$

Now $(E_1 - E_2) = 330$ e.s.u., $\mu = 1.3 \times 10^{-19}$ e.s.u.cm. So that $\delta (\frac{1}{2}mv^2) = 4.3 \times 10^{-17}$ ergs, and $\delta v = (8.6 \times 10^{-17} / 3.3 \times 2.88 \times 10^{-22})^{\frac{1}{2}} = 3 \times 10^2$ cm. per second, or about 1.5 per cent. of the original velocity.

As this is small it will not affect the results to the order of accuracy obtained here, but it would have to be allowed for if the accuracy were to be increased. It also makes it clear that this change in velocity can be used for determination of electric or other moments in a way which would probably prove easier than the one described here.

[*Note added in proof.*—The same apparatus could be used for determination of magnetic moments if, instead of raising the wire to a high potential, a current were passed through it, when it would be surrounded by an inhomogeneous magnetic field. The calculation is the same except that ξ , the acceleration at unit distance, becomes $2I\mu/m$, I being the current through the wire.]

The experiments forming the subject of this paper were done in the Cavendish Laboratory, and the writer has to thank Prof. Sir E. Rutherford for very kindly placing the facilities of the laboratory at his disposal, and Dr. D. M. Morrison for a great deal of help with the experiments.

Further Studies in the Emission of Electrons from Cold Metals.

By T. E. STERN, B. S. GOSSLING,* and R. H. FOWLER, F.R.S.

(Received May 22, 1929.)

§ 1. *Introduction.*

Fowler and Nordheim† and Oppenheimer‡ have already independently studied the theory of the emission of electrons from cold metals under the effect of an intense electric field, and have obtained results in good qualitative agreement with experiment. The formula for this "auto-electronic" current density, $-I$, obtained by the former authors is

$$I = \frac{\epsilon}{2\pi\hbar} \frac{\mu^{\frac{1}{2}}}{(\chi + \mu)\chi^{\frac{1}{2}}} F^2 e^{-i\epsilon\chi^{\frac{1}{2}}/F} \quad (1)$$

at ordinary temperatures. In this formula $\kappa^2 = 8\pi^2m/\hbar^2$; μ is the parameter of the metallic electron distribution in the Fermi-Dirac statistics; χ is the thermionic work function for the metal; $-\epsilon$ is the charge on the electron; \hbar is Planck's constant and $-F$ is the derivative of the potential energy of the electron along the outward normal at the cathode surface; I , F and ϵ are then all positive. When the unit of energy is the electron-volt and the unit of current density is amperes per square centimetre this reduces to

$$I = 6.2 \times 10^{-6} \frac{\mu^{\frac{1}{2}}}{(\chi + \mu)\chi^{\frac{1}{2}}} F^2 e^{-6.8 \times 10^7 \chi^{\frac{1}{2}}/F}. \quad (2)$$

In the original paper of Fowler and Nordheim equation (2) is given with the numerical mistake of 2.1×10^8 instead of 6.8×10^7 . This correction is important and favours the satisfactory interpretation of the experimental results.

An extensive preliminary survey of existing material by the present authors using (2) persuaded them that the theory was on the right general lines, but that further more detailed investigations were required and might be profitable. To appreciate the point of these investigations it is necessary to consider the nature of the comparison possible between (2) and the quantities actually observed. These are the *total current* passing between the electrodes and the

* Research Laboratories of the General Electric Company, Wembley.

† Fowler and Nordheim, 'Roy. Soc. Proc.,' A, vol. 119, p. 173 (1928).

‡ Oppenheimer, 'Phys. Rev.,' vol. 31, p. 66 (1928); 'Proc. Nat. Acad. Sci.,' vol. 14, p. 303 (1928). See also Nordheim's "Zusammenfassende Berichte," 'Phys. Z.,' vol. 30, p. 177 (1929).

applied voltage. The theory in (2) states a relation between the *current density* and the *surface field*. If the effects of space charge may be neglected the surface field must be proportional to the measured voltage, and the ratio is controlled by geometry alone. If the emitting area* is constant (but not otherwise) the current and the current density are proportional. If in addition the theory is correct, then a straight line should result from plotting logarithms of the observed current against reciprocals of the applied voltage. It is now well known that such straight line plots are found.† To derive, however, the maximum information from the comparison of the observed quantities with equation (2) we can make it determine both the emitting area A , and the ratio of the surface field to the applied voltage.‡ This ratio depends, of course, not only on the large scale geometry of the apparatus, but also on the micro-geometry§ of the irregularities of the cathode surface. The ratio due to the former factor we may suppose known. We derive in this way what we may call F_m , the *measured field*. The extra factor due to surface irregularities we shall call β . Schottky has shown very clearly how large values of β may be accounted for by a superposition principle. For example, if the emitting area were really a hemispherical boss on a cathode which on the scale of the boss is effectively an infinite plane, it is easy to show that $\beta = 3$. If the emitting area lies on a second hemispherical boss lying on the first and is small compared with it, then $\beta = 3^2$, and so on. The interest lies in the values of A and β which can be derived from (2) and the observations.

If C is the measured current we have (using natural logarithms)

$$\frac{d \log C}{d F_m^{-1}} = -2 F_m - \frac{6.8 \times 10^7 \chi^{\frac{1}{2}}}{\beta} \quad (3)$$

Equation (3) determines β from the slope of the plot assuming that χ is known ; it is independent of the value of A . Again

$$\log A = 12.0 + \log C - \log \frac{\mu^{\frac{1}{2}}}{(\chi + \mu) \chi^{\frac{1}{2}}} - 2 \log (\beta F_m) + \frac{6.8 \times 10^7 \chi^{\frac{1}{2}}}{\beta F_m}, \quad (4)$$

* Actually the current density will not be accurately constant over any emitting region, and the total current will be $C = \int I ds$ over this region. The "area" to be considered is accordingly a weighted mean area.

† For example Millikan, Eyring and Mackeown, 'Phys. Rev.', vol. 31, p. 900 (1928); Pierson, 'Phys. Rev.', vol. 31, p. 441 (1928). Our preliminary work has amply confirmed this. See also fig. 1 here. Strictly, logarithms of {current/(voltage)²} should be plotted. The difference is usually insignificant, but in § 1.1 we describe some cases in which it is necessary to use {current/(voltage)²}.

‡ See also Hall, 'Proc. Nat. Acad. Sci.', vol. 15, p. 241 (1929).

§ Schottky, 'Z. Physik,' vol. 14, p. 63 (1923).

which determines A when β is known, or better, in terms of the slope,

$$\log A = 10.0 + \log C - \log \frac{\mu^{\frac{1}{2}}}{(\chi + \mu)\chi^{\frac{1}{2}}} - 2 \log (\beta F_m) - \frac{d \log C}{F_m dF_m^{-1}}. \quad (5)$$

It should be observed that β is relatively unimportant in the determination of A , for the important last term in (5) is fixed by C and F_m , and is independent of β and χ which therefore only affect $\log A$ through their logarithms. We assume, of course, that χ and μ are known; μ is obviously quite unimportant, and we take it to be 5 volts in all of our calculations. Using data furnished by various experiments* β is found to vary from about 1.5 to 115. There is, of course, in the majority of the published experiments some uncertainty in the proper value of χ to be used. In an experiment of Gossling, fig. 1, curve 2, the cathode was the end of a fine tungsten wire, pointed and apparently

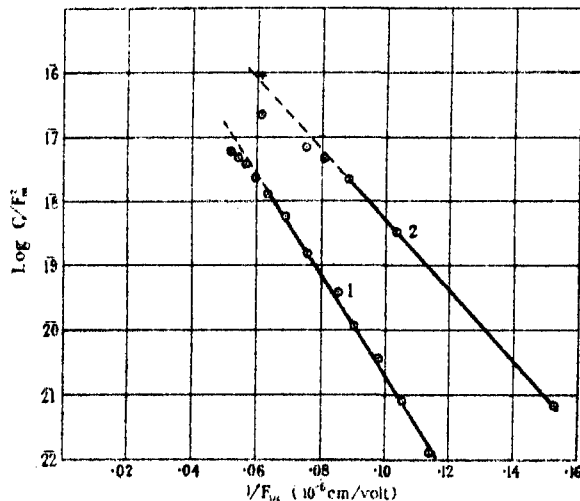


FIG. 1.

polished by violent electrolytic action. Taking for χ an "intermediate" value of 3 (the reasons for this choice will be more obvious after the latter part of the paper has been read) we find by (3) that β was 2.68 and that A was 6.3×10^{-8} cm.². By direct measurement, assuming the point to be hemispherical, its whole area was 1.2×10^{-7} cm.². For fig. 1, curve 1, which represents the same readings as fig. 5, curve 3, and refers to a less finely pointed

* Gossling, 'Phil. Mag.', vol. 1, p. 609 (1926) and other experiments first recorded in this paper. Rother, 'Ann. Physik,' vol. 81, p. 317 (1926); Millikan and Eyring, 'Phys. Rev.', vol. 27, p. 51 (1926); Millikan, Eyring and Mackeown, *loc. cit.*, vol. 31, p. 900 (1928); Del Rosario, 'J. Franklin Inst.', vol. 205, p. 103 (1928).

wire the value of χ was very probably a little less than 4; and using this, β is found from (3) to be 2.9. The emitting area again is found to agree with the dimensions of the cathode. Actually several experiments were made using finely pointed wires, of which one specimen is shown, and all gave similar results. It is satisfactory to have found such examples in which the phenomenon appears to be fully accounted for by the simple original theory. It is generally found that the emitting area derived from (5) is very small, of order ranging from 10^{-8} cm.² to 10^{-13} cm.²; of these the smaller apparent areas are not necessarily true emitting areas, but are underestimated owing to a film effect as we shall explain later in this paper.

The values of β in the preceding theory are increased by including not merely the geometry of the point but also the effect of the image forces in reducing the field necessary for a given emission. This effect has been calculated by Nordheim.* The factors concerned are not large and we shall not refer to them further here beyond recording that in the still more exact theory the values of β derived from the analogue of (3) are somewhat smaller than the values we quote here, and in fact some are most satisfactorily near the natural value unity.

Comparison of the simple theory with observation having reached this stage, with fairly satisfactory results except for the surprisingly small emitting areas derived, it seemed clear that two extensions of the theory would repay investigation. These were (i) an examination of the space charge effect, and (ii) an examination of the effect of surface films on the emission coefficient. These examinations are undertaken here.

(i) It is found that space charge effects are negligible and do not upset the analysis of the observations which we have used and propose to use in this paper. For example if W is the applied voltage and there were no space charge the surface field of the cathode would have the form

$$F_m = W/\alpha,$$

where α is a length fixed by the geometry of the apparatus. When space charge effects are included this is altered to

$$F_m = \frac{W}{\alpha} (1 - \tau).$$

We can, and do, calculate an upper limit for τ which we call T . We find in

* Nordheim, 'Roy. Soc. Proc.,' A, vol. 121, p. 626 (1928). Equation (56) of this paper should contain the same exponential factor as equation (1) here. The factor 3 in the denominator has been accidentally omitted.

analysing those experiments of Gossling used in this paper that in all but two curves, $T \leq 0.03$, even when C , W and F_m are taken from the *high current-density* portions of the experimental ranges. In two cases T becomes large when so calculated, but upon using values of C , W and F_m taken from the middle-portions of the curves (which were actually used for our later calculations) we find that $T \leq 0.03$ in these two cases also. The errors introduced into F_m and so into β and A by a value of τ as great as 0.03 are negligible. This justifies fully the use we have made of the straight line part of the current-voltage relationship. In view of the high current densities with which we deal, even in these middle portions of the curves, this use could hardly be accepted without some such detailed investigation.

Since we only calculate upper limits to τ we cannot discuss quantitatively examples, if any, in which the space charge has a visible effect, excepting perhaps in the case of a certain experiment of Rother using parallel plane electrodes. Its effect is to prevent F_m and therefore βF_m and C from increasing as fast with the applied voltage as one would expect. The plot of $\log C$ against $1/W$ will therefore fall away below the straight line towards the end for smaller values of $1/W$. We have found one or two examples of such plots, and we shall discuss Rother's in some detail farther on.

(ii) Having assured ourselves on this point we obtain a formula for the emission through a surface layer under an applied field, and use this new formula to analyse the observations more exactly. We are able to draw some deductions as to the nature of the surface layer which we think may be of some interest.

It is observed in experiments* that if the cathode is of clean tungsten a much higher field must be applied to obtain a given auto-electronic emission than when the cathode is covered with a layer of sodium, barium, caesium or other electro-positive impurity. The condition of a particular cathode can in fact be varied during an experiment by admitting more and more impurity into the tube between the determinations of the current-voltage relation. In the usual plot resulting from the kind of experiment we are now considering a family of straight lines is obtained with gradually diminishing slopes. There is no reason to suspect a change of β so that the change of slope can be naturally and elegantly interpreted as due to a decrease of χ as the surface layer builds up. The sequence of changes can be reversed by heating the filament to a series of increasing temperatures between further determinations of the current-voltage curve, thus evaporating the surface layer. Such experiments have

* Gossling, *loc. cit.*, and in this paper, De Bruyne, 'Phil. Mag.', vol. 5, p. 574 (1928).

been fully described by Gossling (*loc. cit.*). In fact equation (3) seems to be a reliable and feasible way of determining changes of χ .

If then we are concerned in such phenomena with alteration of the work function by surface layers it is necessary to revise the theory before equations (2) and (4) can be used quantitatively, for it has been shown by Nordheim* and in greater detail by Fowler† that theory and experiment agree in predicting changes of the thermionic emission coefficient parallel to the changes in χ . It is found that such changes persist in the emission coefficients of the auto-electronic effect. The result is to lower the theoretical current density and increase the calculated area considerably when the emission takes place through a surface layer which lowers χ . This leads to more satisfactory interpretations of the experiments. In certain examples there is, according to the simple theory, an apparent change of emitting area while a surface film is being removed or built up. We now find that if a suitable thickness is assigned to the film—a thickness which is *a priori* entirely reasonable—the revised theory fits satisfactorily with a constant emitting area. In short, we think we may claim that the revised theory gives a satisfactory account of the phenomenon and promises to throw much light on the structure of surface films.

§ 1.1. *Methods of Plotting Observations.*

According to the theory, for very wide ranges of variation of C and F_m the relation between $\log C/F_m^2$ and $1/F_m$ should be more accurately linear than the relation between $\log C$ and $1/F_m$. In a number of Gossling's experiments reproducible currents have been obtained covering a range of over 100,000 to 1. The widest range obtained up to the present is that given by Millikan and Eyring‡ in whose fig. 3 a reproducible curve covering from 10^{-11} to 6×10^{-4} amp. is shown. When this curve is replotted using $\log C/F_m^2$ the agreement with the linear relation over the whole range is very close indeed and well within the accuracy to which it is possible to read the published curve. If $\log C$ is used instead of $\log C/F_m^2$ there is a distinct departure from the linear relation equivalent to a factor of 1.6 in the current.

The two curves (Gossling) shown in fig. 1 extend rather further in the direction of higher current. The linear relation can be seen to hold very well up to a point representing a current of about 10^{-3} amp., but above this there is in both cases a progressive departure. This might at first sight be ascribed

* Nordheim, 'Z. Physik,' vol. 46, p. 833 (1928).

† Fowler, 'Roy. Soc. Proc.,' A, vol. 122, p. 36 (1929).

‡ Millikan and Eyring, 'Phys. Rev.,' vol. 27, p. 51 (1926).

to the space charge effect which we shall discuss later, but can, however, be satisfactorily explained as being due to an incipient pulsation of the high voltage supply derived from a transformer and rectifying valves. It was possible in the case of the highest point of curve 2 to calculate the correction for this pulsation assuming the continuance of the linear law. The value of the current corresponding to the voltage maximum, *i.e.*, to the value of $1/F_m$ plotted so calculated, gives the point X which lies close to the straight line through the lower points; here also the agreement is better for $\log C/F_m^2$ than for $\log C$.

The value of the current maximum corresponding to X is 2.45×10^{-2} amp. The relation between current and field expected from equation (1) thus holds in this experiment from 2.5×10^{-2} amp. to 3×10^{-3} amp. and in Millikan's experiment from 6×10^{-4} amp. to 10^{-11} amp.

In other diagrams in this paper the observations cover ranges too short for the distinction between $\log C$ and $\log C/F_m^2$ to appear and the actual values of the currents are also of interest. We have therefore in all the figures subsequent to fig. 1 plotted $\log C$ against $1/F_m$.

§ 2. *The Effect of Space Charge in Discharges under Strong Fields.*

It is ideally desirable to calculate the effect of space charge in limiting any auto-electronic current which is to be exactly analysed, but such a course would be tedious. Fortunately it is possible to obtain a simple criterion for determining when the effect is negligible, which is satisfied in most of the experiments analysed.

The effect of space charge in limiting thermionic emission has been investigated more than once.* But in most of the investigations known to us the potential gradient at the emitting surface is assumed to be zero, and none of them covers the conditions we require. This assumption is perfectly correct for thermionic emission, but it cannot be justified *a priori* for any type of emission; and it obviously is wrong here where the initial potential gradient controls the current emitted. Our treatment then will differ from Langmuir's principally in having an important non-zero field at the surface of the cathode.

Let us consider the simple example of two plane parallel electrodes a distance D apart, with a difference of potential W . Let $-\rho(x)$ be the charge density at a point distant x from the cathode and v the velocity of the electrons there,

* Langmuir, 'Phys. Rev.', vol. 2, p. 450 (1913); Langmuir and Blodget, 'Phys. Rev.', vol. 22, p. 347 (1923), vol. 24, p. 49 (1927); Schottky, 'Phys. Z.', vol. 15, p. 526 (1914); Jaffé, 'Ann. Physik,' vol. 75, p. 391 (1924).

so that $v(0)$ is the initial velocity, if any. Let $V(x)$ be the potential difference between the point and the cathode, so that $V(0) = 0$, $V(D) = W$. If we assume that the space charge is continuous, then the equation of continuity gives

$$I = v\rho. \quad (6)$$

Equation (6) makes $\rho(0)$ infinite if $v(0) = 0$, and is incorrect because it ignores the statistical distribution of the electrons in time. To determine more accurately the statistical density at the cathode surface consider an area emitting on the average n electrons per second with velocity $v(0)$ and acceleration f . The chance that after a given emission there is a gap of at least t seconds before the next is e^{-nt} . The chance that the interval between successive emissions lies between t and $t + dt$ is therefore $e^{-nt} n dt$. The average distance s travelled by an electron before the next electron leaves is therefore given by

$$s = \int_0^\infty (tv(0) + \frac{1}{2}t^2f) ne^{-nt} dt,$$

and this represents the average volume associated with each electron at the cathode surface. The charge density is therefore given by

$$\rho(0) = \epsilon/s.$$

Since $n = I/\epsilon$, $f = F^*\epsilon/m$, where F^* is the electric intensity at and towards the surface, this reduces to

$$\rho(0) = \frac{I^2}{v(0)I + F^*\epsilon^2/m}. \quad (7)$$

The charge density is therefore exaggerated by (6) and as we are concerned in calculating an upper limit to its effects we shall proceed as if (6) were correct.

The mass of the electron may be assumed constant for the velocities with which we are concerned. Therefore

$$v(x) = \left\{ \frac{2V(x)\epsilon}{m} + v^2(0) \right\}^{\frac{1}{2}}, \quad (8)$$

and Poisson's equation becomes

$$\frac{d^2V(x)}{dx^2} = \frac{4\pi I (m/2\epsilon)^{\frac{1}{2}}}{\{V(x) + mv^2(0)/2\epsilon\}^{\frac{1}{2}}}. \quad (9)$$

Putting $V' = V(x) + mv^2(0)/2\epsilon$, and dropping accents, we obtain

$$\frac{d^2V'}{dx^2} = BV'^{-\frac{1}{2}}, \quad (10)$$

which is to be solved subject to

$$V(0) = \frac{mv^2(0)}{2e}, \quad \frac{dV(0)}{dx} = F^*, \quad V(D) = W + mv^2(0)/2e, \quad B = 4\pi I \left(\frac{m}{2e} \right)^{\frac{1}{2}}. \quad (11)$$

This presents no difficulty. We may further simplify the result by putting $v(0) = 0$, for this again can only exaggerate the effect of the space charge. We thus obtain

$$D = \frac{F^{*3}}{6B^2} + \frac{1}{2B^{\frac{1}{2}}} \left[\frac{1}{3} \left(W^{\frac{1}{2}} + \frac{F^{*2}}{4B} \right)^{\frac{3}{2}} - \frac{F^{*2}}{B} \left(W^{\frac{1}{2}} + \frac{F^{*2}}{4B} \right)^{\frac{1}{2}} \right]. \quad (12)$$

Now $BW^{\frac{1}{2}}/F^{*2}$ is usually small. Assuming it is small we can expand D in powers of this quantity, obtaining a convergent series of which the first few terms are

$$D = \frac{W}{F^*} \left(1 - \frac{1}{3} \frac{BW^{\frac{1}{2}}}{F^{*2}} + 3 \frac{B^2W}{F^{*4}} - 8 \frac{B^3W^{\frac{3}{2}}}{F^{*6}} + \dots \right). \quad (13)$$

But W/D is the value of F^* which one would have if there were no space charge at all. Hence we may write

$$F^* = \frac{W}{D} \left(1 - \frac{1}{3} \frac{BW^{\frac{1}{2}}}{F^{*2}} + \dots \right), \quad (14)$$

and assert that the effect of the space charge between plane parallel electrodes is negligible if T is small, where

$$T = \frac{1}{3} \frac{BW^{\frac{1}{2}}}{F^{*2}} = \frac{16\pi}{3} \left(\frac{m}{2e} \right)^{\frac{1}{2}} \frac{CW^{\frac{1}{2}}}{AF^{*2}}. \quad (15)$$

Inserting numerical values,

$$T = 2.5 \times 10^5 \frac{CW^{\frac{1}{2}}}{AF^{*2}}, \quad (16)$$

where C is in amperes, W is in volts, A is in square centimetres, and F^* is in volts per centimetre.

If the discharge is not from a plane cathode to a parallel plane anode, the criterion will still apply, for then the electrons will spread out on leaving the cathode and the density of the space charge will be everywhere diminished. If in any example T is not small we can, of course, deduce little since our approximations have everywhere exaggerated the effect, and an exact calculation would be necessary, except perhaps in the case of a plane-parallel discharge.

One may notice in passing that in the opposite limit when T is very large, equation (12) reduces to

$$D = \frac{2}{3} \frac{W^{\frac{1}{2}}}{B^{\frac{1}{2}}}$$

approximately. With the help of (11) we derive

$$I \propto \frac{W^{\frac{1}{2}}}{D^{\frac{1}{2}}}.$$

Thus in the limiting case of large space charge the current-voltage relation of the auto-electronic discharge is the same as that of the space-charge limited thermionic discharge, as we should expect.

Table I gives an abstract of the calculations of T for the high current-density portions of such current-voltage curves as we discuss in detail later in this paper, and also some values for lower fields in those cases where T as previously found is large. They bear out the general remarks made in § 1 and need not be further discussed. Since the electrodes are not in general parallel planes the length D of formulæ (13) and (14) cannot in general be taken as the distance apart. We do not, however, need to use D . We can apply formula (16) using observed values of C and W and the value of A deduced from (5). We must take as our F^* in (16) F_m , the measured field; for from equation (13) it follows that the space-charge effect is due largely to electrons comparatively remote from the cathode; and, moreover,

$$1/F_m^2 > 1/(\beta F_m)^2.$$

It might seem from the high value of T in experiment 2, curve 1, that the drooping downwards of the $\log C - 1/F_m$ curve, apparently indicated by some observed values of C and W , was caused by space-charge, but as stated in § 1.1 another explanation must be preferred. T , after all, is only an upper limit of τ . Similarly in experiment 3, curve 4, the experimental conditions at high currents were not very satisfactory; and in this case, besides, T is quite small. Thus Gossling's experiments do not show any well-established cases of space-charge limited auto-electronic currents. But a curve, fig. 6, obtained from data published by Rother† may perhaps show the space-charge limiting the auto-electronic discharge. The experiment referred to made use of two parallel plane electrodes of tantalum, 0.005 cm. apart. In view of the shape, one might expect that in this case T and τ would not differ by as much as they would in discharges from points. We find that T , for the place where the curve starts to droop considerably, is 0.25. Although the space-charge limitation is here a possibility, we do not wish to urge it as being necessarily the actual reason for the droop, for the curve may not have been a reversible one.

† Rother, *loc. cit.*

Table I.—Space-charge Criteria.

Experiment.	Curve.	Current (amperes) for which T is calculated.	Emitting area, cm. ²	Current density amps./cm. ²	T.
1	1	1.4×10^{-8}	5.1×10^{-9}	2.7×10^3	0.03
1 (Fig. 3)	2	5.5×10^{-8}	5.1×10^{-9}	1.1×10^4	0.20
	2	6.3×10^{-8}	5.1×10^{-9}	1.2×10^4	0.03
	3	6.5×10^{-8}	5.1×10^{-9}	1.3×10^4	0.006
2	1	2.5×10^{-8}	1.2×10^{-10}	2.1×10^7	2.0
2	1	1.2×10^{-8}	1.2×10^{-10}	1.0×10^8	0.03
2 (Fig. 4)	3	2.5×10^{-8}	1.2×10^{-10}	2.1×10^8	0.0006
	4	1.2×10^{-8}	1.2×10^{-10}	1×10^4	0.03
	5	1.8×10^{-7}	1.2×10^{-10}	1.5×10^8	0.004
3	1	8×10^{-8}	8×10^{-8}	1×10^8	0.00004
3 (Fig. 5)	2	1×10^{-8}	8×10^{-8}	1.2×10^2	0.00003
	3	1×10^{-8}	8×10^{-8}	1.2×10^4	0.0015
	4	2.3×10^{-8}	8×10^{-8}	2.9×10^4	0.003
Fig. 1	2	0.025	6.3×10^{-8}	4.0×10^8	0.025
Rother	Taf. X	2.5×10^{-6}	4.9×10^{-10}	5.1×10^8	0.25

§ 3. The Emission Coefficient under a Strong Field through a Surface Layer.

To represent the effect of a surface layer on the emission in the simplest reasonable way we will use a potential energy near the surface of the form shown in fig. 2. The potential energy V of the electron is assumed to have the form

$$\begin{aligned} V &= 0 & (x < 0), \\ V &= C_1 - F_1 x & (0 < x < a), \\ V &= C_2 - F_2 (x - a) & (a < x). \end{aligned}$$

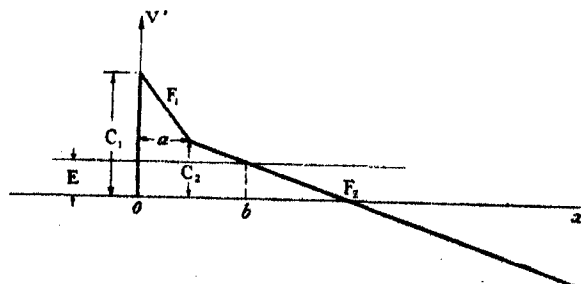


FIG. 2.

The region $0 < x < a$ is the surface film which lowers the effective work function. F_2 is the externally applied potential energy gradient. It is first

necessary to calculate $D(E)$, the fraction of electrons incident on the boundary from within the metal with kinetic energy E normal to the boundary which leave the metal. The energy E may be assumed to be such that neither $C_1 - E$ nor $C_2 - E$ is small compared with C_2 . It is fairly easy to guess the result in a convincing way. When $F_1 = F_2$ the problem reduces to that already worked out by Fowler and Nordheim,* and the result is

$$D(E) = \frac{4 \{E(C_1 - E)\}^{\frac{1}{2}}}{C_1} e^{-\frac{2}{3}\kappa(C_1 - E)^{\frac{3}{2}}/F_1}, \quad (17)$$

where

$$\kappa^2 = 8\pi^2 m/\hbar^2.$$

When $F_1 \neq F_2$ we know† that the exponent in (16) must be replaced by

$$-2\kappa \int_0^b (V - E)^{\frac{1}{2}} dx,$$

which is obviously equal to

$$-\frac{4}{3}\kappa(C_1 - E)^{\frac{3}{2}}/F_1 + \frac{4}{3}\kappa(C_2 - E)^{\frac{3}{2}}/F_1 - \frac{4}{3}\kappa(C_2 - E)^{\frac{3}{2}}/F_2. \quad (18)$$

The method of Jeffreys which yields (18) does not tell us anything about the first factor in (17) but one may fairly guess that the kink at $x = a$, at a considerable height above the level E , will not affect this factor and therefore that

$$D(E) = \frac{4 \{E(C_1 - E)\}^{\frac{1}{2}}}{C_1} \exp \left[-\frac{4}{3}\kappa \left\{ \frac{(C_1 - E)^{\frac{3}{2}}}{F_1} - \frac{(C_2 - E)^{\frac{3}{2}}}{F_1} + \frac{(C_2 - E)^{\frac{3}{2}}}{F_2} \right\} \right], \quad (19)$$

with sufficient accuracy, provided each of the three terms in (18) is large compared with unity. To verify this guess (which is correct) we have, however, computed $D(E)$ exactly by solving the wave equation for the motion of electrons through this layer in terms of Bessel's functions of order $\frac{1}{2}$. The calculations are a little long, but a quite straightforward extension of the calculations of Fowler and Nordheim. If the complete wave function is

$$\Psi = \psi e^{-2\pi i Et/\hbar},$$

it is best to use representations of ψ in terms of the following functions :

$$\begin{aligned} (x < 0) & \quad e^{\pm i\kappa\sqrt{E}x}, \\ (0 < x < a) & \quad \left(\frac{C_1 - E}{F_1} - x \right)^{\frac{1}{2}} \frac{I_{\frac{1}{2}}}{K_{\frac{1}{2}}} \left\{ \frac{2}{3}\kappa\sqrt{F_1} \left(\frac{C_1 - E}{F_1} - x \right)^{\frac{3}{2}} \right\}, \\ (a < x) & \quad \left(x - a - \frac{C_2 - E}{F_2} \right)^{\frac{1}{2}} H_{\frac{1}{2}}^{(1)} \left\{ \frac{2}{3}\kappa\sqrt{F_2} \left(x - a - \frac{C_2 - E}{F_2} \right)^{\frac{3}{2}} \right\}. \end{aligned}$$

* Fowler and Nordheim, 'Roy. Soc. Proc.,' A, vol. 119, p. 173 (1928).

† Nordheim, 'Z. Physik,' vol. 46, p. 833 (1928).

We omit further details, which it is hoped to publish in the 'Proc. Camb. Phil. Soc.'

The current density $-I$ is given by

$$I = e \int_0^{\infty} N(E) D(E) dE, \quad (20)$$

where $N(E) dE$ is the number of electrons hitting unit area of the boundary from inside in unit time with an energy normal to the surface between E and $E + dE$. It has been shown by Nordheim that

$$N(E) = \frac{4\pi mkT}{h^3} \log \left[1 + \exp \left(- \frac{E - \mu}{kT} \right) \right]. \quad (21)$$

At the temperatures concerned it is sufficiently accurate to take

$$N(E) = \frac{4\pi m}{h^3} (\mu - E) \quad (E < \mu), \quad (22)$$

$$= 0 \quad (E > \mu). \quad (23)$$

Therefore

$$I = \frac{16\pi m e}{h^3 C_1} \int_0^{\mu} E^{\frac{1}{2}} (\mu - E) (C_1 - E)^{\frac{1}{2}} \exp \left[- \frac{1}{2} \kappa \left\{ \frac{(C_1 - E)^{\frac{1}{2}}}{F_1} - \frac{(C_2 - E)^{\frac{1}{2}}}{F_1} + \frac{(C_2 - E)^{\frac{1}{2}}}{F_2} \right\} \right] dE. \quad (24)$$

We can now approximate to this integral, after writing $C_1 - \mu = \chi_1$, $C_2 - \mu = \chi_2$, $\eta = \mu - E$, by using the fact that the dominant contribution comes from small values of η . Thus

$$I = \frac{16\pi m e}{h^3 (\chi_1 + \mu)} \mu^{\frac{1}{2}} \chi_1^{\frac{1}{2}} \exp \left[- \frac{1}{2} \kappa \left\{ \frac{\chi_1^{\frac{1}{2}}}{F_1} - \frac{\chi_2^{\frac{1}{2}}}{F_1} + \frac{\chi_2^{\frac{1}{2}}}{F_2} \right\} \right] P, \quad (25)$$

where

$$P = \int_0^{\mu} \left(1 - \frac{\eta}{\mu} \right)^{\frac{1}{2}} \left(1 + \frac{\eta}{\chi_1} \right)^{\frac{1}{2}} \eta \exp \left[- 2\kappa \left\{ \frac{\chi_1^{\frac{1}{2}}}{F_1} - \frac{\chi_2^{\frac{1}{2}}}{F_1} + \frac{\chi_2^{\frac{1}{2}}}{F_2} \right\} \right] d\eta, \\ = \frac{1}{4\kappa^2 \left\{ \frac{\chi_1^{\frac{1}{2}}}{F_1} - \frac{\chi_2^{\frac{1}{2}}}{F_1} + \frac{\chi_2^{\frac{1}{2}}}{F_2} \right\}^2}, \quad (26)$$

very nearly. Hence the current density is given by

$$I = \frac{e}{2\pi h} \frac{\mu^{\frac{1}{2}} \chi_1^{\frac{1}{2}}}{\chi_1 + \mu} \frac{\exp \left[- \frac{1}{2} \kappa \left\{ \frac{\chi_1^{\frac{1}{2}}}{F_1} - \frac{\chi_2^{\frac{1}{2}}}{F_1} + \frac{\chi_2^{\frac{1}{2}}}{F_2} \right\} \right]}{\left\{ \frac{\chi_1^{\frac{1}{2}}}{F_1} - \frac{\chi_2^{\frac{1}{2}}}{F_1} + \frac{\chi_2^{\frac{1}{2}}}{F_2} \right\}^2}. \quad (27)$$

For practical purposes we may replace F_1 by $(\chi_1 - \chi_2)/a$, and denote F_2 simply by F , the applied field. Then (27) reduces to

$$I = \frac{e}{2\pi h} \frac{\mu^{\frac{1}{2}}}{(\chi_1 + \mu) \chi_1^{\frac{1}{2}}} F^2 e^{-1} e^{\chi_1^{\frac{1}{2}}/F} \times \frac{\chi_1 \exp \left[-\frac{1}{3} \kappa a \frac{\chi_1 + \chi_2 + (\chi_1 \chi_2)^{\frac{1}{2}}}{\chi_1^{\frac{1}{2}} + \chi_2^{\frac{1}{2}}} \right]}{\chi_2 \left(1 + \frac{aF}{(\chi_1 \chi_2)^{\frac{1}{2}} + \chi_2} \right)^2}. \quad (28)$$

For values of F with which we are concerned we can generally replace the factor

$$1 + \frac{aF}{(\chi_1 \chi_2)^{\frac{1}{2}} + \chi_2}$$

by unity. The result of this investigation is that for the analysis of observations we must replace equations (3) and (4) by

$$\frac{d \log C}{d F_m^{-1}} = -2F_m - \frac{6.8 \times 10^7 \chi_2^{\frac{1}{2}}}{\beta}, \quad (29)$$

$$\begin{aligned} \log A = 12.0 + \log C - \log \frac{\mu^{\frac{1}{2}}}{(\chi_1 + \mu) \chi_1^{\frac{1}{2}}} - 2 \log \beta F_m \\ + \frac{6.8 \times 10^7 \chi_2^{\frac{1}{2}}}{\beta F_m} - \log \frac{\chi_1}{\chi_2} + \frac{1}{3} \kappa a \frac{\chi_1 + \chi_2 + (\chi_1 \chi_2)^{\frac{1}{2}}}{\chi_1^{\frac{1}{2}} + \chi_2^{\frac{1}{2}}}. \end{aligned} \quad (30)$$

§ 4. *The Effect of Film Thickness (a) on the Current-voltage Curves and the Derived Emitting Area.*

It is now easy to see how neglect of film-thickness has modified the emitting areas derived from a family of current-voltage curves, and how equation (30) may be used to remove this modification and to fix approximately the thickness of the film. As a film is built up which decreases the effective work function from χ_1 to χ_2 , a will increase from zero to a value comparable at least with atomic diameters. For example for a sodium film on tungsten which reduces the work function from 4.5 to 2 volts, the last term in (29) has the value

$$1.8 \times 10^8 a.$$

If this term is neglected in the analysis of the observations the calculated value of A will usually be much smaller for the smaller χ . This corresponds in the figures showing current-voltage plots to the fact that the plots of one family with different slopes (χ 's) do not intersect on the axis but to the right of it, showing an apparent decrease of the emitting area with decrease of the work function.

Table II.

Experiment.	Curve.	β .	χ electron volts.	A' cm. ²	A cm. ²	a cm.
1	3	19.4	4.5	5.1×10^{-8}	5.1×10^{-8}	—
1 (Fig. 3)	1	19.4	2.81	4.6×10^{-10}	5.1×10^{-9}	1.5×10^{-8}
1	2	19.4	1.58	1.8×10^{-10}	5.1×10^{-9}	2.5×10^{-8}
2	1	6.72	4.5	1.2×10^{-10}	1.2×10^{-10}	—
2 (Fig. 4)	3	6.72	1.41	4.8×10^{-12}	1.2×10^{-10}	3.9×10^{-8}
2	4	6.72	1.50	1.5×10^{-10}	1.2×10^{-10}	0.5×10^{-8}
2	5	6.72	1.52	8.7×10^{-12}	1.2×10^{-10}	2.2×10^{-8}
3	4	2.9	4.5	8×10^{-8}	8×10^{-8}	—
3 (Fig. 5)	3	2.9	3.95	3.9×10^{-8}	8×10^{-8}	0.4×10^{-8}
3	2	2.9	2.85	4.1×10^{-9}	8×10^{-8}	1.8×10^{-8}
3	1	2.9	2.33	8×10^{-10}	8×10^{-8}	2.8×10^{-8}
Fig. 1.	2	2.68	3.0	—	6.3×10^{-8}	—
Rother	Taf. X	115	4.0	—	4.9×10^{-10}	—

Table II shows values of β , χ , A' , A and a for the experiments under discussion. A' is the "apparent" emitting area calculated by the formula (5) and neglects the film effect. A is the "true" emitting area and is equal to A' for discharge from cathodes free of films. Otherwise, as a rule, $A' < A$. β is calculated from (3) in the film free curve of each experiment; χ_2 is then calculated from (29); a is found from expression

$$a = \frac{1}{6.8 \times 10^7} (\log A + \log \chi_1 - \log A' - \log \chi_2) \frac{\chi_1^{\frac{1}{2}} + \chi_2^{\frac{1}{2}}}{\chi_1 + \chi_2 + (\chi_1 \chi_2)^{\frac{1}{2}}}. \quad (31)$$

In the computation of Table II, χ for tungsten has been taken to be 4.5 volts, and the assumption has been made that the steepest members of the families of lines in experiments 1, 2 and 3 correspond to nearly clean states of the cathode, with this value of 4.5 as the thermionic work function. If this assumption is in any experiment false, then our calculated areas, and the values of χ found for the other members of the same family, will be slightly in error; but the changes in the areas and film thicknesses would not be large. In the computation of the Rother curve and of fig. 1, curve 2, the elementary theory, without films, has been used.

The results collected in Table II justify very well the assumption that the form of the emitting spot, *i.e.*, the value of β , remained constant throughout each experiment, for the range of χ found on this assumption, *viz.*, 4.5 to 1.4, agrees reasonably well with the change from tungsten to sodium. The

value of χ for sodium is not very definitely known but is probably rather less than 2.0. Experimentally the severe treatment required to produce the tungsten surface might be expected to make the emitting eminence a little less sharp. If an allowance for this were introduced into the calculation the range of χ would be less than that shown. If the form of the emitting spot remains constant it may fairly be assumed that its area also remains constant, and it thus becomes possible to calculate, as we have done, the film thickness from the apparent diminution in area. The film thicknesses for particularly stable films in experiments 1 and 2 are respectively 2.5×10^{-8} cm. and 2.2×10^{-8} cm. In experiment 3 a film which was rather less complete and less stable gave a similar thickness of 2.8×10^{-8} cm. Since in developing the theory we assumed a continuous surface film with a uniform internal field, all of which must be regarded as a rough approximation, these "film-thicknesses" can have no very precise physical meaning; they are, however, of the same order of magnitude as the distance 3.7×10^{-8} cm. between the closest sodium atoms in the crystal of metallic sodium.* From the nature of our idealised film we should expect its "thickness" to be less than this interatomic distance. In the case of the intermediate curves which have intermediate values of a we must suppose that the films are incomplete and we find that their "thicknesses" are considerably less than those of the stable films, but without knowledge of the structure of the film no meaning can be assigned to these small thicknesses. In the case of curves 3 and 4 of fig. 4, where the thicknesses are 3.9×10^{-8} and 0.5×10^{-8} respectively, but the χ is the same as for the stable film of thickness 2.2×10^{-8} of curve 5, the circumstances of the formation of the film were peculiar, involving a resting period of four years. We shall refer to other similar examples of variation in structure without change of χ in a later section.

§ 5. *Detailed Discussion of the Experiments.*

We now come to consider in more detail what is the support afforded to the theory by the existing experimental data.

As already stated the curves obtained by plotting observed values of $\log C$ against $1/F_m$ fall into families of lines which are very nearly straight; those members of a family which correspond to the weaker fields have the smaller slopes when so plotted, and vice versa for the stronger fields and steeper slopes. The family thus consists of a set of straight lines which when produced upwards are seen to have a short envelope and so seem to radiate approximately from

* Hull, 'Phys. Rev.' vol. 10, p. 661 (1917).

a common intersection situated near to but definitely not actually on the axis of infinite field.

Since the value of the work function χ corresponding according to equation (3) to any particular curve is not independent of the value of the correction factor β , it is clearly necessary that the experimental circumstances of the transition from the one extreme of a family to the other should be so far known that this transition can fairly be ascribed to a change of χ without change of β . For this reason those experiments are to be preferred in which a deliberate introduction of sodium is followed by a transition in the direction corresponding to a decrease in χ . We shall describe two experiments of this type.

A number of experiments showing transition in the opposite direction—that of increasing χ —are available from several sources. The use of these for our present purpose involves the additional assumption of an initial surface film of low χ . Effects of this kind are, however, so far usual in the early stages of any experiments that it is preferable to seek independent support for the presumption of such an initial surface film. We think that such support can be found in O. W. Richardson's investigations of the positive thermionic emission from freshly heated surfaces of various metals.* He showed that whatever the anode metal might be, the positive ions were always those of potassium which might be followed after longer heating by sodium. Our own experiments† have also shown that sodium salts adhering to the anode can be decomposed by electron bombardment and transferred to the cathode by sputtering or heating the anode. The last traces of such salts would in any case be difficult to eliminate, and they might even then be replaced by distillation from the glasswork when this is heated during the exhaust. In the experiment of this type which we shall describe there was, in addition to these general grounds, a definite reason for expecting the initial presence of a small quantity of sodium.

Experiment No. 1.—The tube used in this experiment had as cathode a loop of fine pure tungsten wire. Only a few current-voltage curves were taken, the original object being to study the effect of changes of cathode temperature and particularly the conditions of disappearance of the temperature effect; most of the observations were made at constant voltage. The curves shown in fig. 3 represent two extreme members of a family with one intermediate

* O. W. Richardson, 'Roy. Soc. Proc.,' vol. 89, p. 507 (1914).

† Gossling, *loc. cit.*, p. 620.

member. The tube behaved very steadily throughout, that is, erratic spontaneous changes in the current were very rare.

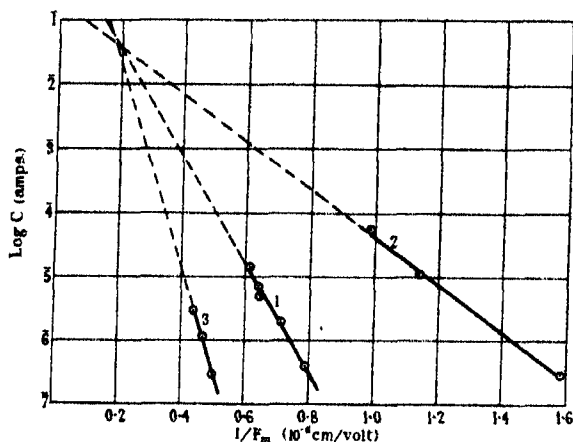


FIG. 3. (Experiment No. 1.)

The details of the experiment were briefly as follows :—

The cathode, a loop of pure tungsten wire of diameter 0.0016 cm. was heated in a slightly moist mixture of nitrogen and hydrogen with the object of fixing its shape before assembling the tube ; but with the more important result, from the present standpoint, of removing the complicated surface layers with which a freshly drawn wire is coated. Adherent shreds and scales of tungsten would, however, not be removed.* The anode was a nickel disc which had been used previously in a similar experiment and was coated afresh with sodium phosphate to serve as a source of sodium. The exhaust of the tube followed the procedure now common ; the tube was sealed on to a liquid air trap and exhausted by a mercury condensation pump. During the exhaust the whole tube (of lead glass) was heated in an oven to 400° C. for 5 hours. The anode was then heated by induced high frequency currents until its gases were very largely removed. The tube was connected to the pump during the whole experiment. Curve 1 of fig. 3 was then obtained before any further heating of the cathode. It represents, as will be seen later, an intermediate state.

After currents of 10 to 20 microamperes had been passed for some time, resulting in the decomposition of the salt on the anode and transference of

* Cf. Avery and Smithells, 'Proc. Phys. Soc.', vol. 39, p. 85 (1927).

sodium to the cathode as described in detail in a former paper,* a rapid transition took place to a point on curve 2. A new steady state was thus established and curve 2 was obtained. During a number of subsequent observations at constant voltage there was a further but relatively slight increase of current; the current was observed finally to be independent of the cathode temperature up to 1750° K. This is taken as showing that the cathode had attained a very stable state. Curve 2 thus represents a close approach to the low voltage extreme of the family.

A number of observations were now made on the Schottky effect showing the influence of strong fields on thermionic currents. In course of these, the cathode was repeatedly heated to 2100° K., and in the middle there was an interruption during which condensible gases to a pressure of a few thousandths of a millimetre were admitted to the tube from the liquid air trap. Before resuming the auto-electronic experiment, the anode was again inductively heated.

After all this it was found that the state of curve 2 no longer existed; there was a gradual transition through various intermediate states, starting from near that of curve 1 and proceeding in the reverse of the former direction until curve 3 was obtained.

Our interpretation of these changes is, first, that the change from the temporary state of curve 1 in the direction of decreasing voltage to the stable state of curve 2, a change which we have found to be characteristic of all tubes into which a source of sodium has been introduced, represents the building up of a sodium layer on the original tungsten surface. This layer is held in such a way as not to be readily volatilised even at 1750° K., and since a thick sodium layer would be volatile, we conclude that the state of curve 2 is that of a thin non-volatile layer. The effect of subsequent heating to higher temperatures together with the exposure to condensible gases was to remove and oxidise the sodium responsible for the first change, the result being the transition from curve 2 to curve 3, which latter curve we take to represent an approach to the high-voltage extreme of the family.

We shall now proceed to apply the results of the theory to the extreme curves 2 and 3. In this and the succeeding experiments the permanence of the emitting spot is supported by the intermediate curves, which are consistent with the assumed constancy of the local field correction factor β and of the emitting area. Assigning to the state of curve 3 the value 4.5 for χ representative of a tungsten surface, we find from the slopes of the curves that the value

* *Res. Labs. of G.E.C. (Gossling), loc. cit., p. 620.*

of β common to the two curves is 19.4 and χ for curve 2 has the value 1.58. The intermediate value of χ for curve 1 is 2.81. The value of the area A for curve 3 is 5.1×10^{-9} cm.². The apparent values A' for curves 2 and 1 where surface films are present are 1.8×10^{-10} and 4.6×10^{-10} respectively, but using equation (31) we determine the thicknesses of the films responsible for these apparent decreases to be 2.5×10^{-8} cm. for curve 2 and 1.5×10^{-8} cm. for curve 1. These results are tabulated in Table II.

Experiment No. 2.—The general course of this experiment was similar to the foregoing. The cathode, however, consisted of a brush of about 20 ends of pure tungsten wire 0.0020 cm. in diameter mounted on a stouter tungsten loop. The ends of wire had been roughly cut with scissors, and although they may have been somewhat smoothed by sputtering a fairly high value of the field correction factor, based on a smooth ellipsoidal end, must be considered probable from the macroscopic form of the end alone. Comparison of the currents obtained with those from cathodes with only single similar ends of wire shows, as might be expected, that only one end was active in the present case. The anode was a nickel disc which had previously been largely freed from gas by thermionic bombardment before the tube was opened and the brush fitted to the cathode. The anode was again coated with sodium phosphate to serve as a source of sodium. The procedure in the early stages of the exhaust was as in experiment No. 1, but in this case the anode was heated by auto-electronic bombardment, the conditions as regards current and voltage varying within the range later described. At one point the brush was heated by passing current through the loop on which it was mounted. The tube was finally sealed off from the pump.

After sealing, the voltage required for a given current was found to be about as high as had ever been required during the exhaust. After a small progressive transition in the direction of higher voltage the currents became reproducible and curve 1 of fig. 4 was obtained representing the high-voltage extreme of the family. This state was stable for the time being, even for currents of several milliamperes.

During the continued passage of currents of about a milliampere the progressive transition, characteristic of tubes with introduced sodium, in the direction of decreasing voltage set in. In the early stages of this a sodium glow could be seen on the cathode system. When a new fairly steady state had been reached curve 2 was taken.

After this the tube lay idle for about four years. Continuing the experiment after this interval the low-voltage state was found to have persisted, curves 3,

4 and 5 being obtained in succession, of which curve 5 appears to represent the normal low voltage extreme, curve 2 taking an intermediate place.

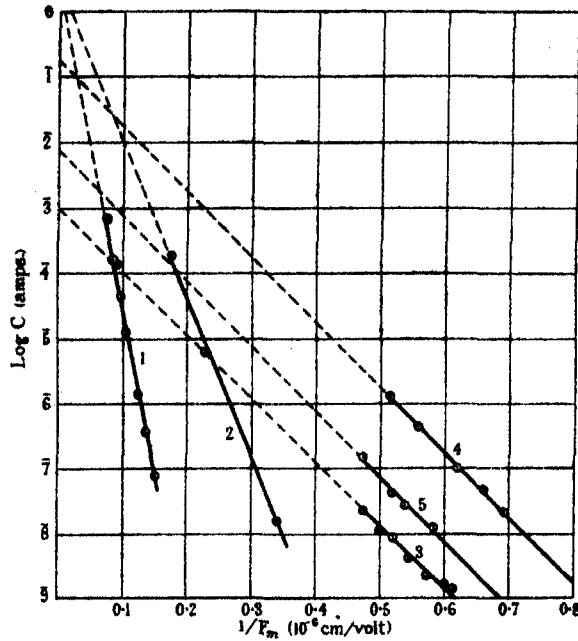


FIG. 4. (Experiment No. 2.)

Curves 3 and 4 showed instability for values of the current higher than those plotted. During the transition from curve 3 to curve 4 a considerable number of readings were obtained which group themselves in the neighbourhood of curve 5 which, therefore, appears to represent a relatively stable state. In this experiment the operation of sealing off and the accompanying liberation of traces of oxidising gases from the fusing glass seem, as in other similar cases, to have resulted in a temporary removal of free sodium. The final stages of the process were actually observed, and curve 1 is therefore taken as representing an approximation to a tungsten surface. The subsequent transition, as before, represents the building up of a sodium layer; in the present case there were visible evidences of the transfer of sodium to the cathode. The long idle interval favoured the completion of the process, probably by absorption of the remaining traces of oxidising gases. During the final stage, the main supply of sodium was not drawn upon because the power expended in the anode was not, as previously, sufficient to heat it. For this reason, the extreme low voltage state of curve 4 was not very stable. Proceeding as

before to analyse the results in the light of the theory we obtain the results shown in Table II.

Experiment No. 3.—This experiment differs from both the foregoing in that there was no deliberate provision for a continual supply of sodium. The cathode, however, which consisted of a single end of pure tungsten wire, had had its edges rounded by etching in fused sodium nitrite; decomposition of residues of this salt may, therefore, have provided a limited supply of sodium, the dispersal and ultimate failure of which proceeded in this case rather more slowly and regularly than in tubes containing only chance traces of sodium. The end of the cathode as viewed under a microscope showed the form of a blunt flattened point with smooth, well rounded edges; since the form assumed for calculation was an ellipsoid of revolution, the field correction factor may be somewhat in error owing to the departure of the macroscopic form of the surface from that assumed. The anode was a nickel disc which had been partly freed from gas by thermionic bombardment in a previous experiment.

The procedure in exhaust was as previously described, the anode being heated by auto-electronic currents of the order of a milliamperes at 10,000 volts. In the later stages there was a marked transition in the direction of lower voltages. Conditions were not steady enough for a curve to be obtained but the general values of $1/F_m$ were about 1.4 times those shown in curve 1 of fig. 5. After a final bombardment with several milliamperes of current the tube was sealed off and the first readings lay between curves 1 and 2 of fig. 5. These were

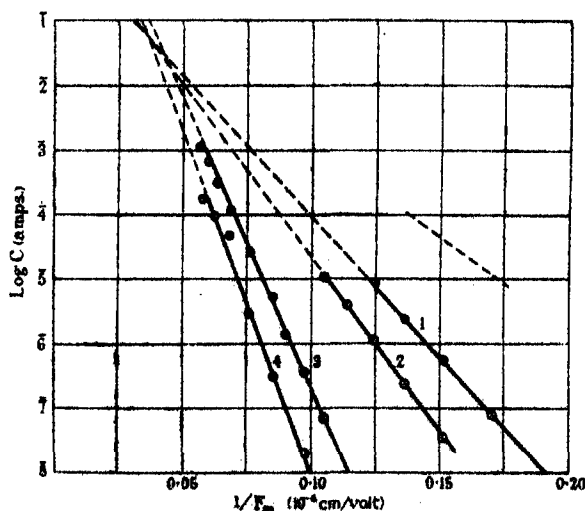


FIG. 5. (Experiment No. 3.)

followed by a slight transition in the direction of lower voltage and a temporarily stable state gave the reproducible readings shown in curve 1. On passing heavier currents there was a progressive transition in the high voltage direction and curve 2 representing four sets of readings was obtained. The passage of still heavier currents for a short time resulted in a further transition resulting in the state of curve 3 which also repeated. Finally a longer period at about 1 milliamperes produced the state of curve 4.

The four curves shown thus represent the high voltage half of a family of which the low voltage extreme is represented by the earlier readings for which the values of $1/F_m$ were about 1.4 times those of curve 1. That the low-voltage state should have survived at all the severe conditions of exhaust by auto-electronic bombardment shows that more than a mere trace of sodium was initially available, but that there was no permanent supply is clear from the direction of the successive transitions following the passage of heavy currents, this direction being here opposite from that observed in the two cases previously described. The results of the analysis of the observations are shown in Table II.

In addition to the three experiments which have just been described mention should be made of the numerous experiments described by various authors* in which cylindrical cathodes have been used with results indicating the initial presence and progressive failure of traces of sodium. In these wherever sufficient curves are available there is an evident tendency to give mixed families of curves, and even occasionally a passage in the course of a single curve from one straight line to another intersecting it (*cf.* fig. 6). Such results are natural, for in the case of a cylindrical or of a plane cathode the total area subjected to the intense field is immensely greater than in that of a pointed cathode, and the probability of more than one local area being in or near the emitting state is also much greater. Further, with a limited and fluctuating supply of sodium no one area remains in a constant state very long, but first one area will predominate and then another. In spite, however, of these uncertainties the "apparent area" as calculated without allowance for the film effect tends generally to be lower for the low voltage (and presumably low χ) curves than for the high voltage and high γ . The results of such experiments can, therefore, be held to give further general confirmation of the theory of the film effect.

In the discussion of these experiments we have ignored effects due to the presence of gas films on the cathode surface; this course was forced on us in

* Gossling, Millikan and Eyring, Del Rosario, Piersol, *loc. cit.*

the absence of evidence from the experiments themselves as to the extent of any such effects. It must, however, be admitted that here, as in all work on

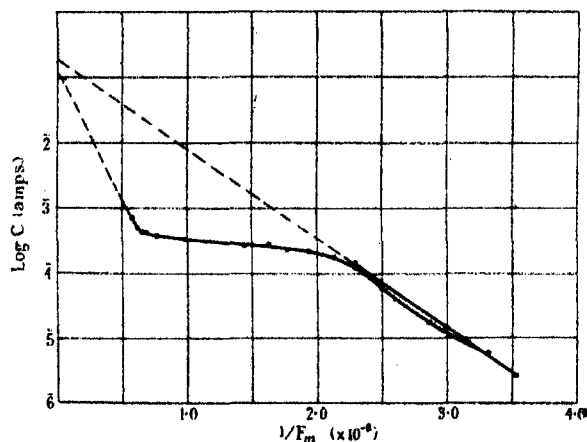


FIG. 6. (From Rother, *loc. cit.*)

metal surfaces which have not recently been strongly heated, there is a certain presumption in favour of gas films. No experimental technique can be considered complete which does not include measures for eliminating them. De Bruyne* has shown that air at a fairly high pressure, 0.0005 to 0.0008 mm., will depress the current to an extent which, though marked, is much smaller than the variations we have been considering; hydrogen gives a smaller effect still. He shows also that even at such pressures prolonged passage of quite small discharge currents results in the diminution both of the pressure of the free gas and of the depression of the current. From this we conclude that the stability of these as of other films depends on a sufficient supply of material being available; especially if the discharge currents are high, 10^{-4} amp. or more. In the experiments discussed the vacuum conditions were good and the readings generally stable at high currents; it is therefore not very likely that the results were appreciably affected by gas films on the cathode.

§ 6. *The Fugitive Temperature Effect.*

The proof that the structure of the surface can have a marked effect on the value of the emission constant enables us to attempt an explanation of the fugitive temperature effect. This, it should be understood, is not the very small and under certain circumstances negligible effect discussed by Fowler

* De Bruyne, 'Phil. Mag.', vol. 5, p. 574 (1928).

and Nordheim,* and more explicitly by Houston,† but the very conspicuous though transitory effect described by Gossling,‡ who observed cases in which a rise of 1000° C. in the cathode temperature increased the current as much as a hundredfold. The magnitude of the effect was found to depend on the experimental conditions, indeed in the case of the fully-developed sodium film in experiment No. 1, curve 2, it was inappreciable. With fresh wires, however, heated for the first time, a relatively small rise of temperature, 300° C. or so, may affect the current. In the later stages a greater rise, 700° C. or more, may be required. Since the rise of temperature renders the state of the cathode still less stable and makes it intolerant of large currents, reproducible readings were difficult to obtain. In the best cases, however, the rise of temperature appears to have increased the current in the same proportion whatever the value of the field. This would correspond to a change in the emission constant (*i.e.*, the factor before the exponential in the emission formula) without a change of the work function. The change is reversible if not carried too far. The maximum reversible change depends on the state of the cathode and varies between 10 and 100 times the values of the currents at room temperature. There is some evidence of a time lag of a few seconds before a steady state is reached when the temperature is changed. Changes of this order of magnitude could be caused by changes in film thickness of order not exceeding the diameter of a sodium atom. It is not, however, suggested that a change in film thickness is actually responsible. The circumstances in which the effect is observed indicate the presence of an incomplete film for which the value of χ is intermediate between those for sodium and tungsten; the change can also be reversible and would, therefore, seem more likely to be due to a rearrangement of the surface structures rather than to the loss and regain of material. This rearrangement must in many cases be such as to affect the value of the emission constant much more than that of χ , just as in the case of curves 3, 4 and 5 of fig. 4, experiment 2, previously discussed.

* *Loc. cit.*

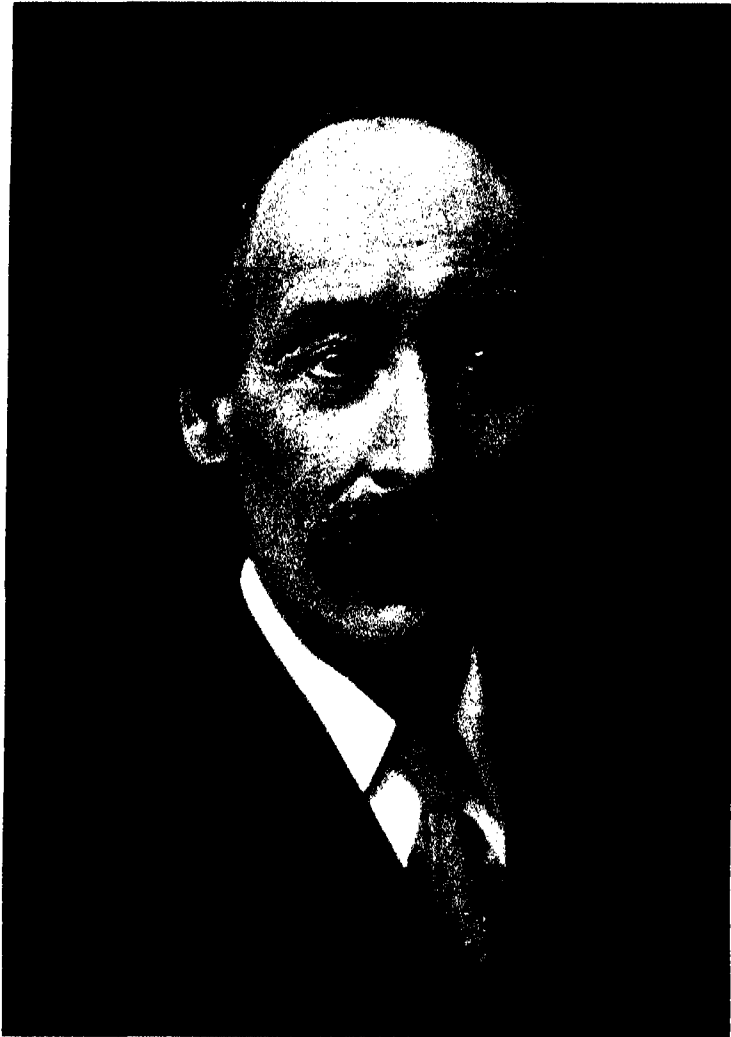
† Houston, 'Phys. Rev.', vol. 33, p. 361 (1929).

‡ *Loc. cit.*, p. 623.

OBITUARY NOTICE.

CONTENTS.

	PAGE
MICAHIAH JOHN MULLER HILL (with portrait)	i



U. J. M. Hill

MICAIAH JOHN MULLER HILL, 1856-1929.

MICAIAH JOHN MULLER HILL was the eldest son of the Rev. Samuel John Hill and was born at Berhampore, Bengal, on February 22, 1856, during the stormy days of the Indian Mutiny, in which he narrowly escaped death. He was educated at the School for the Sons of Missionaries, Blackheath, and entered University College, London, as a student in October, 1872. His academic career in London was one long sequence of brilliant successes and at the same time an arduous struggle against financial difficulties which he could overcome only by winning such scholarships as the College and the University of London had to offer in those days—rare and coveted distinctions which fell to the lot of very few.

In 1874 he took his B.A. degree in London, obtaining the first place in the Mathematical Honours List, a feat he accomplished in only two years and which he followed up in 1876 by winning the Gold Medal in the M.A. Examination. By this time he had entered as an undergraduate at Peterhouse, Cambridge. In 1879 he was Fourth Wrangler and Smith's Prizeman. He then returned to University College for a few months as assistant in the Department of Mathematics, and, in 1880, at the age of twenty-four, was elected to the Chair of Mathematics at Mason College, as it then was, now the University of Birmingham.

It was during his tenure of the Chair at Birmingham that Hill produced his earliest research work, which dates from 1883. In that year he published three papers, one on a generalisation of Tesseral Harmonics for more than two variables, another on the equation giving the anharmonic ratios of the roots of a quintic, and the third, which started an important group in Hill's earlier work, on a generalisation of the equations of Hydrodynamics for space of n dimensions. This was immediately followed by a paper developing the theory of cylindrical vortices of finite section, moving in an infinite fluid, in particular of the elliptic cylindrical vortex. This paper is notable as being Hill's first contribution to the Transactions of the Society.

In 1884 Hill was called from Birmingham to fill the Chair of Mathematics at University College, London, in succession to R. C. Rowe. His colleagues at the time included T. G. Bonney, Carey Foster, Charles Graham, L. F. Vernon Harcourt, Victor Horsley, Alexander Kennedy, Ray Lankester, Henry Morley, and G. D. Thane. Two, namely, Karl Pearson, who was appointed in the same year (1884) to the Chair of Applied Mathematics, and A. F. Murison, who held the Chair of Roman Law, were to remain his colleagues during the forty years of his teaching life at University College.

The life of a professor in a University College in those days was very

different from that to which we are now accustomed. Endowed Chairs were the exception and stipends largely consisted of professors' shares of fees, so that there was a strong inducement to make one's teaching popular rather than profound, a temptation fortunately resisted in most cases, certainly in the case of Hill. Assistants were few, and often paid by the professor. When Hill first took up his duties, the department of Mathematics boasted only a single assistant. The bulk of the routine work of undergraduate teaching, such as the correction of students' exercises, fell upon the professor, and this work Hill, trained as he had been in a hard school, performed with unflagging energy and zeal, and an unselfish devotion which won him the affection and admiration of generation after generation of students. To the last, although many other duties supervened and the general improvement of conditions enabled him to be relieved of such routine work, he insisted on retaining a proportion in his own hands, seeing in it the indispensable means for gaining that personal touch with his students which he felt to be a most important duty and a valued privilege.

It will be readily understood that the prosecution of mathematical research, under such conditions, was no easy task. Nevertheless Hill found time to continue his work on Hydrodynamics, begun at Birmingham, and to publish a few minor papers on Pure Mathematics, largely arising out of his teaching.

It was not until 1888 that he was able to produce really important fresh research work; he then attacked, for the first time, the subject of singular solutions of Differential Equations, a subject for which he always retained a particular liking, for he returned to it in his later years and published a paper on it as late as 1917. In a series of investigations between 1888 and 1893 he dealt fully with the various loci connected with the differential equation of the first order and its complete primitive, extending and consolidating the work of Cayley on the p - and c -discriminants of these equations, and discussing the mode of appearance of the envelope, node-, cusp-, and tac-loci, and important cases of exception. This led him to discuss the more general question of the appearance of loci of singular points in the case of the locus of ultimate intersections of a family of surfaces*; and here Hill broke entirely fresh ground and obtained a variety of new and valuable results.

Hill's later papers (1916-1921) on Differential Equations may be mentioned here, as they belong logically to the same group. In these papers he considers the classification of integrals of ordinary differential equations of the first order and of partial differential equations of Lagrange's form, and in particular the problem, whether the complete primitive and the singular solution obtained by the ordinary rule do in fact exhaust the possible solutions in the case of the ordinary differential equation of the first order.

In 1891, and again in 1894, he returned for a time to Hydrodynamical

* 'Phil. Trans.,' A, vol. 183, pp. 141-273 (1892).

problems ; in the latter year he published the solution for his well-known spherical vortex. This was, however, with the solitary exception of a paper on the Connecting Rod, published in the Proceedings of the Institution of Civil Engineers in 1895, his last excursion into the realm of Applied Mathematics. In view of the success of his earlier Hydrodynamical work, this must remain a matter for regret ; but Hill always drew much of his inspiration from his teaching and his Chair was, in effect, limited to Pure Mathematics. Moreover, his mind had a strong bent towards rigour ; he was at his best in tasks which demanded critical examination of first principles, and he sometimes expressed, in private conversation, doubts as to the validity of many methods which the applied mathematician is apt to use without question.

It was in 1897 that Hill published, in the Cambridge Philosophical Transactions, his first paper on a subject which he was to make peculiarly his own, namely, the critical re-examination of the Vth and VIth Books of Euclid. He was first led to this by difficulties which he encountered in the attempt to teach beginners the theory of proportion, and, during the next thirty years of his life, much of his mathematical activity was spent in trying to unravel the problems presented by the work of the great Greek geometer, in the form in which it has reached us. In this study of Euclid's Vth Book, Hill followed the tradition of his own great predecessor, Augustus de Morgan, of whom he always spoke with the greatest admiration.

His ideas on the subject are set forth in five papers, published between 1897 and 1922 in the Cambridge Philosophical Transactions, in an edition of the Vth and VIth Books of Euclid, and in a book on the Theory of Proportion, published in 1914. In these he practically reconstructed Euclid's treatment, simplifying many of the proofs, and eliminating unnecessary axioms and definitions. In particular he based his treatment on the view that the definition of *equal* ratios should be adequate for the proofs of all properties of such ratios, and he succeeded in showing that Euclid's appeal to the definition of *unequal* ratios for this purpose was unnecessary. This idea, and the use of the axiom of Archimedes, form the groundwork of his treatment, which is largely permeated by Dedekind's conception of the nature of the irrational number.

It was unfortunate that this work of Hill's coincided with the movement for omitting the study of Euclid from the school curriculum. The philosophical significance of the Vth Book really lies in the fact that it provides a theory of numerical measurement of physical quantities, a fact which was never brought out in the old teaching. Those of us who learnt their mathematics at school on the old lines well remember the feeling of bewilderment which came over us when confronted by that awe-inspiring definition of equal ratios. Had Hill's investigation appeared a few years earlier and been properly appreciated, it might have done much to preserve for the school curriculum one of the finest logical disciplines to be found in elementary mathematics.

The work on the Vth Book did not by any means exhaust Hill's later mathematical activities. In a series of papers on the continuation of Power Series, the last of which dates from 1917, he succeeded in demonstrating that the step by step continuation of a number of such series (including those for $(1+x)^n$, $\arctan x$, $\arcsin x$ and the hypergeometric series), round a singularity, actually leads to the well-known interchange of branches, usually obtained directly from the function which the series represents in its first domain of convergence. A number of isolated papers deal with a variety of subjects ranging from the axioms of geometry to the theory of functions. In all Hill's mathematical output comprises nearly fifty original publications.

The mere recital of his contributions to mathematics, however, would give a quite inadequate idea of his position and influence in the academic world. As a teacher he had, to an extraordinary degree, that infinite capacity for taking pains in which Carlyle saw the mark of genius; and he possessed that rare quality, which students so keenly appreciate, of never slurring over difficulties: time spent on making a demonstration perfect was always to him time well spent. And he showed great sympathy with the occasionally devious mental processes of beginners and would even, sometimes, adapt his demonstrations to them. The writer remembers, in his student days, sending up to him a solution which, alas! meandered through as many pages as it should have taken lines, arriving at the desired result by a singularly laborious and inelegant process. Hill read patiently and carefully every line, and in the end his only (and characteristic) comment was that it was a "very courageous" solution!

Above all, he loved his students, a feeling which was universally and deeply reciprocated. When he retired in 1924 from the Chair of Mathematics, his friends asked him in what way he would wish them to commemorate his long connection with University College; and he then, remembering the financial struggle of his early years, expressed the desire that any subscriptions received should be devoted to establishing a Loan Fund by means of which the difficulties of students in straitened circumstances might be temporarily relieved, while their spirit of independence was to be preserved by an undertaking of eventual repayment, so soon as they felt able to do so. It was done according to his wishes, and, indeed, no more fitting memorial could have been found of a life spent in the unselfish service of studious youth.

Hill was one of those who fought for the establishment in London of a real teaching University; and from the re-constitution of the University in 1900 until 1926, when ill-health compelled his retirement, he was a member of its Senate, in which his balanced judgment, ever-courteous modesty, and, above all, his transparent honesty of purpose and that moral atmosphere which radiated from him and impressed all, even the bitterest opponents of his policy, who came into contact with him, soon gained for him a position of ascendancy. For ten years he was Chairman of the Academic Council, the acknowledged

leader and spokesman of the internal side; and for two years (1909–1911) he was Vice-Chancellor of the University, an honour which has only twice been given to a professor. To his initiative were due many important developments, the full effects of which are only now beginning to be felt, such as the establishment of proper machinery for appointments to Chairs and Readerships and various improvements in the status and qualifications of teachers of the University. His work for the University continually absorbed more and more of his time, and his friends often regretted that he should have accepted such heavy burdens at the expense of his mathematical work. He himself felt this growing difficulty and would often express his sorrow that time was lacking to keep pace in his reading with modern research. That under the circumstances he was able, during the years 1900–1926, to produce as much mathematical work as he did is remarkable; what he would have accomplished, had his scientific activities not been hampered by administrative work, must remain a matter for speculation, but that the loss was great cannot be doubted.

Hill was elected a Fellow of the Society in 1894 and served on the Council in the years 1911–1913. In addition to his London degrees he held the Sc.D. of Cambridge and Hon. LL.D. of St. Andrews. He served on the Council of the London Mathematical Society in 1886 and again for the ten years 1891–1901, being Vice-President in 1894 and 1895. In 1927–8 he was President of the Mathematical Association.

Hill married, in 1892, Minnie Grace, daughter of Marriott Ogle Tarbotton, of Nottingham. There were three children of the marriage, two sons and one daughter, all of whom survive him. Those who were privileged to have access to his home circle appreciated its warm and happy atmosphere, where he found the peace of mind necessary for his arduous tasks. He had the great joy of seeing both his sons pass unscathed through the perils of the War, after winning distinction in the front line with the Royal Flying Corps. His last years were, however, darkened by the loss in 1920 of a beloved and devoted wife and, later, by an illness which culminated, during the last fifteen months of his life, in total blindness. He bore this new trouble with characteristic courage and patience, and, in spite of this handicap, actually completed and delivered, in January, 1928, his second Presidential Address to the Mathematical Association. Almost to the day of his death he continued at work, contending with surprising success against well-nigh insuperable obstacles, and planning a book on the foundations of Geometry.

The end came swiftly and comparatively painlessly on January 11th, 1929.

L. N. G. F.

INDEX TO VOL. CXXIV. (A)

- Adsorbed gas and emission of soft X-rays (Nakaya), 616.
 Adsorption of electrolytes, influence of pH (Phelps and Peters), 554.
 Alpha particles, radioactive decay and nuclear penetration (Fowler and Wilson), 493.
 Analysis by X-ray spectroscopy (Eddy and others), 249.
 Asundi (R. K.) The Third Positive Carbon and Associated Bands, 277.
 Asundi (R. K.) *See also* Johnson and Asundi.
 Atom, many-electron, relativistic theory (Gaunt), 163.
 Bhagavantam (S.) The Magnetic Anisotropy of Naphthalene Crystals, 545.
 Bickley (W. G.) Hydrodynamic Forces acting on a Cylinder in Motion, and the idea of a "Hydrodynamic Centre," 296.
 Brunt (D.) The Transfer of Heat by Radiation and Turbulence in the Lower Atmosphere, 201.
 Catalysis by silver of the union of hydrogen and oxygen (Chapman and Hall), 478.
 Caywood (W.) *See* Patterson and others.
 Chapman (D. L.) and Hall (W. K.) A Study of the Catalysis by Silver of the Union of Hydrogen and Oxygen, 478.
 Clark (R. J.) On the Direct Determination of the Electrostatic Moments of Molecules, 689.
 Combination of hydrogen and oxygen (Thompson and Hinshelwood), 219.
 Curie point and magnetostriction (Fowler and Kapitza), 1.
 Darwin (G. C.) A Collision Problem in the Wave Mechanics, 375.
 Davidson (P. M.) *See* Richardson and Davidson.
 Davies (L. P.) The Soft X-Ray Emission from Various Elements after Oxidation, 268.
 Dispersion in metals, quantum theory (Kronig), 409.
 Duncan (W. J.) *See* Frazer and Duncan.
 Eddy (C. E.), Laby (T. H.) and Turner (A. H.) Analysis by X-Ray Spectroscopy, 249.
 Einstein's unified field theory (McVittie), 366.
 Electrical condition of hot surfaces during adsorption (Finch and Stimson), 356.
 Electrons, emission from cold metals (Stern and others), 699.
 Finch (G. I.) and Hodge (D. L.) Gaseous Combustion in Electric Discharges, III, 303.
 Finch (G. I.) and Stimson (J. C.) The Electrical Condition of Hot Surfaces during the Adsorption of Gases, III, 356.
 Flint (H. T.) The First and Second Order Equations of the Quantum Theory, 143.
 Fowler (R. H.) and Kapitza (P.) Magnetostriction and the Phenomena of the Curie Point, 1.
 Fowler (R. H.) and Wilson (A. H.) A Detailed Study of the "Radioactive Decay" of and the Penetration of α -Particles into a Simplified One-Dimensional Nucleus, 493.
 Fowler (R. H.) *See also* Stern and others.
 Frazer (R. A.) and Duncan (W. J.) On the Criteria for the Stability of Small Motions, 642.
 Freeman (L. J.) Further Investigations of the Spectrum of Ionised Nitrogen, 654.

- Gaseous combustion in electric discharges (Finch and Hodge), 303.
- Gaunt (J. A.) The Relativistic Theory of an Atom with Many Electrons, 163.
- Germanium, arc spectrum (Rao), 465.
- Gillam (A. E.) and Morton (R. A.) The Absorption Spectra of Halogens and Inter-halogen Compounds in Solution in CCl_4 , 604.
- Gossling (B. S.) See Stern and others.
- Grace (S. F.) Internal Friction in certain Tidal Currents, 150.
- Hall (W. K.) See Chapman and Hall.
- Halogens and inter-halogen compounds, spectra (Gillam and Morton), 604.
- Hargreaves (J.) The Effect of a Nuclear Spin on the Optical Spectra, 568.
- Hartree (D. R.) See Waller and Hartree.
- Havelock (T. H.) The Dispersion of Double Refraction in Quartz, 46.
- Helium, metastable, action on metal (Oliphant), 228.
- Hill (M. J. M.), obituary notice, i.
- Hinshelwood (C. N.) See Thompson and Hinshelwood.
- Hodge (D. L.) See Finch and Hodge.
- Howland (R. C. J.) Stress Systems in an Infinite Strip, 89.
- Hurst (H. E.) The Suspension of Sand in Water, 196.
- Hydrocarbon chain compounds, structure and properties (Müller), 317.
- Hydrodynamic centre and forces on a cylinder in motion (Bickley), 296.
- Hydrogen ion concentration, influence on adsorption (Phelps and Peters), 554.
- Hydrogen spectrum, parhelium bands (Richardson and Davidson), 50, 69.
- Infra-red investigations of molecular structure (Snow and others), 442, 453.
- Ionisation by collision in monatomic gases (Townsend and MacCallum), 533.
- Iron, behaviour at Ac_3 point (Quinney), 591.
- Johnson (R. C.) and Asundi (R. K.) The Structure of the High Pressure Carbon Bands and the Swan System, 668.
- Kapitza (P.) See Fowler and Kapitza.
- Kronig (R. de L.) The Quantum Theory of Dispersion in Metallic Conductors, 409.
- Laby (T. H.) See Eddy and others.
- Lyons (C. G.) and Rideal (E. K.) On the Stability of Unimolecular Films, 322, 333, 344.
- MacCallum (S. P.) See Townsend and MacCallum.
- McVittie (G. C.) On Einstein's Unified Field Theory, 366.
- Magnetic anisotropy of naphthalene (Bhagavantam), 545.
- Magnetostriction and the Curie point (Fowler and Kapitza), 1.
- Molecules, electrostatic moments (Clark), 689.
- Monatomic gases, ionisation by collision (Townsend and MacCallum), 533.
- Morton (R. A.) See Gillam and Morton.
- Mott (N. F.) On the Interpretation of the Relativity Wave Equation for Two Electrons, 422. The Scattering of Fast Electrons by Atomic Nuclei, 425.
- Müller (A.) The Connexion between the Zig-Zag Structure of the Hydrocarbon Chain and the Alternations in the Properties of Odd and Even Numbered Chain Compounds, 317.
- Nakaya (U.) On the Emission of Soft X-Rays by Different Elements, with reference to the Effect of Adsorbed Gas, 616.

- Naphthalene, magnetic anisotropy (Bhagavantam), 545.
- Night sky, method of measuring light (Rayleigh), 395.
- Nitrogen, ionised, spectrum (Freeman), 654.
- Nuclear spin in optical spectra (Hargreaves), 568.
- Obituary notice :—M. J. M. Hill, i.
- Oliphant (N. L.) The Action of Metastable Atoms of Helium on a Metal Surface, 228.
- Patterson (H. S.), Whytlaw-Gray (R.) and Cawood (W.) The Process of Coagulation in Smokes, 502. The Structure and Electrification of Smoke Particles, 523.
- Perturbation theory in quantum mechanics (Wilson), 176.
- Peters (R. A.) See Phelps and Peters.
- Petroleum, theory of cracking (Wilson), 16.
- Phelps (H. J.) and Peters (R. A.) The Influence of Hydrogen Ion Concentration on the Adsorption of Weak Electrolytes by Pure Charcoals, 554.
- Quantum theory, first and second order equations (Flint), 143.
- Quantum theory of dispersion in metallic conductors (Kronig), 409.
- Quartz, dispersion of double refraction (Havelock), 56.
- Quinney (H.) A Comparison between the Behaviour at the Ac_3 Point of Single Crystal Iron and Polycrystal Iron, 591.
- Radiation heat transfer and turbulence (Brunt), 201.
- Radioactive decay (Fowler and Wilson), 493.
- Rao (K. R.) The Arc Spectrum of Germanium, 465.
- Rawlins (F. I. G.) See Shaw and others.
- Rayleigh (Lord) A Photoelectric Method of Measuring the Light of the Night Sky with Studies of the Course of Variation through the Night, 395.
- Richardson (O. W.) and Davidson (P. M.) The Spectrum of H_2 : the Bands analogous to the Parhelium Line Spectrum, 50, 69.
- Richardson (O. W.) and Robertson (F. S.) The Emission of Soft X-Rays by Different Elements at Higher Voltages, 188.
- Rideal (E. K.) See Lyons and Rideal, and Snow and others.
- Robertson (F. S.) See Richardson and Robertson.
- Scattering of fast electrons by nuclei (Mott), 425.
- Smoke particles, structure and electrification (Patterson and others), 523.
- Smokes, coagulation (Patterson and others), 502.
- Snow (C. P.), Rawlins (F. I. G.) and Rideal (E. K.) Infra-Red Investigations of Molecular Structure, II, 453.
- Snow (C. P.) and Taylor (A. M.) Infra-Red Investigations of Molecular Structure, I, 442.
- Spectra, absorption, of halogens and inter-halogen compounds (Gillam and Morton), 604.
- Spectra of third positive carbon band (Asundi), 277.
- Spectra, optical, effect of nuclear spin (Hargreaves), 568.
- Spectrum, arc, germanium (Rao), 465.
- Spectrum, high pressure carbon bands (Johnson and Asundi), 668.
- Spectrum of H_2 , parhelium bands (Richardson and Davidson), 50, 69.
- Spectrum of ionised nitrogen (Freeman), 654.
- Stability of small motions, criteria (Frazer and Duncan), 642.
- Stern (T. E.), Gossling (B. S.) and Fowler (R. H.) Further Studies in the Emission of Electrons from Cold Metals, 699.

Stimson (J. C.) *See* Finch and Stimson.

Stress systems in an infinite strip (Howland), 89.

Suspension of sand in water (Hurst), 196.

Taylor (A. M.) *See* Snow and Taylor.

Taylor (G. I.) The Criterion for Turbulence in Curved Pipes, 243.

Thompson (H. W.) and Hinshelwood (C. N.) The Influence of Nitrogen Peroxide on the Combination of Hydrogen and Oxygen, 219.

Tidal currents, internal friction (Grace), 150.

Townsend (J. S.) and MacCallum (S. P.) Ionisation by Collision in Monatomic Gases, 533.

Turbulence in curved pipes (Taylor), 243.

Turner (A. H.) *See* Eddy and others.

Unimolecular films, stability (Lyons and Rideal), 322, 333, 344.

Waller (I.) and Hartree (D. R.) On the Intensity of Total Scattering of X-Rays, 119.

Wave equation for two electrons (Mott), 422.

Wave mechanics, collision problem (Darwin), 375.

Whytlaw-Gray (R.) *See* Patterson and others.

Wilson (A. H.) Perturbation Theory in Quantum Mechanics, 176.

Wilson (A. H.) *See also* Fowler and Wilson.

Wilson (H. A.) The Theory of Cracking Petroleum, 16.

X-ray, soft, emission (Davies), 268.

X-ray spectroscopy, analysis by (Eddy and others), 249.

X-rays, intensity of total scattering (Waller and Hartree), 119.

X-rays, soft and adsorbed gas (Nakaya), 616.

X-rays, soft, emission at higher voltages (Richardson and Robertson), 188.

Zig-zag structure and properties of the hydrocarbon chain (Müller), 317.

I. A. R. I. 75.

IMPERIAL AGRICULTURAL RESEARCH
INSTITUTE LIBRARY
NEW DELHI.

[illegible]